

# Reservoir Sedimentation Handbook



**DESIGN AND MANAGEMENT OF  
DAMS, RESERVOIRS, AND WATERSHEDS  
FOR SUSTAINABLE USE**

Gregory L. Morris • Jiahua Fan

# ELECTRONIC VERSION

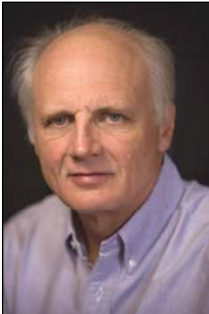
Ver. 1.01

September 2009

Cite as: Morris, Gregory L. and Fan, Jiahua. 1998. *Reservoir Sedimentation Handbook*, McGraw-Hill Book Co., New York.

Electronic version of the original 1998 publication by McGraw-Hill Book Co. This fully-searchable version contains minor corrections.

© Gregory L. Morris and Jiahua Fan



Gregory L. Morris, P.E., Ph.D.  
Gregory L. Morris Engineering  
P.O. Box 9024157  
San Juan, Puerto Rico 00902  
Tel. (787) 723-8005  
gregmorris@attglobal.net  
gregmorris@reservoirsedimentation.com



Jiahua FAN  
China Inst. Of Water Resources & Hydropower Research  
20 West Chegongzhuang Road  
Beijing, China  
fan-jiahua@sohu.com

---

# RESERVOIR SEDIMENTATION HANDBOOK

---

Design and Management  
of Dams, Reservoirs, and Watersheds  
for Sustainable Use

---

**Gregory L. Morris**

*Gregory L. Morris & Assoc.  
San Juan, Puerto Rico, USA*

**Jiahua Fan**

*Professor and Senior Engineer  
Institute of Water Conservancy and  
Hydroelectric Power Research  
Beijing, China*

**McGraw-Hill**

New York San Francisco Washington, D.C. Auckland Bogotá  
Caracas Lisbon London Madrid Mexico City Milan  
Montreal New Delhi San Juan Singapore  
Sydney Tokyo Toronto

**Library of Congress Cataloging-in-Publication Data**

Reservoir sedimentation handbook : design and management of dams,  
reservoirs, and watersheds for sustainable use / Gregory L. Morris  
: Jiahua Fan.

p. cm.

Includes bibliographical references (p. ) and index.

ISBN 0-07-043302-X

1. Reservoir sedimentation. I. Morris, Gregory L. II. Fan,  
Jiahua.

TD396.R473 1997

627'.86—dc21

97-1065

CIP

**McGraw-Hill**



A Division of The McGraw-Hill Companies

Copyright © 1998 by The McGraw-Hill Companies, Inc. All rights reserved.  
Printed in the United States of America. Except as permitted under the United  
States Copyright Act of 1976, no part of this publication may be reproduced or  
distributed in any form or by any means, or stored in a data base or retrieval system,  
without the prior written permission of the publisher.

1 2 3 4 5 6 7 8 9 0 DOC/DOC 9 0 2 1 0 9 8 7

ISBN 0-07-043302-X

*The sponsoring editor for this book was Larry Hager, the editing supervisor was  
Peggy Lamb, and the production supervisor was Pamela A. Pelton. It was set in  
Times Roman by Estelita F. Green of McGraw-Hill's Professional Book Group  
composition unit.*

*Printed and bound by R. R. Donnelley & Sons Company.*



This book is printed on recycled, acid-free paper containing a  
minimum of 50% recycled, de-inked fiber.

McGraw-Hill books are available at special quantity discounts to use as premiums  
and sales promotions, or for use in corporate training programs. For more informa-  
tion, please write to the Director of Special Sales, McGraw-Hill, 11 West 19th  
Street, New York, NY 10011. Or contact your local bookstore.

Information contained in this work has been obtained by The McGraw-Hill Companies, Inc. ("McGraw-Hill") from sources believed to be reliable. However, neither McGraw-Hill nor its authors guarantees the accuracy or completeness of any information published herein and neither McGraw-Hill nor its authors shall be responsible for any errors, omissions, or damages arising out of use of this information. This work is published with the understanding that McGraw-Hill and its authors are supplying information but are not attempting to render engineering or other professional services. If such services are required, the assistance of an appropriate professional should be sought.

*For Daniel, Richard...*

*And others of the next generation.*

---

# **CONTENTS (abbreviated)**

---

**Chapter 1. Introduction**

**Chapter 2. Reservoirs and Sustainable Development**

**Chapter 3. Engineering Features of Dams and Reservoirs**

**Chapter 4. Concepts of Reservoir Limnology**

**Chapter 5. Sediment Properties**

**Chapter 6. Erosion**

**Chapter 7. Sediment Yield from Watersheds**

**Chapter 8. Fluvial Morphology and Sediment Sampling**

**Chapter 9. Hydraulics of Sediment Transport**

**Chapter 10. Sediment Deposits in Reservoirs**

**Chapter 11. Modeling of Sediment Transport and Deposition in Reservoirs**

**Chapter 12. Reduction in Sediment Yield**

**Chapter 13. Sediment Routing**

**Chapter 14. Turbid Density Currents**

**Chapter 15. Flushing**

**Chapter 16. Sediment Evacuation**

**Chapter 17. Decommissioning of Dams**

**Chapter 18. Environmental and Regulatory Issues**

**Chapter 19. Case Study: Cachí Hydropower Reservoir, Costa Rica**

**Chapter 20. Case Study: Loíza Reservoir Case Study, Puerto Rico**

**Chapter 21. Case Study: Gebidem Dam and Reservoir, Switzerland**

**Chapter 22. Case Study: North Fork Feather River, California**

**Chapter 23. Case Study: Sefid-Rud Reservoir, Iran**

**Chapter 24: Case Study, Sanmenxia Reservoir, China**

**Chapter 24. Case Study, Heisonglin Reservoir, China**

---

# PREFACE TO ELECTRONIC VERSION

---

Ver. 1.01

Sediment issues at reservoirs are growing, as is the world community's awareness to this issue. To further the dissemination of information on this topic, the authors are making the Reservoir Sedimentation Handbook freely available in searchable electronic form.

This document was prepared from scans of the original, which were converted to text and then re-formatted to match as closely as possible the original book. All figures, tables and headings fall on the same page as in the original, but paragraph breaks are not exactly the same. This version includes a correction to Figure 9.11, typographical and grammatical errors have been corrected, and hopefully the errors introduced by the text recognition software have themselves all been found and fixed. The original index has not been reproduced, since the text is now fully searchable.

The authors gratefully acknowledge the assistance of Richard Morris and Julian and Christopher Libby in the tedious work of preparing the electronic version.

*Gregory L. Morris*  
*San Juan*

*Jiahua Fan (FAN Jiahua)*  
*Beijing*

---

# PREFACE

---

When the first author began researching problems of reservoir sedimentation many years ago, the lack of a book-type treatment of the subject became immediately apparent. While there is a significant amount of literature, it is widely scattered, written in several languages, and much of it is "gray literature" published in the form of engineering reports and conference proceedings which is not readily accessible. This handbook is an outgrowth of the need for a comprehensive treatment of this complex subject.

An in-depth treatment of each of the major technical topics is, of course, impossible within the context of a single handbook, and the treatment herein is by no means comprehensive and all-inclusive. The topics in each chapter are themselves of sufficient complexity to warrant book-length treatment. It is hoped that this conceptual overview of the major themes in each topic area, supported with a list of references and case studies, will facilitate the readers' comprehension of existing and potential problems at their own particular reservoir and watershed, and the types of remedial actions that have proved useful at other sites. The authors strongly feel that the most fundamental problem is to properly diagnose a sedimentation issue and select the conceptually appropriate course of action. Once the nature of the problem has been conceptually identified and one or more feasible courses of action identified, the approach to be used for subsequent detailed technical studies will usually be clear.

The first author's research on reservoir sedimentation topic was sparked by Ariel Lugo, and a discussion of problems at Puerto Rican reservoirs several years later with A. Santiago Vazquez. Both authors would like to express their special thanks to María Margarita Irizarry who, during her term as Executive Director of the Puerto Rico Aqueduct and Sewer Authority, started sediment management activities at the Loía reservoir. Work at this site initiated the collaboration between the co-authors that eventually resulted in this handbook.

Many workers from around the world, too numerous to name individually, have been very helpful in providing time, insight, information, material, photographs, and permission to reproduce material. We are particularly indebted to those who provided detailed information on case studies: Esmail Tolouie (Sefid-Rud); Gian Rechsteiner (Gebidem); Alexis Rodríguez, Ake Sundborg, and Margareta Jansson (Cachí); Xia Mading (Heisonglin); Richard Webb and Allan Zack (Loíza); and Donna Lindquist, Clay Clifton, Larry Harrison, Howard Chang, and Scott Tu (Feather River). Alain Petitjean and Jean-Pierre Bouchard at Electricité de France provided information on French reservoirs. Contributions by Shou-shan Fan at the U.S. Federal Energy Regulatory Commission are greatly appreciated. Robert MacArthur, George Annandale, Robert Strand, Vic Galay, Andrea Handler-Ruiz, Tom Skelly, Rollin Hotchkiss, and Kathleen Wilson were all particularly helpful. Professionals at the following institutions also provided invaluable information and assistance: China Institute of Water Resources and Hydropower Research (Beijing), Northwest Hydrotechnical Institute (Xian), U.S. Bureau of Reclamation, U.S. Army Corps of Engineers, U.S. Geological Survey, U.S. Natural Resources Conservation Service, U.S. Forest Service, Puerto Rico Aqueduct and Sewer Authority, and Los Angeles County Public Works Department. Editorial support from McGraw-Hill was outstanding.

Production of this handbook also represents a 2-year team effort by personnel at Gregory L. Morris & Assoc. We could not have made it through the long ordeal of manuscript preparation without the capable editorial assistance of Marco Flores, and graphic materials prepared by Elias Castro, Ada Sotto, Sebastian Garcia, Pully Torres, and Miguel Menar helped keep the office running throughout the long writing process. Former employees Guangdou Hu and G.T. Anderson discussed ideas and performed literature searches at university libraries.

The first author greatly appreciates the support by his wife, Miriam, and sons Daniel and Richard, who graciously accepted the long hours and forfeited hiking and kayaking trips. Also gratefully acknowledged are the many years of dedication by his parents, and guidance by many excellent teachers. The second author greatly appreciates more than 45 years of support and help in his sediment research for water resources development by his wife, Song Xiuzhen, and the support of his daughters Ying, Bing, and Xing.

We hope that society will benefit from our collected thoughts about water and sediment management.

*Gregory L. Morris*

*San Juan*

*Jiahua Fan (FAN Jiahua)*

*Beijing*

---

# CHAPTER ONE

---

## INTRODUCTION

---

### 1.1 Need For Sediment Management

---

Most natural river reach are approximately balanced with respect to sediment inflow and outflow. Dam construction dramatically alters this balance, creating an impounded river reach characterized by extremely low flow velocities and efficient sediment trapping. The impounded reach will accumulate sediment and lose storage capacity until a balance is again achieved, which would normally occur after the impoundment has become “filled up” with sediment and can no longer provide water storage and other benefits. Declining storage reduces and eventually eliminates the capacity for flow regulation and with it all water supply and flood control benefits, plus those hydropower, navigation, recreation, and environmental benefits that depend on releases from storage. The Camaré reservoir in Venezuela (Fig. 1.1) offers an example of the consequences of sedimentation; less than 15 years were required for loss of all storage. This site differs from most other reservoirs in only one aspect, the speed at which storage capacity was lost. Sediment management was not practiced at this site.

Storage loss is but one of many sedimentation problems that can affect reservoirs. Operation of storage reservoirs is severely impacted by the time half the volume has been sedimented, but severe sediment-related problems can appear when only a small percentage of the storage capacity has been lost. As reservoirs age and sediments continue to accumulate, sediment-related problems will increase in severity and more sites will be affected. At any dam or reservoir where sustainable long-term use is to be achieved, it will be necessary to manage sediments as well as water. This is not a trivial challenge.

Many type of sediment-related problems can occur both upstream and downstream of dams, and sediment entrainment can also interfere with the beneficial use of diverted water. Sediment can enter and obstruct intakes and greatly accelerate abrasion of hydraulic machinery, thereby decreasing its efficiency and increasing maintenance costs. Turbid density currents can carry sediments tens of kilometers along the bottom of the impoundment, eventually entering deep intakes and accumulating in front of low level outlets. Localized sediment deposits in the delta region and streambed aggradations upstream of the reservoir can produce flooding, cause soil water logging and salinization, impair navigation, alter ecological conditions, inundate powerhouses discharging into delta areas, and bury intakes (Fig. 1.2). In arid regions the growth of phreatophytic vegetation on delta deposits can significantly accelerate water loss. The combination of sediment trapping and flow regulation also has dramatic impacts on the ecology, water transparency, sediment balance, nutrient budgets, and river morphology downstream of the reservoir; dam construction is the largest single factor influencing sediment delivery to the downstream reach. The cutoff of sediment transport by the dam can cause stream-



(a)



(b)

**FIGURE 1.1** Fully sedimented Camaré irrigation reservoir in Venezuela: (a) overview, (b) looking upstream from the spillway showing incipient formation of floodplain deposits above the spillway elevation on either side of the channel. The water surface in the photo is at the spillway crest elevation (G. Morris).



**FIGURE 1.2** Sedimented water supply intake in the delta region upstream of Khasm El Girba Dam on the Atbara River, Sudan (*R. Hotchkiss*).

bed degradation, accelerate rates of bank failure, and increase scour at structures such as bridges. The streambed will coarsen and become armored, degrading or eliminating spawning beds. Even coastal processes can be affected; accelerated coastal erosion affecting the Mississippi and Nile deltas is attributed to sediment trapping behind dams more than 1000 km upstream.

Based on the inventory published by the International Commission on Large Dams (ICOLD, 1988) and the current rate of dam construction, as of 1996 there were about 42,000 large (over 15 m tall) dams worldwide. There are several times as many lesser structures. An overwhelming majority of these structures are designed and operated to continuously trap sediment, without specific provisions for sustained long-term use. Neither current nor projected levels of population and economic activity can be sustained if today's inventory of storage reservoirs is lost to sedimentation, and, as population and economic activity grow, reliance on the services provided by dams is increasing. Reservoir-dependent societies range from technically advanced urban and agricultural systems in the western United States to village irrigators on the Indian peninsula. Sudden loss of the world's reservoir capacity would be a catastrophe of unprecedented magnitude, yet their gradual loss due to sedimentation receives little attention or corrective action.

Reservoirs have traditionally been planned, designed, and operated on the assumption that they have a finite "life," frequently as short as 100 years, which will eventually be terminated by sediment accumulation. Little thought has been given to reservoir replacement when today's impoundments are lost to sedimentation, or to procedures to maintain reservoir services despite continued sediment inflow. There has been the tacit assumption that somebody else, members of a future generation, will find a solution when today's reservoirs become seriously affected by sediment. However, sedimentation problems are growing as today's inventory of reservoirs ages, and severe sediment

problems are starting to be experienced at sites worldwide, including major projects of national importance. Sediment management in reservoirs is no longer a problem to be put off until the future; it has become a contemporary problem.

Traditional approaches to sediment management have not considered the need for sustained use. Large initial storage volumes and erosion control have traditionally been recommended to reduce sediment inflow and delay the eventual "death" of reservoirs, but erosion control alone cannot achieve the sediment balance required to stabilize reservoir storage capacity and achieve sustainable use. Furthermore, many erosion control programs are poorly conceived and implemented, and fail to achieve the desired reductions in sediment yield. As a result, reservoirs worldwide are losing storage capacity rapidly, possibly as fast as 1 percent per year (Mahmood, 1987). Reservoir construction requires sites having unique hydrologic, geologic, topographic, and geographic characteristics, and existing reservoirs generally occupy the best available sites. Because of the high cost and multiple problems associated with sediment removal and disposal on a massive scale, the sedimentation of large reservoirs is to a large extent an irreversible process. If future generations are to benefit from essential services provided by reservoirs it will be largely through the preservation and continued utilization of existing reservoir sites, not the continued exploitation of a shrinking inventory of potential new sites. The water supplies and other benefits derived from reservoirs do not constitute renewable resources unless sedimentation is controlled.

## **1.2 ELEMENTS OF SEDIMENT MANAGEMENT**

---

Conversion of sedimenting reservoirs into sustainable resources which generate long-term benefits requires fundamental changes in the way they are designed and operated. It requires that the concept of a reservoir life limited by sedimentation be replaced by a concept of managing both water and sediment to sustain reservoir function. Sustainable use is achieved by applying the following basic sediment control strategies:

- 1. Reduce sediment inflow.** Sediment delivery to the reservoir can be reduced by techniques such as erosion control and upstream sediment trapping.
- 2. Route sediments.** Some or all of the inflowing sediment load may be hydraulically routed beyond the storage pool by techniques such as drawdown during sediment laden floods, off-stream reservoirs, sediment bypass, and venting of turbid density currents.
- 3. Sediment removal.** Deposited sediments may be periodically removed by hydraulic flushing, hydraulic dredging, or dry excavation.
- 4. Provide large storage volume.** Reservoir benefits may be considered sustainable if a storage volume is provided that exceeds the volume of the sediment supply in the tributary watershed. The required sediment storage volume may be included within the reservoir pool or in one or more upstream impoundments.
- 5. Sediment placement.** Focus sediment deposition in areas where its subsequent removal is facilitated, or where it minimizes interference with reservoir operation. Configure intakes and other facilities to minimize interference from transported or deposited sediments.

The cost and applicability of each strategy will vary from one site to another and also as a function of sediment accumulation. However, even the largest reservoirs will eventually

be reduced to small reservoirs by sedimentation and, sooner or later, will require sediment management.

### 1.3 HANDBOOK APPROACH

---

This handbook seeks to generate an awareness of sedimentation problems, outlining practical strategies for their identification, analysis and management. Basic concepts and tools are presented which, when applied in an integrated manner, can achieve what we will term *sustainable sediment management* in reservoirs. Sedimentation is the single process that all reservoirs worldwide share in common, to differing degrees, and the management strategies and techniques presented herein are applicable to reservoirs of all ages, types, and sizes. An understanding of these principles will also aid in the effective design and management of sediment-trapping structures such as debris basins and detention ponds. Although complex mathematical and physical modeling studies may often be required to finalize the design and operational procedures for sediment management, this handbook makes no attempt to provide an in-depth treatment of these analytical methods or sediment transport theory. Extensive treatments of these topics are already available by others (Yang, 1996; Simons and Senturk, 1992; Julien, 1995; Chang, 1988; Vanoni, 1975; Graf, 1971). Rather, this handbook presents a broader view of basic principles and methods essential for the conceptualization and assessment of sedimentation issues associated with reservoirs, and for identifying management strategies to be explored in subsequent detailed and site-specific studies.

Sedimentation problems and management techniques vary widely from one site to another, and by studying specific sites one can appreciate the complexity of sediment problems and the manner in which they can be addressed. Seven chapters have been devoted to detailed case studies. These cases have been selected to demonstrate a variety of management techniques and cover a wide range of geographic and hydrologic conditions. Case study reservoirs range in size from 2 to 1700 Mm<sup>3</sup> (2 to 1700 × 10<sup>6</sup> m<sup>3</sup>). Two sites are located in the United States, two in China, and one each in Costa Rica, Switzerland, and Iran.

China has 82,000 reservoirs which are losing storage capacity at an average annual rate of 2.3 percent, the highest rate of loss of any country in the world (Zhou, 1993). China's Yellow River has the highest sediment concentrations of all the world's major river systems, and China also has half of the world's large dams. Not surprisingly, China has considerable experience in the management of reservoir sedimentation. This handbook has made a particular effort to distill useful lessons from the Chinese experience.

Finally, this handbook introduces the overall concept of sustainable sediment management with the goal of converting today's sedimenting reservoirs into resources that will benefit future generations as well as our own. Whereas the twentieth century focused on the construction of new dams, the twenty-first century will necessarily focus on combating sedimentation to extend the life of existing infrastructure. This task will be greatly facilitated if we start today.

---

## CHAPTER 2

---

# RESERVOIRS AND SUSTAINABLE DEVELOPMENT

---

---

## 2.1 WATER SUPPLY AND WATER SCARCITY

---

### 2.1.1 Global Water Resources

Natural lakes and rivers worldwide contain about 93,000 km<sup>3</sup> of fresh water, about 0.27 percent of the earth's total fresh water resource (Table 2.1). While the absolute volume of groundwater storage is large, it is much less accessible than surface waters because most is located too deep or in formations of insufficient permeability for economic exploitation, the rate of replenishment is much slower than surface water, and extraction from coastal areas is limited by saline intrusion. Thus, groundwater is much less important than surface supplies. For example, total groundwater availability in 21 Arab countries is estimated at only 14.8 percent of total streamflow (Shahin, 1989). Groundwater recharge in India has been variously estimated at 15 and 25 percent of total runoff, and in the United States and Russia respectively groundwater use accounts for 20 and 9.3 percent of total withdrawals (Gleick, 1993). In the long run, withdrawals from either surface or groundwater sources cannot exceed runoff, defined as rainfall minus evapotranspiration, except to the extent that water is reused. However, reuse potential is not large because the most voluminous water use, irrigation, is consumptive.

Water storage in natural lakes (91,000 km<sup>3</sup>) plus reservoirs (7000 km<sup>3</sup>) is slightly less than the annual global precipitation of 119,000 km<sup>3</sup> over land areas, and about twice the annual runoff into the ocean of 47,000 m<sup>3</sup>, a figure which includes surface water, groundwater, and glacial discharges. The remaining 41 percent of global precipitation is returned to the atmosphere as evapotranspiration. Runoff is unevenly distributed both

**TABLE 2.1** World Water Resources

	Volume, 10 <sup>3</sup> km <sup>3</sup>	Relative amount of	
		Total water, %	Fresh water, %
Saline water:	1,350,939.4	97.47	
Oceans	1,338,000.0	96.54	
Lakes	85.4	0.01	
Groundwater	12,854.0	0.93	
Fresh water:	35,028.6	2.53	100.00
Antarctic ice	21,600.0	1.56	61.66
Other ice and permafrost	2,764.0	0.20	7.89
Groundwater	10,546.0	0.76	30.11
Lakes	91.0	0.01	0.26
Swamps	11.5	0.00	0.03
Atmosphere	12.9	0.00	0.04
Rivers	2.1	0.00	0.01
Saline water:	1,350,939.4	97.47	
Oceans	1,338,000.0	96.54	

geographically and in time. While the Amazon basin accounts for 15 percent of global runoff, Australia, with a slightly larger land area, accounts for only 0.7 percent (Shiklomanov, 1993). Seasonal variation is particularly evident in areas such as India, projected to be the world's most populated country by year 2050, where the monsoon season lasts 3 months or less and the remainder of the year is essentially dry.

### 2.1.2 Water Scarcity

The amount of fresh water circulating through the hydrologic cycle is fixed, but the demand for water use has grown rapidly during the twentieth century and fresh water is becoming an increasingly scarce resource. Modern society is, above all else, a hydraulic society. Population and economic activity are increasingly tied to the diversion of fresh water to human use, particularly as agricultural expansion becomes increasingly dependent on irrigation. Water withdrawals in the United States grew more rapidly than population through the twentieth century, but withdrawals have slowed since the 1970s, reflecting the increasing efficiency of water use because of scarcity (Fig. 2.1). Recog-

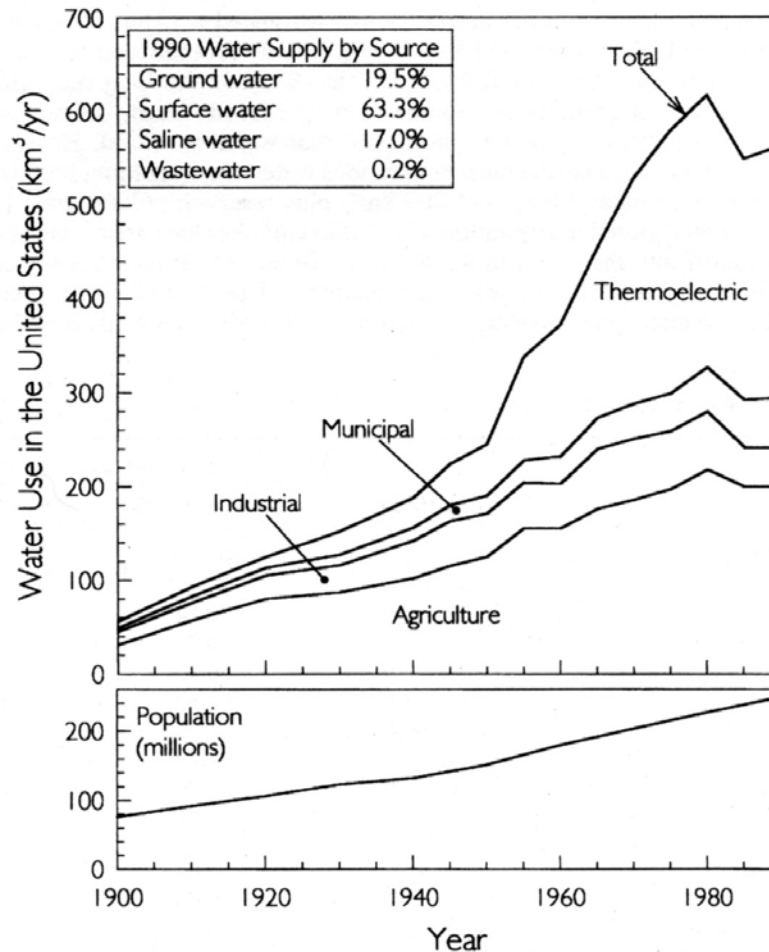


**FIGURE 2.1** Water withdrawals in the United States over time, as compared to population (*data from USGS Water Summary and Census of Population*).

dition that there is inadequate water to pollute freely has led to increasing levels of wastewater treatment, greater efficiency in use, and recycling in the industrial sector. Scarcity has also led to increasing irrigation efficiency in the agricultural sector, and new plumbing codes are gradually taking the United States from 20-L (5-gal) to 6-L (1.6-gal) flush toilets. Municipal water rationing has been imposed not only in dry areas such as southern California but also in humid areas ranging from Florida to New York. Increasing efficiency of use, combined with low rates of population growth, are also generally characteristic of highly industrialized nations in Europe.

The patterns of increasing water scarcity evident in the United States are also occurring on a global scale, but in many regions the scarcity is much more acute. Most of the world's population growth is occurring in less developed countries, especially in areas of low rainfall with high and increasing dependence on irrigation, which greatly increases per capita water requirements since food and fiber must be produced from runoff diverted to agricultural use rather than natural precipitation on rain-fed cropland. Thus, in Sweden it is possible to maintain one of the world's highest standards of living with water withdrawals of only 620 m<sup>3</sup>/capita/yr, whereas in irrigation-dependent Arab countries withdrawals of 1205 m<sup>3</sup>/capita/yr are needed to produce an individual's annual requirement of 375 kg of fruits and vegetables, 35 kg of meats and poultry, 125 kg of cereals, plus 55 m<sup>3</sup> for domestic use (Falkenmark and Lindh, 1993).

Total runoff can be used to give a crude, and admittedly optimistic, estimate of the total volume of water that could be made available if water supplies are fully developed for human use, leaving little if any water to sustain natural aquatic or wetland ecosystems. Engleman and LeRoy (1995) used a per capita runoff of 1700 m<sup>3</sup>/yr as a benchmark for "water stress" and 1000 m<sup>3</sup>/yr as a benchmark for "water scarcity," and combined national data on total runoff with the 1994 United Nations medium population projection by country (summarized in Table 2.2 by continent) to compute runoff per capita. This was compared to the benchmark values to examine trends in water availability. By year 2050 some 58 nations containing nearly 4.4 billion people will be experiencing either water stress or scarcity, as compared to a population of less than 0.4 billion so classified in 1990 (Fig. 2.2). Population and water availability for several countries are compared in Table 2.3, where it can be seen that the United States, despite large deserts, as a whole is a water-rich nation. Israel, with only 461 m<sup>3</sup>/capita, employs the world's most technologically advanced and efficient water management system.

The continuously sustainable or *firm yield* from unregulated stream diversions generally ranges from zero to 20 percent of the mean annual discharge, with the lower values applicable to more and smaller watersheds. Reservoirs are necessary to divert

**TABLE 2.2** Projected Global Population Growth

Continent	Population, millions by year				Growth rate 1990-2050, annual %
	1950	1990	2020	2050	
Europe	549	722	723	678	- 0.1
North America	166	278	358	389	0.6
Oceania	13	27	40	46	0.9
Asia	1,403	3,186	4,744	5,741	1.0
Latin America	166	440	676	839	1.1
Africa	224	633	1,348	2,141	2.1
World Total	2,521	5,286	7,889	9,834	1.0

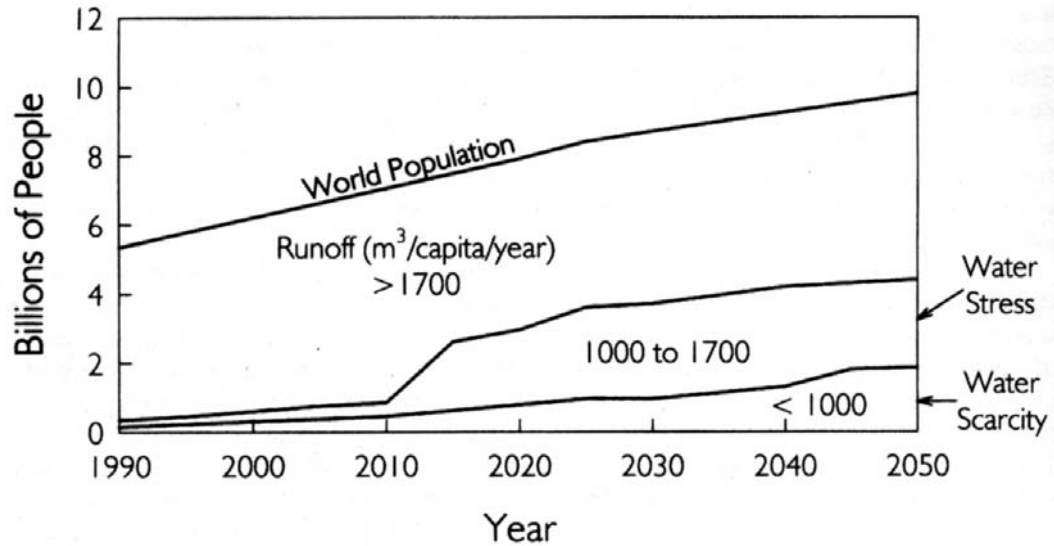


**FIGURE 2.2** Current and projected world population, showing the population in nations having different levels of runoff per capita (after Engleman and LeRoy, 1994)

**TABLE 2.3** Runoff per Capita for Selected Countries

Country	Runoff depth, mm	Population millions		Runoff per capita, m <sup>3</sup>	
		1990	2050	1990	2050
Israel	104	4.7	8.9	461	241
Algeria	7	24.9	55.7	690	309
Egypt	59	56.3	117.4	1,046	502
Ethiopia	98	47.4	194.2	2,320	566
Morocco	573	24.3	47.9	1,151	585
Haiti	396	6.5	18.6	1,696	593
Nigeria	333	96.2	338.5	3,203	910
Pakistan	582	121.9	381.5	3,838	1,227
India	634	850.6	1639.9	2,451	1,271
Dominican Republic	410	7.1	13.2	2,813	1,519
China	293	1155.3	1606.0	2,424	1,743
Turkey	260	56.1	106.3	3,619	1,910
United Kingdom	492	57.4	61.6	2,090	1,947
Mexico	182	84.5	161.5	4,224	2,211
France	338	56.7	60.5	3,262	3,059
Germany	561	79.4	64.2	2,520	3,113
Iran	72	58.9	163.1	4,428	4,972
Japan	1448	123.5	110.0	4,428	4,972
United States	253	249.9	349.0	9,915	7,101
Russia (former U.S.S.R.)	248	280.4	318.9	19,493	17,142
Brazil	816	148.5	264.3	46,809	26,291

*Source:* Adapted from Engleman and Leroy (1994).

a greater percentage of the surface runoff to human use on a continuous basis by equalizing irregular stream flow; water is stored during periods of high flow and delivered during periods of low flow. As water demand increases relative to runoff the reservoir storage volume available for flow equalization must increase, and as demand centers grow it also becomes necessary to develop increasingly distant water sources. Because the most easily developed resources are used first, each additional cubic meter of sustained water yield typically requires more effort to extract than the previous one because of the law of diminishing returns. The cost of each new project; the marginal cost of water supply, tends to increase over time. Biswas (1991) states that the unit cost of water from the next generation of domestic water supply projects is often 2 or 3 times higher than the present generation; nearly all the easily available sources of water have already been or are now under development. With many of the best irrigable areas already in use, the real cost of new irrigation schemes in Asia has also doubled or tripled between the mid-1950s and mid-1980s (Table 2.4).

In summary, there is a clear trend toward increasing water scarcity relative to its traditional uses. Reservoir sedimentation will exacerbate this scarcity by reducing the yield from already-developed supplies.

---

## CHAPTER 3

---

# ENGINEERING FEATURES OF DAMS AND RESERVOIRS

---

This chapter describes basic characteristics of dams and reservoirs and introduces nomenclature and concepts concerning their design and operation.

---

### 3.1 HISTORICAL PERSPECTIVE

---

#### 3.1.1 Dams in Antiquity

The oldest reservoir in operation today is the 100-Mm<sup>3</sup> Afengtang reservoir, constructed west of Shanghai during 589 to 581 B.C. The original dam, reportedly constructed of alternating layers of earth and straw held into place with chestnut piles, no longer exists and has been reconstructed. However, the record for longest service is apparently held by the Mala'a reservoir in Egypt, originally constructed by King Amenemhet III (1842 to 1798/95 B.C.) in the Faiyum depression 90 km southwest of Cairo and reconstructed in the third century B.C. with a dam 8 km long and 7 m high. It stored up to 275 Mm<sup>3</sup> of water diverted from the Nile and remained in operation until the eighteenth century, a span of 3,600 years. The oldest continuously operating dam still in use is the Kofini flood control diversion dam and channel constructed in 1260 B.C. on the Lakissa River upstream of the town of Tiryns, Greece, which it continues to protect. The original structure is still in operation, and while floodwaters have on occasion approached the crest, it has never been overtopped. Remains of other ancient dams have been located at various sites bordering the Mediterranean, the Near and Middle East, Sri Lanka, and in Central America where the first dam is dated at 700 B.C. (Schnitter, 1994).

Dam construction was undertaken on a wide scale by the Romans. Schnitter lists 79 Roman dams, the dimensions of which are known today: 47 in Spain, Portugal, and France; 12 in North Africa; 18 in the Near and Middle East; but only 2 in Italy. The 20.5m-tall Harbaqa Dam and its heavily sedimented reservoir near Palmyra, Syria, constructed by the Romans for irrigation supply, is an example of the relative permanence of sediment deposits upstream of a dam (Fig. 3.1). Although the dam was breached centuries ago, the gullies that traverse the deposits have removed only a fraction of the total sediment deposits. In contrast, the Prosperina dam in Mérida, Spain, also built by the Romans during either the first or second century, has remained in essentially continuous service for more than 1800 years. This 6-Mm<sup>3</sup> reservoir has only a 7-km<sup>2</sup> tributary watershed and is augmented by small canals diverting flow from an additional 13 km<sup>2</sup> of watershed. Because of its large storage capacity relative to watershed area, equivalent to 860 mm of soil denudation, the lack of development or intensive agricultural activity in its gently rolling watershed, and small diversion canals, it was not

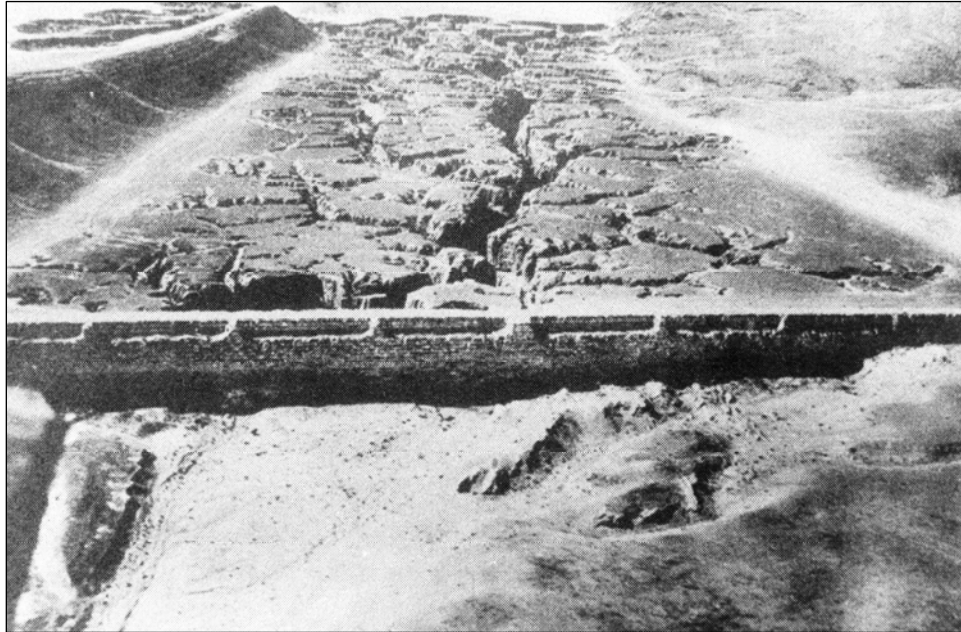


**FIGURE 3.1** Harbaqa Dam constructed by the Romans 80 km from Palmyra, Syria. Despite centuries of erosion, most of the sediment still remains trapped upstream of the dam(*DeBoysson*).

heavily silted. The small diversion canals cannot transport significant flow into the reservoir during major sediment-producing runoff events. During the early 1990s, the reservoir was drained, the Roman dam rehabilitated, sediment excavated, and the reservoir was returned to service.

Little is known about sediment control measures in ancient dams. The earliest record of specialized structures and techniques for sediment management mentioned by Smith (1971) or by Schnitter (1994) are associated with the Almansa Dam in Alicante, Spain, constructed in 1384 for irrigation and provided with a low-level outlet more than 3m in area for emptying and flushing. The flushing tunnel was closed at its upstream end with timbers and the reservoir was impounded for a period of years until a significant amount of sediment had accumulated. To initiate flushing, a worker was sent into the tunnel to cut away the supports restraining the wooden gate. If the sediment accumulation before the dam was sufficiently deep and compacted, the worker could exit the tunnel once the gate was cut away, then pierce through the sediments from the top of the dam with a long rod to initiate the flow that would empty the reservoir and scour away the sediments. However, this was a hazardous procedure since inadequate sediment depth or strength in front of the bottom outlet caused premature blowout, killing anyone in the tunnel. In the absence of flushing the reservoir would fill completely with sediment after several decades (Fernandez Ordonez, 1984). Utilization of a low-level outlet for intermittent flushing was incorporated into many historic Spanish dams and is occasionally referred to as the *Spanish method* of flushing (McHenry, 1974).

The histories of dam building compiled by both Schnitter (1994) and Smith (1971) underscore the potential longevity of these structures, if sedimentation can be controlled. Most ancient dams fell into ruin because of lack of structural maintenance as a result of changing economic or political conditions, or accumulation of sediments. A minority experienced catastrophic failure due to floods, and this often after a long period of neglect.

### 3.1.2. Modern Dam Construction

Large-scale impounding of the world's rivers was not undertaken until the twentieth century, and most dams have been constructed since 1950. The number of large dams (over 15 m tall) worldwide in the inventory maintained by the International Committee on Large Dams (ICOLD, 1988) grew as follows: 427 in 1900, 5268 in 1950, and about 39,000 in 1986. The average annual rate of dam construction for various periods summarized in Table 3.1 shows the slow rate of construction prior to 1950, the frenzy of dam construction from about 1950 to about 1980, especially in China, and the reduced rate of dam construction since 1980.

**TABLE 3.1** Rate of Large Dam Completions Since 1950

Period	Large dams commissioned per year		
	Excluding China	China	World
1900-50	97	0	97
1951-77	357	611	968
1978-82	335	420	755
1983-86	209	56	265
1987-90	NA	NA	NA
1991-94	187	122	309

*Source:* ICOLD. Data for 1987-90 not available.

Rates of dam construction within each country reflect greater variation than the world totals. Data from the United States and Mexico are presented in Fig. 3.2 and illustrate a period of rapid dam construction followed by a decline. The United States undertook

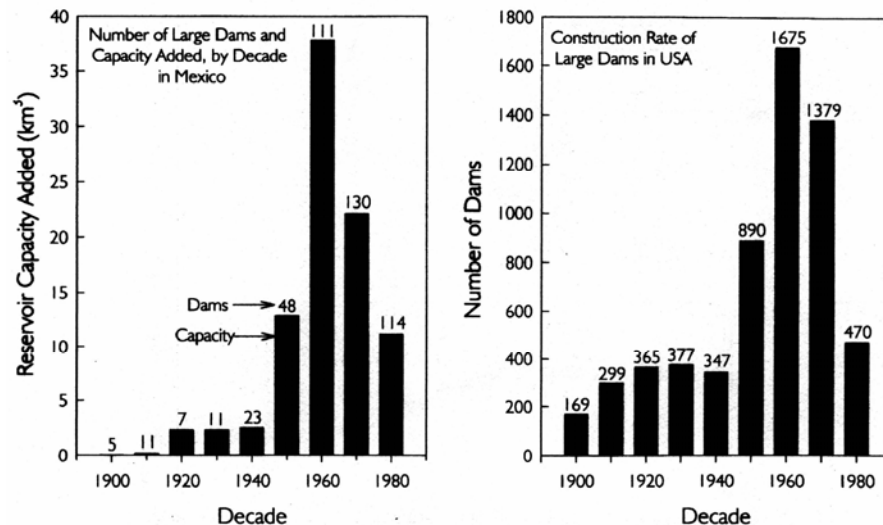


**FIGURE 3.2** Rates of large dam construction in the United States and Mexico (data from large U.S. Army Corps of Engineers and ICOLD, 1984 and 1988). able

sites developed, the rate of dam construction has declined to low levels. A similar pattern is evident in the data from China (Table 3.1) and in many other countries.

## 3.2 CHARACTERISTICS OF DAMS

### 3.2.1 Functions of Dams

The term *dam* can refer to any barrier erected to obstruct or control the flow of water. Three functional classes of dams may be defined: (1) storage dams, (2) barrages, and (3) diversion dams. These structures regulate, respectively: (1) head upstream and discharge released downstream, (2) head but not discharge, and (3) neither head nor discharge. Storage dams impound water to create a permanent pool, or regulate discharge by varying pool level as in the case of water supply, flood control, and storage-based hydro. A barrage is a low structure in which gate operation is used to control water level but does not regulate discharge by storing and then releasing water. A barrage does not have significant storage capacity and its gates are operated to balance inflow and outflow to maintain a target upstream water level, typically for delivery to an intake or for navigation (Fig. 3.3). Diversion dams are constructed for the sole purpose of diverting water, without the intent of regulating either discharge rate or water level.

Both storage dams and barrages elevate the water surface profile, deepen the flow depth, reduce flow velocity, and cause sediment to accumulate upstream of the barrier. Both types of structures can be adversely affected by sediment accumulation. However, the gates in a barrage extend to the riverbed level and both suspended and bed loads are passed through the structure. Because of their small hydrologic size, limited impact or flood flows, and gate placement, the impounded river reach upstream of a barrage may reach a new sediment equilibrium within a few years or decades, whereas storage reservoirs may require many centuries.

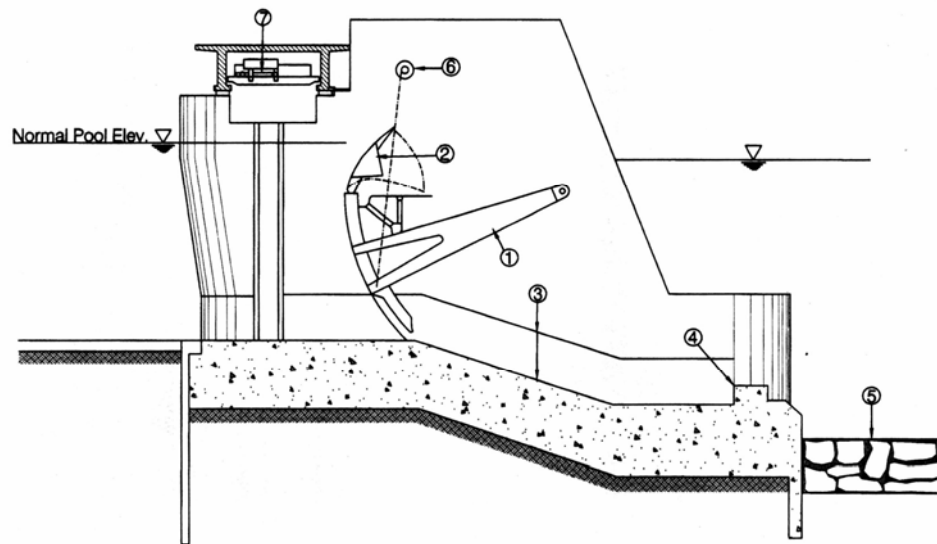


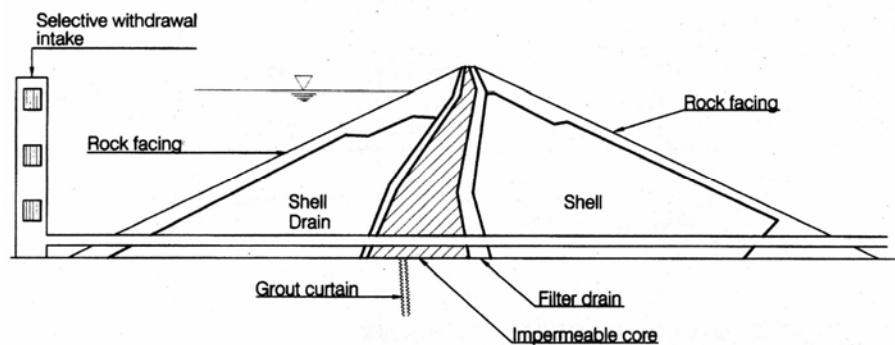
**FIGURE 3.3** Section view of Saint Pierre de Beouf Barrage, Rhone River, France, showing: (1) radial gate; (2) overspill flap gate; (3) armor for abrasion protection; (4) energy dissipation block; (5) scour protection; (6) chain hoist for gate; (7) hoist for stop logs.

of earth or rock designed to resist the lateral forces imposed by the reservoir pool at its maximum stage, plus an impermeable barrier such as clay or concrete usually located within the embankment, but sometimes constructed as an impermeable membrane on the upstream face. A cross-section view of an embankment dam is shown in Fig. 3.4. Embankment dams are extensively used for structures in the 15- to 30-m height range, where they represent nearly 90 percent of the total number, but they represent only 25 percent of the dams exceeding 200 m in height. However, the world's tallest dam is an embankment dam. The largest dams are listed in Table 3.2 for various categories.

### 3.2.3 Concrete Dams

Dams constructed of concrete may employ a variety of methods to withstand hydrostatic forces. A concrete gravity dam resists overturning and sliding forces by the gravitational mass of the concrete structure. Figure 3.5 illustrates the configuration of a concrete gravity dam with a hydropower station. The most recent major advancement in the construction of concrete dams is the application of roller-compacted concrete (RCC), a zero slump mixture of cement, aggregate, water, and, optionally, pozzolan, which is normally placed continuously in lifts of about 0.5 m and compacted with a vibratory roller. It combines the benefits and safety of a concrete gravity dam with the rapid and economical placement methods used in embankment dam construction (Hillebrenner, 1993). This technology has several important advantages over conventional concrete construction including lower cost, less potential for damage by flooding, and shorter construction time (Prendergast, 1992).

In narrow gorges having competent rock on either abutment, an arch dam may be constructed in which the hydrostatic forces are transmitted along the axis of the dam and into the rock abutments. Arch dams have much thinner sections than gravity dams. Although constituting less than 5 percent of dams worldwide, they account for half of all dams over 150 m high.



**Embankment Dam**

**FIGURE 3.4** Cross-sectional view of an embankment dam. The upstream face is protected with stone or other material to prevent erosion by wave action, and internal drains control seepage and avoid piping. A selective withdrawal or multilevel intake tower is also shown.

**TABLE 3.2** Largest Dams for Various Categories

Category and name	River	Country/ state	Height, m	Storage capacity, 10 <sup>6</sup> m <sup>3</sup>	Power capacity, MW	Year
World						
Highest dams						
Rogun	Vakhsh	Russia	335	13,300	-	UC
Nurek	Vakhsh	Tajikistan	300	10,500	2,700	1980
Grand Dixence	Dixence	Switzerland	285	401	-	1961
Inguri	Inguri	Georgia	272	1,100	-	1980
Largest reservoirs*						
Bratsk	Angara	U.S.S.R.	125	169,000	4,500	1964
High Aswan	Nile	Egypt	111	162,000	2,100	1970
Kariba	Zambezi	Zimbabwe	128	160,368	-	1959
Akosombo	Volta	Ghana	134	147,960	-	1965
Largest hydropower projects						
Itaipu	Parana	Brazil	196	29,000	12,600	1983
Guri	Caroni	Venezuela	162	135,000	10,300	1986
Sayano	Yenisei	Russia	245	31,300	6,400	1989
Grand Coulee	Columbia	USA	168	11,795	6,180	1942
United States						
Highest dams						
Droville	Feather	California	230	4,670	644	1968
Hoover	Colorado	Nevada	221	34,850	1,434	1936
Dworshak	N.Fork Clearwater	Idaho	219	4,260	400	1973
Glen Canyon	Colorado	Arizona	216	33,300	1,042	1966
Largest reservoir						
Hoover	Colorado	Nevada	230	34,850	1,434	1936
Glen Canyon	Colorado	Arizona	216	33,300	1,042	1966
Garrison	Missouri	North Dakota	64	27,920	517	1954
Oahe	Missouri	South Dakota	75	27,430	640	1958
Largest hydropower projects						
Grand Coulee	Columbia	Washington	168	11,795	6,180	1942
Chief Joseph	Columbia	Washington	72	752	2,467	1955
John Day	Columbia	Oregon	70	617	2,160	1968
Bath County Upper	Little Back Ck	Virginia	143	44	2,100	UC

UC = uncompleted.

\*208.8-km<sup>3</sup> Owen Falls on White Nile, Uganda, not included, as it impounds a natural lake.

Source: ICOLD (1984, 1988).

### 3.3 RESERVOIR CHARACTERISTICS AND OPERATION

#### 3.3.1 Reservoir Size

Reservoir volume may be expressed in absolute units, such as millions of cubic meters (Mm<sup>3</sup>), or relative to mean annual flow. From the standpoint of sediment management the relative size, termed *hydrologic size* or *capacity to inflow (C:I) ratio*, is more important than absolute size and is computed as the ratio of total reservoir volume to mean annual inflow.

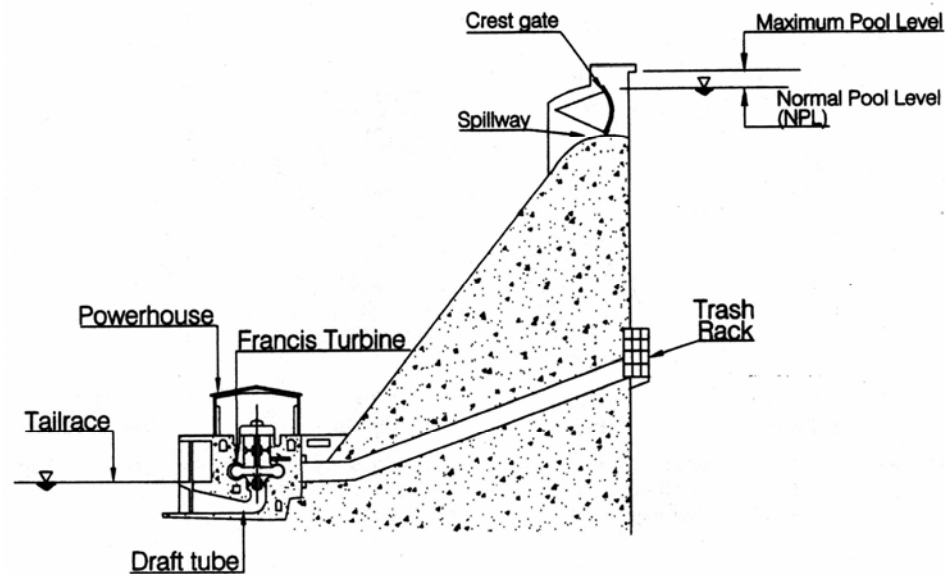


**FIGURE 3.5** Section view of concrete gravity dam with a hydropower station, showing the various terms used to describe system.

Hydrologic size is a primary factor influencing the rate of sediment accumulation (Brune, 1953) and is also a primary determinant of the types of sediment management techniques that can be used. Hydrologically small reservoirs have short residence times and typically spill a significant part of the streamflow downstream during floods. They can be manipulated in a variety of ways to encourage the release of sediments together with that part of the annual discharge that is spilled. A reservoir having a capacity inflow ratio exceeding 50 percent may be considered hydrologically large and may have significant year-to-year carryover storage capacity. Having a large capacity relative to runoff, these reservoirs spill little water, and there is limited opportunity to periodically draw down or empty these larger reservoirs for sediment management because the associated water loss would be unacceptable. However, as large reservoirs fill with sediment and their capacity decreases, a wider range of sediment management techniques will become applicable. At some sites it appears feasible to maintain a reservoir capacity of approximately 20 to 30 percent of mean annual flow using sediment flushing (Tolouie, 1993; Xia, 1987).

The terms *hydraulic residence time*, *turnover time*, and *detention period* all refer to the time required to replenish the water in the reservoir computed from the actual storage volume (which varies as a function of pool elevation) and the inflow rate over a specified time period (rather than the long-term mean inflow). The hydraulic residence time in a hydrologically small reservoir can vary from under an hour during a major flood to many months during the dry season. Because of hydraulic short-circuiting, the actual hydraulic residence time for a particular parcel of water may be very different from the average value computed from the inflow rate and reservoir storage.

### 3.3.2 Pool Geometry

Reservoir pool geometry has a major influence on hydraulic behavior and the pattern of sediment transport within the impoundment. The pool configurations shown in Fig. 3.6 illustrate the wide range of pool planforms that occur.

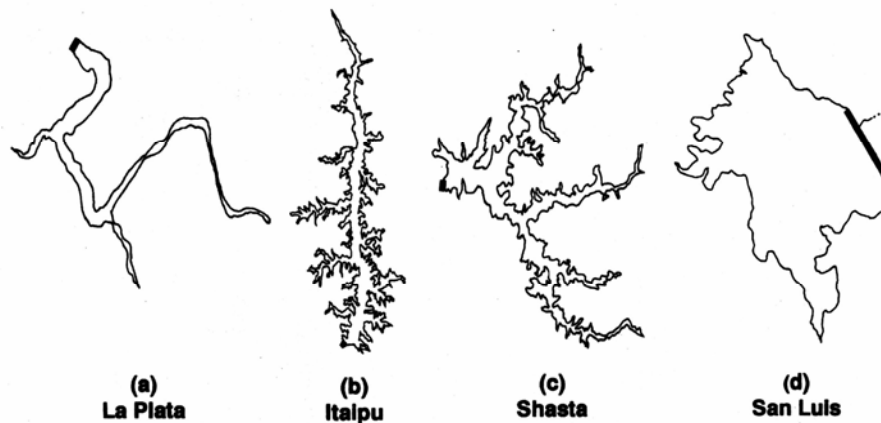


**FIGURE 3.6** Pool configurations for various reservoirs: (a) La Plata, Puerto Rico; (b) Itaipu Brazil/Paraguay; (c) Shasta, California; (d) San Luis, California. The San Luis configuration is typical of reservoirs in areas of low relief requiring a long dam and creating a relatively shallow lake.

### 3.3.3 Pool Allocation

Several water levels may be defined for reservoirs. The *full reservoir level* (FRL) is determined from the crest elevation of the ungated spillway or the design normal water level against the crest gate. During floods the water level in the reservoir may rise above the full level, and this higher design level is termed the *maximum water level*. The minimum operating level is determined from the requirements of the particular intake design and is the minimum level at which the lowest-level intake can be operated.

The *total storage volume* created upstream of a dam may be divided into several zones based on the placement of outlet structures and operational assignments (Committee on Hydropower Intakes, 1995). As illustrated in Fig. 3.7, *dead storage* is the volume that is below the invert of the lowest-level outlet and which cannot be drained by gravity. *Live storage* is the total volume below full reservoir level less dead storage. In projects with a flood control component, *flood storage* is the upper portion of the pool dedicated to flood detention. *Active* or *conservation storage* is the volume that can be manipulated for beneficial use, but excluding flood storage. It lies above the minimum operating level and below the bottom of the flood storage pool. The size of the flood storage pool may be varied seasonally depending on flood hazard, and the *joint use pool* is the volume that may be dedicated to flood control part of the year and for conservation storage during other periods. *Inactive storage* is the lower part of the conservation pool that is normally not used. For example, drawdowns may normally be limited to benefit recreational users, but may become necessary during a prolonged drought.

### 3.3.4 Stage-Storage Relationships

Reservoir storage characteristics are quantified using stage-storage and stage-storage graphs. The accumulation of sediment displaces volume within the reservoir, causing both the storage and area curves to shift, as shown in Fig. 3.7. Sediment tends to accumulate at all levels within the reservoir, with the specific accumulation pattern varying from one site to another. Although the dead storage volume is often termed a *sediment storage pool*, this is inaccurate because only a portion of the sediment inflow will be deposited in the dead storage zone. In some cases, such as in long reservoirs

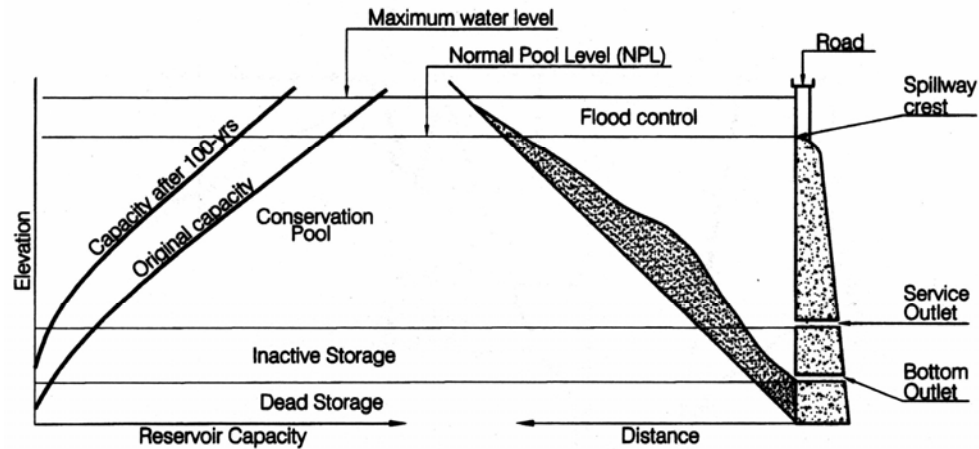


FIGURE 3.7 Shift of stage-storage and stage-area curves due to sedimentation.

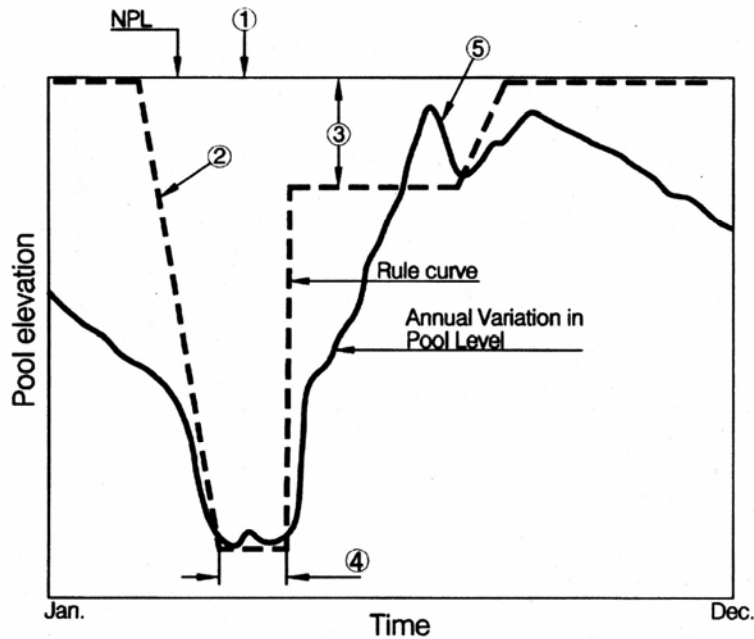
absent turbidity currents or where most sediments are deposited in delta areas, virtually all of the initial sedimentation will be focused in the higher-elevation active pool area, with little accumulation in dead storage.

### 3.3.5 Types of Reservoir Operation

A reservoir storage pool operated for water conservation captures irregular runoff flows to make subsequent deliveries to users at scheduled rates. A hydrologically small municipal water supply reservoir will normally remain at a high level, except during drought when it will drop to low levels. A hydrologically small irrigation reservoir may deliver all stored water to farmers on an annual basis and may be emptied at the end of each irrigation season. In contrast, hydrologically large reservoirs having carryover storage are characterized by water levels that gradually fluctuate over a wide range in response to series of wet and dry years. In recreation reservoirs it is normally desirable to have a continuously high and stable pool level, although some water manipulation may be desirable for purposes such as the control of aquatic vegetation, enhancement of fisheries, or consolidation of muddy sediments by desiccation (Cooke et al., 1993).

Operation for hydropower production seeks to balance two conflicting objectives. To maximize energy yield per unit of water, the pool should be maintained at the highest possible level, yet the pool elevation should be low enough to capture all inflowing flood runoff for energy generation. The resultant operation represents a compromise between high-head and storage requirements, and will often result in significant seasonal water level variations as water captured during the flood season is released to generate power during periods of low water inflow.

A reservoir operating rule guides the allocation of variable inflow over time and among different uses. The concept of a rule curve is presented in Fig. 3.8, which illustrates a seasonally variable flood control pool with an annual drawdown at the beginning of the flood season for sediment removal. The seasonally variable flood



- ① Top of gates
- ② Guide curve for maximum pool level
- ③ Flood control storage
- ④ Drawdown period for sediment flushing
- ⑤ Flood detention and release

**FIGURE 3.8** Conceptual reservoir operating curve showing: (1) top of gates; (2) guide curve for maximum pool level; (3) flood control storage; (4) drawdown period for sediment flushing; (5) flood detention and release.

control pool provides flood storage only in the season of flood hazard, and allows this portion of the pool to be filled for conservation storage at the end of the flood season. Many variables can influence operations, and the operating schedule of a hydropower reservoir may be determined by factors including actual and anticipated power load, water level, anticipated inflow (e.g., snowmelt), current and projected cost of power from alternative sources, recreational demands (e.g., lake boating or downstream kayaking and rafting), and environmental requirements affecting downstream releases and upstream pool levels. Multipurpose reservoirs have an operating regime that reflects the evolving compromise between the potentially conflicting uses, and nominally single-purpose projects may significantly alter their operation to meet new demands (e.g., recreation) or to address environmental problems. Management issues can become highly complex and politicized in systems containing multiple reservoirs extending over many hundreds of kilometers along rivers shared by several states, such as the controversy between upper-basin and lower-basin states along the Missouri River in the United States. Upper-basin states prefer higher water levels in upper-basin reservoirs for recreational purposes, whereas lower-basin interest prefer releases to enhance navigation.

### 3.4 OUTLETS AND GATES

Outlets to control the release of water from a reservoir may be located at high, intermediate, and low levels. Water quality characteristics such as dissolved oxygen, suspended solids, and temperature vary as a function of depth, and a multiple-level intake structure allows the selective withdrawal of water from different depths to better control the quality of released water. Bottom outlets may be used to drain the reservoir and release sediments. Inadequate outlet capacity is one of the principal causes of dam failure, and most dams provide overflow spillways to safely discharge extreme floods. Few dams are designed as nonoverflow structures with the entire flood flow designed to pass through low-level gates. An ungated overflow spillway will begin discharging as soon as the water overtops the spillway crest, whereas water normally stands above the spillway crest in a gated spillway and both the discharge and pool level are controlled by gate operation. The design flood criteria differ from one country to another, and also depend on the downstream hazard and type of dam, but spillway capacity is typically based on flood events having return intervals in the range of the 1,000 to 10,000 years (Berga, 1995).

Gates controlling the release of water may be classified according to their direction of opening as bottom-opening or underflow gates, or as top-opening or overspill gates. They can also be classified by mechanical configuration (e.g., radial, vertical lift, flap), and placement level (e.g., crest, bottom). Several basic types of gate mechanisms are illustrated in Fig. 3.9. The bottom-opening radial or sector gate, also called *Tainter gate* after its inventor, inscribes a sector of a circle and may be installed either as a crest gate or as a bottom gate. They are normally operated by a chain hoist mechanism, although hydraulic actuators are used in high-head, low-level installations. They are sometimes provided with a counterweight. Vertical lift gates have a leaf which travels along vertical slots. They may be constructed as slide gates, or in larger sizes may be equipped with rollers to reduce friction, and may be operated by a hydraulic actuator or by a hoist and wire rope (Fig. 24.5).

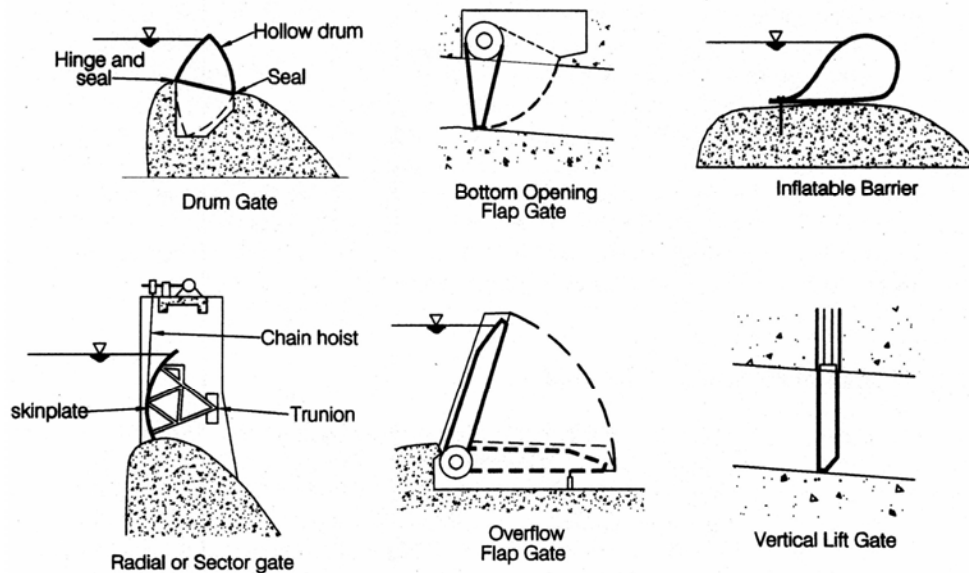


FIGURE 3.9 Types of gates frequently used in dams

Overspill gates are unsuited for sediment passage for two reasons: (1) when partially open they discharge from the water surface where sediment concentration is lowest, and (2) bed material can become trapped in the gate recess. However, they are well-suited for passing floating debris and ice. Some radial gates may be equipped with overspill flaps to provide the sediment-passing characteristics of a bottom-opening gate, while still retaining overspill capacity for release of floating debris (Figs. 3.3 and 3.13). Both radial and bottom-opening flap gates are well suited for the closure of a sediment discharge conduit because neither requires guide slots or mechanical equipment in the channel that conveys the sediment. Gate seals for the flap gate are flush with the conduit, and the seal on the radial gate faces downstream, where it is not subject to scour by sediment and stones. Vertical lift gates require a guide slot along either wall to the base of the gated opening, and there is the possibility of stones lodging in the slot. The slots used in vertical sluices can also produce cavitation problems at high flow velocities. For all types of gates passing coarse sediment, the grade on the apron in the immediate vicinity of the gate should be designed so that stones are not deposited in the area of the seal during decreasing flow, thus preventing complete gate closure (Bouvard, 1988).

Low-level outlets are normally constructed with two gates in series, the downstream gate being used for normal operations and the upstream gate serving as an emergency gate which can be closed to allow repair of the downstream gate. Because the flushing of coarse sediment through bottom outlets can erode gate seals, separate gates for flow modulation and for watertight closure should be considered, as described in the Gebidem case study.

## 3.5 HYDROPOWER PLANTS

---

### 3.5.1 Nomenclature

A hydropower facility is schematically shown in Fig. 3.5. *Trashracks* consist of steel bars that strain debris from water entering the intake. Shallow trashracks are generally set at an incline and use vertical bars so that they can be cleaned by a rake. The *penstock* is the pressure conduit connecting the intake to a powerhouse. In some facilities water is conveyed to a point above the powerhouse through a canal or low-pressure tunnel on a low gradient, which feeds into a short, steep, high-pressure penstock. The *powerhouse* contains the hydraulic turbines, generators, hoists, and control room. Flow exiting reaction-type turbines enters the *draft tube*, which is designed to decelerate flow velocity and recover kinetic energy, creating a negative pressure on the downstream side of the turbine runner. The draft tube discharges to the *tailrace*, which conducts flow back into the river. Headwater and tailwater elevations respectively refer to water surface in front of the intake and in the tailrace at the exit of the draft tube.

### 3.5.2 Types of Hydraulic Turbines

Hydrostatic head is converted into mechanical energy by hydraulic turbines, which can be classified into three types: impulse (Pelton wheel), Francis reaction, and propeller reaction. The propeller-type turbine may have blades of either fixed or variable pitch, the Kaplan turbine being an example of the latter. Basic turbine configurations are shown in Fig. 3.10, and a Pelton wheel is shown in Fig. 3.11. All turbines consist of two elements, a static guide (or nozzle in the case of the impulse turbine), which converts the static head partially or wholly into velocity, and a revolving part, called the *runner*.

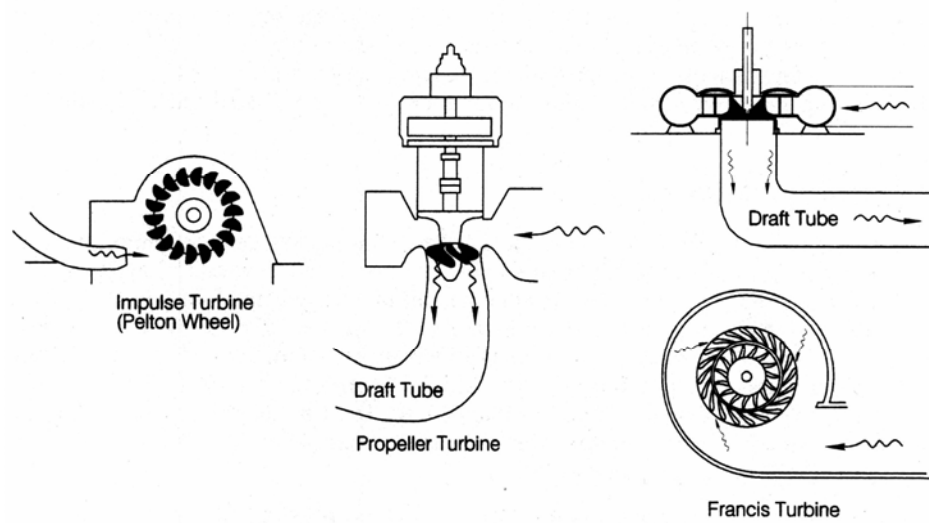


**FIGURE 3.10** Types of hydropower turbines: (a) Pelton wheel; (b) propeller turbine; (c) Francis turbine.

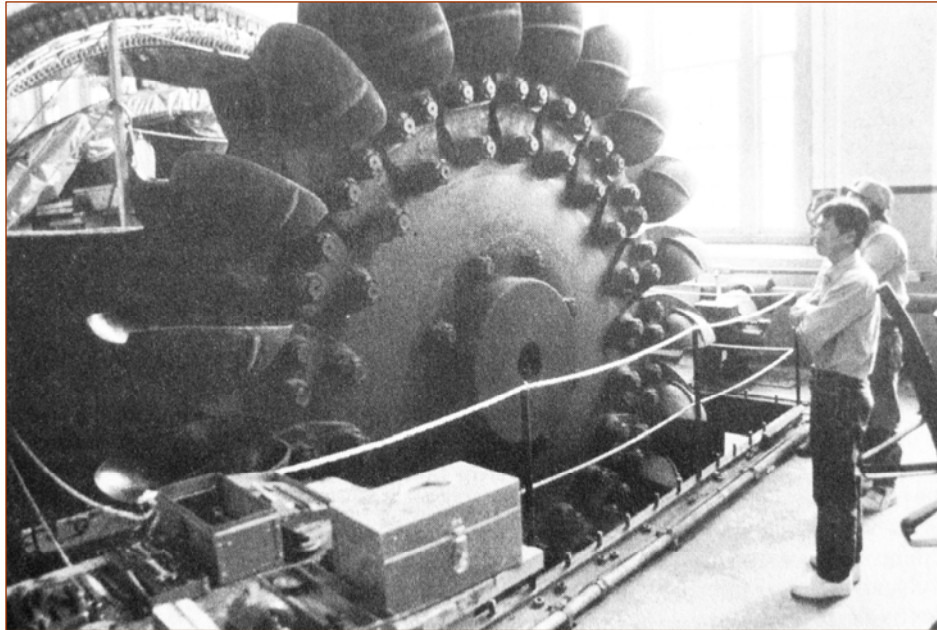


**FIGURE 3.11** Pelton wheel impulse turbine with casing removed (*G. Morris*).

The nozzle in the impulse turbine converts the entire static head into velocity head, and atmospheric pressure surrounds both the jet issuing from the nozzle and the bucket wheel. Impulse turbines are generally used for installations with static head exceeding 150 m. The guide case for reaction-type turbines converts only a portion of the head into

velocity, producing an overpressure between the guide case and the runner. The flow continues to accelerate as it passes through the throat of the runner, and the draft tube generates a negative pressure on the downstream side of the runner which increases energy transfer. Reaction-type turbines are generally used at heads of less than 300 m, and the propeller-type turbine is more suited for high-volume, low-head applications.

### 3.5.3 Energy Relations

Energy is the ability to do work, computed as force times distance. The unit of measure for energy is the joule (J) which is equivalent to a force of 1 newton (N) acting over a distance of 1 meter. In the English system the unit of energy is the foot-pound (ft•lb), a force of 1 pound acting over a distance of 1 foot (1 J = 0.7376 ft•lb). The potential energy in a volume of water is the product of weight and static head. Power is the rate of work, or work done per unit of time and may be expressed in watts (W), the unit equivalent to energy expenditure at the rate of 1 J/s. In hydroelectric practice kilowatts or horsepower are used to express power, and the kilowatt-hour (kWh) is used to express energy. These may be computed as follows:

$$1 \text{ kWh} = 3.6 \times 10^6 \text{ J} = 2.655 \times 10^6 \text{ ft}\cdot\text{lb}$$

$$1 \text{ hp} = 745.7 \text{ W} = 550 \text{ ft}\cdot\text{lb/s}$$

The potential energy available in 1 m<sup>3</sup> of water (1000 kg) at 1 m head is 9800 J = 7228 ft•lb = 2.722x 10<sup>-3</sup> kWh. Power output may be related to flow as follows:

$$\text{Power (kW)} = 9.8 \times Q \text{ (m}^3\text{/s)} \times \text{head (m)}$$

$$\text{Power (hp)} = Q \text{ (gal/min)} \times \text{head (ft)}/3,960$$

Hydraulic turbines can operate at efficiencies exceeding 90 percent based on head loss across the turbine. One of the important effects of sediment on hydropower stations is the erosion of turbine runners, which causes substantial declines in efficiency and increasing maintenance.

### 3.5.4 Sediment Impact on Tailwater

The *gross head* at a hydropower plant is the difference between headwater and tailwater elevation when the plant is not operating. The *net head* or effective head is the total net height of the water column effective on the turbine runner when it is generating power. It represents the gross head less all friction and turbulent losses before and after the turbine, and the increase in tailwater level caused by the turbine discharge plus any sediment accumulation in the river in the vicinity of the power house. Sedimentation problems affecting tailwater elevation are exemplified by the 3.4-Mm<sup>3</sup> Ralston Afterbay Reservoir on the American River in California.

Since closure of Ralston Dam in 1966, sediment has accumulated at an average rate of 43,200 m<sup>3</sup>/yr, and about 30 percent of the reservoir capacity had been sedimented by 1990. The general layout of this system and the pattern of sediment accumulation is illustrated in Fig. 3.12. The 79,200-kW Ralston power plant discharges 2.6 km upstream of the dam in an area affected by delta deposition, and bed aggradation raises the tailwater elevation. When tailwater reaches 358.7 m, backsplash within the impulse turbine discharge chamber causes vibration and reduces turbine efficiency because of increased drag. Peak load diminishes as tailwater rises to 360.0 m, at which point the unit must be shut down. At the Oxbow intake located about 360 m up stream of the dam, sediment

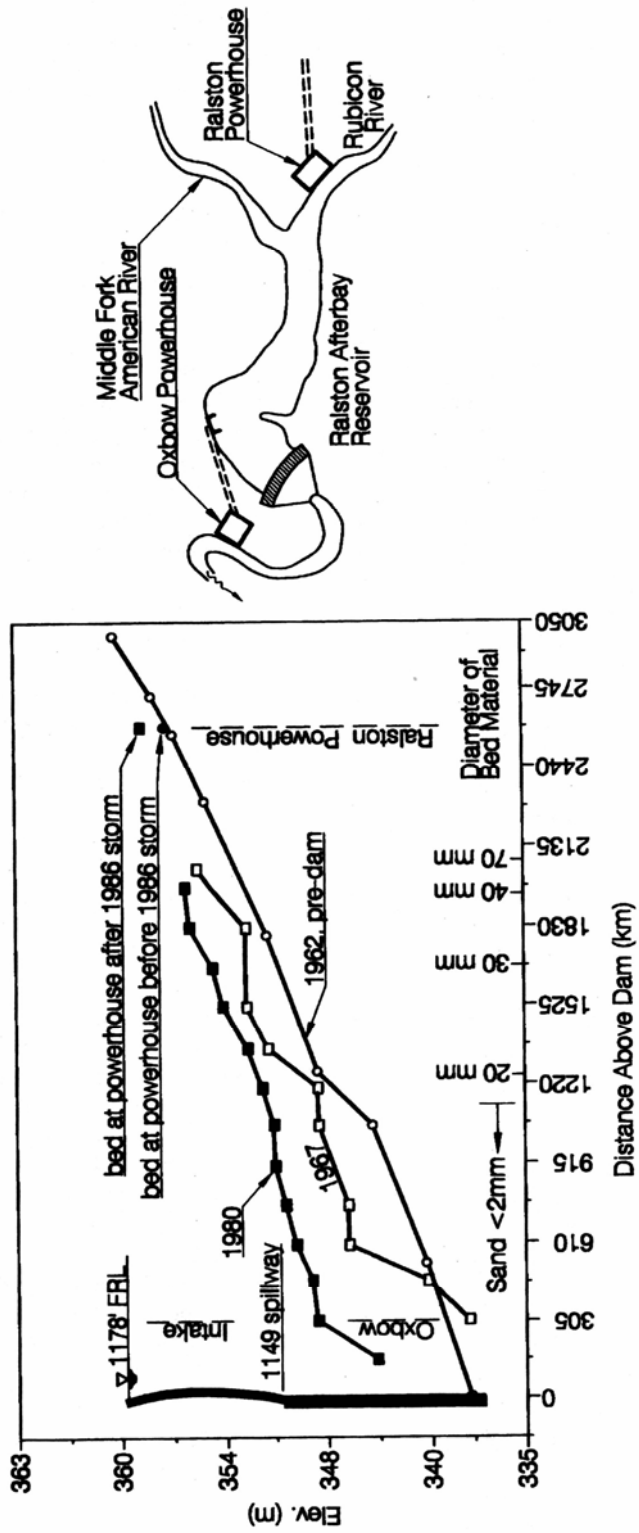


FIGURE 3.12 Schematic layout and sedimentation pattern in Ralston Afterbay Reservoir (after Plumas County, 1990, with permission by Plumas County).

**TABLE 3.3** Sediment Excavation at Ralston Afterbay Reservoir

Year	Excavation volume, m <sup>3</sup>	Base year for costs	Excavation cost, 1990 \$/m <sup>3</sup>
1984	9,990	1990	7.32
1985	9,200	1990	5.20
1986	34,400	1990	15.47
1986	61,200	1990	4.82
1989	24,900	1990	8.04
1994	58,900	1994	23.77

*Source:* Plumas County (1990); Jones (1996).

entrainment during high flows overloads the strainers in the cooling water supply for the generators. The amount of power lost due to shutdowns at Ralston and Oxbow is variable, with larger amounts being lost during wet years.

Sediment accumulation to date has been controlled by excavation (Table 3.3), and excavation volume is expected to increase with time as sedimentation continues. Large amounts of coarse sediment were transported by the 1986 flood, causing 2.4 m of bed aggradation along the river in the vicinity of the powerhouse discharge and requiring larger excavation volumes. Excavation costs may be expected to increase over time as nearby disposal sites become filled up. The extremely high unit cost for sediment excavation from the delta area in 1994 reflected the cost of a 5-km haul with an elevation gain of 365 m to reach the disposal site, where the material was used to construct a dry dam. Regulatory agencies have not allowed placement of excavated material back into the stream channel below the dam, despite more than 2 m of channel degradation at the gage station located 2.5 km below the dam since dam closure. The owner is presently examining alternatives to route sediment through the reservoir to reduce or eliminate reliance on mechanical removal (Jones, 1996).

## 3.6 ABRASION AND CAVITATION

### 3.6.1 Abrasion of Turbines

Sediment entrained in water can severely abrade hydraulic machinery of all types, causing efficiency declines in turbines and pumps and also affecting valve and gate seals. In extreme cases sediment can render hydraulic machinery useless in a matter of weeks (Bouvard, 1992). Grain sizes over 0.1 mm should be excluded for heads exceeding 50 m, and for heads exceeding 200 m even silts should be excluded (Raudkivi, 1993). Angular quartz particles are particularly abrasive and are generally abundant in glacial melt streams, posing a particular problem for hydraulic equipment in this environment. Francis turbines are highly sensitive to wear, often starting in the labyrinth where it causes higher leakage and requires dismantling for repair. In Pelton wheels the abrasion is focused on the needle and nozzle tip, both of which can be easily replaced, a factor that favors their use in installations when abrasion is a possibility. However, abrasion increases rapidly as a function of head, especially above 400 m, and high-head Pelton wheels can be abraded by 0.05-mm quartz in suspension (Bouvard, 1992).

### 3.6.2 Abrasion of Concrete Structures

Sediment will abrade spillways, aprons, and outlets that pass coarse bed material load, which may range from sand to boulders. Conventional concrete has limited abrasion

resistance and may be faced with a variety of abrasion-resistant materials such as dressed stone, steel (at least 2 cm thick, not including anchors), timber, fiber-reinforced concrete, or concrete with a coarse granite aggregate. When dressed stone is used, each block should be shaped like a molar tooth, consisting of "roots" 0.5 to 0.7 m long capped with squared vertical faces at least 15 cm deep which will be exposed to wear. The blocks should be laid with the smallest possible joints, and jointing should be arranged perpendicular to the flow to prevent the development of preferential paths for erosion. Dressed dense granite is highly resistant to both abrasion and shock, but costly. It may be considered in areas where facing replacement would be extremely costly, even if it could not be afforded elsewhere in the project. Oak or larch timbers 10 to 15 cm thick have been extensively used in the French Alps to line outlet works on streams transporting gravels and pebbles, including structures discharging as much as 1000 m<sup>3</sup>/s during floods. Wood is both elastic and smooth and has a service life on the order of 10 to 15 years (Bouvard, 1992). Railroad rails placed parallel to the flow line and interfilled with concrete have been used in a variety of projects, although the concrete between the rails can be eroded by gravel. An example of abrasion protection at a small project is shown in Fig. 3.13.

The Compagnie Nationale du Rhone (CNR) operates 18 barrages on the Rhone River between Switzerland and the Mediterranean Sea. Abrasion is a significant problem at these sites, which pass sands and gravels through gates and across aprons. Dams on the Rhone have used epoxy-resin concrete covered with a 2-cm-thick layer of pitch epoxy resin corundum on aprons and metal linings on the lower 2 or 2.5 m of piers (Bouvard, 1992). Pierrre and Fruchart (1995) reported on shock and abrasion tests performed by CNR on various substances including Abraroc, a proprietary concrete-based material formulated for use in abrasive environments (Table 3.4). In these tests shock resistance was measured as the volume of material eroded from a sample by a 1-kg metal ball 7 cm in diameter falling from 1 m, at 15 strikes per minute, for a period of 3 h. Abrasion resistance was measured by jetting water entraining 99 percent pure silica sand, 1.0 to 2.2 mm in diameter, at a 45° angle against a submerged sample.

### 3.6.3 Cavitation

Areas of negative pressure can occur in high-velocity flows, causing water to separate into liquid and gas phases, forming bubbles that subsequently collapse. The dynamic energy released by cavity collapse is highly erosive and cavitation can cause serious damage to hydraulic equipment and structures. Cavitation noise can be used as an indicator of potential cavitation damage. Raudkivi (1993) states that suspended sediments cause cavitation damage and noise to increase compared to clear water for sediment concentrations up to about 100 g/L, with the maximum effect at about 25 g/L of sediment concentration. At sediment concentrations above 100 g/L, cavitation is reduced compared to clear water.

Liu (1987) reported on the effect of sediment concentration on cavitation, using a cylinder cavitation test and silts from the Yellow River with a  $d_{50}$  diameter of 0.014 mm. In the experimental setup the length of the cavitation cavity downstream of the cylinder could be observed and noise level was measured with a transducer. The difference between the cavitation number  $K$  in clear and sediment-laden water, for constant values of cavity length or noise level, was interpreted as the effect of sediment on cavitation. Compared to clear water, cavitation was initiated more readily for suspended sediment concentrations up to about 15 g/L, and cavitation noise was increased for sediment concentrations up to about 7 g/L. Cavitation was reportedly less than in clear water at higher sediment concentrations (Fig. 3.14).

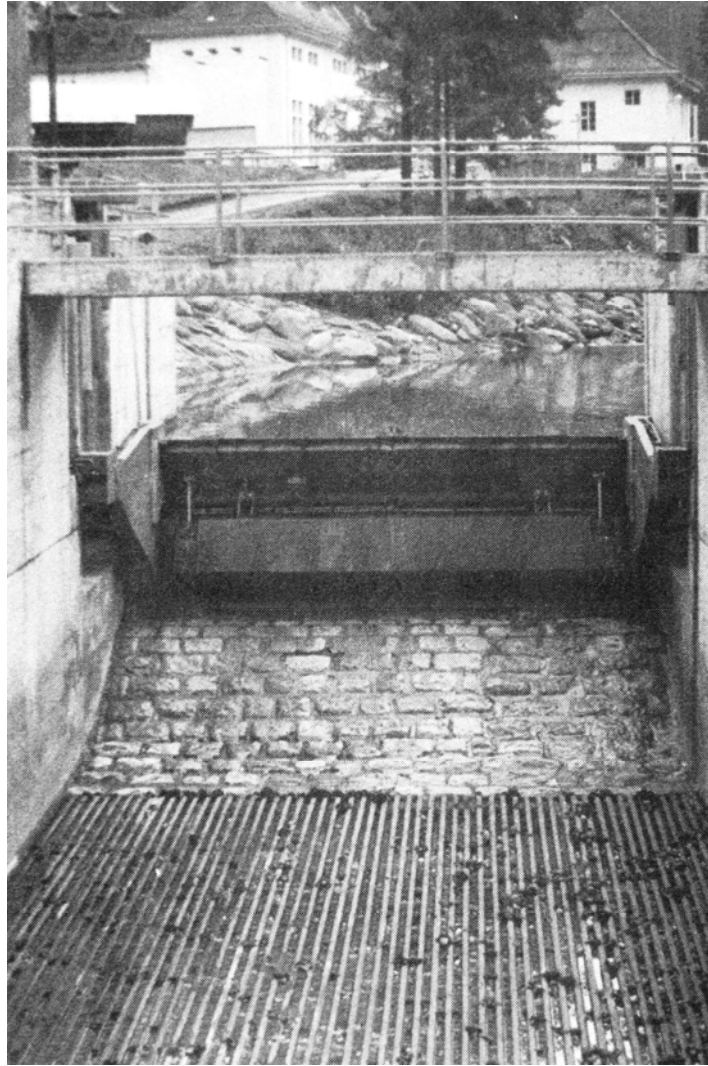


**FIGURE 3.13** The small La Peuffeyre hydroelectric diversion dam, Bex, Switzerland, is located on a steep gravel-bed stream. The spillway is fitted with a radial gate with an overspill bascule for passing floating debris. The spillway is armored with granite blocks and the apron below with railroad rails. Note the erosion of the unprotected concrete between the rails (*G. Morris*)

**TABLE 3.4** Shock and Abrasion Resistance of Selected Materials

Material	Shock resistance, cm <sup>3</sup>	Abrasion, cm <sup>3</sup>
Steel	—	0.02-0.04
Granite	<100	0.35-0.80*
Abraroc	175	0.4
Very resistant concrete	< 150	<1
Resistant concrete	150-250	<2
Common concrete	250-400	2-3
Mediocre concrete	>400	>4

\* Depending on origin

*Source:* Perrier and Fruchart (1995).

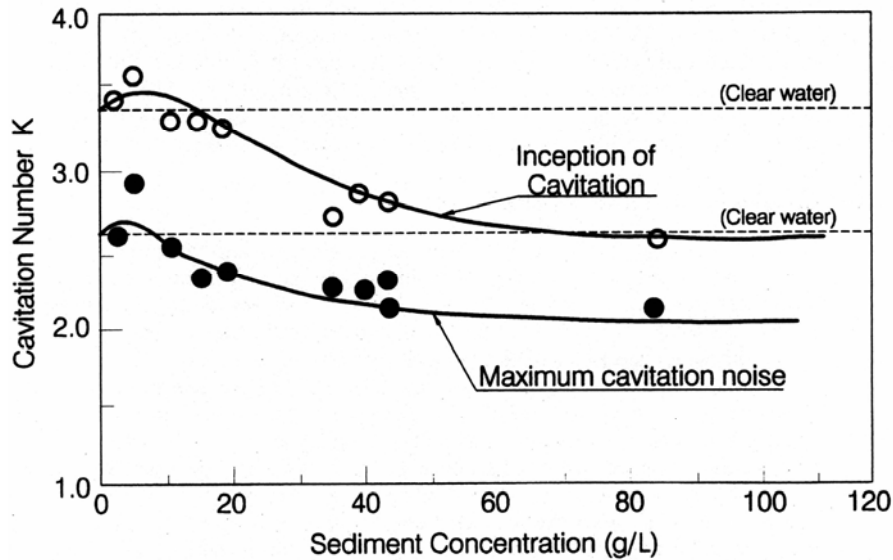


FIGURE 3.14 Effect of sediment concentration on cavitation number (after Liu, 1987).

### 3.7 RESERVOIR BACKWATER AND FLOOD ROUTING

During floods the water surface profile above a dam will be elevated above the level-pool elevation at full reservoir level. The backwater curve corresponding to any flow condition can be computed from the stage-discharge characteristics of outlets, as regulated by gate operation; geometry and hydraulic characteristics along the impounded reach; and the unsteady discharge characteristics of the inflowing hydrograph. Backwater profiles can be computed by using either steady-flow models such as HEC-2 (U.S. Army, 1990) or unsteady flow models such as UNET (U.S. Army, 1992) and DAMBRK (Fread, 1988). These hydraulic models use fixed streambed geometry. However, reservoir geometry is altered by sediment accumulation, and delta deposits can infill the upper reaches of the reservoir and also cause the streambed to aggrade upstream of the normal pool level. The subsequent growth of brush or trees on delta deposits, which increases hydraulic roughness, can substantially increase the backwater profile as compared to initial non-sedimented conditions. The modification of in-channel geometry and roughness due to sedimentation and vegetation should be considered in backwater computations.

When unsteady flood flows are routed through reservoirs, the temporary storage of floodwater will significantly reduce the flood peak at the dam. Sedimentation that reduces flood storage will not only increase backwater levels above the dam due to rising bed level, but it will also increase the peak discharge at the dam. In this manner, extensive sedimentation may cause the spillway design capacity to be exceeded.

### 3.8 RESERVOIR YIELD

Reservoir yield varies as a function of available storage volume in the conservation pool and will decline over time as this volume is lost to sedimentation. The impact of sedimentation management alternatives on reservoir yield should be quantified before selecting a sediment management strategy. McMahon and Mein (1986) summarize yield

analysis technique emphasizing rivers and individual reservoirs, while Basson et al. (1994) describe techniques developed and used in a complex 50-reservoir system. McCuen (1993) provides an overview of a number of statistical techniques for hydrologic analysis and includes diskettes with programs and sample datasets. Time series modeling is reviewed by Salas et al. (1980).

### 3.8.1 Storage-Yield Relationship

Reservoir inflow is stochastic, and yield is expressed as the withdrawal rate that can be sustained at a stated probability level without emptying the storage pool. Thus, a municipal supply reservoir designed to deliver 1 m<sup>3</sup>/s of water at the 99 percent level of reliability may deliver a lesser flow rate on 1 percent of the days (36 days per decade). Failure occurs when the desired yield cannot be sustained for more than 1 percent of the time over the long run. In the simplest case, the reservoir is drafted at a constant rate until empty, at which point the rate of withdrawal will be limited to the rate of inflow. Firm yield is the maximum uninterruptable amount of water that can be continuously withdrawn from a reservoir for a given (e.g., historical) inflow series and subject to a given set of operational rules and a fixed storage volume.

However, supply reservoirs may not be drafted at a constant rate until empty; water rationing may be imposed when the pool level drops to a certain point. Thus, the total conservation pool may be divided into an upper active pool and a lower inactive pool which functions as the reserve pool, with water rationing being triggered once the active pool is depleted.

The yield at zero storage is the minimum streamflow at the stated exceedance level (the unregulated streamflow equaled or exceeded 99 percent of the time in the municipal example). Reservoir yield increases as a function of storage volume for any stated level of reliability. For a given hydrologic sequence, a unique relationship exists between storage volume, yield, and service reliability. Yield increases as a function of storage, but additional increments in storage volume generate less yield than the previous storage increments producing storage-yield relationships having the asymptotic pattern shown in Fig. 3.1. Because the slope of yield curve steepens as storage volume declines, if conservation storage declines at a constant rate, the rate of yield decline will accelerate.

### 3.8.2 Gould's Gamma Method for Estimating Yield

Hydrologic datasets are often short at existing or proposed dam sites, and it is both convenient and necessary to use approximate methods to estimate yield as a function of conservation storage. Even when apparently adequate data are available, it is useful to use an independent method to check yield estimates for reasonableness. McMahon and Mein (1986) present Gould's gamma method for making a preliminary estimate of the constant rate of withdrawal sustainable from a single reservoir, as a function of probability of failure, given information on the mean ( $\bar{x}$ ) and standard deviation ( $\sigma$ ) of annual streamflow discharge. This method incorporates the assumption that the sequence of annual flows is gamma-distributed, but for the sake of computational simplicity it uses the normal distribution and a correction factor to approximate the gamma distribution.

The equation for determining the storage volume required for each combination of yield and level of reliability is:

$$\tau = \{Z_p^2 / [4(1 - D)] - d\} C_v^2$$

where  $\tau$  = storage volume expressed as hydrologic size ( $C/I$  ratio)

$C_v$  = coefficient of variation of annual flows ( $C_v = \sigma / \bar{x}$ )

$Z_p$  = standardized normal variate at  $p\%$

$D$  = withdrawal rate as ratio of the mean annual discharge rate

$d$  = correction factor ( Table 3.5)

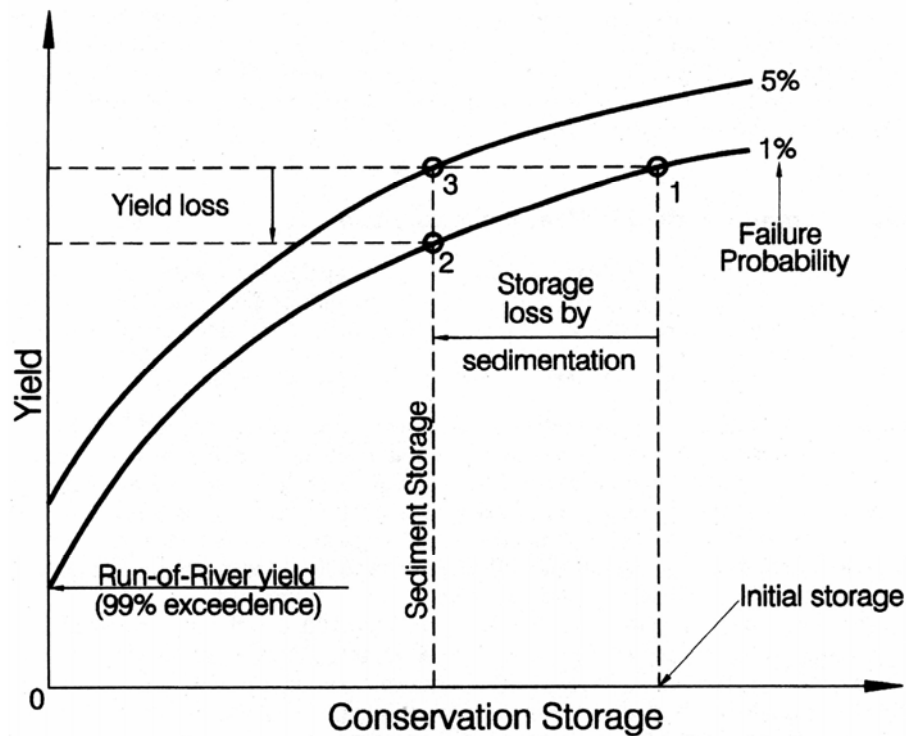


**FIGURE 3.15** General shape of a reservoir storage-yield curve, in which yield asymptotically approaches the mean watershed yield, less evaporative and seepage losses, as storage becomes very large. Two yield curves are shown for different levels of service. The impact of sediment accumulation in the conservation pool may be expressed as either a reduction in yield at a given level of reliability (point 1 to 2) or a reduction in reliability at a fixed yield (1 to 3).

**TABLE 3.5** Values of Gould's Correction Factor  $d$  as a Function of  $Z_p$

Lower $p$ percentile value*	$Z_p$	Correction factor $d$
0.5	3.30	$d$ not constant
1.0	2.33	1.5
2.0	2.05	1.1
3.0	1.88	0.9
4.0	1.75	0.8
5.0	1.64	0.6
7.5	1.55	0.4†
10.0	1.28	0.3†

\* Probability of failure.

† Gould's Gamma method not recommended for use in this range.

Source: McMahon and Mein (1986)

As an example, consider a stream with  $C_v = 0.60$ , a desired draft ratio equal to 50 percent of the mean annual discharge ( $D = 0.50$ ), and a 1 percent probability of failure (probability  $p = 1\%$  and  $Z_p = 2.33$  from the table of normal distribution). From table 3.5 the value of  $d = 1.5$ , and the equation is solved for a capacity inflow value of  $\tau = 0.437$  for the conservation storage pool.

### 3.8.3 Computing Yield by Behavior Simulation

The yield from single or multiple reservoirs may be analyzed by iteratively solving water mass balance across the impoundments for a given storage volume, inflow series and operating rule, using a continuity equation having the following general form:

$$\text{Storage}_t = \text{storage}_{t-1} + \text{inflow} - \text{withdrawals} - \text{losses}$$

Storage is the volume of water in the impoundment at the end of each time step. Inflow includes all natural plus regulated inflows. Withdrawals include all controlled release including diversions, minimum streamflow releases, and releases for sediment management. Losses include all uncontrolled releases including spills, evaporation, and seepage. By expressing reservoir geometry using stage-area and stage-storage curves, behavior simulation can also provide information such as water levels, available power head and evaporative losses at each time step.

The mass balance equation is solved iteratively over the duration of the entire hydrologic sequence, executing at each time step the operating rule which specifies parameters such as the rate and seasonality of withdrawal, rationing or allocation rules when storage drops below stated minimum levels, operating requirements associated with sediment management, etc. At each time step, information on delivery rate, pool elevation, power generation, spills and other parameters generated by the simulation are recorded, and can subsequently be analyzed to determine the probabilistic characteristics of the system behavior. Time steps of 1 month are frequently used in reservoir yield simulations, but at sites where sediment management requires drawdown periods that are not even-month multiples or last only a few days per year, shorter time steps will be required. Sediment management activities using only water that would otherwise be spilled, such as sediment routing described in the Loiza and Feather River case studies, do not require yield analysis. However, real-time modeling of reservoir behavior during short time steps (e.g., 15 minutes) may be necessary for analysis and implementation this procedure.

A behavior analysis for a single reservoir using historical datasets can be performed using an electronic spreadsheet. Both simple and complex systems, including multiple watershed, multiple-reservoir, multiple-use systems, can be analyzed by computer models such as HEC-5 (U.S. Army, 1982) and the Ackers Reservoir Simulation Program (ARSP) distributed by Boss International (1993).

### 3.8.4 Hydrologic Time Series

The historical data series available for any analysis will not be repeated exactly in future, but may be interpreted and manipulated to provide insight into potential future hydrologic patterns. If a short-term streamflow record contains a drought of sufficient intensity, as documented by long-term rainfall records, the historical dataset may provide a reasonable estimate of the long-term yield. The historical series is used to generate and subsequently

verify the reasonableness of synthesized dataset and their resulting simulation, and may also be used to establish the initial operating rule to be subsequently tested with multiple synthetic datasets constructed using statistical parameters computed from the historical datasets.

Fundamental to this procedure is the assumption that hydrologic conditions are stationary (not changing with time) and that historical conditions are representative of the future. However, both streamflow and sediment delivery may be affected by many variables, including upstream storage and diversion projects, deforestation, reforestation, and other land use changes that influence water yield, and both natural and human-induced climatic change. Reforestation of a degraded watershed will decrease both sediment and water yield (Bosh and Hewlett, 1982).

### 3.8.5 Sedimentation Effect on Yield

Sedimentation can affect system yield in three ways: it reduces conservation pool volume, sediment management may require that reservoir operation be altered, and watershed management for sediment control may affect water yield. The first two impacts can be readily evaluated within the framework of behavior analysis modeling, while the third requires modeling of watershed processes.

In a single reservoir the decline in yield (or the decline in reliability at a fixed yield) may be predicted from the storage-yield relationship by subtracting sediment accumulation from the conservation pool to predict future storage. In a system containing multiple reservoirs, each site will contribute only a portion of the total water yield or other benefit and the rate of storage loss will also vary among the sites. Selection of the most efficient means to sustain yield from the entire system requires information on the

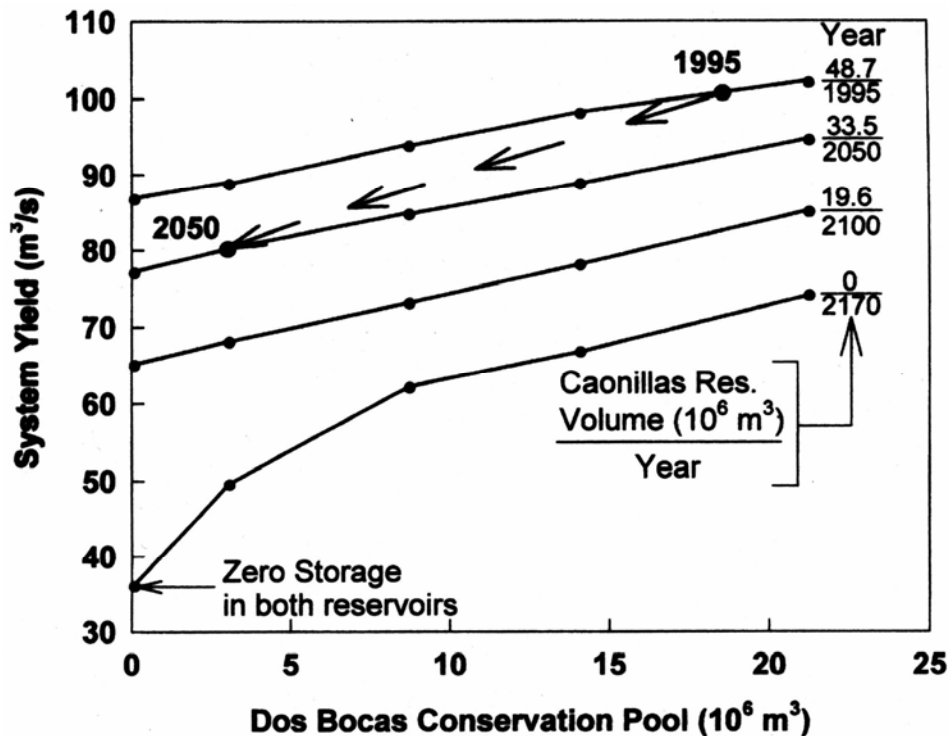


FIGURE 3.16 Effect of sedimentation on yield in a two-reservoir system (Morris, 1996).

cost and yield impact of different sediment management alternatives at each site. Limited economic resources should be focused on those sites and activities that generate the greatest net benefit, subject to environmental and other constraints.

Analysis of a multiple reservoir system may be performed by analyzing different storage capacities, to define the impact of storage loss (or recovery) at each site on the overall system yield. Model runs are used to define the relationship between system yield and reliability for various storage combinations, and the resulting yields and service levels are plotted to fit a continuous curve. Results for a simple two-reservoir system are plotted in Fig. 3.16. The yield impact of storage loss or recovery in either of the two reservoirs can be estimated by holding the capacity of one reservoir constant and computing the change in yield caused by different amounts of sedimentation in the other reservoir. The anticipated yield reduction caused by simultaneous sedimentation in both reservoirs is illustrated in the figure. A similar approach can be used for systems containing more than two reservoirs, in which case the graph would illustrate the effect of storage loss in any single reservoir on the system yield.

---

## CHAPTER 4

---

# CONCEPTS OF RESERVOIR LIMNOLOGY

---

Environmental impacts associated with dams and reservoirs influence both the design and "success" of engineering projects. Both physical and biological within-lake processes influence the pattern of organic sediment deposition, which can affect oxygen and nutrient budgets within the impoundment and in released water. This makes it important for engineers to understand some of the basic concepts and terminology of limnology, that branch of science which encompasses the study of physical and biological processes in inland water bodies. The limnology of natural lakes is described in several texts including those by Home and Goldman (1994), Wetzel (1983), and Cole (1994). The characteristics of reservoirs are rather distinct from natural lakes, and reservoir limnology has been summarized by Thornton et al. (1990).

---

### 4.1 COMPARISON OF LAKES AND RESERVOIRS

---

#### 4.1.1 Summary Differences

Great differences exist within the population of both natural and impounded lakes. Both include water bodies ranging from deep, nutrient-poor, seasonally ice-covered alpine lakes to warm, shallow lakes experiencing high sediment and nutrient loads. Characteristics of natural and artificial lakes may be similar if they occupy similar climatic zones and have comparable hydraulic residence time, nutrient and sediment loading, depth, and water level variation. Both lakes and reservoirs are populated by many of the same species and have many similar physical and biological characteristics. However, in comparisons of one population against the other there emerge several fundamental differences, summarized in Table 4.1 and Fig. 4.1. Differences also occur because reservoirs are often located in climatic zones or geologic environments having few, if any, natural lakes.

#### 4.1.2 Hydrologic Size and Loading Rate

A fundamental difference between natural lakes and reservoirs is their disparity in hydrologic size, expressed as the mean hydraulic retention time or CI (Capacity:Inflow) ratio. Cassidy (1989) argued that reservoirs will not be similar to natural lakes unless their mean hydraulic detention period exceeds 1 year ( $CI > 1$ ), and pointed out that of 2650 reservoirs in the United States having a total storage capacity exceeding  $6.17 \text{ Mm}^3$ , only 20 percent had  $C:I > 1$  while 45 percent had  $C:I < 0.3$ .

**TABLE 4.1** Summary Differences between Natural Lakes and Reservoirs

Parameter	Natural Lake	Reservoir
Hydrologic size (C:I ratio)	Large	Small
Age	1000s of years	10s of years
Water level variation	Small	Moderate to extreme
Discharge level	Surface*	Surface and deep
Watershed: lake area ratio	Small	Large
Sediment and nutrient loading	Low	High
Shape	Oval/circular	Linear/dendritic
Primary productivity	Lower	Higher
Species diversity	Higher	Lower
Senescence	Slow	Rapid
Transparency	Higher	Lower
Impact of watershed activities	High	Extreme
Water quality gradients	Weak/concentric	Strong/longitudinal
Shoreline: area ratio	Low	High

\* Except lakes primarily exchanging water with the groundwater system

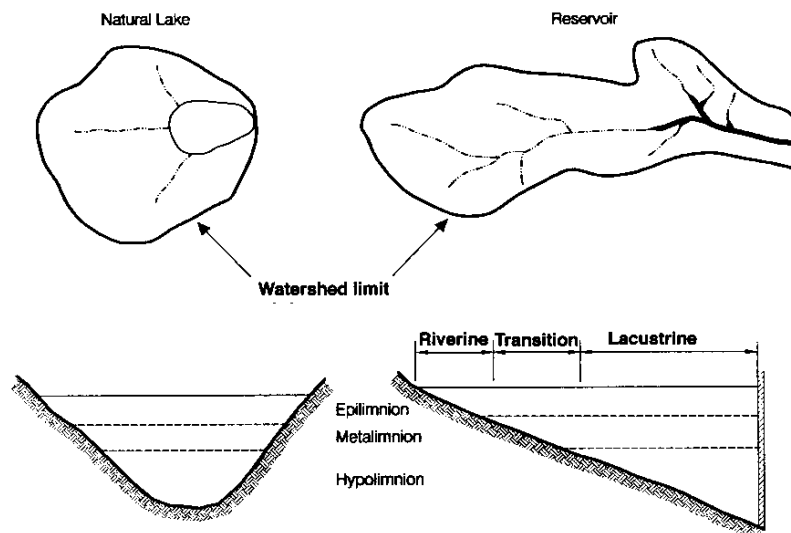


**FIGURE 4.1** Comparison of natural lakes and reservoirs.

Natural lakes characteristically have relatively small drainage areas contributing, nutrients and sediment, and a significant part of the watershed may drain directly into the lake via ephemeral streams. Although this reduced watershed area limits the hydraulic loading and detention time on the lake, water quality conditions in lakes

are nevertheless heavily dependent on conditions in the watershed. In contrast, reservoirs are constructed across streams draining large watersheds, producing comparatively high loading rates for sediment and nutrients. Reservoir water quality reflects watershed processes to an even greater degree than do natural lakes. Hydrologic size has another important impact on reservoir biology; in reservoirs having short hydraulic residence times due to small impoundment volume or hydraulic manipulation, water will be flushed from the impounded reach faster than some species can reproduce. Thus, a hydrologically small reservoir may remain at a state of "arrested" ecological succession compared to natural lakes, supporting populations of only those species that can reproduce rapidly prior to being washed downstream. Planktonic species that drift with currents are particularly sensitive in this respect.

#### 4.1.3 Age and Senescence

Over time, both natural and artificial lakes experience sediment accumulation, decreasing water depth, and nutrient enrichment as organic and inorganic sediments accumulate. This process continues until the lake is converted into a shallow marsh and ceases to exist as an open body of water. Shallow oxbow lakes formed by meander cutoffs in sediment-laden rivers can experience high sediment loading and may have life spans of only a few decades or centuries. At the other end of the spectrum are extremely ancient lakes, such as Lake Baikal in Russia, the world's deepest (1620 m) and largest (23,000 km<sup>3</sup>) freshwater body, which contains more than 3 times the total capacity of all reservoirs worldwide. However, natural lakes more typically have ages on the order of tens of thousands of years, many of them dating from the last glaciation. In contrast, most reservoirs are extremely young, only a few decades old, and are subject to high or extreme rates of sediment loading and greatly accelerated senescence processes compared to natural lakes.

#### 4.1.4 Geometry and Longitudinal Gradients

Natural lakes are typically oval-shaped as a result of either geologic factors influencing their formation (such as nearly circular sinkhole lakes) or the gradual infilling of embayments or dendritic branches with sediment. Lakes are typically shallow around the edge and deepen toward the middle. Reservoir geometry is dramatically different. Reservoirs typically have highly elongated geometries, shallow at the upstream end with regularly increasing depth toward the dam. This produces strong longitudinal gradients in the physical, water quality, and biological characteristics in reservoirs which are largely absent in natural lakes. These gradients must be considered in the development of sampling programs for reservoirs (Thornton et al., 1982). The presence of multiple reservoirs along a stream can also result in a water quality gradient from reservoir to reservoir.

Lakes and reservoirs receive inputs of water, sediment, nutrients, and both dissolved and detrital organic material from their tributary streams. The term *allochthonous* is used to designate the external material inputs into the lake. The term *autochthonous* refers to material produced within the lake itself, such as the organic material produced by phytoplankton or nutrients resuspended into the water column from lake sediments. Reservoirs may be longitudinally divided into the three zones illustrated in Fig. 4.1 (Thornton, 1990). The upstream *riverine zone* is an area of narrow geometry and shallow water characterized by significant flow velocities and transport of silts and clays, while the coarse fraction of the inflowing sediment deposits to form a delta. Allochthonous riverborne organic detrital material predominates in this zone. Despite potentially

significant organic loading, the water column is aerobic because of its limited depth, the absence of stratification, and the inflow of oxygenated river water. Light penetration may be limited by high turbidity from suspended solids delivered by the river, or high algae population sustained by high nutrient concentrations in the river inflow. The *lacustrine zone* occur closer to the dam and exhibits characteristics more similar to natural lakes including clearer water, lower sediment loads, and a stratified water column. The food chain in the pelagic (open water) zone closer to the dam will depend more heavily on autochthonous organic matter produced by plankton. Primary production may be nutrient-limited rather than light-limited. These two zones are separated by a *transition zone*.

#### 4.1.5 Shorelines and Water Level Variation

Reservoirs having irregular or dendritic planforms are characterized by very long shore lines per unit of surface area. Given a stable water level, this could produce an extensively vegetated littoral zone which could significantly influence the reservoir biology. However, many reservoirs are characterized by wide water level fluctuations, including complete emptying every year, which eliminates the possibility of establishing littoral vegetation. Limited water level manipulations to control aquatic vegetation, to consolidate sediment, and to promote fisheries have been described by Cooke et al. (1993) However, the large drawdown or emptying used to manage sediments can severely limit the species that can populate the reservoir.

#### 4.1.6 Sediment Loading

One of the most significant differences between natural lakes and reservoirs is the increased sediment loading, which not only greatly accelerates shallowing and related senescence processes in reservoirs, but also produces higher turbidity. Natural lakes often have a zone of light penetration, the *photic* or *euphotic* zone, many or even tens of meters deep. In contrast, the euphotic zone in reservoirs is more typically on the order of only a few meters deep. High turbidity levels can be caused by sediment inflow or the resuspension of bottom sediment by wave action, and can produce euphotic zones as shallow as 1 m. Vertical mixing in this environment can keep algae below the euphotic zone for prolonged periods, resulting in very low populations of primary producers and associated zooplankton. During seasonal runoff events the inflow of turbid water may reduce the euphotic zone to a fraction of a meter in depth, especially in the upstream riverine zone of reservoirs.

## 4.2 TEMPERATURE AND STRATIFICATION

---

### 4.2.1 Stratification

Water bodies more than a few meters deep have a strong tendency to stratify because of changes in fluid density caused by differences in temperature and suspended solids. Temperature stratification is a ubiquitous phenomenon, the result of solar heating of surface water which produces a three-layer system consisting of: (1) a vertically mixed layer of warmer and well-oxygenated surface water termed the *epilimnion*, (2) a zone of rapid temperature and density change called the *metalimnion*, and (3) the colder, darker, and oxygen-depleted profundal zone or *hypolimnion* (Fig. 4.2). The *thermocline* is defined as the relatively narrow zone where the temperature gradient equals at least 1 °C per

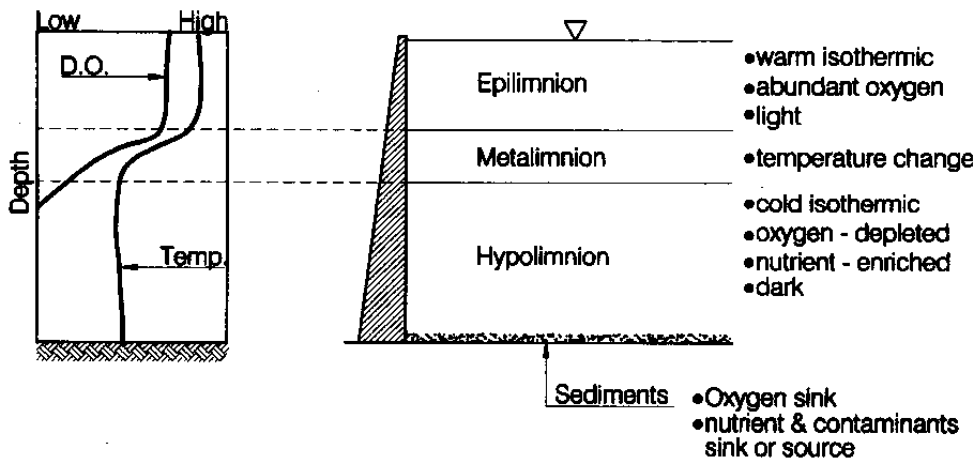


FIGURE 4.2 Vertical structure of reservoirs and lakes

meter of depth, whereas the *metalimnion* is generally understood to encompass the thermocline and the adjacent water column characterized as transitional between the surface and profundal waters. In more productive lakes, the hypolimnic water which is trapped beneath the thermocline will become anaerobic because of the oxygen demand imposed by decomposers and organic sediments.

The density difference per degree centigrade of temperature change increases as a function of temperature. For example, the density difference caused by a 1° change in temperature at 24°C (75°F) is 3 times greater than the density change at 9°C (48°F). Thus, tropical reservoirs may be strongly stratified despite temperature gradients much smaller than those in temperate zone reservoirs. The potential density differences due to suspended solids are an order of magnitude larger than those due to temperature differences and can cause warm turbid inflow to plunge beneath colder water and travel along the length of a reservoir as a turbid density current. In some reservoirs, turbidity currents can transport a significant amount of sediment to the dam, as discussed in Chap. 14.

### 4.2.2 Seasonality of Stratification

Lake stratification is driven by seasonally variable forces: solar energy, inflowing water temperature, and variable suspended solids concentrations. If temperature profiles are measured year round, temperate zone lakes and reservoirs will demonstrate strong summer stratification due to solar heating of surface waters, but isothermal conditions occur during the winter, eliminating the density gradient and allowing the entire water column to mix vertically, a process called turnover. During turnover, nutrients which have accumulated in the deeper water are returned to the surface where they can promote algal growth in the spring as temperatures rise, ice cover disappears, and daylight hours lengthen. The seasonal variation in temperatures throughout the water column in Lake DeGray, Arkansas, is shown in Fig. 4.3. Lakes which have a single period of annual mixing and do not freeze, such as Lake DeGray, are termed monomictic. Lakes that mix twice, once in the fall and once in the spring, with ice cover in the winter, are classified as dimictic. Shallow lakes that are frequently or even continuously mixed are termed *polymictic*

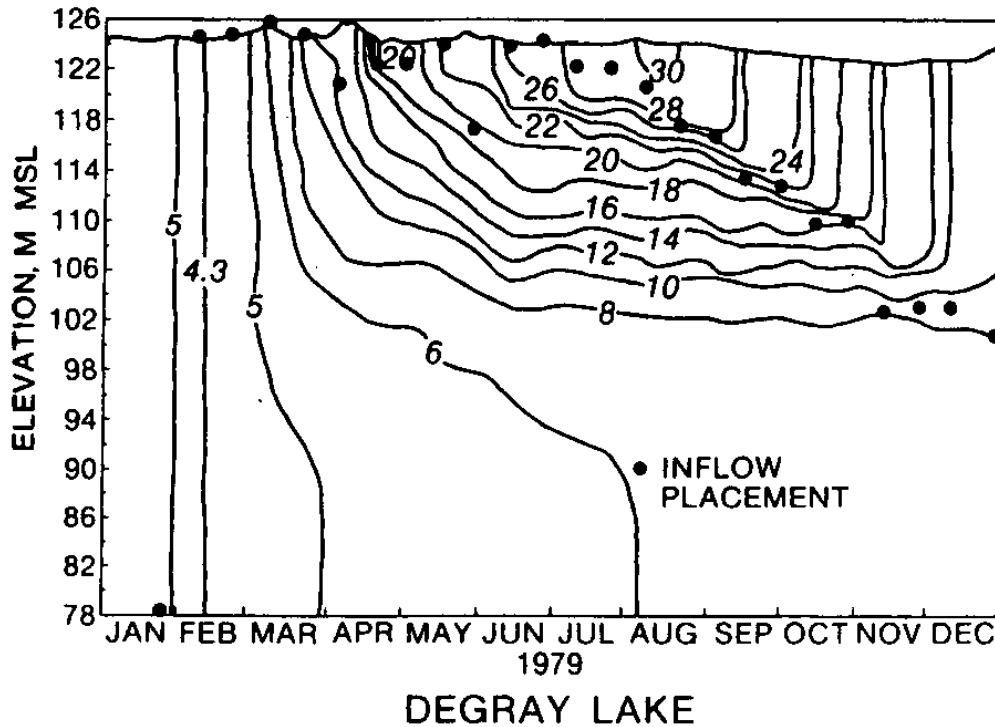


**FIGURE 4.3** Seasonal variation in temperature stratification (°C), Lake DeGray, Arkansas (Kennedy and Nix, 1987).

Wind is the primary factor causing vertical circulation in lakes, and higher winds will cause deeper circulation and increase the depth of the epilimnion. The thermal structure of a lake can also be subject to significant temporal and spatial differences as a result of varying wind direction and velocity. Winds of sufficient strength, duration, and fetch will overcome temperature-induced stratification and completely mix the water column. Reservoirs are subject to the same wind-induced forces as natural lakes. However, hydrologically small reservoirs will additionally be subject to large inflows that can flush out the impoundment, replacing the entire body of water with flood inflow. After the flood the newly impounded water will again stratify as sunlight heats the surface water.

#### 4.2.3 Density of Water

The following water density equations, based on Ford and Johnson (1983) and Chen and Millero (1977), will determine density to within 0.02 kg/m<sup>3</sup> of the true value over the range of 0 to 30°C, 0 to 600 ppm TDS, and 0 to 180 bars pressure. The density of water may be expressed as the temperature-dependent density of the fluid plus the additional density imparted by suspended and dissolved solids:

$$\rho = \rho_T + \Delta\rho_{TDS} + \Delta\rho_{SS} \tag{4.1}$$

where  $\rho$  = density (kg/m<sup>3</sup>) with subscripts T = temperature, TDS = total dissolved solids, and SS = suspended solids. The maximum density of water is 1000 kg/m<sup>3</sup> at 3.98°C. The density of pure water as a function of temperature in °C may be computed by the following equation:

$$\rho_T = 999.8395 + 6.7914 \times 10^{-2}T - 9.0894 \times 10^{-3}T^2 + 1.0171 \times 10^{-4}T^3 - 1.2846 \times 10^{-6}T^4 + 1.1592 \times 10^{-8}T^5 \quad (4.2)$$

The density increment due to dissolved solids may be estimated from:

$$\Delta\rho_{TDS} = C_{TDS} (8.221 \times 10^{-4} - 3.87 \times 10^{-6}T + 4.99 \times 10^{-8}T^2) \quad (4.3)$$

where  $C_{TDS}$  = total dissolved solids (mg/L) and  $T$  = temperature ( $^{\circ}\text{C}$ ). The density increment due to suspended solids is:

$$\Delta\rho_{SS} = C_{SS}(1-1/G) \times 10^{-3} \quad (4.4)$$

where  $G$  = specific gravity of the solids and  $C_{SS}$  = suspended solids in  $\text{g/m}^3$  or  $\text{mg/L}$ .

When  $G = 2.65$ , the equation is reduced to:

$$\Delta\rho_{SS} = 0.00062 C_{SS} \quad (4.5)$$

The modification of density as a function of pressure is given by:

$$\rho_P = \rho / (1 - P/K) \quad (4.6)$$

where  $P$  = pressure in bars (1 bar  $\approx$  10.2 m of water depth) and  $K$  is given by:

$$K = 19652.17 + 148.376 T - 2.329T^2 + 1.3963 \times 10^{-2}T^3 - 5.90 \times 10^{-5}T^4 + (3.2918 - 1.719 \times 10^{-3}T + 1.684 \times 10^{-4}T^2) P + (-0.8985 + 2.428 \times 10^{-2}T + 1.114 \times 10^{-2}P) C_{TDS} \times 10^{-3} \quad (4.7)$$

Temperature differences will be the predominant mechanism creating density differences in reservoirs when inflowing turbidity is low. At  $25^{\circ}\text{C}$  the density difference caused by a  $1^{\circ}\text{C}$  difference in temperature is equivalent to the effect of approximately 420 mg/L of suspended solids with a specific gravity of 2.65.

### 4.3 HYDRAULIC SHORT-CIRCUITING

If reservoirs were plug-flow-type reactors, the hydraulic retention time for any parcel of inflowing water could be computed by dividing the total volume by the inflow rate. However, the flow entering a reservoir may pass directly from inlet to the outlet as a discrete current flowing along a path that is restricted or *focused* both horizontally and vertically, thus limiting the mixing with water in the impoundment. This process is termed *hydraulic short-circuiting* and is a common phenomenon in reservoirs. Hydraulic short-circuiting is influenced by three factors: (1) density differences between the impounded and inflowing water which cause stratification and vertical focusing of inflow, (2) reservoir geometry that horizontally focuses flow, and (3) the opening of an outlet in the dam at a location and discharge rate appropriate to release the focused flow.

#### 4.3.1 Horizontal Focusing

When flood flow enters a reservoir, the flow will tend to bypass dendritic branches, side storages, or other hydraulically "dead" zones as it flows toward the outlet. This phenomenon of horizontally focused flow has been documented along the length of Lake DeGray (Fig. 4.4). Because of horizontal focusing, storage areas off the main channel will receive much less sediment loading than the main reservoir. For example, Lowe and Fox

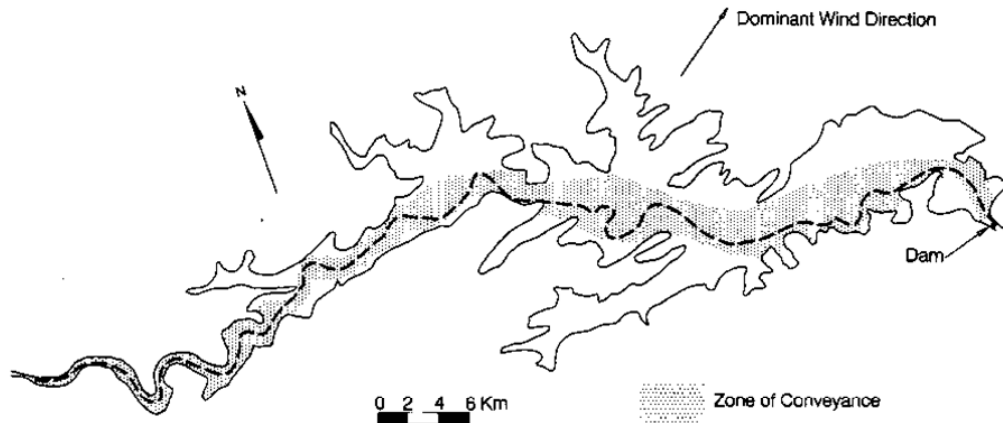


**FIGURE 4.4** Lake DeGray, Arkansas, illustrating horizontal focusing of flow (after Gunkel *et al.*, 1984), the meandering thalweg, and the sampling locations used by James and Kennedy (1987).

(1995) noted that insignificant sedimentation has occurred in the portion of Pakistan's Tarbela reservoir that is off channel, although the main reservoir body itself faces severe sedimentation problems.

In reservoirs having a deep, well-defined submerged river channel, bottom density currents will be horizontally constrained by the channel geometry. If the reservoir submerges an uncut forest, the "channel" constraining density current movement may be defined by the stream corridor running through the still-standing but submerged forest. However, as sediment deposition from turbid density currents infill the original river channel, this horizontal focusing effect will be reduced or eliminated and the density current will tend to spread out laterally and dissipate.

#### 4.3.2 Vertical Focusing

Stratification can cause inflowing water to pass through a reservoir as overflow, interflow, or underflow, depending on the relative density of the inflow and the vertical density structure of the impounded water (Fig. 4.5). Warm water will flow across cooler water as overflow, water of intermediate temperature will flow across the surface of the thermocline, and cool or sediment-laden inflow will flow beneath warmer water as a bottom current. The combination of stratification plus inflow can produce complex vertical profiles in reservoirs, such as that shown in Fig. 4.6, created by the plunging of turbid, oxygenated storm runoff within a tropical reservoir. The depth at which water is released from a dam will also influence the flow patterns through the reservoir upstream of the outlet.

The presence of inflow focusing does not guarantee that hydraulic short-circuiting will occur. A high degree of short-circuiting will occur only if outlets are opened at the appropriate depth, time, and discharge rate to intercept and release the current passing through the reservoir. Consider the case of cold or turbid water entering a warm reservoir, resulting in a strongly stratified system and a bottom density current that reaches the dam. Hydraulic short-circuiting will occur if the inflow is released through a bottom outlet. However, if a surface discharge is used there will be no short-circuiting in the outflow because only the warm surface water will be discharged while the inflow accumulates in the bottom of the impoundment.

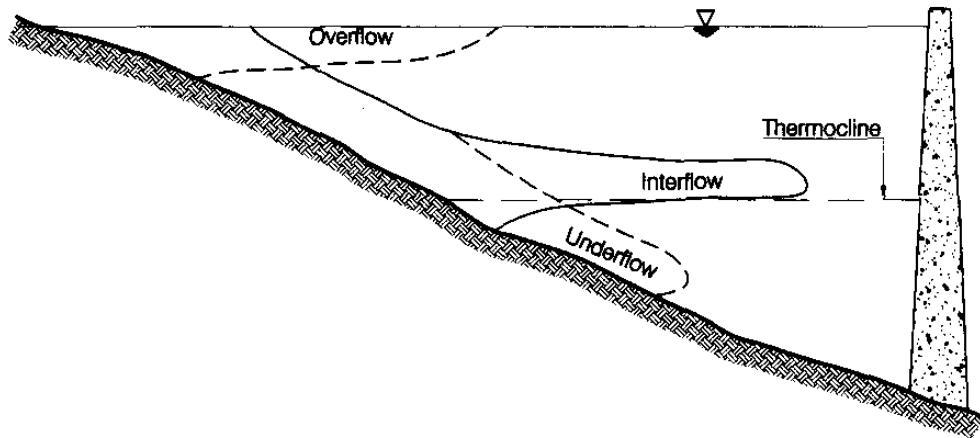


**FIGURE 4.5** Vertical focusing of flow in a stratified reservoir. The flowthrough pattern may be characterized as overflow, interflow, or underflow depending on the density of the inflowing water relative to the vertical stratification structure of the impoundment (Kennedy and Nix, 1987).

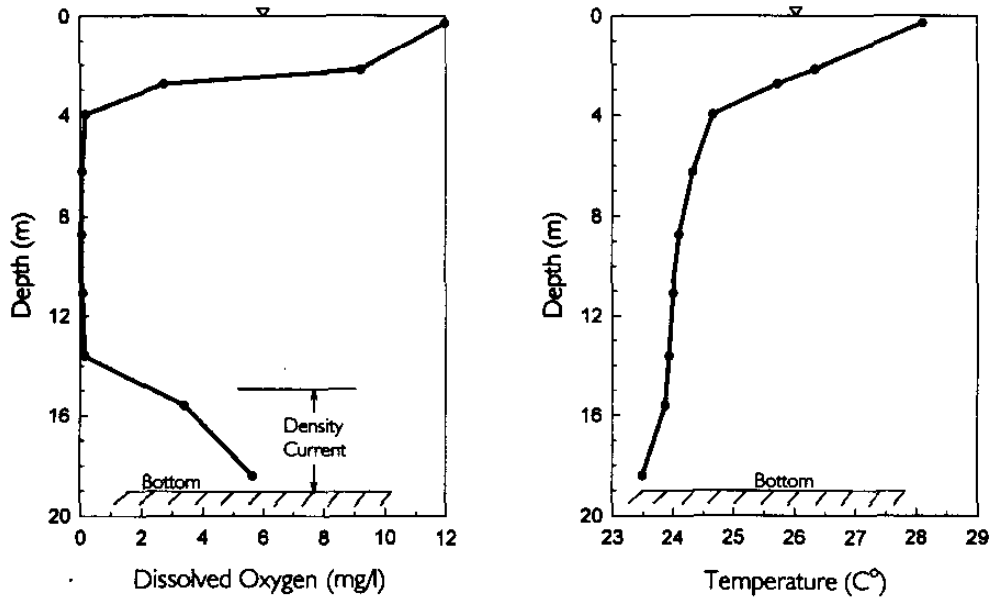


**FIGURE 4.6** Vertical profile of the eutrophic and oxygen-depleted La Plata Reservoir, Puerto Rico, showing a bottom density current of turbid, oxygenated river inflow.

#### 4.4 SELECTIVE WITHDRAWAL

Water quality within an impoundment varies with depth, and an intake structure which allows water to be withdrawn from any of several levels can be used to modify the quality of water discharged from the dam or delivered to users. The highest level of control is achieved with an intake that allows water from different levels to be mixed in variable proportions. A review of selective withdrawal techniques is provided by Cassidy (1989).

Selective withdrawal can improve water quality for a variety of uses. Anaerobic profundal water quality is generally not desirable for municipal water use, potentially creating taste and odor problems and objectionable levels of dissolved iron and manganese that will form staining precipitates when oxidized. Cold irrigation water can affect temperature-sensitive crops such as rice. Anaerobic decomposition of organic matter on the bottom of a reservoir can produce hydrogen sulfide gas which can corrode hydropower equipment and is toxic to aquatic life. The quality of water discharged to the river downstream of a dam heavily influences the biological conditions in the regulated river reach, with the two principal parameters being temperature and dissolved oxygen. Without selective withdrawal capability, the temperature of water released from a reservoir cannot be controlled and thermal shock can be created downstream. Selective withdrawal allows the temperature of releases to be regulated by the controlled mixing of colder hypolimnic water with warm epilimnic water. A vertical array of temperature sensors in the reservoir can help operators select gate openings to achieve the desired temperature.

It may be desired to vent turbid density currents from the reservoir, to withdraw water from sediment-free zones in the reservoir, or both. The selective withdrawal structure described in the case study of glacial-fed Gebidem dam was added to allow water to be withdrawn near the surface where both suspended solids concentration and grain size will be reduced compared to that in the existing fixed deep inlet, reducing wear on turbine runners. The inlet structure at Lost Creek Lake (Fig. 4.7) combines both selective withdrawal with a conduit for venting turbidity currents. The turbidity conduit is intended to allow the rapid release of turbid water during and after large flood events, with the idea of rapidly clarifying surface waters and thereby allowing clear water releases to be reinitiated as soon as possible. This measure was implemented to reduce impacts on downstream anadromous fisheries (Cassidy, 1989)



**FIGURE 4.7** Outlet structures at Lost Creek Lake, Oregon. The Low-level outlet is on the left of the photo, and the selective withdrawal tower and the turbidity conduit connected to its base are visible on the right. (Courtesy U.S. Army Corps of Engineers)

## 4.5 LIGHT AND TRANSPARENCY

---

Lake transparency has traditionally been measured by recording the disappearance depth of a Secchi disk, a white disk 20 cm in diameter, which is lowered into the water between 10 A.M. and 2 P.M. on the shaded side of the boat. This is one of the most basic of all limnologic parameters measured in the field; the method is simple, and a Secchi disk is low-cost, portable, and virtually indestructible. Extensive Secchi disk data have been collected at numerous sites over many years. In an oligotrophic alpine lake, such as Lake Tahoe on the California-Nevada border, Secchi disk transparencies can attain 40 m, whereas in highly turbid water the disk may disappear at a depth of only a few centimeters. Secchi disk transparency will vary seasonally and spatially as a result of turbid inflows and variations in algal populations.

Turbidity can be measured by submersible sondes instrumented with turbidimeters and data loggers. These instruments, which have become widely available at relatively low cost, can provide rapid data collection and reduction, can be used under any ambient light conditions, and can measure the variation in turbidity with depth. This last capability is quite important since the vertical distribution of turbidity is not uniform, being affected by turbid density currents, settling of suspended solids, and planktonic organisms which can be concentrated at specific depths and migrate vertically. If turbidity is correlated to suspended solids concentration based on water sampling at different depths and locations, turbidity data can be used to quickly map the suspended solids structure within the impoundment and to monitor its changes, including the movement of turbid density currents. A sonde used for turbidity profiling would also normally include additional parameters such as temperature, dissolved oxygen, depth, and pH, allowing several important profile parameters to be measured and recorded simultaneously. When turbidimeters are used it is a good idea to use a Secchi disk for comparative purposes. Also, different types of turbidimeters can give different readings for the same natural water sample despite proper calibration against a formazin standard (see Sec. 8.4.3).

Incident solar radiation is polychromatic, and different wavelengths are absorbed at different rates. Red and infrared wavelengths are absorbed most rapidly, and blue light has the greatest penetration. Over half the incident light is usually transformed into heat within the upper meter of the water column. Light intensity is attenuated in both ocean and lake waters according to the Beer-Bouguer law having the form:

$$I_z = I_0 e^{-kz} \quad (4.8)$$

where  $I_0$  = incident light intensity at the water surface  
 $I_z$  = light intensity at depth  
 $z$  = depth, m  
 $k$  = *extinction* coefficient

The relative rate of extinction can be determined by assigning  $I_0 = 1.0$ , or the absolute value of irradiance at any depth can be determined by expressing  $I_0$  in units such as of  $W/m^2$  or  $kcal/m^2$ . The adsorption coefficient for polychromatic solar radiation can be estimated from the Secchi disk transparency  $Z_D$  by the relationship  $k = 1.7/Z_D$ . Coefficient values for monochromatic wavelengths, summarized by Wetzel (1983), range from 2.45 at 760 nm (infrared) to 0.0181 at 473 nm (blue). As a precautionary note, the terminology for the extinction coefficient used here follows the nomenclature of Cole (1994), who points out that the term *absorption coefficient* also applies to the Beer-Bouguer law, but formulated for base 10 logarithms. Thus, the value of the absorption coefficient is 2.3 times the value of the extinction coefficient. Not all authors conform to this nomenclature and there is Potential for confusion.

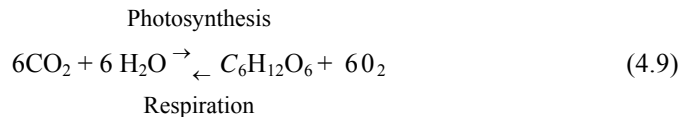
In most systems, photosynthesis is negligible when light intensity declines to about 1 percent of the intensity at the surface. Light reflected to the observer from a submerged Secchi disk has to travel both directions through the water column, and as a rule of thumb the depth of the euphotic zone, the level of 1 percent irradiance, is about 3 times the Secchi disk depth (2.7 times for the Beer-Bougouer law and the relationship  $k = 1.7/Z_D$ ). However, in some lakes and in highly turbid waters, the euphotic zone can be as much as 5 times the Secchi disk depth.

## 4.6 PRODUCTIVITY AND EUTROPHICATION

---

### 4.6.1 Primary Production

The primary producers or *autotrophs* create organic material from inorganic substances using sunlight as an energy source. The process of primary production, the conversion of radiant solar energy into chemical energy, can be represented by the simplified photosynthetic equation:



This equation represents the continual cycling of carbon between inorganic and organic forms. The organic matter in turn feeds heterotrophic and decomposer organisms.

The linkages of energy transfer pathways, from primary producers to herbivores, and ultimately to carnivores, is termed the *food chain*. Each level in a food chain is termed a *trophic level*, with the primary producers occupying the first level. Only about 10 to 20 percent of the energy available at each trophic level is passed to the next, which usually limits ecosystems to about four trophic levels. All food chains may be conceptualized as pyramids with a few carnivores such as largemouth bass at the top, supported by lower trophic levels containing more numerous populations and greater total biomass. An example of a simple grazing food chain is given in Fig. 4.8, which shows energy pathways through the system. Food chains are of two basic types: *grazing* food chains are based on the direct consumption of green plants by herbivores, and *detrital* food chains are based on the decomposition of nonliving organic matter by microbes, with the microbe-enriched material subsequently being processed by *detritivores*, which also shred the detritus into smaller particles.

The organic material that forms the base of the food chain in aquatic ecosystems may be autochthonous material produced within the lake by littoral or floating vegetation, aquatic plants, and microflora including diatoms and algae. The microflora may be either attached to submerged surfaces (*periphytonic*) or floating within the water column (*planktonic*). Allochthonous organic inputs may be delivered by inflowing streams or from adjacent terrestrial ecosystems and include colloidal or dissolved material, organic detritus, and terrestrial animals that fall prey to lake-dwelling organisms.

### 4.6.2 Diurnal Variations in Dissolved Oxygen

As indicated by the photosynthetic equation, there is a net release of oxygen (and consumption of  $\text{CO}_2$ ) during photosynthesis, and the opposite occurs during respiration. Algae and other primary producers release oxygen into the water column during the day, and the respiration by the algae and heterotrophs at night depletes oxygen, resulting in

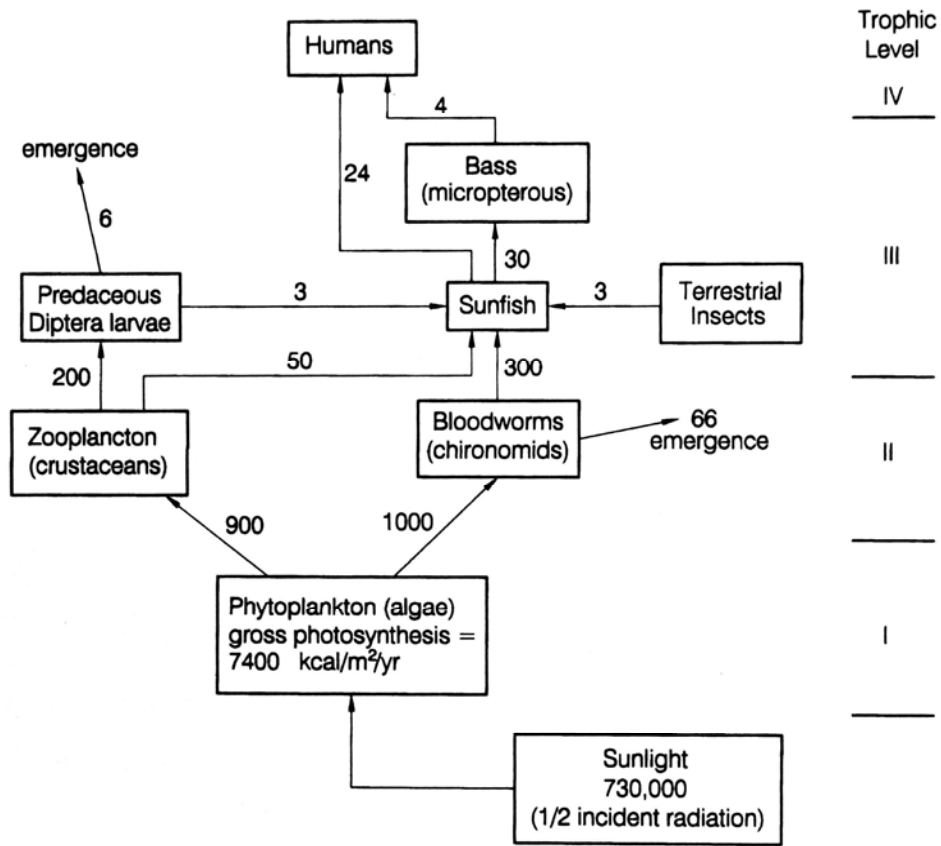


**FIGURE 4.8** Principal energy flow pathways through a simplified food chain in a Georgia (United States) pond managed for sport fishing. Numbers are energy flow between each compartment in kcal/m<sup>2</sup>/yr. (Modified from Odum, 1971.)

a diurnal variation in oxygen concentration in the epilimnion. The diurnal range of oxygen variation increases as a function of increasing primary productivity, and in hypereutrophic water bodies characterized by high algal biomass the dissolved oxygen levels may be supersaturated by day and sufficiently depleted by night to cause fish kills. Oxygen levels required for the survival of different species varies significantly, and oxygen depletion will eliminate the most oxygen-sensitive species (often desirable game species) from an impoundment.

**4.6.3 Productivity**

The gross primary productivity, or simply productivity, is the total rate of organic matter formation, adjusted to include losses such as respiration, grazing, and excretion. The net primary productivity refers to the rate of change in organic material, or net growth, which equals the gross primary productivity less the respiration or metabolic consumption by the primary producers.

The productivity, expressed in terms of gross carbon fixation, is measured in aquatic systems using the light-dark bottle technique. In this technique, a water sample is withdrawn from a desired water level and placed into three glass-stoppered biological

oxygen demand (BOD) bottles. One of these is transparent [the light bottle (LB)], a second is entirely wrapped with black electrical tape [the dark bottle (DB)], and the third [the initial bottle (IB)] is immediately analyzed to determine initial dissolved oxygen (DO) concentration. The LB and DB containing the original water sample and its planktonic population are placed back into the water column at the sampled depth to incubate until a significant oxygen change occurs, but without reaching oxygen depletion in the dark bottle. Incubation times can be less than 1 h in eutrophic waters, whereas 8 h of incubation may not significantly change oxygen levels in oligotrophic waters. After the light and dark bottles are recovered, their oxygen content is measured. The net oxygen depletion in the dark bottle represents the respiration in the aquatic community, while the net oxygen increase in the light bottle represents net production. Gross production (GP), or simply production, equals net production plus respiration and can be computed from the oxygen levels in the bottles as follows:  $GP = LB - DB$ . Oxygen is then converted to carbon equivalent to express production over the measurement period, which is then time adjusted to (g C)/m<sup>2</sup>/day. Carbon uptake may be measured directly in the light-dark bottle method by adding isotope-labeled <sup>14</sup>CO<sub>2</sub> to the sample, then filtering and measuring the radioactivity contributed by <sup>14</sup>carbon absorbed in the filtered phytoplankton. This method is more sensitive than oxygen measurement and can be used for short incubation periods or in oligotrophic waters where productivity is too low for the oxygen measurements. Rates of carbon production and selected other parameters as a function of trophic status are compared in Table 4.2. From a comparison of productivity data from 64 reservoirs and 102 natural lakes, Kimmel et al. (1990) concluded that reservoirs tend to be more productive (more eutrophic) than natural lakes.

Productivity may also be expressed in terms of the conversion of solar energy. The productivity of several ecosystem types is compared in Table 4.3 in energetic terms, and several useful energy conversions relating to primary productivity are summarized in Table 4.4.

#### 4.6.4 Factors Limiting Primary Production

The rate of primary production in aquatic ecosystems may be limited by a variety of factors. Limiting factors may include the rate of light extinction in turbid water, concentration of available forms of necessary nutrients, temperature, and toxins. The primary factors limiting the rate of primary production in aquatic ecosystems may change continuously over time scales ranging from hours to years.

#### 4.6.5 Trophic Status

Lakes and reservoirs may be classified in accordance with their trophic status, which reflects the nutrient concentration and rate of primary productivity within a body of water. An *oligotrophic* lake is characterized by low levels of nutrients and biological activity per unit of volume, resulting in high water clarity and high levels of dissolved oxygen throughout the entire water column. Alpine lakes and reservoirs with small watersheds in areas of erosion-resistant granitic parent material lack significant inputs of nutrients and sediments and are typically oligotrophic. A *eutrophic* lake has high levels of nutrient inputs and high rates of primary productivity, including algal blooms and in some cases prolific growths of submerged or floating vegetation. Water clarity is low, the substrate may become smothered in organic mud as a result of increased primary production, anaerobic conditions occur in deeper water, and temporary oxygen depletion can occur even in shallow water, causing fish kills. In highly eutrophic lakes, sustained anoxia can occur at depths less than 2 m. Eutrophic conditions are normally found in both

**TABLE 4.2** General Ranges of Primary Productivity of Phytoplankton and Related Characteristics of Lakes of Different Trophic Categories

Trophic type	Mean primary productivity,* (mg C)/m <sup>2</sup> / day)	Phyto-plankton, density cm <sup>3</sup> /m <sup>3</sup>	Phyto-plankton, biomass, mg• C/m <sup>3</sup>	Chloro-phyll a, mg/m <sup>3</sup>	Dominant phytoplankton	Light extinction coefficients, k/m	Total organic carbon, mg/L	Total P, µg/L	Total N, µg/L	Total inorganic solids. mg/L
Ultraoligotrophic	<50	<1	<50	0.01-0.5		0.03-0.8		<1-5	<1-250	2-15
Oligotrophic	50-300		20-100	0.3-3	Chrysophyceae, cryptophyceae, dinophyceae, bacillariophyceae	0.05-1.0	<1-3			
Oligomesotrophic		1-3						5-10	250-600	10-200
Mesotrophic	250-1000		100-300	2-15		0.1-2.0	< 1-5			
Mesoeutrophic		3-5						10-30	500-1100	100-500
Eutrophic	>1000		>300	10-500	Bacillariophyceae, cyanophyceae, chlorophyceae, euglenophyceae	0.5-4.0	5-30			
Hypereutrophic		>10						30->5000	500->15,000	400-60,000
Dystrophic	<50-500		<50-200	0.1-10		1.0-4.0	3-30	<1-10	<1-500	5-200

\* Referring to approximately net primary productivity, such as measured by the <sup>14</sup>carbon method. **Source:** After Wetzel (1983)

**TABLE 4.3** Productivity of Aquatic and Terrestrial Ecosystems. \*

Site	Gross Primary Production, kcal/m <sup>2</sup> /yr	Total for the World, 10 <sup>11</sup> kcal/yr
Estuaries and reefs	20,000	4
Tropical forest	20,000	29
Fertilized farmland	12,000	4.8
Eutrophic lakes	10,000	-
Eutrophic seasonal wetlands	10,000	-
Unfertilized farmland	8,000	3.9
Coastal upwellings	6,000	0.2
Grassland	2,500	10.5
Oligotrophic lakes	1,000	-
Open oceans	1,000	32.6
Desert and tundra	200	0.8

\* Net carbon production converted to gross energy values, where necessary, by multiplying by 20. Source: After Horne and Goldman (1994)

**TABLE 4.4** Biological Productivity Energy Conversions

To convert	To	Multiply by	Reciprocal
g O <sub>2</sub> released	kcal	3.510	0.285
g CO <sub>2</sub> absorbed	kcal	2.553	0.392
g C fixed	kcal	9.361	0.107
Kcal	kJ	4.187	0.239
kcal/s	kW	0.239	4.187

Source: After Cole (1994)

natural and artificial lakes that receive runoff or waste discharges from agricultural or urban areas, or shallow water bodies in which nutrients in bottom sediments can be continually brought to the surface water by processes such as wave action. A *mesotrophic* lake has characteristics intermediate between oligotrophic and eutrophic. *Eutrophication* refers to the process by which biological productivity increases within an aquatic ecosystem, as compared to natural conditions, typically as a result of human disturbances which increase the availability of limiting nutrients and results in greatly increased populations of algae or macrophytes. The eutrophication process can affect lakes at all trophic levels.

## 4.7 NUTRIENTS

### 4.7.1 The Concept of Limiting Nutrients

It is now widely recognized that phosphorus and nitrogen are the primary nutrients limiting productivity in most lakes and reservoirs. Of these, phosphorus is the

least abundant of the major nutritional and structural components of biota, is considered to be the primary factor limiting primary production in many freshwater ecosystems, and has been the focus of many control efforts.

Phosphorus is removed from aquatic systems rather rapidly and becomes stored in sediments, where its concentration may be 2 orders of magnitude greater than the concentration in the overlying water. Continued inputs of phosphorus are necessary to maintain enhanced productivity in many oligotrophic and mesotrophic lakes. Manipulation of water levels and sediments will potentially impact phosphorus levels and productivity in the reservoir and downstream ecosystems, making it important to have a conceptual understanding of the phosphorus cycle and its relationship to lake sediments. The phosphorus cycle in lakes is described in basic limnology texts.

The ratios of major elements found in aquatic organic matter, including both algae and aquatic macrophytes are:

1P : 7 N : 40 C per 100 units dry weight

1P : 7 N : 40 C per 500 units wet weight

Thus, if phosphorus is limiting, the addition of phosphorus in assimilable form can theoretically generate 500 times its weight in living cell mass. Phosphorus is naturally supplied to lakes from the atmosphere and soils in the watershed, plus human activity including the discharge of detergents containing phosphorus. A generalized relationship between nutrient concentration and trophic status is summarized in Table 4.5.

**TABLE 4.5** Eplimnic Phosphorus and Nitrogen Concentrations in Neutral Lakes, Related to Trophic Status

Trophic Condition	Total P, $\mu\text{g/L}$	Inorganic N, $\mu\text{g/L}$
Ultraoligotrophic	<5	<2000
Oligomesotrophic	5 - 10	200-400
Mesoeutrophic	10 - 30	300 - 650
Eutrophic	30 - 100	500 - 1500
Hypereutrophic	>100	>1500

### 4.7.2 Phosphorus

Most phosphorus in natural aquatic environments is contained in particulate form, primarily in *seston*, which is both the living and nonliving organic particulate matter suspended in water. The dissolved phosphorus fraction consists of the material passing a 0.5- $\mu\text{m}$  filter and includes dissolved inorganic orthophosphate ( $\text{PO}_4^{-3}$ ), the only inorganic form available for uptake by algae, and organic phosphate in a colloidal state. The orthophosphate fraction usually constitutes about 5 percent or less of the total phosphorus in natural water. When orthophosphate is added to water, its rate of assimilation by algae is extremely rapid, on the order of minutes, with uptake tending to be faster in oligotrophic systems having the most severe phosphorus deficiency. In systems with higher concentrations of phosphorus, algae can assimilate phosphate in quantities significantly exceeding their actual needs, a process termed *luxury consumption*.

The particulate fraction includes phosphorus contained in or adsorbed onto seston and/or inorganic complexes such as clays, carbonates, and ferric hydroxides. Phosphorus data from aquatic systems usually refers to either the total or the soluble inorganic phosphorus (orthophosphate) without further differentiation of its various forms. While

most phosphorus in natural lakes is associated with seston, in reservoirs experiencing significant sediment loads much phosphorus may be associated with sediment, primarily the fine fraction that has a large surface area in relation to mass. The total concentration and fractionation of phosphorus will vary seasonally.

The phosphorus contained in organic material is recycled through both algal and bacterial waste products into forms that can be assimilated. However, sedimentation of the particulate fraction and its incorporation into sediments effectively removes phosphorus from the water column, and sedimentation is the primary sink for phosphorus. The rate of phosphorus sedimentation in reservoirs is significantly higher than in natural lakes, attributed by Canfield and Bachmann (1981) to the association of phosphorus with the higher settleable sediment load delivered to reservoirs. Littoral vegetation also plays an important role in both the uptake and release of phosphorus in natural lakes. It may also be important in smaller reservoirs with stable water levels, significant vegetated shallows, and dendritic geometry that produces an elongated shoreline. However, littoral vegetation may be insignificant or absent in larger impoundments, in arid or alpine zones, and where steep slopes or variation in pool elevation precludes significant vegetative growth.

Under aerobic conditions, phosphate combines with iron to form ferric phosphate and can also be absorbed onto ferric hydroxide and calcium carbonate. These chemical equilibria produce highly insoluble forms of phosphorus causing oxygenated sediment to act as a phosphorus sink. However, sediments with a significant organic content will become anaerobic below the surface, and reduction reactions involving iron cause dissolved iron and phosphate to be released simultaneously into the interstitial water. A layer of oxidized surface sediment less than 1 cm thick can be very effective in preventing the release of soluble phosphorus from the interstitial waters into the water column, but when anoxic or reduced conditions extend to the sediment surface (e.g. because of anoxia in the hypolimnion), the dissolved phosphorus is no longer trapped and over a period of several months phosphorus can migrate into the water column from a depth of at least 0.1 m within eutrophic muds. The rate of phosphorus release can be further accelerated (e.g., doubled) by agitation from turbulence, but biological activity by bottom-feeding fish and burrowing fauna seem to have little impact (Wetzel, 1983) The potential for biological activity that disturbs P-enriched muds is reduced or eliminated by anaerobic conditions in the bottom waters.

As a result of these interactions between phosphorus, sediment, and the water column, oligotrophic lakes with a well-oxygenated hypolimnion show little variation in phosphorus content with depth. There is a limited supply of phosphorus in the system and the oxygenated sediments serve as a phosphorus sink. By contrast, in eutrophic lakes with oxygen-depleted profundal water and anaerobic sediments, soluble phosphorus is continuously released from sediments into the water column, and the phosphorus concentration increases significantly with depth. Thus, water released from the hypolimnion of productive reservoirs tends to be nutrient-enriched, and circulation patterns within reservoirs that draw deeper anaerobic water into the epilimnion can increase nutrient availability, productivity, and the loading of organic sediments (Fig 4.9). Because of the longitudinal gradients characteristic of reservoirs, the significance of internal nutrient cycling can vary from one location to another. These dynamics may be summarized by stating that surface discharge reservoirs tend to trap nutrients and export heat, whereas reservoirs with deep discharges tend to export nutrients and trap heat (Wright, 1967).

Lijklema et al. (1994) examined nutrient dynamics and light-shading associated with the resuspension of sediment by wave action in shallow lakes in the Netherlands. They pointed out that turbulent resuspension of sediments can increase productivity in the overlying water because of the recirculation of phosphorus, but it can also reduce primary

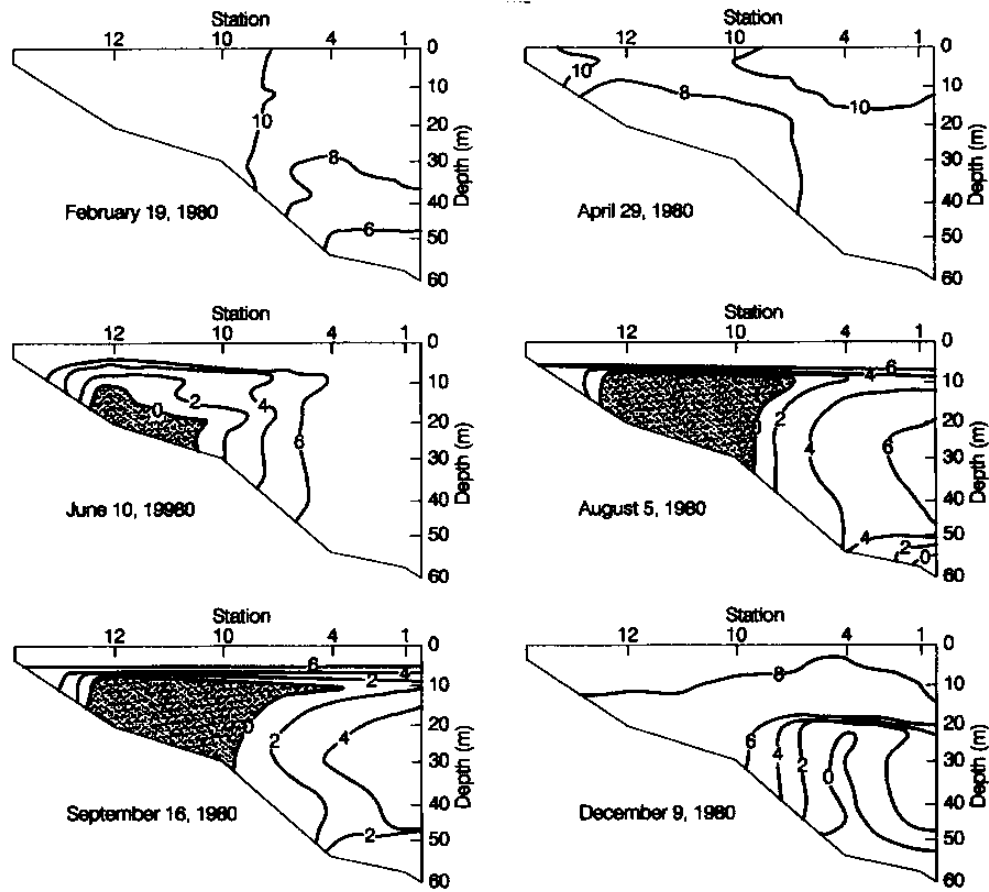


**FIGURE 4.9** Seasonal variation in dissolved oxygen distribution in Lake DeGray, Arkansas, showing seasonal anoxia in the upstream zone of the reservoir receiving the highest rate of organic loading, and the transport of nutrient-enriched anoxic water due to runoff events entering the reservoir as interflow. (Kennedy and Nix, 1987)

productivity as a result of turbidity shading. They modeled sediment erosion, transport, and deposition in a variable-depth system consisting of a generally shallow lake containing deep pits or channels into which suspended sediments would collect, but which were too deep for wave action to resuspend the sediments. It was found that the pits would act as a trap for fine sediments and their associated nutrients, which could be subsequently dredged, thereby removing nutrients from the lake. This modeling simulated the size-dependent settling rate of the sediment, and the preference of phosphate for the fine-sized fractions

### 4.7.3 Nitrogen

Elemental nitrogen ( $N_2$ ), the most abundant element in the atmosphere and the most abundant form of nitrogen in aquatic systems, is biologically nonreactive except for nitrogen-fixing organisms. Nitrate ( $NO_3^-$ ) is commonly the predominant form of reactive nitrogen in aquatic systems. Other forms include ammonia ( $NH_4^+$ ), nitrite ( $NO_2^-$ ), and

both particulate and dissolved organics. Unlike phosphorus, nitrogen is very mobile and is not highly absorbed by soil, and only ammonia ( $\text{NH}_4^+$ ) tends to be adsorbed by clay or organic particles.

Nitrogen is commonly a limiting nutrient in the ocean and lakes in warm climates. Inputs of biologically reactive forms of nitrogen into reservoirs and other aquatic systems are derived from atmospheric sources (precipitation and dry fallout), from runoff (including pollutants), and by fixation of molecular nitrogen by blue-green algae and *photosynthetic* bacteria. The bacterial reduction of nitrate to nitrite and then to elemental nitrogen, a process termed *denitrification*, occurs in areas of oxygen deficit including the hypolimnion and sediments. It is an important process for the removal of biologically reactive nitrogen from aquatic ecosystems. Many aquatic systems experience regular seasonal variations in nitrogen levels (Home and Goldman, 1994).

The nitrogen cycle is complex, and nitrogen may exist simultaneously in many forms in the water column. Nitrogen transformations are controlled largely by microbes. The rate of nitrogen exchange between sediment and the water column varies greatly as a function of various factors including redox potential and sediment composition, and Wetzel (1983) characterized the nitrogen dynamics of sediments as "poorly understood."

#### 4.8 GRADIENTS, SEDIMENTATION, AND BIOLOGICAL PROCESSES

---

A large fraction of the organic matter and nutrients delivered to reservoirs is in particulate form and subject to the same sedimentation processes that affect suspended mineral particles. Allochthonous inputs of both detrital organics and nutrients are delivered to the impoundment by the inflowing river. Both living and dead suspended organic particulate material, the seston, will settle out by physical processes, and a sedimentation gradient would normally be expected from the headwater to the dam. Dissolved nutrients in the water will be incorporated into the algal biomass, or floating macrophytes (e.g., water hyacinth) in some tropical reservoirs, which will also contribute to the sedimentation of organic material as these organisms die and sink. Thus, seston from both allochthonous and autochthonous origin contributes to the total organic sediment load, and in hydrologically large reservoirs this organic load may be expected to be higher in the headwater region and lower nearer the dam.

Gradients in the nutrient content in the water and the resulting deposition rate of organic sediments can have important ecological consequences from the standpoint of oxygen distribution, nutrient cycling, and reservoir metabolism. In reservoirs that are longitudinally short, hydrologically very small, or subject to periodic emptying, these gradients may not be pronounced. However, in larger reservoirs these gradients can be a primary factor controlling ecological conditions. The existence of a sedimentation gradient and several ecological consequences were documented at Lake DeGray by James and Kennedy (1987).

The 808-Mm<sup>3</sup> Lake DeGray impoundment on the Caddo River in Arkansas is hydrologically large lake with C:I = 1.2. The mean depth is 9 m, maximum depth is 60 m, and the 1162 km<sup>2</sup> watershed is mostly forested. The reservoir configuration is shown in Fig. 4.4. Sediment deposition was monitored by triplicate traps suspended in the water at depths of 5 and 15 m, with an additional 45-m trap near the dam. Trap deployment periods ranged from 20 to 48 days. Upon retrieval the samples were recovered, the traps were cleaned and redeployed, and the triplicate samples were mixed and analyzed.

Because of sedimentation, the sediment loading rates measured in the traps declined in the direction of the dam (Table 4.6). Although deposition at the extreme upstream end of the reservoir was limited by high flow velocity that can entrain the low-density organic material and transport it farther downstream, considerable deposition occurred in the vicinity of the plunge point. As nutrient-rich river water moved through the reservoir in early spring, uptake by algae and removal by sedimentation progressively decreased nutrient concentrations down-reservoir, thereby limiting productivity near the dam. Storm events were found to account for about 95 percent of the annual suspended solids loading. The generalized pattern of production and sedimentation of organic matter from both allochthonous and autochthonous sources is summarized in Fig. 4.10.

**TABLE 4.6** Composition of Trapped Sediment as a Function of Location in lake DeGray, Arkansas (mg/m<sup>2</sup>) during the Study Period

Parameter	Headwater	Middle	Dam
Dry weight	8550	2980	1520
Carbon	456	202	123
Nitrogen	45	22	15
Phosphorus	18	5	2
Iron	269	103	50
Chlorophyll <i>a</i>	2.93	0.92	0.23

Source: James and Kennedy (1987)

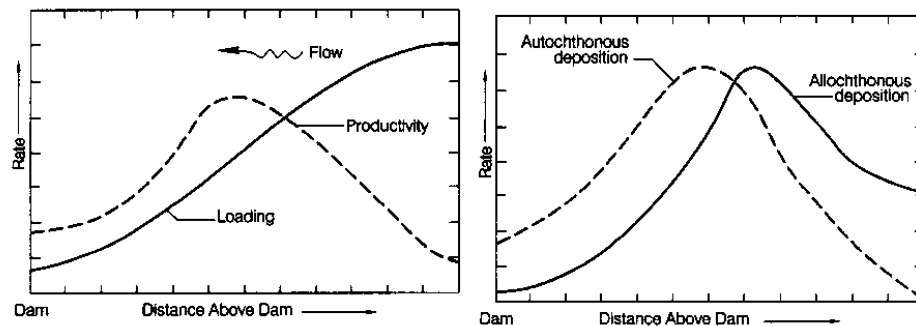


**FIGURE 4.10** Generalized longitudinal pattern of organic matter production and sedimentation.

Kennedy and Nix (1987) studied oxygen dynamics in Lake DeGray, which were found to be related to the longitudinal pattern of sediment deposition. When the reservoir was impounded it submerged a mixed pine-hardwood forest. Oxygen demand from submerged vegetation and soils resulted in severe oxygen depletion within the hypolimnion during the first years of impounding. However, as the readily oxidizable materials were consumed, oxygen dynamics in the lake came to be controlled by allochthonous and autochthonous organic materials. Anoxia is initiated near the headwater region of the reservoir, the zone where organic inputs are greatest from riverborne detritus plus increased photosynthetic activity in the lake due to higher nutrient levels.

Dissolved oxygen in the headwater region is depleted rapidly in the spring because of the limited volume in the hypolimnion plus the high rate of organic loading in that zone. Organic sediments in the headwater zone release nutrients when subject to anoxic conditions. Subsequent streamflow entering the reservoir as interflow transports anoxic water and its associated nutrients deeper into the reservoir, thereby extending longitudinally the zone of higher productivity in the epilimnion (Fig. 4.9).

## **4.9 CLOSURE**

---

Little justice can be done to the field of limnology in a single condensed chapter. Readers are encouraged to acquire a basic college text in limnology, and pursue a basic understanding of the fundamental physical and biological processes occurring in reservoirs.

---

## CHAPTER 5

---

# SEDIMENT PROPERTIES

---

### 5.1. SIZE CLASSIFICATION OF SEDIMENT

---

#### 5.1.1. Size of Sediment Grains

The size of sediment particles transported by water ranges over 7 orders of magnitude from individual clay platelets to boulders. Grain size is the most important parameter describing sediment behavior in water, and a variety of terms may be used to describe the size characteristics of individual grains and composite samples. The term *coarse* normally implies sand and larger grains; *fine* refers to silts and clays. We will use the size classification system recommended by the American Geophysical Union, which is a geometric scale based on a ratio of 2 between successive sizes (Lane, 1947). This classification method is presented in Table 5.1 along with sieve sizes. The phi ( $\phi$ ) classification scale used by many researchers is a geometric grade scale in which particle diameter in millimeters is expressed as the base 2 exponent (phi sizes for grains 0.5, 1, 2, and 4 mm in diameter are -1, 0, 1, and 2 respectively). The phi size for a particle is computed as

$$\Phi = -\log_2 d = 3.3219 \log_{10} d \quad (5.1)$$

where  $d$  = diameter in mm. The phi scale was adopted to facilitate application of conventional statistical methods to sediment-size particles (Krumbein, 1934). Differences occur between the size scales used internationally, especially for coarse sediment (Fig. 5.1). Some size-dependent characteristics of sediments are summarized in Fig. 5.2, along with size ranges for several other types of particles.

Sediment particles are never exactly spherical and the term "diameter" only approximates their size. Several methods are used to determine and express grain diameter. Grains may be measured along three mutually perpendicular axes of which there will be a longest, an intermediate, and a shortest axis. The *triaxial diameter* is the arithmetic average of the three axes. *Sieve diameter* is the length of the side of a square sieve opening through which a particle will just pass and closely approximates the intermediate axis. Sands and fine gravels are normally sized with sieves, and the reported diameter is characteristically the sieve diameter. Individual larger particles, such as gravel or cobbles, can be directly measured by using a scale and the intermediate axis length is reported as the nominal diameter. *Sedimentation diameter* is the diameter of a sphere which, in the same fluid, has the same terminal settling velocity as the particle. The reported diameter values for silts and clays are actually sedimentation diameters, since the size of these minute particles is determined by their fall velocity in water. When analyzing the settling properties of small particles, including clays which are more plate-like than spherical and whose settling velocity is often strongly influenced by flocculation, the sedimentation diameter is the most appropriate measure. *Nominal diameter* is the diameter of a sphere having the same volume as the particle.

**TABLE 5.1** Grain Size Classes

Size class	Grain diameter, mm		Sieve size retained on	
	Min.	Max.	Tyler	U.S. Standard
Boulders:				
Very large	2048	4096		
Large	1024	2048		
Medium	512	1024		
Small	256	512		
Cobbles:				
Large	128	256		
Small	64	128		
Gravel:				
Very coarse	32	64		
Coarse	16	32		
Medium	8	16		
Fine	4	8	5	5
Very fine	2	4	9	10
Sand:				
Very coarse	1	2	16	18
Coarse	0.5	1	32	35
Medium	0.25	0.5	60	60
Fine	0.125	0.25	115	120
Very fine	0.062	0.125	250	230
Silt:				
Coarse	0.031	0.062		
Medium	0.016	0.031		
Fine	0.008	0.016		
Very fine	0.004	0.008		
Clay:				
Coarse	0.002	0.004		
Medium	0.001	0.002		
Fine	0.0005	0.001		
Very fine	0.00024	0.0005		

### 5.1.2. Particle Shape and Roundness

The *shape factor* (SF) is an expression of the "sphericity" of a particle and may be computed from the relative lengths of the longest (*a*), intermediate (*b*), and shortest (*c*) particle axes:

$$SF = \frac{c}{\sqrt{ab}} \quad (5.2)$$

The shape factor for a sphere is 1.0 and for natural sands is usually about 0.7 (Interagency Committee, 1957).

*Roundness* is defined as the ratio of the average radius of the corners and edges of a particle to the radius of a circle inscribed in the maximum projected area of the particle.

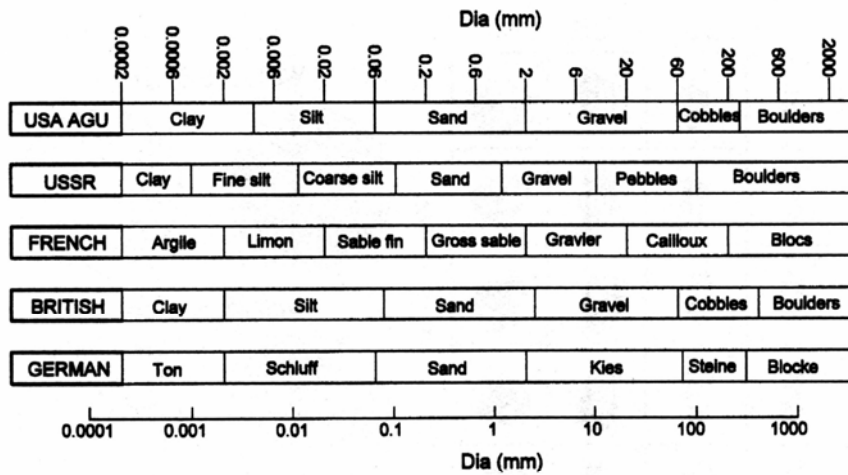


FIGURE 5.1 Comparison of national scales for particle sizes.

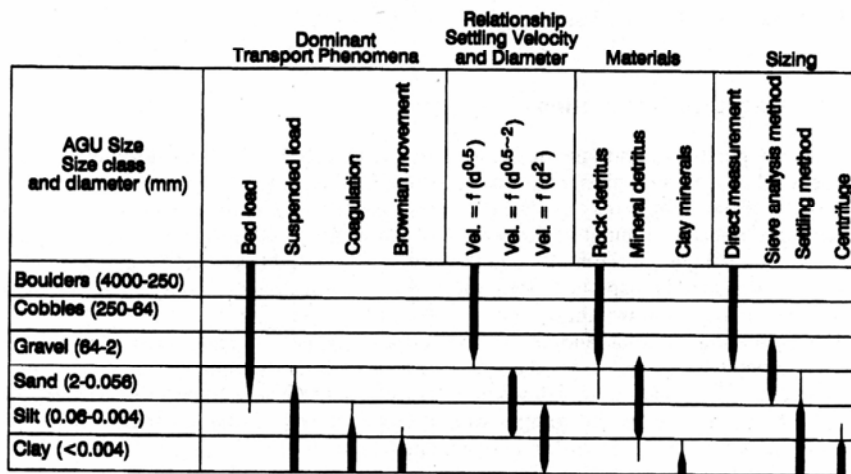


FIGURE 5.2 Comparative sizes of sediment and other small particles (various sources).

It is geometrically independent of sphericity and has a relatively small effect on the hydraulic behavior of the particle, but it is of primary importance in determining the abrasiveness of a particle to hydraulic equipment. Freshly weathered particles have highly angular structures and become more rounded over time as a result of interparticle abrasion. Thus, sands in streambeds tend to be more angular in headwaters and less angular farther downstream. Aeolian (wind-transported) sands are typically more rounded than fluvial sands because the impact and abrasive forces between grains transported by air is greater than between sands transported in water. A visual representation of *roundness* and *sphericity* is shown in Fig. 5.3.

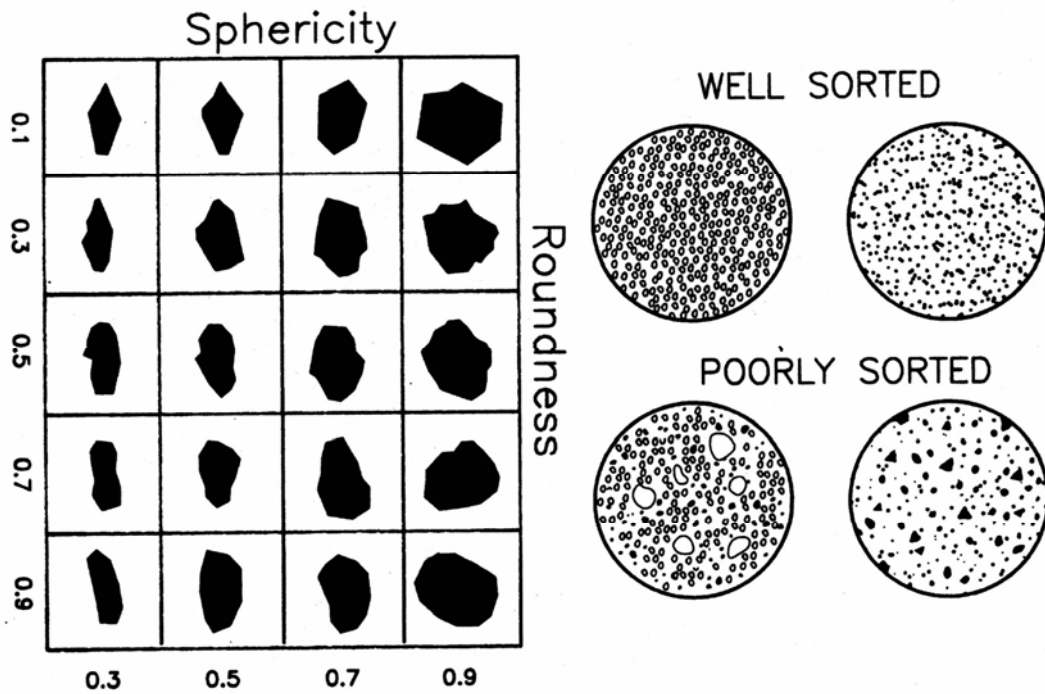


FIGURE 5.3 Sphericity, roundness, and sorting of sediment grains.

### 5.1.3. Grain Size Distribution

Sediment deposits have a range of grain sizes, and both field and laboratory techniques can be used to separate sediment grains according to their size. The granulometric characteristics of the sample may be described by a *grain size distribution curve* (Fig. 5.4) which represents the cumulative dry weight of the sample in each size fraction. The particle size is displayed horizontally and the cumulative weight percent of grains smaller than the stated size is displayed along the vertical axis. In a sieve analysis the vertical axis corresponds to the weight percent passing each screen size.

For both computational and descriptive purposes, it is frequently desirable to use a single diameter which describes the behavior of a sediment sample containing a range of grain sizes. The median ( $d_{50}$ ) diameter is most frequently used to describe a sediment sample. Fifty percent of the sample weight is composed of grains smaller than the median diameter. However, different researchers have proposed using "representative" sizes ranging from  $d_{35}$  to  $d_{max}$  to describe the transport and related properties of sediment mixtures. Stelczer (1981) states that the movement of bed load of mixed sediments is best predicted by the particle size around  $d_{80}$ , with both the coarser and finer fractions of the bed being set into motion almost simultaneously, at the same critical velocity as the  $d_{80}$  fraction. The  $d_{16}$ ,  $d_{84}$ , and  $d_{90}$  diameters are also frequently used to describe sediment mixtures.

Assuming the grain size curve is a cumulative distribution function (CDF) following a normal (Gaussian) distribution, which is often approximately the case, the S-shaped CDF can be converted into a straight line on normal probability paper. For a normal distribution, the  $d_{16}$  and  $d_{84}$  diameters may be used to compute the standard deviation  $\delta$  of the grain size of the sample:

$$\delta = \left( \frac{d_{84}}{d_{16}} \right)^{1/2} \tag{5.3}$$

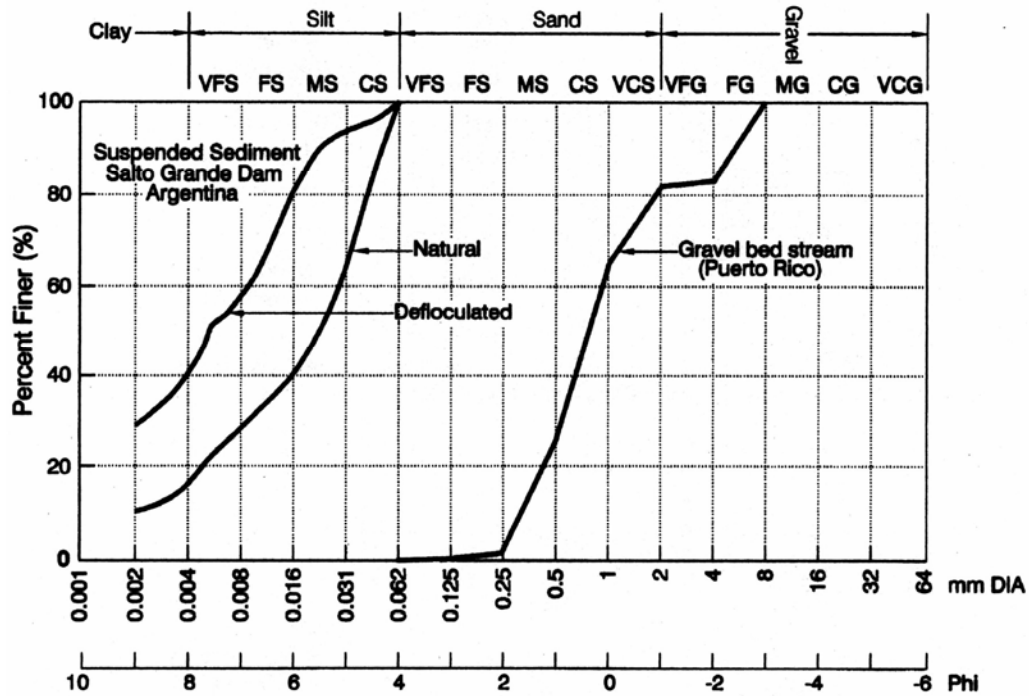


FIGURE 5.4 Grain size distribution curve.

Sediment size distributions usually only approximate a normal distribution, and may be skewed rather than centered on the median size. The *gradation coefficient* (Gr) defines the departure from the sample median value as follows:

$$Gr = \frac{1}{2} \left( \frac{d_{84}}{d_{50}} + \frac{d_{50}}{d_{16}} \right) \tag{5.4}$$

These distribution parameters should be used only if the grain size distribution curve is S shaped.

The slope of the grain size distribution curve reflects the uniformity of the grain sizes in the sample. Steep size-distribution curves are produced by samples which are more uniform in size (well-sorted); flatter size-distribution curves are produced by samples having a wide range of grain sizes (poorly sorted). The concept of *sediment sorting* is visually presented in Fig. 5.3.

#### 5.1.4. Classification by Mode of Transport

The movable bed consists of the sediment found on the streambed that is transported by water, especially during high flows. Not all the material found in streambeds is considered movable, such as large-diameter avalanche debris or deposits of cohesive clays. Stream sediments may be classified by relative grain size and abundance in the movable streambed and by mode of transport (Einstein, 1964). The basic concepts of transport classification based on relative size and mode of transport are summarized in Figs. 5.5 and 5.6. *Suspended load* refers to (1) the material moving in suspension and sustained in the water column by turbulence or in colloidal suspension or (2) the material collected in or computed from a suspended-load sampler. *Wash load* is the portion of

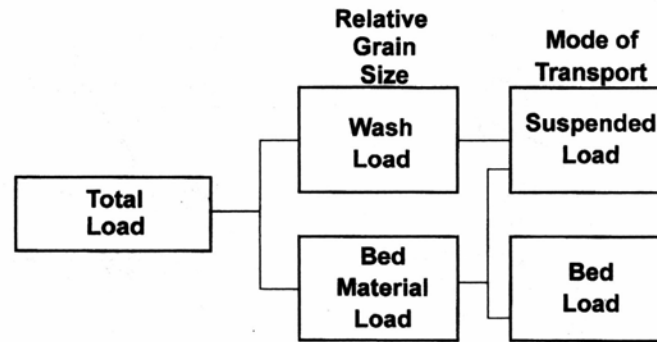


**FIGURE 5.5** Classification of sediment transport by grain size relative to the streambed and by mode of transport.

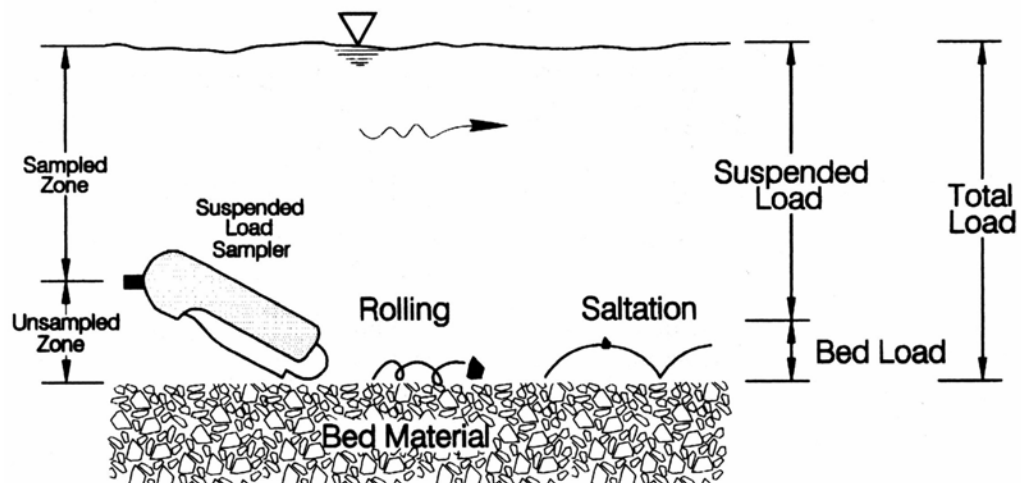


**FIGURE 5.6** Schematic representation of sediment transport and sampling zones in a stream.

the sediment load composed of grains smaller than those found in appreciable quantities in the movable bed, often taken as the smallest 10 percent of the bed material by weight. The wash load is normally transported in suspension. These small sediments are washed through the fluvial system without significant interaction with the bed. *Bed material* consists of the grain sizes which are predominantly represented in the movable bed of a stream. *Bed load* may be used to designate either (1) coarse material moving in continuous or intermittent contact with the bed or (2) material collected in or computed from samples collected in a bed-load sampler or trap. The bed load includes particles rolling or sliding along the bed plus the *saltation load*, which consists of grains bouncing along the bed or particles moved by the impact of the bouncing particles. The *bed material load* is that portion of the total sediment load composed of bed material, whether transported in suspension or as bed load.

Classification by mode of transport depends on both grain size and turbulence within the stream. Clays and fine silts are probably always transported in suspension, and most gravel and cobbles as bed load. However, depending on the turbulent energy, sand may be stable on the bed, may roll or bounce along the bottom, or may be carried in suspension. Thus, the suspended load in a stream may consist entirely of silts and clays at low

discharges, but include sands at high discharge, causing the grain size distribution of the suspended load to coarsen as discharge increases. In many streams the bed material load constitutes a small fraction (less than 15 percent) of the total load.

## **5.2. CHARACTERISTICS OF SEDIMENT GRAINS**

---

Sand, silt, and clay particles behave distinctly and have characteristics that are readily identifiable in the field.

### **5.2.1 Sand**

The term sand refers to a specific size particle, not a particular mineral. Thus, sand-size particles in lowland rivers may consist exclusively of quartz particles, dark basaltic particles predominate in the streams of many oceanic islands, and beach sands may consist of quartz crystals, volcanic or basaltic fragments, or carbonate fragments of shells, urchins, calcareous algae, reef rubble, or carbonate precipitates (oolites). Sand grains are too small to measure individually without use of magnification, yet are large enough to be counted with the unaided eye and can visibly be observed to settle rapidly in water. Sands are normally size-classified by sieves, and the smallest sands (0.062 mm) are the smallest grains that, as a practical matter, can be mechanically sieved. Terrigenous sand-size particles consist of small rock fragments or crystals, but especially silicates, quartz being the most common form. Feldspar follows silicates in abundance. Silicates are abundant crustal minerals and also the most solution-resistant, and remain intact after the surrounding rock matrix has eroded or dissolved away. In mountainous areas where the parent material is being actively decomposed, the sand-size particles will consist of freshly eroded rock fragments, whereas in areas distant from the parent material sand-size particles may consist exclusively of quartz grains. The composition of the sands in a streambed reflects not only the composition of the source material, but also the physical, chemical, and biological processes acting on the sediment. A generalized idea of the effects of climate and topography on the erosional and weathering processes affecting the composition of sands is presented in Fig. 5.7.

### **5.2.2 Silt**

Silts consist of particles in the range of 0.004 to 0.062 mm. All but the largest particles are too small to be individually discerned with the naked eye, but a small sample placed between the teeth will feel gritty. Individual silt grains are small mineral fragments, essentially smaller versions of sand grains, but silt-size particles suspended in water may also consist of flocs formed from clay-size particles. Silts settle much more slowly than sand, and the settling rate of a silt suspension in a graduated cylinder may be barely discernible. When silts are deposited, water can become trapped between grains, and if saturated silt deposits are agitated they will liquefy, causing phenomena such as quicksand. Loess soils are deposits of windblown silt.

### **5.2.3 Clay and Clay Flocculation**

Clay is too fine for its structure to be detected between the teeth. However, a moist sample containing a significant percentage of clay can be rolled into a ribbon by hand, its

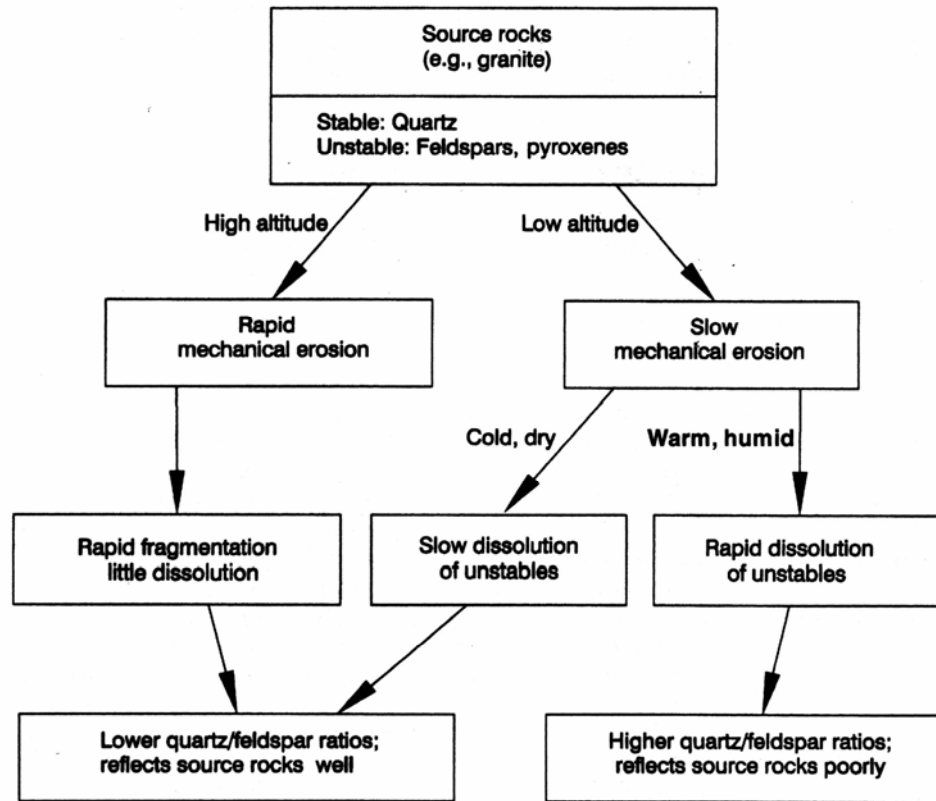


**FIGURE 5.7** Generalized effects of climate and topography on the processes of chemical weathering and mechanical erosion and its influence on quartz/feldspar ratio in residual sands (after Siever, 1988).

"stickiness" caused by interparticle cohesion. Unlike the larger grains, clays are not simply minutely abraded rocks but are minerals typically consisting of sheets of silica tetrahedra cross-linked with alumina octahedra. Individual clay particles can be conceptualized as sheet-like or disk-like and are termed *platelets*. Nonclay minerals are generally not smaller than 0.002 mm, and this size is frequently used to split between the clay and nonclay fraction.

A *cohesive sediment* is one which contains a concentration of fines and colloids sufficient to impart plastic properties at some water content, and the ability to resist shear stress at some other water content, a property termed *cohesion*. The plastic and cohesive properties of clay are due to colloids, particles with a specific surface area (area per unit weight) so large that behavior is controlled by surface rather than gravitational forces. To illustrate the large surface associated with small particles, assume all particles are spherical and compute the surface area for 1 cm<sup>3</sup> of solid material as a function of grain diameter. The undivided diameter is 1.24 cm and the surface area is 4.84 cm<sup>2</sup>, but, if subdivided into 0.001-mm-diameter spheres, the same mass of sediment will have a surface area of 60,000 cm<sup>2</sup>. The electrochemical surficial forces may be 106 times stronger than gravitational forces in 0.001-mm clay platelets (Partheniades, 1962). Deposited clays can gain strength over periods of time ranging from minutes to years as the individual particles become rearranged into more stable positions.

Clays have extremely low settling velocities, and without turbulence or Brownian (thermal) motion a 0.001-mm clay particle will require about 2 weeks to settle 1 m.

However, as a result of Brownian motion, individual clay particles may be very stable even in quiescent water, and remain dispersed for months. Short-distance van der Waals forces cause all particles to be attracted to one another and are responsible for the aggregation of clays and other minute particles into flocs large enough to settle at appreciable velocities. At near-neutral pH values, most particles suspended in water, including clays and organics, are characterized by negative surface charges. In a neutral suspension, each particle with a negative surface charge must be surrounded by a cloud of positively charged ions to achieve electroneutrality. The concentration of the positively charged particles is greatest at the particle surface and becomes more diffuse as a function of distance from the particle, giving rise to an electrical double layer around each particle. Because the charges in the diffuse cloud surrounding the suspended particles are of like sign, when particles approach one another the like-sign charges in the diffuse double layer tend to repel each other, thereby impeding the particles from approaching to within the short distances required for attractive van der Waals forces to dominate.

The facility with which clay particles can combine to form flocs depends on the balance between the attractive van der Waals and the repulsive electrostatic forces, and one of the principal mechanisms for destabilization of clays and other colloids is to compress the double layer thickness by increasing the ionic strength of the solution. The greater the concentration of ions in the solution, the smaller the thickness of the diffuse layer around the charged particle necessary to maintain electroneutrality (Fig. 5.8). The use of trivalent aluminum or iron salts ( $Al^{+3}$ ,  $Fe^{+3}$ ) as coagulants in water filtration plants, and the destabilization of riverine colloids when discharged into seawater, are two examples of destabilization by double-layer compression. The rate of destabilization is also a function of the rate of interparticle collisions resulting from Brownian motion, turbulence, or differential settling velocities. In quiescent water, floc particles may agglomerate by differential settling rates, with larger particles sweeping downward, overtaking, and enmeshing smaller slower-settling particles, causing settling velocity to increase over time as a result of floc growth. Ultimate floc size is limited by the turbulent shear stress that tears the larger floc particles apart. Destabilization of clays and other colloids can also occur as a result of adsorption to produce charge neutralization, enmeshment in a precipitate, and interparticle bridging caused by certain organic polymers (Amirtharajah and O'Melia, 1990).

Most clays do not exist in aquatic systems as individual platelets, but instead are flocculated by naturally occurring salts. Coagulation refers to the process of destabilizing the particles in a solution, and flocculation refers to the process of continued mechanical contact between particles which enables them to adhere to one another to create larger particles. Flocculated clay particles can settle several orders of magnitude faster than individual clay platelets and may exhibit sedimentation velocities characteristic of silts. Clay flocculation is a common phenomenon and is responsible for the rapid clarification of most natural waters. The grain size distributions in Fig. 5.4 show two curves for a single sample corresponding to settling analysis with and without a dispersant to deflocculate the clay fraction. For sedimentation studies, the grain size distribution for conditions of natural flocculation would normally be used.

## **5.3 BULK PROPERTIES OF SEDIMENT**

---

### **5.3.1 Sediment Density and Weight**

The mass density of a solid particle  $\rho_s$  is the mass per unit volume and is expressed in units of  $g/cm^3$  or  $kg/m^3$  (slugs/ft<sup>3</sup>). The specific weight of solid particles  $\gamma_s$  is the weight

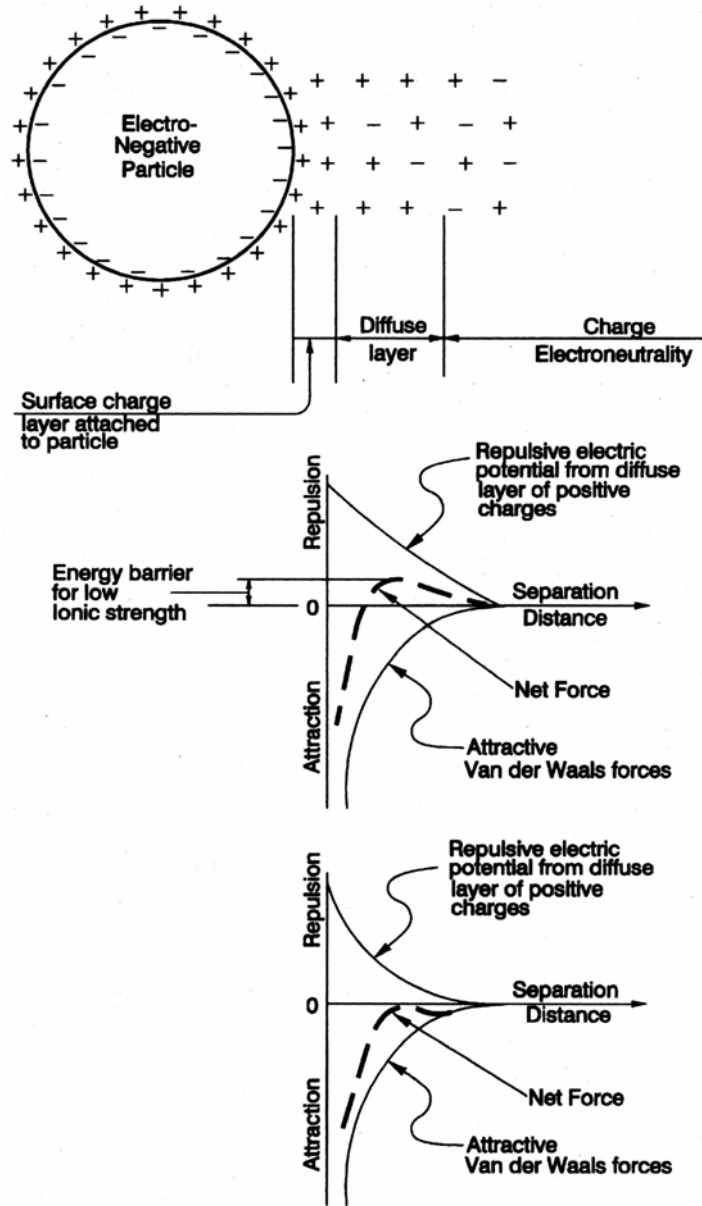


FIGURE 5.8 Double-layer and clay flocculation mechanisms.

per unit of volume. Weight is the product of mass and gravitational acceleration and the specific weight is the mass density multiplied by gravitational acceleration:  $\gamma_s = \rho_s g$ . It is expressed in units of  $\text{kg}/(\text{m}^2 \cdot \text{s}^2)$  or  $\text{N}/\text{m}^3$ . For sediment with a specific gravity of 2.65,  $\rho_s = 2650 \text{ kg}/\text{m}^3$  and  $\gamma_s = 25988 \text{ kg}/(\text{m}^2 \cdot \text{s}^2)$ . The submerged specific weight of a particle  $\gamma'_s$  is expressed as the difference between the specific weights of the solid  $\gamma_s$  and the surrounding fluid  $\gamma$ :

$$\gamma'_s = \gamma_s - \gamma \tag{5.5}$$

The specific gravity  $G_s$  of a solid is expressed as the dimensionless ratio of the specific weights or of the density of the solid and of distilled water at 4°C, the temperature of maximum water density.

$$G_s = \frac{\gamma_s}{\gamma} = \frac{\rho_s}{\rho} \quad (5.6)$$

### 5.3.2 Unit Weight or Bulk Density of Sediment

Unit weight, specific weight, and bulk density are all used to express the dry weight per unit volume of a bulk sediment sample, including both solid grains and voids, after drying to a constant weight at 105°C. Drying time may vary from a few hours for sands to several days for hygroscopic clays. Accurate bulk density values depend on obtaining representative, undisturbed in situ samples of the sediment. Under submerged conditions, samples of predominantly fine-grain reservoir deposits will normally be collected by a piston-type sampler. Some submerged sediments will be so weak that a core can be pushed through several meters of material by hand, and in poorly compacted sediment a piston core or a large diameter gravity core (e.g., 10 cm or 4 in) may give more accurate results than smaller diameter gravity cores. Representative sampling of submerged deposits of fines can be difficult, where alternating layers of coarse and fine sediments occur, since denser material in the core barrel may push through finer sediment layers without capture. Carefully compare the length of core penetration versus length of the core captured to check for problems such as compaction and core loss.

In sampling from nonsubmerged sediments, a metal ring or box can be driven into sediments, the surrounding sediments cleared away, and the sample of known volume then carefully removed. This method can be used on both horizontal and vertical sediment surfaces. In the sand replacement method (Bureau of Reclamation, 1987) a 0.5-m square is leveled, the sample is excavated from within this horizontal surface, and then the in-situ volume of the sample is determined by refilling the hole with calibrated sand. In noncohesive soils, the sample hole will necessarily taper toward the bottom. The calibrated sand should be air-dried, passing No. 16 and retained on No. 30 sieve, and of known unit weight. Sample volume is determined as the difference in weight of the calibrated sand in the container before and after filling the hole.

Bulk densities for surface soils classified as clay, clay loam, and silt loam typically fall in the range of 1.0 to 1.6 g/cm<sup>3</sup>, whereas sandy soils typically range from 1.2 to 1.8 g/cm<sup>3</sup>, with the higher value corresponding to uniformly graded silica sand. Bulk densities for compact subsoils may exceed 2.0 g/cm<sup>3</sup> (Brady, 1974). There is a wide difference in bulk densities in reservoir sediments, both between sites and within the same reservoir. Highest densities typically occur in coarse delta deposits and lowest densities occur in fine sediment near the dam. Lara and Pemberton (1963) published data from 1129 samples in 101 reservoirs, mostly in the United States. Bulk densities ranged from 0.30 to 1.88 g/cm<sup>3</sup>. The average deposit bulk density for 800 U.S. reservoirs was 0.96 g/cm<sup>3</sup> (60 lb/ft<sup>3</sup>), as reported by Dendy and Bolton (1976).

### 5.3.3 Angle of Repose

The angle of repose is the slope angle formed with the horizontal by granular material at the critical condition of incipient sliding. The angle of repose for both dry and submerged noncohesive material, as a function of grain size, may be determined from Fig. 5.9. When sediment has accumulated against a low-level outlet, and the outlet is opened, the angle of repose can be used to describe the side slope of the cone which is excavated within the

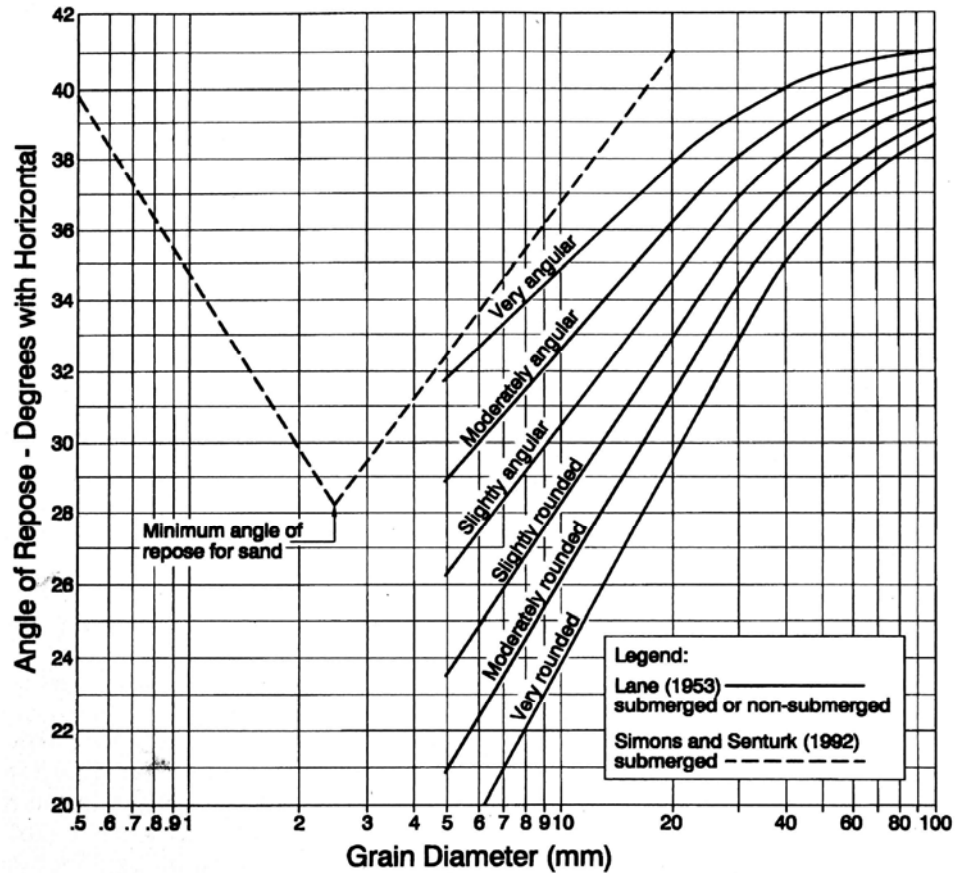


FIGURE 5.9 Angle of repose for uniform noncohesive sediment (Lane, 1953).

sediment, if cohesive materials are absent. When cohesive sediments are present, slopes can be steeper than the angle of repose for cohesionless material. Also, sediment can liquefy and flow under certain conditions, such as earthquake shaking, producing slopes much lower than the angle of repose.

## 5.4 SEDIMENT WATER MIXTURES

### 5.4.1 Void Space

A fluid-sediment mixture consists of solid particles (subscript *s*) and void space (subscript *v*), where the voids between the sediment grains are understood to be occupied by the fluid. The volumetric ratio of voids ( $Vol_v$ ) to sediment grains ( $Vol_s$ ) in a sample is termed the *porosity*  $p$  and is defined as

$$p = \frac{Vol_v}{Vol_{total}} \tag{5.7}$$

Porosity should not be confused with *permeability*, which is the rate at which a medium will transmit a fluid when subject to a pressure gradient. A clay sample may have a porosity value equal to that of a gravel sample, but whereas the gravel will readily transmit water, and is thus said to be highly permeable, the clay will be very impermeable because the pores between grains are too small to transmit water at an appreciable rate. The *void ratio*  $e$  is the ratio of voids to solids and is given by

$$e = \frac{\text{Vol}_v}{\text{Vol}_s} = \frac{p}{1-p} \quad (5.8)$$

#### 5.4.2 Sediment Concentration

Three different methods may be used to compute the concentration of sediment in water (Julien, 1995). Concentration by mass  $C_m$  refers to the sediment mass per unit volume of water-sediment mixture and, by definition:

$$C_m = \frac{\text{sediment mass}}{\text{volume of mixture}} = \frac{\rho_s \text{Vol}_s}{\text{Vol}_s + \text{Vol}_v} \quad (5.9)$$

Values of  $C_m$  are usually expressed in units of mg/L, but units of g/L (or kg/m<sup>3</sup>) are more convenient for high concentrations (1 g/L = 1 kg/m<sup>3</sup> = 1000 mg/L).

The concentration by volume  $C_v$  is the dimensionless ratio of the sediment volume to the mixture volume  $\text{Vol}_{\text{mix}}$ :

$$C_v = \frac{\text{sediment volume}}{\text{volume of mixture}} = \frac{\text{Vol}_s}{\text{Vol}_s + \text{Vol}_v} = \frac{C_m}{\rho_s} = 1-p \quad (5.10)$$

The volume concentration can be computed knowing the mass concentration and sediment density. For  $C_m = 10,000$  mg/L and  $\rho_s = 2.65$  g/cm<sup>3</sup>, adjust all units to kg and m<sup>3</sup> to solve for  $\text{Vol}_s / \text{Vol}_{\text{mix}} = (10 \text{ kg/m}^3) / (2650 \text{ kg/m}^3) = 3.77 \times 10^{-3}$ . Volume concentration may be converted into mass concentration using

$$C_m = \rho_s C_v \quad (5.11)$$

$$C_{\text{mg/L}} = \rho_{s,\text{g/cm}^3} C_v \times 10^6 \quad (5.12)$$

Concentration by relative weight  $C_w$  is the sediment weight divided by the total weight of the water-sediment mixture:

$$C_w = \frac{\text{sediment weight}}{\text{weight of mixture}} = \frac{\gamma_s \text{Vol}_s}{\gamma_s \text{Vol}_s + \gamma \text{Vol}_v} = \frac{C_v G_s}{1 + (G_s - 1) C_v} \quad (5.13)$$

Concentration by relative weight is usually reported in units of parts per million (ppm) where  $C_{\text{ppm}} = C_w \times 10^6$ . For low concentrations there is little difference between mg/L and ppm; the difference exceeds 1 percent when concentration exceeds about 16,000 ppm for sediment having a specific gravity of  $G_s = 2.65$ . The following equation may be used to convert ppm into mg/L:

$$C_{\text{mg/L}} = \frac{G_s C_{\text{ppm}}}{G_s + (1 - G_s) 10^{-6} C_{\text{ppm}}} \quad (5.14)$$

The water: sediment ratio is frequently used to describe the volume of water required to remove a unit volume of sediments during flushing operations, in which case the eroded deposit volume includes both sediment grains and voids. To compute the average

mass concentration in the sediment-water mixture resulting from these operations, first compute concentration by volume [ $C_v$  from Eq. (5.10)], then compute mass concentration  $C_m$  from Eq. (5.11) using the dry bulk weight of the deposit instead of the specific weight of the solid sediment particles. Thus, for a deposit composed of sediment particles with a specific gravity of 2.65 and 30 percent voids, use a bulk weight of  $1.86 \text{ g/cm}^3$  rather than  $2.65 \text{ g/cm}^3$ . For a 25:1 water: sediment ratio with the water volume measured prior to mixing with sediment, compute  $C_v = 1/(25 + 1) = 0.038$  and  $C_m = 71,500 \text{ mg/L}$ .

### 5.4.3 Density of Water-Sediment Mixtures

The density of a sediment-water suspension is greater than the density of water alone and may be computed by the following equation:

$$\rho_{\text{mix}} = C_m + \rho \left( 1 - \frac{C_m}{\rho_s} \right) \quad (5.15)$$

where  $\rho_{\text{mix}}$  = density of mixture,  $C_m$  = sediment concentration by mass in the mixture,  $\rho_s$  = sediment density, and  $\rho$  = liquid density. Express all quantities in consistent units of mass per unit volume (e.g.,  $\text{g/cm}^3$ ,  $\text{kg/m}^3$ ). Example: for a suspended solids concentration of  $32,100 \text{ mg/L}$  ( $= 0.0321 \text{ g/cm}^3$ ), with  $\rho_s = 2.65 \text{ g/cm}^3$ , and  $\rho = 1 \text{ g/cm}^3$ , the density of the mixture is  $1.020 \text{ g/cm}^3$ .

## 5.5 SETTLING VELOCITY OF SEDIMENT GRAINS

---

Settling velocity is a primary determinant of sediment behavior in a fluid. A sediment particle can be transported in suspension only if its settling velocity is less than the vertical component of hydraulic turbulence. Settling velocity is also a primary determinant of the percentage and grain size of the inflowing load that becomes trapped in a reservoir, and the pattern of sediment distribution along the length of a reservoir. The fall velocity of sediment particles depends on characteristics such as size, shape, and density, and also on fluid characteristics such as temperature, salinity, and sediment concentration which affect both the fluid density and viscosity. To make comparisons between the intrinsic sedimentation properties of particles, without differences imposed by the fluid, the standard fall velocity is computed as the average rate of descent for a particle falling alone in quiescent distilled water at  $24^\circ\text{C}$ . The standard fall diameter of a particle is the diameter of a sphere having the same specific weight and the same standard fall velocity as the given particle (Interagency Committee, 1957).

### 5.5.1 Fluid Viscosity

Viscosity is a measure of fluid resistance to deformation. Higher-viscosity fluids have Greater shear strength and are more resistant to deformation, causing particles to fall more slowly in media such as oil, seawater, and cold water, as compared to lower-viscosity warm fresh water. Shear  $\tau$  in a fluid is proportional to the velocity gradient  $du/dy$  at a given point:

$$\tau = \mu \left( \frac{du}{dy} \right) \quad (5.16)$$

where  $\mu$  = dynamic viscosity. The unit of dynamic viscosity, also termed absolute viscosity or simply viscosity, is the Pascal-second ( $\text{Pa}\cdot\text{s} = \text{N}\cdot\text{s}/\text{m}^2 = \text{kg}/\text{m}\cdot\text{s}$ ), defined as a shear stress of 1 Pa ( $1 \text{ N}/\text{m}^2$ ) developed in a homogeneous medium, in laminar flow, between two plane layers 1 m apart and moving at a relative velocity of 1 m/s. In the cgs system the poise (P) is the unit of dynamic viscosity and may be converted to SI units as follows:  $1\text{P} = 10^{-1} \text{ Pa}\cdot\text{s}$ . Kinematic viscosity  $\nu$  is equal to the dynamic viscosity divided by the fluid density:

$$\nu = \frac{\mu}{\rho} \quad (5.17)$$

Kinematic viscosity has units of  $\text{m}^2/\text{s}$ . Liquid viscosity decreases as temperature increases, as shown in Table 5.2. The dynamic viscosity  $\mu$  of water in units of  $\text{Pa}\cdot\text{s}$  at temperature  $T$  in kelvin can be estimated within about 1 percent from the following equation (White, 1979):

$$\ln\left(\frac{\mu}{\mu_o}\right) \approx -1.94 - 4.80\left(\frac{T_o}{T}\right) + 6.74\left(\frac{T_o}{T}\right)^2 \quad (5.18)$$

where  $T_o = 273.16^\circ\text{K}$  ( $0^\circ\text{C}$ ) and  $\mu_o = 0.001792 \text{ kg}/(\text{m}\cdot\text{s})$ .

**TABLE 5.2** Physical Characteristics of Water as a Function of Temperature

	Temp, °C							
	0	5	10	15	20	25	30	40
Viscosity or dynamic viscosity ( $\mu$ , $10^{-3} \text{ Pa}\cdot\text{s} = 10^{-3} \text{ N}\cdot\text{s}/\text{m}^2$ )	1.781	1.518	1.307	1.139	1.002	0.890	0.798	0.653
Kinematic viscosity ( $\nu$ , $10^{-6} \text{ m}^2/\text{s}$ )	1.785	1.519	1.306	1.139	1.003	0.893	0.800	0.658
Density of pure water ( $\rho$ , $\text{kg}/\text{m}^3$ )	999.8	1000.0	999.7	999.1	998.2	997.0	995.7	992.2
Specific weight of pure water ( $\gamma$ , $\text{N}/\text{m}^3$ )	9805	9807	9804	9798	9789	9777	9764	9730

### 5.5.2 Reynolds Number

The Reynolds number  $Re$  indicates the ratio of inertial forces to viscous forces and determines whether hydraulic forces at the particle boundary which resist sediment motion are laminar or turbulent. Different equations are applicable in each case. Laminar flow occurs when the fluid viscosity significantly affects flow, such as the low velocity flow through porous media and the settling of small (silt and clay) particles. The Reynolds number is used as the criterion for differentiating between the laminar and turbulent flow range, and its value is expressed as a function of fluid velocity  $V$ , a characteristic length  $D$ , and kinematic viscosity  $\nu$ :

$$Re = \frac{VD}{\nu} \quad (5.19)$$

Different characteristic lengths are used with different hydraulic sections, and thus the absolute values of Re associated with the transition from laminar to turbulent flow also vary depending on the characteristic length used. For discrete particles settling in a fluid, the particle Reynolds number is computed as

$$\text{Re} = \frac{\omega d}{\nu} = \frac{\rho \omega d}{\mu} \quad (5.20)$$

where the characteristic length is the particle diameter  $d$ , the terminal velocity of the particle relative to the fluid is  $\omega$ , and fluid density is  $\rho$ .

### 5.5.3 Settling Velocity of Silts and Clays

The settling velocity of silts and clays falls in the laminar range. Terminal fall velocity ( $\omega_t$ ) of fine sediment varies directly with the difference in specific weights of the sediment and the fluid, and the square of the particle diameter, as given by Stokes' equation:

$$\omega_t = g \frac{d^2(\rho_s - \rho)}{18\mu} \quad (5.21)$$

This corresponds approximately to a particle Reynolds number less than 1. Stokes' equation predicts the terminal velocity for discrete particles large enough to overcome Brownian motion, with smooth rigid boundaries, approximately spherical in shape, and settling at a uniform velocity in a quiescent fluid where fluid viscosity is the only force resisting the falling particle. The settling diameters of small particles as determined from column settling tests are computed from the observed fall velocity and Stokes' equation. This procedure determines the sedimentation diameter of small particles, normally the parameter of interest in transport studies, rather than their true size or shape. From Stokes' equation, the settling velocity for the largest-size silt particle ( $60 \times 10^{-6}$  m) can be computed as  $3.2 \times 10^{-3}$  m/s in water at  $20^\circ\text{C}$  where  $\mu = 1.007 \times 10^{-3}$  kg/(m•s) and  $(\rho_s - \rho) = 1.65 \times 10^3$  kg/m<sup>3</sup>. The particle Reynolds number for this condition may be computed as 0.5.

### 5.5.4 Settling Velocity of Coarse Grains

The fall velocity  $\omega$  of a sphere over the full range of Reynolds numbers may be expressed as a function of the drag coefficient  $C_D$ , gravitational constant  $g$ , particle diameter  $d$ , and specific weight  $\gamma$  by:

$$\omega^2 = \frac{4gd}{3C_D} \left( \frac{\gamma_s - \gamma}{\gamma} \right) \quad (5.22)$$

For laminar flow, the drag coefficient is given by  $C_D = 24/\text{Re}$ , and in this range settling velocity is not greatly affected by particle shape. However, in the turbulent range the drag coefficient cannot be expressed analytically and the settling velocity must be determined experimentally. Figure 5.10 may be used to determine the fall velocity of coarse sediment.

### 5.5.5 Simplified Equations for Fall Velocity

Rubey (1931) developed an equation to estimate terminal fall velocity over the full range of particle diameters, which may be expressed in the following form:

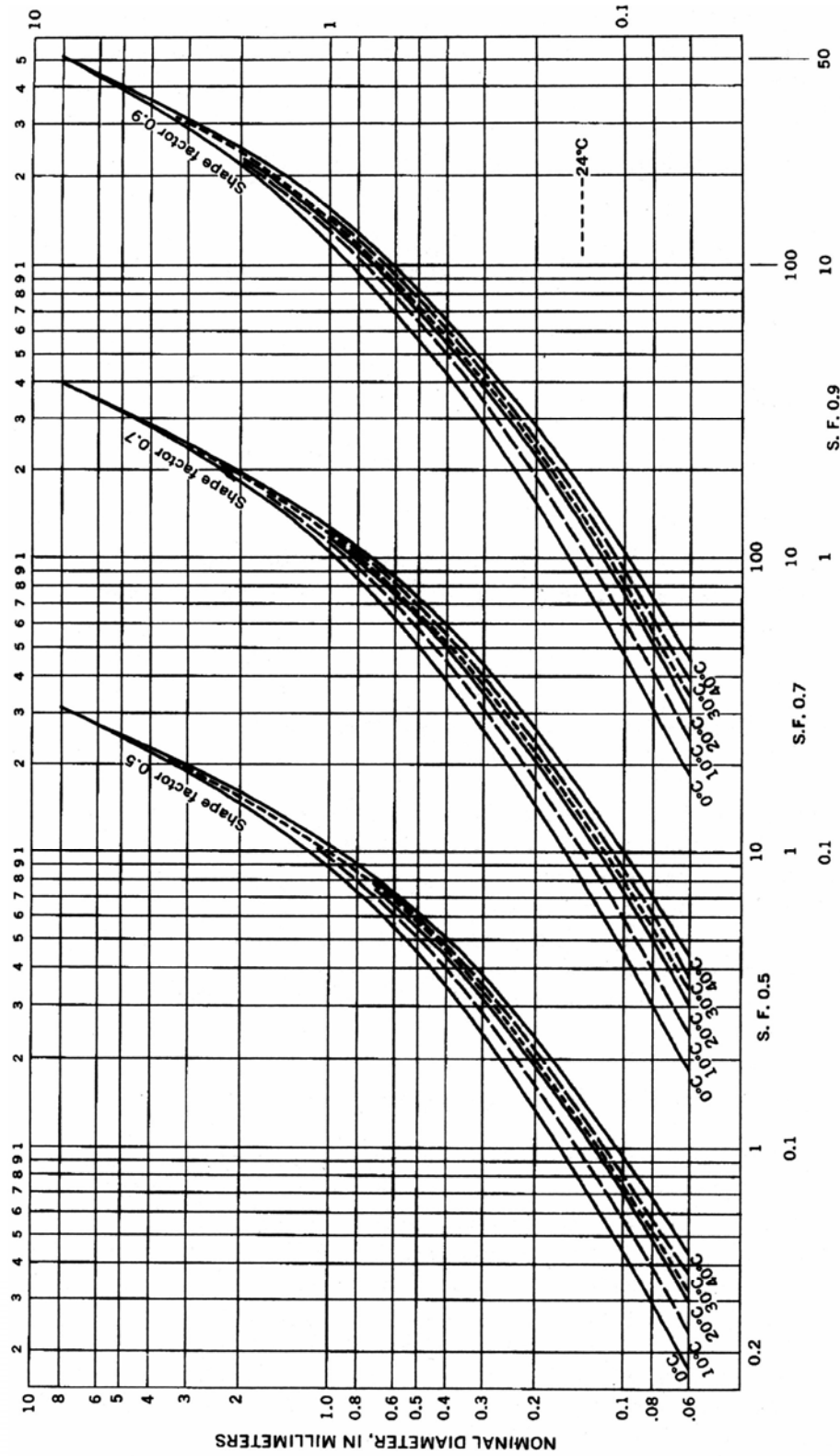


**FIGURE 5.10** Settling velocity of natural sands (Guy, 1969).

$$\omega = \frac{[1636(\rho_s - \rho)d^3 + 9\mu^2]^{0.5} - 3\mu}{500d} \quad (5.23)$$

where  $\omega$  = terminal fall velocity, m/s;  $\rho_s$  and  $\rho$  = density of sediment and water respectively, kg/m<sup>3</sup>;  $\mu$  = viscosity or dynamic viscosity, (N•s)/m<sup>2</sup>, and  $d$  = particle diameter, m. This equation is best used in a programmable calculator. The following is an example computation for  $d = 1$  mm at 20°C.

$$\begin{aligned} \omega &= \frac{[1636(2650 - 1000)(0.001)^3 + 9(1 \times 10^{-3})^2]^{0.5} - 3(1 \times 10^{-3})}{500(0.001)} \\ &= \frac{(0.00270 + 0.00001)^{0.5} - 0.00300}{0.5} = 0.098 \text{ m/s} \end{aligned}$$

Values of viscosity are given in the appendixes.

For grain diameter  $d$  greater than 2 mm, the fall velocity can be approximated by the following equations:

$$\omega = 3.32d^{0.5} \quad \omega \text{ in m/s, } d \text{ in mm} \quad (5.24)$$

$$\omega = 6.01d^{0.5} \quad \omega \text{ in ft/s, } d \text{ in ft} \quad (5.25)$$

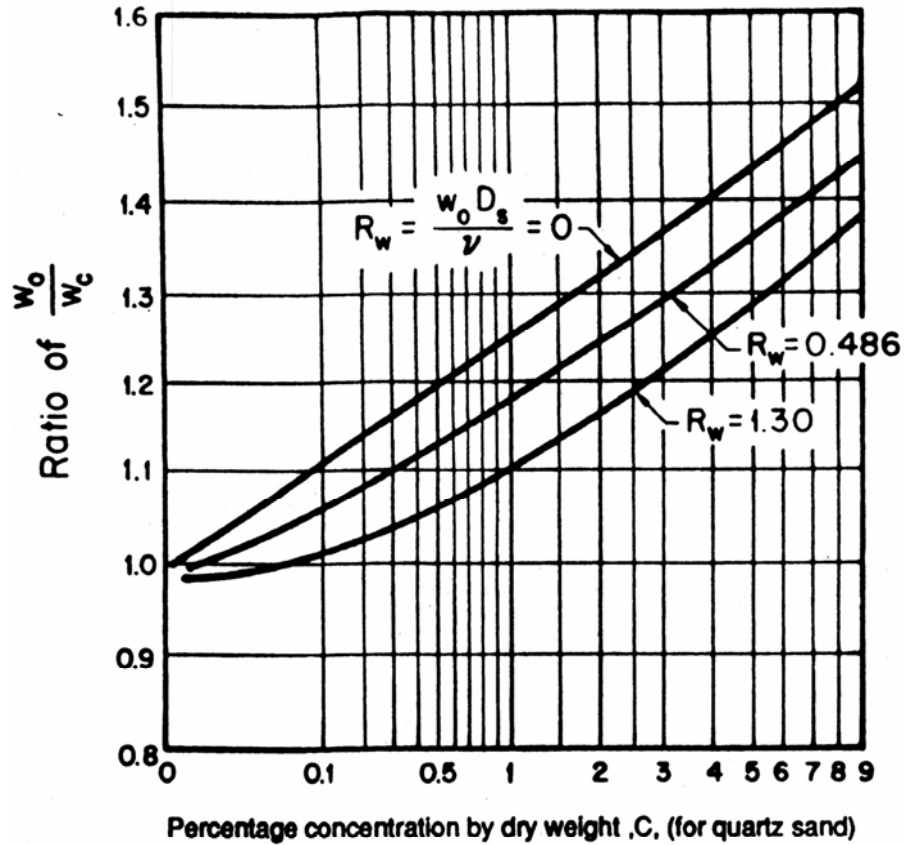
where  $\omega$  = terminal fall velocity of the particle (Yang, 1996). For water, changes in viscosity (temperature) have a negligible effect on the fall velocity of particles in this size range.

### 5.5.6 Effect of Concentration on Settling Velocity

If suspended sediment is dispersed throughout the water column, sediment particles will settle more slowly than in clear water, and the settling rate is said to be *hindered*. The decrease in fall velocity caused by an increase in sediment concentration may be estimated from Fig. 5.11 (McNown and Lin, 1952), which shows the ratio of particle settling velocity  $\omega_0$  in clear water to the settling velocity  $\omega_c$  for sediment concentrations up to 9 percent by weight, and for Reynolds numbers less than 1.3 (i.e., laminar flow). These curves are based on laboratory experiments of quiescent settling of sediments not affected by flocculation and may not be directly applicable to field conditions.

### 5.5.7 Sweep Flocculation and Hindered Settling

Particles settling through the water column can agglomerate into flocs as the larger and faster-settling particles sweep downward, overtaking and entraining the smaller ones. Through this process the settling velocity can increase over time as a result of floc growth. Similarly, if sediment concentration increases with depth because of the settling of sediment from above, the settling velocity can become increasingly hindered with depth by the higher concentration. In either case, the settling velocity will be variable over time. McLaughlin (1959) devised a method to measure the average settling velocity, and to also determine whether settling is hindered or accelerated by floc growth. This method only measures the growth of sweep floc due to sedimentation. It does not provide information on the extent of flocculation that exists before the test begins. Although the procedure is outlined as a laboratory test, it might also be adapted to field measurements in a reservoir, without interferences such as density currents.



$w_0$  = Settling velocity in  
a clear fluid

$w_c$  = Velocity in suspension  
of concentration (C)

FIGURE 5.11 Effects of suspended solids concentration on the fall velocity of sediment in water (McNowen and Lin, 1952).

**Error! Bookmark not defined.** Consider sediment in a settling column (Fig. 5.12a). Sediment flux in the vertical ( $z$ ) direction is  $\bar{w} C$ , where  $\bar{w}$  is the local instantaneous mean sediment settling velocity and  $C$  is the local instantaneous sediment concentration. Consider a thin slice of water within the cylinder and a small time step. Continuity of mass across this slice requires that the change in the rate of sediment flux, the difference between the amount of sediment falling into the slice from above less that falling out the bottom of the slice, must equal the change of sediment concentration within the slice. This may be expressed as

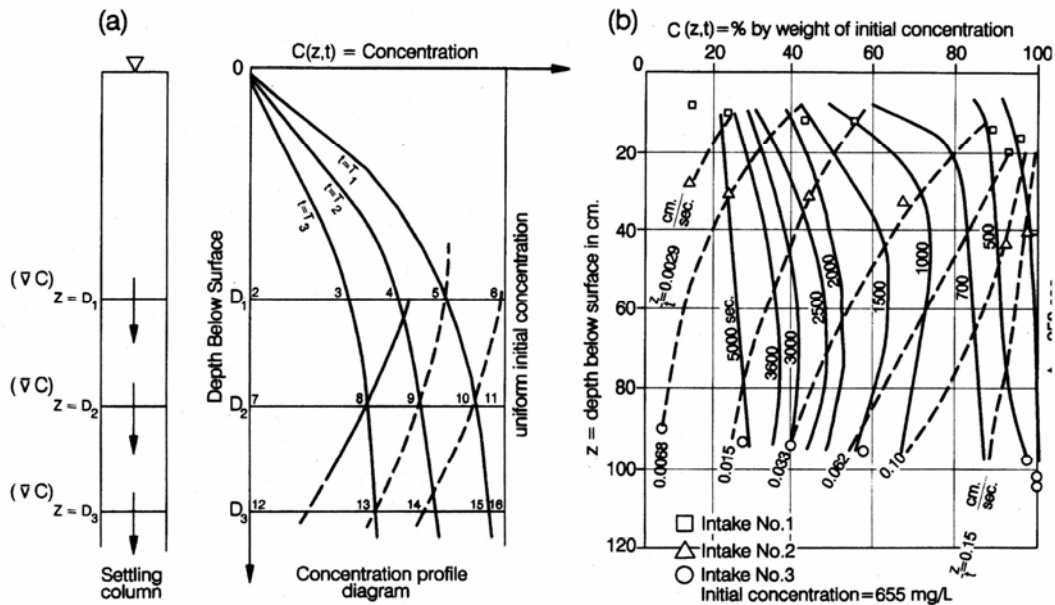


**FIGURE 5.12** (a) An idealized settling column with three measurement locations is shown on the left. The right shows a concentration profile diagram in which instantaneous concentration profiles are shown as solid lines, and lines of constant settling velocity are dashed. (b) Concentration profile diagram for bentonite clay and alum in water (after McLaughlin, 1959).

$$\frac{\partial C}{\partial t} + \frac{\partial(\bar{w}C)}{\partial z} = 0 \tag{5.26}$$

This relationship may be rearranged as:

$$(\bar{w}C)_{z=D} = - \int_0^D \frac{\partial C}{\partial t} dz = - \frac{\partial}{\partial t} \int_0^D C dz \tag{5.27}$$

and in this form it can be used to calculate  $\bar{w}$ , the mean settling velocity of the suspension.

The experimental apparatus consists of a settling column from which a sequence of samples are removed by pipet or withdrawal ports at different levels. The sample is agitated at time  $t = 0$  so that it has a uniform initial concentration equal to 100 percent of the mean sample concentration. At subsequent points in time, the concentration at the surface is taken as zero and the concentration at different depths is measured by withdrawing samples. These samples may be extracted from all levels simultaneously at times  $t_1, t_2,$  and  $t_3$ , thereby creating concentration profiles  $T_1, T_2,$  and  $T_3$  (Fig. 5.12a), or they may be extracted at different points in time and the concentration profiles at different points in time determined by interpolation (Fig. 5.12b). In the concentration profile diagram, solid lines show the concentration profile at different moments in time, and dashes indicate lines of equal settling velocity. Because the liquid volume is being reduced, for each sample the adjusted depth is recorded and the average settling velocity  $z/t$  computed. Dashed isovelocity lines are then interpolated. An experiment performed by McLaughlin using alum and bentonite clay in a 1.2-m-tall cylinder with three withdrawal ports produced the concentration profile diagram shown in Fig. 5.12b. If this settling rate of the sediment is neither hindered nor accelerated by flocculation, the dashed isovelocity lines will be vertical. If flocculation causes the settling rate to increase, the dashed isovelocity lines will slope toward the left, but if settling is hindered

they will slope to the right. In Fig. 5.12b flocculation is the predominant effect.

To compute settling velocity at any depth, such as  $z_i$  in Fig. 5.12a, the areas defined by the polygons 025, 024, and 023 are calculated and the values plotted against times  $t_1$ ,  $t_2$  and  $t_3$ , respectively. If this is performed for a sufficient number of concentration profiles at a given depth, a smooth curve will result, the slope of which at any point in time is the right side of Eq. (5.27). Since the concentration is known from the diagram, the fall velocity can be computed as a function of time. Such a plot is presented in Fig. 5.13, corresponding to the concentration profile diagram in Fig. 5.12b. In this sample, settling velocity increased with time, peaked simultaneously at all depths, then decreased.

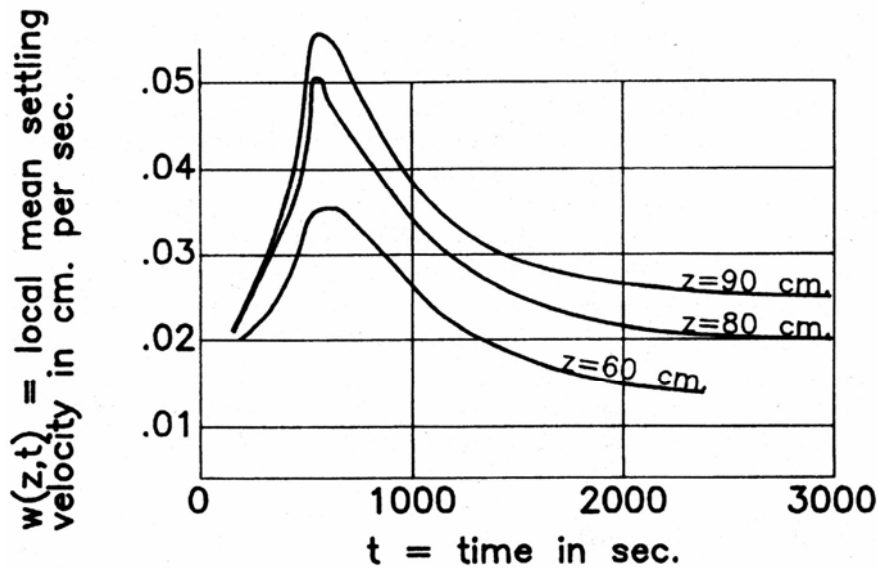


**FIGURE 5.13** Local mean settling velocity as a function of time for bentonite clay and alum in water (McLaughlin, 1959).

## 5.6 LABORATORY AND FIELD ANALYSIS OF SEDIMENT CONCENTRATION

Streambeds in hilly or mountainous areas often contain beds consisting of gravel, cobbles, and boulders. These are termed gravel-bed streams, even though the grains may be larger than gravel size. It is usually neither practical nor necessary to transport large-diameter sediments from gravel-bed streams to the laboratory, and sediment larger than about 0.5 cm is normally sized in the field by direct measurement, as described in Sec. 8.8 and 8.9.

The total suspended sediment concentration in a sample, including both coarse and fine sediment, may be determined by filtration, evaporation, or specific gravity. All methods will measure both the organic and inorganic fractions unless they are previously separated. In eutrophic systems, organisms and organic matter suspended in the water column may contribute significantly to the suspended sediment if solids concentrations are very low.

### 5.6.1 Filtration Method

In the filtration method, the water sample is passed through a preweighed filter, such as a

glass fiber filter in a Gooch crucible. The filter containing the sediments is then oven-dried, cooled in a desiccator, and weighed. Sediment weight is computed as the final less the original (tare) weight. Filtration has the advantage of eliminating the need to compensate for dissolved solids in the water, and it can also be more rapid than the evaporation method. However, filter media will quickly become clogged if more than several hundred milligrams per liter of fines is present.

### 5.6.2 Evaporation Method

In the evaporation method, the sample is first allowed to settle to the bottom of the sample bottle. Settling time depends on the nature of the sediment; for clays, settling may require weeks and small amounts of flocculant may have to be added. Samples should settle in the dark to prevent biological growth. After settling, the supernatant is discarded and the residual aliquot of native water (usually about 20 to 50 mL) is poured into an evaporating dish, and distilled water is used to rinse the remaining sediment. After the water is evaporated without boiling, the dry sample is heated to 110°C for at least 1 h, then cooled in a desiccator and weighed. A correction for dissolved solids should be made in waters high in dissolved solids or low in suspended solids. The weight of dissolved solids is determined by evaporating a sample aliquot of settled or filtered water. If dissolved solids constitute a significant percentage of the total solids in the sample, a correction should be made. In environments having relatively stable dissolved solids levels, using a constant-volume aliquot of native water in all samples that are evaporated produces a constant correction factor.

### 5.6.3 Specific Gravity Bottle

With the specific gravity of water known as a function of temperature, the sediment content in a sample can be measured as the difference between the weight of clear native water (not distilled water), and of the sample when weighed in a specific gravity bottle. This method has the advantage of providing almost instantaneous values of sediment concentration because it does not require sample desiccation. It is therefore well-suited for field monitoring during operations such as reservoir flushing. It can be used with any size of sediment. The tare weight of each bottle should be recorded when it is filled with clear native water, all bubbles must be carefully eliminated from within the stoppered bottle, and the bottle exterior must be carefully dried before weighing. For field use, the balance must be placed in an area completely unaffected by vibration, such as may occur in machinery buildings. Because this method measures the small differences in weights between 100 mL of clear water and the same volume of turbid water, contained in a bottle weighing about 40 g, it is best used for sediment concentrations exceeding 250 mg/L.

### 5.6.4 Sediment Volume

In streams where most or all sediments are sands, the sediment can be settled in an Imhoff cone, and the sediment content expressed as milliliters per liter. This method is useful in monitoring sediment release events because results can be obtained after short settling time, on the order of 1 min. However, this method requires that a calibration curve be constructed for each site where this method is used, to develop a relationship between settled sediment volume and sediment mass. During every event when this method is used, several samples should be collected and analyzed in a laboratory to confirm the original calibration. Because the grain size distribution can change significantly over the course of an event, it is also important that samples be taken at different periods as the calibration curve may shift during an event. In addition to speed, this method has the advantage of simplicity in equipment and procedure.

### 5.7 LABORATORY ANALYSIS OF SEDIMENT SIZE

Particle size analysis is required to determine the settling and transport characteristics of both suspended and deposited sediments. The laboratory sequence for size analysis of sediment samples is summarized in Fig. 5.14, and the applicability of various techniques for size classification are summarized in Table 5.3. The type of analysis to be performed depends on the amount of sediment available and the grain size limits.

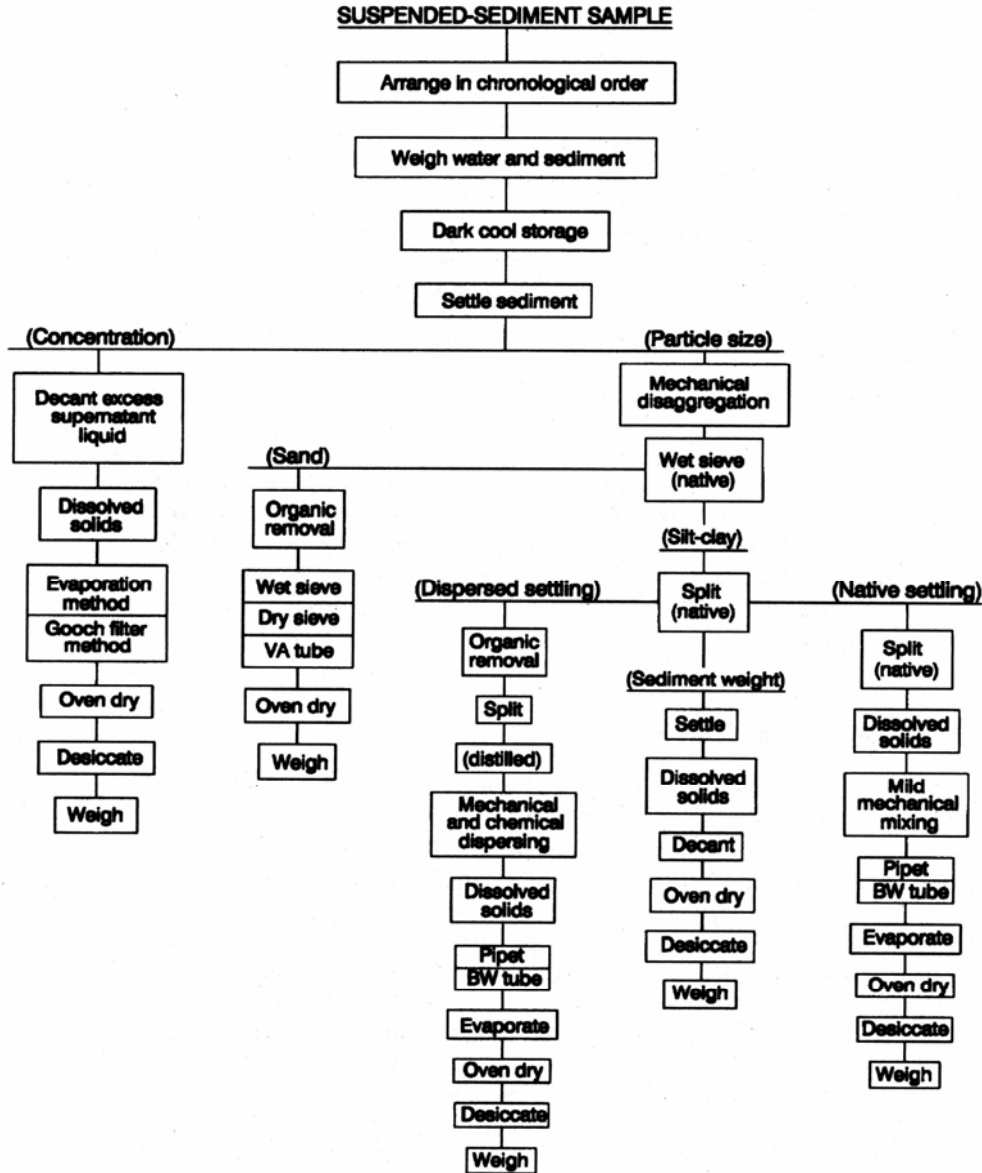


FIGURE 5.14 Generalized flow diagram for concentration and grain size analysis of suspended sediment samples. These procedures may be modified as appropriate for sample characteristics and study requirements (Guy, 1969).

**TABLE 5.3** Application Range for Sediment Test Methods for Grain Size Analysis

Method	Size range, mm	Sample size, mm	Concentration range, g/L
Direct measurement	>5	Single grains	--
Immersion	>5	Single grains	--
Sieves	0.062 - 32	>0.05	--
Pipet	0.002 – 0.062	2-5	2.0 – 5.0
VA Tube*:	0.062 – 2.0		--
L = 120, D = 2.1	0.062 – 0.25	0.05 – 0.8	--
L = 120, D = 3.4	0.062 – 0.40	0.4 – 2.0	--
L = 120, D = 5.0	0.062 – 0.60	0.8 – 4.0	--
L = 120, D = 7.0	0.062 – 1.0	1.6 – 6.0	--
L = 180, D = 10.0	0.062 – 2.0	5 – 15	--
BW tube †	0.002 – 0.062	0.5 – 1.8	1.0 – 3.5
Hydrometer	0.002 – 0.062		>30

\* L = tube length, D = tube diameter, cm. Size ranges are given as sieve diameters.

† May be extended to the range of 0.03-0.35 mm by increasing the concentration in the tube up to 10 g/L, with higher concentrations tending to give more accurate results. For sizes over 0.25 mm, results of the first withdrawal for the fastest-settling particles become erratic, and are undependable for diameters over 0.35 mm.

‡ Depends on hydrometer.

*Source:* Adapted from Guy (1969).

Suspended sediment samples may contain less than a gram of sediment whereas deposit samples may contain hundreds of grams of material for sizing. Samples having both coarse and fine sediments must be split and analyzed using two methods, such as sieve-pipet, VA tube-pipet, or BW tube-VA tube. (VA stands for visual accumulation; BW stands for bottom withdrawal.) Guy (1969) provides a detailed description of sediment laboratory techniques.

### 5.7.1 Use of Deflocculants

Fine silts and clays may occur in nature either in dispersed or flocculated forms, and the tendency for riverine sediments to flocculate may vary as a function of season or stage. Sedimentation studies typically require information on the settling velocity in natural waters, and the use of a deflocculant and distilled water can give very misleading results by producing a grain size classification much finer, and sedimentation velocities much slower, than occur in native water. In sedimentation and transport studies it is generally inappropriate to use a deflocculant to characterize suspended sediments, since the analysis seeks to determine the settling characteristics of the sediment in the reservoir with natural water and not the exact size of individual grains. When clays naturally occur in a flocculated state and have settling velocities more typical of fine silts, it is necessary to use this higher settling velocity in sedimentation modeling. On the other hand, substances such as pesticides and nutrients such as phosphorus are adsorbed largely on to clay particles because of their high surface area. Knowledge of the clay fraction in suspended or deposited material, independent of its settling velocity, can be important for tracking environmentally reactive substances. Thus, in some types of studies, information on both the sedimentation size of the flocculated particles and the size of their component grains can be important. In every case, it is essential to state whether or not a deflocculant was used in the sizing of fines, and split samples should be run with

and without a deflocculant to determine the importance of flocculation. In analyzing the settling velocity of sediment mixtures in the natural state, native water should be used for the settling test and in all intermediate steps (such as wet sieving); use of distilled water can significantly alter flocculation mechanisms and settling characteristics.

### 5.7.2 Organic Material

Suspended organic material including algae may be present in suspended sediment samples. The organic component of a sediment sample may be determined as loss on ignition, which represents the difference between the weight of the oven-dried sample and the weight after organics are volatilized at 500°C in a muffle furnace. Organic matter may also be oxidized within a water sample by the addition of a 6 percent solution hydrogen peroxide at the rate of approximately 5 mL per gram of dry organic matter contained in a 40-mL aliquot of water. Stir, cover, and allow to sit. When the reaction nears completion, heat to 93°C and stir, adding more hydrogen peroxide if necessary to complete the reaction (Guy, 1969). This procedure will influence results when the settling rates of fines are to be measured in native water, since organics can influence flocculation.

### 5.7.3 Separation of Sand and Fines by Sedimentation

The coarse and fine fractions may be separated by the sedimentation method in which the sample is introduced into the top of a sedimentation tube. After a time interval sufficient for all the particles greater than 0.062 mm in diameter to reach the bottom, computed from Stokes' equation on the basis of fall depth and water temperature, the settled portion of the sample may be withdrawn and analyzed in a VA tube and the remainder by the pipet method. Simple sedimentation will not give sharp separations between fine sand and coarse silts, and silts and clays can settle rapidly as a turbidity current within the column. Multiple sedimentation separations may be required to overcome these problems. An alternative method, wet sieving, may be used.

### 5.7.4 Dry Sieving

The grain size distribution of sands and gravels is normally determined by mechanically sorting a representative sample using sieves. The sieve diameter approximates the nominal grain diameter. Larger-diameter sieves [203 mm (8 in)] and mechanical vibrators are normally used to sort large-volume samples, but smaller sieves [e.g., 76-mm (3-in) diameter] are more appropriate for small sample volumes such as those obtained from suspended sediment sampling. The analysis requires a balance having a sensitivity equal to 0.1 percent of the total sample weight. Sieves are arranged with the coarsest size on top, and the dry sample is passed through the stacked sieves by mechanical agitation for a minimum of 5 min by a combination of rotational and jarring action, but the sediment is never manipulated by hand. After agitation, all the sediment retained on each sieve is removed, including grains trapped in the wire mesh. The weight of the sediment passing the finest sieve is weighed first, and then the sediment retained on each successive sieve is added to the first and weighed. The resulting cumulative weights are converted into percent of total weight and then plotted to produce the grain size distribution curve.

If the sample size is too large, one or more of the sieves will become overloaded, inhibiting the passage of fines through the mesh and producing an erroneously coarse distribution. Samples too large for sieving may be reduced by commercially available sample splitters or the quartering method (Fig. 5.15). The split must be performed on the entire sample volume collected in the field to obtain an accurate subsample, since agitation during transport and handling sorts the grains by size within storage containers. Sample splitting can be a source of significant error and must be performed carefully.

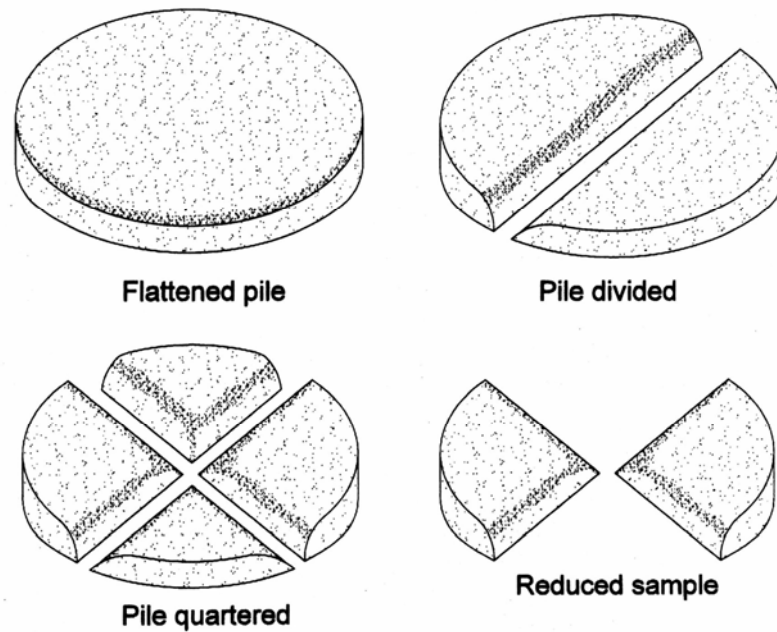


**FIGURE 5.15** Quartering method for splitting a dry sample (after Driscoll, 1986).

### 5.7.5 Wet Sieving

When appreciable fines are present it will be necessary to split the fines from the coarser material, then use different methods to size each fraction. Dried samples containing mixtures of sand and fines can form hard clumps, making the sample unsuitable for dry sieving. In this case wet sieving can be used to separate the fine and coarse particles and to size-classify the latter. All sieves are washed with a wetting solution, rinsed, then immersed in a shallow water-filled container so the screen is about 0.5 cm below the water, taking care that no air remains trapped, and if necessary breaking the surface tension at one corner of the screen by blowing through a straw to allow the release of trapped air. The sample is passed through one sieve at a time, starting with the coarsest mesh. The material passing each screen is captured in the container and applied to the next smaller screen, and the material retained is dried and weighed. This procedure continues to the 0.062-mm screen, and the fines passing this sieve are analyzed separately. If total sand is less than 20 percent of the sample, wet sieving can be accomplished by using a gentle jet of water to wash the sample through a set of stacked sieves (Guy, 1969).

### 5.7.6 Direct Measurement of Nominal Diameter

The nominal diameter of larger grains may be determined by immersion into a cylinder with a volumetric scale. The cylinder diameter should not exceed twice the grain diameter. Compute nominal diameter from the displaced volume and the equation for the volume of a sphere:  $V = (4/3) \pi r^3$ , or  $d = (6V/\pi)^{1/3}$

### 5.7.7 Visual Accumulation Tube

The visual accumulation (VA) tube method provides a fast, economical, and accurate method of determining the fall velocity (and thus the sedimentation diameter) of sand size sediments. Unlike sieves, which measure particle physical dimensions from which hydraulic properties must be computed, the VA tube measures fall velocity directly. The sand should be separated from the finer material by wet sieving or sedimentation, and the fine fraction of the sample sized by the piper method. In the VA tube analysis, all sediments are introduced simultaneously at the top of the water column and become stratified within the column according to differences in fall velocity. Grains reaching the bottom at any instant are of the same sedimentation size, and the size gradation is based on the standard fall diameter. Taller and larger-diameter tubes are required to analyze larger-volume samples containing larger-diameter grains. The accumulation depth of sediment at the bottom of the tube is monitored visually, recorded, and graphed to determine the amount of sediment as a function of sedimentation diameter.

### 5.7.8 Pipet Method

Sediments smaller than 0.062 mm may be size-classified by the pipet method. This method determines the concentration of a suspension at a series of predetermined depths as a function of settling time. A pipet is used to withdraw water at intervals from about 30 s to 3 h (depending on water temperature), and the solids concentration from each sample is determined by evaporation. Larger, faster-settling particles pass beyond the sampling point, and the maximum sedimentation diameter of each sample is determined from Stokes' law. When sand-size particles are present in the sample, they are separated by wet sieving, then mechanically classed by dry sieving.

### 5.7.9 Bottom Withdrawal Method

The bottom withdrawal (BW) tube method is normally used to measure fines, but can measure sands up to 0.35 mm in diameter if a higher initial sediment concentration is used in the tube. For analyzing a large number of samples, the pipet method is less time consuming and possibly more accurate than the BW method (Guy 1969). The BW tube method is based on drawing volumes of water from the bottom of an 80- or 100-cm column of water-sediment mixture at intervals over a period up to about 8 h, with the duration of the test and withdrawal intervals dependent on water temperature (viscosity) and size distribution in the sample. Each withdrawal represents the amount of sediment in a given sedimentation diameter class. The withdrawn samples are transferred to evaporating dishes, dried, weighed, and used to size-classify the sample.

### 5.7.10 Hydrometer

A hydrometer may be used to determine the grain size distribution of fine-grained sediment. Because a large sample size is required, it is suitable for size-classification of samples of bottom sediments, or of suspended sediments at high concentrations (greater than 30,000 mg/L). In this test, about 50 g (dry weight) of sediment is placed into a 1-L sedimentation cylinder and intensely agitated for 1 min by inverting the stoppered cylinder back and forth once per second. Dry samples should initially be soaked 16 h in water prior to testing. Hydrometer measurements are read at intervals of 2, 5, 15, 30, 60, 250, and 1440 min following agitation. The hydrometer is carefully placed in the cylinder about 20 s prior to each reading and is removed immediately thereafter and cleaned by spinning in demineralized water. A correction for hygroscopic water is made by comparing air-dried to oven-dried (110°C) weights of a 20-g subsample of the material. The percentage of the total sample remaining in suspension, at the level at which the

hydrometer is measuring the density of the suspension, is calculated from equations specific to each type of hydrometer. Stokes' law is used to compute the sedimentation diameter corresponding to each reading.

---

## CHAPTER 6

---

# EROSION

---

Most sediments enter reservoirs as a consequence of rainfall erosion and subsequent transport by streams. Successful reduction of sediment yield requires accurate conceptual and quantitative models of the erosion and transport processes responsible for sediment delivery to the impoundment. Watershed management programs frequently fail to reduce sediment yield, despite large expenditures, because the physical nature of the problem is not properly diagnosed, or the economic and cultural conditions leading to accelerated erosion are not addressed and erosion control practices are abandoned as soon as subsidies are removed. Furthermore, because eroded sediments may be flushed downstream through stream channels over a period of decades or longer, it is essential to differentiate between the volume of material eroded from the land surface and the amount which is actually transported into the reservoir, the *sediment yield*. Both erosion and delivery processes must be understood to assess erosion impacts on downstream reservoirs.

Erosion processes have been intensively studied for many decades, with much of the original impetus for scientific erosion research arising from the dust bowl conditions in the midwestern United States during the 1930s. Today the computational tools for modeling soil erosion and related watershed processes are undergoing rapid change and enhancement, the product of decades of research combined with microcomputer technology. This chapter introduces basic erosion concepts and measurement techniques, outlines several modeling techniques available for estimating soil erosion, and describes the linkages between erosion and sediment yield. Sediment yield is addressed in Chap. 7, and erosion control practices are outlined in Chap. 12.

---

### 6.1 CONCEPTS AND DEFINITIONS

---

*Weathering* is the process of chemical and mechanical activity which causes rock to change in character, decay, and finally crumble into soil. Physical weathering involves particle fragmentation and may be caused by freezing and thawing, abrasion during transport, and biological activity. Chemical weathering involves dissolution of the earth's crust by water, and is accelerated when water is acidified by carbon dioxide released during respiration by plant roots and soil fauna. The rate of chemical weathering depends heavily on water availability and is slow and incomplete under arid conditions, leaving physical weathering to predominate. As a result, soils formed under arid conditions are more likely to be coarse-grained. Physical processes such as freeze-thaw cycles and glaciation also prevail in high mountains. Chemical processes are more important in humid regions, and clay soils predominate. Quartz is the most chemically stable mineral found in abundance in crustal rocks and is extremely resistant to dissolution by water. It is the primary constituent of most sands and their morphological counterparts such as streambeds and beaches

*Erosion* is the process whereby earth or rock material is loosened or dissolved and

removed from any part of the earth's surface. Whereas weathering involves only the breakdown of rock, erosion additionally entails the detachment and transport of weathered material from one location to another, denuding the earth's surface and delivering sediment to the fluvial system. Erosion rates are frequently measured on small fractional-hectare plots.

The landscape and associated fluvial transport system may be divided into zones where either erosive or depositional processes dominate (Fig. 6.1). Erosional processes predominate in mountainous environments while deposition predominates on floodplains, although both erosion and depositional processes occur simultaneously in virtually all environments. Thus, material eroded from mountain slopes may be deposited in alpine valleys, and floodplain deposits are eroded by stream channels.

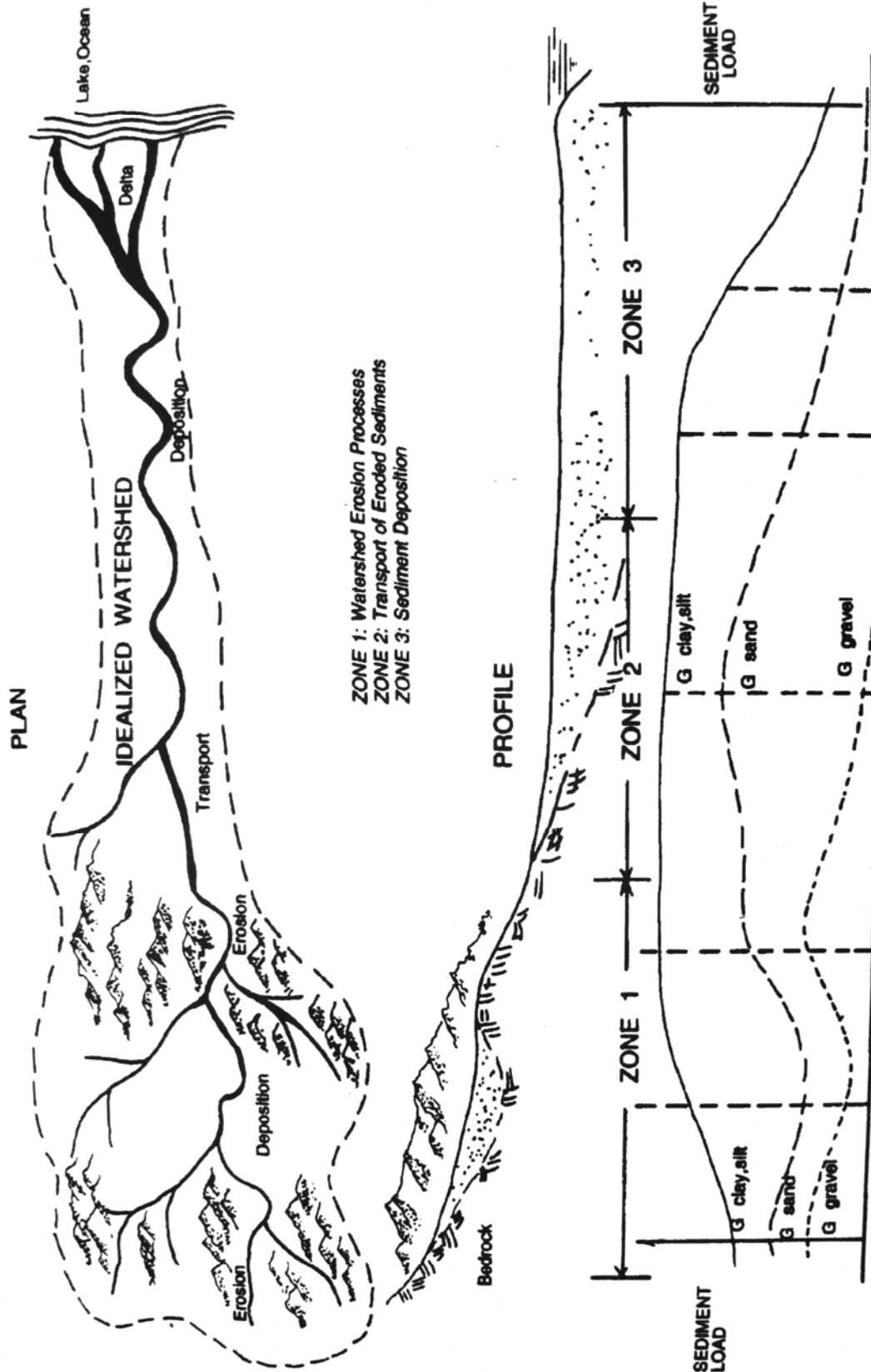
On a global scale and under natural conditions, the denudation of the earth's surface by the chemical solution of rocks by water and biological processes is more important than the mechanical erosion. In general, the long-term rate of soil formation may be considered to balance the natural or *geologic rate of erosion*. Human activity that eliminates protective vegetative cover, destroys the soil structure, and concentrates runoff so that gullying occurs can *accelerate erosion* by 2 or 3 orders of magnitude compared to the geologic rate of erosion. The *recovery period* is the time required for a disturbed site to become re-vegetated and stabilized, and return to erosion rates more typical of natural conditions.

*Sediment yield* is the amount of eroded sediment discharged by a stream at any given point. It represents the total amount of fluvial sediment exported by the watershed tributary to a measurement point, and is the parameter of primary concern in reservoir studies. Because much eroded sediment is re-deposited before it leaves a watershed, the sediment yield is always less than, and often much less than, the erosion rate within that same watershed. The ratio between the erosion rate and sediment yield is the *sediment delivery ratio*.

The susceptibility of a soil to erode is termed *erodability* and depends on the size and physical characteristics of the particles and the nature of the organic and inorganic materials that bind them together. The *erosive forces* acting on a soil are determined primarily by rainfall intensity, slope angle and length, and cover (e.g., vegetation) which protects the soil against direct raindrop impact.

Erosion may be classified according to the erosive agent (water or wind), the erosion site (sheet, rill, interrill, gully, channel), or the erosive process (e.g., raindrop, channel, mass wasting). *Interrill erosion* or *sheet erosion* is the detachment and transport of soil particles due to rainsplash and shallow prechannel flow. *Rill erosion* is the detachment and transport of soil particles by concentrated flow in small channels or rills not more than a few centimeters deep that are eliminated by normal cultivation techniques (Fig. 6.2). Interrill erosion delivers sediment to rills, which in turn discharge to gullies or channels. Both interrill and rill erosion have traditionally been treated as a single process, since most erosion plots measure the combined effects of both. However, interrill and rill erosion processes are quite distinct, as is the soil's resistance to each type of erosion. Measurements on 56 soils using simulated rainfall showed that rill and interrill erosion rates on the same soil for the same rainfall are poorly correlated, and recent research has been focused on separately determining interrill and rill erosion rates (Laften et al., 1991b). A gully is an erosional channel, usually ephemeral, too large to be removed by normal cultivation techniques or to be crossed by a wheeled vehicle.

*Gully erosion* and *channel erosion* may refer to either the gradual or the massive erosion of the beds and banks of gullies and stream channels. *Mass wasting* refers to erosion



DISTANCE ALONG RIVER

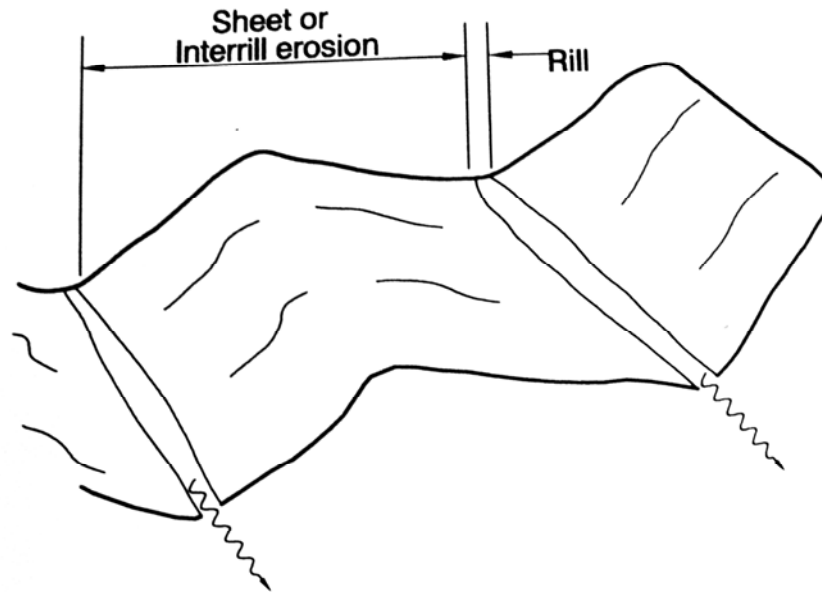


**FIGURE 6.2** Definition sketch of interrill or sheet erosion and of rill erosion.

associated with slope failures, including landslides and similar slope movements. *Wind erosion* refers to movement of soil particles by wind. Wind erosion may be important in arid or semiarid regions as an agent that can transport sediment from ridges into depressions from which it can subsequently be transported by runoff (Rooseboom, 1992).

*Total erosion* or *gross erosion* within a catchment is the sum of all types of erosion: interrill, rill, gully, channel, and mass wasting. The relative importance of different types of erosion varies from one area to another. Sheet and rill erosion normally predominate where the land surface has been denuded and disturbed, such as grazing and cropped lands and construction sites. Glymp (1957) compiled data from 113 U.S. watersheds, 0.25 to 1132 km<sup>2</sup> in area, and concluded that sheet and rill erosion accounted for 90 percent or more of the sediment yield in half of the watersheds. The 1977-79 national erosion inventory of nonfederal lands in the United States conducted by the Natural Resources Conservation Service estimated total erosion of  $4.8 \times 10^9$  t/yr by source, as summarized in Table 6.1. Erosion from large areas of federally owned range and forest lands, about 22 percent of the nation's land area excluding Alaska, are not included in the table, and streambank erosion includes the effect of naturally meandering streams. Although construction sites contribute only small amounts of the total erosion on a national scale, they can be locally very important because of their high erosion rate per unit of land area. In some areas gullying and channel processes account for most erosion, especially in loessial soils or in forested lands. Mass wasting is important in mountain areas, and in special cases piping can be important (Barendregt and Ongley, 1977). The 1992 natural resources inventory for the United States (Kellogg et al., 1994) estimated erosion rates on nonfederal lands nationwide on the basis of about 800,000 statistically

**TABLE 6.1** Erosion Sources on Nonfederal Lands in the United States, 1977-79

Erosion source	Percent of total erosion
Cropland	37.6
Rangeland	26.5
Streambank	10.6
Forest	8.3
Pasture	6.6
Gullying and streambed	5.7
Roads and roadsides	3.2
Construction sites	1.5

*Source:* Holeman (1981).

**TABLE 6.2** Land Use and Erosion Rates in the United States

Land use	Land area, 10 <sup>2</sup> km <sup>2</sup>		Erosion rate, t/km <sup>2</sup> /yr		Total erosion, 10 <sup>9</sup> t/yr	
	1982	1992	1982	1992	1982	1992
Sheet and rill erosion						
Cropland	1.704	1.547	920	690	1.568	1.067
Pastureland	0.554	0.510	240	220	0.133	0.112
Rangeland	1.655	1.614	220	220	<u>0.364</u>	<u>0.355</u>
Subtotal					2.065	1.534
Wind erosion						
Cropland	Same	Same	740	560	1.261	0.866
Pastureland	Same	Same	22	22	0.012	0.011
Rangeland	Same	Same	1054	986	<u>1.744</u>	<u>1.591</u>
Subtotal					3.017	2.468
Combined erosion						
					5.082	4.002

\*Excludes Alaska, includes Puerto Rico and U.S. Virgin Islands.

*Source:* Natural Resources Conservation Service (1995).

Selected sampling locations, where sheet and rill erosion was determined by the USLE model and wind erosion by the WEQ (Wind Erosion Equation) model (Table 6.2). Other types of erosion were not reported. About a 25 percent reduction in erosion rate was registered between 1982 and 1992, primarily from two causes: improved conservation practices on cropland and conversion of cropland to noncropland uses, including erodible land withdrawn under the Conservation Reserve Program which encourages farmers to plant grass or trees on highly erodible cropland through 10-yr contracts with the U.S. Department of Agriculture.

## 6.2 CONSEQUENCES OF SOIL EROSION

---

### 6.2.1 On-Site Impacts

Accelerated erosion creates adverse consequences at the site of soil loss and off-site impacts downstream. On-site impacts are related to reduced productivity on farm, grazing, and forest lands caused by loss of topsoil, reduction of soil depth, and soil crusting and sealing. Lal (1994) compiled "frightening" statistics from a variety of sources indicating that: soil erosion has cumulatively destroyed 430 million ha of productive land; 3 million ha of agricultural land is lost annually to erosion and another 2 million ha to desertification: the yield of rain-fed agriculture may decrease by 29 percent over the next 25 yr because of erosion. El-Swaify and Dangler (1982) called soil erosion the most serious form of land degradation throughout the world.

Erosion accelerates the loss rate of both nutrients and organics from the upper soil layer. Fines are eroded more rapidly than coarse material, and the loss of fines plus reduction in soil depth reduces soil moisture retention capacity. When raindrop impact breaks apart soil aggregates, dispersed clay particles can collect in cracks and pores in the soil matrix and as a thin (1- to 5-mm) layer on the soil surface that dries to a hard dense crust of very low porosity which greatly enhances runoff, even on gentle slopes. This seal can also physically inhibit seedling emergence and reduce oxygen transfer into the soil. Although the problem occurs in many areas of the world, it is most serious in the subhumid to semiarid tropics (Sombroek, 1985). Laboratory work by Morin et al. (1981) showed that the hydraulic conductivity of soil crusts can be 3 to 4 orders of magnitude smaller than the saturated hydraulic conductivity without soil sealing. Reduction in moisture availability due to physical changes in the soil structure and reduced infiltration is a primary cause of productivity declines in eroding soils.

In less developed countries, on-farm economic impacts of erosion tend to exceed off-site impacts. This reflects the lower level of downstream infrastructure development, less concern about water quality, and the heavy dependence of small farmers on natural levels of soil fertility. McIntire (1993) noted that, in less developed areas, the onset of significant erosion can lead to a pattern of rapid land degradation in which declining yields and vegetative cover lead to shortened fallow periods, overgrazing, and further erosion and land degradation.

### 6.2.2 Off-Site Impacts

Off-site erosion impacts include higher turbidity in rivers, lakes, reservoirs, and coastal waters and sediment deposition in these same environments and on floodplains. Reduction in soil infiltration due to erosion will also increase downstream runoff and flooding, and high sediment concentrations increase the cost of flood damages compared to clear water flooding. Aquatic ecosystems are heavily affected: sediment loads can clog spawning gravels, smother the benthos, and adversely affect estuarine and coastal ecosystems.

Off-site economic impacts tend to predominate in more developed countries because of the large amount of downstream infrastructure such as reservoirs and waterways that will be affected by sedimentation, plus adverse water quality impacts on water-based recreation. In the United States, where water-based recreation is a large economic activity, impairment of recreational use, and boating in particular, has been estimated to be the most important single off-farm economic component (Clark, 1985). For example, a survey of recreational boaters by Robertson and Colletti (1994) revealed that 45 percent of the respondents decreased their use of Red Rock Reservoir in central Iowa because of high turbidity, despite its lack of crowding compared to other area reservoirs. On-farm impacts in industrial countries are mitigated by the availability of fertilizer and other

inputs to offset erosion impacts on soil nutrient levels. Also, in industrialized countries crop production conservation techniques are well-developed and actively implemented. Production occurs on mechanizable soils with low slopes, and steep erodible slopes are not cultivated.

Several issues associated with the economic evaluation of erosion impacts have been reviewed by Sanders et al. (1995). From the standpoint of accounting for off-site costs at reservoirs, they point out that the immediate economic impacts of sediment deposits in reservoirs depends on whether deposition is focused in the active storage zone or the dead pool. Because a long time horizon is required to measure soil erosion impacts on crop productivity in the field, they recommended the use of a calibrated biophysical simulation model such as EPIC to facilitate research on the physical and economic benefits of soil conservation alternatives. The EPIC model (Williams et al., 1984) is a multiyear, multicrop model which simulates crop growth and yields subject to erosion and variable inputs. The model is data-intensive, operating on a daily timestep, using up to 10 soil layers, and having 21 parameters for each soil layer. It simulates weather, surface and subsurface hydrology, erosion, nutrient budget, plant growth, agronomic practices including tillage, and soil temperature. The data required to run the model are not presently available for crops in many parts of the world, and the model's extensive data and validation needs tend to increase rather than diminish the reliance on field data from agricultural research stations. However, once validated it allows researchers to rapidly assess the relationship between crop yield and agronomic and conservation practices.

### 6.3 EROSION RATE

Erosion rate is expressed in terms of mass of soil removed per unit of time ( $1 \text{ t/km}^2/\text{yr} = 2.855 \text{ short tons/mi}^2/\text{yr}$ ). It may also be expressed as the denudation rate of the earth's surface, measured in soil depth per unit of time. Twelve of the 14 estimates of the average global rate of denudation summarized by Lal (1994) fell between 0.06 and 0.16 mm/year. The most comprehensive study was reportedly that of Walling (1984) with a computed global rate of 0.088 mm/yr. Assuming a unit weight of  $1.5 \text{ g/cm}^3$  for soil, this is equivalent to an erosion rate of  $132 \text{ t/km}^2/\text{yr}$ . Smith and Stamey (1965) reviewed data on the natural or geologic rates of erosion from many soils planted with thick vegetation, and found that the geologic rates of erosion from well-vegetated sites are commonly less than, and usually much less than,  $60 \text{ t/km}^2/\text{yr}$ .

Over much of the earth's surface, the most significant determinant of modern erosion rates is human activity. The potential impact of human activity in accelerating erosion is summarized in Table 6.3. Changes in the nature and intensity of land use influence long-

**TABLE 6.3** Representative Rates of Erosion from Various Temperate Zone Land Uses

Land use	Erosion rate		Relative erosion rate
	short tons/mi <sup>2</sup> /yr	t/km <sup>2</sup> /yr	(forest = 1)
Forest	24	8	1
Grassland	240	84	10
Abandoned surface mines	2,400	840	100
Cropland	4,800	1,680	200
Harvested forest	12,000	4,200	500
Active surface mines	48,000	16,800	2,000
Construction sites	48,000	16,800	2,000

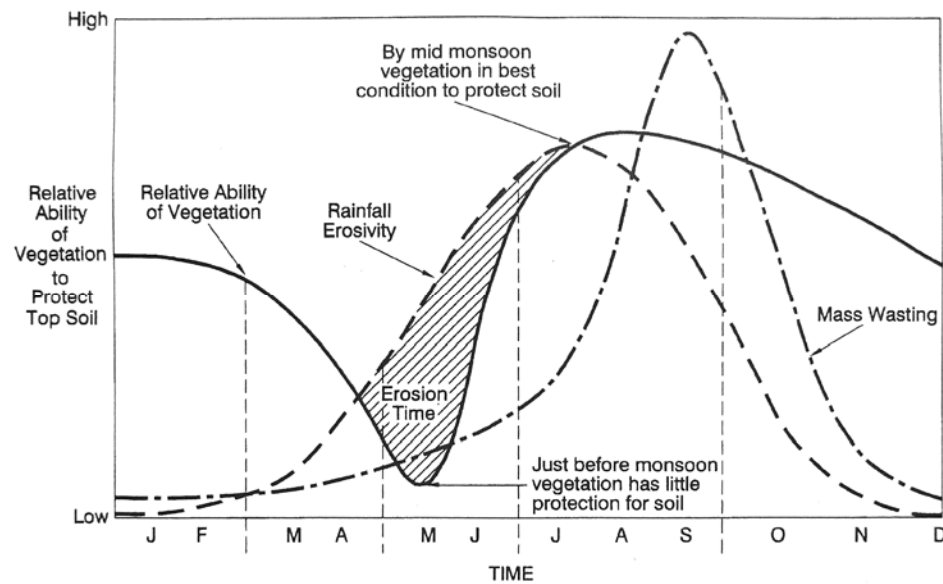


**FIGURE 6.3** Seasonality of erosion in Nepal (after Galay, 1987).

term erosion rates. Trimble (1974) showed that erosion rates in the Piedmont area of the southeastern United States rose to very high levels during periods of maximum agricultural exploitation during the nineteenth and early twentieth centuries, and have since abated because of abandonment of agriculture in many areas and implementation of soil conservation practices, starting in the 1930s, in areas remaining under cultivation.

Large seasonal variations in erosion rate are caused by factors such as increase in the supply of readily erodible sediment after a prolonged dry period, changes in soil cover, and seasonal variation in rainfall intensity. The influence of ground cover is particularly evident in seasonally dry climates where vegetation is subject to heavy grazing pressure, or where lands are ploughed prior to the onset of rains. The seasonality of erosion in Nepal is illustrated in Fig. 6.3 showing high surface erosion rates at the onset of the monsoon when there is limited ground cover on cropped and overgrazed land. Later in the season, vegetative cover has become well-established and the supply of readily erodible loose surface sediment has been exhausted, so surface erosion rates decline, but higher soil moisture increases the rate of slope failure.

## 6.4 INTERRILL AND RILL EROSION

### 6.4.1 Interrill Erosion

Interrill erosion entails two distinct steps: detachment and transport. The primary cause of detachment is the impact of rainfall on a soil surface deprived of protective vegetative cover. Raindrop impact mechanically breaks apart the granular structure of the soil and produces particles small enough to be transported by shallow prechannel flow, and also physically transports particles through the process of rainsplash (Fig. 6.4). Raindrop impact can splash some particles as far as 0.5 m from the impact site. Successive raindrops continue the dislodgement and splash transport process until the particle is splashed into a small stream of flowing water, or until there is enough water on the soil to initiate particle transport by surface flow. Interrill transport distances are normally limited to a few meters, or shorter distances in furrowed fields, before the flow is focused into rills.



**Figure 6.4** Raindrop impact on soil. The force of the impact detaches particles from the soil matrix, breaks apart soil aggregates, and transports detached particles by rainsplash. (courtesy of Natural Resources Conservation Service.)

Soil fines broken apart by rainfall but not transported away from the site can form a soil crust or seal.

Ground vegetation, organic litter, and mulch all protect the soil against the force of direct raindrop impact, thereby greatly reducing the opportunity for dislodgement and subsequent soil sealing. Under some circumstances surface stones can also protect the underlying soil from raindrop erosion, but stones also tend to reduce infiltration rate and focus runoff into channels, thereby potentially enhancing flow channelization and transport.

#### 6.4.2 Rainfall

The energy imparted to the soil as a result of rainfall is dependent on drop size, fall velocity, and rainfall intensity. Drop size increases as a function of rainfall intensity. Defining the median drop diameter  $D_{50}$  as the size in millimeters at which half the volume of rainfall is contained in both larger and smaller drops, the median drop size can be related to rainfall intensity by:

$$D_{50} = 1.24 I^{0.182} \quad (6.1)$$

where  $I$  is the rainfall intensity in mm/h (Laws and Parsons, 1943). Representative raindrop size distributions are illustrated in Fig. 6.5. A rainstorm will have only a few drops significantly larger than the median, but many smaller drops. Based on the drop size distribution determined by Laws and Parsons, and terminal drop velocities, an equation for the rainfall energy as a function of intensity was developed by Wischmeier

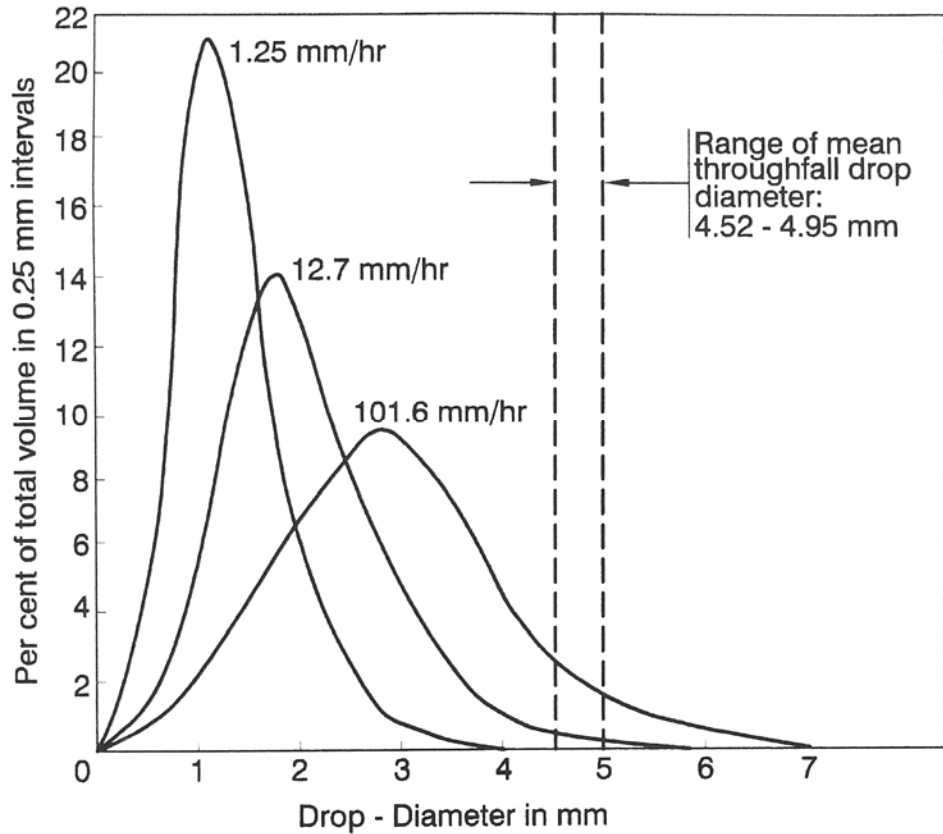


**FIGURE 6.5** Size distribution of raindrops measured for three different rainfall intensities. (*Lars and Parsons, 1943*), compared to the range of median drop size for canopy throughfall drops beneath a leafy canopy (*Brandt, 1990*). The canopy tends to increase drop size for all but the most intense rainstorms.

and Smith (1958) and was expressed in SI units by Foster et al. (1981). The kinetic energy per unit of rainfall  $E_k$ , in units of megajoules per hectare per millimeter of rainfall (MJ/ha•mm), for rainfall intensity  $I$  (mm/h), is given by:

$$E_k = 0.119 + 0.0873 \log_{10} I \tag{6.2}$$

Multiply by 100 to express the results in  $J/m^2 \cdot h$ . Computations for three rainfall intensities are summarized in Table 6.4, illustrating the dramatic increase in rainfall energy as a function of intensity.

### 6.4.3 Rill Erosion

When flow becomes concentrated in rills the bed shear is capable of detaching soil particles. Rills can grow, capture additional flow, and eventually grow into gullies. Like larger channels, the sediment transported by rills includes both the material eroded by channel processes plus the sediment delivered to the rills by interrill erosion.

**TABLE 6.4** Rainfall Characteristics

Type of rainfall	Intensity		Median drop Diameter, mm	Kinetic energy, J/m <sup>2</sup>	
	in/h	mm/h		per mm	per h
Drizzle	0.1	2.5	1.5	15.4	38
Heavy rain	1	25	2.2	24.1	602
Cloudburst	4	100	2.9	29.4	2940

#### 6.4.4 Size of Eroded Particles

Particle size is an important parameter controlling the initiation and maintenance of sediment transport and is used in some erosion-prediction models. Few soils behave as a loose aggregation of grains, like sand on a beach. Rather, granules of many different sizes form a matrix held together by chemical and organic bonding, especially when the soil has a significant clay content.

Meyer (1985) used simulated rainfall to analyze the relationship between the grain size distribution of surface soil and eroded sediment for 17 soil types. Eroded sediment tended to be enriched with respect to the clay content compared to the original surface soil. Because of the formation of particle aggregates, an average of 46 weight-percent of the two clay soils tested produced aggregate particles in the sand size (greater than 0.062 mm), whereas only 18 weight-percent of the eroded particles from eight silty loam samples fell into the sand size. The large size of the eroded particles from clay soils as compared to silty soils is illustrated in Fig. 6.6. The silty loams not only produced the smallest particles of all soils tested, but were also the easiest to erode. This general

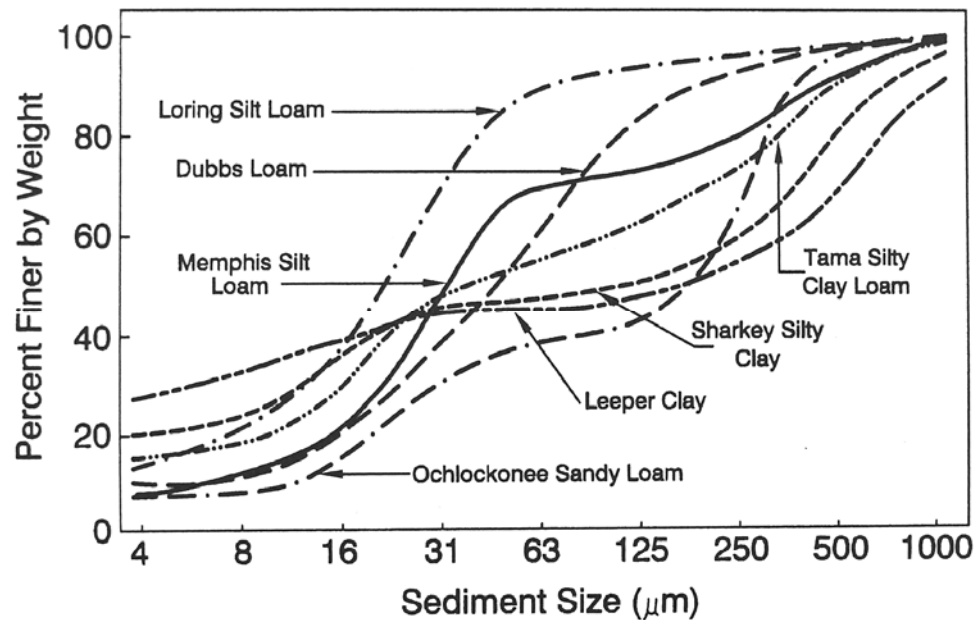


**FIGURE 6.6** Size classification of eroded particles, showing that aggregation in cohesive clay soils causes them to produce more coarse particles (larger than 63  $\mu\text{m}$ ) than silty soils (Meyer, 1985).

pattern was confirmed by subsequent laboratory size testing of 21 soils from across the United States (Rhoton and Meyer, 1987), where it was shown that simple laboratory techniques for sizing bulk samples of surface soils, which eliminates the use of a dispersant, can provide reasonable predictions of the size distribution of eroded particles.

## 6.5 GULLY EROSION

### 6.5.1 Gully Erosion Process

A gully is an erosional channel too large to be eliminated by normal cultivation techniques or crossed by a wheeled vehicle, and active gullies are characterized by a steep or vertical erosional scarp. Gully erosion occurs where erodible soil is exposed to concentrated runoff from rainfall or snowmelt, and may be initiated by enlargement of a rill, when flow is concentrated by a structure such as a trail, road, ditch or drain, or when runoff is increased by upstream land use change. Roads intercept and concentrate downslope flows and are prime agents in gully formation. Even off-road vehicles can accelerate gully erosion, since they leave continuous imprints in the soil which channelize overland flow during rainstorms, subsequently creating continuous rills and gullies as opposed to the often short and discontinuous channels formed naturally and which allow runoff energy to be dissipated (Heede, 1983). Although gully erosion is commonly associated with disturbed lands in semiarid areas, extensive gully erosion can also occur in humid areas when vegetation is removed.

Water plunging into a gully over a vertical headwall creates a plunge pool and erodes the foot of the headwall, causing it to collapse and move farther upstream, creating the pattern of gully growth shown in Fig. 6.7. Additional nickpoints may erode upstream along the gully floor, causing it to deepen. Headwall heights can range from a fraction to many meters in height. Gullies typically become more mature and stable below the actively eroding area of headcut. However, erosion can be reinitiated below the headcut if the base elevation is lowered, causing the formation of new nickpoints and retrogressive erosion upstream along the gully floor, deepening and widening the original gully. Gullies may be discontinuous or may expand until an interconnected or continuous channel network is formed, and their growth may be either regular or erratic.

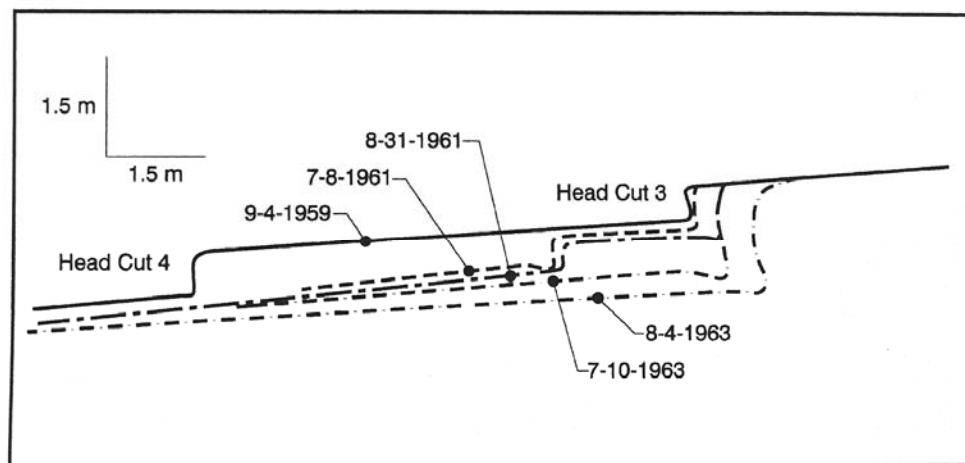
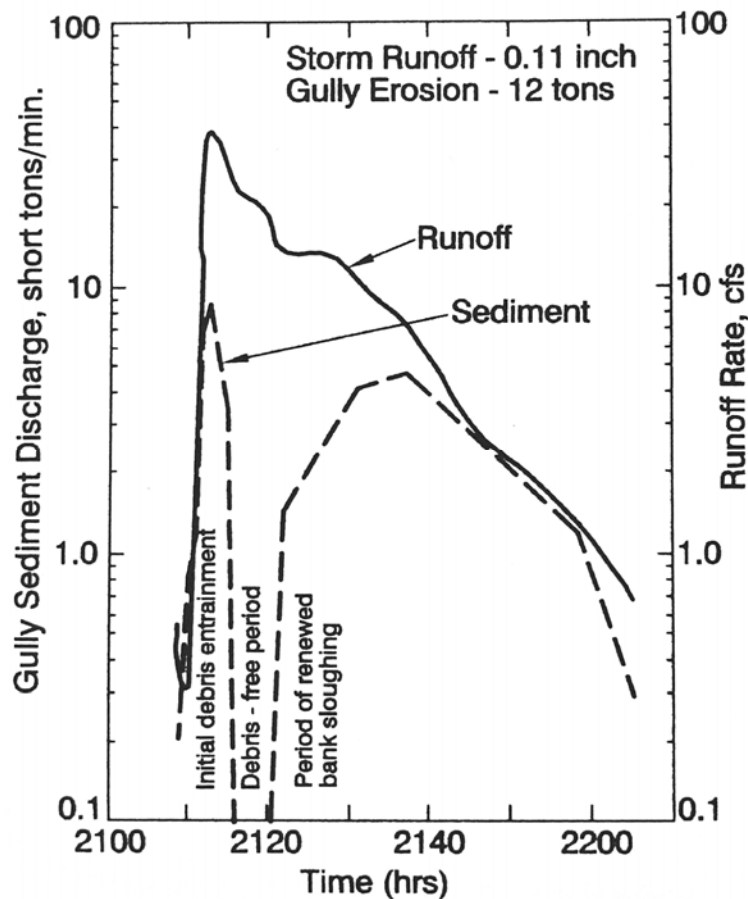


FIGURE 6.7 Longitudinal profile of gully growth (Heede, 1975).

related,

demonstrating that processes in addition to hydraulic shear at the channel boundary influence gully erosion rate. Four gullies in Iowa eroding loessial soils to an underlying layer of more resistant glacial till were intensively monitored by Piest et al. (1975b) with gaging stations above and below each gully to determine the variation in erosion rates over time. The watersheds tributary to the gullies varied from 30 to 61 ha in size; two were in conventional cropping sequences with corn and two were managed for conservation. The two gullies below the conservation watersheds had stabilized as a result of reduced rates of surface runoff and adequate channel vegetation. Sediment discharge from the eroding gullies frequently peaked and then declined dramatically prior to the peak discharge (Fig. 6.8). During some events the conventionally cropped watersheds delivered more sediment than could be transported, causing sediment to temporarily accumulate within the gully. From these and other observations it was concluded that gully erosion is a two-stage process consisting of: (1) production of sediment debris and (2) sediment transport. At the test site the debris production was controlled primarily by block failure of gully walls, whereas transport was related to hydraulic transport capacity. Other patterns of gully erosion may be important in other geographic settings. For example, with an erodible channel floor, the rate of gully erosion may be more closely related to channel hydraulics. Heede (1975) observed similar irregularities in the rate of sediment export by gullies.



**FIGURE 6.8** Rate of gully erosion determined by suspended sediment gaging upstream and downstream of the gully reach, illustrating the dependence of gully erosion on two processes: (1) production of erodible sediment debris and (2) hydraulic transport of debris out of the gully (Piest et al., 1975b)

Schumm et al. (1988) concluded that all gullies follow essentially the same evolutionary path with eventual development of relatively stable conditions, and outlined four stages of gully evolution, presented below in a modified form.

**Stage 1 Initiation.** The channel gradually cuts through the upper (A and B) soil horizons. This is the stage at which erosion control measures can most easily be implemented.

**Stage 2 Headcutting and deepening.** This stage is characterized by upstream migration of the headcut and plunge pool, caving of walls, and channel deepening as the gully erodes weak underlying parent material. This stage ends when the longitudinal channel profile becomes stabilized due to some type of base level control, and the erosion rate declines.

**Stage 3 Widening and healing.** Widening of the gully top width occurs, slopes on the gully walls are reduced by weathering and mass wasting, and revegetation occurs.

**Stage 4 Stabilization.** The side slopes and base level stabilize and soils accumulate and develop on older scarred surfaces. When the channel walls have reclined to approximately 45° and have been vegetated, the gully can be considered to be stable unless further disturbed.

These four stages may be applied to an entire gully system or to different reaches of a single gully from head to mouth. Reversion to stage 2 conditions and renewed erosion can occur during stages 3 or 4 because of lowering of the base level or upstream disturbance.

### 6.5.2 Quantification of Gully Erosion

Gully growth tends to be both rapid and erratic, and both the growth rate and configuration of gullies is highly dependent on local soil and hydrologic conditions. There is no general method for predicting rates of gully formation and growth. All estimates of gully erosion must be based on field measurements in the study area. Erosion rate within a watershed may be approximated by using a time series of air photos to determine the areal extent and growth rate of gullies, and number of gullies per unit area, in combination with ground reconnaissance to determine wall heights. Gully erosion from larger watersheds may be estimated as the sum of erosion rates prepared for smaller sub-basins. In areas with few gullies, the sediment contribution by gully erosion may be small enough to be ignored.

Regression equations have been developed to explain the rate of headwall advance in individual gullies within specific regions. Watershed area tributary to the gully is the single most important explanatory variable, and the rate of gully advance varies as approximately the 0.5 power of tributary area. Based on studies in 210 gullies east of the Rocky Mountains, the U.S. Department of Agriculture (1977) determined that at least six factors significantly influenced the rate of headcut advance: tributary watershed area, storm precipitation, soil erodibility, slope of approach channel above the headcut, groundwater level, and changes in runoff due to land use changes above the gully. The tributary watershed area and precipitation were found to best explain the rate of gully headcut advance, according to the following relation:

$$R = 0.36 (A)^{0.46} (P)^{0.20} \quad (6.3)$$

where  $R$  = rate of headward advancement, m/yr;  $A$  = tributary watershed area, ha; and  $P$  = annual precipitation, mm, on days with precipitation in excess of 12.7 mm/day. This relationship does not apply to arid regions with annual precipitation less than 500 mm.

When the historical rate of gully advancement can be determined from field measurements, interviews, or air photos, the future rate of headcut advancement can be predicted by restating Eq. (6.3) on the basis of the principle of proportions as

$$R_f/R_p = (A_f/A_p)^{0.46} (P_f/P_p)^{0.2} \quad (6.4)$$

where the subscript  $f$  refers to future conditions and  $p$  to past conditions. For example, as the gully headwall advances upstream, the tributary drainage area will decline. A gully head moving up a small tributary will also have a smaller drainage area than the main gully. Similarly, rainfall over a short historical period (less than 10 years) may have differed significantly from the long-term average. The future rate of gully advance is estimated from the historical period by substituting future and historical values, without factors such as land use change and interception of different geologic material which will affect the rate of gullying. The rate of headcut advancement will be decreased if erosion carries the gully into more cohesive and erosion-resistant soils.

The total volume of material eroded by a gully will be influenced by the upstream migration of secondary nickpoints and the widening of the gully floor, in addition to the rate of headwall advance. Each of these should be considered separately. One method to project future gully widening is to project headward advance, and assume that the top width planform of the existing gully will move upstream with the headcut. Alternatively, widening can be estimated from measurements in older nearby gullies to determine base level gradient, depth, and topwidth:depth ratios. As a rule of thumb, in cohesive materials gully topwidth is about 3 times gully depth and in noncohesive material gully topwidth is about 1.75 times depth (Heede, 1976).

## 6.6 CHANNEL EROSION

### 6.6.1 Processes

Channel and streambank erosion occur along the bed and banks of streams. Actively eroding banks are often nearly vertical with freshly exposed roots, and bank vegetation generally offers no protection when bank undercutting occurs below the root zone. Channel erosion is associated with the natural process of channel meandering as well as accelerated erosion due to channel incision and widening. The downstream impacts associated with these processes are quite distinct.

Alluvial rivers continuously meander across their floodplain, scouring sediment from the outer side of one meander bend and depositing a portion of this load on point bars farther downstream, while maintaining the same channel width and longitudinal profile. The process of meander migration documented by Leopold et al. (1964) in Fig. 6.9 illustrates that the river width and thalweg depth remain essentially constant, and that the point bar fills back to the level of the original floodplain. Sediment eroded from

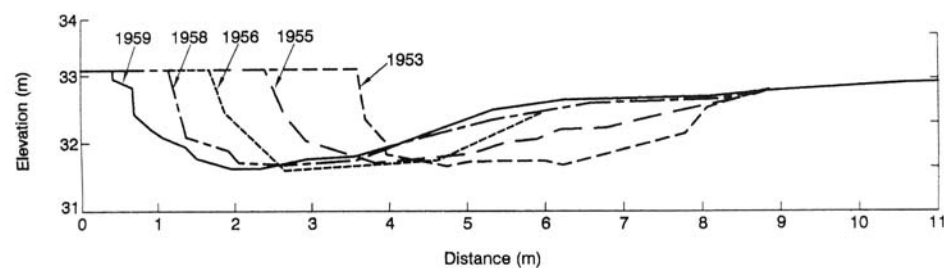


FIGURE 6.9 Process of meander migration (modified from Leopold et al., 1964).

meanders is not necessarily exported, since it may be redeposited a short distance downstream. During floods a meandering river reach can become a net depositional environment because of floodplain sedimentation. The rate of channel bank erosion is not indicative of net sediment yield unless accompanied by channel widening or incision. Much of the channel bank protection activity throughout the world has been directed at stabilizing meandering rivers to improve navigation and protect properties in erosion-prone areas. This converts naturally meandering streams into fixed streams controlled by hard structures such as revetments and dikes. The Rhine is an example of a highly regulated river which has been confined to a fixed channel by erosion control structures along either side, and can now erode only vertically.

Degradation and incision of streambeds cause channel widening and the net export of potentially large volumes of sediment because of hydraulic forces which erode and transport sediment, plus bank failures initiated by undercutting. Channel incision can be initiated or accelerated by increased peak flows caused by upstream land use changes, deeper flow due to diking or levee construction, reduced supply of bed material due to trapping in upstream reservoirs, reduction in hydraulic roughness and increase in channel slope due to stream channelization and straightening, removal of streambank vegetation and mechanical breakdown of banks by livestock, and in-stream mining of sand and gravel. A period of channel erosion can also follow a period of channel deposition during a period of increased sediment supply. Examples of channel incision and erosion are described in Chap. 22, the Feather River case study.

The process of channel incision is quite distinct from meander migration: it involves both a lowering of base level and the incision of a new wide floodplain within the older deposits. This erosion process can remove large volumes of valley sediment until a new meandering channel within an entrenched floodplain becomes stabilized at a lower base level (Fig. 6.10). A classic example of channel degradation and massive sediment export is the Rio Puerco, summarized by Schumm et al. (1988). Rio Puerco drains a 19,000-km<sup>2</sup> watershed in north and central New Mexico and is a major sediment source affecting Elephant Butte reservoir on the Rio Grande. A sediment concentration of 327,000 ppm in Rio Puerco, 40 percent of which was sand, was documented by Nordin (1963) at a discharge of 30 m<sup>3</sup>/s. From historical records and photographs, it is known that prior to 1885 Rio Puerco and its tributary channels were small and the valley was apparently stable with a few discontinuous gullies. A combination of climatic and human impacts, which are not well understood, triggered the process of channel incision which resulted in the net erosion of 48.7 Mm<sup>3</sup> of sediment from the channel between 1887 and 1928. After initial deepening the channel migrated laterally and meandered, creating a widening floodplain entrenched within the former floodplain.

### 6.6.2 Quantifying Channel Erosion

Sediment volumes removed by channel erosion may be computed from the change in channel geometry over time as recorded by repeated aerial photography or field measurements of bank height (or river profile) and the width of the eroded area consisting

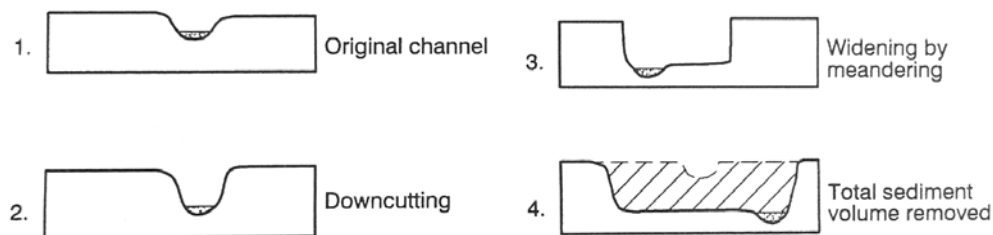


**FIGURE 6.10** Conceptual process of channel incision and widening.

of the active channel and the adjacent incised floodplain. Streambank erosion rates may be expressed in terms of tons per stream kilometer per year, and multiplied by the total stream length in the study area to estimate total streambank erosion. In quantifying streambank erosion, relatively long time periods and long stream reaches should be used because channel adjustment is not a continuous or uniform process, and responds to the episodic nature of hydrologic events. If aerial photography or other data are available at regular intervals, bank erosion can be computed on an annual basis and graphed as a function of either total or peak discharge during each period.

Channel deposition and erosion also exhibits seasonal cycles. Differences between discharge in upstream and downstream fluvial gage stations were used by Miller and Shoemaker (1986) to detect seasonal changes in sediment storage along a 33-km reach of the Potomac River in the United States. Temporary channel-bottom, channel-margin, and channel-island deposition of fine sediment amounted to 14.3 percent of the annual suspended sediment load.

## 6.7 SLOPE FAILURE

---

This section discusses slope failures as a source of sediment in watersheds. Slope failures occurring directly in reservoirs are discussed in Chap. 10.

Slope failures include phenomena such as landslides, slumps, and debris flows. These events can produce large volumes of sediment, but they are difficult to quantify because they tend to occur episodically and in response to extreme events. The initial sediment load is contributed at the time of slope failure, and additional sediment is contributed thereafter by rainfall on denuded landslide scars and the mass of destabilized material. Sediment contribution by slope failure can be measured by using sequences of air photos to determine the frequency of occurrence and the surface area of the watershed affected. Large-scale landslide activity is triggered by intense rainfall, and the triggering of landslide activity within a region can be related to rainfall duration and intensity. Development of a regional relationship in a humid tropical area of Puerto Rico was performed by Larsen and Simon (1993) based on the analysis of 256 intense rainfall events. The landslide threshold was developed by comparing rainfall characteristics of storms that produced landslides with those that did not, resulting in the following relationship:

$$I = 91.46D^{-0.82} \quad (6.5)$$

where  $I$  is rainfall intensity, mm/h, and  $D$  is storm duration, h. The resulting intensity relationship for Puerto Rico is illustrated in Fig. 6.11. Similar relationships have been developed in other areas of the world.

Landslide scars are relatively common on steep slopes in the humid tropics, even in areas of undisturbed forest, and represent an important source of sediment. Erosion studies underway in the moist Luquillo Experimental Forest in Puerto Rico when hurricane Hugo struck documented the impact of the hurricane rainfall and resulting landslides. The experimental forest occupies steeply sloping volcanic soils on the Luquillo Mountains with a maximum elevation of 1000 m and is essentially undisturbed except for a sparse network of well-maintained paved roads. Average precipitation in the forest during this storm was 267 mm, and high-intensity rainfall (over 30 mm/h) was sustained for about 7 h. The return interval of this rainfall was about 10 yr. Aerial photography was used to identify 285 landslides in 6474 ha of the forest, of which 66 percent were concentrated in a 1031-ha area closest to the passage of the hurricane's eye. The surface area of individual landslides ranged from 18 to 4502 m<sup>2</sup>, with a median of 148 m<sup>2</sup>. In the 1031-ha area of intense landslide activity, landslides affected 0.65 percent of the land

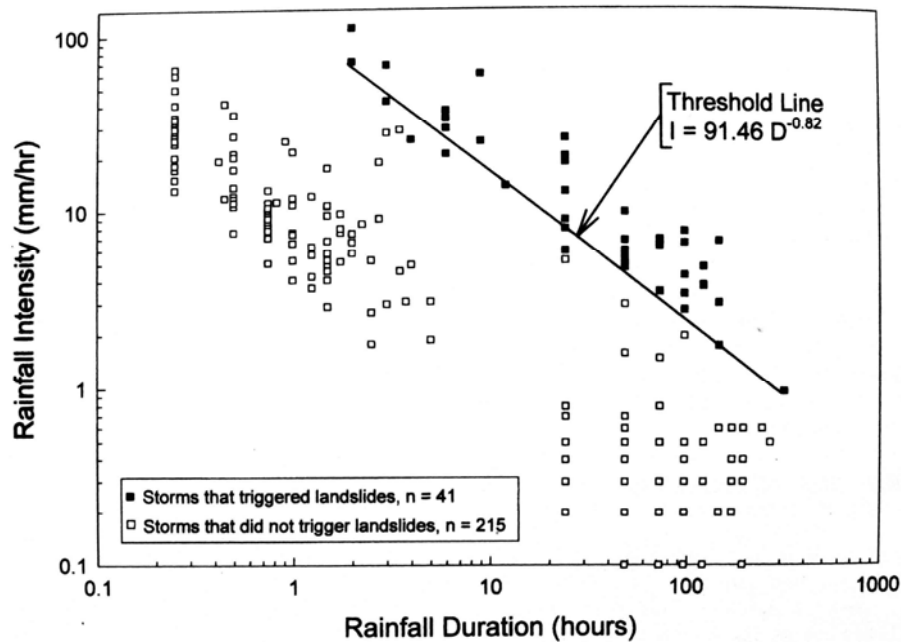


**FIGURE 6.11** Intensity of rainfall that triggered landslides in Puerto Rico based on 256 storms over the period 1959 to 1991. (After Larsen and Simon, 1993).

surface. Shallow soil slips (0.5 to 1.5 in deep) and debris flows (1.5 to 2.0 m deep) were the predominant forms of slope failure and together accounted for 91 percent of landslides, the remaining 9 percent being slumps. Virtually all the mapped landslides occurred in areas receiving over 200 mm of rain during the storm (Larsen and Torres-Sanchez, 1992). However, extensive channel or valley floor modification was not observed in the forest area, nor did any of the road culverts fail despite debris clogging (Scatena and Larsen, 1991).

The analysis of aerial photography for the Luquillo moist tropical forest spanning the period of 1941 to 1990 showed that small mass movements with a median area of 156 m<sup>2</sup> could be expected to affect about 0.64 percent of the land area per century. The resulting rate of mass wasting on forested slopes was estimated at 188 m<sup>3</sup>/km<sup>2</sup>/yr or 239 t/km<sup>2</sup>/yr. By comparison, suspended sediment export from forest streams ranges from 159 to 203 t/km<sup>2</sup>/yr, and the combined suspended and bedload from another similar forest stream is 300 t/km<sup>2</sup>/yr (Larsen, 1991). On the basis of <sup>10</sup>beryllium measurement, Brown et al. (1995) estimated that about 55 percent of the sediment exported from the forest is mobilized by mass wasting and the remainder from sheet erosion.

## 6.8 FIELD MEASUREMENT OF EROSION

Erosion rates are measured in the field to provide the data needed to construct and calibrate erosion prediction models, to test the effectiveness of alternative erosion control measures, and to demonstrate erosion and control processes to audiences such as farmers and policy makers.

### 6.8.1 Erosion Plots

In agricultural practice, sub-hectare plots are used to measure the rate of soil loss under different conditions of soil type, slope, cropping pattern, and climate. Tens of thousands of plot-years of data are now available and have been used to calibrate the USLE and RUSLE models (described in Sec. 6.9). The standard USLE agricultural plot is 22.6 m long along a 9 percent slope axis and is about 4 m wide (plot width is adjusted to an even multiple of row widths). Plots of other dimensions and slopes are also used. Sheet metal borders are driven into the ground around the plot to exactly define its size. All runoff is captured and passed through tanks where the sediment is trapped, then removed and weighed. Field plot techniques are described by Mutchler et al. (1994), who emphasize the importance of the USLE standard plot because of the extensive existing database collected in a generally uniform manner and the proven usefulness of the USLE/RUSLE equations.

For the separate calibration of interrill and rill erosion rates as required for the newer WEPP model, Laften et al. (1991*b*) measured interrill erosion in multiple plots 0.5 m wide and 0.75 m long, and rill erosion was measured in plots 0.5 m wide and 9 m long, under simulated rainfall. Soil loss from small sloping areas can also be measured with troughs, or pairs of troughs upstream and downstream of the sampled portion of the slope. All trough runoff is directed into sediment traps.

### 6.8.2 Fabric Dams

Fabric dams represent an inexpensive method of comparing erosion rates from different land uses and, because the results are readily visible, they are also useful for demonstrations. As a disadvantage, runoff volume cannot be measured. Dissmeyer (1982) described fabric dam construction for monitoring of forestry practices using rot-resistant posts, hogwire or similar coarse wire mesh, and geotextile or other filter fabric (Fig. 6.12). The filter fabric is selected for the soil size it is intended to trap and the expected runoff volume. Sediment is trapped by the pores in the fabric plus the reduced flow velocity behind the dam. Plot size should be adjusted to prevent dam overtopping, and in areas of mechanically disturbed soils, such as construction areas, plot length should normally not exceed 30 m. Plot widths of about 10 m are recommended, with space between adjacent plots. Plots comparing results of different treatments should be established in areas having similar soils and slopes, and rainfall should be measured. Sediment accumulation may be measured by repeated topographic survey or using a square grid of stakes on 0.5 m centers, with lengths marked from zero upward along each stake. Core the full depth of sediment, dry, and weigh to determine the volume to weight conversion to express erosion rates in terms of mass per unit surface area.

### 6.8.3 Experimental Watersheds

Some agricultural studies and most forestry studies employ instrumented watersheds ranging in area from 1 to over 100 ha, in combination with smaller plot studies to analyze local erosion sources such as logging roads. Forestry is normally practiced on soils having steep and irregular slopes, and the erosion rates from haul roads is typically orders of magnitude higher than from the forest floor. The resulting pattern of soil disturbance caused by logging is much more irregular than by mechanized agriculture. The use of small instrumental watersheds instead of sub-hectare plot studies helps to even out some

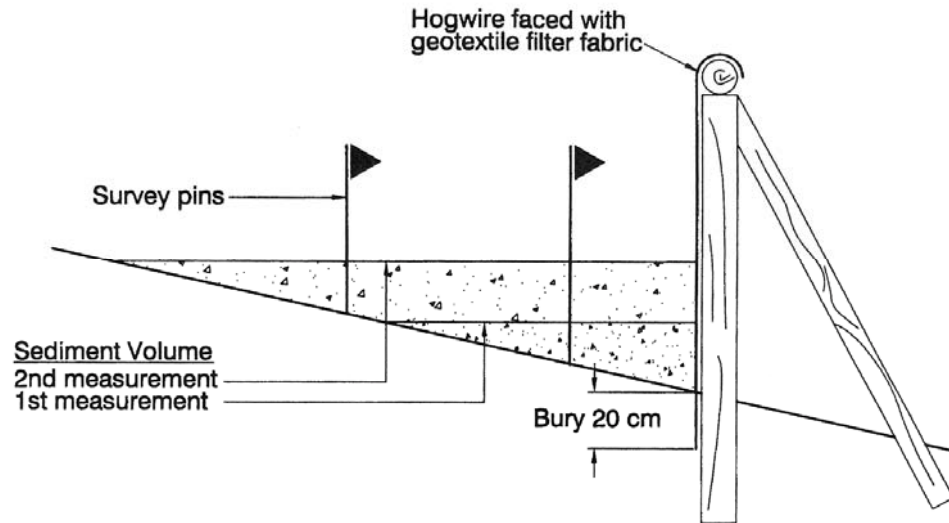
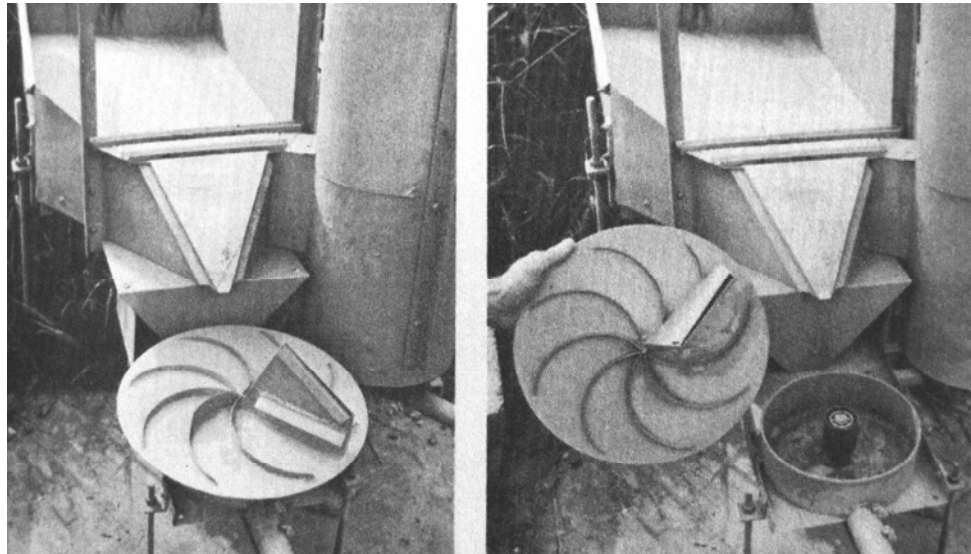


FIGURE 6.12 Fabric darn for erosion control studies (adapted from Dissmeyer, 1982).

of this inherent variability to allow a better comparison of the impacts of alternative forest management techniques. Data from experimental watersheds provide information on sediment yield which is not strictly comparable to the erosion rate measured in small plots, and differences in drainage area size and delivery ratio must be considered in comparing data from the two sources.

#### 6.8.4 Measurement Equipment

Measurement equipment and sampling strategies must be selected on the basis of the study requirements. Total runoff collection devices are not generally feasible for areas other than small plots because storage requirements are excessive. Inadequate storage can produce overflow and sediment loss during large events responsible for the highest erosion rates, which are most important to sample accurately. Sample volume may be reduced by using a slotted flow divisor to obtain a storm-integrated or discharge-weighted sample of the runoff. The multi-slot divisor equally divides the flow among an odd number (from 3 to 13) of stationary slots. The Coshocton wheel sampler uses a revolving slot to sample between 0.33 and 1 percent of the flow (Fig. 6.13). Flow divisors are typically placed downstream of an H-type flume which measures total discharge. This flume has a flat bottom that reduces clogging by sediment and is simple to build. Construction details for samplers, flumes, and other devices including the "Walnut Gulch supercritical flume" developed for the measurement of ephemeral, flashy, and sand- and gravel-laden streams, are provided by Brakensiek et al. (1979). Modified sampling equipment is described by Replogle and Johnson (1963).



**FIGURE 6.13** Coshocton wheel sampler and H flume (*Wendy et al., 1979*).

The timewise variation in suspended sediment discharge during individual runoff events can be sampled using a continuous stage recorder and automatic sampler, as described in Chap. 8. In forested watersheds discharging coarse channel sediment and woody debris, a debris basin with an overflow weir and suspended load sampler represents a good measurement option. The discharge of coarse sediment is measured by repeated surveys of the debris basin to determine the volume trapped, and the measurement is corrected for the amount of woody debris.

### 6.8.5 Simulated Rainfall

Rainfall simulators have been used in substitution for natural rainfall in field erosion studies on plots up to about 1 ha and in laboratory studies of microscale erosion phenomena (Meyer, 1994). The field simulator consists of an array of nozzles or other drop-forming devices suspended in the air on a framework of pipes or other structural members, and fed by pumps and hoses. Because of their large water requirements, the larger simulators are usually supplied from a pond or other local water body.

The ideal simulator should produce drops having a size distribution near that of natural rainstorms, the drops should fall nearly vertically, and the application should be nearly continuous and uniform over the study area at the simulated storm intensities. The simulator should be capable of producing any simulated storm repeatedly on different plots, and should wet an area large enough to provide realistic results. The system should be portable for movement from one plot to another and operate satisfactorily in a variety of field conditions. Additionally, the simulated rainwater should be free of sediment and its chemical characteristics should be sufficiently similar to natural rainfall so that soil aggregation characteristics are not significantly altered. No simulator achieves all these goals perfectly, and tradeoffs are inevitable. There is no accepted standard for rainfall simulators; a variety of custom devices have been developed for different applications.

Rainfall simulators do not substitute for natural storms but have important advantages in certain types of work. They can obtain erosion data from small sites without the time and expense of establishing a long-term monitoring program. The effect of intense storms can be simulated immediately as opposed to potentially waiting for years for such an event to occur under natural conditions. Detailed instrumentation can be installed to monitor intense simulated storms that would not be possible under natural conditions. Simulators also allow the response of many types of soils or types of treatments to be compared under controlled and repeatable conditions over a relatively short period of time. Simulators may also be useful as an educational or demonstration tool (Dillaha, 1988). However, considerable interpretation is necessary to transform simulator results into annual erosion values, such as those used in USLE, and rainfall simulators are not substitute for long-term field plots subjected to natural climatic and rainfall conditions.

### 6.8.6 Other Methods

Radioactive  $^{137}\text{cesium}$  generated by fallout from nuclear atmospheric testing has been used to measure and trace erosion and deposition processes on the land and in reservoirs. Significant fallout of this isotope started in the late 1950s, peaked in 1964, and declined quickly after the nuclear test ban treaty, although areas of Europe received additional inputs from the Chernobyl reactor accident.  $^{137}\text{Cesium}$  is tightly sorbed onto clays and penetrates only a short distance (on the order of 10 cm) into the soil column. It may be used to trace the movement of fallout-contaminated surface soils through a watershed, along channels, and to reservoirs and other points of deposition. By measuring rates of  $^{137}\text{cesium}$  activity as a function of depth in the soil profile, it is possible to determine whether sites are erosional or depositional, and determine deposition depths. It has been used in numerous studies to examine soil erosion and sediment budgets (Wilkins and Hebei, 1982; Campbell et al., 1988; Whitelock and Loughran, 1994) and has also been used to determine the sources of eroded sediment by the "fingerprinting" process discussed in Chap. 7. However, Fredericks et al. (1988) have pointed out that in soil erosion studies the  $^{137}\text{cesium}$  method is most suited as a research tool rather than for routine analysis. Soil samples exhibit a high degree of spatial variability in their  $^{137}\text{cesium}$  levels due to factors such as differences in soil characteristics and highly localized variations in rates of fallout deposition and soil erosion. Consequently, a large number (e.g., more than 20) soil samples must be analyzed from each site to reduce the standard error of mean activity counts to acceptable values. Studies involving over 100 samples are not uncommon, and counting times in a gamma-ray spectrometer typically run 8 to 16 h per sample. This tracer has also been frequently used for the dating of reservoir sediments, an application where the spatial variability is less critical since the objective is merely to identify the most active horizon in a continuously depositional environment, and not to compare activities among the samples. The use of  $^{137}\text{cesium}$  for dating reservoir sediments is described in Chap. 10.

Erosion monitoring using pins or nails with washers has been described by Lal et al. (1990). Erosion pins, or nails with small washers, are set out on a grid across a field and the decline in soil level is measured over time relative to each nail and averaged across the study site. This method is inexpensive and unattractive to vandals. However, it is difficult to obtain representative data since the nail itself obstructs soil movement, cultivation can artificially displace soil around the nail, and the erosion rate can be masked in swelling soils. This technique is suitable only for intensely monitored small plots where the primary interest is in relative rates of erosion and deposition.

The long-term rate of soil denudation can be determined from biological evidence, such as the exposure of roots on trees, the age of which is determined by counting annual growth rings (LaMarche, 1967). Biological indicators, such as freshly exposed roots, are also useful in identifying areas of recent channel erosion in the field.

## 6.9 EROSION MODELING WITH USLE AND RUSLE

---

Erosion modeling is fundamental to soil conservation because it allows the likely effectiveness of alternative conservation treatments to be tested on various landscape units to determine their impact on soil loss. When combined with economic data on the costs of alternative methods, the most economically efficient means to reduce erosion can be identified. The key to erosion modeling is the ability to extrapolate erosion rates measured at selected research sites to farms and small watersheds. Impacts on larger landscape units are computed as a sum of the erosion rates in multiple smaller areas, with an adjustment for delivery ratio.

The Universal Soil Loss Equation (USLE) is the method most widely used around the world to predict long-term rates of interrill and rill erosion from field or farm size units subject to different management practices. Wischmeier and Smith (1965) developed the USLE based on thousands of plot-years of data from experimental plots, and although the initial focus was oriented primarily to conditions in the middle and eastern United States, the USLE has been extended and applied worldwide. Metric conversions for the USLE have been summarized by Foster et al. (1981). The predictive accuracy of the USLE was checked against 2300 plot-years of soil loss data from 189 field plots at widely scattered locations by Wischmeier (1975). Average soil loss was 25 t/ha and mean prediction error was 1.3 t. For the evaluation of forestry practices, Dissmeyer and Foster (1980) combined the *C* and *P* factors into a cover-management factor for utilization of the equation to predict interrill and rill erosion from forest areas during the recovery period following logging. In forests the rate of soil loss from logging roads, skid roads, and channels and gullies is typically higher than sheet and rill erosion. These losses are not computed in the USLE and must be computed separately by a different method.

In 1987 work began on the development of a Revised USLE (RUSLE) to incorporate more recent research and technology (Renard et al., 1994). The RUSLE model was released in 1995 and is distributed as a computer program and manual. (The Windows-based RUSLE2 software can be downloaded from:

[http://fargo.nserl.purdue.edu/rusle2\\_dataweb/RUSLE2\\_Index.htm](http://fargo.nserl.purdue.edu/rusle2_dataweb/RUSLE2_Index.htm) ). While it retains the same basic structure as USLE, algorithms for computing individual factors have been changed significantly and computerized methods assist in determining individual factors.

The USLE/RUSLE model is an empirical multiple-regression-type equation which incorporates the parameters that influence erosion, without making any attempt to simulate the actual erosion process. Both USLE and RUSLE have the following form:

$$A=R \times K \times LS \times C \times P \quad (6.6)$$

The equation is said to be universal because it includes the four principal factors which influence soil loss: (1) the inherent erodibility of the soil is expressed by *K*, (2) erosive rainfall forces are expressed by *R*, (3) gravitational forces affecting runoff are given by the hillside length-slope factor (*LS*), and (4) cover factors modifying erosive forces are expressed by *C* and *P*. In the equation, *A* is annual long-term (20+ years) rate of soil loss.

The *rainfall erosion index R* is computed as the average erosional potential of rainfall measured as the product of rainfall kinetic energy and maximum 30-min rainfall intensity for all significant storms (greater than 12.7 mm, 0.5 inches) during an average year.

The *soil erodibility factor*  $K$  indicates the susceptibility of soil particles to detachment. This value is measured experimentally and published values are available for soils in the United States from the Natural Resources Conservation Service and soil survey reports. Several methods for estimating  $K$  values on unstudied soils are provided in the RUSLE program. Values represent average soil loss from a 72.6 ft (22.1 m) plot length on a 9 percent slope, per unit of rainfall erosion index  $R$ , for bare soil in continuous fallow.  $K$  values depend primarily on soil texture and are modified by parameters including structure, organic matter, and permeability.

The *length-slope factor* (LS) indicates effect of slope length and gradient, with  $LS = 1$  for a 22.1 m long experimental plot on a 9 percent slope.

The *vegetative cover factor*  $C$  is the ratio of soil loss under specified conditions to bare tilled soil. Values may range from 1 to 0.01.

The parameter for *erosion control practice*  $P$  compares the conservation techniques against a value of  $P = 1$  for straight rows tilled perpendicular to the slope.

Several important improvements over USLE have been incorporated into the RUSLE. The rainfall erosivity  $R$  values have been computed in more detail and incorporate the reduction in erosivity due to ponding on flat soils. Soil erodibility is varied seasonally, and alternative methods are presented for estimating  $K$  values on soils where data from field plots are not available. The length-slope factors are evaluated by using four different length-slope relationships and can incorporate freeze-thaw phenomena. Also, the slope can be divided into segments to represent complex slopes. Crop cover  $C$  and conservation practice  $P$  factor values were updated to better represent present agricultural practice and now incorporate conservation practices on rangeland.

The USLE/RUSLE model has a large database of plot studies, there are published values for model parameters, and many workers are familiar with its use. Although originally developed and calibrated for soil conditions in the United States, the USLE/RUSLE model has been used successfully in many countries. It has been used to study watersheds up to several hundred square kilometers in areas where reservoir sedimentation or fluvial sediment data are available to help determine the delivery ratio (Stall and Lee, 1980). However, use of the USLE/RUSLE model may lead to large errors unless values developed for the United States are adapted to conditions in other regions and confirmed with field studies. For example, Bollinne (1985) found that erosion from smaller rainfalls (less than 12.7 mm), which are excluded from rainfall erosivity computations in the United States, produce 33.5 percent of the annual runoff from bare soil near Brussels and therefore contribute significantly to erosion. Cover and other factors also required adjustment. In Costa Rica, Cuesta (1994) reported that while the USLE was at least partially adapted to conditions in that country, it still appears to overestimate erosion rates by approximately an order of magnitude on some steeply sloping soils. The adoption of the model to steeply sloping soils is a particularly important issue: the equation was originally developed and calibrated for use on mechanizable soils with lower slopes, but in the tropics the steep and nonmechanizable soils may also be intensely cultivated and erosion prediction in this environment is quite important. The model also may not properly account for nonstandard farm practices. For example, Jackson (1988) argued that the USLE tended to overestimate soil loss from Amish farms in the Pennsylvania area, which are cultivated exclusively by animal power and include long rotations in forage.

As a limitation the USLE/RUSLE model predicts long term (e.g., 20+ year) interrill and rill erosion from field- and farm-size units, but no depositional processes are included. Additional sources of erosion such as gullying and mass wasting are not considered and must be computed separately. The model is poorly adapted to determine short-term variations in sediment yield, since it does not simulate physical processes. The

soil erodibility factor  $K$  is an average value, but in reality the  $K$  value can be expected to change because of differences in antecedent soil moisture, storm characteristics, and the timewise dependence between erosion events. Erosion events are not independent of each other; one erosion event can deplete the supply of readily detached soil available for the subsequent event. Such antecedent conditions are not considered in the equations and can introduce significant error in predicting individual storm events. Single-event simulation can be important in reservoir analysis when it is desired to apportion sediment yield among the various reservoir inflow events that occur during a year.

## 6.10 EROSION MODELING USING WEPP

---

The Water Erosion Prediction Project (WEPP) was initiated in 1986 as a cooperative effort among four federal agencies: Agricultural Research Service, Natural Resources Conservation Service, Forest Service, and Bureau of Land Management. The objective was to replace the USLE with a new generation of erosion prediction technology to incorporate current understanding of the erosion process. The WEPP model and documentation is available in compact form from the USDA National Soil Erosion Laboratory at <http://www.ars.usda.gov/Research/docs.htm?docid=10621>.

The WEPP model simulates the physical processes affecting erosion. It uses a daily time step to update plant growth, litter production, soil characteristics, and hydrologic conditions important for determining runoff and erosion processes. When runoff occurs the model computes soil detachment, transport, and deposition at multiple points along the soil profile, in channels, and in small reservoirs. There are three versions of the model: profile, watershed, and grid. The profile version is a direct replacement of USLE with important additional capabilities, including the redeposition of eroded sediment and timewise simulation of erosion with a daily time step. The watershed version is a field-size model, which also incorporates the profile model and estimates sediment delivery to channels. The profile model is used to simulate erosion processes from different types of land uses and treatments. The eroded sediment is routed to the basin outlet by components in the watershed model which simulate processes of erosion and transport in ephemeral channels, and through detention reservoirs which trap sediment. The grid model is designed for application to geographical areas which do not correspond to watershed limits. Sediment can be delivered from one grid element to another and routed to multiple discharge points.

WEPP simulates three erosion processes: detachment, transport, and deposition. Interrill, rill, and channel erosion is simulated as a function of hydraulic shear. It does not simulate classical gullying, where processes other than hydraulic shear at the channel boundary are important, nor does it simulate erosion of perennial streams. The size of the area that can be simulated with the model depends on the erosion processes within the landscape unit. Thus, in areas of loessial soils where classical gullying may be the primary form of erosion, the WEPP model may be limited to pre-gully flows from areas less than 1 km<sup>2</sup>, whereas on other soils it might be applied to areas on the order of 10 km<sup>2</sup> without encountering significant erosive processes not simulated by the model.

The model simulates the hydrologic components important for predicting erosion. It can use either measured or simulated daily climatic data for storm rainfall amount and duration, peak:average rainfall intensity ratio, daily temperature range, wind velocity and direction, and solar radiation. Snow, snowmelt, frost, freezing and thaw depth, infiltration, and water loss during winter conditions are computed. Plant growth and decomposition is simulated daily for both cropland and rangeland, estimating values for variables including canopy cover and height, live and dead biomass above and below the

soil, leaf area index, basal area, and organic residue. Information on the dates and types of farming operations are input into the model. Daily water budget computations include precipitation. Evapotranspiration, infiltration, surface ponding, and deep percolation. Hydraulic shear forces on the soil surface have been computed assuming rectangular rills spaced about 1 m apart, using the kinematic wave equations and their approximations. Soil properties estimated each day include random roughness, ridge height, bulk density, saturated hydraulic conductivity, and soil erodibility parameters for rill and interrill areas, and critical hydraulic shear. These parameters are adjusted to account for factors including tillage, plant growth, and rainfall.

Of particular interest to the simulation of processes affecting reservoirs, the WEPP model can provide detailed simulation of individual storm events, predicting not only the amount of sediment eroded but also the grain size distribution of the sediment that enters downstream channels.

Because WEPP simulates both interrill and rill erosion processes, separate erodibility data on interrill and rill erosion rates are needed. The initial dataset obtained from 56 representative sloping cropland and rangeland soils across the United States under simulated rainfall revealed that there was little correlation between the two erosion rates. This reflects the different processes and forces involved in these two erosion processes and reinforces the need to simulate these two processes separately in erosion modeling. It was also found that soil erodibility values showed little quantitative resemblance to the USLE  $K$  values determined for these same soils (Laften et al., 1991b).

Interrill erosion is the detachment and transport of soil by raindrops and shallow overland flow. Sediment delivery from interrill areas is estimated to vary as the square of rainfall intensity by the following relationship:

$$D_i = K_i G C S I^2 \quad (6.7)$$

where  $D_i$  is sediment delivery from the interrill area to the rill,  $\text{kg/m}^2/\text{s}$ ;  $K_i$  is interrill erodibility;  $I$  is the effective rainfall intensity,  $\text{mm/s}$ ;  $G$  and  $C$  are adjustment factors for ground cover and canopy cover respectively; and  $S$  is a slope adjustment factor.

Rill erosion is the detachment and transport of soil particles by concentrated flowing water. The rill detachment capacity  $D_c$  in WEPP is estimated for clear water as a linear function of the hydraulic shear  $\tau$  in excess of the critical shear stress  $\tau_{\text{crit}}$  required to initiate detachment:

$$D_c = K_r (\tau - \tau_{\text{crit}}) \quad (6.8)$$

where  $K_r$  is rill erodibility. The actual rate of detachment in a rill is diminished as sediment concentration increases within the rill flow. This actual rill detachment rate  $D_r$  is related to the detachment capacity for clear water by:

$$D_r = D_c (1 - G/T_c) \quad (6.9)$$

where  $G$  is the sediment load. Transport capacity  $T_c$  is estimated using an approximation of Yalin's sediment transport equation having the form:

$$T_c = K_t \tau^{3/2} \quad (6.10)$$

where  $K_t$  is the transport coefficient (Finkner et al., 1989).

## 6.11 SEDIMENT DELIVERY RATIO

### 6.11.1 Basic Delivery Ratio Concepts

Models such as RUSLE and WEPP determine erosion rates in small areas, and not the amount of eroded material that is actually delivered to a downstream reservoir. The

sediment delivery ratio represents the fraction of the material eroded from a particular site or watershed which reaches a downstream point where sediment yield is measured. When the term is applied to an entire basin, it represents the ratio of gross erosion within a watershed to the sediment yield during the same period. The delivery ratio may be expressed in either decimal or percentage forms, and values may range from a few percent to nearly 100 percent (Boyce, 1975) with larger delivery ratios generally applying to smaller watersheds with steeper slopes and finer-grained material. Delivery ratios may be computed for any desired time interval.

Determining the sediment delivery ratio is a critical step in converting estimates of soil erosion within a basin into a quantifiable value of sediment yield. The problems associated with estimating delivery ratio have been summarized by Walling (1983). Sediment yield estimate can be highly sensitive to the sediment delivery ratio, as illustrated by Walling (1994) using six watersheds in Nigeria, Mali, and Algeria. Erosion rates from these watersheds ranged from 100 to 1500 t/km<sup>2</sup>/yr, whereas measured sediment yield averaged 211 t/km<sup>2</sup>/yr with a maximum value of 483 t/km<sup>2</sup>/yr. The sediment delivery ratio in these basins was about 10 percent, and a 1 percent error in estimating the delivery ratio would have the same impact on the yield estimate as a 10 percent error in the erosion rate estimate.

### 6.11.2 Causes of Reduced Sediment Delivery

Sediments and associated pollutants mobilized by sheet and rill erosion may be redeposited by a variety of mechanisms prior to reaching stream channels, where transport processes are generally more efficient. Redeposition processes have been summarized by Novotny et al. (1986):

1. Rainfall impact detaches soil particles and maintains them in suspension, but as rainfall intensity declines the excess particles in suspension are deposited.
2. Overland flow detaches and transports particles. The sediment content of overland flow is at or near the saturated state, and the sediment-carrying capacity of overland flow is directly proportional to discharge. As flow is reduced during the receding portion of the hydrograph, excess sediment is deposited.
3. Vegetation retards flow and filters out particles during shallow flow conditions.
4. Infiltration reduces overland flow, causing sediment to be filtered out or deposited.
5. Small depressions, ponding, and retardance by vegetation and litter reduce flow velocity and cause sediment to be deposited.
6. Slope reduction at the base of hillslopes or near channels reduces flow velocity and causes sediment to be deposited.

After flow enters channels there are still opportunities for redeposition, including deposition during periods of overbank flooding, trapping by vegetation, and channel aggradation. Erosion processes on disturbed slopes can deliver sediment to channels faster than it can be transported, resulting in aggradation as described by Laird and Harvey (1986) on burned chaparral lands in Arizona. Sediments may also be stored temporarily on either channel bottom or in channel bars and islands (Miller and Shoemaker, 1986), or in navigational pools and riparian wetlands (Bhowmik, 1988).

Six major factors which influence the long-term sediment delivery ratio from a basin are described below, based on Renfro (1975).

**1. Erosion process.** The delivery ratio will generally be higher for sediment derived from channel-type erosion (including that from roads) which immediately places

sediment into the main channels of the transport system, as compared to sheet erosion.

**2. Proximity to basin outlet.** Sediment delivery will be influenced by the geographic distribution of sediment sources within the basin and their relationship to depositional areas. Sediment is more likely to be exported from a source area near the basin outlet as compared to a distant sediment source, since sediment from the distant source will typically encounter more opportunities for redeposition before reaching the basin outlet.

**3. Drainage efficiency.** Hydraulically efficient channel networks with a high drainage density will be more efficient in exporting sediment as compared to basins having low channel density, meandering low-gradient channels, or channels clogged with debris. Concrete-lined urban drainage systems have a sediment delivery ratio near 100 percent unless sediment-trapping structures (e.g., debris basins) are included in the design.

**4. Soil and cover characteristics.** Finer particles tend to be transported with greater facility than coarse particles, resulting in a higher delivery ratio for soils which produce fine-grained erosion particles. Because of the formation of particle aggregates by clays, silts tend to be more erosive and produce higher delivery ratios than clay soils.

**5. Depositional features.** The presence of depositional areas, including vegetation, ponds, reservoirs, and floodplains, will decrease the delivery ratio. Most eroded sediment from large watersheds may be redeposited at the base of slopes, as outwash fans below gullies, in channels, or on floodplains. Broad valleys with meandering streams may trap considerable sediment, and there may be field evidence of channel, channel bank, and floodplain aggradation. Wilkins and Hebei (1982) reported that non-cultivated areas of natural or forest vegetation at field borders often serve as highly efficient sediment traps, despite relatively steep slopes. Conversely, in narrow steep mountain valleys with gravel-bed channels, there may be limited opportunity for sediment redeposition and the sediment delivery ratio for fine sediment in such environments may approach unity once the eroded particle enters a channel.

Widespread use of conservation measures, such as terraces, farm ponds and grass filter strips will increase sediment trapping. Reservoirs can be highly efficient sediment traps which will influence the sediment delivery ratio. In a study of paired 180-km<sup>2</sup> basins in Wales, Great Britain, receiving 1500 to 1800 mm of annual precipitation, Grimshaw and Lewin (1980) concluded that reservoir construction reduced sediment yield by an order of magnitude as a result of sediment trapping, plus the effect of flow regulation which reduced both peak discharge and bed material transport in the channel below the dam.

**6. Watershed size and slope.** A large, gently sloping watershed will characteristically have a lower delivery ratio than a smaller and steeper watershed. From an evaluation of 252 sites in the urbanizing Anacostia watershed north of Washington, D.C., Coleman and Scatena (1986) concluded that whereas erosion is controlled principally by land use, the transport of sediment from erosion sites to stream channels is controlled principally by local topography and buffer vegetation.

Field observation of floodplains and stream channels, combined with documentary, photographic, and oral historical information, can help to indicate the long-term patterns of sediment accumulation or erosion in valleys. This information, combined with measured delivery ratio data from similar watersheds, can aid in determining a reasonable delivery ratio value.

### 6.11.3 Measurement

The sediment delivery ratio cannot be measured directly because gross erosion is never measured in a watershed; erosion rate is extrapolated from smaller plots or computed from modeling. Thus, *sediment delivery ratio* is actually the ratio of measured yield to the estimated erosion rate based on USLE or some other erosion prediction methodology. Delivery ratios much greater than unity have been reported by some researchers, and reflect the inability of erosion prediction models to account for all the erosion processes upstream of the point of yield measurement.

To the extent that the erosion estimate is changed by applying different methodologies, the delivery ratio will be affected. This may be illustrated by the following scenario. Consider a delivery ratio computed in a gaged watershed where the erosion rate has been determined by using the USLE model. Subsequently this same delivery ratio is applied to a similar-sized ungaged watershed where the erosion rate is estimated by a different technique, producing erosion estimates significantly different from what USLE would have predicted. The resulting sediment yield estimate will be biased because the sediment delivery ratio actually gives the relationship between USLE-predicted erosion and measured sediment yield, not the relationship between the erosion rate predicted by the new model and the sediment yield. The potential for difficulties in estimating soil loss over large areas was underscored by McIntire (1993), who stated that two studies in Mexico, which used the same basic dataset but different methodologies, arrived at two very different estimates of the average national rate of soil loss: 270 versus 4700 t/km<sup>2</sup>/yr.

### 6.11.4 Variation in Delivery Ratio

Values of delivery ratio can vary widely, and in large watersheds can be surprisingly low. Trimble (1974, 1977) examined erosion and sediment delivery from 10 large (2650 to 19,400 km<sup>2</sup>) river basins in the Piedmont region in the southeastern United States covering the period 1760 to present. The Piedmont area is a gently sloping region about 250 km wide and 1200 km long, lying at elevations from about 100 to 500 m between the Atlantic coastal plains and the Blue Ridge Mountains. It was an area of extensive cultivation, erosive land use, and high rates of soil loss from the mid-1800s to the 1930s. Although soil loss amounted to about 95 mm of denudation per century, the sediment yield was only 5.3 mm per century, equivalent to a sediment delivery ratio of 5.6 percent per century. Because the transport capacity of the stream network was low in relation to the sediment load applied by accelerated erosion, most of the eroded material was deposited as colluvial deposits at the base of slopes, as alluvial deposits on flood-plains, or as channel deposits. A similar study covering the 1853 to 1938 period in the Wisconsin Driftless area produced a long-term sediment delivery ratio of 6 percent (Trimble, 1981).

Two examples of the effect of sediment storage in valley streams and floodplains were described and photographed by Trimble (1974). In the Middle Oconee River, Georgia, sediment deposition in the channel caused overflow and a rising water table, making the adjacent bottomland too wet to farm. Ditching was ineffective, since the channel quickly refilled with eroded sediment. In Hall County, Georgia, a 3.6-m-tall mill dam built around 1865 had become completely buried beneath more than a meter of channel sediment by 1930, and the growth of natural levees by sediment deposition from the river had elevated riverbanks by 3 m. As a result of decreased upland erosion and sediment supply, the stream channel began degrading in 1955, and by 1972 the top meter of the dam was again exposed. In summary, this stream aggraded nearly 5 m during a 90-year period, and then degraded by 2 m over the subsequent 20 years.

Happ (1975) concluded that valley sedimentation may account for as much as 75 percent of the sediment yield in some agricultural watersheds, and illustrated the rapid aggradation of a valley floor caused by the redeposition of eroded sediment using data from the Whitewater River (Fig. 6.14). When upland sources of erosion are reduced, aggraded channels will begin to incise and slowly export the accumulated sediments. However, eroded sediments that have deposited outside the area affected by channel erosion may not be remobilized.

Under some circumstances, low sediment delivery ratios can occur even in very small watersheds. Whitelock and Loughran (1994) examined a 14.1-ha urbanizing basin and computed total erosion for the 1954 to 1991 period as 714 t and 832 t using the  $^{137}\text{cesium}$  and USLE methods respectively. From  $^{137}\text{cesium}$  dating of channel sections in the stream draining the watershed, it was determined that the accumulation of coarse material accounted for 571 t of the eroded sediment, and the amount of sediment actually exported from this small basin represented a sediment delivery ratio of 20 to 31 percent, depending on the erosion estimate used.

The sediment delivery ratio can vary dramatically over both long and short time spans. Long-term changes will occur as a result of changing land use and the construction and operation of upstream reservoirs. As long as reservoirs are trapping sediment, the downstream sediment yield and the delivery ratio will be reduced. However, when reservoir operation is changed to release sediment, or as the total storage capacity becomes filled up with sediment, the delivery ratio downstream of the reservoir will increase.

Sediment delivery ratio can vary dramatically from one event to another, even from a small area. This may be illustrated using 7 years of data reported by Piest et al. (1975a) from two Iowa watersheds about 30 ha in area, contour-planted in corn. Average annual values of sediment delivery ratio varied from 4 to 67 percent in one watershed and 6 to 61 percent in the other. The delivery ratios computed for 55 individual events over the 7-yr period reflected even more dramatic variation. For instance, one 14-mm rainfall in May produced a delivery ratio of 554 percent, while a 17-mm July rainfall, in another year in the same watershed, produced a delivery ratio of only 1 percent. Seasonal change in crop cover is a major factor causing these extreme variations. Delivery ratios in excess of 100 percent were reported for 24 of the 55 events, reflecting the limited ability of USLE to predict total erosion from individual runoff events.

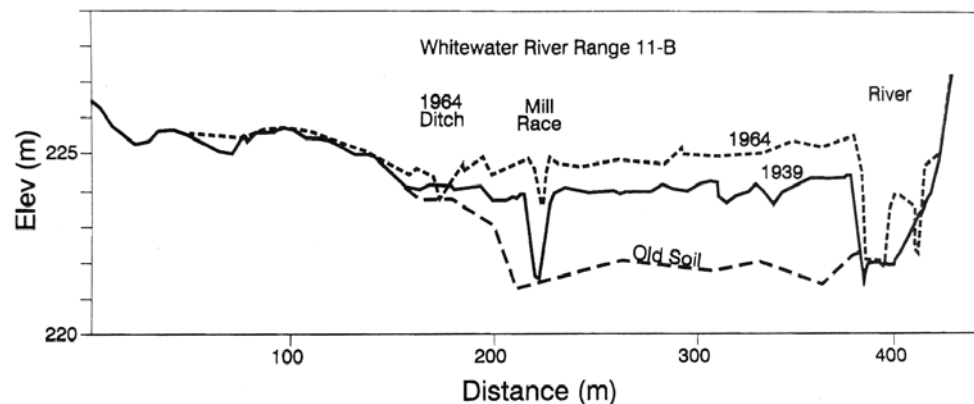


**FIGURE 6.14** Sediment redeposition and valley floor aggradation on the floodplain of Whitewater River, Minnesota, due to accelerated upland erosion (Happ, 1975).

### 6.11.5 Estimating Sediment Delivery Ratio

While established methods are available for estimating the rate of erosion from farm-size areas, there is no generally accepted method for determining the percentage of eroded sediment that will be delivered to the basin outlet. Haan et al. (1994) pointed out that the degree of understanding of sediment delivery ratios is probably less than any other area of sedimentation.

Within some physiographic regions, a power relationship may be developed between delivery ratio and basin area which plots as a straight line on log-log paper. For example, the dataset presented by Renfro (1975) for the Blackland Prairie area in Texas produces an equation for percent sediment delivery ratio (SDR) in the form  $SDR = 62.1 (\text{area})^{-0.1419}$  for areas from 1 to 250 km<sup>2</sup>. Boyce (1975) stated that the relationship of sediment-yield to drainage area usually differs from the sediment-delivery to drainage area relationship by only a constant, and summarized several relationships for sediment delivery ratio (Fig. 6.15). In regions having uniform landforms and the data required to construct a regional relationship, this can represent a reliable approach available for estimating sediment delivery. However, generalized delivery ratio versus area curves do not take into account topographic, geologic, climatic, land use, and other differences that affect delivery ratios, and caution must be used to apply these relationships only to landscapes similar to those for which the relationship was developed. When estimating sediment yield based on delivery ratio data from other watersheds, compare conditions in the watersheds to look for conditions such as reservoirs (including farm ponds) which may significantly influence delivery ratios. Where an upstream reservoir is present, the sediment delivery may be computed to the reservoir, and the sediment discharge below the reservoir computed on the basis of sediment release efficiency determined from the Brune curve. Problems will arise if this method is used to assign delivery ratios to sub-watersheds, since the sum of the delivered sediment from the sub-watersheds will exceed that computed for the entire basin.

Some researchers have estimated delivery ratios based on a description of channel or land use conditions. In the Ryan Gulch basin in northwestern Colorado, a semiarid undeveloped watershed receiving 330 to 510 mm of average annual rainfall moving from an elevation of 1860 to 2620 m, Hadley and Shown (1976) developed the sediment delivery ratios given in Table 6.5. For a suburban basin in Wisconsin, Novotny et al. (1979) presented the delivery ratio guidelines given in Table 6.6.

The U.S. Forest Service (1980) has developed a method to estimate sediment delivery ratio for a single storm based on USLE/RUSLE estimates of erosion, using the stiff diagram shown in Fig. 6.16. The surface runoff term (ft<sup>3</sup>/s/ft) represents peak discharge per unit of slope width. The texture of eroded material is expressed as the percentage that is smaller than sand. Ground cover factor is the percentage ground cover between the erosion source and the nearest channel and includes both living plants and litter, with a value of zero corresponding to bare soil. The slope shape between the source area and the nearest channel is defined as 0 for a convex slope, and 4 for a concave slope, which has a greater tendency to trap sediment. Delivery distance is measured from the source area to the channel. Surface roughness values for the soil are assigned on a subjective basis with using 0 for a smooth surface and 4 for a very rough surface. Slope gradient is the average slope from the source area to the nearest channel. After all the values have been plotted on each axis, the plotted points are connected to form a polygon and the percentage of the total area of the rectangle contained within the polygon is measured. This percentage area from the stiff diagram is applied to the curve in Fig. 6.17 to determine the sediment delivery ratio. This procedure applies only to the sheet erosion processes predicted by the USLE/RUSLE model for small land management units. Channel erosion, including roads, is often the primary erosion source in forests and must be analyzed separately, as

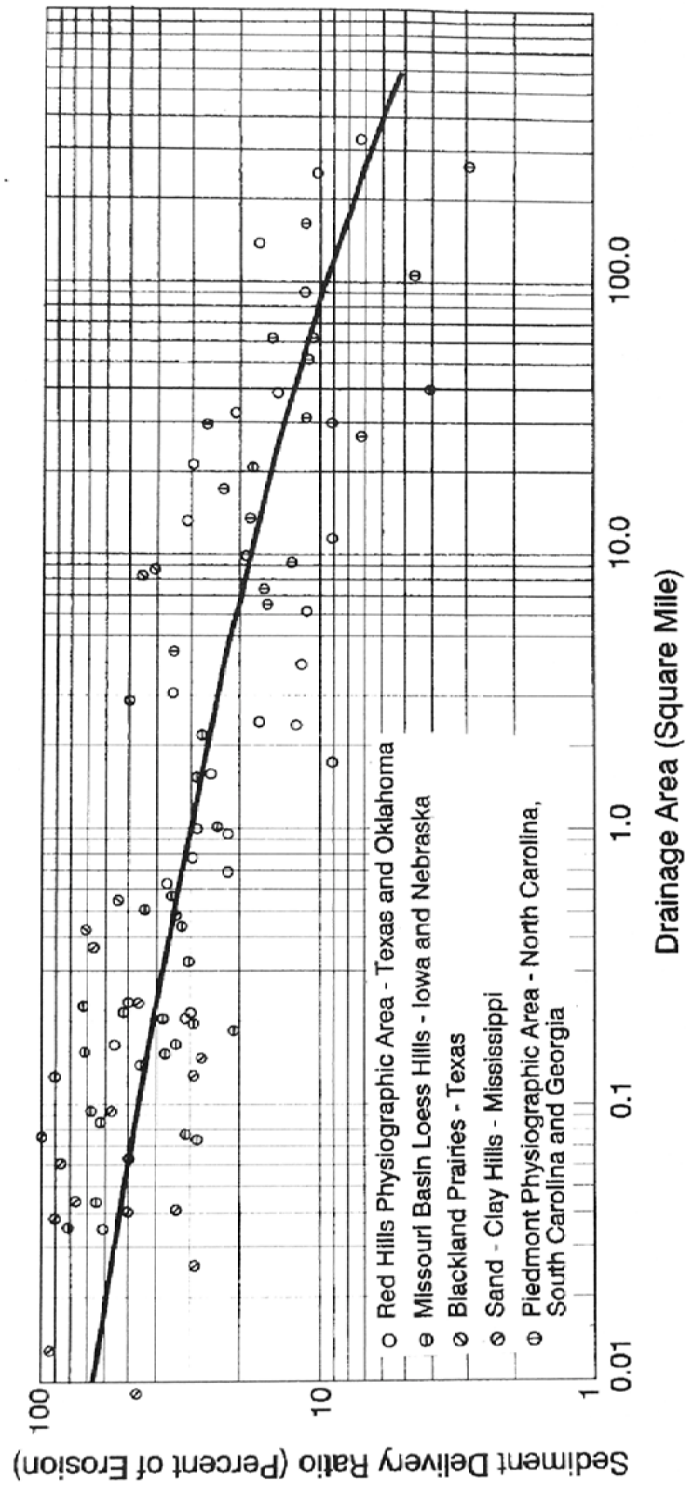


**FIGURE 6.15** Sediment delivery ratios from selected areas in the United States (Boyce, 1975).

**TABLE 6.5** Guidelines for Evaluating Relative Sediment Delivery in Ryan Gulch basin, Colorado

Delivery ratio	Channel condition
1.0	Unvegetated gullies with no deposition
0.75	Unvegetated gullies with sediment deposits
0.5	Gullies healed with vegetation indicating shallow flows
0.3-0.5	Channels, intermittent gullies
0-0.4	Shallow, vegetated, ungullied, or braided channels with evidence of deposition such as active alluvial fans or sediment deposits on bottomlands where flows spread naturally or are used for irrigation.

*Source:* Hadley and Shown (1976).

**TABLE 6.6** Sediment Delivery Ratios Estimated for Land Uses in Menomonee River Basin, Wisconsin

Sub-basin type	Impervious area	Degree of storm sewerage, %	Sediment delivery ratio, %
Agricultural	<5	0	1-30
Developing-construction	<5	20-50	20-50
Low-density residential, unsewered	<20	0	<10
Parks	<10	0	<3
Medium-density residential, partially sewerage	30-50	<50	30-70
Medium-density residential, sewerage	30-50	>50	70-100
Commercial, high-density residential, sewerage	>50	80-100	100

*Source:* Novotny et al. (1979).

well as downstream deposition processes in channels and floodplains. Erosion rates reported from unsurfaced roads are given in Table 6.7.

### 6.11.6 Sediment Sorting and Enrichment

Use of a single delivery ratio value obscures the complex processes involved in the transport and sorting of sediment from the source area, through the basin, and into a reservoir. These processes not only produce wide spatial and temporal variability in the rate at which eroded sediment is delivered to a downstream point, but through selective transport and deposition, the character of the transported material also changes as compared to the erosion source (Walling, 1983). The selective erosion and transport of the finer-grained material, and preferential deposition of the larger grains, causes eroded

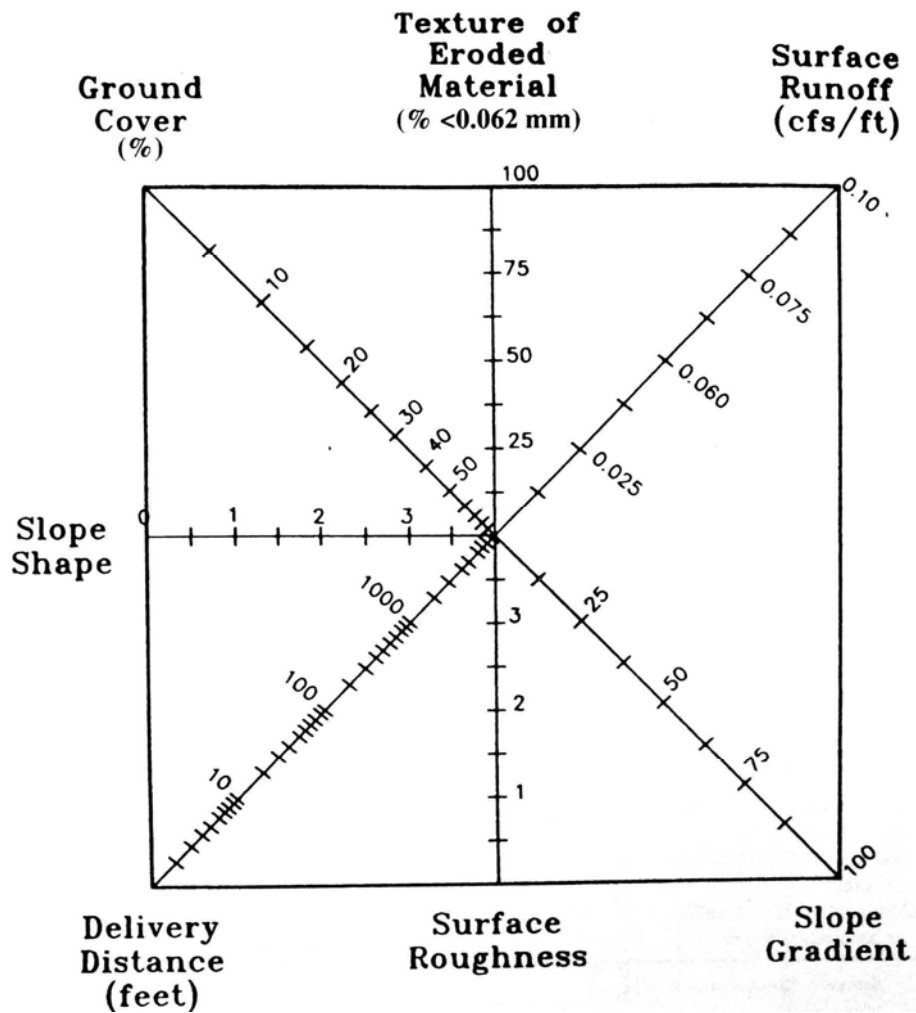


**FIGURE 6.16** Stiff diagram (used with Fig. 6.17) to estimate sediment delivery in forested areas from the USLE model (U.S. Forest Service, 1980).

sediment to become enriched with respect to the clay fraction and the associated organics, nutrients, and contaminants as compared to the erosion source. The *enrichment ratio* of a given constituent is the ratio of concentration in the eroded material and its concentration in the source material. The enrichment ratio may be either greater or less than unity, and for any constituent the enrichment ratio and delivery ratios tend to be inversely related (Fig. 6.18). As a result of enrichment, the sediment delivered to a reservoir tends to be finer than the material at the point of erosion.

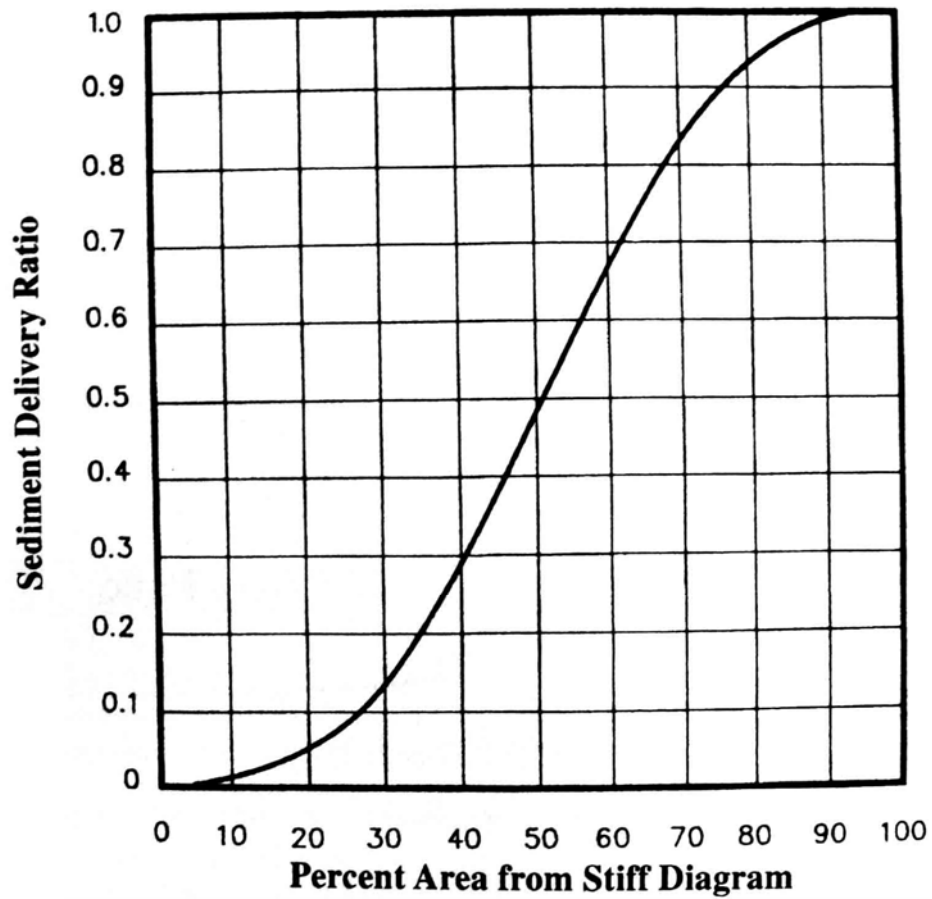


**FIGURE 6.17** Conversion curve, to be used in conjunction with the stiff diagram in Fig. 6.16 for estimating sediment delivery to channels, from erosion rates estimated in forested areas using the USLE model (U.S. Forest Service, 1980).

**TABLE 6.7** Erosion Rates Reported for Unsurfaced Roads

Location	Approximate erosion rate, t/km <sup>2</sup> road surface/yr
Idaho	2,000
Southeastern United States	800-12,000
Coweeta, North Carolina	3,700
California	2,500
Washington, use-dependent	300-66,000

Source: Ward (1985).

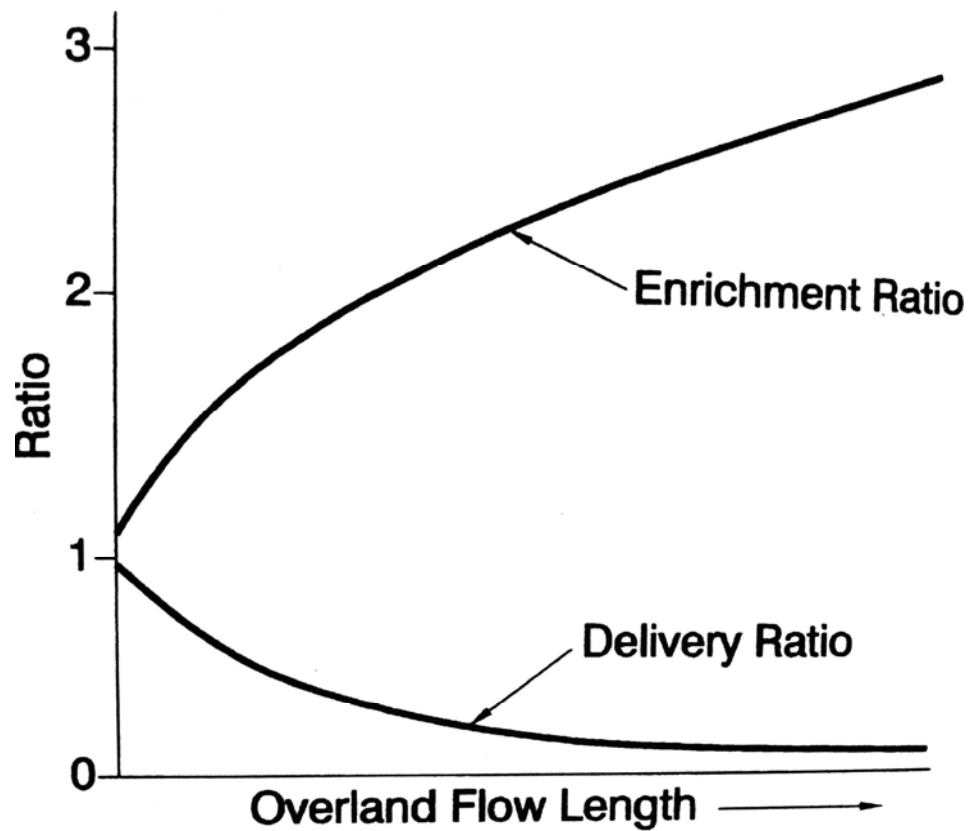


*FIGURE 6.18 Sediment delivery and sediment enrichment (after Novotny and Olem, 1994).*

## 6.12 CLOSURE

Erosion processes are complex and can vary dramatically in both space and time. Existing erosion prediction techniques can provide reasonable estimates of long-term erosion rates for different land uses. However, prediction of single-event erosion and sediment delivery from complex watersheds is less reliable. Prediction of the sediment delivery ratio remains the most uncertain step in the estimation of sediment yield based on erosion models.

---

## CHAPTER 7

---

# SEDIMENT YIELD FROM WATERSHEDS

---

*Sediment yield* refers to the amount of sediment exported by a watershed basin over a period of time, which is also the amount which will enter a reservoir located at the downstream limit of its tributary watershed. The *specific sediment yield* is the yield per unit of land area. The correlation of sediment yield to erosion is complicated by the problem of determining the sediment delivery ratio, which makes it difficult to estimate the sediment load entering a reservoir on the basis of the erosion rate within the watershed. This underscores the need to monitor sediment yield with fluvial gage stations and sediment surveys in reservoirs.

Estimates of long-term sediment yield have been used for many decades to size the sediment storage pool and estimate reservoir life. However, these estimates are often inaccurate, and many reservoirs have accumulated sediment more rapidly than originally planned. Most sediment is exported from watersheds during relatively short periods of flood discharge, and these events must be accurately monitored to provide information on the long-term yield as well as the timewise variation in load needed to evaluate sediment routing strategies. Knowledge of the spatial variation in yield is required to focus yield reduction efforts on the landscape units that deliver most sediment to the reservoir. Long-term trends in sediment yield occurring over a period of decades may also influence sediment management in reservoirs.

This chapter describes fundamental concepts of sediment yield, emphasizing the variable nature of yield over both time and space and monitoring strategies which are useful to document both the variability and long-term magnitude of the sediment load entering a reservoir. Sediment sampling techniques are discussed in Chap. 8, and methods for reducing sediment yield are presented in Chap. 12.

---

### 7.1 SPATIAL VARIABILITY IN SEDIMENT YIELD

---

The process of erosion and the delivery of sediment to the exit of a basin is never a spatially uniform process. When virtually any landscape unit is examined, at any scale, there will typically be large variations in the specific sediment yields. The large variability in specific sediment yield worldwide was summarized by Jansson (1988) in an analysis of suspended sediment data from 1358 gaging stations with tributary watersheds between 350 and 10,000 km<sup>2</sup>, and totaling 16 × 10<sup>6</sup> km<sup>2</sup> of land area. Stations were divided in six yield classes (Table 7.1). The highest yield class, with specific sediment yields exceeding 1000 t/km<sup>2</sup>/yr, represented only 8.8 percent of the total land area in the global dataset but contributed 69 percent of the total sediment load. In contrast, basins with specific yields less than 50 t/km<sup>2</sup>/yr constitute nearly half the total land area but contributed only 2.1 percent of the total sediment yield.

**TABLE 7.1** Worldwide Sediment Yield

Yield class, t/km <sup>2</sup> /yr	Number of gage stations	Percent of gaged land area	Percent of total gaged load
0-10	230	21.3	0.3
11-50	285	25.6	1.8
51-100	172	11.9	2.1
101-500	426	25.6	14.7
501-1000	145	6.9	21.0
>1000	179	8.8	69.1

*Source: Jansson (1988)*

Extremely high sediment yields, in the range of 10,000 to 50,000 t/km<sup>2</sup>/yr, have been reported at some stations in China, Java, Kenya, New Guinea, and New Zealand (Walling, 1994). Taiwan discharges more sediment to the ocean per unit of land area than any area of the world. Streams draining the Central Range of Taiwan produced average suspended-sediment yields of 13,760 t/km<sup>2</sup>/yr, and one small basin exported 31,700 t/km<sup>2</sup>/yr of suspended sediment (Li, 1976). Taiwan's total sediment discharge to the ocean is nearly 5 times larger than the sediment discharge from the entire continent of Australia, although the area of Australia is 210 times larger. Australian discharge is low because it is mostly desert which does not discharge to the ocean. Extremely high sediment yields in Taiwan, Philippines, Indonesia, New Guinea, and New Zealand reflect active tectonism and volcanism, steep slopes, heavy rainfall, and soil disturbance by agriculture and logging (Milliman and Meade, 1983). In contrast, extremely low long-term (e.g., 1000-year) sediment yields of 2 t/km<sup>2</sup>/yr have been documented in small undisturbed alpine catchments with erosion-resistant granitic parent material (Owens and Slaymaker, 1994).

The world's largest rivers in terms of sediment discharge are summarized in Table 7.2. The high-yielding Yellow River in China drains extremely erosive loess soils, and the Ganges/ Brahmaputra drains the tectonically active and glaciated Himalayas. Human disturbance is also important in both basins. Areas with extremely low sediment yield

**TABLE 7.2** Ranking of the World Rivers by Sediment Load Discharged to the Ocean

River and country	Average sediment discharge, 10 <sup>6</sup> t/yr
1. Ganges/Brahmaputra, India	1670
2. Yellow, China	1080
3. Amazon, Brazil	900
4. Yangtze, China	478
5. Irrawaddy, Burma	285
6. Magdalena, Colombia	220
7. Mississippi, United States	210
8. Orinoco, Venezuela	210
9. Hungo (Red), Vietnam	160
10. Mekong, Thailand	160

include streams draining flat areas, arid areas with inadequate streamflow to transport large sediment volumes, and arctic regions which usually have low relief, little precipitation, and low human impact. Sediment trapping by dams can have a large impact on sediment discharge, even in large rivers. The pre-impoundment Colorado River transported  $135 \times 10^6$  t/yr through the Grand Canyon, and the pre-impoundment Nile discharged  $100 \times 10^6$  t/yr, but because of sediment trapping at upstream dams both rivers now discharge negligible amounts of sediment (Milliman and Meade, 1983). Both the Nile and the Mississippi River deltas are now being eroded because of sediment trapping by upstream dams.

Geology, slope, climate, drainage density, and patterns of human disturbance all affect sediment yield, and no single parameter or simple combination of parameters explains the wide variability in global yields. Using data from 61 gage stations in southern Kenya, Dunne (1979) demonstrated that land use is a dominant factor explaining variability in sediment yield. Several researchers have correlated sediment yield to precipitation, and a sample of these relationships is summarized in Fig. 7.1. General relationships can be observed within some specific geographic regions, such as the relationships for the conterminous United States developed by Langbein and Schumm (1958) from gage station data, and by Dendy and Bolton (1976) based on resurvey data in 800 reservoirs. Within the 48 states, yield from drier areas tends to be limited because of low runoff and yield in wetter areas is limited by the protective soil cover and reduced erodibility of humid zone soils. However, such relationships are highly generalized and do not reflect the wide scatter in the underlying data, and they cannot be extended to other geographic areas. For instance, the Langbein-Schumm relationship breaks down if extended to include all of North America, since the low-precipitation areas of tundra in northern Canada and Alaska have extremely low sediment yields. On a global basis, there is no apparent relationship between precipitation and specific sediment yield. However, sediment concentrations in arid zone rivers tend to exceed concentrations in humid zones. That this does not cause an increase in sediment yield from arid regions is attributed to the reduced discharge volume.

The wide variation in specific sediment yield in the global dataset is also reflected at all levels of analysis: national, regional, and within-watershed. Regional comparisons of specific sediment yields using gaged watersheds showed that yields varied by a factor of 500 in Thailand (Jantawat, 1985), 800 in South Africa (Rooseboom, 1992), 400 in Kenya (Dunne, 1979), and 70 in Zimbabwe (Van Den Wall Bake, 1986). Sediment yields for selected physiographic regions in the United States (Fig. 7.2) illustrate both the variation between regions as well as the wide variation of measured rates within regions.

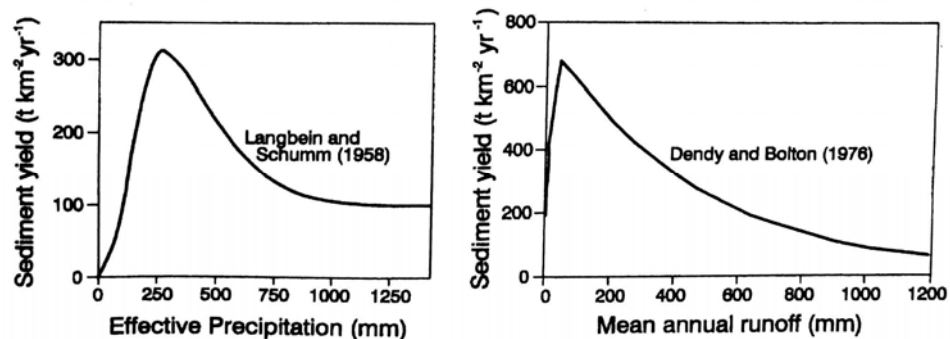


**FIGURE 7.1** Relationships between sediment yield and rainfall development for the conterminous United States.

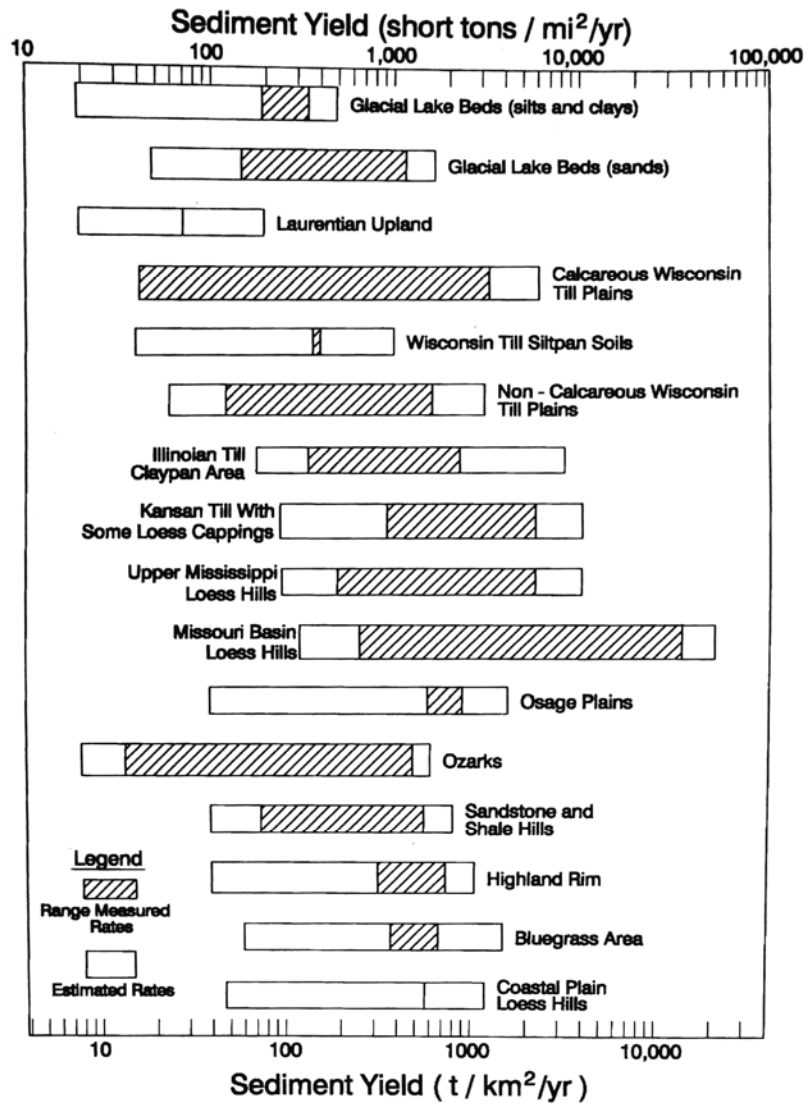


FIGURE 7.2 Comparative sediment yields in selected areas of the United States (Vanoni, 1975).

Within a single watershed only a small fraction of the landscape is usually responsible for a large percentage of the sediment yield. Dividing total sediment discharge by total basin area to determine the average yield can be grossly misleading because it masks the underlying variability in sediment yield from individual sub-watersheds or land parcels (Campbell, 1985). Dramatic variations in sediment yield can occur even within small watersheds, especially when subject to disturbance, as illustrated in a 4.0 ha mountain watershed in Idaho studied by Megahan (1975). Logging increased sediment yield from the watershed by a factor of 150 compared to undisturbed conditions. However, erosion rates were accelerated by a factor of 550 on logging roads affected by mass wasting and only 1.6 on forest soils with disturbance limited to tree falling and skidding (Table 7.3). The increase in sediment yield from the watershed reflected the presence of limited land areas with a high sediment yield rather than a general increase in sediment yield across the entire landscape. To be effective, control efforts must be focused on the high-yield areas.

**TABLE 7.3** Mean 6-Year Sediment Production from Surface and Mass Erosion Caused by Logging

Type of disturbance	Sediment yield, m <sup>3</sup> /km <sup>2</sup> /yr	Ratio to undisturbed land
Undisturbed land	42	1
Average for disturbed watershed	6,325	155
Sub-watershed by type of disturbance:		
Tree felling and log skidding only	65	1.6
Roads (surface erosion)	8,966	220
Roads (mass erosion)	22,417	550

Source: Megahan (1975)

## 7.2 TEMPORAL VARIABILITY IN SEDIMENT YIELD

### 7.2.1 Temporal Focusing of Sediment Yield

Being the product of discharge and solids concentration, sediment yield exhibits greater variability and is more focused in time than streamflow. For example, a stream draining disturbed hilly lands may experience a thousand-fold increase in both sediment concentration and liquid discharge between minimum and peak flow. This will cause a million-fold increase in the instantaneous rate of sediment discharge if both concentration and discharge peak simultaneously. Under these conditions the sediment load during 15 minutes of peak discharge will equal the sediment load during 28 years of low flow.

Extreme variability in sediment yield has been reported by a number of workers. Milliman and Meade (1983) cited the case of the 4100-km<sup>2</sup> Santa Clara River basin in Southern California which discharged  $50 \times 10^6$  t of sediment during a single flood event in 1969, more than 700 times the measured average annual load of  $69 \times 10^3$  t/yr. Grant and Wolff (1991) reported on a 30-year study in three experimental forest watersheds totaling 4.3 km<sup>2</sup> in the Cascade Mountains of Oregon, selected for their proximity and similarities in size, aspect, and topography. The forest receives about 2300 mm/yr of precipitation and was dominated by old-growth Douglas fir. Watersheds 1 and 3 were logged between 1962 and 1966, and watershed 2 was a control. Cumulative sediment yield as a function of time is shown in Fig. 7.3, illustrating the effect that a large storm can have on the pattern of long-term yield. Slope failures in watershed 3 resulted in the delivery of 88 percent of the 30-year sediment yield during a single event, probably within only a few hours. About 90 percent of this material originated from logging roads.

High temporal variability in sediment transport is a general feature of river systems worldwide. For rivers in the United States, Meade and Parker (1984) have shown that 50 percent of the annual sediment load is discharged in only 1 percent of the time, and 90 percent of the load is discharged in only 10 percent of the time. A similar concentration in time was reported by Walling and Webb (1981) on the basis of continuous measurements in River Creedy near Devon, United Kingdom, and by Summer et al. (1994) for the Danube River in Austria. The cumulative sediment load ranked as a function of either time or discharge can be represented on a semilog plot similar to Fig. 7.4.

### 7.2.2 Within-Storm Variation in Suspended Load

Suspended solids concentration will usually vary widely over the duration of a runoff event. The timewise variation in suspended sediment concentration and discharge during

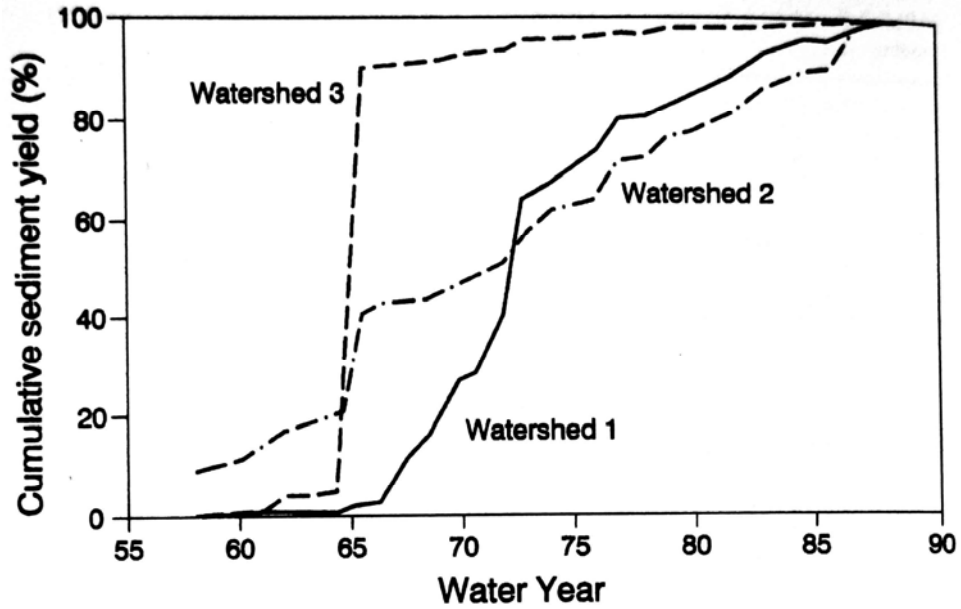


FIGURE 7.3 Cumulative sediment yield with time three small forest watersheds, showing the dramatic impact of slope failures and debris flows in watershed 3 caused by a single storm during the 30 year period (after Grant and Wolff, 1991).

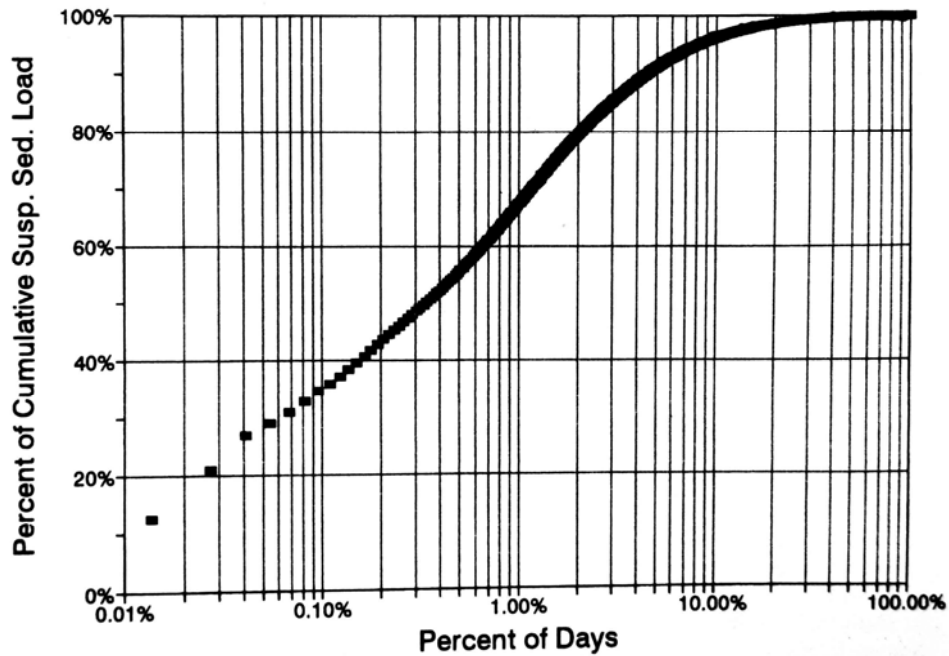
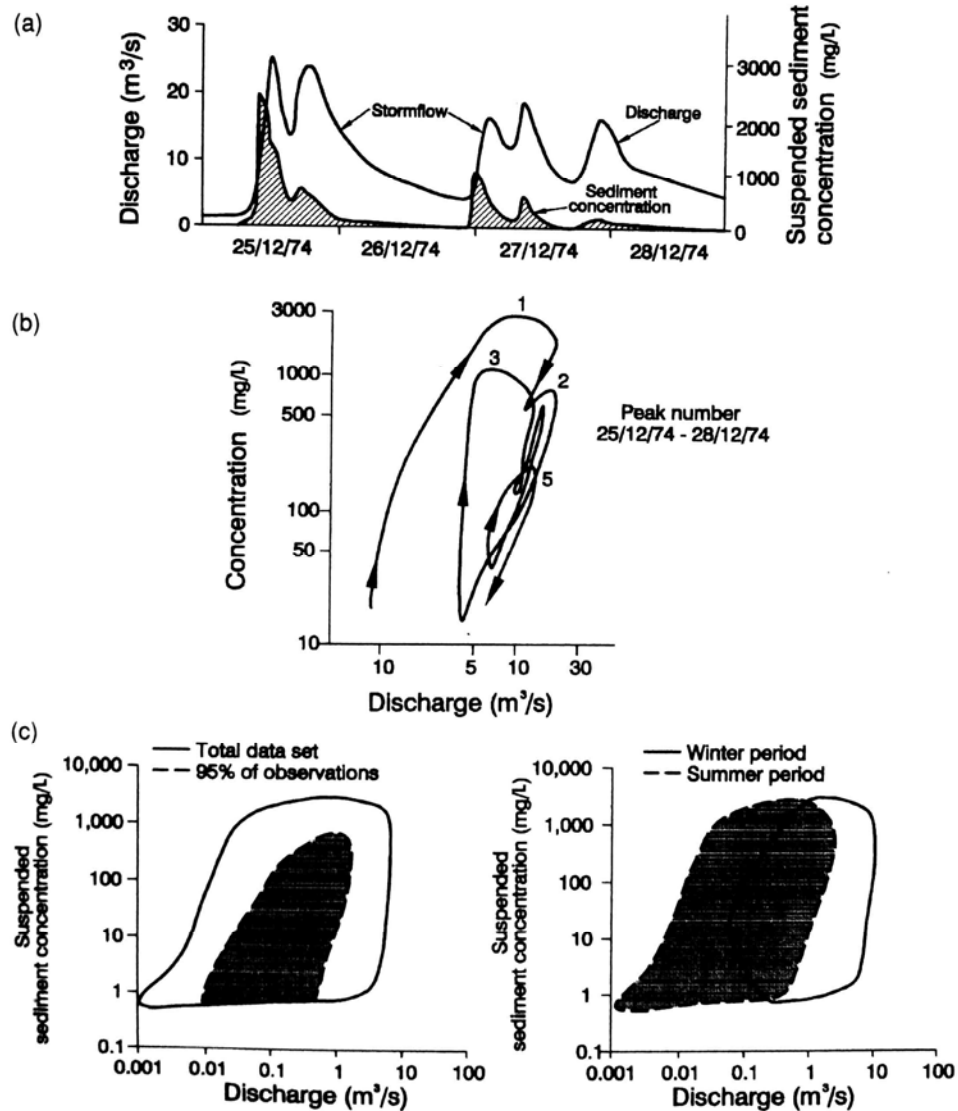


FIGURE 7.4 Ranked cumulative sediment yield from Río Tanamá, Puerto Rico, as a function of time, illustrating the timewise focusing of sediment discharge. Only 1 percent of the days account for 67 percent of the sediment discharge over the 21-year sediment discharge record. Sediment discharge would have been even more tightly focused in time had hourly rather than daily data been available for preparation of this plot (prepared from USGS daily data).

a multiple-peak event is illustrated in Fig. 7.5a, showing the reduction in concentration during subsequent peaks due to exhaustion of sediment supply. The concentration  $C$  and discharge  $Q$  data pairs from this event are plotted in Fig. 7.5b in the form of an event  $C$ - $Q$  graph with a clockwise loop. When concentration and discharge data pairs from many events are superimposed they create a scatter plot (Fig. 7.5c) of the type commonly used to construct sediment rating curves. Note that a better fit is obtained when the period-of-record  $C$ - $Q$  data are subdivided into seasonal datasets. The degree of scatter illustrated in the rating curve is typical of conditions in many streams.



**FIGURE 7.5** Suspended sediment and discharge relationships for River Dart, United Kingdom (after Walling and Webb, 1988). (a) Timewise variation in discharge and concentration showing sediment exhaustion over this multiple peak storm. (b) Multiple clockwise loops in the  $C$ - $Q$  graph resulting from sediment exhaustion. (c) General shape of  $C$ - $Q$  relationship incorporating instantaneous data from multiple storms.

Williams (1989) has classified single event  $C-Q$  graphs into five categories:

Name	Characteristic	Occurrence
Class I	Single-value line	Rare
Class II	Clockwise loop	Common
Class III	Counterclockwise loop	Common
Class IV	Single line plus loop	Rare
Class V	Figure Eight	?

The form of each class is illustrated in Fig. 7.6, showing the basic relationship between the timewise variation in discharge and sediment concentration, and the resulting single-event  $C-Q$  graph configuration.

If sediment concentration varies directly as a function of discharge, then it will be possible to construct a single-value relationship relating sediment concentration (and sediment load) to water discharge. This condition is represented by the Class I curve in which discharge and concentration rise and fall simultaneously, and, when skewed, both discharge and concentration are symmetric. The Class I curve implies uninterrupted sediment supply through the flood, and sediment concentration should be directly related to hydraulic factors alone. This condition is not typical; the temporal graphs of water and sediment discharge in most field data are not symmetric. However, most sediment rating curves are constructed by using one or several single-value functions.

The Class II, or clockwise hysteresis loop, is well-known and occurs commonly. This pattern usually occurs when sediment concentration peaks before discharge, but under certain conditions a clockwise loop can occur when the concentration and discharge peaks occur simultaneously. Clockwise  $C-Q$  loops may be attributed to three causes: (1) The readily erodible material in the watershed or the sediment accumulated in the channel since the previous flood is washed out prior to the storm peak, and sediment load becomes increasingly supply limited over the duration of the event. (2) Sediment supply available from the bed may become limited prior to the peak discharge because of the development of an armor layer. (3) Variations in rainfall and erodibility across the watershed can concentrate sediment discharge from areas of high sediment production near the basin outlet during the rising limb of the hydrograph. Some methods of routing sediment through reservoirs take advantage of clockwise loops, passing, sediment-laden water through the impoundment during the rising limb of the hydrograph, and storing the clearer water from the falling limb. In urban water-quality detention basins, the opposite effect is desired: sediment-laden first-flush water from the rising limb is captured while cleaner water from the remainder of the storm is discharged to the environment.

Class III  $C-Q$  relationships, counterclockwise loops, may also be attributed to three causes. (1) In longer rivers the change in discharge tends to increase as a function of wave velocity, which is generally faster than the mean flow velocity of the stream (which is also the transport velocity of the sediment), causing sediment to lag increasingly behind the discharge peak as the flood wave moves downstream. This difference is magnified when floods pass through lakes or other detention areas which can have high wave velocities but slow sediment movement. (2) High soil erodibility in conjunction with prolonged erosion during the flood, including gully erosion, have been reported to cause counterclockwise loops in erodible loessal soils. (3) Variability in rainfall and erodibility across the watershed can cause high sediment discharge from distant portions of the watershed to arrive during the declining limb of the hydrograph. The complex Class IV pattern combines causal factors associated with Classes I and either II or III.

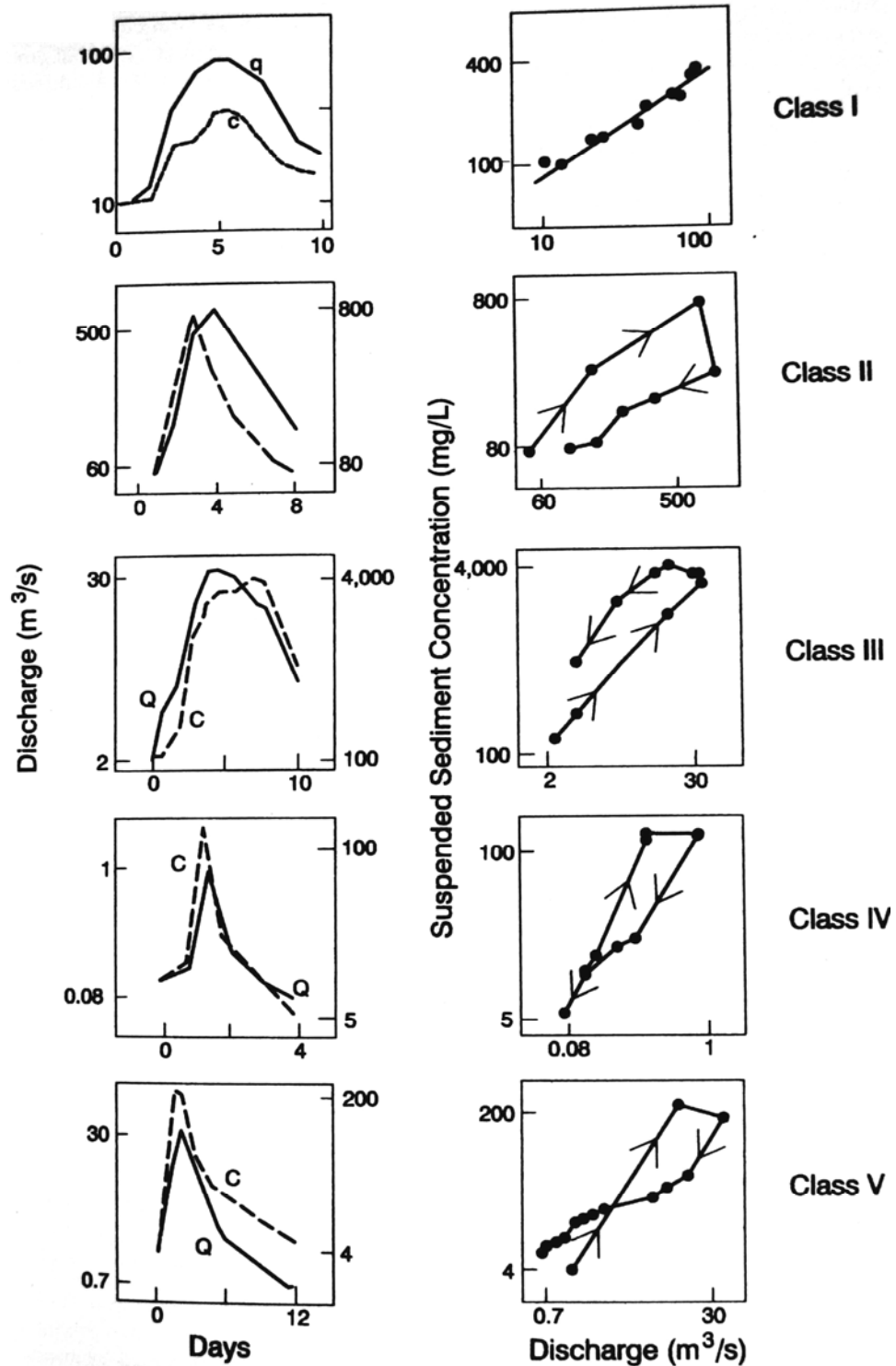


FIGURE 7.6 Concentration-discharge (C-Q) graphs (after Williams, 1989) illustrating relationships between discharge and concentration observed in storm hydrographs. The temporal graphs are arithmetic plots and the C-Q relationships are log-log plots.

Class V, a figure-eight loop, combines features of both clockwise and counter-clockwise loops, with the key feature being that relatively high sediment concentrations must be sustained while discharge drops. Under some conditions, a sediment peak preceding the discharge peak can produce a figure-eight pattern.

The  $C-Q$  relationship for a particular stream is not a fixed parameter of the watershed but can exhibit considerable variation from one storm to another depending on factors including the intensity and areal distribution of the rainfall, and changes in the supply of readily erodible sediments. When discharge-concentration data pairs from many events are combined, the resulting scatter may be large and preclude the development of a consistent rating relationship.

### 7.2.3 Seasonal Variability in Sediment Yield

Suspended sediment yield can exhibit a regular seasonal variation due to processes within the watershed. At the onset of a rainy season there may be a large supply of readily erodible sediment, and the protective vegetative cover may be largely eliminated by cultivation and overgrazing, producing early season runoff having a higher sediment concentration than late season runoff. Seasonal variation of erodibility in Nepal was illustrated in Fig. 6.3. In some areas wind plays an important intermediary role, transporting fine sediments from ridges into depressions where it becomes available for fluvial transport at the onset of rains (Rooseboom, 1992). In large basins, such as the Nile, subregions having different erosional characteristics may contribute runoff at different times of year, creating strong seasonal variations in sediment load.

Seasonal variations in sediment load can be important for reservoir sediment management. If reservoir emptying for sediment flushing is scheduled to coincide with the season of highest sediment load, the large sediment load that enters during this period can be routed through the reservoir without deposition. This routing strategy was used at the Old Aswan Dam on the Nile, which was equipped with 180 bottom sluices for sediment release. The Nile at Aswan has two main tributaries, the White Nile and the Blue Nile. The White Nile originates in the area of Lake Victoria and is characterized by relatively small changes in discharge between flood and nonflood season, and low sediment yield. However, floods in the Blue Nile and Atbara Rivers originate in the erosive Ethiopian highlands and contribute most of the sediment load, producing highly seasonal variations in both discharge and sediment concentration (Fig. 7.7). During the early part of the Nile flood, the bottom sluices were opened to pass this runoff and its associated sediment through the reservoir, minimizing sediment deposition. Today's Aswan High Dam controls 100 percent of the Nile runoff, and sediment release is no longer practiced. Seasonal flushing at numerous reservoirs in China is also scheduled to coincide with periods of high sediment discharge.

### 7.2.4 Interannual Variability in Sediment Load

Large year-to-year variations in annual sediment discharge is characteristic of streams in both wet and dry areas. Walling and Kleo (1979) graphed the coefficient of variation in annual sediment discharge for 256 stations worldwide having a minimum of 7 years of data and found no significant difference in annual sediment yield variability between wet and dry climates.

### 7.2.5 Long-Term Changes in Sediment Yield Due to Disturbances

Changes in sediment yield over periods of thousands of years due to postglacial climate changes have been deduced from sediment deposits in natural lakes (Owens and

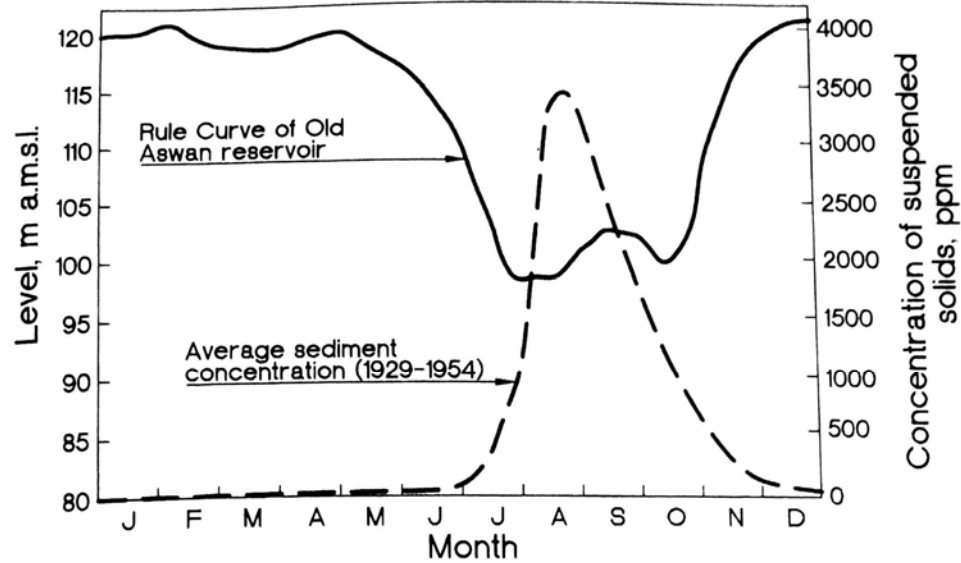


**FIGURE 7.7** Seasonal variation in discharge and sediment concentration in Nile River at Aswan, and the operating rule used at the Old Aswan Dam which minimized impounding and trapping of the heavy sediment load (Shahin, 1993).

Slaymaker, 1994). However, from an engineering standpoint, a long-term change can be any trend evident over a period of decades. Sediment yield is increased over time by activities that reduce or destroy the vegetation cover, disturb the soil, or increase the peak or total runoff. Sediment yield is decreased by the construction of upstream ponds and reservoirs that trap sediment, protection of exposed erodible surfaces with either vegetative or hard cover, and exhaustion of the supply of erodible sediment. When records are based on a short period that is unusually wet or dry or contains an extraordinary flood, the period-of-record sediment yield may depart significantly from the true long-term conditions, giving the false appearance of a trend.

Using the graph in Fig. 7.8 of 40 years of suspended sediment data from the lower Orange River in South Africa, which transports mostly fine sands and silts and has the longest sediment record in that country, Rooseboom (1992) concluded that the declining sediment yield in the Orange River probably reflected two processes: exhaustion of the supply of readily erodible sediment and sediment trapping by farm ponds. Trends in sediment yield may be best analyzed by constructing a double-mass diagram of the cumulative liquid and solid discharge, which helps compensate for apparent changes in load due to streamflow variability alone, as in Fig. 7.13.

Long-term changes in sediment yield accompany land use conversion, such as from natural to commercially harvested forest, from forest to agriculture, or from agriculture to urban use. Some of these conversions may be reversible, such as the conversion of forest land to agricultural use and subsequent recovery of the forest following abandonment of farms. The downstream sediment yield due to cycles of disturbance and recovery will be modified by the temporary storage of eroded sediment. As described by Trimble (1977), farmland in the southeastern United States experienced soil loss on the order of 1 mm/yr over a period of more than 150 years, yet the export of sediment by rivers accounted for less than 0.06 mm/yr because 94 percent of the eroded sediment was redeposited as colluvium at the base of slopes, or as channel and alluvial floodplain deposits (as much as 6 m deep in some areas). Today streams are downcutting through these historical deposits and exporting sediments eroded from farms during the previous century.

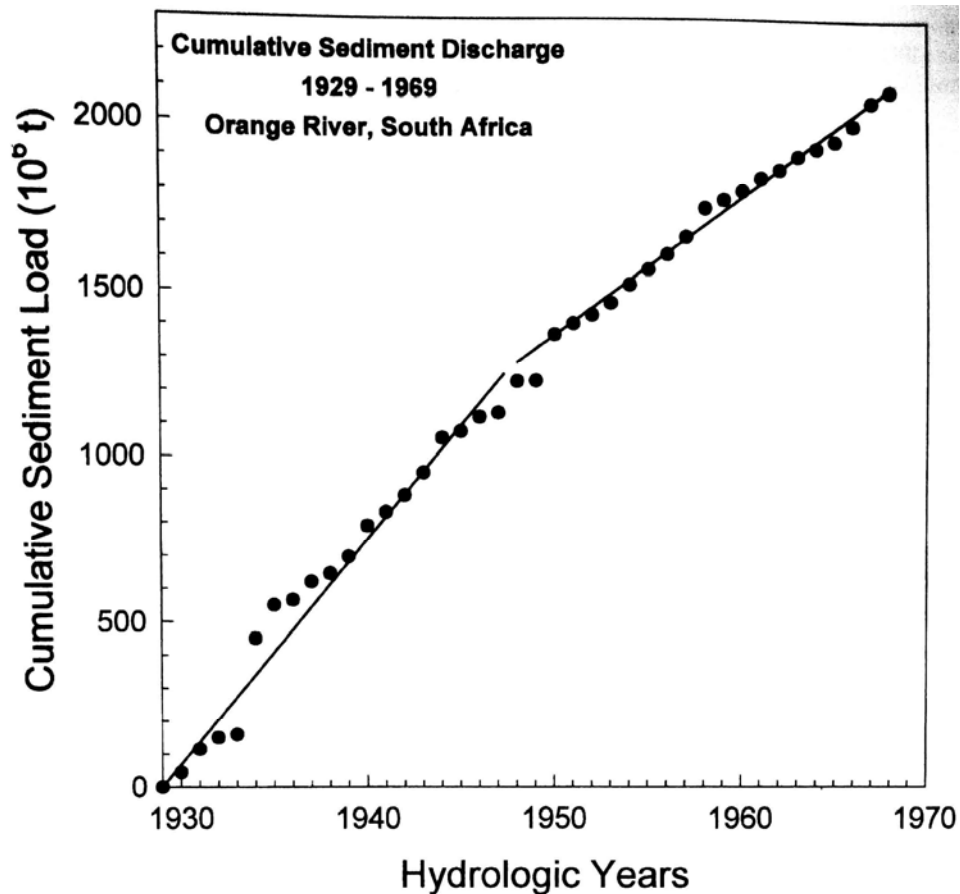


**FIGURE 7.8** Cumulative sediment discharge for Orange River, South Africa, showing a long-term decline in sediment yield, apparently due to the construction of upstream farm ponds plus exhaustion of the readily erodible sediment supply because of soil loss (Rooseboom, 1992).

Similar phenomena were reported by Sutherland and Bryan (1988) in a detailed sediment budget analysis of a small (0.30-km<sup>2</sup>) semiarid basin in Kenya, in the watershed tributary to Lake Baringo. Land misuse and overgrazing since the 1930s led to severe soil erosion and degradation in the region; bedrock and parent material were exposed on slopes and much of the material eroded from slopes accumulated as temporary colluvial deposits at the base of the slopes. After rapid erosion from hillslopes was no longer possible because of topsoil exhaustion, the colluvial deposits constituted the primary source of sediment discharged to the stream channel system. Monitoring of sediment production and deposition using 441 erosion pins, Gerlach troughs, and repeated cross-section surveys of stream channels, revealed that colluvial deposits were exporting sediment to stream channels at a rate of 7030 t/km<sup>2</sup>/yr, as compared to only 922 t/km<sup>2</sup>/yr for denuded primary source areas. The fine-grained sediments eroded from the colluvium were efficiently delivered to the channel system and exported, and 96 percent of the sediment exported from the basin was in the form of suspended load. It was estimated that this erosion would remove 83 percent of the colluvial sediment reservoir over a period of 43 years.

Sediment yield from urbanizing areas will proceed through a cycle as land use progresses from: (1) low-yield pre-development land uses to (2) high-yield construction

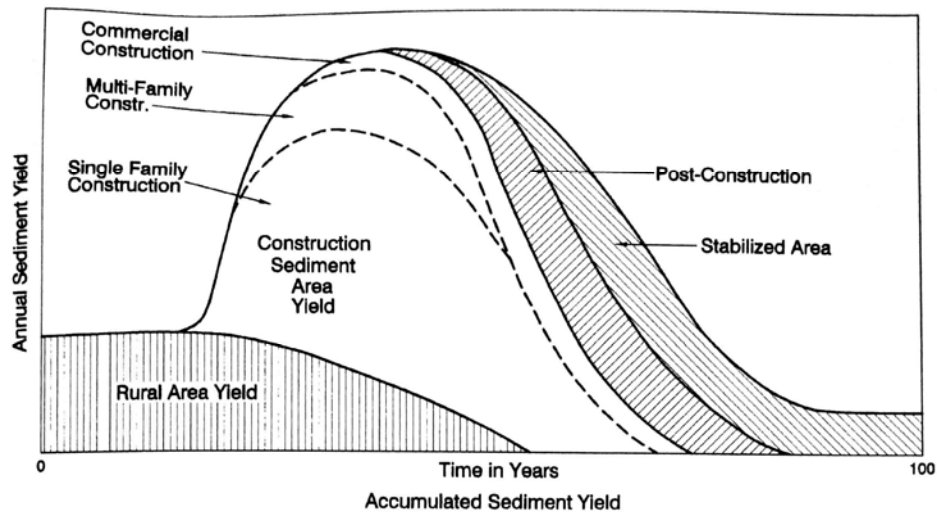


**FIGURE 7.9** Schematic sequence in the change in sediment yield with time due to the urbanization of a rural watershed (Livesey, 1975).

sites characterized by disturbed soil and a high efficiency storm drainage network, to (3) protected soil cover (Fig. 7.9). Increased peak discharge from urban areas will also increase long-term channel erosion downstream. When roads in urban areas are not paved, sediment yield may be continuously high.

The reason for sediment yield trends can be obvious in smaller watersheds where cause-effect relationships may be readily evident and in areas where natural sediment yield variability is not extreme. However, in larger watersheds where multiple activities occur simultaneously, in basins where a large percentage of the eroded sediment is stored between the point of erosion and the basin exit, and when natural variation in sediment yield is very high, the understanding and prediction of long-term trends can be problematic. Day (1988) reported that one of the principal objectives of the Canadian sediment monitoring program was to provide data for trend analysis to better understand the impacts of upstream land use change and water resource construction activities. However, success was limited by problems including less-than-ideal station locations, major flow diversions within basins, the difficulty of discerning between natural and human-influenced changes, and the paucity of data on land use activities across large basins. Generally, as basin size increases, the data on land use become increasingly sparse. However, as basin size decreases the sediment yield becomes increasingly variable, making it difficult to distinguish between human-induced and natural causes. Only the downstream effects of sediment trapping by reservoirs was clearly noticeable.

When published land use data are available, the land use classification may say little about actual erosion conditions in a watershed as a result of activities such as logging, grazing, and fuelwood harvest, as suggested by the highly degraded "forest" area shown in Fig. 7.10. Extreme variability in sediment yield in semiarid climates can frustrate studies even in small watersheds, where the cause-effect relationship between land use change and sediment yield would be expected to be clearly evident.

Multiyear departures from long-term conditions can also result from disturbances such as fire. The effect of fire on the sediment yield from the highly erodible soils in the brush-dominated watershed tributary to Gibraltar reservoir at Santa Barbara, California, is illustrated in Fig. 7.11. However, fire does not necessarily increase sediment yield. Mohrman and Ewing (1991) examined changes in suspended sediment load following the



**FIGURE 7.10** Area called as “forest” in Andhra Pradesh, India, but devastated by overgrazing, fuelwood harvesting, etc. (*G. Morris*).

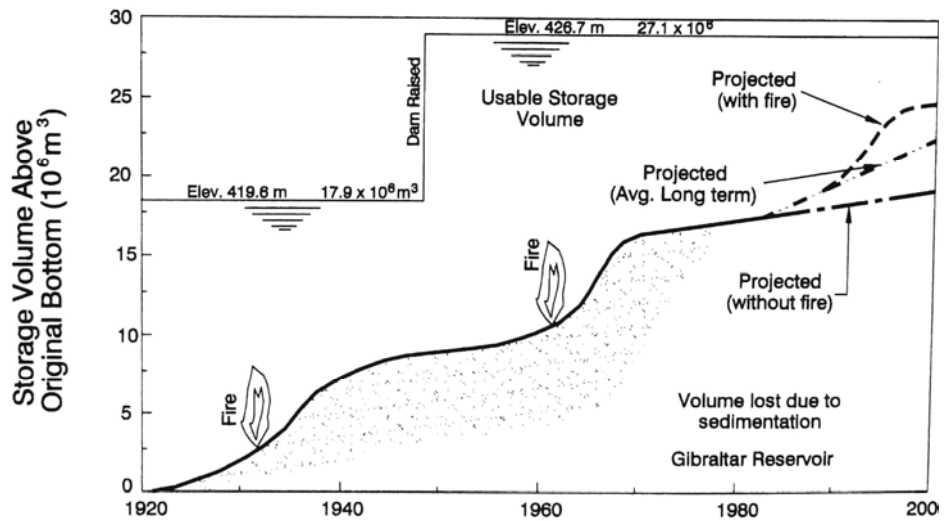


**FIGURE 7.11** Effect of fire on sediment yield, as exemplified by the drainage area tributary to Gibraltar Reservoir, Santa Barbara, California (*modified from City of Santa Barbara, 1987*).

large forest fires in Yellowstone National Park during 1988. From a comparison of data during 1985-86 and 1988-89 for gages on Yellowstone River at Corwin Springs (4140 km<sup>2</sup>) and Lamar River at Tower Junction (1690 km<sup>2</sup>), with 30 percent and 38 percent of the total watershed burned respectively, they concluded that the fires produced no major changes in sediment loading. The largest sediment load in the 4-year record examined was in a prefire year.

### 7.2.6 Changes in Long-Term Yield Due to Geomorphic Factors

Long-term changes in sediment yield are exemplified by the case of Elephant Butte reservoir on the Rio Grande in New Mexico. Constructed in 1915, this 3250-Mm<sup>3</sup> reservoir lost capacity at an annual rate of 30 Mm<sup>3</sup> during the first 5 years after construction, but the rate of storage loss declined, and since 1940 storage loss has averaged 4 Mm<sup>3</sup> per year (Fig. 7.12). This period has also seen a large reduction in sediment yield from Rio Puerco, a major sediment contributor, attributed to factors including changes in river channel morphology. The reservoir was constructed toward the end of a period of river channel incision. Upstream reservoirs also reduced the unregulated tributary area (Orvis, 1989). The effect of long-term geomorphic factors is suggested in the Rio Puerto data (Fig. 7.13), which illustrates the clear trend of decreasing suspended sediment concentration. Sediment load at this gage station has not been affected by upstream reservoir construction.

Sediment yield has declined since 1940 across the Colorado basin as a result of geomorphic processes. Arroyos within the basin incised rapidly and produced large amounts of sediment during the late nineteenth and early twentieth centuries. For example, Chaco River in northwestern New Mexico was 2.4 m wide and 0.5 m deep in 1849, but by 1925 had enlarged to 46 to 137 m in width and 6 to 9 m in depth. The reason for the onset of the entrenchment process, with attendant high rate of sediment production due to channel erosion and subsequent reduction in sediment yield, is not well-understood.

Different researchers have attributed changing channel erosion patterns to increased grazing pressure in the late nineteenth century, changes in suspended measurement techniques in the Colorado River in the 1940s, climate variations including periods of drought and of intense storms, erosion control activities in the watershed including construction of reservoirs and stock ponds, and geomorphic factors. These factors were summarized by Gellis et al. (1991), who concluded that all of the mentioned factors contributed to the process with the exception of changes in measurement techniques,

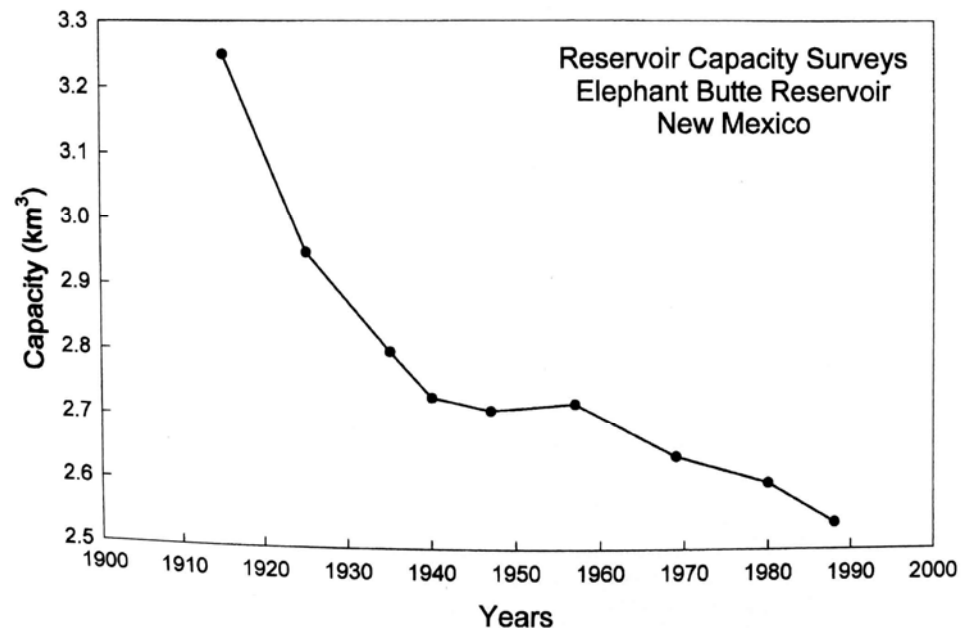


**FIGURE 7.12** Long-term storage loss in Elephant Butte Reservoir, Rio Grande River, United States (Gorbach, 1996)

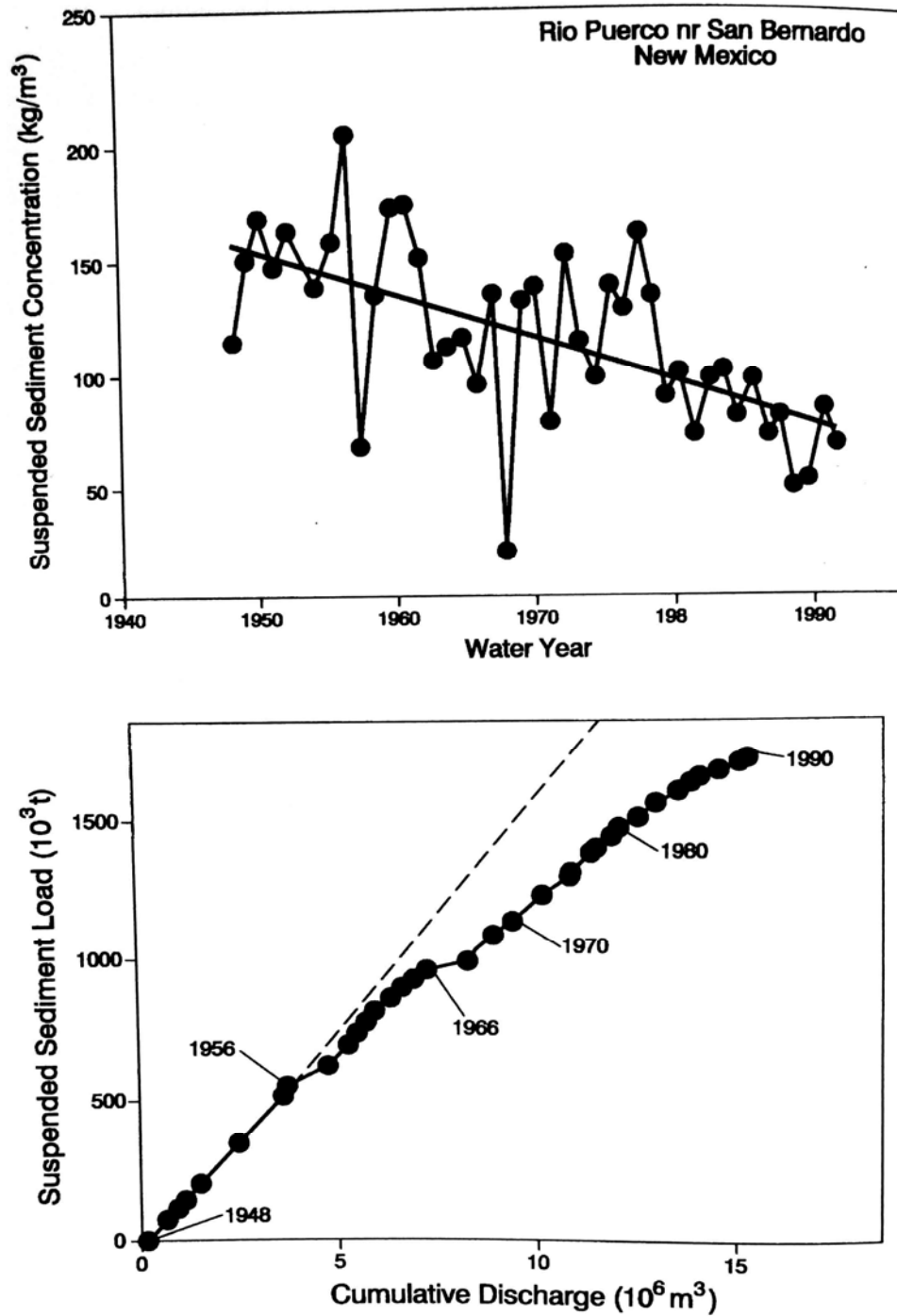


**FIGURE 7.13** Sediment concentration and double mass curve of annual suspended sediment load runoff, Rio Puerco near An Bernardo, just upstream of confluence with Rio Grande (after Gellis, 1991)

since the limited available data suggest that the present sampling instruments would tend to increase rather than decrease the apparent yield. It was concluded that the overall process could be interpreted within the context of a five-stage geomorphic model (Fig. 7.14). In this model, a period of incision (stage 1) is initiated within a basin by a combination of factors, such as drought and increased grazing pressure, which significantly reduce vegetative cover and initiate channel erosion. Subsequently channels incise and enlarge through the gullying process (stage 2) until channel width expands and slope diminishes, to the point that sediments can no longer be eroded. Vegetation then invades the widened channel bottom, increasing hydraulic resistance and decreasing flow velocity, which in turn further encourages sediment deposition and refilling the arroyo. A new disturbance can reinitiate the incision process. Similar processes have been observed in humid climates, where they tend to be accelerated in time. The five-stage model represents a long-term cyclic process which occurs over a period of decades and which can have a profound effect on sediment yields. Depending on its location on the long-term cycle, sediment yield data from any particular time period may not necessarily reflect the long-term condition.

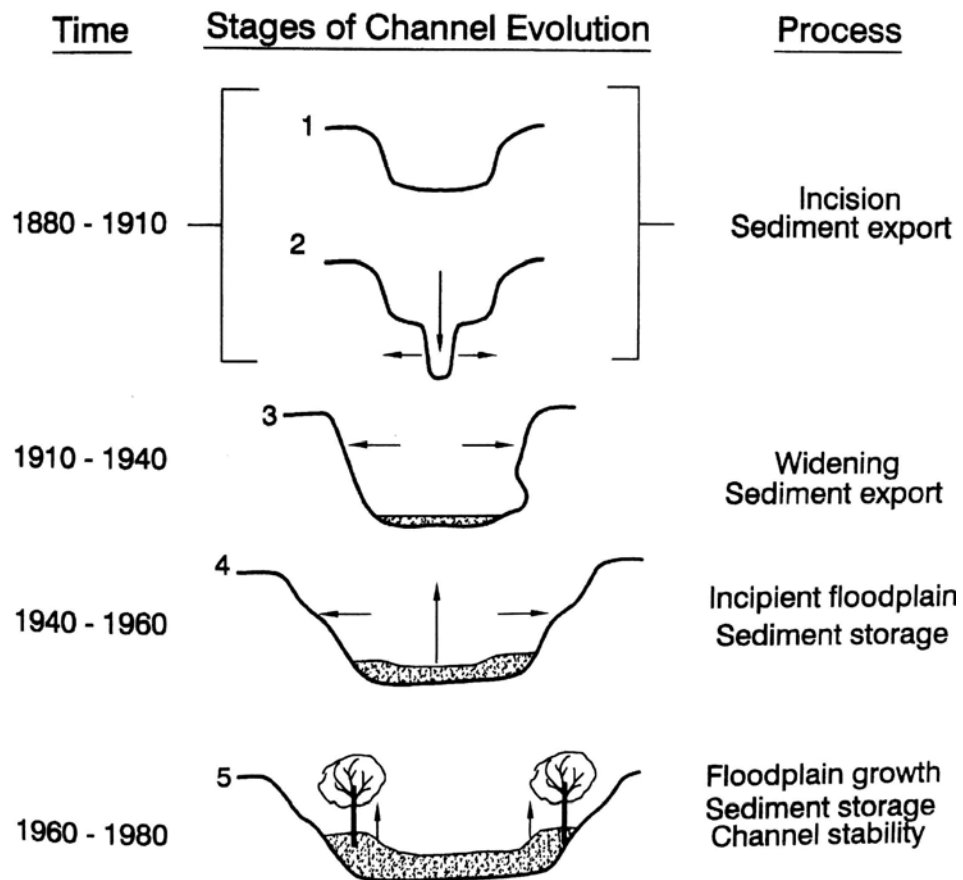


**FIGURE 7.14** Five-stage geomorphic process hypothesized to affect long-term cycles of stream incision in a semiarid climate (adapted from Gellis et al., 1991).

## 7.3 STRATEGIES FOR MEASURING SEDIMENT YIELD

---

Sediment yield can be computed from reservoir surveys or a fluvial sediment monitoring program. Although both methods have potentially important sources of error, reservoir survey data generally represent a more reliable measure of the long-term basin sediment yield. However, reservoir surveys cannot provide data on the short-term variations in sediment delivery, essential information for certain sediment management strategies. Ideally both types of data will be available and can be checked against each other.

### 7.3.1 Reservoir Resurvey

Continuously impounding reservoirs act as excellent sediment traps, and successive reservoir surveys can be compared to determine the sediment volume accumulated during the survey interval. By correcting for trap efficiency, and converting the volume of sediment deposits into sediment mass on the basis of dry bulk density, the total sediment yield from the watershed can be computed. Reservoir survey procedures are described in Chap. 10.

The thickness of sediment deposition is normally determined by repeated bathymetric surveys and must also include areas above the normal pool elevation when deposition occurs in the backwater zone. In reservoirs lacking reliable pre-impoundment topographic data, <sup>137</sup>cesium sampling may be performed in continuously depositional zones of fine sediment accumulation in reservoirs which began impounding several years prior to atmospheric testing in the late 1950s.

Reservoir resurveys offer several important advantages:

1. The method does not rely on a continuous monitoring program, and as long as there is accurate information on the pre-impoundment topography or data from a prior survey, the next resurvey can be made at any time.
2. Measurement during peak flood discharge is not required.
3. Reservoir resurveys are typically much less costly than continuous fluvial sediment monitoring stations. However, the subsoil borings needed to verify deposit unit weights may be costly.
4. Bathymetric surveys can be performed to a high degree of accuracy.
5. The total load, including bed load, is measured.

Several sources of error and limitations are associated with the use of resurvey data to estimate sediment yield, in addition to the geometric errors that can be associated with bathymetric mapping and the difficulty of replicating the original cross-section locations.

1. The most prevalent source of error is the lack of accurate data on sediment unit weight, which is usually estimated rather than sampled. Significant sediment compaction of fine sediment may occur over time, causing unit weights to change from one survey to the next. This is a particular problem associated with surveys early in the reservoir life. Sediment compaction can cause the rate of storage loss to be more rapid during the initial years of impounding as compared to later years, even though the sediment load is constant.
2. In reservoirs with low rates of sediment accumulation, or for short intersurvey periods which produce small sediment accumulation depths, the errors in bathymetric mapping may be relatively large in relation to the intersurvey sediment thickness, making it difficult to determine the volume of sediment accumulation. As a practical matter, reservoir resurvey can normally determine the average sediment yield over a period of several years. However, use of precise techniques in reservoirs with

significant sediment loads can reduce the resurvey period to as little as 1 year, as described in the Cachi case study.

3. Trap efficiencies approaching 100 percent will occur in reservoirs having a large capacity:inflow ratio and high-level outlets, but it may be difficult to estimate the trap efficiency in reservoirs having a small capacity:inflow ratio and low-level outlets, as may occur in mountain hydropower stations.
4. Reservoir resurvey data do not provide information on the variation in sediment yield over short time periods, which can be important for many types of sediment management activities.
5. Both sediment and water can be diverted into or out of the upstream watershed.
6. Sediment removal from the system due to instream mining, at sediment traps operated upstream of the reservoir, or from within the reservoir itself, must be accounted for.
7. Organic sediments can accumulate because of primary production within the reservoir.
8. Finally, the reservoir resurvey method can be used to estimate sediment yield only where there is a preexisting reservoir.

Butcher et al. (1992) have provided a more detailed description of several potential sources of error in reservoir surveys.

In lakes or reservoirs lacking original bathymetric data, or where such data are not reliable, the depth of deposit can be determined by using identifiable and datable horizons within the sediment. One such sediment horizon corresponds to the appearance of man-made radioactive material resulting from atmospheric testing or, in some areas of Europe, the Chernobyl reactor accident. The use of <sup>137</sup>cesium as a datable horizon is described by Ritchie et al. (1973) and McHenry and Ritchie (1980). It is well-suited for use as a horizon because it sorbs rapidly and tightly onto surface sediments which are subsequently washed into the reservoir. Reservoir sediment cores are sectioned and radioactive emissions are counted, producing a profile of "cesium activity as a function of depth. The resulting profile is interpreted to determine the layer corresponding to the large-scale atmospheric tests in the early 1960s, and sediment accumulation above this horizon is measured. By analyzing a number of cores from different areas in the impoundment, the overall depth of deposit may be determined. This method cannot be used in areas where sediments have been reworked following deposition.

The total deposit depth can also be determined by using fully penetrating spud or core samples, with the original bottom being detected by the change in grain size, color, and compaction of the material. If a reservoir was affected by an extreme event, such as a severe flood, an identifiable thick layer of coarser material may have been deposited across much of the impoundment and can serve as an identifiable and datable horizon. Similar layers might be caused by fire in the watershed, volcanic eruption, the initiation or cessation of a major source of pollutants, etc.

Short-term studies of deposition can be performed by using sedimentation plates, which are metal plates placed across the floor of the reservoir and measured the following year to determine the depth of deposition over each plate. Relocation of plates following burial in sediment may be aided using electronic positioning, a metal detector, or by installing a visible wand near each plate. The plate technique is most suitable for reservoirs that are drawn down annually so the plates can be set out and recovered on the dry reservoir bed. Submerged sediment traps may also be used, but have the potential disadvantage of causing localized interference with flow patterns that may affect sediment trapping efficiency.

### 7.3.2 Fluvial Monitoring

Fluvial sediment yield cannot be measured directly, but must be computed from stream discharge and sediment concentration, both of which can vary over 3 orders of magnitude. While the continuous monitoring of discharge typically presents little difficulty, no method is available to continuously measure the discharge-weighted suspended sediment concentration. Fluvial monitoring strategies attempt to work around this limitation by using three principal types of data:

1. Depth-integrated discharge-weighted concentration data collected at discrete points in time, giving particular emphasis to the monitoring of the larger discharge events responsible for most sediment transport.
2. A larger number of single-point pumped samples collected at different times over the hydrograph to better characterize both the rising and falling stage of significant runoff events.
3. Continuous single-point samples of turbidity, which may or may not correlate well to single-point suspended solids concentration, depending on the stream characteristics.

The bed load component is usually not measured but is estimated as a percentage of the suspended sediment load or computed from stream hydraulics and bed load equations. Dedkov and Moszherin (1992) analyzed fluvial sediment data from 1872 mountain rivers worldwide, draining watersheds of 500 to 100,000 km<sup>2</sup>. Of these, bed load data were available for only 158 rivers, or 8 percent of the stations. At these, the bed load component averaged 23 percent of suspended sediment load. Because bed load measurement was presumably neglected at stations where it was considered unimportant, the average bed load transport at all stations was probably significantly less than 23 percent of the suspended load.

The sampled suspended sediment data may be used to compute the sediment load by either of two strategies: extrapolation or interpolation. Extrapolation techniques make the assumption that a relationship determined at one point in time, or over one range of discharges, can be applied to another time period or to discharges greater than those sampled. These assumptions are inherent in the utilization of *C-Q* relationships or sediment rating curves, which are frequently determined from a few years of data and then applied to a much longer discharge record to estimate long-term sediment yield, and which are also frequently extrapolated to cover discharges larger than actually measured. The sediment rating curve may be applied to either flow duration or time series discharge data.

Interpolation makes the assumption that the suspended sediment concentration measured at one point in time is representative of a longer time interval. Interpolation procedures typically combine use of a time series of sediment concentration and discharge values to compute load. The accuracy of this method is heavily dependent on sampling frequency. A 10-min sampling frequency may be required for small flashy streams, and a 24-h interval will produce large underestimates of sediment yield in all but the largest rivers.

Both interpolation and extrapolation techniques have large potential sources of error. Concentration-discharge relationships have a high degree of scatter: concentration can vary by 3 orders of magnitude at a given discharge. This makes short-interval gaging and interpolation of both discharge and sediment concentration the most accurate method available. A monitoring station using this technique would use manual depth-integrated sampling to calibrate the relationship between the discharge-weighted concentration and the point concentration at the inlet to the pumped sampler and turbidity monitor. Both stage and turbidity would be measured at short intervals, and pumped samples would be

withdrawn during both rising and falling stages of each significant event to calibrate the turbidity data. All automatic sampling can be performed by portable battery-operated sampling equipment with a data logger and onboard computer to program the data collection sequences. Sampling programs established as part of a general water-quality monitoring network are inadequate for estimating sediment load.

### 7.3.3 Uncertainty in Sediment Yield

Continuous long-term sediment concentration data are usually not available, and considerable judgment is often required to convert the available data into estimates of sediment yield. The magnitude of error that is possible in estimating sediment loads by different practitioners can be illustrated by the lively discussion between Griffiths (1979) and Adams (1980) concerning sediment yields from rivers draining the Southern Alps on South Island, New Zealand. Both investigators used essentially the same dataset to construct rating curves, but Adam's study resulted in average yields 70 percent higher than Griffiths'. However, on the Cleddau River there was a 48-fold difference in the sediment yield estimates. Adams points out that, because load estimates from point concentration samples may be in error by +100 percent or -50 percent, the importance of the 70 percent difference in yield is uncertain. That both investigators consider their results to be "in general agreement" speaks to the high degree of variability that can occur in fluvial sediment studies.

Galay (1987) reported that the rate of reservoir sedimentation in the Himalayas and in India has often been underestimated for the following reasons. Sediment sampling and analysis programs are generally inadequate to determine long-term sediment loads. Suspended sediment measurements are often unavailable for high discharges, and there are no measurements during catastrophic events. Bed load is not measured, and cannot be measured accurately in large mountain rivers that may be transporting cobbles or even boulders. Older data may reflect watershed conditions prior to extensive deforestation. Field data may have poor quality control or may sometimes be falsified, especially at remote and poorly supervised stations. These same limitations may apply to data from other parts of the world as well.

The episodic nature of sediment discharge can cause yield estimates to be severely underestimated, especially in mountainous areas. An example of this is the case of Jennings Randolph Reservoir on the North Branch of the Potomac River in the Appalachian highlands in Maryland and West Virginia, described by Burns and MacArthur (1996). The sediment yield from the 673 km<sup>2</sup> mountainous watershed was originally estimated at 25,000 m<sup>3</sup>/yr (20 acre•ft/yr), but 2 years after impounding began in 1982, significant sediment deposition was noticed, and in 1986 the flood of record deposited a sediment volume equal to 30 years of sediment inflow according to the original design computations. A resurvey after only 4 years of operation revealed that the reservoir had already accumulated 43 percent of the projected 100-year sediment load of 2.5 Mm<sup>3</sup>.

The original sedimentation estimates had been based on several regional sediment yield studies plus stream sediment samples collected during 1961-62 for river discharges less than 140 m<sup>3</sup>/s, a recurrence interval of about 1 year. In Fig. 7.15 the measured rate of

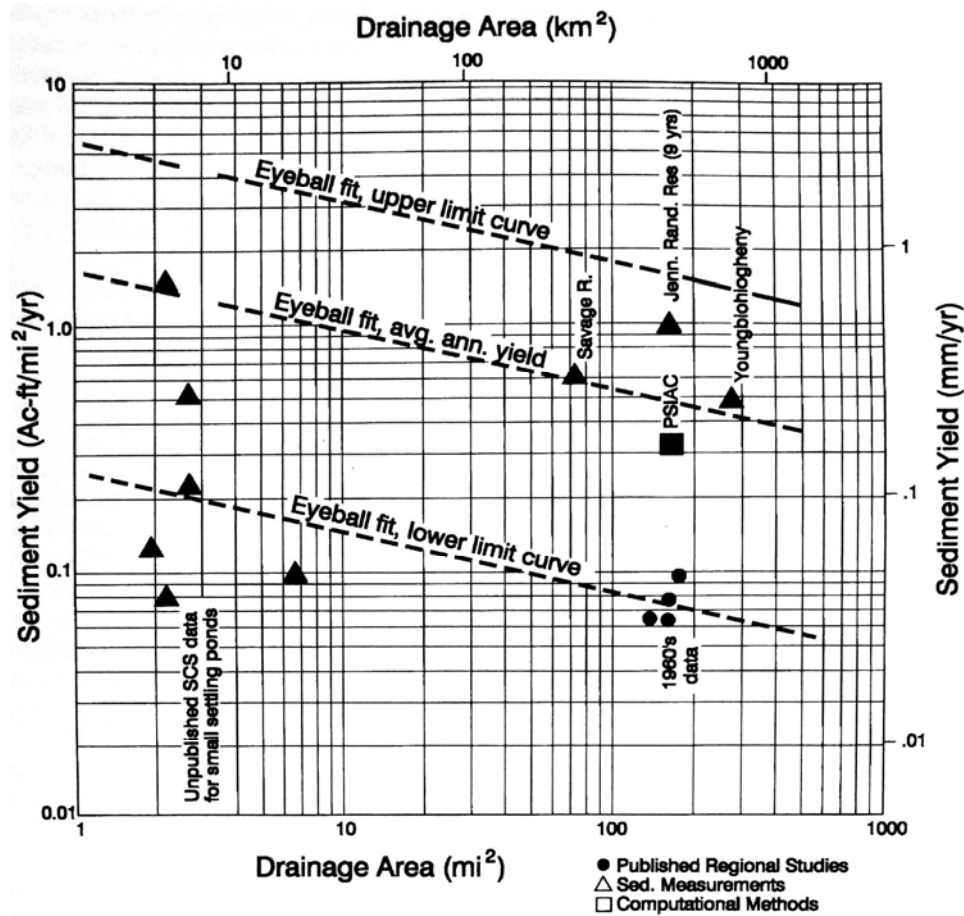


FIGURE 7.15 Various sediment yield estimates associated with Randolph Jennings Reservoir (Burns and MacArthur, 1996).

sedimentation at the site is compared to various regional estimates of sediment yield, sediment surveys at other nearby reservoirs, and an estimate prepared by the PSIAC methodology (see Sec. 7.6.3). The scatter in the data underscores the practical problem of attempting to assign a sediment yield to a site without reliable fluvial monitoring data. The study concluded that the original sedimentation estimate was based on valid data, was computed by accepted methods, and was generally in concurrence with a number of other studies prepared in the area. However, in this mountainous watershed sediment yield tends to be dominated by infrequent large events, and the traditional and accepted methods for computing sediment yield can greatly underestimate sediment yield from a basin dominated by extreme episodic events.

### 7.3.4 Quantifying Interannual Variability in Sediment Load

The year-to-year variation in sediment load is greater than the variation in streamflow. Information on this variability can be used to determine the uncertainty in the estimate of mean annual load as a function of sampling duration. Assuming that errors are not introduced in the sampling or computational procedures, the uncertainty in estimating the

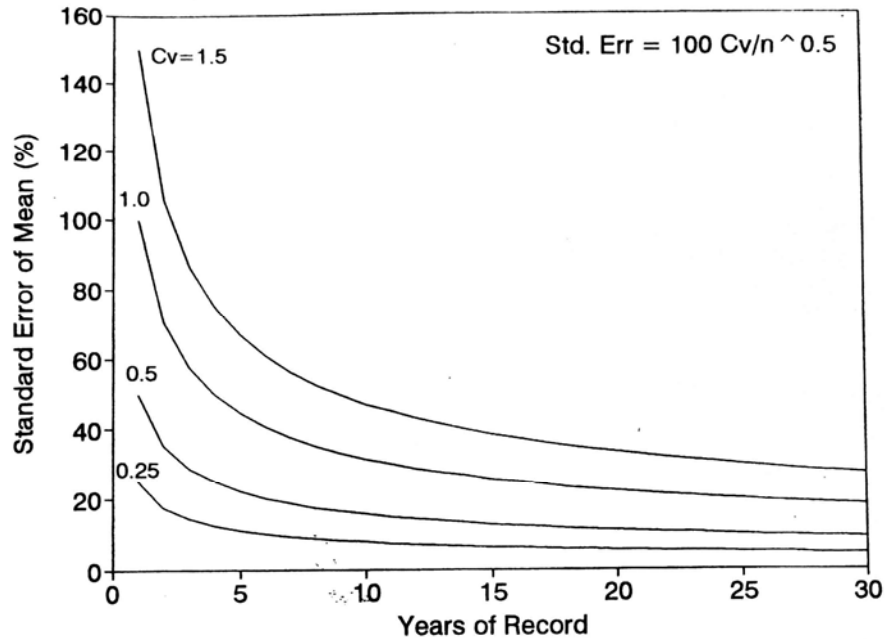


FIGURE 7.16 Timewise variation in uncertainty in estimating the mean sediment discharge.

mean annual sediment load attributable to natural interannual variability can be quantified as the standard error of the mean:

$$SE = 100 C_v/n^{0.5} \quad (7.1)$$

where SE = standard error of the mean suspended sediment discharge, %;  $C_v$  = coefficient of variation computed as the standard deviation divided by the mean; and  $n$  = number of years of record. The timewise solution of this equation for several representative values of  $C_v$  is illustrated in Fig. 7.16, showing that the decrease in the standard error of the mean annual load is initially rapid, but after about 10 years the error declines rather slowly. For a stream with  $C_v = 0.70$ , after 5 years of measurement the standard error of the mean annual sediment load would be  $\pm 31$  percent, after 10 years it would be 22 percent, and after 30 years it would be 13 percent. A 20 percent error in the estimate of the mean due to natural variability is tolerable in most engineering studies and is very small compared to the other types of errors inherent in sediment monitoring programs. The use of a 5- to 10-year monitoring program has been recommended as adequate by a number of authorities (Strand and Pemberton, 1987; Day, 1988; Rooseboom, 1992; Summer et al., 1992). A much longer monitoring period is required to detect trends.

## 7.4 SEDIMENT RATING CURVES

The relationship between sediment discharge and concentration, usually plotted as a function of water discharge on log-log paper, is called a sediment rating curve. Techniques for developing concentration or load versus discharge relationships have been

described by Glysson (1987), who argued in favor of the term *sediment transport curve*, since the term rating suggests a degree of causality that does not really exist. Rating curves are developed on the premise that a stable relationship between concentration and discharge can be developed which, although exhibiting scatter, will allow the mean sediment yield to be determined on the basis of the discharge history.

Two types of relationships are commonly used, concentration versus discharge and load versus discharge. Because sediment yield is the product of both concentration and discharge, in the latter curve the discharge term appears on both axis, and produces an apparent fit which is better than the original dataset. Plots of field data represent essentially instantaneous concentration-discharge data pairs, but curves may also be plotted showing average sediment concentration or load as a function of discharge averaged over daily, monthly, or other time periods.

### 7.4.1 Fitting Sediment Rating Curves

A concentration versus discharge rating curve in some streams may be characterized by a single log-log relationship. When there is a poor relationship between concentration and discharge, a better relationship might be obtained by constructing multiple curves to model different components of the total load. For instance, separate curves may be prepared for the coarse and fine size classes, for summer and winter conditions, for rising and falling stages or for different discharge ranges. A problem inherent in the rating curve technique is the high degree of scatter, which may be reduced but not eliminated. Concentration does not necessarily increase as a function of discharge (Fig. 7.17). Scatter

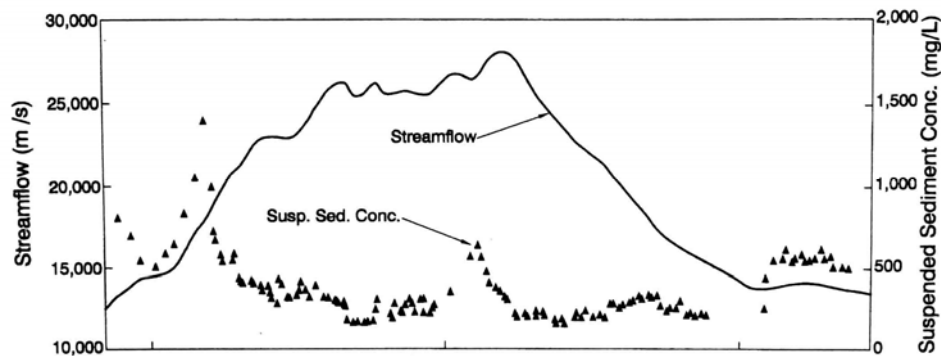


**FIGURE 7.17** Variation in discharge and suspended concentration in the Mississippi River at Chester, Illinois, during the 1993 flood, showing a large drop in suspended solids concentration with increasing discharge (Holmes and Oberg, 1996).

at some stations may be so great as to preclude the development of a reliable rating relationship (Fig. 7.18). A high degree of scatter occurs when sediment delivery to the stream is controlled by processes in the watershed that do not correlate well with the stream discharge.

There is no standard method for rating curve construction, and in some cases visual fitting methods can give better results than mathematical curve fitting. Construction of a rating curve should always begin by analyzing a simple plot of the data to look for relationships (e.g., seasonal effects) that may not be apparent from a mathematical curve-fitting procedure. The case study on Cachí reservoir (Chap. 19) provides a good example of how multiple methods are used to produce rating curves. A good curve fit does not

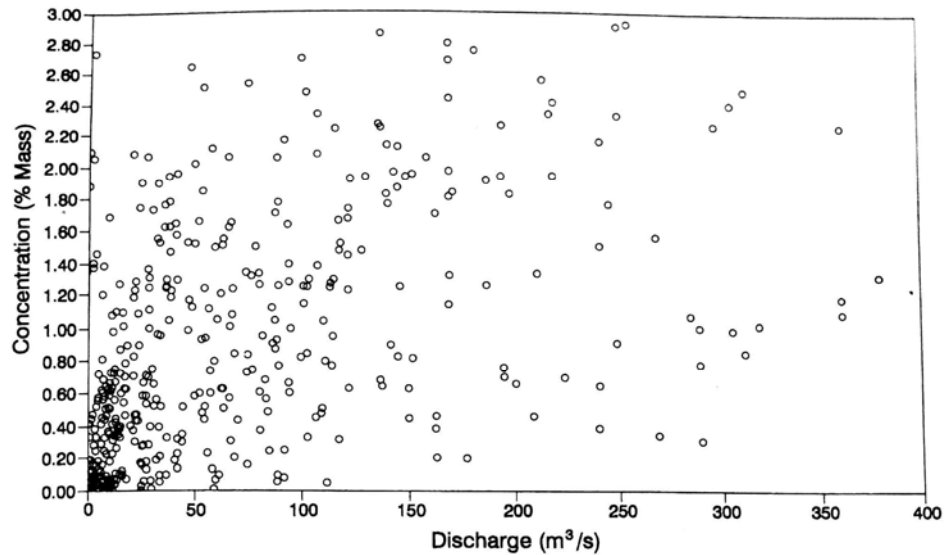


FIGURE 7.18 Suspended sediment concentration versus discharge, Caledon River at Jammersdrift, South Africa (Rooseboom, 1992).

imply an accurate representation of the hydrologic process unless the data: (1) cover the entire range of discharges, (2) include both rising and falling stages of hydrographs from storms during all seasons, (3) are not biased by unusual hydrologic conditions, (4) include points at high discharge for more than a single event.

### 7.4.2 Visual Curve Fitting

Visual curve fitting has long been used for the construction of rating curves and can have several advantages over mathematically fitted curves. High-discharge events which transport most sediment are often poorly represented in sediment datasets, and data from the highest-discharge classes may be absent altogether. Extrapolation into the highest-discharge classes is probably better achieved by visual fitting from an experienced practitioner as opposed to extrapolation of a regression relationship. Complex relationships may also be visually broken into subsets to yield a better relationship than a single fitted curve. Two such strategies are illustrated in Fig. 7.19. Other possible strategies include subdivision of the dataset into rising and falling stages, or preparation of separate rating curves for coarse and fine sediment. The rating curve may also shift significantly following an extraordinary flood which scours out the sediment stored in stream channels.

### 7.4.3 Mathematical Curve Fitting

A rating curve may be constructed by log-transforming all data and using a linear least square regression to mathematically determine the line of best fit. The log-log relationship between concentration (or load) and discharge is of the form  $C_s = aQ^b$ , and the log-transformed form will plot as a straight line on log-log paper:

$$\log C_s = a + b \log(Q) \quad (7.2)$$

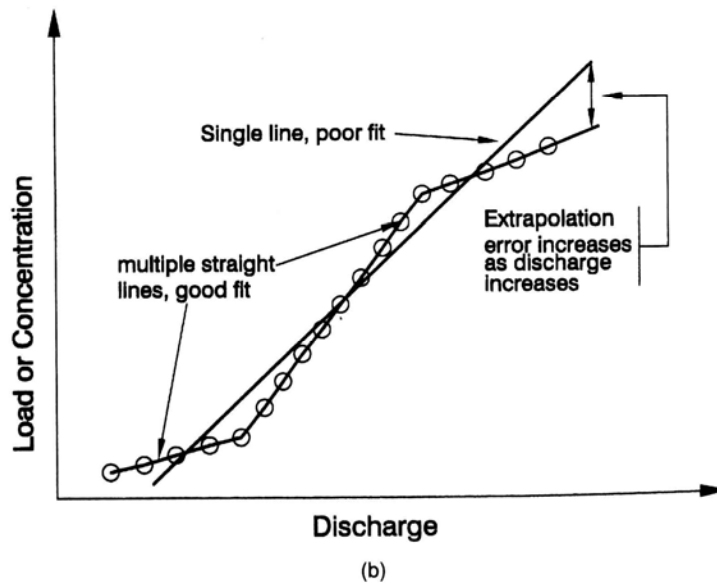
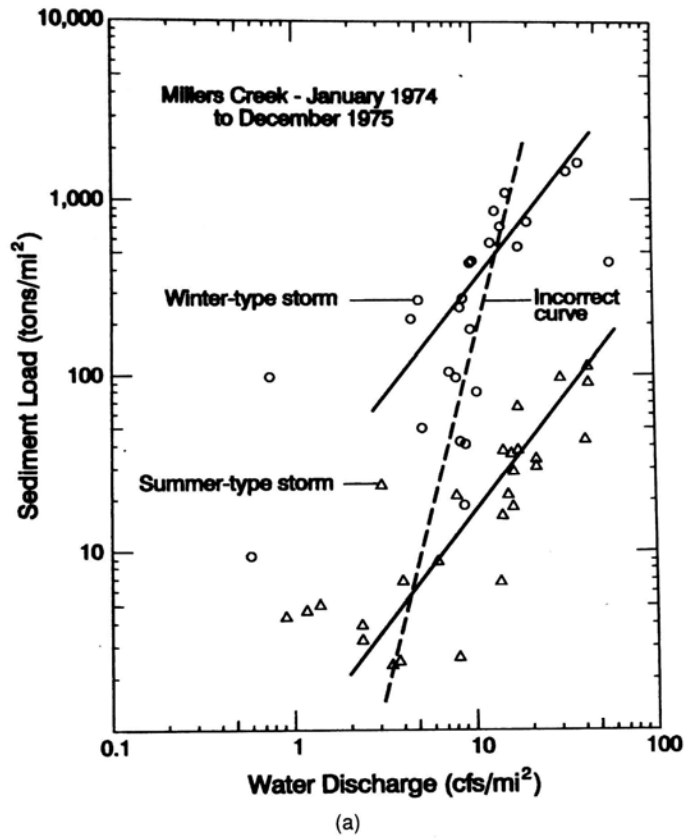


**FIGURE 7.19** Disaggregation of discharge-concentration data pairs into subsets to better define the relationship. (a) Disaggregation of dataset by season or type of storm. (b) Use of multiple line segments to better fit an unusual distribution. This method may be particularly useful when group-averaged data are used (adapted from Glysson, 1987).

However, a regression equation will minimize the sum of the squared deviations from the log-transformed data, which is not the same as minimizing the sum of the squared deviations from the original dataset, and this introduces a bias that underestimates the concentration (or load) at any discharge. To illustrate this effect, consider the values of 10 and 90, which have a mean value of 50. If these values are log-transformed, their logs averaged, and the antilog of the average back-transformed, the resulting mean is 30. Because the geometric mean computed by using the log transforms will necessarily be lower than the arithmetic mean, the result is a negative bias, the magnitude of which increases with the degree of scatter about the regression. Ferguson (1986) reports that this bias may result in underestimation by as much as 50 percent. Ferguson and others have suggested bias correction factors, but their appropriateness is uncertain (Glysson, 1987; Walling and Webb, 1988).

Alternatives to the lognormal transformation are now widely available with microcomputer technology. McCuen (1993) provides a description of several alternative procedures plus software diskettes containing programs and sample datasets, which allow the power model to be fit so that the error term is minimized on the basis of the original unlogged dataset. Another method for testing the goodness of fit of different models against the original dataset of instantaneous concentration-discharge was used by Jansson (1992a) at Cachí reservoir. In this case the total load for the original dataset was computed by assigning an arbitrary duration interval to each sample point. The total load was then recomputed by each model (regression, visual fit, etc.) using all the discharge values contained in the original dataset, to see how accurately each model reflected the total load for the sampled period.

A particular weakness of a mathematically fitted curve is the potentially poor fit at the high extreme, which will be represented by few datapoints. Large errors can occur when mathematical curves (e.g., a log-quadratic) are extrapolated to discharge values greater than those covered in the original dataset, producing unreasonable values. All rating curves should be plotted and examined for reasonableness over the entire range of discharge values to which they will be applied.

The infrequent large-discharge events which account for most sediment load will constitute only a few points in the entire sediment dataset. As a result, the shape of a regression equation fit using the original dataset will be biased by the numerous datapoints at low discharge values, which account for a small percentage of the sediment load. This problem can be overcome by dividing the data into discharge classes, computing the mean sediment concentration within each discharge class, then running the regression model using the means. This technique equally weighs the error minimization scheme over the entire range of the dataset.

#### 7.4.4 Rating Curve Example

As an example, the 8-year  $C-Q$  record at 21 km<sup>2</sup> Goodwin Creek, Mississippi, was divided into 0.076-m (0.25-ft) stage intervals using discharge and suspended sediment data pairs from a gaging flume equipped with a pumped sampler. The dataset was divided between the fine and sand fractions, and the mean suspended sediment concentration for each fraction was determined for each stage interval to produce the plot in Fig. 7.20, which illustrates the clearly separate relationships for sand and fines. Although the resulting relationship appears to imply a high degree of correlation between discharge and concentration, the original dataset displays considerable scatter. The standard deviation of concentration within a stage interval is about as large as the average concentration itself. Application of the averaged data may accurately determine the long-term load, but estimates for individual storms would incorporate large errors. In this

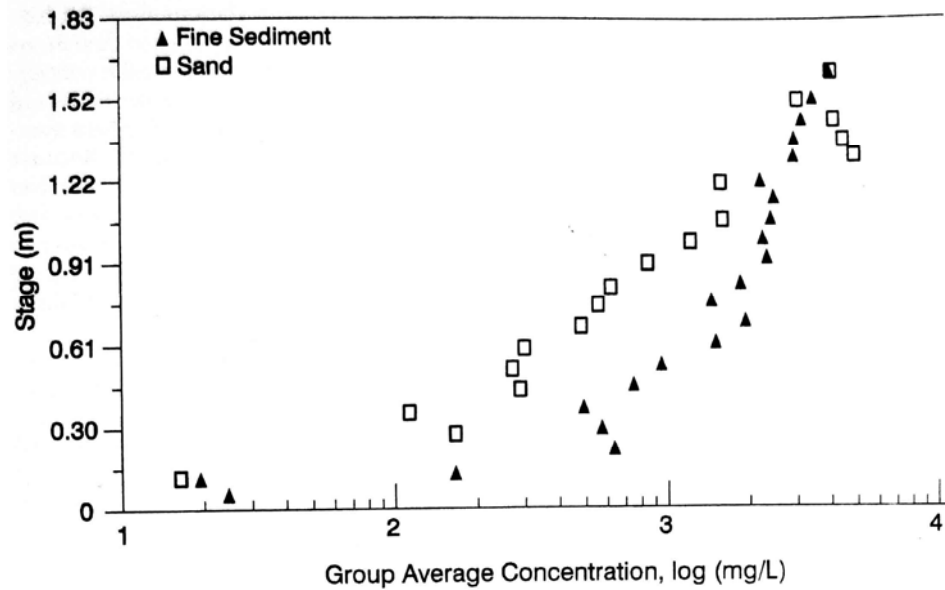


**FIGURE 7.20** Suspended sediment rating relationship for Goodwin Creek, Mississippi, from interval-average datapoints. Note the different relationships for the fine and coarse fractions. (Willis et al., 1989.)

watershed it was possible to obtain more accurate curves for the analysis of seasonal transport rates by constructing four seasonal rating curves for 3-month periods, for both sand and fines, for a total of eight rating curves. There was a greater seasonal effect on the transport of fines than of sand (Willis et al., 1989).

## 7.5 COMPUTING SEDIMENT LOAD

### 7.5.1 Time-Series Sediment Rating Curve Technique

If a reliable rating relationship is available, the suspended-sediment load may be computed by using a rating curve and a time series of discharge data. The product of discharge and discharge-weighted concentration equals load during the computational interval, and daily sediment load  $Q_s$  in either metric tons or short tons may be computed as

Metric units:

$$Q_s = 0.0864CQ_{\text{water}} \quad (7.3)$$

U.S. customary units:

$$Q_s = 0.0027CQ_{\text{water}} \quad (7.4)$$

where  $Q_{\text{water}}$  is in either  $\text{m}^3/\text{s}$  or  $\text{ft}^3/\text{s}$  and suspended sediment concentration  $C$  is in  $\text{mg}/\text{L}$ . Rating curves developed from short periods of sediment gaging are often applied to long-term (e.g., 30-year) streamgage records to determine long-term sediment yield. This time series analysis can be used to determine the seasonality of sediment discharge as well as

the long-term yield. For a seasonal analysis, seasonal shifts in the rating relationship should be incorporated if they are significant.

In sediment yield computations, the time base of rating relationships should always match that of the discharge data for computing sediment yield. Thus, a rating relationship between daily load and mean daily discharge would be used to compute load from a daily discharge series. A rating curve based on instantaneous  $C-Q$  data pairs should be applied to mean daily discharge only when concentration is changing so slowly that an instantaneous value is representative of the 24-h interval. Application of a rating curve constructed from instantaneous  $C-Q$  data to a mean daily discharge series can underestimate sediment yields by 50 percent on smaller streams because the average daily flows do not reflect the peak discharges (Walling, 1977).

### 7.5.2 Load-Interval Flow-Duration Technique

Either annual or seasonal flow-duration data may be used to determine the long-term and seasonal sediment yield. In this case, a load-interval method is used to determine the sediment load within each discharge interval, instead of constructing a rating curve. The load interval procedure consists of two steps:

1. The discharge axis of the rating curve is partitioned into intervals and the average load for each class is calculated as the mean of the individual loads associated with the datapoints in the class. Approximately 20 classes may be used.
2. The total load for the period of record is computed as the sum of the mean load for each discharge interval multiplied by the discharge frequency for the same interval.

This method was found to produce a significant improvement in the accuracy of the period-of-record load estimate compared to the rating curve technique, because the mean load associated with a particular discharge class reflects only samples in that class and is not influenced by trends in adjacent classes as in a rating curve (Walling and Webb, 1981).

### 7.5.3 Interpolation Procedures

Interpolation uses time series sample points for suspended sediment and discharge to compute total load, assuming the measured values represent the mean values in each time interval. When short time intervals are used (e.g., 10 to 15 min. on small streams) this is the most accurate method available for determining load, since it continuously tracks the actual variation in both concentration and discharge. For continuous monitoring, turbidity has been used to gage concentration, and pumped samples may be used to continuously recalibrate turbidity against concentration. Procedures for turbidity monitoring are discussed in Chap. 8. Although the interpolation procedures can be used only over a period in which discharge and suspended sediment are monitored simultaneously, they can be used to construct rating relationships (e.g., daily load versus daily discharge) that can subsequently be applied to a longer-term discharge dataset.

### 7.5.4 Estimating Bed Load

Bed load is usually not measured, but is estimated as a fraction of the suspended sediment load. Strand and Pemberton (1987) present a procedure outlined in Table 7.4 for estimating bed load.

**TABLE 7.4** Bed Load Correction to Suspended Load Data

Suspended sediment concentration, mg/L	Streambed material	Texture of suspended material	Bedload in terms of suspended load, %
<1000	Sand	20-50% sand	25-150
1000-7500	Sand	20-50% sand	10-35
>7500	not sand*	<25%	5-15
Any concentration	Clay and silt	No sand	<2

\*Includes compacted clay, gravel, cobble, and boulder streambeds.

Source: Strand and Pemberton (1987).

## 7.6 ESTIMATING SEDIMENT YIELD

Estimates of sediment yield may seek to determine: the long-term yield, the timewise variability in sediment load for the design and modeling of a sediment routing procedure, or the spatial variability in sources of sediment to better focus yield-reduction efforts. A recent summary of techniques for estimating sediment yield was prepared by MacArthur et al. (1995).

This section introduces methods for estimating sediment yield that can be used at ungaged sites as well as gaged sites. However, even sophisticated computational methods can be based on heavily biased data, such as a nonrepresentative sediment rating curve, and computational sophistication is not synonymous with accuracy. It is always good to use multiple methods as a check. As an example of how multiple methods can be used to estimate sediment yield, MacArthur et al. (1990) used the results from a prior study, data from six nearby reservoirs, a published sediment yield map, and four different computational procedures (flow-duration, PSIAC, Dendy and Bolton drainage area relationship, and computed bed load for the erodible channel) to estimate sediment yield at Caliente Creek in California, an ephemeral stream incised into a semiarid alluvial fan and characterized by highly episodic sediment discharge.

Future conditions can differ from the present. New reservoir construction upstream, sediment release from upstream reservoirs, land use and geomorphic change, and catastrophic events all complicate the issue of long-term yield predictions, and the fallibility of long-term projections must always be kept in mind. Sediment yields usually seem to be underestimated. For example, Tejwani (1984) reviewed sedimentation studies of 21 Indian reservoirs and found that the specific sediment yield was lower than projected in one reservoir, but ranged from 40 to 2166 percent higher than the design value at the remaining 20 sites. Much of the problem was attributed to degradation of the watershed following project design studies. In contrast, the inflow of sediment into Lake Mead on the Colorado River has been far less than originally predicted due to a long-term reduction in sediment yield plus the construction of upstream storage reservoirs.

### 7.6.1 Regional Rate of Storage Loss

The results of reservoir surveys within a region may be used to estimate the overall rate of storage loss per unit of tributary area. This is a simple procedure in which measured specific sediment rates at other reservoirs in the regions (expressed in  $10^3 \text{ m}^3/\text{km}^2/\text{yr}$ , or mm/yr) are plotted against drainage area to develop a regional relationship, as illustrated

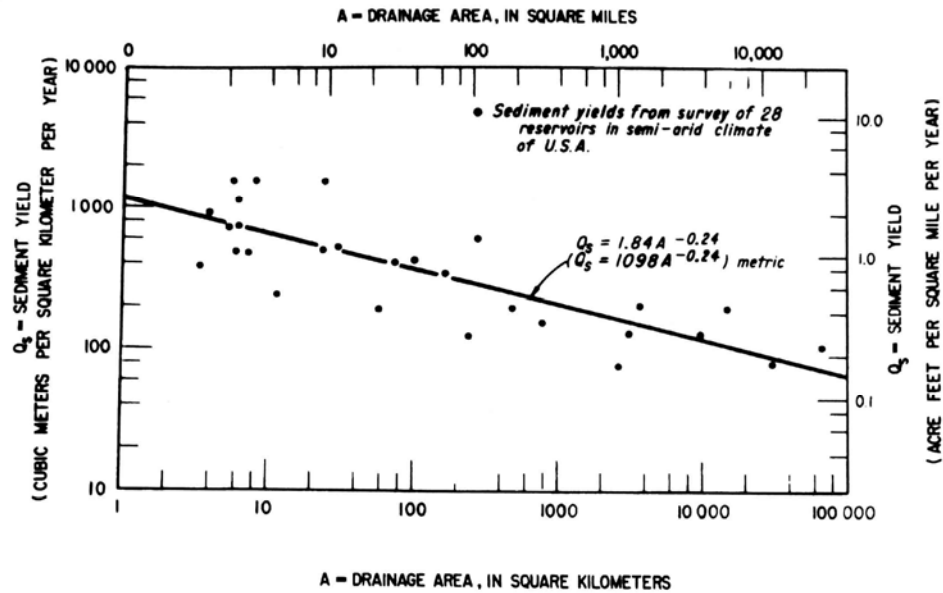


**FIGURE 7.21** Average annual sediment yield versus drainage area size for semiarid areas in the western United States (Strand and Pemberton, 1987).

in Fig. 7.21. The resulting relation will provide a guideline for estimating the anticipated sedimentation rate at the subject site. In preparing a graph of this type it is essential that the reservoirs all occupy watersheds having geologic and land use conditions similar to the site under investigation. Not all reservoirs in a general geographic area will be similar and as a result this approach will produce a very credible relationship in some regions but it may not work at all in others.

### 7.6.2 Regional Regression Relationship

If data on sediment yield and watershed characteristics are available from many sites, it may be possible to develop a regression relationship which describes the sediment yield within the region as a function of independent variables such as watershed area, slope, land use, and rainfall erosivity.

Dendy and Bolton (1976) related specific sediment yield to drainage area using resurvey data from about 800 reservoirs throughout the United States (excluding Florida), for drainage areas from 2.5 to 78,000 km<sup>2</sup> and runoff depths up to 330 mm/yr. Sediment yield was related to drainage area by the following relationship:

$$\frac{S}{S_R} = \left( \frac{A}{A_R} \right)^{-0.16} \tag{7.5}$$

At 505 sites, data were also available on mean annual runoff. It was found that the specific sediment yield peaked at about 508 mm (2 in) of annual runoff, resulting in two equations for predicting sediment yield based on both runoff depth and drainage area. For sediment depths less than 508 mm/yr:

$$\frac{S}{S_R} = C_1 \left( \frac{Q}{Q_R} \right)^{0.46} \left[ 1.43 - 0.26 \log \left( \frac{A}{A_R} \right) \right] \quad (7.6)$$

For runoff depths over 508 mm/yr:

$$\frac{S}{S_R} = C_2 e^{(-0.11Q/Q_R)} \left[ 1.43 - 0.26 \log \left( \frac{A}{A_R} \right) \right] \quad (7.7)$$

In the above three equations the following terms are used with values given in metric (and U.S. customary) units:

- $A$  = watershed area, km<sup>2</sup> (mi<sup>2</sup>)
- $A_R$  = reference watershed area value, 2.59 (1.0)
- $C_1$  = coefficient, 0.375 (1.07)
- $C_2$  = coefficient, 0.417 (1.19)
- $Q$  = runoff depth, mm/yr (in/yr)
- $Q_R$  = reference runoff depth value, 508 mm/yr (2 in/yr)
- $S$  = specific sediment yield, t/km<sup>2</sup>/yr (ton/mi<sup>2</sup>/yr)
- $S_R$  = reference specific sediment yield value, 576 t/km<sup>2</sup>/yr (1645 ton/mi<sup>2</sup>/yr)

Observed versus computed sediment yields for the 505 sites were plotted from Eqs. (7.6) and (7.7), producing a correlation coefficient of  $r^2 = 0.75$ .

These equations express only the general relationship between drainage area, runoff, and sediment yield and should be used only for preliminary planning purposes or as a rough check. Because these equations reflect average conditions across the United States, actual yields will tend to be higher (or much higher) than predicted in erosive areas and lower than predicted in areas of undisturbed watershed. Local site-specific conditions can influence sediment yield much more than drainage area or runoff.

### 7.6.3 PSIAC Method

The Pacific Southwest Interagency Committee (PSIAC, 1968; Shown, 1970) developed a watershed inventory method for use in the western United States to predict order-of-magnitude sediment yields in the range of 95 to 1430 m<sup>3</sup>/km<sup>2</sup>/yr (i.e., 0.095 to 1.43 mm/yr) based on nine physical factors in the watershed. Not all of the prediction factors are independent of one another. This method considers the yield contribution from all types of erosion sources, and not just surface erosion as in the USLE/RUSLE type models (Chap. 6). The methodology was tested by Shown (1970) in 28 drainage basins between 0.05 and 96 km<sup>2</sup> in Colorado, Wyoming, and New Mexico for which sediment data were available, and was found to correlate well with measured sediment yields. The method is intended to provide rough estimates of sediment yield, and it can also be used to determine the general magnitude of changes in sediment yield that might accompany changes within the watershed. The rating system is summarized in Table 7.5. Other weighting factors, or region-specific variables, may be more appropriate outside of the western United States.

A slightly modified weighting table developed by Strand and Pemberton (1987) of the U.S. Bureau of Reclamation is an adaptation of the PSIAC method. By personal communication, Strand indicated that good results had been obtained with the PSIAC-type methodology in the western United States, where it has generally provided better results than the USLE or similar approaches which focus only on sheet erosion processes.

**TABLE 7.5** PSIAC Method for Estimating Yield from Watershed Conditions\*

Sediment yield levels	A. Surface geology	B. Soils	C. Climate	D. Runoff	E. Topography	F. Ground cover	G. Land use	H. Upland erosion	I. Channel erosion and sediment transport
<b>High</b>	(10) a. Marine shales and related mudstones and siltstones	(10) a. Fine textured, easily dispersed; saline-alkaline; high shrinkage-swell. b. Single grain silts and fine sands.	(10) a. Storms of several days' duration with short periods of intense rainfall. b. Frequent intense convective storms. c. Freeze-thaw.	(10) a. High peak flows per unit area. b. Large volume of flow per unit area.	(10) a. Steep upland slopes (>30%). High relief; little or no floodplain development.	(10) Ground cover does not exceed 20%. a. Vegetation sparse; little or no litter. b. No rock in surface soil.	(10) a. More than 50% cultivated. b. Almost all area intensively grazed. c. Entire area recently burned.	(25) a. More than 50% of the area characterized by rill and gully or landslide erosion.	(25) a. Banks eroding continuously or at frequent intervals with large depths and long flow duration.
	<b>Moderate</b>	(5) a. Rocks of medium hardness. b. Moderately weathered. c. Moderately fractured.	(5) a. Medium-textured soil. b. Occasional rock fragments. c. Caliche layers.	(5) a. Storms of moderate duration and intensity. b. Infrequent convective storms.	(5) a. Moderate peak flows. b. Moderate volume of flow per unit area.	(10) a. Moderate upland slopes (<20%). b. Moderate fan or floodplain development.	(10) Cover not exceeding 40%. a. Noticeable litter. b. If trees present, understory not well developed.	(10) a. Less than 25% cultivated. b. 50% or less recently logged. c. Less than 50% intensively grazed. d. Ordinary road and other construction.	(10) a. About 25% of the area characterized by rill and gully or landslide erosion. b. Wind erosion with deposition in stream channels.

**TABLE 7.5** PSIAC Method for Estimating Yield from Watershed Conditions\* (Continued)

Sediment yield levels	I.								
	A. Surface geology	B. Soils	C. Climate	D. Runoff	E. Topography	F. Ground cover	G. Land use	H. Upland erosion	I. Channel erosion and sediment transport
Low	(0)	(0)	(0)	(0)	(0)	(-10)	(-10)	(0)	(0)
	a. Massive, hard formations.	a. High percentage of rock fragments.	a. Humid climate with low-intensity rainfall.	a. Low peak flows per unit area.	a. Gentle upland slopes (<5%).	a. Area completely protected by vegetation, rock fragments, litter.	a. No cultivation.	a. No apparent signs of erosion.	a. Wide shallow channels with flat gradients, short flow duration.
	b. Aggregated clays.	b. High in organic matter.	b. Precipitation in form of snow.	b. Low volume of runoff per unit area.	b. Extensive alluvial plains.	Little opportunity for rainfall to reach erodible material.	b. No recent road construction.	b. Channels in massive rock, large boulders or well-vegetated.	b. Channels in massive rock, large boulders or well-vegetated.
	c. High in organic matter.	c. Arid climate; low-intensity storms.	c. Arid climate; rare convective storms.	c. Rare runoff events.			c. Low-intensity grazing.	c. Artificially controlled channels.	c. Artificially controlled channels.

Numerical Score	Sediment Yield†	
	(mm/yr)	(acre•ft/mi <sup>2</sup> /yr)
>100	1.5	3.0
75-100	0.5-1.5	1.0-3.0
50-75	0.25-0.5	0.5-1.0
25-50	0.1-0.25	0.2-0.5
0-25	<0.1	<0.2

\*Weighting factors in parentheses.

†Exact conversion 1 acre•ft/mi<sup>2</sup> = 0.476 mm depth of soil loss

Source: PSIAC (1968).

Best results are obtained when the methodology is first "calibrated" by using similar nearby basins where sediment yield is known from reservoir resurveys or extensive and reliable stream gaging and sampling. A similar calibration approach should be used in applying the methodology to a humid area.

#### 7.6.4 Sediment Yield Maps

Sediment yield mapping can undertake a variety of forms. The regionalized sediment yield map for India (Fig. 7.22) was developed from reservoir resurvey data from 46 sites. It illustrates the basic strategy of dividing a large heterogeneous geographic region into subareas having presumably more uniform sediment yield characteristics. However, this map also illustrates the problem inherent in the use of yield maps: highly variable within-region sediment yields. Whereas the average rate of sediment accumulation between the highest and the lowest regions in India varies by a range factor of 3, within-region variation has a range factor as high as 81. Many factors other than regional physiography control the rate of sediment accumulation.

Rooseboom (1992) reported on a detailed South African study to characterize and predict sediment yield nationwide which resulted in the preparation of a sediment yield map after other techniques failed to produce usable results. Although the approach used in South Africa cannot eliminate the uncertainty due to yield variations that can occur within each region, the degree of uncertainty is quantified.

The problem confronted in South Africa was that of highly variable specific sediment yields, ranging from 1 to 880 t/km<sup>2</sup>/yr, including large differences even between catchments which otherwise appeared to be nearly identical according to the available data. There was no discernible pattern between drainage area and sediment yield. The relatively dry temperate climate in South Africa, variety of land forms, widespread incidence of accelerated erosion, and reduction in sediment yield in some areas due to

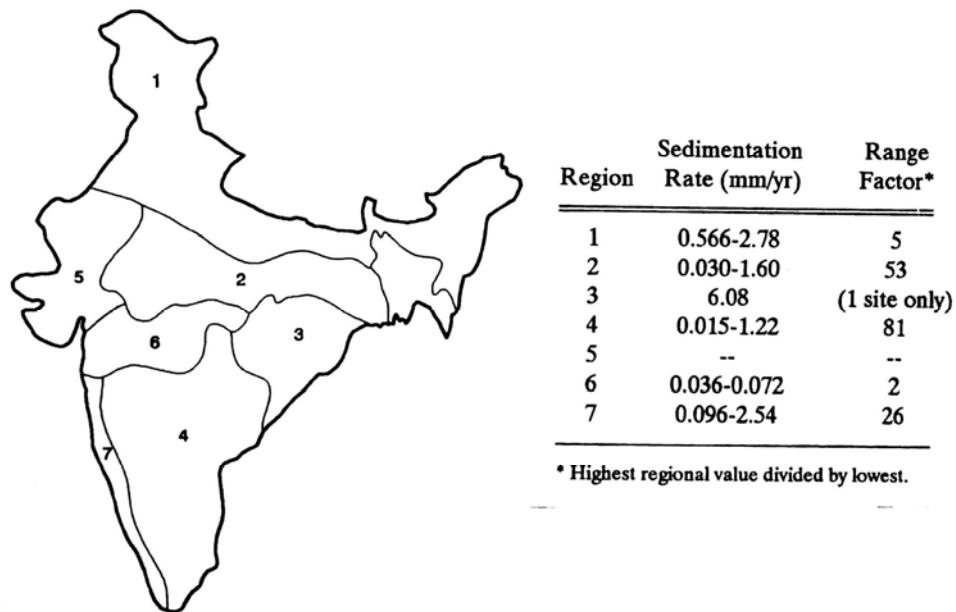


FIGURE 7.22 Sediment yield map for India (Shangle, 1991).

upstream farm ponds and the depletion of readily erodible topsoil further complicated the analysis. Three different methods were used to determine the sediment yield characteristics of the catchments: multiple regression analysis, deterministic runoff modeling, and regionalized statistical analysis. The analytical dataset consisted of 122 reservoirs having between 8 and 82 years of reservoir survey data obtained by the South African Department of Water Affairs. The following independent variables were available for the analysis: watershed area, sediment yield, soil erodibility indices, land use, slopes, rainfall intensity, and rainfall erosivity indices. Other parameters may also have been important but were not available on a countrywide basis.

An attempt to develop a regression relationship was frustrated by very low levels of significance, large standard errors of estimate, multicollinearity, and equations that predicted negative unit yields in some cases. The second method attempted was to construct a deterministic model describing runoff transport capacity from each catchment and to calibrate this model against sediment yield. The rational formula was used to determine runoff discharge, continuity and Chezy equations to convert discharge into flow velocities and depths, and stream power to represent the sediment transport capacity of the discharge. However, this method could not be calibrated to the dataset. Since most of the sediment load in South African rivers is smaller than 0.2 mm in diameter, sediment loads are dependent primarily on the amount of sediment supplied from the catchment rather than instream transport capacity.

The third method, which was adapted, was to produce a sediment yield map by dividing the country into nine regions judged to have relatively uniform yield potential considering: soil types and slopes, land use, availability of recorded yield data, major drainage boundaries, and rainfall characteristics. Regions were then further divided into areas of high, medium, and low sediment yield potential. A constant ratio between yields in the high-, medium-, and low-yield areas in all regions was used. The study resulted in: (1) a national map showing nine major regions with three subregions in each; (2) tabulated mean standardized sediment yield for each yield region; (3) graphs for each region showing the variability of yield data as a function of catchment size (Fig. 7.23); and (4) a table giving the high, medium, and low yield potential in each region.

A four-step procedure is used to estimate sediment yield. First locate the catchment, assign it to a region, and compute the watershed area falling within each subregion. Second, look up the standardized regional yield from a table. Third, adjust the standardized yield for the confidence level. For example, to conservatively estimate the maximum expected sediment yield, enter the graph of yield variability within the region as a function of catchment area and determine the factor at the 90 percent confidence level (a value of 4.0 for a 1200 km<sup>2</sup> watershed in Fig. 7.23). Multiply the standardized regional yield by this factor. Fourth, measure the area of the total watershed within the high-, medium-, and low-yield modifiers and apply the subregional weighting factors to determine the weighted average yield from the heterogeneous catchment area.

### 7.6.5 Erosion Modeling

Formal erosion modeling using USLE/RUSLE, WEPP (see Chap. 6), or some other system can be used to quantify erosion and sediment yield. The fraction of the eroded sediment delivered to the point of interest is determined by applying delivery ratios. Properly applied, this method can provide information on both the type of erosion and its spatial distribution across the watershed. For reliability, the results should be calibrated against sediment yield measurements at one or more points in the study watershed.

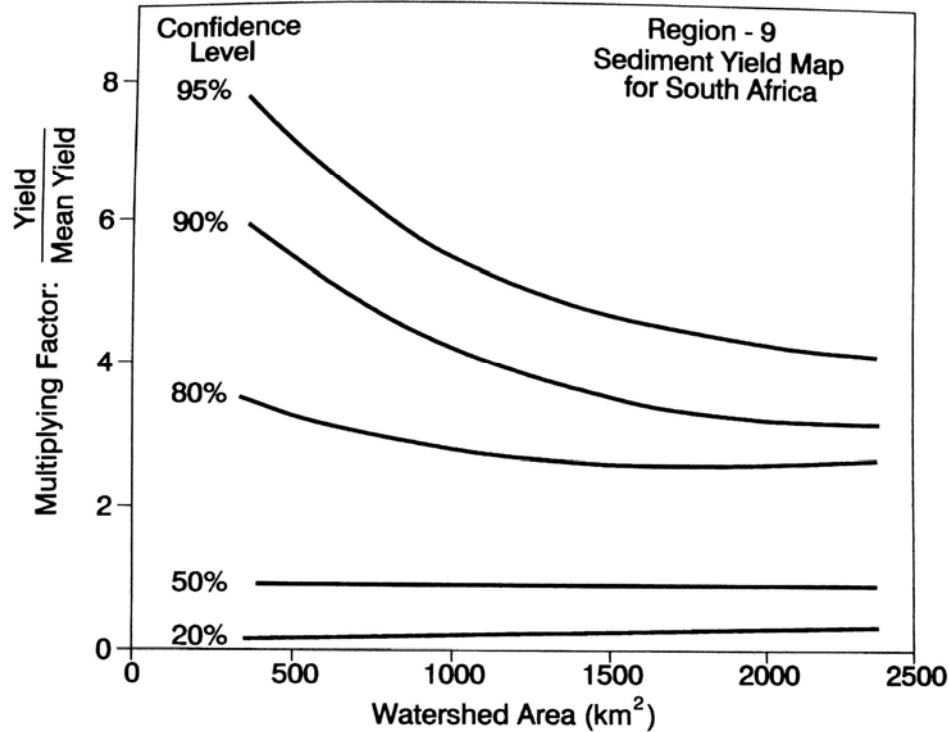


**FIGURE 7.23** Variability of sediment yield as a function of catchment size within each yield area, based on reservoir surveys (Rooseboom, 1992).

## 7.7 GIS AND EROSION PREDICTION

A geographic information system (GIS) is a relational database system that allows management of multiple layers of spatially distributed information. Layers of information can be combined, forming overlays to aid synthesis and interpretation by users (Fig. 7.24). A GIS does not generate new data by itself, but by manipulating the database the user may identify relationships not previously apparent. There are two types of GIS: raster (or grid-based) systems and vector-based systems. Both types are equally powerful tools for specific applications; they are being used for watershed management and are being linked to erosion and hydrologic models (Shanholtz et al., 1990; Vieux and Kang, 1990).

Erosion models can be implemented in a GIS format through user interfaces or shells written in a variety of computer languages (Lal et al., 1990; Pérez et al., 1993). The interface allows a user to: (1) define a study area; (2) select management practices such as crops, rotations, irrigation; (3) select soil and water conservation practices such as contouring, terraces, and strip cropping; (4) access the GIS database to attach attributes to model parameters; (5) execute the model and modify attribute tables; and (6) analyze and display the results. The model spatially displays the amount of soil loss associated with the selected management practices.

AEGIS is one of the first applications linking the crop simulation models in DSSAT1 (Tsuji et al., 1994) to a GIS. Its application in three regions in Puerto Rico is described by

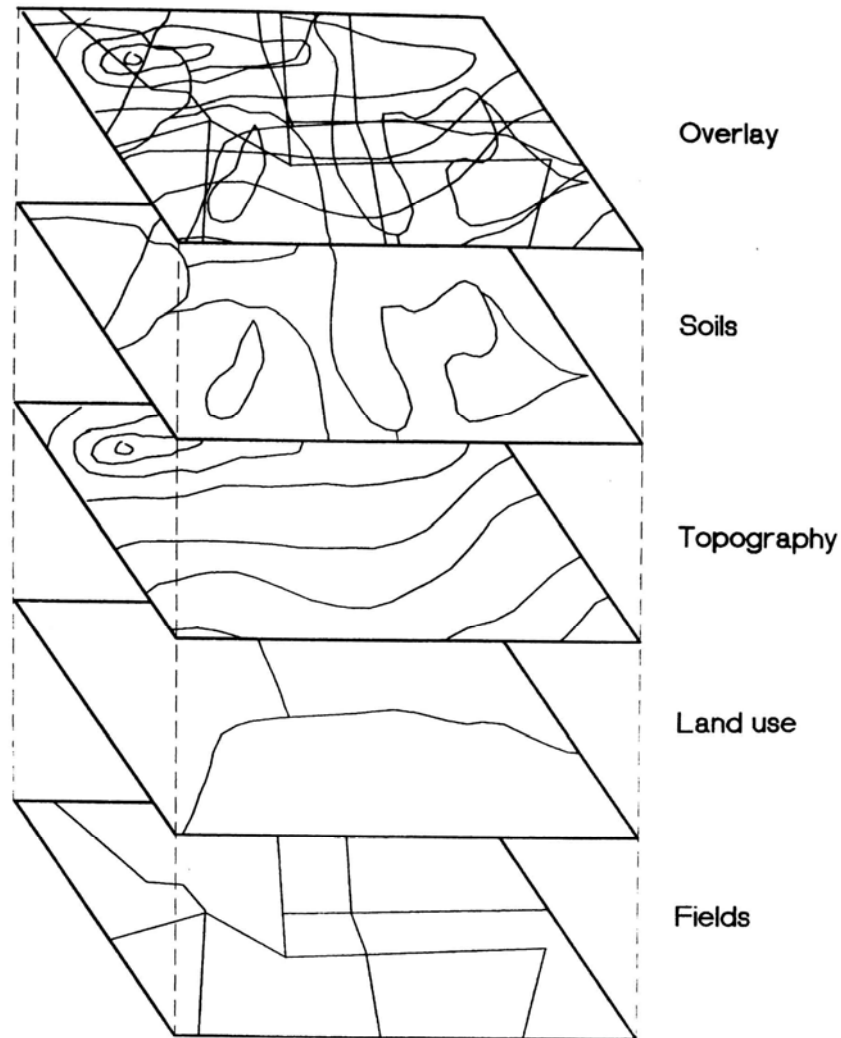


**FIGURE 7.24** Concept of GIS overlays.

Calixte et al. (1992), and subsequent versions of AEGIS allow the user to insert new regions containing the required GIS layers describing soils, topography, and climate. AEGIS has been modified and used for regional planning, such as the study conducted by Bowen (1995) in Albania for USAID to determine fertilizer requirements for achieving minimum wheat production targets. It is currently being applied to the southern coastal plain of Puerto Rico to quantify the soil loss impacts of a shift from sugarcane to more-nutrient-demanding vegetable crops that also maintain less soil cover during the growing season and expose the soil to erosive rain. However, initial versions of AEGIS run the former USLE model in a vector-based GIS system and predict erosion only to the edge of the polygon. The limited ability to predict sediment delivery to channels, and subsequent channel routing, is at present a serious limitation of GIS modeling. However, when a downstream gage station is available, the sediment delivery can be estimated by calibration procedures.

The LISEM model (DeRoo et al., 1994) is an example of a physically based erosion model completely incorporated within a raster GIS system. There are no conversion rou-

tines. The model is completely expressed in terms of the GIS command structure using a prototype modeling language which allows a high level of aggregation; the entire program code contains less than 200 lines, exclusive of comments. The processes modeled in LISEM include interception, infiltration, splash detachment, rill and interrill erosion, storage in microdepressions, and overland and channel flow. The results of the model consist of GIS raster maps of soil erosion and deposition and maps of overland flow at desired time intervals during an event.

Linkage of erosion prediction models and a GIS database containing information such as soil erodibility, slope, land use, and climate offers the potential to examine the impacts of management practices on erosion rates and sediment yield across large landscapes. The potential exists to automatically analyze and predict the impacts of specific storm tracks, including the possibility of linking with weather radar. The major theoretical limitation with this approach is the difficulty of computing sediment delivery from each landscape unit in the database to a downstream point of interest, such as a reservoir.

## **7.8 IDENTIFYING SUSPENDED-SEDIMENT SOURCES**

---

Given the widely variable rates of sediment yield from different landscape units, erosion control methods to reduce the inflowing load should focus on the landscape units responsible for the delivery of most sediment to the reservoirs. Several techniques may be used to identify sediment sources by either: (1) geographic location or (2) erosion type or process, for example, surface erosion or channel erosion. Three basic strategies for determining the source of suspended sediments have been outlined by Peart (1989): indirect determination, direct measurement, and sediment fingerprinting. Sediment sources are usually determined by indirect methods using an erosion inventory or modeling. An erosion inventory consists only of an assessment of relative rates of erosion and sediment delivery, without necessarily quantifying the absolute magnitude of sediment production. Modeling, on the other hand, quantifies erosion rates within the framework of a formal numerical methodology.

### **7.8.1 Indirect Determination**

Methods for erosion modeling based on area-distributed models (RUSLE, WEPP) are suitable for the indirect determination of sediment sources. These techniques have two major limitations. First, most erosion models do not include channel erosion processes, which must be measured and then computed separately. The second limitation is the difficulty of assigning the sediment delivery ratio. Because the rate of surface erosion is much larger than the sediment yield in many systems, the apportionment of sediment loads to different source regions may depend primarily on the subjective assignment of sediment delivery ratios to each source area. Because of these limitations, modeling of source area contributions should be complemented with direct measurement to the greatest extent possible.

### **7.8.2 Direct Measurement**

Sediment production from subareas within a watershed can be directly measured by multiple suspended sediment gaging stations. Direct measurement is an essential part of a sediment monitoring program, especially when the watershed contains soil and land use conditions for which erosion equations have not previously been calibrated by plot studies, and where there is uncertainty concerning the sediment delivery ratio, as is often

the case. The availability of portable, programmable sampling and data-logging equipment incorporating pumped samplers, level recorders, turbidimeters, and tipping-bucket rain gages makes direct measurement of sediment yield at multiple sites within a watershed an increasingly attractive alternative. The cost of this instrumentation is very small compared to the value of the reservoir infrastructure it is desired to protect.

As an alternative, direct measurement at selected points can be used to calibrate regional erosion and sediment delivery models. In either case, sampling stations should be carefully selected beforehand on the basis of, as a minimum, a preliminary assessment of erosion sources within the watershed to identify expected high- and low-yield source areas. A simplified erosion inventory procedure might be used for this initial assessment.

Direct measurement over an interval of years is necessary to determine rates of gully and channel erosion. The database for soil loss measurements may be extended by using historical air photos, historical cross-section surveys at locations such as bridge or pipeline crossings, records of gage shift at streamgage stations, and oral histories, in combination with current measurements and monitoring. The services of a competent fluvial geomorphologist are highly recommended to assist evaluations of the contribution from channel processes.

### 7.8.3 Qualitative Erosion Inventory

Use of a qualitative erosion inventory procedure based on field mapping to identify the nature and spatial distribution of active sediment sources in the urbanizing 330-km<sup>2</sup> Anacostia watershed near Washington, D.C., was described by Coleman and Scatena (1986). Standardized guidelines for assessing the relative importance of erosion sources were prepared in tabular format, a sample of which is shown in Table 7.6. Four types of land use considered to generate high sediment yields were identified: agricultural areas, construction sites, surface mines, and stream channels. Land uses falling into these categories, as identified from a variety of sources, were located on 1:20,000 topographic maps. Each of 252 identified sites was then visited by a two-person inspection team to rank sediment yield at each site as high, medium, or low compared to other land uses in the same category, based on an assessment of both erosion rates and processes affecting the delivery of eroded sediment to stream channels. In addition to information on the types of problems contributing to high sediment yield, the results were also mapped to show the spatial distribution of areas of high and low sediment yield. During inspections the sites were also evaluated with respect to their probable future sediment load, an important evaluation criterion because of the transitional land uses in the urbanizing basin (recall Fig. 7.9).

### 7.8.4 Sediment Fingerprinting

Under favorable conditions, sediment trapped at a downstream point can be identified or "fingerprinted" as to its source on the basis of sediment characteristics distinct to each geographic source area or type of erosion process. Sediment characteristics may be distinguished by geographic variations in geologic parent material or vertical variations caused by weathering or radionuclide deposition. In the case of distinction by weathering, the delivery of surface soil from the upper "A" horizon would be indicative of surface

**TABLE 7.6** Erosion Inventory Assessment Factors for Agricultural Areas

Factor	Factor Importance		
	High (10)	Medium (5)	Low (0)
1. Land use	<ul style="list-style-type: none"> <li>a. &gt;50% crops</li> <li>b. &lt;50% crops, but poorly maintained</li> </ul>	<ul style="list-style-type: none"> <li>a. &lt;25% crops</li> <li>b. Active pasture</li> <li>c. Effective conservation</li> </ul>	<ul style="list-style-type: none"> <li>a. Fallow or abandoned</li> <li>b. Conservation tillage</li> <li>c. Orchard</li> </ul>
2. Topography	Steep upland slopes, 40–100%	Moderate upland slopes, 20–40%	Gentle slopes, 0–20%
3. Soil erodibility	High, $k > 0.37$	Moderate, $0.25 < k < 0.37$	Low, $k < 0.25$
4. Sediment delivery	<ul style="list-style-type: none"> <li>a. Adjacent to water course</li> <li>b. No buffer zones</li> </ul>	<ul style="list-style-type: none"> <li>a. Not adjacent to water course</li> <li>b. Adequate buffer zones</li> </ul>	<ul style="list-style-type: none"> <li>a. Not adjacent to water course</li> <li>b. Effective buffer zones</li> </ul>
General site status			
	Very high	30–40	
	High	20–30	
	Moderate	10–20	
	Low	0–10	

Source: Coleman and Scatena (1986).

erosion whereas the delivery of deeper soils or parent material can indicate channel erosion sources.

Properties used for fingerprinting include clay mineralogy, sediment color, sediment chemistry, mineral magnetic properties, and radionuclide concentrations. The three radionuclides with the greatest promise for use as indicators are the artificial isotope  $^{137}\text{cesium}$ , and atmospherically derived (i.e., nonnatural or "unsupported")  $^{210}\text{lead}$  and  $^7\text{beryllium}$  isotopes. All are gamma emitters with different fallout histories and decay rates and have been dispersed at relatively uniform rates over wide geographic areas. On all, simultaneous nondestructive activity measurements can be made relatively easily by modern high-resolution gamma spectrometry equipment. Because fallout rate is unrelated to parent soil material, radionuclide concentration can be used to differentiate between sediment sources in basins of otherwise homogeneous soils. Fingerprinting techniques using radionuclides are described by Walling and Woodward (1992).

Fingerprinting techniques were used by Peart and Walling (1986) to analyze sediment sources in the small 9.3-km<sup>2</sup> Jackmoor Brook watershed in the United Kingdom with multiple tracers: pyrophosphate iron, dithionite iron, manganese oxide, magnetic susceptibility, saturation isothermal remanent magnetization (SIRM), total P, total N, organic carbon, and  $^{137}\text{cesium}$ . Over 100 samples of surface and streambank soils were collected and the fines ( $d < 0.06$  mm) were separated and analyzed. Suspended sediment from multiple runoff events was also collected from the stream by pumped sampler, centrifuged, and analyzed. The values of all tracer parameters except one were higher in the suspended sediment compared to the soil samples because of enrichment in the fine fraction. Particle size analysis determined that enrichment was primarily restricted to the smaller than 0.010 mm fraction. The enrichment factor for this size fraction was about 1.5 for both channel and surface material but was higher for organic material. Following correction for enrichment, the relative contribution of surface and bank material to the composite suspended load was determined by using a simple mixing model:

$$C_s = \frac{P_r - P_b}{P_s - P_b} \times 100 \quad (7.8)$$

where  $C_s$  = percent contribution from surface soil sources,  $P_r$  = value of selected property for suspended sediment,  $P_s$  = value of selected property for surficial soil, and  $P_b$  = value of selected property for bank material.

To check the error introduced by enrichment calculations, property ratios were also analyzed (e.g., carbon/phosphorus). If property ratios from each source are consistent across all size fractions, this eliminates the need to correct for enrichment computations. The enrichment computations were generally confirmed.

By further subdividing the soil sample dataset into cropland and permanent pasture, it was possible to differentiate between these two sources of surface sediment based on  $^{137}\text{cesium}$  activity. Radioactive cesium is tightly sorbed at the soil surface and penetrates insignificantly into deeper soil layers. Thus, the highest levels of activity corresponded to topsoil in permanent pasture which had been continuously exposed to fallout, intermediate levels of activity occurred in arable soils mixed by ploughing, and the lowest levels were in the deep deposits along channel banks. On the basis of fingerprinting it was concluded that suspended sediments at the gage station were derived from the following sources: 6 percent from channel banks, 24 percent from permanent pasture topsoil, and 70 percent from arable topsoil.

Fingerprinting can potentially be applied to sediments deposited in reservoirs. However, the reconstruction of stratigraphic histories and application of source tracing or fingerprinting techniques to reservoir sediment profiles is complicated by the high variability in sediment deposition patterns. Foster and Charlesworth (1994) analyzed core data from four small (less than 7-ha pool area) artificial impoundments in the United

Kingdom and found that the spatial variability is often greater than downcore variability. The problem of spatial heterogeneity in reservoir sediments due to longitudinal sorting, variable pool level, reworking of sediments, and sediment focusing by density currents must be carefully analyzed in any stratigraphic or source-tracing analysis of deposits.

Under conditions where it is applicable, fingerprinting offers the means to directly determine sediment delivery by source. However, use of this method is complicated by phenomena including enrichment with fines and organics as a result of differential rates of transport, sediment transformations during transport which alter nonconservative sediment characteristics, and the temporary storage and remobilization of sediment within the fluvial system. This makes fingerprinting more applicable to watersheds with rapid sediment export and small amounts of sediment storage in streams. Fingerprinting cannot be employed if sediment tracer characteristics are relatively uniform throughout the basin. However, even when soils are uniform across a watershed, it may be possible to distinguish among erosional sources on the basis of differences in radionuclide deposition. At present, fingerprinting is primarily a research tool.

### 7.8.5 Lake and Reservoir Deposit Histories

Sediment deposits in impoundments may be cored and characteristics of the core material may be interpreted to provide information on the processes responsible for sediment delivery from the watershed. For example, Hereford (1987) examined the depositional history of a small reservoir at the outlet of a 2.8-km<sup>2</sup> high-relief basin in Utah, and from stratigraphic analysis of the alluvium determined that significant sediment deposition occurred in the reservoir only 21 times in 38 years. From the thickness of the deposits, the average sediment load of individual events was determined as 2300 m<sup>3</sup>/km<sup>2</sup> with a standard deviation of 1300 m<sup>3</sup>/km<sup>2</sup>. The variation in sediment yield between events was slightly less than 1 order of magnitude. That this variation was considerably lower than the 3 orders of magnitude variation in annual sediment yield typical of the region suggested that sediment supply was limited by erosion rates on hill slopes rather than transport processes. In landscapes characterized by large episodic sediment yield events, the analysis of natural lake cores may help estimate the frequency of these large events, which may leave a thick layer of coarse sediment or other identifiable and datable features in the lacustrine sediment record. Laronne (1990) describes the use of stratigraphy in small artificial impoundments to determine the recurrence interval of sediment discharge events in the semiarid northern Negev, Israel. They suggest that the availability of event-based sediment yield records may be utilized to predict erosion rates without recourse to rainfall or runoff data.

## 7.9 CLOSURE

---

Sediment yields are highly variable, and most of the sediment entering a reservoir is delivered from only a small fraction of the landscape during short periods of time. The key to effective sediment management, either in the watershed or at the reservoir, lies in identifying and characterizing both the spatial and timewise nature of sediment delivery. This, in turn, will permit control efforts to be focused effectively, and for sustainable use to be achieved.

Fluvial sediment yield is among the most difficult parameters to accurately measure in the field, but accurate measurements are essential to provide the data required to better understand delivery processes, and to support sediment modeling efforts. Due to the highly variable rates of sediment delivery, the results of erosion modeling are not necessarily representative of the sources of sediment actually reaching a reservoir, unless

they can be calibrated with field data. Modern fluvial sampling techniques using portable, microprocessor-driven automatic sampling equipment incorporating stage recorders, turbidimeters, and pumped samplers, can be particularly useful for fluvial sampling. Techniques for sediment sampling are outlined in Chap. 8.

---

## CHAPTER 8

---

# FLUVIAL MORPHOLOGY AND SEDIMENT SAMPLING

---

The quantification of sediment load is fraught with difficulty and the potential sources of error are numerous because of vertical and horizontal variability in sediment transport within the river section, extreme and potentially rapid variation in sediment transport over time, poor correlation of sediment concentration with other hydrologic variables, and logistical problems associated with sampling during flood and hurricane. A basic understanding of fluvial sediment variability in time and space, sampling techniques, bias, and possible sources of error is essential to properly collect and interpret sediment data. This chapter introduces several basic concepts of river morphology, focusing on patterns of sediment variation within the fluvial environment. Sampling techniques for both suspended load, bed load, and bed material are presented, and some of the sources of error that can affect sampling programs are discussed.

---

### 8.1 STREAM FORM AND CLASSIFICATION

---

River morphology is a complex topic, and this section provides only a brief summary of several fundamental concepts which are important from the standpoint of understanding sampling strategies. General concepts are presented by Guy (1970) and a quantitative overview of river morphology from the aspect of fluvial engineering is presented in Chang (1988).

#### 8.1.1 Stream Order

Stream order is a measure of the position of a stream in the hierarchy of tributaries. In 1932, Horton introduced to U.S. practice a stream-ordering system in which the lowest order was assigned to the smallest stream, the reverse of the European practice which assigned the lowest order to the largest rivers. In the Horton method a first-order stream has no tributaries at the mapping scale being used in the analysis, and second-order streams have only first-order tributaries. Third-order streams have only first- and second-order tributaries, etc. This system extends downstream including higher-order streams until reaching the study limit or the sea. In the Strahler method all intermittent streams at the upstream limit of the drainage system are first-order, the confluence of two first-order streams creates a second-order stream, etc. This method may be considered less subjective than Horton's and is widely used. Both methods are illustrated in Fig. 8.1.

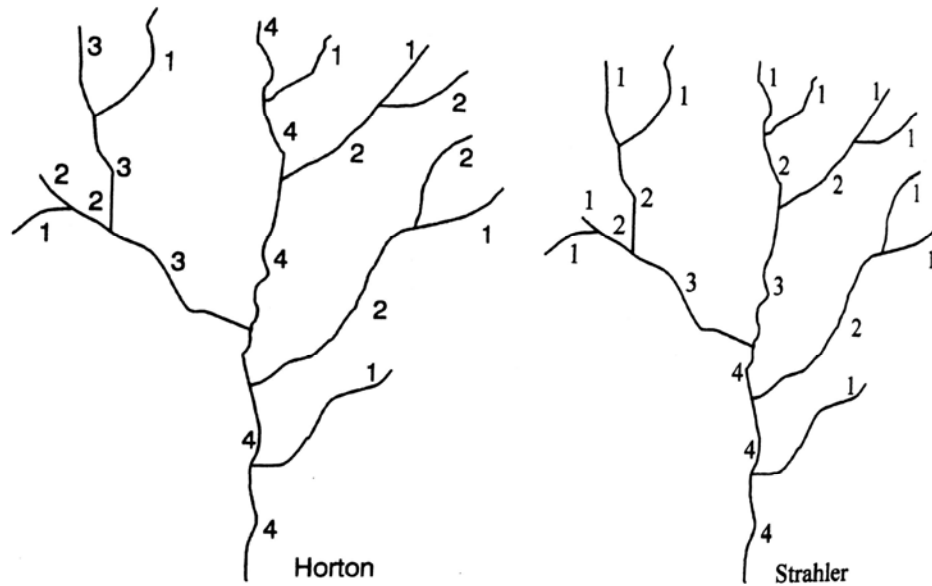


**FIGURE 8.1** Stream-ordering methods proposed by Horton and Strahler. Other ordering schemes are also in use (after Gordon et al., 1992).

Other ordering systems also exist (Gordon et al., 1992). Stream lengths and orders are commonly determined by using topographic mapping at 1:24,000 or similar scale, and stream order determination depends on the mapping scale since smaller tributaries appear at larger map scales. At a scale of 1:62,000 the Mississippi River is of tenth order. Many low-order streams discharge directly into streams two or more orders higher, and building a dam on every third-order stream in a fifth-order network will typically control only about half of the total drainage area. For this reason, schemes to build either sediment or flood retention dams on smaller streams require a large number of structures (Leopold et al., 1964).

### 8.1.2 Drainage Density

*Drainage density* is the total length of streams per unit area within a watershed. Because much eroded sediment is redeposited prior to reaching channels, basins with a high drainage density tend to export sediment efficiently. Drainage density comparisons must be made on the same mapping scale, since greater enlargement reveals smaller tributaries and produces longer total stream lengths. Topographic maps at 1:24,000 or similar scale are generally used for this computation.

#### 5.1.1. 8.1.3 Stream Patterns

Stream patterns reflect geology, sediment load, discharge, and slope. In erodible materials, the stream planform is controlled largely by sediment load and hydraulic forces, modified by erosion-resistant features on the bed and banks such as bedrock outcrops, clay lenses, or similar features that influence both the meander pattern and migration rate. The classification of basic channel patterns is summarized in Fig. 8.2. Stream *sinuosity* is computed as the channel length divided by the straight-line valley length, which may also be expressed as valley slope divided by channel slope. A stream is classified as meandering if sinuosity exceeds 1.5.

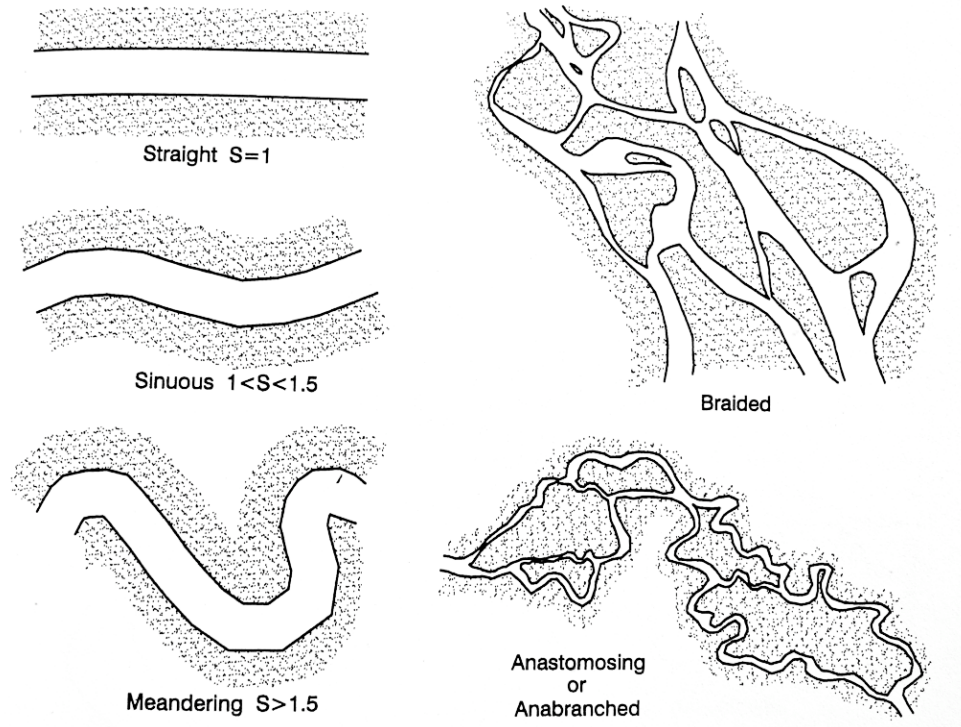


**FIGURE 8.2** Basic river planforms and sinuosity  $S$ . Straight channels occur only when structural controls are present.

#### 8.1.4 Meandering and Stream Migration

Rivers are rarely straight for significant distances, except when constrained by structural controls. Even in laboratory flumes containing uniformly graded material it is impossible to maintain a straight channel; flow irregularities cause differential rates of erosion and initiate meander formation. Stream meandering patterns and bar location are illustrated in Fig. 8.3. Erosive forces are focused on the exterior of bends slightly downstream of the center of curvature. The bed and bank are scoured on the outside of the bend, helical flow patterns are created, and the *thalweg* (the deepest flow line) occupies the exterior of the bend, as shown in section  $B-B'$  of the figure.

The interior of bends is a lower-velocity depositional environment characterized by the formation of a *point bar* which infills behind the migrating meander bend. Pioneer vegetation adapted to depositional environments colonizes the point bar and retards the flow velocity as it crosses the bar, encouraging the deposition of increasingly finer-grained material. Erosion at the meander exterior and deposition on the point bar causes meanders to migrate both laterally and downstream. Erosion from the bend exterior is balanced by deposition on the point bar, and the river maintains a constant width as it migrates across the floodplain. Bank erosion and migration rates are greatly accelerated during periods of high flow. When lateral migration brings two meanders into proximity, causing a meander to cut off, it creates an oxbow lake which will eventually fill with sediment from future floods.

The *thalweg* moves from one side of a river to the other as meanders turn in alternate directions. The zone of *thalweg* crossing between bends typically has a flatter and

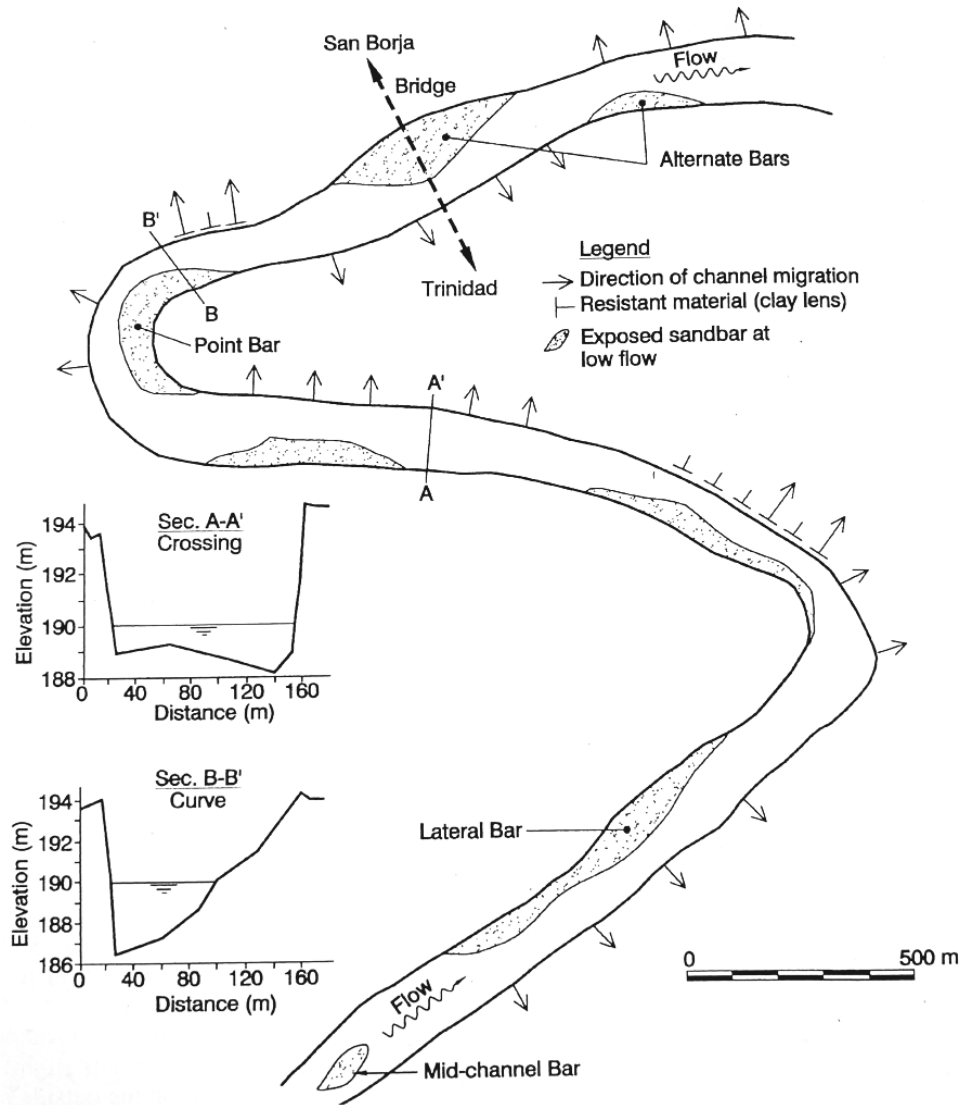


**FIGURE 8.3** Reach of the meandering sand-bed Rio Maniqui in the upper Amazon drainage in Bolivia, showing the main types of bars, direction of meander migration, and the variation in channel cross section between meander bends and crossings. The bed consists primarily of medium to coarse sands, but clay lenses create erosion-resistant areas on the bed and banks which influence the rate and pattern of river migration (after Morris and Ancalle, 1994).

shallower cross section, compared to the meanders, and an unstable thalweg location. As a result, the thalweg profile along a meandering river will be irregular, characterized by deeper water at bends and shallower water at crossings. This same type of irregularity can occur in the thalweg profile of reservoirs having curved reaches and sufficient sediment accumulation for deposits to be affected by scour. An example of such a thalweg profile in Loiza reservoir is presented in Fig. 20.9, where a scour hole has developed in the fine sediment at a sharp curve near km 5.5.

### 8.1.5 Lane's Balance

Alluvial rivers are dynamic systems, continually adjusting to the unsteady hydrologic environment, and river form can change dramatically when certain hydraulic thresholds are crossed. A qualitative geomorphic relationship among the major variables affecting river form was proposed by Lane (1955) in the form of an equilibrium equation:

$$Q_s d \propto Q S \quad (8.1)$$

where  $Q_s$  and  $Q$  refer to sediment and water discharge respectively,  $d$  to grain diameter, and  $S$  to bed slope. This equation may also be visualized in the form of the balance shown in Fig. 8.4. According to this relationship, dam construction which affects a downstream river reach by reducing sediment supply or reducing sediment size can be expected to produce downstream degradation since all of these actions tend to reduce the slope required to maintain equilibrium. In contrast, the reduction in total or peak discharge which typically occurs below the dam, tends to increase the equilibrium slope. Thus, reduced sediment discharge is, to a certain extent, balanced by reduced water discharge. The interplay among these and other factors (armoring, tributary inflows, encroachment by vegetation) will determine the extent and speed of channel adjustment below the dam. Generally, an aggrading channel tends to widen and a degrading channel tends to narrow. Quantitative geomorphic relationships which are an extension of Lane's qualitative approach have been presented by Chang (1988), Yang (1996), and Klaassen (1995).

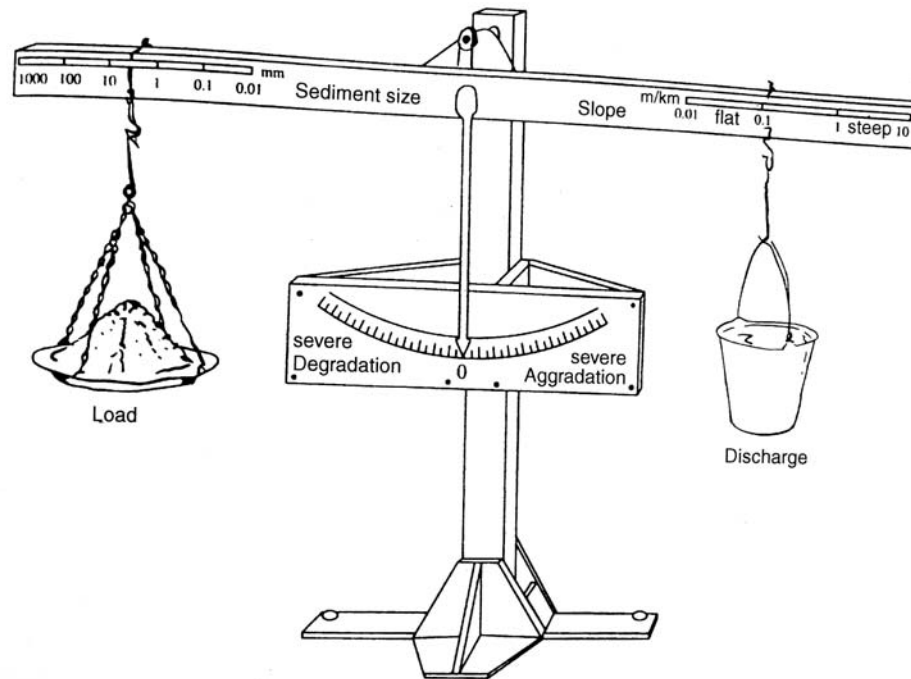


**Figure 8.4** Sediment load x Sediment size  $\propto$  Stream slope x Discharge

**Figure 8.4** Visualization of the factors influencing the geomorphic behavior of an alluvial stream (Lane, 1955)

**8.1.6 Differences between Sand and Gravel Bed Streams**

The grain size in movable bed rivers can range from silts to boulders. For convenience, the continuum of bed material sizes will be divided into sand-bed and gravel-bed rivers, understanding that sand bed also includes smaller noncohesive sediment, and gravel bed includes coarser material. To exhibit all the characteristics of a sand-bed river, the depth of sand deposits in the bed must exceed the maximum scour depth so that additional sand is continuously available for transport at all discharges. Several important differences between sand-bed and gravel-bed rivers are summarized in Table 8.1.

**TABLE 8.1** Selected Differences between Rivers with Sand and Gravel Bed.

Parameter	Sand bed	Gravel bed
Grain size variation in the bed	Small	Large
Bed material transport	Continuous	Episodic
Channel slope	(Velocity) <sup>5</sup>	(Velocity) <sup>3</sup>
Variation in sediment transport	Low	High
Armoring	Ineffective	Significant
Bed forms	Present	Absent
Variation in scour depth	Rapid	Slow
Scour depth	Deep	Shallow
Channel response to changed hydrology	Rapid	Slow

Source: Modified from Simons and Simons (1987).

Movable beds of sand-size material typically have a relatively narrow range of grain sizes. Small amounts of sand are being transported continuously, even at low discharges, and armoring is absent. In contrast, gravel beds may contain grain sizes ranging from sand to cobbles, frequently exhibit bimodal grain size distribution curves (Fig. 8.5), and

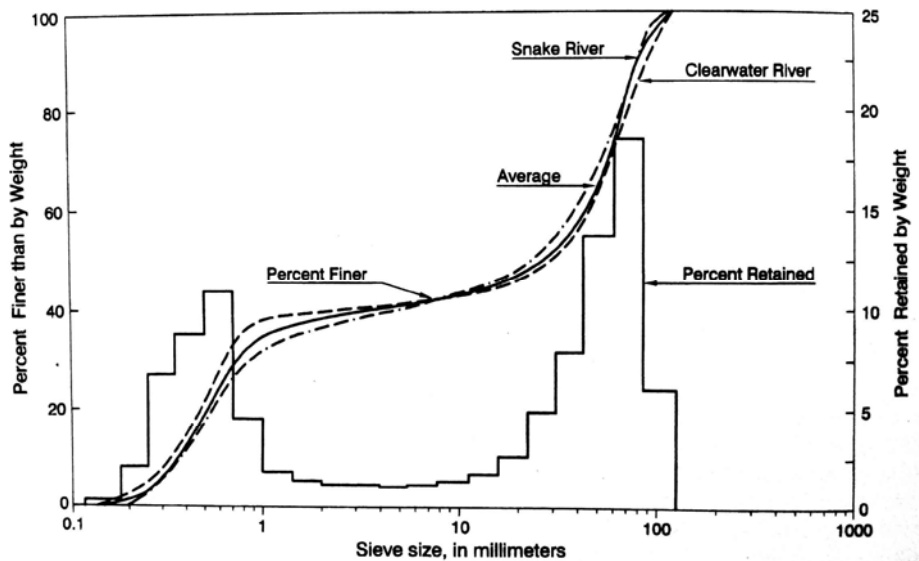


**Figure 8.5** Bimodal grain size distribution for gravel-bed rivers showing grain size as both a histogram and a cumulative frequency distribution (Emmett, 1976)

may have virtually no bed material transport until the gravel bed is mobilized at a high discharge. Both sand- and gravel-bed rivers may transport large amounts of fines as wash load.

### 8.1.7 Armoring

Gravel-bed rivers can exhibit the basic patterns illustrated in Fig. 8.6, depending on the grain size distribution and sediment supply in relation to the available transport energy.

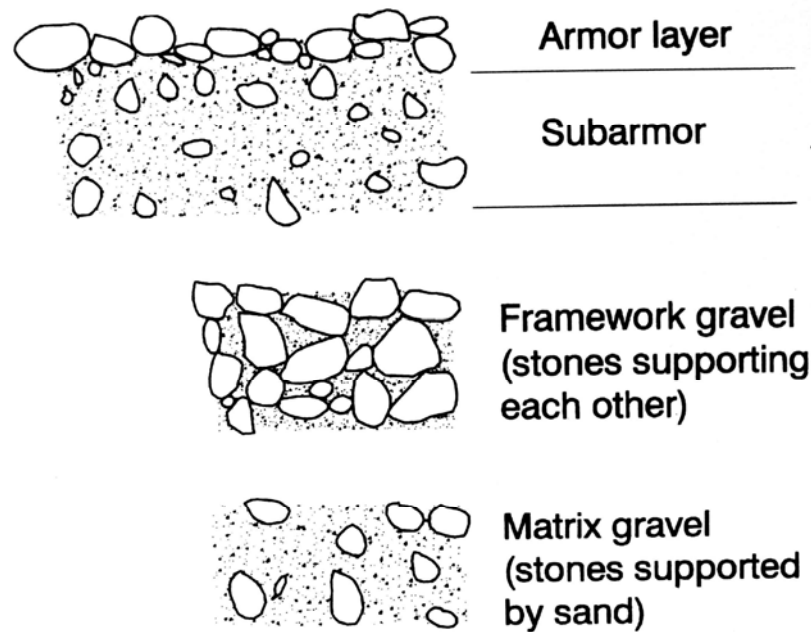


**FIGURE 8.6** Patterns of gravel deposition in streambeds, cross-section view.

The formation of a surface layer of *armor* or *pavement* about one grain thick protects the finer material in the underlying *subarmor* or *subpavement* zone from hydraulic transport until discharge is sufficient to mobilize the armor layer. Armor layers form frequently in gravel-bed rivers and occur when the bed contains a wide variation in grain sizes, when the supply of the finer grains is small compared to the transport energy, and when the largest grain size is transport-limited. Normal discharges will erode smaller grains from the surface of the bed, leaving the larger stones behind and causing the bed surface to coarsen to the point of immobility at that particular discharge. At this point the bed is said to be armored. Bed material transport may approach zero at discharges too low to destroy the armor layer despite the presence of material of transportable size in the subarmor, and sediment discharge will be supply-limited. However, at high discharge the armor layer is mobilized and all underlying sediment will be available for transport. When the armor layer is destroyed, the underlying sands may be transported in suspension.

Armoring is an important process in reducing the degradation of channels downstream of dams and can occur below dams in streams that did not contain enough gravel in relation to the sand load for significant armoring to occur under pre-impound-

ment conditions. When dam construction cuts off the supply of bed material, the sand fraction in the bed material will be transported downstream faster than the gravels, causing the bed to degrade and initiating the armoring process. Armoring can also provide more stability to the bed below dams compared to pre-impoundment conditions if dam operation reduces peak discharges along the downstream reach so that the armor layer is rarely mobilized. Armoring is incorporated into many numerical sediment transport models, which can be used to predict the extent of bed degradation and armoring downstream of dams.

### 8.2 SUSPENDED-SEDIMENT SAMPLING

The relationships between the wash load, suspended load, bed material load, and bed load are illustrated in Fig. 8.7. The suspended-sediment concentration within a stream cross section can be highly nonuniform, especially when sands are being transported. The objective of suspended sediment sampling is to determine the mean discharge-weighted

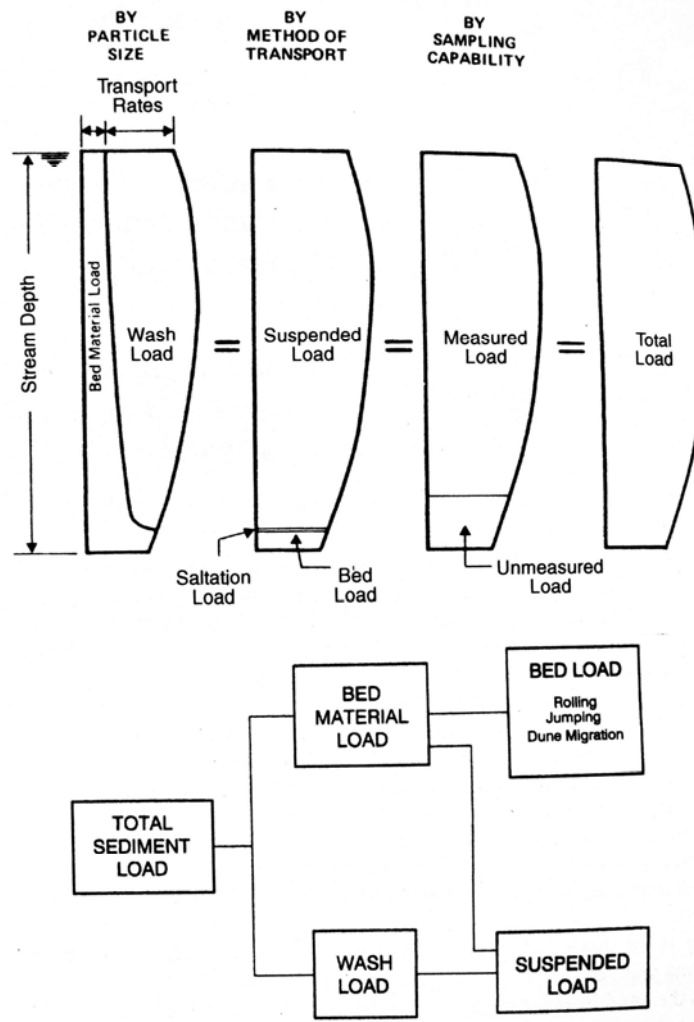


FIGURE 8.7 Components of total sediment load (adapted from Deady et al., 1979).

sediment concentration and grain size in the cross section, despite the variation in sediment concentration and the velocity distribution across the stream and within each sampling vertical. Having sampled the discharge-weighted mean concentration, suspended-sediment load is computed as the product of mean concentration and discharge. Edwards and Glysson (1988) and Guy (1969), should be consulted for more detailed information on sediment sampling procedures.

### 8.2.1 Vertical Concentration Gradient

The tendency for sediment to settle toward the bottom of the stream creates a vertical concentration profile, with lower sediment concentration at the surface and higher concentrations near the bottom. Sediment is maintained in suspension by the vertical component of turbulence in flowing water, which is on the order of about 1 percent of the forward velocity. Random turbulent motion causes equal volumes of water to rise and to sink within the water column, but, because sediment concentration increases as a function of depth, the rising water volume has a higher concentration than the sinking water, creating a net upward motion of sediment which offsets sedimentation and produces the vertical concentration gradient.

In most streams the turbulent component is large compared to the sedimentation rate of silts and clays. These fines are typically transported as wash load, and the concentration of fine sediment particles along a vertical within the water column is nearly uniform. In contrast, rapidly sinking sands normally have a concentration profile that tends to vary logarithmically as a function of depth. Figure 8.8 illustrates the variation in grain size, concentration, and velocity as a function of depth, illustrating that the concentration profile varies as a function of grain size, with large-diameter particles being concentrated closer to the bottom of the vertical profile. The transport rate at any depth is a product of the velocity and concentration at that depth, and the total sediment load is the product of mean flow velocity and the discharge-weighted sediment concentration. Accurate determination of suspended sediment load requires a discharge-weighted sample of suspended sediment along each sampling vertical.

### 8.2.2 Isokinetic Sampling

When a sampling device collects water samples so that water enters the sampler nozzle at the same velocity as the flow in the surrounding fluid, and without changing direction,

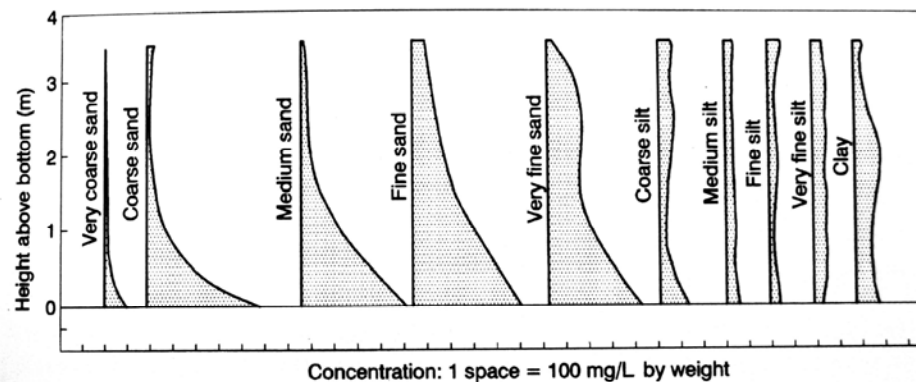


**Figure 8.8** Vertical variation in sediment concentration as a function of grain size (Dendy et al., 1979)

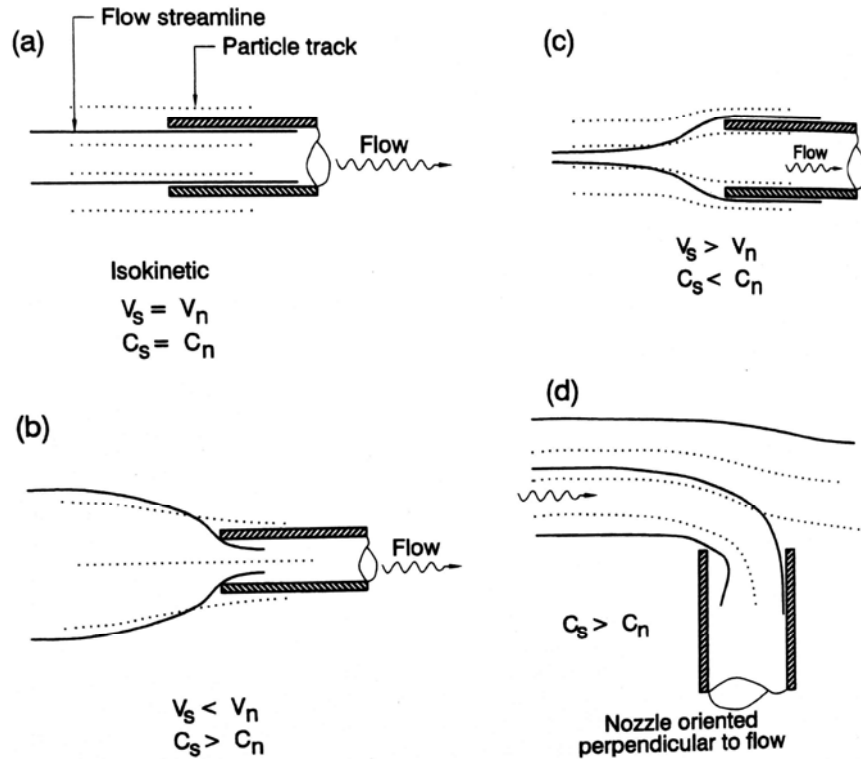


**FIGURE 8.9** Concept of isokinetic sampling and the types of sampling errors created by non-isokinetic sampler intake conditions. In this diagram  $V$  = velocity,  $C$  = concentration, and the subscripts  $s$  = stream and  $n$  = nozzle.

the sampling is said to be *isokinetic*. Under isokinetic sampling, both the flow streamlines and the paths traced by suspended particles entering the sampler are straight and parallel, and the resulting sample will represent the discharge-weighted concentration along the vertical distance sampled if the sampler vertical transit rate is constant. When the flow path is distorted and curving streamlines occur, the particle paths may not follow the streamlines because of the higher density and momentum of the particle compared to the surrounding fluid, as illustrated in Fig. 8.9. Because the departure of the particle path from a curving streamline increases as a function of particle size, the error caused by non-isokinetic sampling also increases as a function of grain size. Errors due to non-isokinetic sampling occur primarily in the sand-size particles; the errors in the sampling of silts and clays are very small.

### 8.2.3 Sampling Location

A sediment data collection site should have a stable cross section to facilitate construction of a stage-discharge relationship and should normally be at or very close to an existing streamgage site. However, not all existing streamgage sites are well-suited for sediment monitoring. An ideal suspended-sediment sampling site would be of uniform depth, straight, and without eddies and have sufficient turbulence to completely mix the

suspended sediment, although this is not normally achieved unless sediment size is rather small. If below a river confluence, the gaging site should be far enough downstream that complete lateral mixing occurs between the tributaries. Areas of backwater should be avoided because this affects both the stage-discharge and the velocity-discharge relationship. For sand-bed rivers in which the ratio of total load to suspended load depends on channel characteristics, the measurement site should normally have a configuration similar to the normal stream geometry.

Gaging stations must be accessible during floods, so sediment stations are frequently located at highway bridges which provide both access and a measurement platform spanning the river. As a disadvantage, bridges normally occur at constricted reaches, can collect debris, can alter streamlines, and in sand-bed rivers can experience significant scour. Samples need to be collected at the same cross-section location throughout the period of record. Avoid sites where channel realignment, a new bridge, or other construction affecting the channel is anticipated over the life of the sampling program (Edwards and Glysson, 1988).

#### 8.2.4 Sampler Designations

Samplers developed by the U.S. Federal Inter-Agency Sedimentation Program are designated by the prefix US, letters, and a two digit number. The letter designators are D = depth integrating, H = hand held, P = point integrating, BM = bed material, BP = battery pack, U or SS = single stage, and PS or CS = pumping type. The last two digits indicate the year the sampler was developed.

#### 8.2.5 Depth-Integrating Sampler

Depth-integrating samplers (Fig. 8.10a) are designed to continuously withdraw an isokinetic sample while transiting a vertical. A sampling station is illustrated in Fig. 19.17. The sampler consists of a bottle fitted with nozzles of various sizes to control the rate of inflow, an exhaust tube to release air from the sample bottle as water enters, and a streamlined "fish" to hold the bottle and maintain the nozzle oriented directly into the current. Both the nozzle and the exhaust tubes are sized to achieve isokinetic flow velocity. For small streams, a sampler attached to the end of a rod is manipulated by hand while the user is wading. Larger samplers for deeper water are raised and lowered by winch. All samplers should be oriented parallel to the flow prior to immersion of the sampler nozzle into the water at the initiation of sampling. The resulting sample is discharge-weighted in the vertical and can be multiplied by the mean flow velocity at the same vertical to obtain the load. The total load across the entire stream is computed by sampling and summing the loads at several verticals.

For round-trip depth-integrated sampling, the sampler is lowered through the water column to the bottom and then raised again at transit rates which are constant in each direction but which need not be equal. The downward transit velocity should be slower than the upward velocity to minimize the possibility of the sampler digging into the bed, and sampler direction should be reversed as soon as it strikes bottom to avoid oversampling the higher-concentration zone near the bed. In sand-bed rivers, duplicate samples should be taken and visually compared for large differences in the amount of sand, and a third sample should be taken if necessary. The transit rate must be adjusted so that an adequate sample size is collected, and yet the bottle must not be allowed to fill completely. Once the bottle is filled, water will continue to circulate, entering the nozzle

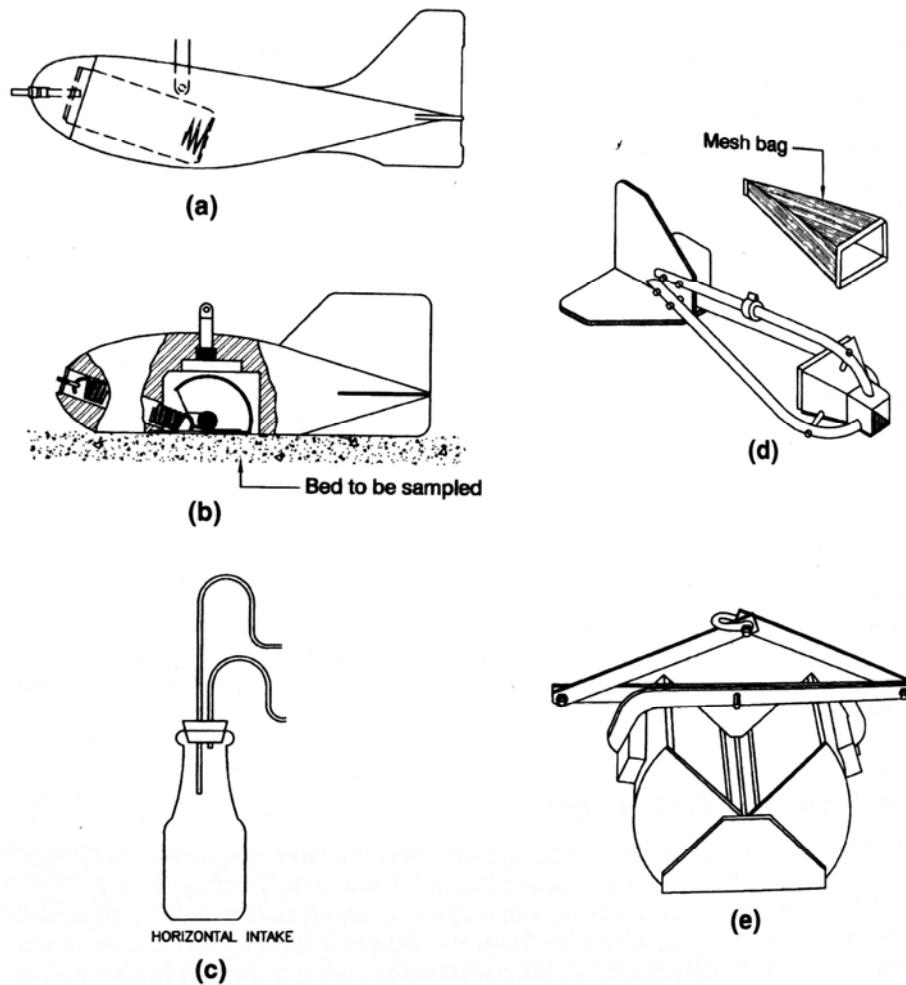


**FIGURE 8.10** Several sediment samplers: (a) Model USD-49 depth-integrating sampler without bottle. (b) USBM-54 bed material sampler using a spring-actuated rotating scoop. (c) single stage suspended-sediment sampler. (d) Helly-Smith bed load sampler, and (e) Ponar dredge.

and exiting the air exhaust, but coarser material will be trapped in the bottle, resulting in a nonrepresentative sample. Different nozzle sizes are available for depth-integrating samplers, allowing the user to adjust the inflow rate to allow deeper streams to be sampled. The largest nozzle size possible should be used, since smaller nozzles have a greater tendency to clog and undersample coarse grains. The vertical transit rate should not exceed 40 percent of the mean flow velocity at the sampling location, which limits the maximum round-trip sampling depth to about 4.5 m when the smallest nozzle is used. Point-integrating samplers must be used in deeper water.

### 8.2.6 Point-Integrating Sampler

Point-integrating samplers are equipped with a remotely operated valve so that the sampler can be lowered to any depth prior to opening of the inlet. This sampler can be used to obtain a time-integrated sample while held at a specific depth (a *point-integrated*

*sample*), or it can be transited vertically to obtain a depth-integrated sample over a transit distance of up to about 9 m. In a stream not exceeding 9 m in depth, a single transit is used. First lower the sampler to the bottom, note the depth, then initiate the upward transit and open the valve simultaneously. A second sample should be taken after inserting a new sample bottle, starting at the surface with the valve open and closing the valve as soon as the sampler touches bottom. In the case of streams deeper than 9 m, two transits may be made for each upward and downward trip, one for the upper half of the river depth and the second for the lower half of the depth.

Multiple points in a vertical may be sampled to approximate the vertical concentration profile, from which the discharge-weighted concentration can be determined. The number of vertical points is a function of water depth, sediment grain size, river stage, and concentration characteristics as determined from prior sampling. Accuracy increases as a function of the number of points, and more points are needed to accurately characterize a stream having a large suspended sand load than one transporting only silt and clay. Edwards and Glysson (1988) recommend 5 to 10 separate point samples to accurately determine the concentration profile along a single vertical. By opening the nozzle for the same duration at each point the sample volumes will be proportional to the flow velocity, and the resulting samples may be composited prior to analysis to determine the discharge-weighted concentration.

Sampling economy can be achieved at stable cross sections by reducing the number of points. Detailed sampling should first be undertaken to determine the minimum number and placement of points required to replicate results obtained with a larger number of points and verticals. Prior sampling can determine the sampling points within a specific cross section that best reflect the discharge-weighted concentration in a stream. Because the distribution can change as a function of discharge, calibration should be performed over the full range of discharges and should be rechecked periodically. Long (1989) suggested point sampling at the following depths (measured from the water surface downward) when abbreviated sampling is performed:

Number of points	Location of vertical (relative depth)
1	0.6
2	0.6, 0.2
3	1.0, 0.5, bottom

### 8.2.7 Sampling in Transverse Direction

Two methods are used to locate multiple verticals across a stream to determine the total discharge-weighted sediment load: the equal-discharge-increment (EDI) and the equal-width-increment (EWI) methods.

In the EDI method the entire cross section is divided into a minimum of 4 or a maximum of 9 increments of equal discharge but unequal width. A vertical sampled at the centroid of each discharge increment is used to represent the mean concentration for that interval. Since each vertical represents an equal percentage of the total discharge, the concentration in all the verticals can be averaged to obtain the mean concentration for the entire cross section. The EDI method uses a smaller number of verticals than the EWI method but requires that the flow distribution across the section be known beforehand to select the measurement points.

The EWI method divides the stream into increments of equal horizontal widths (but unequal discharge), and the sample volume must be proportional to the flow velocity in

each vertical. This requires isokinetic sampling at identical transit velocities at all verticals. A minimum of 10 and maximum of 20 verticals is recommended. The samples in all bottles may be composited to yield a single cross-sectional concentration.

### 8.2.8 Single-Stage Sampler

An automatic single-stage suspended load sampler was described by the Interagency Committee on Water Resources and is shown in Fig. 8.10c. This suspended sediment sampler operates on the siphon principle and automatically collects suspended samples during the rising stage of a flood. Multiple samplers may be mounted at successively higher elevations on a bracket to obtain samples at different stages as water levels rise and each successive bottle is filled. Serious limitations are associated with this sampler: the samples are always collected near the water surface, only the rising limb of the hydrograph can be sampled, the original sample may be altered by subsequent submergence, intake velocities are not isokinetic, and the sample location is usually at the streambank, which is often not representative of the entire cross section (Brakensiek et al., 1979). This sampler is not recommended for use; a pumped sampler should be used instead. Older datasets derived from these samplers should be interpreted with caution.

## 8.3 PUMPED SAMPLERS

---

Because of the logistical problems associated with the manual sampling of sediment at remote locations, and the need for frequent sampling to better define sediment concentrations during runoff events, pumped samplers are frequently employed to complement manual sampling. Pumped samplers do not eliminate manual sampling, which is required to provide the pumped sampler adjustment factor, and the number of samples collected and analyzed as a result of pumped plus manual sampling can be greater than that for manual sampling alone. The principal reason to use an automatic sampler is to improve data reliability.

### 8.3.1 Equipment Description

Pumped samplers typically include: (1) line or battery power supply, (2) intake nozzle and pipe, (3) pump, (4) intake pipe, (5) sample handling system and storage bottles, and (6) microprocessor control unit and data logger, including ports for additional probes. All components other than the intake line and sample probes are located inside an instrument shelter or weatherproof case, and facilities for sample refrigeration may also be provided. The pump is operated intermittently to first flush the line and then to discharge a sample into a sample bottle. The sample bottles are periodically collected and carried to the laboratory for analysis, and multiple samplers can be programmed to operate sequentially to provide more bottles. A commercially available self-contained, portable, battery-operated pumped sampler containing an onboard programmable microprocessor is illustrated in Fig. 8.11.

The pumped sampler control unit is normally connected to a stage recorder which measures the threshold water stages used to initiate event sampling and, when combined with a rating curve, can also provide a discharge record. The onboard computer enables sampling to be preprogrammed for fully automatic operation, or a data link may be provided to enable control from a central station via radio, cellular telephone, etc. Programming strategies for samplers are discussed in a subsequent section of this chapter.

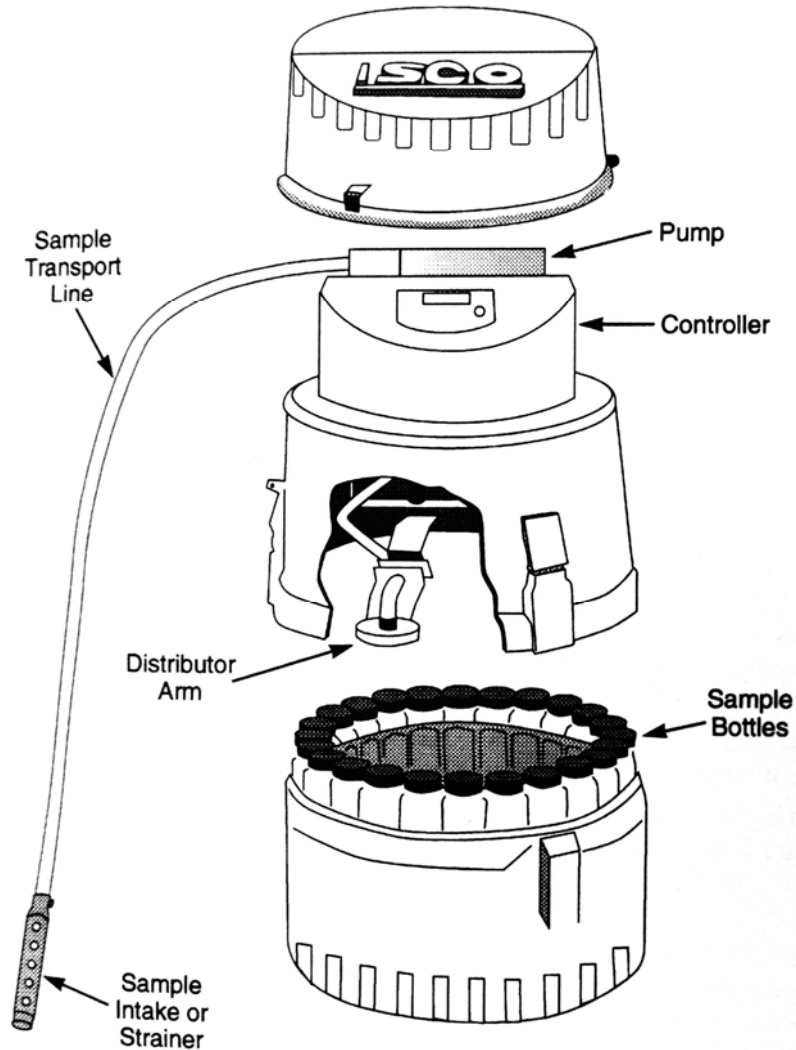


**FIGURE 8.11** Pumped sampler with an onboard programmable microprocessor and data logger. Additional probes for parameters such as stage and turbidity can be attached to the control unit for data collection and to actuate the collection of pumped samples. (Courtesy ISCO.)

### 8.3.2 Sampler Intake Placement

Pumped samplers withdraw water from a single point within the cross section, which would ideally represent the discharge-weighted mean suspended-sediment concentration within the entire cross-section at all discharges. However, when the sampler intake is fixed, the relative depth of the sampling point will vary as a function of stage, and the relationship between the sample point concentration and the mean concentration within the stream may not be stable. As evident from the vertical distributions in Fig. 8.8, while the relative depth of the sampler intake may have a relatively small effect on the measured concentrations of silt and clay, it will have a very large impact on all sands, and possibly even coarse silt in low-gradient streams. The sample intake should be located at a point within the cross section that approximates the mean concentration across the full range of sampled flows, or have a stage-dependent adjustment factor. The following

general principles for the selection of the sampling section and locating the sampler intake within the section have been adapted from Guy and Norman (1970), Edwards and Glysson (1988), and Long (1989).

1. **Tributaries.** Sampling in the vicinity of tributaries should be avoided. A location immediately upstream of a tributary can experience backwater, and a location immediately downstream can experience incomplete horizontal mixing of sediment from the two streams.
2. **Hydraulics.** Ensure consistent hydraulic characteristics. The sample section should have a stable thalweg and be of reasonably uniform width and depth. In meandering alluvial streams, areas of crossings may be affected by a shifting thalweg location, in which case a sampling point at the outside of a bend near the thalweg may provide a location with more stable transport characteristics.
3. **Turbulence.** Provide adequate turbulence. Select the sampling cross section and intake location in an area having good turbulence and adequate flow velocity. This will minimize the variation in sediment concentration across the cross section, reduce deposition on or near the intake, and rapidly remove any particles disturbed during the sampler purge cycle.
4. **Point integration.** Where appropriate, use point-integrated samples to determine the concentration profile for particles finer than 0.25 mm and from this the depth of mean sediment concentration. Use this as a reference depth for determining the depth of the sampler placement.
5. **Submergence.** Adjust the sampler inlet height to provide continuous submergence, if possible.
6. **Bed effects.** Minimize bed effects. Raise the sampler inlet above the bottom so that bed load is not entrained and interference by dune migration is avoided. In shallow streams experiencing large variations in stage, this may require that the intake be above the water surface at the lowest stage, being activated only as stage and discharge increase.
7. **Bank effects.** Minimize bank effects. Place the sampler far enough away from stream banks to eliminate any possible bank effects.

It may be impossible to simultaneously satisfy all these criteria. They should be satisfied to the extent possible to produce the most stable relationship obtainable between the sample concentration and mean concentration in the stream. It is more important that the sampling location be representative of conditions during significant discharge events, which transport most sediment, than at low flows when little sediment is transported.

### 8.3.3 Sampling Depth

The relative depth of a fixed sampling point can vary greatly as a function of changing river stage, representing a potentially large source of error in the sampling of coarse sediment having a significant vertical variation in concentration. An intake barely below the water surface at low flow may be near the bottom of the section and sampling bed load during a high-discharge event. This problem can be reduced by setting the intake at an elevation above the low-flow water surface (when little sediment is discharged), but which will be submerged to an appropriate depth during larger flows. Sample intake placement may also be constrained by pumping lift, which is limited to about 10 m, presenting a problem on rivers with wide fluctuations in stage. This can be overcome by using a submersible pumping unit separate from the sampler.

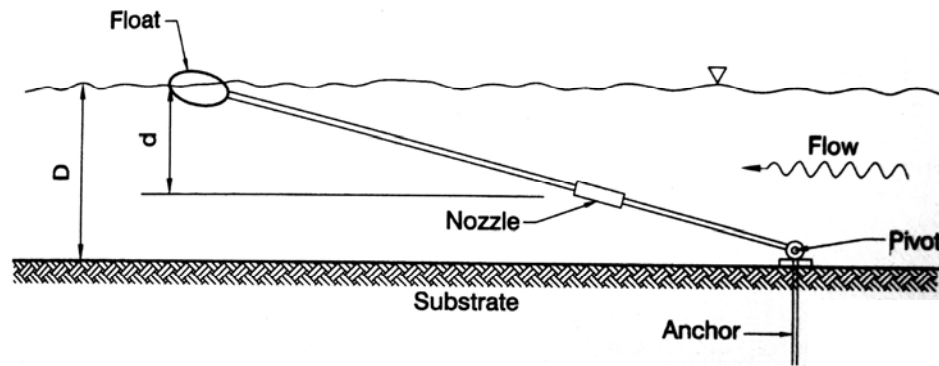


**FIGURE 8.12** Intake boom for use with a pumped sampler which maintains the sampler intake at a fixed proportional depth (e.g., 60 percent of total depth) in small streams (after Eads and Thomas, 1983).

Proportional depth sampling can be achieved in small streams by using a sampling boom anchored to the streambed and fitted with a float at the downstream end as shown in Fig. 8.12. Anchoring the boom on the bottom instead of suspending it from above facilitates the passage of floating debris. The intake nozzle is oriented parallel to the boom, facing downstream, and is set to sample at 60 percent of the stream depth. A test system was found to produce sample concentrations similar to simultaneously measured depth-integrated samples taken by a DH-48 sampler (Eads and Thomas, 1983).

### 8.3.4 Nozzle Orientation

Sampling efficiency is the ratio of the sampled sediment concentration to the stream concentration at the sampling point. Essentially 100 percent sampling efficiency is achieved by using a sampling nozzle pointed in the upstream direction with an intake velocity equal to the ambient flow velocity (isokinetic sampling), but an upstream-facing nozzle is easily clogged and is not recommended for automatic samplers (Edwards and Glysson, 1988).

A nozzle set at an angle to the flow will produce flow curvature, and because sediment particles will not curve as quickly as the water entering the nozzle, decreased sampling efficiency results (Fig. 8.9d). Winterstein (1986) performed flume tests to determine the effect on sampling efficiency of orientation and flow velocity in a 6.35-mm inside-diameter nozzle for 0.06- and 0.20-mm-diameter silica sand, using an upstream-facing nozzle as the reference. It was shown that the size distribution of suspended sediment samples collected by a nozzle set at an angle to the flow will be biased toward smaller sediment sizes. A small sampling error is produced by upstream-oriented nozzles or by a directly downstream-oriented nozzle, but a high degree of undersampling occurs for nozzles oriented at 90°. Fines will be only slightly undersampled, but undersampling error increases as a function of particle size and sampling efficiency may be lower than 50 percent for 0.2-mm sand compared to isokinetic sampling. Winterstein concluded that the high sampling efficiency of the downstream orientation occurred because sand grains were thrown in front of the nozzle by the turbulent wake shed by the nozzle, but cautioned that this high degree of efficiency may not be achieved in the field where the nozzle may not be oriented exactly downstream to the flow. Edwards and Glysson (1988) recommend a downstream orientation for sampling from pumped samplers.

The intakes for commercial samplers are often supplied with strainers designed to exclude debris. Strainers should normally be removed for collecting sediment data, since they can create a zone of reduced turbulence at the intake which may allow sedimentation and undersampling of larger grains.

### 8.3.5 Cross-Section Coefficient

It is necessary to determine the relationship between the pumped sample concentration and the mean sediment concentration in the stream by manual sampling over a large range of flows. Pumped samples should be taken at the start and end of the more time-consuming manual sampling, and the cross-section sample is compared to the average of the pumped samples. Single-point sampling can accurately represent the mean concentration of fine sediments (silts and clays) that exhibit an essentially uniform concentration distribution. However, the measurement of sand load presents a difficult problem and can produce very poor correlation between the point samples and the mean concentration. One possible approach is to separate both pumped and manual samples into fine and coarse fractions, and to establish relationships for each individually.

## 8.4 CONTINUOUS TURBIDITY MEASUREMENT

---

The sediment concentration in streams can vary by orders of magnitude during a flood event and may be poorly correlated to changes in discharge (see Figs 7.5 and 7.17). The use of automated pumped samplers increases the frequency of sediment sampling, allowing more complete sampling of runoff events, especially in flashy streams and at remote sites. However, the larger number of samples increases laboratory costs, yet does not produce the coverage needed to accurately track concentration on a continuous basis. Ideally, a gage parameter would be available which varies directly as a function of suspended sediment, and which could be continuously monitored and logged. A perfect gage parameter for suspended sediment concentration does not exist, but turbidity has gained acceptance as the imperfect parameter of choice for suspended sediment monitoring.

### 8.4.1 Application

Turbidity is generally a better predictor of suspended fluvial sediment concentration than is discharge, and turbidity readings logged at short intervals can continuously track the change in concentration in the rising and falling limbs of runoff events.

Turbidity is well-suited to measurement of changes in suspended sediment concentration in streams where the sediment composition is relatively stable as a function of time and discharge, but its application is more complicated in streams where sediment characteristics (and their optical properties) change significantly. Best results are achieved with the combination of a turbidimeter and pumped sampler. The suspended solids concentration is continuously tracked by using turbidity, and pumped samples are collected to provide the calibration between turbidity and solids throughout the event. This results in fewer samples to be analyzed and better coverage of events. Commercial pumped samplers now offer both stage and turbidity probes, plus extensive programming and data logging capability, greatly facilitating this type of data collection.

The most important advantage offered by turbidimeters is continuous measurement. The number of data points that can be logged is virtually unlimited, enabling the turbidimeter to continuously log events at short time intervals and define the variation in concentration much more clearly than pumped samples alone. Instantaneous instream variations in turbidity can be smoothed by internal routines that time-average multiple data points over periods of several minutes. Lewis (1996) indicated that a 10-min logging interval was adequate for a small flashy northern California stream. By monitoring discharge and turbidity simultaneously, the suspended sediment load can be computed from the logged datafiles by applying the correction relationships developed for the station.

Turbidimeters cannot replace conventional sampling techniques because the relationship between point turbidity and the mean suspended sediment concentration in the cross section is not constant; it requires calibration and periodic checking. Turbidimeters also cannot operate unattended for long periods; they require attention at regular intervals to be checked for clogged lines, to clean optical surfaces, and to collect calibration samples from pumped samplers operating in parallel with the turbidimeter. A 1- or 2-week interval between maintenance visits might be used initially and adjusted according to conditions. In systems equipped to communicate with a base station by cellular telephone or radio, problems can be signaled using the microprocessor at the gage station, or the raw data can be periodically sent to the base station and processed to detect malfunction conditions. This type of reporting system can be used to minimize visits by technicians, spreading routine maintenance visits further apart while responding immediately to malfunctions, thereby minimizing station downtime.

#### 8.4.2 Types of Turbidimeters

Turbidity is a measure of light scattering by the suspended particles in the water. Turbidity values are only approximately related to suspended solids concentration, being influenced by factors such as particle size, shape, mineral composition, organic matter, and color. Turbidity was originally measured with the Jackson candle turbidimeter, an instrument consisting of a tall calibrated glass cylinder with a standard candle beneath, and turbidity was related to the water depth at which the image of the flame was no longer distinguishable. From this was derived the Jackson turbidity unit (JTU), which may be encountered in older literature but is no longer in general use.

Three types of turbidimeters have been used to monitor stream sediment at gage stations. *Attenuance turbidimeters* measure the attenuation of a light beam passing through a fixed distance. Dual beams are frequently employed in field turbidimeters to compensate for lamp aging and biofouling. Turbidimeters measuring changes in transmitted light are relatively insensitive to low scattering intensities, and are subject to multiple-scattering interference at high concentration.

The measurement of scattered light at an angle to the light beam helps overcome these problems and reduces sensitivity to variation in particle size. Instruments measuring scattered light are termed *nephelometers* and are the accepted standard for turbidity measurement as specified by Standard Methods (APHA, 1985). Their readings are expressed as nephelometric turbidity units (NTUs), as opposed to the term formazin turbidity units (FTUs) which is reserved for instruments measuring transmitted or absorbed light (Hach et al., 1990). The different turbidity units are not strictly interchangeable.

Low-power submersible turbidity probes based on both principles are available from commercial suppliers and may be integrated with pumped samplers. The Hach *surface scatter turbidimeter* uses a somewhat different approach in that the light source is directed onto the surface of a water sample continuously pumped into an enclosed housing, and reflection is measured from the surface. Biofouling is essentially eliminated since optical surfaces are not in contact with the water, but this equipment requires a separate pump and line power.

#### 8.4.3 Relationship between Turbidity and Suspended Solids

Suspended particles differ in their optical characteristics, which affect their absolute levels of attenuation and scatter as well as the ratio of attenuation to scatter. Gippel (1995) calibrated both attenuation and nephelometric turbidimeters to the same formazin standard and subsequently measured natural turbidity. The attenuation turbidimeter

typically measured 2.5 times higher turbidity values than a nephelometric turbidimeter for the silt-clay suspensions analyzed. This occurs because the formazin standard has a much higher scattering efficiency than most natural particles. It was also found that dissolved organic color is unlikely to alter turbidity readings by more than 10 percent.

The term *specific turbidity* refers to the turbidity measured in formazin units divided by the mass particle concentration in milligrams per liter. Gippel (1995) also examined the effect of particle size on specific turbidity, and found that particle size variation can cause turbidity to vary by a factor of 4 for the same suspended solids concentration. Differences in specific turbidity as a function of turbidimeter type and particle size are summarized in Fig. 8.13a. Foster et al. (1992) examined the response of two attenuation turbidimeter probes to various concentrations of river silts and clays using both native water and dispersant, and found that the specific turbidity decreased more than tenfold over the range of sediment diameters tested. Larger particles produce less turbidity response per unit of mass.

For a turbidimeter that has been calibrated to give a linear response to a formazin standard, the turbidity of a mixture having a fixed grain size composition will vary linearly according to the function

$$T = aKC_s + b \tag{8.2}$$

where  $T$  = turbidity,  $K$  = specific turbidity, and  $C_s$  = suspended solids concentration. For nephelometric turbidimeters  $a \leq 1$  and is a function of dissolved organic color. For attenuation turbidimeters  $a = 1$ . The constant  $b$  is a function of organic color and has a value of  $b = 0$  for nephelometric turbidimeters. For attenuation turbidimeters  $b = 0$  only when there is no color at zero suspended solids concentration (Gippel, 1995). The experimental relationship between turbidity and suspended solids concentration development by Lewis (1995) in Fig. 8.13b shows both the linearity of the relationship when grain size is constant and the greater specific turbidity associated with the finer particles. The larger sand-size particles produce a relatively small effect on turbidity.

When particle size varies as a function of concentration, the turbidity response will have a nonlinear form :

$$T = a C_s^C + b \tag{8.3}$$

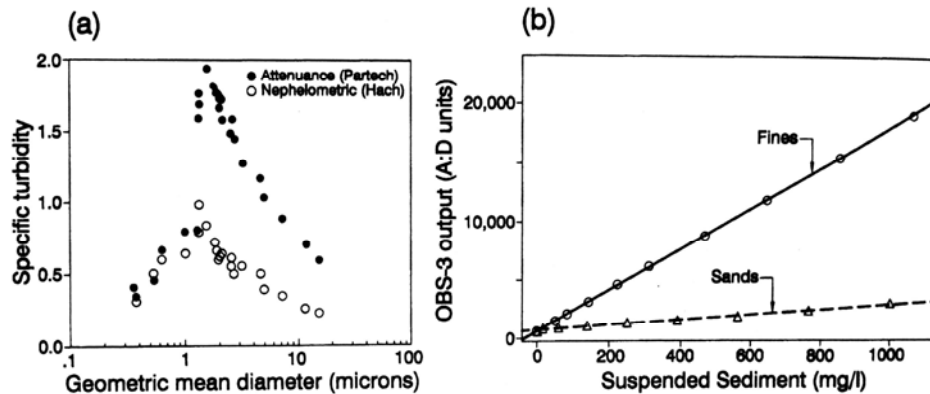


**FIGURE 8.13** (a) Variation in nephelometric and attenuation turbidity as a function of grain size and concentration (after Gippel, 1995). (b) Linear variation in turbidity as a function of concentration for coarse and fine sediment showing the larger specific turbidity response generated by fine sediment (Lewis, 1996).

where  $a$  = a characteristic coefficient. When particle size increases as a function of suspended solids concentration,  $c < 1$  and indicates decreasing specific turbidity. When particle size decreases as a function of concentration,  $c > 1$  (Gippel, 1995).

The relationship between turbidity and suspended solids concentration should be constructed for each stream and for each distinct hydrologic condition (e.g., rising limb, falling limb, runoff from thunderstorms, snowmelt, and high versus low discharge). Numerous close correlations between turbidity and suspended solids concentration have been reported in the literature, which suggests that either the particle size variations are not usually great, or that particle size variations are often associated with systematic variations in suspended solids concentration. The best correlations will occur in environments where sediment properties are likely to remain relatively constant, such as small watersheds, and where there is a wide variation in concentration (Gippel, 1995). Some variance in specific turbidity can be tolerated, since the improved data obtained from a continuous estimate of suspended solids concentration overcomes the problem of infrequent sampling, which is the greatest source of error in estimating sediment loads (Olive and Rieger, 1988).

#### 8.4.4 Limitations of Turbidity Data

Although turbidimeters offer numerous advantages as a complement to traditional sampling techniques, turbidity measurement also has a number of limitations which must be understood and addressed if accurate data are to be obtained.

- Turbidity is a point sampling method and incorporates the limitations associated with the measurement of mean cross section suspended-sediment concentration by sampling a single point. Depth-integrated samples are required to calibrate the point-sampling system. The sampling point must be carefully located to be representative of the entire stream according to criteria previously discussed for point sampling using pumped samplers.
- Because small particles and organics have a much higher specific turbidity than larger sand-size particles, turbidity measurements will tend to track the concentration of the finer fraction of the load while being rather insensitive to the coarse fraction. This makes it difficult to interpret turbidity data from streams with a significant amount of coarse material. It may be helpful to divide calibration samples into fine and coarse fractions to better model the suspended solids-turbidity-discharge relationship in a particular stream.
- Optical components may be subject to biofouling after a period of days or weeks, and the rate of biofouling can be expected to increase as a function of higher water temperature and nutrient content. In smaller streams experiencing a wide range of stage, the turbidimeter may be placed above the low-flow water level to reduce biofouling of optical surfaces. Since little sediment is discharged during low-flow periods, and suspended solids concentration is low, the missing data is of little consequence to load computations. Periodic inspection and cleaning of all optical surfaces is required.
- Logged data should be searched for anomalous conditions, such as large turbidity spikes with little change in discharge. These may be caused by discharge of pollutants from upstream factories or agricultural operations. If a pump is delivering water to a turbidimeter, a change in stream stage without a corresponding change in turbidity may reflect clogging or pump failure. Whereas this would be detected in a pumped sampler by empty sample bottles, the turbidimeter will continue to send signals regardless of what it is measuring. Turbidity trends over periods of days or weeks may reflect fouling of optical surfaces.
- Turbidity measurement does not provide grain size data.

Despite the limitations associated with turbidity measurement, continuous monitoring with some loss of precision can give a more accurate estimate of total sediment load and its timewise variation, compared to a smaller number of pumped samples which fail to accurately track large changes in sediment concentration. The use of a pumped sampler in conjunction with a turbidimeter, as described in the next section, can greatly enhance the reliability of turbidity data in streams where the concentration-turbidity relationship changes during runoff events.

## **8.5 SAMPLING STRATEGIES FOR PUMPED SAMPLERS AND TURBIDITY**

---

Pumped samplers are frequently activated by a stage sensor which initiates a timer that withdraws samplers at fixed intervals during events. The resulting samples are used to construct a rating relationship or to estimate sediment load by interpolation. However, with samplers now containing microprocessors, more sophisticated statistically based sampling plans can be implemented which produce unbiased estimates of both sediment load and variance, and overcome the bias that accompanies the use of traditional nonstatistical sampling schemes. Pumped samplers can also be used to calibrate turbidimeters.

### **8.5.1 Statistically Based Strategies for Pumped Samplers**

When sediment load is to be estimated from pumped samples alone, it is desirable to use stratified or variable-probability sampling strategies that reduce variance by taking advantage of the population structure. Sampling density is increased at high flows by using an onboard microprocessor and stage sensor to select sampling times. Thomas (1985) initially introduced the SALT (selection at list time) sampling scheme, but more recently has proposed time-stratified and flow-stratified sampling schemes which produce lower variance than the SALT sample plan.

Time-stratified sampling (Thomas and Lewis, 1993) partitions a hydrograph into a series of time intervals called *strata*. The duration of each time stratum is predetermined by the operator and varies as a function of hydrograph stage and direction. The sampling strata are programmed into the sampler's computer. At the beginning of a time stratum, the stream stage and direction (rising or falling) are sampled, the corresponding stratum length and sample size are retrieved from memory, the sampling times within the strata are determined, and the sampler is operated at these times. At the end of each time stratum the procedure is repeated.

Flow-stratified sampling (Thomas and Lewis, 1995) stratifies a hydrograph by discharge rather than time. The total flow range is stratified into classes based on stage height and direction, and each class is randomly sampled during the time it is occupied. Under this method noncontiguous samples from the same flow stratum are placed together.

Comparisons among the SALT, time-stratified, and flow-stratified sampling plans using data from a station measuring runoff from 10.4 km<sup>2</sup> of the North Fork Mad River in northern California revealed that time-stratified sampling generally produced the lowest variance for estimating total load from individual storms, but for estimating total load over a longer period with multiple storm peaks the flow-stratified sampling plan produced the lowest variance (Thomas and Lewis, 1995).

### 8.5.2 Sampling Strategies for Turbidimeters

Lewis (1996) described the use of turbidity-controlled sampling for suspended load estimation on a flashy mountainous stream in northern California. Turbidity was monitored continuously and logged at 10-min intervals. A programmable data logger signaled a pumping sampler to collect a suspended sediment concentration sample at specific turbidity thresholds, thereby providing the samples needed to recalibrate the suspended solids versus turbidity relationship. This recalibration during discharge events produced an accurate estimate of the suspended solids load, even though the sand fraction increased as a function of suspended sediment concentration and constituted more than half the sediment load at high concentrations. Turbidity thresholds were uniformly spaced after a log or power transformation of the turbidity scale. Simulations revealed that, for this stream, sampling thresholds that were uniformly spaced on the basis of the square root of turbidity gave better load estimates than cube root or a logarithmic scale, probably because of increased emphasis on high turbidities. To avoid sampling of ephemeral turbidity spikes caused by debris, threshold values were exceeded for two sampling intervals before activation of the sampler. A hydrograph reversal threshold was also established. In the studied stream, 75 percent of the suspended sediment was delivered after the discharge peak so denser sampling thresholds were established for falling turbidities than for rising. The relationship between turbidity and suspended solids for two events is given in Fig. 8.14, showing that hysteresis is important in some storms and absent in others at this site. The particular sampling protocol at any other stream should be selected and adjusted on the basis of continuous turbidity measurements at the site. By personal communication, Lewis indicated that relations between suspended solids and turbidity are generally linear (N. California streams). As compared to reliance on pumped samples alone and a probability-sampling protocol such as SALT, a turbidity-controlled protocol will provide a load estimate of comparable reliability for larger storms with only  $1/6$  as many pumped samples, and turbidity monitoring also gives much more detailed information.

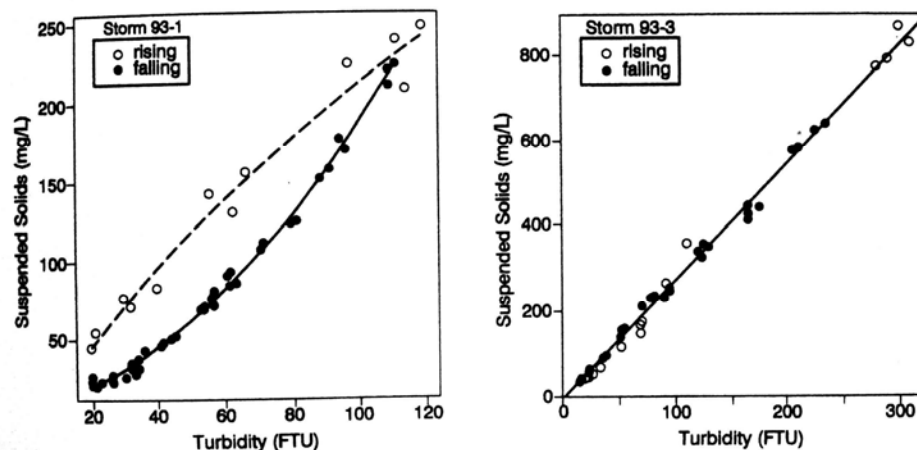


**FIGURE 8.14** Suspended-sediment concentration versus turbidity for two events on the North Fork Mad River, California, illustrating the presence of hysteresis in one event and its absence in another. Periodic recalibration of the concentration-turbidity relationship using pumped samples produced an accurate load estimate (Lewis, 1996).

## 8.6 DURATION OF MONITORING

---

How long must a fluvial sediment station be monitored to obtain useful data? The recommended duration of a monitoring program depends on the program objective. Three situations will be considered: (1) construction of rating relationship, (2) determining mean sediment yield, and (3) detection of trends. Construction of a sediment rating relationship can be performed for a short record, if that record contains data representative of the critical discharge classes responsible for most of the sediment load. However, extremely short monitoring periods covering only a year or two which do not include major runoff events should be used with extreme caution. The problems resulting from a short sediment record have been discussed in Sec. 7.3 with respect to the Randolph Jennings Reservoir. Nevertheless, accurate short-term data are far superior to long-term monitoring which fails to adequately monitor high-discharge events, as illustrated in the Cachi case study (Chap. 19). The Cachi case study illustrates how a flow-duration curve can be constructed and applied to the rating curve to estimate the range of discharges that are most critical from the standpoint of sediment yield (see Fig. 19.9). Although several years of sediment monitoring are normally recommended for development of a rating relationship, at Cachi it was possible to prepare an apparently accurate rating relationship by using continuous turbidity data from a relatively small number of runoff events. However, short datasets (including Cachi) typically do not include large episodic runoff events, and the problem of estimating discharge during these events remains unaddressed. In mountains or arid areas where episodic events can contribute extreme sediment loads, this is an important consideration.

The second objective, determination of the mean sediment yield, may be achieved by using a 5- to 10-year data-collection program. Evaluation of the Canadian sediment sampling program (Day, 1988) suggested that the historical emphasis on long-term data collection, up to 30 years in duration, is not necessary for many engineering purposes. At stations operating continuously for 5 to 10 years, the mean annual sediment discharge may be determined directly without extrapolation to a longer-range discharge record as long as sampled conditions are reasonably representative of long-term conditions. Rooseboom (1992) suggested that a minimum of 6 years of data collection is adequate to determine mean sediment load, but that a much longer record is required to observe trends. Summer et al. (1992) found that 10 years of sediment data collection was adequate to define load parameters for engineering purposes in the Danube River in Austria. Inadequate sampling programs typically underestimate sediment load. The coefficient of variance of the annual loads can be used to determine the standard error of the resulting estimate of mean annual yield using Eq. (7.1); also see Fig. 7.16 and the discussion of uncertainty in sediment yield contained in Sec. 7.3.

The third objective, detection of trends, requires long-term monitoring extending over a period of decades. While long-term trends can be dramatic in some cases, as illustrated in Figs. 7.8 and 7.13, in other cases trends may be difficult to identify or interpret because of factors such as flow diversion, upstream dam construction, and the episodic nature of sediment yield. Difficulties of this nature experienced in the Canadian sediment monitoring program were described by Day (1988) and are briefly summarized in Sec. 7.3.3.

## 8.7 BED LOAD SAMPLING

---

### 8.7.1 Bed Load Transport

The zone close to the bed of the river is not sampled by suspended load samplers and is termed the *unsampled zone* or the *zone of bed load transport* (Fig. 8.7). Transport in the

unsampled zone includes the rolling and jumping material in the bed load, plus some portion of the suspended load, and the amount of material transported in this zone can represent a significant fraction of the total load in sand-bed rivers. Bed load is difficult to measure, and at most gaging stations it is estimated or computed rather than measured directly. Because sediments in arid zones tend to be coarse-grained, bed load generally constitutes a larger part of the total load in streams draining desert areas than those in humid areas.

One common method to estimate bed load is to compute it as a percentage of the suspended sediment load using Table 7.4 or a local relationship determined by sampling. In rivers having a movable bed of coarse sediment, the bed load discharge can be estimated from a bed load formula, but this method itself is subject to considerable uncertainty. When bed load transport is supply-limited, bed load equations cannot be used.

The potential importance of bed load transport was illustrated by Long (1989), referring to unpublished work by Lin Binwen who in 1982 computed the sediment balance along a reach of the Yellow River between the Shaanxian gaging station, just below Sanmenxia dam, and the Tongguan gaging station about 120 km upstream (see Fig. 24.1 for location map). In this reach the river transports primarily silts but has a sandy bed. During the period March–June 1976, when Sanmenxia Reservoir was trapping sediment, the volume of material deposited in the reservoir was computed from the difference in suspended sediment discharge measured at the upstream and downstream stations. Sediment accumulation was also measured using the range method in the reservoir. Sediment grain size data were collected simultaneously, making it possible to compare the two methods not only in terms of total load but also as a function of grain size. Suspended solids monitoring under-estimated deposition by 16 million tons over the 4-month period, and 80 percent of the unmeasured load consisted of sand-size particles larger than 0.05 mm diameter.

### 8.7.2 Bed Load Sampling

Whereas suspended load transport rate is computed as the product of concentration and discharge, the bed load sampler must directly measure the load of particles moving along the bed. One of the major difficulties to be overcome in bed load measurement is the high temporal and spatial variability of the movement of bed material. Numerous researchers have documented highly irregular rates of bed load transport under conditions of constant discharge (Fig. 8.15). At a given discharge, the short-interval bed load transport rate typically varies from near zero to 4 times the mean rate (Hubbell, 1987). Transport rate also varies laterally, and multiple sampling traverses across a stream are required to determine the transport rate. *Sampler efficiency* is defined as the ratio of the mass of bed load collected during any sampling interval to the true mass of bed load that would have passed through the sampler entrance width during the same period had the sampler not been present. Sampler efficiency is determined by calibration in a hydraulic flume, and sampled transport rates are divided by efficiency to determine the true transport rate. Sampler efficiency varies as a function of grain size and transport rate, further complicating bed load measurement.

Early portable bed load samplers interfered with the flow field, resulting in a low sampling efficiency, and sediment tended to accumulate at the sampler entrance. These problems are minimized by a sampler which has an entrance nozzle followed by an expanding section that generates higher velocities in the throat and clears the entrance of entrained sediment. A permeable bag is attached to the downstream end of the expanding nozzle to hold the collected sample. The Helly-Smith type sampler used in the United States (Fig. 8.10d) is based on this principle and is available in two sizes. Bed load

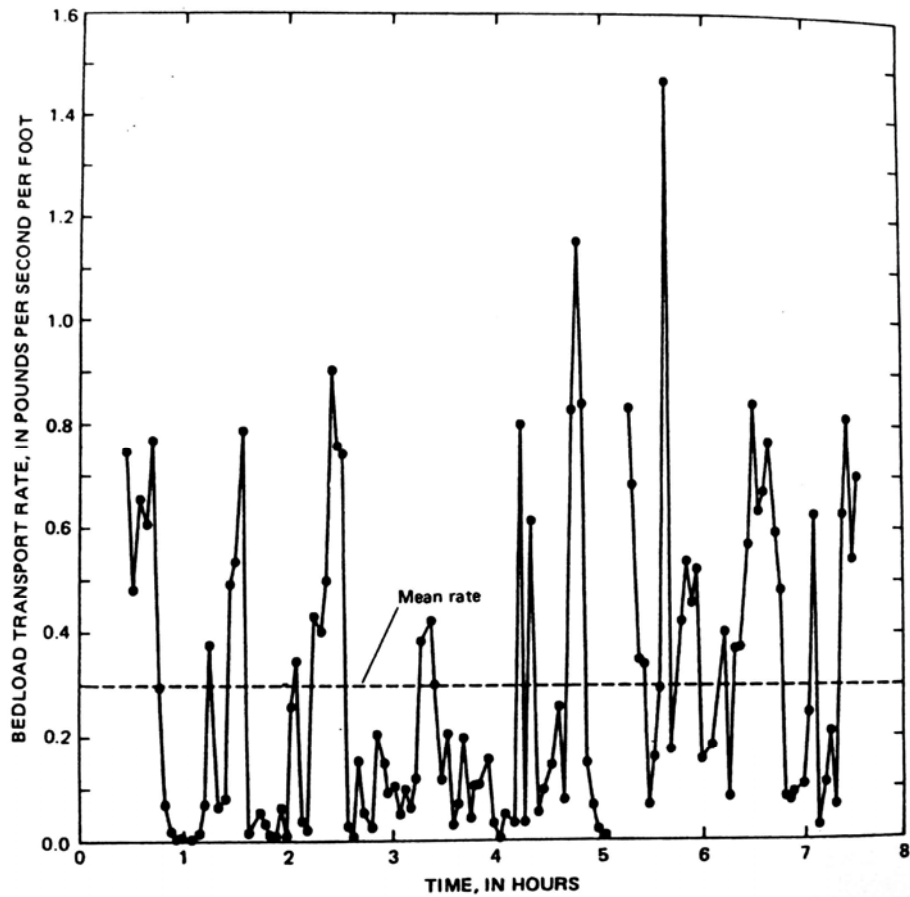


**FIGURE 8.15** Timewise variability in the rate of bed load transport (*Edwards and Glysson, 1988*).

samplers of varying designs are used in different countries, and the resulting loads are not directly comparable. Threefold differences in measured bed load transport rates in the same river but using different samplers were illustrated in the comparison of U.S. and Chinese samplers reported by Childers et al. (1989).

### 8.7.3 Continuous Bed Load Measurement

Continuous bed load sampling is undertaken with a permanent (and costly) structure to sample the entire bed load transported across the sampling section. Designs include a slot in the streambed that allows the sediment to fall into a box where the accumulation is continuously weighted (Laronne et al., 1992), or sediment may be continuously removed from the stream by a vortex tube or by conveyor for weighing and sizing (Tacconi and Billi, 1987). Continuous sediment discharge has also been measured by implanting acoustic sensors in the streambed which register strikes by moving bed material. These stations are costly, and in 1992 Laronne et al. reported that continuous bed load data were available from only six streams worldwide. However, detailed data from these

heavily instrumented research sites help define the characteristics of bed load transport processes.

#### **8.7.4 Grain Tracking**

The downstream motion of individual stones along a streambed can be traced by marking the stones in one section of the stream and relocating them repeatedly over time to determine transport distances and rates. A problem with this method is the difficulty of finding the stones after they have been moved downstream, and simple marking methods such as painting makes it impossible to trace particles that become buried. More sophisticated tracer methods include embedding magnets in stones, which allows recovery despite burial to as much as 0.6 m with commercial metal detection equipment (Schick et al., 1987). Smaller material such as sands can be labeled, released, and recovered at downstream points using a bed load sampler. These methods do not measure total bed load and provide only semi-quantitative information on the motion of material in the size classes marked and subsequently recovered. However, observing the movement of painted stones is a useful method for determining the condition of initiation of motion in different areas of a streambed.

### **8.8 SAMPLING OF COARSE BED MATERIAL**

---

The transport rate for bed material is often determined from the bed material grain size distribution and transport formula, and river sedimentation models require data on bed material as the basis for transport and armoring computations. The composition of the bed material is also required for many type of sediment studies relating to bed stability, initiation of motion, scour, streambed degradation below dams and environmental impact. This section outlines methods to sample the coarse bed material in sand- and gravel-bed rivers.

#### **8.8.1 Sampling Sand Beds**

Sand beds are sampled by obtaining bulk samples which are returned to a laboratory, split as required, and sieved in accordance with procedures outlined in Chap. 5. Sediments in sand bed streams can be sampled by hand at low water when bars are exposed or at shallow depth. In relatively shallow and low-velocity rivers (less than 0.5 m/s) with little or no gravel, a Ponar-type dredge or similar device may be used from a boat. The Ponar dredge (Fig. 8.10*b*) is similar to an Eckman dredge, but is heavier and much better suited to collecting surface sediments sand size or smaller. Where the current is appreciable a bed material sampler based on the rotating bucket principle (Fig. 8.10*6*) may be used, which will scoop a 7-cm-wide sample to a maximum depth of about 5 cm.

#### **8.8.2 The Sampling Problem in Gravel-Bed Streams**

The sampling procedures used in sand-bed streams are generally unsuitable for gravels and larger material. Conditions in gravel-bed rivers present special sampling difficulties, which have been reviewed by Church et al. (1987). There is no sampling equipment

for the collection of gravel or coarser material beyond wading depth (other than use of heavy construction equipment), so samples are normally collected from exposed bars during periods of low water. It is often not practical to bulk sample cobbles or larger bed material because the stones are too large to be carried back to the laboratory, or to be sieved and weighed in the field. Stones larger than 180 mm are difficult to handle and weigh.

Gravel beds generally have wide size ranges, often exceeding 10 phi ( $\phi$ ) units [Eq. (5.1)]. The size distribution may be bimodal, characterized by separate peaks in sand and gravel ranges separated by few grains in the 1- to 4-mm size range (Fig. 8.5). Gravel-bed rivers can also exhibit large spatial variations in grain size. The coarsest material occurs along the leading edge of bars, in riffles, and along the line of the main current; smaller material accumulates toward the trailing edge of bars, in pools, and at progressively higher elevations on point bars. River beds containing significant gravels are typically armored, resulting in a surface layer about one grain thick which is much coarser than the remainder of the deposit, or the subarmor. Sand may be absent from the bed surface while constituting over half the material beneath the armor layer.

Because of the large variation in grain size, a single method cannot be used for sizing bed material in gravel-bed rivers. Fines (smaller than 0.062 mm), if present, are determined by settling tests. Sands and gravels up to about 16 mm are normally sized with laboratory sieves. Stones can be measured with specially constructed sieves or a hand-held sizing template, but more frequently their diameter is measured along the intermediate  $b$  axis. Axis measurement is the only practical method for sizing stones larger than 180 mm. Different grain size distributions are produced by the different methods for selecting and determining the grain size frequency of the sampled stones. Conversion factors to render equivalent the samples collected and analyzed by different techniques are presented in Sec. 9 of this chapter.

### 8.8.3 Selection of Sampling Areas

Because the grain size in gravel-bed rivers exhibits large variations from one point to another, selection of appropriate sampling sites is a critical aspect of a sampling program. There are three dimensions to the problem of sample site selection. Depth: is the armor or the subarmor to be sampled? Longitudinal: sample in riffles or pools, at bends or crossings? Lateral: sample at midchannel or closer to the banks?

Sampling location depends in part on the purpose of the sampling. If information is needed on the initiation of motion or surface roughness, the armor layer should be sampled. If bed material transport is to be computed for discharges large enough to mobilize the armor layer, or if a grain size must be specified in a sediment transport model, then both armor and subarmor should be sampled to define the grain size subject to transport. For environmental and fisheries studies, the finer portion of the bed is typically of great interest, especially with respect to the suitability of spawning gravels because even a relatively small increase in material smaller than 0.85 mm can have a large impact on gravel permeability and the oxygenation of eggs. To analyze impacts of releases for gravel-flushing or channel maintenance, it may be important to have sampling locations representative of different aquatic habitats (e.g., both riffles and pools).

Two patterns will normally be apparent in the longitudinal profile of a gravel-bed river. First, the profile can usually be divided into a series of steps characterized by shallow fast-flowing riffles separated by deeper pools of slower-moving water. Finer sediment tends to accumulate within the pools and is not representative of the bed as a whole or the larger grains that control streambed morphology. Sampling should typically

be focused in riffles, not pools. In bars, the upstream edge will normally contain coarser

material than the downstream edge. Lateral variation in bed material grain size can also be pronounced, especially on point bars. Material toward the center of the stream can be much coarser than material closer to the shoreline. Sampling should normally focus on the area of coarser sediment, avoiding the areas where finer material is deposited because of a localized reduction in hydraulic energy. Consistent criteria must be used for selection of sample locations along the entire reach sampled. Otherwise, the sampled grain size will reflect variations introduced by inconsistent sampling criteria rather than the true longitudinal variation along the stream caused by variations in hydraulic conditions and sources of sediment supply.

Bed material sampling should be timed to coincide with low water so that the bed of the stream will be exposed to the greatest extent possible. If sampling is performed during periods of higher water, the sample sites will be limited to the margins of the stream where the bed material is finer, and sample results may not be representative. There is no suitable method to sample gravels in water more than about knee-deep, since portable sampling equipment will not penetrate the stone bed.

#### 8.8.4 Selection of Sampled Stones

Once the sample areas have been selected, there are three alternatives for selecting the group of stones to be analyzed.

**1. Bulk sampling.** Bulk sampling involves collection of a volume of bed material using a cylindrical sampler (Fig. 18.19*b*), a shovel, backhoe, etc. Samples from submerged deposits should be collected in an enclosed container to prevent fines from washing out.

**2. Grid sampling.** The grid or transect method uses some variant of the pebble count technique described by Wolman (1954). The selection of individual stones from within a sampling area for inclusion in the size distribution is randomized so that the selection probability depends on the exposed surface area of the stone. The grid method includes the selection of each stone at the intersection of a square grid set out using string or wire, linear transects with sampling stations at regular intervals, or a system to randomly select each sample stone such as walking and sampling the grain at the point of each toe, at the point of a tossed stick, etc. Normally the sampled points should be at least two stone diameters apart. However, if the grid is small enough that two grid points fall on the same stone, that stone should be counted twice. If a grid point falls on fines (e.g., smaller than 8 mm), it should be noted as "fines," and a point falling exactly in the crevice between two stones should be discarded. One variant of this method, which has the advantage of also working in shallow water, is to bend over at each sampling point, eyes closed or averted, and select the first stone touched (Leopold, 1970).

**3. Areal sampling.** This method is based on the selection of all surface stones within a perimeter (e.g., 1 m<sup>2</sup>). Another areal-based selection method involves spray painting a portion of the exposed bar and selecting all the painted stones. A third areal sampling method involves sizing of stones by using vertical photographs of the bed, including a scale in each photograph.

Bulk sampling can be used to sample the entire bed including both armor and subarmor, or it can be used to sample the subarmor only after the armor layer has been removed by hand. Bulk sampling is not well-suited for sampling armor because the irregular surface layer one grain thick does not represent a well-defined volume. The remaining techniques are suitable for sampling the surface layer only. All techniques are oriented to randomizing sample collection within a preselected sampling area. However,

the sampling area itself cannot be selected randomly; selection must be based on the stream morphology to ensure that sampling areas are representative.

A variety of more specialized techniques are available for sampling the bed for specific needs, such as studies examining spawning gravels. For instance, bulk samples which preserve the bedding patterns can be obtained by freeze coring, injecting liquid carbon dioxide or liquid nitrogen into the bed through one or more standpipes and recovering the solid block of frozen bed material that forms around the standpipe (Walkotten, 1976).

### 8.8.5 Measurement of Stone Sizes

Bulk samplers are normally size-classed by sieving. However, when a sample contains grains too large to sieve, the oversize stones can be measured individually. Each stone may be oriented so that it has three axis:  $a$  = long,  $b$  = intermediate, and  $c$  = short. One common size classification method is to measure the length of the intermediate or  $b$  axis of each stone with a ruler or calipers, treating this as the nominal or sieve diameter for assigning each stone to a  $\frac{1}{2}$  phi ( $\frac{1}{2}\phi$ ) size class. As an alternative, a square mesh or sizing template cut into metal may be used to size stones by  $\frac{1}{2}$   $\phi$  size classes, similar to sieving. Either method yields similar results. In the case of photographs, because stones usually lay flat with their shortest axis oriented vertically, the  $b$  axis corresponds to the shorter of the two visible dimensions.

### 8.8.6 Frequency by Size Class

Once sorted by size the percentage distribution of stones within each size class can be determined by either counting or weighing the stones:

- **Count.** The number of stones in each size class is counted. This represents the most rapid way to tabulate and record field data.
- **Weight.** The weight of the stones in each size class is determined with a scale in the field or laboratory, or by computing weights from the  $b$ -axis dimension by assuming that the  $b$  axis is equivalent to the nominal diameter and the volume  $V$  of the equivalent sphere is computed by  $V = \frac{4}{3}\pi r^3$ . The volumes are converted to weight by multiplying by specific weight (e.g., 2.65 g/cm<sup>3</sup>). Although there are variations between individual stones, over a sample population use of the  $b$  axis to estimate the weight of stones gives results very similar to direct weighing (Church et al., 1987). In areas having unusual (e.g., flat or elongated) gravel shapes, it is recommended that this conversion be checked by using local samples. The size to weight conversion can also be computed by multiplying the count within each class interval by the mean stone weight in each class interval. However, stones in the largest class should be weighed individually.

The number of stones counted within a size class interval must be multiplied by the average weight of stones for that class interval to obtain the total weights by class. Table 8.2 gives  $\frac{1}{2}$   $\phi$ . size classes and the corresponding diameters and volumes for a sphere representing the mean weight in each class. The diameter of the stone representing the average weight of all stones in the class interval can be estimated very closely by

$$\text{Mean diameter} = \left( \frac{d_u^2 + d_L^2}{2} \right)^{1/2} \quad (8.4)$$

**TABLE 8.2** Mean Grain Sizes for  $\frac{1}{2}$  phi ( $\frac{1}{2}\phi$ ) Size Classes, Based on Weight.

Class limits		Mean diameter, mm	Mean volume cm <sup>3</sup>
Mm	$\phi$		
181 to 256	-7.5 to -8.0	220.6	5621
128 to 181	-7.0 to -7.5	156.0	1988
90.5 to 128	-6.5 to -7.0	110.3	703
64 to 90.5	-6.0 to -6.5	78.0	248
45.2 to 64	-5.5 to -6.0	55.1	27.6
32 to 45.2	-5.0 to -5.5	39.0	31.0
22.6 to 32	-4.5 to -5.0	27.6	11.0
16 to 22.6	-4.0 to -4.5	19.5	3.88
11.3 to 16	-3.5 to -4.0	13.8	1.37
8 to 11.3	-3.0 to -3.5	9.74	0.484

Note:  $\phi = -\log_2 \text{dia (mm)} = -3.3219 \log_{10} \text{dia (mm)}$ .

where  $d_u$  and  $d_L$  are the upper and lower grain diameters in the class interval. If stone diameters or weights are uniformly distributed across a class interval, this equation provides a better estimate of the mean stone volume (or weight) than use of either the arithmetic or geometric mean of grain diameters  $d_u$  and  $d_L$ .

### 8.8.7 Number of Stones Sampled

How many stones must be included in a sample from a gravel-bed stream for it to be representative? Wolman (1954) recommended that at least 100 grains be included, but indicated that a minimum of 60 also gave reliable results. More recent research reviewed by Church et al. (1987) suggests that as few as 50 may be adequate. In the areal method in which all stones are counted, the sampling area should be adjusted for the size of the material to be sampled to obtain the requisite number of stones without excessively large counts. Because the size of bed material varies from point to point within a stream, given a limited sampling effort a better overall picture of the bed material will probably be obtained by collecting smaller samples from more locations as opposed to larger samples from fewer locations.

### 8.8.8 Presentation of Grain Size Results

Either count or weight frequency data may be arranged into histograms or, more commonly, cumulative distribution functions. Both types are illustrated in Fig. 8.5.

### 8.8.9 Truncated Samples

Samples from gravel beds may be truncated through either accident or design. A tenfold change in diameter produces a thousandfold change in the weight of individual grains, and, in gravel beds having a wide range of grain sizes, the smaller particles may constitute an insignificant part of the sample by weight, especially in the surface layer.

Gravel beds may also have a few stones significantly larger than others, which may not be included in normal sampling. Thus, the sample may be truncated at either or both ends. This truncation may be unimportant for modeling bed material transport; the largest stones are infrequent and the smaller may act as wash load and insignificantly affect bed configuration. However, truncation limits and the presence of unsampled material, especially fines, should be indicated in field notes. Although sand or fines may form an insignificant part of the bed from the standpoint of transport hydraulics, their presence may be critical from the standpoint of environmental analysis (e.g., spawning gravels, transport of contaminants associated with fines), and the quantification and modeling of their behavior will be critical in some applications.

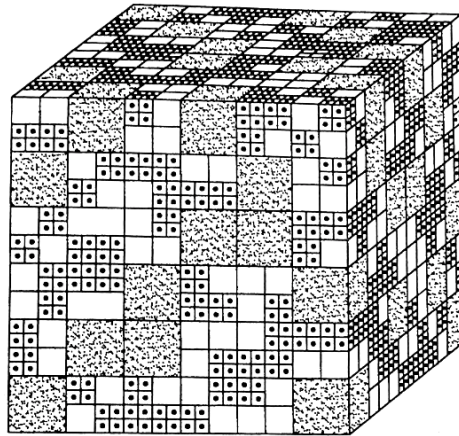
#### 8.8.10 Use of Photographs

Vertical photographs of bed material which include a scale are invaluable in documenting the condition of the bed, and methods for quantifying grain size from photographs have been described by Adams (1979). Vertical photographs can be taken using a handheld 35-mm camera and placing a scale bar with  $\frac{1}{2} \phi$  increments in each photo. This method has the advantage of allowing many sites to be sampled rapidly with highly portable equipment, and provides a permanent visual record of the data collection sites. Photographs may be taken at many sites for comparison or archival purposes, and grain size computed for only a limited number of these sites. The photographs to be analyzed are enlarged to 200 x 250 mm (8 x 10 in) and overlaid with a transparent grid which is used to select stones to construct a distribution curve by the grid-count method described in the next section. Stones are sized by using the sampling bar contained in the photo to measure the shortest visible axis (the  $b$  axis, since the stone will normally lie with the shortest  $c$  axis oriented vertically). As a disadvantage, the photographic method does not measure the true  $b$ -axis length because the  $b$  axis will not always be parallel to the bed (imbrication angle) and because of partial hiding of the stone and shadow effects. Church et al. (1987) concluded that photographic methods for estimating grain size may be adequate for gravel and large material where high accuracy of absolute lengths is not required for size classification. However, photographic measurements should be checked by conventional field techniques in each study area, since packing and imbrication angle can change from one environment to another. Adams (1979) reported that the sizes measured by the photographic method are biased, being about  $0.1 \phi$ , smaller than the equivalent sieve size. The grain size frequency distribution curve for sieve and photographic sizing are of similar shape, but displaced by the amount of bias.

### 8.9 BED MATERIAL GRAIN SIZE CONVERSION FACTORS

---

Hydraulic transport formulas have been based largely on laboratory work in which bulk samples are divided into size classes by sieving and weighing. It is desirable to have gravel-bed samples reported in a manner that is consistent with the bulk-sieve-weight procedure used in laboratory flumes and for smaller grain sizes. Different sample collection and frequency methods will produce different frequency distributions (Leopold, 1970). A system of correction factors that can be applied to different sampling techniques was presented by Kellerhals and Bray (1971) and was subjected to rigorous scrutiny by Church et al. (1987) with both laboratory and field techniques. The latter concluded that the Kellerhals-Bray corrections "yield reasonable results" and recommended their use.



(a)	(b)	(c)	(d)	(e)	(f)	(g)
Particle	Linear Size, $d$	Particle Weight $W$ ,	Volume Count	Class Weight	Surface Count	Surface Area
	1	1	4608	4608	192	192
	2	8	576	4608	48	192
	4	64	72	4608	12	192

**FIGURE 8.16** Cube model for developing sampling conversion factors (after Kellerhals and Bray, 1971).

The Kellerhals-Bray correction scheme was constructed by visualizing the bed as filled with a series of cubes. The cubical model was used only to simplify computations: the method is independent of the exact particle shape. The sample cube is illustrated in Fig. 8.16 along with a tabulation of key geometric features. The conceptual model contains three sizes of stones, and the total weight within each size class is the same (as shown in column  $e$  of the figure) resulting in 33.3 percent of the total sample weight in each size class.

The conversion factors were developed for three types of sampling methods (bulk, grid, and areal) and two types of frequency measurements (weight and count), all described in the previous section. If a grid is placed over the surface, or a vertical photograph of the surface, and each stone falling beneath a grid intersection is assigned to a size class, the resulting frequency count should be directly proportional to the surface area of the exposed stones (col.  $g$  in Fig. 8.16). This grid-count method will produce a grain size distribution identical to a bulk-sieve-weight sample. All other methods require conversion factors to produce a size distribution similar to that which would have been obtained by using the bulk-sieve-weight technique. The conversions as a function of grain (or class) diameter are given in Table 8.3 for the sampling method (bulk, grid, areal) and the frequency measurement (weight or count). Two examples will be given to illustrate use of the conversion factor.

**TABLE 8.3** Conversion Factors for Surface Samples

	Bulk-sieve-weight	Grid-count	Grid-weight	Areal-count	Areal-weight
Bulk-sieve-weight	-	1	$d^3$	$1/d^2$	$d$
Grid count	1	-	$d^3$	$1/d^2$	$d$
Grid weight	$1/d^3$	$1/d^3$	-	$1/d^5$	$1/d^3$
Areal count	$d^2$	$d^2$	$d^5$	-	$d^3$
Areal weight	$1/d$	$1/d$	$d^2$	$1/d^3$	-

Source: Kellerhals and Bray (1971)

**8.9.1 Areal Count to Bulk Sieve Conversion**

For this example consider the cube introduced in Fig. 8.16 and assume that all the surface stones within a perimeter have been sampled and size-classed, and the number within each size class has been counted (areal-count method). In Table 8.4, the first two columns represent the raw field data: counts within each size class. The counts are classified by the smallest limit of the class interval, equivalent to reporting sieved grain sizes by the "retained on mesh size. From these data the values in column 3 are computed, but these percentages will not produce a frequency distribution equivalent to the bulk-sieve-weight method. It is necessary to apply a correction factor of  $d^2$  from Table 8.3. the value of which is computed in column 4. Since the grain size distribution is based on a percentage of the total sample weight or mass, it is not necessary to determine the weight of the stones, only the conversion factors. Applying the column 4 correction factor to the percentages in column 3 yields the corrected numerical values in column 5, from which the percentage distribution in column 6 and the cumulative distribution in column 7 can be computed. In this conversion, the length  $d$  refers to the diameter corresponding to the mean weight of that class interval [Eq. (8.4)].

A second example involves a weight conversion using one of the Kellerhals and Bray field datasets, as summarized in Table 8.5. In this case, all stones within a perimeter were sampled and weighed (areal-weight method). To convert this to either the bulk weight or the grid count format, which are identical, the conversion factor is  $1/d$ . The first two columns in Table 8.5 are obtained from a grain size distribution curve, from which columns 3 and 4 are computed. The weight (column 3) is multiplied by the  $1/d$  conversion factor (using the diameter in column 4) to produce the corrected values of  $W/d$  in column 5. The numerical values in column 5 are used to compute the percentage distribution by

**TABLE 8.4** Areal Count to Bulk-Sieve-Weight Conversion Based On Fig. 8.16

Site $d$	Areal count $C$	Percent of count	$d^2$	Converted counts $Cd^2$	Percent by class	Percent finer
(1)	(2)	(3)	(4)	(5)	(6)	(7)
8						100.0
4	12	4.8	16	0.76	33.3	66.7
2	48	19.0	4	0.76	33.3	33.3
1	192	76.2	1	0.76	33.3	0.0
Sum	252			2.29		

**Table 8.5** Areal Weight to Grid Count Conversion

Size <i>d</i> , mm	Percent finer	Retained weight <i>W</i> , %	Geometric mean dia. <i>d</i> (mm)	<i>W/d</i>	<i>W/d</i> as percent	Percent finer
(1)	(2)	(3)	(4)	(5)	(6)	(7)
87	100					100
62	97	3	73.0	0.041	0.9	99.1
45	81	16	53.0	0.302	6.5	92.7
32	58	23	38.5	0.597	12.8	79.9
23	38	20	27.5	0.727	15.6	64.3
16	21	17	19.5	0.872	18.7	45.7
12	8	13	14.0	0.929	19.9	25.8
8	3	5	10.0	0.500	10.7	15.1
5.8	2	1	6.8	0.147	3.1	12.0
4	1.5	0.5	4.8	0.104	2.2	9.7
2.8	0	1.5	3.3	<u>0.455</u>	9.7	0.0
Sum				4.674		

*Source:* Kellerhals and Bray (1971).

grain size in column 6, from which the corrected grain size distribution in column 7 is computed.

## 8.10 SOURCES OF ERROR

In establishing or evaluating a suspended-sediment monitoring program to address problems of engineering design, operation, or environmental impact, two types of questions must be asked:

1. What are the temporal characteristics of concentration, load, and particle size distribution needed for the design?
2. How well does the existing or proposed sampling program document these characteristics?

This section discusses some of the sources of error which must be considered in designing or evaluating a sediment monitoring program.

### 8.10.1 Sampling Precision and Accuracy

In discussing sampling procedures, the difference between the concepts of precision and accuracy should be understood. The term *precision* refers to the repeatability of measurements. If procedures are precise, the errors in each procedure will occur in a consistent manner, making it possible to subsequently apply correction factors to offset the systematic bias, if it can be quantified. For example, two types of sampling equipment operated side by side may obtain consistently repeatable values but have different means, making it possible to apply a correction factor to offset the bias between the samplers. *Accuracy* refers to how well the measurement reflects the characteristic that is being monitored; precise and repeatable measurements are not necessarily accurate measures of conditions in the stream cross section. Thus, precise measurements of suspended solids

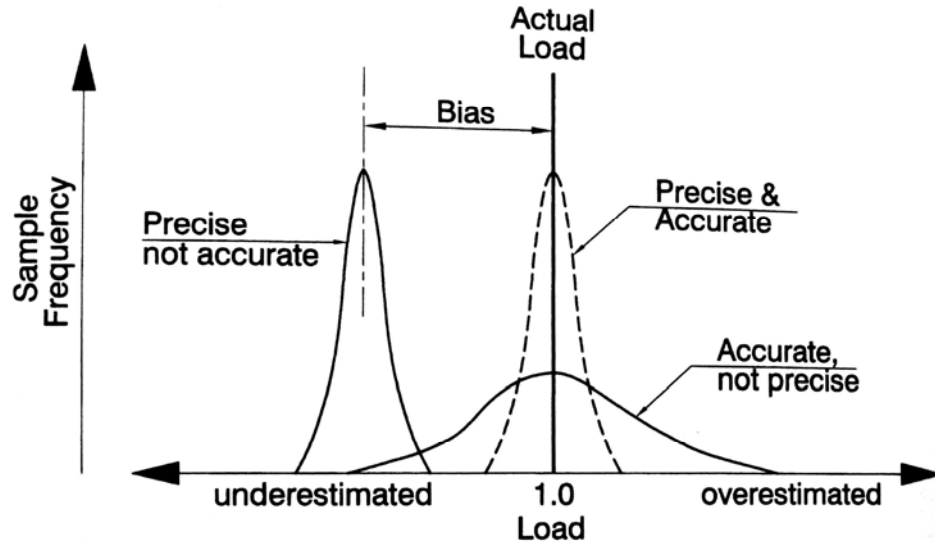


**FIGURE 8.17** Comparison of the concepts of precision and accuracy for measurement of sediment load.

concentration at the water surface will not be an accurate indicator of the total load in a sand-bed river. The concept of precision and accuracy is illustrated in Fig 8.17, which shows hypothetical histograms of a population of samples taken to estimate sediment load.

### 8.10.2 Sampling Equipment

The first potential source of error is the sampling equipment itself. How well does the sampler measure the ambient concentration? Sampling accuracy for suspended sediment samplers is dependent on achieving isokinetic sampling velocities; the water velocity entering the sampling intake should be within 3 to 5 percent of the ambient stream velocity. Intake and exhaust tube diameters and lengths are sized to achieve this condition, and use of nozzles designed for one sampler on a different sampler will produce errors, as will the use of bent or damaged nozzles. The point sampling errors caused when nozzle intake velocity deviates from the ambient velocity affects primarily the sand size material, and increases as particle diameter increases (Edwards and Glysson, 1988). See Fig 8.18. Although standardized dimensions have been established for suspended and bed load samplers, not all samplers use the same **materials, and** variances can occur in some critical dimensions. Each sampler should be calibrated to guarantee performance. Each sampler manufactured for the Federal Interagency Sedimentation Program is flume-calibrated, but many commercial samplers are not.

Gurnell et al. (1992) compared the intake of an ISCO pumped sampler to a USDH41 hand sampler, both placed side by side at a stationary point in the stream. The ISCO nozzle orientation was not reported. It was concluded that the ISCO sampler provided unbiased estimates of suspended sediment concentration in comparison with the USDH48 sampler. As discussed in Sec. 8.3, nozzle orientation has a large influence on sampling, and can influence both the total concentration and the grain size entrained in a pumped sampler. The potential for error due to nozzle orientation increases as a function of grain size.

Suspended-load measurements collected by depth-integrated isokinetic sampling at multiple profiles represents the most accurate standard against which all other suspended

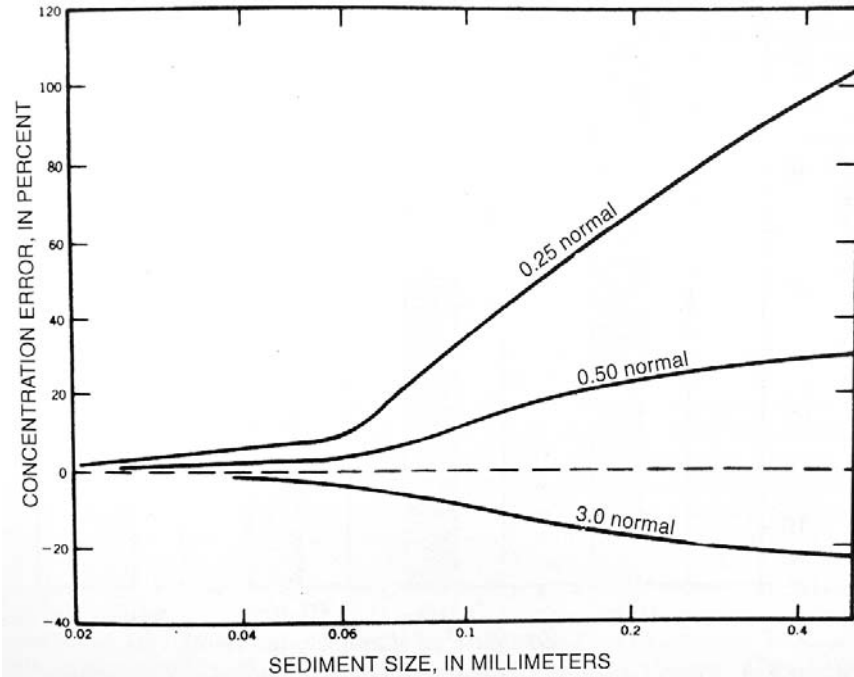


**FIGURE 8.18** Deviation in sediment concentration as a function of grain size when intake velocity is 0.25, 0.50, and 3.0 times stream velocity (Guy and Norman, 1970). Most of the error occurs in the sand size range.

-sediment sampling methods are calibrated. What is the repeatability of the manually collected depth integrated samples? Allen and Petersen (1981) examined the variability of suspended sediment concentration by taking paired equal-transit-rate samples on two Oklahoma streams. The smaller of the two, East Bitter Creek (18 m wide, 3 m deep bankfull), drains 91 km<sup>2</sup> and transports primarily silt and clay. Washita River (55 m wide, 5 m deep bankfull) drains 12,410 km<sup>2</sup> and transports about 30 percent sand. Two sources of sampling error overshadowed all others and both increased sample concentration. The first problem was associated with dipping the sampler nozzle into the streambed; it was caused by an irregular bottom (dunes), excessive downward transit velocity, soft bed, and ploughing into the bed when travel reversal caused the sampler to move upstream. The second problem occurred when the operator was late in reversing the sampler's travel, allowing it to linger in the zone of maximum sediment concentration near the bed. The variability between paired samples was larger for relatively inexperienced operators than for experienced, and also increased as a function of river stage. The variability between sample pairs for measurements at high stage are summarized in Fig. 8.19.

### 8.10.3 Number of Sampling Points

The most accurate measurements of sediment load are obtained if depth-integrated verticals are used across a stream. However, because each additional vertical represents a

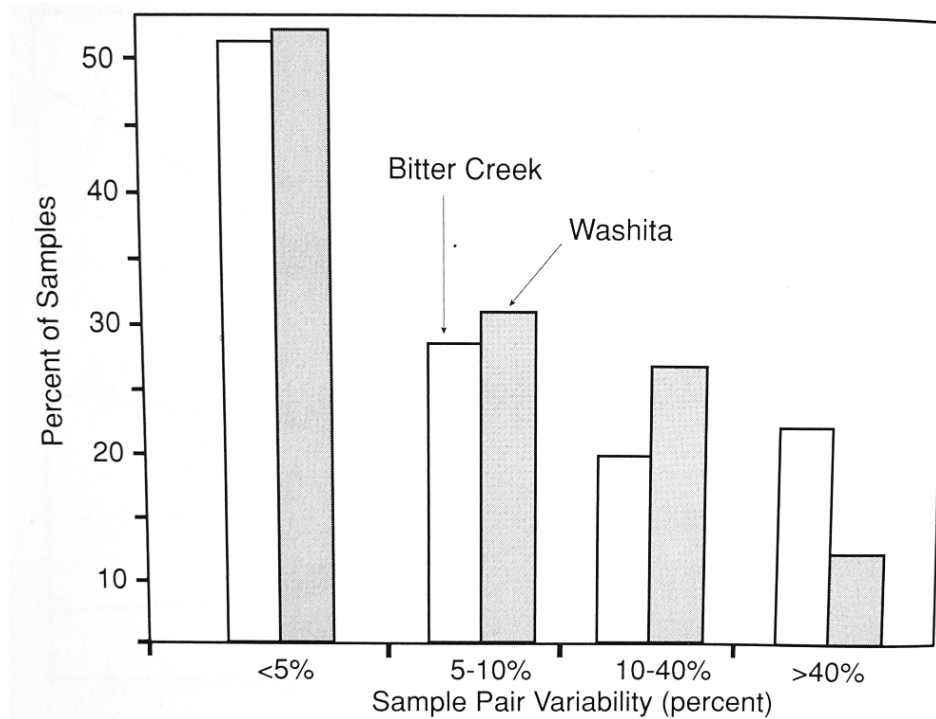


**FIGURE 8.19** Variation in suspended sediment concentration resulting from paired sampling in two Oklahoma rivers using depth integrated samplers (Allen and Peterson, 1981).

significant increase in manual sampling effort and additional samples to transport and analyze in the laboratory, it is desirable to minimize the number of samples collected. In the case of automatic equipment the sample will be withdrawn from only a single point on the cross section. What magnitude of error may be associated with the use of a reduced number of sampling points within a cross section?

The error introduced by reducing the number of verticals can be determined only by field measurements in each individual stream, since the horizontal distribution of sediment transport is unique to each cross section. From repeated sampling at multiple verticals, it may be found that one of the verticals consistently represents the mean characteristics of the entire stream. The suitability of an abbreviated sampling technique must be verified by conventional sampling techniques using multiple verticals, and these calibrations should be repeated periodically and after any large discharge that could alter the channel configuration. Particular care must be exercised to adequately sample large runoff events, since the transport of coarse material can increase greatly in these events and an abbreviated sampling protocol developed for low-flow conditions may not be representative of large discharges.

The magnitude of the error introduced by variations in the sampling protocol will be largest in streams having a large load of coarse sediment. In streams transporting very fine material that is uniformly distributed through the water column, and when the sampling location has sufficient turbulence to generate concentration profiles which are essentially uniform both horizontally and vertically, point samples can be representative of the mean concentration of fines within the stream.

Can midstream samples at or near the surface be substituted for depth-integrated or 60 percent-depth samples? This question may arise in rivers without sand transport, in sampling for water-quality constituents or contaminants that are associated with fine sediment, and during floods when deeper sampling may be made impossible by high

velocity and floating debris. Yuzyk et al. (1992) analyzed results of 436 vertical measurements from six sites on four major Canadian river systems and found that the midstream near-surface sample was within  $\pm 15$  percent of the vertical mean 89 percent of the time at five of the six stations sampled, with the tendency to undercount by about 10 percent. Data from the verticals showed that the concentrations of silts and clays commonly displayed inconsistent and variable patterns of concentration within the cross section, and at four of the six sites, the error in the clay fraction was greater than the error in the silt fraction. An inconsistent vertical variation in the concentration of fines is also evident in Fig. 8.8.

#### 8.10.4 Laboratory Error

Errors may be introduced during the handling, splitting, and laboratory analysis of samples. The differences in dry suspended-sediment weights determined with fast-filtering Whatman 40 (8- $\mu\text{m}$  retention) and Millipore 0.45- $\mu\text{m}$  papers was examined by Gurnell et al. (1992) on glacial discharge, who found that, as suspended-solids concentration decreased, the error increased, from 1 percent at 1000 mg/L to 4 percent at 400 mg/L.

Probably the greatest potential for error occurs when sample splitting is performed. Splitting is normally not required from pumped or single-transit depth-integrated samples. However, in deep rivers large sample volumes may result and it may be necessary to split the composited sample. Yuzyk et al. (1992) concluded that, when suspended sediment samples contain rapidly settling sands, it is not possible to obtain a representative subsample of a larger suspended-sediment sample, even when vigorous mixing procedures are used, and errors on the order of 50 percent can be produced. This sample splitting problem affects only suspended coarse particles, not fines. Chapel and Larsen (1996) compiled information on sample splitting. In general they found that both churn and cone splitters produced errors on the order of about 3 to 6 percent for fines, but more typically in the 15 to 30 percent range for sands, with the splitting error increasing as a function of grain size within the sand size class. Sample splitting is also a potentially large source of error in the preparation of bed material for sieving.

Water chemistry greatly affects flocculation, which in turn controls the settling rate of clays and the apparent grain diameter when computed as the sedimentation diameter. It is always necessary to determine beforehand whether the suspended sediment samples should be analyzed in native water or by using a dispersant, and the results should be clearly marked as to the procedure used to aid in the subsequent interpretation of the resultant grain size distribution.

#### 8.10.5 Rating Curves

Sediment concentration is poorly correlated to discharge, and sediment rating curves typically exhibit a high degree of scatter; suspended-sediment concentration in some streams varies by nearly 3 orders of magnitude at a given discharge. However, the product of the rating curve and a discharge time series can be used to accurately estimate the total load over a long period of time, provided that rating curves are constructed from a dataset that includes both the rising and falling limbs of large discharge events, and for storms in all seasons of the year. A rating curve constructed from an incomplete dataset should not be presumed to be correct.

Rating curves are frequently extended beyond the range covered by data, since historical or synthetic discharge datasets often include discharges much larger than the maximum sampled during the fluvial monitoring program. This extrapolation can be a source of error and uncertainty, since a disproportionate amount of sediment can be transported by extreme discharge events. Rating curve extrapolation should be based on

characteristics of similar streams for which a more complete dataset is available, and the maximum suspended sediment concentrations resulting from extrapolation should be checked for reasonableness.

Sediment load can be seriously underestimated when rating-type relationships are applied without regard to the time base of the underlying dataset. A rating curve based on instantaneous concentration-discharge data pairs should not be applied to average daily discharge values, except when concentration changes so slowly that an instantaneous value indeed approximates the daily average concentration. If average daily discharge data are to be used to compute load, the rating curve should also be constructed from daily loads and mean daily discharges.

### 8.10.6 Sampling Frequency and Computational Error

The most severe and pervasive problem with sampling protocols is the failure of the sampled dataset to represent the full range of rapidly fluctuating sediment concentration. Use of turbidity to gage suspended-sediment concentration is gaining favor, despite its inherent drawbacks, because it allows the variation in sediment concentration to be tracked continuously. In essence, the large error introduced by having no data during most of the monitoring period is replaced by a smaller correlation error between turbidity and suspended solids

Walling and Webb (1981, 1988) used continuous turbidity measurements to monitor actual load in River Creedy, United Kingdom. Nearly 100 independent load estimates were also made for the same period by selecting data subsets to represent alternative periodic sampling strategies, simulating manual sampling at either regular or irregular intervals, including increased sampling frequency during high-flow events. A variety of indirect load-computation techniques based on both timewise interpolation and extrapolation (rating curves) were applied to these data subsets. Sample data subsets for the construction of rating curves of the form  $\text{concentration} = aQ^b$  included regular interval sampling plus regular intervals augmented with random sampling of higher discharge events. Rating curves were constructed from the entire data subset, and also for additional subsets to differentiate between seasons and rising and falling stages. The resulting estimates of suspended sediment load over a 7-year period are compared in Fig. 8.20, illustrating the large error range associated with different combinations of sampling frequency and computational method. Discontinuous sampling techniques frequently underestimated the 7-year sediment load by an average of 60 percent. This analysis underscores the potential for traditional methods of collecting and analyzing suspended sediment data to underestimate the actual yield, a theme echoed by many other researchers. The largest errors corresponded to estimates of sediment loads during short time periods. Some of the sediment discharge characteristics that create errors in construction of sediment rating curves were illustrated in Fig. 7.5.

### 8.10.7 Bias in Curve Fitting

As described in Sec. 7.4.3, if data are log-transformed before a least squares fit of the data, a negative bias will result.

## 8.11 CLOSURE

Sediment sampling depends heavily on the investigator's interpretation of the fluvial environment and design and execution of a suitable to that environment. Sampling

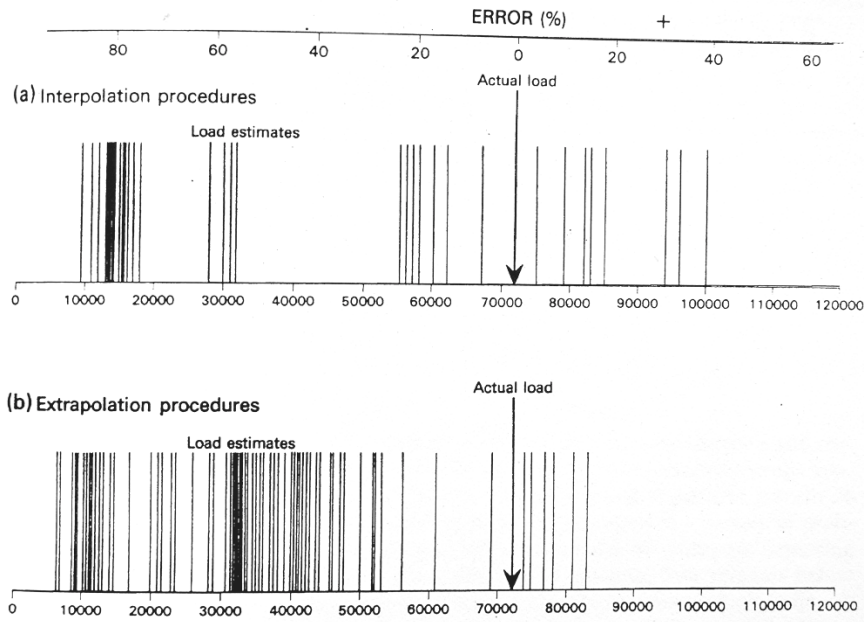


**FIGURE 8.20** Estimates of 7-year sediment load determined by different methods, compared to the true load determined by continuous turbidity measurement (*Walling and Webb, 1981*).

Sampling design must take into consideration both economic constraints and practical logistical problems, while ensuring quality control. The use of newer sampling technologies involving turbidity monitoring and pumped samplers is strongly encouraged, especially at remote sites and in less developed areas, since it can provide an independent source of data useful for checking manually collected data under conditions of possibly limited supervision and quality control. If two independent datasets produce quite different results, this will signal the potential for data problems and the need for more thorough analysis. As demonstrated in the Cachí case study (Chap. 19), continuous turbidity monitoring for even a limited period can greatly enhance the reliability of sediment load estimates by revealing variations in sediment concentration not detected from intermittent manual sampling (see Fig. 19.8). The cost of implementing a proper sediment sampling program is very small compared to the scale of engineering civil works that may be affected by sediment, and given the potential for large errors in sediment sampling and its long-term consequences to many types of engineered structures, cost cutting in the area of data collection is a false economy.

Users of fluvial sediment data should find out as much as possible about the way the data was collected, especially in areas where sampling protocols may not be standardized. Even data provided by organizations such as the U.S. Geological Survey need to be checked to ascertain that the available dataset includes large sediment-producing storms. Did large storms occur during the sampling period, and were these storms adequately sampled (rising and falling limbs), or was sampling at automatic stations abbreviated by equipment malfunction or exhaustion of sample bottles? Problems of this nature are an unavoidable part of a field data collection program, and when they occur they enter into that analysis process loosely called "engineering judgment" that is required to properly interpret the available data and apply it to design problems.

---

## CHAPTER 9

---

# HYDRAULICS OF SEDIMENT TRASPORT

---

This chapter briefly reviews hydraulic formulas for fluid flow in open channels and several fundamental sediment computations. Reservoir sedimentation alters hydraulic conveyance by changing both the cross section (by deposition) and vegetative growth on the delta. The condition of incipient sediment motion is important in a variety of problems associated with reservoir sedimentation. It is fundamental for scour and armoring computations downstream of dams, for the evaluation of flushing flow releases below dams to maintain spawning gravels, for determining conditions under which sediment will be deposited or eroded, for the design of stable channels and protective revetments crossing sediment deposits (e.g., for dam decommissioning), and as a computational parameter in sediment transport equations. Several sediment transport equations are briefly reviewed to provide an overview of the computation of bed material transport, which is the basis for modeling activities.

The field of sediment transport is complex, and workers in this field should refer to more comprehensive texts to better understand the computational basis. Yang (1996) gives an overview and comparison of sediment transport theory and equations, including a coherent presentation of the utilization of unit stream power as a unifying concept for the analysis of a variety of transport phenomena. Julien (1995) gives a good coverage of fundamental equations and applications, using an approach different from Yang. Chang (1988) discusses sediment transport with a strong emphasis on the quantitative aspect of fluvial processes and morphology of alluvial channels. Simons and Senturk (1992) and ASCE Manual 54 (Vanoni, 1975), currently being updated, are extensive references providing a general-purpose overview of the field of sedimentation engineering. Senturk (1994) gives an extensive overview of dam and reservoir hydraulics and presents many worked problems, but gives only limited treatment to sediment issues.

***Special Conditions in Reservoirs.*** Many of the computational methods introduced in this chapter are based on simplifying assumptions such as conditions of steady uniform flow in prismatic channels, and have been developed to analyze cohesionless sediment. Transport computations also assume that the exchange between the fluid and the bed has reached equilibrium conditions. These conditions often do not apply in reservoirs.

During impounding, a reservoir cross section is not prismatic but increases moving downstream. Flow is not uniform. Streams entering a reservoir are depositing sediment load, thereby violating the assumption of equilibrium between the bed and fluid. In many reservoirs, sediment deposits consist largely of cohesive sediments, which present a special problem from the standpoint of sediment transport because of the difficulty in

characterizing the erodibility of cohesive materials, especially since erodibility will vary as a function of time, depth, and operating rule. Inflow into reservoirs receiving drainage from small steep watersheds may be very unsteady. Flow stratification commonly occurs in reservoirs. During flushing events, flow may become hyperconcentrated. Both inflow and flushing procedures may involve a wide range of grain sizes, with clays through gravels being eroded and transported simultaneously. Erosion processes within the reservoir may be further influenced by processes such as meandering and bank failure, which are not included in any mathematical formulation.

In summary, the sediment transport conditions associated with reservoirs are extremely complex. Detailed analysis of many of these problems lies beyond present knowledge, and only qualitative or rough quantitative estimates can be provided. Caution should be used in the application of numerical techniques in either hand calculations or computer models to ensure that the basic assumptions are not grossly violated by the prototype system, and to be aware of the direction and potential magnitude of the error introduced by the assumptions inherent to the computational techniques.

## 9.1 DEFINITIONS AND UNITS

---

In the International System of Units (SI), mass is measured in kilograms (kg). Weight is a force, the product of mass and gravitational acceleration, and is expressed in terms of newtons ( $1 \text{ N} = 1 \text{ kg} \cdot \text{m/s}^2$ ). A mass of 1 kg subject to a gravitational acceleration of  $9.8 \text{ m/s}^2$  at the earth's surface has a weight of 9.8 Newtons, although it is customary to say that it "weighs" one kilogram. However, for dimensional consistency weight must be expressed in newtons for computational purposes. In the U.S. Customary System of units [foot-pound-second (fps)], weight is measured in pounds and mass in slugs. Symbols and units used in this chapter, other than coefficients, are defined below. The fps system units are given in some instances for clarity.

<i>A</i>	Area of the wetted hydraulic cross section ( $\text{m}^2$ )
<i>D</i>	Water depth (m)
<i>d</i>	Particle diameter (m or mm). When subscripted, it refers to the size on the grain size curve. Thus, $d_{90}$ refers to the diameter of the particle larger than 90 weight-percent of the particles in the mixture.
<i>F</i> *	Dimensionless shear stress or Shields parameter. Most authors use the symbol $\tau^*$ for this dimensionless parameter, which can lead to confusion with the absolute value of bed shear, which is also denoted by the letter $\tau$ .
<i>G</i>	Specific gravity (dimensionless), the ratio of the density or specific weight of solid, fluid, or mixture thereof, to the density or specific weight of pure water at $4^\circ\text{C}$ . The specific gravity of most sediment is approximately 2.65.
<i>g</i>	Gravitational constant, $9.81 \text{ m/s}^2$ or $32.2 \text{ ft/s}^2$ .
<i>k</i>	Size of roughness elements (m)
<i>P</i>	Perimeter of the wetted hydraulic cross section (m)
<i>Q</i>	Total discharge ( $\text{m}^3/\text{s}$ ).
<i>q</i>	Discharge per unit width ( $\text{m}^3/\text{s}$ per meter of channel width).
<i>R</i>	Hydraulic radius (m) computed as $R = A/P$ . It may be conceptualized as the average depth of flow over the frictional boundary. In a

channel which is much wider than deep, the hydraulic radius is closely approximated by the water depth and the assumption that  $R = D$  is made frequently.

- $Re_* = dU_* / \nu$  Boundary or shear Reynolds number (dimensionless).
- $S$  Channel or water surface slope (m/m, dimensionless).
- $U_* = (gRS)^{1/2} = (\tau/\rho)^{1/2}$  Shear velocity or friction velocity, is a measure of the intensity of turbulent fluctuations (m/s).
- $V$  Mean flow velocity within a single vertical or across an entire cross section, in which case  $V = Q/A$  (m/s).
- $v$  Local flow velocity at a particular point within a fluid (m/s).
- $VS$  Unit stream power, the time rate of energy dissipation per unit weight of water computed as the product of mean velocity and slope. It has units of (N•m/N)/s[(ft•lb/lb)/s], which simplifies to velocity. See Appendix J.
- $\tau V = (\gamma DS)V$  Stream power or the rate of energy dissipation per unit of surface area N•m/(m<sup>2</sup>•s) or ft •lb/(ft<sup>2</sup> •s)]. Stream power may also be expressed in terms of W/m<sup>2</sup>, where 1 W = 1 J/s = 1 N m/s. See Appendix J.
- $\gamma = \rho g$  Specific weight (N/m<sup>3</sup>, lb/ft<sup>3</sup>). The specific weight of 1 m<sup>3</sup> of water on the earth's surface is (1000 kg/m<sup>3</sup>)(9.81 m/s<sup>2</sup>) = 9810 kg/(m<sup>3</sup> •s<sup>2</sup>) = 9810 N/m<sup>3</sup>. For  $G = 2.65$ , the specific weight of sediment is 2.65(1000 kg/m<sup>3</sup>)(9.81 m/s<sup>2</sup>) = 25,997 N/m<sup>3</sup>.
- $\mu$  Viscosity or dynamic viscosity is a measure of a fluid's resistance to deformation, expressed as the velocity gradient  $dv/dy$  produced by shear stress  $\tau$ , according to the relation  $\tau = \mu(dv/dy)$ . For water at 20°C, the value is  $1.00 \times 10^{-3}$  N•s/m<sup>2</sup>. Values are tabulated in the appendixes.
- $\nu = \mu/\rho$  Kinematic viscosity, the ratio of dynamic viscosity  $\mu$  to fluid density  $\rho$ . For water at 20°C, the value is  $1.00 \times 10^{-6}$  m<sup>2</sup>/s. Values are tabulated in the appendixes.
- $\rho$  Density or mass per unit volume (kg/m<sup>3</sup>, slugs/ft<sup>3</sup>).
- $\phi$  Angle of repose of sediment (degrees). See Fig. 9.1.

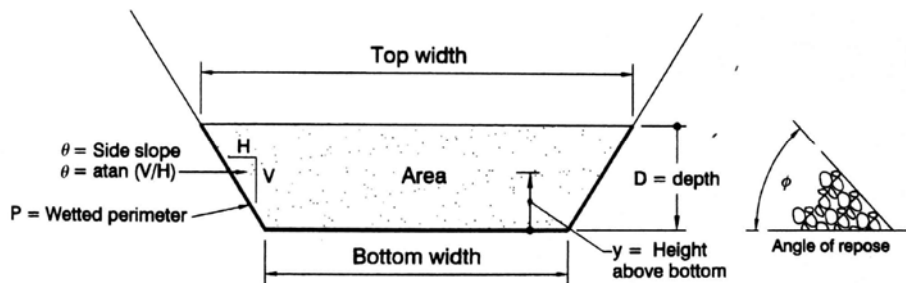


FIGURE 9.1 Definition sketch of geometric properties.

$\tau = \gamma RS = \gamma DS$  Bed shear or tractive force ( $\text{N/m}^2$ ,  $\text{lb/ft}^2$ ). It is the frictional force at the boundary of a moving fluid which resists forward motion. The unit of  $\text{N/m}^2 = \text{kg/m/s}^2$  is also known as the pascal (Pa), the unit of pressure in the SI system. To convert into  $\text{N/m}^2$ : multiply  $\text{g/cm}^2$  by 98; multiply  $\text{dynes/cm}^2$  by 0.1; multiply  $\text{lb/ft}^2$  by 47.88. The term  $\tau_{cr}$  is used to designate the bed shear stress and  $\tau_{cr}$  the critical value of bed shear at the initiation of particle motion.

$\omega$  Terminal fall velocity of a sediment particle in a quiescent fluid (m/s).

Subscripts:

cr	Critical condition of incipient motion
s	Sediment
$\theta$	Side slope

An unsubscripted variable ( $\gamma$ ,  $\rho$ , etc.) refers to the fluid.

Most channels are constructed with a trapezoidal cross section, and for ease of computation many river and reservoir problems can be roughly approximated by using a trapezoidal section. The definition sketch for a trapezoidal section is given in Fig. 9.1.

## 9.2 FLOW RESISTANCE EQUATIONS

---

### 9.2.1 Chézy Equation

In 1775, the French engineer Chézy presented the relationship bearing his name, the first equation to successfully relate uniform open-channel flow to bed resistance. Chézy related the average velocity  $V$  of steady uniform open channel flow to three parameters: channel slope  $S$ , the hydraulic radius  $R$ , and a coefficient which expresses the boundary roughness. The equation is usually written in the form:

$$V = C(RS)^{1/2} \quad (9.1)$$

in which  $C$  is the Chézy coefficient of friction.

### 9.2.2 Manning Equation

The equation developed in 1889 by the Irish engineer Robert Manning may be derived from the Chézy equation if the Chézy friction coefficient is set equal to  $C = R^{1/6}/n$ . The Manning equation has the following form:

$$V = (1/n) R^{2/3} S^{1/2} \quad (9.2)$$

The  $n$  value in the Manning equation represents the roughness or flow-resistance characteristics of the boundary. When written in fps units, this formula includes the unit conversion factor 1.486 in the numerator, giving the following form:

$$V = (1.486/n) R^{2/3} S^{1/2} \quad (9.3)$$

By multiplying both sides of the equation by the wetted cross-sectional area, Manning's equation can be solved for discharge in SI or fps units:

$$Q = (1/n)AR^{2/3}S^{1/2} \quad \text{or} \quad Q = (1.486/n)AR^{2/3}S^{1/2} \quad (9.4)$$

In the English-speaking world, the Manning equation is the most widely used hydraulic resistance equation for open channel flow.

### 9.2.3 Darcy-Weisbach Equation

Originally developed for flow in pipes, the Darcy-Weisbach equation has the following form:

$$V = (8gRS/f)^{1/2} \quad \text{or} \quad V/U_* = (8/f)^{1/2} \quad (9.5)$$

Unlike the friction coefficient in the Chézy and Manning equations, the Darcy Weisbach friction factor  $f$  is dimensionless, and can be read from a Moody diagram.

## 9.3 HYDRAULIC FLOW-RESISTANCE FACTORS

---

Hydraulic flow resistance has two components: grain roughness and form loss. Grain roughness refers to the shear forces created by sediment particles, vegetation, or other roughness elements at the flow boundary. Form loss is the large-scale turbulent loss caused by the irregularity of the channel geometry along its length because of constrictions, expansions, bends, bed forms, and similar geometric features. Both types of flow resistance are important in natural channels. More extensive information on  $n$  value determination may be found in Chow (1959), Barnes (1967), and Arcement and Schneider (1989). Chow includes tables and photographs to aid in the evaluation of the roughness in excavated and natural channels, and also describes the U.S. Soil Conservation Service procedure for estimating the  $n$  value on the basis of vegetal retardance. Barnes presents the Manning roughness values for a range of natural channels, illustrating each channel with color photographs, while Arcement and Schneider provide similar information and photographs for floodplain forests.

### 9.3.1 Grain Roughness

The Strickler formula, developed in 1923, defined Manning's  $n$  value for grain roughness as a function of particle size:

$$n = \frac{d_{50}^{1/6}}{21.1} \quad (9.6)$$

where  $d$  = particle diameter in meters. The Federal Highway Administration (1975) equation to estimate the roughness for gravel beds or riprap has the same form but with a coefficient value of 20.8 in the denominator. Equations of this type are relatively insensitive to changes in grain diameter and do not include the effect of form losses due to irregular channel geometry.

### 9.3.2 Estimating Total Roughness

A tabulation of representative roughness values for common engineering materials and natural channels are summarized in Table 9.1.

**TABLE 9.1** Representative Values of Manning's  $n$  Value for Open Channels

Type of channel	Minimum	Normal	Maximum
Lined channels			
Concrete channels			
Trowel finish	0.011	0.013	0.015
Float finish	0.013	0.015	0.016
Finished, gravel on bottom	0.015	0.017	0.020
Unfinished	0.014	0.017	0.020
Gunite, good section	0.016	0.019	0.023
Gunite, wavy section	0.018	0.022	0.024
On good excavated rock	0.017	0.020	
On irregular excavated rock	0.022	0.027	
Gravel bottom with sides of			
Formed concrete	0.017	0.020	0.025
Random stone in mortar	0.020	0.023	0.026
Dry rubble or riprap	0.023	0.033	0.036
Gabion-lined channels			
Unvegetated	0.025	0.028	0.030
Vegetated channels			
Vegetation erect	0.030		0.500
Vegetation flattened	0.030		0.070
Excavated or dredged channels			
Earth, straight and uniform			
Clean, recently completed	0.016	0.018	0.020
Clean, after weathering	0.018	0.022	0.025
Gravel, uniform section, clean	0.022	0.025	0.030
With short grass, few weeds	0.022	0.027	0.033
Earth, winding and sluggish			
No vegetation	0.023	0.025	0.030
Grass, some weeds	0.025	0.030	0.033
Dense weeds or aquatic plants in deep channels	0.030	0.035	0.040
Earth bottom and rubble sides	0.028	0.030	0.035
Stony bottom and weedy banks	0.025	0.035	0.040
Cobble bottom and clean sides	0.030	0.040	0.050
Dragline-excavated or dredged			
No vegetation	0.025	0.028	0.033
Light brush on banks	0.035	0.050	0.060
Rock cuts			
Smooth and uniform	0.025	0.035	0.040
Jagged and irregular	0.035	0.040	0.050

**TABLE 9.1** Representative Values of Manning's  $n$  Value for Open Channels (*Continued*)

Type of channel	Minimum	Normal	Maximum
Excavated or dredged channels			
Channels not maintained, weeds and brush uncut			
Dense weeds, high as flow depth	0.050	0.080	0.120
Clean bottom, brush on sides	0.040	0.050	0.080
Same, highest stage of flow	0.045	0.070	0.110
Dense brush, high stage	0.080	0.100	0.140
Natural Streams			
Minor streams (top width at flood stage <100 ft)			
Streams on plain			
1. Clean, straight, full stage, no rifts or deep pools	0.025	0.030	0.033
2. Same as above, but more stones and weeds	0.030	0.035	0.040
3. Clean, winding, some pools and shoals	0.033	0.040	0.045
4. Same as above, but some weeds and stones	0.035	0.045	0.050
5. Same as above, lower stages, more ineffective slopes and sections	0.040	0.048	0.055
6. Same as 4, but more stones	0.045	0.050	0.060
7. Sluggish reaches, weedy, deep pools	0.050	0.070	0.080
8. Very weedy reaches, deep pools, or floodways with heavy stand of timber and underbrush	0.075	0.100	0.150
Mountain streams, no vegetation in channel, banks usually steep, trees and brush along banks submerged at high stages			
Bottom: gravels, cobbles, and few Boulders	0.030	0.040	0.050
Bottom: cobbles with large Boulders	0.040	0.050	0.070
Flood plains			
Pasture, no brush			
Short grass	0.025	0.030	0.035
High grass	0.030	0.035	0.050
Cultivated areas			
No crop	0.020	0.030	0.040
Mature row crops	0.025	0.035	0.045
Mature field crops	0.030	0.040	0.050

TABLE 9.1 Representative Values of Manning's  $n$  Value for Open Channels (*Continued*)

Type of channel	Minimum	Normal	Maximum
Natural streams			
Brush			
Scattered brush, heavy weeds	0.035	0.050	0.070
Light brush and trees, in winter	0.035	0.050	0.060
Light brush and trees, in summer	0.040	0.060	0.080
Medium to dense brush, in winter	0.045	0.070	0.110
Medium to dense brush, in summer	0.070	0.100	0.160
Trees			
Dense willows, summer, straight	0.110	0.150	0.200
Cleared land with tree stumps, no sprouts	0.030	0.040	0.050
Same as above, but with heavy growth of sprouts	0.050	0.060	0.080
Heavy stand of timber, a few down trees, little undergrowth, flood stage below branches	0.080	0.100	0.120
Same as above, but with flood stage reaching branches	0.100	0.120	0.160
Major streams (top width at flood stage >100 ft). The $n$ value is less than for minor streams of similar description because banks offer proportionally less effective resistance.			
Regular section with no boulders or brush	0.025		0.060
Irregular and rough section	0.035		0.100

*Source:* Chow (1959) and others.

### 9.3.3 Cowan's Method

Specific procedures that can be used to determine Manning's  $n$  values for channels and floodplains, described by Arcement and Schneider (1989), are based on Cowan's (1956) method, work on channel roughness by Aldridge and Garrett (1973), and floodplain studies. Cowan's procedure determines roughness values using a base  $n$  value which is then modified incorporate additional factors which influence flow resistance. The basic form of the relationship is

$$n = (n_b + n_1 + n_2 + n_3 + n_4) m \quad (9.7)$$

where  $n_b$  = base  $n$  value for a straight, uniform, smooth channel in natural materials

$n_1$  = factor for the effect of surface irregularities

$n_2$  = factor for variations in shape and size of the channel cross section

$n_3$  = factor for obstructions

$n_4$  = factor for vegetation and flow conditions

and  $m$  = factor for channel meandering

The base  $n$  value may be selected from Table 9.2, and then modified according to the

parameters given in Table 9.3 for channels or Table 9.4 for floodplains. The adjustment for meanders in Table 9.3 refers only to the case when flow is contained within the channel; it does not apply to downvalley overbank flow which crosses meanders. For floodplains the base  $n$  value is selected for the natural bare soil surface without considering the vegetative cover. Arcement and Schneider noted that the  $n$  values given in Table 9.2 cover a wide range because the effects of bed roughness are difficult to separate from the effects of other roughness factors. The selection of the base  $n$  value from within the ranges given in the table will be influenced by personal judgment and experience.

For channels, the selection of the base  $n$  value depends on whether the channel bed is unstable or stable. Sand-bed rivers with an unlimited supply of sediment are classified as unstable because bed geometry is affected by bed forms; this classification does not include channels in rock or clay transporting only a thin layer of sand which may be entirely mobilized during large events. Channels which do not develop bed forms are classified as stable and include streams with beds consisting of rock, cohesive alluvial materials, and gravel or larger material. In sand-bed channels the flow regime should be determined by the method in Sec. 9.4. The base roughness values for sand-bed channels in Table 9.2 are given for upper regime. The  $n$  values for transitional- and lower-regime conditions are primarily determined by bed form, are generally much larger than the values shown in Table 9.2, and cannot be assigned reliably using this method. Characteristic

**TABLE 9.2** Guidelines for Selecting Base  $n$  Value in Channels and Floodplain

Bed material	Median size of bed material, mm	Base $n$ value	
		Straight uniform channel	Smoothest possible channel
Unstable channels (sand bed, upper regime):			
	0.2	0.012	—
	0.3	0.017	—
	0.4	0.020	—
	0.5	0.022	—
	0.6	0.023	—
	0.8	0.025	—
	1.0	0.026	—
Stable channels and floodplains:			
Concrete	—	0.012-0.018	0.011
Rock cut	—	—	0.025
Firm soil	—	0.025-0.032	0.020
Coarse sand	1-2	0.026-0.035	0.020
Fine gravel	—	—	0.024
Gravel	2-64	0.028-0.035	—
Coarse gravel	—	—	0.026
Cobble	64-256	0.030-0.050	—
Boulder	>256	0.040-0.070	—

**Notes:** Values for straight uniform channel are from Benson and Dalrymple (1967) and represent conditions close to average. Values for smoothest possible channel are from Chow (1959).

**Source:** Arcement and Schneider (1989).

**TABLE 9.3** Adjustment Values for Factors Affecting Channel Roughness

Channel conditions		<i>n</i> value adjustment	Example
Degree of irregularity ( $n_1$ )	Smooth	0.000	Compares to the smoothest channel attainable in a given bed material.
	Minor	0.001-0.005	Compares to carefully dredged channels in good condition but having slightly eroded or scoured side slopes.
	Moderate	0.006-0.010	Compares to dredged channels having moderate to considerable bed roughness and moderately sloughed or eroded side slopes.
	Severe	0.011-0.020	Badly sloughed or scalloped banks of natural streams; badly eroded on sloughed sides of canals or drainage channels; unshaped, jagged and irregular surfaces of channels in rock.
Variation in channel cross section ( $n_2$ )	Gradual	0.000	Size and shape of channel cross sections change gradually.
	Alternating occasionally	0.001-0.005	Large and small cross sections alternate occasionally, or the main flow occasionally shifts from side to side owing to changes in cross-sectional shape.
	Alternating frequently	0.010-0.015	Large and small cross sections alternate frequently, or the main flow frequently shifts from side to side owing to changes in cross-sectional shape.
Effect of obstruction ( $n_3$ )	Negligible	0.000-0.004	A few scattered obstructions, which include debris deposits, stumps, exposed roots, logs, piers, or isolated boulders, that occupy less than 5% of the cross sectional area.
	Minor	0.005-0.015	Obstructions occupy less than 15% of the cross sectional area, and the spacing between obstructions is such that the sphere of influence around one obstruction does not extend to the sphere of influence around another obstruction. Smaller adjustments are used for curved smooth-surfaced objects than are used for sharp-edged angular objects.
	Appreciable	0.020-0.030	Obstructions occupy from 15 to 50% of the cross sectional area, or the space between obstructions is small enough to cause the effects of several obstructions to be additive, thereby blocking an equivalent part of a cross section.
	Severe	0.040-0.050	Obstructions occupy more than 50% of the cross sectional area, or the space between obstructions is small enough to cause turbulence across most of the cross section.

**TABLE 9.3** Adjustment Values for Factors Affecting Channel Roughness (*Continued*)

Channel conditions		<i>n</i> value adjustment	Example
Amount of vegetation ( <i>n<sub>4</sub></i> )	Small	0.002-0.010	Dense growths of flexible turf grass, such as Bermuda, or weeds growing where the average depth of flow is at least two times the height of the vegetation; supple tree seedlings such as willow, cottonwood, arrowweed, or saltcedar growing where the average depth of flow is at least 3 times the height of the vegetation.
	Medium	0.010-0.025	Turf grass growing where the average depth of flow is from 1 to 2 times the height of the vegetation; moderately dense stemmy grass, weeds, or tree seedlings growing where the average depth of flow is from two to three times the height of the vegetation; brushy, moderately dense vegetation, similar to 1- to 2-year-old willow trees in the dormant season, growing along the banks, and no significant vegetation is evident along the channel bottoms where the hydraulic radius exceeds 2 ft.
	Large	0.025-0.050	Turf grass growing where the average depth of flow is about equal to the height of the vegetation: 8- to 10-year-old willow or cottonwood trees intergrown with some weeds and brush (none of the vegetation in foliage) where the hydraulic radius exceeds 2 ft; bushy willows about 1 year old intergrown with some weeds along side slopes (all vegetation in full foliage), and no significant vegetation exists along channel bottoms where the hydraulic radius is greater than 2 ft.
	Very large	0.050-0.100	Turf grass growing where the average depth of flow is less than half the height of the vegetation; bushy willow trees about 1 year old inter-grown with weeds along side slopes (all vegetation in full foliage), or dense cattails growing along channel bottom; trees inter-grown with weeds and brush (all vegetation in full foliage).
Degree of meandering ( <i>m</i> )	Minor	1.00	Ratio of the channel length to valley length is 1.0 to 1.2.
	Appreciable	1.15	Ratio of the channel length to valley length is 1.2 to 1.5.
	Severe	1.30	Ratio of the channel length to valley length is greater than 1.5.

*Source:* Arcement and Schneider (1989)

**TABLE 9.4** Adjustment Values for Factors Affecting Floodplain Roughness

Floodplain conditions		<i>n</i> value adjustment	Example
Degree of irregularity ( <i>n</i> <sub>1</sub> )	Smooth	0.000	Compares to the smoothest, flattest flood plain attainable in a given bed material.
	Minor	0.001-0.005	Is a flood plain slightly irregular in shape. A few rises and dips or sloughs may be visible on the flood plain.
	Moderate	0.006-0.010	Has more rises and dips. Sloughs and hummocks may occur.
	Severe	0.011-0.020	Flood plain very irregular in shape. Many rises and dips or sloughs are visible. Irregular ground surfaces in pastureland and furrows perpendicular to the flow are also included.
Variation of floodplain cross section ( <i>n</i> <sub>2</sub> )		0.0	Not applicable.
Effect of obstructions ( <i>n</i> <sub>3</sub> )	Negligible	0.000-0.004	Few scattered obstructions, which include debris deposits, stumps, exposed roots, logs, or isolated boulders, occupy less than 5% of the cross-sectional area.
	Minor	0.005-0.019	Obstructions occupy less than 15% of the cross sectional area.
	Appreciable	0.020-0.030	Obstructions occupy from 15 to 50% of the cross sectional area.
Amount of vegetation ( <i>n</i> <sub>4</sub> )	Small	0.001-0.010	Dense growth of flexible turf grass, such as Bermuda, or weeds growing where the average depth of flow is at least two times the height of the vegetation, or supple tree seedlings such as willow, cottonwood, arrowweed, or saltcedar growing where the average depth of flow is at least three times the height of the vegetation.
	Medium	0.011-0.025	Turf grass growing where the average depth of flow is from 1 to 2 times the height of the vegetation, or moderately dense stemmy grass, weeds, or tree seedlings growing where the average depth of flow is from 2 to 3 times the height of the vegetation; brushy, moderately dense vegetation, similar to 1- to 2-year-old willow trees in the dormant season.
	Large	0.026-0.050	Turf grass growing where the average depth of flow is about equal to the height of the vegetation, or 8- to 10-year-old willow or cotton wood trees intergrown with some weeds and brush (none of the vegetation in foliage) where the hydraulic radius exceeds 2 ft, or mature row crops such as small vegetables, or mature field crops where depth of flow is at least twice the height of the vegetation.

**TABLE 9.4** Adjustment Values for Factors Affecting Floodplain Roughness

Floodplain conditions		<i>n</i> value adjustment	Example
Amount of vegetation (n4)	Very large	0.051-0.100	Turf grass growing where the average depth of flow is less than half the height of the vegetation, or moderate to dense brush, or heavy stand of timber with few down trees and little undergrowth where depth of flow is below branches, or mature field crops where depth of flow is less than the height of the vegetation.
	Extreme	0.101-0.200	Dense bushy willow, mesquite and saltcedar (all vegetation in full foliage), or heavy stand of timber, few down trees, depth of flow reaching branches.
Degree of meander (m)		1.0	Not applicable.

**Source:** Arcement and Schneider (1989)

*n* value ranges as a function of bed form given by Simons, Li & Associates (1982) are presented in Table 9.5. They suggest that values in the higher portion of the range be used in applications such as flood control where maximum water depth is the critical parameter of concern, and values near the lower limit of the range be used for velocity-critical applications such as sediment transport, scour, bank erosion, and riprap design. Brownlie (1983) described a method for determining the roughness in sand beds attributable to both grain size and bed forms. His procedure is also explained in Chang (1988).

### 9.3.4 Effect of Vegetation on Flow Resistance

Vegetation presents a special problem in hydraulic computations because the boundary roughness changes greatly as a function of factors such as flow depth, velocity, and the

**TABLE 9.5** Manning's *n* Values for Channels with Beds of Fine to Medium Sand

Bed form	Range	Suggested values	
		Max. depth	Max. velocity
Ripples	0.018-0.030	0.030	0.022
Dunes	0.020-0.035	0.035	0.030
Transition	0.014-0.025	0.030	0.025
Plane bed	0.012-0.022	0.022	0.020
Standing waves	0.014-0.025	0.025	0.020
Antidunes	0.015-0.031	0.030	0.025

**Source:** Simons, Li & Associates (1982)

biomechanical characteristics of the vegetation. Vegetation is also of special interest in problems involving reservoir sedimentation. Delta deposits in reservoirs will raise the backwater profile upstream of the normal pool by changing both the cross-section geometry and hydraulic roughness. Hydraulic roughness effects can be particularly important if the delta becomes vegetated with brush or trees. Vegetation can also enhance sediment trapping on deltas by creating lower flow velocities, plus the physical trapping

action of the vegetation itself. Vegetative roughness can change both seasonally and over the long term as vegetation grows.

The roughness value can change dramatically during flow events as vegetation is inclined or flattened by the flow. Tones (1997) compiled data from 452 experiments in grassed channels with flow depths from 0.018 to 0.81 m, and vegetation height ranging from 0.05 to 0.9 m. As shown in Fig. 9.2, Manning's  $n$  value in vegetated channels is initially high but subsequently drops to a range of about 0.03 to 0.07 for all types of grasses analyzed when flow velocity exceeds about 1 m/s or the water depth  $D$  attains about 3 times the vegetation height 1-4. The  $n$  value for areas with trees and shrubs which are not flattened by flowing water can be affected seasonally by the presence or absence

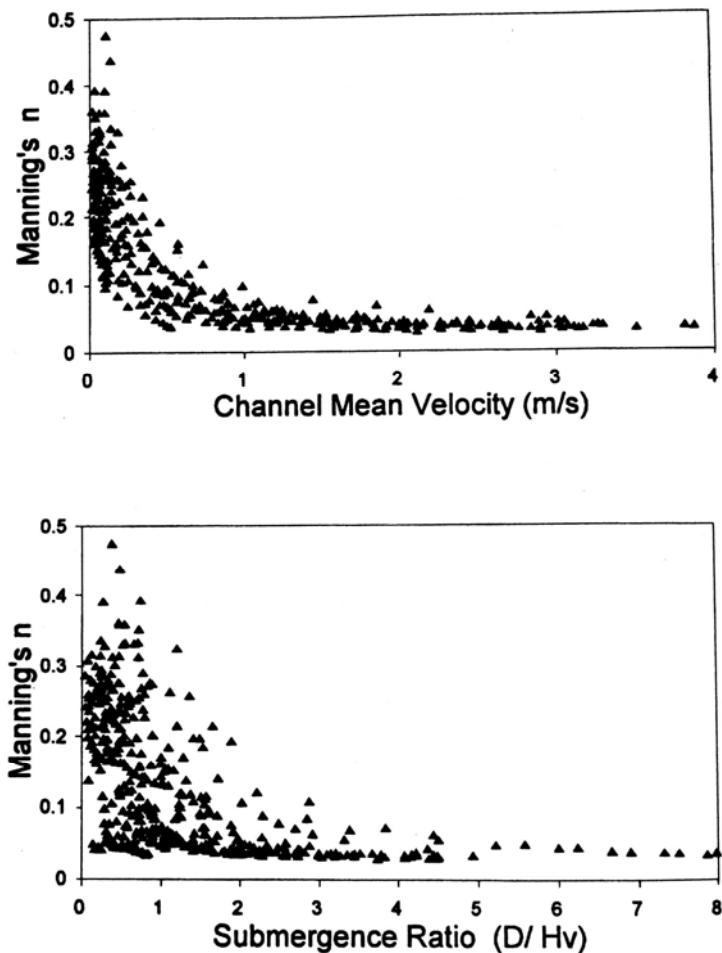


FIGURE 9.2 Variation in Manning's  $n$  value for grass channels (Torres, 1997).

of leaves, which create more drag than bare branches. In problems involving vegetation,

the  $n$  value should be determined for the flow conditions and seasons of the year being analyzed.

### 9.4 BED FORMS IN SAND-BED CHANNELS

Sand-bed channels are deformed by flow and the hydraulic roughness will vary greatly depending on the bed configuration, as illustrated in Fig. 9.3. As flow velocity increases, an initially flat sand bed develops first ripples and then dunes. With additional velocity, the stream subsequently transitions into a plain bed form, and finally forms antidunes with standing (stationary) waves which may or may not crest and break. Transition from the lower flow regime, where bed forms dominate roughness, to the upper regime produces a dramatic drop in roughness and will produce a discontinuous discharge rating curve. For example, Nordin (1964) documented a threefold increase in flow velocity in the Rio Grande near Bemalillo, New Mexico, with no increase in water level, because of changing bed forms (Fig. 9.4). In gravel-bed rivers, bed forms tend to be poorly developed and do not contribute significantly to flow resistance (Chang, 1988).

The relationship between bed form and stream power developed by Simons and Richardson (1966) shown in Fig. 9.5 can be used to determine the flow regime. Because of the nonuniform conditions in natural channels, different flow regimes and bed forms can coexist in different areas of the same channel.

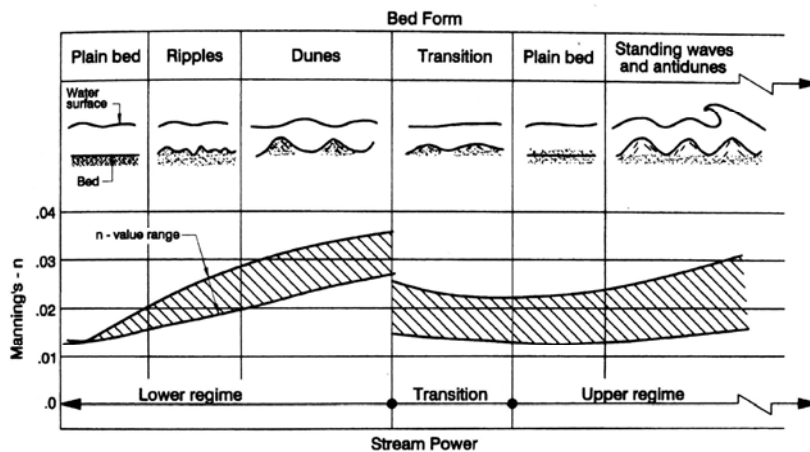


FIGURE 9.3 Bed forms encountered in movable bed streams.

### 9.5 VELOCITY DISTRIBUTION

#### 9.5.1 Reynolds Number

The relation of viscous to inertial forces is expressed by the Reynolds number:

$$Re = \frac{VL}{\nu} \tag{9.8}$$

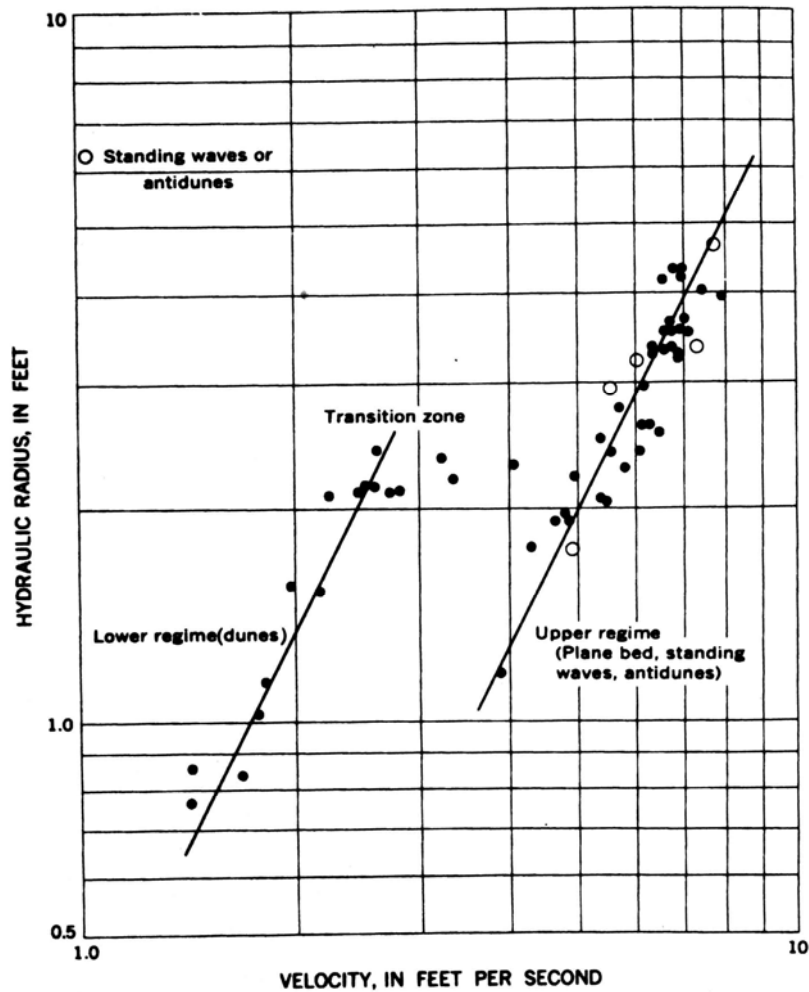


FIGURE 9.4 Discontinuous rating curve on a sand-bed river (Nordin, 1964).

where  $V$  = mean velocity,  $\nu$  = kinematic viscosity, and  $L$  = a characteristic length which depends on the geometric properties of the cross section. Transmission of shear forces at the boundary into the fluid creates a velocity profile in the fluid. When viscous forces predominate, flow is said to be *laminar* and the fluid velocity varies linearly as the function of distance from the boundary. When inertial forces predominate, the flow regime is said to be *turbulent* and velocity varies logarithmically as a function of distance from the boundary. Most civil engineering problems deal with turbulent flow.

The characteristic length is defined as a function of the cross-section geometry. The characteristic lengths are  $L$  = flow depth for an open channel and  $L$  = roughness height or grain diameter for the boundary Reynolds number. Therefore, the absolute values of the Reynolds number which denote the transition from laminar to turbulent flow will depend on the cross-section shape. A transition zone separates the laminar and fully developed turbulent flow regimes. Reynolds number values relevant to open-channel and boundary layer hydraulics are given in Table 9.6.

TABLE 9.6 Reynolds Number

Flow regime	Open channel	Boundary
Laminar	<500	<4
Turbulent	>2000	>70

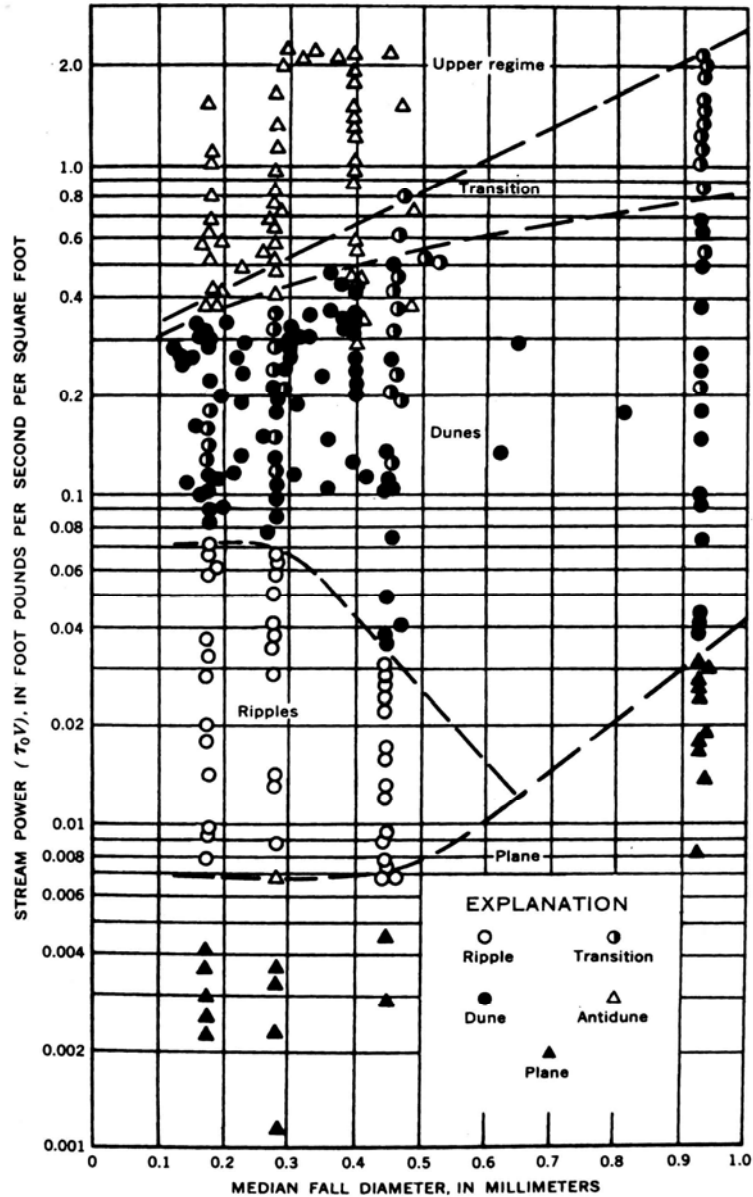


FIGURE 9.5 Prediction of bed form type based on stream power (Simons and Richardson, 1966).

### 9.5.2 Boundary Conditions

Fluid particles in immediate contact with a solid boundary have zero velocity. Even in turbulent channels, a thin layer of laminar flow, termed the *laminar sublayer*, occurs next to the solid boundary, where velocity is low and viscous forces predominate. When the thickness of the laminar sublayer is greater than the height of the surface roughness elements, the boundary is said to be *hydraulically smooth*. However, if the laminar sublayer is thin and surface roughness elements protrude into the zone of turbulent flow, thereby contributing to form drag, the boundary is said to be *hydraulically rough*. These concepts are contrasted in Fig. 9.6. Most civil engineering problems deal with flows in the fully turbulent range, where the laminar sublayer is very thin compared to the size of the roughness elements. In this regime, the frictional resistance is independent of the Reynolds number, but is a function of the roughness element size.

### 9.5.3 Boundary Reynolds Number

The shear velocity Reynolds number or boundary Reynolds number is defined as

$$\text{Re}_* = \frac{U_* k}{\nu} = \frac{(gRS)^{1/2} k}{\nu} \quad (9.9)$$

where  $U_*$  = shear velocity,  $R$  = hydraulic radius,  $\nu$  = kinematic viscosity,  $S$  = slope, and  $k$  = absolute roughness size. The  $k$  value is measured as the distance from the lowest to the highest part of the protuberance into the fluid, but is also affected by the shape and geometric configuration of roughness elements. The particle diameter  $d$  is commonly substituted for  $k$  to compute  $\text{Re}_*$ .

### 9.5.4 Vertical Velocity Distribution

For turbulent, nonstratified flow, the Prandtl-von Kármán universal velocity distribution law expresses the local fluid velocity  $v_y$  at a distance  $y$  from a boundary in the following form:

$$v_y = \frac{1}{\kappa} U_* \ln \frac{y}{y_0} \quad (9.10)$$

where the von Kármán constant  $\kappa = 0.4$  and  $y_0$  is a constant of integration. This relationship may be used to determine the vertical distribution of flow velocity above the bed of a wide prismatic channel.

When the boundary is hydraulically smooth,  $y_0 = m v_y / U_*$ , where  $m$  is a constant having an experimentally determined value of about  $1/9$ . In this regime the roughness

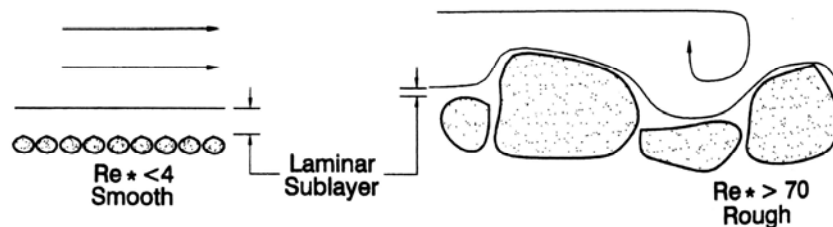


**FIGURE 9.6** At hydraulically smooth boundaries, the roughness elements remain within the laminar sublayer. At a hydraulically rough boundary, the roughness elements protrude through the laminar sub-layer.

elements lie within the laminar sublayer, and therefore the velocity profile is influenced by viscosity but is unaffected by the roughness characteristics. By substitution into Eq. (9.10), the smooth-boundary velocity distribution for the hydraulically smooth regime is

$$\frac{v_y}{U_*} = 2.5 \ln\left(\frac{9yU_*}{\nu}\right) = 5.5 + 2.5 \ln\left(\frac{yU_*}{\nu}\right) \tag{9.11}$$

For flow over a hydraulically rough boundary,  $y_0 = mk$  and the velocity distribution is influenced by the absolute height of the roughness elements  $k$ , but is not influenced by viscosity. In this case the constant  $m$  has a value of about  $1/30$ . By substitution into Eq. (9.10), the rough-boundary velocity distribution can be given by

$$\frac{v_y}{U_*} = 2.5 \ln\left(\frac{30y}{k}\right) = 8.5 + 2.5 \ln\left(\frac{y}{k}\right) \tag{9.12}$$

To use Eqs. (9.11) and (9.12), compute shear velocity  $U_* = (gRS)^{1/2}$ , substituting  $R = D$  as appropriate. In these equations  $y =$  height (m) above the bottom. In rivers and canals the size of roughness elements can be estimated as  $k = 3d_{90}$ , or  $k = 6d_{50}$  if the  $d_{90}$  value is not known (Julien, 1995). When the velocity distribution is known from a minimum of two points in a vertical, the  $k$  value may be computed. The effect of relative roughness height relative to flow depth ( $k/D$ ) on the shape of the velocity distribution for turbulent conditions is illustrated by the vertical velocity profiles in Fig. 9.7.

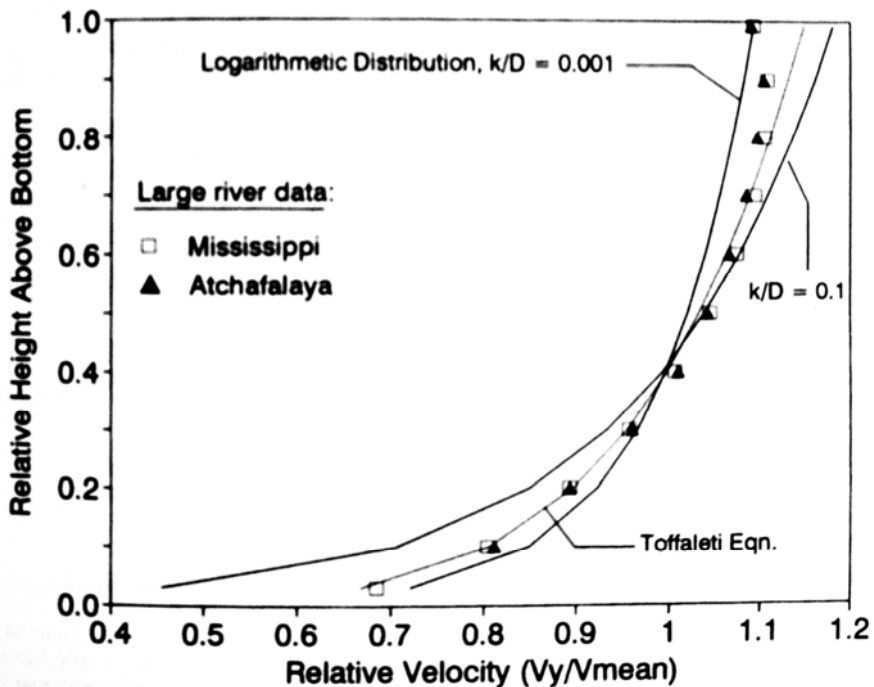


**FIGURE 9.7** Vertical variation in velocity showing the logarithmic variation as a function of relative roughness. The graph also presents data from the Mississippi and Atchafalaya Rivers and the corresponding velocity distribution suggested by Toffaleti (1963).

By studying 973 measured vertical velocity profiles at two stations on the sand-bed Mississippi and Atchafalaya Rivers, Toffaleti (1963) found that the vertical velocity profiles in these two large rivers were essentially identical, but were somewhat different from the profile derived from Eq. (9.12) (see Fig. 9.7). He fit the following velocity profile equation to the data from these two large sand-bed rivers:

$$v_y = 1.15V \left( \frac{y}{D} \right)^{0.155} \quad (9.13)$$

where  $V$  = mean velocity at the cross section,  $y$  = height above the bottom, and  $D$  = total depth. Flow curvature, channel irregularities, tributary inflows, and stratification will all significantly influence the vertical velocity profile. The tangential component of flow can be particularly important at curves and is discussed in more detail by Chang (1988).

### 9.5.5 Velocity Profile Measurement

According to the velocity relation produced by the logarithmic velocity distribution, the mean velocity at a vertical can be estimated by point measurements at specific depths below the water surface. Velocity measurements at the following points can be used to estimate mean flow velocity at a vertical.

1. When one point is used, velocity at 60 percent of total depth will approximate mean velocity.
2. If two points are used, measure at 20 and 80 percent of total depth and average the two velocities.
3. If three points are used, measure at 20, 60, and 80 percent of total depth. First average the 20 and 80 percent velocities, and then average the resultant velocity with the velocity at 60 percent depth:

$$V_{mean} = \frac{V_{20} + V_{80}}{4} + \frac{V_{60}}{2} \quad (9.14)$$

The measurement procedure is repeated at multiple verticals across the cross section to obtain the mean velocity. Single-point measurements may be used in shallow water and multiple points at deeper verticals.

### 9.5.6 Horizontal Velocity Distribution

The horizontal variation in both flow velocity and discharge across a stream will depend on changes in the stream cross section and curvature. There is no general solution for the horizontal variation in flow velocity in irregular natural channels.

## 9.6 VERTICAL DISTRIBUTION OF SEDIMENT CONCENTRATION

Under conditions of steady uniform flow, the tendency for sediment to settle under the influence of gravity is offset by the vertical component of turbulence in the water column, a process known as *turbulent diffusion*. The upward-moving water comes from the deeper zone with higher concentration, partially offsetting the settling of the sediment and creating a vertical concentration gradient which can be described using the Rouse equation:

$$\frac{C_y}{C_a} = \left( \frac{D-y}{y} \cdot \frac{a}{D-a} \right)^z \quad (9.15)$$

where  $C_y$  and  $C_a$  = concentrations of sediment having fall velocity  $\omega$  at vertical distances  $y$  and  $a$  above the bed and  $D$  = total depth. In this equation  $z = (\omega / \kappa U_*')$  where  $\kappa = 0.4$  is von Kármán's constant. This equation can be used to determine the concentration  $C_y$ , at any height  $y$  above the bottom relative to the known concentration  $C_a$  at height  $a$  above the bed. The value of  $z$  will decrease as fall velocity to decreases, producing a more uniform vertical concentration distribution for finer sediment. Thus, a different vertical distribution will exist for each size class. Concentration distributions for several values of  $z$  are illustrated in Fig. 9.8, assigning a concentration  $C_a = 1.0$  at height  $a = 0.05D$ . The equation should not be used at its extreme limits, since concentration calculates as zero at the exact water surface and infinite at the bottom. The Rouse equation applies to equilibrium conditions and may not be applicable to many situations in reservoirs where rivers are depositing their sediment load and are thus not at equilibrium. The vertical distribution of suspended sediment in reservoirs can also be influenced by stratification.

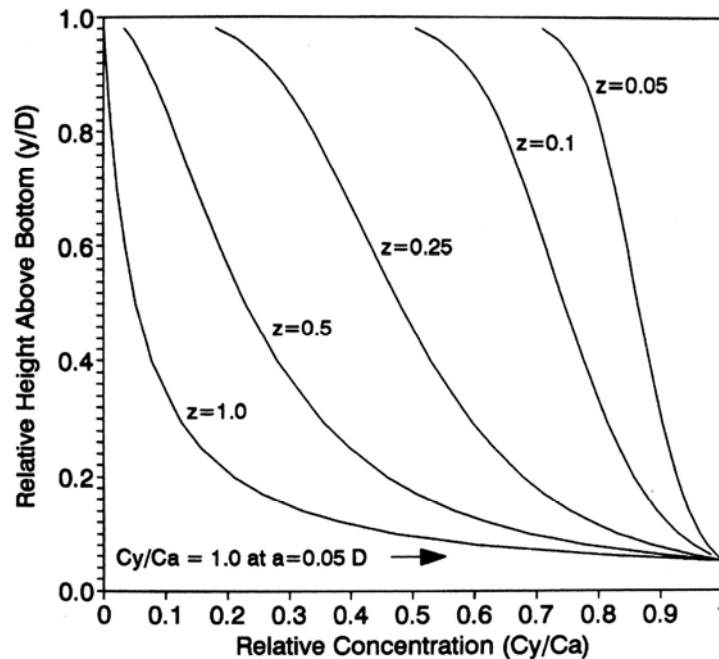


**FIGURE 9.8** Vertical variation in suspended sediment concentration relative to the concentration,  $C_a = 1.0$  at  $a/D = 0.05$ , for different fall velocities. Concentrations are plotted over the range of relative depths  $0.98 > y/D > 0.05$ , and the variation in fall velocity is expressed by the parameter  $z$ .

## 9.7 INITIATION OF MOTION

The motion of a fluid flowing across its bed tends to move the bed material downstream. Below some critical condition, the hydraulic forces will be so small that particles will be

moved very rarely or not at all. However, a slight increase in velocity above this critical condition will initiate appreciable motion by some of the particles on the bed. This critical condition is termed the *condition of initiation of motion*, and is commonly computed in terms of either the critical mean flow velocity in the vertical or the critical bed shear stress (also known as *tractive force*). As pointed out by Lavelle and Mofjeld (1987), there is not truly a precise threshold value for the onset of sediment motion. Rather, sediment transport rate declines continuously as flow velocity declines. The so-called "critical value" actually refers to a very small rate of transport, and has been defined differently by various researchers.

In a cohesionless bed, sediment movement is first initiated by an individual particle which rolls or jumps a short distance before coming to rest. This movement is followed by similar movement of a different particle. As the flow velocity increases, the number of particles in motion and the distance traveled before coming to rest increases, until at some higher velocity the entire bed is completely mobilized. In 1936 Shields defined the critical condition of incipient motion as the point of *zero transport*, as extrapolated from conditions under which measurable transport occurred. Others have defined this point using terms such as *weak movement*, and the condition of incipient motion is somewhat subjective. In a bed containing a range of sediment sizes, at intermediate flow velocities only the smaller particles in the bed will be transported while the larger particles remain stable.

Engineering interest in determining the critical flow velocity which initiates the scour of sediment particles originated in the design of stable (nonscouring and nonsedimenting) earthen canals. Much of the early work in this field was derived from experience gained in the construction of irrigation canals in colonial India and Pakistan. There are two basic approaches to the determination of the critical condition in open channels: the bed shear (tractive force) approach, and the velocity approach. Both approaches have a long history of use and an extensive literature. Although the initiation of motion of bed material is determined by the flow velocity at the water-sediment boundary, velocity at the bed is rarely measured and there is no agreement as to the distance above the bed that should be considered as "bottom velocity." Therefore, as a practical matter, the critical velocity is normally computed from the mean velocity across a vertical or the cross-sectional area.

### 9.7.1 Bed Shear or Tractive Force

For steady uniform flow, the specific weight of a column of water can be divided into two vectors, one oriented perpendicular to the bed and one oriented along the bed in the direction of flow. Under conditions of steady uniform flow, the component of the gravitational force exerted along the slope direction which causes downstream motion is balanced by the bed shear stress or tractive force  $\tau_0$ , which is the frictional force exerted on the moving fluid at its boundary. Bed shear stress is not the force on individual particles, but the force exerted over an area of the channel bed or banks. For the small slopes normally encountered in hydraulic problems, the bed shear stress in a wide channel can be computed as:

$$\tau_0 = \gamma DS \quad (9.16)$$

For the more general case, the depth term is replaced with the hydraulic radius to give:

$$\tau_0 = \gamma RS \quad (9.17)$$

This concept of tractive force was first introduced by duBoys in 1879 in studies of the movable bed of the Rhone River.

### 9.7.2 Approximate Methods

The simplest method for estimating the threshold or critical condition for the movement of cohesionless sediment is using the linear relationship between critical bed shear stress ( $\tau_{cr}$ ) and grain size given by Julien (1995), reproduced below in several different systems of units:

$$\tau_{cr}(\text{N/m}^2) = 0.785d_{50}(\text{mm}) \quad (9.18)$$

$$\tau_{cr}(\text{g/m}^2) = 80d_{50}(\text{mm}) \quad (9.19)$$

$$\tau_{cr}(\text{lb/ft}^2) = 0.0164d_{50}(\text{mm}) \quad (9.20)$$

$$\tau_{cr}(\text{lb/ft}^2) = 5d_{50}(\text{ft}) \quad (9.21)$$

These equations are approximately valid for  $d_{50} > 0.3$  mm ( $d_{50} > 0.001$  ft) and can be used as a quick check against other methods and to help determine the hydraulic roughness regime. A similar linear relationship was suggested in 1955 by Leliavsky (cited by Graf, 1971). Figure 9.11 may also be consulted.

### 9.7.3 Empirical Criteria

The "permissible" velocities in canals do not necessarily correspond to a condition of zero sediment transport, but rather to an equilibrium condition which does not produce objectionable rates of either scour or deposition, even though the canal may be transporting sediment along its bed. A well-known compilation of empirical data based on experience with stable canals was prepared by Lane (1955) for the U.S. Bureau of Reclamation and is a useful practical guide (Fig. 9.9). In using this figure recall the bed shear conversion,  $1 \text{ N/m}^2 = 0.00981 \text{ g/m}^2$ . Curved canal sections tolerate lower velocity and tractive force than straight canal sections.

Lane noted that canal engineers had long observed that nonscouring velocities are higher in large canals than in small ones. Small shallow canals erode at a lower mean velocity than large ones. He argued in favor of the tractive force approach rather than the limiting velocity approach as the basis for canal design because it produced predictions more consistent with these field observations. This effect is demonstrated in the example computations in Secs. 9.7.7 and 9.7.8.

### 9.7.4 Shields Diagram

The Shields diagram (Fig. 9.10) is a widely used method to determine the condition of incipient motion based on bed shear stress. Points lying above the curve representing the critical condition correspond to sediment motion, and points below the curve correspond to no motion. Shields determined that the critical condition could be related to two dimensionless parameters: the *dimensionless shear stress*  $F$ , (also known as the *Shields parameter*), which does not represent the actual shear stress, and the boundary Reynolds number  $\text{Re}_* = U_*d/\nu$ .

The Shields parameter reflects the ratio of the force producing sediment motion to the force resisting motion. The force producing motion is expressed by the product of the bed shear stress  $\tau_0$  and the cross-sectional area of the particle exposed to the flow, represented by the square of the particle diameter  $d^2$ . The force resisting motion is the product of the submerged unit weight of the sediment ( $\gamma_s - \gamma$ ) and particle volume, represented by the

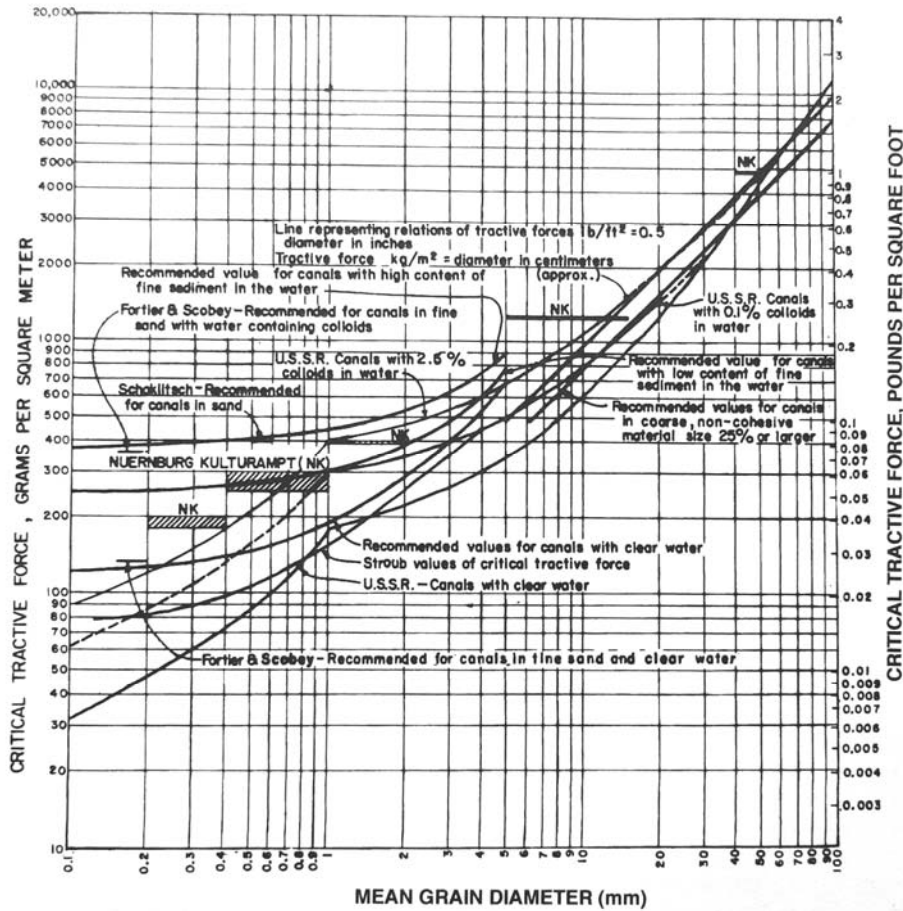
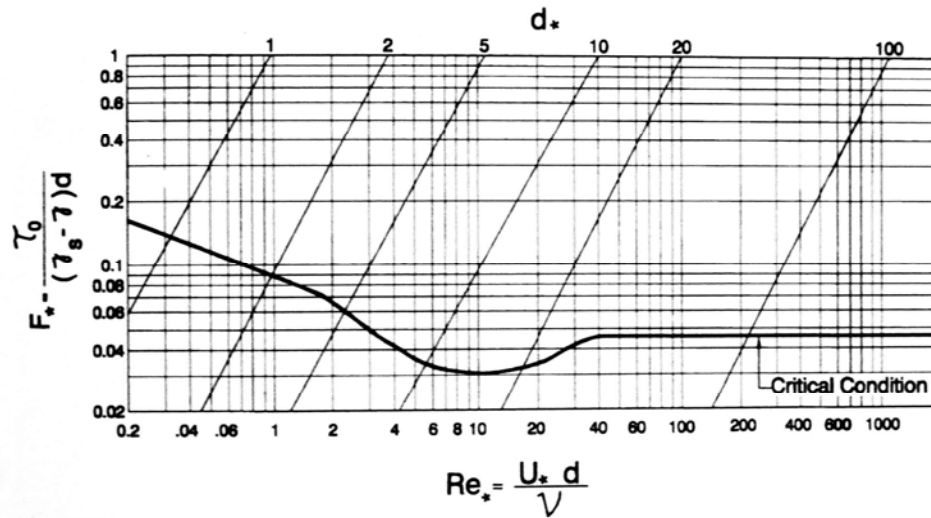


FIGURE 9.9 Allowable tractive force in channels as a function of grain size (Lane, 1955).

particle diameter cubed  $d^3$ . Thus, the Shields parameter  $F^*$  may be computed by:

$$F^* = \frac{\tau_0 d^2}{(\gamma_s - \gamma) d^3} = \frac{\tau_0}{(\gamma_s - \gamma) d} \tag{9.22}$$

The simplified form on the right-hand side is the value of the ordinate axis on the Shields diagram. The relationship between the Shields parameter and the boundary shear Reynolds number for the critical condition has been determined experimentally by testing uniformly graded sediments in hydraulic flumes. In beds of mixed sediment, it has been customary to use the  $d_{50}$  sediment grain size to represent the bed behavior. However, some researchers feel that a diameter larger than  $d_{50}$  is more appropriate for describing the effective initiation of motion in a mixed bed, as discussed in Sec. 9.7.9.



**FIGURE 9.10** Modified Shields diagram for incipient sediment motion showing curves plotted by Yalin and Karahan (1979). An exact value for the Shields parameter cannot be given at any point because there is significant scatter in the experimental data from which the curve is derived, and the exact shape of the resulting curve reflects interpretations by different researchers.

Use of the Shields diagram requires that the critical value of the Shields parameter  $F_{*cr}$  be determined. However, problem-solving with the Shields curve is not straightforward. Since the grain diameter  $d$  appears on both axes, a trial-and-error solution can be required. To facilitate computations when grain size is known, the dimensionless diameter  $d_*$  (top axis in Fig. 9.10) may be computed (Julien, 1995):

$$d_* = d \left[ \frac{(G_s - 1)g}{\nu^2} \right]^{1/3} \quad (9.23)$$

where  $d$  = sediment diameter (m, ft),  $G_s$  = specific gravity of sediment, and  $\nu$  = kinematic viscosity. Because  $d_*$  is dimensionless, Eq. (9.23) may be solved using either SI or fps units. With  $d_*$  determined, the  $F_{*cr}$  value may be read from the Shields diagram, and the critical value for bed shear stress  $\tau_{cr}$  is computed by substituting into Eq. (9.22). Values of critical shear stress as a function of grain diameter, computed using this method, are plotted in Fig. 9.11 and can be used as a guide to estimate the condition of initiation of motion.

When grain diameter is not known, compute the shear stress by Eq. (9.16), estimate the grain diameter [using Eq. (9.18) or Fig. 9.11], and use this to solve for the appropriate  $Re_*$  or  $F_{*cr}$  value, with which  $F_{*cr}$  may be determined from Fig. 9.10. Since many hydraulic engineering problems deal with flow in the turbulent range and sediment having  $d > 1$  mm, computations may often be initiated by assuming that  $F_{*cr} = 0.047$ , the approximate value for the dimensionless shear stress in the range of boundary Reynolds number  $Re_* > 40$  (Yalin and Karahan, 1979). For this condition Eq. (9.22) is rearranged as

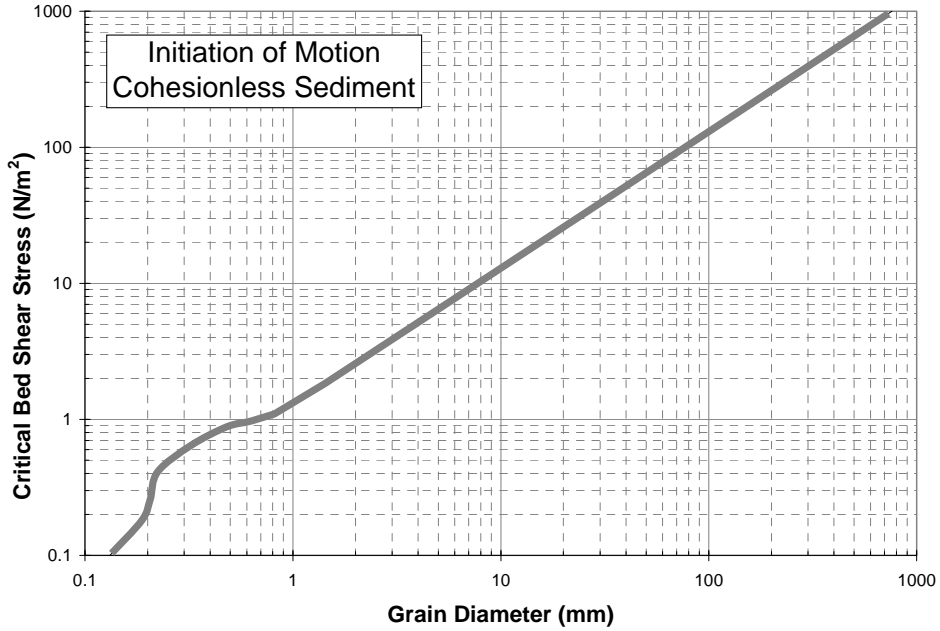


**FIGURE 9.11** Approximate bed shear stress required to initiate particle motion on a uniform bed of cohesionless sediment (based on Julien, 1995) for 20°C, specific gravity of sediment = 2.65.

$$\tau_{cr} = F_*(\gamma_s - \gamma)d = 0.047(\gamma_s - \gamma)d$$

By substitution solve for either  $\tau_0 = \tau_{cr}$  or  $d = d_{cr}$ . Substitute the resulting  $d$  value back into the expression for boundary Reynolds number [Eq. (9.9)] to check the validity of the assumption  $Re_* > 40$ .

### 9.7.5 Velocity Criteria

Yang (1973, 1996) has argued that unit stream power is a better indicator of the condition of incipient motion than the Shields parameter. Yang defined the dimensionless critical velocity  $V_{cr}/\omega$  as the ratio of the average cross-section velocity at the critical condition to the terminal particle fall velocity for the grain size of interest. This ratio was then related to  $Re_*$ , the shear velocity Reynolds number, by experimental data. For the hydraulically smooth and transition zones the incipient motion criteria is given by:

$$\frac{V_{cr}}{\omega} = \frac{2.5}{\log(V_*d/\nu) - 0.06} + 0.66 \quad (9.24)$$

and for the hydraulically rough region the relationship is:

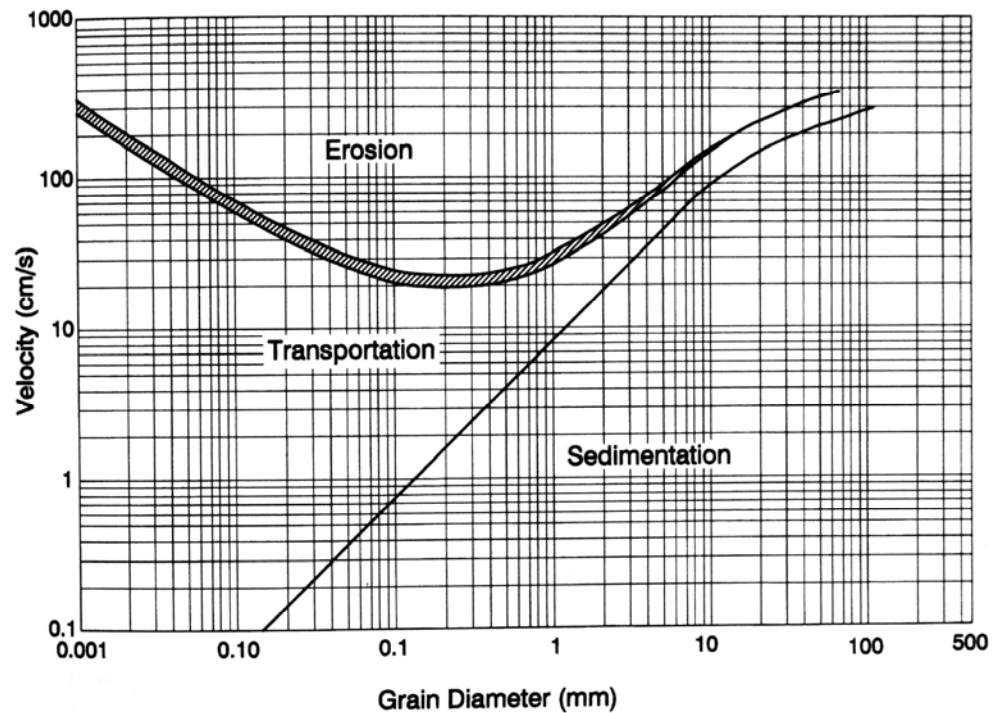


**FIGURE 9.12** Velocity criterion developed by Hjulstrom in 1935 to describe the initiation of erosion and of deposition for uniform particles.

$$\frac{V_{cr}}{\omega} = 2.05 \quad (9.25)$$

In the turbulent range, for  $Re_* > 70$ , Yang's expression [(Eq. 9.25)] states that particles on a bed will begin moving when the average velocity is twice the particle settling velocity. An approximate relationship of this type has long been recognized, and Rubey (1931) cited work by canal engineers extending back to 1857 who observed that the competent (nonscouring) velocities in canals tend to lie between 1 and 2 times the theoretical settling velocity of the bed material. A graphical relationship between critical velocity and grain size (Vanoni, 1975) is presented in Fig. 9.12.

### 9.7.6 Annandale's Erodibility Index Method

The erodibility index method developed by Annandale (1995) may be used to determine the hydraulic conditions under which erosion will be initiated in a wide range of material, including rock, earth with and without vegetation, engineered earth, and granular material. This method has been only recently developed and is not time-tested. However, unlike the other methods presented, it has the interesting potential to analyze the point of initiation of erosion on a wide range of materials, not only loose granular sediments. It has been used to study scour at spillways (Annandale, 1994). Of particular interest to

fluvial applications, the method has been used to analyze the onset of streambank erosion following a flood event at 44 sites along a 27-km stream corridor in Texas, with material including fine silty sand, granular clays, riprap, bagwalls, and vegetated soils. Eroding and noneroding conditions were successfully differentiated by the index method (Fig. 9.13).

The erodibility index method is based on stream power,  $\tau V$  (see Appendix J), the erosive power of water, according to the relationship:

$$\tau V = f(K_h) \quad (9.26)$$

where  $\tau V$  = stream power ( $\text{W}/\text{m}^2$ ), and  $f(K_h)$  is the erodibility index. Erosion will occur when  $\tau V > f(K_h)$ , but not when  $\tau V < f(K_h)$ . The rate of energy dissipation per unit of bed area is computed by:

$$\tau V = \gamma D S V \quad (9.27)$$

where  $\gamma$  = unit weight of water,  $D$  = depth,  $V$  = velocity, and  $S$  = energy slope.

The following equation and parameters are used to determine the erodibility index or the erosion resistance offered by any material:

$$K_h = M_s K_b K_d J_s \quad (9.28)$$

where  $M_s$  = mass strength number, given in Tables 9.7 and 9.8 for granular and cohesive soils, respectively.

$K_b$  = block or particle size number; refers to the mean grain size  $d_{50}$  for granular material and the mean size of blocks. For noncohesive sediment it is computed as  $K_b = 1000d_{50}^3$  for  $d_{50}$  in meters. For vegetated soils it is related to the rooting characteristics.

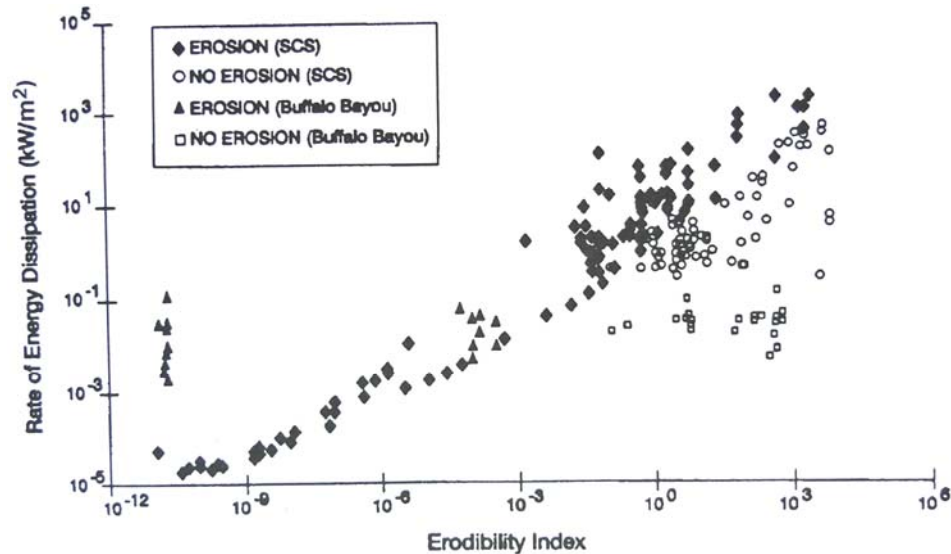


**FIGURE 9.13** Eroding and noneroding conditions based on the erodibility index method (Annandale, 1996).

**TABLE 9.7** Mass Strength Number for Granular Soil ( $M_s$ )

Consistency	Identification in profile	Standard penetration test blow count	Mass strength number $M_s$
Very loose	Crumbles very easily when scraped with geological pick	0-4	0.02
Loose	Small resistance to penetration by sharp end of geological pick	4-10	0.04
Medium dense	Considerable resistance to penetration by sharp end of geological pick	10-30	0.09
Dense	Very high resistance to penetration of sharp end of geological pick; requires many blows of pick for excavation	30-50	0.19
Very dense	High resistance to repeated blows of geological pick; requires power tools for excavation	50-80	0.41

*Source:* Annandale (1995)

**TABLE 9.8** Mass Strength Number for Cohesive Soil ( $M_s$ )

Consistency	Identification	Vane shear strength, kPa	Mass Strength number $M_s$
Very soft	Pick head can easily be pushed in up to the shaft of handle; easily molded by fingers	0-80	0.02
Soft	Easily penetrated by thumb; sharp end of pick can be pushed in 30 to 40 mm; molded by fingers with some pressure	80-140	0.04
Firm	Indented by thumb with effort; sharp end of pick can be pushed in up to 10 mm; very difficult to mold with fingers; can just be penetrated with an ordinary hand spade	140-210	0.09
Stiff	Penetrated by thumbnail; slight indentation produced by pushing pick point into soil; cannot be molded by fingers; requires hand pick for excavation	210-350	0.19
Very stiff	Indented by thumbnail with difficulty; slight indentation produced by blow of pick point; requires power tools for excavation	350-750	0.41

*Source:* Annandale (1995).

$K_d$  = interparticle bond shear strength number, the equivalent residual friction angle from a triaxial or vane shear test. For granular material it may be estimated as  $\tan \phi$  using angle of repose (Fig. 9.1).

$J_s$  = relative ground structure number. It is an expression of rock shape and orientation and has a value of  $J_s = 1$  for granular or soil-type material.

We present here only the technique applicable to cohesionless granular material. For loose granular material (0.1 to 100 mm dia.), the relationship between stream power at the critical erosion condition  $TV$ , and the erodibility index  $K_h$  may be expressed as

$$\tau V_{cr} = 480K_h^{0.44} \quad (9.29)$$

Erosion occurs if stream power exceeds the value of  $\tau V_{cr}$ . For cohesionless granular material, the erodibility index value may be related to grain diameter (in mm) by:

$$K_h = M_s K_b K_d J_s = (0.02)(1000d_{50}^3)(\tan \phi)(1) = 20d_{50}^3 \tan \phi \quad (9.30)$$

where  $\phi$  = angle of repose. A worked example is given in the next section. Refer to Annandale (1995) for guidelines for application to other earth and rock materials.

### 9.7.7 Example 9.1

Determine critical grain size for noncohesive sediment in a wide channel at 20°C ( $\mu = 1 \times 10^{-3}$ ,  $\nu = 1 \times 10^{-6}$ ) with the following characteristics:  $D = 0.6$  m,  $V = 1.2$  m/s,  $n = 0.030$ . Use Manning's equation and assume  $R = D$  since the channel is wide ( $V = n^{-1}D^{2/3}S^{1/2}$ ), and rearrange to compute  $S = 0.0026$ . Solve for bed shear stress:

$$\tau_0 = \gamma DS = 9810(0.6)(0.0026) = 15.3 \text{ N/m}^2$$

**Empirical Relationships.** The simplest relationship is given by Figure 9.11. Use Eq. (9.18) by letting  $\tau_0 = \tau_{cr}$ , compute  $d_{50} = \tau_{cr}/0.785 = 15.3/0.785 = 19$  mm. To use Figure 9.9 it is necessary to perform a unit conversion. Converting into  $\text{g/m}^2$  gives

$$[15.3 \text{ kg} \cdot \text{m}/(\text{s}^2 \cdot \text{m}^2)](\text{s}^2/9.81\text{m})(1000\text{g}/\text{kg}) = 1560 \text{ g/m}^2$$

Or, converting into  $\text{lb}/\text{ft}^2$  gives

$$(15.3 \text{ N/m}^2)(1/47.9) = 0.32 \text{ lb}/\text{ft}^2$$

From Figure 9.9, a diameter of approximately 20 mm is obtained.

Using the diameter, determine the flow regime.

$$\text{Re}_* = \frac{U_* d}{\nu} = \frac{(gRS)^{1/2} d}{\nu} = \frac{0.1237(0.02)}{1 \times 10^{-6}} = 2472$$

It is strongly turbulent; i.e.,  $\text{Re}_* \gg 70$ .

**Yang's Method.** In the turbulent range rearrange Eq. (9.25) to obtain:

$$\omega = \frac{V_{cr}}{2.05}$$

Let  $V = V_{cr}$ ; solve for  $\omega = 1.2/2.05 = 0.585$  m/s. Estimating that the particle diameter is greater than 2 mm, rearrange Eq. (5.24) to solve for the particle diameter:

$$d = \left( \frac{\omega}{3.32} \right)^2 = \left( \frac{0.5852}{3.32} \right)^2 = 0.031m = 31mm$$

A more general case would be to solve for the diameter using the Rubey equation (5.23), which is valid for the full range of particle diameters and includes the temperature-dependent effect of viscosity. However, for particles in this grain size, viscosity effects are negligible.

**Shields Diagram.** Let  $\tau_0 = \tau_{cr}$ . In the turbulent flow range,  $F_{*cr} = 0.047$  (Fig. 9.10). Rearrange Eq. (9.22) to solve for diameter:

$$d = \frac{\tau_{cr}}{F_{*cr}(\gamma_s - \gamma)} = \frac{15.3}{0.047(25,996 - 9810)} = 0.020m = 20mm$$

**Erodibility Index Method.** Compute stream power:

$$\begin{aligned} \tau V &= \gamma D S V \\ &= (9810 \text{ kg/m}^2\text{s}^2)(0.6 \text{ m})(0.0026)(1.2 \text{ m/s}) = 18.4 \text{ W/m}^2 \end{aligned}$$

where  $1 \text{ W} = 1 \text{ N}\cdot\text{m/s}$ . Determine the critical  $K_h$  value from stream power by rearranging Eq. (9.29):

$$K_h = \left( \frac{\tau V}{480} \right)^{2.27} = 6.0 \times 10^{-4}$$

Determine the value of the critical grain diameter by letting  $\tan \phi = 0.8$  and rearranging Eq. (9.30) to solve for diameter:

$$d_{s0} = \left( \frac{K_h}{20 \tan \phi} \right)^{1/3} = \left( \frac{6.0 \times 10^{-4}}{16} \right)^{1/3} = 0.033m = 33mm$$

### 9.7.8 Example 9.2

Conditions in this example are the same as those in Example 9.1, except  $D = 6 \text{ m}$ . The velocity is unchanged at  $V = 1.2 \text{ m/s}$ . Use Manning's equation to solve for  $S = 0.00012$ . Solve for bed shear stress:

$$\tau_0 = \gamma D S = 9810(6.0)(0.00012) = 7.06 \text{ N/m}^2$$

Solve as before using the Shields curve:

$$d = \frac{\tau_{cr}}{F_{*cr}(\gamma_s - \gamma)} = \frac{7.06}{0.047(25,996 - 9810)} = 0.009m = 9mm$$

A similar value is obtained from Fig. 9.9, Fig. 9.11, and using Eq. (9.18).

For the erodibility index method, compute stream power:

$$\begin{aligned} \tau V &= \gamma D S V \\ &= (9810 \text{ kg/m}^2\text{s}^2)(6.0 \text{ m})(0.00012)(1.2 \text{ m/s}) = 8.5 \text{ W/m}^2 \end{aligned}$$

$$K_h = \left( \frac{\tau V}{480} \right)^{2.27} = \left( \frac{8.5}{480} \right)^{2.27} = 1.06 \times 10^{-4}$$

$$d_{50} = \left( \frac{k_h}{20 \tan \phi} \right)^{1/3} = \left( \frac{1.06 \times 10^{-4}}{16} \right)^{1/3} = 0.019 \text{ m} = 19 \text{ mm}$$

The above approaches all predict a reduction in the critical grain size as flow depth increases, with average velocity remaining unchanged. However, mean velocity approaches (as differentiated from the bottom velocity approach) will predict a grain size identical to that in Example 9.1 because the mean velocity remains unchanged between the two examples.

### 9.7.9 Initiation of Motion in Graded Sediments

Stelczer (1981) stated that the critical mean velocity of each size fraction in a mixed bed was virtually identical to that for uniformly graded sediment. This is essentially the assumption incorporated into mathematical sediment transport models which compute transport of material within each size fraction separately. However, the initiation of significant motion within a bed of mixed sediments can be affected by factors such as hiding of smaller grains by the larger ones and armoring. Graf (1971) stated that for sediments which are not uniformly sized or contain cohesive sediment, the critical bed shear stress for incipient motion should be higher than predicted in the Shields diagram. Results from experimental work in glass flumes and in the field led Stelczer (1981) to conclude that: "The movement of bed load comprising several size fractions is controlled overwhelmingly by the particle size around  $d_{80}$ . The smaller fractions and the larger ones are set into motion almost simultaneously (at the same critical velocity) with the  $d_{80}$  fraction. This fraction tends to shield smaller particles, whereas once these are removed, the larger fraction loses support and is scoured by the flow." Additional information on the initiation of motion in mixed beds is given in Sec. 18.6.4.

## 9.8 STABLE CHANNEL DESIGN

The incipient motion criteria discussed above apply to a flat bed. On a sloping surface, such as the side of a channel, sediment will be inherently less stable than on a flat bed. However, the shear stresses on straight channel sides are smaller than on the bed. These factors must be considered to determine the stable material and allowable side slope angle.

### 9.8.1 Shear Stress Distribution

Shear stress is not distributed evenly across a cross section. For a straight prismatic trapezoidal channel, Lane (1953) computed the shear stress distribution shown in Fig. 9.14 and concluded that in trapezoidal channels maximum shear stress for the bottom and sides is approximately equal to  $0.97 \gamma DS$  and  $0.75 \gamma DS$ , respectively.

The boundary shear stress distribution for a curved trapezoidal channel was experimentally measured by Ippen and Drinker (1962), who found that the maximum shear stresses occur at the outer toe of the bank immediately downstream of the curve. Shear stress in the curved reach will be 2 to 3 times greater than the shear in a straight channel. The ratio of maximum shear in a curved reach to the shear stress in a straight channel is given by:

$$\frac{\max \tau_0}{\tau_0} = 2.65 \left( \frac{r_c}{B} \right)^{-0.5} \quad (9.31)$$

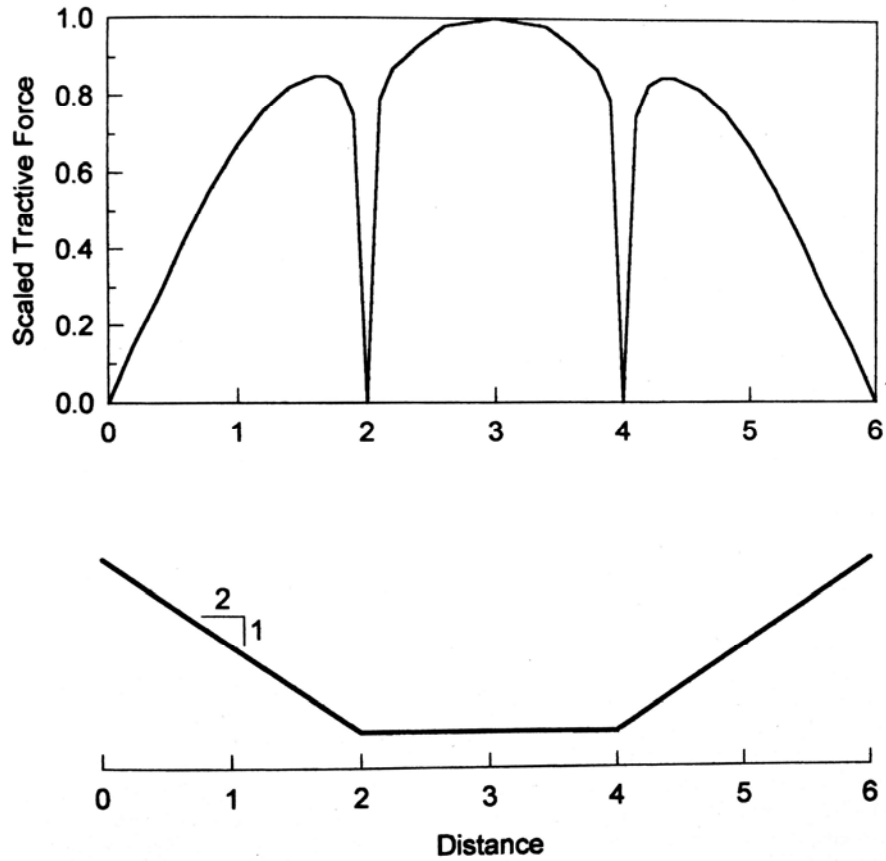


FIGURE 9.14 Variation in shear stress across a trapezoidal channel (Lane, 1955).

where  $\tau_0$  = average boundary shear in the approach channel,  $\max \tau_0$  = maximum local boundary shear in the curved reach,  $r_c$  = centerline radius of the bend, and  $B$  = water surface top width at the upstream end of the curved reach.

**9.8.2 Slope Stability**

A simplified slope stability analysis may be based on the following relationship:

$$\frac{\tau_{\theta cr}}{\tau_{cr}} = \left[ 1 - \frac{\sin^2 \theta}{\sin^2 \phi} \right]^{0.5} \tag{9.32}$$

where  $\tau_{\theta cr}$  = the critical shear stress on the slope consisting of sediment or stone having  $\phi$  = angle of repose and  $\theta$  = channel side slope angle (Fig. 9.1). The side slope is stable when  $\tau_{slope} < \tau_{\theta cr}$ . Although the side slope will tolerate a lower shear stress than the bottom, the sides also receive less shear stress than the bed because of the uneven shear stress distribution. Because the angle of repose increases as a function of stone size, the

angle of the stable slope will also increase. Flow curvature will increase localized forces at channel bends.

## 9.9 BED MATERIAL TRANSPORT

Bed material load consists of coarse material in the streambed which is mobilized by flowing water, and may be transported either in suspension or as bed load. Bed material transport for selected grain sizes may be *supply limited* when transport energy exceeds the supply of material of a transportable size. A shortage of transportable material may occur in a channel in rock which contains a thin bed of sand or gravel, or in a gravel-bed river prior to mobilization of the armor layer, for example. However, when there is an ample supply of transportable material on the streambed, the rate of sediment movement is *transport-limited* and is determined by the available hydraulic energy in the stream.

Equations describing the capacity of flowing water to transport bed material may be divided into two broad groups. *Bed load* equations describe the amount of material transported as bed load, while *total load* equations actually describe the "total bed material load," which includes bed material transported in suspension plus the bed load. The total bed material load is normally the measure of interest in stream transport studies. Wash load concentration and transport rate cannot be predicted from hydraulic conditions in the stream, but depend on the rate of erosion in source areas and delivery rate of fine sediment to stream channels.

Many bed material transport equations have been developed: Alonso (1980) listed 31 equations developed through 1973; the HEC-6 model offers the user a choice of 12 different equations or equation combinations, Yang (1996) includes a program listing and diskette that can be used to compute sediment transport using 13 different "commonly used" equations. Unlike hydraulic equations (e.g., Chezy, Manning, Darcy-Weisbach) which give approximately equivalent results, the application of different sediment transport equations to the same dataset can generate estimates of transport rates ranging over more than 2 orders of magnitude, as illustrated in Fig. 9.15. Results of an analysis can be heavily influenced by the choice of transport equation.

Most river and reservoir sediment transport problems involve the selection and use of transport equations in the context of mathematical modeling. Criteria for selecting a bed material transport equation are discussed in Chap. 11. The remainder of this section briefly presents three transport equations which have been found to be generally reliable when tested against a variety of datasets (Alonso, 1980; Brownlie, 1981; ASCE, 1983). A more detailed description and comparison of these and other transport equations is provided by Yang (1996) and Simons and Senturk (1992).

### 9.9.1 Ackers and White

Ackers and White related the weight concentration of bed material load  $C_s$  to the mobility function  $F_g$  by the following equation:

$$C_s = cG_s \frac{d}{R} \left( \frac{V}{U_*} \right)^n \left( \frac{F_g}{a} - 1 \right)^m \quad (9.33)$$

where  $G_s$  = specific gravity of sediment and  $n$ ,  $c$ ,  $a$ , and  $m$  are coefficients. The mobility number  $F_g$  is computed as

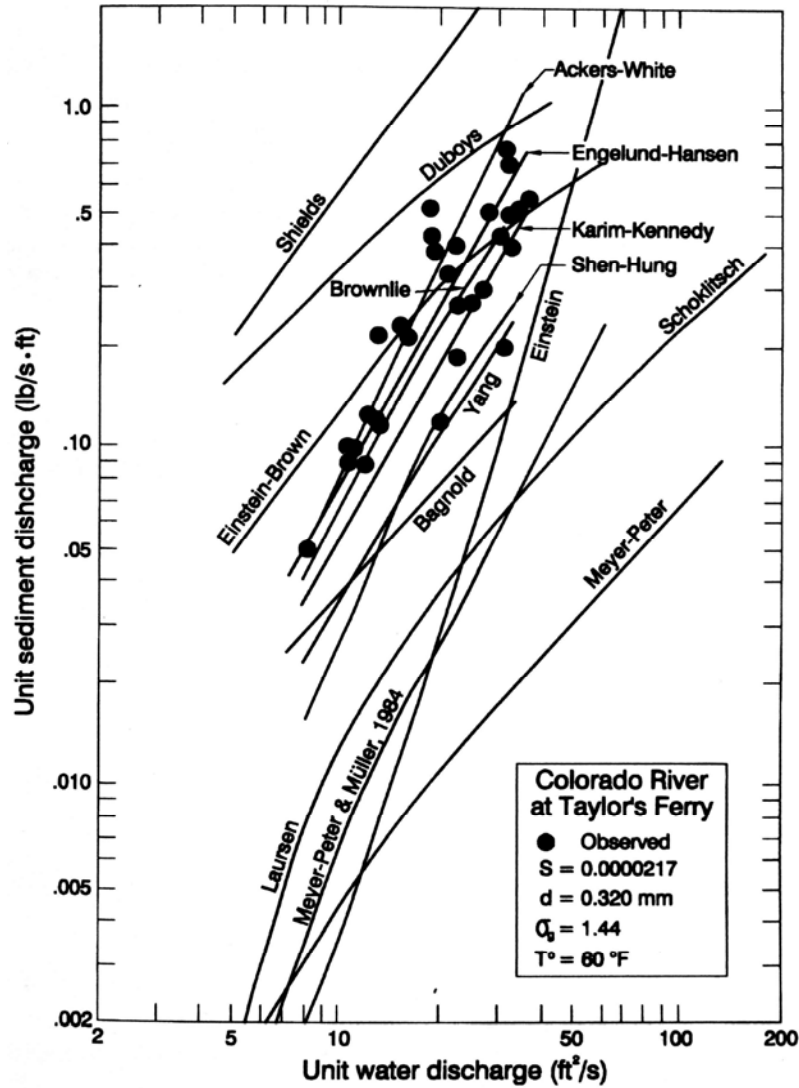


FIGURE 9.15 Measured total sediment discharge in Colorado River at Taylor's Ferry and comparison with several transport equations (after Vanoni et al., 1960).

$$F_g = \frac{U_*^n}{[gd(G_s - 1)]^{1/2}} \left[ \frac{V}{(32)^{1/2} \log(10R/d)} \right]^{1-n} \tag{9.34}$$

Sediment size is expressed by a dimensionless grain diameter,  $d_*$  previously given in Eq. (9.23). The coefficient values were developed based laboratory data for sediment diameters greater than 0.04 mm and a Froude number less than 0.8.

### 9.9.2 Engelund and Hansen

The equation developed by Engelund and Hansen may be expressed in the following form (Vanoni, 1975):

$$q_s = 0.05\gamma_s V^2 \left[ \frac{d_{50}}{g(\gamma_s/\gamma - 1)} \right]^{1/2} \left[ \frac{\tau_0}{(\gamma_s - \gamma)d_{50}} \right]^{3/2} \quad (9.35)$$

This equation is dimensionally homogeneous and can be solved using any set of homogeneous units. In SI units the transport rate  $q_s$  will be given in newtons per meter of width, and it must be divided by the gravitational constant of  $9.8 \text{ m/s}^2$  to express the results in mass units of  $\text{kg}/(\text{s}\cdot\text{m})$ .

### 9.9.3 Yang's Equation for Sand Transport

Yang (1983) observed that most sediment transport equations for bed load or total bed material load are based on correlating sediment transport to a single hydraulic variable using one of the following basic forms (Yang, 1996):

$$q_s = A(Q - Q_{cr})^B$$

$$q_s = A(V - V_{cr})^B$$

$$q_s = A(S - S_{cr})^B$$

$$q_s = A(\tau - \tau_{cr})^B$$

$$q_s = A(\tau V - \tau_{cr} V_{cr})^B$$

$$q_s = A(VS - V_{cr} S_{cr})^B$$

where  $q_s$  = sediment discharge per unit width of channel

$Q$  = water discharge

$V$  = mean velocity

$S$  = energy or water surface slope

$T$  = bed shear stress

$\tau V$  = stream power per unit bed area

$V$  = unit stream power

$A$  and  $B$  = parameters related to hydraulic and sediment conditions and having different values in each equation

Some researchers have also used an empirical regression analysis to correlate sediment transport to hydraulic parameters.

Yang (1983) plotted sediment discharge as a function of each hydraulic parameter using laboratory flume data with 0.93-mm sand (Fig. 9.16). It was observed that more than one sediment discharge rate can occur at a single value of water discharge or water surface slope, making these two parameters poor predictors of transport rate. A single-value relationship exists between sediment discharge and both velocity and shear stress. However, the resulting curves are quite steep, which makes the independent variable a poor predictor. The best correlations were achieved by using stream power. Unit stream power, computed as the product of flow velocity and slope, was the best predictor.

A transport relation was developed based on the rate of energy expenditure per unit weight of water, which is defined as the unit stream power and is computed as the product of velocity and slope,  $VS$ . (See Appendix J.) The equation has the basic form

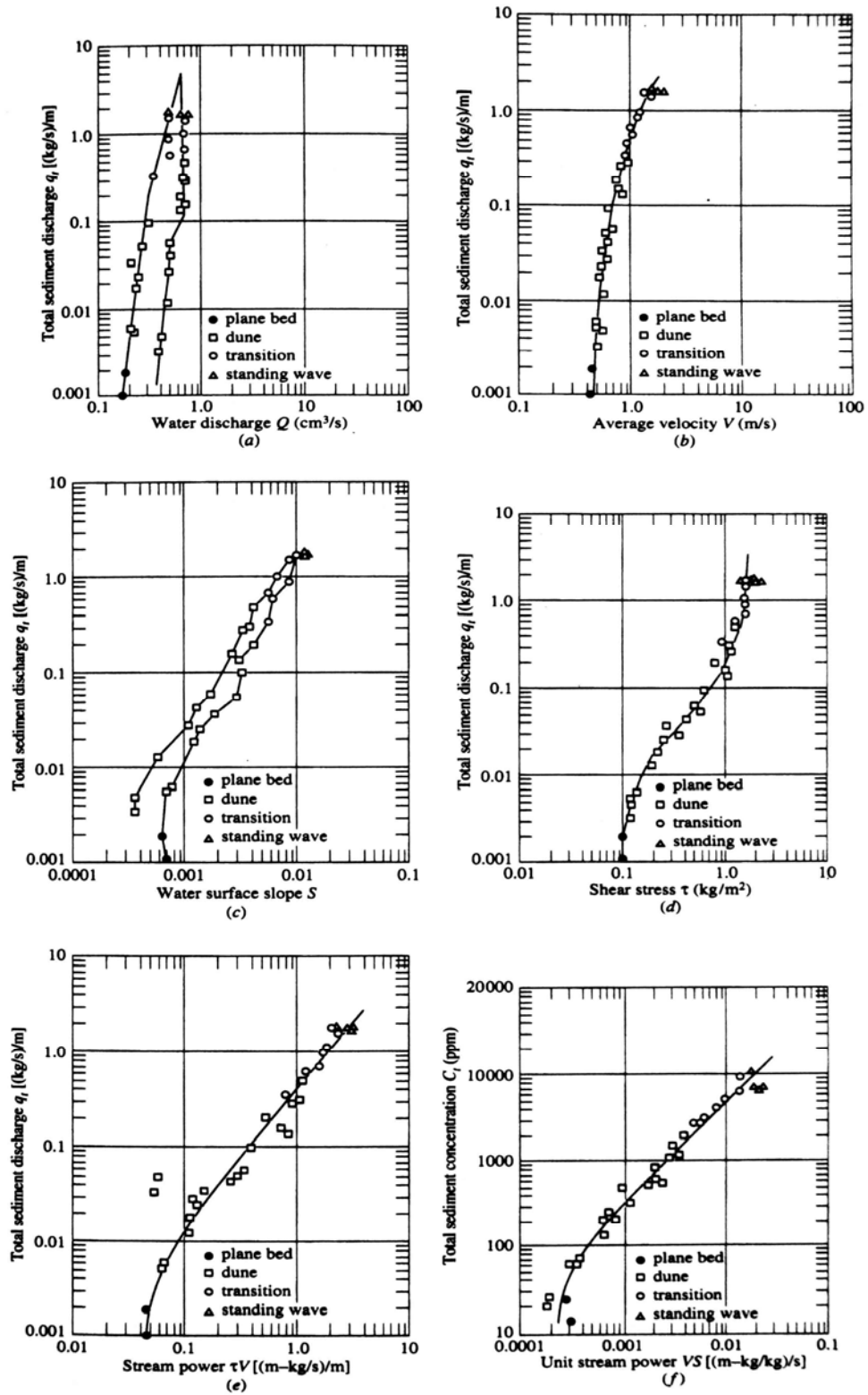


FIGURE 9.16 Relationship between sediment discharge and selected hydraulic parameters for 0.93-mm sand in a 2.4-m-wide flume (Yang, 1983).

$$\log C_{ppm} = I + J \log \left( \frac{VS}{\omega} - \frac{V_{cr}S}{\omega} \right) \quad (9.36)$$

where  $C_{ppm}$  = bed material sediment concentration, excluding wash load (in ppm), and  $I$ ,  $J$  = dimensionless parameters related to flow and sediment characteristics. The coefficient values were determined by regression analysis of 463 sets of laboratory data, producing the following equation for sand transport [Yang (1973)]:

$$\begin{aligned} \log C_{ppm} = & 5.435 - 0.286 \log \frac{\omega d}{\nu} - 0.457 \log \frac{U_*}{\omega} \\ & + \left( 1.799 - 0.409 \log \frac{\omega d}{\nu} - 0.314 \log \frac{U_*}{\omega} \right) \log \left( \frac{VS}{\omega} - \frac{V_{cr}S}{\omega} \right) \end{aligned} \quad (9.37)$$

where  $C_{ppm}$  = total sand concentration (ppm by weight),  $\omega$  = sediment fall velocity,  $\nu$  = kinematic viscosity,  $U_*$  = shear velocity,  $d$  = median particle diameter,  $V_{cr}S$  = critical unit stream power at incipient motion computed using Yang's method [Eq. (9.24) or (9.25)]. When the sediment concentration is more than about 100 ppm by weight, the incipient motion criteria can be eliminated without affecting the accuracy of the equation, resulting in the following relation (Yang, 1979):

$$\begin{aligned} \log C_{ppm} = & 5.165 - 0.153 \log \frac{\omega d}{\nu} - 0.297 \log \frac{U_*}{\omega} \\ & + \left( 1.780 - 0.360 \log \frac{\omega d}{\nu} - 0.480 \log \frac{U_*}{\omega} \right) \log \frac{VS}{\omega} \end{aligned} \quad (9.38)$$

These equations may be solved with either SI or fps units to determine sediment concentration in ppm by weight, which is dimensionless.

#### 9.9.4 Yang's Equation for Gravel

A gravel transport equation using the same form as Eq. (9.37) but different parameter values is given as (Yang, 1984):

$$\begin{aligned} \log C_{ppm} = & 6.681 - 0.633 \log \frac{\omega d}{\nu} - 4.816 \log \frac{U_*}{\omega} \\ & + \left( 2.784 - 0.305 \log \frac{\omega d}{\nu} - 0.282 \log \frac{U_*}{\omega} \right) \log \left( \frac{VS}{\omega} - \frac{V_{cr}S}{\omega} \right) \end{aligned} \quad (9.39)$$

where  $C_{ppm}$  = total gravel concentration (ppm by weight).

#### 9.9.5 Yang's Modification for Water-Sediment Mixtures

The foregoing equations were derived for sediment transport in essentially clear water. The equations must be modified for use with other fluids, or for conditions in which there is an extremely high sediment concentration in the water which requires that the following parameter values be modified: fall velocity, kinematic viscosity, and relative specific weight. Extremely high suspended-sediment concentrations and hyperconcentrated flows can occur in some river systems, such as China's Yellow River, and can also occur during reservoir flushing. This section presents, as an example, an application

specific to the Yellow River. Modification should be expected for use on another system having a different grain size distribution.

Yang (1996) outlined the modification of the sand transport equation given in Eq. (9.38) to include the characteristics of the water-sediment mixture, using the Yellow River as an example. The effect of sediment concentration on fall velocity of fine sands in the Yellow River may be estimated by

$$\omega_m = \omega(1 - C_v)^M \quad (9.40)$$

where  $C_v$  = sediment concentration by volume, including wash load,  $\omega_m$  and  $\omega$  = sediment fall velocity in the mixture and in clear water respectively, and exponent  $M = 7$ .

The kinematic viscosity is a function of temperature, sediment concentration, and size distribution. The expression for the kinematic viscosity of water-sediment mixtures for the grain size distribution encountered in the Yellow River can be expressed by

$$v_m = \frac{\rho}{\rho_m} e^{5.06C_v} \quad (9.41)$$

where  $\rho$  and  $\rho_m$  = densities of clear water and the water-sediment mixture, respectively, and  $v_m$  = kinematic viscosity of the mixture. The density of the mixture is given by

$$\rho_m = \rho + (\rho_s - \rho)C_v \quad (9.42)$$

When revised to incorporate these effects, Yang's equation for sand transport given in Eq. (9.38) is revised to the following form:

$$\begin{aligned} \log C_{ppm} = & 5.165 - 0.153 \log \frac{\omega_m d}{v_m} - 0.297 \log \frac{U_*}{\omega_m} \\ & + \left( 1.780 - 0.360 \log \frac{\omega_m d}{v_m} - 0.480 \log \frac{U_*}{\omega_m} \right) \log \left( \frac{\gamma_m}{\gamma_s - \gamma_m} \frac{VS}{\omega_m} \right) \end{aligned} \quad (9.43)$$

Note that the parameter coefficients are unchanged.

## 9.10 HYPERCONCENTRATED FLOW

Hyperconcentrated flows are sediment-water mixtures having a sediment concentration high enough that the particles interact with one another to create a structural lattice within the fluid of sufficient strength to affect characteristics such as velocity distribution within the flow and particle settling rates. The behavior of the mixture departs significantly from that of clear water, a Newtonian fluid, and is usually described based on the characteristics of a Bingham fluid. High concentrations of cohesive sediments can significantly affect the behavior of the sediment-water mixture as it flows in rivers and enters or exits reservoirs. A comprehensive overview of both practical and theoretical aspects of hyperconcentrated flow has been presented by Wan and Wang (1994).

Hyperconcentrated flow occurs naturally in China's Yellow River and its tributaries. In this river system 300 g/L is the approximate threshold concentration for hyperconcentrated flow to occur, and peak suspended sediment concentrations exceeding 1000 g/L have been reported at some gage stations. Because the hyperconcentration threshold depends on factors including grain size distribution and mineralogy, the threshold concentration will not necessarily be the same in other river systems. Hyperconcentrated

flows are not limited to China, and may be generated during reservoir flushing in river systems that otherwise never experience hyperconcentration. For instance, Ake Sundborg observed hyperconcentrated flows during flushing at Cachi Reservoir, Costa Rica (Chap. 19).

High concentration flows can produce extremely rapid and large changes in the configuration of erodible channels in rivers and reservoirs. Hyperconcentrated floods cause the cross section to become narrower and deeper with the creation of lateral berms. Because of the high sediment concentration they can also cause rapid channel aggradation. The role of hyperconcentrated flows in some Chinese reservoirs has been mentioned in the Sanmenxia and Heisonglin case studies, where they are important in the formation of turbidity currents.

Whether produced naturally or by the erosion of upstream sediment deposits in a reservoir, under favorable conditions hyperconcentrated flows can be passed through a reservoir as a turbidity current with little sedimentation. The high concentrations associated with hyperconcentrated flow produce high-velocity turbidity currents and can transport coarse sediment to the dam, aided by the reduced settling velocity of the coarse sediment within the hyperconcentrated fluid. Once the flow reaches the dam to form a muddy lake, sedimentation within the muddy lake is hindered by hyperconcentration, allowing the fluid to be vented through the dam over a period of several days under favorable conditions. Due to settling and compaction within the submerged muddy lake, the discharge from the muddy lake may have a higher concentration than the inflow.

## 9.11 COHESIVE SEDIMENTS

---

### 9.11.1 Importance of Cohesive Sediments

Reservoir sediments often contain a high percentage of clays, and their mechanical behavior is strongly influenced by the interparticle cohesion caused by electrostatic and related surface forces. These forces, which may be several orders of magnitude larger than gravitational forces, give clay its "stickiness" and influence important phenomena such as flocculation, the rate of sedimentation and compaction, the angle of repose, and erosion resistance.

For coarse noncohesive sediments, characteristics such as settling velocity, condition of incipient sediment motion, and erosion rate are determined by gravitational forces, which can be represented by the grain diameter. However, in fine-grain sediments (smaller than 0.01 mm) surface forces predominate, and the behavior of cohesive sediments cannot be determined based on grain size alone. Colliding fine particles stick together to form agglomerates having settling velocities orders of magnitude larger than those of the individual particles. Thus, the floc rather than the individual particle becomes the settling unit. These same physico-chemical surface forces provide the main resistance to erosion of cohesive sediment deposits (Partheniades, 1986). While grain size influences the surface forces through the relationship between surface area per unit of mass and particle diameter, the strength of cohesive surface forces are also strongly influenced by mineralogy and water chemistry parameters, such as ionic strength.

In 1935 Hjølstrom developed a graphical relationship between mean velocity and grain size which illustrates the areas of sediment erosion, transportation, and deposition (Fig. 9.12). Notice that the line of incipient motion, which separates erosion from transportation, has a minimum value for a grain size around 0.1 mm, and increases for both larger and smaller grains. The increased resistance to erosion for the larger sediment particles is due to gravitational forces, whereas the increased resistance to erosion for fine particles is primarily due to cohesive forces. Also note that for fine sediment there is a

large difference between the thresholds for erosion and deposition. Once a fine particle is eroded, it will not be redeposited unless flow velocity decreases substantially.

For practical applications in reservoirs, the characterization of cohesive sediment properties is complicated by the nonuniform nature of the deposits. Different inflow events will produce deposits having different thicknesses and grain size, and mineralogy can vary as a function of the sediment source area for different inflow events. Differences will also be caused by the fraction of coarse sediments or organics. Variations will occur along the length of the reservoir due to the differential settling rates of the inflowing sediment and other factors. Sediments will become compacted by consolidation and dewatering over time, and deposits which are exposed to the air will experience accelerated compaction and desiccation. As cohesive sediments compact, they become more difficult to erode (Fig. 9.17).

The modeling of erosion processes in cohesive sediments at small French reservoirs upstream of barrages was reported by Bouchard et al. (1989) and Bouchard (1993, 1995). Following extensive sampling of continuously submerged cohesive sediment, the mechanical properties were found to have wide variation both laterally and vertically within the deposits. The mechanical characteristics of the cohesive bed material could be represented in only a very approximate and aggregated fashion. At the very small (200 m long) Kembs reservoir on the Rhine it was impossible to identify a clear succession of

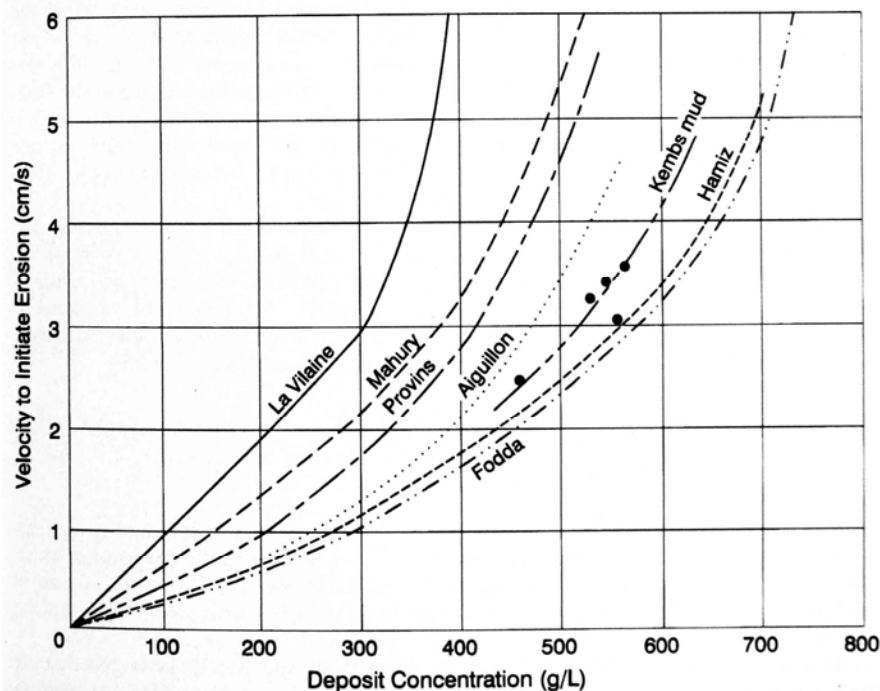


**FIGURE 9.17** Flow velocity required to initiate erosion of cohesive sediments from various sites, as a function of dry bulk density of the sediment deposit (after Migniot, 1977), also showing the muds from Kembs Reservoir reported by Bouchard (1993).

mud layers with a constant composition which could be followed from one bore hole to another. The deposit structure consisted of a set of lenses with little continuity. More uniform conditions may occur at larger reservoirs.

Cohesive sediments in reservoirs may also be characterized by two different grain sizes. At the Kembs reservoir the deposits were characterized by a mixture of clay ( $d = 0.002$  mm) and fine sand ( $d = 0.08$  mm), and the variation in the mean  $d_{50}$  diameter of any sample primarily reflected the variation in the proportion of these two components. Thus, mud characteristics were determined based on sediment concentration and the percentage of dry matter having a diameter greater than 0.04 mm, thereby separating the cohesive and noncohesive sediment fractions (Bouchard, 1995).

### 9.11.2 Settling and Compaction of Cohesive Sediment

The settling velocity of discrete clay particles is given by Stokes's law. As the concentration of clay particles increases, the flocculation produces particle aggregates having much larger effective diameters than discrete clay platelets. Consequently, the settling rate of clay will initially increase as a function of concentration. However, at some higher concentration the flocs begin to contact one another, creating a structural lattice which greatly hinders fall velocity. Metha et al. (1989) indicate that settling rates begin to be hindered when the flocculant suspension exceeds about 5 to 10 g/L in concentration.

Particles settle as a group during the *hindered settling* process, which is characterized by a sharp interface between the overlying clear water and a slowly compacting flocculant mass that is settling uniformly. Coarser particles may be trapped within the flocculant mass and settle together with it. As the flocculant mass compacts, clear water is squeezed out of the structural lattice and makes its way to the interface through vertical channels or small "drainage wells" which conduct water to the surface of the flocculant material, and also along sidewalls when this phenomena is observed in a clear sedimentation column. Pore water trapped within the flocculant mass must migrate upward to the surface for settling to continue. This settling process is conceptually illustrated in Fig. 9.18, where  $C_v$  = concentration by volume.

Primary consolidation ends when the excess pore water pressure has completely dissipated. Secondary consolidation, which is the result of plastic deformation of the structural lattice due to overburden, begins during primary consolidation and may continue long after primary consolidation ends (Mehta et al., 1989). The behavioral characteristics of the sediment will change as it compacts, and the nomenclature used to describe cohesive sediment varies based on the bulk density (Yang and Wang, 1996):

fluid mud	density less than 1.2 g/cm <sup>3</sup>
mud	density between 1.2 and 1.6 g/cm <sup>3</sup>
consolidated mud or clay	density exceeds 1.6 g/cm <sup>3</sup>

Consolidation rates vary widely from one site to another (Fig. 9.19), and in general the concentration in the consolidating mass varies as a logarithmic function of time. There is no general expression for the rate of hindered settling and consolidation of cohesive sediment. It is necessary to determine the settling rate using laboratory settling columns.

Several characteristics of cohesive sediments must be specifically considered in the evaluation of reservoir sedimentation. Flocculation may cause suspended sediment to settle much faster than predicted based on the size of the individual grains, as demonstrated at the Peligre Reservoir in Haiti by Frenette and Julien (1986).

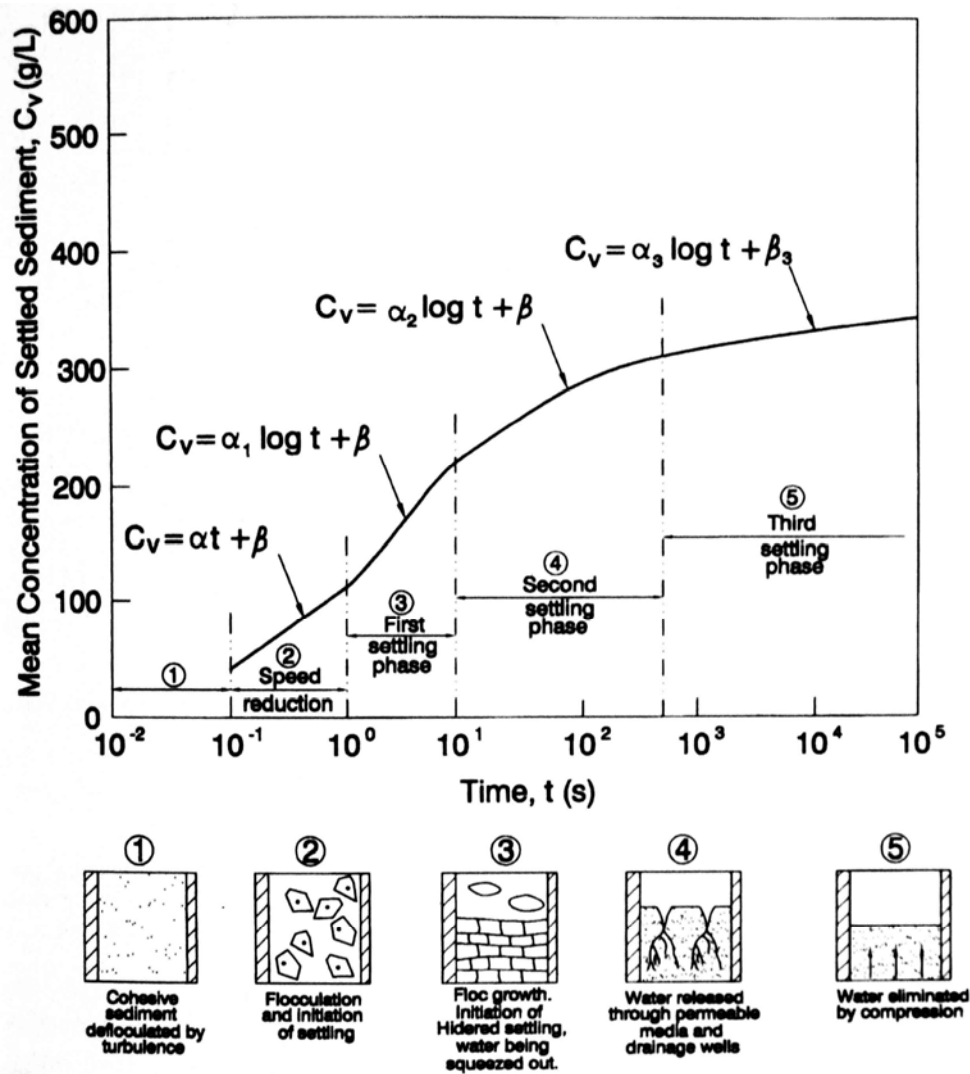


FIGURE 9.18 Settling processes for cohesive sediment (adapted from Migniot, 1968).

In many reservoirs it is observed that the rate of storage loss is initially high and then declines (Murthy, 1977). This phenomena may be explained by the gradual compaction of cohesive sediment: the volume occupied by cohesive sediment during the first year after deposition is greater than the volume it will occupy after many years of compaction. This compaction effect must be taken into account in short-interval volume measurements (see Sec. 10.9.4).

In reservoirs where new sediment layers are being continuously deposited, the upward migration and release of pore water may be retarded by the continued deposition of additional fine sediment layers. Sediment deposition will also cause overburden to increase with time. Because of these factors and others such as variation in the inflowing grain size and surface drying during drawdown, the bulk density of reservoir deposits often do not increase regularly with depth, and sediment density may actually be lower in deeper layers, as illustrated in Fig. 10.17.

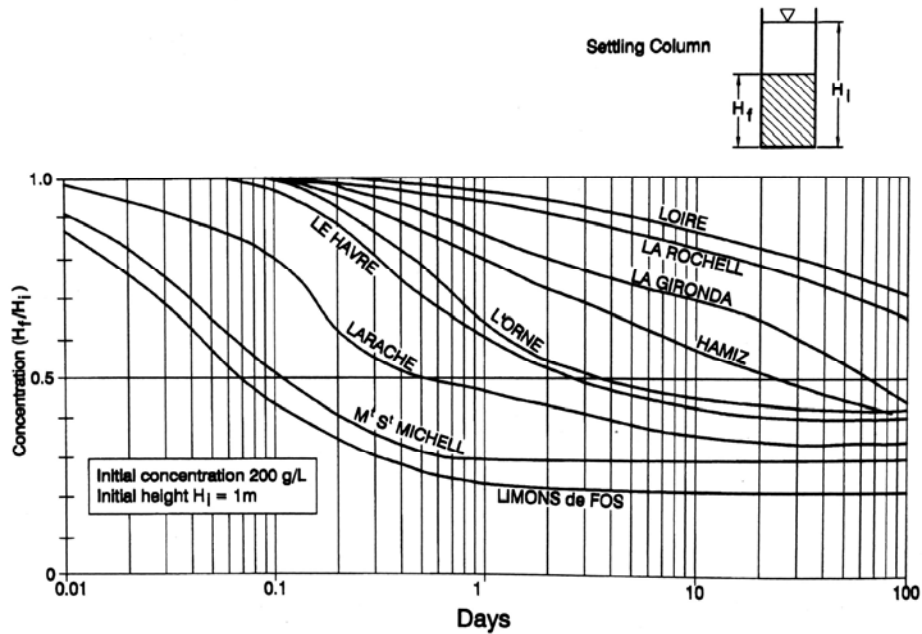


FIGURE 9.19 Variation in the consolidation rate of cohesive sediments (modified from Migniot, 1982).

**9.11.3 Rheology of Cohesive Sediment Mixtures**

In a moving fluid the change in velocity  $v$  as a function of depth  $y$  along a vertical profile, is termed the shear rate. A graph which illustrates the relation between the shear rate  $dv/dy$  and shear stress  $\tau$  is called a rheogram, and the equation describing this relationship is called a rheological equation.

Clear water is a Newtonian fluid because the shear rate is directly proportional to the applied shear stress  $\tau$  at every depth. The rheological equation for a Newtonian fluid is:

$$\tau = \mu \, dv/dy \tag{9.44}$$

where  $\mu$  = dynamic viscosity ( $N \cdot s/m^2$ ). The characteristic shape of the rheogram for a Newtonian fluid, as shown in Fig. 9.20, applies to clear water and sediment-water mixtures of low concentration. These fluids will start moving as soon as the applied shear stress exceeds zero.

At some higher sediment concentration, the suspended particles begin to interact significantly with one another, creating a weak structural lattice within the fluid which resists deformation by an applied shear stress. When this occurs the fluid will remain immobile until the applied shear exceeds a threshold value termed the initial rigidity ( $\tau_B$ ). Water-sediment mixtures of this nature may be represented using the Bingham fluid model, the rheogram of which is also presented in Fig. 9.20. The rheological equation for a Bingham fluid is:

$$\tau = \tau_B + \eta \, dv/dy \tag{9.45}$$

where  $\tau_B$  = Bingham yield stress ( $N/m^2$ ) or initial rigidity, and  $\eta$  = plastic viscosity or coefficient of rigidity, and represents the ratio of stress to shear,  $dv/dy$ , which is constant

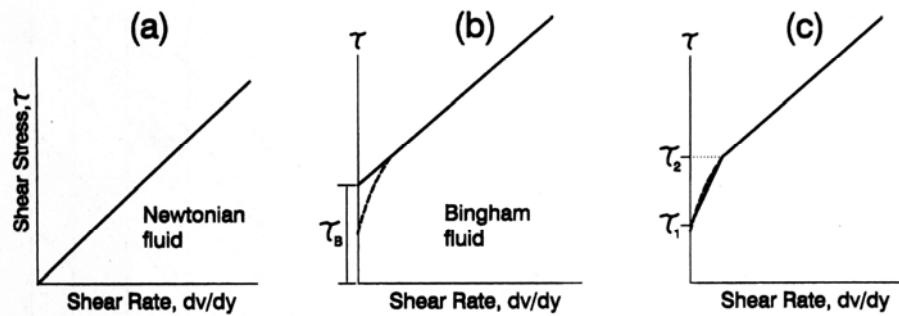


**FIGURE 9.20** Rheograms illustrating the patterns characteristic of (a) Newtonian fluid, such as clear water, (b) Bingham fluid, such as hyperconcentrated sediment-water mixtures and muds, and (c) fluid model used by Otsubo and Muraoka in Fig. 9.23.

in a Bingham fluid. The rheological equation for a Bingham fluid is an empirical formula derived from experimental data and which has proven useful in the analysis of a variety of water-sediment mixtures including hyperconcentrated flows, clay slurries, and debris flows. If the stress/shear ratio is not constant the fluid behavior is termed plastic. A fluid is termed *thixotropic* if shear stress declines with time for a given value of  $dv/dy$ , and *antithixotropic* if shear stress increases over time.

As a practical matter, a slurry may be considered a Bingham fluid when the Bingham yield stress  $\tau_B$  exceeds  $0.5 \text{ N/m}^2$  (Wan and Wang, 1994). The initial rigidity is not constant for a given sample of cohesive sediment, but will increase as a function of sediment concentration due to compaction with time (Fig. 9.21). Several important behavioral characteristics of cohesive sediment have been related to the initial rigidity.

#### 9.11.4 Laboratory Testing of Cohesive Sediment

Several basic laboratory and field tests may be used to characterize the bulk characteristics behavior of cohesive sediment. The *liquid limit* is the moisture content expressed as the weight percentage of oven-dried soil at which the soil will just begin to flow when jarred slightly. The *plastic limit* is the lowest moisture content, expressed as a percentage by weight of the oven-dried soil, at which it can be rolled into threads 3 mm (1/8 inch) in diameter without breaking into pieces. Soils which cannot be rolled into threads at any moisture content are considered nonplastic. The *plasticity index* is the difference between the liquid limit and the plastic limit. It is the range of moisture content in which a soil is plastic. When the plastic limit is equal to or greater than the liquid limit, the plasticity index is recorded as zero. In the *vane shear test* a vane-shear apparatus containing several vanes on a central axis is inserted into either a laboratory or field sample and rotated to test the cohesive strength of the bulk sample (Fig. 9.22a). Torque is applied to the sample through a calibrated spring, and the torque at which sample failure occurs provides a direct reading of the shear stress of the sample.

Several types of tests can be used to directly measure erodibility of cohesive sediment samples. In the *rotating cylinder test* a sediment sample is transferred to a laboratory where it is shaped into a cylinder and inserted into a clear cylindrical container (Fig. 9.22b). The space between the sample and the outer cylinder is filled with water, and the outer cylinder is rotated about the stationary soil sample to produce shear stress across the sample surface. Rotation speed (torque) is increased until the sample surface is observed to fail through cracking, peeling, or sloughing. A change in torque is also observable at this point.

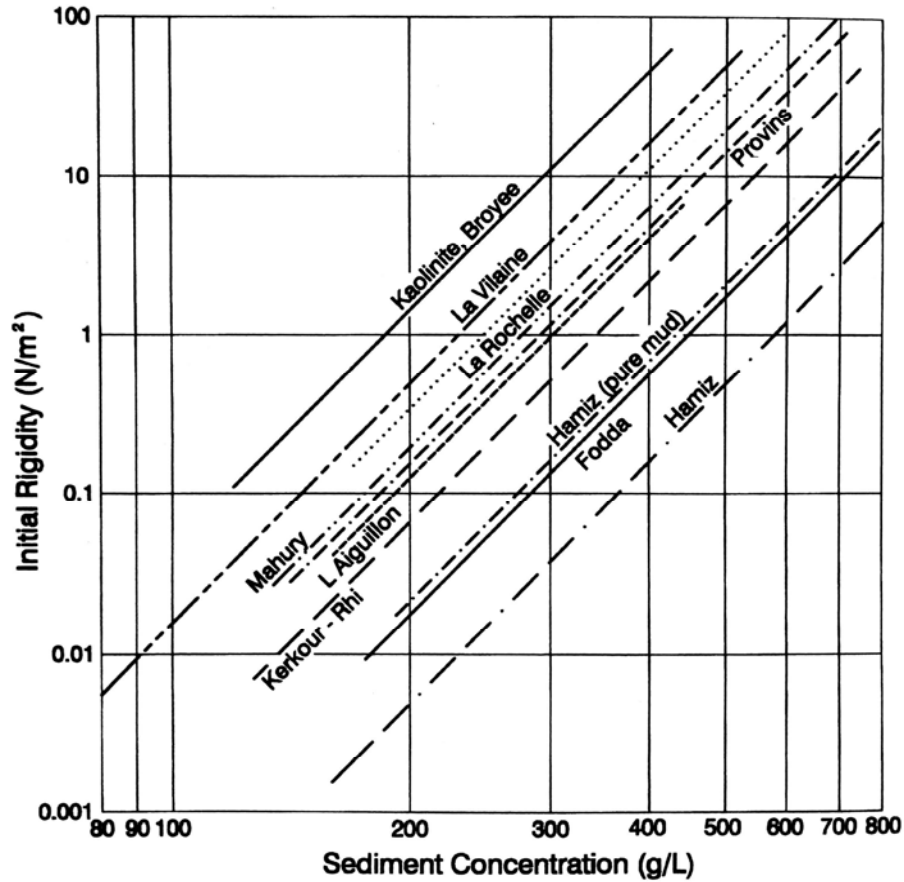


FIGURE 9.21 Increase in initial rigidity as a function of sediment concentration (after Migniot, 1968).

The erosion rate for sediment samples may be measured in a laboratory *flume test*. Samples from the field are molded into a container placed in the bottom of a hydraulic flume so that the sample surface is flush with the bottom of the flume. The erosion rate at a given flow velocity is measured by the rate of weight loss in the sample container, or the increase in solids concentration in the circulating water. Testing of this type can also be performed in a closed rectangular conduit.

The degree of gravity setting or compaction can be measured as a function of time using a *column settling test*. The relationship between the sediment concentration at the onset of hindered settling, and the final sediment concentration after a settling period, has been found to be a useful parameter for estimating several characteristics of cohesive sediment. The procedure described by Otsubo and Muraoka (1988) used a 60 mm i.d. clear cylinder 230 mm high. Samples were added and agitated, allowed to settle for one day, again fully agitated for 5 minutes, and then the test was initiated. The height of the initial sediment interface  $H_i$  was recorded, as well as the interface level  $H_f$  after 144 hours of quiescent settling. The settling ratio  $V_f$  may be computed as

$$\frac{H_f}{H_i} = \frac{C_i}{C_f} \tag{9.46}$$

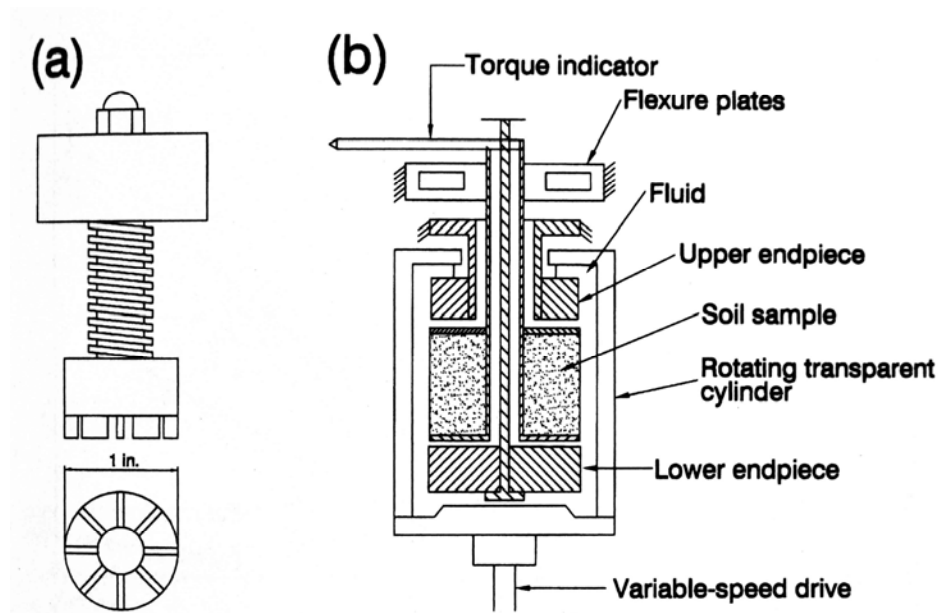


FIGURE 9.22 Devices used for the (a) vane shear test and (b) rotating cylinder test.

where  $H$  is the interface height,  $C$  is the mass sediment concentration ( $\text{kg}/\text{m}^3$ ), and subscripts  $i$  and  $f$  refer to the initial and final condition respectively. Otsubo and Muraoka used pure water in their settling tests; for field applications it may be more appropriate to use native water. They also tested each mud using several different initial concentrations for column settling tests. Mingnot (1968) used 200 g/L as the initial sediment concentration in column settling tests.

### 9.11.5 Erosion Thresholds for Cohesive Sediment

Although absolute thresholds for sediment transport do not actually exist (Lavelle and Mofjeld, 1987), approximate threshold conditions may be defined when erosion rates become readily observable or significant. In the case of cohesive sediment, two erosion threshold values may be defined.

1. *Surface erosion* or *particle erosion* refers to the condition when individual particles or aggregates visibly begin to be removed from the surface of a bed of cohesive sediment. Bulk measures of cohesive sediment mechanical parameters (solids concentration, plasticity, Atterberg limits, etc.) have not been found useful for predicting the critical flow conditions for initiation of surface erosion (Partheniades, 1986).
2. *Mass erosion* occurs at higher values of shear stress (velocity) and is characterized by the removal of large clumps of sediment from the bed.

The onset of mass would normally be of interest in reservoir studies.

Threshold values of bed shear stress for surface erosion  $\tau_{c1}$ , and mass erosion  $\tau_{c2}$  were related to initial rigidity by Otsubo and Muraoka (1988), who performed a series of flume tests using both lake and estuary sediments to develop the relationship shown in (Fig. 9.23). Critical values for initiation of surface or particle erosion  $\tau_{c1}$  are given by

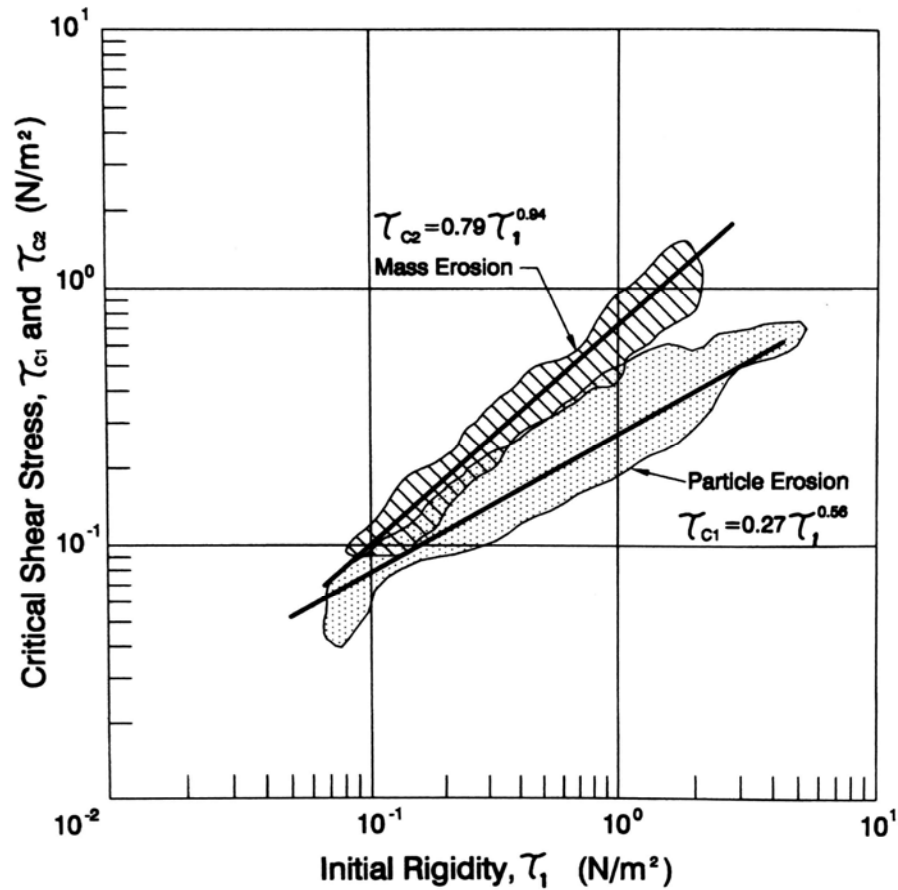


**FIGURE 9.23** Critical values for surface and mass erosion, as a function of initial rigidity as defined in Fig. 9.20c (after Otsubo and Muraoka, 1988).

$$\tau_{c1} = 0.27\tau_1^{0.6} \tag{9.47}$$

Critical values for the initiation of mass erosion  $\tau_{c2}$  are given by

$$\tau_{c2} = 0.79\tau_1^{0.94} \tag{9.48}$$

These relationships were developed for values of bed shear stress ( $\tau_{c1}$  and  $\tau_{c2}$ ) between 0.08 and 3 N/m<sup>2</sup>.

Cohesive sediments compact over time, and the rate and extent of compaction will reflect the mechanical shear strength of the aggregates. Higher cohesive forces will form stronger and denser aggregates, and will in turn exhibit greater resistance to erosion by shear forces. These denser aggregates also resist compaction by gravity within a settling column. Based on this logic, Otsubo and Muraoka (1988) suggested that cohesive settling behavior in laboratory columns might be correlated to erosion characteristics. Use of the settling parameter is advantageous because it is easier to measure than initial rigidity using a viscometer.

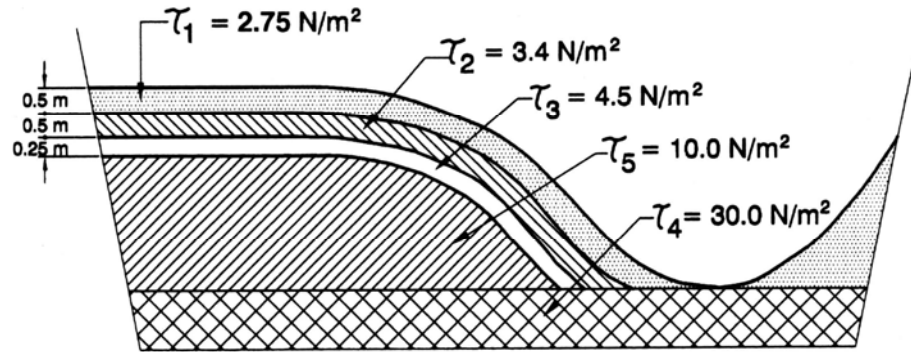


**FIGURE 9.24.** Erosion resistance of successive sediment layers used by Bouchard (1988) to model cohesive sediments in the small Kembs Reservoir on the Rhine.

Their experiments indicated that several parameters could be correlated to the settling ratio given in Eq. (9.47). The relationship between the settling ratio and initial rigidity is given by

$$\log(\tau_B) = 3.58(H_f/H_i) - 3.17 \quad (9.49)$$

valid over the range  $0.65 < H_f/H_i < 0.95$ . The initiation of mass erosion may be directly related to the settling ratio by first solving Eq. (9.50) and then Eq. (9.49).

Based on flume testing of recently deposited sediment, Bouchard used erosion threshold values ranging from 2.75 to 30 N/m<sup>2</sup> for modeling erosion in Kembs reservoir, using the bedding pattern shown in Fig. 9.24.

Bed shear threshold values for mass erosion can vary greatly as a function of the clay characteristics, and sediments that have compacted for many decades and have been subject to desiccation can be very resistant to erosion, as illustrated by flume data using cohesive sediment from several rivers in China (Fig. 9.25).

### 9.11.6 Erosion Rate of Cohesive Sediment

The erosion rate of cohesive sediment has been described by Partheniades (1962).

$$q_e = \alpha \left( \frac{\tau}{\tau_{cr}} - 1 \right) \quad (9.50)$$

where  $q_e$  = mass of sediment eroded per unit area of bed surface per unit of time (kg/s•m<sup>2</sup>),  $\tau$  = shear stress (N/m<sup>2</sup>),  $\tau_{cr}$  = critical stress at which erosion commences (N/m<sup>2</sup>), and  $\alpha$  = coefficient of erodibility.

### 9.11.7 Deposition Rate of Cohesive Sediment

The deposition rate of cohesive sediment can be described using the Krone equation.

$$q_d = C_v \omega \left( 1 - \frac{\tau}{\tau_d} \right) \quad (9.51)$$

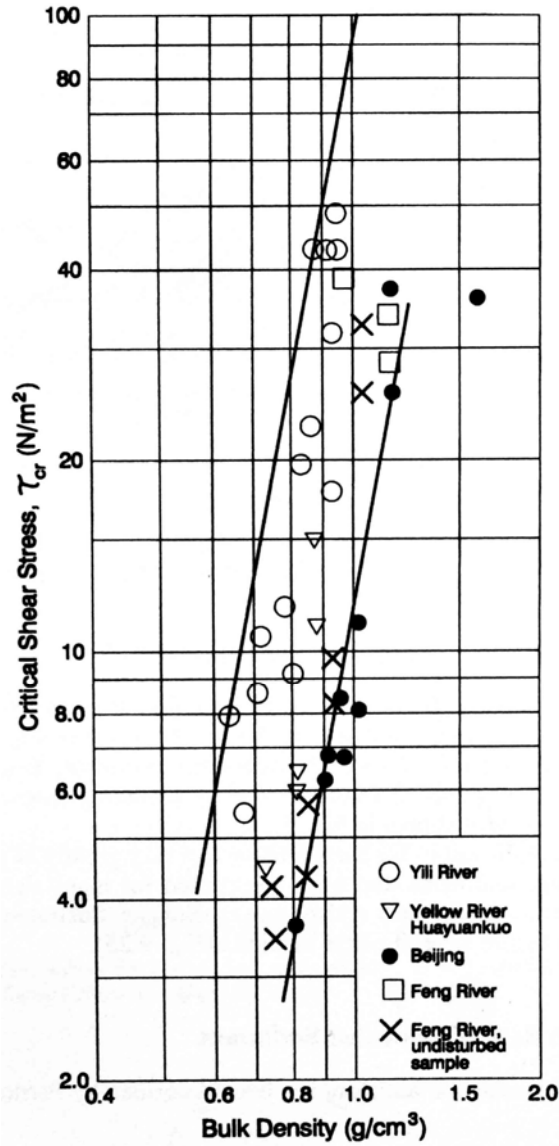


FIGURE 9.25 Critical shear stress values for initiation of mass erosion of cohesive sediment (after Du and Zhang, 1989)

where  $C_v$  = volumetric sediment concentration,  $\omega$  = fall velocity, and  $\tau_d$  = critical stress for sediment deposition.

### 9.11.8 Angle of Repose

The angle of repose of cohesive sediment increases as a function of concentration. At low concentrations the angle of repose will be less than that of cohesionless sediment, but as concentration increases the angle of repose will exceed that of cohesionless sediment.

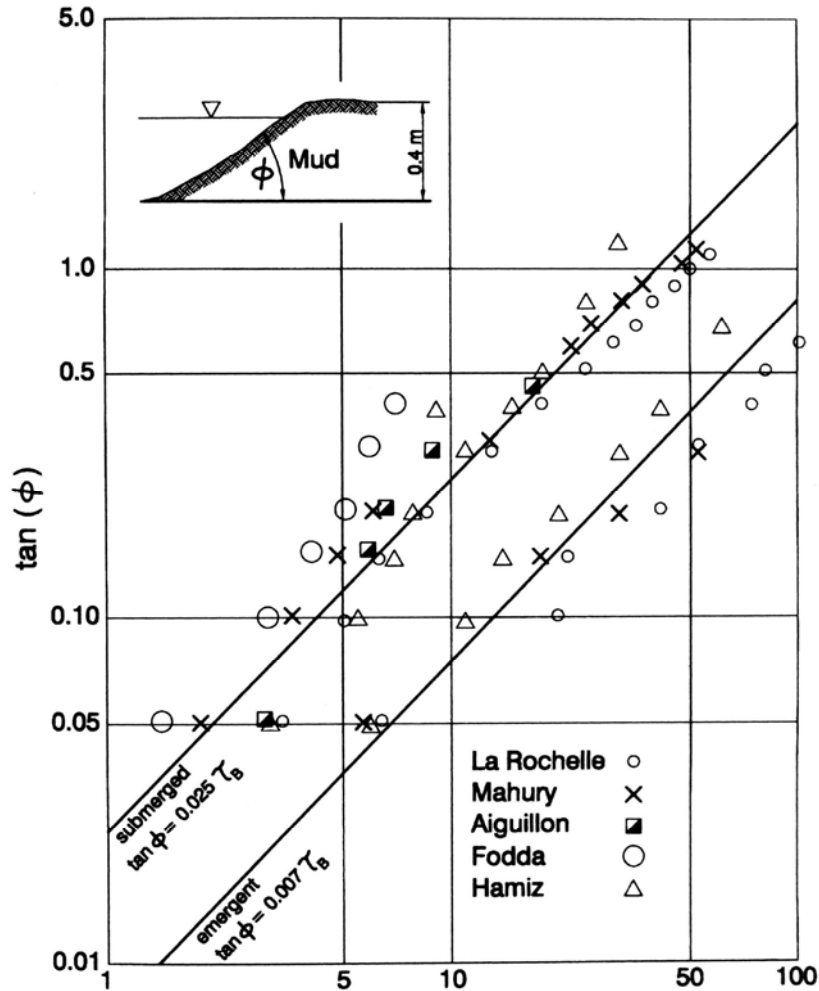


FIGURE 9.26 Angle of repose of cohesive sediment as a function of initial rigidity for emergent and submerged sediments (after Migniot, 1968).

Migniot (1968) has related the angle of repose of cohesive sediment to the initial rigidity ( $\tau_B$ ) for several sediment samples, as shown in Fig. 9.26 for submerged and emergent conditions. The general equation is:

$$\tan \phi = C \tau_B \tag{9.52}$$

where  $\phi$  = angle of repose,  $\tau_B$  = initial rigidity ( $N/m^2$ ), and  $C$  = coefficient with a value of 0.007 for emergent sediment and 0.025 for submerged sediment.

### 9.11.9 Settling of Individual Coarse Particles

The flocculant interaction of fine particles creates the Bingham yield stress, and larger particles having a certain diameter  $d$  can be supported and will not settle in a quiescent

Bingham fluid. The diameter  $d$  of the nonsettling particles is proportional to the Bingham yield stress. This flocculant structure can be disrupted by turbulence, giving rise to the situation in which coarse sediment can be sustained in suspension within a quiescent fluid, yet will settle out when the same fluid begins to move and the turbulence within the fluid partially destroys the flocculant structures. As flow velocity and turbulence increase, sedimentation of the coarse materials will also increase, until the turbulence due to velocity is itself sufficient to entrain and suspend the coarse sediment (Wan and Wang, 1994, p. 59).

The critical condition when the concentration of a suspension is so high that the submerged particle weight is balanced by the yield stress of the flocculant mass is given by:

$$d = K_1 \left( \frac{6 \tau_B}{\gamma_s - \gamma_m} \right) \quad (9.53)$$

where  $d$  = particle diameter (m),  $\gamma_s$  and  $\gamma_m$  are the specific weights of the sediment particles and the mixture respectively ( $\text{N/m}^3$ ),  $\tau_B$  = initial rigidity ( $\text{N/m}^2$ ), and the  $K_1$  coefficient value has been reported in the range of 0.875 to 0.95 by different researchers (Wan and Wang, 1994).

#### 9.11.10 Group Settling of Cohesionless Sediment

Due to particle interaction, the fall velocity of a group of cohesionless coarse particles within a suspension will be smaller than the fall velocity of individual particles in clear water. The gross fall velocity of a group of uniformly sized coarse noncohesive particles is given by the previously introduced equation by Richardson and Zaki (1954):

$$\omega_m = \omega(1 - C_v)^M \quad (9.40)$$

where ( $\omega_m$  = gross fall velocity of uniform discrete particles in a mixture,  $\omega$  = fall velocity of an individual particle in clear water,  $C_v$  = volumetric concentration of particles in the mixture, and  $M$  = exponent value which is a function of the particle Reynolds number (Qian, 1980). Based on data graphed by Wan and Wang (1994), approximately:

$$\begin{aligned} \text{for } \text{Re} \leq 3 & \quad M = 4.65 \\ \text{for } 3 < \text{Re} < 300 & \quad M = 4.65 - 1.075 [\log(\text{Re}) - 0.477] \\ \text{for } \text{Re} \geq 300 & \quad M = 2.5 \end{aligned}$$

Some experimenters have reported values of  $M$  around 7 for sand with  $d_{50} = 0.067$  mm and 0.15 mm. In a water-mixture having nonuniformly sized sediment particles, each grain size will settle at the velocity appropriate to its respective diameter.

## 9.12 CLOSURE

Sediment transport analysis is not an exact science. Even under carefully controlled laboratory conditions there is significant scatter in the data, and field conditions are far more complex. Conditions in reservoirs are more complex than in rivers. Numerical techniques can provide only very approximate estimates of field conditions unless good calibration data are available, which is rarely the case. The quantitative analysis of

cohesive sediments can be particularly challenging. The purpose of these remarks is not to detract from the use of analytical techniques; they constitute the essential foundation of sedimentation engineering. Rather, it is to emphasize the imprecise nature of the results that are to be anticipated, and to emphasize the importance of engineering judgment in the application of numerical methods and interpretation of results.

---

## CHAPTER 10

---

# SEDIMENT DEPOSITS IN RESERVOIRS

---

### 10.1 SIGNIFICANCE OF DEPOSIT PATTERNS

---

Sediment deposition is the principal problem affecting the useful life of reservoirs. Knowledge of both the rate and pattern of sediment deposition in a reservoir is required to predict the types of service impairments which will occur, the time frame in which they will occur, and the types of remedial strategies which may be practicable. Deposition patterns also reflect transport processes in the reservoir and can provide information on sediment delivery and distribution processes that may not be ascertainable from other data. This chapter provides an overview of the types of depositional and erosional patterns which occur in reservoirs and presents basic computational methods related to measuring and predicting deposition.

### 10.2 GENERALIZED DEPOSITION PATTERNS

---

When a tributary enters an impounded reach and flow velocity decreases, the sediment load begins to deposit. The bed load and coarse fraction of the suspended load are deposited immediately to form delta deposits, while fine sediments with lower settling velocities are transported deeper into the reservoir by either stratified or nonstratified flow. A reservoir on a single stream with no major tributaries and operated at a nearly constant high pool level may represent a uniformly depositional environment and represents the simplest sediment deposition pattern. However, even in this case a variety of depositional patterns can occur between one reservoir and another because of differences in hydrologic conditions, sediment grain size, and reservoir geometry. In reservoirs with fluctuating water levels or that are periodically emptied, previously deposited sediments may be extensively eroded and reworked by processes such as downcutting by streamflow, slope failure, and wave action. Further complexity is added when there are significant sediment inputs from tributaries.

Most sediments are transported within reservoirs to points of deposition by three processes: (1) transport of coarse material as bed load along the topset delta deposits, (2) transport of fines in turbid density currents, and (3) transport of fines as nonstratified flow. Because reservoirs typically have long shorelines in relation to their surface area, shoreline erosion and slope failure can also be significant at some sites. The resulting sediment deposition patterns reflect each of these processes. Interpretation of sediment deposition patterns can help determine the transport patterns which are active, especially in the case of density currents which transport sufficient sediment to the dam to produce a distinctive wedge-shaped muddy lake deposit.

### 10.2.1 Depositional Zones

The longitudinal deposition zones in reservoirs may be divided into three main zones as conceptually illustrated in Fig. 10.1. *Topset beds* correspond to delta deposits of rapidly settling sediment. The downstream limit of the topset bed corresponds to the downstream limit of bed material transport in the reservoir. *Foreset deposits* represent the face of the delta advancing into the reservoir and are differentiated from topset beds by an increase in slope and decrease in grain size. *Bottomset beds* consist of fine sediments which are deposited beyond the delta by turbidity currents or nonstratified flow. They may also include autochthonous organic material produced by algae or aquatic plants within the reservoir.

Whereas delta deposits may contain both coarse and fine material, the bottomset beds are characteristically fine-grained. However, tributary inflows, reservoir drawdown, slope failures, and extreme floods can all deliver coarser material into zones where finer-grained material normally predominates, resulting in layering of deposits or localized variations in grain size.

### 10.2.2 Longitudinal Deposit Geometry

Longitudinal deposition patterns will vary dramatically from one reservoir to another as influenced by pool geometry, discharge and grain size characteristics of the inflowing load, and reservoir operation. Deposits can exhibit four basic types of patterns depending on the inflowing sediment characteristics and reservoir operation (Fig. 10.2):

1. **Delta deposits** contain the coarsest fraction of the sediment load, which is rapidly deposited at the zone of inflow. It may consist entirely of coarse sediment ( $d > 0.062$  mm) or may also contain a large fraction of finer sediment such as silt.

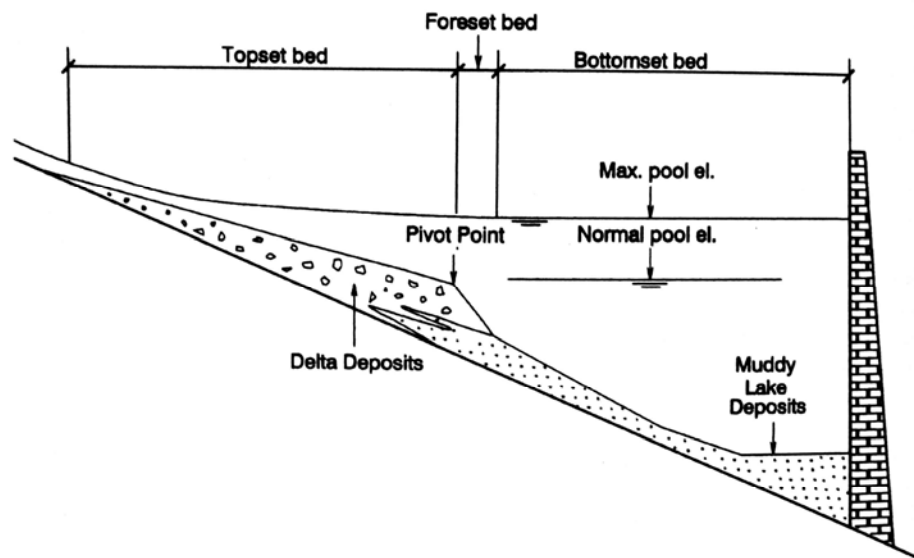
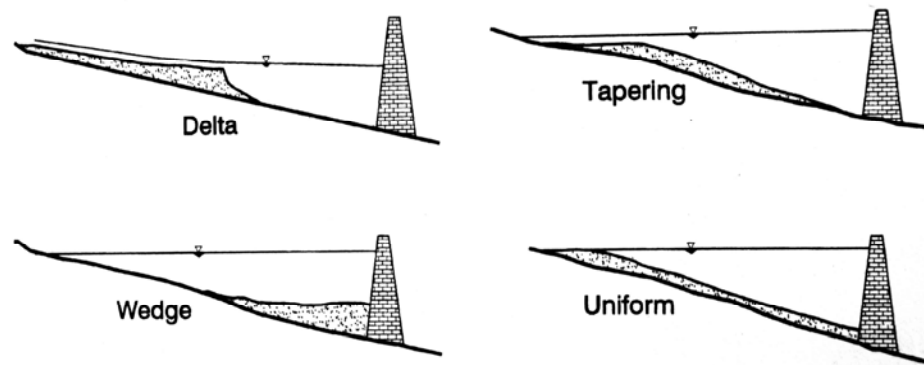


Figure 10.1 Generalized depositional zones in a reservoir.



**FIGURE 10.2** Longitudinal patterns of sediment deposition in reservoirs. Multiple patterns can exist simultaneously in different areas of the same reservoir.

2. **Wedge-shaped deposits** are thickest at the dam and become thinner moving upstream. This pattern is typically caused by the transport of fine sediment to the dam by turbidity currents. Wedge-shaped deposits are also found in small reservoirs with a large inflow of fine sediment, and in large reservoirs operated at low water level during flood events, which causes most sediment to be carried into the vicinity of the dam.
3. **Tapering deposits occur** when deposits become progressively thinner moving toward the dam. This is a common pattern in long reservoirs normally held at a high pool level, and reflects the progressive deposition of fines from the water moving toward the dam.
4. **Uniform deposits** are unusual but do occur. Narrow reservoirs with frequent water level fluctuation and a small load of fine sediment can produce nearly uniform deposition depths.

Reservoirs may exhibit different depositional processes from one zone to another, resulting in a complex depositional pattern, as illustrated in the profile for Sakuma Reservoir in Japan (Fig. 10.3). This figure also illustrates the longitudinal sorting of sediment by grain size.

### 10.2.3 Lateral Deposition Patterns

Sediment deposition is initially focused in the deepest part of each cross section, creating deposits having a near-horizontal surface regardless of the original cross section shape (Fig. 10.4). Where variations from this pattern are observed, it can usually be explained by phenomena such as a local sediment inflow from a tributary, scour at bends, or channel erosion during drawdown and flushing.

Three types of processes can contribute to sediment focusing into the deepest part of the cross section. (1) Turbid density currents transport and deposit sediment along the thalweg. (2) The logarithmic vertical concentration profile within the water column will focus suspended sediment into the deepest part of the cross section. (3) If suspended sediment is uniformly distributed throughout the cross section and settles vertically, sediment deposition will be directly proportional to water depth. This third process would produce a deposit pattern which is much less focused than the patterns normally observed in reservoirs, and indicates the importance of the first two processes in focusing sediment. The relative

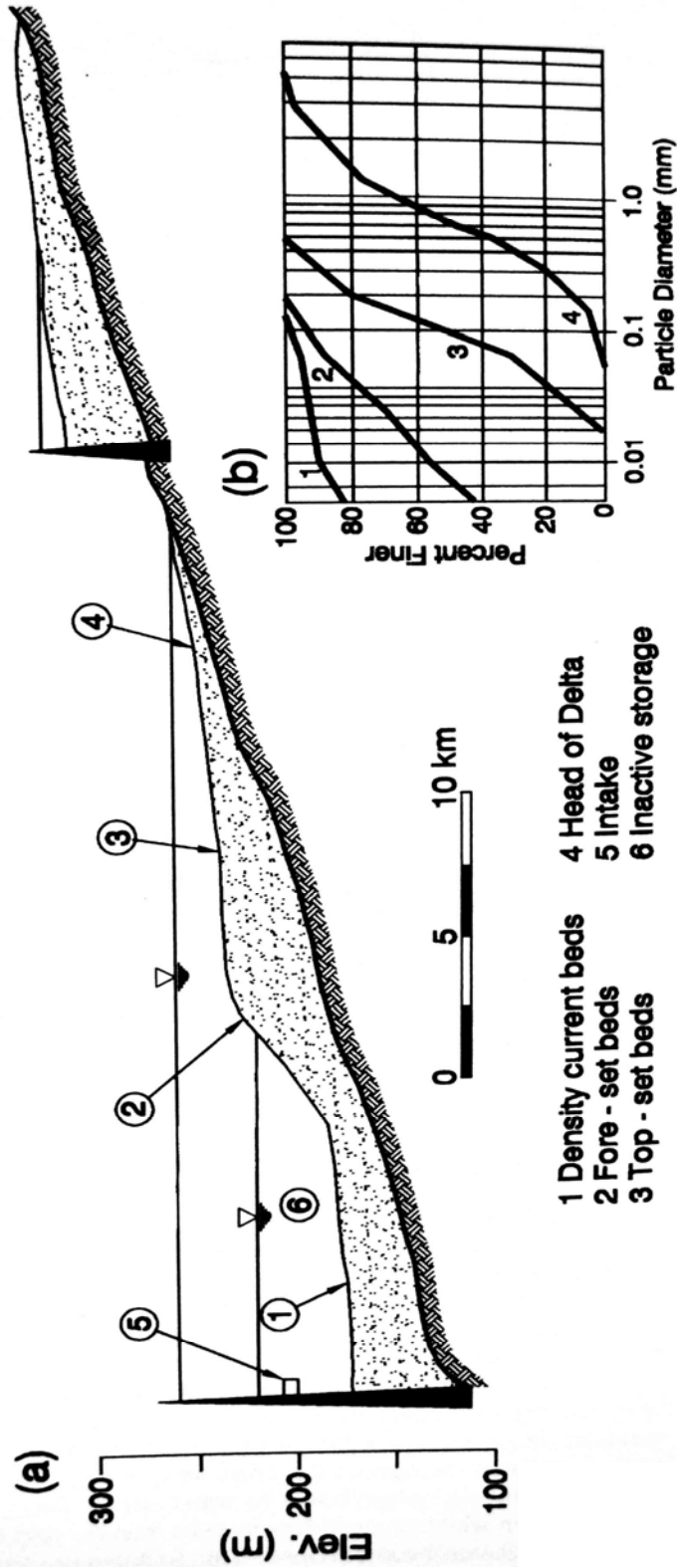
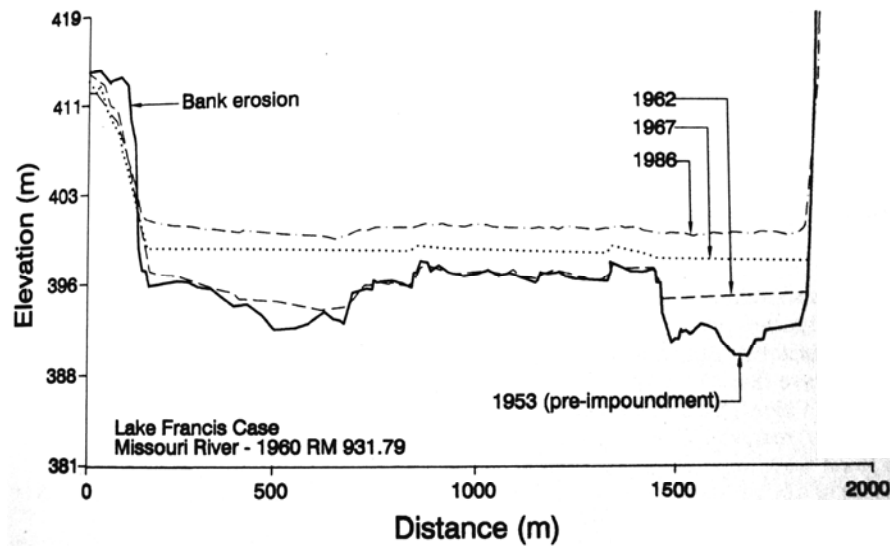


FIGURE 10.3 (A) Longitudinal profile in Sakuma Reservoir, Japan, after 24 years of operation. The thalweg profile shows both delta and turbidity current deposits. (B) Grain size at different points in reservoir (modified from Okada and Baba, 1982).



**FIGURE 10.4** Sediment deposition in Lake Francis Case on the Missouri River. Sediment is focused into the deepest part of the reservoir cross section, creating a flat bottom. Notice that this cross section also shows the impact of shoreline erosion (*Stanley Consultants, 1989*).

importance of these processes will vary from one reservoir to another, but turbid density currents are probably of greater importance in explaining the distribution of fine sediment within a reservoir than has been generally recognized.

#### 10.2.4 Layered Deposits

Sediment is delivered to reservoirs in pulses by large storms, separated by prolonged periods of low flows and smaller events. The pulsed nature of sediment delivery may be recorded in reservoir deposits as alternating layers of coarse and fine sediment. Sediment layers may be either absent or not readily perceptible at the upstream end of the delta, or in areas close to the dam with low sediment loading, but the downstream area of the delta and the upstream zone of the bottomset bed will characteristically have distinct layering. A typical pattern is for lenses of sandy sediment delivered during high inflow to be interbedded between layers of fines deposited during periods of low flow. Layering may be revealed in sediment cores or in areas where channel erosion during drawdown has cut through earlier deposits. Seasonal discharges or accumulation of organic material (seasonal algal blooms or leaf fall from deciduous forests) may also produce a regular sequence of strata. In continuously depositional areas, these sediment sequences may be interpreted to reconstruct the depositional history.

#### 10.2.5 Influence of Regulation Regime

The reservoir operating rule has a large influence on the sediment accumulation pattern, and a change in operating rule can be used to focus sediment deposition. In a pool subject to wide fluctuations in water level, delta deposits at a high pool level can be scoured and redeposited closer to the dam. For example, the rapid advancement of delta deposits

toward Tarbela Dam in Pakistan (Chap. 13) is caused by seasonal drawdown, and one of the sediment management strategies considered at that site is to limit drawdown to focus delta deposition further upstream, thereby delaying adverse impacts on the low level intakes at the dam.

### 10.2.6 Shoreline Erosion and Landslides

Reservoirs generally have long shorelines in relation to their surface area, and in erodible soils shoreline erosion can not only be an important source of sediment loading but it can threaten near-shore structures. Shoreline landslides can be important when a reservoir is first filled, and landslides also represent a special hazard because of the flood wave that can result. The worst disaster of this type was the 1963 landslide at Vaiont (Vajont) Dam in northern Italy, when a massive 240-Mm<sup>3</sup> rock slide fell into the 150-Mm<sup>3</sup> reservoir. The landslide entered the reservoir at a velocity of 30 m/s, creating a flood wave that overtopped the 265-m-tall thin arch dam (the world's tallest) to a depth of 100 m over the spillway crest. Although the dam remained intact, about 2600 people were drowned by the flood wave (Jansen, 1983).

## 10.3 DELTA DEPOSITS

---

Delta deposits may constitute the majority of the sediment accumulation at hydrologically small reservoirs where coarse-grained material predominates, but it is more common for delta deposits to constitute only a small fraction of the total sediment accumulation. However, because delta deposition is focused in the shallow upstream reaches of reservoirs where storage volume is small, even relatively small volumes of deposits can be problematic from the standpoint of upstream aggradation. Delta deposits are also the most visible component of sedimentation.

### 10.3.1 Delta Deposition Patterns

Reservoir deltas have the following basic characteristics (Fan and Morris, 1992a):

1. There is an abrupt change between the slope of topset and foreset deposits.
2. Sediment particles on the topset bed are coarser than on the foreset bed, and there is an abrupt change in particle diameter between topset and foreset deposits.
3. The elevation of the transition zone from the topset to the foreset bed depends on the reservoir operating rule and pool elevation.

In deep reservoirs which have been operated at different levels, distinct deltas may be formed at different water levels. Conversely, in long, narrow reservoirs, the bathymetric profile commonly associated with delta deposits may be absent, but an area characterized by a rapid shift in grain size marking the downstream limit of coarse material deposition may still be present.

Reservoir deltas always grow in the downstream direction, and in some cases their vertical and upstream growth may also be significant. Because the upstream area of the reservoir is shallow and has little storage capacity the longitudinal growth of the delta

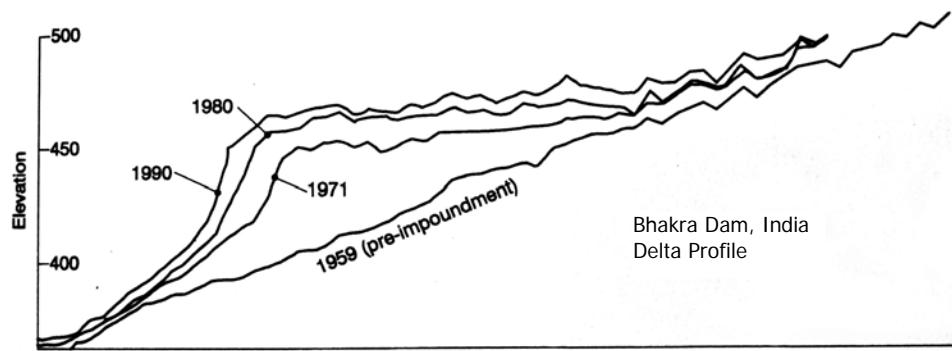


**FIGURE 10.5** Timewise pattern of delta growth upstream of Bhakra Dam, India. The rate of delta advance slows with time because of reservoir geometry, which deepens and broadens in the downstream direction.

may initially be very rapid. At Guanting Reservoir in China, the delta initially progressed downstream at a rate of 3.0 km/yr and simultaneously proceeded upstream at a rate of 2.6 km/yr. As the delta progresses downstream into deeper and wider portions of the reservoir, its rate of longitudinal growth slows. This timewise pattern of delta growth at the Bhakra Dam in northern India is illustrated in Fig. 10.5.

As the delta advances downstream, the topset and foreset deposits prograde over previously deposited bottomset beds of finer sediments. This process can create alternating lenses of coarse and fine material as large events deliver coarse material deep into the impoundment, which may be subsequently overlaid by finer material. In general, fully penetrating cores in an extensively sedimented reservoir will reveal the finest sediment at the bottom, coarsening until the surface level is reached.

Large volumes of sediment deposited in delta areas during periods of flood inflow can be reworked during subsequent periods of drawdown. A remarkable example of delta deposition and the subsequent reworking of these deposits was described at the 85.3-Mm<sup>3</sup> Kulekhani hydropower reservoir in Nepal by Galay and Okaji (1995). During July 1993, the 126 km<sup>2</sup> watershed was affected by a rainstorm with up to 540 mm of precipitation in one day. Slope failures resulting from this storm affected between 4.0 and 9.2 percent of the entire watershed surface area tributary to the dam, and 83 percent of all delivered sediment was estimated to have originated from slope failures within the watershed. This storm delivered about 4.8 Mm<sup>3</sup> of sediment to the reservoir, for a single-event delivery rate of 38,000 m<sup>3</sup>/km<sup>2</sup>. Of this, 2.9 Mm<sup>3</sup> was estimated to consist of fines and the remainder was coarse material.

Coarse material including boulders created a massive delta deposit which extended upstream as the pool level rose during the course of the storm. During drawdown in the subsequent monsoon period, these deposits were reworked and moved downstream, prograding over finer sediment (Fig. 10.6). An oblique aerial photo of the delta deposits exposed at low water is presented in Fig. 10.7, along with a photograph taken on the delta which illustrates the eroding deposits.

Reservoir deltas reflect the interaction between the inflowing stream and the deposited bed material, and the fluvial process affecting deltas is similar to that of an alluvial stream. The bed continuously adjusts to changes in water and sediment inflow and changing base level (the reservoir water level). Stream channels crossing deltas can experience fluvial processes such as meandering, levee formation, channel incision, and armoring. In reservoirs with a fluctuating water level, the pattern of delta development will be heavily influenced by the changing base level and alternating periods of deposition and erosion.

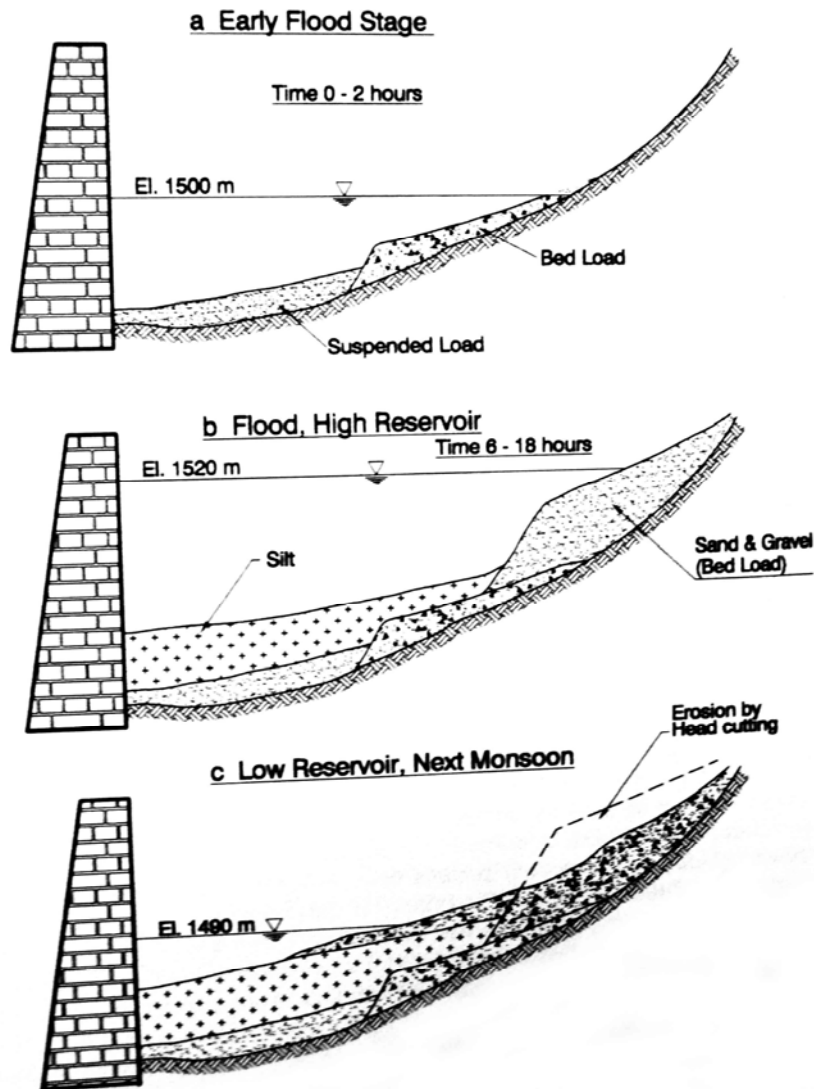


**FIGURE 10.6** Process of sediment deposition and reworking of delta deposits resulting from a massive sedimentation event at Kulekhani Reservoir, Nepal (after Garay and Okaji, 1995).

In lower-gradient environments, the flowing river may meander across the top of delta deposits and, when depositing fines under conditions of stable pool level, the flowing stream can create a fingerlike delta that extends into the reservoir and creates natural levees (Fig. 10.8a), a pattern originally described by Eakin and Brown (1939). Meandering stream platforms also occur on delta deposits as illustrated at Glenmore Reservoir in Fig. 10.8b. The 28-Mm<sup>3</sup> Glenmore Reservoir, built in 1932 to supply water to Calgary, had lost about 10 percent of its total capacity to sedimentation by 1968. Average sediment composition was 35 percent sand, 50 percent silt, and 15 percent clay, and on a volumetric basis about 70 percent of the deposits occurred in the delta area. Gravels were transported about half the distance along the delta as bed load by the stream channel, but the overall volumetric contribution by bed load was considered negligible.

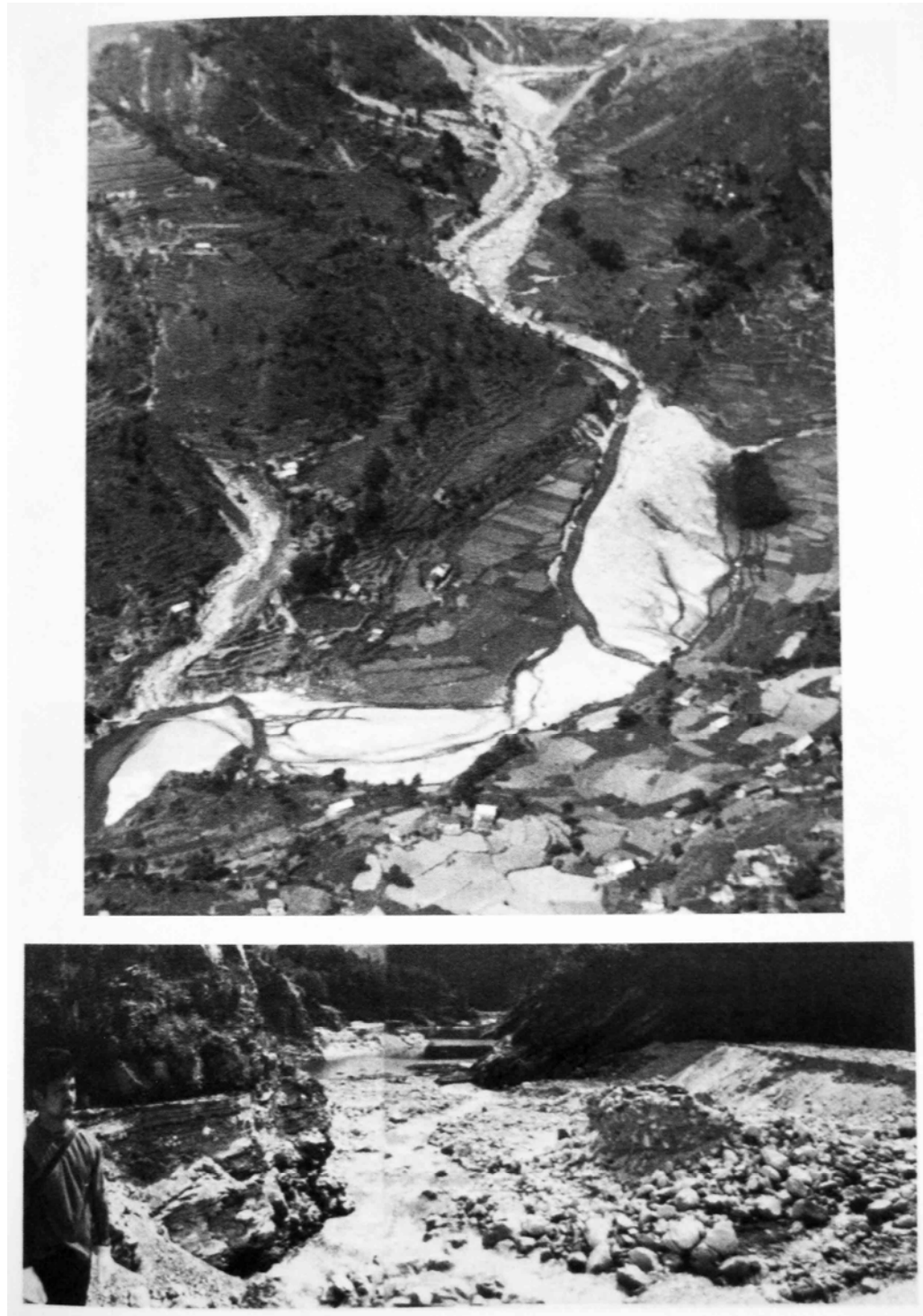
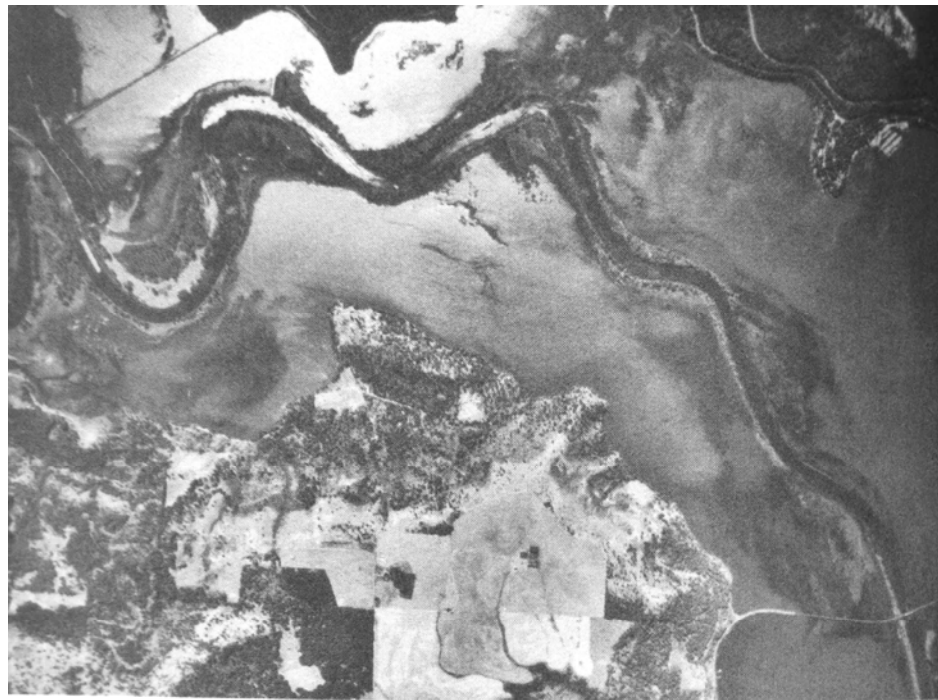


**FIGURE 10.7** Photos of Kulekhani Reservoir, Nepal. The aerial view shows the general extent of delta deposition, and the ground photo illustrates the channel erosion that is reworking deposits farther downstream. Note the large size of the deposited sediment (V. Garay).



(a)



(b)

**FIGURE 10.8** Aerial photographs of meandering channel patterns entering reservoirs. (a) Coew d'Alene Reservoir, Idaho, showing the development of natural levees along either side of the inflowing stream. (b) Glenmore Reservoir, Calgary, Canada, during low pool condition in 1962.

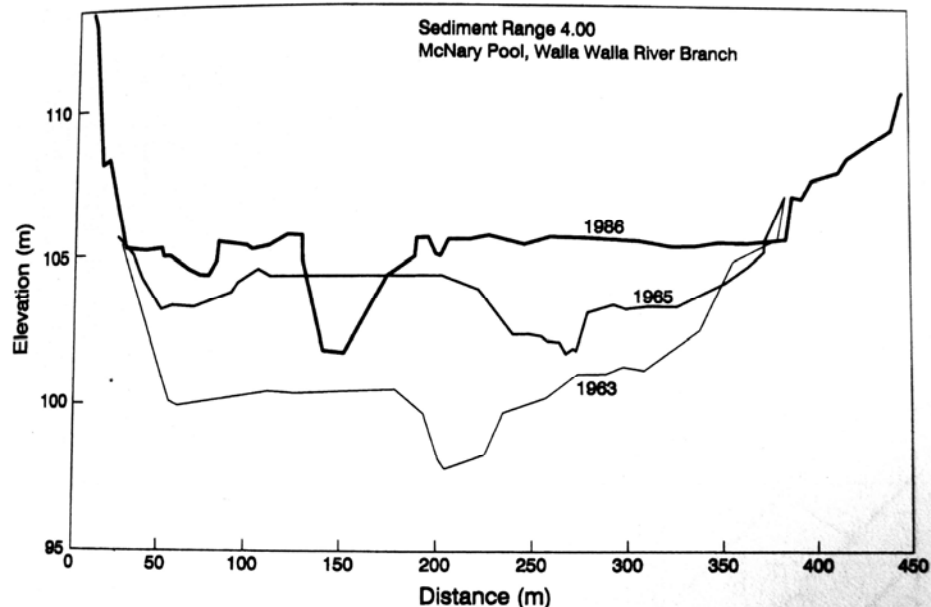


**FIGURE 10.9** Aggradation and lateral channel movement in the area of delta deposition along the impounded Walla Walla River, tributary to McNary Dam on the Columbia River (courtesy U.S. Army Corps of Engineers, Walla Walla District).

The timewise aggradation within the delta reach of the impounded Walla Walla River, a tributary to the Columbia, is illustrated in Fig. 10.9.

### 10.3.2 Slope of Delta Deposits

Knowledge of the slope of delta deposits can be used to predict the extent of delta deposition and consequent rise in flood levels above the reservoir pool. Initially the delta slope will extend upstream from the pivot point defined as the intersection of the topset and foreset beds (Fig. 10.1). In a fully sediment reservoir or debris basin, when the delta deposits extend to the dam, the spillway will define the pivot point. The delta slope is a primary factor determining both the length of upstream aggradation of delta deposits and the volume of sediment that can be stored, and because delta deposits extend upstream at some slope greater than horizontal, a fully sedimented dam can store much more sediment than water. This is an important consideration in estimating the amount of sediment that can be trapped in debris basins, including heavily sedimented reservoirs that may be relied on to reduce sediment yield at downstream reservoirs.

Data from reservoirs in the United States has shown that the slopes of delta deposits range from a relatively flat 20 percent of the original stream slope to nearly 100 percent of the original stream slope (Fig. 10.10). In many reservoirs the top slope of the delta will be about half of the original streambed slope (Borland, 1971), and this is often used as a rule of thumb. However, because a wide range of delta slopes can occur under different conditions, the U.S. Army Corps of Engineers (1989) specifically warns against using rule of thumb values for estimating delta slopes. Numerical modeling is recommended as the most effective method for predicting the ultimate topset slope. Empirical relationships can be useful for estimating slope only when applied to reservoirs having geomorphic and operating conditions similar to the sites used in the empirical dataset.

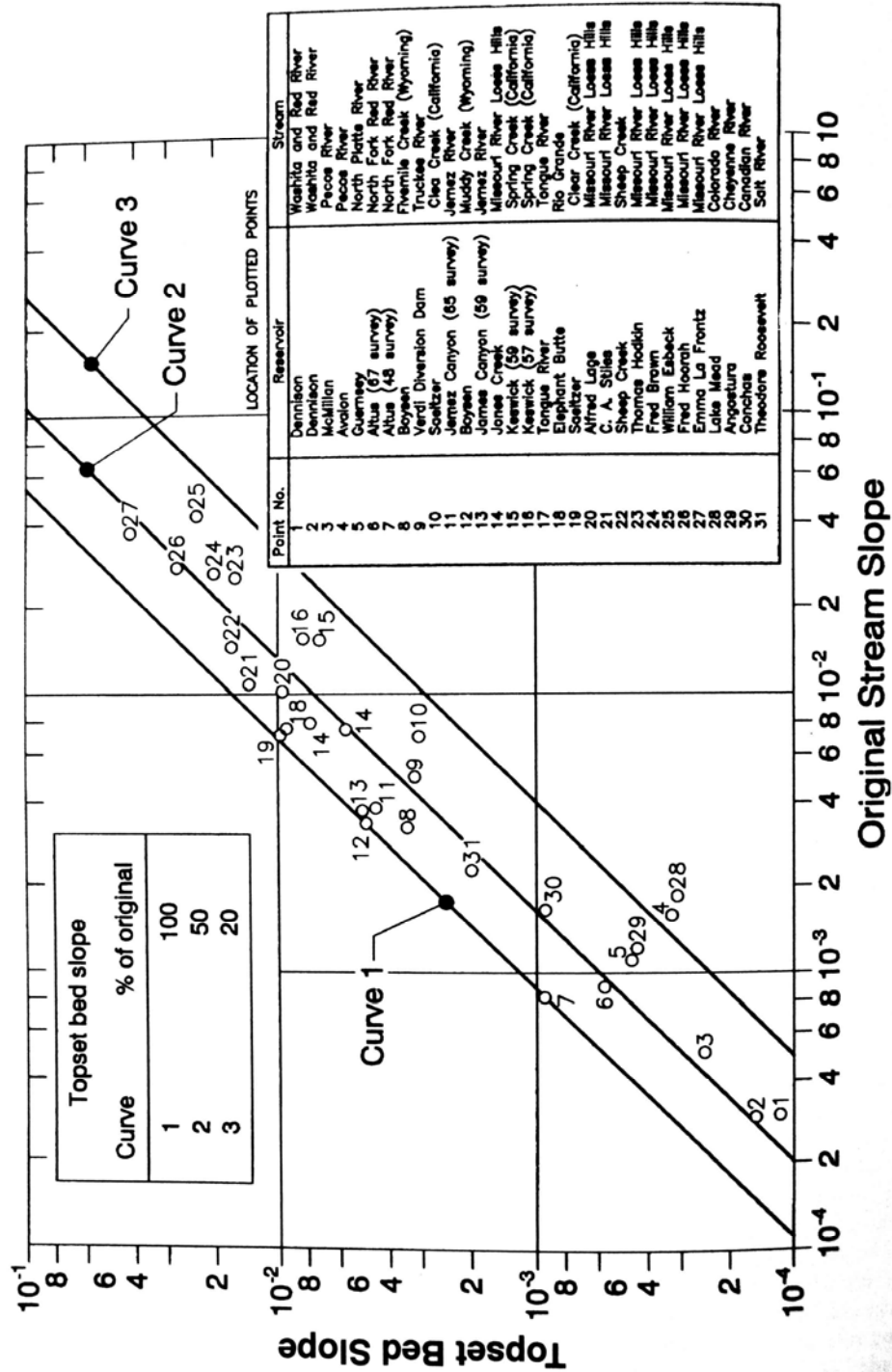


FIGURE 10.10 Topset slope versus original stream slope from existing reservoirs (Strand and Pemberton, 1987).

### 10.3.3 Foreset Slope

Foreset slope is often estimated from empirical relations, but this method is not particularly accurate unless the empirical relationship is derived from similar reservoirs. For example, Strand and Pemberton (1987) report that the average of foreset slopes observed in Bureau of Reclamation reservoir resurveys is 6.5 times the topset slope, but some reservoirs exhibit a foreset slope an order of magnitude greater than this. For example, the foreset slope of the Lake Mead delta is 100 times the topset slope. In contrast, reservoirs on rivers in China with a heavy silt load have foreset slopes about 1.6 times the original river bed slope (Wuhan College of Hydropower, 1982). Generally, deltas composed of coarse granular material (sand, gravel) will have a steep foreset slope, whereas deltas containing fine-grained material will have much lower slopes. Similar patterns are observed in river deltas discharging to the ocean. Sandy sediment that accumulates at the mouth of Rio Senegal has a subaqueous slope of about  $S = 0.017$ , nearly 30 times steeper than the fine-grained Mississippi delta with  $S = 0.0007$  (Coleman, 1982).

## 10.4 MEASUREMENT OF DEPOSITION RATE

---

The rate and pattern of reservoir sedimentation is normally documented by comparison of periodic surveys performed by either the range or contour method. However, alternative methods for estimating volume change or deposition rate may be useful or necessary in some circumstances.

### 10.4.1 Sediment Mass Balance

The amount of sediment deposited in a reservoir can be estimated from the difference between fluvial sediment inflow and discharge over either a short (single-event) or a long time frame. This technique is essential for obtaining detailed information on the process of sediment delivery and trapping in the reservoir, and for evaluating and monitoring the effectiveness of different sediment management techniques. However, reliable long-term results are difficult to obtain, and a mass balance should not be relied on as the sole means of estimating the rate of sediment accumulation and storage loss. A sediment mass balance should always be checked with reservoir surveys.

### 10.4.2 Horizon Tracing Using <sup>137</sup>Cesium

The rate of sediment accumulation can be determined by measuring the depth of deposition above an identifiable and datable horizon. One such horizon is the layer of radioactive <sup>137</sup>cesium which was deposited worldwide by atmospheric nuclear testing. The <sup>137</sup>cesium isotope does not occur naturally; it first appeared in measurable amounts in 1954 and increased rapidly as a result of fallout from Russian nuclear tests from 1962 through 1964. Because it remains tightly adsorbed into the clay lattice structure in freshwater environments, <sup>137</sup>cesium remains in the top layer of soil and can be used to trace surface sediment as it is eroded and redeposited. <sup>137</sup>Cesium emits gamma radiation which can be measured directly in samples, and with a 30-year half-life, it will be possible to measure <sup>137</sup>cesium content of soils and sediment deposits for some years to come. Radioactive cesium is not found in sediments deposited prior to 1954, and peak values occur around 1964, producing two datable layers in the profile. Because the absolute magnitude of <sup>137</sup>cesium counts will vary from one site to another, and as a function of clay content in the

deposits, the method requires that older sediments be deposited below the datable layer to detect the horizon created by the relative increase in activity.

The procedure for dating reservoir sediments based on  $^{137}\text{cesium}$  has been described by McHenry and Ritchie (1980). In reservoirs, an 8-cm-diameter sediment core is extracted and sectioned into increments of 5 to 10 cm. Composites of each depth increment are made if multiple cores are required to obtain adequate sample material. The samples are dried and gamma emissions are counted. Once the depth of the datable layer is located, the rate of sediment accumulation can be determined from the depth to the bottom of the cesium-contaminated layer. The  $^{137}\text{cesium}$  technique can also measure the recent rate of sediment accumulation in natural lakes which may not otherwise have a datable horizon, unlike reservoirs which have an identifiable preimpoundment bottom. For example,  $^{137}\text{cesium}$  has been used to measure modern sedimentation rates in natural lakes along the Mississippi River (Ritchie et al., 1986; McIntyre et al., 1986).

Cesium dating has also been used to monitor soil erosion and to date surface deposits, as reviewed by Walling and Quine (1992).  $^{137}\text{Cesium}$  dating has been used in combination with erosion pins to study sediment movement on hill slopes (Saynor et al., 1994), and to determine rates of valley and channel sedimentation (Whitelock and Loughran, 1994).  $^{134}\text{Cesium}$ , which was not present in bomb fallout, was released by the Chernobyl accident in 1986 and has been used to investigate the rate of floodplain deposition in Europe (Froehlich and Walling, 1994).

### 10.4.3 Sub-bottom Profiling

A sub-bottom profiler is a sonic depth measurement system which combines a high-frequency signal in the 200-kHz range which reflects off a soft bottom and a lower-frequency signal in the 5- to 24-kHz range which will penetrate deeper and reflect from a denser horizon consisting of original soil or rock. Under favorable conditions, sediment thickness exceeding 10 m can be measured. The ability to obtain useful data from sub-bottom profiling is site-specific. In particular, sonic energy is strongly reflected from water-gas interfaces, and the presence of methane gas bubbles produced by the anaerobic decomposition of organic material in the sediment can make it impossible to obtain readings from the original bottom at some sites (as in the Cachi case study). Where conditions permit its use, this technique can rapidly map sediment thickness without knowledge of the original bottom topography.

### 10.4.4 Spud Surveys

The spud survey method is a simple manual technique for measuring the total depth of sediment accumulation. Developed in 1934 and described by Eakin and Brown (1939), the spud method can be used to determine the location of the original bottom and the thickness of sediment deposits, without prior knowledge of the original bottom contour. Because sonic sub-bottom profiles are confounded by gas layers that may occur in sediment deposits, the spud may be used to measure sediment depth in situations where sonic techniques fail. As a limitation, the spud method works only in soft sediments, generally consisting of fines not exposed to air drying and with a maximum thickness of about 4 m.

A spud is a case-hardened steel rod about 2 to 3 m long and about 3 to 4 cm (1 $\frac{1}{4}$  to 1 $\frac{1}{2}$  in) in diameter into which outward-tapering grooves have been machined at regular intervals (Fig. 10.11). The Natural Resource Conservation Service (no date) recommends a sectioned spud that can be assembled up to 5 m in total length to facilitate transport and also notes that a reinforcing bar having a rough coating of concrete to facilitate silt retention may be used.

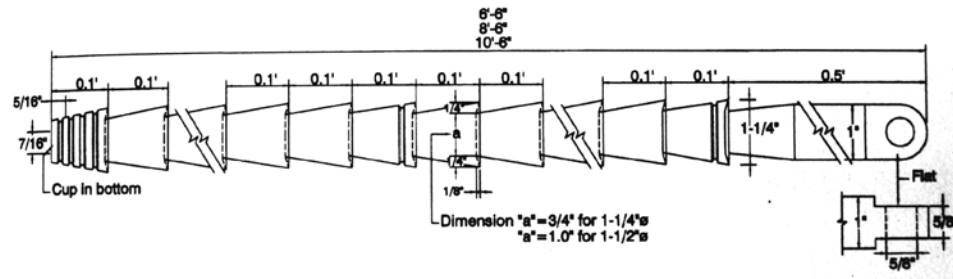


**FIGURE 10.11** Configuration of spud to determine the thickness of soft sediment deposits (*Eakin and Brown, 1939*).

The spud is cast or allowed to fall vertically through the water with force sufficient to penetrate the deposited sediment and into the underlying original soil material, or it is driven by hand in water too shallow for a boat. After the spud depth (spud plus line length) is noted, it is lifted slowly so as not to wash out the sediment captured in the grooves, and it is examined to determine the depth to the pre-impoundment bottom based on a change in texture, color, presence of roots, etc. The depth to the top of the sediment deposits is simultaneously determined by using a sounding weight, and deposit thickness is determined by subtraction. Under favorable conditions, a spud can penetrate sediment a meter or so deeper than its total length. This method is most applicable to water depths less than 30 m, but by coating the bar with heavy grease prior to each measurement to minimize sample washout during recovery, the spud has been used successfully in water up to 60 m in depth (Castle, 1963). The accuracy of the method depends on the operator's experience and skill in determining the depth to the original bottom on the basis of the samples collected in the grooves, but this skill can be rapidly learned (Ritchie and Henry, 1985). In dry reservoirs sediment thickness can be determined by angering.

#### 10.4.5 Sedimentation Plates

Flat plates can be placed at distinct points on the bottom of a reservoir, and the deposit depth over the plates can be subsequently measured at intervals. Flat plates have the advantage over sediment traps in that they do not pose any type of obstruction to the horizontal flow of water or concentrated muds near the bed. In areas where the rate of sediment accumulation is low, on the order of centimeters per year or less, it may be difficult to estimate sedimentation rates from small differences in the surveyed topography across an undulating bed. Sedimentation plates provide a stable datum against which small amounts of sedimentation can be measured on a repeated basis. The plates can be located after they have become buried by sediment by means of wands or posts, electronic surveys, global positioning system, or metal detectors. A magnet can be buried with nonmetallic plates to aid location by a detection device. Sedimentation plates are best suited for use in areas of reservoirs which are periodically drawn down, allowing plates to be set out and remeasured on the dry reservoir bed. As a disadvantage, the setting out and recovery of data from sedimentation plates is labor-intensive. They can provide a general picture of sedimentation rates, but if used should supplement rather than replace reservoir surveys.

## 10.5 RESERVOIR CAPACITY SURVEYS

---

Repeated reservoir capacity surveys are used to determine the total volume occupied by sediment, the sedimentation pattern, and the shift in the stage-area and stage-storage curves. By converting to sediment mass on the basis of estimated or measured bulk density, and correcting for trap efficiency, the sediment yield from the watershed can be computed.

### 10.5.1 Types of Surveys

Reservoir surveys are classified as either contour surveys or range surveys. *Contour surveys* use more complete topographic or bathymetric information to prepare a contour map of the reservoir. They are the most accurate technique for determining volume and also provide the most complete information on sediment distribution. Recent advances in automated survey techniques now make hydrographic contour surveying very economical in smaller and midsize reservoirs, which may require only a few days of field time using automated depth measurement and positioning systems to perform the tightly spaced data-collection traverses required by contouring software.

The *range method* uses a series of permanent range or cross-section lines across the reservoir which are resurveyed at intervals and used to compute the intersurvey volume change in each reach by geometric formulas. Hydrographic survey techniques are used for submerged areas, and standard land surveying or photogrammetric techniques are used above the water level. Range surveys are faster and more economical to perform than contour surveys because field data requirements are greatly reduced compared to contour surveys. They have historically been the most commonly employed technique to monitor sedimentation, but are increasingly being supplanted by automated contour surveying methods. Range surveys are well-suited for tracking changes in storage as a result of sedimentation, with a minimum of field time. Best results are obtained if contour survey methods are used to accurately determine the volume bounded by adjacent range lines, and range end areas are then correlated to this volume. The range method is subsequently used to track changes in storage based on the changes in range geometry. The *constant factor* and *width adjustment* methods are based on this principle.

### 10.5.2 Survey Intervals

The reservoir survey interval should be based on individual site characteristics. At reservoirs losing capacity very slowly, a survey interval on the order of 20 years or even longer may be adequate. By contrast, at important sites which are losing capacity rapidly, or where the impact of sediment management is being evaluated, a survey interval as short as 2 or 3 years might be used. Deposits should be surveyed and sampled after a major flood which has a significant impact on the reservoir or which may provide information for subsequent model calibration, as described in the Feather River case study (Chap. 22). A reservoir should also be surveyed as soon as a new reservoir is closed upstream to provide a baseline for computation of the new sedimentation rate from the reduced area of uncontrolled drainage.

Sedimentation rate is computed as the difference between volume measurements from two surveys. The minimum survey interval depends on the precision of the survey technique and the rate and pattern of storage loss. For instance, if a survey technique incorporates an error on the order of 2 percent of the total reservoir volume, and if the reservoir is losing capacity at 0.25 percent per year, a 4-year survey interval may be too

short to produce reliable information unless most sediment inflow is focused into a small portion of the impoundment. The Cachí case study describes the unusual situation in which a 1-year reservoir survey interval was used. To produce the required level of precision for comparing the two surveys, the change in depth (i.e., change in sediment thickness) was computed for only those points in the two bathymetric datasets which were considered to be exactly coincident in the horizontal plane. Also, at Cachí most sediment deposition was focused along the flushing channel, producing localized deposition depths exceeding 1 m between the two survey dates.

### 10.5.3 Survey Techniques

A bathymetric or hydrographic survey is performed with sonar operating in the 200-kHz range from a moving boat. Current systems typically include real-time positioning systems, data logging onto a portable computer, and postprocessing software for the preparation of digital maps.

If a reservoir is emptied or substantially drawn down, photogrammetric techniques or airborne laser can be used to map the above-water contours.

In a reservoir subjected to a wide range in stage or which is regularly emptied, aerial photography can be repeated at different water levels, measuring the pool surface area at each level to generate the elevation-area relationship for the reservoir. In large reservoirs, the pool area at different water levels can be determined from satellite images. When the inflow and discharge from a reservoir is accurately measured during drawdown, a stage-volume relationship may be constructed from the net volume of water released and the change in water level.

### 10.5.4 Survey Errors

All techniques for estimating reservoir volume incorporate errors. In sedimentation surveys, the objective is to accurately measure the *difference* between successive surveys. This makes computation of sedimentation rate extremely sensitive to small errors in volume estimates, especially when the volume changes are relatively small because of a short intersurvey period or low sedimentation rate, or when reservoirs are new and have not yet lost a significant percentage of their total volume. Errors of only a few percent in the total volume estimate can produce errors of several tens of percent in the computed sedimentation rate. With the range method, volume estimates can vary as much as 10 percent in small reservoirs, depending on the computational method, quantity, and orientation of ranges (Heinemann and Dvorak, 1963). Volumetric differences up to 30 percent along individual reaches have been reported by Murthy (1977), depending on the range computational procedure used. When range methods are used it is essential that range tracks be resurveyed as accurately as possible so that the profile changes represent sediment deposition rather than a meandering survey line. It may not be possible to exactly relocate range lines, and it will then be impossible to exactly reconstruct the original survey lines, resulting in resurveyed ranges having significantly different top widths at the "same" station. Identical computational methods must be used for each survey.

When the reservoir survey technique is to be changed (e.g., from range to contour), the new survey data should be used to compute the volume by both the old and the new techniques to determine the bias between the two methods. This bias can then be used to adjust volumetric estimates prepared at different times in the reservoir life, producing a consistent volumetric time series for estimating sedimentation rate. Changes in the pool level

due to gate modifications should be adequately documented, and, when they occur the entire data series of reservoir volumes should be retabulated for a consistent pool level. In reservoirs with poorly consolidated sediments, the bottom may not be distinct, and submerged forests or other vegetation will also complicate location of the true bottom. Fathometers must be calibrated properly to compensate for the effects temperature stratification and depth of transducer submergence.

### 10.5.5 Reporting

The usefulness of sedimentation studies to workers attempting to manage sedimentation depends heavily on the completeness of the reporting. Recommended contents for a sedimentation report are outlined by Blanton (1982):

General information on the dam, reservoir, and drainage basin.

1. Information on all surveys at the reservoir, past and present.
2. Description of the survey and sampling techniques for the present survey and of special techniques employed.
3. Reservoir map showing all range line locations.
4. Description of all major survey controls, together with a table listing horizontal and vertical control information.
5. A graph showing the reservoir stage fluctuation or stage duration curve.
6. Profiles of all reservoir and below-dam degradation ranges showing the latest survey superimposed on the original profile, and in some instances plots from selected prior surveys.
7. Graphs of sediment distribution in longitudinal profile, in percent depth versus percent sediment volume and in percent depth versus percent distance from the dam.
8. Data in tabular and graphic form describing sediment densities and particle sizes and a map of sampling sites.
9. Revised area and capacity tables and curves resulting from the new survey.
10. Any data on sediment inflow and outflow which may be available for estimating trap efficiency.

The inclusion of these data will greatly facilitate understanding of the sedimentation process. As appropriate, summary data should also be submitted to regional or national databases.

## 10.6 CONTOUR SURVEYS

---

### 10.6.1 Contour Survey Methods

The preferred method for performing reservoir contour surveys is using automated hydrographic surveying equipment. Description of a reservoir contour survey by automated hydrographic survey techniques is given by Webb and Gómez-Gómez (1996). Surveying technology is advancing rapidly, and a variety of computerized hydrographic survey systems are available commercially, such as the portable system shown in Fig. 10.12. A typical system consists of a real-time positioning system such as the differential Global

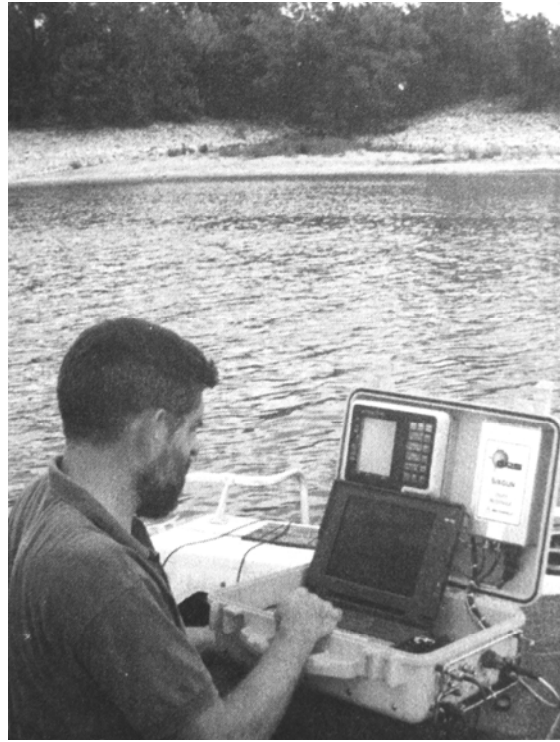


**FIGURE 10.12** Use of portable automated hydrographic survey equipment (*courtesy of Specialty Devices, Inc.*).

Positioning System (GPS) or microwave equipment (range-range or range-azimuth) and a single-beam fathometer operating in the 200-kHz range, which together define the absolute  $x$ ,  $y$ ,  $z$  coordinates of the reservoir bottom during traverses. Typical accuracies are about 0.1 m in depth and from several centimeters to several meters in the horizontal plane, depending on the positioning system used. The data file is post-processed to generate range profiles or a contour plot of the entire reservoir. For the preparation of a contour map, the network of traverses should be much denser than in traditional range survey methods, and manual manipulation should be anticipated to create the final contour map. Closely spaced traverses will minimize interpolation problems during postprocessing, since contouring algorithms perform better as data density increases. In general, for contouring the distance between traverses should be significantly less than the shore-to-shore traverse length to minimize interpolation errors.

Automated survey systems have several important advantages over conventional methods. Large amounts of survey data can be collected rapidly and economically and to a high level of accuracy. Reliance on range markers is eliminated by navigational systems referenced to an absolute coordinate system. Preplanned track lines can be specified, and the system will display real-time navigational instructions to the pilot, greatly facilitating the accurate repositioning of lines when ranges are to be resurveyed. All position and depth data are continuously recorded into a file which can subsequently be postprocessed to plot survey results and automate tedious volume computations. By overlaying bathymetric maps from different survey dates, maps of net depth of deposition or scour can be generated. The hydrographic survey should be performed when the reservoir is at a high water level. Areas above water must be

surveyed by either traditional or photogrammetric methods and merged with the hydrographic survey data.

### 10.6.2 Volume Computations from Contour Data

By using the *stage-area curve method*, the area of each contour within the reservoir pool is determined and used to plot the stage-area curve. The volume between any two adjacent elevations can be determined by integrating the area under the stage-area curve with a planimeter or by trapezoidal approximation, and the resulting volumes summed to create a stage-storage curve.

For computing volumes from contour data, two methods are available for determining the volume between each successive pair of contour lines. The *average contour area method* should be used between range lines, which produces contour surface areas that increase only as a function of reservoir width, while the reach length is constant for all elevations. The equation is

$$\text{Volume} = \frac{H(A_1 + A_2)}{2} \quad (10.1)$$

where  $H$  = elevation difference between adjacent contour lines and  $A_1$  and  $A_2$  are the surface areas enclosed by each contour line.

When surface area increases as a function of two dimensions, length and width, a more accurate estimate of the enclosed volume is obtained by the *modified prismoidal method* in which

$$\text{Volume} = \frac{H[A_1 + (A_1A_2)^{1/2} + A_2]}{3} \quad (10.2)$$

where the symbols are the same as before. Additional computational algorithms are provided in commercial software packages for use with digital mapping.

## 10.7 RANGE SURVEYS

The *range method* has traditionally been the most widely used method to measure reservoir sedimentation. It provides the means to efficiently track sediment accumulation with a minimum of field data. When sediment thickness is known along range lines, the range methods can also be used to compute sediment volumes directly. Methods of computing reservoir volume from ranges are summarized in Vanoni (1975), Strand and Pemberton (1987), Heinemann and Dvorak (1963) and Natural Resources Conservation Service (no date).

### 10.7.1 Location of Ranges

Sedimentation ranges should be laid out both upstream and downstream of a new dam, the upstream ranges to monitor sediment accumulation and the downstream ones to monitor degradation. Below the dam, grain size data should be sampled at each range and at each survey date, to document changes in bed composition. Photography may also be used to document streambed condition. A typical pattern of range locations above the dam is shown in Fig. 10.13, and recommendations for the location of ranges have been adopted from Blanton (1982):

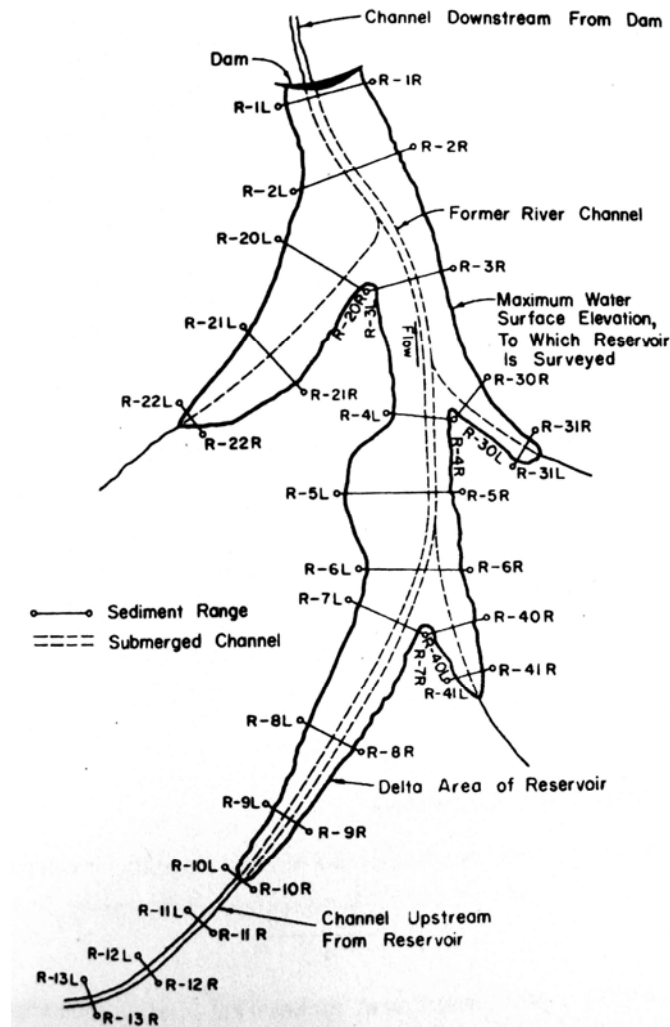


FIGURE 10.13 Location of ranges for measurement of reservoir sedimentation (Borland, 1971)

- Establish range lines perpendicular to the reservoir or tributary axis at locations such that average conditions in the intervening reach will be accurately represented by the average of the two bounding ranges.
- Locate ranges across the mouth of each principal arm or tributary, with additional ranges extending upstream as along the main stem.
- The most downstream reservoir range should be located immediately upstream of the toe of the dam.
- Spacing between ranges may be closer in the delta or areas of special interest, and ranges should also be located at structures or other features that are particularly sensitive to sediment impacts.

Range lines should extend to the anticipated aggradation limit above the pool level, and downstream degradation limit. By convention, range lines are normally assigned numbers

or stations that increase moving upstream, and range lines should be plotted from left to right when looking downstream.

The number of ranges depends on reservoir size and geometry, with a minimum of three ranges required for even the smallest impoundment. As a rough guide, the average number of ranges used by the Bureau of Reclamation in 57 reservoirs from about 30 to 15,000 ha in surface area is given by

$$\text{Number of ranges} = 2.942 A^{0.3652} \quad (10.3)$$

where  $A$  = reservoir surface area, ha. The exponent value is 0.2875 for  $A$  in acres. This relationship provides only a very approximate guideline, as there is considerable scatter in the data. For instance, reservoirs with a surface area around 500 ha had from 12 to 60 ranges (Blanton, 1982).

### 10.7.2 General Considerations for Computing Volumes from Ranges

Several methods are available to compute volumes from ranges. Each of these methods may be applied to range end areas for either water depth or sediment thickness, to respectively compute capacity or sediment accumulation within each reach. Because each computational method will produce different results, it is essential that identical computational methods be used along each reach for each survey so that the changes in the computed volume represent sedimentation rather than differences in computational technique. Automated surveying techniques used for contour surveys are also applicable to range surveys and can largely eliminate errors due to displacement of range lines during data collection.

### 10.7.3 Computing Range End Areas

The end area between adjacent sounding points along a range line is computed by

$$E = \frac{L(D_1 + D_2)}{2} \quad (10.4)$$

where  $D_1$  and  $D_2$  are the depths (or sediment thickness) at adjacent sounding points separated by interval length  $L$ . The total end area of a range line is the sum of the segment end areas so computed. When soundings are approximately equally spaced, the following formula may be used to compute the total end area of the entire range, or along a segment of a range having equally spaced sounding intervals

$$E = L \left( \frac{D_1}{2} + D_2 + D_3 + \dots + \frac{D_n}{2} \right) \quad (10.5)$$

where  $L$  is the equally spaced sounding interval along the range. As is evident, computations are greatly simplified when the spacing between sounding points is uniform.

### 10.7.4 Average End Area

The simplest volume computation method is the average end-area method:

$$\text{Volume} = \frac{L(E_1 + E_2)}{2} \quad (10.6)$$

where  $L$  = length between ranges and  $E_1$  and  $E_2$  are the cross-sectional end areas of the ranges bounding the downstream and upstream limits of the reach. To obtain accurate results with this method requires that the cross sections extend perpendicular across the pool and tributary arms at points representative of the reservoir cross-section area. Because reservoirs commonly have an irregular shape and range lines may not be located in areas representative of the average reservoir cross section, large inaccuracies may result by multiplying the average range end area by the reach length.

### 10.7.5 Surface Area—Average End Area

A more accurate estimate of the volume bounded by ranges may be obtained by using average end areas and top widths to determine the mean water depth below normal pool, and multiplying mean depth by the intervening surface area. It is assumed that the average depth at the ranges is representative of the average depth across the intervening pool area. The equation is

$$Volume = \left(\frac{A}{2}\right) \left(\frac{E_1}{W_1} + \frac{E_2}{W_2}\right) \quad (10.7)$$

where  $A$  = pool surface area between ranges with end areas  $E_1$  and  $E_2$  and top widths  $W_1$  and  $W_2$ .

If there is only one range in a segment, such as will occur above the most upstream range along each tributary, locate a point at the upstream limit of the tributary and treat it as a range line having zero cross-sectional area ( $E_2 = 0$  and  $W_2 = 0$ ). For the reach between the most downstream cross section and the sloping face of an embankment dam, compute the volume by:

$$V = A \left(\frac{E}{W}\right) - V_0 \quad (10.8)$$

where  $V_0$  is the volume displaced by the upstream face of the dam.

#### 5.1.1. Constant Factor Method

The constant factor method (Burrell, 1951; Borland, 1971) is a range method in which a constant factor relationship is computed between the range end areas and the total volume in each segment. It has the advantage of a high level of precision for computing the incremental volume loss due to sedimentation, and also computes volume loss as a function of elevation, allowing the stage-capacity relationship to be revised.

To apply this procedure first compute the volume and range end areas for each reach and for each elevation increment, based on a contour survey. The constant factor is then computed as

$$C_0 = \frac{V_0}{E_0} \quad (10.9)$$

where  $V_0$  = original capacity of the reach,  $E_0$  = original sum of end areas for the reach, and  $C_0$  = constant factor. In practice, this means that once the volume of a segment has been computed, the new volume may be computed following sedimentation by applying the constant factor to the new end areas computed within each elevation increment. The change in the volume of sediment deposits is determined by applying the constant factor to the change in the end area between surveys:

$$V_s = C_0 E_s = C_0 (E_0 - E_1) \quad (10.10)$$

where  $E_0$  is the sum of end areas from the original survey and  $E_1$  is from the subsequent survey,  $V_s$  = sediment volume deposited in (or scoured from) the reach, and  $E_s = (E_0 - E_1)$  = sum of sediment end areas bounding the reach.

This method is illustrated with computations for the reach between ranges 3 and 4 at Panchet Hill Reservoir in India (Table 10.1). Columns 1 to 5 are data from the original survey, and the constant factor  $C_0$  in column 6 is computed from  $C_0 = V_o/E_0$  using data in columns 4 and 5 for each depth increment. The new end areas are obtained from subsequent survey and are summed in column 9. The sum of sediment end areas is computed as  $E_s = E_0 - E_1$ , the sediment volume is computed as  $V_s = C_0 E_s$ , and the new capacity is computed as  $V_1 = V_0 - V_s$ .

### 10.7.7 Width Adjustment Method

The width adjustment method (Blanton, 1982) is a range method used by the Bureau of Reclamation and derived from the constant factor described previously. To use the constant width method the new contour area  $A_1$  between two ranges is computed for an adjustment factor defined as the ratio of the new average width to the original average width for both the upstream and downstream ranges at the specified contour. The computational basis for a single depth increment within a reach is illustrated in Fig. 10.14. After all reaches have been computed, the reach areas at each contour elevation are summed across the entire reservoir to construct the revised stage-area curve.

## 10.8 RESERVOIR RELEASING AND TRAPPING EFFICIENCY

---

The *sediment release efficiency* of a reservoir is the mass ratio of the released sediment to the total sediment inflow over a specified time period. It is the complement of trap efficiency:

$$\text{Release efficiency} = 1 - \text{trap efficiency} \quad (10.11)$$

Churchill (1948) based his empirical relationship on the concept of sediment releasing, whereas Brune (1953) used the concept of sediment trapping which has come into more common use. However, sediment release efficiency is the more useful concept from the sediment management standpoint because it can also be used to evaluate flushing, which can release more sediment than enters, thereby producing a release efficiency in excess of 100 percent. If expressed in terms of trap efficiency, this would yield a negative value, which is difficult to conceptualize. Because the sediment trapping or releasing efficiency can be computed over any time period (e.g., single-event or long-term) the time frame should be specified.

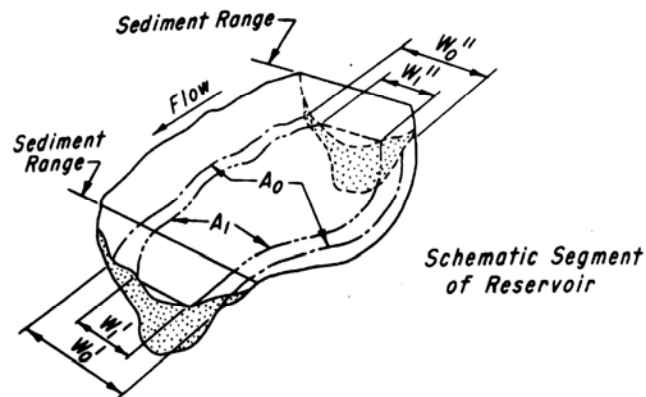
Both Brune's and Churchill's empirical relationships have been widely used and found to provide reasonable estimates of long-term releasing or trapping efficiency, but Borland (1971) notes that the Churchill method is more applicable for estimating sediment retention in desilting and semidry reservoirs. Both methods are based on the ratio of volume to inflow, and neither method specifically considers features such as the grain size of the inflowing sediment load and the outlet configuration. The effects of reservoir operation are included only to the extent that they are reflected in the selection of the operation are included only to the extent that they are reflected in the selection of the pool volume use in the computations. Judgment is required to adjust these methods to specific conditions. For instance, Frenete

**TABLE 10.1** Sample Computation for Constant Factor Method along a Reach of Panchet Hills Reservoir, Bihar, India

Elev. range, m	Original end areas*		Sum of original end areas $E_{o1}$ , m <sup>2</sup>	Original capacity $V_o$ , Mm <sup>3</sup>	Const. factor, $C_o$	New end areas*		New sum of end areas $E_{n1}$ , m <sup>2</sup>	Sum of Sediment end areas $E_{s1}$ , m <sup>2</sup>	Sediment volume $V_s$ , Mm <sup>3</sup>	New capacity $V_{n1}$ , Mm <sup>3</sup>
	$D/S$ , m <sup>2</sup>	$U/S$ , m <sup>2</sup>				$D/S$ , m <sup>2</sup>	$U/S$ , m <sup>2</sup>				
340-350	1600	1,900	3,500	0.92	262	900	200	1,100	2400	0.63	0.29
350-360	2000	3,000	5,000	1.77	354	1800	2400	4,200	800	0.28	1.48
360-370	2300	3,400	5,700	2.38	418	2000	3500	5,500	200	0.08	2.30
370-380	3400	3,900	7,300	2.96	405	2700	3600	6,300	1000	0.41	2.55
380-390	3700	5,500	9,200	3.54	385	4500	4900	9,400	-200	-0.08	3.61
390-400	5100	6,300	11,400	4.14	363	5100	6200	11,300	100	0.04	4.10
400-410	5900	7,200	13,100	4.73	361	5400	7000	12,400	700	0.25	4.48
410-420	6800	8,400	15,200	5.32	350	7400	8000	15,400	-200	-0.07	5.39
420-430	8300	10,100	18,400	5.97	325	8800	8500	17,300	1100	0.36	5.62
				31.729						1.900	29.829

\*U/S = upstream, D/S = downstream.  
 Source: Modified from Murthy (1977).

and Julien (1986) used Brune's, Churchill's, and other empirical methods at Peligre Reservoir in Haiti and found all methods significantly overestimated release efficiency. This was attributed to the high rate of clay flocculation, producing sediment fall rates much higher than the rate for discrete particles. A predominance of slowly settling fine sediment and a low-level outlet will tend to increase sediment release, while predominantly coarse inflow will reduce sediment release compared to "average" reservoirs. Empirical methods incorporating particle size as a variable have also been developed (Borland, 1971; Chen, 1975). Mathematical modeling is required to provide information on single-event behavior and the effect of changed operating rules on sediment release.



<i>Initial Survey</i>	<i>New Survey</i>
$A_0$ = Contour Area	$A_1$ = Contour Area (Computed)
$W_0'$ = Downstream Width	$W_1'$ = Downstream Width
$W_0''$ = Upstream Width	$W_1''$ = Upstream Width

$$A_1 = A_0 \left( \frac{\frac{W_1' + W_1''}{2}}{\frac{W_0' + W_0''}{2}} \right)$$

**WIDTH ADJUSTMENT METHOD FOR REVISING CONTOUR AREAS IN COMPUTATION OF RESERVOIR SEDIMENTATION**

FIGURE 10.14 Width adjustment method used by U.S. Bureau of Reclamation for revising contour area (Blanton, 1982).

**10.8.1 Brune Curve**

Brune (1953) developed an empirical relationship for estimating long-term trap efficiency in normally impounded reservoirs based on the correlation between the capacity to inflow ratio (C:I) and trap efficiency observed in Tennessee Valley Authority reservoirs in the southeastern United States (Fig. 10.15). This is probably the most widely used method for estimating the sediment retention in reservoirs, and gives reasonable results from very limited data: storage volume and average annual inflow. As a limitation, the method is applicable only to long-term average conditions. Brune noted that significant departures can occur as a result of changes in the operating rule.

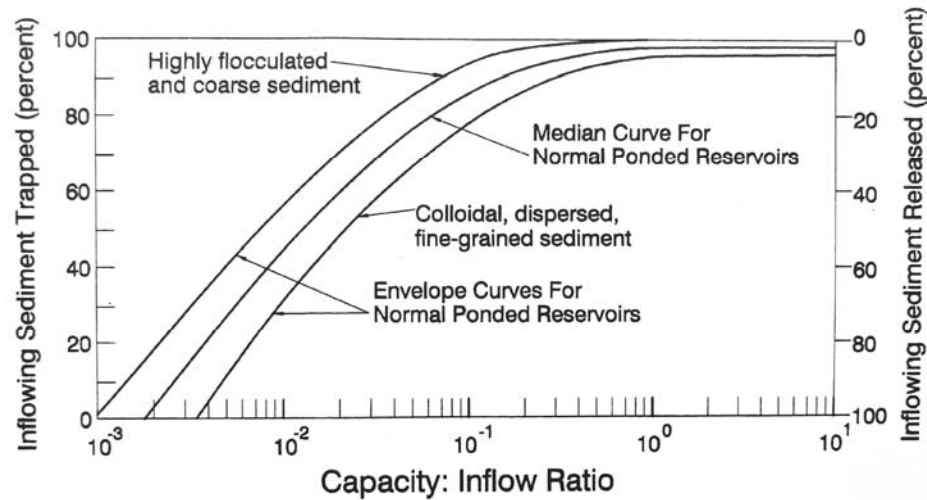


**FIGURE 10.15** Brune curve for estimating sediment trapping or release efficiency in conventional impounding reservoirs (*adapted from Brune, 1953*).

Normally dry reservoirs tend to be less efficient at trapping sediment, and shallow sediment-retention basins designed for the express purpose of trapping sediment can operate much more efficiently than indicated by the curve. For instance, the All-American Canal desilting basins in Arizona would have negligible sediment trapping efficiency based on their C:I ratio, but the basins operate at a trapping efficiency of 91.7 percent. Trapping efficiency also depends on the actual storage level at which the reservoir is held during flood periods (as opposed to its nominal storage capacity), and the placement of outlets.

### 10.8.2 Churchill Method

Churchill (1948) developed a relationship between the sediment release efficiency and the sedimentation index of the reservoir, defined as the ratio of the retention period to the mean flow velocity through the reservoir (Fig. 10.16). The minimum data required to use this method are storage volume, annual inflow, and reservoir length. In applying the Churchill method, the following definitions are used:

**Capacity.** Reservoir capacity at the mean operating pool level for the analysis period ( $\text{m}^3$  or  $\text{ft}^3$ )

**Inflow.** Average daily inflow rate during study period ( $\text{m}^3/\text{s}$  or  $\text{ft}^3/\text{s}$ )

**Retention period.** Capacity divided by inflow rate (s)

**Length.** Reservoir length at mean operating pool level (m or ft)

**Velocity.** Mean velocity computed by dividing inflow by average cross-sectional area. The average cross-sectional area can be determined by dividing reservoir capacity by length ( $\text{m}/\text{s}$  or  $\text{ft}/\text{s}$ ).

**Sedimentation index.** Retention period divided by velocity.

The sedimentation index computed from the above definitions is applied to the curve in Fig. 10.16 to estimate the sediment release efficiency. Churchill's method can be used to

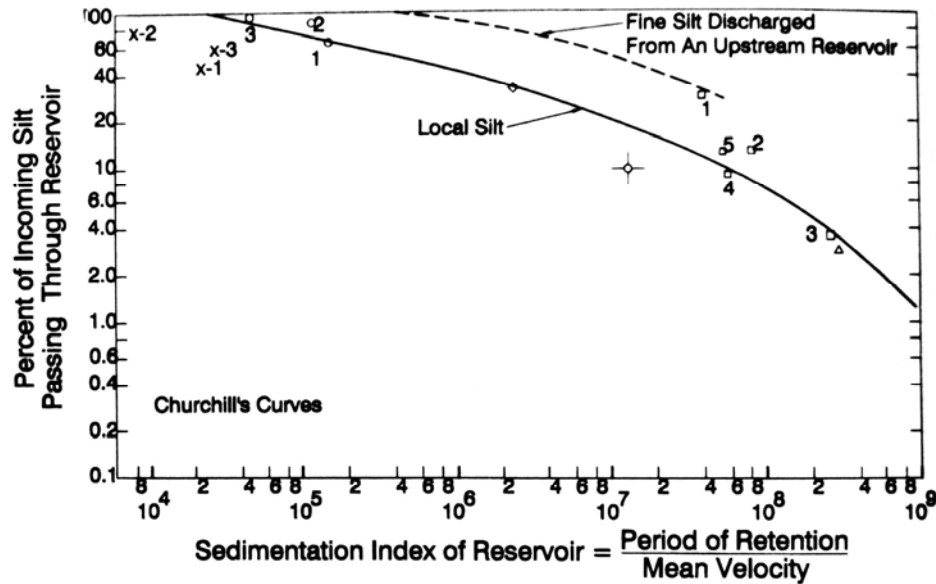


FIGURE 10.16 Churchill curve for estimating sediment release efficiency (adapted from Churchill, 1948).

estimate the release efficiency in settling basins, small reservoirs, flood retarding structures, semidry reservoirs, or reservoirs that are continuously sluiced.

## 10.9 SPECIFIC WEIGHT OF RESERVOIR DEPOSITS

Inflowing sediment load is measured in terms of its mass. To predict storage depletion, sediment mass is converted to volume based on deposit density. Conversely, the volume of surveyed sediments in an existing reservoir must be converted into mass to estimate sediment yield from the watershed. The dry weight of a deposit per unit volume is variously called the *specific weight*, *unit weight*, or *dry bulk density*. The specific weight of a sediment deposit is estimated in a two-step process: (1) the initial specific weight is estimated and (2) the effect of consolidation with time is computed. Methods for converting the volume of deposited sediment to units of mass have been reviewed by Heinemann and Rausch (1971).

### 10.9.1 Compaction Processes

Specific weight is determined by grain size, deposit thickness, and whether the deposit has been exposed to the air and allowed to dry. Consolidation is a time-dependent process which increases specific weight, and reservoir sediments may consolidate for decades because of self-weight plus overburden from additional sedimentation.

Coarse sediment particles rest directly against one another as soon as they are deposited, and the void spaces between coarse grains are large enough that water can freely escape from between the grains. As a result, coarse sediments achieve essentially ultimate density as soon as they are deposited, and the subsequent rearrangement of the grains and compression of the deposit is negligible. Silts and clays, however, typically settle initially

into a loose matrix with interparticle bridging, resulting in a large volume of small water-filled voids. As additional layers of sediment are deposited, additional pressure is applied and the interparticle bridges can collapse, compressing the sediment. However, the overlaying sediments which compress the deposit also act as a confining layer which retards the vertical migration and escape of the void water, thereby impeding and prolonging the compaction process. The poor permeability of clay can also cause deposits of higher density to overlay layers of lower density, causing a reversal of the vertical density gradient, as reported for deposits in Lake Mead (Fig. 10.17). Grain size variation will also cause bulk density to vary with depth. Bulk density is highest in the coarse materials deposited in the delta region of the reservoir, and decreases in the direction of the dam as the deposits become finer-grained.

### 10.9.2 Range of Unit Weights

The density of solid sediment particles is approximately  $2.65 \text{ t/m}^3$ . The dry bulk densities for 1129 samples of reservoir sediments reported by Lara and Pemberton (1963) ranged from  $1.8$  to  $3.0 \text{ t/m}^3$ . The guidelines in Table 10.2 developed by the U.S. Natural Resources Conservation Service illustrate the range of specific weights commonly encountered in reservoirs as a function of both grain size and consolidation processes.

### 10.9.3 Lara-Pemberton Method for Initial Bulk Density

Lara and Pemberton (1963) developed an empirical method for estimating the initial specific weight of sediment deposits based on the analysis of some 1300 sediment samples from

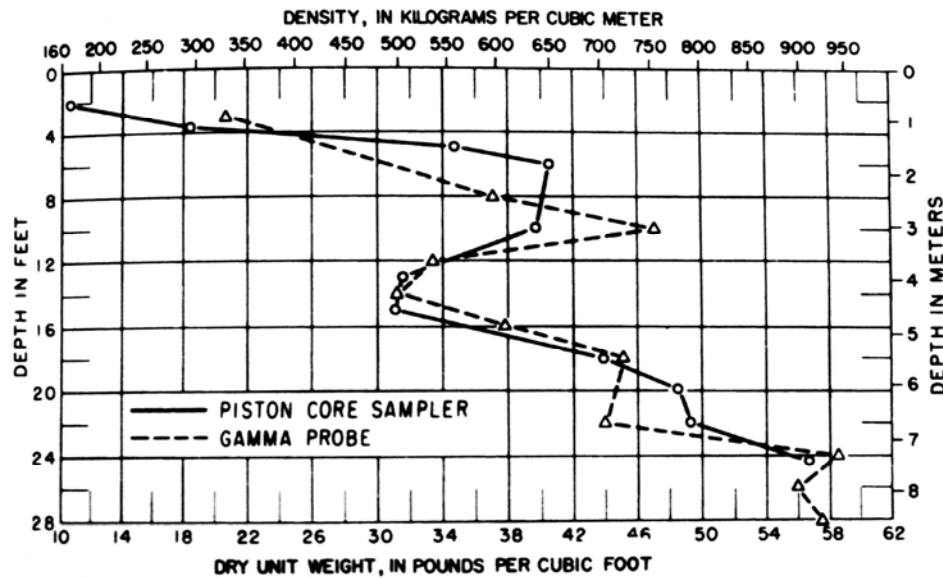


Figure 10.17 change in dry bulk density of reservoir sediment as a function of depth, sampling location 5, Lake Mead (Standard and Pemberton, 1987).

**Table 10.2** Typical Specific Weights for Reservoir Deposits

Dominant grain size	Always submerged	Aerated
Metric (t/m <sup>3</sup> or g/cm <sup>3</sup> ):		
Clay	0.64 to 0.96	0.96 to 1.28
Silt	0.88 to 1.20	1.20 to 1.36
Clay-silt mixture	0.64 to 1.04	1.04 to 1.36
Sand-silt mixture	1.20 to 1.52	1.52 to 1.76
Sand	1.36 to 1.60	1.36 to 1.60
Gravel	1.36 to 2.00	1.36 to 2.00
Poorly sorted sand and gravel	1.52 to 2.08	1.52 to 2.08
U.S. Customary Units (lb/ft <sup>3</sup> ):		
Clay	40 to 60	60 to 80
Silt	55 to 75	75 to 85
Clay-silt mixture	40 to 65	65 to 85
Sand-silt mixture	75 to 95	95 to 110
Clay-silt-sand mixture	50 to 80	80 to 100
Sand	85 to 100	85 to 100
Gravel	85 to 125	85 to 125
Poorly sorted sand and gravel	95 to 130	95 to 130

*Source:* Geiger (1963).

reservoirs and rivers. This method incorporates the two primary factors influencing bulk density: (1) grain size distribution taking into account the presence of clays and (2) reservoir operation which affects consolidation and air drying. Data on the bulk density of deposits from subsequent reservoir resurveys by the Bureau of Reclamation have supported the Lara and Pemberton equation (Strand and Pemberton, 1987).

To estimate initial specific weight, classify the reservoir operation into one of four categories: (1) sediment always submerged or nearly submerged, (2) normally moderate to considerable drawdown, (3) normally empty reservoir, and (4) riverbed sediments. The sediment composition must also be divided among the sand, silt, and clay fractions. The specific weight computation is performed by using the values in Table 10.3 and the following equation:

$$W = W_c P_c + W_M P_M + W_S P_S \quad (10.12)$$

where  $W$  = is the deposit specific weight (kg/m<sup>3</sup> or lb/ft<sup>3</sup>);  $P_c$ ,  $P_M$ ,  $P_S$  = the percentages of clay, silt, and sand, respectively, for the deposited sediment; and  $W_c$ ,  $W_M$ ,  $W_S$  = the

**TABLE 10.3** Coefficient Values for Lara-Pemberton Equation

Operational Condition	Initial weight kg/m <sup>3</sup> (lb/ft <sup>3</sup> )		
	$W_c$	$W_M$	$W_S$
Continuously submerged	416 (26)	1120 (70)	1154 (97)
Periodic drawdown	561 (35)	1140 (71)	1154 (97)
Normally empty reservoir	641 (40)	1150 (72)	1154 (97)
Riverbed sediment	961 (60)	1170 (73)	1554 (97)

initial weights for clay, silt, and sand, respectively. As an example, in a continuously submerged zone within the reservoir which traps 23 percent clay, 40 percent silt, and 37 percent sand, the solution is

$$W = (416)(0.23) + (1120)(0.40) + (1550)(0.37) = 1117 \text{ kg/m}^3$$

Because sediment composition can vary dramatically from one area of the reservoir to another, and higher-elevation areas may be air-dried whereas deeper layers may be continuously submerged, the reservoir should be divided into the appropriate zones for a more accurate estimation of overall initial weight.

### 10.9.4 Sediment Compaction

It may be desired to know: (1) the bulk density of a sediment deposit at the end of a specified consolidation period or (2) the average weight over a time interval. Lane and Koelzer (1953) presented an empirical formula for the density-time relationship which takes into account the grain size of the sediment and the method of operating the reservoir:

$$W = W_1 + B \log t \tag{10.13}$$

in which  $W$  = specific weight of a deposit with an age of  $t$  years;  $W_1$  = initial weight, usually taken to be the value after 1 year of consolidation; and  $B$  = constant. Both  $W_1$  and  $B$  are functions of sediment size and they are defined for four operational conditions: (1) sediment submerged continuously or almost continuously, (2) normally moderate reservoir drawdowns, (3) normally considerable reservoir drawdown, and (4) reservoir normally empty. Parameter values are given in Table 10.4. For sediment containing more than one

**TABLE 10.4** Coefficient Values for Consolidation Calculation

Operational condition	$B, \text{ kg/m}^3 \text{ (lb/ft}^3\text{)}$		
	Sand	Silt	Clay
Continuously submerged	0	91 (5.7)	256 (16)
Periodic drawdown	0	29 (1.8)	135 (8.4)
Normally empty reservoir	0	0	0

size class, the weighted value of the coefficient  $B$  should be computed. For the previous example of continuously submerged sediment with 23 percent clay, 40 percent silt, and 37 percent sand:

$$B = (0.37)(0) + (0.40)(91) + (0.23)(256) = 95.3 \text{ kg/m}^3$$

In computing the average compaction over a period of time, each year's sediment deposits will have a different compaction time. The average density of all sediment deposited during  $t$  years of consolidation may be computed using the equation presented by Miller (1953):

$$W_t = W_1 + 0.4343B \left[ \frac{t}{t-1} (\ln t) - 1 \right] \tag{10.14}$$

Where  $W_t$  = average specific weight after  $t$  years of consolidation,  $W_1$  = initial specific weight, and  $B$  = constant as given in table 10.4. For the previous example, with  $W_1 = 1117 \text{ kg/m}^3$  and  $B = 95.3$ , the average specific weight of the deposit after 100 years is computed by

$$W_{100} = 1117 + (0.4343)(95.3)[(100/99)(4.61) - 1] = 1268 \text{ kg/m}^3$$

This equation incorporates the assumption that sediment accumulates at a constant rate every year. The error introduced by this assumption is negligible over a period of many years, but over shorter periods in environments with highly irregular sediment inputs, year-by-year computations can be made with an electronic spreadsheet and Eq. (10.14)

## **10.10 EMPIRICAL PREDICTION OF DEPOSITION PATTERNS**

---

Sediments are deposited in reservoirs at all elevations, causing the stage-capacity curve to shift. Empirical methods have been developed to distribute sediment deposits within a reservoir as a function of depth, thereby projecting the shift in the stage-storage curve. These methods are much quicker and easier to use than mathematical modeling and also require less data. When sediment survey data are available for an existing reservoir, the observed deposition pattern can be used to select the proper empirical relationship to compute the future shift in the stage-area and stage-capacity relationships. As a limitation, empirical methods do not identify the specific locations in a reservoir which will be affected by sediment; they predict only the change in the stage-area and stage-capacity curves. A significant shift in the operating regime, such as implementation of sediment management, will affect the deposition pattern. Empirical methods cannot be used to simulate these effects, and the evaluation of management alternatives requires numerical modeling.

### **10.10.1 Deposits in Flood Control Pool**

Reservoir levels are normally held below the flood control level, resulting in small amounts of sediment accumulation in the portion of the impoundment between the normal and maximum (flood) pool levels. However, large amounts of sediment can be delivered during floods, and if the pool level is held above the normal pool for a significant period of time a substantial amount of sediment may be deposited in this zone. Data from 11 reservoirs in the Great Plains area of the United States are plotted in Fig 10.18, which shows the percentage of total sediment inflow trapped within the flow control pool as a function of the flood pool index, computed as

$$\text{Index} = \left( \frac{\text{Depth of Pool}}{\text{Depth Below Flood Pool}} \right) \quad (\text{percent of time in flood pool})$$

The graphed relationship is only a rough guideline and reservoirs having different geometry (e.g., mountain reservoirs) may depart from this relationship.

### **10.10.2 Area-increment and Empirical Area Reduction Methods**

Empirical methods to distribute sediment below the normal pool elevation developed by the U.S. Bureau of Reclamation have been widely used. They are based on a four-step process:

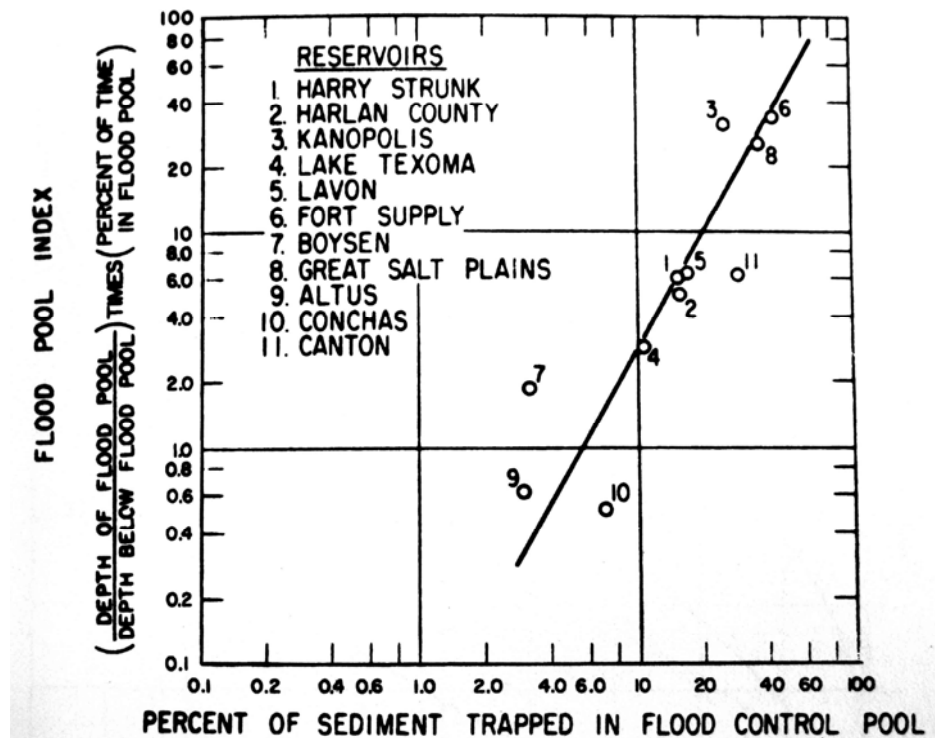


FIGURE 10.18 Percent of sediment trapped within flood control pool in 11 reservoirs in the U.S. Great Plains region (Strand and Pemberton, 1987).

1. Determine the amount of sediment to be distributed. In an existing reservoir, the volume of sediment might be estimated by assuming that the observed historical rate of volume loss will continue into the future. At a new site, volume loss would be estimated from the predicted inflowing load, sediment release efficiency, and deposit specific weight.
2. On the basis of the site characteristics, select the appropriate empirical curve for sediment distribution. In an existing reservoir with surveyed sediment deposits, the historical deposition pattern is used as the basis for selecting the empirical curve for distributing future sediment deposition.
3. Determine the height of sediment accumulation at the dam, termed the *new zero-capacity elevation*.
4. Use the selected empirical curve to distribute sediment as a function of depth above the new zero-capacity elevation. These values are then subtracted from the original stage-area and stage-capacity curves to produce the adjusted curves.

This entire procedure is repeated for each sediment volume to be analyzed. These computations are readily adapted to solution by electronic spreadsheet.

The first empirical method developed was the *area-increment method*, which uses the assumption that an equal volume of sediment will be deposited within each depth increment in the reservoir. From resurveys of many reservoirs, the Bureau found that the deposition pattern varied from one site to another in a somewhat predictable fashion. Reservoir geometry, operation, and sediment grain size all affect sediment distribution

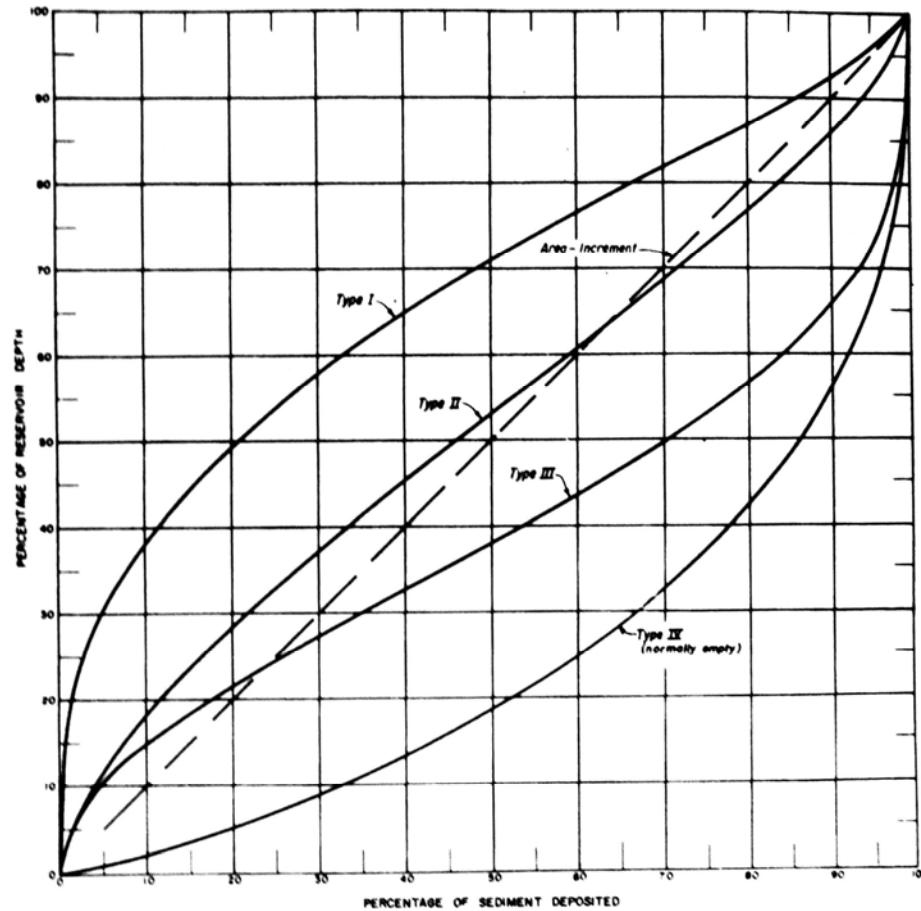


FIGURE 10.19 Type curves for the empirical area-reduction method for estimating storage loss due to sediment deposition (Strand and Pemberton, 1987).

within the impoundment, and four different empirical type curves were developed on the basis of these characteristics. Use of the appropriate type curve can produce a more realistic sediment distribution than the area increment method. The four type curves developed from reservoir resurvey data are shown in Fig. 10.19 along with the curve corresponding to the area-increment method. Notice that the area-increment curve is very similar to the Type II curve. Both empirical methods were described by Borland and Miller (1958). The *empirical area reduction method* was revised by Lara (1962), and the example given here using the Theodore Roosevelt Dam located on the Salt River upstream of Phoenix, Arizona, is based on Strand and Pemberton (1987).

Data for the example computations at Theodore Roosevelt Dam are given in Table 10.5. The dam was constructed in 1902 with an original capacity of  $1888 \text{ Mm}^3$  to the top of the conservation pool, located 71.3 m above the original streambed elevation at the dam. The original stage-area and stage-capacity curves are given in columns 1, 2, and 3 of Table 10.5. The sediment survey conducted in 1981 determined that  $239 \text{ Mm}^3$  of sediment had accumulated during the 72.4 years since closure. In the example problem the distribution for 100 years of sediment accumulation will be calculated.

TABLE 10.5 Empirical Area Reduction Method, Sample Computations, Theodore Roosevelt Dam

Elevation h, m (1)	Original survey data		Relative				Computed Sediment Distribution				Revised	
	Area A, ha (2)	Capacity $V_r$ , $10^6 \text{ m}^3$ (3)	F value (4)	Depth p (5)	Area a (6)	Area, ha (7)	Volume increment, $10^6 \text{ m}^3$ (8)	Cumulative volume, $10^6 \text{ m}^3$ (9)	Area, ha (10)	Capacity, $10^6 \text{ m}^3$ (11)		
651.05	7197.6	1887.87		1.000	0.000	0.0	2.59	330.08	7197.6	1557.8		
649.22	6962.1	1758.37		0.974	0.546	283.0	10.57	327.49	6679.1	1430.9		
646.18	6546.8	1552.42		0.932	0.795	412.1	13.75	316.92	6134.7	1235.5		
643.13	6108.9	1359.58		0.889	0.944	489.7	15.77	303.17	5619.2	1056.4		
640.08	5707.9	1179.79		0.846	1.050	544.2	17.21	287.40	5163.7	892.4		
637.03	5361.1	1010.57		0.803	1.127	584.2	18.27	270.19	4776.9	740.4		
633.98	4831.7	855.20		0.761	1.184	613.9	18.99	251.92	4217.8	603.3		
630.94	4305.2	716.16		0.718	1.225	635.3	19.60	232.93	3669.9	483.2		
627.89	3837.4	591.99		0.675	1.254	650.1	19.96	213.33	3187.3	378.7		
624.84	3343.6	482.55		0.633	1.271	658.8	20.15	193.37	2684.8	289.2		
621.79	2875.8	388.09		0.590	1.277	662.3	20.18	173.22	2213.5	214.9		
618.74	2515.6	305.92		0.547	1.274	660.8	19.99	153.04	1854.8	152.9		
615.70	2139.2	234.78		0.504	1.263	654.6	19.80	133.05	1484.6	101.7		
612.65	1725.6	176.27	0.125	0.462	1.242	643.9	19.40	113.25	1081.7	63.0		
609.60	1434.3	128.02	0.198	0.419	1.212	628.6	18.87	93.84	805.7	34.2		
606.55	1110.5	89.25	0.304	0.376	1.174	608.6	18.18	74.98	501.9	14.3		
603.50	803.3	60.28	0.471	0.333	1.126	583.8	19.83	56.79	219.5	3.5		
<b>600.00*</b>	<b>549.1</b>	<b>36.97</b>	<b>0.748</b>	<b>0.284</b>	<b>1.059</b>	<b>549.1</b>	<b>36.96</b>	<b>36.97</b>	<b>0.0</b>	<b>0.0</b>		
597.41	412.8	24.35	1.038	0.248	0.999	412.8	24.35	24.35	0.0	0.0		
594.36	274.0	13.97	1.618	0.205	0.918	274.0	13.97	13.97	0.0	0.0		
591.31	169.6	7.27	2.669	0.162	0.821	169.6	7.27	7.27	0.0	0.0		
588.26	91.9	3.37		0.120	0.704	91.9	3.37	3.37	0.0	0.0		
585.22	47.3	1.31		0.077	0.558	47.3	1.31	1.31	0.0	0.0		
582.17	21.0	0.26		0.034	0.358	21.0	0.26	0.26	0.0	0.0		
579.73	0.0	0.00		0.000	0.000	0.0	0.00	0.00	0.0	0.0		

New zero-capacity elevation.  
Source: After Strand and Pemberton (1987).

Either the area-increment method or the empirical area reduction method can be solved by performing the following steps. The difference between the methods is the type curve selected to distribute sediment.

1. **Determine sediment inflow.** The sediment volume to be distributed within the reservoir must be determined. At the Theodore Roosevelt Dam, the sediment survey data were extrapolated to determine an average volume loss of 330 Mm<sup>3</sup> per 100 years.
2. **Select design curve.** Plot the original depth-capacity relationship on log-log paper and calculate the slope  $m$  of the fitted line, which is the reciprocal of the slope of the depth versus capacity plot (Fig. 10.20). Use the resulting slope  $m$  to classify the reservoir shape using the table below.

Reservoir shape	Type	$m$
Lake	I	3.5-4.5
Floodplain-foothill	II	2.5-3.5
Hill and gorge	III	1.5-2.5
Gorge	IV	1.0-1.5

The type curves in Fig. 10.19 reflect the tendency for sediment in lake-type reservoirs to accumulate in shallower water and in gorge-type reservoirs to accumulate in deeper water.

When the slope  $m$  does not plot as a straight line, use the shape type corresponding to the predominate overall slope, or the slope in the area of the reservoir where most of

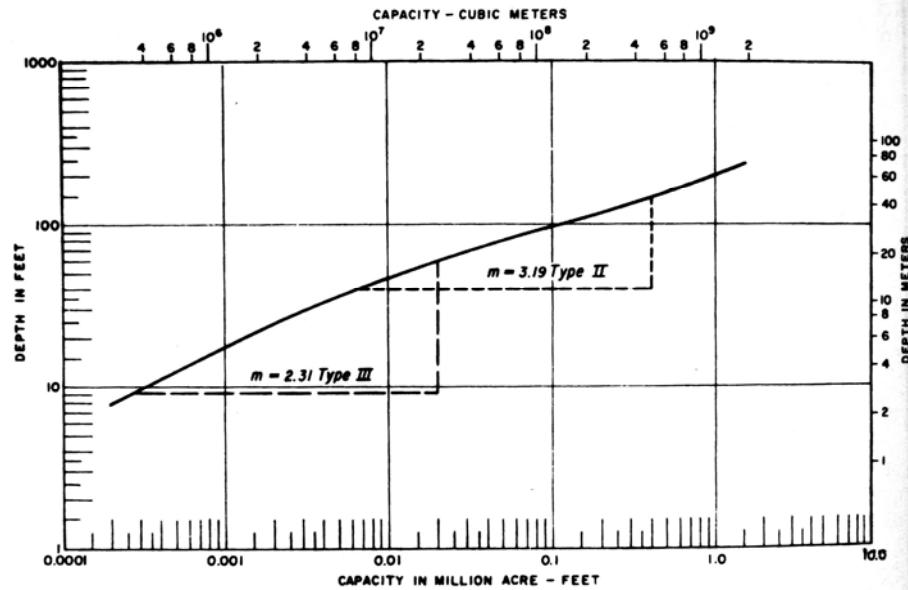


**FIGURE 10.20** Reservoir depth-capacity relationship as used in the empirical area-reduction method (Strand and Pemberton, 1987).

the sediment will deposit. Strand and Pemberton state that the reservoir does not change type with continued sediment deposition, unless reservoir operation changes. Thus, the stage-capacity plot should be based on the original reservoir bathymetry, not the bathymetry following sediment accumulation.

Classify the reservoir operation as stable pool, moderate drawdown, considerable drawdown, or normally empty. Giving equal weight to reservoir shape and reservoir operation, determine the weighted reservoir type from the table below.

Reservoir Operation	Operational class	Shape class	Weighted class
Sediment submerged (continuous high pool level)	I	I	I
		II	I or II
		III	II
Moderate drawdown	II	I	I or II
		II	II
		III	II or III
Considerable drawdown	III	I	II
		II	II or III
		III	III
Normally empty	IV	All	IV

Where a choice of two types is given, or in borderline situations, select the type according to whether reservoir shape or reservoir operation is felt to be more influential at the site. For the Theodore Roosevelt Dam, a Type II classification was chosen. Sediment grain size may also be considered using the following guideline:

Predominant Grain size	Type
Sand or coarser	I
Silt	II
Clay	III

In most river basins the grain size distribution has been found to be the least important factor influencing sediment distribution, and grain size should be used as an auxiliary variable to select the weighted type curve only in those cases when there is a choice between two type numbers.

For an existing reservoir having a sediment survey, plot the survey results on Fig. 10.19 to determine which empirical curve should be used. By plotting the data from Theodore Roosevelt Dam, it was confirmed that the Type II empirical curve should be used at that site.

**3. Compute new zero-capacity elevation at dam.** Use the original elevation-area and capacity curves to compute the value of the dimensionless function  $F$  at several different pool elevations in the deeper part of the reservoir:

$$F = \frac{S - V_h}{HA_h} \tag{10.15}$$

where  $S$  = total sediment deposition ( $330 \text{ Mm}^3$ ),  $V_h$  = reservoir capacity ( $\text{m}^3$ ) from column 3 at each elevation  $h$  from column 1,  $H$  = original depth of reservoir below normal pool (71.3 m),  $A_h$  = reservoir area ( $\text{m}^2$ , from column 2) at a given elevation  $h$ . Note that hectares must be converted to square meters before computing. Also compute decimal values for the relative depth  $p$  as

$$p = \frac{h - h_{\min}}{H} \tag{10.16}$$

where  $h_{\min}$  = original bottom elevation (579.73 m). Plot the resulting  $F$  and  $p$  values (columns 4 and 5) on the type curves presented in Fig. 10.21. The intersection of the

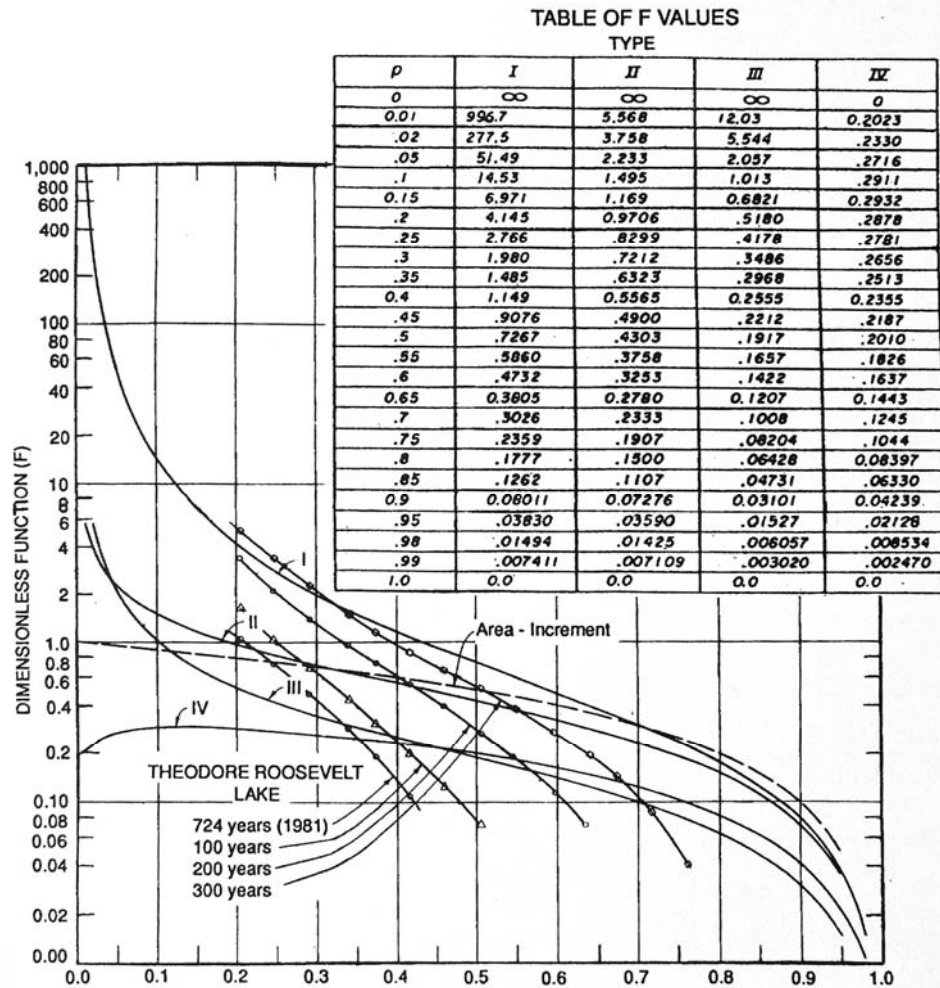


**FIGURE 10.21** Type curves for determining the new zero depth at the dam based on the dimensionless  $F$  function. The values for each of the type curves are shown in both graphical and tabular form (Strand and Pemberton, 1987).

plotted  $F$  values with the type curve selected for the reservoir defines the  $p_0$  value for the new zero-capacity elevation at the dam. The example intersection occurs at  $p_0 = 0.284$ .

The new zero-capacity elevation is given by  $h_0 = (p_0H + h_{min}) = (0.284)(71.3) + 579.73 = 600.0\text{m}$ . The zero-capacity elevation is included as a row in Table 10.5, and the corresponding area is computed from the original area-elevation curve as  $A_0 = 518.5$  ha.

The area-increment curve is often also used to compute the intersection point because it will always intersect the  $F$  curve and offers a good method to check the new zero-capacity elevation.

**4.Distribute sediment.** The specified volume of trapped sediment is distributed within the reservoir according to the selected type curve. Compute the values for relative sediment area  $a$  (Col. #6) at each relative depth  $p$  using the appropriate equation:

$$\text{Type I:} \quad a = 5.047p^{1.85}(1-p)^{0.36} \quad (10.17)$$

$$\text{Type II:} \quad a = 2.487p^{0.57}(1-p)^{0.41} \quad (10.18)$$

$$\text{Type III:} \quad a = 16.967p^{1.15}(1-p)^{2.32} \quad (10.19)$$

$$\text{Type IV:} \quad a = 1.486p^{-0.25}(1-p)^{1.34} \quad (10.20)$$

Also compute the relative sediment area  $a$  at the new zero elevation. (For the example use Type II, resulting in  $a = 1.059$  when  $p = 0.284$ .) Compute the area correction factor as  $A_0/a = 549.1/1.059 = 518.5$  ha.

Compute the area at each pool elevation occupied by sediment (column 7) by multiplying the area correction factor by the relative sediment area (column 6) at each level above the new zero-capacity elevation. In the fully sedimented part of the reservoir extending from the new zero-capacity elevation down to the original bottom, the sedimented pool area equals the original pool area.

Compute the sediment volume for each stage increment above the new zero-capacity elevation using the end area method (column 8). For example, at elevation 603.50 the computation is  $(549.1 + 583.8)(10^4)/2(603.50-600.0) = 19.83 \times 10^6 \text{ m}^3$ . From the zero-capacity elevation to the reservoir bottom, the sediment volume equals the original reservoir capacity, since this zone is entirely sedimented. The cumulative volume of deposited sediment (column 9) is computed by summing the values in column 8. The total sediment volume should match the predetermined sediment volume from step 1 ( $V_s$ ) within about 1 percent.

Compute the revised area and capacity curves (columns 9 and 10) by subtracting the sediment area (column 7) and cumulative sediment volume (column 9) from the original area and capacity values (columns 2 and 3).

The original and adjusted curves for Theodore Roosevelt Dam for the example and other points in time are presented in Fig. 10.22.

## 10.11 SAMPLING SEDIMENT DEPOSITS

---

Sediment sampling equipment is required to obtain undisturbed samples of reservoir deposits for determining parameters such as bulk density, grain size distribution, and chemical characteristics. The selection of sediment sampling technique depends on the parameter to be measured, sediment grain size and consolidation (which affects core penetration), water depth, and sediment thickness. Sediment sampling can be performed from a boat, raft, or ice cover. Aquatic sampling techniques are reviewed by Mudroch and MacKnight (1991).

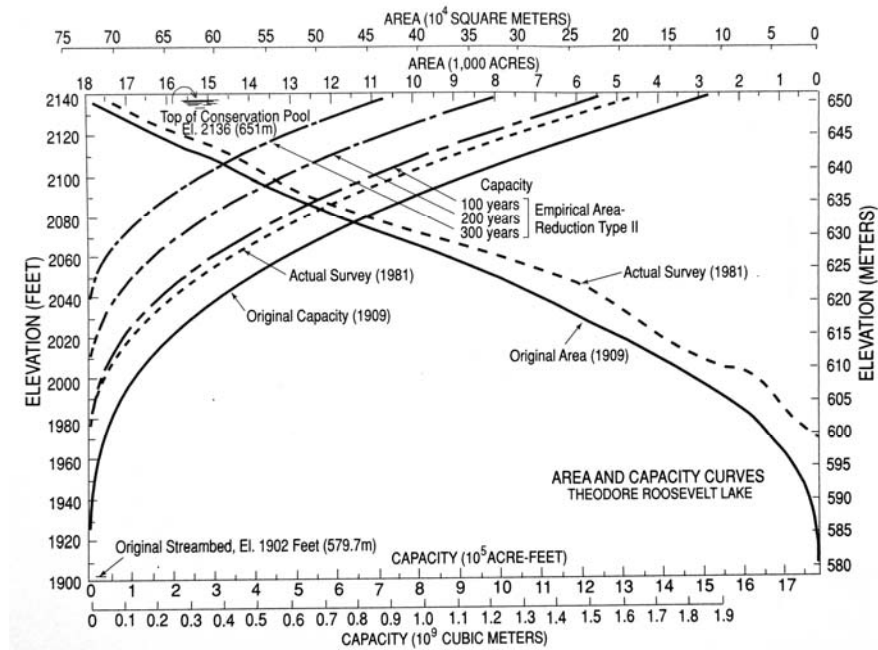


**FIGURE 10.22** The original and adjusted stage-capacity and stage-area curves for Theodore Roosevelt Dam. Also, the curve from the 1981 reservoir survey is compared to the relationship computed from the Type II empirical distribution, indicating good overall agreement (*Strand and Pemberton, 1987*).

### 10.11.1 Planning the Sampling Program

In design of the sampling program, several considerations in addition to cost are important. The sediment volume required depends on the tests to be performed. For example, <sup>137</sup>cesium counts tend to require large samples, indicating the use of cores on the order of 8 cm in diameter. In sampling for contaminants associated with fine sediment, it may not be necessary to use coring equipment capable of collecting sands because the contaminants of interest are not associated with sands. Deeper sand layers and deeper cores may produce a very different picture of deposit composition compared to surface sampling with a Ponar dredge, for example, which will sample only the most recently deposited material. In sampling for any type of contaminants required by regulatory agencies, the most important preparatory task will be the development of a sampling plan specifying sampling locations, depths of penetration, sample collection and handling protocols, and laboratory methods agreeable to all parties involved. This may be the most difficult part of the sampling program.

### 10.11.2 Sampling for Chemical Contaminants

In sampling sediments for contaminants, including a variety of organic chemicals and heavy metals, special sample collection and preservation protocols are required to ensure the integrity of samples to be analyzed for trace contaminants. For specialized sampling consult the pertinent regulatory agency (e.g., U.S. Environmental Protection Agency) for

the most recent protocol covering both sample collection and laboratory techniques appropriate for the contaminants of interest and which meet the specific regulatory requirements of concern.

### 10.11.3 Surface Dredges

Samples of the sediment on the surface of the deposits may be recovered with a Ponar dredge (Fig. 8.10e) or similar equipment. This type of equipment will sample only superficial deposits a few centimeters deep. Surface samples will not be representative of deposits which exhibit significant layering. This equipment has the important advantage of ease of use; smaller dredges can easily be managed by hand, although larger ones require use of a winch. The Ponar dredge can sample both sands and fines, and works better for sediment grain-size sampling than the lighter Eckman-type dredge. However, a box-type or core sampler should be used to determine specific weights.

### 10.11.4 Gravity Corers

Sediment cores are frequently obtained by gravity coring devices consisting of a cutting head, barrel, thin-wall plastic core liners, weight, and stabilizing fins, as shown in Fig. 10.23. The core barrel has a check valve at the top which allows water to flow out of the

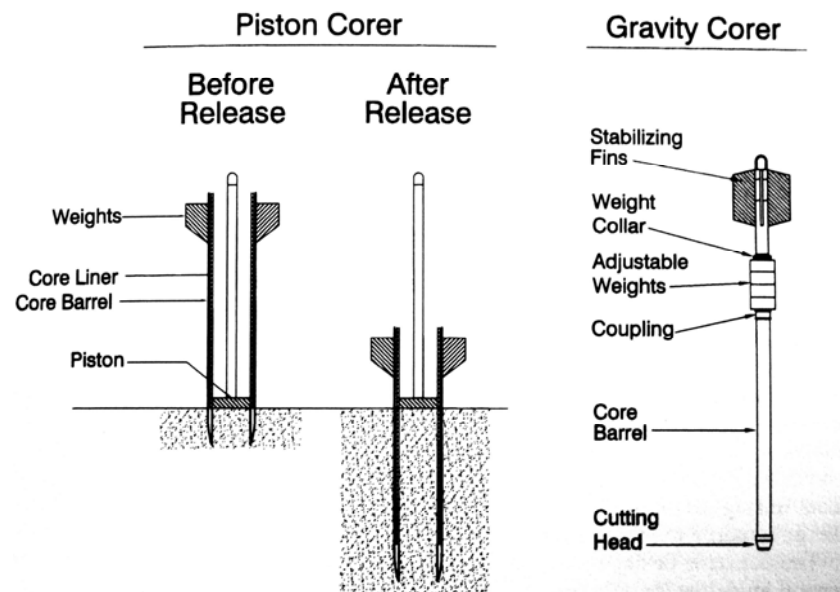


FIGURE 10.23 Piston and gravity corers.

core during descent, but which closes once the core has penetrated into the sediment and downward descent is stopped. This creates a vacuum which holds fine sediment in the core when removed. A core catcher will prevent sandy sediment from falling out of the barrel upon recovery, but in soft sediment it will reduce sediment capture and should not be used. After penetration, the corer is raised to the boat, the cutting shoe is removed, a cap is placed over the exposed end of the core liner, and the core is withdrawn, labeled,

and prepared for transport to the laboratory. The recovery depth of a gravity corer is limited by wall friction inside the coring tube, which can also compress softer sediment

#### **10.11.5 Piston Corer**

A piston corer consists of an inner piston that fits inside the core liner, an outer core barrel, drive shoe, and weights (Fig. 10.23). The corer is lowered to the bottom, bringing the piston into proximity or contact with the sediment surface, at which point the outer core barrel is released and is driven into the sediment by self-weight while the piston remains in a fixed position. The downward movement of the core barrel tends to create a vacuum at the lower face of the piston, which in turn helps draw the sample into the coring tube and offsetting wall friction, thereby recovering sediment at greater depth than with a gravity corer.

#### **10.11.6 Other Methods**

Conventional drilling equipment mounted on a raft can be used to obtain fully penetrating cores of sediment deposits, including coarse sediment that will not be penetrated by either gravity or piston cores. Vibracore techniques have also been used to obtain sediment cores in lakes and work well in both sandy and soft sediment. A vibracore consists of a thin-walled tube which is worked through the sediments by vibration of the core barrel to overcome friction. Some types of vibracore equipment requires scuba divers to operate equipment on the submerged sediment and float the core to the surface on bags filled with compressed air.

### **10.12 CLOSURE**

---

Volumetric surveys have historically been conducted at most reservoirs for the purpose of passively observing sedimentation and predicting "useful life" of the impoundment. Data needs expand considerably when the management focus shifts from passive observation, to active management of the sedimentation process to extend reservoir life or achieve sustainable use. In addition to information on sediment volumes, it may also be necessary to determine the active zones of sediment deposition, the grain size distribution, the presence of potentially toxic substances, cohesive sediment characteristics, and to undertake detailed monitoring of the sediment inflow and deposition processes which occur during periods as short as a single storm. Additional data collection effort may also be required to monitor and minimize downstream impacts of sediment release.

The concepts of deposition patterns and processes presented herein provide only a general guideline for analyzing sediment behavior at any particular reservoir. Each site has unique geometry, hydrology, sediment loading, and operational characteristics. Management and regulatory issues are potentially complex. To adequately characterize sediment behavior, and to identify effective management alternatives, requires the collection of sufficient and reliable field data specific to each site. Management recommendations can be no more reliable than the data upon which they are based.

---

## CHAPTER 11

---

# MODELING OF SEDIMENT TRANSPORT AND DEPOSITION IN RESERVOIRS

---

### 11.1 INTRODUCTION

---

To manage any system requires a model which predicts future behavior and response to perturbation. All models are born as mental images and, depending on the situation, they may grow in complexity to include graphics, desktop calculations, numerical simulations, and physical scale modeling. Real-world or "prototype" hydrologic systems are complex, and their behavior is analyzed with models which are greatly simplified and do not reproduce system behavior exactly. In engineering analysis this uncertainty is offset by applying informal or formal safety factors, to convert approximate modeling results into acceptable design parameters.

The principal sediment modeling problems analyzed in reservoirs can be divided into four major categories.

1. Water and sediment yield from the watershed
2. Rate and pattern of sediment transport, deposition, or scour along the reach above the dam under different operating rules.
3. Localized patterns of deposition and scour in the vicinity of hydraulic structures
4. Scour, transport, and deposition of sediment in the river below the dam

Sediment yield is typically modeled using a sediment rating curve, erosion modeling, or related procedures. Techniques for estimating, modeling, and measuring erosion and sediment yield are discussed in Chaps. 6, 7, and 8. The remaining problem categories are addressed by using numerical and physical models to simulate hydraulic and sediment transport behavior in the fluvial system. This chapter briefly outlines hydraulic and sediment transport modeling approaches, and some of the available modeling tools are described. Problems such as bank erosion, slope failure, landslide hazard, and wind erosion from reservoir deposits during drawdown may be important in some individual cases but are not discussed here.

### 11.2 MODELING PROTOCOL

---

Both numerical and physical modeling procedures may be organized into an eight-step protocol. There is no clear consensus within the modeling community concerning the

proper use of the terms *calibration*, *verification*, and *validation*, and the meaning of these terms should always be interpreted within the context of its usage. The usage presented below follows that of Anderson et al. (1992).

**1. Problem identification.** All modeling work begins as a question or a perceived problem which may be initially defined by management, technical staff, or regulatory requirements.

**2. Conceptual model.** Once a problem has been identified, construct a conceptual model which will define the analytical approach. Formulation of a workable conceptual model requires one or more site visits, collection of the available historical data, geomorphic interpretation, and possibly the collection of field data.

Fluvial systems are dynamic and, in addition to obtaining information during site reconnaissance, it is also important to define the historical events and trends affecting the geomorphic behavior of the system. The fluvial system may be degrading and coarsening because of a cutoff of sediment supply by upstream dams or aggregate mining, aggrading because of erosive land uses or upstream flow diversion, or recovering from a recent extreme discharge event which scoured the channel. Information on channel changes, meandering, landslides, and areas of frequent overbank flow should also be ascertained. A number of data sources may be available to ascertain historical conditions. Streamgage records can be checked for historical large events and gage shift, which is the gradual change in the streambed relative to the gage datum. Ensure that any observed gage shift is caused by a general change in the streambed rather than localized conditions such as bridge scour. Historical air photos, maps, and reports should be consulted. Old cross-section surveys for bridges, for example, may provide useful data if the original datum can be ascertained and the effects of general change in streambed elevation can be distinguished from localized changes due to bridge scour. Interviews can provide qualitative information.

**3. Define Modeling Purpose, Scope, and Methodology.** On the basis of the conceptual model, define the specific objectives to be addressed by subsequent modeling activities.

Problem formulation should identify the study reach, the sediment-related problems of concern, and the grain size and hydrographs of interest. The study limit should extend upstream of any anticipated project impacts, and in reservoirs it should extend upstream of the limit of backwater deposition. Important tributaries influencing sediment inflow or hydrology should be included. Location of the downstream limit will depend on the particular study, but should generally extend beyond the area where project impacts are anticipated to be significant, should include sediment-sensitive areas or structures, and should include gage stations which may be useful during calibration. A downstream hydraulic structure or point of bedrock control may constitute a convenient downstream model boundary. Considering the nature of the problem and the constraints of time, budget, and data availability, select the modeling approaches and tools to be used. In general, select the least complicated modeling tools suitable for the problem: do not add unnecessary complexity to the problem at hand.

**4. Model construction and calibration.** Using the historical data and additional field data collection as required, construct and calibrate the model according to historical conditions. *Calibration* is the process of adjusting model parameters within a range of reasonable values to cause the model to accurately reproduce conditions observed in the prototype system. Many parameters including hydraulic roughness, geometry, inflowing sediment load, and grain size, as well as transport equations, may require adjustment during the calibration process.

**5. Verify existing condition model.** The process of ascertaining that the existing condition model accurately simulates the prototype system by using a dataset independent of that used for calibration is termed *verification*. A model calibrated using one event should be verified using another independent event or time period. Verification events should: (1) involve phenomena in the prototype system pertinent to the goals and objectives of the proposed model study, (2) be continuous and of reasonable duration, and (3) consist of extreme events only if the simulation of extreme events is to be addressed in the modeling. In general, the greater the difference between the modeled conditions and the verification conditions, the greater the uncertainty in the modeling results (French, 1985). In practice, two independent datasets are frequently unavailable, making formal model verification impossible.

**6. Predictive simulation.** Once the model has been calibrated and verified, it can be run using "future" hydrology and geometry to analyze different structural or operational alternatives. Models of existing and proposed conditions should normally be compared by using the same input data series, except when future hydrology needs to incorporate the effects of future upstream projects and proposed operating rules. If sediment load is expected to change in the future, because of an upstream dam, for example, this should also be reflected in the future conditions.

Sensitivity is defined as the change in an output parameter with respect with the change in an input parameter. For a function of the general form  $Y_i = f(X_1 \dots X_n)$ , the coefficient of sensitivity corresponding to a change in the independent parameter  $X_i$  may be given by:

$$S_i = \frac{Y_i - Y_0}{Y_0} \times 100\% \quad (11.1)$$

where  $S_i$  = coefficient of sensitivity expressed in percentage form,  $Y_0$  = value of dependent parameter for the base condition, and  $Y_i$  = value of dependent parameter obtained using a changed value of the independent parameter  $X_i$ . The sensitivity of model results to different input parameters may be determined by changing each input by the same percentage amount and comparing the percentage changes in the output parameter. Close attention should be given to any parameter which, when changed by a small amount, causes a significant change in the result. If results are highly sensitive to a given input factor, the uncertainty caused by the sensitive parameter may be reduced by further researching that parameter to determine its value with greater confidence, or by application of a safety factor (Molinas and Yang, 1991).

**7. Conclusions and recommendations.** It is always necessary to interpret model results within the context of a conceptual model to draw conclusions and make recommendations. As the amount and quality of calibration data declines, interpretation will become increasingly dependent on conceptual modeling and engineering judgment. In the absence of reliable calibration data, if two different models are applied to the same problem by two different modelers, quite different results may be anticipated, as illustrated in Fig. 11.1. The uncertainties associated with sediment transport modeling underscore the importance of conceptual modeling as a guide throughout the modeling process and as the means of determining which procedures and results are to be accepted as "realistic" and which are to be discarded as "unreasonable." Reliance on conceptual modeling and engineering judgment will be reduced, but not eliminated, if good calibration and verification data are available.

**8. Validation.** A model is validated when it accurately predicts conditions different from the calibration conditions, such as the effect of a hydraulic structure. For example, a model developed to predict long-term impacts may be rerun with actual hydrology

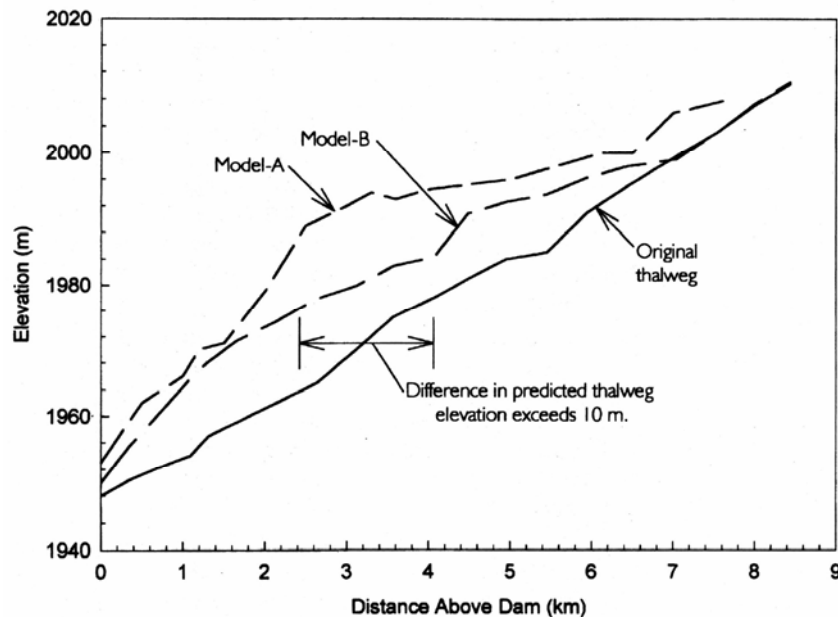


**FIGURE 11.1** Thalweg profiles above a proposed dam after 41 years of operation with annual flushing, as predicted by two different researchers using two different one-dimensional models. The two predicted thalwegs differ by more than 10 m in elevation over 20 percent of the modeled reach. This was due to differences in the input hydrograph time step used in the two models, computational differences, and the lack of data for model calibration.

following the first several years of project operation, and compared to field conditions to determine how well the model is predicting postproject conditions. Ideally the model would be improved by incorporation of the new data, and its usefulness as a future management tool would be enhanced. Validation may be considered particularly important in projects with deficient calibration data, or in situations where postproject conditions depart significantly from calibration conditions.

### 11.3 CONCEPTUAL MODELING

Conceptual modeling involves mental visualization of the fluvial system and perturbations thereof. Conceptualization may be supported by graphics, field data, and desktop calculations. The formulation of accurate conceptual models lies at the foundation of all engineering analysis and is the basis for engineering judgment. Conceptual modeling determines which potential problems are insignificant and may be ignored, which are to be analyzed in more detail, and which analytical approach and assumptions are to be used in subsequent analysis. Numerical and physical modeling supplement rather than replace conceptual modeling, which continues to be the basis for interpreting conflicting or unexpected results encountered during modeling, and for converting modeling results into specific design recommendations. Conceptual modeling provides the ultimate "reality check" against which all other modeling results must be compared.

In projects having a generous budget for data collection and modeling, extensive calibration data may be available and reliance on conceptual modeling may be reduced. More frequently, projects have tightly constrained budgets and time frames,

the available calibration dataset is extremely limited, and it is desired to analyze processes which can be simulated only approximately by current modeling tools. Under these conditions, results can depend heavily on conceptual modeling.

Accurate conceptual modeling proceeds from three types of knowledge: fundamental understanding of fluvial and sediment behavior, experience from other sites, and site-specific information. Fundamental concepts of hydraulics and sediment transport may be learned through both formal and individual study. The interpretive skills of fluvial geomorphology are particularly relevant to the interpretation of natural environments and development of conceptual and semiquantitative models of the fluvial systems. Experience is gained through one's own practice complemented by a review of case studies and site visits.

The site visit is a singularly important component of all modeling work. The following procedures can improve the information obtained during site visits.

- **Timing.** The initial site visit should be undertaken at the very beginning of a project, before formulating the problem and selecting the modeling tools. In rivers, the site visit should be timed to coincide with low water when the bars are exposed and may be sampled. An existing seasonally emptied reservoir should be visited during maximum drawdown to better observe geometry and deposition patterns.
- **Mapping and aerial photography.** The combination of mapping and aerial photography provide the initial basis for understanding the fluvial system. Both should be reviewed prior to a site visit and taken to the field. An overflight of the project area is highly recommended. Oblique 35-mm photographs from an aircraft shot in an overlapping sequence can be a highly useful visualization tool, especially when combined with ground photography. For example, see the photos reproduced in Fig. 10.7.
- **Ground Photography.** Always take more film and photographs than will be needed, and photograph everything. Overlapping panorama-type photos can be very useful. Ground photography should also be used to illustrate riverbed characteristics, and in gravel-bed systems the photographic technique outlined by Adams (1979) and described in Sec. 8.8.10 can also provide quantitative grain size information for the armor layer.
- **Sampling.** Points of bed material sampling should be selected by the modeler. However, in some cases the modeler will not be directly involved in the collection and analysis of samples, but may be supplied with grain size curves based on sampling performed by others. Sample collection by the modeler during site visits is highly recommended, even if not part of the formal sampling program. The primary purpose of this sampling is to help the modeler observe bed conditions and grain size variations during the site visit. These observations will be more focused if the modeler attempts to collect representative samples, compared to a walkover or "windshield" reconnaissance. Informal samples collected by modelers need not be large, and for sands need not exceed 30 cm<sup>3</sup> in size (about the size of a 35 mm-film canister). The modeler's samples should be analyzed for grain size distribution and compared with the grain size curves provided by others to better correlate field conditions to the size distribution curves, and check for possible anomalies in the supplied data.
- **Interviews.** Residents, fishermen, utility workers, and others who have many years of familiarity with the system should be interviewed. They can provide valuable information on trends or unusual events that might otherwise be overlooked.

In summary, field time should be used to collect as much information as possible about the system, from every available source. Visit as many sites along the rivers as possible, not just bridges. Where possible, travel the study reach by boat. Collection of representative field information is the single most important activity leading to a reasonably accurate conceptual model of the prototype system.

## 11.4 NUMERICAL MODELING

---

Numerical sediment transport models are available to simulate flows in one, two, and three dimensions. However, most modeling is performed with one-dimensional models, which are far more robust than their two- and three-dimensional counterparts. Molinas and Yang (1986) noted that two- and three-dimensional models require extensive amounts of computer time and calibration data, and may not be desirable for solving engineering problems with limited data and resources when the problem can be analyzed within the context of a one-dimensional model. Because river systems and most reservoirs have highly elongated geometry, the assumption of one-dimensional flow is appropriate for the analysis of many types of sediment problems. The following discussion reflects the capabilities and requirements of one-dimensional models.

One-dimensional mathematical models are used to analyze sediment transport along long reaches of rivers or in reservoirs where essential transport processes can be simulated with a one-dimensional flow field. They are applied to problems such as sediment accumulation in reservoirs as a function of the operating regime, sediment pass-through, and scour below dams. Numerical models have several important advantages over physical models: lower cost, ease of re-running to simulate a variety of different conditions, ability to simulate some types of problems numerically that are unsuitable for physical modeling because of the scaling laws involved (e.g., sediment cohesion), portability, and reproducibility. Mathematical models may be copied onto magnetic or optical media, transported and reproduced on compatible computers anywhere worldwide, and stored for any length of time and then re-run.

The initial geometry of the model is established by using river cross sections and specifying the width, depth, and grain size distribution of the movable bed. The grain size and load of inflowing sediment at the upstream limit of the model must also be defined. Movable bed numerical models solve hydraulic and sediment transport equations iteratively through a series of time steps. In one-dimensional models, the hydraulic parameters are computed at the start of each time step, typically using the assumption of steady flow, and calculations proceed in the upstream direction according to the standard step method. The resulting hydraulic parameters are then used to solve sediment transport equations to determine sediment transport capacity along each reach during each time step. This transport capacity is then compared to the inflowing load and the bed condition to determine the amount and grain size of the sediment that is either deposited or scoured. A sediment balance is computed for each reach starting at the upstream limit of the model and proceeding downstream. The movable bed geometry is adjusted in accordance with net sediment scour or deposition along each reach, and the new bed geometry is then used in the hydraulic computations for the subsequent time step. These models usually incorporate a sediment bed consisting of multiple layers, allowing the process of armor formation to be simulated.

Most of the commonly used numerical sediment transport models were originally developed for the analysis of movable bed rivers having coarse sediments and employ sediment transport equations developed from flume and river data. In contrast, reservoir problems may involve the analysis of grain sizes ranging from cobbles in the delta area to clays near the dam. The silts and clays which normally behave as wash load in most rivers, and which are ignored in many river sedimentation models, often constitute the majority of the total sediment load in a reservoir. Unlike riverine systems, reservoirs are normally depositional environments. However, during drawdown, reservoirs may experience retrogressive erosion, hyperconcentrated flow, and modification of deposit erodibility by sediment cohesion. A relatively small percentage of cohesive material can

significantly decrease the erosion rates for coarse sediment, as discussed in the Sefid-Rud case study (Chap. 23). These phenomena are atypical of river environments and can be simulated only in a very approximate manner by current numerical models.

Present numerical models are not well-suited to modeling sediment transport in complex curvilinear or three-dimensional flow fields, complex flows around structures, transport phenomena associated with turbid density currents, and problems involving river morphology. Numerical modeling of sedimentation problems only approximates the behavior of the prototype and does not substitute for professional experience and judgment, as model results typically require considerable interpretation. Mathematical models have also historically been limited in their ability to demonstrate results visually compared to physical models, although postprocessors that provide tools such as contour mapping, animation, and particle-tracing greatly enhance visualization, when two and three-dimensional models are used.

## 11.5 CONSTRUCTION AND CALIBRATION OF NUMERICAL MODELS

Several aspects of preparing and calibrating one-dimensional models are outlined in this section. Detailed information on the application of specific numerical models is available from user manuals, model vendors, and short courses. The site visit and related activities discussed under conceptual modeling should be undertaken before initiating model development.

### 11.5.1 Hydrology

In most one-dimensional models, the inflowing hydrograph is specified as a series of constant-discharge intervals, as illustrated in Fig. 11.2. Because sediment transport is

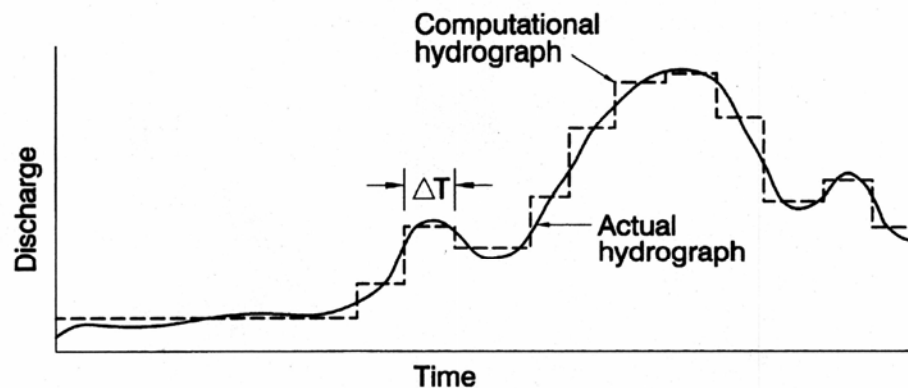


**FIGURE 11.2** Stepwise approximation of a continuous discharge time series for input into a numerical sediment transport model.

concentrated in periods of higher discharge, low flows may be simulated by a long period of constant discharge, or flows below a threshold considered to have negligible effect on sediment transport may be simply ignored. Proposed condition hydrology may be modified by a change in operating rules which influences the flow-duration characteristics of the stream.

### 11.5.2 Geometry

To represent the behavior of a fluvial system in a one-dimensional model requires that the system geometry be specified in a manner that reproduces the essential prototype hydraulic behavior. Model geometry must be configured to simulate a one-dimensional flow path followed by sediment and water moving toward the dam, and cross-section locations should be selected to reflect reach-averaged hydraulic conditions.

There is no rule of thumb for the distance between cross sections, and, depending on the study purpose, cross sections may be located several kilometers apart or only a single river width apart. The key objective is to reproduce the hydraulic characteristics of the reach. Cross-section geometry at a specific point may require adjustments to better simulate the hydraulic characteristics of the reach. Hydraulically ineffective areas of the reservoir lying outside the main flow path should be eliminated from the model, as illustrated in Fig. 11.3. Similarly, surveyed sections in rivers may be truncated to eliminate areas of ineffective flow caused by obstructions (Fig. 11.4). Whether a given discharge is contained within the movable channel boundary or can overflow onto the floodplain can have a significant impact on sediment transport, and overbank elevations may be adjusted to reflect values representative of the reach when survey lines intersect localized depressions in the floodplain.

In addition to defining the initial hydraulic geometry of the cross section, it is also necessary to define the width and depth of the movable bed. Field inspection should give particular emphasis to the identification of bedrock or clay lenses that may limit the scour depth and sediment supply during large events. Horizontal limits of the movable bed should be based on field inspection and indicators such as vegetation. A generalized idea of the sensitivity of one-dimensional sediment transport models to input parameters is given in Table 11.1.

### 11.5.3 Selection of Transport Equation

The use of different bed material transport equations in a numerical model can produce significant differences in the simulation results. For example, Gist et al. (1996)

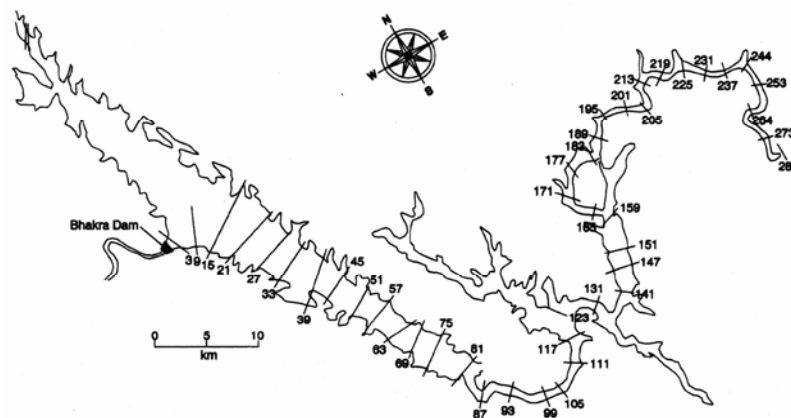


**FIGURE 11.3** Bhakra dam, India, illustrating the layout of the cross sections used to simulate sedimentation processes by a one-dimensional mathematical model (after Mandnwrnft et al., 1992)

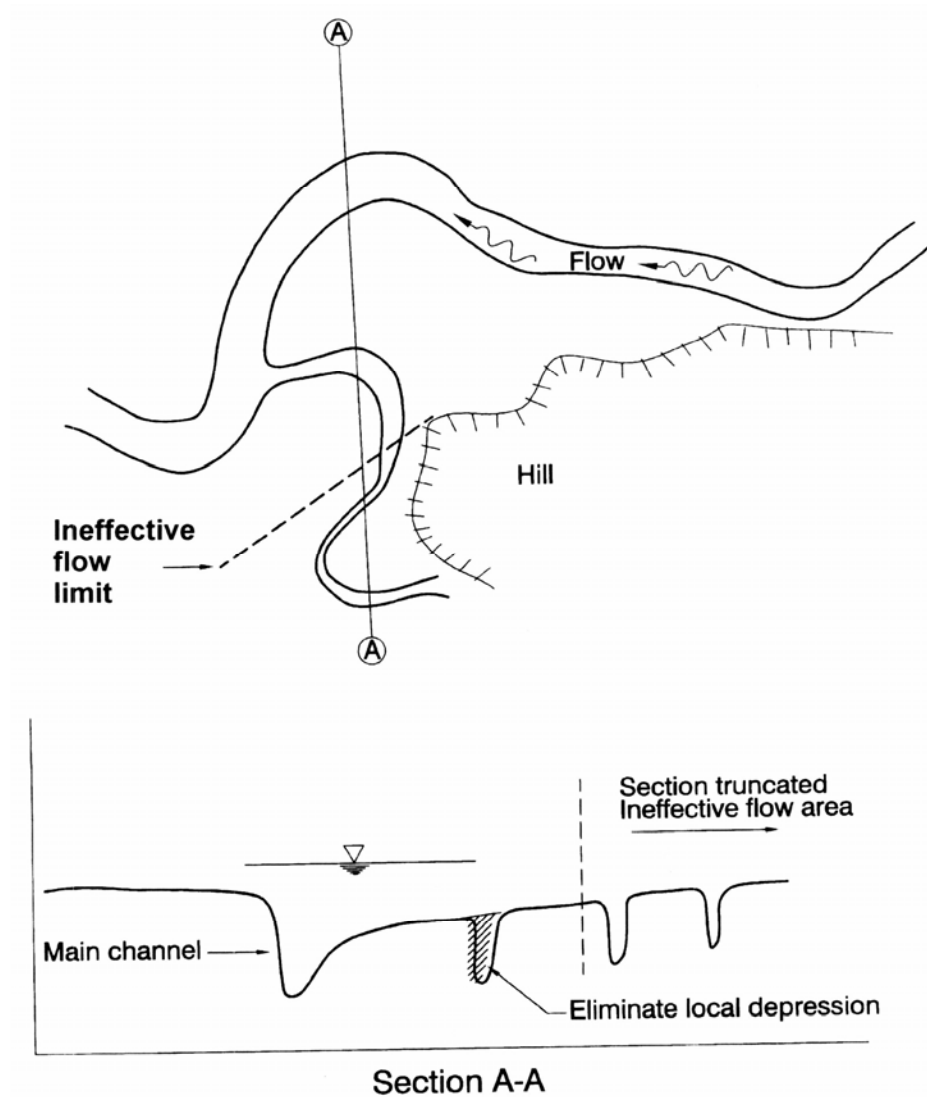


**FIGURE 11.4** Modification of cross-section hydraulic geometry to eliminate areas of ineffective flow during overbank flooding.

Tested three different sediment transport functions in a HEC-6 model of sediment trapping in a debris basin. Different equations produced a four-fold variation in total sediment transport and more than a two-fold difference in the amount of sediment trapped during a single-event analysis. When measured bed material load data are available, transport equations should be compared to the measured values to select the applicable equation. In existing reservoirs with appreciable sediment accumulation or a suitable calibration event, the historical depositional and scour process should be simulated with different equations and the transport relation that best reproduces the observed historical pattern should be selected.

**TABLE 11.1** Relative Influence of Input Parameters on Sediment Routing Models

Description of Data	Relative importance of data		
	High	Medium	Low
Physical parameters:			
Roughness coefficients	X		
Sediment inflow	X		
Water inflow	X		
Variation of bed elevation		X	
Sediment size distribution		X	
Water temperature			X
Cross-section geometry	X		
Active layer thickness	X		
Coefficients of losses			X
Operational parameters:			
Sediment transport equation	X		
Time step duration	X		
Number of stream tubes		X	
Number of time iterations			X
Stream power minimization			X
Roughness equation	X		

*Source:* Molinas and Yang (1991).

Most numerical models allow a customized sediment transport equation to be used if none of the equations provide a good fit. In this case, Simons and Senturk (1992) suggest the following procedure. Using the existing data collected from a river station, plot sediment load or concentration as a function of water discharge, velocity, slope, depth, shear stress, stream power, and unit stream power. The least scattered curve without systematic deviation from a one-to-one correlation between the dependent and independent variables should be selected as the sediment rating curve for the station. In constructing a rating curve, ensure that the time scales for sediment transport and the hydrologic data series are compatible. For example, if the sediment transport model uses a hydrologic series in which one day is the smallest time step, the sediment rating curve and other hydrologic variables should be computed for average daily values.

Often field data on transport rates are not available, and in the case of new reservoirs there will be no historical deposition pattern to guide modeling. In these cases measurements at other sites and engineering judgment can contribute to the selection of an appropriate transport function. Comparisons have shown that some transport equations tend to be better predictors of transport rates than others when applied to diverse datasets. These comparisons provide one starting point for the selection of an appropriate equation. Final selection of the transport equation will depend on calibration results,

Brownlie (1981) compared the ability of 14 transport equations to predict measured transport rates, in 5263 records from laboratory flumes and 1764 field data records, as summarized in Fig. 11.5. The Brownlie equation gave the best fit of all equations for this particular dataset because its parameter values were calibrated from this dataset, and it would not be expected to perform as well when verified for an independent dataset. In a comparison of measured sediment transport rates for field and laboratory datasets by

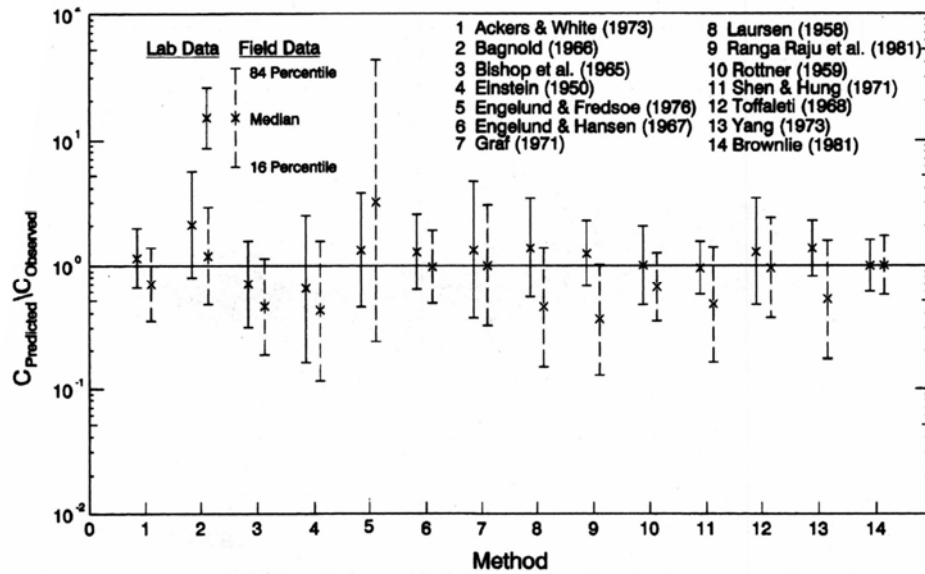


**FIGURE 11.5** Comparison of the ability of 14 different sediment transport equations to predict measured transport rates in rivers and laboratory flumes (*Brownlie, 1981*).

Alonso (1980), ASCE (1982), and Yang and Wan (1991), the Yang equation gave the best overall results. Brownlie also plotted the goodness of fit of each individual equation for the test dataset. The plot for Yang's equation in Fig. 11.6 shows that a much better agreement is achieved with the flume data than with the field data. This same pattern occurred with most of the equations tested.

Transport equations may also be selected based on a comparison of conditions in the study area against the dataset used in the development of each equation. The range of the basic data used to develop selected equations is given in Table 11.2. Regime or regression equations should be used only when the flow and sediment conditions are similar to those from which the regression coefficients were derived. More formal methods may be used to compare the applicability of specific transport equations to a given fluvial environment. Williams and Julien (1989) suggested an applicability index based on the relative roughness  $Z = d/D$ , Shields parameter  $F_*$ , and dimensionless grain size  $d_*$ . The range of these parameter values in the calibration dataset for each transport equation is compared to the range of each of these same parameters in the prototype system to determine each equation's likely applicability.

When fine sediments are simulated by numerical models, recall that the settling is controlled not by the grain size of individual particles, but by the extent of flocculation. The settling rate or sedimentation diameter for fines should be analyzed in native water.

#### 11.5.4 Calibration

In existing reservoirs, data may be available which document grain size and geometric change over time. Calibration may be performed using these data (see Fig. 20.14). However, calibration against a period of continuous deposition will not guarantee that the model will accurately simulate the effect of a new operating rule that initiates scouring of these deposits.

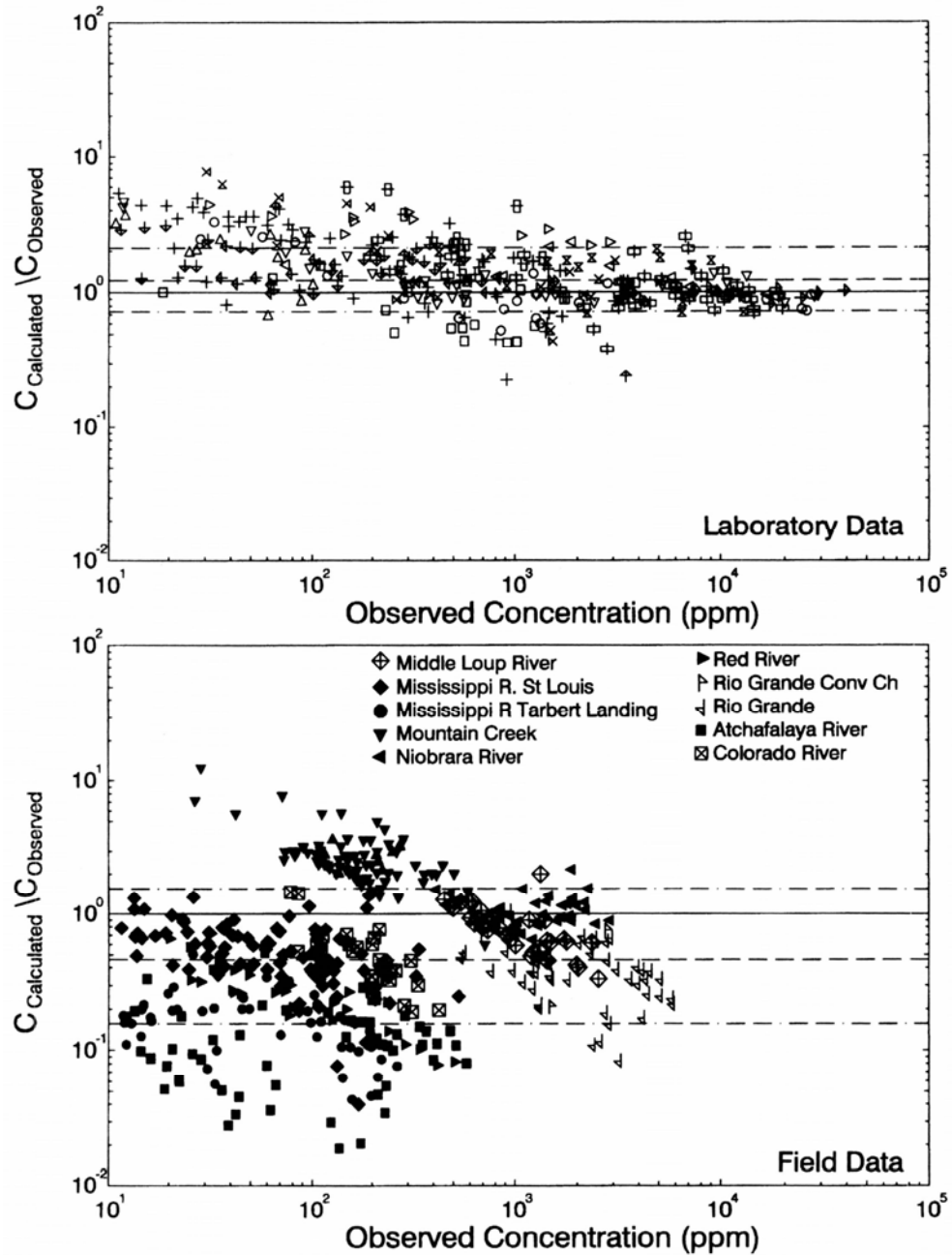


**FIGURE 11.6** Ability of the Yang sand transport equation to predict sand transport rates (*top*) measured in laboratory flumes and (*bottom*) measured in rivers (Brownlie, 1981)

In rivers lacking transport data, and at proposed reservoir sites, the model should be calibrated by simulating the existing condition, reproducing the existing streambed slope and grain size characteristics along the study reach, including any observed trends of bed aggradation or degradation. For example, in the modeling of Waimea River on Kauai, Hawaii, Copeland (1991) selected the transport equation for its ability to simulate the

**TABLE 11.2** Range of Data Used to Construct Selected Sediment Transport Equation.

Equation	Type	Uniform grain Size	Size range, mm	Data sources ( $D$ = depth, ft)
Meyer-Peter and Muller	Bed Load	Yes	0.4-30	Flumes, $D < 1.2$ m
Laursen	BMT	No	0.011-4.08	Flumes and rivers
Toffaletti	BMT	No	Fine sand 0.1-1.3	Flumes and rivers, $0.1 < D < 50$
Ackers-White	BMT	Yes	1-3	Flumes and lowland rivers
Yang (sand)	BMT	Yes	0.152-1.35	Flumes and rivers, $0.1 < D < 50$
Colby	BMT	Yes	0.1-0.8	Flumes and rivers, $1 < D < 100$
Shen and Hung	BMT	Yes	Sands	Flumes and shallow rivers
Modified Einstein	Total load	No	0.28	Niobara and Middle Loup River, flumes
Einstein	BMT	No	0.785-28.65	

BMT = Bed Material Transport.

Source: Adapted from Williams (1990).

direction of bed aggradation and degradation observed in different reaches. In this case, modeling results type indicated that equilibrium conditions did not prevail under all flow conditions. Rather, the system was supply-limited at high discharges, causing the study reach to degrade during infrequent large events. Aggradation occurred during smaller events.

For a proposed reservoir site the numerical model may be used to simulate a similar existing reservoir in the region. This exercise can demonstrate the model's ability to simulate the pertinent processes, and aid in the selection of transport equations and parameter values. For example, Zarn (1992) modeled a chain of five planned hydro stations along the upper Rhine River in Switzerland, using the MORMO one-dimensional steady-flow numerical model (not publicly distributed) which uses 21 grain sizes to account for bed material processes including transport, scour, deposition, sorting, and armoring of sediment sizes ranging from 0.01 to 300 mm. Sediment release at the existing Reichenau hydropower station, located 39 km upstream of the proposed project, was simulated by modeling and verified against field data. The model was then used to simulate sediment accumulation and the effects of different sediment pass-through options at the proposed power stations.

In general, model construction should proceed by first entering several cross sections and then running the model in a fixed-bed mode (hydraulics only, no sediment). Once the first model segment functions, continue adding cross sections until the model is completed. Use fixed-bed mode to perform hydraulic calibration for low, bankfull, and high flows before calibrating for sediment. Roughness values can change as a result of sedimentation, vegetative growth, and change in water depth. In elongated reservoirs, the roughness value selection can have a significant impact on upstream water levels, as described with reference to the Three Gorges Dam in Chap. 13. Perform calibration adjustments proceeding in the same direction as the computational sequence. Thus, for subcritical standard step hydraulic computations, start hydraulic adjustments at the downstream limit of the model and proceed upstream. In contrast, sediment is entered at the upstream end of the model and is transported downstream by the computational sequence. Thus, when calibrating for sediment, start adjustments at the upstream end of the model and work downstream. The upstream limit of the model should consist of a reach having stable characteristics throughout all simulations for both existing and proposed conditions.

## 11.6 DESCRIPTIONS OF SELECTED NUMERICAL MODELS

---

Many mathematical models have been developed for simulation of sediment behavior. In a compilation of U.S. models, Fan (1988) obtained information on 48 private and government models in the following categories: 34 stream-, 18 watershed-, and 20 reservoir-sedimentation models. Multifunction models were listed in multiple categories. Many additional models have been developed and are used in other parts of the world. In summarizing the status of the available U.S. models, Fan (1988) made the following generalizations. All computer stream sedimentation models include three major model components: water routing, sediment routing, and special function modules. Most models include the option of selecting alternative sediment transport formula, but none provides criteria for making that selection. Most models use the finite difference method and simulate unsteady *flows* as a series of steady *flows*. Most are equilibrium transport models in which sediment transport is assumed to reach equilibrium conditions during each model time step. Different models may produce significantly different results, even when run with the same set of inputs. All models are strongly data-dependent and require adequate data for calibration and verification, but in practice the field data required for this purpose are often lacking. All models require a great deal of professional judgment and field experience for interpretation of their outputs. Dawdy and Vanoni (1986) stated that the choice of a modeler is probably more important than the choice of a model because of the many judgmental factors involved.

The remainder of this section briefly describes several sediment transport models that may be useful for analyzing sedimentation issues associated with reservoirs. The models described illustrate the types of numerical tools currently available for use on microcomputers, and show that each model will have certain features that can make it attractive compared to others in certain situations. There is no general-purpose model that is "best" for all conditions, and there are many good models in addition to those mentioned here.

### 11.6.1 HEC-6

The U.S. Army Corps of Engineers HEC-6 model (U.S. Army, 1991) is probably the most widely used model in the United States for the simulation of sediment transport in rivers and reservoirs. Developed by William Thomas at the Army's Hydrologic Engineering Center, it was first distributed for use within the Corps in 1973. The model has been modified and enhanced through new releases, and the current version handles both deposition and scour of sediment sizes from clay to boulders. A list of model vendors is available from the Hydrologic Engineering Center, 609 Second St., Davis, California 95616.

HEC-6 is a one-dimensional movable-boundary open-channel flow model that computes sediment scour and deposition by simulating the interaction between the hydraulics of the flow and the rate of sediment transport. The model incorporates the assumption that equilibrium conditions are achieved between the flow and the bed material transport within each time step, an assumption also made in most other sediment transport models. This assumption may be violated during rapidly rising and falling hydrographs, which can limit the model's ability to simulate single events. For this reason the HEC-6 program documentation specifically states that the model is designed for the analysis of long-term river and reservoir behavior. However, in practice it has also been used to simulate single events (for example, Gist et al., 1996)

HEC-6 can simulate a main river plus tributaries and local inflows. The hydraulic

profile is simulated by the standard step method and Manning's equation to solve the one-dimensional energy equation, with the user specifying  $n$  values for both channel and overbank areas at each cross section. It supports the use of both downstream and internal rating curves, expansion and contraction losses, flow, containment by levees, levee overtopping, ineffective flow areas, and conveyance limits in a fashion similar to the HEC-2 model, but it does not handle split flow or have special routines for bridges. Supercritical flow is approximated by normal depth, and sediment transport in supercritical reaches is not explicitly computed.

At each time step, the hydraulic computations are initiated at the downstream boundary of the model and proceed upstream. Then sediment computations are initiated at the upstream boundary and proceed downstream. The bed elevation and grain size is adjusted throughout the modeled reach, and hydraulic computations for the next time step are initiated. Sediment transport capacity is calculated at each time interval. Transport potential is calculated for each grain size class in the bed as though that size comprised 100 percent of the bed material. This transport potential is then multiplied by the fraction of each size class present in the bed to determine the transport capacity for each size class.

HEC-6 model geometry is established by defining a series of cross sections, using the same geometric input format as the HEC-2 hydraulic model. The user is required to establish the limits of the erodible bed, which will not change over the course of the simulation. The initial bed geometry is assumed to raise and lower uniformly as a result of deposition or sedimentation (Fig. 11.7), except that for simulating reservoir

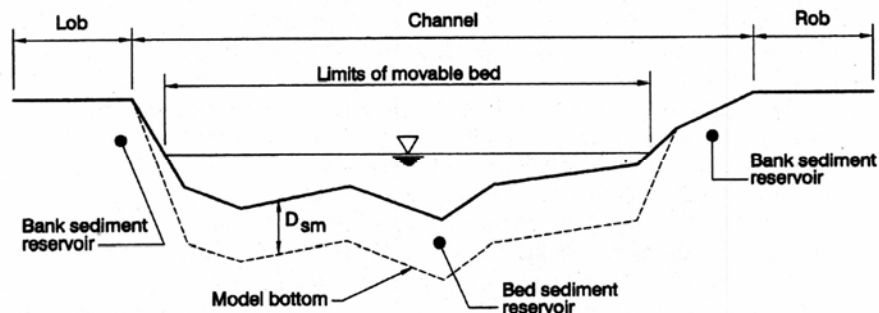


**FIGURE 11.7** In the HEC-6 model, aggradation and degradation cause the entire movable bed to raise or lower (U.S. Army, 1991).

sedimentation the model will allow all sediment to be focused into the bottom of each cross section, producing horizontal sediment layers. Both sedimentation and scour can occur within the movable channel limits, but only deposition can occur in the overbank floodplain area. Armoring processes are simulated. The model incorporates 12 different transport equations or equation combinations, plus a user-specified transport function. Gee (1992) notes that the impact of using different transport equations will most likely be greater on transport rates than on geometry changes. Fines, consisting of silt and clay-size particles, are scoured according to Ariathuri's (1976) adaptation of Partheniades' (1965) method. Deposition of fine sediment is based on Krone's (1962) relationship.

Key advantages of this model include good documentation (U.S. Army, 1991; Gee, 1992), continuing support and development by the Hydrologic Engineering Center, a long history of use, familiarity to many reviewing agencies, and the availability of training through the Corps of Engineers and university short courses. A particular strength

of the HEC-6 model for reservoir analysis is its ability to simulate both deposition and scour for a wide range of grain sizes, including silts and clays. Many other stream sedimentation models do not incorporate the capability to simulate fines.

In the future this model will be incorporated into the River Analysis System (HEC-RAS), which consists of an integrated system of hydraulic analysis software consisting of a graphical user interface, hydrologic and geometric database, separate hydraulic analysis components, data storage and management capabilities, and graphics and reporting facilities. When fully implemented the system will contain three one-dimensional hydraulic analysis components: (1) steady-flow water surface profile computations, replacing HEC-2 which will no longer be supported by the Corps; (2) unsteady-flow simulation based on the UNET model; and (3) movable boundary sediment transport, eventually replacing HEC-6. A key feature of this system is that all three computational modules will use a common geometric and hydrologic database.

### 11.6.2 GSTARS

The General Stream Tube Model for Alluvial River Simulation (GSTARS) was developed by the U.S. Bureau of Reclamation (Molinas and Yang, 1986) and is available from Ted Yang, MS D8540, U.S. Bureau of Reclamation, P.O. Box 25007, Denver, CO 80225. GSTARS is a steady-, nonuniform-flow, one-dimensional model which simulates certain aspects of two-dimensional flow by using the stream tube concept for hydraulic computations. It is also capable of solving for channel width as an unknown variable, based on the concept of stream power minimization. A version which will incorporate routines specifically designed to simulate reservoir sedimentation processes is under development.

Hydraulic computations may use the Manning, Darcy-Weisbach, or Chezy equation, and computations can be carried through both subcritical and supercritical flows without interruption. Geometry is specified by channel cross sections, and roughness coefficients are specified as a function of distance across the channel.

The model uses stream tubes to compute the lateral variation in hydraulic and sediment transport conditions within the cross section. Stream tubes are imaginary channels within the wetted cross section bounded by streamlines. Since flow does not cross streamlines, each stream tube has the same discharge (Fig. 11.8). The bed elevation in each stream tube is allowed to move vertically up or down depending on transport conditions, and one stream tube may be eroding while another parallel stream tube is aggrading, providing a more realistic pattern of channel erosion and degradation than in models in which bed geometry is fixed. Stream tube boundaries are computed at each cross section at each time step to provide equal hydraulic conveyance within each stream tube. The user determines the number of stream tubes to be used, and when a single stream tube is used, the model becomes one-dimensional in the conventional sense.

The model simulates armoring by using a multiple-layer bed. Some transport equations (Yang, Ackers and White, Engelund and Hansen) compute total load without breaking it into size fractions, but to track the composition of the bed and for armoring computations it is necessary to determine transport rates by size class. In the GSTARS model, the sediment load is computed for each size class individually as if the entire bed consisted of that size. The resulting load is multiplied by the fraction of bed material corresponding to that particle size to give the bed material load for each size class. Up to 10 user-specified size classes may be used in the model, but the model will not simulate the scour and deposition of silts or clays.

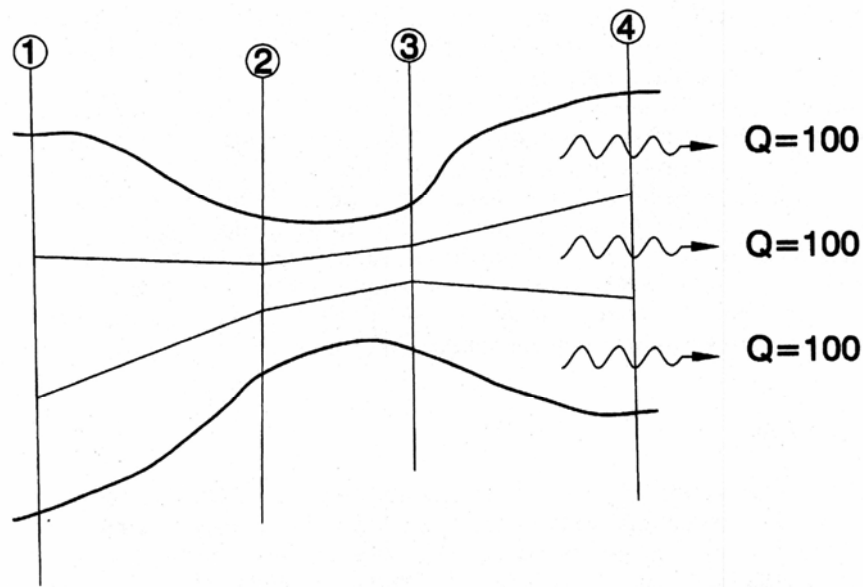


**FIGURE 11.8** Illustration of the stream tube concept used in the GSTARS model.

Changes in channel width can be computed by the model based on minimum stream power theory which states (Chang, 1980):

For all alluvial channels, the necessary and sufficient condition of equilibrium occurs when the stream power per unit length of channel,  $\tau QS$ , is a minimum subject to given constraints. Hence, an alluvial channel with water discharge  $Q$  and sediment load  $Q$  as independent variables, tends to establish its width, depth, and slope such that  $\tau QS$  is a minimum.

This concept is implemented into the model by integrating the value of stream power ( $\tau QS$ ) along the channel. At a given time step, if alteration of the channel width results in lower total stream power than raising or lowering the channel bed, then channel adjustments are made in the lateral direction instead of vertical. Thus, erosion can either deepen or widen a channel. Similarly, depositing sediment accumulation can be placed on the bottom or on the banks. Channel widening or narrowing computations are restricted to the stream tubes adjacent to channel banks, and the bed of interior stream tubes can move only vertically.

### 11.6.3 FLUVIAL

The FLUVIAL model is a private one-dimensional model developed by and available from Howard Chang (P.O. Box 9492, Rancho Santa Fe, CA 92067; Fax (619) 756-9460; email [changh@mail.sdsu.edu](mailto:changh@mail.sdsu.edu)). The fundamental characteristics of the FLUVIAL model are described by Chang (1988) and its use to analyze reservoir sedimentation is described in the Feather River case study (Chap. 22).

The FLUVIAL model contains five major components: (1) hydraulic routing, (2) sediment routing, (3) changes in channel width, (4) changes in channel bed profile, and (5) changes in transverse bed geometry due to curvature. A particular feature of this model is its ability to simulate the development of the transverse bed slope in a curved

reach, provided calibration data are available. The application of this feature is illustrated in the Feather River case study (Fig. 22.13).

Model geometry is specified by a series of cross sections. Bed material composition is specified at the upstream and downstream boundaries of the model and may be specified at other locations as well. Hydraulics, sediment transport, and bed and width adjustment are simulated iteratively. Hydraulic routing can be performed as a series of steady approximations by the computationally faster standard step method, or as dynamic-wave unsteady flow. Bed roughness can be input in the form of Manning's  $n$  values, or Brownlie's (1983) formula can be used to predict alluvial bed roughness. Six different sediment transport formulas are incorporated into the model, and armoring computations are performed. The model does not simulate silts and clays.

#### 11.6.4 TABS

TABS-2 is a collection of generalized computer programs and utility codes integrated into a numerical modeling system for analyzing two-dimensional hydraulics, transport, and sedimentation problems in rivers, reservoirs, bays, and estuaries (Thomas and McAnally, 1985). There are three basic components: RMA-2 computes two-dimensional hydraulics, STUDH computes sediment transport, and RMA-4 which computes water-quality parameters.

RMA-2 is a finite element solution of the Reynolds form of the Navier-Stokes equations for turbulent flows. Friction is calculated by Manning's equation and eddy viscosity coefficients are used to define turbulence characteristics. The model automatically recognizes dry elements and corrects the mesh accordingly. The sedimentation model STUDH solves the convection-diffusion equation with bed source terms, and is structured for either sand or cohesive sediments. Clay erosion is based on work by Partheniades and the deposition of clay utilizes Krone's equations. Deposited material forms layers, and bookkeeping within the STUDH code allows up to 10 layers at each node for maintaining separate material types, deposit thickness, and deposit age. Transport calculations with RMA-4 are made with a form of the convection-diffusion equation that has general source-sink terms. Up to seven conservative or decaying substances can be routed.

Whereas one-dimensional models specify geometry by cross sections, two- and three-dimensional models use a finite element mesh to establish model geometry (Fig. 11.9). Multidimensional models have much greater computational requirements than one-dimensional models because they solve more, and more complex, equations at every node and time step. Therefore, it is desired to minimize the number of nodes while adequately reflecting the significant features of the hydraulic geometry. A microcomputer version of TABS-2, with pre- and post-processing software for mesh generation and flow visualization, is available from vendors such as Boss International, 6612 Mineral Point Road, Madison, WI 53703 (Internet <http://www.bossintl.com>).

#### 11.6.5 SSIIM

The SSIIM model developed by Nils Olsen uses a finite volume method to solve the Navier Stokes equations in three dimensions on a general nonorthogonal grid. Another three-dimensional finite volume model is used to calculate sediment concentration within the reservoir by solving the diffusion/convection equation for sediment concentration. The primary motivation for development of this model was the difficulty of simulating fine sedi-

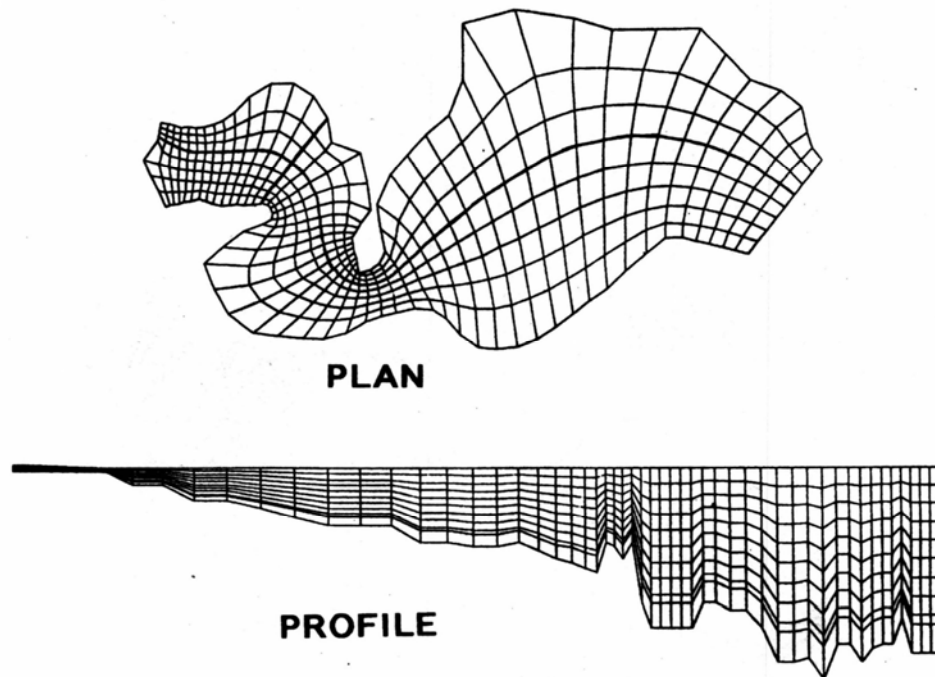


**FIGURE 11.9** Example of a geometric mesh used in a three-dimensional model of Angostura Reservoir, Costa Rica (*courtesy of N. Olsen, SINTEF, Trondheim, Norway*).

ments in physical models. Particle animation is provided to aid flow visualization. Application of this model to the analysis of sediment accumulation at two hydropower reservoirs in Costa Rica has been reported by Olsen et al. (1994). Flow fields simulated by this model are illustrated in Fig. 11.10. The model, which runs under the OS/2 operating system, is available at no cost to the developer, Nils Olsen at the Norwegian Institute of Technology, and the program and documentation can be downloaded from the Internet. It may be located by conducting a search for SSIIM 13.ZIP or SSIIM using an Internet search tool.

## 11.7 PHYSICAL MODELING

---

A physical model is a scaled physical representation of the prototype system which uses a fluid and sediment to simulate prototype behavior. Water is almost always used as a fluid, although in some instances air models have been used for analysis of problems such as groyne locations for river training. Model sediment may consist of natural grains or artificial material such as plastics or walnut shells. Basic concepts of physical modeling and scaling are summarized by French (1985) and Borg (1993). A physical model used to analyze reservoir flushing is shown in Fig. 11.11.

Physical models can generally be classified into four categories: (1) undistorted fixed-bed model in which both vertical and horizontal scales are equal, (2) distorted fixed-bed model with a larger vertical than horizontal scale, (3) undistorted movable-bed model, and (4) distorted movable-bed model. Physical models

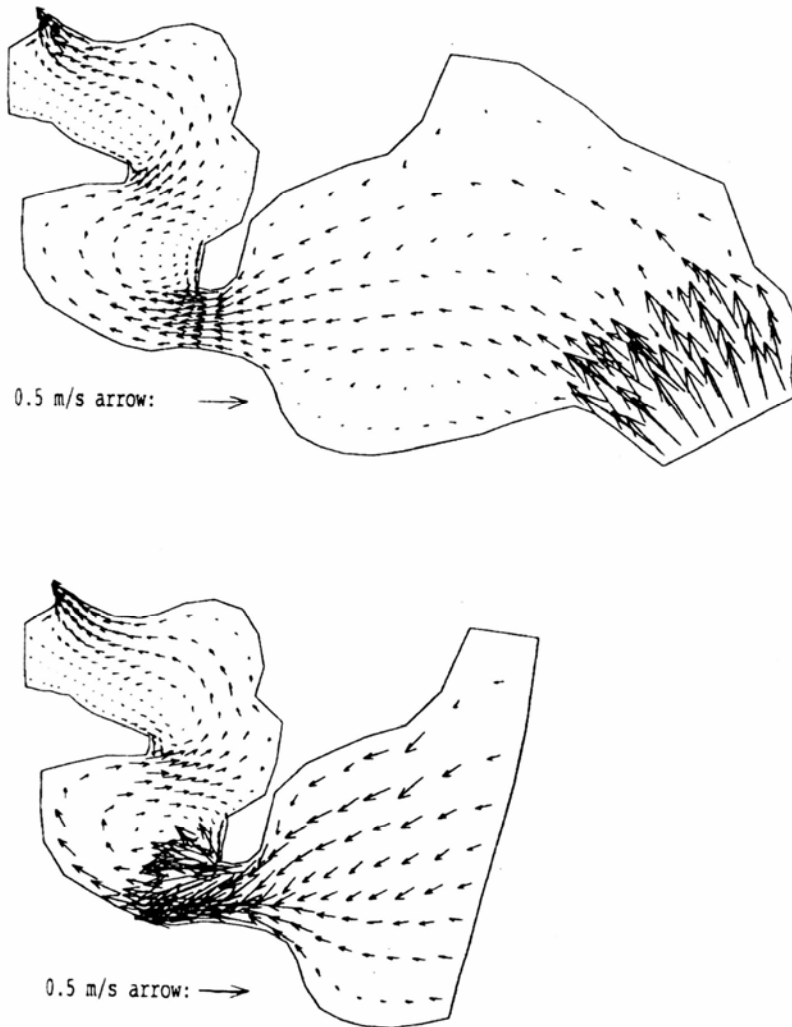


**FIGURE 11.10** Simulation of change in flow velocities due to sediment accumulation in the proposed Angostura reservoir in Costa Rica. Top: Initial condition. Bottom: condition after 6.8 years of sedimentation. (Olsen *et al.*, 1994).

must be both geometrically and dynamically similar to the prototype system and should maintain the proper relationship between the forces influencing water and sediment movement: gravity, fluid friction, viscosity, surface tension, and sediment cohesion. However, a geometric scale model does not produce true dynamic similarity because the ratios between these forces are not preserved when physical dimensions are scaled. Thus, model scales are selected to preserve the scale ratios of the most important forces, while allowing some deviation in less important parameters. In a distorted model, the vertical scale is exaggerated to produce adequate flow depths. Distortion is required in hydraulic models when the physical size of the prototype system is such that large model scales must be used (e.g., the 1:2000 scale model of the Mississippi River). Without vertical distortion flow depths would become too small to measure satisfactorily, and the shallow flow may be laminar and also affected by surface tension. In models using a scale factor on the order of 1:50, problems due to scaling of forces are minimized because gravity is the



**FIGURE 11.11** Physical model at 1:50 scale used to simulate the formation of a flushing channel using an 8m diameter low-level outlet at the Changma Dam on Shule River in the Gobi Desert. Model constructed by the Northwest Hydrotechnical Science Research Institute under contract to Ganzu Provincial Government, China (G. Morris)

primary force influencing open-channel hydraulics in both the prototype system and at the model scale; out-of-scale forces such as fluid friction and surface tension do not introduce significant error.

The design and operation of movable bed models is much more complex than fixed-boundary hydraulic models. Boundary roughness in a movable bed model may be influenced by bed forms as well as grain size, the model must simulate the motion of sediment as well as water, and fine sediment cohesion cannot be scaled properly. The need for vertical distortion occurs frequently in movable-bed models, since the slopes and velocities characteristic of an undistorted hydraulic model are often too small to move any of the model materials used to simulate stream sediment. Exaggeration of the vertical scale produces greater flow depths and higher tractive forces.

### 11.7.1 Applicability of Physical Models

Physical models are well suited for analyzing problems involving complex geometry, river morphology, or flow curvature which result in sediment concentration profiles and deposit pattern varying in both the transverse and longitudinal directions. Problems of this type involve the design of sluice gates and low-level outlets for sediment flushing, flow training structures, scour and deposition patterns in the vicinity of structures, and sedimentation in navigation channels and locks. Turbidity currents may also be simulated.

As an advantage, physical modeling has traditionally been more visual and intuitive than mathematical modeling, since the physical scale model provides the direct and immediate representation of flow features and sediment patterns. Processes may be visually documented with a video camera. A visit to a hydraulic laboratory to view a

physical model is impressive, and the physical results can be understood in an intuitive manner by non-modelers.

### 11.7.2 Disadvantages of Physical Models

Key disadvantages of physical models include high cost, long time periods required to run extended simulations, and immobility. A physical model is constructed at a single laboratory and cannot be transported or easily reproduced, and it cannot be stored for a long period since it occupies laboratory space needed for other studies. Contracts for physical modeling work typically include a clause specifying the period after work is completed that the model will be maintained in operable condition, in case a review indicates the need for further modeling activities. Physical models are not capable of accurately scaling cohesive sediment behavior. When a question can be adequately addressed by either a mathematical model or a physical model, it is generally less costly to use mathematical modeling. Physical modeling tends to focus on the analysis of situations where the flow fields are too complex for mathematical modeling, for analysis of bed morphology, or where it is important to have an intuitive physical representation of the system.

## 11.8 COMBINING NUMERICAL AND PHYSICAL MODELS

---

Reservoir problems frequently require the application of both physical and numerical models. Numerical modeling is used to simulate sediment movement along the long impounded reach and to simulate scour and armoring in the reach below the dam. Physical modeling is used to simulate the details of the complex flow field and sediment movement in the vicinity of the structure. The numerical model can be used to simulate the amount and grain size of sediment delivered into the vicinity of the dam. The physical model routes the inflowing sediment through the structure, analyzing patterns of deposition and scour. The conjunctive use of both physical and numerical models is illustrated in the Feather River case study.

## 11.9 EXAMPLES OF PHYSICAL MODEL SCALING AND OPERATION

---

A physical modeling study on California's Feather River is described in Chap. 22. The Feather River study involved the modification of an existing small structure for which there was a well-documented calibration event, and required the analysis of bed material load only. This section presents an example of a complex physical modeling study for the Gezhouba Project on China's Yangtze River involving the simultaneous analysis of bed load, suspended load, and density currents, for a wide range of sediment diameters, for the design of new structure on a major river. The physical modeling work was reported by Dou (1977), Li and Jin (1981), Tang and Lin (1987), and Tang (1990). The physical model and prototype system are compared in Fig. 11.12.

The Gezhouba Project is a multipurpose dam on China's Yangtze River, 47 m high, impounding a 1580-Mm<sup>3</sup> reservoir. Mean annual runoff is 542,900 Mm<sup>3</sup>, and the average annual sediment load includes 520×10<sup>6</sup> tons of suspended load, 6×10<sup>6</sup> tons of sand-size

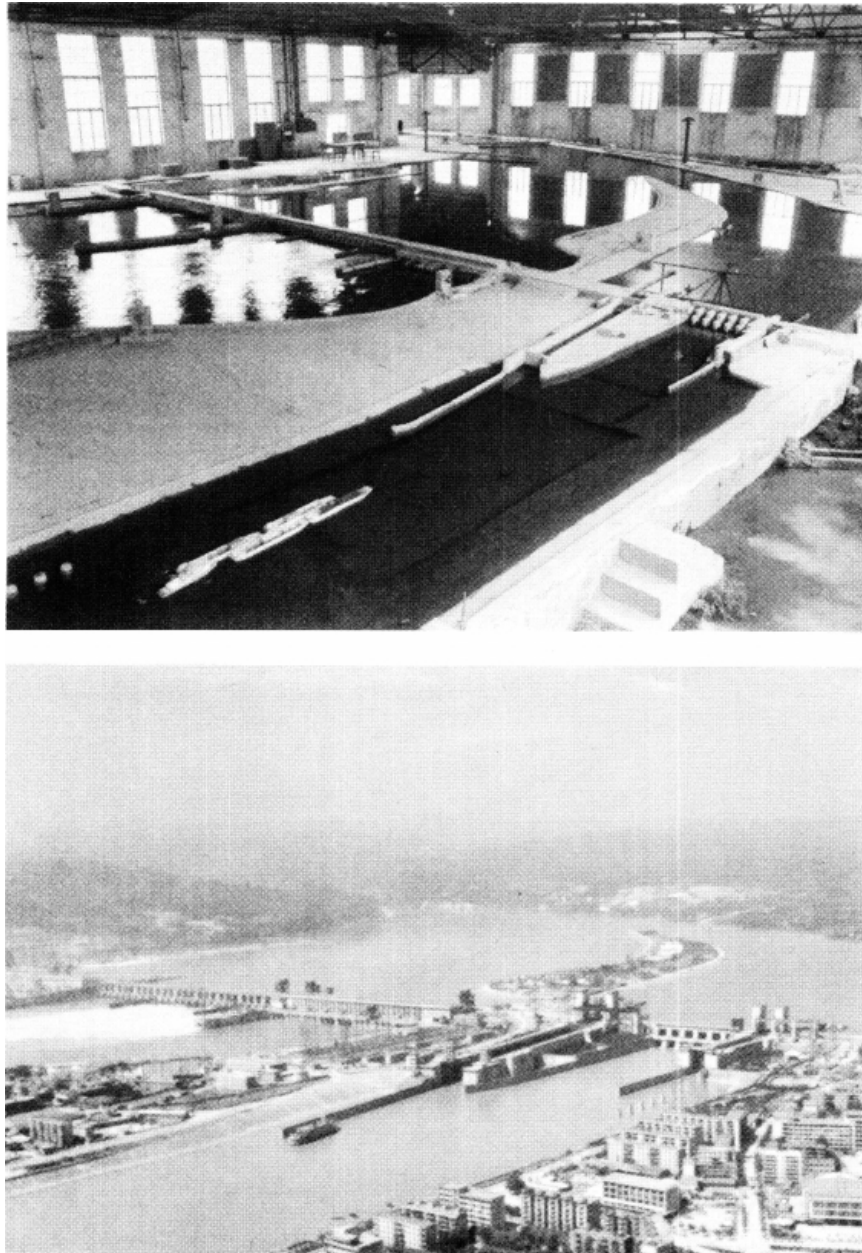


**FIGURE 11.12** Physical model (top) and aerial view of completed project (bottom) at Gezhouba Dam, Yangtze River, China (*courtesy Yangtze River Academy of Science*).

bed load, and 700,000 tons of gravel bed load. The median diameter of suspended sediment is 0.034 mm, and the gravel portion of the bed load has a median diameter of about 24 mm. The dam is situated 2.8 km downstream of the Nanjinguan Gorge, below the famous Three Gorges reach. At this point the main current direction turns almost 90° to the right, the river width increases from 300 m at the Nanjinguan Gorge to 2200 m near the dam axis, and the river form transitions from a single narrow channel to three channels with a wide cross section (Fig. 11.13). Given the large flood discharge and limitations imposed by navigation requirements, the main sluice structure was located in the middle channel and Gezhouba Island was partially excavated to improve the approaches to the flood sluices. Power plant intakes and navigation locks were placed on either side of the sluices.

**11.9.1 Problem Identification**

Three main sediment management problems needed to be solved for this project. First, it was necessary to determine the general layout of hydraulic structures along the dam

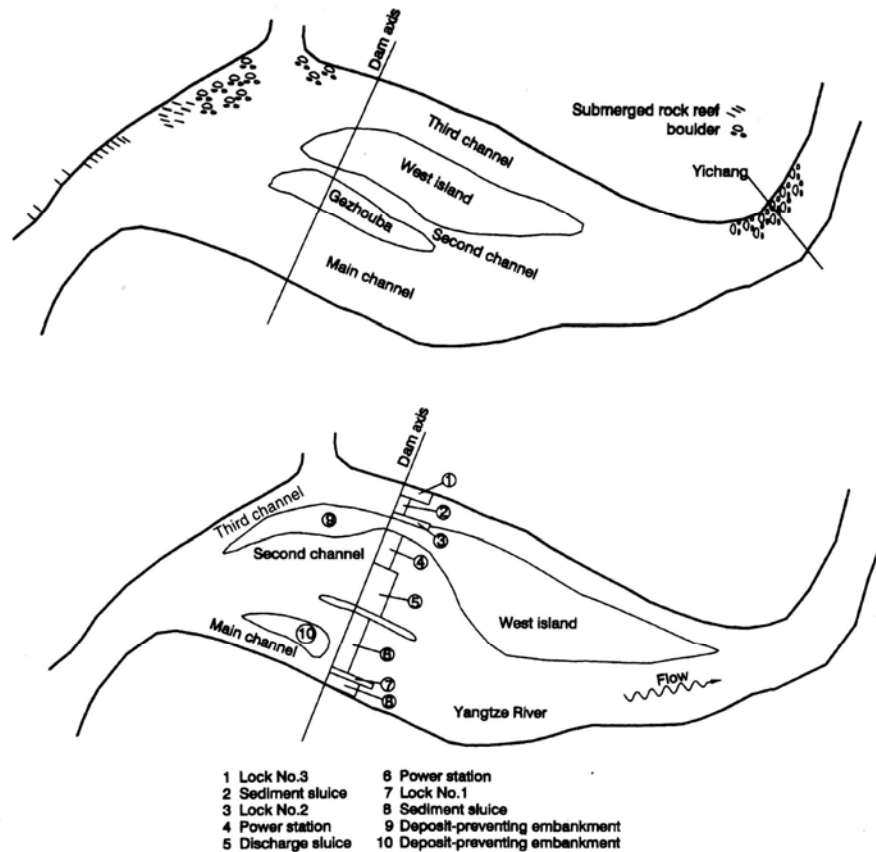


**Figure 11.13** configuration of preproject Yangtze River in the vicinity of the Gezhouba Dam site (top). Layout of the Gezhouba Project as constructed (bottom)

axis: flood sluices, sediment sluices, power intakes, and navigation locks. Second, there were sedimentation issues to be addressed at the navigation locks and their upstream and downstream approach channels, including the mechanics of sediment deposition in blind channels and desiltation measures. Third, it was necessary to determine details of the layout approach of sediment sluices beneath the power intakes, which would pass the coarser fraction of the sediment load and decrease the amount of sediment passing through the hydro turbines.

### 11.9.2 Model Type and Scales

The physical model simulated a 16-km river reach and was designed as a movable bed model which was supplied both suspended and bed material at the upstream boundary. Given the available laboratory space and water supply, a distorted model was selected with a horizontal scale ratio of 1:200 and a vertical scale of 1:100. Prototype flow conditions were very complex and included the transport of a wide range of particle sizes: bed load, suspended load, and density currents were to be simulated simultaneously in a single model. Not all similarity conditions could be satisfied simultaneously, so the main scale parameters were satisfied while some deviation was allowed on secondary scales. The scale ratios used are listed in Table 11.3.

**TABLE 11.3** Computed Scale Ratios

	Parameter	Symbol	Scale ratio
Geometric parameters	Length	$L_r$	200
	Water depth	$h_r$	100
Flow parameters	Velocity	$v_r$	10
	Roughness	$\eta_r$	1.52
	Discharge	$Q_r$	200,000
	Suspended load	Settling velocity	$w_r$
Suspended load	Sediment diameter	$d_r$	1.1
	Critical velocity	$(v_0)_r$	10
	Concentration	$s_r$	0.46
	Dry Specific weight	$(\gamma_0)_r$	2.25
	Time scale	$(t_s)_r$	98.3 (computed)
			96 (adopted)
	Density current	Velocity	$(v_0)_r$
	Time of deposition	$(t_s)_r$	98.3
Bed load (sand)	Sediment diameter	$d_r$	1.25
	Critical velocity	$(v_0)_r$	10
	Sediment transport rate	$(q_{bs})_r$	459
	Dry specific weight	$(\gamma_0)_r$	2.25
	Time scale	$(t_{bs})_r$	98.3 (computed)
		96 (adopted)	
Bed load (gravel)	Diameter	$d_r$	12.5
	Critical Velocity	$(v_0)_r$	10
	Sediment transport rate	$(q_{bg})_r$	320
	Dry specific weight	$(\gamma_0)_r$	1.89
	Time scale	$(t_{bs})_r$	118 (computed)
			96 (adopted)

### 11.9.3 Establish the Initial Boundary Conditions and Scale Sediment

To select an appropriate model sediment, flume tests were made on the initiation of motion of many artificial sediments before selecting bakelite (plastic) powder with a specific weight of  $1.4 \text{ t/m}^3$ . The bakelite powder had a wide range of grain sizes, from 0.01 to 10 mm, making it possible to simulate the full range of sediment found in the prototype system, from suspended load to gravels. The  $d_{50}$  for the model bed load was about 0.14 mm with a Manning roughness of 0.016, and a velocity for initiation of motion of about 6 to 7 cm/s. Field measurement and computations indicated that the critical velocity for initiation of bed load motion in the prototype was 0.6 m/s, which is about 10 times the critical velocity for the model, satisfying the corresponding scaling criteria.

### 11.9.4 Model Construction

The model was constructed as an accurate scale replica of the prototype. The physical model was 80 m long, equivalent to 16 km in the prototype system. The simulated bed load of sand and gravel was introduced at the upstream end of the model, and a recirculation system was used for the suspended load. During tests the concentration profiles and grain size distribution of suspended sediment were measured in the model, and inflow and outflow concentrations were measured at 15-min intervals. Sediment feed was adjusted as required to maintain the proper sediment inflow conditions.

### 11.9.5 Calibration

Model scales and roughness were calibrated by measuring vertical velocity distribution and water levels. Patterns of flow, sediment deposition, and erosion in the model were calibrated against conditions observed in the field in 1971, and conditions with cofferdams across the left and right channels in 1972. Water levels were calibrated for discharges varying from 5300 to 33,500  $\text{m}^3/\text{s}$ , and extra roughness was added in some areas to make the water surface profile in the model better match the prototype. The velocity distribution in both the prototype and the model were measured to check that the vertical mean velocities across cross sections and vertical velocity distributions were similar. Variations in transverse and vertical suspended sediment concentrations were also measured and compared. When discharges exceeded 20,000  $\text{m}^3/\text{s}$ , turbidity currents were observed in the model.

Gravels are not transported through the Nanjinguan Gorge for discharges less than 20,000  $\text{m}^3/\text{s}$ , and at higher flows they are transported primarily along the right-hand channel. Gravels equivalent to a prototype grain diameter of 100 mm could be transported throughout the entire length of the model.

Similarity of topography and the grain size distribution of sediment deposits between the prototype and the model must be achieved by adjusting the sediment inflow rate and grain size distribution to match the suspended sediment concentration, bed load transport, grain size distribution, outflow sediment characteristics, and sediment transport time scale observed in the prototype. Model scale ratios were adjusted by trial and error until the topographic features and grain size distribution of deposits in the prototype system were reproduced satisfactorily by the model. Topographic calibration is the most complex and difficult problem in model tests. Calibration periods consisted of a 3 month flood season and an entire year. Model results were compared to prototype topographic surveys which indicated both the configuration and volume of the deposits. There were 31 model runs for the purpose of topographic calibration, of which 29 were preparatory model runs and two were formal test runs. The 29

preparatory runs were made to adjust (1) the roughness, load, and size distribution of the inflowing sediment, and (2) the time scale, by observing the effect on deposit patterns. The last two formal test runs were conducted under identical operating conditions to examine the degree of similarity and the stability of model behavior. Tests showed that the total prototype deposit volume was simulated adequately by the model.

	Test 1	Test 2	Prototype
3-month deposit, Mm <sup>3</sup>	2.82	2.71	2.9
1-year deposit, Mm <sup>3</sup>	2.77	2.83	2.55

There are two time scales in the model, one for the flow of water and another for sediment, the latter being used for model operation. On the basis of the results of topographic calibration, a model time scale of 96 was adopted (1 day of model operation equivalent to 96 days in the prototype system). The topographic distribution of deposits in the model reasonably approximated the prototype behavior except in the reaches immediately upstream of the cofferdam. From this work, it was concluded that the model could be used to predict flow patterns and sediment features after construction of the dam.

#### 11.9.6 Predictive Simulation

Proposed project conditions were simulated by adding a scaled model of the hydraulic structures that reproduced topographic and structural details and the roughness of wetted surfaces. The flow patterns and sediment regimes caused by alternative structural arrangements were tested extensively in hundreds of test runs performed from 1974 to 1980. Problems analyzed included: general layout of hydraulic structures, flow regime for navigation and realignment of the navigational channels, scour and deposition in navigational channels, location and quantity of sediment erosion and deposition, and the grain size and concentration of sediment entering the hydropower plant.

#### 11.9.7 Design Recommendations

On the basis of model testing, the navigation approach channels and locks were designed to incorporate guide dikes to improve flow conditions and to reduce sediment load entering the approach channel. Sediment sluices were set adjacent to the navigation locks to flush accumulated sediment twice annually: once during the flood season and once at the end of the flood season. Residual sediment deposits remaining in dead zones after flushing are removed by dredging. The flood sluices were designed to pass floodborne sediment, and modeling indicated that about 95 percent of the total gravel load would be discharged in this manner. Sediment release through flood sluices reduces the sediment load on the navigation and power systems, and the coarse sediment load entering the turbines was reduced by placing bottom outlets immediately beneath the power intakes.

#### 11.9.8 Validation

For validation, the model is operated to simulate an event which affects the prototype system, but which is different from the calibrated conditions, to ensure that the model accurately simulates prototype response. The first phase of dam construction was com-

pleted in the winter of 1980 and a major flood during the autumn of 1981 caused large changes to the river bed upstream and downstream of the dam. Model validation tests were made using 1981 field data for the inflow hydrograph and bed topography. Tests showed that the amount of sedimentation, the spatial and grain size distribution of the deposits, and outflow concentration, were in satisfactory agreement with prototype data.

## **11.10 CLOSURE**

---

Modeling is an essential process for understanding and managing the behavior of a fluvial system. Mathematical modeling can be very helpful, even when calibration data are extremely sparse, by providing additional insight into the probable behavior of the system and by focusing investigations within the context of a formal analytical framework. Sensitivity analysis can help identify critical issues. However, it should always be recalled that formal modeling supplements, but does not replace, conceptual modeling and engineering judgment. Site visits, prior experience, review of case studies, and a geomorphic evaluation and identification of significant historical events and trends are all essential components of modeling studies

---

## CHAPTER 12

---

# REDUCTION OF SEDIMENT YIELD

---

### 12.1 INTRODUCTION

---

There are only two strategies to reduce the sediment yield entering a reservoir: either prevent erosion or trap eroded sediment before it reaches the impoundment. This chapter outlines basic principles of erosion control and sediment trapping.

The rehabilitation of degraded watersheds can dramatically reduce the rate at which sediment, nutrients, and other contaminants are delivered to a reservoir. There is an extensive literature on watershed management and erosion control. This chapter focuses on erosion control, whereas the term watershed management encompasses a wide variety of measures with objectives such as enhancing water quality, reducing flooding, and improving wetland habitat. Watershed management programs may include both point and nonpoint sources, such as New York City's \$750 million program announced in 1993 to improve water quality in the city's drinking water reservoirs, with the objective of avoiding the much higher cost of constructing water filtration plants under the EPA's Surface Water Treatment Rule. New York's watershed management program will include the implementation of stricter watershed regulations, land purchases, upgrading of sewage treatment plants, and agricultural pollution management (AWWA, 1995).

#### 12.1.1 Applicability

Programs to prevent and correct erosion problems are invariably recommended to limit reservoir sedimentation and enhance water quality, and at most reservoirs this is the only measure recommended. However, many erosion control programs have been spectacularly unsuccessful, despite large expenditures, because they were improperly planned and executed, and lacked the long-term support and commitment of the land users. Many reservoirs designed under the assumption that sediment yield will be controlled by upstream erosion control practices have not only seen that promise unfulfilled, but have seen sediment yield accelerate as population density and land degradation increased in the watershed.

In many developing areas, the progressive deforestation and cultivation of steep slopes is the only survival option for the rural poor, and about 10 percent of the world's population cultivates steeply sloping soils. These slopes may be worked by hand or by animals such as oxen which can plow extremely steep hillsides. Where there are marked wet and dry seasons, soil plowing may be done prior to the arrival of rains, thereby maximizing the potential for erosion (Fig. 12.1). Even when conservation measures are employed on steep soils, there can still be a lot of erosion.



**FIGURE 12.1** Recently ploughed sloping soils in the Dominican Republic, prior to the onset of the wet season (*G. Morris*).

It is both costly and difficult to implement improved land use practices over watersheds of any size, and particularly in watersheds covering thousands of square kilometers with multiple political jurisdictions and with tens of thousands of land users. Nevertheless, land use improvement to reduce erosion and sediment delivery is often the best method, and perhaps the only method, that is feasible for combating sedimentation at many reservoirs, especially at hydrologically large reservoirs which are continuously impounding.

Damage to reservoirs by sedimentation represents only a small part of the cost of erosion. Estimates by Clark et al. (1985) suggest that loss of storage capacity in reservoirs accounts for only 11 percent of the total cost of erosion in the United States (Table 12.1). This table underestimates the cost of reservoir sedimentation because it assumes that existing reservoir capacity can be replaced at the same cost per unit volume used for new reservoir construction, which is obviously not the case, especially for high-cost operations such as dredging. However, it does point out that many users can be severely affected by erosion, and the control of reservoir sedimentation is often not the principal reason for implementing soil conservation measures. Measures to reduce erosion and sediment yield typically benefit many parties in addition to dam operators, and a dam owner attempting to combat erosion in the watershed may have many potentially helpful alliances.

### 12.1.2 Limitations

Even when successful, erosion control does not necessarily represent a complete solution to sedimentation problems. Some environments have naturally high rates of sediment yield. Erosion control requires a long-term commitment, and produces long-term rather

**TABLE 12.1** Summary of Damages Due to Soil Erosion in the United States (Millions of 1980 Dollars)

Type of Impact	Single-value estimate	Cropland's contribution
Instream effects:		Not estimated
Biological impacts		
Recreational	2000	830
Water storage facilities	690	220
Navigation	560	180
Other instream uses	900	320
Subtotal	4200	1600
Offstream effects:		
Increased flood damages	770	250
Water conveyance facilities	200	100
Water treatment facilities	100	30
Other off-stream uses	800	280
Subtotal	1900	660
<b>Total</b>	<b>6100</b>	<b>2200</b>

*Source:* Clark et al (1985).

than short-term results. Land use changes which reduce erosion may not produce a short-term reduction in downstream sediment yield. For instance, Faulkner and McIntyre (1996) did not detect any reduction in sediment yield from the 1150 km<sup>2</sup> Buffalo River in Wisconsin, 20 years after a transition to less-erosive land use within the basin. Finally, because erosion can never be reduced to zero, erosion control alone cannot achieve a sediment balance across a reservoir. Additional measures will eventually be required to remove sediment if the reservoir is to remain in operation, although erosion control can greatly delay this requirement.

### 12.1.3 Additional Sources of Information

Moldenhauer and Hudson (1988) and Morgan (1995) provide good overviews of erosion control issues and strategies in less developed areas. Schwab et al. (1993) is a basic agricultural engineering text on erosion control techniques which focuses on structural measures used in the United States. Sediment control in the urban environment is covered by Goldman et al. (1986), Urbonas and Stahre (1993), and Haan et al. (1994). Publications and extension support are available from the Natural Resources Conservation Service within the U.S. Department of Agriculture, which has local offices nationwide (Internet: [www.nrcs.usda.gov](http://www.nrcs.usda.gov)). Internet access to publications from the U.S. Environmental Protection Agency can be obtained at [www.epa.gov](http://www.epa.gov).

A CD-ROM containing an extensive description of Best Management Practices (BMPs) and a database on water utilities which have implemented watershed protection programs is available through the American Water Works Association (6666 W. Quincy Ave., Denver, CO 80235, Internet: [www.awwa.org](http://www.awwa.org)). An electronic listing of 800 watershed management programs and contacts throughout the United States, plus information on BMPs, is available from the Conservation Technology Information Center (address below). Several organizations with publications, periodicals, and software related to soil conservation are:

The Soil and Water Conservation Association  
7515 NE Ankeny Rd., Ankeny, IA 50021-9764 Internet: [www.swcs.org](http://www.swcs.org).  
Focus: Agricultural soil conservation, United States and worldwide

North American Lake Management Society  
One Progress Blvd., Box 27, Alachua, FL 32615 Internet: [www.nalms.org](http://www.nalms.org)  
Focus: Water quality issues in lakes and reservoirs

The International Erosion Control Association  
P.O. Box 774904, Streamboat Springs, CO 80477-4904 Internet: [www.ieca.org](http://www.ieca.org)  
Focus: Urban areas and construction industry

Conservation Technology Information Center  
1220 Potter Dr., Room 170, West Lafayette, IN 47906-1383 Internet:  
[www.ctic.purdue.edu](http://www.ctic.purdue.edu)  
Focus: Mechanized agriculture in the United States

Metropolitan Washington Council of Governments  
777 North Capitol St. NE, Suite 300, Washington, DC 20002-4201 Internet:  
[www.mwcog.org](http://www.mwcog.org)  
Focus: Urban best management practices

## 12.2 BASIC TECHNICAL PRINCIPLES

---

### 12.2.1 Technical Strategies for Erosion Control

Literally hundreds of specific structural and nonstructural management practices can be used to reduce sediment yield. In the United States, recommended control practices are termed *Best Management Practices* (BMPs). Many additional practices have been developed and applied successfully in other countries, including indigenous terrace systems in some parts of Asia and in the Andes which have been in continuous use for over 1000 years. The wide variety of techniques employed worldwide to reduce soil erosion and sediment yield may be synthesized into 10 basic strategies:

**1. Fit the activity to the soil, climate, and terrain.** Human activities ill-adapted to the local soils and climate can produce erosion on a massive scale. In agriculture, avoid the most erodible areas, and apply agronomic systems and land husbandry techniques that are suited to the local soils and climate. In logging, avoid road construction on highly erodible slopes, and select logging methods suitable for the slopes involved. In urban construction, adjust development to the terrain by minimizing cut and fill. Erosion control measures must also be matched to local conditions; some erosion control techniques that work well in one region may increase erosion under different soil and climatic conditions.

**2. Minimize the area and duration of soil disturbance.** The greater the soil area that is disturbed, the greater the rate of erosion. In the agricultural sector, conservation tillage can be used to minimize soil disturbance. In logging, different yarding methods can produce a ten-fold difference in the soil area disturbed. On construction sites the areal extent and length of time that disturbed soils are exposed to erosive rains can be limited by proper scheduling of the work.

**3. Protect denuded soils.** Denuded soils are highly susceptible to erosion by direct raindrop impact and rilling by prechannel flows. Protection may be provided to agricultural soils by mulching with crop residue and related conservation tillage

techniques. Skid trails in forests can be covered with slash. Temporary protection at construction sites can be provided by either natural or synthetic mulches, and permanent erosion protection is provided by vegetation or impervious cover such as concrete and asphalt.

**4. Maximize vegetative cover.** A good vegetative cover provides the best, least-cost, long-term protection against erosion by insulating the soil against direct raindrop impact, enhancing infiltration, and other methods. Even an incomplete cover of vegetation or mulch can produce a dramatic reduction in the erosion rate (Fig. 12.2).

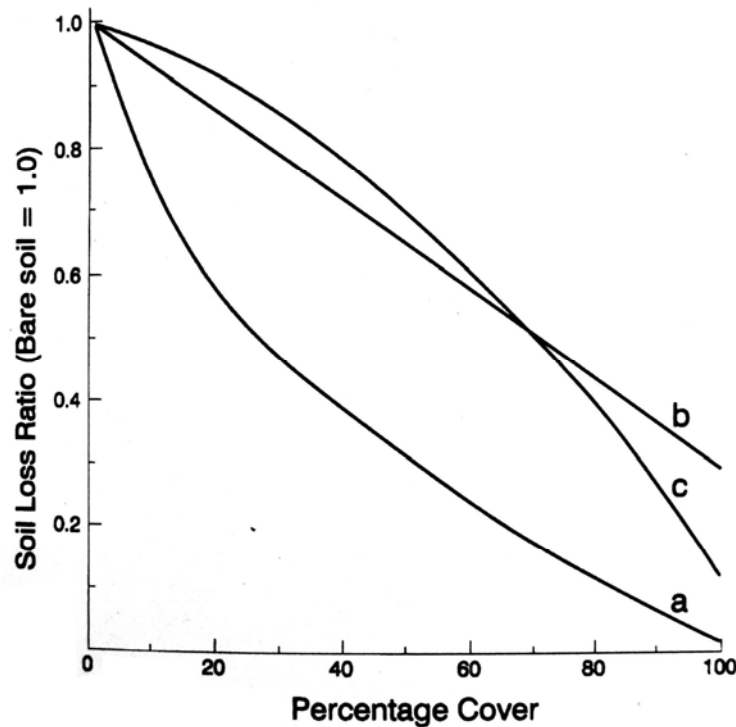


**FIGURE 12.2** Reduction in erosion rate compared to bare soil, as a function of vegetative cover, for: (a) ground-level vegetation, (b) vegetative canopy 1 m above ground level, and (c) oat straw mulch. Note that a large reduction in erosion can be achieved prior to full coverage (*redrawn from Styczen and Morgan, 1995*).

For all types of land use, the rapid reestablishment of vegetative cover following disturbance is essential to reducing erosion. The principal erosion control measure on rangeland is to manage stocking levels and grazing patterns to maintain adequate vegetative cover, especially in riparian areas.

**5. Maximize infiltration.** Rainfall which infiltrates the soil does not appear as erosive surface runoff, and is also available to support plant growth. Measures which retard runoff by adjusting slopes (contouring, terraces) and by improving soil structure and permeability (maintenance of organic matter, maintenance of vegetative cover, use of mulches) all improve infiltration capacity. Maintenance of infiltration capacity is a critical measure on agricultural soils.

**6. Manage slopes to prevent flow concentration.** Channel erosion processes are initiated and sustained by concentrated flows on sloping soils. Erosion control techniques such as flow diversion, terracing, and cross drains on roads may be used to divert runoff away from erosive slopes and to counteract the natural tendency for runoff to become concentrated and cause channel erosion (Fig. 12.3). Erosion potential is also reduced by limiting slope length and steepness.

**7. Prepare drainageways to handle concentrated flows.** Concentrated flows are highly erosive, and adequate protection is required where runoff becomes concentrated into channels. Use a low channel slope to reduce erosion hazard, and provide channel protection in accordance with the channel slope, geometry, and discharge. Bed slope may be controlled by orienting diversion channels across the slope, and by using check dams or drop structures for downslope channels. Commonly used channel protection materials include grass, geosynthetic mattings, stone, and concrete.

**8. Trap sediment before it leaves the site.** Use every opportunity to trap sediment in runoff from disturbed areas. Broad filter strips of grass or woodland areas at the limits of plowed fields, logging areas, and construction sites can infiltrate runoff, retard flow velocity, and trap sediment from prechannel flows. Vegetated stiff grass hedges and silt fences retard flow so that sediment will settle. Sediment transported by channel flow can be trapped using sediment detention ponds.

**9. Protect and preserve vegetation in natural riparian buffers.** Sediment delivery to stream channels by sheet flow can be reduced by maintaining a broad strip of riparian vegetation, either grass or forest, between areas of disturbed soil and stream



**FIGURE 12.3** Concentrated runoff released downslope produces rill and channel erosion. Avoid this type of erosion by diverting flows away from unprotected slopes and providing protection where the flow is released downslope (*G. Morris*).

channels. Avoid activities that will disturb the stability of natural stream channel banks and the adjacent riparian zone.

**10. Plan, monitor, and maintain control measures.** Develop soil and water conservation plans to facilitate implementation within the requirements of each land use and site layout. Monitoring is necessary to schedule maintenance, and to identify which strategies work and which do not. Periodic inspections are required to assure that control measures are properly installed and maintained.

In the preparation of any conservation plan it is useful to review these 10 issues and ask how satisfactorily each has been addressed.

### 12.2.2 Classification of Erosion Control Techniques

Techniques to reduce erosion and sediment yield may be broadly classified into three categories.

*Structural or mechanical measures* control the movement of water over the earth's surface to reduce the flow velocity, increase the storage of surface water, and safely dispose of runoff (Morgan, 1995). Included in this category are: (1) all types of structural terraces; (2) diversion channels, grassed waterways, and other flow conveyance structures; (3) channel protection and stabilization measures such as riprap, gabions, and check dams; and (4) sediment traps including debris basins, detention basins, and reservoirs. Structural measures are characterized by high construction cost and the requirement for maintenance over an indefinite period. Structural linings are required to protect channels when the flow velocity (bed shear stress) exceeds critical thresholds.

*Vegetative or agronomic measures* rely on the natural regenerative properties of vegetation or the management of crop and crop residue (mulch) to protect the soil. Contour vegetated hedges can also form natural terraces. Vegetation is inexpensive and self-renewing, and its use can minimize or virtually eliminate long-term maintenance concerns. However, a significant effort may be required for the initial establishment of vegetation, particularly on severely degraded sites and in semiarid areas. Vegetation alone may be incapable of controlling erosion by concentrated flows.

*Operational measures* are management and scheduling measures employed to minimize erosion potential. This includes strategies such as scheduling construction to minimize the area of exposed soil and scheduling timber harvest activities to avoid periods of excessive soil moisture. The focus of operational measures is inherently preventive, seeking to avoid erosion and minimize the requirements for either vegetative or structural remediation. Vegetative and operational measures are both classified as nonstructural controls.

### 12.2.3 Types of Sediment Trapping Structures

Hydraulic structures which trap sediment may be broadly classified in the following categories:

- A *check dam* is a small grade control structure designed to trap bed load only and used to prevent bed degradation and arrest gully erosion. Check dams normally do not exceed about 2 m in height. They reduce stream slope to reduce the flow velocity and channel erosion. Coarse sediment is trapped above each dam as the bed adjusts to the new grade established by multiple check dams installed along the watercourse.

- A *debris basin* is used to trap coarse sediment before it enters a downstream channel, the performance of which would be adversely affected by sedimentation (Vanoni, 1975). They may also be used to trap hyperconcentrated debris flows (Mizuyama, 1993). Unlike a sediment detention basin, which is designed to maximize sediment retention, a debris basin is designed to trap only the larger-diameter sediment that will not pass through the downstream system as wash load, or the massive amounts of sediment associated with debris flows. They are often sized to trap the sediment transported by a single large design event. Provision is made for periodic sediment removal to maintain sediment trapping volume.
- A *sediment detention basin* is designed to trap suspended sediment for water quality control, protecting downstream aquatic environments and structures from both suspended and bed material load, and the associated pollutants. They are occasionally used in rural areas, and are widely used for controlling sediment in runoff from urban areas and construction sites. Sediment detention basins can also provide additional benefits such as reduction in peak discharge and the creation of wetland habitat.
- Most *reservoirs* are presently operated as efficient sediment traps, although sediment trapping is not the intended purpose for their construction, and in most cases is considered objectionable. Reservoirs are normally much larger than detention basins. In some cases reservoir operation may be modified in the future to enhance the downstream release of sediment.

Systems to remove coarse sediment from a water diversion, such as for hydropower production, are discussed under *sediment excluders* (Chap. 13).

#### 12.2.4 Sediment Trapping in Upstream Reservoirs

Although constructed for other purposes, upstream reservoirs of all sizes act as de facto sediment traps, and downstream sites will experience greatly reduced sediment loading. There are, for instance, 39 major structures along the Paraná River and its tributaries in Brazil, above the Yacyretá dam below Posadas, Argentina. These upstream dams, including Itaipú, currently the world's largest hydropower site, are responsible for dramatically decreased sediment yields at the Yacyretá Dam site. What is less commonly recognized is that smaller structures can also have a significant impact on sediment yield when constructed in large numbers across the watershed. The National Inventory of Dams for the United States lists over 74,000 reservoirs having over 60,000 m<sup>3</sup> of storage. However, the U.S. Natural Resource Conservation Service estimates that there are 2 million farm ponds nationwide (see Table 2.5). Large numbers of smaller reservoirs and ponds have been constructed in many other countries as well.

Sediment trapping by upstream dams is the most important factor controlling sedimentation in many reservoirs. There are, however, two potential disadvantages to this strategy as a long-term protection measure. First, the sediment-retention capacity of upstream reservoirs may be limited. Second, owners of upstream sites may alter their operation to pass sediment downstream.

#### 12.2.5 Sediment Trapping versus Erosion Control

Under favorable conditions, sediment trapping can be a highly effective method for reducing sediment yield. An engineered structure can provide reliable and predictable sediment trapping as soon as it begins operation, eliminating the uncertainties associated with implementation of an erosion control program. However, there are a number of disadvantages to sediment trapping.

- **High cost.** All structural measures are very costly to construct. The lower cost of small check dams is offset by the large number of structures that is typically required. Larger sediment detention structures must be properly engineered from the standpoint of dam safety, spillway capacity, and long-term operation. Structures of all sizes will eventually fail without maintenance. Because the cost per unit of storage volume tends to decline as a function of dam height, to trap a given volume of sediment, a few larger structures will be more cost-effective than many smaller structures. The least costly measure might be to enlarge the reservoir itself.
- **Siting.** With the exception of check dams, which are located within the gully floor, a sediment detention pool will occupy a significant amount of land area. Sites appropriate for a sediment detention structure may be difficult to locate and costly to acquire.
- **Sustainability.** For detention to represent a sustainable long-term sediment control strategy, one of two criteria must be satisfied: (1) sediment must be removed from the detention basin or (2) the sediment retention structure must continue to hold the trapped sediment for an indefinite period. If sediment is to be removed periodically, scale economies could make it less costly to remove sediment from the reservoir itself rather than to construct and operate upstream detention basins. The long-term integrity of sediment detention structures is a critical issue, because when a structure fails the trapped sediment will be exposed to erosive forces and may be released. For example, Gellis et al. (1995) examined detention structures and check dams constructed in the 1930s on the semiarid Zuni Reservation in New Mexico. Of the 23 rock and brush check dams investigated along 800 m of a single arroyo, 22 had failed. Of the 47 rock or earthen detention structures located within a 172-km<sup>2</sup> quadrant, 60 percent had failed by embankment breaching or erosion around the end of the embankment. This situation is not unusual; the western United States is littered with failed detention structures and check dams.
- **Limited benefits.** Accelerated erosion is caused by unsustainable land use practices, and reservoirs are only one of the many uses affected by erosion. Soil and water conservation measures within a watershed can have many benefits beyond the protection of reservoir storage, and many different interests and institutional resources may be enlisted to combat watershed degradation. Conversely, sediment detention structures will benefit only certain downstream users, but not the upstream lands where the erosion problem originates. Economic resources assigned to sediment detention structures will not be available to help cure the underlying problems in the watershed, which may generate a wider range of long-term benefits to the society.

Sediment detention structures are commonly used at construction sites, and for water quality enhancement and flood detention in urban areas. However, they are infrequently used specifically for the control of reservoir sedimentation because of the disadvantages mentioned above.

## **12.3 FORMULATING AN EROSION CONTROL STRATEGY**

---

### **12.3.1 What Causes Erosion?**

Accelerated erosion is the earth's natural and predictable response to inappropriate land use and poor management practices. Nobody sets out with the intent of accelerating erosion, yet its occurrence is widespread. While many highly effective erosion control techniques can be readily demonstrated on test plots or in small, closely controlled watersheds, it is quite another matter to convince a community of land users to implement these practices on a sustained basis.

Implementation can be highly problematic in less developed areas, where a tributary watershed containing several thousand square kilometers of sloping and highly erodible soils may be cultivated and grazed by tens of thousands of subsistence farmers. Most subsistence farmers use wood for fuel, which also places woodlands under continuous harvest pressure (see Fig. 7.10). About 90 percent of the population in Africa uses fuelwood for cooking (Anderson, 1987). Factors that make erosion so difficult to control include the large number of people and activities contributing to the problem and, in many areas, the lack of consistent or effective government policy oriented toward soil and water conservation. Napier (1990) pointed out that the implementation of soil conservation measures over a large area is very expensive, and it is unrealistic to believe that effective soil conservation programs can be implemented in any society without a permanent, adequately funded service infrastructure staffed by trained professionals committed to soil conservation goals. A good overview of the socioeconomic barriers to the adaptation of soil conservation measures by farmers of all income levels and on every continent is provided by Napier et al. (1994).

### 12.3.2 Identifying and Prioritizing Sediment Sources

As pointed out in Chap. 7, sediment yield varies widely across watersheds of all sizes, and most sediment will typically be contributed by a relatively small portion of the total tributary area. To focus erosion control efforts, it is necessary to identify the geographic areas and specific land use practices that are the major sediment contributors. In developed areas, considerable information may already have been collected for the project watershed, or for similar watersheds. In contrast, in less developed areas there may be virtually no formal information on conditions in the watershed, no useful water quality records, and incomplete mapping and photographic coverage.

Sediment sources can be characterized by modeling and sampling techniques discussed in Chaps. 6 and 7. The importance of sampling is emphasized because of the difficulty in converting erosion estimates to actual sediment yield, given the difficulty in determining sediment delivery ratios. Even when formal analysis is not performed, a screening analysis can differentiate between areas that produce little sediment and those that produce large amounts of sediment. Lands of low or moderate slope with good vegetative cover and an absence of gullying characteristically have low sediment yield. Disturbed soils, especially those on high slopes or which deliver sediment directly to stream channels, can be expected to have high sediment yield. Many types of sediment sources should be obvious even to untrained observers. However, even low rates of sheet erosion over a wide area can generate large amounts of sediment. An erosion depth of only 1 mm across 1 ha represents  $10 \text{ m}^3$  of annual soil loss, or about 16 tons of sediment. Use particular caution in the interpretation of channel erosion. Incising channels with expanding cross-sectional area can produce large volumes of sediment. However, channel erosion by rivers having a stable cross-sectional area while meandering across a floodplain will produce little net export of sediment downstream, and the river-floodplain system is usually a zone of net sediment deposition.

Identify specific land use practices that are important contributors to erosion. On farms, certain practices or selected crops may be much more important as sediment sources than others. On construction sites, problems such as the lack of adequate enforcement may be the principal problem (Fig. 12.4). In forests, high erosion rates may be associated with specific types of yarding methods or specific aspects of logging road design.

In assessing erosional impacts on a reservoir, examine trends over periods of many years or decades, and focus erosion control efforts in areas where the greatest benefits can be anticipated within this time frame. For instance, in an area which is already



**FIGURE 12.4** Eroding soil at a construction site in the watershed tributary to Loiza Reservoir. In addition to obvious sheet and rill erosion on bare slopes, the stream passing through the site has also been affected by earth movement. Although Puerto Rico has regulations requiring erosion and sediment control at construction sites, enforcement is lacking (*G. Morris*).

severely degraded, future sediment yield may be limited by the supply of erodible soils. Previously eroded material may already have collected in intermediate storage points in the watershed, from which it will be delivered to the reservoir over the coming years or decades, regardless of the improvements made in the upstream watershed. At the same time, there may be another area of the watershed where destructive land uses are only starting. It may make more sense to focus limited control efforts on stabilizing the area of the watershed where soils have not yet suffered severe degradation.

Identify the land users who will need to change their actions. Does this group consist of a dozen land developers in an urbanizing area, or a population of a million supported by subsistence agriculture on steep slopes?

Erosion control is not primarily a "technical" problem, and factors limiting the implementation of erosion control measures need to be identified. Cook (1988) identified three types of factors that can contribute to erosion problems – informational, institutional and technological – all of which must be tackled simultaneously for successful implementation. Informational constraints may include inadequate extension services and non-awareness of appropriate technology. Institutional problems may include lack of enforcement; perverse legal, regulatory, and policy environments; and a wide range of subsidy programs that promote resource exploitation and degradation. Technological problems may include the lack of an erosion control package which is both technically effective and economically attractive to land users.

### 12.3.3 Identification of Partners

Having characterized the problem of erosion and sediment yield from the standpoint of reservoir operation, look for partners with whom to join forces to achieve improved management within the watershed. A dam owner attempting to reduce sediment yield from a watershed may join forces with governmental and nongovernmental institutions, individuals, and grass roots organizations, who can in turn provide training, install control measures, pass regulations, perform enforcement actions, and access a variety of sources for cash and in-kind contributions to the erosion control effort. In the United

States, a logical first point of contact is the local office of the Natural Resources Conservation Service within the Department of Agriculture. The electronic listing of watershed organizations mentioned in the introduction to this chapter can provide numerous contacts in the field, and watershed organizations can also be located on the Internet. Erosion control is generally not a burden that the dam owner carries alone, and well-directed contributions by the dam owner may catalyze sustained changes within the watershed, making this an attractive long-term option. This approach is described in the Feather River case study (Chap. 22).

#### **12.3.4 Economic Costs, Benefits, and Erosion Control Strategies**

Erosion damages may be broadly apportioned between on-site costs which affect the eroding area itself, and off-site costs that accrue to downstream users or in distant areas. The question of who bears the cost of erosion, and how large those costs are, is highly relevant to the selection of an erosion control strategy.

The on-site costs of erosion on farms may include reduced crop yields, increased cost of inputs such as fertilizer, damage to plants and fields by channelized water, gullying of farm roads, and desiccation of local streams used for water supply. On hillside farms with shallow soils and high erosion potential, the on-site cost of erosion is typically very high. Agriculture cannot be sustained for many decades on shallow soils that are rapidly eroding. If subsistence farmers on eroded soils migrate to urban slums, erosion may impose a high cost to the urban sector as well.

Agronomic practices that trap moisture and nutrients to improve yields will also reduce erosion. When these productivity-enhancing erosion control practices become an integral part of the farmer's agronomic practices, they become self-sustaining. Shaxson (1988) has referred to this as "erosion control by stealth," and described as an example of the conservation approach taken on tea estates on sloping soils in Malawi. Managers were told that production costs could be reduced significantly by reorganizing the road system to allow uninterrupted access to the tea gardens during the rains, the main production and harvest period. In areas of new plantings or replantings the dirt roads were realigned along topographic crestlines whenever possible, where they would not be subject to washout by cross-flows. Adequately drained lateral roads were extending along the contour or controlled gradients, adjacent to conservation banks that controlled runoff. The tea rows were then realigned parallel to the contoured roads, rather than in straight lines, thereby impeding downslope runoff. Mulching was found to be beneficial to young tea plants for agronomic reasons, but it simultaneously protected the soil against raindrop impact. While the initial cost of developing this contoured system was higher than the traditional practice, subsequent maintenance costs were much lower because of reduced runoff which damaged roads, carried off soil and fertilizer, and clogged drainage channels and conservation banks. Thus, while the changes in agricultural practices responded to economic incentive, they simultaneously reduced land degradation.

A different economic balance between on-site and off-site costs occurs on mechanized farms. The on-site cost of erosion on deep, gently sloping soils is typically small, despite soil and nutrient losses which may be significant from the standpoint of downstream users. The on-site cost of erosion is also perceived to be small in the forestry and construction sectors: loggers and contractors are on the site for a very short period of time, and erosion does not normally interfere significantly with their operations. However, in developed areas, the off-site costs of erosion can be high because of the larger inventory of downstream infrastructure such as reservoirs and navigation channels and the high value assigned to stream quality for water supply, recreational, aesthetic, and environmental reasons. In a competitive economic environment, few operators are

willing or able to incur significant costs for altruistic reasons, and when the on-site costs of erosion are small it is necessary to resort to subsidies, informal or formal coercion, or both, to implement and maintain effective erosion control measures for the benefit of society as a whole.

Subsidies have been widely used to implement soil conservation measures in both industrialized and less developed countries. However, subsidies should be used with utmost caution, since they can create perverse incentives that may run counter to the intended purpose. Lutz et al. (1994) cite an example of a reforestation incentive program in Costa Rica that unintentionally encouraged farmers to deforest their land so they could qualify for a reforestation subsidy. Farmers may also delay conservation practices in the expectation of future subsidies for their implementation, and allow conservation measures to fall into disrepair when subsidies end. In the United States, subsidies have been used to temporarily retire erosive land from agricultural production. However, this is not only very costly (see sec. 12.6), but the benefits are only temporary since the land is often returned to production when the subsidies end (Napier, 1990).

In the construction and forestry sectors, erosion control has increasingly focused on formal regulatory approaches. The U.S. Environmental Protection Agency now requires sediment detention storage equal to 2.54 cm (1 in) of runoff depth from the disturbed area of construction sites exceeding 4 ha, and a number of states now have erosion control requirements at construction sites which exceed federal standards (Gilbert, 1996). In the forestry sector some states have only voluntary guidelines for good timber harvest practices, but enforceable standards are established in other areas. Timber harvest on federal lands requires the preparation of a timber harvest plan which includes specification of the appropriate erosion control measures which must be adhered to.

Nonregulatory techniques that can be helpful in combating erosion include:

1. Education and training of agency personnel, engineers, foresters, and operators
2. Promulgation of standards of practice by professional organizations
3. Adverse publicity, as might occur when a school biology class visits a stream below a badly eroding site, and invites the local television news crew to film the event
4. Civil suits bought by parties injured by the erosion
5. Peer pressure

## **12.4 EROSION CONTROL MEASURES ON FARMS**

---

This section provides a brief description of several basic erosion control strategies widely used on farms. Many variations of these techniques have been developed to fit soil, climate, crop, and socioeconomic conditions around the world, and local sources should be consulted for information on specific techniques. Although not specifically discussed in this handbook, wind erosion is also important in many agricultural areas, and some measures which reduce erosion by water, such as strip cropping and reduced tillage, can also protect against wind erosion.

### 12.4.1 Contouring

The practice of orienting field operations such as plowing and planting along the contour is called *contouring*. It reduces surface runoff by trapping water in small depressions and decreases the incidence of rill formation.

### 12.4.2 Strip Cropping

The practice of growing alternate strips of different crops in a field is called *strip cropping*. For water erosion control the strips may be aligned along the contour, and the crops follow a different rotational sequence so that the entire field is never bare. Buffer strips may also be used to protect sensitive areas of the field from erosion, or to create areas which will retard runoff and trap sediment.

### 12.4.3 Grass Filter Strips

A grass filter strip is a broad vegetated area, aligned on the contour insofar as possible, which will filter sheet flow from cropped areas. Filter strips can trap both sediment and the associated pollutants, including agricultural chemicals. The effectiveness of the filter strip depends on factors including slope, filter strip width and soil infiltration rate, sediment grain size, and amount of runoff. Filter strips are ineffective in treating concentrated flows. Being a vegetative measure, filter strips tend to be self-maintaining. However, they require a significant amount of space and can reduce the amount of land available for crop production. They might be used for forage.

### 12.4.4 Conservation Tillage

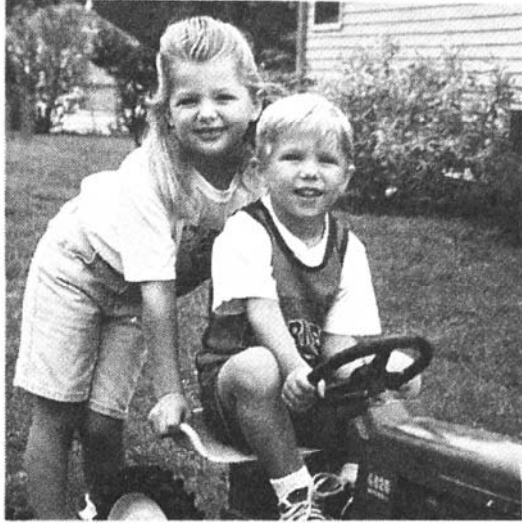
One of the most important agricultural conservation measures being adopted in many areas of the world in recent years is the reduction in tillage (turning of the soil). In the United States the term *conservation tillage* encompasses a variety of specific techniques such as no-till, mulch-till, ridge-till, and strip-till, all aimed at reducing the frequency and surface area of the field subject to tillage. Approximately 40 million hectares (100 million acres) of U.S. cropland (about 20 percent of the total) had been converted to conservation tillage by 1996.

Under conservation tillage, the crop stubble is left standing and residue is evenly spread across the field as mulch instead of being plowed under. Weeds are controlled by cutting and herbicide. Compared to conventional tillage, conservation tillage can increase soil organic matter, reduce erosion by as much as 90 percent, enhance infiltration, and reduce moisture loss. When implemented across a watershed, the enhanced infiltration can reduce peak discharge and downstream flood damages.

Of greatest importance from the standpoint of sustained implementation are the tangible short-term benefits to the farmer. On mechanized farms in the United States, conservation tillage practices which greatly reduce erosion are "sold" to farmers, by emphasizing their economic advantages in terms of reduced machinery costs and labor (Fig. 12.5). On a 200-ha (500-acre) mechanized farm, Hill (1996) estimates that the reduced number of passes through the field with equipment translates into an annual savings of 225 hours of the farmer's labor and 1750 gallons of fuel, plus \$2500 in reduced mechanical wear on machinery. The equipment required for no-till agriculture is lighter and lower-horsepower than machinery required for heavy plowing, which produces fur-

**Really want them  
to own the farm  
someday?**

**Find out how  
conservation  
tillage  
pays!**



**Send for this publication.**  
*Conservation Tillage: A Checklist for U.S. Farmers*  
 is 36 pages of management and benefits  
 information. Send \$4.00, to cover postage  
 and handling, to:  
 Conservation Technology Information Center  
 1220 Potter Drive, Rm. 170  
 West Lafayette, IN 47906-1383  
 Phone: (317) 494-9555,  
 FAX: (317) 494-5969  
 E-mail: [ctic@ctic.purdue.edu](mailto:ctic@ctic.purdue.edu)



**Visit our web site! <http://www.ctic.purdue.edu>**

**FIGURE 12.5** Advertisement promoting conservation tillage in the United States based on its cost advantages to farmers. The key to the successful and sustained implementation of conservation measures is making them productive to the farmer (*Conservation Technology Information Center, by permission*).

ther cost savings. Colacicco et al. (1989) indicated that farmers may be attracted to conservation tillage more for its cost savings rather than for the purpose of soil conservation.

#### 12.4.5 Grassed Waterways

A grassed or vegetated waterway is a shallow drainageway in which vegetation protects the channel against erosion, thereby increasing the permissible (nonerosive) velocity compared to bare soil. Maximum permissible velocities depend on the type of grass, but are generally limited to about 1.2 m/s and slopes not exceeding 5 percent. For streams that have a base flow, a stone center is provided. Scour resistance may be enhanced by geosynthetic reinforcement. Various grassed waterway configurations are illustrated in Fig. 12.6.

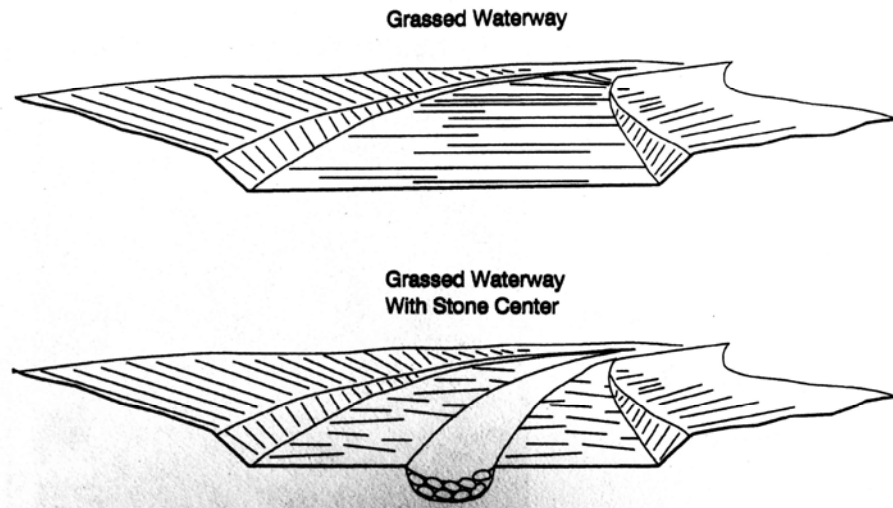


**FIGURE 12.6** Grassed or vegetated waterways. Either trapezoidal (as shown) or parabolic cross sections may be used. An inner channel lined with stone is used when there is sustained base flow.

#### 12.4.6 Terraces

The use of terraces is an ancient technique, and some terrace systems in Asia and the Andes have been in service for over 1000 years. Beach and Dunning (1995) have hypothesized that ancient Mayan agriculture in Central America, which sustained a population much larger than today's population of subsistence farmers in the same area, was based on the extensive use of terraces, of which only the faintest vestiges remain today. Terraces work against gravity, interrupting the tendency of water to flow downslope. The layout and configuration of terrace systems or earthen bunds will depend on the farming system, soils, crops, climate, etc. Several alternative terrace configurations are illustrated in Fig. 12.7. Terraces are normally designed to discharge the collected runoff to a lined channel or drain which carries excess water downslope. Because structural terraces collect and concentrate water, the failure of a terrace can release a concentrated flow of water which can cause gulying. While terraces can be highly efficient at trapping both soil and water, and are required for sustained production on steeply sloping soils, structurally formed terraces of earth or stone are costly to construct and maintain.

#### 12.4.7 Contour-Grassed Hedges

Because structural measures are costly to construct, and will fall into disrepair and fail without continual maintenance, considerable attention has been given recently to the use of self-sustaining stiff grass hedges. Natural terraces can be created by planting a dense hedge of stiff grass on the contour, which retards runoff and causes water to pond and deposit sediment on the uphill side of the hedge (Dabney et al., 1995). Because it is living, the grass hedge will become stronger with time and can grow as sediment collects and the terrace height increases (Fig. 12.8). Deposited sediment fills in low spots, runoff tends to become more evenly dispersed and less erosive with time, and the hedge tends to naturally build terraces that follow the contour (Dewald et al., 1996). Contour grass hedges differ from grass buffers and filter strips because they are narrow, are

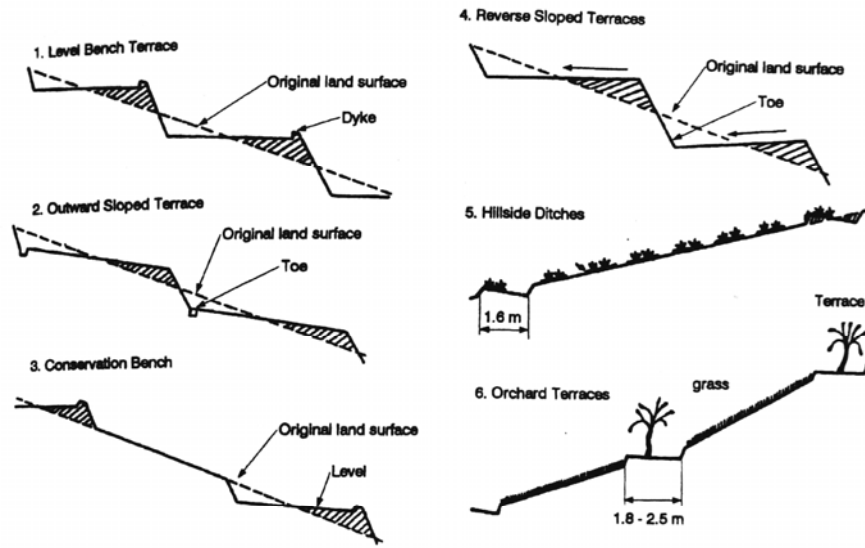


FIGURE 12.7 Several types of structural farm terrace systems used to impede downslope runoff and enhance the infiltration of water into the soil.

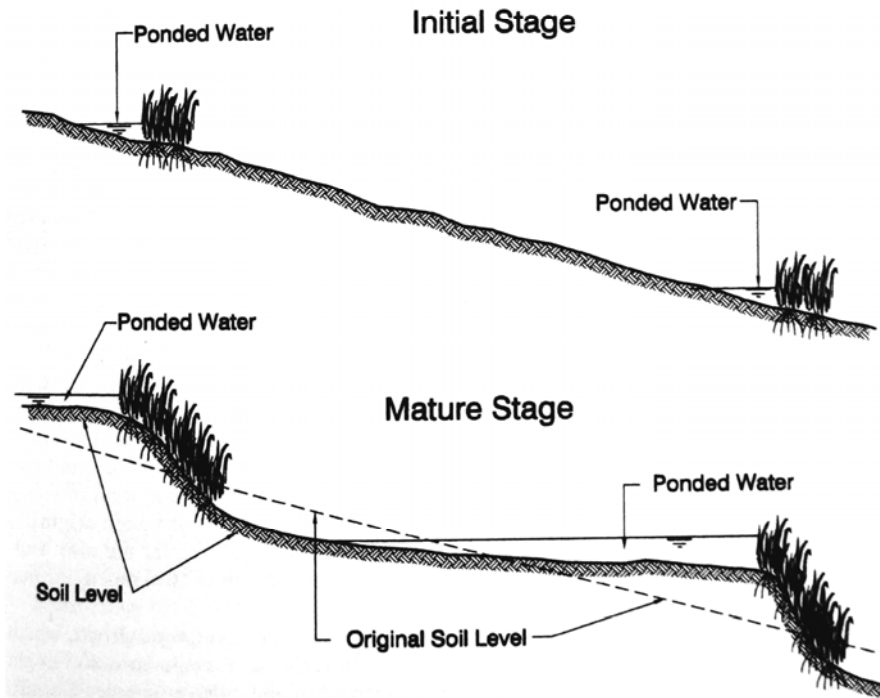
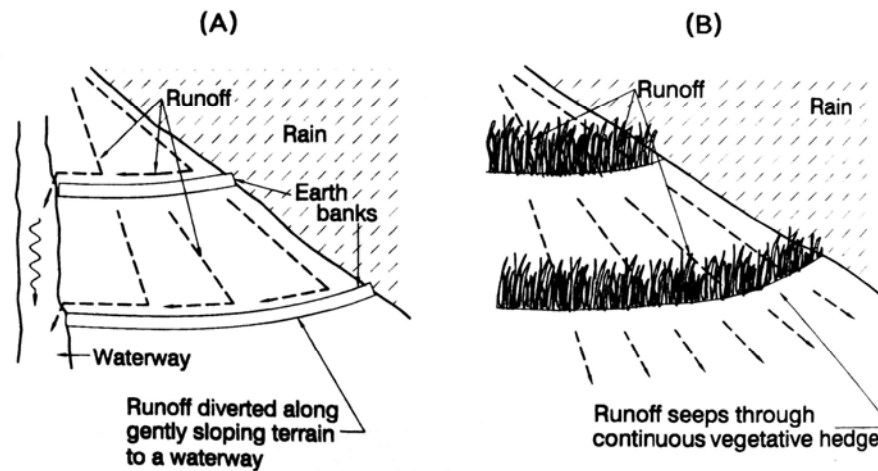


FIGURE 12.8 Slope profile illustrating the mechanism by which a stiff grass hedge will pond water and cause sedimentation, resulting in the creation of self-sustaining terraces (after Dabney et al., 1995).

planted with stiff, erect grasses, and maximize the formation of berms or terraces due to sediment deposition. Unlike structural terraces, which deliver a concentrated flow to a grassed waterway or structural conduit, the grassed hedge allows water to seep through (Fig. 12.9).



**FIGURE 12.9** Runoff management on terraces. (a) Because structural terraces are impermeable, they direct intercepted runoff to a grassed waterway, lined channel, or drain for transport downslope. (b) The contour stiff grass hedge is permeable, and disperses runoff across the slope instead of concentrating it into a channel. (After Grimshaw and Helfer, 1995.)

The success in creating a vegetated hedge which forms natural self-sustaining terraces owes much to the properties of the grass itself. Vetiver grass (*Vetiveria zizanioides*) has been found to be a remarkably functional species in tropical and subtropical areas (Grimshaw and Helfer, 1995). Vetiver grass, a wetland plant native to northern India, grows under an exceptionally wide range of soils and climates. Neither vetiver nor its roots are inherently spreading, and if planted in long lines it will create a dense but compact hedge. It has been used successfully in areas receiving from 500 to 5000 mm of annual rainfall. It survives prolonged inundation, grows rapidly, has a rooting depth exceeding 3 m, is resistant to fire, will become established on extremely degraded soils, and will tolerate soil temperatures as low as  $-10^{\circ}\text{C}$ . It is relatively unpalatable and is not damaged by grazing by either cattle or goats, although young shoots can be harvested for forage. It is easy to propagate and requires virtually no maintenance. There are examples of vetiver hedges in southern India that are 200 years old, and erosion control lines planted over 30 years ago in Fiji have developed a system of stable noneroding terraces on steeply sloping soils, with no maintenance. Although originally developed to control sheet erosion, the remarkable properties of vetiver are also well-adapted for use in gully and channel stabilization, and for erosion control on engineered slopes such as road embankments.

It is essential to use the proper "domesticated" south Indian vetiver cultivar, which does not produce seeds. The wild variety from north India sets fertile seed and might become a pest in some areas. Information on vetiver grass and cultivar sources is available from Grimshaw and Helfer (1995), National Research Council (1993), and the Vetiver Network (15 Wirt St. NW, Leesburg, VA 20176; Internet [www.vetiver.org](http://www.vetiver.org)). Dewald et al. (1996) have described the use of switchgrass (*Panicum virgatum* L.) and eastern gamagrass (*Tripsacum dactyloides* L.) for the

planting of stiff grass hedges in temperate climates. Both vetiver and switchgrass form a dense hedge of stiff stems, effectively ponding water to depths of 0.3 m or more.

## 12.5 IMPLEMENTING EROSION CONTROL ON FARMS

---

### 12.5.1 Types of Farms

In discussing erosion problems on farms, it is necessary to distinguish between mechanized and subsistence farms. Mechanized farms occupy generally flat or gently sloping soils which often have a relatively low erosion hazard. These farmers typically produce cash crops, use machinery, and buy their food in supermarkets. This group includes most of the farmers in developed countries, and the wealthier farmers who occupy the flat soils in less developed countries.

Subsistence farmers cultivate small plots, eat what they grow, and dedicate only a limited part of their land to cash crops. They generally occupy lands too steep for mechanization, or areas too remote to enable crops to be marketed. Much of the farm work may be performed by women, especially when the men work off-farm to generate cash income.

The two groups of farmers have many features in common, and the basic soil and water conservation techniques have similar objectives regardless of the size and type of farm. However, specific implementation measures and strategies are quite different for the two systems, and will be discussed separately.

### 12.5.2 Criteria for Successful Erosion Control

Measures for the successful implementation of conservation practices on farms are synthesized below from Moldenhauer and Hudson (1988), Hudson and Cheatle (1993), Lutz et al. (1994), and Napier et al. (1994).

- **Successful conservation programs must be long-term.** Successful soil and water conservation requires that farmers in a region change their agronomic practices, a process which occurs only gradually. Conservation can be achieved only if sponsors and governments are committed to supporting long-term programs. Short-term projects have proved to be ineffective. If conservation practices are to be effective in reducing long-term sediment yield, they must be implemented permanently. This means they must be either profitable for farmers, or enforceable. However, profitability alone may not be sufficient. Problems such as land tenure, lack of credit, poorly implemented extension programs, and perverse legal and institutional arrangements may also need to be corrected.
- **Grass roots involvement and relevance is required.** Work from the ground up to develop a program that is relevant to local needs. Involve farmers, families and communities in the planning and implementation of resource conservation activities. It is particularly important to build on local social structures, cultural patterns, knowledge, and practices. Conservation measures not relevant to the needs of the land users may not be implemented, except with subsidies, and will not be sustained in the long run.

- **Develop technically sound and economic conservation measures.** Successful and sustainable conservation measures will produce tangible short- and long-term benefits to farmers and will fit within the farmer's economic and managerial capabilities. To be sustained, conservation practices must be seen by farmers as ways to minimize their risks, increase return, and reduce labor or other inputs. Focus on agronomic practices which reduce the cost of inputs and labor and enhance crop production, while also controlling erosion. Structural control measures can be costly to construct and maintain, and land degradation is better controlled through improved land husbandry than by engineering-based maintenance-intensive soil conservation measures. Subsidies may be required to achieve large-scale implementation of some measures, but should be used with extreme caution and carefully targeted since they can also be counterproductive.
- **Training and communication.** Appropriate forms of communication must be used, such as adequately trained and motivated extensionists, appropriate technical publications, and teaching by example. In less developed areas, the training of extensionists from within each community can be an attractive alternative for programs having a limited funding period from donor agencies, since the extensionist's knowledge and skills are more likely to stay within the community after funding ends. Although mass media can provide awareness, they are not an effective tool for promoting conservation.
- **Flexibility.** The program must be flexible, with periodic reviews to discard unsuccessful approaches and adopt and improve the strategies that work in each local setting. Rigid plans with fixed timetables and targets are generally inappropriate.
- **Start small and grow systematically.** A small success is always better than a large failure. Successful projects start small, using the initial stage to test and perfect techniques, and then expand gradually and systematically. The rate of expansion will depend on the rate at which land users are prepared to change and the resources available to the project.
- **Recognize and work within socioeconomic constraints.** The adoption of conservation practices appears to depend at least as much on socioeconomic factors as on the technical effectiveness of the practices. The project must be fully aware of the existing cultural, economic, and land tenure system, and tailor the program to fit that system.
- **Administrative structures.** Utilize existing organizations and administrative structures, and strengthen them to the extent possible. In less developed areas, the programs implemented by nongovernmental organizations (NGOs) have developed many sound strategies for working with the rural poor and can serve as excellent catalysts for general change, in contrast to the disappointing results often achieved by government agencies. However, for widespread implementation the programs need to become institutionalized within local government structure. Avoid the use of special administrative units established to facilitate and administer the program, because they tend to disappear when project funding ends.

In contrast to the strategies recommended above, several features appear repeatedly in programs that have failed. Unsuccessful programs:

1. Have a top-down orientation and do not adequately consult the local communities
2. Do not consider the short-term needs of farmers
3. Do not provide for maintenance and follow-up to conservation works
4. Attempt to expand the program too rapidly

5. Are inflexible
6. Create political antagonism within the local community or the government

## **12.6 EROSION CONTROL ON MECHANIZED FARMS**

---

Soil conservation was initiated in the United States in the 1930s, when dust bowl conditions in the midwest were merely symptomatic of the lack of conservation that characterized agriculture nationwide at the time. Soil conservation technology was in its infancy, and farmers generally lacked knowledge of erosion control techniques. Land abuses were widespread and readily apparent, not different from many less-developed areas of the world today. Farms were literally being washed away by rain and blown away by wind.

Present conditions are remarkably different in the United States, as in most other mechanized agricultural areas in the world, where the most obvious soil erosion problems have been controlled. On the basis of conditions in the mid-1980s, Colacicco et al. (1989) estimated that two-thirds of U.S. cropland will suffer no yield loss over the next 100 years, since most land is eroding at less than the tolerable rate and suffers no productivity loss. Despite erosion, productivity losses on the remaining lands can be largely offset by increased fertilization.

Successful implementation of erosion control techniques across the diverse U.S. landscapes is the product of many efforts: erosion control research in experiment stations, sustained implementation efforts nationwide for some 60 years by the Soil Conservation Service (now renamed Natural Resources Conservation Service), increased public awareness and demand for enhanced water quality, an increasingly stringent regulatory environment, and of great importance, the elimination of cultivation on steeply sloping soils. Nevertheless, erosion, runoff quality, and reduced infiltration rates are problems that still require more work in many areas. Two recently formed watershed groups in Illinois were profiled by CTIC (1996), and are representative of the approaches and concerns of watershed management in agricultural areas of the United States. Both watershed groups are composed of area landowners, interested citizens, and locally active personnel from a variety of government agencies, and were organized to address problems of local significance.

In the watershed tributary to Lake Springfield, which had been dredged (Sec. 16.5.1), the two key issues were continued sedimentation and contamination of the drinking water reservoir with a herbicide widely used by local farmers. Floods in 1994 deposited a volume of sediment equal to about 10 percent of the volume dredged, and represented about \$1 million in future dredging costs. Remediation includes best management practices such as no-till, erosion control structures, filter strips, streambank vegetation, and improved herbicide application practices.

Flooding during 1993 was the key problem that initiated watershed protection activities in the Embarras River watershed. A nonprofit river management association was formed to provide local landowners with the organizational structure needed to implement a comprehensive resource plan developed for a 12-county watershed. Although flooding catalyzed action, the list of concerns grew to include: log jams, water quality, erosion, drainage, wildlife, better communication and accountability, loss of the natural character of the river, private property rights, instream sedimentation, recreation, water supply, land use change, wetlands, small bridges and culverts, and funding sources. Implementation of conservation tillage on 75 percent of the 450,000 ha of farmland in the watershed is expected to reduce peak flood discharge by 10 percent, and normally dry

flood control dams will provide an additional 15 percent reduction in peak discharge. Together these measures are expected to reduce soil loss by about 1.5 million tons a year.

Farmers are reluctant to implement soil conservation measures unless there is an economic incentive to do so in terms of reduced production costs, increased yield, or subsidies. Conservation tillage is often implemented as a cost-saving measure rather than for erosion prevention. Sloping soils which cannot be tilled with tolerable rates of erosion are recommended for permanent pasture or woodland, in accordance with the land capability classification system, but farmers may be unwilling to take land out of crop production. Because the on-farm cost of erosion is relatively low in the United States, and off-farm costs may be more than double the on-farm costs, erosion prevention has relied heavily on subsidies paid to farmers (Napier, 1990). Under the Conservation Reserve Program initiated in 1985, farmers were paid an annual rent plus half the cost of establishing a conserving land cover, in exchange for the retirement of highly erodible or other environmentally sensitive land from crop production under 10-year contracts. By 1993 some 36.5 million acres, or about 8 percent of U.S. farmland, was included in the program at an average cost of \$122/ha/yr (Table 12.2). The program was

**TABLE 12.2** Conservation Reserve Program in the United States

Parameter	Value	
Contracts	377,000	
Enrollment, ha (acres)	$14.8 \times 10^6$	$(36.5 \times 10^6)$
Total erosion reduction t/yr (tons/yr)	$635 \times 10^6$	$(700 \times 10^6)$
Total rental cost, \$/yr	$1.8 \times 10^9$	
Average annual rental cost, \$/ha (\$/acre)	122	(50)
Area planted in trees, %	6	

*Source:* Osborn (1993).

estimated to have reduced erosion by 635 million tons/yr, an average of 43 tons/ha, representing a 22 percent reduction in the total erosion from cropland nationwide. A limitation of this and similar subsidy-based programs is that when the subsidies expire, the land may be returned to crop production (Osborn, 1993). This cost of avoided erosion is about \$2.83/ton, which is close to the cost of dredging sediment from reservoirs. This makes it a very costly approach for curing reservoir sedimentation, especially if the sediment delivery ratio is low.

Given the cost of subsidies for conservation set-asides, coupled with budgetary limitations, Ervin (1993) postulated that erosion control in the agricultural sector may be expected to gradually abandon subsidies and move increasingly into the regulatory arena, as the demand for environmental quality increases and political power shifts away from agricultural groups.

## 12.7 EROSION CONTROL ON SUBSISTENCE FARMS

Issues related to the implementation of soil and water conservation on subsistence farms are discussed in Moldenhauer and Hudson (1988), Hudson and Cheatle (1993), and Napier et al. (1994).

### 5.1.1. 12.7.1 Erosion Control Strategy

Hudson (1988) has pointed out that one of the keys to erosion control in the United States is the system of land capability classification, which identifies slopes steeper than 12 percent as unsuitable for open cultivation. Adherence to this criterion is possible in the United States, with its abundance of fertile lands on low slopes and dispersed pattern of land ownership. However, in many tropical areas this system is entirely irrelevant because the area of flat soils is small, the best lands are concentrated into large landholdings, and the expanding population of the poor is forced onto soils of ever-increasing slopes for survival.

When an erosion problem is identified in a watershed, there is a tendency to develop and implement a "soil conservation" program. However, this top-down approach has largely been ineffective against erosion, as evidenced by the failure of projects of this type worldwide. Farmers control the use of the land they till, and are rarely willing to implement costly soil conservation measures, or change their production practices, unless there are tangible benefits to themselves and their families. The application of structural erosion-control measures on subsistence farmers has often been unsuccessful; the measures have not been maintained, and in some cases they were even dismantled by the people they were supposed to benefit. Shaxson (1988) cites an example of well-meaning conservation programs in some African countries requiring the construction of contour banks on cultivated land. This provoked severe resentment of government officials, especially when farmers who did not perform the required work were fined or jailed. People were especially embittered when they saw that even where the banks were installed, erosion did not end. In Nicaragua, Obando and Montalvan (1994) reported that machinery was used to construct structural conservation measures on farms in the watershed south of Lake Xolotlan to provide flood protection for the city of Managua. These measures, which were constructed at no cost to the farmers, generally interfered with common cultivation practices in the area. Many of the structures were either abandoned or undermined by the farmers, who returned to their traditional practices. This and other similar experiences noted in the literature underscore the importance of the socioeconomic aspect of erosion control and involvement of the local people. An important challenge is to develop conservation practices that not only reduce erosion but also increase land productivity.

Successful erosion control projects will focus on practices that improve the farmer's condition while simultaneously conserving soil and water. This concept has been termed *conservation farming* or *land husbandry* by Hudson (1988). Conservation measures are most likely to be profitable, and thus implemented, when they are cheap and simple, or when they allow improved agronomic practices to be implemented. Even when the principal impact of soil loss is offsite (e.g., reservoirs), the farm-level approach is still appropriate because conservation measures must be implemented and sustained by farmers themselves.

### 12.7.2 Terracing

The retardance of runoff and trapping of sediment is a key management practice on sloping soils. Terraces (or earthen bunds) have been widely used and represent the basis of sustained agricultural production in many areas of the world. Terraces may be constructed of stone, or of earth with permanent vegetative cover to protect and stabilize the terrace slope. Terraces are costly (labor-intensive) to construct and maintain, and will not be sustained by the farmer unless there are tangible benefits. However, once the benefits are realized, farmers will construct and maintain terrace systems. In Ecuador (Nimlos and Savage, 1991), poor farmers constructed terraces because it was

part of an agronomic package that generated dramatic yield increases (more than double for some crops), and the level soil was also easier to farm. In some areas of Kenya terraces are required to trap enough moisture to prevent crop failure in dry years (Wenner, 1988).

The benefits of terracing are highly site-specific. In drier climates terraces may be required to trap enough water to undertake crop production, but on heavy clay soils, terraces can create waterlogging and decrease crop production. Contour-grassed hedges of vetiver may function much more satisfactorily than traditional structural terraces in many situations.

Research and experiment stations have tended to favor terracing and similar soil conservation methods which have high levels of technical efficiency, rather than methods having high levels of cost-effectiveness to the farmer. Although terracing is a highly effective method for reducing erosion, it is also costly to implement and maintain, and because terracing may take some land out of production it may actually reduce the short-term yield (Lutz et al., 1994). Terracing may also disturb the soil in a manner that brings less productive soil to the surface. Depending on the setting, these costs can make terrace construction economically unattractive to farmers. Structural measures have been successfully employed in a number of regions, but are not the answer to all sloping soil erosion problems. Methods such as construction of contour ditches and use of grass strips and organic fertilizers are conservation measures that are less costly to implement than terraces and may be considered more beneficial by farmers.

### **12.7.3 Agronomic Strategies to Reduce Erosion**

Good agronomic practices produce a soil having a high infiltration capacity, achieved by maintaining high levels of organic matter and soil cover in the form of either vegetation or mulch. Sloping soils are modified to create terraces which retard runoff, thereby enhancing infiltration and providing more water to sustain plant growth, and also trapping soils and nutrients which would otherwise be lost with the runoff. Level soils are also easier to cultivate than steep slopes. Retarding runoff and providing proper drainage channels also helps preserve farm roads. All of these practices both benefit the farmer and reduce erosion.

Agronomic conservation strategies used on subsistence farms focus on techniques such as tillage reduction and intercropping to maintain a continuous cover of vegetation or mulch, return organic material to the soil, and maximize water infiltration. Nitrogen-fixing legumes are planted to improve soil fertility. Compost prepared from crop residue and animal manure is spread back on the field as fertilizer. Crops are planted on the contour, and strip cropping is used. Grass buffer zones which may be used for cut-and-carry forage are set on the contour to trap sediment from fields, and stiff grass hedges may be used to build natural terraces. Multiple cropping and multilayer cropping systems tend to produce a more ecologically balanced environment, reducing both soil erosion and pest problems. These systems can also reduce risk to the farmer, as when two crops with somewhat differing tolerance to extreme wet or dry conditions, such as maize and sorghum, are planted together in areas subject to drought to ensure against total crop failure. The two following examples illustrate the application of these principles.

### **12.7.4 The World Neighbors Program in Honduras**

World Neighbors (Vecinos Mundiales) is a nongovernmental organization (NGO) that works in poor rural communities and extends knowledge about soil conservation and

other subjects. The organization's experience with soil conservation projects in Honduras has been summarized by López-Vargas and Pío-Carney (1994).

In the initial stage of work with communities, farmers often do not believe in soil conservation. Many claimed that breaking up the soil was foolishness, that constructing ditches on the contour was for burying people, that collecting dung for composting was a dirty job, and that because nothing grows on eroded lands it is better to move elsewhere when the land becomes exhausted. The farmers may also not be familiar with new or alternative crops.

Technical training must initially make individuals aware that they are the only persons responsible for resolving their own problems and, above all, that they have the capacity and intelligence to do so with a little effort. For long-term effectiveness farmers must come to understand contributions of air, sunlight, water, nutrients, and soil organisms to the formation of the crop, as well as the role that the forest plays in the entire system and in human life. They must realize the responsibility they have to be good administrators of nature and the potential they have to make nature useful and to provide a better life, not only in the present but also in the future and for future generations.

Practical and simple techniques are recommended for conserving soil structure, moisture-retention capacity, and fertility. Diversion ditches are designed to reduce the speed of flowing water, and in dry areas level ditches are used to capture runoff and encourage infiltration. Vegetative barriers filter soil from water flowing downslope, and the gradual accumulation of soil helps form natural bench terraces over years. Vegetative barriers can also produce forage for livestock and vegetative material for organic fertilizer. On rocky soils, rock barriers are constructed on the contour. Where possible, minimum tillage techniques are used since they are less labor-intensive than traditional tillage and also reduce erosion by minimizing the area of soil disturbance. Organic fertilizers are prepared by composting vegetable matter and fresh dung from livestock, and after composting the fertilizer is applied at the rate of 2 to 4 kg/m<sup>2</sup>. Dung is not applied directly to crops without composting because it can attract insect pests. Legumes such as velvet bean are planted as green fertilizers, since they not only fix nitrogen but also produce seeds that can be processed to produce flour and tortillas, and vegetable matter for incorporation into organic fertilizer. Simple conservation structures such as diversion ditches, maximum use of organic material, narrow furrows with minimal soil disturbance, and the minimal use of chemical fertilizer are the key elements to the program.

The Vecinos Mundiales project workers start in each community on a small scale by recommending a few simple techniques and applying them on small plots using native varieties and tools. They build on existing local knowledge and techniques, and seek to achieve gradual change. The objective is to slowly but surely alter production techniques, incorporating the best traditional techniques with new ones as appropriate. More people will become interested and the program will grow as the initial results are proven in the field. Farmers are encouraged to share with others, and local extensionists are recruited from those farmers who effectively practice what they preach. Total acceptance is not expected, but participation levels of 60 to 80 percent are customary.

### **12.7.5 Implementation in Ecuador**

Nimlos and Savage (1991) described the USAID-funded Sustainable Land Use Management Project in Ecuador, which seeks to introduce sustainable soil conservation practices and a conservation ethic to indigenous Quechua farmers cultivating steeply sloping lands. The fertile level lands at lower elevations are owned by wealthy

landowners and are used mostly for grazing; poor subsistence farmers have access only to marginal lands. The project area is located at elevations between 2300 and 4500 m, slopes of 50 to 70 percent are common, and 80 percent of the parcels are less than 1 ha in size. The men often travel to the city to seek work, leaving women to work the fields.

The program used 60 extensionists with 2 to 6 years of technical education, who trained about 3500 farmers. About 9000 ha received conservation treatment, and the area under improved cropping (strip-cropping, intercropping, crop rotation, contour cultivation, and green manuring) approximately doubled every year. Construction of conservation structures including hillside ditches, bench terraces, and earthen reservoirs increased by about 70 percent per year. The program also provided assistance in the safe management of pesticides, use of fertilizer, agroforestry, and native forest management. Crop production increased dramatically: garlic by 92 percent, peas 421 percent, barley 216 percent, onions 80 percent, beans 47 percent, potatoes 260 percent, melloco (a native fruit) 475 percent. The implementation rate for conservation treatments was highest in areas where the increase in crop production was the most dramatic. The program was a success and soil-conserving practices were expanded because the needs of poor farmers were addressed and conservation practices increased yields.

Terracing was used to trap soil, and the combination of terracing and green manure enabled farmers to grow crops in areas that had previously been unusable because of severe erosion. Terraced lands are much easier to irrigate and cultivate, trap more moisture, and produce much higher yields. In the project area, unterraced land was valued at \$160/ha, but its value increased to \$2200/ha when terraced.

## 12.8 EROSION CONTROL AND FORESTRY PRACTICES

---

### 12.8.1 Definitions

A *silvicultural system* refers to the methods in which trees are harvested and the stand is regenerated. They include clear-cutting and variations thereof which produce even-aged stands of timber, and single-tree or group selective-cutting techniques which maintains an uneven-age stand structure. A *logging system* refers to the method used to fell trees, cut them into logs, and transport the logs from the stump to a temporary storage area (the *log landing*), from whence they are transported to the mill. The *yarding system* refers to the method of transporting logs from the stump to the log landing and is the most critical aspect of the logging system from the standpoint of erosion. Logs can be transported to the landing by dragging or *skidding* with a tractor, a ground-level cable and winch, or animals such as oxen and elephants. There are several types of *skyline* yarding systems which either partially or wholly suspend logs in the air during transport, greatly reducing soil disturbance. If a helicopter is used to remove logs, the method is termed *aerial yarding*.

In some areas of the United States it is necessary to assess the cumulative impact of timber harvest and other activities on water quality. The cumulative effect is the total environmental impact resulting from the incremental impact of a proposed action, when added to all other past, present, and reasonably foreseeable future actions, regardless of who undertakes those actions. The idea behind a cumulative impact assessment is that sensitive downstream uses, such as fishery habitat, can tolerate only a limited degradation in stream quality. Therefore, all contributors to water quality degradation should be considered when determining whether or not additional degradation is acceptable (Cobourn, 1989; Sidle and Hornbeck, 1991).

Forest harvest activities, including erosion control measures, should be planned in advance by preparing a timber harvest plan. A timber-harvest plan includes maps, sketches, or photographs of the area to be logged. It specifies the logging methods to be used, landing locations, the stream areas to be protected with buffer strips, and the width of the buffers. It gives specifications for the construction, use, and maintenance of a well-designed transport system, and it will also specify the methods to be used to repair and stabilize logged areas, log landings, and roads upon completion of the harvest operation. As part of timber harvest planning, areas of high erosion potential should be identified and road construction avoided in these areas. Some flexibility should be retained to allow adjustment to conditions encountered in the field.

### 12.8.2 General Strategies for Erosion Control

Natural forest represents the best type of vegetative cover available: forest soil is highly permeable, and a layer of litter protects the soil from direct raindrop impact. Because of the high infiltration rate, only rare and extreme rainfalls are capable of producing surface flows. On steep slopes, a large percentage or even the majority of the long-term erosion from forests can originate from slope failures during extreme rainfall events.

Commercial timber harvest disturbs a limited area of the forest floor for a very short period of time, after which there is a cycle of regeneration and growth which may last from 20 to 100 years before the next harvest. With timber harvest rotations of 20 years or longer, and provided that vegetation recovers rapidly, the period of high erosion rates due to sheet erosion is limited. Most sediment from timber harvest is derived from haul roads and skid trails. Ill-designed and poorly constructed forest roads concentrate flows, create gullying, and produce sediment for a period of many years. Consequently, sediment control methods are oriented to: (1) reducing the amount of land that is disturbed by roads and skid trails, (2) preservation of riparian stream corridors, (3) proper road design and construction, and (4) rapid regeneration to protect the soil. General principles of erosion control have been summarized from Gilmour (1977), Hyson et al. (1982), Meghan (1983), and Wisconsin Department of Natural Resources (1990).

### 12.8.3 Yarding Methods

Large differences in impacts can be associated with different yarding systems, because of the large difference in the amount of soil surface disturbed by the various systems (Fig. 12.10). In general, the yarding system that minimizes the area of disturbed soil will produce the least erosion, other factors being equal. Specific recommendations for yarding are given below.

- Yard logs uphill rather than downhill, since this produces a pattern of skid trails that tends to disperse runoff rather than to concentrate it (Fig 12.11).
- Avoid stream channels insofar as possible in all phases of the yarding operation. Never locate skid trails along stream corridors, and drain muddy water in skid trails away from streams. Use temporary log or metal culverts at stream crossings, and, when skyline yarding, lift logs across streams rather than dragging them.
- Suspend logging on rainy days and periods immediately following rains when soils are saturated. Operate logging equipment only when soil moisture conditions are such that excessive soil damage will not occur.
- Avoid tractor yarding on soils exceeding 30 percent slope, or 25 percent on soils of high erosion hazard.

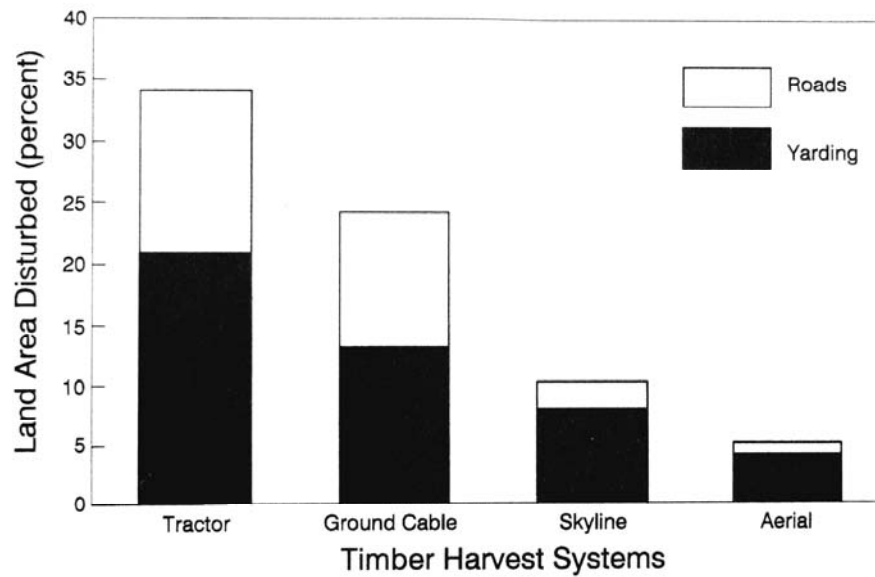


**FIGURE 12.10** Average soil disturbance attributed to roads and yarding for different logging systems, based on 16 studies in the United States and Canada (Megahan, 1981).

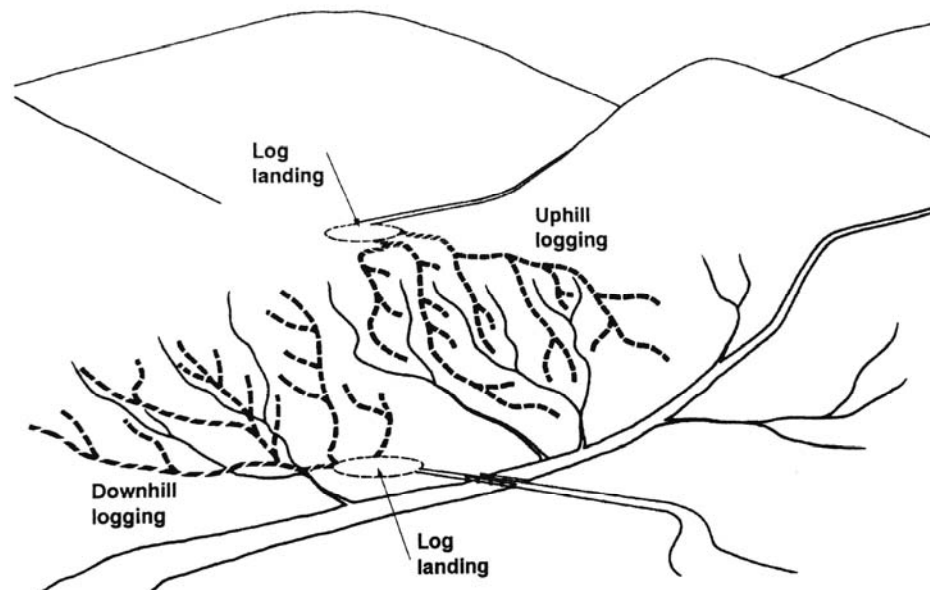


**FIGURE 12.11** Yarding in the uphill direction creates a pattern of skid trails that tends to disperse rather than concentrate runoff (redrawn from Gilmour, 1977).

- Minimize logging roads and skid trails on very steep slopes or fragile soils by using a skyline or aerial yarding system.
- Obliterate and stabilize all skid trails by mulching and reseeding immediately upon completion of logging. If necessary, also construct cross drains on abandoned skid trails to divert runoff onto the forest floor and prevent gullyng.

#### 12.8.4 Log Landings

Log landings are relatively flat areas where logs are temporarily stored before being transported to the mill.

- Locate landings so that skid trails leading to landing areas will minimize impacts on natural drainage channels.
- Landings should be located on areas of gentle slope such as ridge tops or widened road areas. Locate landing areas on firm ground away from stream channels, and drain landings into well-vegetated buffer areas.
- Landings and other intensive work areas should be kept free of chemicals and fuel, and should be located away from streams, springs, and lakes, and outside of riparian areas.
- Upon abandonment, ditch and mulch the landing area to prevent erosion. If the landing will be used repeatedly for thinning operations, plant with herbaceous material. If it will not be used again for many decades, as in a clear-cut area, plant trees.

#### 12.8.5 Riparian Buffer Strips

Undisturbed strips of native vegetation which are preserved between streams and areas disturbed by road construction or logging will reduce the quantity of sediment and logging slash that enters the stream. Maintaining the environmental integrity of a riparian buffer zone (also called a *streamside management area*, SMA) is highly beneficial to water quality and aquatic habitat, and to terrestrial species as well. The riparian zone should be maintained in native vegetation to provide bank stability, and to provide shade that maintains low stream temperatures needed for the survival of some fish species. The buffer should be of sufficient width to trap sediment and nutrients in the runoff from adjacent disturbed areas. When trees in the buffer strip are to be harvested, fell trees away from the stream and remove logs carefully to minimize disturbance. Large and older trees should be maintained in this zone as a source of woody debris that is an important component of the stream ecosystem. Slash and other logging residue should never be deposited in streams or in the riparian buffer zone.

One of the purposes of a riparian buffer strip is to trap sediment that originates in an upslope area, before it enters a stream. The recommended width of buffer strips will vary depending on site conditions, but a minimum width of 25 m on each side of the stream may be used as a guideline (Megahan, 1977). Strips might be narrower in areas of low slope with careful control in adjacent logging areas, but much wider in heavily disturbed areas with unstable soils. Buffer widths recommended by various states within the United States generally vary from about 10 to 60 m on each side of the stream, with larger widths required on soils having steeper slopes and more erodible soils. The widths recommended by Maine (Table 12.3) are representative.

**TABLE 12.3** Recommended Filter Strip Widths in the State of Maine

Land slope, %	Width of strip along slope	
	m	ft
0	7.6	25
10	13.7	45
20	19.8	65
30	25.9	85
40	32.0	105
50	38.1	125
60	44.2	145
70	50.3	165

*Source:* AWWA (1995).

### 12.8.6 Logging Roads

Logging produces a high density of roads, on the order of 2 km of road per square kilometer of logged area. Roads concentrate runoff and can create long-term problems of gully erosion if runoff is not handled properly. Important sediment sources related to roads typically include stream crossings, fill slopes, poorly designed road drainage structures, and roads close to streams. Roads run across the slope and intercept any downslope runoff, and contribute additional runoff from the relatively impervious road surface. This flow can become quickly concentrated along unlined ditches and can cause gullying along the road; it can also cause gullying when it is diverted downslope. Practices to reduce erosion from logging roads have been summarized by Megahan (1977):

- Design the transportation system and locate landings to minimize total mileage, considering both skid trails and haul roads.
- Design roads and skid trails to follow natural contours. Avoid the use of switchbacks in steep terrain by using an alternative road layout. Avoid stacking roads by using longer-span cable harvest techniques.
- Space cross drains to provide adequate drainage and prevent the concentration of roadside flows into erosive torrents.
- To improve slope stability, design cut-and-fill slopes for stable angles less than the normal angle of repose. If the terrain is too steep for this to be practicable, use engineered slope stabilization techniques.
- Use existing roads wherever practical when they meet adequate erosion control standards, or can be upgraded to meet those standards, thereby minimizing the amount of new disturbance and construction.
- Orient road crossings at right angles to streams. Cross streams along straight reaches having stable bank material. Size permanent culverts or bridges to pass large storms (e.g., 25-year). At temporary crossings, remove metal or log culverts and reconfigure, mulch, and replant the streambank as soon as operations are completed.

Characteristics of poor and good road design and maintenance are schematically compared in Fig. 12.12.

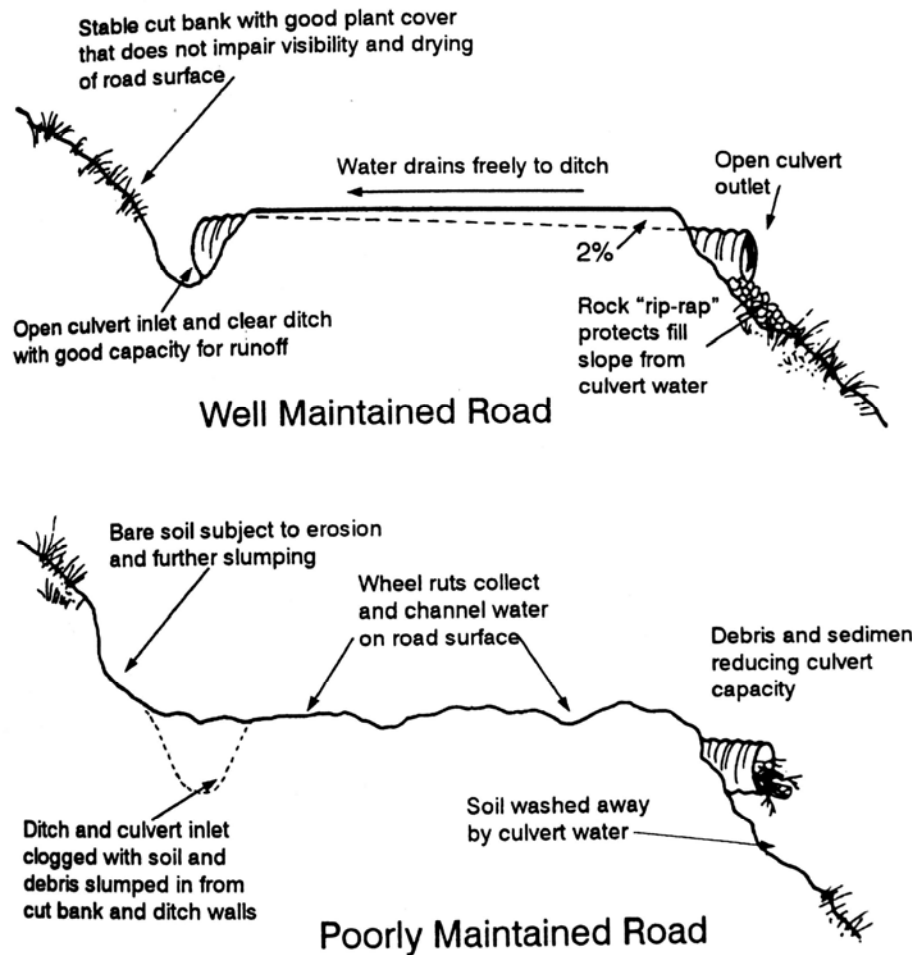


FIGURE 12.12 Examples of some important differences between well-maintained and poorly maintained woodland roads (Adams, 1991).

## 12.9 RESERVOIR SHORELINE EROSION

Reservoirs typically have extremely elongated shorelines compared to natural lakes, and also more variable water levels. Shoreline erosion can be significant. Shoreline erosion and slope failures are most prevalent during the first months or years of impounding, and in rare cases slope failure and the resulting flood wave can endanger the structure or cause flooding. A geotechnical evaluation is required to identify these types of problems prior to dam construction.

Lyons (1996) surveyed shoreline problems at Bureau of Reclamation Reservoirs. Erosion was reported at 114 of 154 reservoirs surveyed, and affected 4224 of 15,586 km (27 percent) of the shoreline in reservoirs for which data were available. Much of the shoreline damage was reported as "minor." The most common potential impacts of shoreline erosion were to archaeological sites, government property, water quality, and fish and wildlife. However, at 14 sites shoreline erosion was considered of sufficient severity to affect project life.

Shoreline erosion problems in clay, glacial till, and silt at Berlin Lake, Ohio, were reviewed by Hammel and Sekela (1995). At this site, land acquisition extended only 0.6 m above the flood pool level at the time of dam construction. Private recreational structures built around the periphery of the reservoir not only encroached too closely to the banks, but subsurface drainage from septic tanks and waves from power boats further contributed to natural causes of shoreline erosion such as water level variation and wind waves.

In some cases it may be feasible to modify the operating plan to reduce water level fluctuations and resultant erosion. Otherwise, because of the long length of shoreline, it is not generally feasible to protect against shoreline erosion except in localized areas where high-value property or structures are threatened. Practices to stabilize shorelines in specific localities may include the use of riprap, sheet piling, or other conventional engineering measures, and reduction of boat speeds to minimize wake.

## **12.10 CONTROL OF CHANNEL EROSION**

---

### **12.10.1 Types of Channel Erosion**

There are several types of channel erosion, and different control strategies are required for each. One type of channel erosion results from the natural tendency of rivers to meander. In this case the "problem" is usually related to the encroachment of human activities onto naturally unstable floodplain areas, and the desire to essentially freeze the active channel along a set course. As pointed out in Sec. 6.6, a stream channel which naturally meanders across a floodplain does not exhibit a change in cross-sectional area (Fig. 6.9) and is not a significant source of downstream sediment load. Rather, floodplains are usually depositional environments. River stabilization techniques are not discussed here, but can be found in Przedwojski et al. (1995) and Petersen (1986).

A second type of channel erosion occurs when natural stream channels incise, thereby increasing their cross-sectional area and exporting large volumes of sediments (Fig. 6.10). The causes of stream incision can be complex and poorly understood, and while incision may be triggered by land use changes within the watershed, it may also be part of longer-term natural cycles of sediment storage and release.

The third type of channel erosion involves gullying, a widespread and easily recognized erosion phenomenon that affects primarily ephemeral drainage on all types of land use (Fig. 12.13). For the purpose of this discussion, gully erosion is differentiated from natural stream incision in the following manner: stream incision may be partially or largely a component of a natural process, whereas the principal agent of gullying is land use degradation or other human activity that increases runoff, concentrates flows, or lowers the base level of a stream.

### **12.10.2 Basic Strategy for Gully Control**

The gully erosion cycle was outlined in Sec. 6.5. Erosion control measures in gullies seek to convert the eroding system into a stable condition as quickly and economically as possible, creating an environment in which self-perpetuating vegetation becomes established to permanently control erosion. Because gullies are characterized by high erosion rates due to concentrated channel flows, it may be necessary to alter hydraulic conditions before vegetation can become established (Heede, 1976).

Gully erosion control may involve the following measures:



**FIGURE 12.13** Gully erosion at a construction site (*G. Morris*).

1. Diversion of concentrated flows away from the advancing gully headwall
2. Reduction of gully slope by using structural check dams
3. Planting vegetation on the gully floor to retard runoff, trap sediment, and anchor the soil
4. Sloping vertical gully sidewalls to create stable slopes which are then vegetated
5. Installation of nonerodible channel lining

Permanent control structures such as a series of check dams and structural lining may be the only option in channels where upstream land use has permanently changed (e.g., urban development), greatly increasing peak discharges. The combination of measures selected will depend on factors such as gully size, slope, climate, and the available economic resources.

### 12.10.3 Check Dams

Possibly the first large-scale use of check dams for sediment trapping was by the Nabatean civilization, which occupied arid lands in present day Israel and Jordan and established the City of Petra as its capital in 312 B.C. In the 130-km<sup>2</sup> area around Avdat, 115 km south of Jerusalem, the Nabateans constructed 17,000 check dams (130 per square kilometer), each typically about 2 m high, 40 to 50 m long, and provided with a spillway. When silted up these dams increased the amount of arable land in the region fifteenfold (Schnitter, 1994). An interesting and richly illustrated account of runoff management by Nabateans and Israelites in the Negev Desert, and a modern reconstruction of their runoff farming system, is provided by Evenari et al. (1971).

Check dams are grade stabilization structures used to reduce the gradient and flow velocity along a channel. Sediment deposition widens the gully floor and also traps moisture, assisting the establishment of vegetation and providing more sustained base flows. The objective of check dam construction is to convert the eroding gully reach into a depositional zone which will trap bed material, retain moisture, and support vegetation.

There are two serious disadvantages to check dams: they are expensive to build, and if not maintained they will eventually fail. If vegetation does not propagate and stabilize the gully prior to check dam failure, the erosion process can be reinitiated and the check dams may have no long-lasting impact. In practice check dams are often constructed as a one-time erosion control measure, and maintenance is neglected. They should be used only when vegetative measures alone cannot be used.

For grade control Heede (1976) recommends the use of numerous small check dams not more than 0.5 m tall and spaced head-to-toe, the toe of one check dam at the head of the deposition zone of the next dam downstream (Fig. 12.14a). Spacing as a function of dam height and stream gradient is shown in Fig. 12.14b. Check dams spaced farther

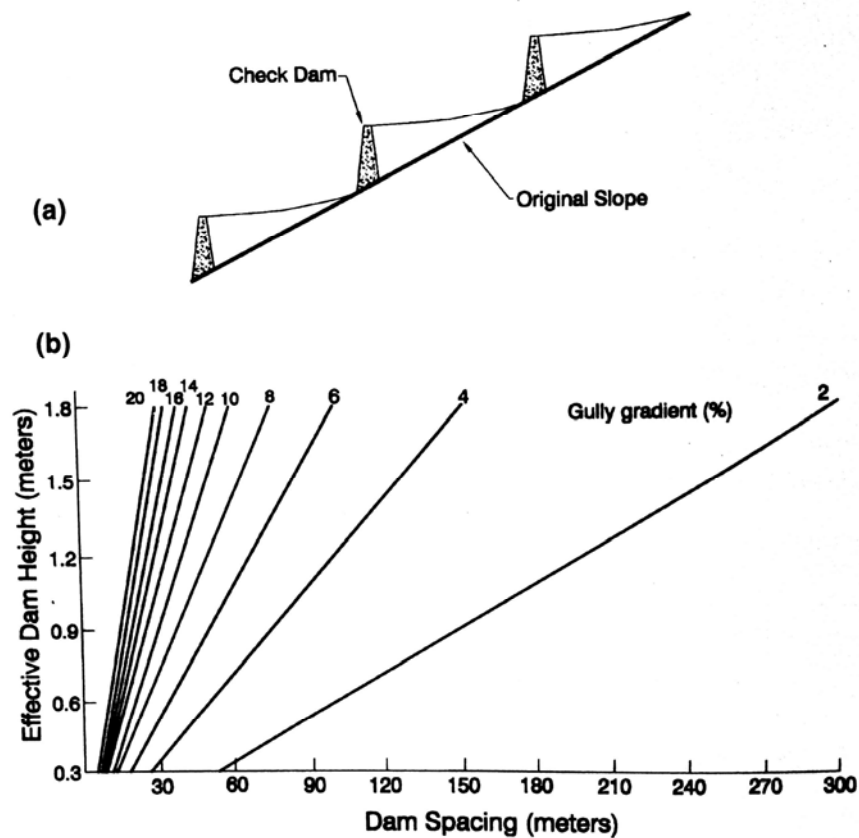


**FIGURE 12.14** (a) Head-to-toe arrangement of check dams along a gully. (b) Distance between check dams as a function of dam height and gully slope. (redrawn from Heede, 1976.)

apart are more efficient for sediment trapping because they will be taller and have greater storage capacity, but smaller structures placed closer together are more effective for reducing channel gradient. Computational procedures for check dam design are described by Heede and Mufich (1974).

Check dams may be constructed of many different locally available materials: stone, brush, sandbags, logs, concrete, etc. Selection of the material may depend, in part, on how rapidly revegetation is expected to occur. The basic components of a stone check dam are shown in Fig. 12.15, and Heede (1976) provides a detailed description of the

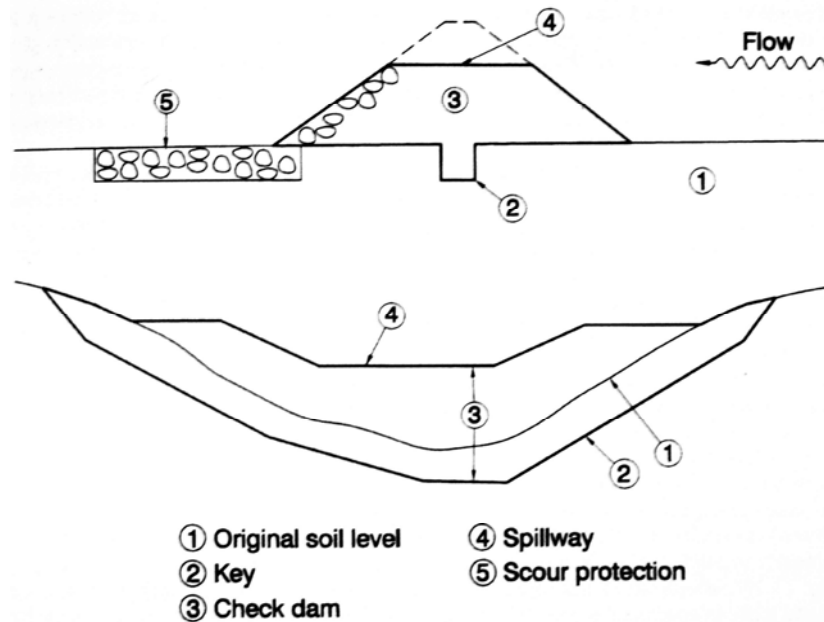


FIGURE 12.15 Basic configuration of a rock check darn (after Heede, 1976).

construction of rock check dams. It is particularly important to provide scour protection below each dam, to depress the center part of the spillway, and to properly key and protect the sides to prevent erosion beneath and around the end of the structure.

In areas severely affected by gully erosion, control works within the gullies themselves can provide a far more effective means of reducing sediment yield than treatment of slopes. For example, multiple types of erosion yield treatments were installed across 34.4 percent of the 70.1-km<sup>2</sup> Chiuyuan Gully watershed, Shaanxi Province, China (Gong and Jiang, 1979). Fields on sloping soils were terraced. Abandoned farms, steep slopes, and some gullies were afforested with trees and shrubs useful for fuel, fodder, and green manure. Grasses were planted on abandoned land and incorporated into crop rotations. Check dams were built at 317 sites, and some flood waters were diverted to irrigation use. Over a 17-year period these measures reduced sediment yield by 55 percent. Of this, 46 percent was attributed to the check dams alone, which trapped sediment and reduced channel erosion by reducing the slope of the gully floor. The remaining 9 percent reduction in sediment yield was attributed to the control measures installed on the slopes above the gullies. Of these, terracing was the most effective measure.

#### 12.10.4 Vegetative Control of Gullying

Under favorable conditions vegetation alone can be used to control gullying. Desirable vegetation will be stiff enough to provide significant hydraulic resistance, thereby

retarding flow velocity and encouraging sediment deposition. The selection of vegetation should be matched to the climatic and gully characteristics.

Vetiver grass has been successfully used to control gullying (Grimshaw and Helfer, 1995). Among the many advantages of vetiver are its deep roots (in excess of 3 m), rapid stabilization, ease of propagation, and the ability to plant it in stiff, compact hedges oriented perpendicular to the channel where it will retard channel flow and encourage sediment to accumulate. Unlike "dead" check dams which deteriorate with time, the protection provided by living vegetation will improve with time as the plants grow and strengthen, provided that channel flows do not wash away the plants. Vegetative controls are particularly susceptible to damage by large flow during the establishment stage; repeated replantings may be required in critical areas and should be anticipated in project budgets.

Heede (1976) cautioned against the use of trees in smaller gullies, since they might create so much hydraulic resistance that flow would be diverted out of the gully and erode adjacent areas. However, in larger gullies trees can be highly effective. The loess soils in the watershed of China's Yellow River include some of the world's most spectacularly gullied landscapes, with gullies having vertical walls many tens of meters tall. Reforestation of gully floors has been demonstrated to be an effective gully erosion control measure in this area by Li (1993).

The study area consisted of undulating hills dissected by deep gullies. The mean annual sediment concentration in runoff from ridges, slopes, and farmland ranged from 20 to 90 g/L. In contrast, the sediment concentration in gully channels averaged 500 to 700 g/L and typically occurred as hyperconcentrated flow. The effectiveness of gully afforestation is illustrated by data from trials involving two similar gullies, an untreated 1.15-km<sup>2</sup> control watershed, and a 0.87-km<sup>2</sup> watershed which was reforested starting in 1954 using four different tree species. Reforestation was undertaken on the gully floor, which had more moisture than the ridgeland but was unsuitable for crops because of flooding. Tree planting was initiated in smaller lateral gullies away from the main eroding flood channels, and was subsequently expanded downstream into the main channels. As seen in the double mass plot (Fig. 12.16), afforestation dramatically decreased both water and sediment yield from the treated gully as compared to the control: between 1958 and 1965, sediment yield from the afforested gully was reduced 92 percent compared to the untreated gully. The economic welfare of the region was also improved by the availability of forest products. Several mechanisms were responsible for reduced sediment yield. Roots helped stabilize and anchor the soil, and the hydraulic resistance of the stems reduced flow velocities, resulting in the net deposition of approximately 0.5 m of soil in the afforested gully. In contrast, channels incised at a rate of 5 m in 30 years in untreated gullies. Increased infiltration also reduced runoff and subsequent channel erosion.

### 12.10.5 Channel Linings

Lining materials such as grass, stone, geosynthetically reinforced turf, and concrete can be used to prevent channel erosion and gullying. Considerable recent attention has been given to geosynthetically reinforced turf (available from several manufacturers), which provides more rapid and higher erosion resistance than grass alone and can be substituted for stone or concrete in appropriate situations (Williams et al., 1996). Because of high cost, linings are primarily used in urban areas or along transportation corridors.

## 12.11 EROSION CONTROL STRATEGIES FOR RANGELAND

---

Pasture is land that could be suitable for growing crops or trees, but which is managed for forage production and grazing. Rangeland is land which is used for cattle grazing or wild-

### Water and Sediment Yield, Two Gullies Middle Reach Yellow River, China

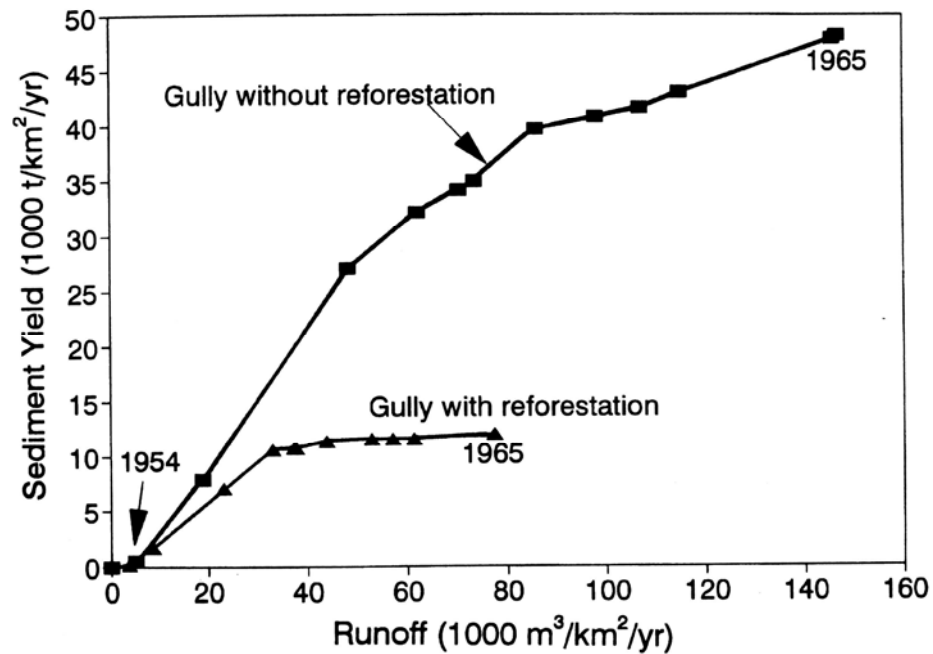


**FIGURE 12.16** Cumulative yield of water and sediment from two gullies in China, illustrating the effectiveness of gully reforestation (*drawn using data from Li, 1993*).

life habitat rather than cultivated, usually because it is too dry or too steep, or has some other limitation making it unsuitable for crop production. These limitations, and especially limited vegetation, tend to make rangelands particularly susceptible to erosion. The economic productivity of rangelands depends on maintaining a natural and productive vegetation cover. Because of the low economic unit value of rangeland, the options for erosion control treatment are normally very limited.

Grazing management tends to focus on: (1) limiting livestock stocking rates; (2) proper scheduling of grazing, including periods of rest and recovery; (3) livestock distribution and exclusion from sensitive areas such as riparian corridors by fencing; and (4) allocation of forage between livestock and wildlife. The mechanical action of cattle can be particularly destructive to the riparian zone, especially since animals tend to congregate in this zone for water, forage, and shade. For both pasture and rangelands, areas of livestock watering, salting, and shade should be located well away from riparian areas. Fencing of riparian areas is an effective, although costly, method of controlling livestock access. For example, in a 13-year study of an unimproved pasture watershed in Ohio, Owens et al. (1996) found that the annual average flow-weighted sediment concentration was reduced by 57 percent, and total sediment yield by 40 percent, after the riparian area was fenced, even though the herd size was the same as during the unfenced period, and storm flow was 30 percent greater during the fenced period. An example of the impact of livestock in a riparian zone is described in Chap. 22.

## 12.12 EROSION CONTROL STRATEGIES IN URBANIZING AREAS

---

Sediment yields are typically low from fully developed urban areas where land surfaces are covered by vegetation and pavement. In contrast, the sediment yields from construction sites can be very high. The total sediment yield from an urbanizing area represents the sediment from the surrounding rural or agricultural land that is not yet developed, construction sites, and fully developed urban sites. The generalized change in sediment yield from an urbanizing area as a function of land use and time was schematically illustrated in Fig. 7.9. Although the total amount of sediment from an urban area will normally be low once fully developed, the runoff may continue to have pollutants which can compromise water quality in downstream water bodies. The increased peak discharge from an urbanized area will also increase channel erosion downstream.

Erosion control and related water quality requirements in urban environments and construction sites are normally established by regulation, and both local and federal ordinances may apply. Because of the regulated nature of this activity, region-specific best management practices and design standards will often apply. Urban BMPs for stormwater quality control have been reviewed by Goldman et al. (1986), Schueler (1987), and Urbonas and Stahre (1993).

The 10 general strategies outlined in Sec. 12.2 are all applicable to construction sites. Of particular importance are (1) work scheduling to minimize the surface area and duration that bare soil is exposed to rainfall at any point in time, (2) protection of exposed surfaces with mulch, vegetation, or pavement as rapidly as possible following earth movement, (3) use of lined channels and on-site storm drains to reduce channel erosion, and (4) detention and sediment trapping of site runoff prior to discharge.

Several techniques have been used to trap or otherwise prevent the discharge of pollutants with stormwater runoff from urban areas. The only feasible strategy for drainage areas of any significant size (exceeding about 1 ha) is stormwater detention with plain sedimentation of solids, aided by biological processes when the stormwater pond includes wetlands. The effectiveness and longevity of different urban stormwater management practices were reviewed by Schueler et al. (1992). Use of wet ponds and wetland detention ponds were found to be an effective and long-lived sediment removal technique. However, the pollutant removal efficiency of normally dry detention ponds was not always reliable. Methods other than detention can be used to treat small-area flows, such as that from an individual parking area. Schueler et al. (1992) found that surface filtration by sand beds can work well, provided that the sand can be raked, removed, and replaced as required to maintain infiltration capacity. In contrast, many systems in which the filtration medium is not removed failed because of clogging problems after several years. These included infiltration basins, deep filtration systems such as gravel-filled trenches, and porous pavements. Paving systems designed as turf reinforcement systems were not studied. Grassed swales can prevent erosion, but have very low pollutant removal efficiencies when there is appreciable flow velocity. Vegetated filter strips have worked well in agricultural applications, but were generally found to perform poorly in urban environments because of problems such as excessive slope (greater than 15 percent), inadequate strip width, uneven terrain which caused flow channelization, and poor vegetative cover.

One pervasive problem at construction sites is the need to protect bare slopes. The use of mulches and geotextiles for erosion control on slopes has been reviewed by Rickson (1995). Contour plantings of vetiver grass (see Sec. 12.4.7) have been found to be an effective means to vegetatively stabilize road cuts and fills in moist tropical and subtropical areas. The silt fence is a widely used (and misused) control techniques

designed to retard the flow velocity of sheet runoff, thereby causing sediment deposition. It is effective only in the control of sheet flow; once flow becomes concentrated a silt fence is useless. Because flows tend to rapidly become channelized on construction sites, detention basins are usually recommended, in combination with upstream erosion control measures, to reduce the amount of sediment that leaves the site.

Techniques for the design of detention basins are given in the next section of this chapter, and are applicable to treating runoff from construction sites as well as developed urban areas. When a basin which provides detention and sediment trapping during the construction phase will also be used after the project is completed, the trapping efficiency may be expected to change because of the change in the grain size of the suspended solids load between the construction and post-construction period.

## 12.13 SEDIMENT DETENTION BASINS

This section outlines design strategies for sediment detention basins. More detailed discussions are presented by Haan et al. (1994), Urbonas and Stahre (1993), and U.S. EPA (1986).

### 12.13.1 Design Philosophy

Basic design strategies for maximizing sediment retention are the opposite of those outlined in other parts of this handbook, and oriented to minimizing sediment deposition within impoundments. The most important differences are summarized in Table 12.4. Because sediment traps will eventually become filled, periodic sediment removal is just as important as proper design to maintain long-term trapping efficiency.

Sediment yield from impervious urban surfaces is distinctly different from soil. The erosion rate from soil is related to rainfall intensity and runoff rate. Sediment concentration tends to increase as a function of rainfall intensity, and exceptional loads may be produced by large storms which initiate gullying and slope failures. However, on impervious surfaces the sediment and other particulate matter that collect on the surface are washed into the stormwater drainage system by the initial part of the runoff, the so-called *first flush* effect. Thus, most of the sediment may be washed from the streets and other impervious areas by the initial runoff, and subsequent rainfall will generate relatively small amounts of sediment, regardless of the storm intensity.

First flush effects are obvious to even a casual observer in the visual change in runoff quality from a small impervious drainage area over the course of a prolonged or multiple-event storm. However, Urbonas and Stahre (1993) have noted that they appear not to

**TABLE 12.4** Major Differences between Sediment-Trapping and Sediment-Excluding Impoundments

Design parameter	Sediment-trapping impoundments	Sediment-excluding impoundments
Hydraulic short-circuiting	Minimize	Maximize
Outlet structures	High level	Low level
Detention time	Maximize	Minimize
Portion of hydrograph to trap	First	Last
Water level during flood	High	Low

occur in some urban areas. First flush effects may not be apparent in a smaller storm of insufficient volume or intensity to wash most of the surface pollutants into and through the storm drainage system, when the point of measurement includes runoff from widely dispersed areas with large differences in the time required for runoff to reach the measurement site, and when first flush effects from paved areas are masked by runoff from construction sites or undeveloped areas tributary to the monitoring site. Because of variations in storm intensity and travel times, first flush effects should be more pronounced from a small urban drainage area (such as a single parking area or facility) compared to the aggregate drainage from a larger urban area.

To maximize the retention of sediment and the pollutants associated with fine sediment, detention basins should trap and hold runoff from smaller events for a prolonged period, and provide adequate detention for larger events. A schematic diagram of the storage compartments in a wet sediment detention basin are presented in Fig. 12.17. Operation of the basin is described with respect to the outlets and storage areas shown in the figure.

**1. Small runoff events.** A small runoff event is one which does not exceed the live storage volume. These events would normally be described in terms of a runoff depth (e.g., 1 or 2 cm across the tributary area). The total volume of small runoff events should be detained in the live storage zone for the longest time possible to maximize the trapping of fine sediment. However, it should also be drained from the live storage zone fast

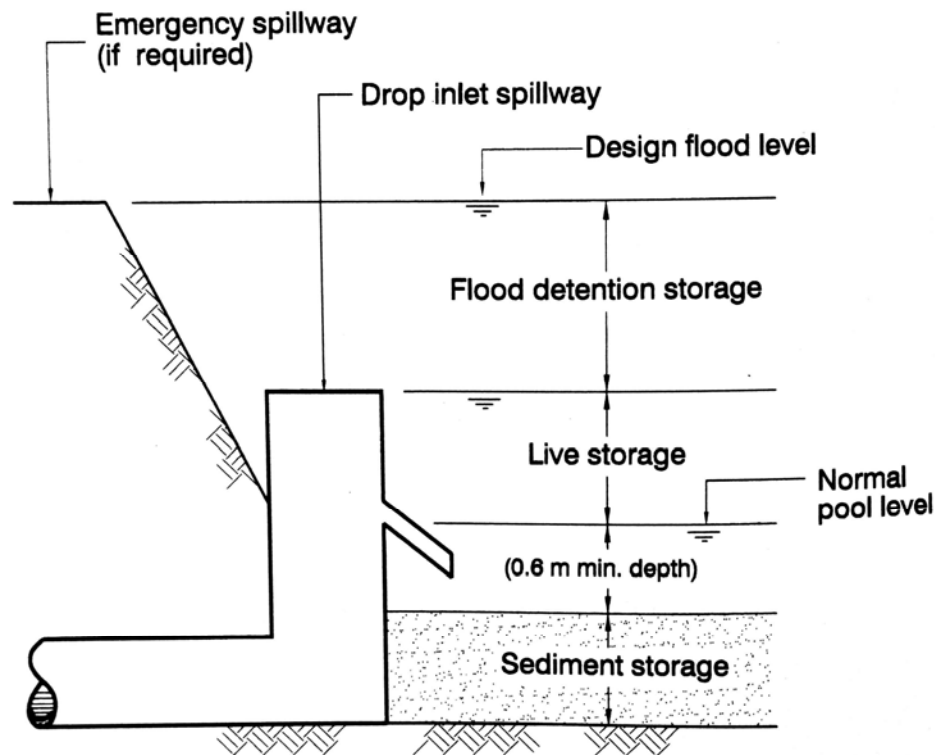


**FIGURE 12.17** Allocation of storage in a wet detention pond. A wet pond could contain open water or wetland species, depending on the normal water depth.

enough (e.g., 24 hours) to make storage space available for the subsequent storm event. A downward sloping pipe is used to drain the live pool to reduce the potential for clogging by floating debris, which can be a problem with a horizontal pipe or orifice (Schueler et al., 1992)

**2. Design sedimentation event.** Achieve a stated removal efficiency (based on the surface loading rate) during runoff from the design sedimentation event, with discharge over the spillway. Design storm intensities ranging from 2- to 10-year events are typically used in different areas.

**3. Design flood.** Provide sufficient flood surcharge storage and spillway capacity to pass the design flood without endangering the structure or causing flood damages. Selection of the design storm will depend on the size of the structure and its hazard rating, and in the case of dams (as opposed to excavated ponds), spillway design may be regulated by state dam safety bodies. The minimum design storm for the spillway rating would normally be the 100-year event, and in the case of an embankment structure a much larger event may be appropriate.

**4. Dewatering.** Provide a low-level outlet for dewatering the basin and its sediment, to facilitate periodic cleanout. The configuration of the dewatering outlet will depend on local factors. For example, if coarse sediment is present, it may be advantageous to have the dewatering drain located at the inlet where the more permeable sediment will accumulate, instead of at the outlet where the accumulated sediment will be finer and more difficult to dewater.

The adaptation of this concept to specific areas will depend on local hydrologic and sediment conditions, plus local regulatory requirements.

### 12.13.2 Detention Basin Geometry

Detention basin surface area is established from the design sedimentation event and the surface loading rate. Surface area may also be influenced by the flood and live storage volumes, which will depend on both the surface area and pool depth. Basin depth is the sum of freeboard, flood surcharge, live storage, and sediment storage (Fig. 12.17). Freeboard requirements are usually related to the downstream risks, size of structure, embankment construction material (e.g., earth or concrete), and in larger structures factors such as wave action and ice (MacArthur and MacArthur, 1992).

The live storage volume and drainage rate represents a compromise between the desire to maximize detention time for sedimentation, and the need to empty the live storage pool quickly to trap a subsequent rainfall event. A water budget model can be run with 15-minute or hourly rainfall data to analyze basin function, to determine what percentage of the runoff will be trapped in the live pool. A simplified procedure for this analysis has been described by Urbonas and Stahre (1993) for hourly rainfall data. However, these models do not account for the variation in water quality that may occur over time. According to Urbonas and Stahre (1993), a 24-hour drain time appears to represent a good compromise between the requirements for sediment trapping and the desire to empty the basin prior to the subsequent event. As a practical matter, storage volumes are frequently set by regulatory agencies based on runoff volume.

Hydraulic short-circuiting occurs when there are dead zones in the basin, thereby allowing a portion of the inflow to pass to the basin outlet in a time period less than (or much less than) the nominal detention period. Discharge entering a basin as a jet from a single inlet will gradually expand, and at the outlet zone the active flow field constricts in the vicinity of the discharge weir. An inlet pipe entering a basin and pointing directly at the basin outlet may effectively short-circuit a large fraction of the basin area. The dead storage volume

in a basin can be quantitatively evaluated by tracer studies in the field, or by physical or computer modeling. Because of the effort involved, tracer testing and modeling of detention basins are most suitable for critical sites, or the evaluation or development of standardized design guidelines or criteria.

The following strategies may be employed to reduce hydraulic short-circuiting within a settling basin.

- Use an elongated basin. Length:width ratios should always exceed 2:1, and larger values are preferred.
- Use interior baffles to extend the effective length:width ratio, and to obstruct the inflowing jet.
- If the basin is triangular in shape, locate the inlet at the narrow end so that the flow expands with the basin geometry.

The detention basin configurations in Fig. 12.18 illustrate the use of baffles to reducing hydraulic short-circuiting. However, in a system which has a very accentuated first flush

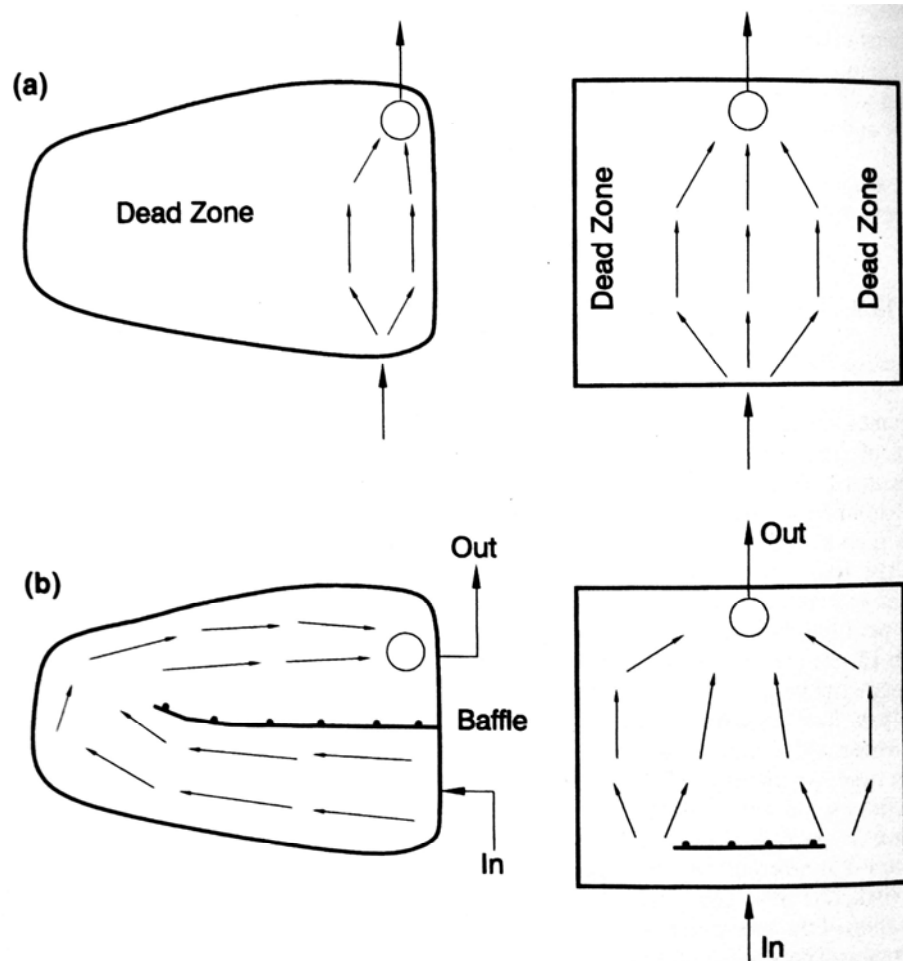


**FIGURE 12.18** (a) Hydraulic short-circuiting in detention basins creates large dead zones. (b) Use of baffles minimizes the dead zones in the basin. Baffles may be constructed of posts and exterior plywood, roofing panels, heavy plastic, or other water- and wind-resistant material.

effect, such as runoff from a paved area, it may be desirable to trap the first-flush water in the live storage, and hydraulically short-circuit the cleaner discharge from the remainder of the event to the flood discharge outlet.

The volume and depth of the sediment storage pool are based on the anticipated sediment loading rate and the planned period between sediment removal. At a construction site with potentially high rates of sediment yield, the basin may be cleaned several times a year or after a major storm. In a developed urban area, where the basin is incorporated into project landscaping and may support a wetland habitat, the dewatering and cleaning interval should be on the order of several years or longer. In a wet basin, leave a minimum water depth of 0.6 m between the top of the design sediment storage pool and the normal pool level.

Shallow areas in a wet detention pond will become colonized by wetland plants, either by design or as a result of natural processes, and detention areas can serve as wetland habitat. Wetland design in stormwater systems has been reviewed by Kadlec and Knight (1995) and Schueler (1993). In determining the water depths in detention areas, the colonization depth of wetland vegetation must be taken into consideration. For instance, cattail (*Typha domingensis*), a common, aggressive, and less-desirable wetland plant, can colonize water to depths on the order of 1 m. Depths greater than this may be required to maintain open water unless vegetative control efforts are undertaken.

### 12.13.3 Design Computations for Plug Flow

Sediment retention ponds are subject to widely varying rates of inflow, and the settling characteristics of the inflowing sediments may change as a function of season, and over longer periods of time because of land use change. The extent of hydraulic short-circuiting will normally be unknown, and may also change over time as trapped sediments accumulate and vegetation grows, altering storage volume and other hydraulic characteristics. As a result, engineering procedures for sedimentation pond design provide only a rough approximation of actual performance.

**Inflow Hydrology.** To size the basin surface area and the flood spillway, the inflow must be estimated for the design sedimentation event as well as the spillway design discharge. For small basins, simple procedures can be used—for example, the rational formula, which has the form:

$$Q = CIA \quad (12.1)$$

where  $Q$  = discharge ( $\text{m}^3/\text{s}$ ,  $\text{ft}^3/\text{s}$ ),  $I$  = rainfall intensity ( $\text{m}/\text{s}$ ,  $\text{in}/\text{h}$ ) for a duration equal to the time of concentration for the tributary drainage area,  $A$  = tributary drainage area ( $\text{m}^2$ , acres), and  $C$  = dimensionless runoff coefficient, which is the same in either system of units. Representative coefficient values are given in Table 12.5. Local hydrologic design guidelines may adopt other values.

Sediment detention structures may also be used for flood detention, in which case the outlet structure should be designed with unsteady-flow modeling tools to generate and route stormwater hydrographs. Many stormwater modeling tools are available from commercial software vendors, which are suitable for performing runoff and hydraulic routing computations in detention ponds.

Drop inlet spillways will draw down the water level in the vicinity of the weir, which tends to attract floating debris. Placement of a solid skirt or baffle around the inlet, which extends above and below the weir crest (Fig. 12.19a), will minimize the problem of debris entrainment. The inlet top may then be covered. However, sediment deposition can encroach on the flow area below the inlet. Use of a baffled inlet structure

(Fig. 12.19*b*) which minimizes this problem is described by the Soil Conservation Service (1983).

**TABLE 12.5** Representative Coefficient Values for Rational Formula

Type of drainage area	Runoff coefficient, <i>C</i>
Lawns:	
Sandy soil, flat, 2%	0.05-0.10
Sandy soil, average, 2-7%	0.10-0.15
Sandy soil, steep, 7%	0.15-0.20
Heavy soil, flat, 2%	0.13-0.17
Heavy soil, average, 2-7%	0.18-0.22
Heavy soil, steep, 7%	0.25-0.35
Business:	
Downtown areas	0.70-0.95
Neighborhood areas	0.50-0.70
Residential:	
Single-family areas	0.30-0.50
Multi units, detached	0.40-0.60
Multi units, attached	0.60-0.75
Suburban	0.25-0.40
Apartment dwelling areas	0.50-0.70
Industrial:	
Light areas	0.50-0.80
Heavy areas	0.60-0.90
Parks, cemeteries	0.10-0.25
Playgrounds	0.20-0.35
Railroad yard areas	0.20-0.40
Unimproved areas	0.10-0.30
Streets:	
Asphaltic	0.70-0.95
Concrete	0.80-0.95
Brick	0.70-0.85
Drives and walks	0.75-0.85
Roofs	0.75-0.95

**Determine Pond Surface Area.** The quiescent sedimentation of discrete particles within an idealized rectangular settling tank can be conceptualized by using the diagram in Fig. 12.20. The basin's inlet and outlet zones are considered to be completely mixed. The critical fall velocity  $\omega_c$  in this basin is the fall velocity of the smallest-size-class (slowest-settling) particle which will be completely removed by plain sedimentation, as illustrated in the figure. All particles with a higher fall velocity will also be completely removed. The critical settling velocity  $\omega_c$  of the smallest-size-class particle that is 100 percent sedimented in the idealized basin is given by:

$$\omega_c = \frac{Q}{A_b} \quad (12.2)$$

where  $Q$  = discharge and  $A_b$  = basin surface area. The ratio  $Q/A_b$  (the *surface loading rate*) indicates that sediment removal is dependent on the surface area of the settling basin, but not its depth.

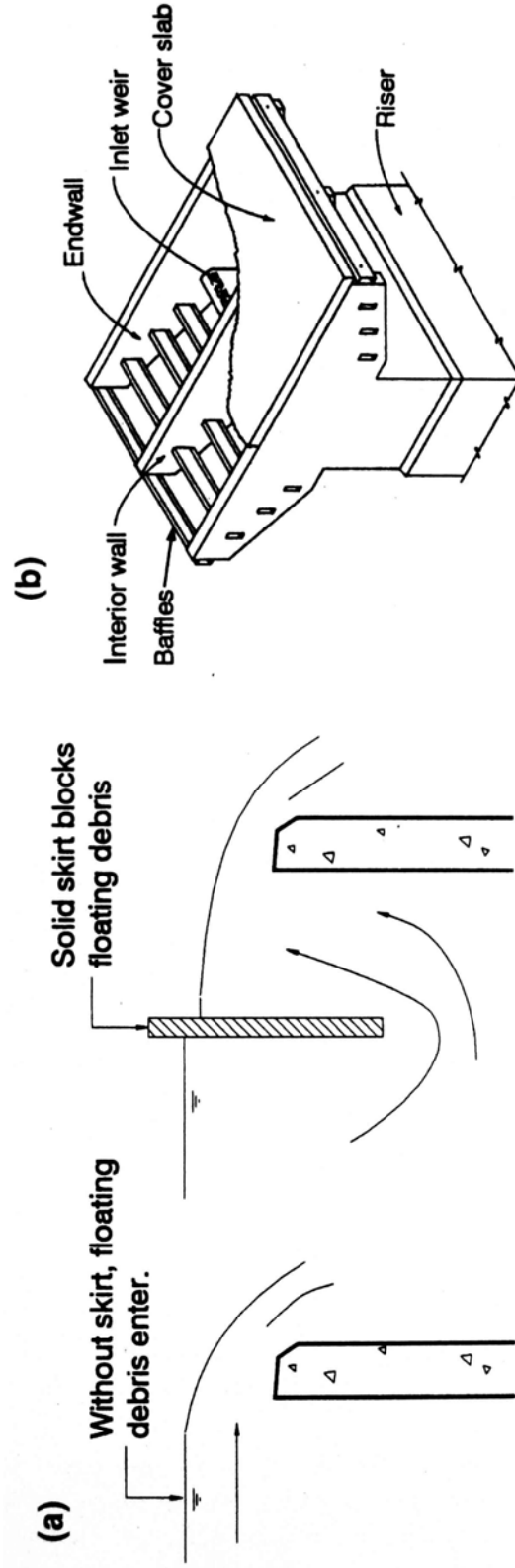


**FIGURE 12.19** (a) Placement of a solid skirt or baffle around a drop inlet will minimize the attraction and entry of floating debris. However, when this type inlet is covered, sediment accumulation can impair its hydraulic performance. (b) Covered baffled inlet which minimizes debris entrainment and obstruction by sediment. (*Soil Conservation Service, 1983.*)

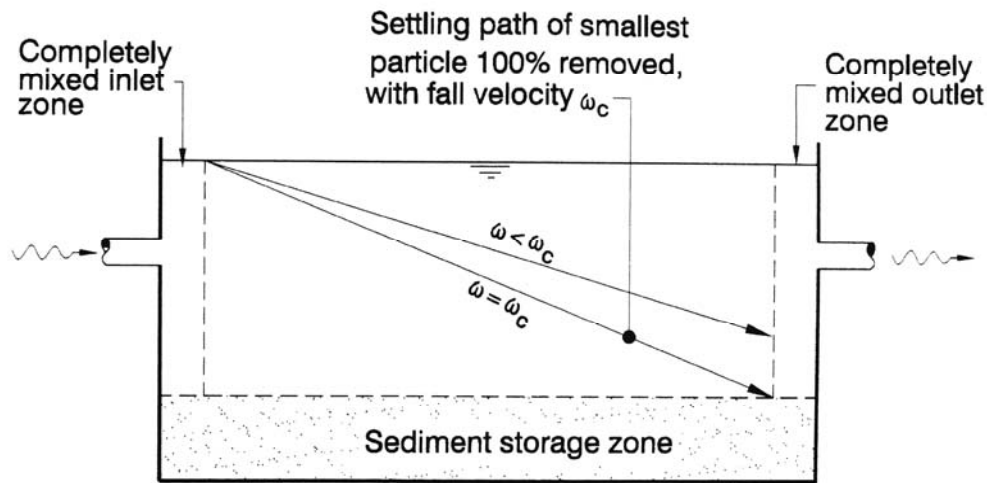


FIGURE 12.20 Particle settling in an idealized sedimentation basin.

Inflowing sediment load exhibits a range of grain sizes and settling velocities, and particles in size classes with a fall velocity less than the critical fall velocity ( $\omega < \omega_c$ ) will be only partially removed. The trapping efficiency  $E$  of this slower-settling sediment is given by the ratio of settling velocities:

$$E = \frac{\omega}{\omega_c} \quad (12.3)$$

where  $\omega$  = fall velocity of the particles in a class size where  $\omega < \omega_c$ .

The surface loading rate and the trap efficiency as a function of the inflowing grain size distribution may be used to determine the sediment removal and, from this, the grain size distribution of released sediment in the effluent. Sediment trapping computations for an idealized sedimentation basin are illustrated in the following example for a 1-ha (10,000 m<sup>2</sup>) basin with an inflow rate of 1 m<sup>3</sup>/s, water temperature of 20°C, and the inflowing grain size distribution given in Fig. 12.21.

1. Compute the surface loading rate to determine the settling velocity of the slowest-settling particle size class that will be 100 percent removed:

$$\omega_c = \frac{Q}{A} = \frac{1 \text{ m}^3/\text{s}}{10,000 \text{ m}^2} = 1 \times 10^{-4} \text{ m/s}$$

The particle diameter  $d$ , corresponding to the critical settling velocity  $\omega_c$  is estimated at 0.0105 mm by the Rubey equation [Eq. (5.23)].

2. Referring to the inflowing grain size distribution, subdivide the particles smaller than  $d$  into classes, as shown in Fig. 12.21, and determine the mean settling velocity for each class.
3. Compute the trap efficiency for each sediment size class as  $E = \omega/\omega_c$ . For the inflowing sediment with settling velocity  $\omega$  greater than  $\omega_c$  the trap efficiency will be 100 percent (i.e.,  $E = 1$ ). Compute release efficiency as  $1 - E$ .
4. Compute the overall trap efficiency for the inflowing sediment load by multiplying the weight percent in each class by the corresponding trap efficiency for each class, and summing.

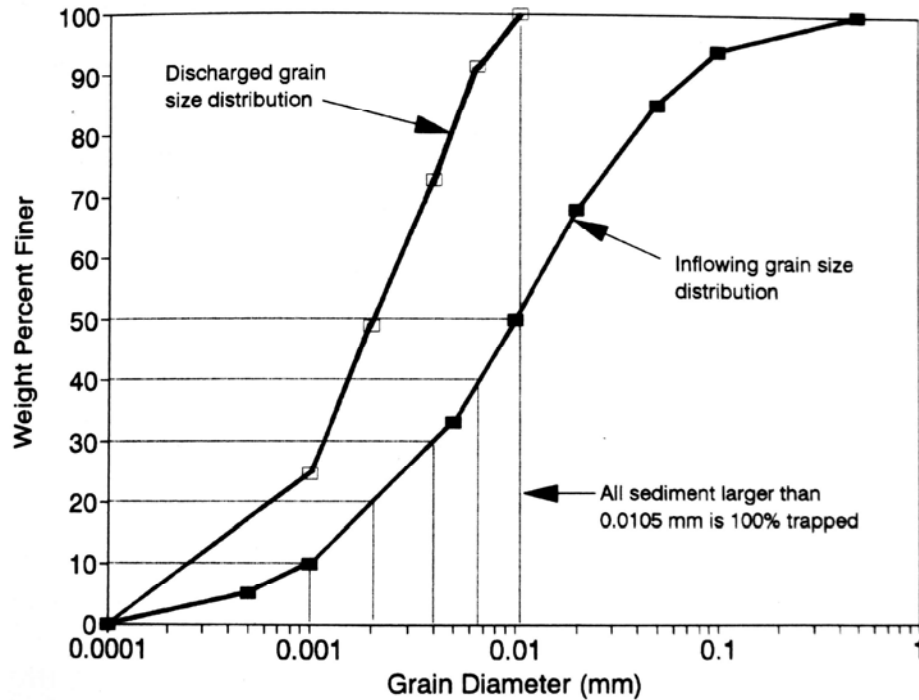


**FIGURE 12.21** Inflow and outflow suspended-sediment grain size distribution for example detention basin computations. The dotted lines indicate the grain size class intervals for the portion of the inflowing sediment load with a trap efficiency of less than 100 percent.

5. Compute the size distribution in the water discharged from the basin, as illustrated in Fig. 12.21.

Numerical computations for this example problem are summarized in Table 12.6. In the example basin, all sand and coarse silt is completely trapped, but the trapping rate of clays is insignificant. This procedure can be modified to size a basin to achieve a given level of removal efficiency given the inflowing grain size distribution.

**TABLE 12.6** Sediment Trapping Computations for an Idealized Detention Basin

Class interval, weight %	Class Size, Weight %	Lower Particle Diameter, mm	Upper Particle Diameter, mm	Mean Class Particle Diameter, mm	Mean Class Call Velocity, m/s	Fall Velocity Ratio $\omega/\omega_c$	Release Efficiency By class, decimal	Cumulative Release By class % of inflow	Released Sediment Grain Size Distribution, % finer
0-10	10	0.0001	0.0010	0.0006	$3.2 \times 10^{-7}$	0.003	0.997	9.97	25
10-20	10	0.0010	0.0020	0.0015	$2.0 \times 10^{-6}$	0.020	0.980	19.77	49
20-30	10	0.0020	0.0040	0.0030	$3.6 \times 10^{-6}$	0.036	0.964	29.41	73
30-40	10	0.0040	0.0065	0.0053	$2.5 \times 10^{-5}$	0.250	0.750	36.91	91
40-50	10	0.0065	0.0105	0.0085	$6.5 \times 10^{-5}$	0.650	0.350	40.41	100

### 12.13.4 Sedimentation under Turbulent Nonidealized Conditions

Real basins are not plug flow reactors, and even basins designed to optimize sedimentation may have a significant volume of dead space and secondary currents circulating within the basin. Under turbulent and nonideal conditions, the trap efficiency as a function of the settling velocity ratio  $\omega/\omega_c$ , can be given by (Urbonas and Stahre, 1993):

$$E = 1 - \left[ 1 + \frac{1}{n} \frac{\omega}{\omega_c} \right]^{-n} \quad (12.4)$$

where  $E$  = trap efficiency of sediment in the size class corresponding to particle fall velocity  $\omega$ ,  $n$  = a factor which depends on the hydraulic efficiency of the basin, and  $\omega_c$  = critical fall velocity as defined in Fig. 12.20. Suggested values of  $n$ , based on settling characteristics, are

$n = 1$	Poor settling characteristics
$n = 3$	Good performance
$n > 5$	Very good performance
$n = \text{infinity}$	Ideal performance

For very large values of  $n$ , this equation reduces to the equation for idealized sedimentation under turbulent conditions:

$$E = 1 - e^{-\omega/\omega_c} \quad (12.5)$$

A graph of settling characteristics as a function of grain size for  $n = 3$  (good performance) is provided in Fig. 12.22 and may be used to estimate the removal efficiencies. The difference between good and poor performance has a relatively small impact on the settling curve in the area of low removal efficiencies ( $\omega$  much less than  $\omega_c$ ), but significantly affects the removal of particles with settling velocities close to the critical velocity  $\omega_c$ .

### 12.13.5 Dewatering Orifice

The discharge orifice should be sized to dewater the live storage zone within a stated time period, such as 24 hours. The discharge rate through an orifice is given by:

$$Q = CA\sqrt{2gh} \quad (12.6)$$

where:  $C$  = orifice coefficient  
 $A$  = orifice area ( $\text{m}^2$ ,  $\text{ft}^2$ )  
 $g$  = gravitational constant ( $\text{m/s}^2$ ,  $\text{ft/s}^2$ )  
 $h$  = head above the orifice (m, ft)

This equation is dimensionally consistent and the orifice coefficient is independent of the system of units. Several orifice coefficient values are given in Table 12.7.

As the pond dewater the orifice will operate under continuously decreasing head. For a basin with vertical sides and zero inflow during the dewatering period, the time required to dewater the volume above the orifice may be determined by using a discharge rate equal to half the discharge at the maximum head (i.e.,  $Q_{\text{max}}/2$ ). The time required to dewater a basin through an orifice can also be given by:

$$T = \frac{B\sqrt{2h}}{3600AC\sqrt{g}} \quad (12.7)$$

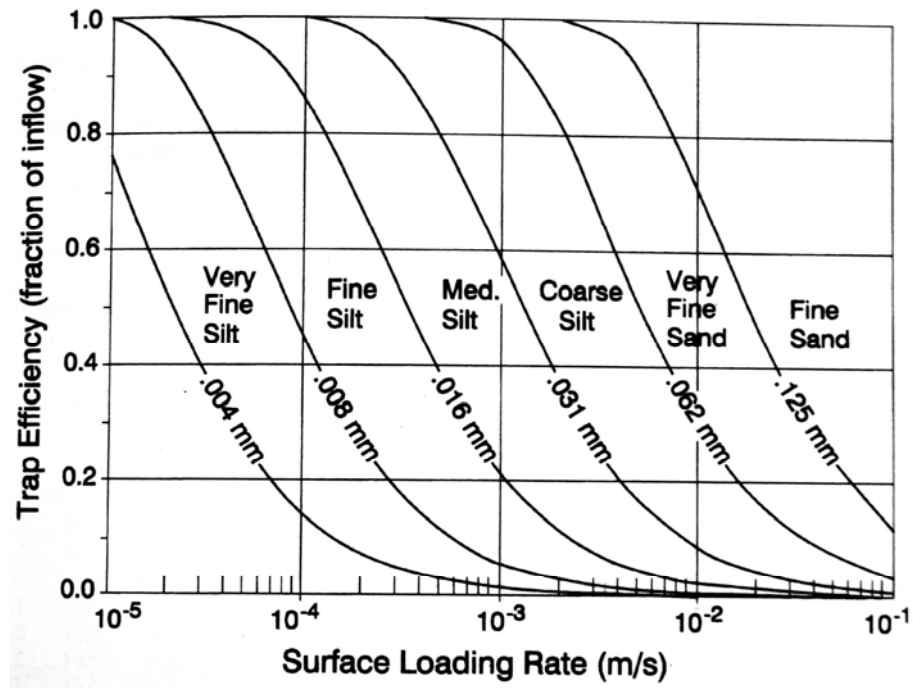


FIGURE 12.22 Settling characteristics as a function of grain size for estimating the efficiency of a settling basin with "good" hydraulic characteristics [ $n = 3$  in Eq. (12.4)].

TABLE 12.7 Orifice Coefficient Values

Condition	Coefficient $C$
Sharp edge, circular or square	0.6
Short tube (length = 2 or 3 times diameter) flush with wall	0.82
inward projecting	0.75
Borda's mouthpiece (length = 'A diameter)	0.51

Source: King and Brater (1963).

where  $T$  = time to dewater (hours),  $B$  = basin surface area, and  $h$  = initial head above the orifice (Goldman et al., 1986).

### 12.13.6 Weir Discharge

Horizontal weirs are often used to discharge floodwater from detention structures. The general equation for discharge over a horizontal broad-crested weir is

$$Q = CLH^{3/2} \quad (12.8)$$

where:  $Q$  = discharge ( $\text{m}^3/\text{s}$ ,  $\text{ft}^3/\text{s}$ )

$L$  = length of the weir (m, ft)

$H$  = head upstream of the weir (m, ft)

The value of the coefficient  $C$  depends on the weir geometry and the system of units. Coefficient values may be converted between SI units and the fps system by

$$C_{SI} = C_{fps} / 1.81$$

Coefficient values for broad-crested weirs are summarized in Table 12.8, where the breadth of the weir crest is measured parallel to the direction of flow.

**TABLE 12.8** Coefficient Values for Broad-Crested Weirs

Head (ft)	Breadth (ft)										
	0.5	0.75	1	1.5	2	2.5	3	4	5	10	15
0.2	2.80	2.75	2.69	2.62	2.54	2.48	2.44	2.38	2.34	2.49	2.68
0.4	2.92	2.80	2.72	2.64	2.61	2.60	2.58	2.54	2.50	2.56	2.70
0.6	3.08	2.89	2.75	2.64	2.61	2.60	2.68	2.69	2.70	2.70	2.70
1.0	3.32	3.14	2.98	2.75	2.66	2.64	2.65	2.67	2.68	2.68	2.63
2.0	3.32	3.31	3.30	3.03	2.85	2.76	2.72	2.68	2.65	2.64	2.63
3.0	3.32	3.32	3.32	3.32	3.20	3.05	2.92	2.73	2.66	2.64	2.63
5.5	3.32	3.32	3.32	3.32	3.32	3.32	3.32	3.32	2.88	2.64	2.63

Head (m)	Breadth (m)										
	0.15	0.23	0.30	0.46	0.61	0.76	0.91	1.22	1.52	3.05	4.57
0.06	1.55	1.52	1.49	1.45	1.40	1.37	1.35	1.31	1.29	1.38	1.48
0.12	1.61	1.55	1.50	1.46	1.44	1.44	1.43	1.40	1.38	1.41	1.49
0.18	1.70	1.60	1.52	1.46	1.44	1.44	1.48	1.49	1.49	1.49	1.49
0.30	1.83	1.73	1.65	1.52	1.47	1.46	1.46	1.48	1.48	1.48	1.45
0.61	1.83	1.83	1.82	1.67	1.57	1.52	1.50	1.48	1.46	1.46	1.45
0.91	1.83	1.83	1.83	1.83	1.77	1.69	1.61	1.51	1.47	1.46	1.45
1.68	1.83	1.83	1.83	1.83	1.83	1.83	1.83	1.83	1.59	1.46	1.45

*Source:* King and Brater (1963).

## 12.14 DEBRIS BASINS

Debris basins are designed primarily to trap coarse sediment which would otherwise cause objectionable deposits in channels or other downstream areas. They may also be used to trap hyperconcentrated debris flows originating in mountainous areas.

### 12.14.1 Debris Basin Configurations

Debris basins may be constructed as conventional dams with overflow spillways, as basins equipped with perforated risers, as dams with a permanently open sluice, or as excavated pits in the streambed. For hyperconcentrated debris flows, there are additional techniques for protecting downstream areas, such as construction of channels and protective walls. Several strategies for protection against hyperconcentrated debris flows are illustrated in Fig. 12.23. Stonestreet (1994) and Gist et al. (1996) describe the design of a series of excavated pools for use for trapping of floodborne debris on San Timoteo Creek

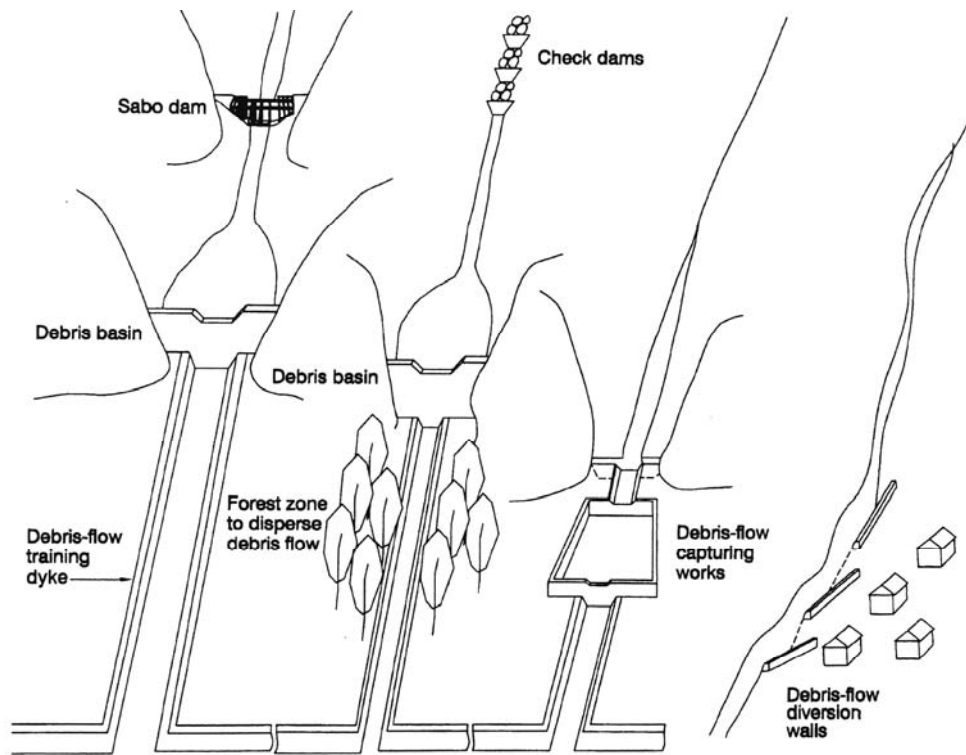


FIGURE 12.23 Strategies for the control of debris flows (modified from Mizuyama, 1993).

in southern California (Fig 12.24). Excavated basins were analyzed at this site instead of a conventional structure because of limited space within the constricted canyon, which was shared with a railway line, and local objections to the installation of a 13-m-tall conventional dam-type debris basin in the canyon.

### 12.14.2 Sediment Trapping by Debris Basins

Unlike sediment detention basins, which seek to trap as much sediment as possible from all runoff events, a debris basin is designed to trap only the coarse load, or only the hyperconcentrated load associated with debris flows. To efficiently trap only a selected part of the total load, debris basins tend to be hydrologically small with very low capacity:inflow ratios. Debris basins have limited sediment storage capacity, and the accumulated sediment must be removed if they are to provide long-term protection. An oversized basin which traps the target grain size, plus a large volume of finer sediment, is undesirable; it will increase the volume and cost of sediment removal.

Debris basin design is a three-step process: (1) determine the critical sediment size or other critical aspect of the inflowing sediment load that should not be exceeded during the design event for the downstream conveyance system to work properly, (2) determine the grain size distribution and volume of the inflowing load, and (3) determine the

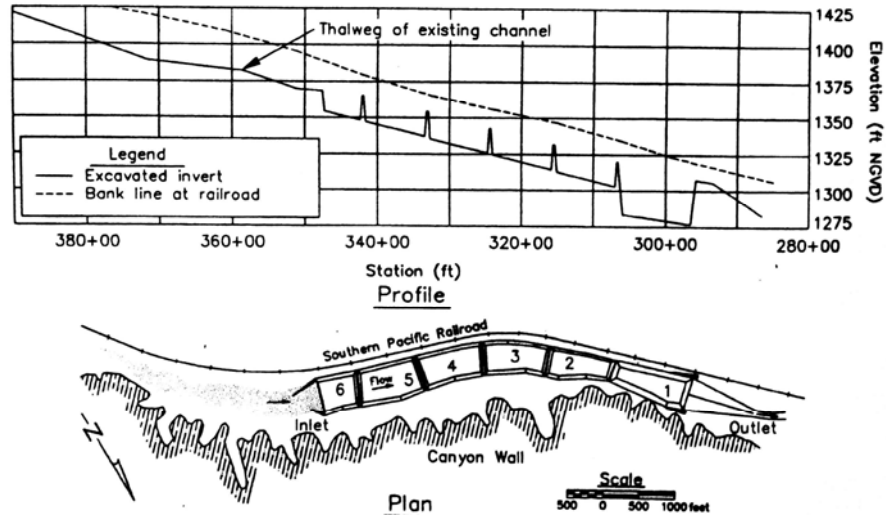


FIGURE 12.24 Plan and profile of in-channel debris basin (Stonestreet, 1992).

hydraulic characteristics of the basin required to trap the target grain size without excessive trapping of finer material. Because debris basins may be designed to protect against a variety of hazards, there is no "standard" design technique.

The critical grain size will be determined from sediment transport studies and modeling of downstream channels. The loading on a debris basin may be derived from either watershed processes or channel processes. In southern California, debris flows are most likely to be associated with heavy rainfall on recently burned hillsides, which causes either extreme sediment loads or slope failures. In this case the debris yield is primarily a function of watershed processes rather than stream hydraulics. Sediment yield data and past experience in southern California indicate that the single-event debris yield is the critical design condition in this environment, rather than long-term accumulation. A method to compute single-event debris yield in this region has been presented by Gatwood et al. (1992). This method is based on a multiple linear regression developed from historical debris yield measurements and the following parameters: relief ratio, drainage area, unit peak flow or 1-hour precipitation, and a fire factor. In other environments the sediment to be trapped may consist of bed material and may be modeled on the basis of stream hydraulics. Woody debris may be important in some regions, and absent in others. Determination of debris loadings depends heavily on information from past experience. Volcanic activity can produce extreme sediment loads and require unique designs (U.S. Army, 1986).

Once the sediment load has been determined, the actual hydraulic performance of the basin can be modeled by numerical modeling tools. For instance, the HE-6 model was used to analyze the sediment-detention characteristics of the excavated debris basins shown in Fig. 12.24 for a 100-year design event.

The debris storage volume will depend on the size of the design event and the cleanout interval. Debris basins should be designed to provide protection during the largest design event, and should be cleaned regularly, or when accumulated sediment occupies a predetermined fraction of the design sediment storage volume (e.g., 25 percent). Therefore, in most instances the issue of deposition above the spillway elevation is not an important consideration. However, in an analysis of fully sedimented Japanese dams designed to trap debris flows, Maita (1993) found that the stable slope of the deposits upstream of the

dam was usually one-half to two-thirds the original stream slope. During an extreme sediment-transporting event, the slope will steepen and the sediment will accumulate above the already-filled structure, whereas smaller subsequent events which deliver less sediment from upstream will tend to scour the deposits, reducing the slope above the dam. Under this condition even "fully sedimented" structures may provide some residual sediment trapping during critical large events.

### 12.14.3 Debris Basin Cleanout

There are two basic alternatives for accomplishing debris basin cleanout: mechanical removal and hydraulic removal. Debris basins are generally designed as normally dry impoundments with some type of dewatering outlet. Mechanical sediment removal is normally done with conventional earth moving equipment after the sediment has dewatered, and the excavated sediment is used for fill (Fig. 12.25). Cost data for debris basin cleanout presented in Table 16.1 show that costs can vary widely as a function of both the sediment volume and the haul distance.

For hydraulic removal, the sediment which accumulates during a large event would be removed by emptying and flushing during smaller events. In mountainous areas of Japan threatened by hyperconcentrated debris flows, Mizuyama (1993) reports that considerable emphasis is being given to the construction of *sabo dams*, which are dams consisting of concrete abutments with an open steel framework in the central portion (Fig. 12.26). The steel grid is spaced to provide sufficient retardance to hold back the debris flow, while allowing smaller flows to pass through the structure without accumulating sediment. This alternative was found to be superior to conventional concrete gravity structures, which had the disadvantage of filling with sediment from smaller runoff events prior to the arrival of a large debris flow.



**FIGURE 12.25** Cleanout of a debris basin operated by Los Angeles County, California. Note the perforated riser for drainage of the basin (*M. Bolander*).

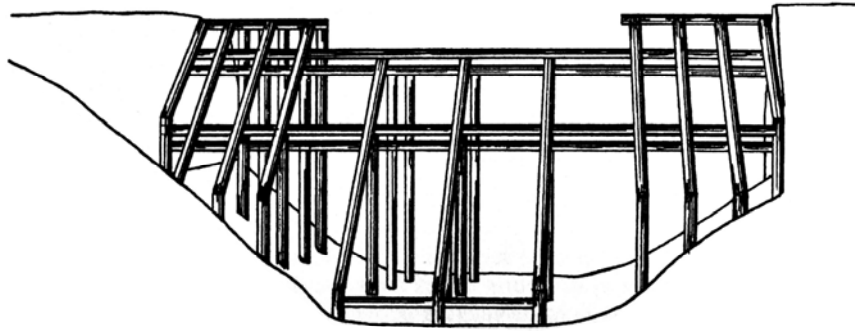


**FIGURE 12.26** Open sabo-type dam used in Japan to control debris flows. The open structure in the middle of the dam is sized to arrest the motion of a large debris flow, but to pass smaller events. This prevents premature sedimentation of the storage basin (*redrawn from Mizuyama, 1993*).

Although the hydraulic removal of accumulated debris is conceptually attractive, it has important impediments. First, the fraction of the deposit that can be removed will depend heavily on the reservoir geometry. Erosive flows will create a flushing channel through the deposits, and the long-term storage capacity that can be maintained will be limited to the volume of the flushing channel. In a narrow debris basin much of the original capacity might be recovered by flushing, but in a broad basin the flushing channel may comprise only a small percent of the original volume. Flushing is discussed in Chap. 15. Second, there may also be downstream limitations. Sediment eroded from the debris basin may be redeposited further downstream, which may be objectionable for operational or environmental reasons.

## 12.15 CLOSURE

---

Long-term sediment yield is heavily influenced by two factors: the construction of upstream reservoirs which trap sediment, and land use practices in the tributary watershed. Many less developed areas of the world, especially in the tropics, are experiencing a startling degradation of their forest and land resources, and travelers in these regions will be struck by the paucity of soil and water conservation practices. Deforestation, erosion, and degradation stalk the landscape, and in many areas it would seem that erosion will be controlled only when the supply of erodible soils is exhausted. The destruction of even the Amazon, shrouded in the smoke of its burning trees, would seem to be only a matter of time.

In an article aptly titled "An Explosion of Green," McKibben (1995) argues that one of the most dramatic environmental phenomena of this century has been the reforestation of the eastern United States, following more than a century of land degradation. A cleric traveling the 380 km route from New York to Boston in the early nineteenth century reported that not more than 30 km of forest had withstood the assaults of farmers and loggers. Today this same corridor is remarkable for its abundance of trees.

Reforestation of the eastern United States has been largely accidental; it is nature's response to the abandonment of farming, especially on sloping soils. Important contributing factors include increasing agricultural productivity on better (flatter) soils, the development of large-scale irrigation projects in the western deserts, increasing

employment opportunities in the urban/industrial economy which drew workers away from the farms, and a reduction in the population growth rate as the nation passed through the demographic transition. Land use changes, coupled with soil conservation efforts on all types of land use, enable the eastern United States to support today a larger population at a much higher standard of living than it did during the nineteenth century, while also sustaining a much larger forested area and generating much less soil erosion.

A transition of this type is hopefully not impossible to achieve in many of today's developing economies. But if achieved, factors such as population control and socioeconomic transformation will probably be of greater importance than soil conservation itself. Any soil conservation work that helps to promote this transition will be doubly effective.

---

## CHAPTER 13

---

# SEDIMENT ROUTING

---

### 13.1 CONCEPT AND APPLICATION

---

#### 13.1.1 Overview

Sediment routing includes any method to manipulate reservoir hydraulics, geometry, or both, to pass sediment through or around storage or intake areas while minimizing objectionable deposition. The sediment load in a stream is highly variable in time and can also vary significantly within the stream cross section; most inflowing sediment is contained in only a fraction of the inflowing water. Routing techniques seek to identify the sediment-laden portion of the inflow, and to manage it differently than clear water inflow to prevent, minimize, or focus sediment deposition.

Although some routing procedures may involve reservoir emptying, they are fundamentally different from flushing techniques, which also involve reservoir emptying. Sediment routing focuses on either minimizing deposition or balancing deposition and scour during flood periods, whereas flushing removes accumulated sediments after they have been deposited. Routing preserves the timewise pattern of sediment transport along the stream, whereas flushing modifies it significantly. The operational strategies and consequences of reservoir drawdown or emptying under the two methods are quite distinct and should not be confused.

#### 13.1.2 Classification of Techniques

The storage area being protected from sedimentation may be located in the original stream channel, off-channel, or in permeable subsurface deposits created in the impoundment from which water may be extracted by drains or wells. Sediment routing techniques may be classified into the following categories:

##### *Sediment Pass-Through*

1. Seasonal drawdown
2. Flood drawdown by hydrograph prediction
3. Flood drawdown by rule curve
4. Venting turbid density currents

### *Sediment Bypass*

1. On-channel storage
2. Off-channel storage
3. Subsurface storage

Routing techniques may also focus sediment deposition within selected areas of the impounded reach to minimize their interference with beneficial uses or to facilitate their subsequent removal. This chapter describes all routing techniques except density current venting, which is covered in Chap. 14.

Concepts of sediment bypass and sediment pass-through are compared in Fig. 13.1. The concept of sediment routing is summarized by the Chinese slogan, "Discharge the muddy water, impound the clear water." Of the four techniques classified as pass-through, three involve reservoir drawdown to maximize flow velocity to pass sediment through the impounded reach without deposition. The key distinguishing characteristic among the three drawdown techniques is the method of hydraulic control. Seasonal drawdown involves prolonged drawdown or emptying of the reservoir for periods of weeks or months, typically based on a calendar schedule. In contrast, the two flood drawdown procedures involve lowering of water level or operation of gates only during flood events. Density current venting does not require drawdown, but releases turbid underflow from low-level outlets at the dam.

From among the case studies, Sanmenxia, Heisonglin, Cachi, Gebidem, and SefidRud all employ reservoir emptying for sediment management. Sanmenxia is an example of sediment routing because the reservoir is empty during the flood seasons, with the primary emphasis placed on passing sediment through the impoundment without deposition. Heisonglin represents a combination of routing plus flushing; although emptying occurs during flood season, the detention and resultant sediment deposition imposed by the low discharge rate requires that flushing techniques also be employed to preserve capacity. At Cachi and Gebidem, only flushing is performed because reservoir emptying is not synchronized with flood inflow, and sediment management aims to remove sediment after it has been deposited. The Loiza and Feather River case studies (Chaps. 20 and 22) are examples of sediment routing in reservoirs that are not emptied.

### 13.1.3 Advantages and Disadvantages

Sediment routing partially preserves the natural sediment-transport characteristics of the river, whereas flushing usually changes these characteristics dramatically. Generally speaking, routing is the most environmentally benign sediment management strategy, while flushing is potentially the most damaging. Some routing techniques can transport coarse as well as fine sediments beyond the dam, largely eliminating the impacts to streambed profile. At some sites routing can be implemented at very low cost, but at others

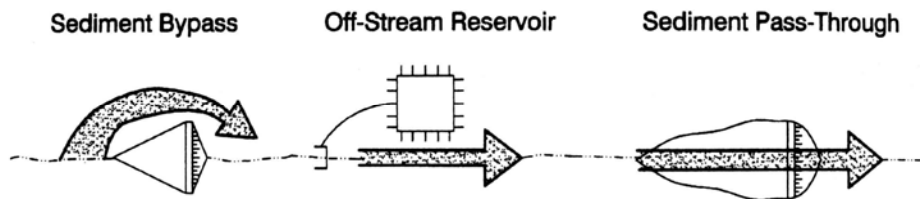


**FIGURE 13.1** Classification of sediment routing strategies.

costly modifications to the dam will be required to provide large-capacity low-level outlets.

A major disadvantage of sediment routing is that a significant amount of water must be released during floods to transport sediments. Sediment routing is most applicable at hydrologically small reservoirs where the water discharged by large sediment-transporting floods exceeds reservoir capacity, making water available for sediment release without infringing on beneficial uses. Some routing operations require the use of real-time hydrologic forecasting. Sediment routing may not be able to remove previously deposited sediment or pass the coarsest part of the inflowing load beyond the dam. Thus, routing needs to begin as early as possible after dam construction to preserve capacity, and supplemental measures (e.g., flushing, dredging) may also be required.

## **13.2 SEDIMENT PASS-THROUGH BY SEASONAL DRAWDOWN**

---

### **13.2.1 Technique**

A reservoir operated under seasonal drawdown is either partially or completely emptied during the flood season. Seasonal drawdown is conducted during a predetermined period each year, as opposed to flood routing, which requires that the reservoir level be drawn down to pass individual flood events whenever they occur.

### **13.2.2 Partial Drawdown**

Under partial drawdown, the reservoir is maintained at a lower pool elevation during the flood season to increase flow velocity and decrease detention time and sediment trapping. The pool may temporarily be drawn down even further to route specific events through the impoundment. Sediment release efficiency is determined by the sediment transport capacity along the full length of the impoundment, including any backwater area in front of the dam which will accumulate sediment until an equilibrium profile is established. Under appropriate conditions, a sediment balance can be achieved with year-round uninterrupted reservoir operation by using partial drawdown.

### **13.2.3 Partial Drawdown at Three Gorges Project**

An example of partial drawdown is the Three Gorges Project (TGP) on the Yangtze River in China. General project information is described by Changjiang Water Resources Commission (1994) and Lu (1995), and sedimentation issues have been described by Lin et al. (1989, 1993) and Chen (1994).

Construction of the controversial Three Gorges Project began in 1993 and is projected to require 17 years. When completed it will be the world's largest hydropower project with 18,200 MW of installed capacity in 26 generating units of 700 MW powered by Francis-type turbines rated at 940 m<sup>3</sup>/s with minimum and maximum operating heads of 71 and 113 m, respectively. Many aspects of the project are both massive and extremely challenging. The concrete gravity dam, powerhouse, and locks will require over 100 Mm<sup>3</sup> of rock and earth excavation, 30 Mm<sup>3</sup> of embankment construction, and 27 Mm<sup>3</sup> of concrete. At 175 m, the dam is not unusually tall, but it must be constructed across a river 60 m deep with a mean discharge of 14,300 m<sup>3</sup>/s. The 1084 km<sup>2</sup> reservoir area will

submerge 632 km<sup>2</sup> of upland area, of which 278 km<sup>2</sup> is agricultural land, and will require the relocation of over 1 million people. In addition to hydropower production, it is designed to provide 22 km<sup>3</sup> of flood control storage, and to enhance navigation upstream of the dam by submerging rapids and downstream of the dam by increasing minimum flows from around 2770 m<sup>3</sup>/s to over 5000 m<sup>3</sup>/s.

A primary design objective is to achieve long-term sustainable use. This requires that sedimentation be managed to prevent long-term loss of storage capacity in the flood control pool, to enable continued navigation along the entire length of the reservoir by 10,000-ton tows, and to minimize sediment entrainment into the turbines and accumulation in the vicinity of navigation locks at the dam. The navigation criteria require continuous maintenance of a channel along the entire length of the reservoir at least 3.5 m deep, 100 m wide, and having a minimum radius of curvature of 1000 m. These objectives are achieved by constructing a hydrologically small reservoir and operating in a seasonal drawdown mode. Design and operational parameters were analyzed in numerous physical and numerical sediment transport modeling studies performed over a period of decades.

Despite its large absolute total storage capacity of 39 km<sup>3</sup>, the TGP reservoir is hydrologically small compared to the 451 km<sup>3</sup> annual discharge of the Yangtze River; it has a capacity:inflow ratio of only 0.087. The 600-km-long reservoir will not exceed 1 km in width along 85 percent of its length, and will have a maximum width of about 1.7 km (Fig. 13.2). Thus, the reservoir will continue to be confined within the narrow Yangtze gorge and most places will be narrower than the equilibrium channel width, esti-

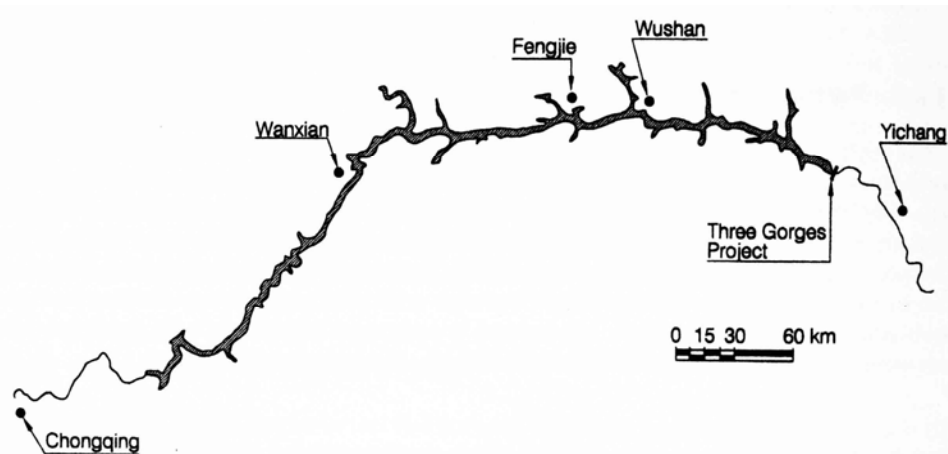


**FIGURE 13.2** Plan view of Three Gorges Project reservoir, currently under construction (after Linet *et al.*, 1989).

mated at 1300 m. The Three Gorges Project differs from the Sanmenxia Dam on the Yellow River, which experienced severe sedimentation problems, in that sediment concentration on the Yangtze averages only 1.2 g/L, as opposed to 37 g/L on the Yellow River, and the discharge of the Yangtze is about 10 times larger than that of the Yellow River. In the TGP reach the Yangtze River transports  $526 \times 10^6$  t/yr of suspended sediment with a median diameter of 0.033 mm, plus  $8.6 \times 10^6$  t/yr of bed load.

A flood control and sediment routing level of 145 m will be maintained during the wet season and a normal pool level of 175 m will be maintained during the remainder of the year to provide increased head for power production (Fig. 13.3). The lowered reservoir level during the flood season not only empties the flood control pool, but is also required to generate the flow velocity necessary to route sediment through the reservoir.

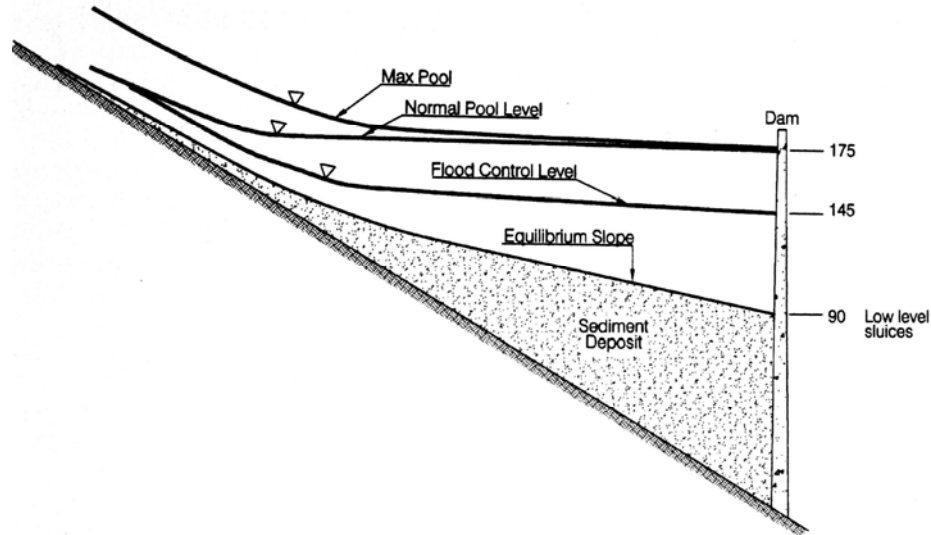


**FIGURE 13.3** Three Gorges Project on Yangtze River in China, showing the routing profile (modified from Lin *et al.*, 1989).

The dam has been designed with 23 low-level bottom outlets at an elevation of 90 m and 22 high-level sluices at an elevation of 158 m, in addition to penstocks, and will be able to discharge  $60,900 \text{ m}^3/\text{s}$  at a pool elevation of 145 m. The maximum discharge capacity of the dam is  $116,000 \text{ m}^3/\text{s}$ .

The flood season, from June to September, accounts for 61 percent of the river discharge and 88 to 90 percent of the annual sediment load. High velocities created by the low pool elevation will pass sediment finer than 0.01 mm through the reservoir pool without deposition, and will also allow the development of an equilibrium bed profile that will preserve between 85 and 92 percent of the original storage capacity. The reservoir will have very little effect on the shape of the hydrograph, passing both water and sediment in a seasonal pattern very similar to natural conditions (Fig. 13.4). Preservation of the natural hydrograph is a key feature of sediment routing, and may be contrasted to hydrographs of flushing presented in Fig. 15.1. After approximately 100 years, the inflowing load and the sediment discharged from the dam are expected to reach equilibrium with respect to both total amount of sediment and grain size distribution. However, there will be variations in the pattern of sediment deposition and scour from one year to another. Simulations have shown that large floods can be expected to deposit sediment in the backwater reach, but in the subsequent year this deposit will be scoured from the upstream reach and moved closer to the dam until discharged through the low-level outlets. If unanticipated deposition occurs, the large capacity of the low-level outlets ( $51,780 \text{ m}^3/\text{s}$  at 130-m pool elevation) will allow additional drawdown to promote scouring of deposits.

Sediment passage through the dam will help offset bed degradation in the downstream reach. Initially the reservoir will trap bed material, causing channel degradation below the dam, until limited by the formation of a gravel armor layer. After approximately 60 years, the combination of armoring and increased bed material discharge through the dam is expected to halt and possibly reverse downstream degradation. However, significant aggregate mining is occurring in the channel below the dam, which may deplete armor-size material and increase downstream bed degradation.

Drawdown will not solve all sediment-related problems. Gravels will continue to accumulate in the impounded reach and will need to be dredged, but the amount is antici-

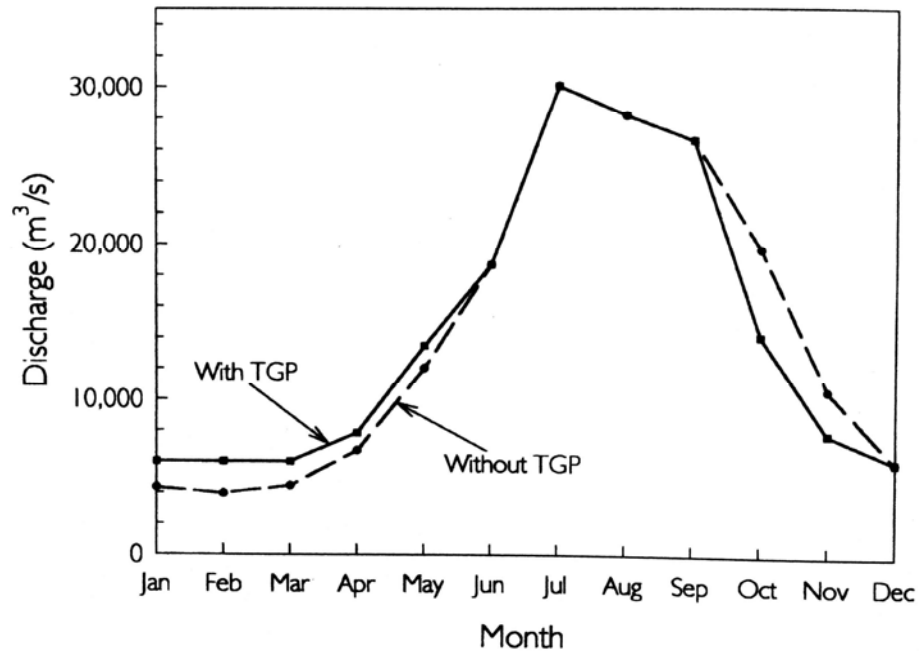


**FIGURE 13.4** Hydrograph of Yangtze River below Three Gorges Project, showing that the natural hydrograph is largely preserved to route sediments through the impounded reach (*redrawn from Chen, 1994*).

puted to be small, on the order of  $170,000 \text{ m}^3/\text{yr}$ . Significant deposition is anticipated in the vicinity of the ship locks and the rate of deposition will increase over time, reaching approximately 1 or  $2 \text{ Mm}^3/\text{yr}$  when sediment equilibrium conditions are achieved. This deposition will be removed by dredging. River training works are also anticipated in some locations to facilitate navigation, especially in zones where the channel naturally switches from one side of the river to the other in different seasons. River training works will also be required to limit sediment deposition around shipping terminals in the port of Chongqing at the upstream limit of the reservoir.

Despite decades of study and numerous numerical and physical modeling studies, there still remain uncertainties. For instance, it is not possible to precisely predict the hydraulic roughness when the reservoir is in operation, since the existing bed of gravel and bedrock will be covered with sediment and the now-exposed walls of the gorge will become submerged. An error of  $\pm 10$  percent in estimating the hydraulic roughness coefficient for these new conditions will produce an error of  $+2.1 \text{ m}$  or  $-2.8 \text{ m}$  in the stage along the backwater reach for the flood having the 1 percent recurrence interval (Lin et al., 1993). All projections also depend to some degree on the unpredictable sequence and magnitude of floods following construction, and future sediment yield. As operation begins the reservoir will be filled by increments, and the response of the river system will be observed at each stage to detect potential problems and adjust operation accordingly.

#### 13.2.4 Seasonal Emptying of Reservoir

When a reservoir is seasonally emptied for sediment routing the effect is similar to flushing, since emptying will cause a channel to be eroded along the thalweg and sediment will be eroded. Reservoir emptying may be classified as sediment routing when the low-

level outlets remain open through essentially the entire flood season, so that most sediment is released by routing rather than by erosion of previously deposited sediment. The appropriate classification in some cases will be ambiguous.

An important advantage of seasonal emptying for sediment pass-through is that the peak concentration of sediment released downstream can be smaller than if the reservoir is operated for flushing. This can be critical from the aspect of environmental impact on the downstream river system and other users. At a sensitive site, sediment routing may be feasible whereas flushing is not. For this reason a distinction should be made between routing and flushing operations, even when both involve reservoir emptying.

The case study of Sanmenxia Reservoir on China's Yellow River provides an example of a large multipurpose seasonally empty reservoir operated with the primary objective of sediment routing. The case study of Heisonglin irrigation reservoir combines elements of both routing and flushing. Sediment accumulation is minimized by the short detention period for each flood, and sediment deposited during the detention period is flushed during free-flow periods between floods.

In some cases a community may be served by an unregulated stream diversion which has inadequate capacity during the dry season, yet the water demand is not large enough to justify a large conventional reservoir. In such a case a seasonal-use reservoir may also be operated in conjunction with the unregulated stream diversion to augment the dry season water supply. During the flood season, all deliveries are made from the stream diversion while the reservoir remains empty for sediment routing. Near the end of the flood season, the reservoir is refilled to provide a regulated water supply during the dry season. Because sediment is routed through the small reservoir, it may be sized according to hydrologic needs and without providing additional volume for sediment storage. This strategy permits the construction of a smaller and more economical structure as compared to a conventional reservoir when the amount of additional yield required is not large.

### **13.2.5 Normally Empty Reservoir**

A third type of seasonal-use reservoir is a normally empty single-purpose flood detention structure constructed with an ungated bottom outlet. This type of reservoir fills temporarily only during larger floods. These impoundments will never have a Stage 1 continuously depositing phase (see Fig. 2.5), and a channel-floodplain configuration can begin developing as soon as the structure begins operating. Sediments deposited in the channel may be transported downstream during nonimpounding periods while sediment deposited in floodplain areas will tend to accumulate continuously. A method to compute long-term sediment deposition in a flood detention structure, but which does not include the effect of main channel scour, has been described by Annandale (1996).

## **13.3 FLOOD DRAWDOWN**

---

### **13.3.1 Technique**

Most sediment enters a reservoir during flood events. Flood drawdown seeks to discharge as much sediment as possible from a reservoir by lowering the pool level and increasing flow velocities during individual flood events. Two hydraulic control techniques may guide gate operation for sediment routing during flood events:

- **Rule curve.** In reservoirs which are hydrologically very small, gate operation may be controlled using a rule curve and discharge measurements at the dam or an upstream gage station.
- **Hydrograph prediction.** In reservoirs having significant storage or limited discharge capacity, the pool may be drawn down or emptied in anticipation of flood arrival, releasing water from the rising limb of the hydrograph and refilling the reservoir with water from the hydrograph recession. This approach requires real-time prediction of the inflowing hydrograph to guide gate operation.

These two methods of hydraulic control are discussed in subsequent sections.

### 13.3.2 Sediment Balance by Flood Routing

Full long-term sediment equilibrium is attained when sediment inflow and discharge are balanced with respect to both sediment quantity and grain size distribution. This is rarely achieved: the coarsest fraction of the load will typically continue to accumulate. However, under favorable conditions pass-through can achieve a sediment balance for all but the largest inflowing grain sizes, while sustaining a desirable profile extending upstream from the dam. Even when a sediment balance cannot be achieved, sediment pass-through can reduce the frequency, cost, and environmental impacts associated with complementary techniques such as dredging or flushing, or can extend the life of a reservoir where sediment removal is not considered practical. One example of this technique is provided in the Feather River case study (Chap. 22). An example on the Isar River in Germany is described in Sec. 18.3.4.

Sediment release efficiency, the ratio of sediment release to sediment inflow, can vary widely in drawdown routing. It will exceed 100 percent when there is net scour from the reservoir of previously deposited material. If storage capacity is to be stabilized, sediment deposited within the reservoir by smaller events outside of the routing period must be mobilized and transported beyond the dam during pass-through events, and the sediment release efficiency during the routing period must exceed 100 percent. The adverse environmental impact of this increase in solids may be small or negligible because increased sediment loads will occur during periods of naturally high sediment concentration and transport capacity, and dilution by flood discharge will limit the increase in solids concentration. This is different from flushing, which tends to release sediment during periods of relatively low flow and produces high sediment concentrations.

To achieve a sediment balance for a particular grain size, pass-through periods must produce bed shear values adequate to transport the target material through the entire length of the impoundment and beyond the dam. The duration of the discharge must also be adequate to release the total inflowing load in the target grain size that is delivered to the reservoir between routing events. Generally, for a given discharge and flow duration, the entire inflowing sediment load smaller than a certain diameter can be discharged through the impounded reach at the same rate it is delivered. Somewhat larger grains will be transported but at a rate slower than the delivery rate. A yet larger size will not be transported at all once it enters the pool, because of backwater above the outlet at peak discharges. These two larger sizes will continue to accumulate in the reservoir despite successful pass-through of finer material (Fig. 13.5). Larger diameter sediments can be transported by increasing either discharge or flow velocity (i.e., more drawdown), and the amount of transportable material that is released can be increased by prolonging the duration of routing flows.

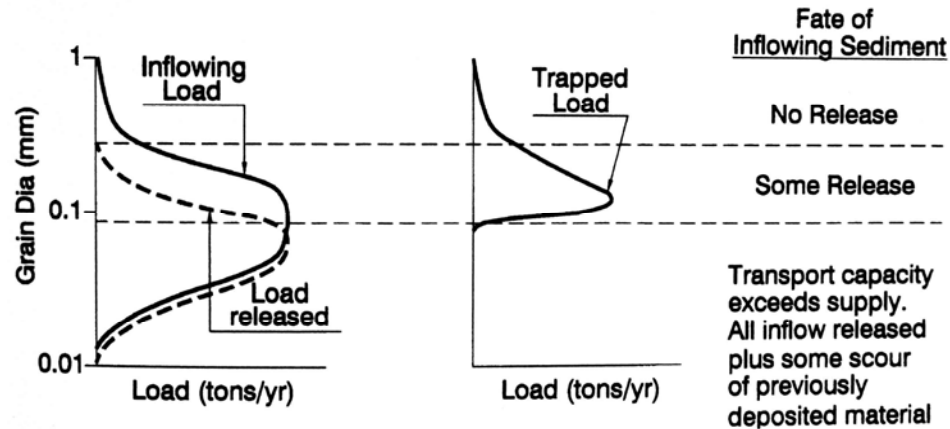


**FIGURE 13.5** Conceptual diagram showing variation in grain size of inflowing load of sediment released from an impoundment by sediment pass-through or by flushing.

Sediment balance is achieved when transport capacity through the reservoir matches or exceeds the inflowing load. For streams in which the rate of sediment transport is supply-limited (rather than transport-limited), the transport capacity required to successfully pass sediment through the impounded reach will not be as large as the inflow transport capacity. If inflowing sediments create a deposit along the length of the reservoir, sediment movement along the impounded reach may be transport-limited while movement along the reaches upstream and downstream of the reservoir is supply-limited.

Deposits within the impounded reach may evolve toward an equilibrium condition by an episodic process. In narrow impoundments, the finer material that is initially deposited can be partially washed out by a high-discharge event, as described at Rock Creek Reservoir in Chap. 22. Over time the grain size on the surface will gradually increase. In an impounded reach wide enough to develop a channel-floodplain configuration, the channel bed will coarsen while floodplain deposits continue to consist of fine-grained sediment. The accumulation of coarse material within the scour channel can encourage the channel to erode adjacent fine-grain deposits, laterally shifting its course.

### 13.3.3 Sediment Adjustments under Routing

Conversion of a conventionally operated reservoir to a sediment routing operation will change the sediment deposition pattern within the impoundment. The longitudinal deposit profile can change both in geometry and grain size distribution as coarser material is transported to the area of the dam. Existing delta deposits may be mobilized and moved downstream, and coarse material delivered by the stream plus remobilized delta deposits may prograde over fines closer to the dam. Depending on the grain size distribution and other factors, erosion of existing delta deposits may be limited by armoring and coarse bed material may continue to be trapped.

As a result of flood routing, the sediment discharge downstream of the dam will mimic but not necessarily match natural conditions. Pass-through causes sediment release below the dam to be more episodic than inflow. Sediments will accumulate above the dam during impounding periods and will be released only during infrequent flood routing periods.

The transport of detrital organic material represents a small but ecologically important component of the sediment in rivers. This organic detritus, which is a source of food and nutrients to downstream riverine and estuarine ecosystems, may be efficiently trapped during the impounding period even in reservoirs which have otherwise achieved a sediment

balance. Sediment release during infrequent routing events may deliver short-term pulses of particulate material to downstream aquatic systems, separated by long periods with limited export of organic detritus. Organics exported from the reservoir outside of the routing period can be expected to be quite distinct from the form of detrital material (leaves, etc.) exported by the watershed. Organic material from the reservoir will already have been processed by reservoir organisms, and may be replaced with algae and zooplankton specific to the reservoir environment. Thus, the ecological impact on downstream food chains may be large, even though a complete sediment balance is otherwise achieved on an annual basis.

#### **13.3.4 Modeling Considerations**

Pass-through operations are analyzed with numerical models simulating long-term patterns of sediment delivery and transport through the impounded reach. The long-term sediment release efficiency may be simulated for alternative operating rules which specify both the extent and duration of drawdown, subject to operational constraints particular to each site. Numerical modeling can simulate the overall behavior of the reservoir including patterns of sediment accumulation, evolution of the grain size distribution of the deposits, and the material discharged from the dam. Armoring can be important, and it may be necessary to simulate a wide range of grain sizes including both fines and coarse material. Physical modeling may be required to address questions concerning three-dimensional scour and deposition phenomena in the immediate vicinity of hydraulic structures such as gates and intakes, or the effect on river training structures such as dikes. Physical modeling can also be used to analyze sediment accumulation, evolution of the grain size distribution of the deposits, and grain size and quantity of sediment discharged under different operating rules. Examples of modeling are provided in the Feather River and Loiza case studies (Chaps. 22 and 20, respectively).

### **13.4 FLOOD DRAWDOWN BY HYDROGRAPH PREDICTION**

---

#### **13.4.1 Technique**

Sediment can be routed through the pool by drawing down the reservoir to a low level before arrival of a flood, passing the rising limb of the flood through the impounded reach, and refilling the reservoir with water from the hydrograph recession, which often has a lower suspended sediment concentration than the rising limb. Between flood events the reservoir is operated in conventional impounding mode.

#### **13.4.2 Application**

When a reservoir pool is lowered, the discharge must necessarily exceed inflow. Early drawdown is necessary at sites where reservoir level cannot be lowered during a flood because of limited low-level gate capacity or to avoid increased flood damage downstream caused by releases which significantly exceed inflow. Early drawdown may be particularly useful for enhancing the pass-through of suspended sediment, especially where velocities are too low to remobilize sediment once deposited on the bed.

#### **13.4.3 Operational Sequence**

Drawdown for individual floods is feasible in a storage reservoir when the combination of

flood forecast lead time, reservoir volume, and gate capacity permit drawdown prior to the arrival of a flood wave. For maximum effectiveness, the reservoir is brought to a minimum level before the arrival of the flood, all gates remain fully open during the flood, and gates are closed when the flood recession contains only enough water to refill the reservoir. This operation requires real-time information on the volume of water tributary to the dam, consisting of two components: (1) the volume of water in the reservoir and (2) the runoff volume contained in the flood hydrograph which has not yet reached the reservoir. The volume in the reservoir can be continuously monitored by reporting level gages at different points along the impoundment, and the water volume in the hydrograph recession can be continuously predicted with real-time reporting raingages and hydrologic modeling. This routing procedure is described below and illustrated in Fig. 13.6.

1. **Impounding.** Between flood events the reservoir is impounded normally. Weather forecasts are checked regularly to anticipate meteorological conditions that could produce high runoff.
2. **Lowering.** When potentially significant rainfall begins, gate opening is initiated to lower the pool as far as possible, without allowing the total water volume upstream of the dam (reservoir storage plus predicted hydrograph volume) to fall below the reservoir storage capacity. Because releases are made only as rainfall is received in the watershed, if rainfall tapers off at any point during the drawdown process the gates are closed and the reservoir is refilled.
3. **Full drawdown.** Full drawdown is achieved when all gates are fully open, producing the lowest water level and the highest flow velocity possible at the given discharge.

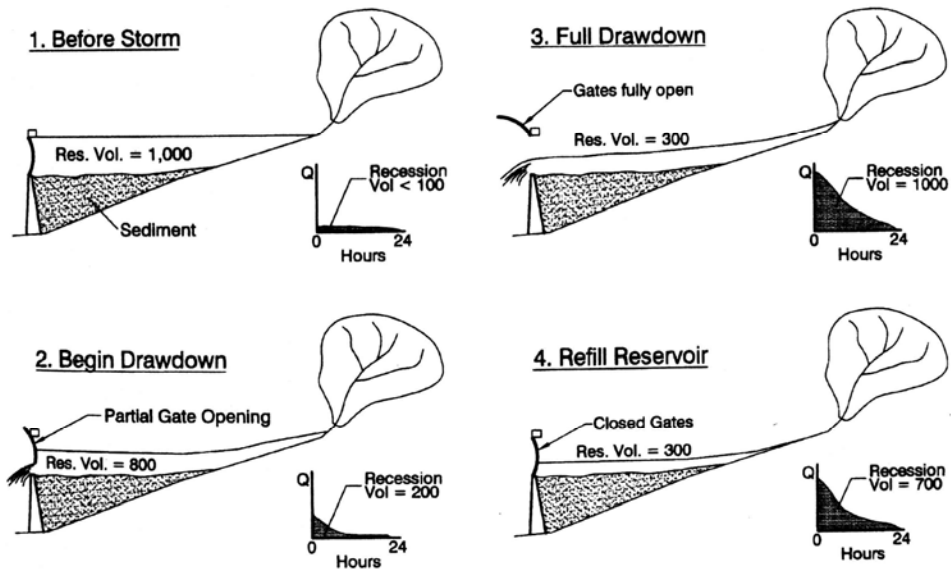


**FIGURE 13.6** Operational sequence to pass suspended sediment through a hydrologically small reservoir without removing it from service, based on flood drawdown by hydrograph prediction.

4. **Refill.** The tributary water volume (reservoir storage plus hydrograph volume) is continuously monitored. When the storm recedes and the tributary volume (reservoir storage plus watershed hydrograph) declines to a value equal to total reservoir volume, gates are closed and the reservoir is refilled from the hydrograph recession.

This technique, described in the Loíza case study (Sec. 20.6), has the potential for wide applicability in hydrologically small reservoirs, including reservoirs rendered hydrologically small by sediment accumulation. Advances in instrumentation, telemetry, and computer modeling technology provide the tools needed to implement an economical real-time hydrologic forecast system for suspended sediment routing.

#### 13.4.4 Monitoring Reservoir Volume

Because the water surface will slope appreciably during routing, the stage-storage relationship developed for level pool conditions cannot be used to estimate the volume in the impounded reach during a flood. The hydraulic gradient will vary along the length of the impoundment and over the duration of the routing event. To estimate storage volume while retaining the simplicity of a single-value stage-storage relationship, the reservoir may be divided into a number of lengthwise segments and a separate level-pool stage-storage relationship developed for each segment. Each segment might, for example, represent the volume contained between successive cross-section survey stations. Data from two or more reporting level gages along the length of the reservoir may be used to determine the water surface profile, using interpolation to generate the water levels at each of the intermediate segments for which a stage-storage relationship has been developed. The total reservoir storage at any point in time is given by the summation of the storages in each segment. Computational accuracy may be enhanced by increasing the number of stage-storage segments, increasing the number of level sensors, and developing more sophisticated algorithms for interpolating the levels measured at discrete points.

#### 13.4.5 Hydrograph Prediction

The essential elements required for hydrograph prediction are antecedent and real-time hydrologic data (e.g., precipitation and river stage) and calibration datasets. Data on snowpack, temperature, operation of upstream reservoirs, and other parameters may also be important. Runoff hydrograph volume may be predicted from upstream river gages or rainfall data and hydrologic models which incorporate soil moisture accounting and route runoff from each subcatchment to the reservoir. Examples include the Sacramento model (Burnash et al., 1973) and the SSARR model and antecedent precipitation index (API) rainfall-runoff models incorporated in the U.S. National Weather Services River Forecast System (Page and Smith, 1993). The World Meteorological Organization has reviewed a number of operational hydrologic models suitable for real-time forecasting (Becker and Serban, 1990) and has compared the operational capability of 14 models (WMO, 1992). The following features are important regardless of the model that is used:

- Adequately account for antecedent soil moisture and, in temperate climates, snowmelt (especially rain on snow events).
- Automatically adjust for the loss of one or more stations from the gaging network during an event due to damage by lightning, wind, flood, etc.
- Adjust or recalibrate during a prolonged event on the basis of observed runoff at a gage station.

- Range alarms and consistency checks to help detect gages which may continue to send signals despite erroneous data.
- Presentation of results in a format that facilitates operational use.

Calibration should give primary emphasis to predicting total hydrograph volume, and particularly hydrograph recession at the end of the storm. Because failure to refill the reservoir can create a critical condition, a safety factor should be incorporated which ensures there is a low probability that the reservoir will not be refilled completely. The safety factor should be revised periodically, since model accuracy should increase with time as data from re-calibration events become available. Operation can also be improved by use of meteorological forecasts and tools such as weather radar to monitor rainfall intensity.

## **13.5 FLOOD DRAWDOWN BY RULE CURVE**

---

### **13.5.1 Technique**

In smaller reservoirs or barrages with large gate capacity, the water level can be lowered during a flood event to pass sediment, with gate operations guided by a rule curve and discharge measurements at the dam or an upstream gage station. Lower-level and longer duration drawdowns will increase sediment transport through the impounded reach and can also increase the grain size of the material transported. The amount and grain size of the material mobilized can be controlled by the rule curve. For example, in the small reservoirs on the Feather River in California described in the case study (Chap. 22), because of downstream environmental considerations it was desired to stabilize reservoir capacity but not to flush previously deposited material from the impounded reach. The rule curve was developed to meet this criteria, although the gate capacity could allow additional drawdown and flushing of previously deposited material.

### **13.5.2 Operational Example**

The 44-m-tall Cowlitz Falls Dam is a run-of-river hydropower facility equipped with two Kaplan units capable of discharging  $297 \text{ m}^3/\text{s}$ . Located on the Cowlitz River about 23 km downstream of Randle, Washington, the dam was completed in 1994. Its storage capacity of  $12.6 \text{ Mm}^3$  is equivalent to a capacity to inflow (C:I) ratio of only 0.3 percent.

The cofferdam upstream of the dam was left in place after dam construction to deflect sediment into the sediment bypass channel during routing events and prevent its entry into the turbines. The sediment bypass terminates at two low-level sluices, each  $3.6 \times 4.9 \text{ m}$  with upstream-sealing wheel gates. There are four radial crest gates and an emergency spillway is also provided. The project layout is illustrated in Fig. 13.7.

Sediment transport along 30 km of river plus the impoundment was analyzed using the HEC-6 sediment transport model with 37 river cross sections. Sediment transport through the bypass channel and gates was analyzed by physical modeling. Sediment management is only one of several parameters that will influence the development of a rule curve, and at Cowlitz Falls four criteria were important:

1. The 100-year flood level in the upstream area of the reservoir cannot exceed the pre-dam flood level. This established a minimum flood control drawdown curve.

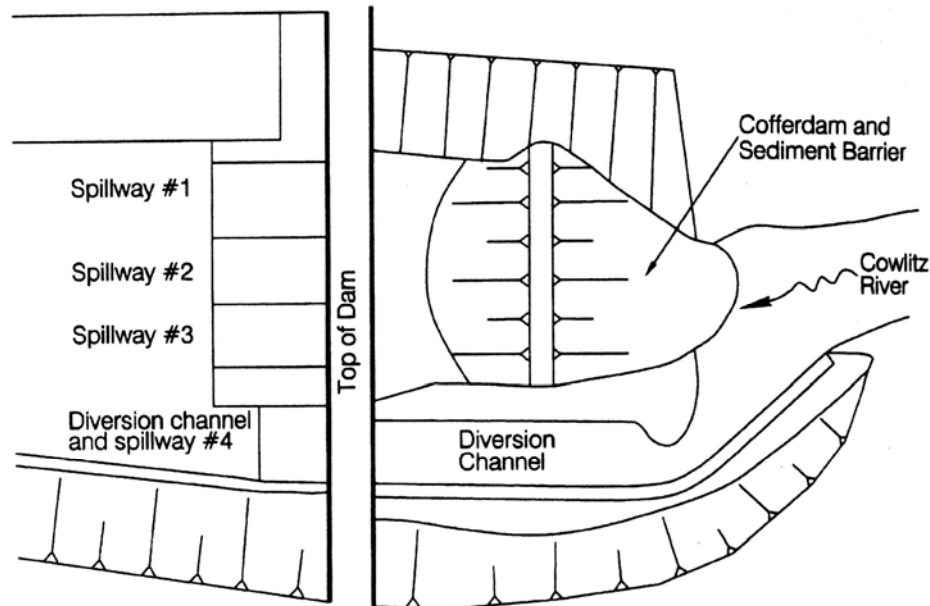


**FIGURE 13.7** Layout of the Cowlitz Falls Dam showing location of submerged upstream cofferdam which diverts sediment-laden flow into the diversion channel and low-levels outlets (after Locher and Wang, 1995).

2. Prevent sediment deposition in the upstream portion of the pool that would cause upstream flood levels to increase, and pass as much sediment as possible beyond the dam.
3. Allow continuous operation of the turbines throughout routing events by maintaining pool level above the top of the cooling water intake for generating units.
4. Fully open crest gates as early as possible during floods to facilitate the passage of floating debris.

The rule curve meeting these criteria is presented in Fig. 13.8.

The unusual sawtooth configuration produced by the Cowlitz Falls rule curve results from the following operational sequence:

1. Normal pool elevation (262 m) is maintained up to  $297 \text{ m}^3/\text{s}$  with all releases through the turbines, and between 297 and  $652 \text{ m}^3/\text{s}$  the turbine release is augmented with sluicing through the diversion channel and low-level outlet.
2. Between 652 and  $765 \text{ m}^3/\text{s}$  the reservoir is drawn down in accordance with upstream flood control criteria by using turbines and sluices.
3. Between 765 and  $1190 \text{ m}^3/\text{s}$ , the crest gate in spillway 4 is opened as required to maintain a water surface elevation of 257 m.
4. At  $1190 \text{ m}^3/\text{s}$ , bay 4 is fully opened. When flow increases to  $1615 \text{ m}^3/\text{s}$ , bay 1 is also opened. Bays 2 and 3 are opened when discharge exceeds  $2550 \text{ m}^3/\text{s}$ .

The longitudinal profile of the river reach upstream of the dam is somewhat unusual, having an area of very steep gradient near the dam. During drawdown, velocities will continue to be low in the deep pool area near the dam, which will restrict the grain size that can be passed through the dam to material not larger than fine sands (Locher and Wang, 1995).

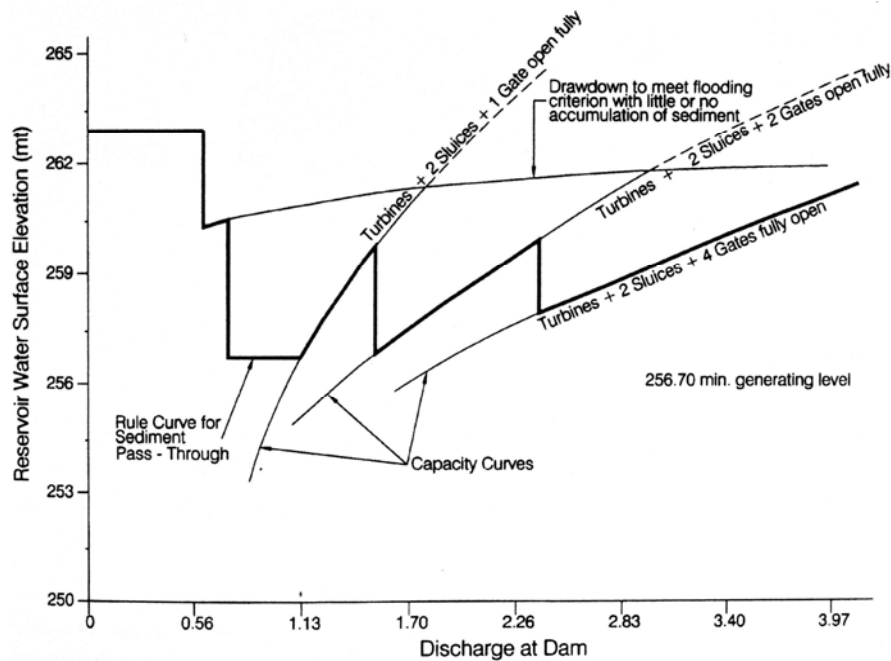


**FIGURE 13.8** Rule curve for sediment pass-through operation at Cowlitz Falls Dam (after Locher and Wang, 1995).

## 13.6 SEDIMENT BYPASS FOR INSTREAM RESERVOIRS

### 13.6.1 Technique

When topographic conditions are favorable, a large-capacity channel or tunnel can be constructed to bypass sediment-laden flow around an instream storage reservoir. This configuration eliminates the need for a large-capacity spillway at the main dam since flood flow is diverted.

### 13.6.2 Application

Sediment bypass around an instream impoundment has been reported at the Nagle Reservoir in South Africa (Annandale, 1987) and is proposed at the Ho-Ku Reservoir in Taiwan (Hwang, 1985). At the Nagle Reservoir (Fig. 13.9) the storage pool is located in a river meander and floods are bypassed through a channel across the meander bend. The flood gates control flow along the flood channel and are normally closed, allowing inflow to overtop the flood weir and enter the storage pool. During floods, the gates are opened and the flood weir diverts sediment-laden water into the bypass channel, which simultaneously flushes sediment from the reach upstream of the flood weir. Located in shallow water at the upstream end of the reservoir, the flood weir is much smaller than the main dam. This strategy may be used to bypass both suspended and bed load.

The sediment bypass configuration proposed at Nan-Hwa Reservoir in Taiwan described by Hwang (undated) is based on a similar concept (Fig. 13.10). In this instance

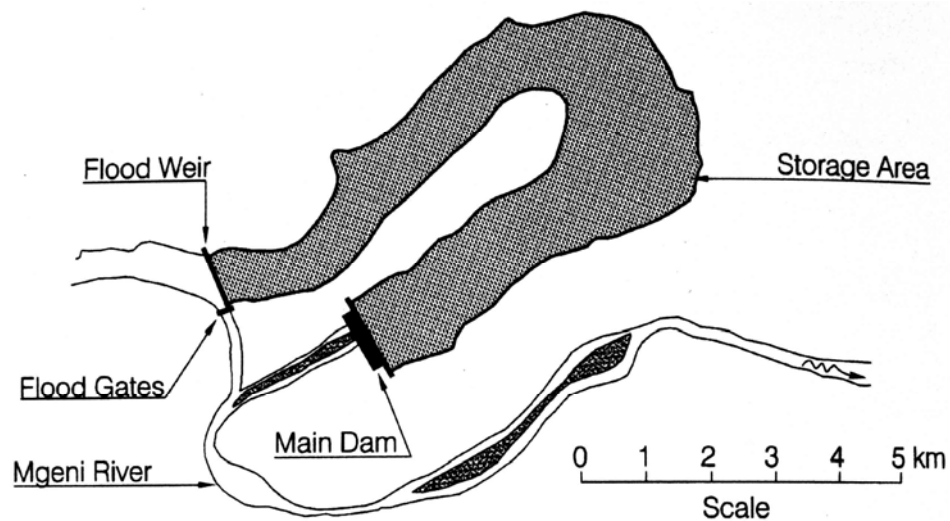


**FIGURE 13.9** Sediment bypass configuration at Nagle Reservoir in South Africa (after Annandale, 1987)

instance the forebay receives runoff from the main stream and from an intake on another stream. Water enters the storage afterbay only after it has passed through the forebay area, which acts as a sedimentation basin. Sediment deposited in the forebay is removed by intermittent flushing.

## 13.7 OFF-STREAM RESERVOIRS

### 13.7.1 Technique

An off-stream reservoir is any impoundment constructed off the main river and which is filled with diverted water of low sediment concentration. Several methods may be used to reduce the sediment load on the offstream reservoir: (1) sediment-laden discharge from large floods can be partially or entirely excluded from the reservoir by limiting the hydraulic capacity of the intake structure or selective operation of the intake gate, (2) the intake structure can be designed to exclude coarse sediments, and (3) the diversion dam can be operated as a sediment trap for diverted water, with trapped sediment being subsequently removed by flushing. An off-stream reservoir can be constructed as a diked impoundment, using a conventional dam across a small tributary with low sediment yield, or on the floodplain paralleling the main channel. These strategies are schematically illustrated in Fig. 13.11. Tributary arms of existing reservoirs may also receive relatively little sediment compared to the main river branch, thereby acting as off-channel storage pools within existing impoundments.

Since inflow can be controlled at the diversion point, an off-stream reservoir does not require a large and costly spillway structure. The reduced sediment loading can largely eliminate the need to provide a sediment storage pool and reduces future maintenance costs (e.g., dredging), further reducing costs compared to a conventional reservoir. Because it never receives high sediment loads, the off-stream reservoir can also provide consistently high quality water to quality-sensitive users such as municipal water supplies.

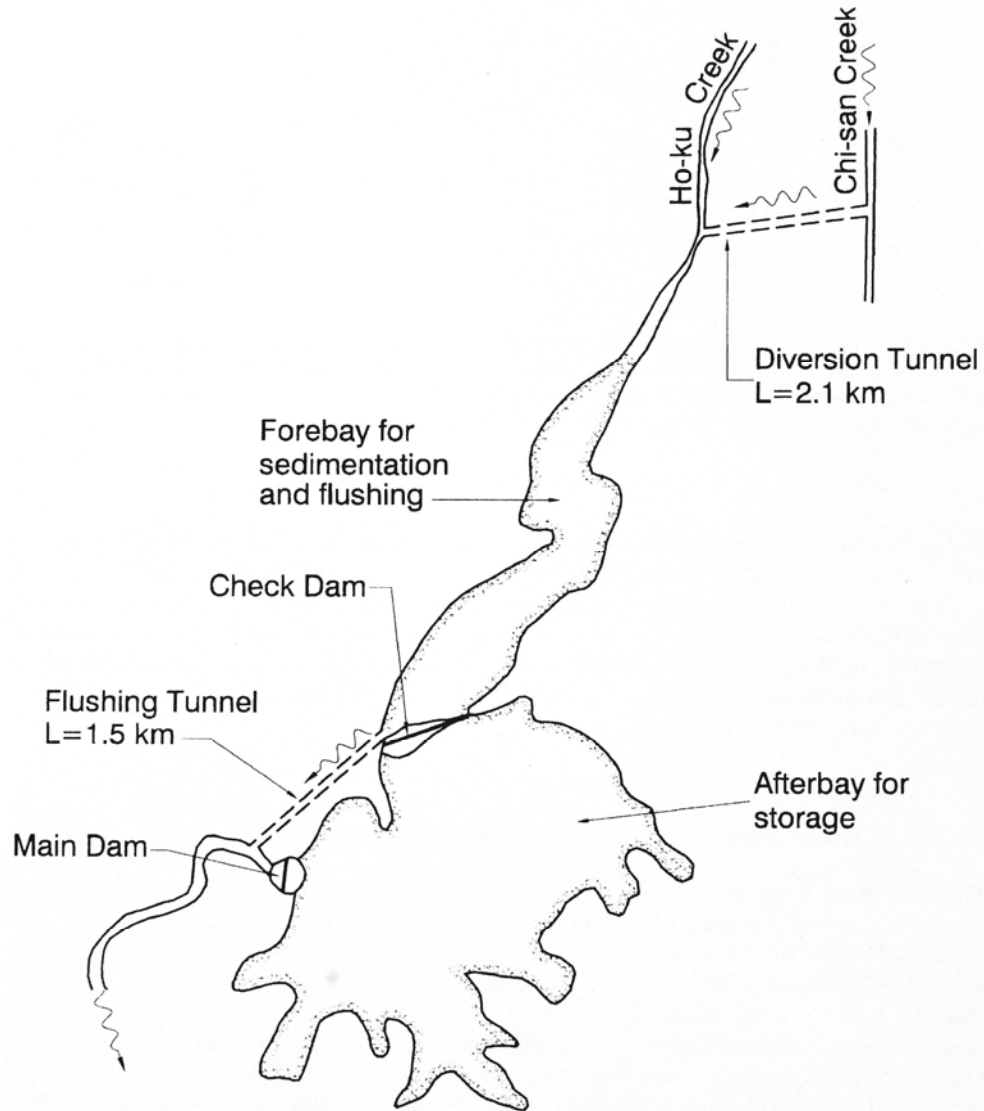


**FIGURE 13.10** Proposed Nan-Hwa reservoir in Taiwan, showing the compartment of the reservoir into an upstream forebay for sediment trapping and diversion, and an afterbay for sediment storage (after Hwang, undated).

Off-stream reservoirs can also provide important environmental benefits compared to conventional structures. Depending on the design, they may not require a large instream barrier at the intake site, and the downstream transport of bed material can be maintained.

### 13.7.2 Application

Of the 33 major reservoirs in Taiwan, 9 are offstream structures designed to bypass sediment. Data on two of these structures were summarized by Wu (1991), who reported

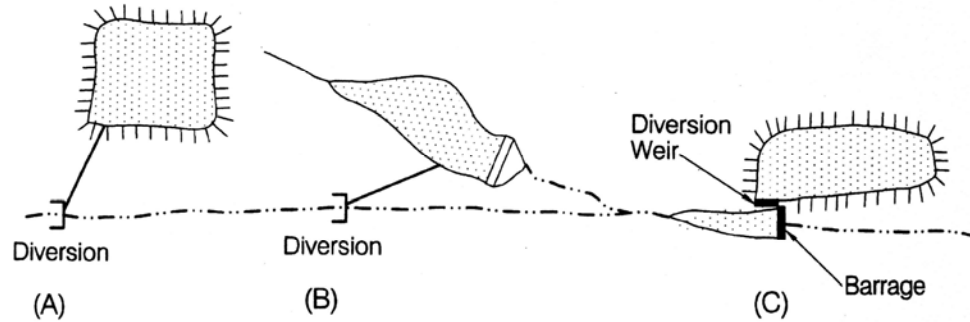


**FIGURE 13.11** Alternative configurations for off-stream reservoirs. Limited-capacity intake diverting flow into: (a) an excavated or diked impoundment, or (b) an impoundment located on a small tributary with a low sediment load. (c) Use of a barrage to control flow over a diversion weir and into an off-stream impoundment, as suggested by Urlapov (1977).

that at Sun Moon Reservoir, 49.5 percent of total streamflow was diverted into the reservoir but only 3.5 percent of the stream sediment was diverted. At Coral Lake Reservoir 29.6 percent of the streamflow was diverted but only 12.2 percent of the sediment. The large difference in sediment diversion at these two structures was attributed to the configuration of the diversion dam. The diversion dam at the Sun Moon Reservoir had a higher sediment trap efficiency, and was thus more efficient in preventing sediment delivery to the reservoir.

### 13.7.3 Computation of Reservoir Yield and Sediment Exclusion

Whereas yield from an on-stream reservoir can be expressed as a function of storage capacity alone by a storage-yield curve, in the off-stream configuration reservoir yield is also affected by the limited hydraulic capacity of the stream diversion and conveyance channel or pipeline between the intake and the reservoir. A larger diversion capacity will allow the off-stream reservoir to refill more rapidly, which can be important on flashy streams. However, the increased intake capacity comes at the cost of higher sediment loading because a larger percentage of total diversions will consist of sediment-laden flood flows. Flow into the off-stream impoundment will always be limited to the lesser of streamflow or the diversion capacity. In the sediment bypass system, this inflow constraint does not exist because the reservoir impounds the original stream channel and inflow rate is not restricted.

To minimize sediment loading, the off-stream reservoir should be designed to receive no additional inflow when it is full. Sediment inflow during floods is thus limited by both the restricted intake capacity and the higher probability of the reservoir being full during flood periods. For further reduction in sediment inflow, a gate could be operated at the stream diversion to manually or automatically select water for diversion or exclusion on the basis of reservoir level, stream turbidity, and possibly other criteria.

A performance comparison of a conventional on-stream impounding reservoir and an off-stream reservoir was made using 21 years of daily discharge data from the USGS gage at Rio Fajardo, Puerto Rico (Morris, 1996). This small (38.6 km<sup>2</sup>) moist watershed receives about 2500 mm/yr of rainfall which is rather well distributed throughout the year, although streamflow is flashy. Sediment yield is 814 t/km<sup>2</sup>/yr, and a rating curve of sediment concentration of the form  $C_{mg/L} = aQ^b$  was established for the four available years

of mean daily discharge and load data published by the USGS. A daily simulation analysis was run to determine the yield available on 99 percent of the days in the 21-year dataset, and to compute sediment accumulation in the reservoir from the average daily suspended sediment concentration, the volume of water diverted each day, and assuming 100 percent trap efficiency in the off-stream reservoir.

The simulated system consisted of a stream diversion having various capacities, combined with various storage volumes in the off-stream storage compartment (Fig. 13.11a). Simulation results are summarized in Table 13.1, expressing both storage and yield values as the dimensionless fraction of the average daily flow (ADF) over the simulation period. By comparison, the 99 percent run-of-river flow exceedance at this gage station for the analyzed dataset is 0.057 x ADF. Sediment inflow is expressed as percent of total sediment load. For reservoirs on this stream with storage volumes up to 90 days of mean flow (25 percent of mean annual runoff), there was essentially no difference in yield between a conventional reservoir and an off-stream reservoir with an inlet rated at 3 x ADF. Use of a smaller inlet capacity rated at 1 x ADF produced a small decrease in yield and a larger decrease in sediment inflow as compared to the larger inlet. The smallest inlet, rated at 0.5 x ADF, had a significant impact on yield for larger storage volumes but not for smaller. By comparison, a 100-year sediment pool for a conventional reservoir at this site with a 90 percent trap efficiency will require 5.6 Mm<sup>3</sup> of storage volume, equivalent to 33 days of ADF.

Depending on the configuration, sediment inflow into this off-stream reservoir is 80 to 98 percent less than a conventional (onstream) reservoir at the same location. For a given yield, the off-stream reservoir can be much smaller than the conventional reservoir because the sediment pool is practically eliminated. While sediment accumulation is not entirely eliminated from the off-stream reservoir, the rate of accumulation is reduced to such low levels that activities such as dredging become economically attractive. This illustrates that in some streams a dramatic reduction in sediment loading can be achieved using off-stream storage, without a significant penalty in terms of yield.

**TABLE 13.1** Yield and Sediment Load for Conventional and Off-Stream Reservoir, Río Fajardo, Puerto Rico

Reservoir storage volume, days at ADF	Reservoir Configuration						
	A yield, ADF	B Yield, ADF	B Load, %	C Yield, ADF	C Load, %	D Yield, ADF	D Load, %
5	0.145	0.145	2.1	0.145	2.1	0.140	2.1
10	0.220	0.220	3.5	0.220	3.5	0.220	3.5
15	0.285	0.285	5.2	0.285	4.9	0.275	4.6
30	0.425	0.425	10.2	0.385	7.7	0.340	5.9
60	0.545	0.545	16.3	0.500	11.1	0.380	6.7
90	0.610	0.605	20.5	0.530	12.0	0.390	6.8

*Notes:* ADF = Average daily flow = 1.93 m<sup>3</sup>/s. Storage volume is expressed as days of discharge at ADF, where 1 day ADF = 166,700 m<sup>3</sup>.

Load = percent of total river suspended sediment load trapped over the simulation period.

A = conventional impounding reservoir, sediment inflow is 100% of river load.

B = off-stream reservoir, inlet capacity = 3.0 x ADF.

C = off-stream reservoir, inlet capacity = 1.0 x ADF.

D = off-stream reservoir, inlet capacity = 0.5 x ADF.

### 13.8 SUBSURFACE RESERVOIR

Deposits of coarse sediment contain voids which can store water, and under favorable conditions a *trap dam* may be constructed to accumulate coarse sediment, extracting water from the subsurface storage by a pipe through the base of the dam and which extends through the permeable deposits (Fig. 13.12). Use of these systems as for small local water

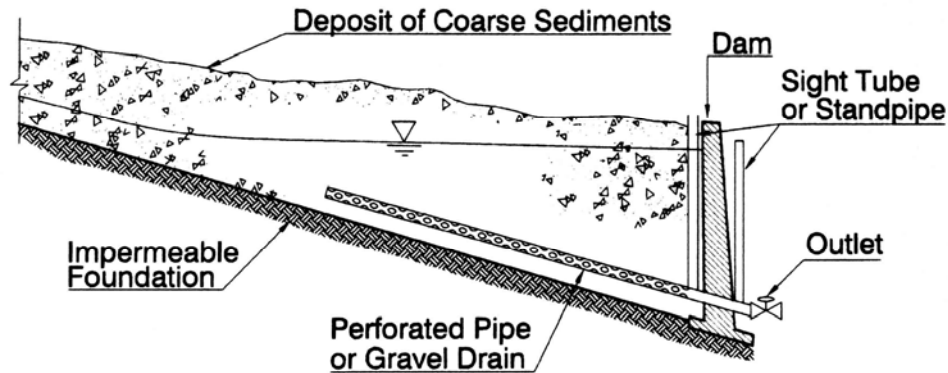


**FIGURE 13.12** Schematic configuration of sediment routing by trap dam and subsurface reservoir.

supply systems in Africa has been described by Baurne (1984), who also states that evidence from Libya suggests these types of structures have been used for at least 1000 years. Important advantages include freedom from sedimentation, water quality improvement for drinking supply as a result of filtration through porous media, and elimination of evaporative losses once the water level is more than about 0.6 m below the surface.

The volume of water that can be stored can be estimated from the impoundment geometry and measurement of the porosity in the local bed material, which may be as high as 30 percent. Because the water level cannot be visually observed, a standpipe and float, transparent plastic tube, or pressure gage may be placed at the outlet to monitor the static water surface within the media. Collection of water at the outlet should be facilitated by placing a perforated pipe or gravel drain extending into the deposits from the outlet pipe.

Construction of a trap dam to create a subsurface reservoir requires that the stream carry a significant load of coarse bed material and have an impermeable foundation. Because only a fraction of the total impoundment volume is occupied by water, a "minor" seepage loss may represent a significant fraction of the total supply from a subsurface reservoir. Watertightness is essential. The dam should not be raised faster than the impoundment can be filled with coarse material, and it may be necessary to raise the dam in annual increments to match the rate of coarse sediment accumulation. This may be facilitated by constructing the foundation and abutment elements during the first construction season, leaving a wide weir to be elevated incrementally during subsequent years.

Although subsurface storage reservoirs have been reported to date only for smaller village-size water supplies, they may represent a means to obtain a limited water supply from sites that are otherwise hopelessly sedimented. For example, reconstruction of Gibraltar Dam in California to meet dam safety standards occurred during a severe 5-year drought. There was no source of water for preparing the concrete mix; streams in the area



**FIGURE 13.13** Well drilled into empty Gibraltar Reservoir, California, during drought. The photograph also shows dredging equipment left stranded by the drought (*G. Morris*).

were dry as was the heavily sedimented reservoir. The required water supply was obtained from wells drilled through the silty reservoir deposits and into the permeable gravels in the original river bed (Fig. 13.13).

### 13.9 SEDIMENT EXCLUSION

---

A sediment excluder is a device or system designed to route sediment along the river, bypassing the intake. These intakes are an important feature at many water supply intakes and hydropower diversion dams, and may also be used to supply offshore reservoirs. Use of an intake configuration which minimizes sediment entrainment is an important component of design. Sediment exclusion is discussed in more detail by the Committee on Hydropower Intakes (1995), Raudkivi (1993), and Bouvard (1992). Complex three-dimensional flow patterns occur in the vicinity of intakes, and physical modeling is frequently employed in the design of large intake structures.

The distribution of coarse suspended sediment within moving water is not uniform but tends to decrease exponentially as a function of distance above the bed. Sediment excluders are designed to take advantage of this vertical variation in sediment concentration to consistently withdraw water from zones within the flow field characterized by relatively lower sediment content. The greater the variation in sediment concentration within the water column, the more effectively an excluder will operate. Exclusion will not be effective on slowly settling fines that are almost uniformly distributed across the flow field. Zones of low sediment concentration may exist naturally in the river or may be created by intake geometry. Suspended sediment exclusion can be achieved by employing either flow curvature or flow partitioning to reduce suspended sediment concentration in the intake.

### 13.9.1 Sediment Exclusion by Flow Partitioning

If water level can be maintained at a nearly constant elevation, upstream of a barrage for example, the flow can be partitioned vertically. For example, vertical partitioning may be accomplished by a two-level intake across a flow path and perpendicular to the direction of flow, at the end of a straight reach. The upper-level intake is used to divert clear water and the sediment-laden bottom water is discharged downstream through a low-level outlet, as schematically illustrated in Fig. 13.14. Similarly, a submerged weir running parallel to the direction of flow will allow surface water to overflow toward the intake while the deeper water and bed load continues downstream and bypasses the intake.

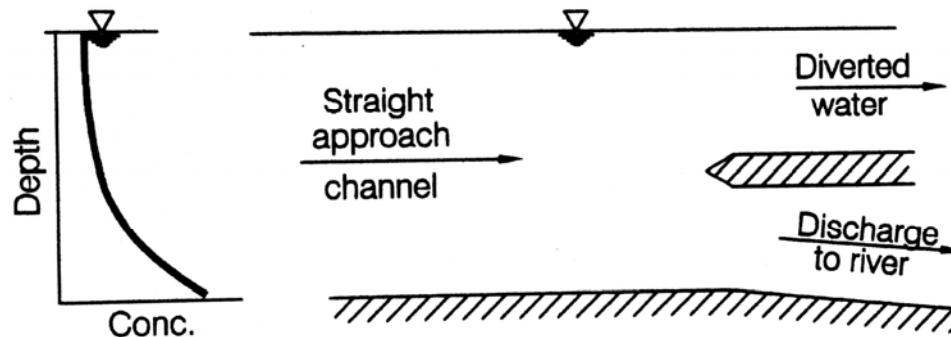


**FIGURE 13.14** Sediment exclusion by vertical flow partitioning. Surface water with lower sediment content is diverted to use while sediment-laden bottom water is discharged back to the stream.

### 13.9.2 Sediment Exclusion by Flow Curvature

When flowing water is diverted at a curve, the water surface will become elevated at the exterior of the curve because of momentum forces. Water at the surface flows faster than water at the bottom, and the greater momentum of the surface water carries it into the exterior of the curve and forces the slower-moving bottom water out of the curve, creating a transverse current. When this transverse current is superimposed on the downstream direction of flow, the resulting current is helicoidal. As a result of this flow pattern, an intake located at the outside of this curve will be continuously fed with surface water while bottom water with higher sediment concentration is pushed out of the bottom of the curve. This principle was employed 2000 years ago in constructing the Dujiangyan irrigation diversion from the Min River in China.

The basic principle of flow curvature can be employed to construct a variety of intake configurations, as illustrated in Fig. 13.15. Submerged vanes (e.g., Iowa vanes) can also be used to produce flow curvature and otherwise modify sedimentation patterns in the vicinity of intakes and can also modify current patterns to deflect erosive currents and help stabilize the river in the vicinity of structures (Odgaard and Wang, 1991).

### 13.9.3 Gravel Sluice

Gravel is not normally transported in suspension, but its gradual accumulation upstream of a low dam which diverts water into an intake will eventually block the intake. This block-

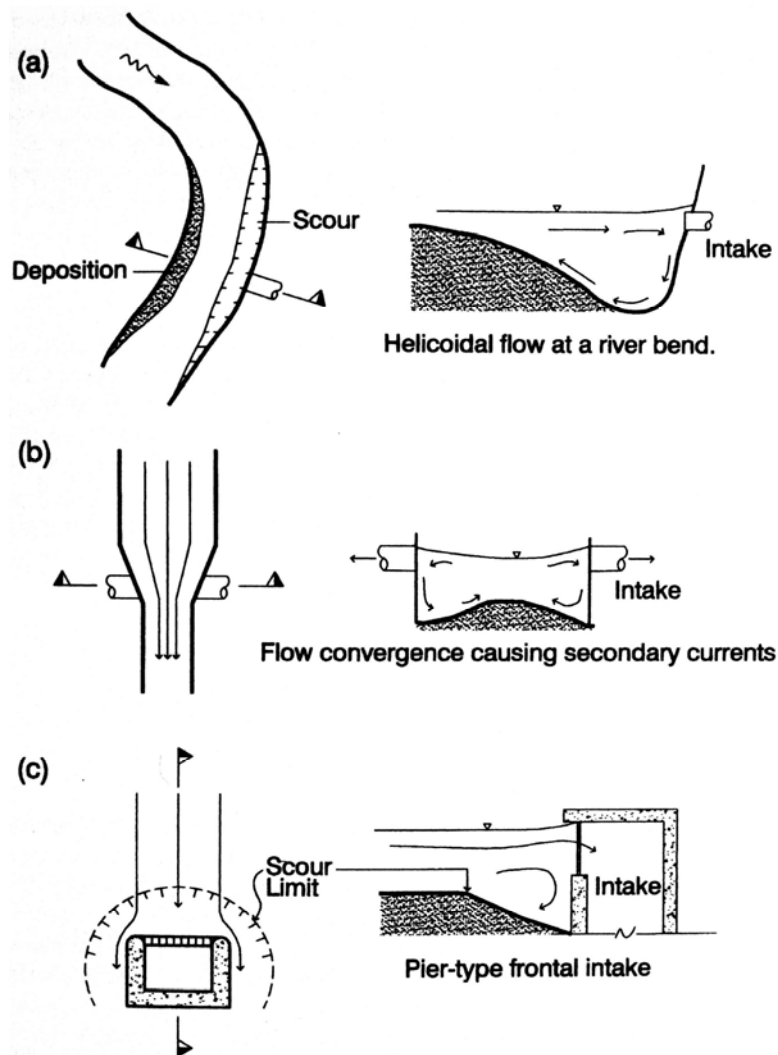


**FIGURE 13.15** Sediment-excluding intake configurations based on flow curvature: (a) helicoidal flow at a river bend, (b) flow convergence, and (c) pier-type frontal intake.

age can be prevented by periodically flushing gravel from the immediate vicinity of the intake using a sluicing system such as that illustrated in Fig. 13.16. In this illustration, the low dam has a vertical sluice controlling flow along a sluice channel that passes immediately in front of the intake. Opening the sluice removes bed material from the vicinity of the intake, but no attempt is made to halt or otherwise manage the accumulation of bed material behind the dam.

### 13.9.4 Intakes at Large Dams

Intake structures at dams should be designed to minimize problems of sediment entrainment and eventual blockage by deposits. In some reservoirs, sediment can affect low-level intakes soon after the dam is closed because of turbidity currents which reach the dam. As the reservoir fills with sediment, delta deposits will eventually reach the dam,

and coarse sediments can be transported to the vicinity of the intake as bed load. Several strategies may be used to reduce sediment entrainment into intakes at the dam. Low-level outlets may be established to facilitate hydraulic scour of sediment from the vicinity of the intake, employing a concept similar to that illustrated in Fig. 15.18. Deep sluices can be placed immediately below or adjacent to power intakes at the dam, and can be operated on either a continuous or intermittent basis to reduce sediment entrainment into the intake, as at Cachi Reservoir (Fig. 19.6).

### **13.9.5 Sediment Removal from Diverted Water**

When sediment exclusion does not eliminate all the grains below the maximum allowable size, exclusion may be complemented by systems to remove sediment from diverted water. These systems are generally sized on the basis of the plain sedimentation of discrete particles, but may also involve circular flow in which centrifugal force also aids in the removal of sediment. Settling sediments are typically focused into a narrow slot or series of orifices along the bottom of a sedimentation tank, then removed by either continuous or intermittent discharge. A conceptual drawing of a rectangular sedimentation tank is illustrated in Fig. 13.17.

## **13.10 COMPARTMENTED AND SERIAL RESERVOIRS**

---

### **13.10.1 Reservoir Compartmentation**

Operational flexibility for sediment management can be provided by dividing the total storage volume into two components by using internal dikes or multiple reservoirs. For example, use of a single seasonally empty reservoir may be infeasible because some regulating storage is required during the nominally wet season. As an alternative, it may be feasible to construct a larger seasonal-use on-stream impoundment which will receive a heavy sediment load and a smaller offstream impoundment. During the wet season, only the off-stream reservoir would be used while the on-stream reservoir remains empty for sediment routing. Both would be available for dry season service. The off-stream impoundment may consist of an arm of the reservoir that receives limited sediment input.

### **13.10.2 Reservoirs in Series**

When more than one reservoir is constructed along a river, sediment released from an upstream impoundment will be redeposited downstream unless all sites are managed together. Sediments should be routed progressively through all reservoirs in series to minimize the amount of redeposition in downstream impoundments. The reservoir pool elevation at the downstream site affects the location of deposits, and one operational objective for multiple reservoirs in series may be to focus deposition into areas which facilitate subsequent removal. At some sites, such as small mountain hydropower diversions upstream of a hydrologically large storage reservoir, it may not be feasible to manipulate the downstream site and the released sediment may simply accumulate in the downstream pool. This is the case for the reservoirs along the Feather River discussed in Chap. 22; all the sediment routed through the small hydropower dams simply accumulates in the large Oroville Reservoir further downstream.

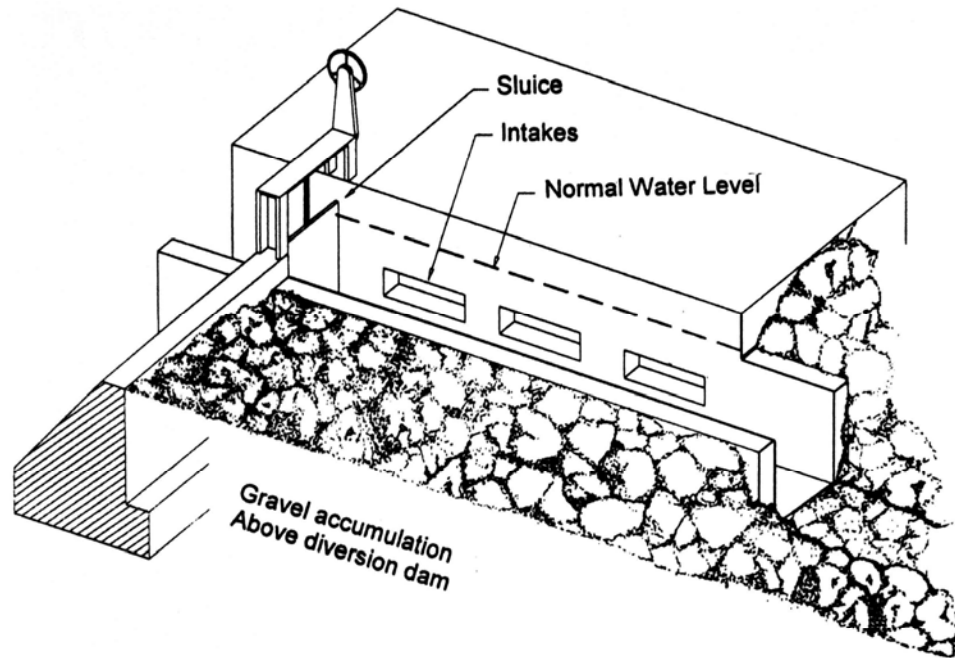


FIGURE 13.16 Gravel sluice for a small intake.

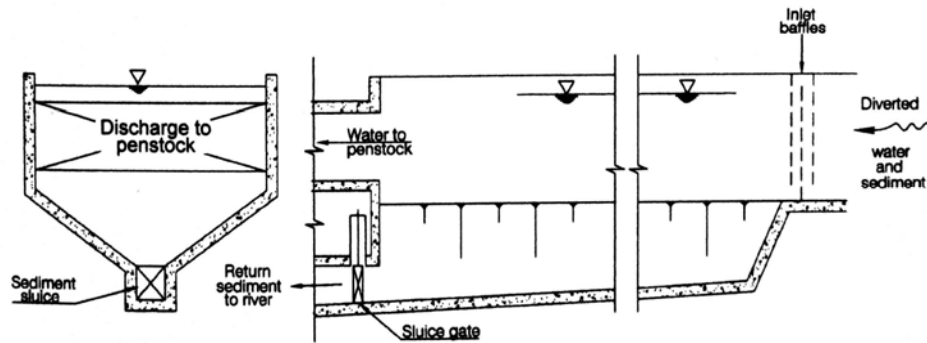


FIGURE 13.17 Schematic diagram of rectangular settling tank or desander.

### 13.11 CLOSURE

A wide variety of routing strategies are available to achieve a sediment balance or to minimize the rate of sediment accumulation. Routing strategies represent the least environmentally disruptive method for maintaining long-term storage capacity in reservoirs while minimizing the environmental impacts on fluvial systems. However, environmental impacts cannot be entirely eliminated and may continue to be significant, especially at in-stream reservoirs.

---

## CHAPTER 14

---

# TURBID DENSITY CURRENTS

---

Stratification due to density differences is a near-ubiquitous feature of the fluid environment. Stratified flow occurs frequently in reservoirs because of density differences between the inflowing and the impounded water caused by differences in temperature, dissolved solids, turbidity, or combinations thereof. Basic patterns of stratified flow were introduced in Chap. 4. Because of the high densities imparted by high turbidity levels, turbidity currents plunge and flow along the bottom of a reservoir, regardless of the temperature regime. Turbid density currents are important in explaining the movement and distribution of sediment within reservoirs. Turbidity currents which reach the dam may be vented through low-level outlets, reducing the sediment accumulation within the impoundment without drawing down the pool level.

This chapter describes basic characteristics of turbid density currents and uses field data from reservoirs to illustrate their behavior, their role in reservoir sedimentation, and management strategies. Methods to compute several characteristics of density currents are also presented. The occurrence and management of turbidity currents is also discussed in the Heisonglin and Sanmenxia case studies (Chaps. 25 and 24), and turbid density currents are important in the sediment balances at Cachi and Sefid-Rud Reservoirs (Chaps. 19 and 23).

### 14.1 INTRODUCTION

---

A density current is the gravity-induced movement of one fluid under, through, or over another fluid, caused by density differences between the two fluids. Temperature-induced stratification occurs commonly in lakes and oceans because of solar heating of surface water. In reservoirs, density differences cause warm water to flow as a surface current across the top of colder and denser water in the impoundment, cool water to plunge to the top of the thermocline and travel across the top of the colder bottom water as interflow, and high-density cold or turbid water to flow as a bottom current beneath the overlaying layer of warmer water (Fig. 4.5).

Turbidity transported in reservoirs by temperature-induced density currents are *density currents transporting turbidity*. Density currents caused primarily or entirely by the presence of the turbidity are *turbidity currents*. The term *turbid density current* will be applied to either type of current.

Turbidity currents occur when sediment-laden water enters an impoundment, plunges beneath the clear water, and travels downstream along the submerged thalweg. As the current travels downstream, it will generally deposit the coarser part of its sediment load along the bottom, and, if enough sediment load is deposited, the density

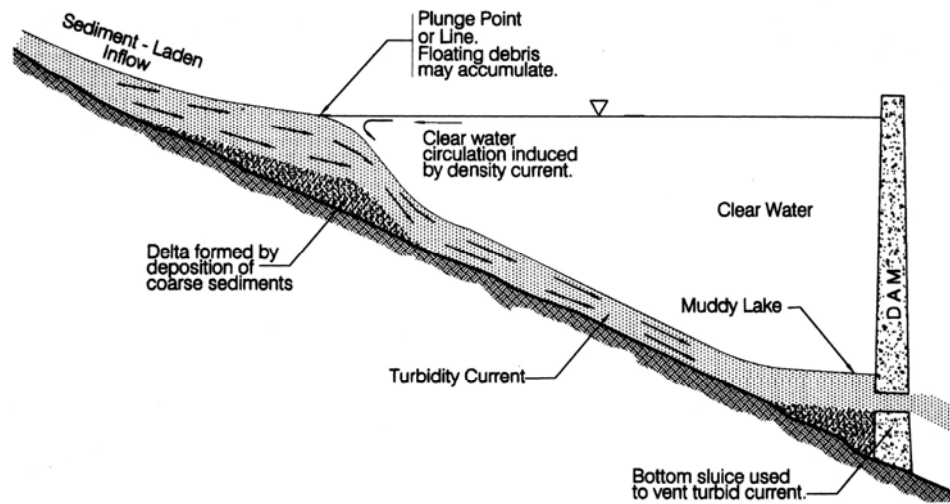


**FIGURE 14.1** Schematic diagram of the passage of a turbid density current through a reservoir and being vented through a low-level outlet.

current will dissipate along the way to the dam. If the current reaches the dam, it will accumulate to form a submerged muddy lake, and the turbid water reaching the dam can be vented if low-level outlets are opened. An idealized sketch of a turbidity current passing through a reservoir is illustrated in Fig. 14.1, which shows the plunging flow, passage along the bottom of the impoundment, accumulation as a submerged "muddy lake" before the dam, and release through a low-level outlet. A turbidity current can be sustained only as long as inflow continues; if the duration of the turbid inflow is less than the travel time required to reach the dam, the current will dissipate.

Turbidity currents were first reported by Swiss scientists in the 1880s who observed that turbid waters of the Rhine and Rhone Rivers plunged beneath the clear waters of Lake Constance and Lake Geneva (Forel, 1885). An aerial photograph of the plunging Rhone River is shown in Fig. 14.2. Plunging was attributed to both temperature and turbidity differences, but it was recognized that the density difference due to turbidity was the most important factor. This initiated the scientific study of density current phenomena in lakes.

The earliest records of turbidity current releases from a reservoir were made in July 1919 at Elephant Butte Reservoir on the Rio Grande in the United States, where the inflow suspended-sediment concentration was 72 g/L and discharge from the low-level outlet at the dam was 41 g/L. Similar observations were made in 1921, 1923, 1927, 1929, 1931, 1933, and 1935 (Lane, 1954). The passage of turbid water through Lake Mead during 1935-36 was described by Grover and Howard (1938), and numerous subsequent turbidity current events were monitored by the U.S. Bureau of Reclamation (1948). Under favorable conditions, turbidity currents can travel long distances in reservoirs and be released through low-level outlets. Turbidity currents in Lake Mead traveled for distances of 129 km to reach the dam, the longest recorded travel distance for a reservoir turbidity current. In China, systematic measurements of turbidity currents were made in Guanting Reservoir on the Yongding River near Beijing in the 1950s, and at Sanmenxia Reservoir in the 1960s and at Lujiaxia Reservoir in the 1970s, both on the Yellow River.

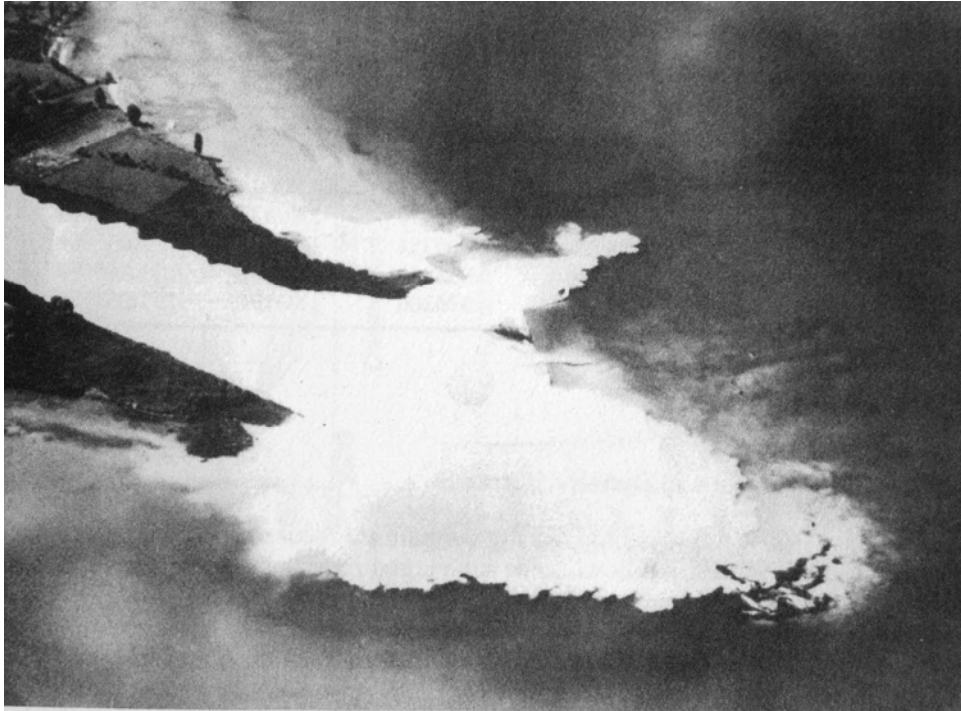


**FIGURE 14.2** Aerial photograph of turbid water from the Rhone plunging beneath the waters of Lake Geneva (*Swiss Federal Institute, Lausanne*).

Bell (1942) suggested that turbidity currents could be vented from Lake Mead to reduce the rate of reservoir sedimentation. Although Bell's suggestions were not implemented at Lake Mead, at some reservoirs in Algeria and China over half the inflowing sediment load from individual flood events has been passed through the impoundment as a turbidity current and vented from the dam through low-level sluices. At other sites with different sediment and geometric characteristics, turbidity currents do not reach the dam and there is no opportunity for their release, but they continue to be important in distributing sediment within the reservoir.

## 14.2 GENERAL CHARACTERISTICS

---

### 14.2.1 Variation in Density

Differences in both temperature and suspended solids contribute to stratification in reservoirs. When inflowing water has a higher solids concentration and lower temperature than impounded water, both turbidity and temperature will make the inflow relatively more dense and cause it to plunge. Turbid water is often warm and will plunge beneath colder water, since suspended solids can have a much greater influence on density than temperature. Densities for several water and sediment mixtures are given in Table 14.1, illustrating the large effect of suspended solids on density.

**TABLE 14.1** Density of Water and Sediment Mixtures As a Function of Temperature and Suspended Solids

Temperature, °C	Pure water	Water + sediment		
		1 g/L	10 g/L	100 g/L
0	0.999868	1.000491	1.006095	1.062137
4	1.000000	1.000623	1.006226	1.062264
10	0.999728	1.000351	1.005955	1.062002
20	0.998232	0.998855	1.004465	1.060562
30	0.995676	0.996300	1.001919	1.058103

Source: Washburn (1928).

### 14.2.2 Configuration of Density Currents

Being a gravity-driven flow, turbid density currents are focused into the deepest part of the cross section, generally following the submerged river thalweg. Isolines of concentration and velocity measured in a turbidity current at Sanmenxia Reservoir illustrating this effect are shown in Fig. 14.3. In reservoirs where trees were not removed prior to impounding, turbid density currents may be further focused along stream channels by the submerged floodplain forest (Ford and Johnson, 1983). Flood discharge, suspended-sediment grain size, and concentration all vary over the duration of a flood. Consequently, turbid density currents are unsteady with respect to discharge, sediment concentration, grain size distribution, velocity, and thickness.

### 14.2.3 Plunging Flow

The zone where the inflowing turbid water entering a reservoir plunges beneath the clear water, thereby producing stratified flow, is called the *plunge point* or *plunge line*. In a narrow reservoir the plunging flow will form a line across the width of the reservoir; the surface water will be turbid upstream of this line and clear downstream of this line. However, when a sediment-laden flow discharges into a wide reach, the turbid surface water may extend into the reservoir as an irregular tongue-like current which can shift from one side of the impoundment to the other.

As nonstratified flow entering the reservoir moves toward the plunge line, the depth increases and velocity decreases, and the maximum thickness of the turbid current occurs at the plunge point. The transition from nonstratified to stratified flow is illustrated in Fig. 14.4. Plunging flow establishes a weak countercurrent in the overlying clear water just downstream of the plunge line, causing clear surface water to travel upstream. Since both downstream-moving and upstream-moving currents converge along the plunge line, floating debris carried by the flood typically accumulates immediately downstream of the plunging flow, a readily observable indicator of the plunging phenomena. Bell (1942) observed an accumulation of driftwood and other floating debris in Lake Mead on May 3, 1940, so extensive that it created a floating barrier completely blocking the canyon section of the reservoir between 137 and 145 km above the dam. In Switzerland, during the winter when the colder turbid Rhone flows into and plunges beneath surface waters of Lake Geneva, the plunge line is defined by a zone of ice accumulation characterized by the sound of ice being grated together by the countercurrent (de Cesare, 1995).

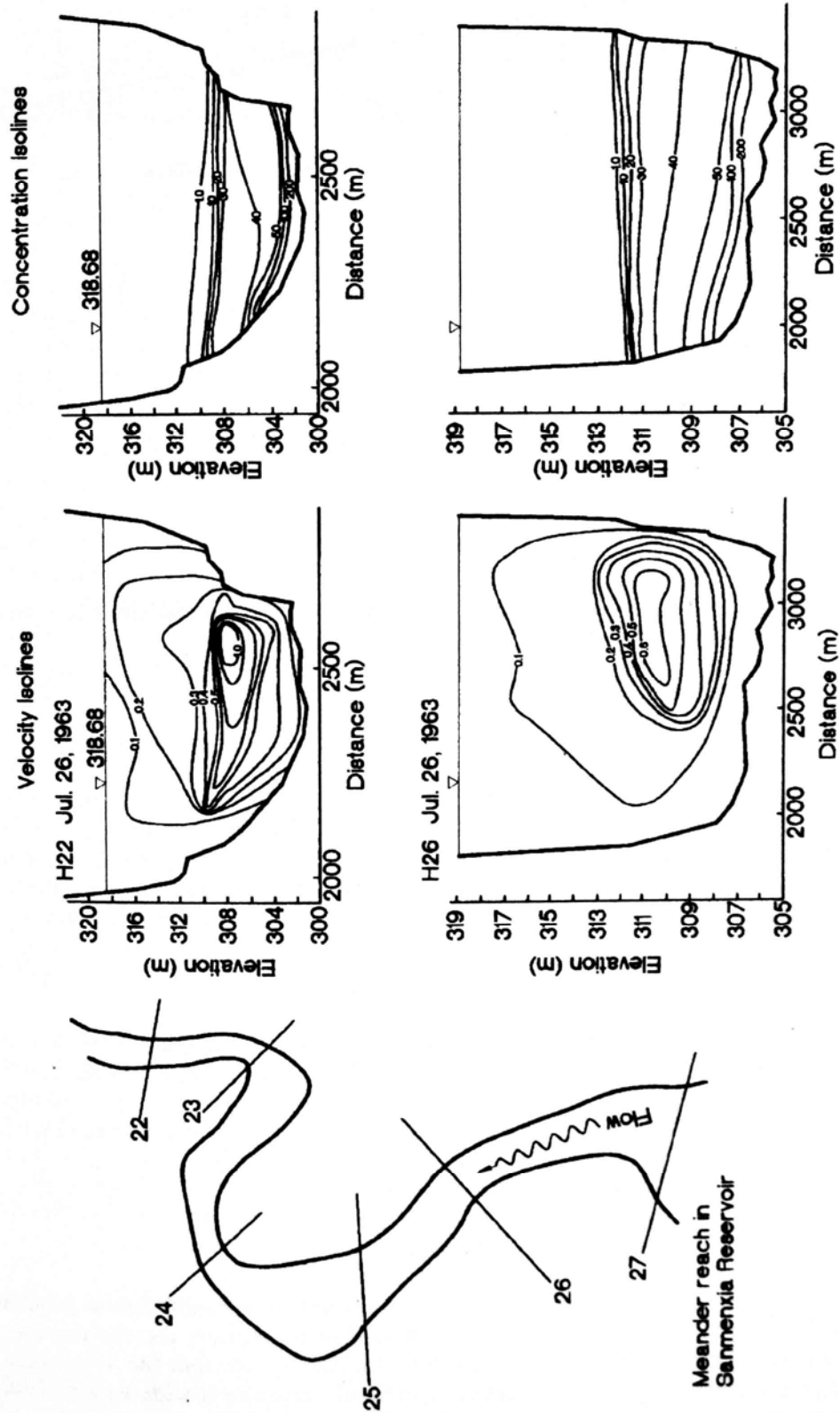
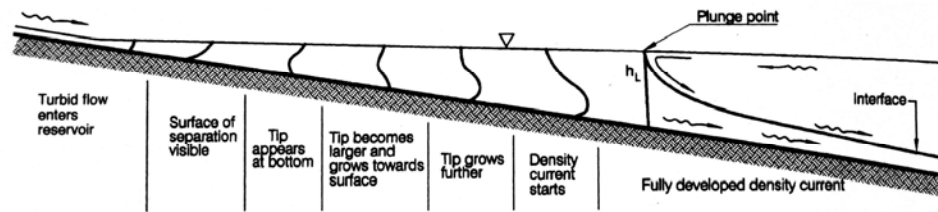


FIGURE 14.3 Isolines of velocity and concentration for a turbidity current passing through Sanmenxia Reservoir, China. Notice the exaggerated vertical scale; the density current is actually about 6m thick and 500 m wide.



**Figure 14.4** Transition from nonstratified to stratified flow (modified from Singh and Shan, 1971)

The plunge line is typically located at the downstream limit of the zone of delta deposition, but its location is not fixed, being determined by pool level, discharge, suspended sediment concentration, and reservoir geometry. Even if the water level remains constant, the plunge point location can shift upstream and downstream a distance of many kilometers during different parts of a flood as discharge and sediment concentration vary. An increase in discharge or a decrease in sediment concentration will cause the plunge point to move downstream into deeper water.

#### 14.2.4 Plunge Point Location

The water depth at the plunge point can be estimated based on the densimetric Froude number at the plunge point ( $F_p$ ):

$$F_p = \frac{V}{\sqrt{\frac{\Delta\rho}{\rho} gh}} \quad (14.1)$$

where  $V$  is the mean velocity,  $h$  is the water depth at the plunge point,  $\rho$  is the density of the impounded clear water,  $\rho'$  is the density of the turbid water, and  $\Delta\rho = \rho' - \rho$ . The equation for the densimetric Froude number [Eq. 14.1] can be rearranged to determine the depth  $h$  at the plunge point by assuming a rectangular cross section with a bottom width  $B$  and substituting the continuity equation in the form  $V = Q/Bh$ , to produce

$$h = \left( \frac{Q}{F_p B} \right)^{2/3} \left( \frac{\Delta\rho}{\rho} g \right)^{-1/3} \quad (14.2)$$

Both flume tests and measurements in reservoirs indicate that the densimetric Froude number has a value of about 0.78 at the plunge point. Values of densimetric Froude numbers reported by various researchers are summarized in Table 14.2. Several other methods for computing the plunge point location were discussed by Ford and Johnson (1983).

#### 14.2.5 Turbidity Current Forward Motion

To travel long distances, the velocity of a turbid current must be sufficient to generate the turbulence required to maintain its sediment load in suspension, thereby maintaining the density difference between the gravity-induced current and the surrounding fluid. When a turbidity current is initiated, it typically contains a wide range of suspended particle sizes, including particles that cannot be maintained in suspension by the turbulence within the current but which have not yet settled out of suspension. Settling of larger par-

**TABLE 14.2** Densimetric Froude Number  $F_p$  at Plunge Point

Author	Laboratory or field data	$F_p$
Bu et al., 1980	Liujiaxia reservoir, Tao River	0.78
Fan, 1991	Guanting Reservoir	0.5-0.78
Fan, 1960	Turbid water flume tests, 3-19 g/L	0.78
Cao et al., 1984	Turbid water flume tests:	
	10-30 g/L	0.55-0.75
	100-360 g/L	0.4-0.2
Singh and Shan, 1971	Saline water	0.3-0.8
Farrel and Stephan, 1986	Cold water	0.67

ticles reduces fluid density and the gravitational forces which maintain the flow, causing velocity to decrease. Lower velocity means less turbulent energy and less sediment-carrying capacity, which induces additional settling and further reduces the gravitational driving force and velocity. This process of sediment loss and velocity reduction continues until motion stops. This same process also causes a longitudinal reduction in the grain size of the suspended solids carried by the current and deposited along the bottom of the reservoir; grain size decreases along the direction of turbidity current movement. Turbidity current flow can be maintained over long distances only when it contains an adequate concentration of slowly settling fine-grained sediment that can be maintained in suspension by the current velocity.

A turbidity current having a potential travel distance greater than the length of a reservoir may be passed through low-level outlets in the dam and released from the impoundment. This requires that the flood have a duration exceeding the turbidity current travel time between the plunge point and the dam, since the flow of a turbidity current is maintained by the continued supply of sediment-laden water. When the inflow ceases, the turbidity current will dissipate.

The transition from nonstratified to stratified flow and subsequent movement of a turbidity current along Sanmenxia Reservoir is illustrated in Fig. 14.5. In this case the current formed as sediment settled in the backwater reach, causing deeper flow to accelerate in relation to the surface water, which continued moving downstream at a lower velocity. At range R1 near the dam, the flow field is further distorted by the release from low-level outlets at elevation 300 m, and the sediment concentration becomes hyper-concentrated near the bottom. Particle size decreases regularly in the downstream direction. Near the upstream area of Sanmenxia Reservoir, discharge from the sediment-laden Wei River has also been observed to produce turbid underflows moving both upstream and downstream beneath the current of the Yellow River. Conversely, when the Yellow River has higher sediment concentration, it plunges and flows upstream beneath the Wei River. Conditions in Sanmenxia Reservoir are discussed in more detail in that case study (Chap. 24).

### 14.2.6 Turbidity Current Behavior at a Bend

Flume tests (Fan et al., 1959) revealed that the centrifugal forces at a bend cause the turbidity current interface to rise at the exterior of the bend and decline at the interior of the bend. Similar behavior has also been observed in Sanmenxia and Guanting Reservoirs. The Yellow River has a meandering reach between Range H26 and H22 in

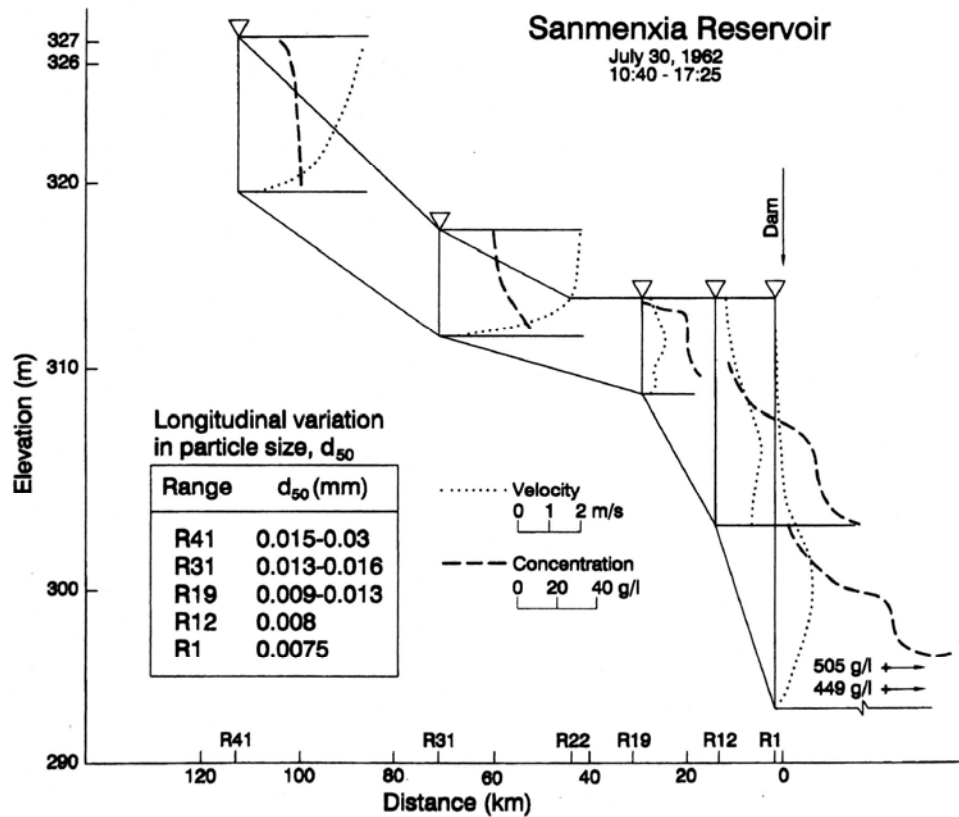


FIGURE 14.5 Passage of turbidity current through Sanmenxia Reservoir when held at a low pool elevation.

Sanmenxia reservoir with radii of curvature between 1.3 and 2.8 km (Fig. 14.3). Field measurements of velocity and concentration showed that the submerged current tended to be focused on the outside of each meander bend. At sharper bends in Guanting Reservoir, turbidity isolines were also elevated at the exterior of the bend.

### 14.2.7 Submerged Muddy Lake

When a turbidity current reaches a barrier such as a dam, the forward velocity is converted into head and the current will rise up against the face of the barrier, and subsequently fall back down to initiate formation of a muddy lake. When a turbid density current reaching the dam is not vented, or is vented slowly, the accumulating turbid water forms a submerged muddy lake having a sharp interface with the overlying clear water. The surface of this muddy lake will extend along a nearly horizontal profile upstream from the dam. The volume of the muddy lake will increase and the interface will rise, as long as turbid inflow exceeds losses by (1) venting and (2) the upward seepage of clear water from within the muddy lake due to sedimentation and compaction of the solids. The muddy lake interface may suddenly rise in response to fresh inflow and slowly fall due to hindered settling. The variation of the muddy lake interface in Lake Mead over a 25-month period is shown in Fig. 14.6. Changes in density with depth are also shown, illustrating the slow settling and compaction of the solids in the submerged muddy lake. Muddy lake formation can also occur upstream of other submerged obstacles such as a cofferdam.

Sedimentation within the muddy lake causes sediment concentration and fluid density to increase with depth, and subsequent turbid inflows will spread across the top of the higher density fluid in the muddy lake. The inflowing density current is thus converted from underflow to interflow in areas affected by muddy lake accumulation. Interflow conditions observed in Sanmenxia Reservoir are illustrated in Fig. 14.7. In this case, the muddy lake was not formed by the main dam but by accumulation behind a landslide deposit which acted as submerged barrier.

### **14.3 TURBIDITY CURRENTS AND SEDIMENT DEPOSITS**

---

Turbidity currents reaching the dam create two types of sediment deposits. Thalweg deposits due to sedimentation from the turbidity current extend downstream from the plunge point and are formed by currents that reach the dam as well as those that dissipate. Horizontal deposits of fine-grained material extending upstream from the dam can be formed only by turbidity currents that reach the dam and create a muddy lake.

#### **14.3.1 Thalweg Deposits**

As turbid density currents travel along the thalweg, they deposit sediment that fills the cross-section from the bottom up, first occupying submerged river channels, and when the channel is filled it produces a relatively flat layer of deposits. Cross-section data from reservoirs worldwide consistently show that most deposition is focused along the thalweg, while sites a short distance away and only marginally shallower generally receive little sediment deposition. This phenomenon is an indication that turbid density currents are important mechanisms controlling the transport and deposition of fine-grained sediment.

Sediment begins depositing from turbidity currents immediately downstream of the plunge point and continues depositing until the current dissipates. These deposits are typically thickest and contain the coarsest material near the plunge point, and both grain size and deposit thickness decrease moving downstream. The resulting deposit may be described as wedge-shaped, since it is thickest at the upstream limit and becomes progressively thinner moving toward the dam. Deposits from turbidity currents consist of material significantly finer than the delta deposits, even in reservoirs where most of the inflowing load consists of fines. For example, at Guanting Reservoir most inflowing sediment is silt (less than 0.062 mm). However, whereas the diameter of sediment particles in the delta reach is usually greater than 0.03 mm, turbidity currents typically carried sediments with  $d_{90}$  diameters of 0.010 to 0.020 mm and deposited these finer sediments downstream of the delta.

#### **14.3.2 Muddy Lake Deposits**

When turbid density currents reach the dam and form a muddy lake, a characteristic deposition pattern is created which consists of sediment deposits extending nearly horizontally upstream from the dam. One example of such deposits is shown in

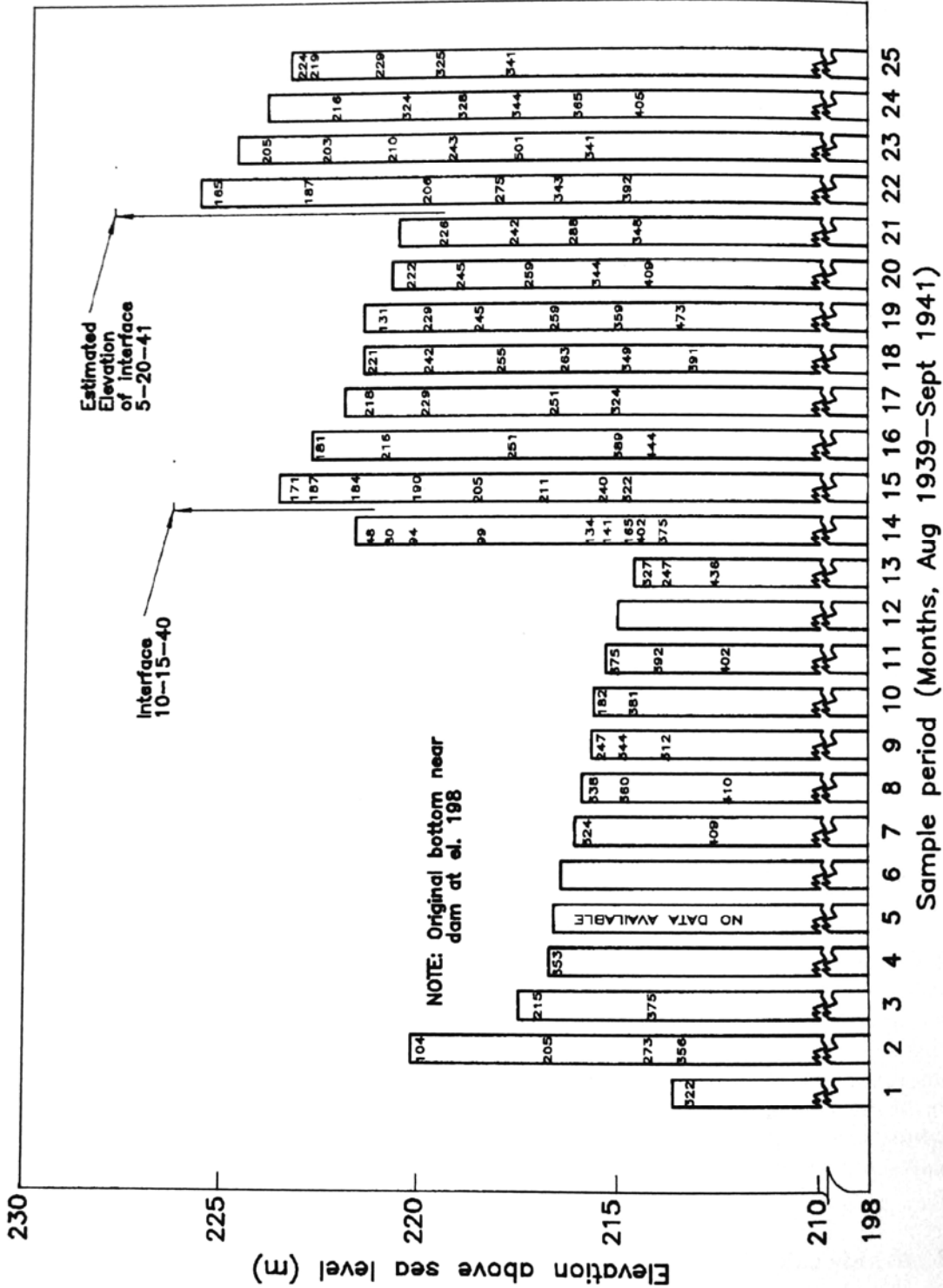
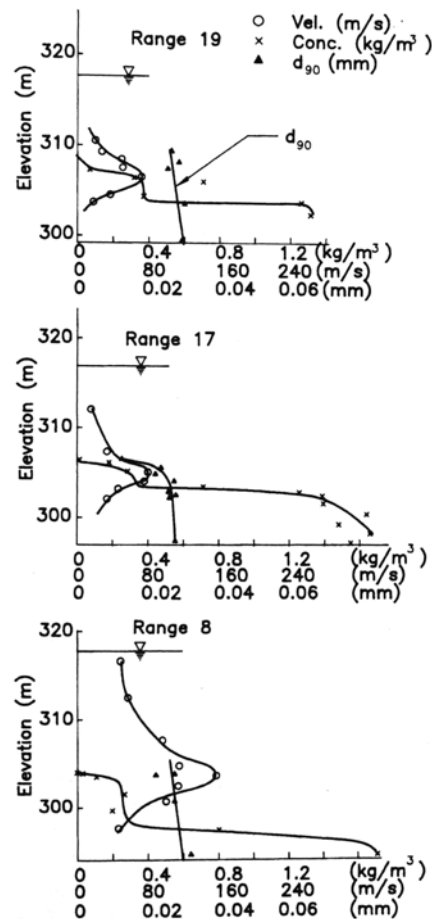


FIGURE 14.6 Dynamic behavior of the muddy lake in Lake Mead based on monthly measurements over a 2-year period. The inflow of new turbidity current events causes the lake level to rise abruptly, and sedimentation causes the interface to settle slowly. Sediment concentrations (g/L) are shown as a function of depth within the bars (adopted from Bell, 1942).



**FIGURE 14.7** Vertical profiles of velocity, concentration, and  $d_{90}$  for a turbidity current flowing over a denser submerged muddy lake in Sanmenxia Reservoir (*Sanmenxia Hydrologic Exp. Sta., 1962*).

Longitudinal profiles of the 100-Mm<sup>3</sup> Sautet Reservoir in France (Fig. 14.8a), with inflow suspended solids concentrations typically in the range of 1 g/L (Nizery & Bonnin, 1953). Even though the turbid density currents had very low concentrations, they still formed muddy lake deposits before the dam. Horizontal muddy lake deposits are also evident in longitudinal profiles in Steeg Reservoir on the Oued Fodda in Algeria with inflowing sediment concentrations on the order of tens of grams per liter (Fig. 14.8b). The absence of horizontal deposits extending upstream from a dam indicates that turbid density currents dissipate or deposit most of their load before reaching the dam.

Because coarser sediments settle fastest within the muddy lake, under appropriate conditions this can create layered muddy lake deposits which are graded coarse to fine, moving from the bottom to the top of the sediment layer associated with each major flood.

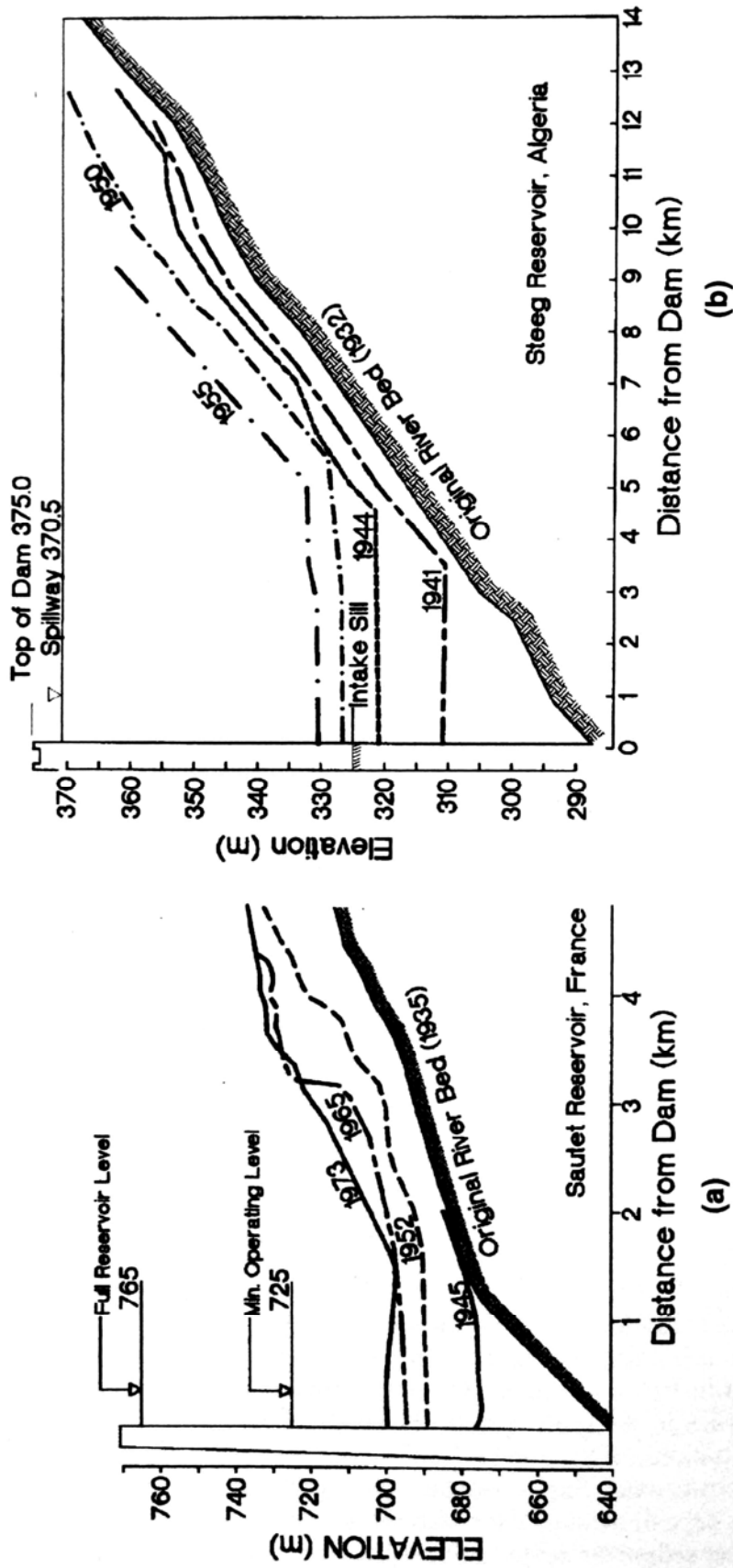


FIGURE 14.8 Bottom profile of reservoirs showing the horizontal pattern of sediment accumulation behind the dam characteristic of muddy lake deposits. (a) Sautet Reservoir, France (Comité Française, 1976). (b) Steeg Reservoir, Oued Fodda, Algeria (Thévenin, 1960).

### 14.3.3 Deposit Effects on Turbidity Currents

Sediment deposition changes reservoir geometry and can alter the ability of turbidity currents to travel to the dam. Two types of geometric changes reduce the ability of turbidity currents to travel to the dam, even though inflow conditions are unchanged. First, thalweg deposition infills the original river channel along which density currents flow, creating a broad and flat reservoir bottom which causes the turbidity current to flatten out. This reduces the thickness and increases the width of the current, increasing both bed and interface friction and also enhancing entrainment of clear water across the density interface. Second, muddy lake deposits replace the original sloping bottom with a nearly horizontal surface extending upstream from the dam. This reduction in bottom slope reduces the gravitational force driving the current forward. Periodic flushing of a reservoir which maintains a channel along the thalweg is an effective means of combatting both processes, preserving reservoir geometry conducive to the propagation of turbid density currents.

Turbidity current movement to the dam can possibly be enhanced by delta deposition that shortens the effective length of the reservoir and moves the plunge point closer to the dam, reducing the travel distance for the density current and possibly increasing bed slope downstream of the delta.

## 14.4 INDICATORS OF TURBIDITY CURRENTS

---

Several observable phenomena indicate the presence of turbid density currents in a reservoir. Turbid water may be discharged from a low-level outlet while surface waters in the reservoir are clear. Continuous suspended solids monitoring immediately above the reservoir and at the dam can indicate the presence of turbidity currents and also establish their travel time to the dam. Bottom water can be continuously discharged through a low-level outlet and monitored below the dam to observe the arrival of turbid water.

A muddy flow that enters and disappears at the upstream limit of a reservoir, a phenomenon frequently observed from the air, is an indication of plunging flow. The plunge line may be observed as a sharp transition between clear and turbid water and by the accumulation of floating debris. Longitudinal bathymetric profiles revealing nearly horizontal deposits extending upstream from the dam represent sediment deposits from a muddy lake, and indicate that significant amounts of sediment are being transported to the dam by turbidity currents (Fig. 14.8). The presence of turbid density currents or a submerged muddy lake may also be determined by sampling water quality profiles during or following runoff events. The presence of density currents of all types may be measured by sonic or other velocity profiling methods or by monitoring of water quality parameters such as temperature and dissolved oxygen which distinguish the inflowing and impounded waters (see Fig. 4.6).

## 14.5 TURBIDITY CURRENT PROBLEMS IN RESERVOIRS

---

### 14.5.1 Blockage of Low-Level Outlets

Turbidity currents can transport appreciable amounts of sediment along the bottom of a reservoir, causing sediment accumulation in front of the dam which interferes with the

operation of low-level outlets. This is not an unusual phenomena in hydropower reservoirs in mountainous areas.

The 208-m-tall Luzzone Darn in Switzerland, completed in 1963, impounds 36.5 km<sup>2</sup> of the mountainous watershed of the Val Blenio River to create an 87 Mm<sup>3</sup> hydropower reservoir. Although the total amount of sediment deposition in this reservoir is not large, about 35,000 m<sup>3</sup>/yr, turbid density currents transport sediments into the immediate vicinity of the dam where they accumulate and interfere with operation of low-level outlets. By 1983, these deposits had accumulated to a depth of one-third the height of the low-level power intake, and dredging was performed to remove 17,000 m<sup>3</sup> of deposits near the intake. In 1985, the reservoir was emptied for flushing and about 0.3 Mm<sup>3</sup> of sediment was released.

In 1992 vertical instrumented arrays were deployed to measure density current movement (Sinniger et al., 1994). Profile 5 was located 250 m upstream of the dam and profile 10 was located 1100 m upstream of the dam, at a point about halfway between the dam and the upstream pool limit. By examining some of the results summarized in Table 14.3, it will be seen that only 8 percent of the sediment inflow during the smaller

**TABLE 14.3** Summary Measurements of Turbid Density Currents, Luzzone Reservoir

Date	Weight, kg		Volume, m <sup>3</sup>	
	Profile 5	Profile 10	Profile 5	Profile 10
Aug. 4, 1992	10,267	123,479	9	103
Aug. 29, 1992	29,325	245,971	24	205
Aug. 31, 1992	1,026,852	5,235,728	856	4,363

*Source:* Sinniger et al. (1994).

August 4 inflow event reached the dam, whereas 20 percent of the upstream flow reached the dam during the large August 31 event. Turbidity currents repeatedly entered and traveled along a low-level outlet pipe at the dam, causing sediment to accumulate at the valve which was located some distance downstream of the entrance to the conduit. On one occasion the accumulation was so great that it completely blocked the conduit and water would not flow after the valve was opened, despite high hydrostatic head. This phenomenon was examined by Boillat and DeCesare (1994) using a physical model (Fig. 14.9).

### 14.5.2 Turbidity Currents at a Confluence

Many reservoirs impound river confluences, and sediment-laden discharge from one tributary can create a turbidity current that affects the other tributary. An extreme example of this phenomenon occurs at the Liujiaxia hydropower plant, the second largest in China.

The Liujiaxia Dam across the Yellow River is located 1.6 km below the confluence with the tributary Taohe River. Sediment-laden discharge from the tributary plunges beneath the impounded Yellow River and then flows as a turbidity current both upstream and downstream along the floor of the reservoir, dropping its sediment load and dissipating. Over the course of many events, this created a localized sand bar that grew

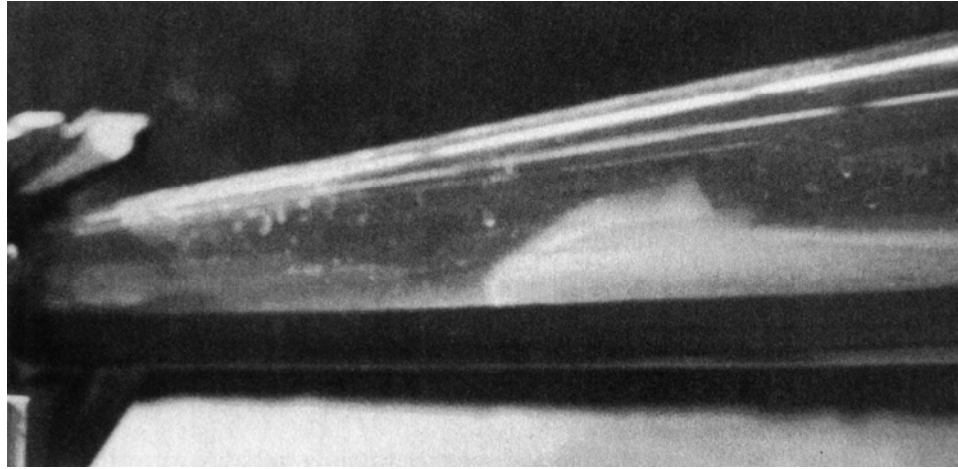


**FIGURE 14.9** Photograph of a turbidity current advancing toward the left along a physical scale model of a low-level circular conduit at Luzzane Dam, Switzerland. The bulbous-shaped nose at the front of the advancing current is typical of density underflows (*C. DeCesare*).

until it prevented the diversion of water for power generation at low pool levels. Sediments in the downstream-traveling turbidity current also entered the power intake causing abrasion of turbines and gate recesses. Longitudinal profiles of turbidity current deposition along both the Yellow and Taohe Rivers are shown in Fig. 14.10. During 15 years of impounding operation, serious deposition at the confluence twice caused an abrupt increase in the elevation of the sand bar. The first event occurred during the 1973 flood season when 14.7 m of deposition occurred. In this case the silt inflow from the Taohe River was  $52.3 \times 10^6$  tons, twice the average annual discharge, and the outlets at

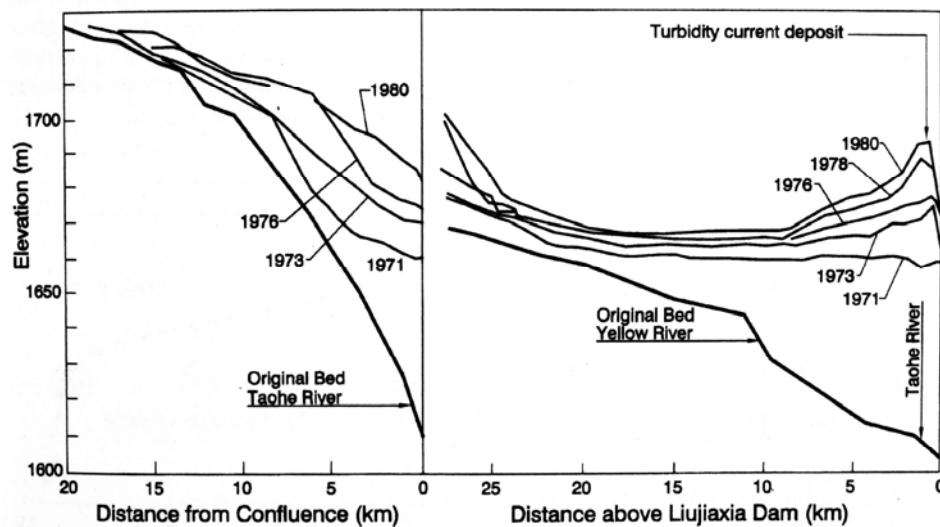


**FIGURE 14.10** Change in longitudinal deposit profiles upstream of Liujiaxia Dam on the Yellow River, caused by localized deposition of sediment from turbidity currents entering from the tributary Taohe River (*Fan, 1991*).

the dam were not opened in time to vent the turbidity current as it entered. Deposition occurred in both the Taohe and Yellow Rivers. The second event occurred during 1978 and 1979; the deposit thickness increased an additional 15.6 m during this period.

## 14.6 VERTICAL STRUCTURE OF TURBIDITY CURRENTS

In a turbidity current the density interface (which is also the turbidity interface) will approximately coincide with the velocity interface. However, when density differences are imparted mainly by temperature, the turbidity may become concentrated in the lower part of the flow or may largely settle out even though the temperature-driven current continues flowing. Atypical conditions may also occur as the current is fading away and depositing the remaining sediment load.

Vertical profiles of concentration and velocity within a turbidity current are illustrated in Fig. 14.11. The vertical structure will vary as a function of hydraulic parameters including roughness and Froude number. In a turbidity current, a significant vertical variation in sediment concentration will normally be observed only in the vicinity of the plunge point, where the current is in the process of rapidly depositing its coarse fraction. After the coarser particles have been largely deposited and only finer-grained sediments remain in suspension, the vertical concentration profile is usually quite uniform in terms of both grain size and concentration as observed in flume tests (Fan et al., 1959; Michon et al., 1955) and also in reservoir data. An inflection point on the concentration profile occurs near the interface, and above the interface the concentration is always very low. Figure 14.12 illustrates vertical profiles of velocity and turbidity measured over the course of 5 days in Sanmenxia Reservoir showing the growth and dissipation of a turbidity current. During this event, the water in the Yellow River was also moving downstream along the reservoir, resulting in forward motion in overlying water as well as in the faster-moving turbidity current. Several features of a turbidity current event are illustrated by these data: (1) the turbidity interface is sharp over the duration of the event, (2) the zone of forward velocity is always within the turbid water zone except at the end of the event as flow is dissipating, and (3) the unsteady behavior of the turbidity current over the duration of the event. An appreciable concentration of fine sediment may remain in suspension even after the current has ceased moving.

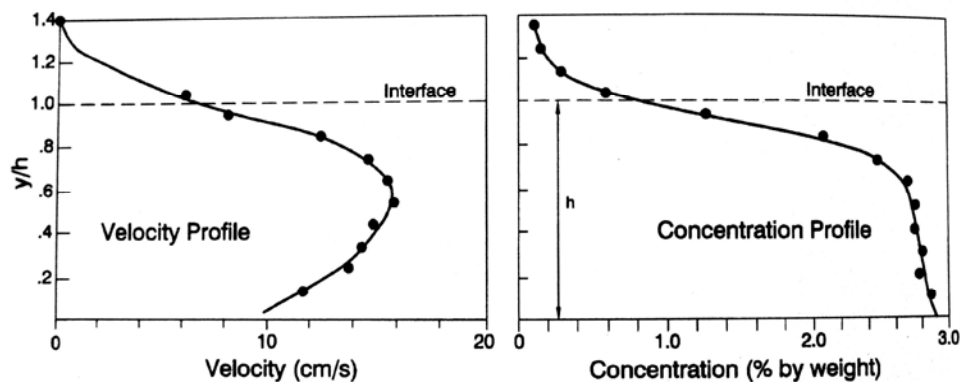


**FIGURE 14.11** Vertical profiles of velocity and concentration within a turbidity current (Ashida and Egashira, 1975)

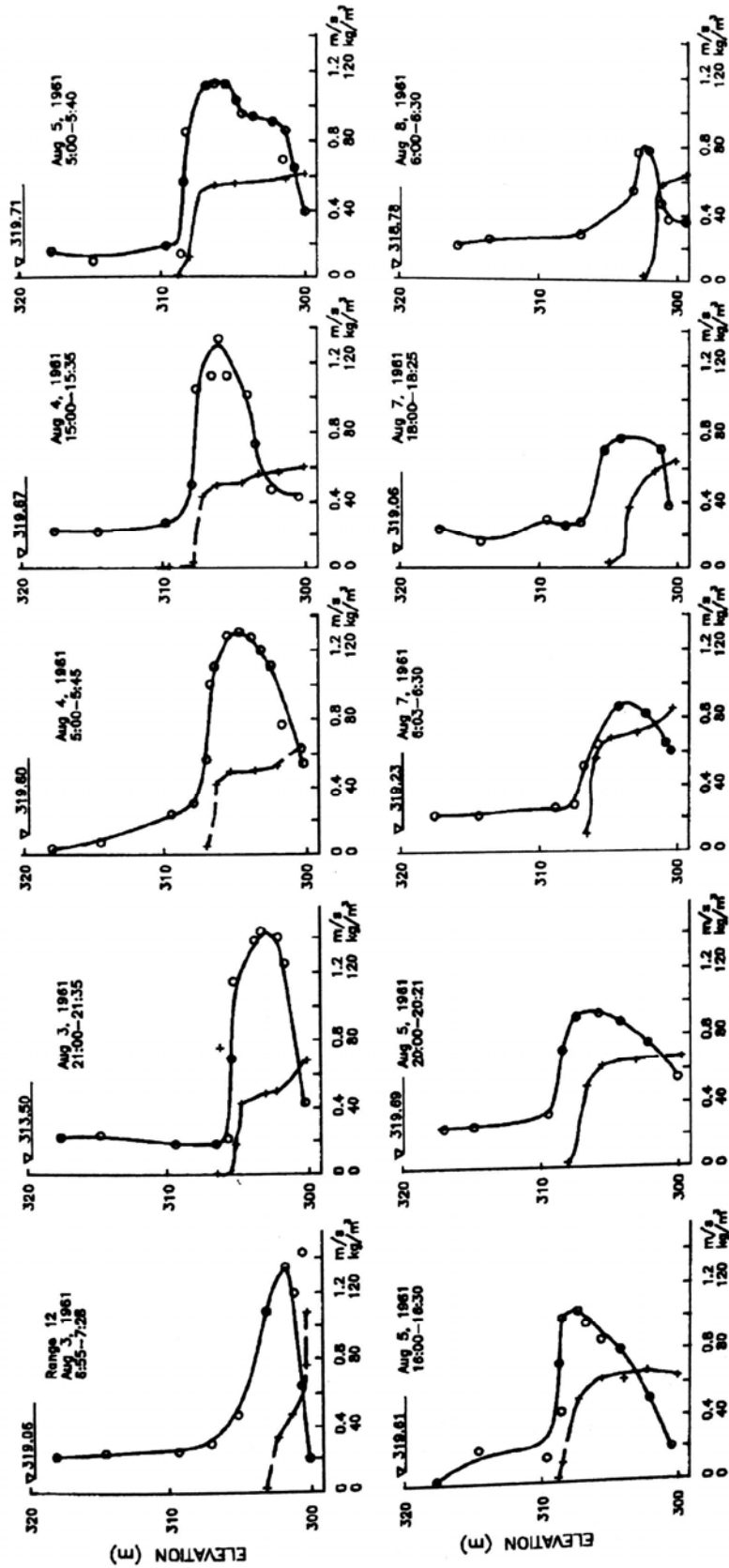


**FIGURE 14.12** Vertical profiles of concentration (crosses) and velocity (circles) for a 5-day turbidity current event at range 12 in Sammenxia Reservoir, showing the growth and fading away of the current (*Fan, 1991*).

## 14.7 VENTING OF TURBIDITY CURRENTS

---

### 14.7.1 Overview

Turbidity currents can be vented from reservoirs by opening a low-level outlet at the dam, and at some reservoirs it has been possible to release more than half the total sediment load in an individual flood by venting the turbidity current. Successful venting depends on properly located low-level outlets, which are opened in time to release the current using a discharge rate that matches the turbidity current inflow. However, it will not be possible to vent turbidity currents in many reservoirs, and the efficiency of releasing turbidity currents can decline over time as deposition which fills the submerged channel changes the reservoir bathymetry and impedes propagation of the turbidity current.

Turbidity currents may also be vented for environmental reasons. For example, at the Lost Creek reservoir in Oregon it was desired to release turbid water from the pool during large inflowing storms, flushing turbid water along the river and to the ocean over a short period of time, rather than to trap turbid water in the reservoir where it would be released more gradually over a longer period of time. In this stream it was considered more desirable to have a short high-turbidity period followed by normal low-turbidity flows, as opposed to a prolonged period of elevated turbidity. The turbidity conduit for this reservoir is shown in Fig. 4.7.

### 14.7.2 Venting Efficiency

A turbidity current will flow only as long as there is a continued input of turbid water at the upstream end of the reservoir, and it will stop as soon as the inflow ends. Thus, when inflow ends, the portion of the current spread out along the length of the reservoir will stall and the turbidity will settle in place. This portion of the current cannot be vented. As a rough approximation, the maximum amount of an inflowing turbidity current that can be vented will equal the total inflow volume less the volume of the density current retained along the length of the reservoir.

Based on this conceptual model, Fig. 14.13 presents the relationship between releasing efficiency  $W_o/W_i$  and reservoir length  $L$ , giving also the  $Q_o/Q_i$  value for each venting event, where  $W_i$  and  $W_o$  represent, respectively, the inflowing and outflowing (vented) turbidity current, and  $Q_o$  and  $Q_i$  represent the average flow rates for inflow and turbidity release. Venting efficiency tends to increase as the reservoir length decreases and as the  $Q_o/Q_i$  ratio increases. In practice, the venting efficiency is heavily influenced by the timing of gate openings and their arrangement at the dam. The effect of timing of gate operations on venting efficiency is discussed in the Heisonglin case study (see Table 25.4). Venting efficiency exceeding 100 percent has occasionally been reported, but is usually related to either: (1) entrainment of additional sediment by scour of deposits between the upstream monitoring station and the plunge point and (2) release of unconsolidated sediments within a muddy lake created by a prior event.

### 14.7.3 Timing and Duration of Releases

To efficiently vent a turbidity current, it must be known when the current arrives at the dam and when it ends, to time the opening and closing of gates. Turbidity current motion may be measured in situ by instrument arrays, or it may be estimated from inflow conditions and previous measurements. The in situ measurement of turbidity currents can today be conducted without great expense by deployment of reporting sensors, such as



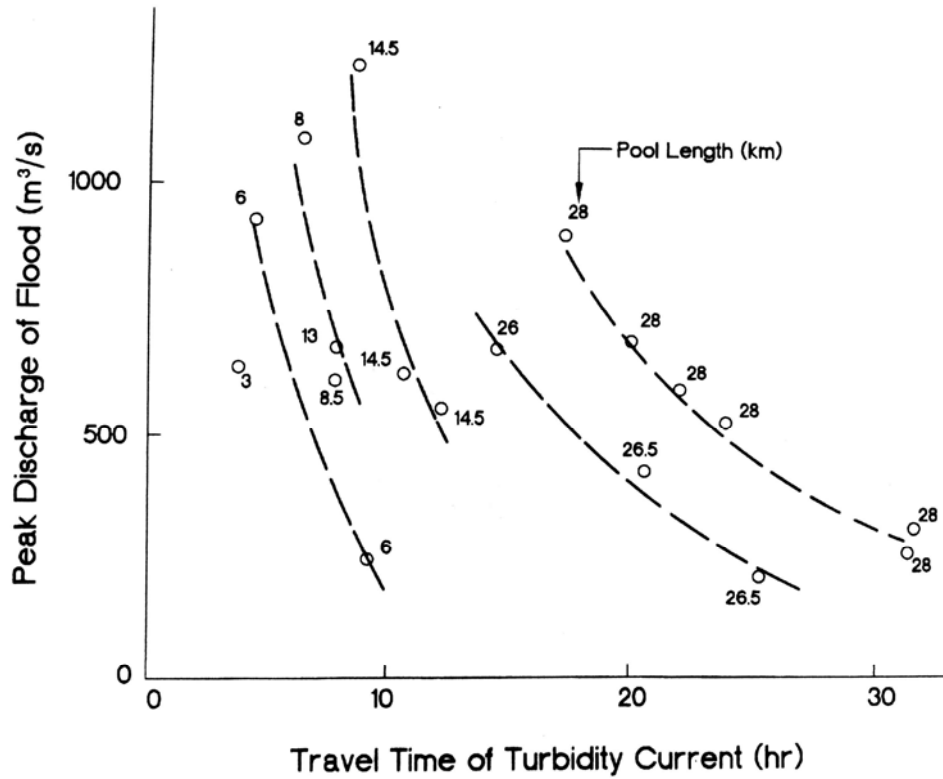


FIGURE 14.14 Variation of turbidity current travel time with peak flood discharge and pool length, Guanting Reservoir (Fan and Jiao, 1958)

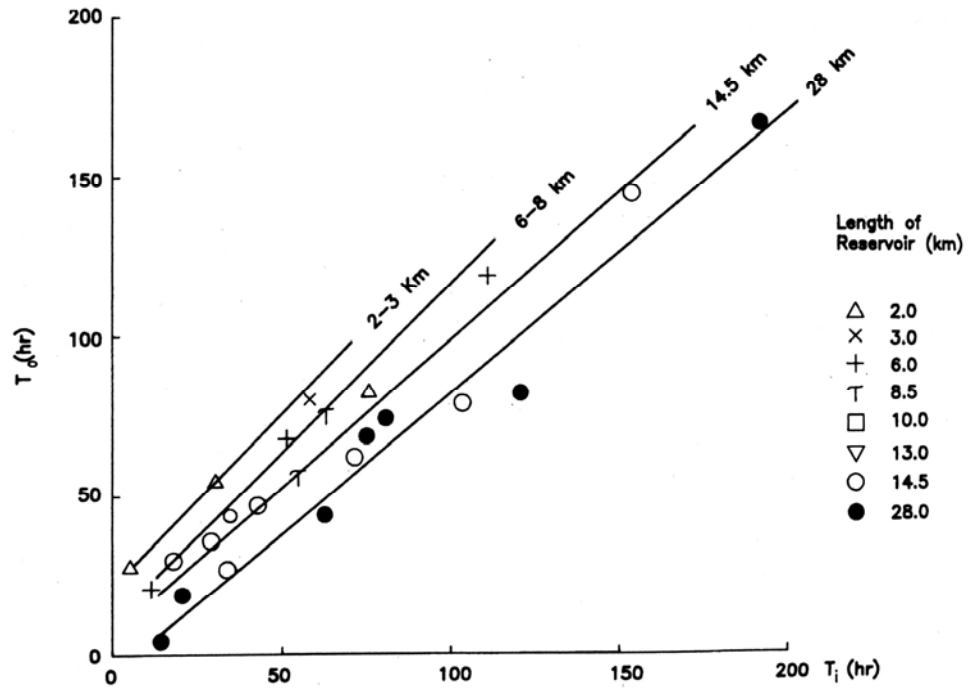


FIGURE 14.15 Relationship between duration of turbidity current release ( $T_0$ ) and inflow period ( $T$ ) as a function of pool length, as measured in Guanting Reservoir at various pool levels (Fan and Jiao, 1958).



**FIGURE 14.16** Photograph of turbid water from the muddy lake being discharged from the low-level outlet at Steeg Reservoir, Oued Fodda, Algeria.

### 14.7.5 Height of Aspiration

When a turbidity current reaches a dam and is vented, water will be aspirated from levels both above and below the outlet level. There is the potential to entrain clear water from the layer above the turbidity current, releasing clear water when it is not necessary. Similarly, when an intake is operated at a level above a muddy lake, it is possible to entrain turbid water from the muddy lake. A definition sketch illustrating these phenomena is shown in Fig. 14.17, and symbols are defined below.

- $Q$  total discharge through orifice,  $\text{m}^3/\text{s}$
- $q$  discharge per unit width of slotted outlet,  $\text{m}^3/\text{s}$
- $h_L$  height of aspiration, m, as in definition sketch
- $g$  gravitational constant =  $9.8 \text{ m/s}^2$
- $F_2$  two-dimensional densimetric Froude number for slot aspiration
- $F_3$  three-dimensional densimetric Froude number for orifice aspiration

The limiting height of aspiration is the point at which clear or turbid water first starts to be released or aspirated through the outlet.

A theoretical analysis of the limiting height of aspiration  $H_L$  of a density current was made by Craya (1946), resulting in the following expression:

$$\frac{\Delta\rho}{\rho} \frac{gh_L^3}{q^2} = \frac{27}{8\pi^2} = 0.34 \quad (14.3)$$

Experiments to determine the limiting height of aspiration were conducted using slots or orifices in laboratory flumes. A slot produces a two-dimensional flow field, and an

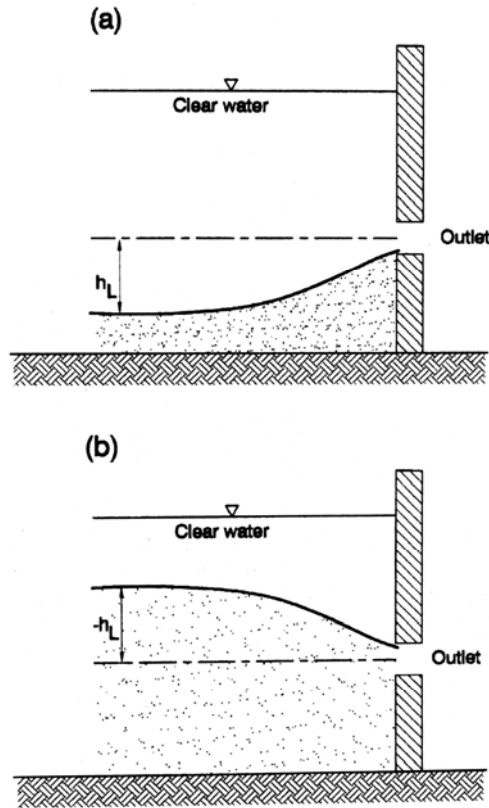


**FIGURE 14.17** Definition sketch showing interface configuration at the limiting condition for: (a) aspiration of turbid water from muddy lake through a low-level outlet, and (b) aspiration of clear water when venting a turbidity current.

orifice produces a three-dimensional flow field. Based on experiments with saline water, Gariel (1946, 1949) obtained the relationship for the limiting height of aspiration for a slot:

$$\frac{\Delta\rho}{\rho} \frac{gh_L^3}{q^2} = 0.43 \quad (14.4)$$

The following equation was obtained for an orifice:

$$\frac{\Delta\rho}{\rho} \frac{gh_L^5}{Q^2} = 0.154 \quad (14.5)$$

Fan (1960) performed flume tests using turbidity currents and described the mixing pattern in the vicinity of an orifice. Mixing with the overlying water can be violent because of the existence of a vertical vortex at the outlet, which produces a second mixing zone extending above the turbidity interface. The aspiration height was measured and expressed in terms of the densimetric Froude number. For a slot, the limiting depth for aspiration of turbid water from below the slot axis is given by:

$$F_2 \left[ \frac{\Delta\rho}{\rho} \frac{gh_L^3}{q^2} \right]^{1/3} = 0.75 \quad (14.6)$$

and the aspiration height at which clear water begins to be entrained from above the slot is given by:

$$F_2 = \left[ \frac{\Delta\rho}{\rho} \frac{g(-h_L)^5}{q^2} \right]^{1/3} = -0.75 \text{ (by extrapolation)} \quad (14.7)$$

For an orifice, the limiting depth for aspiration of turbid water from below the axis is

$$F_3 = \left[ \frac{\Delta\rho}{\rho} \frac{gh_L^5}{Q^2} \right]^{1/5} = 0.8 \quad (14.8)$$

and the aspiration height at which clear water begins to be entrained from above the orifice axis is given by:

$$F_3 = \left[ \frac{\Delta\rho}{\rho} \frac{g(-h_L)^5}{Q^2} \right]^{1/5} = -1.2 \quad (14.9)$$

During 1961 and 1962, turbidity currents were released from Sanmenxia Reservoir through 12 gates, each 3 m wide and 8 m tall, located at an elevation of 300 m. The original riverbed at the dam was 280 m, but because of sediment accumulation it rose to about 290.5 to 292 m during 1961, and to 294 to 295 m during 1962. From these tests, and with 304 m as the axis elevation, the following values of  $F_3$  were determined by using the orifice equations (14.8) and (14.9):

$F_3 = 0.9$  lower aspiration limit ( $h_L$ ) in 1961

$F_3 = 1.1$  lower aspiration limit ( $h_L$ ) in 1962

$F_3 = -0.4$  clear-water aspiration limit ( $-h_L$ ) in both years

The data from Sanmenxia Reservoir may be used to estimate aspiration height (either  $h_L$  or  $-h_L$ ) by rearranging Eq. (14.9) to solve for aspiration height for an orifice:

$$h_L = F_3 \left[ \frac{Q^2}{(\Delta\rho / \rho)g} \right]^{1/5} \quad (14.10)$$

The appropriate values of  $F_3$  may then be substituted directly. The clear-water aspiration height  $-h_L$ , was significantly less than  $h_L$ , possibly because of the large cross-sectional area of the outlet gates and the shallow water depth before the dam. The flow pattern was quite different from that simulated in the laboratory flume.

## 14.8 COMPUTATIONS

---

Density current computations are complicated by the unsteady nature of the flow resulting from variable inflow and water levels and continuous deposition of sediment and entrainment of clear water, which changes the density within the current. Reservoir bathymetry is also nonuniform in the longitudinal direction, and will also gradually change over time as a result of sediment accumulation. This section presents several equations which may be used to make a preliminary evaluation of the potential for turbidity currents to reach the dam.

### 14.8.1 Computational Strategy

Hand computations can be used to give a rough idea of the potential for turbidity currents to reach the dam. To make a preliminary evaluation of whether turbid density currents can transport material to the dam, the following procedure is recommended. Because inflowing discharge varies with time, an "average" discharge value for the flood duration should be used. Computations should be performed for the larger events which transport significant amounts of sediment.

1. Compute the water depth at the plunge point [Eq. (14.2)] to provide the first indicator of the potential for turbidity currents to occur, and to indicate the area within a reservoir where a turbid density current can form as a function of the density difference between the impounded and inflowing water, and the discharge.
2. Compute the velocity of the turbidity current based on the suspended solids concentration of the inflow.
3. Based on the velocity, determine the maximum grain size that can be transported.
4. Remove all larger grains, then return to step 2 and recompute for the grains remaining in suspension.

By performing the recomputation of steps 2, 3, and 4 through several iterations it will become evident whether the current can be sustained with a significant sediment concentration or will rapidly fade away.

It is important to recall that the computational procedure assumes a steady state at each reiteration, and does not reflect the time required for the sediment to settle out. If the travel time to the dam is short, and the settling velocity of the sediment within the current is low, the current may transport a significant amount of material to the dam under nonequilibrium conditions. If these preliminary computations suggest the potential for significant turbidity transport to the dam, further analysis would be performed with field measurements and numerical modeling.

### 14.8.2 Flow Velocity of a Turbid Density Current

The flow velocity of a density current can be determined in a manner similar to that for open channel flow. In open-channel flow:

$$V = \sqrt{\frac{8}{f} gRS} \quad (14.11)$$

where  $V$  = velocity,  $f$  = friction coefficient,  $R$  = hydraulic radius, and  $S$  = bed slope. In a density current the gravitational acceleration should be modified to express the gravitation force exerted by the density difference  $\Delta\rho$  between the turbid water and the stationary clear water, resulting in the following equation for density current velocity:

$$V = \sqrt{\frac{8}{f} \frac{\Delta\rho}{\rho} gRS} \quad (14.12)$$

Assuming the depth is much less than the width, we can substitute depth of the density current  $h$  for the hydraulic radius  $R$ . Assuming a rectangular density current cross section with a width of  $B$ , we can substitute the continuity equation  $h = Q/BV$  to obtain:

$$V = \sqrt[3]{\frac{8}{f} \frac{\Delta\rho}{\rho} g \frac{Q}{B} S} \quad (14.13)$$

The friction coefficient  $f$  represents the total interfacial frictional effects including the channel bed plus the boundary with the overlying stationary fluid. In Chinese reservoirs, the friction value is typically in the vicinity of  $f = 0.025$ .

### 14.8.3 Grain Size That Can Be Transported

On the basis of field data, Fan (1986) presented the relationship shown in Fig. 14.18 for roughly predicting the maximum grain diameter that can be transported by a turbid den-

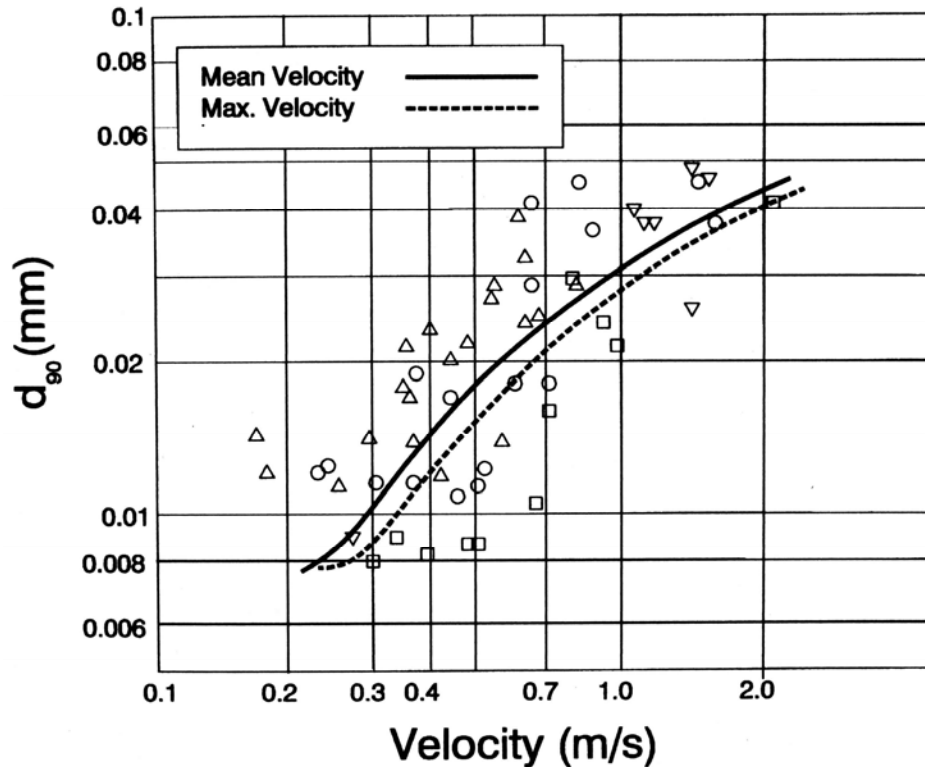


**FIGURE 14.18** Relationship between turbidity current velocity and the grain size that can be maintained in suspension (after Fan, 1986).

sity current, as a function of forward velocity. In short reservoirs the slowly settling sediment may not have the opportunity to settle out of the moving current, and larger material may be transported to the dam than predicted because of delayed sedimentation. Somewhat different conditions may also apply in reservoirs having different sediment characteristics. For example, Toluie (1993) reported that density currents in the large Sefid-Rud Reservoir transported grain sizes larger than those reported in Chinese reservoirs, as discussed in that case study (Chap. 23). At high concentrations, sedimentation can be significantly retarded by hindered settling. The settling rate can also be influenced by flocculation mechanisms within the turbid water.

## 14.9 MONITORING DENSITY CURRENT MOVEMENT

When it is desired to evaluate the potential to release turbid density currents from an existing reservoir, detailed monitoring is recommended. Modern monitoring technology allows accurate, cost-effective measurements to be obtained from automated equipment. The typical monitoring arrangement would consist of an inflow station immediately above the point where the stream enters the reservoir, plus one or more stations along the length of the impoundment. If the pool is at a low level, previously deposited sediment may be scoured from the bottom of the reservoir and the suspended solids concentration at the plunge point may be significantly greater than measured at the inflow

station. This phenomenon should be considered when selecting monitoring stations and interpreting data.

Submerged turbidimeters can be used to detect the arrival of the advancing current at each lake station, thereby determining its forward velocity. Either a closely spaced array of turbidimeters or dipping sondes may be used to determine the thickness of the current. Because the inflowing current will drop the coarsest fraction of the load, and because turbidimeters are highly sensitive to small grain sizes but not to coarser particles, water from the current will need to be sampled if turbidity readings are to be used to estimate suspended solids concentration. Samples collected from an existing outlet at the dam can be used to determine the arrival time at the dam plus the grain size that is transported to the dam. However, because of the potential problem of clear-water aspiration, if a high-discharge outlet is used the suspended solids concentration in the outlet is not necessarily indicative of the sediment concentration within the current.

The grain size transported by the current may also be determined from shallow bottom cores or surface sediment samples immediately following a turbidity current event. Cores that penetrate through the material deposited by several events may be interpreted to determine the grain size that "normally" reaches the dam.

## **14.10 CLOSURE**

---

Turbidity currents are of great importance in distributing sediment along the length of a reservoir, and focusing sediment deposition within the deepest portion of each cross section. In some cases turbidity currents can be used to release large volumes of sediment from reservoirs. However, the behavior of turbid underflows in reservoirs is not easy to quantify, and field measurement represents the best method to document their behavior.



---

## CHAPTER 15

---

# FLUSHING

---

---

### 15.1 CONCEPT AND APPLICATION

---

#### 15.1.1 Overview

Hydraulic flushing involves reservoir drawdown and emptying by opening a low-level outlet to temporarily establish riverine flow along the impounded reach, eroding a channel through the deposits and flushing the eroded sediment through the outlet. Unlike sediment routing, which attempts to prevent deposition during flood events, flushing uses drawdown and emptying to scour and release sediment after it has been deposited. However, sediment entering the reservoir during flushing periods will also be routed through the impoundment and released.

There are two key features that distinguish flushing from sediment routing. Flushing operations (1) remove previously deposited sediment and (2) the timewise pattern of sediment release below the dam differs significantly from sediment inflow. The change in the pattern of sediment release is greatest when flushing is conducted during the non-flood season, as illustrated in Fig. 15.1. However, the sediment release pattern will also differ from sediment inflow when flushing is conducted during a portion of the flood season. A large volume of accumulated sediment will be released during a short period of time, generating extremely high sediment concentrations. In contrast, sediment routing largely maintains the natural seasonality of sediment transport along the river, as was illustrated in Fig. 13.4

The channel scoured through the deposits is maintained by repeated flushing, usually at annual intervals. In wide reservoirs the flushing channel will erode only a narrow channel through the deposits, to produce a channel and floodplain-type geometry (Fig. 15.2). While sediment deposited in the channel each year can be eroded during the subsequent flushing period, sediment deposited on the floodplains during impounding periods will continuously accumulate. Auxiliary flushing channels may be used in addition to the main flushing channel to remove a portion of the floodplain sediment. Generally, a large flushing discharge through low-level outlets is necessary to preserve long-term storage capacity.

#### 15.1.2 Classification of Techniques

Fan (1985) has classified flushing into two general categories: (1) *empty* or free flow flushing, which involves emptying the reservoir to the level of the flushing outlet with riverine flow through the impoundment, and (2) *pressure flushing*, which requires less drawdown but is also less effective. The second method is not commonly used.

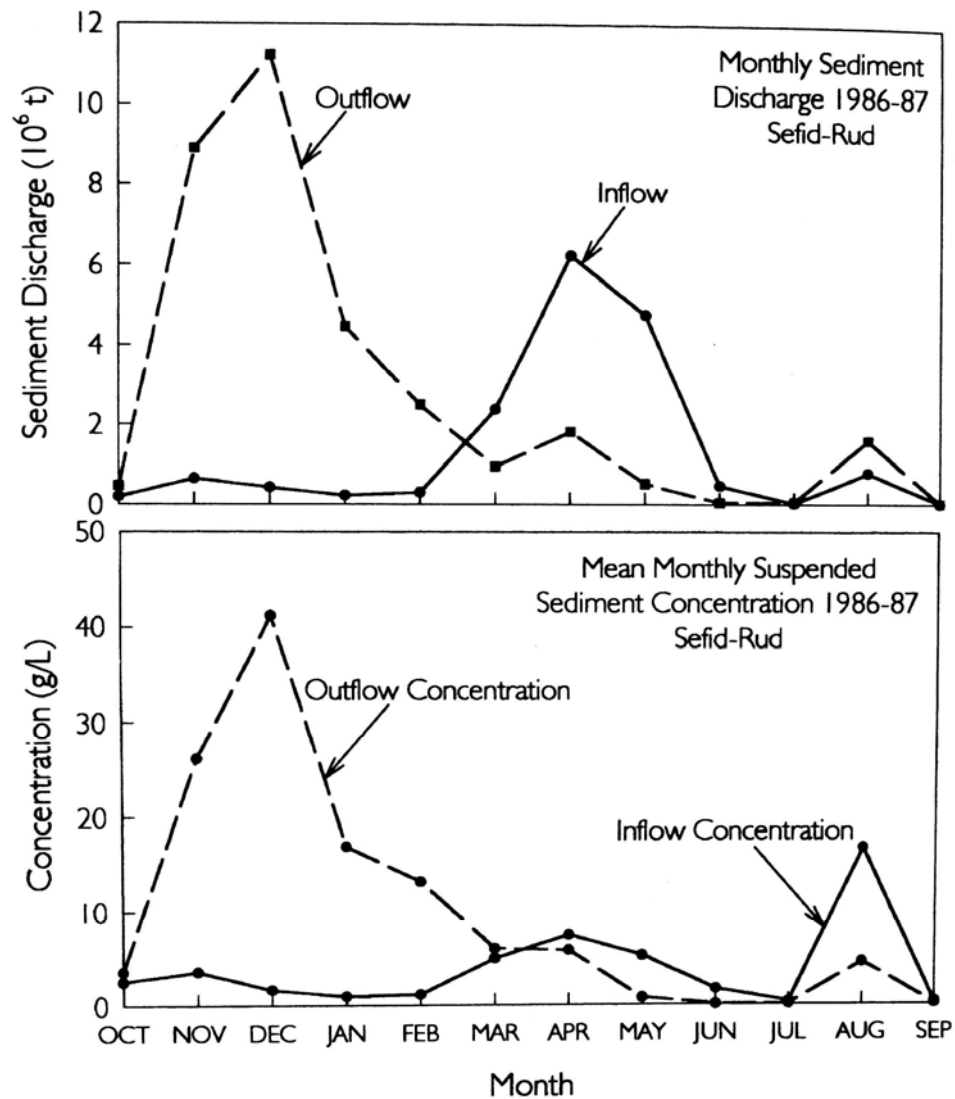


**FIGURE 15.1** Change in the seasonality of sediment delivery below Sefid-Rud Reservoir, Iran, caused by flushing (data from Tolouie, 1993).

Empty flushing can also be classified according to whether it occurs during the flood season or the nonflood season. While both strategies have been employed successfully, flood season flushing is generally more effective because it provides larger discharges with more erosive energy, and floodborne sediments may be routed through the impoundment.

### 15.1.3 Applications

Flushing can be used to reduce or halt sediment accumulation and to recover reservoir capacity, and has been successfully applied at numerous hydropower and irrigation reservoirs which are drawn down for periods ranging from days to months. It has been

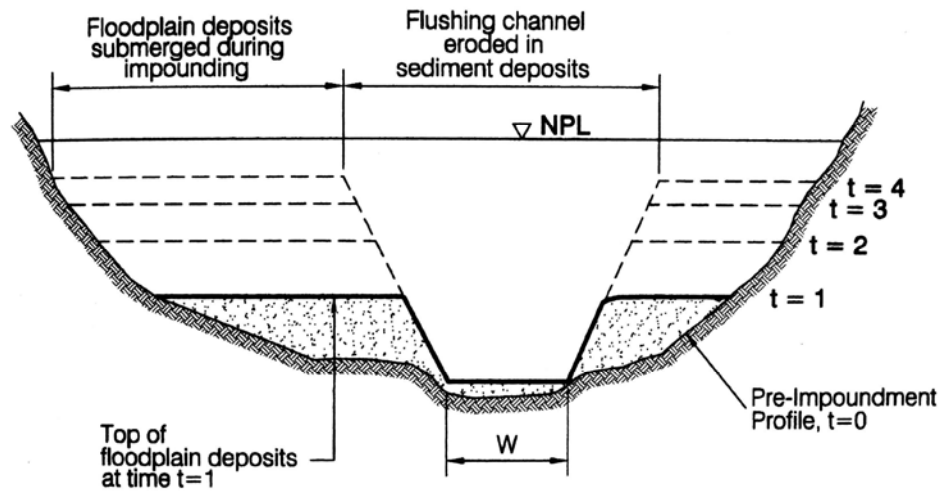


**FIGURE 15.2** Reservoir cross section showing development of flushing channel and adjacent flood-plain deposits that are submerged during normal impounding. The floodplain level will rise over time as deposition continues, but the rate of rise will decrease. In a narrow reservoir, the main channel may span the width of the impoundment and floodplains may be absent.

successfully employed at reservoirs having a wide range of physical sizes but all having a small hydrologic size [a capacity to inflow (C:I) ratio typically less than about 0.3], allowing the reservoir to be refilled quickly when the bottom outlet is closed to terminate flushing. It can also be used at hydrologically larger sites that have been reduced in size by sediment accumulation. Sediment sizes removed by flushing have ranged from clay to gravel. Details of flushing operations at the small Cachi and Gebidem hydropower reservoirs and at the large Sefid-Rud irrigation reservoir are described in their studies, and the combination of sediment routing and flushing is described in the Sanmenxia and the Heisonglin case studies.

#### 15.1.4 Limitations

There are two main limitations to flushing. First, it is necessary to draw down or empty the reservoir. This limits flushing to hydrologically small reservoirs without carryover storage, that can be removed from service during the flushing period. Second, flushing causes sediment to be released from the reservoir at a much higher concentration than occurs in the natural fluvial system. The initial period of flushing, with a duration **ranging** from a few hours to several days, depending on the size of the reservoir, is characterized by extremely high sediment concentrations, typically exceeding 100 g/L at the dam site and in some cases even exceeding 1000 g/L. These extreme concentrations can create unacceptable impacts downstream. Extreme sediment concentrations can clog irrigation canals and heat exchangers for industrial cooling systems, they are unsuited for hydropower use, they can exceed the solids handling capacity of water purification plants, and the combination of turbid water and muddy deposits severely impairs recreational use. Environmental harm can be great; the combination of high sediment concentration (which smothers benthic organisms and clogs gills) and anoxia can kill virtually all the organisms in a stream. Sediment deposits along the streambed may continue to affect the stream benthos long after the flushing has been completed and may also impair navigation and increase flood hazard by reducing channel capacity. Sediment

released from an upstream reservoir will accumulate in a downstream reservoir unless all the reservoirs are managed conjunctively. The environmental consequences of reservoir emptying and potential remedial measures are discussed in Chap. 18.

## 15.2 FEATURES OF FLUSHING

---

### 15.2.1 Flushing Channel Geometry for Fine Sediment

Flushing scours a single main channel through beds of fine sediment while floodplain deposits on either side of the channel are unaffected by erosion. The plan and longitudinal view of a flushing channel is illustrated in Fig. 15.3. During impounding, both channel and floodplain are submerged, and continued sedimentation causes floodplain deposits to increase in height while the main channel is maintained by repeated flushing as previously shown in Fig. 15.2. The bottom width  $W$  of the flushing channel is determined by hydraulic conditions, and the slope of the channel wall is determined by the angle of repose of the deposits. In areas of fine sediment deposits, the main channel usually follows the original pre-impoundment river course.

### 15.2.2 Accumulation of Coarse Sediment Deposits during Flushing

Flushing periods do not necessarily coincide with major floods, as in the case of a reservoir which is flushed during the first month of a 3-month wet season, and a significant amount of bed material can be delivered to and trapped within the reservoir during impounding periods. This is quite different from sediment routing or pass-through for bed material in which large-capacity gates are operated during flood events, whenever they occur, to maintain transport capacity through the impounded reach when the inflow of bed load is significant. As a result, the accumulation of coarse sediment in the form of delta deposits can become a serious problem, even though the accumulation of fine sediment is successfully controlled by flushing.

Flushing is conducted during only part of the year, and sediment transport capacity through a reservoir operated for flushing is less than in the upstream channel. If flushing flows are of insufficient discharge and duration to transport all of the inflowing load, coarse material above a certain diameter and which is supply-limited in the river reach above the reservoir, will become transport-limited and accumulate within the impounded reach. The zone of coarse sediment accumulation within a reservoir that is flushed will depend on the water level during large discharge events, which is a function of impounding operations and the backwater produced by the flushing outlet. The zone of deposition for bed material can also be influenced by previous delta deposition which elevates the base level of the stream, reducing stream slope and causing deposition upstream of the delta regardless of the water level during a flood event.

Patterns of coarse sediment accumulation in reservoirs subject to flushing have rarely been documented. At several flushing sites bed material has been observed to deposit as a delta in the upper portion of the reservoir, similar to the pattern commonly observed in conventionally operated impounding reservoirs. Chen and Zhao (1992) describe the case of the gorge-shaped  $10.2 \text{ Mm}^3$  Nangin irrigation reservoir in Shaanxi Province, China, which experienced a major flood in 1975, its second year of operation. This flood mobilized gravels in the streambed and created backwater deposits 3 to 4 m thick 1 km above the original pool limit, and the zone of deposition extended 2.2 km above the 4.0 km long reservoir pool. The original bed slope averaged 0.006, and the slope in the area of deposits ranged from 0.0014 to 0.0056. As bed material was deposited in the upstream

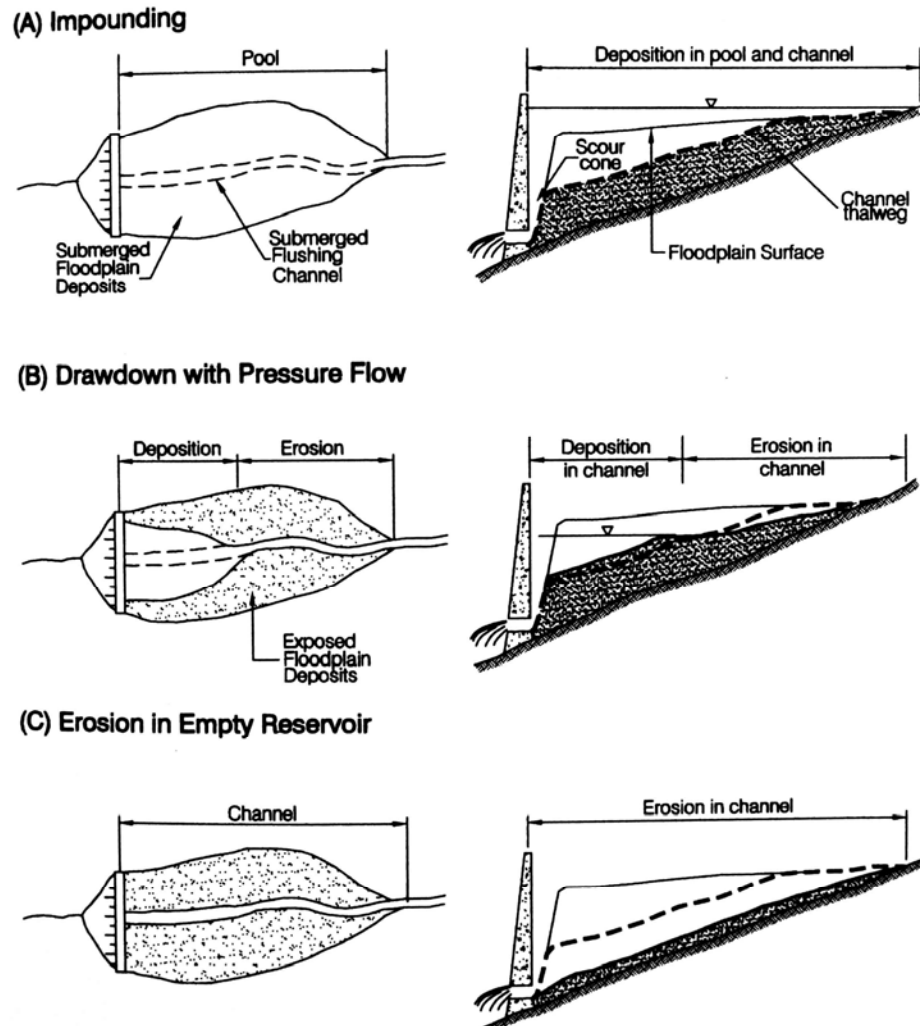


**FIGURE 15.3** Plan and thalweg profile for flushing operations illustrating longitudinal pattern of sediment redistribution during a flushing event: (a) impounding period with deliveries to downstream users; (b) drawdown with erosion in the upper reach of the flushing channel and redeposition near the dam, with pressure flow through the bottom outlet; (c) complete drawdown causing erosion along the length of the reservoir with free flow through bottom outlet.

reach, degradation of previously deposited material occurred further downstream. Over a period of years it was observed that large inflow events caused aggradation of the bed due to the large inflowing sediment load, and these deposits were scoured during years lacking large floods. However, because the rate of scour was low, there is a net accumulation of gravels.

At Cachí Reservoir, coarse material accumulates in the form of a delta at the upstream limit of the normal pool because the annual inflow of coarse sediment exceeds the volume removed during flushing (1 month of drawdown and 3 days flushing). The delta gradually advances toward the dam, burying both the floodplain deposits and the flushing channel. The upper basin of Cachí reservoir accumulated 4 to 6  $\text{Mm}^3$  of coarse material between 1966 and 1990. Despite annual flushing, these deposits have grown to 8 to 12 m

in thickness. Coarse bed materials are also encroaching at Hengshan Reservoir, China, in the form of a broad delta containing sand and gravel. The contrast in deposition conditions in the delta area and near the dam is evident in Fig. 15.4. Although flushing has been effective in removing silts from Hengshan reservoir, the delta is continuously aggrading. At both Cachí and Hengshan Reservoirs the flushing flow crosses the coarse delta deposits as a braided or wide and shallow stream, instead of the deep incised channel typical of the downstream portion of the reservoir.

A second pattern which is also anticipated, but not known to have been documented, is the gradual increase along the bed elevation of the flushing channel downstream of the delta due to the deposition of coarse sediment. The accumulation of coarse bed material in the flushing channel may cause lateral shifting of the flushing channel as its bed elevation rises and fine-grain floodplain deposits on the channel banks are eroded.

The rate of delta accumulation varies widely between reservoirs, depending on the difference between the rate of coarse sediment delivery and its removal by flushing flows. Armoring can limit the erosion rate of delta deposits by flushing discharge. The volume and grain size of the coarse sediment released by reservoir flushing can increase over time as deposits advance toward the dam, increasing the slope and transport capacity of the flushing channel. Additional bed material accumulation upstream of the delta should also be anticipated.

### 15.2.3 Channel Formation and Maintenance

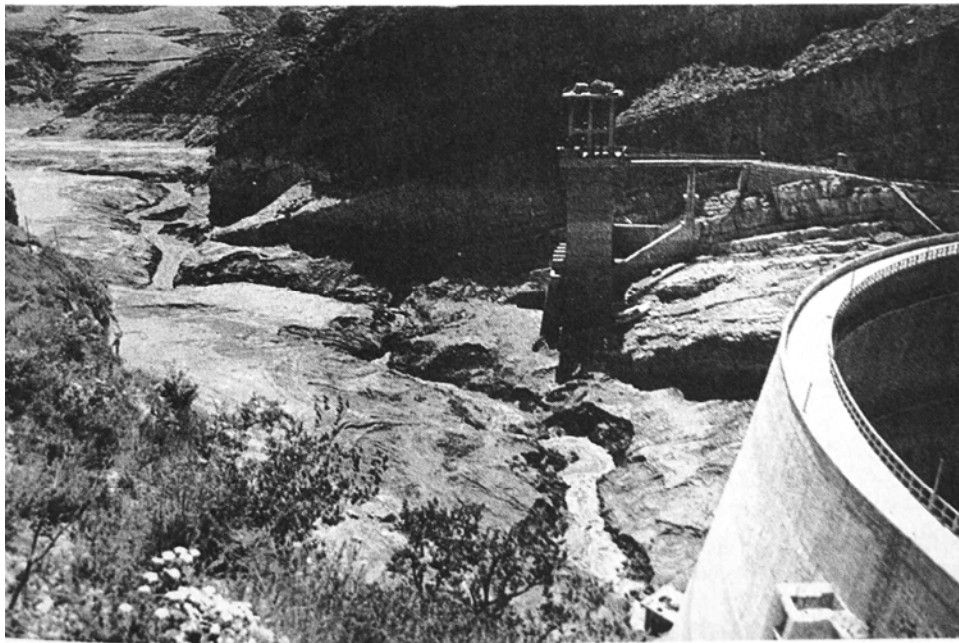
When flushing is initiated at a reservoir that has been accumulating sediment for a number of years, two distinct flushing phases may be identified. During the first, or *channel formation*, phase, existing deposits are eroded to create the main flushing channel, plus any auxiliary lateral or longitudinal flushing channels. During this phase a portion of the reservoir capacity can be recovered. During the second, or *channel maintenance* phase, the flushing channels have already reached their equilibrium size and only recently deposited sediment is flushed out of the channels. Maintenance flushing is typically practiced on an annual basis, although both shorter and longer intervals have been used. Depending on site characteristics and flushing flows, channel formation may require several years of flushing operations. Maintenance flushing must continue indefinitely to sustain sediment control benefits.

During impounding periods much of the fine sediment entering a reservoir tends to deposit in the lowest part of each cross section, especially when turbidity currents are present. When a channel is maintained by flushing, sediment deposition becomes focused within the channel and can be removed during the next flushing event. There are four mechanisms by which flushing reduces sediment accumulation: (1) previously deposited material is removed; (2) sediment entering the reservoir during the flushing period will be routed along the channel and released through the low-level outlet; (3) while impounding sediment deposition is focused in the channel, from which it can be scoured during the next flushing event; and (4) the flushing channel geometry facilitates the movement of turbidity currents toward the dam where they can be released.

The potential importance of the flushing channel in focusing suspended sediment inflow is illustrated by data from the Cachí Reservoir case study. Cachí Reservoir is divided into upper and lower pools by a natural constriction. Because delta deposition of coarse sediment affects most of the upper pool but not the lower, only the lower pool is used in these computations. The flushing channel at Cachí occupies only 9.5 percent of the total surface area of the lower reservoir pool, yet 71 percent of the total inflowing solids load (76 percent of suspended load) either flows as a turbidity current along the submerged channel to the dam where it is discharged through the power intake, or is deposited within the channel and subsequently removed by flushing. The remaining



(a)



(b)

**FIGURE 15.4** Hengshan Reservoir, China. (a) View looking downstream across the delta that is encroaching into the reservoir. Although flushing is effective in removing the silts, this delta containing coarse material is continuously advancing toward the dam. (b) View of flushing channel in deposits of silty material near the dam.

sediments are deposited on the submerged floodplain that occupies 90.5 percent of the reservoir area. The percent of inflowing sediment deposited in the flushing channel depends on site characteristics such as the top width of the channel compared to the full reservoir cross section, the tendency for turbid density currents to form, the hydraulic capacity of the flushing channel, and the operational rule. This question has not been researched in detail.

#### 15.2.4 Flushing Procedures

Each flushing event has three distinct stages: *drawdown*, *erosion*, and *refill*. The characteristic behavior of hydraulic and sediment parameters during flushing are summarized in Fig. 15.5. Reduction in water level to initiate flushing, the drawdown stage, may

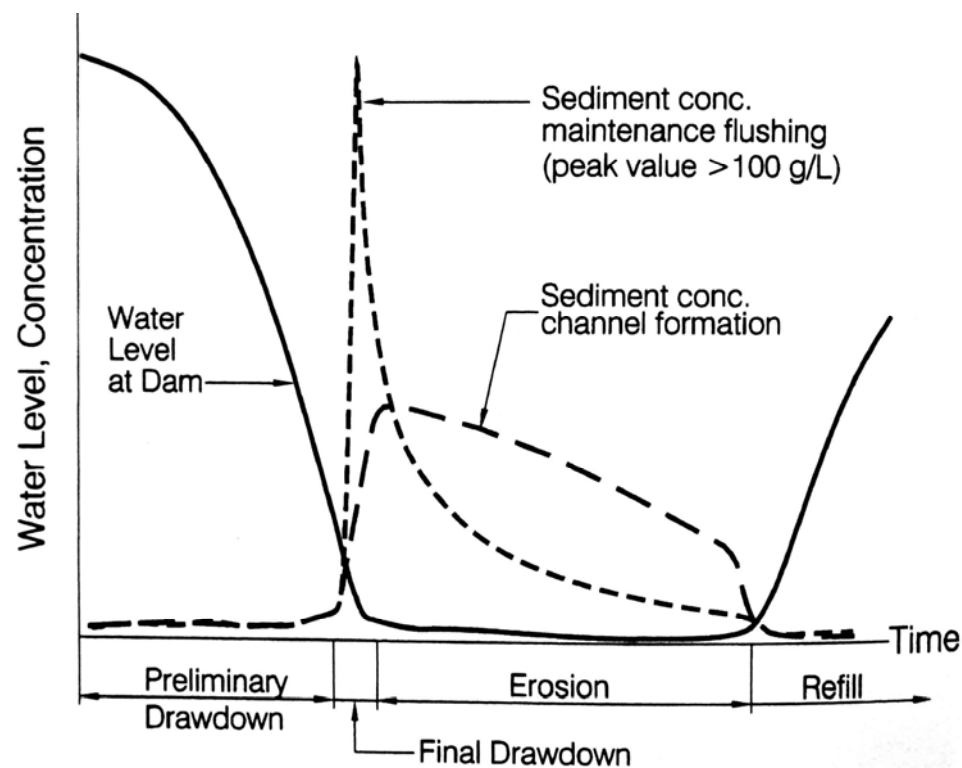


**FIGURE 15.5** Hydraulic and sediment characteristics for channel formation and channel maintenance flushing events at constant discharge.

usually be divided into two parts. *Preliminary drawdown* brings the reservoir to the minimum operational level by delivering water to users or hydropower turbines and typically occurs over a period of days or weeks. *Final drawdown* involves rapid emptying of the reservoir below the minimum operational level using the bottom outlets and usually occurs over a short period of time, on the order of a few hours in smaller reservoirs.

Complex patterns of sediment movement can occur during drawdown. During drawdown, sediments from the upper end of the reservoir can be mobilized and transported downstream where they will be redeposited in the lowered pool, as illustrated by the adjustment in the sediment profile in Fig. 15.3b. A turbidity current may also be formed

**TABLE 15.1** Several Periods of Drawdown Flushing with Density Current Venting at Sanmenxia Reservoir, China, 1962

	Period, 1962					
	1 3/21-4/9	2 4/9-4/20	3 5/16-6/16	4 8/20-8/27	5 9/8-9/25	6 10/15-11/8
Water level, m	308.6	306.0	303.8	310.1	308.5	309.4
Inflow $Q$ , m <sup>3</sup> /s	1120	780	446	1400	1380	1610
Outflow $Q$ , m <sup>3</sup> /s	1200	768	428	1625	1290	1460
Concentration at selected ranges, g/L:						
R41	16.3	18.9	12.7	19.9	27.2	17.1
R31	49.2	27.2	14.8	14.7	18.2	16.7
R22				16.2	20.4	16.6
Outflow	17.7	7.6	5.3	11.7	14.1	9.5
$d_{50}$ at selected ranges, mm:						
R41	0.063	0.064	0.043	0.043	0.062	0.050
R31	0.038	0.048	0.025	0.032	0.023	0.038
R22				0.023	0.031	
Outflow	0.008	0.008	0.008	0.011	0.012	0.011

R41 = 114 km above dam, R31 = 74 km above dam, R22 = 42 km above dam.

Source: Fan (1991).

by the eroded sediment. Individual sediment particles may experience multiple episodes of erosion and deposition during the draw down period.

Measurements made during partial drawdowns at Sanmenxia Dam during 1962 are summarized in Table 15.1. During the March-May period, sediment concentration increased while grain size decreased moving downstream from range R41 to R31, located respectively 114 and 72 km above the dam (location map, Fig. 24.1). This reflects the additional entrainment of fine sediment between the two sections, and possibly the simultaneous deposition of coarser grains. Downstream of R31, the current encountered the pool impounded by the dam and plunged to form a turbidity current that was vented at the dam. There was a significant decrease in both grain size and solids concentration moving downstream as coarser sediment settled out of the turbidity current.

The *erosion stage* occurs when riverine flow is established along the full length of the impoundment, producing high flow velocities that scour fine sediment from the channel and transport the eroded sediments through the dam. Erosion may continue for a few days or for weeks, depending on the site, with longer flushing periods required for higher sediment loads or lower flushing discharges. The *refill stage* begins on closure of the bottom outlet, and rising backwater causes sediment to deposit within the impoundment. Water having a lower sediment concentration may be released during this period to help scour deposited sediment out of the river channel below the dam.

## 15.3 EMPTYING AND FLUSHING

### 15.3.1 Empty Flushing during Flood Season

Some irrigation reservoirs in China are emptied for flushing during the first part of the flood season, passing early-season floods through the impoundment without significant detention. The reservoir is refilled during the latter part of the flood season. By incor-

porating elements of both sediment routing and sediment flushing, this strategy can be more effective than either routing or flushing used alone. Downstream irrigation intakes are supplied from run-of-river flow while the reservoir is empty. Because of the high sediment concentrations that can be released during the flushing period, the downstream irrigation canals must be designed to operate at high non-sedimenting velocities.

Seasonal emptying is also feasible when water demand is seasonal, as in the case of some food processing industries. The Jansenpei (Gen-San-Pee) Reservoir in Taiwan was constructed to supply a sugar mill that operated only 6 months of the year. Originally operated to impound water year-round, the reservoir rapidly lost capacity. After 17 years of conventional operation, a bottom outlet was installed and the reservoir was converted to seasonal operation, allowing free flow through the reservoir during the part of the year the mill was not in operation. The operating rule is presented in Fig. 15.6*a*. As apparent from the sedimentation history of this reservoir (Fig. 15.6*b*), this strategy dramatically reduced the rate of storage loss (King, 1957; Hwang, 1985).

A photograph of the seasonally empty Dashikou irrigation reservoir in China is shown in Fig. 15.7. Operators at the dam reported that the reservoir began to fill with sediment rapidly. An outlet about  $1.5 \times 3$  m was installed with a single vertical sluice on the upstream side. During the initial part of the flood season the reservoir remains empty, passing all inflow through the low-level outlet. Near the end of the flood season the outlet is closed to impound for winter irrigation. This procedure was effective in arresting significant additional deposition and allowed previously deposited material to be flushed out.

### 15.3.2 Empty Flushing during Nonflood Season

Flushing can also be successful during the nonflood season, but will typically require a longer flushing period than flood flushing because of the lower discharge. Limited discharge and inability to route inflowing floods can enhance the tendency for coarse sediment to accumulate, and, because flood season inflow is not routed through the flushing channel, the rate of sediment deposition on floodplain areas can also be expected to be higher. A detailed description of flushing during the nonflood season is provided in the Sefid-Rud case study (Chap. 23).

## 15.4 FLUSHING WITH PARTIAL DRAWDOWN

---

Flushing is most effective in preserving reservoir storage when outlets are placed near the original streambed and the reservoir is completely emptied. However, constraints may limit either the allowable drawdown or the invert elevation of the flushing outlet, requiring that flushing be undertaken with only partial reservoir drawdown. Two examples of this strategy are given. The first is the concept of pressure flushing that was studied but not implemented at Gebidem Reservoir in Switzerland. In this method the reservoir is repeatedly drawn down to the minimum operating level and sediment is evacuated by pressure flow through the bottom outlet. The second example is flushing with a high-level outlet channel placed at or above the intake level, seasonally diverting flow from the intakes to the high-level outlet. In this second method, water deliveries are halted during the flushing period.

### 15.4.1 Pressure Flushing

Under pressure flushing the reservoir is drawn down to the minimum operating level and then the bottom outlets are opened, allowing the development of a conical scour hole in

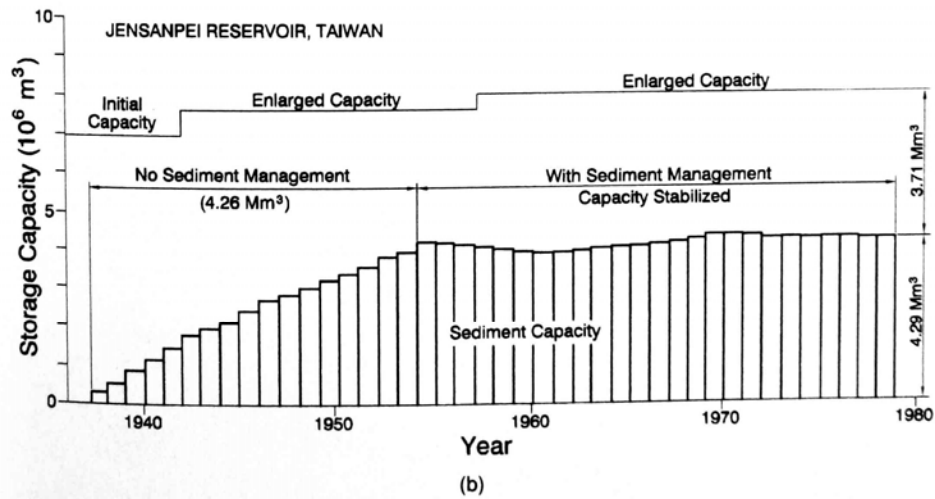
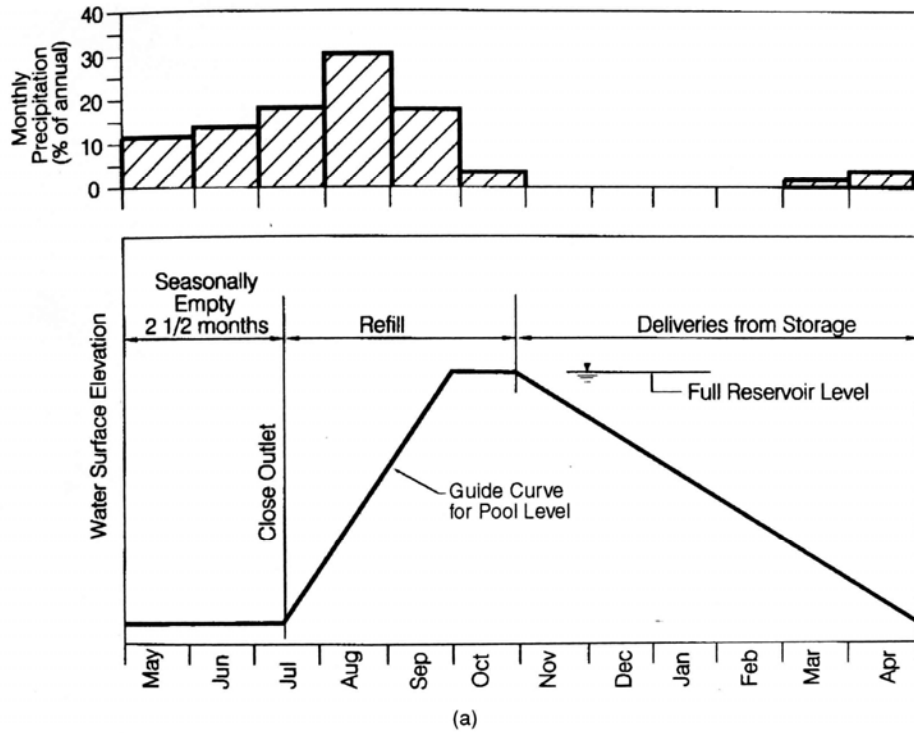


**FIGURE 15.6** Jensanpei Reservoir in Taiwan: (a) operating rule for flood season emptying and flushing, and (b) sedimentation history (after Hwang, 1985).

front of the outlet while maintaining the minimum operating level (Fig. 15.8). Sediment from the upper portion of the reservoir is transported toward the dam during drawdown, but only material in the scour hole in front of the outlets can be evacuated. At Gebidem Reservoir, model tests indicated that the scour hole could be evacuated in only 2 to 3 hours, but it would take 20 to 30 hours to refill the hole with sediment. To discharge the

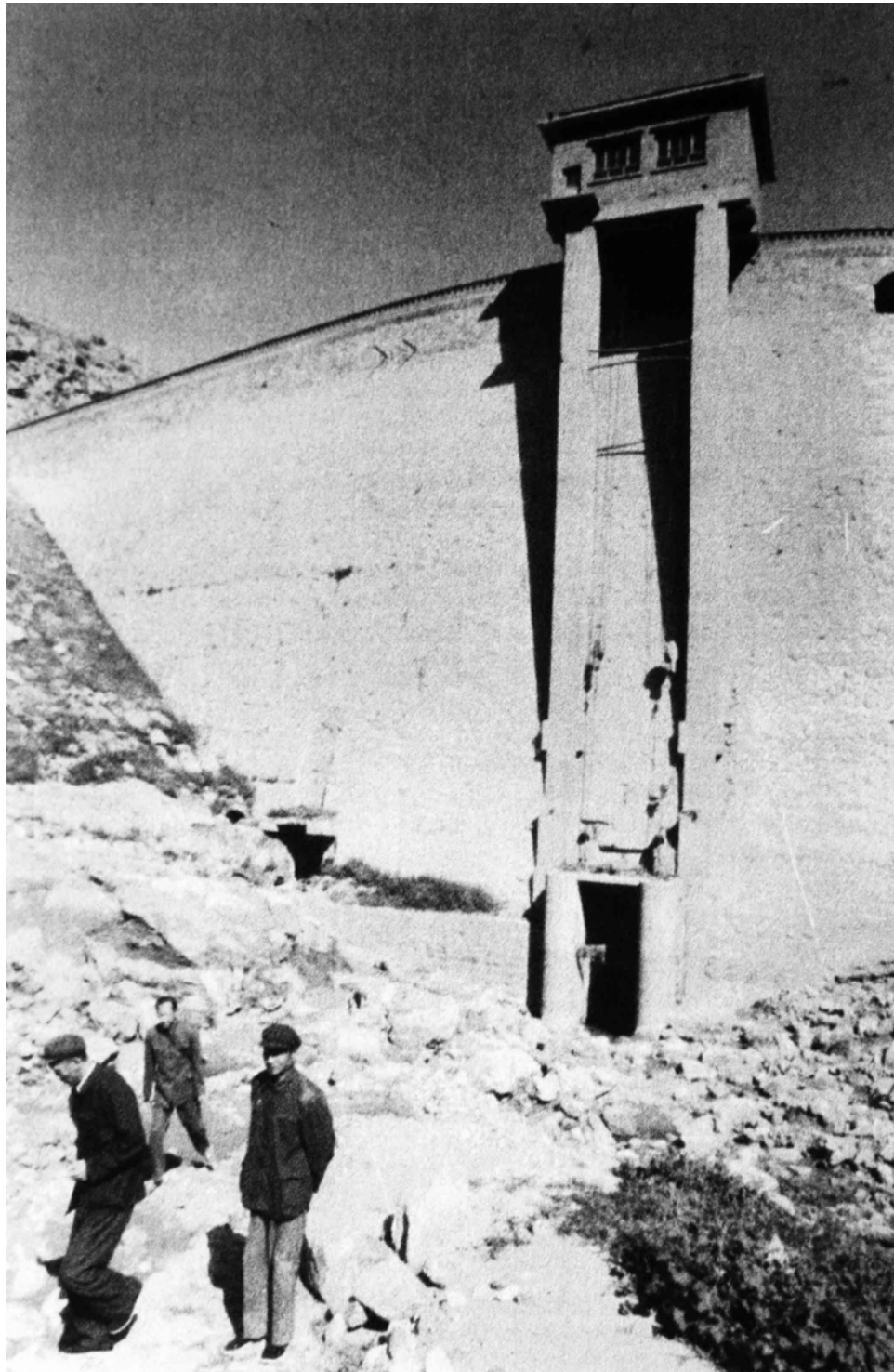


**FIGURE 15.7** Dashikau irrigation reservoir in China, emptied during the early part of the flood season for sediment release (*G. Morris*).

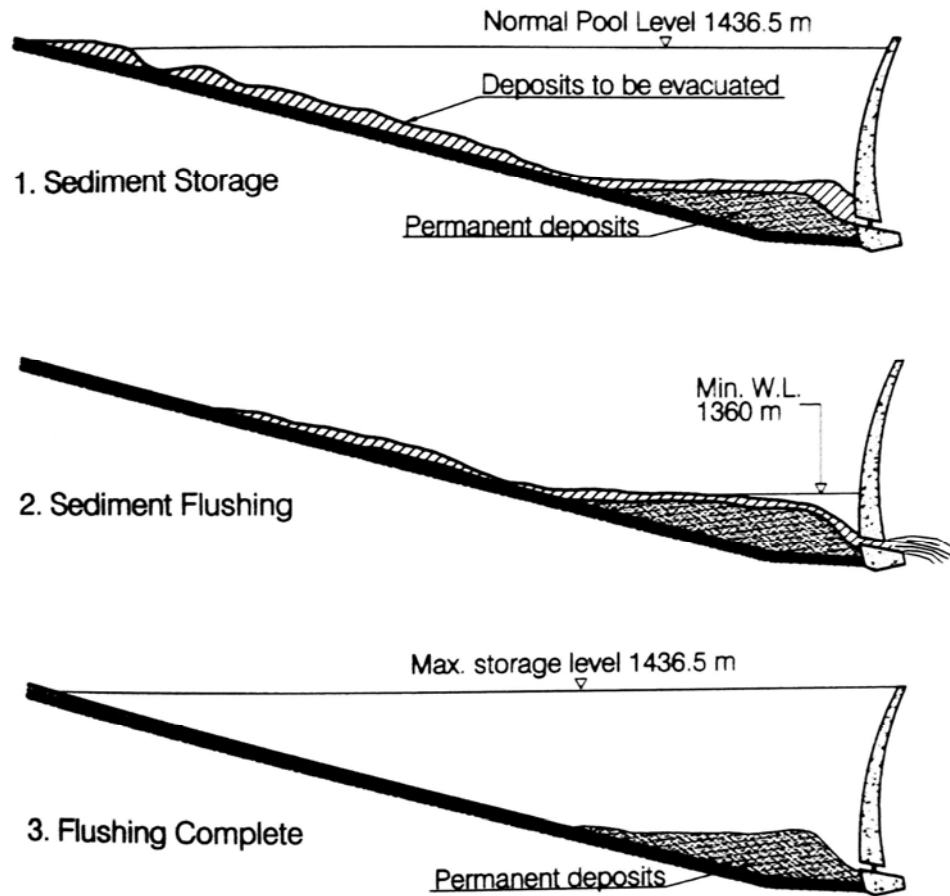


**FIGURE 15.8** Pressure flushing sequence (after Ullmann, 1970).

anticipated 400,000 to 500,000 m<sup>3</sup>/yr of sediment inflow at this site, 10 to 15 drawdowns would be required annually (Ullmann, 1970). This is generally not an effective flushing technique.

#### 15.4.2 Flushing with High-Level Outlet

A proposed method for flushing sandy bed material around Tarbela Dam in Pakistan using partial drawdown has been described by Lowe and Fox (1995). Tarbela is a 137 m high embankment dam on the Indus River used for hydropower production (3750 MW installed capacity) and making up to 5000 m<sup>3</sup>/s of irrigation deliveries. Total capacity was 14,300 Mm<sup>3</sup> at closure in 1974, but 17.4 percent of the total volume had been lost to sedimentation by 1992. The original project was designed for a 50-year economic life with no provisions for the eventual management of the inflowing sediment load of about 208 million tons per year. The consequences of sedimentation at this site are extraordinary.

- Peak summer discharges at Tarbela frequently exceed 8500 m<sup>3</sup>/s. Passage of sand over spillways, with maximum velocities exceeding 30 m/s in the spillway chutes

and flip buckets, could result in catastrophic erosion and spillway disintegration.

- Passing sand through power and irrigation tunnels would create severe erosion, requiring a continuous and extensive maintenance program.
- Sand discharged immediately downstream of the dam would tend to accumulate in the channel, elevating the tailwater and reducing power production. A continuous large-scale dredging program may be required.
- A bedrock acceleration of 0.12g (equivalent to a magnitude 5 earthquake at Tarbela) can liquefy loose saturated deposits similar to those on the foreslope of the Tarbela delta. The final slope at rest after liquefaction failure would be about  $s = 0.005$ . If the toe of the delta is within 8 km of the dam, the liquefied sediments could reach, enter, and clog the intakes, putting the irrigation and electrical generation system out of service for 6 to 12 months.

The inflowing sediment consists of 59 percent fine sand, 34 percent silt, and 7 percent clay. Approximately 99 percent of the inflowing load is trapped and accumulates, primarily in the form of a delta deposit which is advancing toward the dam (Fig. 15.9). Delta topset beds have a slope of about  $s = 0.0006$  to  $0.0008$ . Most sediments are deposit-

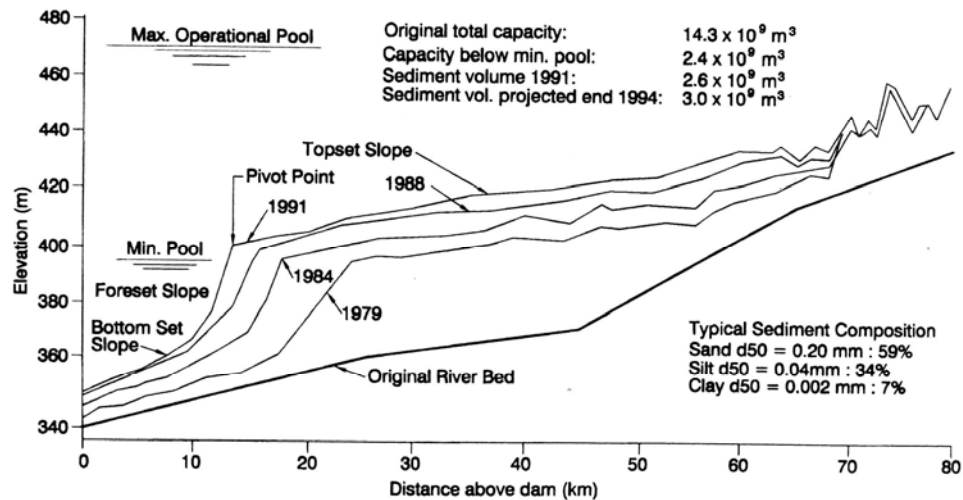


FIGURE 15.9 Advancement of delta deposits toward Tarbela Dam, Indus River, Pakistan (after Lowe and Fox, 1995).

ed on the topset bed as the reservoir fills and levels rise during the wet season, but when the reservoir is drawn down for irrigation deliveries, the river reworks and transports these deposits downstream, extending the delta toward the dam. Most sediment is transported to the face of the delta at the onset of the wet season when the pool level is still low and discharge is increasing from 1500 to 4500  $\text{m}^3/\text{s}$ .

Several sediment management strategies have been considered. Erosion control in the watershed, which drains the tectonically active Himalayas, is not technically feasible. Construction of an upstream dam could temporarily trap sediment, but no such project is ready for construction. Dredging has been discarded because of the extraordinary volume of sediment involved, about  $150 \text{ Mm}^3/\text{yr}$ . A normally-submerged rock embankment or dike constructed upstream of the intakes, and submerged at normal pool level, can temporarily prevent encroachment of the toe of the delta into the intakes. By gradually raising the minimum pool elevation, all delta deposition can temporarily be focused into

areas more than 8 km above the dam. These last two measures, used together, can delay serious sediment problems by as much as 40 years. Nevertheless, continued long-term operation of the project can be realized only by developing a system to pass sediments beyond the dam.

Under the proposed long-term sediment management strategy, coarse sediment would be trapped in the upper part of the pool during impounding periods. The deposited material would be flushed through a high-level bypass channel around the dam at the beginning of the subsequent flood season by lowering the pool following irrigation season deliveries. Because this strategy involves temporary sediment storage and remobilization, it is classified as a flushing technique rather than sediment routing. The invert elevation of the flushing channel would be set more than 80 m above the original streambed elevation, and also above the level of the hydropower intakes. This high invert elevation reflects cost and technical considerations associated with construction of the large-capacity (4500 m<sup>3</sup>/s) bypass channel. A normally submerged dike would be constructed around the power intakes, thereby allowing delta deposits to approach the vicinity of the dam and enter the high-level flushing channel without entering the intakes. The concrete-lined trapezoidal flushing channel would have a 60 m bottom width and 15 m depth, with its upstream invert about 20 m below the dike crest. This layout is conceptually presented in Fig. 15.10, which shows the normally submerged semicircular dike which protects the intakes from bed material and also diverts water and sediment into the bypass channel when the reservoir is drawn down for flushing. The channel would discharge sediment during a 20- to 30-day period of low reservoir levels at the beginning of each wet season, and sediment concentration in the diverted water is expected to run between 1 and 5 g/L based on field measurements of sediment concentration in the river as it flowed across the delta deposits. Reservoir volume would be stabilized at a size significantly smaller than the original capacity. All power production would necessarily cease during the flushing period. Because Tarbela is a major source of electrical energy in Pakistan, an alternative power supply is required to sustain electrical service during flushing periods.

## **15.5 EROSION PROCESSES DURING FLUSHING**

---

Flushing releases are characterized by both extreme and highly variable sediment concentrations. Channel erosion and slope failures within reservoir deposits dominate during the flushing process, and sheet erosion of deposited floodplain sediment is insignificant.

### **15.5.1 Slumping at the Dam**

When a bottom outlet is first opened to initiate flushing, and if poorly consolidated fine sediment have accumulated above the outlet, slope failure can be initiated in the vicinity of the outlet with slumping and plastic flow of the deposits. This slumping is illustrated in the photograph at the small Santa Maria Dam in Guatemala (Fig. 15.11). A similar pattern has been observed by the first author at small reservoirs in Puerto Rico. At Hengshan Dam in China, mud on the floodplain surface within 350 m of the dam slid gradually into the channel and was released through the bottom outlet over a period of several days (Fan, 1985). At the 20-MW Mangaho River project in New Zealand, 59 percent of the storage capacity had been lost after 45 years and the bottom outlet was buried under 13 m of silt after 25 years without sluice operation. There was no flow during the first day the gate was opened, but on the second day silt began to extrude from the

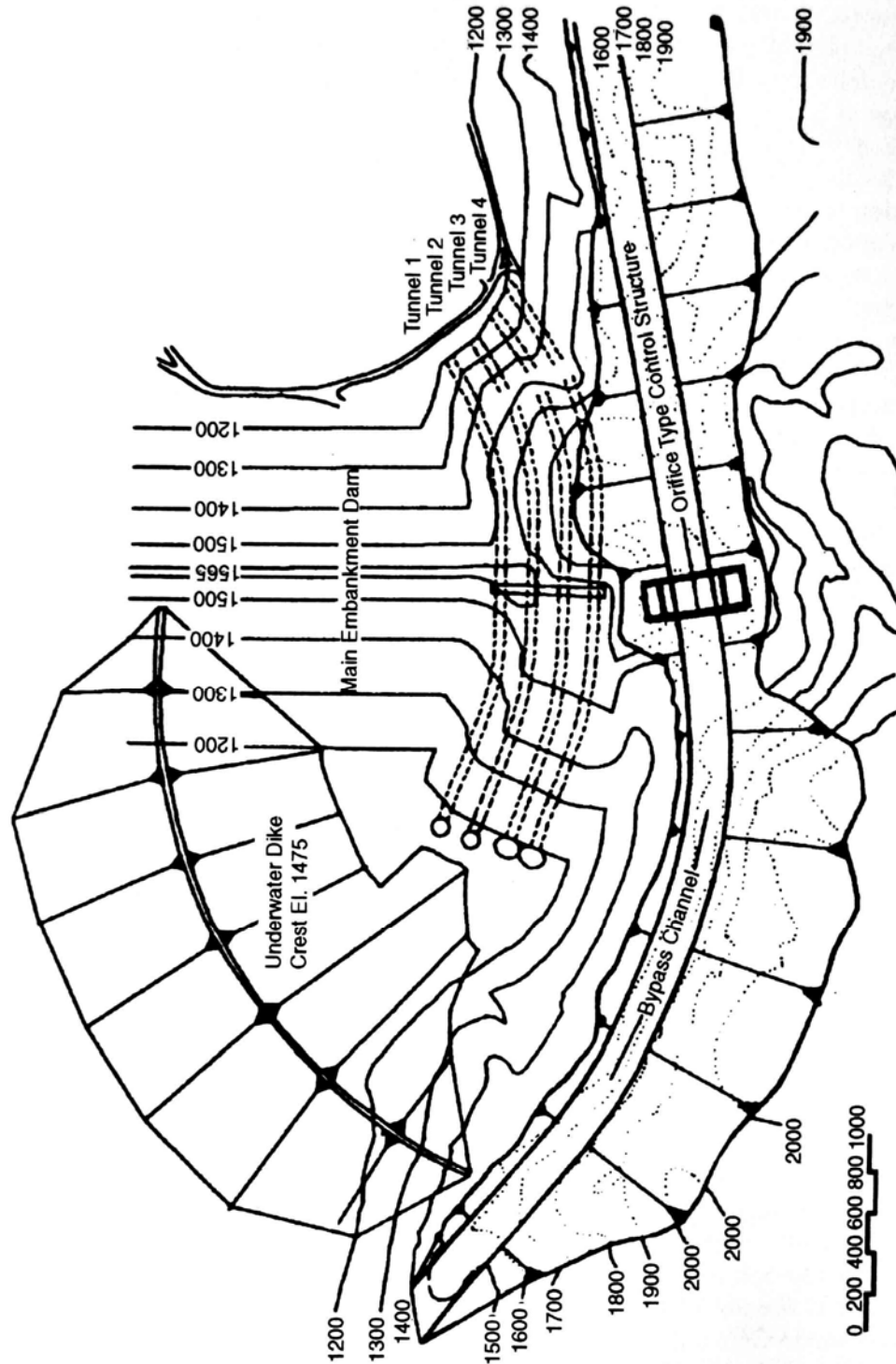


**FIGURE 15.10** High-level Sediment bypass system proposed at Tarbela Dam (after Lowe and Fox, 1995). The underwater dike is used to allow delta deposits to reach the high-level bypass channel, without entering the power intakes. Elevations and distances in feet.



**FIGURE 15.11** Slumping of fine-grained deposits near the dam in the small 285,000 m<sup>3</sup> Santa Maria reservoir on Río Samala, Guatemala, as sediment is discharged through bottom outlets. Sediment slumping was accelerated and removal enhanced by closing gates to temporarily inundate the deposits, then draining the reservoir a second time (V. Galay).

bottom outlet, emptying the reservoir and leaving a crater-like depression above the sluice entrance. About 75 percent of the accumulated sediment was flushed during the subsequent month. During this period it was necessary to haul out logs and tree stumps that blocked the sluice entrance. Thereafter flushing was undertaken annually (Jowett, 1984).

### 15.5.2 Slope Failure

The erosion of flushing channels produces unstable banks which will slump or slide into the channel, and bank failure is the primary mechanism involved in the widening of flushing channels. The main flushing channel may deepen until it encounters the armored bed of the preimpoundment river, after which further erosion can occur only by widening

of the channel by bank failure. The type of slope failure and the stable angle of repose will depend on the sediment characteristics. Examples of several forms of bank slides observed during flushing at Sefid-Rud are illustrated in Figs. 23.19, 23.21, and 23.22.

### 15.5.3 Retrogressive Erosion

A channel erosion process characterized by a zone of high slope and rapid erosion, moving upstream along a channel having a lower slope and erosion rate, is termed *retrogressive erosion*. This process is illustrated in Fig. 15.12a, based on observations in a laboratory flume, and in Fig. 24.14 as observed in Sanmenxia Reservoir. The highest rate of erosion occurs along the steep drop at the downstream end of the deposit, causing this area of maximum erosion to move upstream through a headcutting process similar to gully erosion. The point of slope change or headcut may be visually apparent as shown in

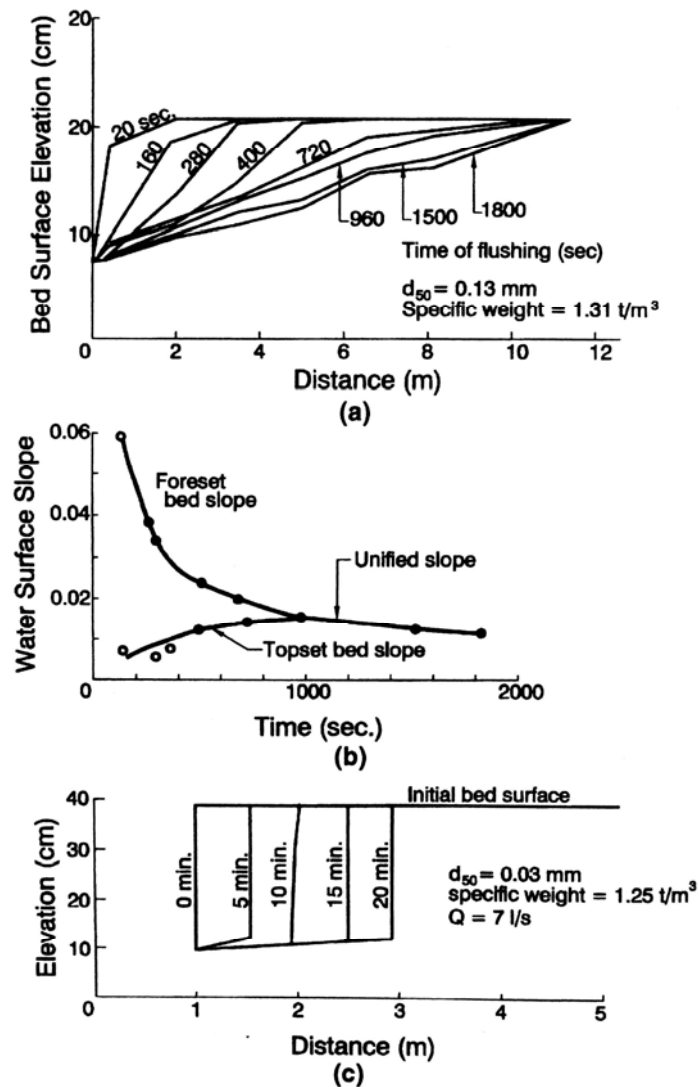


**FIGURE 15.12** Characteristics of retrogressive erosion from flume tests. (a) Longitudinal profile in unconsolidated deposits. (b) Transition toward a unified slope over time, corresponding to flume test shown in a. (c) Longitudinal profile in consolidated sediments.

Figs. 23.20 and 25.13. The point of slope change is also called the *pivot point* or the *nickpoint*, and the term *nickpoint erosion* is also used to describe retrogressive erosion. Multiple headcuts can be formed along the length of an eroding channel.

Retrogressive erosion is the principal method for the formation of flushing channels through reservoir deposits. The opening of deep outlets – which establishes flow across deposits having a relatively mild slope, with an abrupt drop or even a waterfall at the downstream end – initiates retrogressive erosion, creating a nickpoint that can move upstream rapidly depending on the nature of the deposits and the erosional forces. At Sanmenxia Reservoir on the Yellow River, a reach extending 80 km upstream from the dam was affected by retrogressive erosion between October and November 1964, the longest such phenomenon recorded in a reservoir (Fig. 24.14). In contrast, retrogressive erosion lasts less than 24 hours in erodible silt deposits in smaller reservoirs in China such as the 2-km-long Hengshan Reservoir. In more consolidated deposits, retrogressive erosion will move upstream more slowly. Erosion moved upstream at the rate of 100 m/day in cohesive sediments at Sefid-Rud Reservoir (Tolouie, 1993).

Retrogressive erosion results from the change in hydraulic energy caused by the discontinuous longitudinal profile, and it is not dependent on any specific grain size in the deposit, although erosional patterns are influenced by the deposit characteristics. Retrogressive erosion can occur in coarse sediments on a river delta (Randle and Lyons, 1995) and also in fine-grained and cohesive sediments. In noncohesive or unconsolidated cohesive sediments retrogressive erosion tends to proceed upstream as shown in Fig. 15.12a. In consolidated deposits the eroding face tends to be more nearly vertical as in Figure 15.12c. The creation of a stepped erosion face created by alternating layers of cohesive and noncohesive sediment was observed at Sefid-Rud Reservoir (Fig. 23.14). As retrogressive erosion proceeds there is a gradual transition of the foreset and topset slopes to a unified slope, as shown in Fig. 15.12b. The most intense erosion occurs in the area of highest slope and the pivot point (or nickpoint) continuously moves upstream, causing the foreset slope to decrease. At the same time channel erosion causes the topset slope to increase, until a unified slope is achieved. At this point retrogressive erosion has ended and the erosion process may now be termed *progressive erosion*. Jiang (1992) reports that sediment transport computations based on unit stream power have been used to predict rates of retrogressive erosion.

#### 15.5.4 Progressive Erosion

The term *progressive erosion* refers to a channel erosion process which occurs uniformly or progressively along the length of a channel instead of being concentrated at the downstream end. In general, when the suspended-sediment concentration in flowing water is less than the sediment carrying capacity, the flow will entrain sediment from the channel bed. When clear water enters a zone of erodible deposits having uniform slope and grain size, it will progressively entrain sediment by eroding the deposit. The rate of bed erosion will initially be rapid because of the large available sediment-carrying capacity of clear water. As the flow progresses downstream and entrains sediment, its capacity to erode and transport additional sediment will decrease, eventually reaching zero. In this manner progressive erosion can cause a high rate of bed erosion at the upstream end of a deposit and less erosion at the downstream end. This erosion pattern can be offset in reservoirs by the tendency for deposits to be coarser and less erodible at the upstream end.

### **15.6 VARIATION IN EROSION RATE AND SEDIMENT RELEASE**

The rate of channel erosion may be limited by either the erosive hydraulic forces or the available sediment supply in the channel, and in the riverine environment the discharge of

sediment of different grain sizes may be characterized as either transport-limited or supply-limited. The wash load is typically supply-limited, since the load of fine sediment is almost always limited by the rate of supply from the watershed rather than hydraulic transport capacity. Conversely, the load of coarse bed material is transport-limited, since hydraulic transport capacity rather than sediment abundance is the limiting factor. The same concept applies to the rate of sediment release during the flushing process and can be used to explain variations in the concentration and grain size of sediment release during flushing events.

### 15.6.1 Within-Event Variability

Flushing events are characterized by large changes in the rate of channel erosion and the suspended-solids concentration in the flow exiting the dam, as illustrated in Figs. 15.5, 19.18, 21.6, 23.15, and 25.8. These variations primarily reflect changes in the availability and erodibility of fine sediment during the flushing event.

Channel formation and channel maintenance tend to produce two distinct patterns of sediment release. Material deposited in previous years or decades is continuously scoured during *channel formation*, producing sediment concentrations which are initially high and decline gradually (Fig. 15.5). The maximum concentration and rate of sediment release is limited by the erodibility of the deposit, which has become consolidated over time. Concentration variations will occur over the course of a flushing period because of changing inflow rate and variations in the rate of sideslope failures along the flushing channel.

During *maintenance flushing* the channel will contain only recently deposited materials which are readily mobilized, including recently reworked sediment. The transition from drawdown to riverine flow during a maintenance flushing event is characterized by a dramatic increase in the sediment concentration discharged from the dam as the unconsolidated fines in the submerged channel near the dam are rapidly evacuated, generating short-term sediment concentrations of hundreds of grams per liter. However, as the readily eroded material is washed out, the concentration of fines becomes supply-limited, depending on the rate of bank erosion and collapse. In contrast, the discharge of coarse material (e.g., sands) may be transport-limited throughout the flushing event and may be much more uniform over time. Thus, during a maintenance flushing event, the release of fine sediment may be initially transport-limited and subsequently supply-limited, and will typically exhibit extreme variations in concentration and rate of release. In contrast, the discharge of coarse bed material (including sediment eroded from delta deposits) may be transport-limited throughout the event and experience much smaller variations in concentration and rate of release. As a result, in a reservoir having a significant load of both fine and coarse sediment, short flushing periods may be effective in removing fines but longer flushing periods and larger flushing flows will be required to remove the inflowing load of coarse material.

### 15.6.2 Between-Event Variability

During channel formation the discharged sediment is derived from the erosion of older and more consolidated deposits. Sediment concentrations remain high during the entire flushing event as the flow continuously erodes deposits. In contrast, maintenance flushing erodes the recently deposited and poorly consolidated fines from the channel, producing a short period of extreme sediment concentration including hyperconcentrated flow, until the channel sediment supply is exhausted. These contrasting mechanisms can cause wide between-event variations in sediment concentration. Peak concentrations in channel maintenance events at Sefid-Rud were almost double the concentrations during channel formation events (Table 15.2). Variation in the delivery of fines to the reservoir also

causes sediment discharge to be highly variable between events, as illustrated by the high variability between maintenance flushing events at Cachí Reservoir, also shown in Table 15.2. The high load evacuated in 1988 at Cachí reflects increased sediment input from flooding and a landslide (Jansson, 1992a). The high variability at Sefid-Rud and Cachí have occurred even though both sites been operated in a consistent manner over the period covered by the data, subject to normal operational variations caused by natural events such as floods. These data illustrate the difficulty of accurately predicting sediment release during flushing.

**TABLE 15.2** Variation in Sediment Discharge and Concentration During Flushing

Year	Cachí		Sefid-Rud	
	Peak Concentration, g/L	Sediment Removal 10 <sup>6</sup> t	Peak Concentration g/L	Sediment Removal 10 <sup>6</sup> t
1981		0.477	170*	24
1982		0.386	180*	12
1983		0.545	145*	52
1984		0.665	195	68
1985			344	142
1986			330	46
1987			292	27
1988	430	1.266	305	57
1989	170	0.482	398	54
1990	280	0.653	284	32

\*Channel formation stage. All other events are maintenance flushing.

Source: Sefid-Rud data from Tolouie (1993); Cachí data from Ramirez and Rodriguez (1992).

Data from 38 flushing events with full drawdown at the Zemo-Afchar hydropower station located downstream of the Kura and Aragvi Rivers in the former Soviet Union were reported by Gvelessiani and Shimaltsel (1968) and again reflect a high degree of variability. During the first 2 years of operation the reservoir lost 44 percent of its capacity, another 32 percent was lost in the next 8 years, and 4 percent was lost in the next 18 years (1937 to 1954). Prior to 1939 the reservoir had been operated with limited drawdown for flushing, but this was not effective. From 1939 through 1966 a total of 38 flushing events were conducted with full drawdown, for which data from 36 were reported. Flushing frequency varied from once to as many as four times a year. The relationship between mean suspended sediment concentration and mean discharge below the dam (Fig. 15.13) shows that larger discharges tended to remove more sediment, yet produced lower mean sediment concentrations. The highest mean sediment concentrations were associated with the shortest flushing duration because the highest solids concentration occurs at the beginning of the event and then declines. There is a wide range of variability from one event to another because of factors including flushing duration and sediment accumulation between flushing events. Peak discharge concentrations, reported for only two events, were 270 and 370 g/L.

### 15.6.3 Effect of Discharge on Erosion Rate

Guo and Li (1984) analyzed flushing at the Hengshan Reservoir in China and noted that lower (base flow) discharges tended to cut a narrow deep channel, but a wider channel

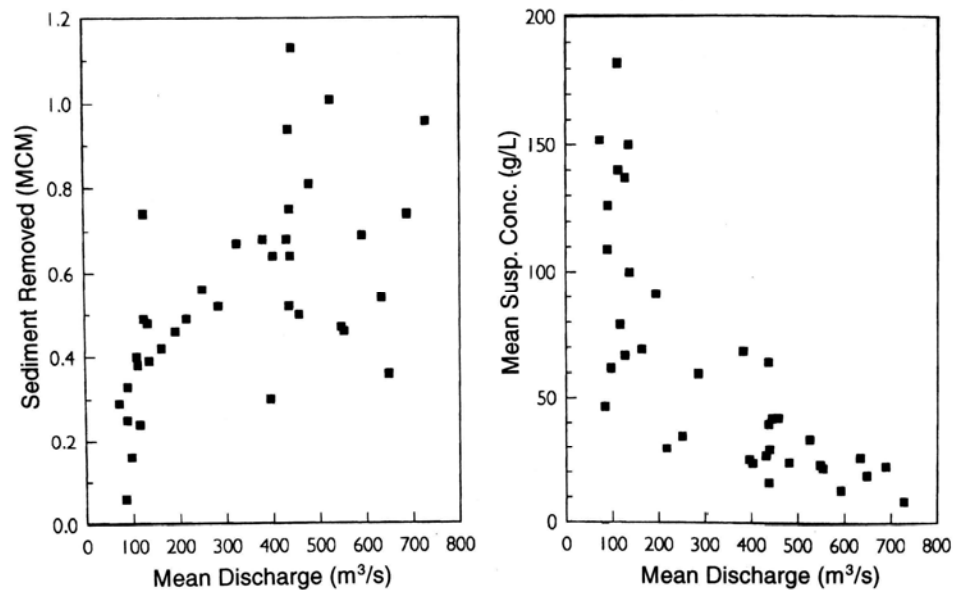


**FIGURE 15.13** Flushing discharge relationships for 36 flushing events at Zemo-Afchar reservoir in the former Soviet Union (data from Gvelessiani and Shimaltsel, 1968). Mean discharge refers to the duration of the flushing event. MCM = 106m<sup>3</sup>.

can be produced with a larger flow. Actually, the channel may be deepened by using either smaller or larger flows, but widening is achieved by large flows only. In China it was found that the flushing effect is maximized if a reservoir is emptied immediately prior to the arrival of floods so that the flood flow can exert its erosive force on deposits which have not yet had the opportunity to fully dewater and consolidate after emptying the reservoir. The phrase used to describe this strategy is "Deepen by small flow, widen by flood flow." That larger flows widen flushing channels has also been observed in sediments with a high clay content (Tolouie, 1993) and in coarse noncohesive delta deposits (Randle and Lyons, 1995). On the basis of work in Algeria, Duquenois (1956) described the use of a small storage dam upstream of a reservoir to temporarily store and then rapidly release water, converting a continuous inflow into a series of larger pulsed flows. The pulsed flow scoured delta deposits and created turbid density currents to transport sediment closer to the dam.

## 15.7 FLUSHING EFFICIENCY

### 5.1.1. 15.7.1 Definition

The term *flushing efficiency* ( $F_e$ ) is defined as the ratio of deposit volume eroded to the water volume used during flushing over any specified time interval. For inflow and outflow water volumes  $V_i$  and  $V_o$  (m<sup>3</sup>), inflow and outflow total sediment concentrations  $C_1$  and  $C_o$  (kg/m<sup>3</sup>), and deposit bulk density  $\rho$  (kg/m<sup>3</sup>), flushing efficiency  $F_e$  may be computed by:

$$F_e = \frac{(V_0 C_0 - V_i C_i) / \rho}{V_0} \quad (15.1)$$

During empty flushing when  $V_0$  and  $V_i$ , and if  $C_i$  and  $\rho$  are constant, flushing efficiency is directly related to  $C_0$ , the total solids concentration in the discharge. An alternative expression for flushing efficiency is the *water: sediment ratio* (Qian, 1982), which is the inverse of flushing efficiency ( $1/F_e$ ).

### 15.7.2 Flushing Efficiency with Partial Drawdown

Reservoir drawdown during flushing may be limited by operational requirements, or by the elevation of the available outlets if no bottom outlets are provided. When flushing flow is discharged through outlets located significantly above the level of the deposits, resulting in a pool of impounded water before the dam, the flushing efficiency is typically very low. Flushing efficiencies for several reservoirs where sediment was released through high-level outlets are summarized in Table 15.3. Flushing under conditions of partial drawdown may erode upstream sediments and redeposit them closer to the dam, and, if a low-level outlet is opened, some of the eroded sediment may be vented as a turbidity current, but this is an inefficient means of removing sediment from a reservoir. Effective sediment removal through a high-level outlet can be achieved only after the bed of the deposits has risen close to the level of the outlet, as described at Tarbela Dam in Sec. 15.4.2.

Flushing with partial drawdown may be useful under specific circumstances. For example, drawdown and sediment release through a high-level outlet was undertaken at the Guernsey Reservoir in Wyoming to deliver fine sediment to a downstream unlined irrigation canal. The sediment partially sealed the canal bottom and reduced canal seepage losses. Although sediments were scoured from the upper portion of the reservoir during the 1961, 1962, and 1963 drawdowns, the suspended solids concentration in water discharged from the reservoir never exceeded 0.8 g/L (Jarecki and Murphy, 1963). The principal effect of these and subsequent drawdowns has not been to release sediment, but

**TABLE 15.3** Overflow Drawdown Flushing

Reservoir	Outflow situation	Years of operation	Discharge, m <sup>3</sup> /s	Duration	Flushing efficiency	Water:sediment ratio
Guernsey, U.S.A.	Overflow spillway	1960-1962	56.6 - 198	10-18 days	0.00017	5880
Warsak, Pakistan	Overflow spillway	1976-1979, 5 flushings	1410	Total 490.5 h	0.00169	592
Liujiaxia, China	Overflow and outlets; water level lowered = 4.4-7.8 m	1981,1984, 1985,1988	1660 - 2090	103 - 177 h	0.0023 - 0.0071	435-141
Shuicaozi China	Overflow spillway	1965,1966, 1974, 1978, 1980, 1981	21.4-230	3-4 days	0.012 - 0.043	83-23

*Source:* Fan (1995).

to redistribute sediment within the reservoir by removing it from the upper pool and redepositing it closer to the dam (Lara, 1973)

### 15.7.3 Flushing Efficiency with Emptying

The flushing efficiency achieved at several sites under conditions of reservoir emptying is summarized in Table 15.4. These are mean values for the entire event, including the period of extremely high sediment removal at the beginning of the event as well as the subsequent period of lower-concentration discharge and low flushing efficiency. Reported values for flushing efficiency vary widely and are heavily influenced by flushing duration, and will also be heavily influenced by the amount of sediment inflow during the preceding impounding period. For example, flushing efficiency during 36 events at Zemo-Afchar varied from 0.006 to 0.12 (computed with data from Gvelessiani and Shimaltsel, 1968). In laboratory tests of reservoir flushing by Lai and Shen (1996), about half the total volume of sediment removed was eroded during the first third of the flushing period, producing a pattern of flushing efficiency which was initially high (about 0.10) when retrogressive erosion was initiated, and declined asymptotically to a lower level (about 0.025).

A high flushing efficiency is not necessarily synonymous with desirable or effective sediment management. For example, the flushing efficiency for the removal of coarse material will necessarily be lower than for fines, and if a site is operated to maximize flushing efficiency it may continuously accumulate coarse sediment. High flushing efficiency may also generate sediment concentrations downstream which are excessive from the standpoint of other users or the environment.

**TABLE 15.4** Flushing Efficiency for Reservoir Emptying

Reservoir	Years of Operation	Discharge, m <sup>3</sup> /s	Duration of Flushing	Flushing efficiency	Water:sediment ratio
Gebidem, Switzerland	1969-1994	35	35 h/yr	0.048-0.060	21-17
Barenburg, Switzerland	1985	90	20 h	0.06	17
Ferrera, Switzerland	1985			0.026	38
Gen-shan-pei, China	1958-1983		53 days/yr	0.0897	11
Santo Domingo, Venezuela	1978	8-10		0.09-0.13	11-8
Donfanghong, China	1984	51		0.056-0.083	18-12
Sefid-Rud, Iran	1980-1987		61-157 days	0.022-0.067	45-15
Zemo-Afchar, U.S.S.R.	1939-1966	72-688	13-76 h	0.015-0.096	67-10
Chirurt, U.S.S.R.	1968	400-500	5 days	0.04	25

## 15.8 AUXILIARY FLUSHING METHODS

Natural processes that erode floodplain deposits include tributary stream channels that enter the reservoir and direct rainfall impact on deposits exposed during flushing. Neither causes significant erosion of deposits, and, when floodplain sediments are exposed to air during flushing events, their surface layers can become hardened thereby increasing their resistance to erosion. The only effective hydraulic means to remove floodplain deposits is by erosion using auxiliary flushing channels arranged either laterally or longitudinally across the sediment deposits. Auxiliary channels can scour sediment from a larger portion of the reservoir than the single main channel. Sediment removal can also be assisted by mechanical methods.

### 15.8.1 Lateral Erosion

The use of auxiliary flushing channels which drain laterally across floodplain deposits, from the sides of the reservoir into the main flushing channel, is termed *lateral erosion*. This technique was first implemented and described by Xia (1989) at Heisonglin Reservoir in China (sec. 25.8). Figure 15.14 illustrates the principal components of the system including the upstream diversion dam, supply channel, and lateral channels for scouring sediment.

Lateral erosion is undertaken by diverting river flow into a supply channel following the margin of a reservoir, releasing this flow at various points, and allowing it to flow across floodplain deposits toward the main channel. Lateral erosion can only be performed after a flushing channel has been established. The desired scour pattern may be laid out beforehand by digging a series of shallow pilot trenches extending across the sediments from the supply channel to the main flushing channel. These may be excavated while the reservoir is empty or during impounding periods using a dredge. Sediment excavated from the pilot channels may be placed on the adjacent channel banks, since they will collapse and the sediment will be carried away as the lateral channel is deepened and widened.

Lateral erosion has the advantage of using relatively short channels with high slopes between the supply channel turnout and the main channel invert. Sediment removal can

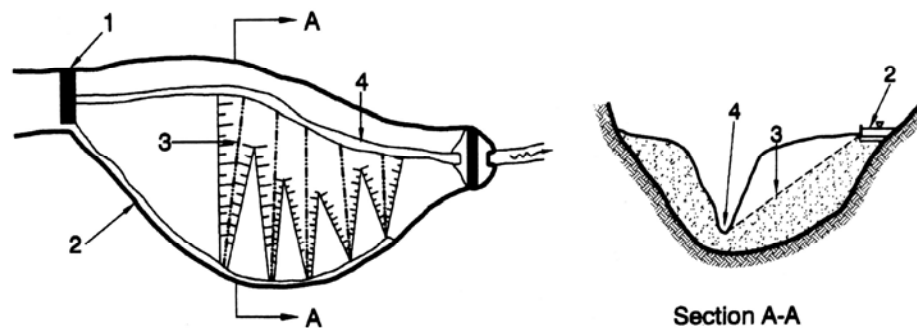


**FIGURE 15.4** Conceptual layout of auxiliary channels for lateral erosion. (1) Diversion dam. (2) Diversion channel. (3) Thalweg of lateral channel. (4) Main flushing channel. Based on layout at Heisonglin Reservoir, China.

be achieved with relatively low discharges, especially in silty deposits. However, because erosion rate is greatly accelerated and a wider channel can be created by using higher flow rates, the supply channel and turnouts should be designed to use the highest flow rate possible. The Sefid-Rud case study (sec. 23.5) describes the use of piping to establish lateral erosion channels in areas of cohesive sediment overlying permeable sands.

Data on lateral erosion at several sites in China are summarized in Table 15.5. The 3.5-Mm<sup>3</sup> Hongqi Reservoir in Shaanxi Province, China, lost 36 percent of its storage capacity within 5 years, and a variety of methods for removing the silt deposits were tested and compared, as summarized in Table 15.6. The high efficiency of lateral erosion, as reflected in the high discharge concentration, was attributed to the high lateral slopes that could be developed between the supply channel and the flushing channel invert. Lateral slopes were 4 to 15 times greater than the longitudinal slope at this site (Zhang et al., 1992).

### 15.8.2 Longitudinal Erosion

The concept of longitudinal erosion by a diversion channel is similar to that of lateral erosion, but uses a different geometry. One or more longitudinal pilot channels excavated parallel to the main channel are eroded by using water from a tributary or by diversion of the main river. Flow along the pilot diversion channel erodes sediment as in the original formation of the main flushing channel. This method was field-tested using a single large channel at the Sefid-Rud Reservoir and is described in Sec. 23.6.

**TABLE 15.5** Lateral Erosion at Selected Chinese Reservoirs

Reservoir	Sediment inflow, m <sup>3</sup> /yr	Reporting period, years	Total erosion duration, months	Mean erosion discharge, m <sup>3</sup> /s	Mean sediment removal, m <sup>3</sup> /day	Total sediment removed, m <sup>3</sup>
Heisonglin	530,000	1980-85	6.8	0.2	4000	816,000
Guanshan	120,000	1984-88	3.9	0.29	2900	344,000
Shiaodaokuo	415,000	1982	2	0.15	1400	80,000
Hongqi	148,000	1988-90	2.8	0.1-0.3	2100	175,000

*Source:* Fan (1995).

**TABLE 15.6** Comparison of Silt Removal Methods Used at Hongqi Reservoir, China

Method	Range of flow, m <sup>3</sup> /s	Average discharge concentration, g/L	Cost, yuan/m <sup>3</sup>
Lateral erosion	0.14-0.23	219-271	0.037
Emptying and flushing	0.12	34-57	
Hand labor and flushing*	0.12-0.24	116-232	0.02-0.10
Siphon dredge	0.3-0.82	61-250	0.16
New reservoir			1.00

\*Hand labor used to direct flow and facilitate bank collapse

*Source:* Zhang et al. (1992).

Because sediment deposits slope laterally, pilot excavation is required to define the desired course of a longitudinal channel and to maintain the required horizontal distance between channels. Diverted flow enlarges the pilot channel until the entire flushing flow passes through the auxiliary channel at the highest flow rate possible, thereby maximizing channel width. A fully developed system would consist of a series of longitudinal channels, submerged during impounding and exposed during flushing. Once the channels have been scoured, they would be maintained by rotating the diversion flow through each channel at regular intervals, possibly on the order of once every several years. The use of multiple parallel longitudinal diversion channels, conceptually illustrated in Fig. 15.15, has not yet been reported.

In narrow reservoirs with steep banks, it may be possible to construct a longitudinal channel along one side of the deposits. Over time, the channel may move laterally (down the reservoir sideslope) as it erodes, thereby increasing the amount of sediment removed. Use of this technique was observed by the first author in deposits of fine sediment in the small (2 Mm<sup>3</sup>) Prieto Reservoir in Puerto Rico.

Longitudinal erosion has the advantage of being able to erode large volumes of material with a single channel. However, it must be carefully planned and implemented to ensure that the channels remain parallel and do not intersect as a result of bank failure, channel migration, and overflow of pilot channels. The presence of poorly consolidated sediments can make it virtually impossible to create multiple parallel longitudinal channels, and once the floodplain has been divided up into a series of channels, access with equipment to repair any breaches becomes difficult. Significant spacing will be required between the diversion channels to prevent them from merging by channel migration. Any spillage will flow laterally to an adjacent channel or to the main channel, scouring a lateral channel that cuts off the downstream end of the planned longitudinal channel. This problem is either minimal or absent from lateral erosion since the auxiliary channels are oriented downgradient across sediment beds.

### 15.8.3 Flow Diversion

Both lateral and longitudinal erosion use flushing flows diverted from the main channel. The construction and use of an ungated earthen diversion dam is described in the Sefid-Rud case study (Chap. 23). In that case, the diversion dam was designed to pass the entire river discharge and to be submerged by the reservoir pool before the onset of large floods to prevent failure by overtopping. The upstream limit of the diversion channel feeding

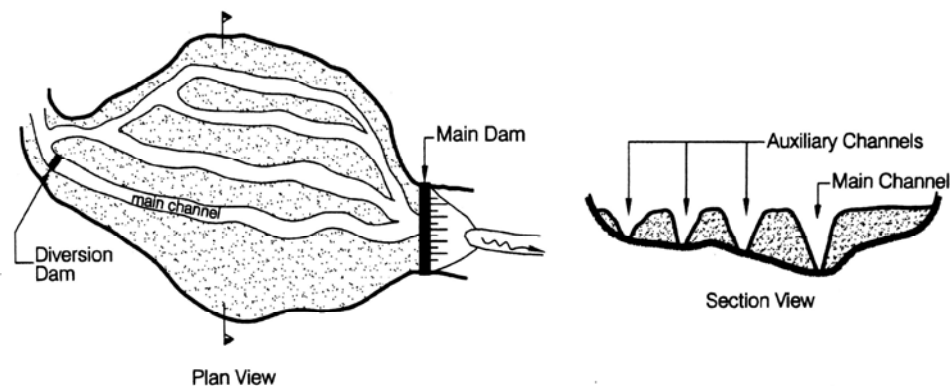


**FIGURE 15.15** Conceptual layout of diversion channels for longitudinal erosion.

either lateral or longitudinal channels must be located at the diversion dam, which itself must be constructed in an area far enough upstream to have sediment deposits of adequate strength yet beyond the area of delta deposition which could bury the diversion structure. It may also be feasible to construct the diversion system above the normal pool elevation. Construction of a diversion dam can interfere with the passage of turbid density currents along the main channel. Since sediment focusing into flushing channels is an important aspect of sediment control by flushing, the diversion system should facilitate the continued passage of turbidity currents during impounding to minimize deposition on floodplain areas.

#### 15.8.4 Mechanically Assisted Flushing

Mechanical equipment such as bulldozers has been used to push sediment deposits into the flushing channel, thereby removing sediment faster than would occur by erosion alone and also removing sediment from an area wider than the flushing channel itself. In 1992 Los Angeles County used flushing to sluice  $1.7 \text{ Mm}^3$  of sediment from the San Gabriel debris basin over a 5-month period, using bulldozers to push the sediment into the flushing channel. The cost of this operation was about  $\$0.93/\text{m}^3$ , mostly bulldozer costs. A similar but smaller-scale pilot sluicing operation at Morris Dam cost  $\$1.42/\text{m}^3$ . This sediment sluicing method has since been discontinued because of downstream environmental concerns related to sediment discharge (Kumar, 1995). If banks of a flushing channel are high, their collapse can be accelerated by excavation at the base of deposits by pressurized water or explosives. Although the use of explosives was considered at Sefid-Rud, as described in the case study (sec. 23.3.3), there is no record to date of its successful utilization to assist flushing in any reservoir.

### 15.9 STORAGE HISTORY CURVES

The long-term variation in reservoir storage when flushing is used to combat sedimentation depends on: (1) the rate of sediment accumulation on floodplain deposits, (2) the storage volume in main and auxiliary flushing channels, and (3) the accumulation of coarse material that is not removed by flushing. Assuming a reservoir is operated in conventional impounding mode for a number of years, and that flushing is initiated when half the storage capacity has been lost, the timewise variation in storage may follow the generalized storage history curves shown in Fig. 15.16. The curves in Fig. 15.16a illustrate the condition in a reservoir where there is no net accumulation of coarse material;

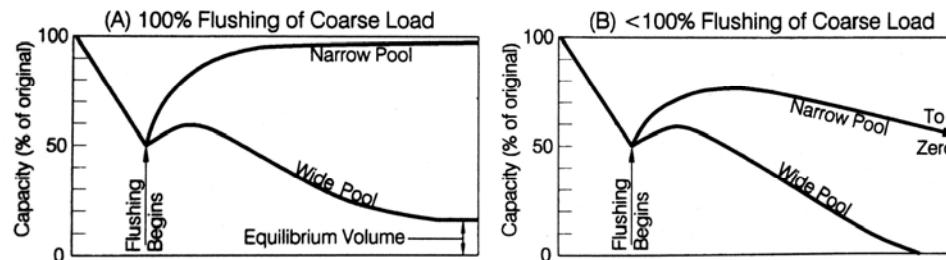


**FIGURE 15.16** Long-term variation in reservoir storage with flushing, as a function of reservoir geometry, for two bed load conditions: (a) all inflowing bed load is released by flushing and (b) coarse load continuously accumulates.

that is, the entire inflowing load is removed by flushing. There is an immediate increase in capacity associated with flushing channel formation. In a narrow reservoir where the flushing channel occupies virtually the entire pool width, it is possible to restore and maintain most of the original storage volume. In a wide reservoir, a single flushing channel will produce only a temporary increase in capacity, and continued sediment deposition on submerged floodplains will cause the reservoir to decline to some stable volume, equal to the volume within the main flushing channel. The rate of storage loss declines as soon as flushing is initiated because sediment deposition is focused in the flushing channel. This reduces the rate of sediment deposition on floodplains as compared to continuous impounding. The rate of deposition on the floodplain will decline over time, as will the rate of rise in floodplain height. Sediment inputs become more focused within the channel as bank height increases and water depth over the floodplain decreases (Fig. 15.2). The use of auxiliary flushing channels has the effect of producing a curve intermediate between that for a wide and a narrow reservoir.

The curves in Fig. 15.16*b* show the same wide and narrow reservoirs as before, but with the accumulation of coarse material that is not removed by flushing because the flushing discharge is too small or of insufficient duration. Although bed material is typically a small fraction (e.g., 10 percent) of total sediment inflow, its volume may be large compared to the flushing channel volume. To the extent that coarse bed material deposition becomes focused in or along the flushing channel, its overall impact on sediment accumulation can be much larger than suggested by simply comparing the volume of bed material to the total reservoir volume. If the coarse fraction of the inflowing load is not removed by flushing, the capacity of both the narrow and the wide reservoir will eventually decline to zero, although at a slower rate than without flushing. The deposition of coarse material may be countered, but not necessarily eliminated, by increasing the discharge and duration of flushing flows. Flushing discharge may be limited by factors such as the natural inflows during the flushing season, outlet capacity, or downstream channel capacity.

## 15.10 SCOUR CONE GEOMETRY

---

When sediment accumulates in the area of outlets which are maintained in service by continued withdrawals, a scour cone will develop through the sediment deposits. As a first approximation, the bottom of this cone may be estimated to be approximately as large as the outlet cross section and located at the outlet invert elevation. Actually, some scour does occur immediately in front of the outlet, influenced by factors including submerged angle of repose of the sediment, inflow and outflow of water and sediment, outlet geometry, and local obstructions or other conditions that obstruct the flow field. Scour cone geometry is not fixed, but is influenced by changing discharge conditions (Jin, 1992). Both Jin (1992) and Fang and Cao (1996) reported that the angle of repose in reservoir scour cones is smaller in the direction extending upstream from the dam along the longitudinal axis ( $a$  axis), compared to the transverse sediment slopes perpendicular to the outlet axis, the  $b$  axis as illustrated in Fig. 15.17. Fang and Cao reported that laboratory studies show the side slopes for scour cones to be approximately equal to the submerged angle of repose of the sediment. However, field data for scour cone slope angles in silty sediments at several Chinese reservoirs subject to drawdown (Table 15.7) are considerably smaller than the slope angles determined from laboratory hydraulic models. The scour cone angle in these reservoirs was influenced by drawdown. In reservoirs not subject to drawdown the scour cone may be estimated by the submerged angle of repose for granular sediment (Fig. 5.9). The angle of repose for continuously

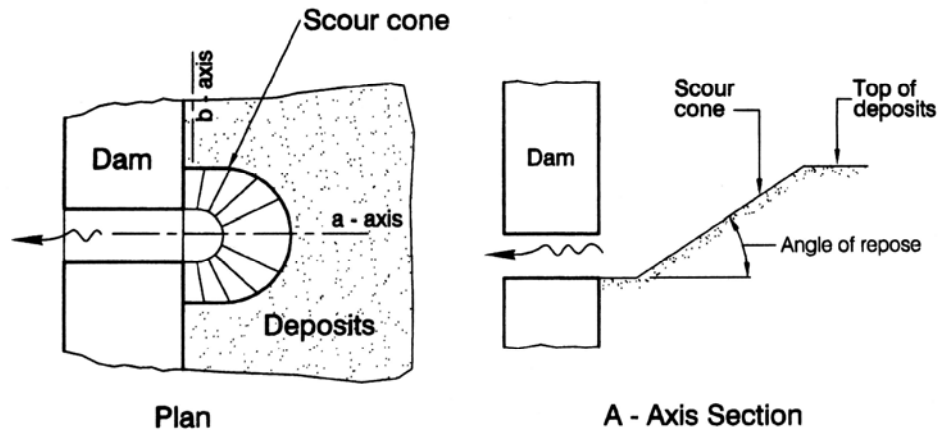


FIGURE 15.17 Sketch of scour cone upstream of a submerged outlet.

TABLE 15.7 Field Data on Scour Cone Slope Angles for Chinese Reservoirs

Reservoir	Annual sediment load, $10^6 \text{ m}^3$	Initial storage volume, $10^6 \text{ m}^3$	Scour cone angle, degrees	
			a axis	b axis
Kongazhue	33.7	357	6	—
Bikou	18.9	512	3.4-5.4	8-17
Qington Gorge	139	606	4-7	9-4
Fen He	17.8	702	9.5-11	13-17
Yan Gou Gorge	58.5	216	7-9	11-15

Source: Fang and Cao (1996)

submerged cohesive sediment may be significantly steeper than for noncohesive sediment, as observed from unpublished reservoir measurements in Switzerland (DeCesare, 1995). If the bottom outlet is not operated during periods of significant inflow the scour cone can become filled with sediment, burying the outlet. If the reservoir is emptied and flushed with free flow through the bottom outlet, there will be a channel extending upstream from the outlet rather than a localized cone.

### 15.11 COMPARTMENTED AND MULTIPLE RESERVOIRS

A reservoir in which the total storage volume is divided into two independently operating storage units is termed a *compartmented reservoir*. The compartments may be contiguous, may consist of a smaller compartment inside a larger one, or may consist of two separate storage areas operated as a single system. Storage compartmentation allows the two portions of the total storage pool to be operated separately to enhance overall sediment management.

### 15.11.1 Parallel Storage Compartments

If a storage reservoir is divided into two sides, one side may be operated for storage while the other side is emptied for flushing. The Dalingkou Reservoir in Hebi Province of China took advantage of local topography by building two parallel reservoirs connected by a water supply tunnel. The reservoir in the smaller watershed with better vegetation was mainly used as clear-water storage for water supply while the other was used for flood retention. This layout permitted continuous storage for water supply in one reservoir while sediment flushing was conducted at the other (Xia, 1983).

### 15.11.2 Reserve Storage Compartment

Some reservoirs may have multiple uses with large differences in water demand, such as a reservoir making seasonally large irrigation deliveries and smaller but continuous deliveries to a potable water system. Reservoir compartmentation may be required to enable the main storage pool to be seasonally emptied or flushed, while continuing to supply water from a small storage compartment created by damming a tributary branch receiving low sediment loading.

### 15.11.3 Reservoirs in Series

When several reservoirs are located in series along a stream, sediment released during flushing at an upstream site will simply accumulate in the downstream site unless both are managed conjunctively. An example of sediment management at three reservoirs in series is provided by the flushing experience at the Rioni hydropower reservoirs in the Republic of Georgia. Best results were obtained when flushing was initiated at the downstream reservoir, scouring out a main channel to transport through the impoundment the sediments subsequently released by flushing the upstream sites. If the upstream reservoir is flushed first and a channel has not been scoured through the bed of the downstream reservoir, the sediments released from the upstream site will spread out and settle on the floodplain deposits in the downstream reservoir (Kereselidze et al., 1985).

At Jiaojiazhuang in the Hebi Province of China, two reservoirs were constructed in series, 2.5 km apart. The initial stage of the flood containing high sediment concentrations is allowed to pass through the upper reservoir and the gates are closed to retain the clearer water in the falling limb of the hydrograph. The muddy flow passing through the upstream reservoir is captured at the downstream site. After the water in the downstream reservoir has been diverted to beneficial use, the clear water from the upstream reservoir is released to scour the deposited sediment from the downstream site (Zhang et al., 1976).

## 15.12 PLANNING AND IMPLEMENTATION

---

Before undertaking flushing, it would normally be desired to answer questions such as: what volume of storage can be recovered, how much water will be released, what will be the downstream sediment concentration, how large should bottom outlets be, and what is the recommended flushing schedule? These questions can be addressed only approximately, and field conditions can depart significantly from predictions and modeling results.

### 15.12.1 Downstream Impacts

A critical issue to be addressed in any reservoir emptying or flushing operation is that of downstream impacts. Sediment released by flushing will be redeposited somewhere downstream: in the stream channel, a downstream reservoir, water intakes and delivery systems, the sea, etc. Flushing is not feasible at many sites because of downstream water quality impacts. Furthermore, the discharge required to prevent excessive localized accumulation downstream of the dam may be more critical in determining the hydraulic requirements for flushing than the discharge needed to erode sediment from the reservoir itself. Problems associated with downstream redeposition are described in both the Sanmenxia and Gebidem case studies (Chaps. 24 and 21). Potential impacts to downstream infrastructure and the environment due to flushing are reviewed in Chap. 18.

### 15.12.2 Scheduling of Flushing

The optimal flushing schedule from the standpoint of sediment removal may create significant operational conflicts, and selection of a workable flushing schedule will normally be reached through a process of compromise. The flushing schedule and procedures should be modified according to monitoring data to minimize adverse impacts while achieving sediment management objectives. Monitoring data should include downstream impacts as well as sedimentation processes in the reservoir.

At many reservoirs in China, flushing occurs during the first part of the flood season when large flushing discharges are available and downstream irrigation requirements can be supplied from run-of-river diversions. The large sediment inflows during this period can also be routed through the empty impoundment. The use of high-velocity irrigation canals can minimize the problem of sediment deposition despite high sediment concentrations in the flushing flow.

At reservoirs with regular seasonal variations in water level, emptying for flushing will logically be scheduled during the period of low pool level. The flushing period at Sefid-Rud was selected to coincide with the period of low reservoir level and to avoid delivery of sediment-laden water to the seasonally operated irrigation intakes downstream, which were not designed to handle high sediment concentrations. At Cachi Reservoir, the 3-day flushing period is set months in advance to coincide with wet season flows to allow rapid refilling and to also coincide with a long holiday weekend when electrical demand is low. At the Dashidaira Dam in Japan, winter was selected for flushing to minimize turbidity impacts on fishing, irrigation, and tourism (Wada, 1995). Flushing may also be initiated when specific hydrologic conditions occur, such as adequate dilution volume in a downstream river as described in the Gebidem case study (Chap. 21). It may also be desirable to schedule flushing to provide a clear-water discharge following flushing to help wash the released sediment through the downstream fluvial system, as performed at some sites in France.

Flushing may not be undertaken every year. The Hengshan Reservoir (Fig. 15.4) is a 13.3-Mm<sup>3</sup> gorge-type impoundment with a 69-m-high dam used for flood control and irrigation. Because this reservoir is in an arid zone and water supplies are scarce, emptying and flushing is delayed until the main channel has been filled by density current siltation, an interval of every 3 or 4 years. Following the first 8 years of impounding, from 1966 to 1973, 3.19 Mm<sup>3</sup> of sediment had accumulated and deposits at the dam were 27 m thick. The reservoir was emptied for 37 days in 1974 and a storage capacity of 800,000 m<sup>3</sup> was recovered. In 1979, the reservoir was emptied a second time and 1.03

Mm<sup>3</sup> of capacity was recovered. The third and fourth emptying and flushing operations were undertaken in 1982 and 1986. During the initial period of free flow, the outflow concentration usually reaches 1000 g/L, regardless of the discharge, and in 1974 the outflow concentration exceeded 1000 g/L for over 16 hours. The fines removed at this site consist of silts (Guo and Li, 1984).

### 15.12.3 Sizing and Location of Bottom Outlets

In general, flushing sluices should be located as deep as possible and should be as wide as possible. Two side-by-side sluices are preferred to two sluices at different levels, since the former arrangement will produce lower backwater at a given discharge. To maximize effectiveness, flushing should also be performed with the largest discharge possible (Paul and Dillon, 1988). Sluices should be designed to produce full drawdown and free flow conditions through the dam. Because flushing dates are often determined by operational constraints, the outlet capacity would normally be sized to minimize backwater during the highest flows anticipated during the period selected for flushing. Selection of the design capacity of outlets and backwater during the design flow should be determined by modeling.

The placement of both sluices and service intakes should be planned so that the service intakes will be maintained free of sediment by sluice operation, as conceptually illustrated in Fig. 15.18. If intake structures are located outside the area to be maintained sediment-free by flushing from the main channel or a lateral channel, mechanical removal will eventually be required. When geologic or other conditions make it impossible to place the flushing outlet below the service intakes, it may be feasible to divert the flushing flow into the vicinity of the service intakes by constructing a low dike partway across the channel upstream of the dam, thereby directing the flushing channel along the desired alignment (Fig. 15.19). A physical model test to determine the flushing channel alignment in the vicinity of the dam is described in Chap. 11.

### 15.12.4 Sediment Release and Concentration

The amount of sediment released during flushing, and the maximum sediment concentration during a flushing event, is highly variable. At present there is no generally applicable method to accurately predict the rate of sediment release, channel formation, or peak sediment concentrations during flushing. Empirical relationships have been developed to estimate sediment release in some reservoirs. For example, Fan and Jiang (1980) developed the following equation from field data for the discharge of fine sand ( $d_{50} = 0.06$  to  $0.09$  mm) from Sanmenxia Reservoir during erosion in 1963 and 1964:

$$Q_s = 3.5 \times 10^{-3} Q^{1.2} (S \times 10^4)^{1.8} \quad (15.2)$$

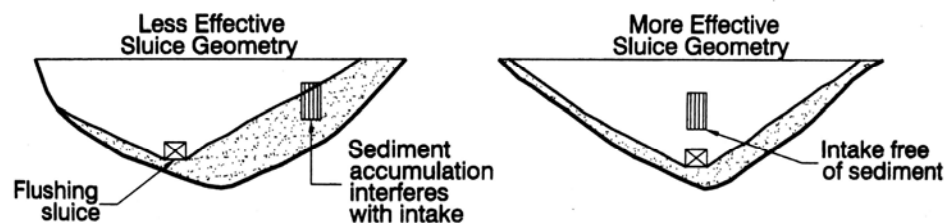


**FIGURE 15.18** Placement of sediment sluice below intake to avoid sediment buildup that interferes with water deliveries.

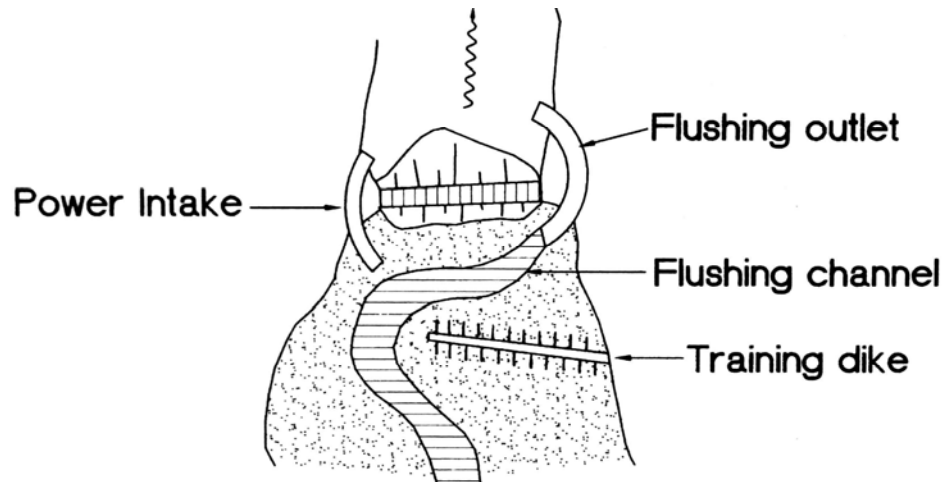


**FIGURE 15.19** Use of dike to train the path of a flushing channel into the vicinity of a service intake to maintain the intake area free of sediment. The dike would be submerged during impounding.

where the sediment discharge  $Q_s$  (t/s) is predicted from water discharge  $Q$  ( $\text{m}^3/\text{s}$ ) and water surface slope  $S$ .

Based on field data during periods of empty flushing and retrogressive erosion in Chinese reservoirs, the following empirical relationship was developed to describe the rate of sediment release (Xai, 1983).

$$Q_s = \frac{E Q^{1.6} S^{1.2}}{B^{0.6}} \quad (15.3)$$

The range of values for the dataset are given for each term:  $Q_s$  = outflow sediment discharge (range 0.0006 to 777 t/s),  $Q$  = water discharge (range 0.1 to 5730  $\text{m}^3/\text{s}$ ),  $S$  = bed or water surface slope (range 0.00006 to 0.016), and  $E$  = erodibility coefficient. A high value of  $E$  corresponds to easily eroded sediment, whereas a low value of  $E$  corresponds to deposits of coarse or consolidated sediment. A plot of field data and representative values of  $E$  are given in Fig. 15.20. Lai and Shen (1996) extended Curve III of this relationship to laboratory flume experiments using walnut shell grit as a sediment.

Field experience at a variety of sites indicates that peak suspended sediment concentrations exceeding 100 g/L should be anticipated for emptying and flushing when sediment beds contain significant fines, but much smaller values may occur when only coarse noncohesive sediment deposits are eroded. Zarn (1992) was able to accurately predict the maximum sediment concentration of noncohesive sediment released from deposits above Reichenau hydropower station in Switzerland using the one-dimensional MORMO code, a research model.

In 1985 the Dashidaira Dam was built on the Kurobe River in Japan. This, the first Japanese dam with large-scale flushing outlets in the bottom of the structure, was first flushed in 1992. Both physical and numerical modeling was undertaken to predict the flushing behavior at the dam, where it was planned to flush 600,000  $\text{m}^3$  of sediment over 9 days, producing suspended-solids concentration of 2800 ppm in the river below the dam, not significantly higher than natural levels peaks during floods. However, sediment was released more than twice as fast as predicted, suspended-solids levels reached 4400 ppm, and dark gray turbid water having an offensive odor reached the sea 36 km downstream of the dam. The odor was apparently caused by the accumulation and

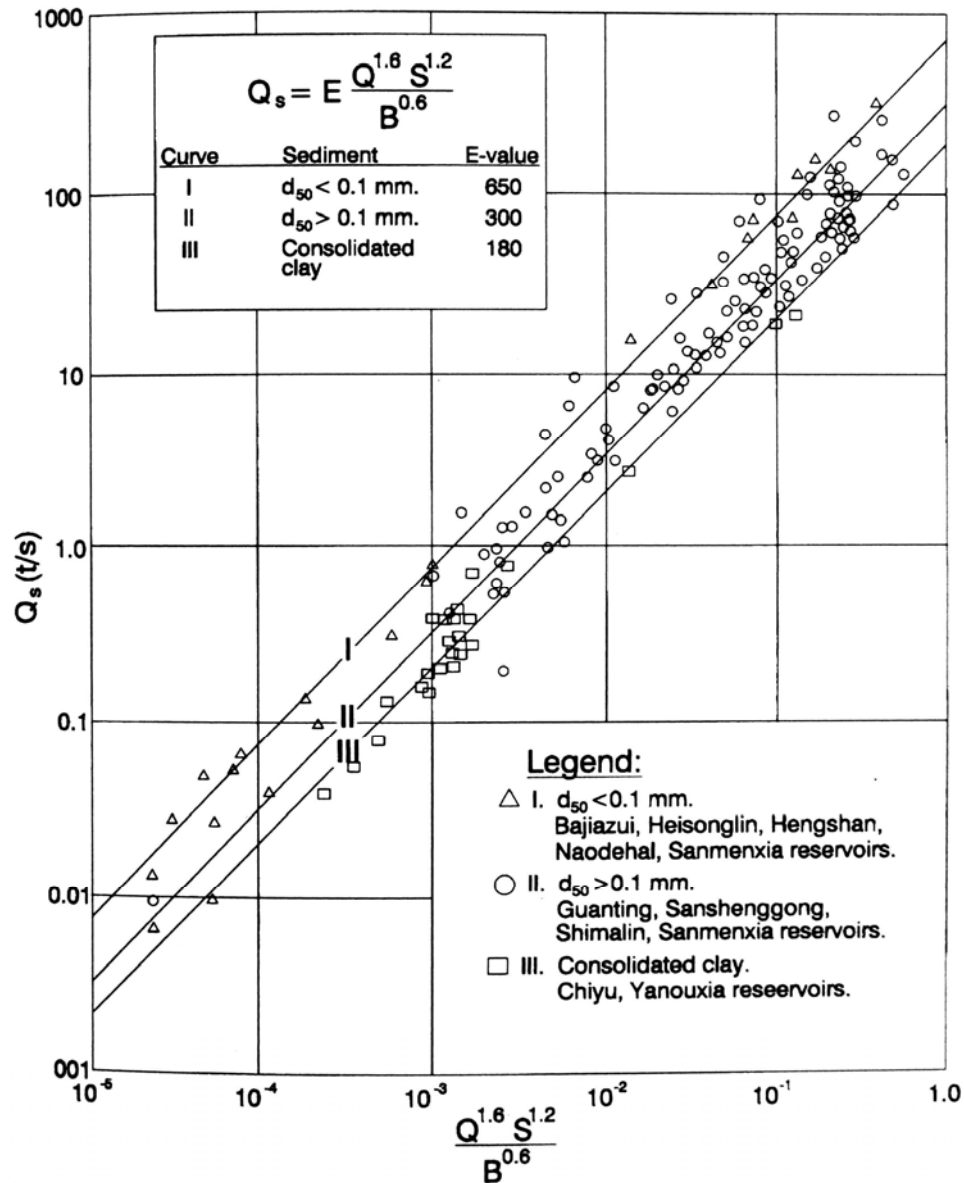


**FIGURE 15.20** Rate of sediment release during retrogressive erosion, based on empirical data from Chinese reservoirs during emptying and flushing (Xai, 1983).

anaerobic decomposition of organic material in the sediment. The flushing operation was halted after 3 days.

The erosion of cohesive sediment was modeled by Bouchard (1995), who pointed out that the sediment properties of noncohesive sediment are difficult to assess, and the sliding of unstable banks can be an important phenomenon for supplying sediment to the channels compared to erosion of the channel bed.

During maintenance flushing, the total quantity and peak concentration of sediment released is determined by factors such as the amount and grain size of sediment that has accumulated since the previous flushing event, flushing flow rate, drawdown procedure

(i.e., release of turbidity currents during drawdown), and sediment consolidation. The wide range in values that occur in practice are discussed in Sec. 15.6 and the Cachi case study (Table 19.2). A sediment budget approach is necessary to estimate the volume of sediment to be released during maintenance flushing.

### 15.13 LONG-TERM STORAGE CAPACITY

---

To estimate the volume of material that can be eroded by flushing and the volume that can be maintained for long-term use, it is necessary to determine the geometry of the main and, if present, the auxiliary flushing channels. This requires knowledge of: (1) the channel planform layout across the deposits, (2) invert profile of each flushing channel relative to the deposit geometry, and (3) the bottom width and side slope of each channel to determine its volume.

In deposits of fine-grained sediment, the planform of the flushing channel will tend to develop along the pre-impoundment river channel. However, in deposits of coarse material the flushing channel can develop an actively meandering braided channel. Stream planforms and the type of geometric control can change along the length of the reservoir, moving from coarse delta deposits to deposits of fine sediment. The planform location and length of auxiliary flushing channels will be established during their design.

Determination of channel slope and cross-section geometry will be complicated at many sites by the complex configuration of the deposits, which will vary from the delta to the dam and may include layered and cohesive material. Only approximate solutions may be expected. Numerical modeling may be undertaken to analyze the probable configuration of the flushing channel over time. Both FLUVIAL12 and GSTARS are one-dimensional sediment transport models capable of adjusting channel width in accordance with the concept of streampower minimization. They may represent useful tools to analyze the development of flushing channel geometry in reservoirs, but the application of these models for flushing studies has not yet been reported. The HEC-6 model requires that the user specify the channel width beforehand. A number of one-dimensional models have been developed in China, but they are essentially research tools and are not available for distribution.

In China, the stream channel relationship developed by Altunin (1964) has been used to estimate channel width:

$$B = \frac{1.5 Q^{0.5}}{S^{0.2}} \quad (15.4)$$

where  $B$  is channel bed width, m;  $Q$  is discharge, m<sup>3</sup>/s; and  $S$  is bed slope.

Tolouie (1993) examined the problem of defining the cross-sectional geometry of a flushing channel at the Shahrud longitudinal diversion channel in Sefid-Rud Reservoir. After comparing a variety of equations against field data, he developed the procedure outlined below for estimating the size of a flushing channel. The description of the Shahrud diversion channel in the Sefid-Rud case study (sec. 23.6) provides more information on the site at which this analysis was developed.

The geometry of the flushing channel, or the volume of material that can be removed, can be established if the following geometric channel properties are known: length, bank profile, angle of repose, thalweg profile, and bottom width. The length is determined from the thalweg distance or the layout of a pilot channel, and the bank profile will be given by the elevation of the deposit surface. The angle of repose can be estimated or

measured from the deposit geotechnical characteristics. This leaves two unknowns: thalweg profile (slope) and bottom width.

The invert elevation at the downstream limit of the thalweg is determined by the elevation of bottom outlets, or in the case of lateral or longitudinal erosion by the invert of the main flushing channel at the terminus of the auxiliary channel. Initially the slope of the flushing channel will follow the original stream, but this slope can be modified by the accumulation of coarse material and the advancing face of delta deposits. The slope can also be modified by sediment layering, and in the Shahrud channel Tolouie made separate slope computations for the top cohesive layer and the final channel slope. The slope may also be modified by topographic features buried beneath the sediment. With the slope estimated from the site characteristics, the problem is reduced to the computation of bottom width.

The following types of data are required to determine bottom width, and the numerical values given are those used in the example computation.

$S$  slope (0.0054)

$Q$  discharge (8 m<sup>3</sup>/s)

$\rho$  liquid density (1000 kg/m<sup>3</sup>)

$P_s$  density of sediment grains (2650 kg/m<sup>3</sup>)

$T$  age of deposit (25 years)

$P_s$ , percent of silt and clay in deposit (50 percent)

$g$  gravitational constant (9.81 m/s<sup>2</sup>)

$I_p$  plasticity index (not applicable to this sample; use 0)

$Li$  liquidity index = water content/liquid limit (not applicable to this sample)

$\nu$  kinematic viscosity (1.14×10<sup>-6</sup> m<sup>2</sup>/s at 15°C)

$d_{50}$  grain diameter (0.08 mm = 8×10<sup>-5</sup> m)

$B$  bottom width, m

The first computational step is to determine the critical tractive force of the deposit, which is the bed shear at which erosion is initiated. Two equations are proposed. For noncohesive beds and for alternating beds of cohesive and noncohesive material:

$$\tau_c = 0.052(\rho_s - \rho)gd_{50}[1 + (I_p^{0.90} + P_{sc}^{0.84} \log(9 + T))] \quad (15.5)$$

The first term is that of White (1940) and the second is based on field observations in the Shahrud diversion channel. For the example condition this may be solved for  $T_c = 2.8$  N/m<sup>2</sup>.

$$\tau_c = 0.052(2650 - 1000)(9.81)(8 \times 10^{-5})[1 + 0 + 50^{0.84} \log(34)] = 2.8 \frac{N}{m^2}$$

In reservoir deposits, fines are often mixed with coarse sediments, imparting significant cohesion to nominally cohesionless deposits. Thus, reservoir deposits tend to be more erosion-resistant than pure sands. The second term in Eq. (15.5) accounts for this additional cohesion. To estimate the critical tractive force for layered sediment beds, use the characteristics of the cohesionless sediment layer in the first term and the cohesive layer characteristics for the second term. Tolouie notes that, in beds consisting entirely of cohesive sediment, this equation probably underestimates the critical tractive stress (and will thus overestimate bottom width).

For unconsolidated silt and clay deposits such as the weak, low density deposits

encountered closer to the dim, the following equation may be applied:

$$\tau_c = 4L_i^{-1.25} [\log(9 + T)]^{0.5} \quad (15.6)$$

Based on the work of Lane (1953), the shear stress acting on the sides of the channel and causing it to widen may be estimated as 0.7 times the shear stress on the bottom. Using this criterion, and having determined the critical shear stress in the previous step, rearrange Eq. (9.16) to solve for flow depth at the critical condition:

$$\tau_c = \gamma D_c S = \rho g D_c S \quad (9.16)$$

$$D_c = \frac{\tau_c}{0.7 \rho g S} = \frac{2.8}{(0.7)(1000)(9.81)(0.0054)} = 0.076 \text{ m} \quad (15.7)$$

Determine the critical shear velocity:

$$U_{*c} = \left( \frac{\tau_c}{\rho} \right)^{1/2} = \left( \frac{2.8}{1000} \right)^{1/2} = 0.053 \text{ m/s} \quad (15.8)$$

The equation proposed by Keulegan (1938) was found to give an appropriate value for the critical mean velocity  $V_c$ :

$$\frac{V_c}{U_{*c}} = 5.75 \log \left( \frac{U_{*c} D_c}{\nu} \right) + 3.25 = 5.75 \log \left( \frac{(0.053)(0.076)}{1.14 \times 10^{-6}} \right) + 3.25 = 23.7 \quad (15.9)$$

From this we may compute  $V_c = 1.25$  m/s. From continuity  $Q = AV$ , and because the section is wide and shallow  $A = BD$ . Combining gives

$$B = \frac{Q}{V_c D_c} = \frac{8}{(1.25)(0.076)} = 84 \text{ m} \quad (15.10)$$

These equations were developed and tested in the Sefid-Rud Reservoir and may not be applicable at other sites.

## 15.14 CLOSURE

Sediment flushing has been performed regularly at a limited number of reservoirs and has been well-documented at only a few sites. However, interest in this procedure is increasing as reservoirs accumulate sediment and improved data are starting to become available. Downstream impacts are large and effort needs to be directed toward mitigation of these impacts. This important topic has received much less study than flushing procedures themselves. Also, at some reservoirs receiving a wide range of grain sizes, flushing has successfully removed fines but coarse material continues to accumulate. This underscores the need to consider the long-term accumulation of coarse materials as well as fines in the implementation of flushing systems. While the general features of flushing are well-known, there are no proven methods for computing many important parameters relating to erosion rates, sediment concentrations, channel dimensions, sediment focusing, and long-term storage capacity. These parameters can be predicted only approximately. Modeling techniques for flushing processes are not well-developed, and the behavior of coarse sediments in reservoirs which are flushed has received little attention. There is considerable research opportunity in this area.

---

## CHAPTER 16

---

# SEDIMENT EXCAVATION AND DREDGING

---

### 16.1 INTRODUCTION

---

Sediment deposits may be mechanically removed from reservoirs by hydraulic dredging or dry excavation. Selection of the excavation method will depend on factors including sediment volume, grain size and geometry of the deposit, available disposal and reuse options, water levels, and environmental criteria, all of which will affect the feasibility and cost of alternative methods of excavation. All methods of mechanical excavation are costly because of the large volumes of material involved and, frequently, the difficulty of obtaining suitable sites for placement of the excavated material within an economic distance of the impoundment. However, once sediments are deposited in a reservoir, excavation is often the only management option available.

The removal of significant volumes of sediment from lakes or reservoirs characteristically entails *dredging*, the lifting of sediment from the bottom to the surface of a water body and deposition at another location. Most dredging is performed to construct and maintain commercially navigable waterways. Dredging in the United States amounts to about 500 Mm<sup>3</sup>/yr. The Corps of Engineers performs or contracts about 230 Mm<sup>3</sup> of dredging annually, of which about 90 percent consists of dredging in coastal waters.

Dredging in lakes and reservoirs not used for commercial navigation has historically been undertaken on a small scale, rarely involving more than 1 Mm<sup>3</sup> of sediment removal per site. In smaller impoundments dredging has been focused on removal of silts and organic sediments originating from accelerated erosion in the watershed and eutrophication. The fine-grained and possibly organically enriched sediments contribute to shallowing of the lake, impair fisheries, detract from recreational activities such as bathing, and may continually recycle nutrients back into the water column thereby sustaining high algae populations and aquatic weed growth even after external nutrient inputs are reduced. In larger reservoirs dredging has focused on the cleaning of specific areas such as hydropower intakes, navigational channels, and recreational areas. In some cases dredging has been used to create or enlarge reservoirs, such as the water supply reservoir for the City of Bradenton, Florida, which was enlarged by dredging sandy soils.

As sediment continues to accumulate in reservoirs, both the frequency and size of reservoir dredging projects are increasing. At this writing the largest-scale reservoir dredging project to our knowledge completed in the United States involved the removal of 2.3 Mm<sup>3</sup> from Lake Springfield, Illinois, during the period 1986-1990, while the lake was simultaneously used as a public water supply source for the City of Springfield. A

contract for the removal of 6 Mm<sup>3</sup> from the Loíza water supply reservoir in Puerto Rico was awarded in 1996.

This chapter describes sediment removal from reservoirs by both dry excavation and dredging. More detailed information on dredging engineering is provided by Herbich (1992), and Turner (1996) provides an overview of hydraulic dredging practice. The most comprehensive information on containment area management is available from the Dredging Research Program of the U.S. Army Engineer Experiment Station, P.O. Box 631, Vicksburg, Mississippi 39180. Cooke et al. (1993) discuss dredging and a wide variety of other lake and reservoir management and restoration techniques. The Center for Dredging Studies at Texas A&M University offers an annual dredging short course.

## 16.2 DRY EXCAVATION

---

Dry excavation is typically used for the cleanout of debris basins which are normally empty and contain coarse sediments which dewater quickly. However, dry excavation by conventional earth-moving equipment was also used to remove 2.3 Mm<sup>3</sup> of silt from Cogswell Reservoir near Los Angeles, which was emptied for this purpose (Fig. 16.1).



**FIGURE 16.1** Photograph of sediment removal at Cogswell Reservoir (*courtesy Los Angeles County*).

### 16.2.1 General Considerations

Several factors limit the use of dry excavation in reservoirs. Most important, it requires that the reservoir be dewatered, limiting its use to impoundments which are seasonally dry or which can be dewatered for a prolonged period. Conventional land equipment will sink in thick deposits of inadequately dewatered fine sediment, and, depending on the characteristics of the deposits, dewatering may require more than a year. Storm inflow can inundate the work area. However, in reservoirs that are drawn down or emptied annually, each year's accumulation of fine sediments may be desiccated and consolidated, producing deposits that can be readily handled with conventional equipment. At Sefid-Rud Reservoir (Chap. 23) the pilot channels for flushing were excavated across seasonally dry sediment deposits by conventional equipment, 'although fine sediment deposits near the dam were too soft for equipment access even after several years of seasonal drawdown for flushing.

When a bottom outlet at the dam is opened to dewater sediment, the river flowing across the deposits will scour the deposits, thereby producing downstream impacts similar to emptying and flushing unless mitigation measures are implemented. Several methods may be used to reduce downstream sediment release during excavation.

1. Initially perform only partial drawdown while excavating sediment from higher elevations within the impoundment. The lowered pool will act as a sediment trap.
2. Construct sediment traps below the dam in areas which are readily accessible for subsequent dewatering and cleanout.
3. Minimize the period of full drawdown, and time the initial full drawdown to coincide with the dry season to minimize scouring of deposits and maximize the efficiency of downstream sediment traps.
4. Close the lowest outlet and maintain a sediment-trapping pool above the dam during periods of high inflow.
5. Divert dry season flows around or across sediment deposits with a lined channel or temporary pipeline.

Dry excavation tends to be more costly than hydraulic dredging, but the comparative economics will depend on the job characteristics. Excavation of dewatered sediment with conventional equipment and trucks eliminates the problem of dewatering a dredge slurry, reduces sediment bulking compared to hydraulic dredging, and can be used to deliver sediment to many small and widely dispersed containment or reuse sites. Environmental permitting requirements for dry excavation may also be simpler than for dredging. Unit costs will vary widely, depending on the volume of material, haul distance, and elevation difference between the points of excavation and disposal. Costs for debris basin excavation are summarized in Table 16.1, and dry excavation costs at reservoirs are given in Tables 16.4 and 3.3.

### 16.2.2 Cogswell Reservoir

The 11-Mm<sup>3</sup> Cogswell rockfill dam in Los Angeles was constructed in 1933 for flood detention and water conservation. At this site, water conservation is practiced by slowly releasing floodwaters to maximize groundwater recharge in the downstream riverbed. During 1994-1996, 2.4 Mm<sup>3</sup> of sediment, primarily silt, was excavated from Cogswell Reservoir (Fig. 16.1). All the finer sediment in the main part of the reservoir was removed, leaving behind only the coarse sediment deposited far upstream along tributaries. The maximum haul distance was about 2 km, with a maximum uphill haul (bottom of reservoir to top of fill) of 230m.

**TABLE 16.1** Cost of Sediment Removal from Debris Basins During 1993 in Los Angeles County, California

Basin name	Volume removed, m <sup>3</sup>	One-way haul, km	Unit cost	
			\$/m <sup>3</sup>	\$/yd
1 Dunsmuir	8,412	0.8	\$5.23	\$4.00
2 Halls	10,532	6.1	\$7.41	\$5.66
3 Gould	3,581	11.3	\$7.83	\$5.99
4 Kinneloa East	2,891	1.9	\$8.65	\$6.61
5 May No. 1	4,791	0.8	\$9.39	\$7.18
6 Las Flores	12,543	3.1	\$9.52	\$7.28
7 Brand	6,600	4.8	\$10.00	\$7.65
8 May No. 2	3,157	0.8	\$10.52	\$8.04
9 Wildwood	5,133	12.6	\$11.10	\$8.49
10 Blanchard	6,691	5.2	\$11.66	\$8.91
11 Aliso	14,876	11.3	\$12.12	\$9.27
12 Mullally	1,279	7.7	\$13.29	\$10.16
13 Devils M-1 DRI	11,846	4.8	\$14.10	\$10.78
14 Browns M-1 DRI	3,431	2.6	\$14.86	\$11.37
15 Deer	2,218	9.2	\$15.32	\$11.71
16 Kinneloa West	4,935	1.9	\$17.22	\$13.17
17 Lincoln	2,297	0.5	\$17.41	\$13.32
18 Turnbull	10,826	10.0	\$19.75	\$15.10
19 Sunset Upper	2,753	4.8	\$22.38	\$17.11
20 Vallecito	1,736	31.6	\$23.04	\$17.62
21 Hay	2,446	9.3	\$24.09	\$18.42
22 Linda Vista	369	13.2	\$24.37	\$18.63
23 Barkentine	1,032	10.1	\$27.12	\$20.74
24 Fieldbook	373	35.4	\$29.70	\$22.71
25 Oakmont View	134	6.0	\$49.32	\$37.71

*Source:* Courtesy Los Angeles County Dept. of Public Works.

Excavated material was placed in an adjacent canyon as engineered fill. The unit cost for excavation and disposal was \$5.60/m<sup>3</sup>. Engineering, environmental permitting, and mitigation work cost about \$2 million more (an additional \$0.87/m<sup>3</sup>). Environmental mitigation activities included revegetation of the fill, fish population studies downstream of the reservoir, water quality and other monitoring costs, and sediment removal from pools below the dam.

The project was designed to minimize the downstream release of sediment. To minimize sediment release the reservoir was only partially drawn down during the first years of excavation; full drawdown was timed to coincide with the dry season, and sediment traps were dug within the reservoir area immediately upstream of the outlet and below the dam. The trap upstream of the outlet was excavated in the deposits by heavy equipment supported on the soft sediment by mats. Below the dam, in the area of the plunge pool and at several sites within about 0.5 km below the dam, sediment traps were constructed by building temporary instream barriers about 1 m tall using sandbags. Because of these measures, only 5000 m<sup>3</sup> of sediment was deposited in pools beyond the last instream sediment basin below the dam. Fine sediment that escaped downstream and deposited in pools was subsequently suction-dredged by portable equipment.

### 16.3 TYPES OF DREDGES

Several types of dredging equipment can be used in reservoirs, and the siphon dredge has been developed specifically for reservoir use. Dredging systems can be classified into two broad categories: hydraulic and mechanical. In hydraulic dredging the sediment is mixed with water and transported from the point of extraction to the point of placement as a sediment-water slurry. Mechanical dredges use buckets to dig and lift sediment to the surface with minimal water entrainment. Dredged material may be discharged into a containment area or, in some countries, discharged to the river below the dam.

#### 16.3.1 Hydraulic Suction Dredges

The hydraulic dredge with a rotating cutterhead at the end of the suction line is the most widely used type of dredge in reservoirs (Fig. 16.2). Advantages of hydraulic dredges include low unit cost for sediment removal, high rates of production, and ability to work in a reservoir without interfering with normal impounding operation. A slurry pipeline is a clean and convenient method to transport sediment from the dredging site to the containment area. Hydraulic dredges are widely available and versatile, can pump long distances with the aid of booster pump stations, and can efficiently handle material from fine sediment through coarse sand. Larger material can also be dredged hydraulically, but at higher unit costs because of the high pipeline velocities (and high friction losses) required to maintain the material in suspension, plus increased wear on equipment. The principal disadvantages of hydraulic dredging are the bulking of fine sediment and the requirement for sediment dewatering.



**FIGURE 16.2** Photograph of a 25-cm hydraulic dredge with the cutterhead raised (*courtesy Ellicott International*).

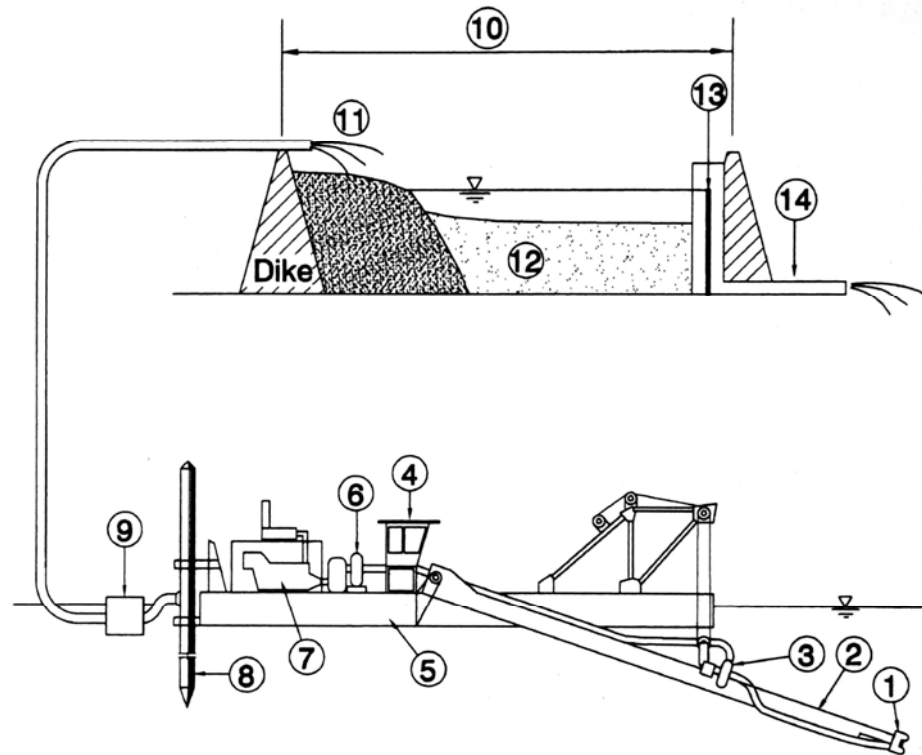


**FIGURE 16.3** Schematic diagram of a hydraulic dredge and disposal area illustrating: (1) cutterhead, (2) ladder, (3) ladder pump, (4) controls, (5) hull, (6) main pump, (7) engine, (8) spud, (9) float and discharge pipeline, (10) disposal or containment area with perimeter dike, (11) inlet zone where coarse sediment tends to accumulate and mound, (12) fine sediment deposits, (13) adjustable effluent weir, (14) discharge of clarified effluent.

Figure 16.3 schematically illustrates a hydraulic dredging system. Hydraulic dredges are sized according to the diameter of their suction pipeline (e.g., a 25-cm dredge), or a combination of suction and discharge diameter. The cutterhead consists of a series of blades on a variable-speed drive, rotating between about 15 and 30 r/min. The cutter-head is worked back and forth across the active face to dislodge the sediment, which is picked up by the suction line. Many cutterhead variations are available, and in flowable material a plain suction end without a cutterhead may be used. Some small dredges use a horizontal auger to deliver fine sediment to the suction line, with a hood to reduce turbidity generation (Fig. 16.4).

The pumping unit may consist of a centrifugal pump located on the dredge or a submerged ladder pump. The advance of the dredge across the deposits may be controlled by pivoting on the spuds, which are alternately lifted and set to produce the pattern shown in Fig. 16.5. Lateral swing is controlled by guy wires tied to anchors or the shore. Cables may also be used to control the motion of the dredge without the use of a spud. The dredge shown in Fig. 16.4 is winched forward along its track by a cable anchored on the shore.

In conventional suction dredges, the pump is located within the dredge hull at the water surface. However, because the specific gravity of the slurry is higher than the surrounding water, when excavation depths exceed about 10 m, or at lesser depths in

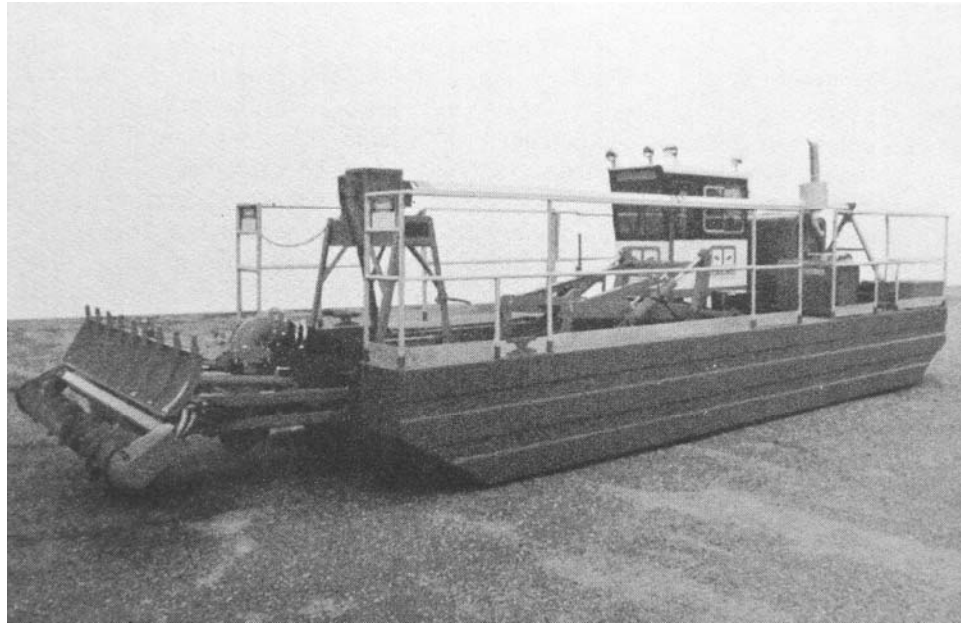


**FIGURE 16.4** Small portable dredge with auger-type cutterhead suitable for use in unconsolidated fine sediment (*courtesy Elliott International*).

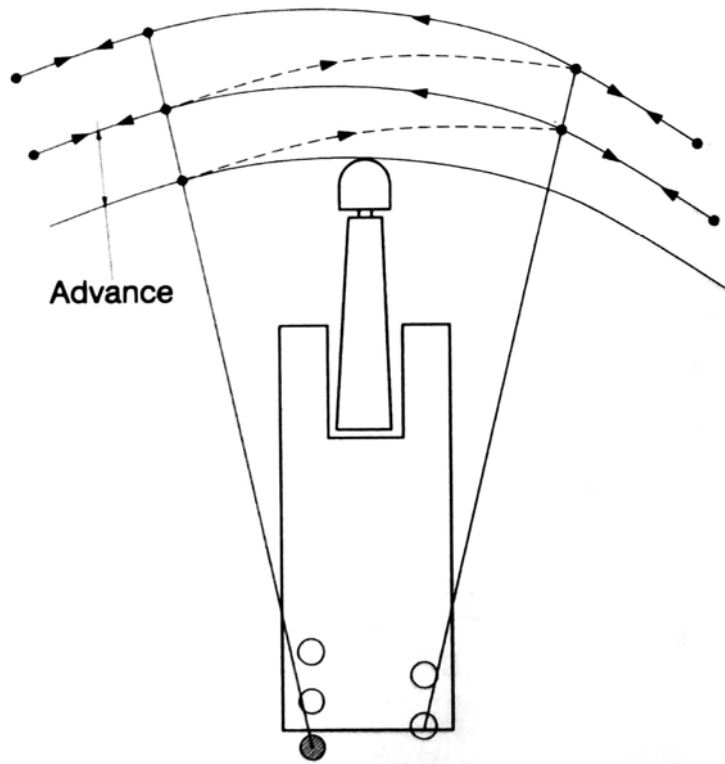


**FIGURE 16.5** Forward motion of a cutterhead dredge pivoting on spuds.

ons can

significantly reduce efficiency and induce pump cavitation. As a rule of thumb, the maximum output of a conventional cutterhead dredge at 15 m digging depth is about half of its output at 3 m digging depth (Turner, 1996). The suction head limitation may be overcome and production increased by locating a pump below the water surface on the ladder supporting the cutter-head, a configuration termed a *ladder pump* dredge and illustrated in Fig. 16.3.

Along rivers which have been impounded for navigational purposes, large dredges may be towed to the dredging site. However, at landlocked reservoirs it is necessary to use transportable dredges which can be broken down and trucked to the site. The largest transportable dredges have a 760-mm (30-in) suction with a 5000-hp pumping unit and a solids-handling capacity of about 2300 m<sup>3</sup>/h (Turner, 1995). For large and prolonged dredging projects, dredges are assembled at the reservoir for permanent use.

### 16.3.2 Siphon Dredge

Siphon dredges are differentiated from a conventional hydraulic dredge by the absence of a pump, and a discharge line that is continuously submerged. The slurry is forced through the pipeline by the differential head between the water surface in the reservoir and the discharge point, located at the lowest possible point on the dam (Fig. 16.6a).

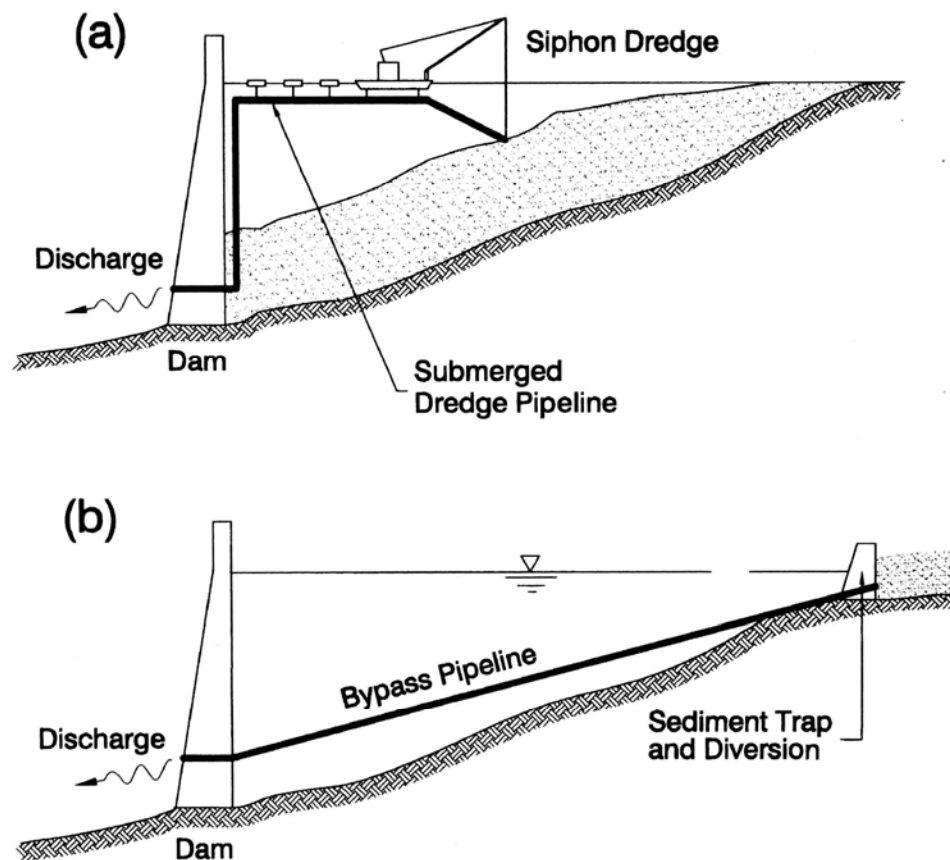


FIGURE 16.6 (a) Mobile siphon dredge. (b) Fixed sediment bypass pipeline.

another to suction fine sediment. Siphon dredges may be configured with a plain suction end or a mechanical cutterhead; the cutterhead-type siphon dredge installed at Valdesia Reservoir is described later in this chapter. There are two principal limitations to siphon dredging. First, because of the low available head, deployment is generally limited to areas rather close to the dam (e.g., 2 km). This distance will vary as a function of dam height, pipe diameter, and the material being dredged. Second, siphon dredges discharge to the river below the dam, a practice not generally permitted in industrialized countries because of environmental concerns.

The potential use of a permanent siphon-type arrangement to pass sediment beyond a dam has been reviewed by Hotchkiss and Huang (1995), and represents a possible approach for bypassing sand over short distances. A permanent sand bypass system (Fig. 16.6*b*) can be environmentally superior to intermittent flushing, and was proposed but not implemented at Spencer Dam on the Niobrara River (Sec. 18.4.9). Limitations inherent in systems of this type include: (1) the lack of a reliable system to deliver sand to the pipe without clogging by debris or heavy floodborne sediment loads and (2) limited hydraulic gradient. For successful operation, a permanent bypass station would probably need to have a movable suction, plus a pump if coarse sediment were to be transported. Because of the irregular sediment transport rate, a bypass station would probably need to be installed at a sediment trap. Sediment bypassing was analyzed by Eftekharzadeh and Laursen (1990). The authors know of no permanent bypass installation in a reservoir, other than a conventional siphon dredge arrangement.

### 16.3.3 Jet Pump

In a jet pump, high-pressure water is jetted through a nozzle, creating a suction which entrains water and sediment. Pumps of this type have no moving parts and thus offer improved ability to pass debris. These pumps have been used for coastal sand bypassing systems, and might be useful for a similar type of application in a reservoir. In most systems, the pumps are deployed from a jetty by a crane which moves the pump from one location to another. The cost of a sand bypassing system at Nerang River entrance, Australia, averaged \$2.38/m<sup>3</sup> for the pumping of 1.3 Mm<sup>3</sup> of sand a distance of 1.2 km during 1987-1989 (Clausner, 1989 and 1990).

### 16.3.4 Cable-Suspended Dredge Pumps

A number of specialized proprietary dredging systems are available which use cable-suspended dredge pumps, including systems which also use a submerged video monitor for precision dredging (Fig. 16.7*a*). A system of this type was used for dredging at depths of nearly 200 m at Luzzzone Reservoir in Switzerland, eliminating the need to lower or empty the reservoir with the attendant loss in hydropower generation. These systems also generate very low turbidity, making them useful for the excavation of contaminated sediment or where severe turbidity restrictions are established. Both hydraulic and pneumatic pumps have been used in these systems. Harrison and Weinrib (1996) describe the application of the EDDY pumping system for the demonstration dredging of 7833 m<sup>3</sup> of medium and fine sand from Cresta Reservoir in California (Chap. 22). This system uses a hydraulic pump to create a suction vortex, similar to a tornado, which suctions sediment from the bed without a cutterhead. Unlike pneumatic pumps, this system was able to successfully handle woody debris and stones. A disadvantage, however, is that

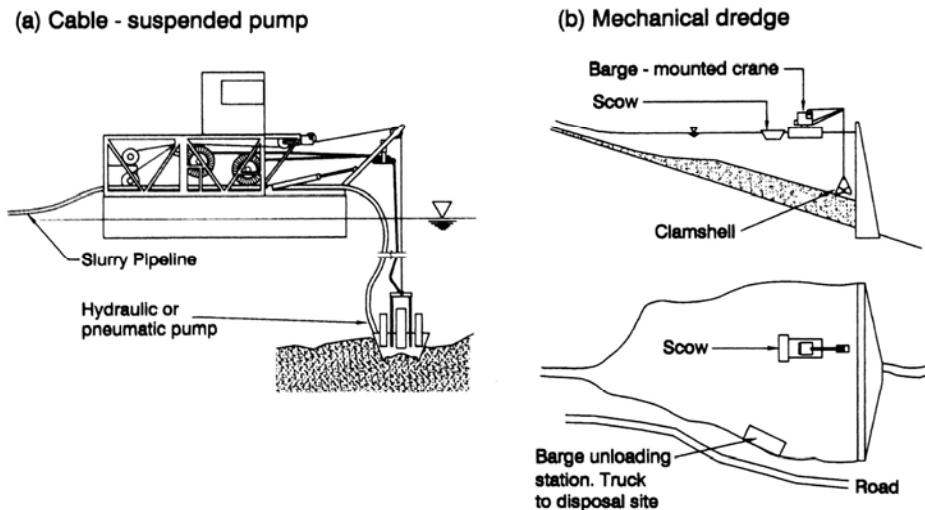


**FIGURE 16.7** (a) Cable-suspended dredge pump, capable of dredging to depths of 200 m. (b) Clamshell mechanical dredge showing the associated barge required to transport sediment to the shoreline.

unit excavation costs for these specialized pumping systems are significantly higher than for conventional hydraulic dredges.

A cable-suspended pneumatic pump was used to dredge  $0.55 \text{ Mm}^3$  of silt from Gibraltar Reservoir at Santa Barbara, California, over a 3-year period. The sediment was dredged and delivered to a containment site about 30 m above the reservoir level at an average cost of  $\$7.69/\text{m}^3$  or  $\$5.85/\text{yd}^3$  (City of Santa Barbara, 1987). A more detailed description is provided by Cooke et al. (1993).

### 16.3.5 Mechanical Dredges

A mechanical or bucket dredge excavates submerged sediments with a bucket (Fig. 16.7b). A barge-mounted *clamshell* may be used to excavate both fine and coarse material. A fully enclosed clamshell design has been developed which can reduce turbidity generation compared to the nonenclosed bucket. Mechanically dredged sediment is deposited into a scow tied alongside the dredge, then is subsequently towed to the edge of the reservoir for mechanical unloading and transport to the disposal sites. Compared to hydraulic dredges, mechanical dredges deliver a product having low water content, but the production rate is low. The *bucket ladder* dredge consists of a continuous chain of open buckets and is used principally in the alluvial mining industry. It may be suitable for use in a reservoir where gravels or larger material predominate. A bucket ladder dredge will generate considerable turbidity.

### 16.3.6 Sediment Removal by Explosives

Explosives have been used to excavate or rehabilitate small stock ponds in rural areas of the United States. The use of explosives to remove sediments in reservoirs has been proposed at several sites, but the authors know of no site where any explosive technique has been attempted on a significant scale. This section briefly reviews the status of explosive techniques in reservoirs.

A search of publications available in the Institute of Hydroelectric Power Research and Water Conservancy in Beijing conducted by Guangdou Hu in 1988 revealed only a few small-scale examples of the use of explosives in China. Explosives were used at the small, seasonally empty Dashikau irrigation reservoir to break boulders so they could be passed through a bottom sluice (this reservoir is shown in Fig. 15.7). Explosives were also used on a pilot scale to excavate fine-grained material from exposed sediment beds during reservoir emptying. Limited testing in China indicates that clayey sediments rapidly attenuate shock, and a relatively small amount of material is moved in relation to the explosive used. The blast-induced vibration propagates much better in saturated Yellow River silts. For floodplain deposits in the Xiaolangdi Reservoir, it was estimated that 0.67 kg of dynamite would be required to excavate 1 m<sup>3</sup> of channel volume on the flood plain, and about half this amount of explosive for the side slopes of the channel.

Tolouie (1989) described a proposal to use explosives at the Sefid-Rud Reservoir in Iran to hasten the collapse of channel banks during hydraulic flushing in the emptied reservoir (Fig. 23.8). While this method could accelerate the rate of bank collapse, it is not clear that it would significantly increase the total amount of sediment removal compared to natural erosive processes. This method was not employed.

*Explosive mobilization* is a conceptual technique in which an underwater explosion suspends sediment during a period of high-velocity flow, such as a sediment routing event, which carries the resuspended sediment out of the reservoir. This strategy was suggested by Allan Zack and analyzed by the first author at the Loiza Reservoir in Puerto Rico, but was not recommended for testing or implementation. Several conditions must be met for explosive mobilization to be successful:

- Sediment removal will be significantly increased only when fine sediments, which otherwise would not be eroded or would be eroded very slowly, are mobilized into the flowing water. The explosion should suspend sediment as a cloud of fine particles that can be carried away by the current, rather than as large clumps which would settle back to the bottom.
- Explosives emplaced in dewatered sediments before the flood season may remain submerged for a prolonged period prior to detonation. Conventional techniques using underwater electrical connections are not suitable for this application. A suitable explosive technology might be based on the use of nitromethane, an extremely stable industrial solvent which can be buried in drums and activated by an onshore detonator, with blast transmission along a polyurethane pipeline filled with the solvent (Trocino, 1991).
- Many potential security, safety, and environmental issues must be addressed.

The best opportunity for successful explosive mobilization would occur where the timing and rate of inflow are controlled by an upstream reservoir. However, it is unclear to what extent the use of explosives might increase sediment removal over other methods, and the possible economic advantages of using explosives have not been analyzed. This is a highly unconventional technique, and any work in this area should obviously be initiated on a pilot scale.

## **16.4 CONSIDERATIONS FOR RESERVOIR DREDGING**

---

A dredging job can be considered in terms of four basic components: (1) the sediment to be removed, i.e., the dredge site; (2) the equipment to remove and lift the sediment,

i.e., the dredge; (3) the means to transport the dredged material, i.e., a pipeline for hydraulic dredging; and (4) the dredged material disposal site.

#### 16.4.1 Dredge Site

The site from which sediments are to be removed is defined in terms of both area and depth. When the purpose of reservoir dredging is to establish a navigational channel, the contractor must ensure that all sediment within the dredging template is removed, but the contractor is not paid for the removal of sediment beyond a certain overdepth limit. In contrast, reservoir dredging may be oriented to removal of a specified sediment volume within a specified contour interval, rather than the attainment of precise geometry. In this situation, greater tolerance may be specified for deviation from the planned dredging template without contractor penalty, and areas with woody debris and hard material may be avoided.

It is essential to know the grain size characteristics of the sediment to determine the percentage of coarse sediment to be removed, based on boring data. Grain size determines the minimum velocity required in the pipeline for solids transport and the settling characteristics of the sediment in the disposal area. Because sediment can be deposited in layers, it is essential to verify the grain size composition of the sediments from borings which extend through the entire depth of the zone to be dredged. Surficial sampling will not reveal the existence of these layered deposits. In small jobs, sediments may be probed with a rod to determine their thickness and consistency. Sediment sampling will also frequently be required for environmental monitoring. Because regulatory requirements and the pollutants of concern will vary greatly from one area of the world to another, the best strategy is to consult with the appropriate regulatory agencies early in the planning stage, to ensure that all the required samples are collected, and that the sampling and testing protocols are in compliance with agency requirements.

A hydraulic dredge also requires a staging area with an all-weather access road. The staging area will typically be used to assemble and maintain dredging equipment, work-boat access and docking, fuel and equipment storage, and contractor offices and parking.

Reservoirs may be subject to large and rapid changes in water levels, and in narrow reservoirs floating equipment may be subject to high flow velocities during large floods. Floating equipment or pipelines which are carried downstream by flood flow may become lodged against gates. Flood conditions should be anticipated, and the contractor must be able to properly secure equipment and pipelines in the event of flood.

#### 16.4.2 Dredging Equipment

Almost all reservoir dredging is done with conventional hydraulic dredges. Special situations that may require more specialized equipment (and warrant higher unit costs) include removing contaminated sediments, dredging gravel and larger sediment, and digging at depths exceeding about 15 m.

The dredge size required at a particular reservoir will depend on factors including the desired production rate, digging depth, and distance and elevation change between the dredge and the point of discharge. Figure 16.8 may be used to obtain a preliminary idea of the relationship between dredge size and production rate for a conventional cutter-head dredge without a ladder or booster pump. The typical horsepower range as a function of dredge size is illustrated in Fig. 16.9. The maximum pumping rate may also be limited by the surface area in the containment area; effluent turbidity will increase as a function of

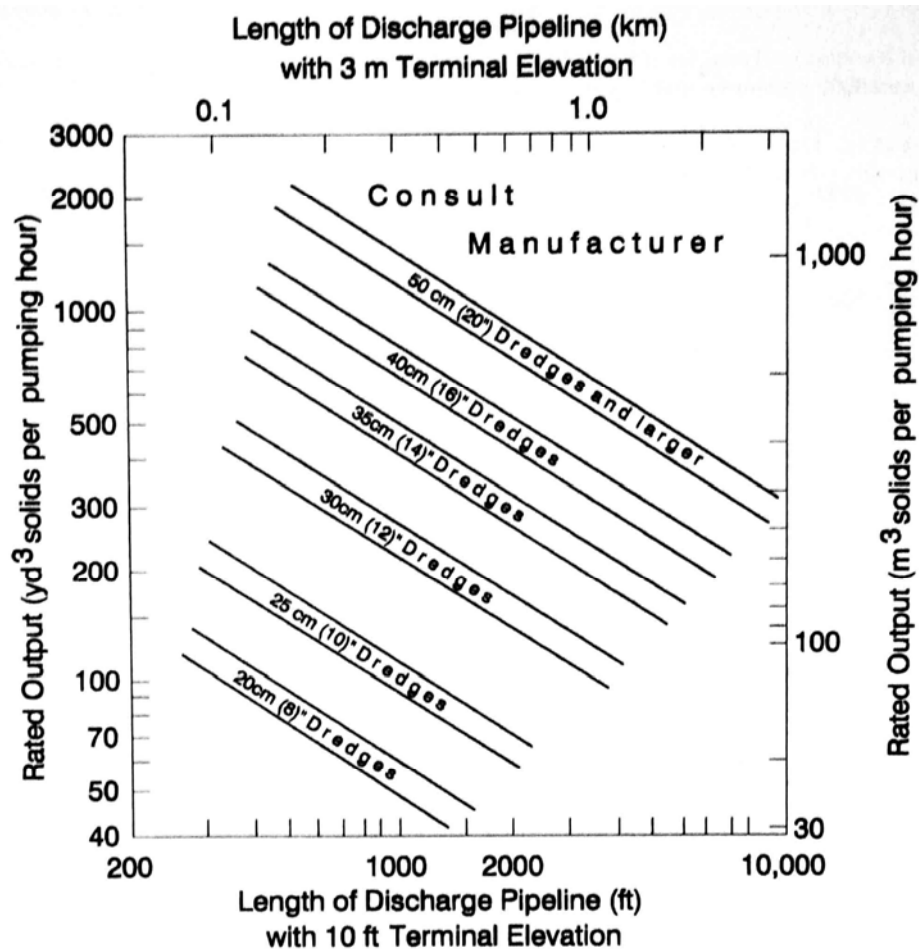


**FIGURE 16.8** Approximate relationship between dredge size and production rate (redrawn from Herbich, 1992).

the hydraulic loading rate (discharge per unit surface area), and a large dredge pumping into a small containment area can produce an effluent of unacceptable quality. A hydraulic dredge pumps much more water than sediment, and if the dredge discharges below the dam this may adversely affect the reservoir water balance.

Dredge sizing may also depend on local operational conditions. For instance, in some cases an owner (or lake association) may prefer a small dredge with low capital costs and simplified operation, and operate the machine for a period of several years to remove a large volume of sediment. Or, a small dredge may be used to remove sediment at approximately the same rate it is delivered to the reservoir.

Production time refers to the amount of time that the dredge is actually digging and pumping slurry. Hydraulic dredges are usually operated 24 hours a day, but actual dredging time will normally not exceed about 18 hours/day because of time spent in activities such as equipment moves and maintenance. Using this guideline and knowing the volume of sediment to be removed, the time to complete the job may be computed as

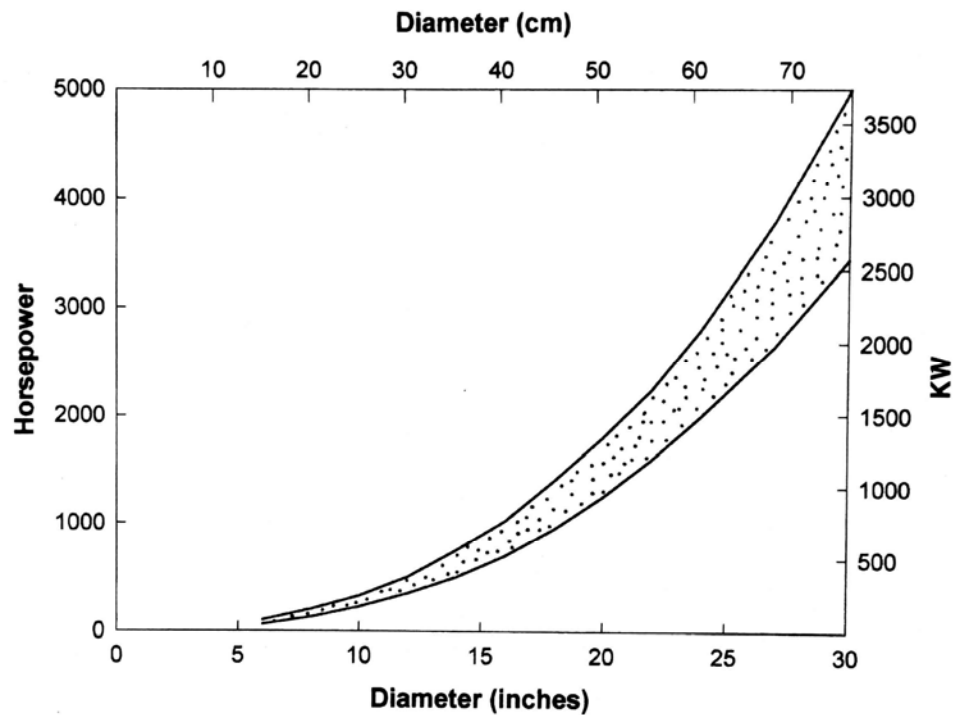


**FIGURE 16.9** Typical size of pumping units as a function of dredge suction diameter (based on Turner, 1996).

a function of the dredge production rate. If there is a significant amount of debris, or considerable aquatic or wetland vegetation in shallow areas, the actual production time may be significantly reduced. Dredges smaller than about 50 cm (20 in) may be particularly susceptible to reduced productivity because of roots from vegetation (Turner, 1996).

### 16.4.3 Pipeline System

A pipeline transports the sediment slurry from the dredging site to the point of discharge, and, for a long pipeline, one or more booster pumps may be used. Pipelines may be made of steel and supported on pontoons, or they may be made of sections of heat-welded high-density polyethylene pipe, which has the advantage of being flexible and noncorrosive. Having a specific gravity of about 0.95, the polyethylene pipe will float when filled with water, but will sink when conveying slurry and thus requires the use of floats. Pipeline wear (abrasion) is greatest when the pipe is transporting coarse sands and gravels, and minimal when transporting fines.

Locating the pipeline route may be straightforward in a rural area, but in urban areas it may be complicated by features such as development patterns, easements, road and railroad crossings, etc. Whereas the dredge will move from one area to another, a booster pump station may not be moved for the duration of the job. Booster pump locations should be selected to minimize inconvenience and potential noise impacts, and appropriate mufflers should be specified for pumps with diesel drives.

#### 16.4.4 Disposal Site

There are two basic strategies for the disposal of dredged sediment: *riverine disposal* to the channel below the dam, or *off-stream disposal* into a diked upland containment area.

**Riverine Disposal.** The discharge of sediment below the dam is often the most economical option from the standpoint of the dam owner. This may be especially true in mountainous areas where large-capacity disposal sites are not readily available, such as at Amaluza Reservoir on Ecuador's Paute River (Fig. 16.10), where dredged sediments are discharged below the dam. Riverine discharge has been used at a number of reservoirs in less industrialized areas, and siphon dredging requires discharge below the dam.

From the aspect of maintaining the continuity of sediment transport along the river system, the disposal of dredged material into the river downstream of the dam would appear to represent the best option. However, the year-round discharge of dredged material is completely different from the episodic nature of sediment discharge under natural conditions and can create large downstream impacts. Because the dredged material will typically consist of fines from the area near the dam, rather than coarse material deposited in the delta region that is most distant from the dam, the discharge of dredged sediment will typically not remedy problems of riverbed degradation associated with the trapping of coarse material above the dam. Riverine disposal is usually prohibited in industrialized areas, and may also be infeasible in areas where otherwise permitted by regulatory agencies because of adverse downstream impacts.

Sediment discharged below the dam and settling into downstream navigation channels, intakes, or canals will need to be dredged again (usually by a different party).

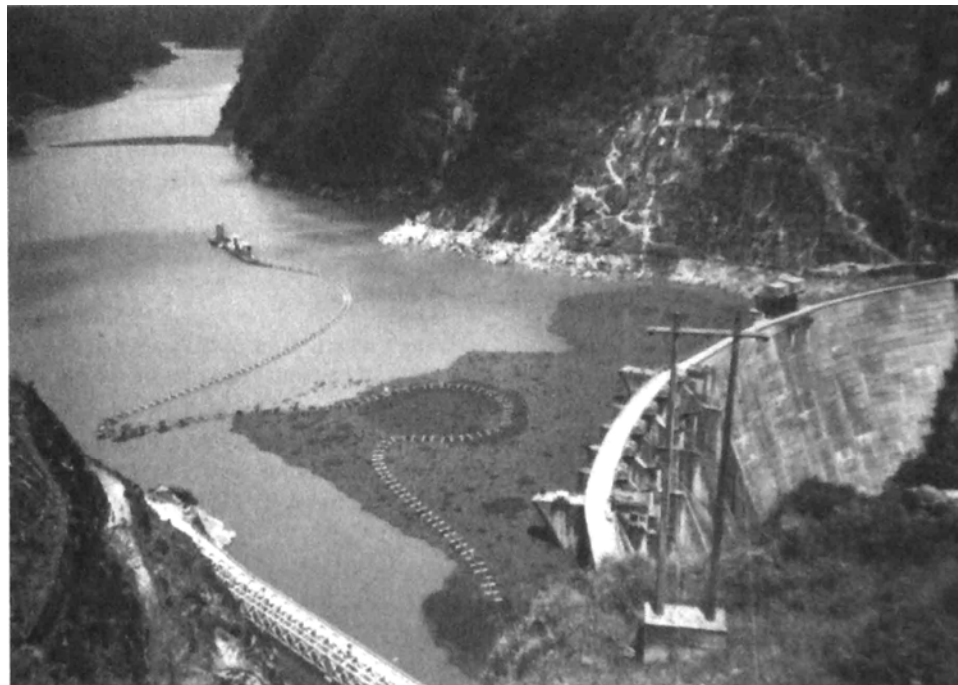


**FIGURE 16.10** Dredging at Amaluza hydroelectric reservoir in Ecuador during 1995, with discharge to the river below the dam (A. Sotto).

This merely moves the sediment problem from one place to another. Sediment deposition can cause the riverbed to aggrade and overflow its banks, obstruct water supply and irrigation intakes, increase treatment costs at water filtration plants, clog permeable river beds supplying infiltration galleries, and impair recreational and aesthetic uses. In addition, the clogging of coarse bed material with fine sediment can severely affect or destroy aquatic ecosystems. Sedimentation within the downstream channel should be expected to be particularly severe in relatively low-gradient streams where sediment accumulation has already become a problem because of the reduction in peak downstream discharges following dam construction.

In some cases sediment discharge to the river below the dam may be a logical alternative, especially if undertaken as a continuous long-term process which matches sediment discharge below the dam to the rate of sediment inflow. However, the consequences of discharge below the dam should always be analyzed very carefully because of the large downstream impacts which can be caused. This analysis will rely heavily on a responsible environmental impact analysis, since the negative below-dam impacts will typically affect third parties, while the owner of the dam reaps the economic benefits. The authors have not yet found an example of a detailed monitoring study examining the impacts of the discharge of dredged material below a dam.

***Off-Stream Disposal.*** For off-stream disposal, hydraulically dredged sediment is pumped into an upland diked containment area where the sediments are allowed to settle, and the supernatant water is discharged into the environment (often back into the lake being dredged). After dredging ends, the containment area is dewatered, sediments are allowed to dry, and the site is (1) dedicated to a new use or (2) reused for additional future sediment deposition by either heightening dikes or excavating the dried sediments. In some cases it might be feasible to dam a shallow tributary arm of the reservoir, discharging sediment into that area and filling it well above the reservoir level.

A number of criteria in addition to the lease or purchase price will be important to consider in selecting an off-stream disposal site:

1. Provide adequate volume to store the dredged material following bulking and adequate surface area for solids settlement to meet the effluent standards, based on the settling characteristics of the sediment.
2. For economy, the disposal site should be located as near as possible to the area to be dredged and close to the lake elevation. However, nearby disposal sites are not always available.
3. Limit the cost of dikes by selecting a site with favorable topography and suitable borrow material for dike construction. The construction of containment area diking is a potentially large cost item.
4. Avoid areas considered environmentally sensitive such as wetlands and streams, historical sites, and river floodway. As an exception, it may be feasible to impound a tributary stream, subsequently converting the containment area into a wetland with a permanent drop structure.
5. Minimize adverse hydrologic impacts. To minimize impacts on the lake's water budget, the settled effluent from the disposal area should drain back into the reservoir. Avoid areas where seepage from the containment area can cause an undesired increase in groundwater levels, or provide for remedial measures such as drains.
6. Isolate the site from urban areas where the disposal dikes, pipelines, and other equipment may be considered a nuisance, a safety hazard, aesthetically unpleasant, and may conflict with existing zoning, roads, and rights-of-way.

7. In arid regions, consider the long-term impacts of wind-blown silt that can originate from the disposal area after it dries.
8. The site should provide the operational flexibility needed for the job, such as the ability to discharge dredged material at different points as the dredge moves.
9. The site should be suitable for future reuse.

The large volumes of sediment associated with major dredging work can represent a difficult siting problem, and the "best" site may not be optimal from the standpoint of all the above criteria. The locations of disposal sites selected for the discharge of 6 Mm<sup>3</sup> of hydraulically dredged sediment from Loiza Reservoir are illustrated in Fig. 16.11. Because of topographic limitations and the presence of river floodways, urban land uses, wetlands, and other restrictions, these were the closest feasible sites. Contrast this to the siting that was possible at Lake Springfield (Fig. 16.12).

#### 16.4.5 Long-Term Use and Sustainable Dredging

If a reservoir is dredged once, it will probably need to be dredged again. Dredging represents a long-term management alternative only as long as disposal sites are available.

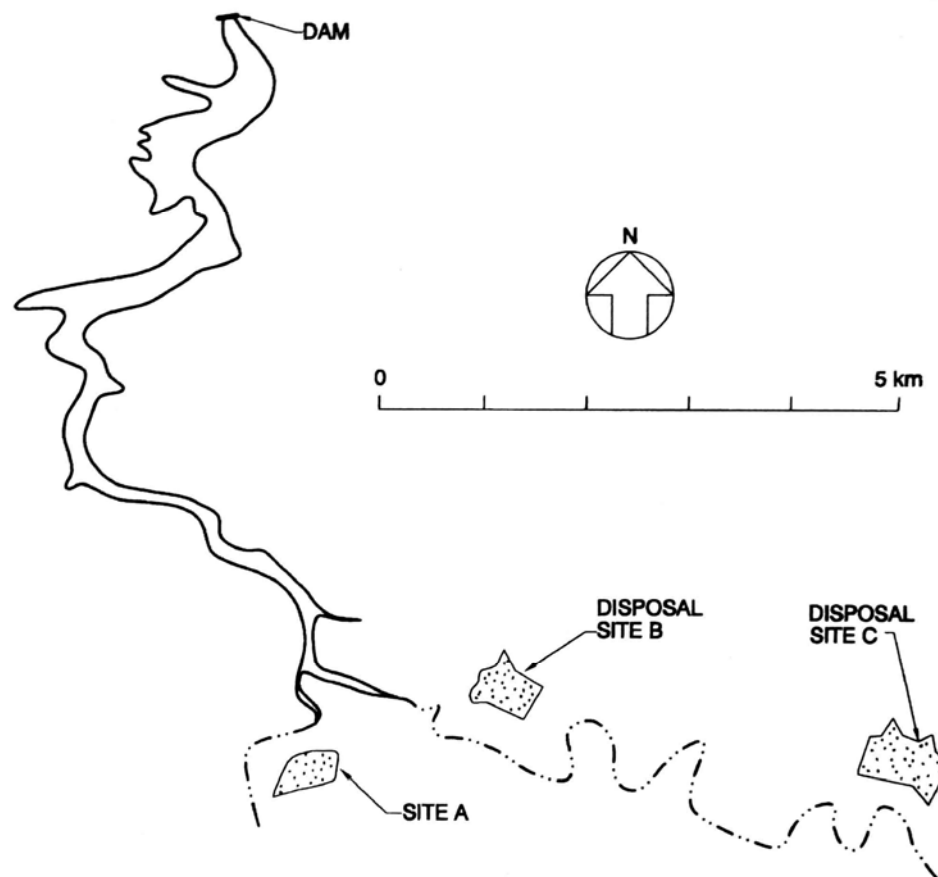


**FIGURE 16.11** Location of disposal areas for 6 Min<sup>3</sup> of sediment to be dredged from Loiza Reservoir, Puerto Rico.

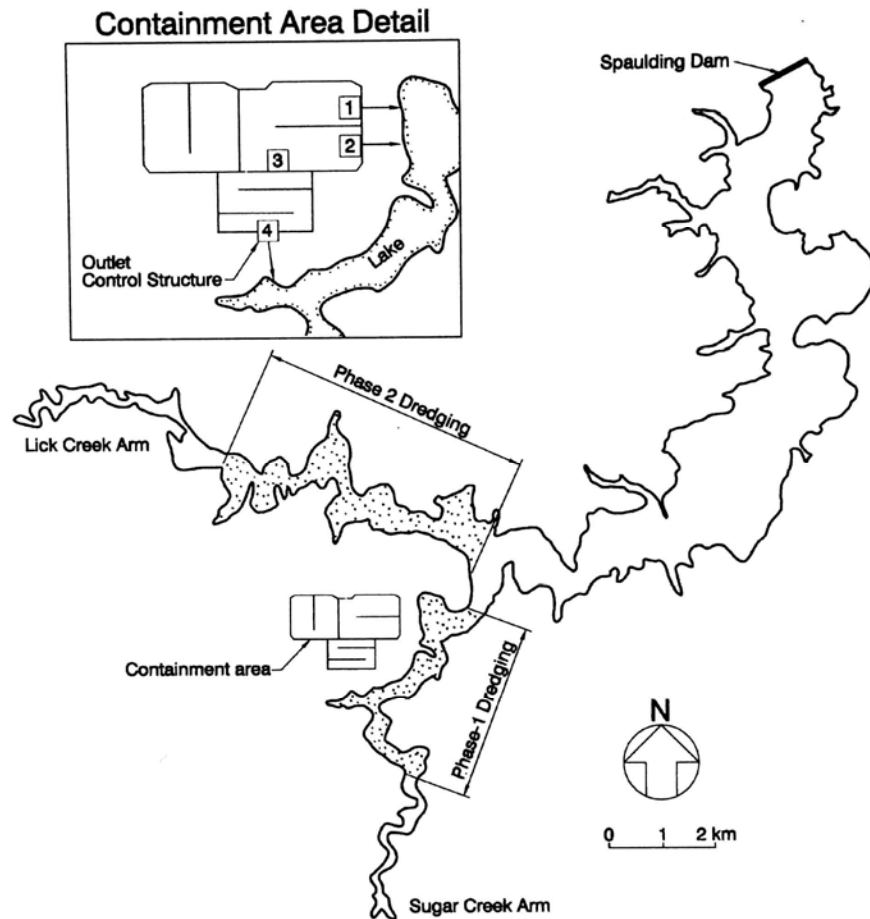


**FIGURE 16.12** Location and layout of disposal areas used for 2.3 Mm<sup>3</sup> of sediment dredged from Lake Springfield, Illinois

The need for repeated future dredging should be carefully considered in the selection and design of a spoil area, providing the option for future reuse of the site insofar as possible. Site reuse can be achieved by excavating and trucking the dredged material after it has dewatered, or by raising the dikes. Disposal area reuse has been discussed by Montgomery et al. (1978).

Containment areas are often dedicated to agricultural use after a year or two of dewatering. Containment areas may also be converted into a natural or parkland area. When wet or ponded, containment areas have rapidly developed wetland vegetation and become significant wildlife habitats.

#### 16.4.6 Dredging Contracts

General considerations for dredging contracts have been reviewed by Sanderson (1992). Dredging is normally performed under one of three types of contract forms. A *unit price* contract is based on measurement of the volume of material removed, and payment is based on this measurement. A *rental contract* pays for the number of hours the dredge is in operation, with additional payment schedules for idle, standby, and moving time.

Contract specifications in this case should give considerable attention to the capacity and condition of the dredging equipment. The least-used type of dredging contract is a *lump sum* contract which specifies the work to be performed for a fixed price within a stated time period.

Sanderson has observed that contracts and the pre-contracting process are almost always given less attention than they deserve, and many disputes could be avoided by more careful preparation of contracts and specifications. Several recurrent issues in the preparation and administration of dredging contracts were identified.

**1. Differing Site Conditions.** Dredging involves the excavation of unseen material, and the conditions encountered during the work may be different from those expected by either the owner or the contractor during the contracting phase. There is a high potential for unforeseen conditions to arise, leading to claims for differing site conditions.

In preparing specifications for dredging work, the recommended procedure is to provide a detailed description of the field testing performed, and the results of that testing. Other known conditions which may affect the work should be factually presented (e.g., submerged obstructions and anticipated seasonal variations in water level, which may dramatically affect pumping costs). However, the data presented should not be interpreted by the owner, least it be interpreted to warrant conditions at the site. Interpretation should be the bidder's responsibility. Unpredictable water level variation due to drought is a potentially critical aspect of reservoir dredging, and should be addressed in the contract. Another potential problem in some sites involves debris, which may be concentrated in certain areas of a reservoir and may not be detected during sampling.

**2. Records.** From the standpoint of contract administration, a singularly important task is the proper documentation of the facts relating to work progress, and a factual description of the nature of any problems encountered. The contractor should maintain a daily log of dredging operations, and the owner should prepare inspection reports on a regular basis. Good field records form the essential basis for the settlement of subsequent claims and disputes which may arise on the job.

**3. Authority.** The contract documents typically establish specific individuals who shall serve as the owner's and contractor's representative for issues relating to contract decisions and notifications, and certain types of decisions can be made only with persons having the proper legal authority. For example, an inspector may be authorized only to make reports and lack authority to require any type of operational change. Both the contractor and owner must understand and rigorously follow the procedures and chain of command established in the contract documents.

**4. Corps of Engineer Contracts.** As the largest contractor of dredging services in the United States, the Corps of Engineers is recognized as the premier authority on dredging matters. The Corps exerts a strong influence on the standards of industry practice, and thereby will influence the manner in which private dredging contracts may be subsequently interpreted by arbitrators or the court. Private dredging contracts should adhere to the Corps principles wherever possible in the writing and interpretation of contract clauses. Copies of dredging contracts may be obtained from Corps of Engineers offices, or a complete set of Federal Acquisition Regulations may be obtained from the Superintendent of Documents.

**5. Dispute Resolution.** Recourse to litigation for resolving disputes is both time-consuming and very costly. In response, voluntary alternative dispute resolution techniques have emerged. *Mediation-based techniques* use the intercession of a third party to help the parties reach a mutually satisfactory agreement. Mediation works best when the two parties desire to continue a business relationship. *Arbitration-based*

*techniques* are more formal than mediation, but faster and less formal than litigation. Under arbitration the dispute is submitted to a third party or a panel that reviews the evidence and arguments presented, and renders a decision. Arbitration proceedings are private and the matter and settlement is confidential. Although arbitration is voluntary, the parties may agree to binding arbitration, and it may be made a condition of the contract using an arbitration clause:

*Any controversy or claim arising out of or relating to this contract, or the breach thereof, shall be settled by arbitration in accordance with the Commercial Arbitration Rules of the American Arbitration Association, and judgment upon the award rendered by the arbitrator(s) may be entered in any court having jurisdiction thereof.*

Information on both mediation and arbitration may be obtained from The American Arbitration Association ([www.adr.org](http://www.adr.org)), 1633 Broadway, 10th Floor, New York, New York 10019.

#### 16.4.7 Permit Requirements

The following list of permits is based on those required for the Lake Springfield dredging, described in the next section. These are typical of the permits required in the United States for dredging in waters classified as nonnavigable with sediment discharge to an upland area.

- **Army Corps of Engineers.** A dredging permit was not required because the reservoir is not classified a navigable waterway. A nationwide permit was obtained for disposal of hydraulic dredged material to an upland area. As part of the Army permit, a cultural resources study was required in the proposed containment area. Depending on the site characteristics, a jurisdictional determination may be required at the spoil area site to determine the extent of wetland areas to be affected by the fill activity, and thus subject to permitting.
- **Environmental Protection Agency.** A water quality permit was required from the state, which has primacy under the National Pollution Discharge Elimination System. The disposal site was considered a treatment system and the effluent was limited to a maximum suspended-solids concentration of 15 mg/L. The lake sediments to be dredged had objectionable levels of pesticides, which had washed into the lake with topsoil from farms in the catchment area. There was concern that dredging would cause these pesticides to be released, and the water quality permit required biweekly monitoring of selected pesticides in the disposal area supernatant. Concentrations never exceeded the detection limit.
- **State.** A state dam safety permit was required for the spoil embankment, which was classified under Illinois regulations as a Class 1 site because of its proximity to a residence.
- **Local.** It was necessary to change the zoning classification of the site from agricultural to landfill because of the presence of pesticides in the dredged sediments, even though the dredged material had lower pesticide levels than the farmland it covered or the adjacent fields.

The permit issued by the Army Corps of Engineers encompasses the permitting requirements of and review by that agency plus the Environmental Protection Agency, the Fish and Wildlife Service, and National Marine Fisheries Service. Endorsement by the State Historic Preservation Office is also required, based on an assessment of the site to determine the presence or absence of cultural resources.

Permitting requirements will be more complex when navigational waterways are involved, when sediments affect significant wetland areas (which will typically require development and implementation of a mitigation plan), when threatened or endangered species are present, where toxic sediments may be involved as may occur in urban lakes, or under similar complicating situations. Preparation of a full environmental impact statement may be anticipated for large dredging jobs or those considered to have potentially significant impacts.

## 16.5 EXAMPLES OF RESERVOIR DREDGING

---

### 16.5.1 Lake Springfield, Illinois

Predredging conditions at Lake Springfield were summarized by Bhowmik et al. (1988), and the initial phase of dredging was described by Buckler et al. (1988). Built in 1934, Lake Springfield supplies municipal drinking water to the City of Springfield, Illinois, and cooling water to the city's thermoelectric power plant. It is a shallow 1635-ha impoundment on the Sugar Creek tributary to the Sangamon River, extensively used for recreation, and has about 700 residences around its periphery. The lake has a tributary area of 686 km<sup>2</sup>, and its original capacity was 73.9 Mm<sup>3</sup> for an average depth of only 4.5 m. By 1984, the capacity had been reduced by about 13 percent, a storage loss of about 9.5 Mm<sup>3</sup>.

Sediment accumulation not only reduced storage volume, but also impaired recreational use, rendering some boat ramps and the two principal arms of the reservoir inaccessible to boats and fishermen. Lake fishing contributed an estimated \$1.1 million annually to the community's economy. Property values adjacent to the area with greatest sedimentation were reduced some 20 percent compared to similar properties on the main body of the lake. The major benefits of reservoir dredging in the tributary arms of the reservoir where recreational and property values were most impaired were identified as:

1. Restoring sediment trapping capacity in upper arms of the lake, thereby protecting the main body of the lake from sedimentation
2. Increase water storage by 2.3 Mm<sup>3</sup>
3. Reclamation and reuse of high-quality eroded topsoil that had accumulated in the lake
4. Reduction of aquatic plant problems
5. Improved fisheries management, including spawning and desirable aquatic habitat development
6. Increased recreational use such as pleasure boating, water skiing, and fishing

Recovery of full lake capacity was not contemplated because of high cost.

Nineteen candidate upland containment sites were analyzed for sediment disposal on the basis of proximity to both areas to be dredged; availability of soil suitable for dike construction; relatively flat topography; proximity to lake level to reduce pumping head; potential for more than one discharge weir location; and isolation from nearby residences or infrastructure to minimize safety, nuisance, and right-of-way conflicts for the pipeline (Buckler et al., 1988). The configuration of the selected 199-ha disposal site is shown in Fig. 16.12.

The dredging project was divided into two phases, one for each arm of the reservoir. Dredging began in 1987, after being delayed by low water which left inadequate depth under the prescribed cut to float the dredge. Dredging was undertaken 5 days per week, 24 hours per day, from April into December, with a conventional cutterhead-type dredge and a flexible high-density polyethylene pipeline. Dredging was not feasible in the middle of winter because the upper arms of the lake ice over. The dredge, booster pump, pipeline, and other equipment used on this job were transported to the site in 17 tractor-trailers. A staging area with good road access was provided at the edge of the lake for the contractor to use for equipment setup and launching, and for storage of equipment and supplies for the job.

The first dredging phase did not need a booster pump because it was close to the containment area. The second phase used a single barge-mounted diesel booster pump at the edge of the lake to pump dredged material into the containment area. Hospital-class mufflers were specified for the booster, since the lake is lined with residences. Despite the numerous residences and 24-hour operation, there were no noise complaints during either phase of the work. Dredging reportedly generated a very small turbidity plume which caused no problems. Deposited sediments in the lake averaged 66 percent clay, 33 percent silt, and 1 percent sand (Fitzpatrick et al., 1985). Because dredging was concentrated in the upstream portion of the reservoir the dredged sediment contained more silts and sands than the main body of the lake.

Because of the variable site topography, containment dikes varied from 1.2 to 7 m in height. The dikes were originally wide enough to drive around on top, but wave erosion during the prolonged dredging project subsequently made them too narrow for driving in some areas. Toe drains were required in some areas to control seepage. The containment area provided 7 to 14 days of water retention, and was compartmented with outlet structures at different locations for flexible operation, since the slurry pipe would enter at different areas depending on the place the dredge was working. Supernatant met the 15-mg/L effluent standard for suspended solids about 75 percent of the time, problems occurring primarily when it was windy. Emergent wetland vegetation began to grow as some of the compartments filled with sediment. It was found that by routing the supernatant through these shallow vegetated areas prior to discharge, the effluent turbidity levels were greatly reduced, resulting in turbidities on the order of 1 to 2 mg/L for prolonged periods. Supernatant from the containment area was discharged back into the reservoir. In addition to the development of wetland vegetation, the containment area cells saw extensive use by waterfowl. At the completion of dredging, the containment area was allowed to dewater and consolidate for 2 years, by which time it was suitable for agricultural use. The land was then leased to a local farmer for the production of corn and soybeans (Skelly, 1996).

The project began in 1987 and required 4 years to complete. A total of 2.28 Mm<sup>3</sup> was dredged at a unit cost of \$3.02/m<sup>3</sup> (\$2.31/yd<sup>3</sup>), which included the cost of purchasing and constructing the containment area. Project characteristics are summarized in Table 16.2 and costs are summarized in Table 16.3.

### **16.5.2 Valdesia Reservoir, Dominican Republic**

The concrete-gravity Valdesia Dam, a hydropower facility owned by Corporación Dominicana de Electricidad, was constructed in 1976 approximately 80 km west of Santo Domingo. Two hurricanes damaged the dam and deposited large volumes of sediment, which prompted subsequent dredging operations. Information for this example is based on a site visit in November 1990, including discussions with engineers and operators.

**TABLE 16.2** Summary Characteristics of Lake Springfield Dredging

	Phase 1	Phase 2
Dredge pump	1000 hp	675 hp
Booster pump	None	1000 hp
Pipeline	35 cm (14 in)	40 cm (16 in)
Pumping distance, km	0.8 to 2.0	1.2 to 3.6
Operation	24 h/day, 6 days/week	24 h/day, 5 days/week
Start	June 1987	April 1989
End	August 1988	July 1990
Sediment removed, yd <sup>3</sup>	1.38X 10 <sup>6</sup> yd <sup>3</sup>	1.6X 10 <sup>6</sup> yd <sup>3</sup>
Sediment removed, m <sup>3</sup>	1.05 X 10 <sup>6</sup> m <sup>3</sup>	1.22 X 10 <sup>6</sup> m <sup>3</sup>
Cost	\$1.8 million	\$2.7 million

*Source:* City of Springfield.

**TABLE 16.3** Summary of Dredging Costs, Lake Springfield, Illinois

Item	Cost, \$
Land purchase	1,272,000
Earthwork, Phase 1 retention area	637,000
Earthwork, Phase 2 retention area	483,000
Phase I dredging	1,800,000
Phase II dredging	2,700,000
Total cost	6,892,000
Unit cost	\$3.02/m <sup>3</sup>

Total volume dredged = 2.28 x 10<sup>6</sup> m<sup>3</sup>.

*Source:* City of Springfield.

During September 1979 the Dominican Republic was hit by hurricanes David and Frederick within the space of several days. The radial gates were not opened before the storm knocked out both sources of power supply, and the unopened gates were overtopped for 4 days and were destroyed. Large amounts of sediment and debris, including full-grown trees, washed into the reservoir during the storm and became lodged against the dam, blocking the bottom sluices. Soundings revealed sediment and debris accumulations up to 17 m deep within 1 km upstream of the dam. Cranes were used to grapple material away from the bottom sluice, but even though the bottom sluice would begin to flow it would become clogged again by more woody debris within a matter of hours. After several months of work, the attempt to reopen the bottom sluice was abandoned.

Dredging was undertaken to remove the accumulated sediment, using a 700-mm siphon dredge, designed by the Italian firm GEOLIDRO, with a hydraulically operated basket tooth-type cutterhead. This dredge, donated by the Italian government in the form of international aid, is the largest siphon dredge ever employed in a reservoir (Fig. 16.13). The discharge line was connected to a circular sluice drilled through the base of the dam; the hydrostatic head thus discharged silt through the pipeline without the aid of a pump.

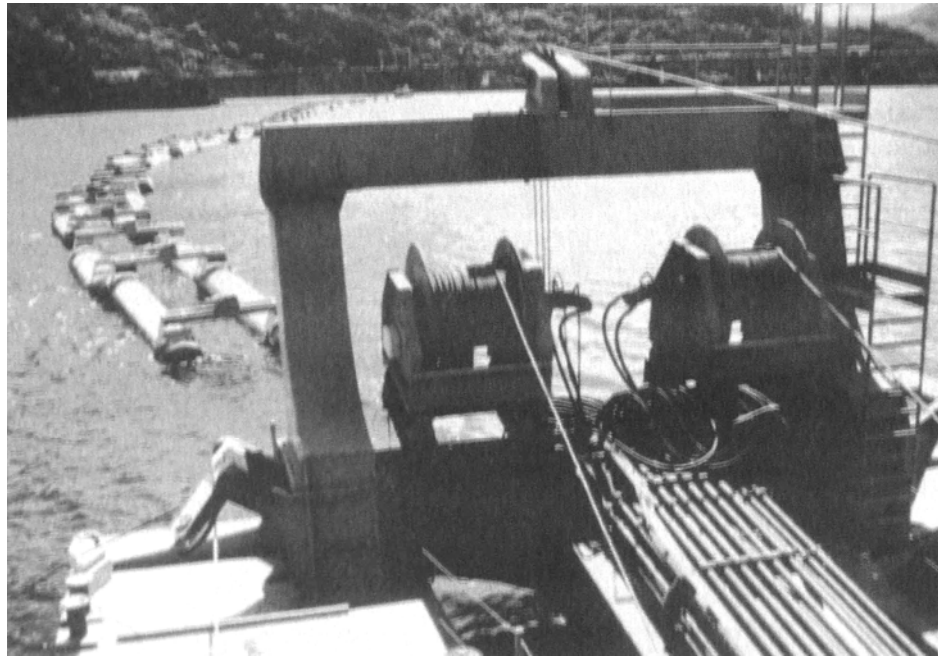


**FIGURE 16.13** Discharge line of 700-mm siphon dredge at Valdesia Reservoir, Dominican Republic. Note that the discharge line is suspended underwater beneath the floats. (*G. Morris.*)

Dredging began in November 1988 and continued on a regular basis for 11 months and on an intermittent basis for the following year. Because of lack of records, the amount of sediment removed is not known. Intermittent operation was attributed to a combination of low water level due to drought plus an inadequate inventory of spare parts (cables, pulleys, etc.). According to the dredge operator, there was relatively little problem with clogging by woody debris. On two occasions woody debris clogged the pipeline, which was uncoupled to remove the obstruction. The cutterhead itself was clogged on a number of occasions, and in each case the cutterhead was lifted, rotation reversed, and woody material removed by hand. Clogging problems were encountered only in limited areas of the reservoir most affected by the hurricane-driven debris.

The dredged slurry was discharged directly to the river downstream of the spillway. The dredged sediments had accumulated in the stream channel below the dam to a thickness of over a meter and were covered with both wetland and upland vegetation. Because the power penstock discharges more than 1 km downstream of the dam, dredged sediments accumulated in the normally dry riverbed below the dam. These sediments would be scoured and washed downstream only during a flood that produced spillway discharges. Because the area immediately below the dam is a semiarid zone without agricultural or other development, a temporary change in the flood level caused by sediment deposition below the dam is not a critical issue. Downstream irrigation intakes would also not be affected, since deposited sediments would be scoured only during major floods.

### 16.5.3 Bai-Ho Reservoir, Taiwan

Sediment excavation at the 25-Mm<sup>3</sup> Bai-Ho Reservoir in southern Taiwan has been described by Wang et al. (1995). The reservoir was built in 1965 with a design life of 100

years, and is used for municipal and irrigation water supply. A high rate of sediment delivery from the 26.55-km<sup>2</sup> watershed area resulted in an average rate of storage loss of 0.3538 Mm<sup>3</sup>/yr, for a 1.4 percent annual loss. The dam lacks a low-level outlet and sediment sluicing was not conducted.

Limited volumes of sediment have been removed from this reservoir over a period of several years by both excavation and hydraulic dredging. Generally, hydraulic excavation was used near the intake and dry excavation in upper (delta) areas of the reservoir. A severe drought in 1994 produced extremely low water levels, and this condition was used to undertake large-scale dry excavation to depths of about 3.3 m over an area of 0.87 km<sup>2</sup>. During the drought an average of 5500 m<sup>3</sup>/day of sediment was removed and delivered to a disposal site about 2 km from the reservoir with 6 hydraulic backhoes, 2 bulldozers, and 25 trucks. Sediment removal costs are reported in Table 16.4. The large

**TABLE 16.4** Sediment Excavation Costs at Bai-Ho Reservoir, Taiwan

Year	Type of operation	Volume, 1000 m <sup>3</sup>	Unit cost, US\$/m <sup>3</sup>
1991	Hydraulic dredging	35	6.60
1991	Dry excavation	300	6.00
1992	Dry excavation	212	5.40
1992	Hydraulic dredging	42	1.41
1993	Hydraulic dredging	8	4.20
1994	Dry excavation	283	4.30
All years	Hydraulic dredging	85	3.80
All years	Dry excavation	795	5.24

Source: Wang et al. (1995).

variation reported for hydraulic dredging cost reflects accounting procedures under which the capital cost of the hydraulic dredge was assigned to some years, whereas only fuel and labor costs were assigned to other years.

## 16.6 CONTAINMENT AREA DESIGN

### 16.6.1 Volume for Initial Storage

The volume of a containment area required for the initial sediment storage volume includes: (1) the volume occupied by the sediment at the end of dredging and prior to dewatering; (2) ponding depth, usually about 0.6 m; and (3) freeboard, also typically about 0.6 m. The volume reserved for sediment storage must be larger than the *in situ* sediment volume in the reservoir because of sediment *bulking* resulting from the entrainment of water during dredging. Sediment volume must be determined separately for fine sediment with a high bulking factor and for coarse sediment, which will exhibit very little bulking.

The *bulking factor* is the dimensionless ratio of the volume occupied by the sediment after deposition in the containment area to the *in situ* volume of the same material prior to dredging, as given by:

$$B = \frac{V_c}{V_i} = \frac{\gamma_c}{\gamma_i}$$

where  $B$  = bulking factor,  $V$  = volume,  $\gamma$  = dry unit weight, and subscripts  $c$  and  $i$  refer to the containment area and *in situ* conditions, respectively.

The bulking factor for a particular sediment may be determined in two ways: (1) it may be estimated from prior experience and the type sediment to be excavated or (2) it may be determined by using the column settling tests described in the next section. Table 16.5 summarizes the typical range of bulking factors experienced as a function of type of sediment. For clays, the bulking factor will depend heavily on the degree of flocculation, and higher bulking factors also tend to be associated with clays of higher initial density and higher plasticity. Coarse sediment (sand) has a bulking factor close to 1.0.

Sediment composition will vary from one part of a reservoir to another, and so will the bulking factor. The bulking factor also depends on the time allowed for consolidation. If a thin (e.g., 1 m) layer of sediment is deposited in a containment area one year, and is allowed to dry prior to discharge of additional dredged material the following year, the bulking factor will be lower than for continuous discharge. These effects are considered in establishing the *sizing factor*, which is the ratio of total containment volume to the total dredged volume. If there are multiple containment areas, the sizing factor may differ for each. Dredging in the delta region of a reservoir may produce a slurry containing a high percentage of coarse material and a low bulking factor. In contrast, material dredged farther downstream may consist of clays which dewater very slowly and have a high bulking factor.

### 16.6.2 General Containment Area Considerations

On level ground, a containment area which is approximately square will minimize the length of the required dike construction per unit of volume. However, it will produce a configuration with a high degree of hydraulic short-circuiting, which reduces effective residence time and thus sedimentation efficiency. The use of one or more interior dikes will provide the hydraulic barrier required to produce an elongated flow path which reduces the effect of hydraulic short-circuiting (Fig. 16.14). The containment area configuration will also be influenced by factors including local topography, operational requirements, and long-term management objectives (e.g., future reuse).

**TABLE 16.5** Bulking Factors for Various Sediments

Material	Sedimented dry bulk density, kg/m <sup>3</sup>	Bulking factor		
		USAE	Huston	Others
Clay	480-1250	1.2-3.1	1.45	
Recent clay deposits				1.3
Silty clay				1.4-1.7
Sandy clay			1.25	
Clayey sand				1.3
Silt		1.1-1.4	2.0	1.3
Silty fine sand				1.1
Sand	1490	1.0-1.2	1.0	

USAE = U.S. Army Corps of Engineers.

Source: Adapted from Herbich (1992).

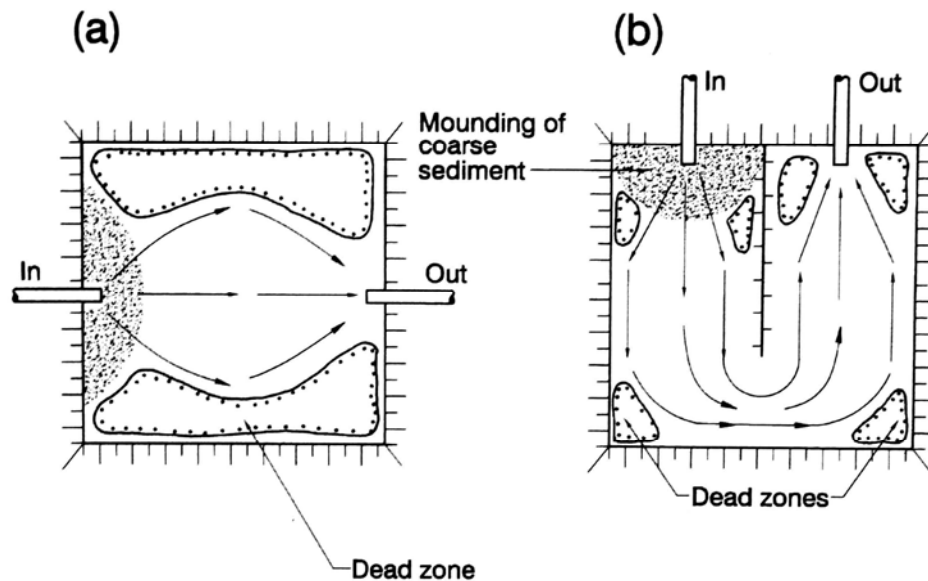


**FIGURE 16.14** Use of interior dikes to reduce the amount of hydraulically dead zones within containment areas by limiting hydraulic short-circuiting. (a) High degree of short-circuiting. (b) Use of interior dike to reduce short-circuiting

In a long-duration project dredging clays that have a high bulking factor and that dewater and compact slowly, the tendency for the sediment to compact under self-weight as additional material is added will be offset by the poor permeability of the fine material. The fine sediment having a high void ratio will resist compaction, and a large percentage of the containment area will be occupied by voids rather than sediment. If land area is limited it can be advantageous to divide the containment area into multiple compartments. The dredge may pump into different containment areas, or different cells within a single containment area, on rotating sequence. Within any given containment area the first lift of dredged material (perhaps 1 m thick) would be allowed to dewater and compact for a season before a subsequent lift is added (Fig. 16.15). Vegetative growth assists dewatering when the roots penetrate and extract water from deeper in the soil column. For more information on dewatering strategies, see U.S. Army (1987), Haliburton (1978), and Montgomery et al. (1978).

When sediment enters the disposal area, the coarse material will settle out near the pipeline discharge point, and fines will settle across the remainder of the basin, as illustrated in Fig. 16.3. Under favorable conditions this coarse material may be used to build up the dikes.

## 16.7 COLUMN SETTLING TESTS

Column settling tests may be used to determine the settling and compression characteristics of dredged sediments. Reservoir sediments often exhibit *zone* or *hindered settling* characteristics, meaning that a sharp interface forms between the settling sediment and the clear supernatant, typically within 24 hours. The sediment mass is slowly compressed as its internal flocculant structure collapses under self-weight, and water seeps upward to the surface, often through small vertical pipes. Particles remaining in the supernatant will settle individually.

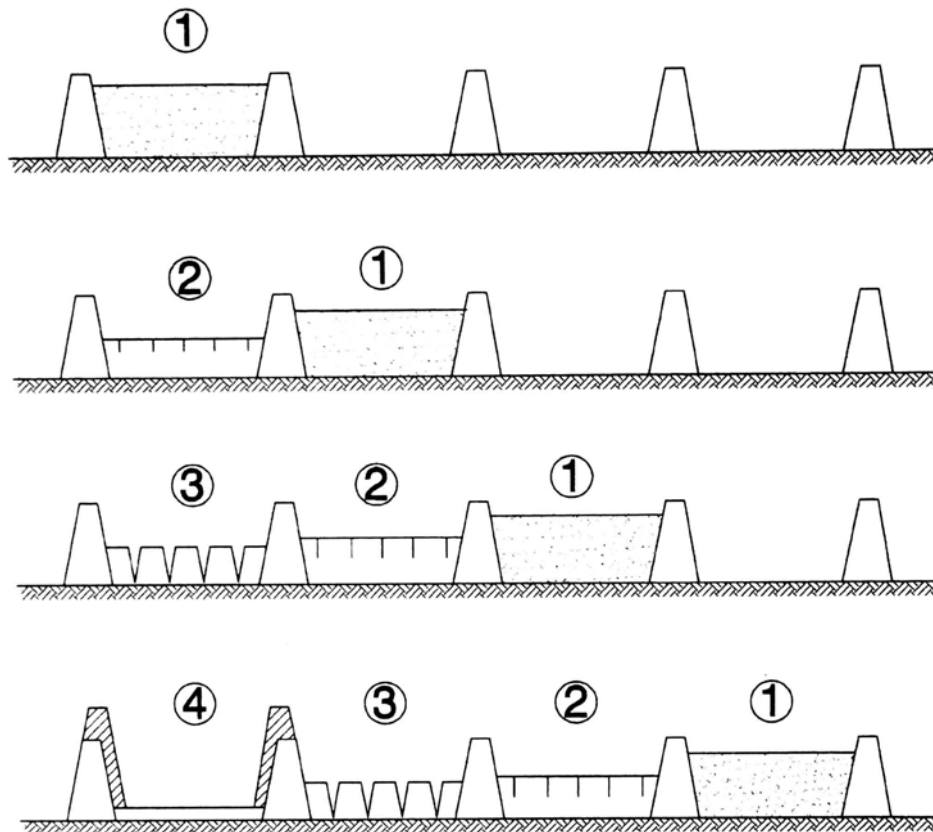


**FIGURE 16.15** Containment area management to dewater sediment. (1) Fill with slurry; (2) dewatering; (3) desiccation; (4) use dried sediment to raise dikes to repeat cycle. (Modified from U.S. Army Corps of Engineers, 1987.)

In the hydraulic sizing of a containment area two factors are of primary importance: the volume needed to store the dredged sediment, and the surface area needed to meet effluent standards. Design criteria for both can be determined from a single column settling test. These tests should be conducted with a slurry concentration equal to that expected during dredging (usually about 150 g/L for fines).

### 16.7.1 Column Test Procedure

The U.S. Army (1987) describes a procedure which uses about 50 L of sediment and a settling column approximately 2 m tall and at least 20 cm (8 in) in diameter. The Army recommends against the use of a smaller-diameter column because of wall effects. The Army's procedure describes zone, compression, and flocculant settling tests, the last of which requires withdrawal ports at several levels in the column and the construction of concentration profiles (previously described in Sec. 5.5.7). The procedure described below is a simplification of the Army procedure in that samples for flocculant settling are withdrawn from only one level. The procedure is as follows:

1. Construct a 20-cm-diameter Plexiglas settling column with an air supply introduced at the bottom to mix the slurry prior to the test. To construct a sediment concentration profile multiple ports will be required (Fig. 16.16).

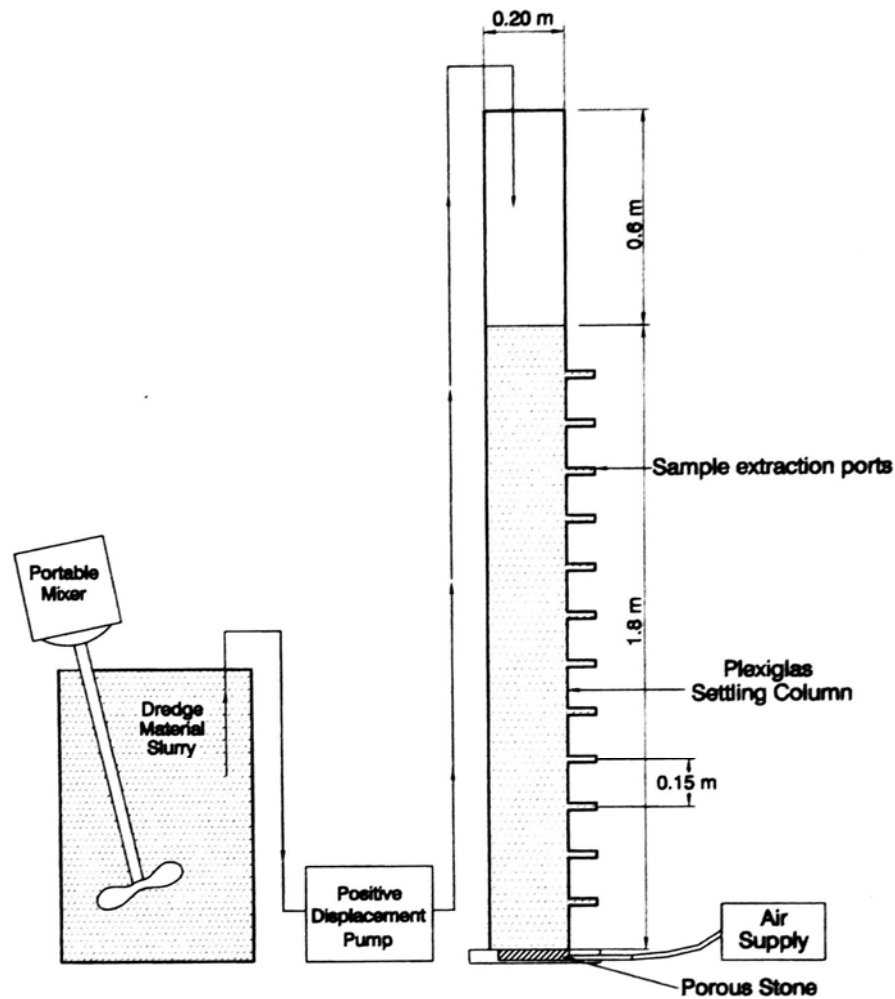


**FIGURE 16.16** Equipment for column settling test of dredged sediments (after U.S. Army Corps of Engineers, 1987).

2. Collect approximately 55 L of sediment, which may be a composite taken from several different areas. If sediment characteristics change appreciably from one area to another in the reservoir, and this sediment will be discharged into different containment areas, sample and test source material for each containment area separately.

3. Mix sediment with native water and allow coarse material to settle out. This simulates conditions in the disposal area where the coarse sediment settles out near the inlet pipe and the fines settle and compact separately.

4. Conduct a pilot settling test in a 4-L graduated cylinder using a slurry concentration of about 150 g/L. If an interface forms within several hours, the slurry mass is exhibiting zone settling. Record the settling rate of the interface over time. The break in the settling curve (Fig. 16.17) will define the concentration at which compression settling begins. If

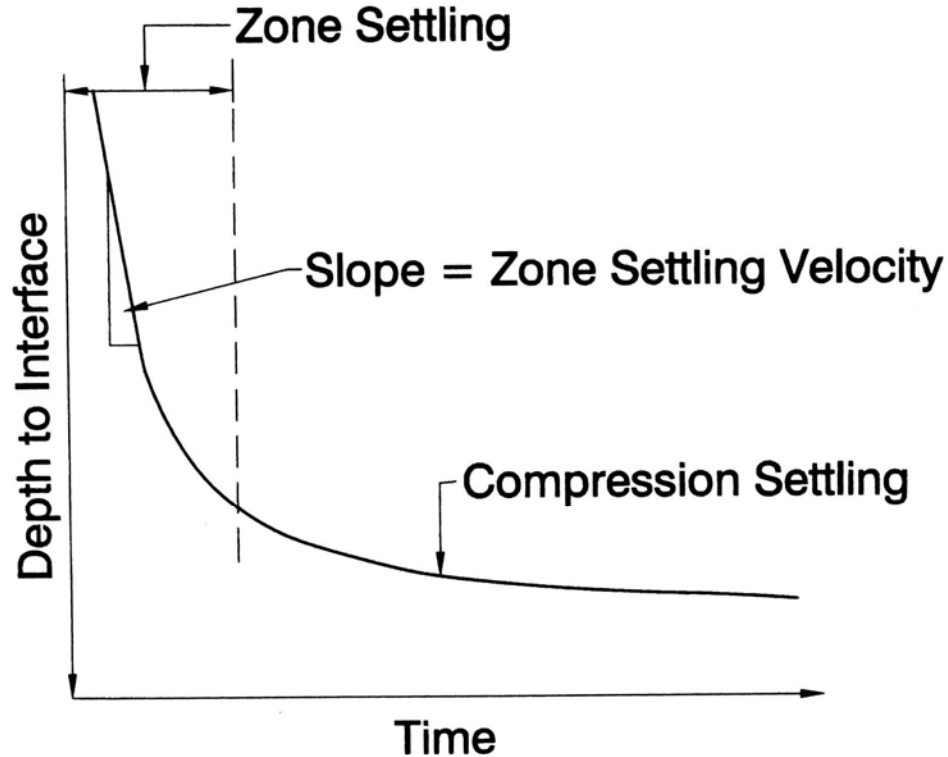


FIGURE 16.17 Plot of the settling of the sediment interface over time in column settling test (after U.S. Army Corps of Engineers, 1987).

no break occurs, sedimentation began in the compression zone and the test should be rerun using a lower-concentration slurry. If no interface is observed within the first several hours, the slurry is experiencing flocculant settling. Use this test to define the initial sediment concentration to be used in the 20-cm column.

5. Run the settling test in the 20-cm column with a concentration less than that associated with compression settling in the 4-L pilot column. Fill the large column with slurry of the appropriate dilution, air-agitate to achieve a uniform mixture. To begin the test, stop agitation and immediately withdraw a 50-mL sample to determine the initial solids concentration.

6. Record the height of the sediment-water interface at various points in time. Because settling rate declines over time, the following intervals may be used for sampling: 1, 2, 4, 6, 12, 24, 48, 96 hours, etc., for at least 15 days. These sampling times may be adjusted. If a sediment-water interface forms in less than an hour, this should be recorded. In other cases many hours may be required for the formation of a distinct interface.

7. At each sampling time, withdraw 50-mL supernatant samples from 0.3 m below the surface (representative of discharge over the weir) and analyzed for suspended solids. From these data three types of design determinations can be made.

### 16.7.2 Zone Settling Test

When zone settling occurs, the zone settling test defines the minimum surface area required for effective settling and retention of the sediment. The supernatant above the interface may continue to have sediment concentrations of several grams per liter, and a

surface area much greater than that determined by zone settling may be required to attain the required effluent water quality standards.

Plot the depth to the sediment interface over time, and compute the zone settling velocity as the slope of the initial straight part of the curve in Fig. 16.17. For zone settling, the minimum ponded area required for separation of solids from the clear supernatant liquid is given by:

$$A = \left( \frac{Q_i}{V_s} \right) C_h \quad (16.1)$$

where  $A$  = area required for setting,  $m^2$ ;  $Q_i$  = inflow rate,  $m^3/h$ ;  $V_s$  = zone settling velocity from the settling test,  $m/h$ ; and  $C_h$  = correction factor for hydraulic efficiency, discussed below (U.S. Army, 1987).

The zone settling velocity is equivalent to the *surface loading rate*, defined as the discharge divided by surface area. This is demonstrated by rearranging Eq. (16.1) in the following form:

$$V_s = \frac{Q_i}{A} \quad (16.2)$$

Whereas the hydraulic retention time will vary as a function of water depth, the surface loading rate is constant for a given basin geometry and is a better indicator of the sedimentation efficiency of a shallow basin than retention time.

### 16.7.3 Compression Settling Test

The compression settling test is used to estimate the volume required for initial storage of dredged material, prior to dewatering. This uses the same graph as the zone settling test, but extended for 16 days to determine the compression settling rate (Fig. 16.17).

The volume that will be occupied by the dredged sediment can be determined from the average suspended solids concentration in the settled sediment. The mean sediment concentration below the sediment-water interface can be computed from the interface height at any time by:

$$C_t = \frac{C_i H_i}{H_t} \quad (16.3)$$

where  $C$  = slurry concentration,  $g/L$ ;  $H$  = height of interface from bottom of column,  $m$ ; and subscripts  $i$  and  $t$  represent initial and subsequent points in time. The computed concentration values at each point in time are then plotted as a function of time on a log-log scale (Fig. 16.18), and this plot can then be used to determine the average sediment concentration in the settled sediment. Solids in the supernatant above the interface are neglected.

Once the rate of consolidation has been determined, the bulking factor is determined from the void ratio. For sizing a containment area, the bulking factor should be based on a time period equal to half the dredging time; half the sediment will be stored for a longer time and half for a shorter time. The dredging time is determined by dividing dredge production rate into the volume of sediment to be dredged.

Use the log-log graph of concentration versus time (Fig. 16.18) to determine the mass concentration of sediment  $C$  in the disposal area at time equal to one-half the dredging time. This, the design concentration, is then used to compute the average void ratio of fine-grained sediment in the containment area at the completion of dredging by:

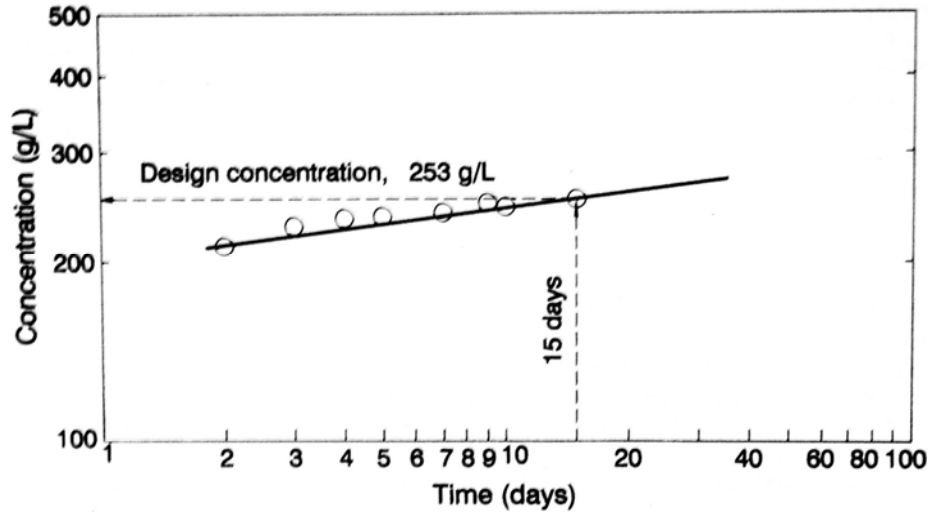


FIGURE 16.18 Timewise increase in fine sediment concentration within a containment area (after U.S. Army Corps of Engineers, 1987).

$$e = \frac{G_s \rho}{C - 1} \tag{16.4}$$

where  $e$  = void ratio;  $G_s$  = specific gravity of sediment (usually 2.65);  $\rho$  = density of water, g/L; and  $C$  = mass sediment concentration, g/L. Compute the volume occupied by fine sediment in the containment area at the end of dredging,  $V_o$ , in  $m^3$  by:

$$V_o = V_r \left( \frac{e_o - e_r}{1 + e_r} \right) + 1 \tag{16.5}$$

where  $e_r$  = average in situ void ratio of sediment in the reservoir prior to dredging based on data from cores;  $e_o$  = void ratio computed for containment area; and  $V_r$  = in situ volume of sediment to be dredged from the reservoir,  $m^3$ . To compute the total volume required for sediment storage in the containment area, add the volume occupied by coarse sediment using the assumption that no bulking of coarse sediment will occur (U.S. Army, 1987).

#### 16.7.4 Achievement of Strict Effluent Standards

Regulatory agencies may require that suspended solids levels of 50 mg/L or lower be achieved in the effluent from the disposal area. The individual suspended particles in the supernatant above the sediment interface within the water column will exhibit flocculant settling, and the surface loading rate required to achieve a low level of suspended solids in the effluent can be much lower than that required for zone settling. Under favorable conditions these levels may be attained in disposal area effluent by plain sedimentation, given adequate sedimentation time. In Lake Springfield, for example, an effluent quality standard of 15 mg/L was regularly achieved.

A high-quality effluent can usually be achieved by a combination of: (1) adequate detention time, or low surface loading rate, without hydraulic short-circuiting; (2) low

weir overflow rates; and (3) water level manipulation. The following design procedure for achieving high effluent standards by plain sedimentation within the containment area is based on design experience at reservoir dredging projects in the midwestern United States (Berrini, 1996).

1. Conduct the column settling test as described above, withdrawing suspended samples at a constant depth of about 0.15 m below the water surface. This represents, approximately, the average quality of the water that will be discharged over the weir with a minimum 0.6 m ponding depth.
2. From the samples, determine the detention time  $t$  required to achieve the required effluent standard.
3. Compute the required surface area of the basin,  $A$ , based on hydraulic detention time,  $t$ , and a 0.6-m minimum ponding depth,  $D$ , using  $A = Qt/D$ . Alternatively, compute the surface loading rate by  $V = D/t$ , and from this compute the required surface area by  $A = Q/V$ , where  $Q$  = pumping rate. Both methods produce the same surface area.
4. Design an adjustable effluent weir with stop logs to permit water level management. As a rule of thumb, limit the depth of overflow across the weir to 0.15 m, which is equivalent to a weir overflow rate of about 0.09 m<sup>3</sup>/s per meter of weir length (1 ft<sup>3</sup>/s per foot or 7.5 gal/min per foot).

Sediment and water chemistry conditions in some areas can produce clay suspensions that resist settling, and in windy areas wave action can continually resuspend shallow sediment. There are three basic alternatives. The first alternative is to pass the effluent through a shallow vegetated polishing pond, which will have better settling characteristics than an open water body. The second alternative is to increase ponding depth. The third alternative is to use a chemical flocculant. When a flocculant is used, the containment area would be constructed with a final basin, and the flow would enter this final basin through a static mixing device where the flocculating polymer is added. The flocculated sediment will settle into this last compartment and clarified water discharged over a weir. The injection of polymer at the exit of the dredge discharge line is not recommended.

### 16.7.5 Hydraulic Efficiency

The nominal residence time in a containment area may be computed as the water volume divided by discharge rate. However, hydraulic short-circuiting can reduce the true hydraulic detention time or surface loading rate to a value significantly less than the nominal value determined by geometric computations. In a perfect plug flow reactor, the detention time of all inflowing water will equal the nominal detention time. However, because of hydraulic short-circuiting, the detention period will vary and some of the water and its suspended sediment will pass rapidly to the outlet, while other parts of the basin act as dead zones (Fig. 16.14). This section outlines a procedure for estimating the deviation from theoretical conditions (U.S. Army Corps of Engineers, 1987).

The correction factor for hydraulic efficiency of a basin,  $C_h$ , is the ratio of the nominal residence time  $T$  to the field residence time  $T_f$ :

$$C_h = T/T_f \quad (16.6)$$

In an existing basin a tracer test may be used to determine the field residence time in the basin and, from this,  $C_h$ . Tracer test procedures are outlined by the U.S. Army Corps of Engineers (1987). For new containment areas the following equation can be used:

$$\frac{1}{C_h} = \frac{T_f}{T} = 0.9(1 - e^{-0.3(L/W)}) \quad (16.7)$$

where  $L/W$  is the length:width ratio of the proposed basin. Configurations which produce a more elongated flow path, or the use of several compartments in series, will reduce the effect of short-circuiting compared to a square basin. The effective  $L/W$  ratio can be increased by using internal dikes.

### 16.7.6 Weir Length

In practice the overflow weir will not merely skim off the surface layer of water, but it will also draw water up from deeper depths. The greater the discharge rate per linear meter of weir, the greater will be this aspiration effect and the deeper the depth of upwelling in front of the weir. The required weir length will depend on the settling characteristics of the sediment and the effluent quality standards.

The U.S. Army Corps of Engineers (1987) developed a nomograph for the relationship between the maximum weir overflow rate and ponding depth, presented below as equations in both the International System of Units (SI) and U.S. Customary Units:

For zone settling:

$$SI: \quad D = 0.06 + 6.56 Q_w \quad (16.8)$$

$$U.S. \text{ Customary:} \quad D = 0.2 + 2 Q_w \quad (16.9)$$

For flocculant settling:

$$SI: \quad D = 0.34 + 6.56 Q_w \quad (16.10)$$

$$U.S. \text{ Customary:} \quad D = 1.1 + 2 Q_w \quad (16.11)$$

In these equations  $D$  = ponding depth at the weir (m, ft) and  $Q_w$  = discharge per unit length of weir ( $\text{m}^3/\text{s}$  per linear meter,  $\text{ft}^3/\text{s}$  per linear foot). These equations may be used for weir loading rates not exceeding  $0.14 \text{ m}^3/\text{s}$  per linear meter ( $1.5 \text{ ft}^3/\text{s}$  per linear foot), which corresponds to a maximum water depth over the weir of about 0.2 m.

Because the sediment surface will tend to slope from the inlet zone to the outlet weir, the ponding depth at the weir can be expected to be deeper than the average ponding depth. The ponding depth at the weir can be estimated by:

$$D_w = D_{ave} + 0.0005 L \quad (16.12)$$

where  $D_w$  = ponding depth at the weir,  $D_{ave}$  = average ponding depth for the entire detention area, and  $L$  = length of ponded surface between inflow and weir.

The "effective" weir length will depend on weir geometry, with the idea being to minimize the approach velocity. The effective length of a horizontal or a rectangular weir extending from the dike into the containment area is equal to the total weir length. Use of a labyrinth weir in this application will not reduce the approach velocity. For a shaft-type weir, the weir should be located far enough away from dikes to allow flow to enter unobstructed from all sides. This criterion is met when the distance from the nearest dike or other flow obstruction is 1.5 times the required weir length determined by using the nomograph [Eqs. (16.8) through (16.11)].

### 16.7.7 Retention Time for Flocculent Settling in Supernatant Water

When zone settling occurs, flocculant settling of the individual particles in the supernatant above the solids interface will determine the solids concentration in the effluent, and will control detention area design to meet effluent water quality requirements. The normal test procedures for flocculant settling are performed, except only the portion of the water column above the sediment interface is used. Computations are as before, producing a family of curves of mean retention time versus percentage solids removal, one curve for each depth (each sample port).

## 16.8 FLOW CONDITIONS IN SLURRY PIPELINES

---

### 16.8.1 Flow Regimes

The hydraulics of sediment-water mixtures or slurries flowing in pipelines have been previously summarized by Graf (1971) and Herbich (1992). The flow of sediment-water mixtures in pipelines may be divided into three regimes based on the composition of the mixture and pipe diameter.

**1. Pseudo-homogeneous** regime occurs when all particles are in suspension and there is little variation in the concentration from the top to the bottom of the pipe. This condition generally requires that flow velocity within the pipe be at least two orders of magnitude greater than the particle sedimentation rate. Mixtures consisting of sediments having particle diameters smaller than about 0.03 mm may be considered to be nonsettling and will characteristically exhibit pseudo-homogeneous flow characteristics.

**2. Heterogeneous** regime occurs when all particles are in motion but the vertical sediment distribution is not uniform. At higher velocities within the heterogeneous flow regime, all the particles travel in suspension at essentially the same speed as the fluid. At lower velocities within this regime, the larger grains form a bed of saltating particles which move at a slower velocity than the remainder of the flow, but which do not form a stationary deposit within the pipeline.

**3. Stationary bed** regime occurs when the coarse fraction of the sediment load forms a stationary bed with bed load transport along the surface of the deposit. Bed forms such as ripples and dunes can form on the stationary bed.

Each of these conditions is schematically illustrated in Fig. 16.19, along with the equation defining the approximate transition point between each regime. The boundaries between these regimes are not distinct and the transition from one to another is gradual. Furthermore, conditions can change from one regime to another as the dredge excavates through sediment layers having different grain size characteristics. Therefore, in dredging of coarse material it is not generally possible to continuously operate at an optimal zone with respect to pipeline hydraulics.

The general shape of the curve of head loss as a function of discharge for different sediment concentrations is illustrated in Fig. 16.20. The point of minimum head loss at a given concentration, and therefore the most economical operating point for a slurry pipeline, will correspond to the lowest velocity at which all the sediment remains in motion, i.e., the lowest velocity in the heterogeneous flow regime. At lower velocities, sediment settles to create a stationary bed, reducing the pipeline cross-sectional area and increasing head loss. Graf (1971) has pointed out that a slurry pipeline should normally be operated at a higher velocity to prevent deposition of bed and the potential for blockage.

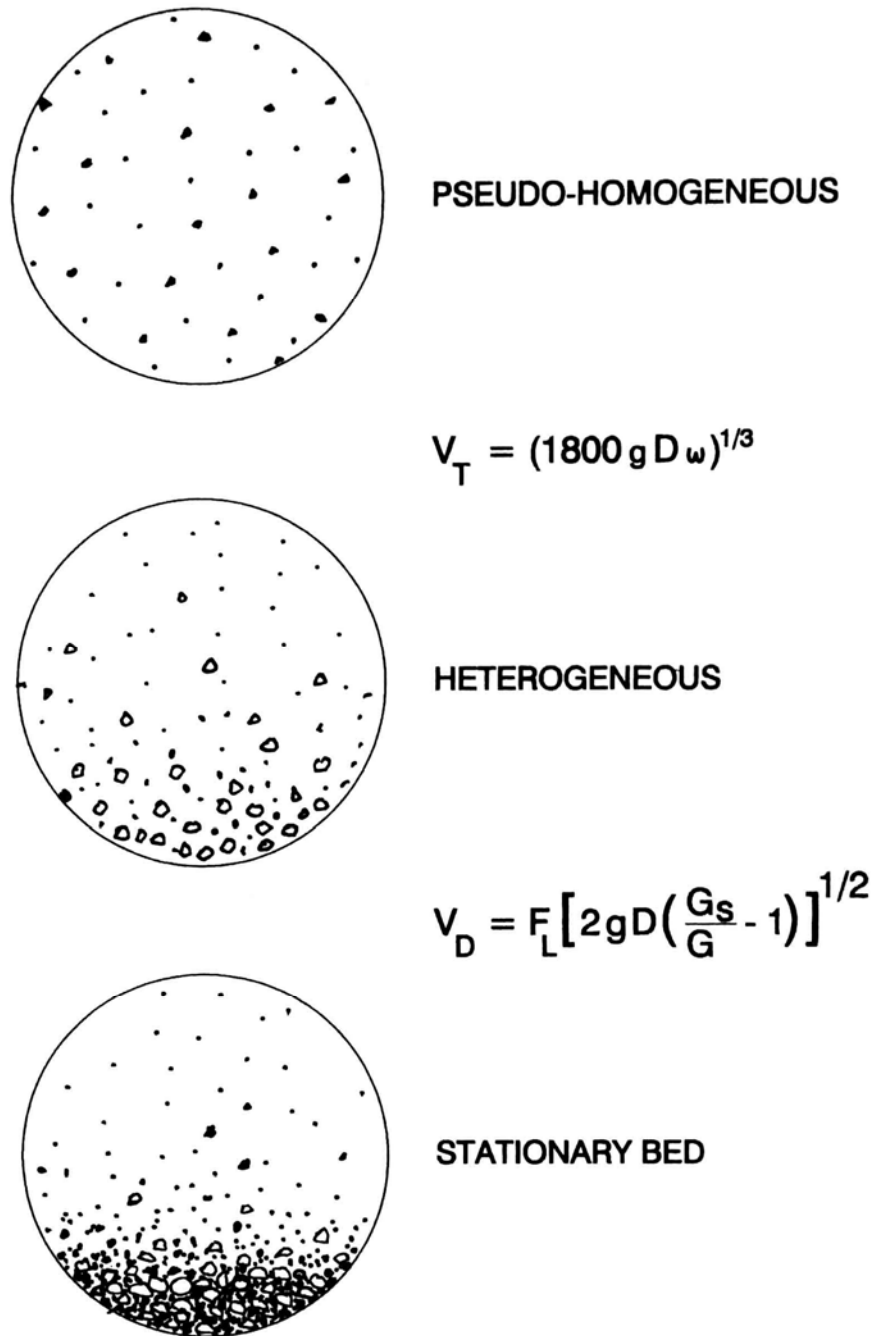


**FIGURE 16.19** Transport regimes for sediment transport in pipelines based on Graf (1971). The vertical distribution of fine, nonsettling sediment remains homogeneous for all flow conditions. Coarse sediment may exhibit a vertical concentration profile, depending on the flow velocity. Equations for the transition velocity between each regime are shown. At higher velocities within the heterogeneous regime all sediment will be in suspension, and at lower velocities within this regime coarse material will be transported as bed material which rolls or bounces along the pipeline without forming a stationary bed.

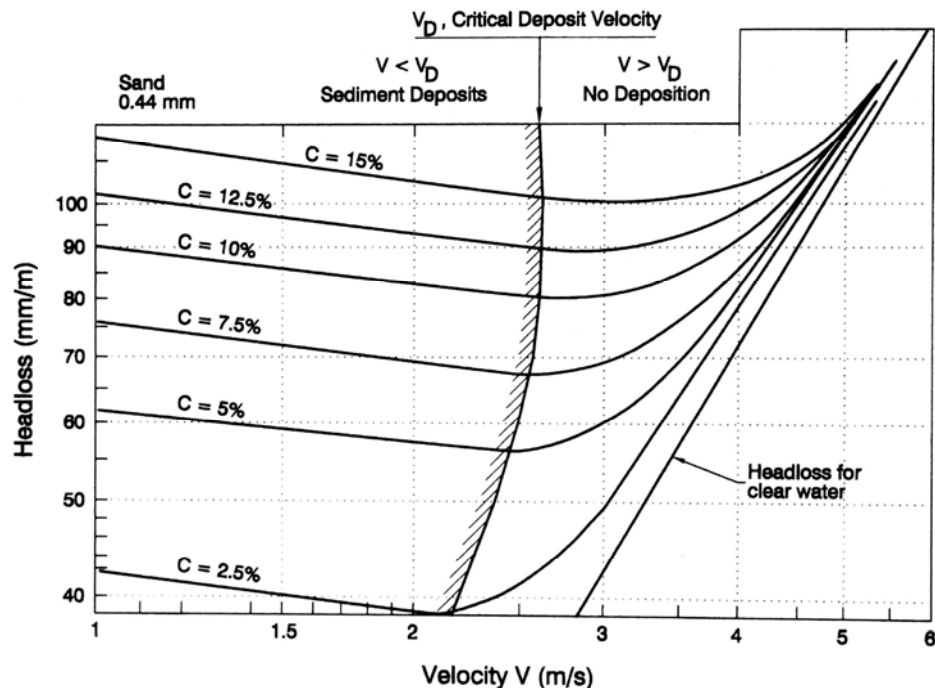


**FIGURE 16.20** Head loss as a function of velocity for different sediment concentrations. Minimum head loss occurs at the critical deposit velocity, the lowest velocity that sustains all material in motion without forming a stationary bed (redrawn from Condolios and Chapus, 1963).

Pipeline blockage can occur when  $V < V_D$ , and may be caused by: an increase in the concentration or grain diameter of the material being dredged, if flow velocity decreases or stops while the pipeline contains solids, or because of pipeline leakage. In selecting pumping units, or designing a gravity system, it is important that the head-discharge characteristics of the system be compared to the head loss curves for the pipeline system corresponding to the maximum grain size and concentration that can be expected, to ensure that the system always operates within the nonsettling region. Much lower pipeline velocities can be safely used for pumping fine-grain, nonsettling material, as compared to coarse sediment.

The Durand-Condolios relationship defines the *critical deposit velocity*, which separates the heterogeneous (deposit-free) regime from the moving bed regime. The critical deposit velocity  $V_D$  is given by:

$$V_D = F_L \left[ 2gD \left( \frac{G_s}{G} - 1 \right) \right]^{1/2} \quad (16.13)$$

The coefficient value  $F_L$  may be estimated from Fig. 16.21. The transition point from heterogeneous to homogeneous flow is given by:

$$V_T = (1800gD\omega)^{1/3} \quad (16.14)$$

In these equations  $V$  = mean flow velocity (m/s, ft/s);  $C$  = volumetric concentration of sediment expressed as a decimal value;  $d$  = sediment diameter (mm);  $D$  = pipe diameter (m, ft),  $g$  = 9.8 m/s or 32.2 ft/s;  $\omega$  = sediment fall velocity (m/s, ft/s); and  $G$  and  $G_s$  =

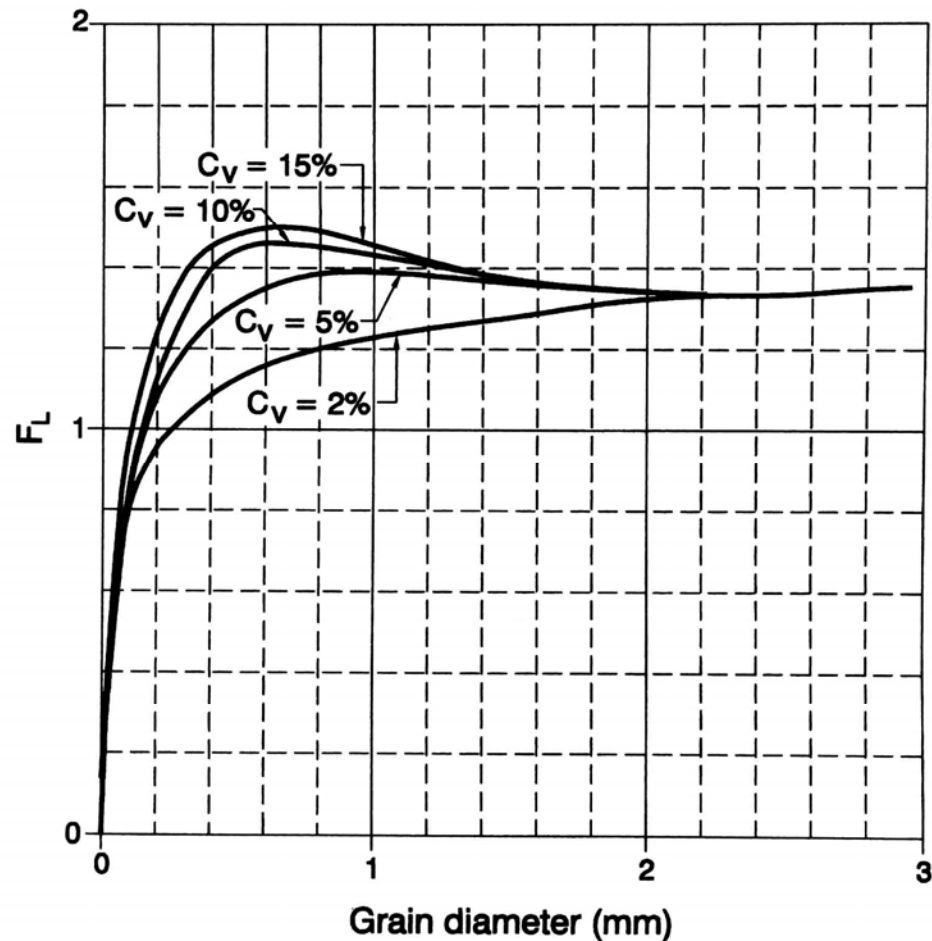


FIGURE 16.21 Variation of coefficient  $F_L$  as a function of grain diameter (Durand, 1953).

specific gravity of the fluid and sediment grains, respectively. These velocity equations are dimensionally homogeneous. For example, for  $D = 0.25$  m,  $d = 2$  mm (coarse sand),  $G_s = 2.65$ ,  $G = 1.0$ ,  $g = 9.8$  m/s<sup>2</sup>,  $C_v = 0.15$ , and taking a value of  $F_L = 1.34$  from Fig. 16.21, compute  $V_c = 3.8$  m/s from Eq. 16.13. Compute the setting velocity  $\omega = 0.147$  m/s from the Rubey equation (Eq. 5.23), and compute  $V_T = 8.6$  m/s from Eq. 16.14.

## 16.9 PIPELINE HEAD LOSS

There is no simple and clear-cut method for determining slurry head losses in hydraulic dredging pipelines. Dredge slurries typically contain a range of grain sizes. Furthermore, the grain size distribution, density, and viscosity can all change rapidly as the dredge moves through nonhomogeneous beds of sediment. Some silt-clay mixtures exhibit properties of a Bingham fluid, which is quite different from a newtonian fluid. A number of researchers have found that the presence of a significant concentration of clay in the slurry can decrease friction losses compared to coarse sediment alone. Accordingly, methods for estimating head loss in dredged pipelines only approximate field conditions.

### 16.9.1 Friction Losses by Slurry Density Approach

One approach to computing the friction head loss in a slurry pipeline is to use the Darcy-Weisbach friction loss equation, but express head loss in terms of the equivalent column of slurry instead of clear water (Herbich, 1992). The Darcy-Weisbach equation may be expressed as follows:

$$H_f = f \left( \frac{L}{D} \right) \left( \frac{V^2}{2g} \right) \quad (16.15)$$

To express unit friction loss  $S$  in terms of the column of slurry with a specific gravity of  $G_m$ , the equation may be rearranged as:

$$SG_m = \frac{fV^2}{2gD} \quad (16.16)$$

To solve for friction loss based on discharge in a circular pipe:

$$SG_m = \frac{fQ^2}{0.6169D^5(2g)} \quad (16.17)$$

where  $S$  = friction loss per unit length of pipe (m/m or ft/ft),  $G_m$  = specific gravity of the mixture or slurry,  $Q$  = discharge (m<sup>3</sup>/s, ft<sup>3</sup>/s),  $D$  = pipe diameter (m, ft),  $f$  = Darcy-Weisbach friction factor, and  $g$  = gravitational constant. The Darcy-Weisbach equation may be solved with any dimensionally consistent units.

In this method the specific gravity of the fluid being pumped is the only variable; it does not account for differences in the grain size of the slurried material. The specific gravity of the mixture  $G_m$  may be computed from the volumetric sediment concentration  $C_v$  as

$$G_m = C_v (G_s - G) + G \quad (16.18)$$

where  $G$  = specific gravity of water and  $G_s$  = specific gravity of sediment particles.

Methods to compute the friction factor in a slurry pipeline were presented by Schiller (1992). Little error is introduced by assuming that the Darcy-Weisbach friction factor  $f$  for a slurry is the same as for clear water, as read from the Moody diagram. Because of the abrasive action of sediment, which polishes the pipeline interior, the value of the Darcy-Weisbach friction factor  $f$  may be determined from the Moody diagram for "smooth pipe" conditions, or by the following equations. For laminar flow in circular pipe ( $Re < 2000$ ):

$$f = \frac{64}{Re} \quad (16.19)$$

For smooth pipe in the turbulent range ( $Re > 4000$ ), the value off may be determined by iteration using the following equation:

$$\frac{1}{f^{0.5}} = 2.0 \log (Re f^{0.5}) - 0.8 \quad (16.20)$$

This equation can be easily solved using a hand calculator having an iterative equation solver. For the range of Reynolds numbers from 40,000 to 60,000,000, the solution may be approximated by:

$$f = 0.10408 (\text{Re} - 22,000)^{-0.157} \quad (16.21)$$

### 16.9.2 Minor or Local Losses

Minor head losses  $H_m$  at bends and valves may be computed as a function of velocity  $V$  by:

$$H_m = \frac{KV^2}{2g} \quad (16.22)$$

using the head loss coefficient values of  $K$  shown in Table 16.6. It is more convenient to convert minor losses into an equivalent length of straight pipeline, which is added to the

**TABLE 16.6** Coefficient Values for Minor Losses

System component	K
Plain end suction	1.0
Globe valve, wide open	10.0
Angle valve, wide open	5.0
Gate valve, wide open	0.2
T, through side outlet	1.8
Elbows:	
90° short radius	0.9
90° long radius	0.6
45° elbow	0.4
Stern swivel	1.0
Ball joints:	
Straight	0.1
Medium cocked	0.4 to 0.6
Fully cocked (17°)	0.9
Discharge	1.0

Source: Adapted from Herbich (1992)

total pipeline length for the purpose of frictional head loss computations. The equivalent length is given by:

$$L_e = \frac{KD}{f} \quad (16.23)$$

where  $K$  = sum of all  $K$  values for the individual components along the pipeline.

### 16.9.3 Turner's Friction Loss Graph

Friction loss in a slurry pipeline will vary as a function of the sediment grain size. Turner (1996) recommends use of the Hazen-Williams equation and the friction coefficient  $C$  values shown in Fig. 16.22 to estimate friction loss in a slurry pipeline transporting

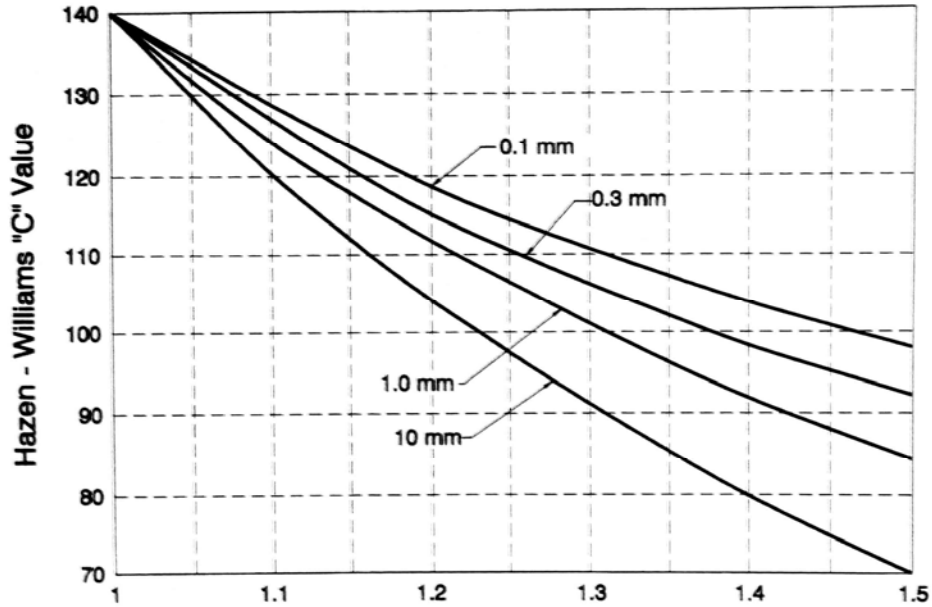


**FIGURE 16.22** Variation in the Hazen-Williams friction coefficient  $C$  for a dredge slurry pipeline, as a function of grain size and specific gravity of the slurry (redrawn from Turner, 1996).

coarse sediment. The  $C$  values in the graph reflect the variation in friction losses as a function of the grain size of coarse sediment as well as the specific gravity of the slurry. Silts have a somewhat lower friction value than fine sand. For silts use the slurry density approach described in section 16.9.1, applying a  $C$  coefficient appropriate for clear water and multiplying head loss by the specific gravity of the slurry. The  $C$  coefficient for clays is difficult to determine without specific field data. The "lubricating" effect of clays, observed under some conditions, is elusive and should not be planned on without specific data.

The Hazen-Williams equation can be expressed in the following form:

$$S = B \left( \frac{100}{C} \right)^{1.85} \left( \frac{Q^{1.85}}{D^{4.8655}} \right) \tag{16.24}$$

where  $S$  = friction loss in column of water (not column of slurry) per unit length of pipe (m/m, ft/ft),  $C$  = Hazen-Williams coefficient for friction loss,  $Q$  = discharge,  $D$  = pipeline inside diameter, and  $B$  = coefficient value depending on the system of units, as given below.

Coefficient $B$	Units		
	$Q$	$D$	$S$
$2.13 \times 10^{-3}$	m <sup>3</sup> /s	m	m/m
$2.08 \times 10^{-3}$	gal/min	in	ft/ft
$9.43 \times 10^{-4}$	ft <sup>3</sup> /s	ft	ft/ft

The curves in Fig. 16.22 have been developed from practical data acquired over many years from many sources. On the basis of field observations, the  $C$  value of 140 for clear water is considered representative of both steel and polyethylene pipelines after they have been subject to wear. Because these values are based primarily on field experience rather than laboratory data, they should not be considered precise. This is especially true because the slurry discharged from a dredge never has a constant composition. Also, a significant concentration of clay can have a lubricating effect and reduce friction losses, thereby increasing the  $C$  value by as much as 10 points. On the basis of practical experience, Turner also indicates that local losses from fittings along a dredge pipeline often approximate 10 percent of the frictional losses for straight pipe.

#### **16.9.4 Total Pipeline Head Loss**

The computation of total head losses along a dredge pipeline includes friction losses, local or minor losses at bends and valves, entrance and exit losses, and static head. In a slurry pipeline, the static head must be computed for the specific gravity of the slurry, not pure water, and a positive static head is required to lift the column of slurry in the pipeline from the bottom to the surface of the water body.

### **16.10 CLOSURE**

---

Sediment excavation is a costly method for sediment management and the recovery of reservoir capacity, but it may be required in many circumstances. The magnitude and frequency of sediment excavation can be minimized by reducing erosion in the tributary watershed, and employing design and management techniques such as sediment routing to minimize sediment deposition in the impoundment.

The potential for the continued excavation of sediments depends on the availability of sediment disposal sites, and if excavation or dredging is to be relied on as a long-term management tool, disposal areas of adequate capacity or with reuse potential must be available.

---

## CHAPTER 17

---

# DECOMMISSIONING OF DAMS

---

---

### 17.1 INTRODUCTION

---

As dams age, decommissioning becomes an issue that must be considered by some owners. Decommissioning of dams and hydroelectric projects requires that they be rendered inoperative in a manner that is safe and environmentally acceptable. In some cases it may entail decommissioning of appurtenances while the dam is left intact, and in other cases the dam may be partially or completely removed. The requirements for decommissioning will be determined by unique conditions at each site.

Decommissioning may be implemented to satisfy either economic, environmental, or regulatory requirements. When projects become uneconomic to operate, owners may voluntarily decide to decommission. In other cases, the demand to decommission may be determined by environmental or regulatory requirements. At some sites in the United States and Europe, project decommissioning and dam removal is being considered to restore fisheries (e.g., salmon). The U.S. Federal Energy Regulatory Commission (FERC) declared in a policy statement before Commissioners on December 4, 1994 that the Commission has the right to demand decommissioning of a project when considering an application for relicensing.

Decision making to determine the feasibility of voluntary decommissioning and dam removal is a complex process, especially when fluvial conditions are to be reestablished along the previously impounded reach, potentially mobilizing sediment that has accumulated for many decades. Decommissioning also includes consideration of a number of issues in addition to sediment management. Various decommissioning and dam removal options can be evaluated by making use of decision-making systems such as the Analytical Hierarchy Process (Saaty, 1990). A worked example of how this process can be applied to make such decisions is published in the American Society of Civil Engineers' *Guidelines for Retirement of Dams and Hydroelectric Facilities*, currently in preparation.

Sediment management is a significant part of the decommissioning process. The cost of sediment management for the proposed decommissioning of the Elwha River dams

on the Olympic Peninsula, Washington State (U.S. Department of Interior, 1994) represents nearly half the total construction cost of the proposed decommissioning project. Pansic et al. (1995) found that sediment management cost is a major portion of the total cost of decommissioning (Fig. 17.1).

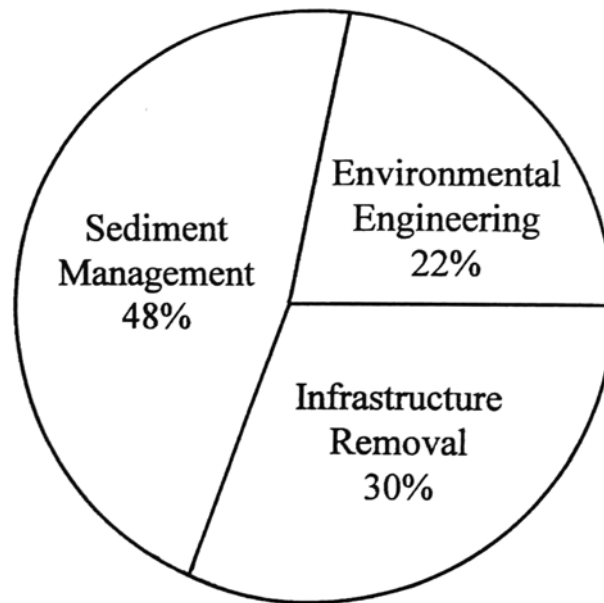


**FIGURE 17.1** Relative magnitude of costs associated with decommissioning of dams.

This chapter provides an overview of the types of sediment management issues typically associated with the decommissioning of dams. Basic sediment management options are discussed and examples are presented.

## **17.2 DAM REMOVAL OPTIONS**

There are three basic structural alternatives for decommissioning a dam. The dam can be left in place, partially breached, or completely removed. Either partial or complete removal may be accomplished as a staged process extending over a period of years to reduce the rate of sediment release.

Selection of the appropriate sediment management strategy is intimately related to the dam removal strategy, and, given the importance of sediment management, it will typically be a primary factor determining which dam removal strategy is to be implemented.

The basic sediment management options can be classified into four basic categories:

1. Leave the sediment in place;
2. Allow natural erosion to remove some or all of the sediment;

3. Construct a channel through the deposits while off-channel deposits are stabilized and maintained in place; or
4. Remove all sediment deposits by mechanical excavation or hydraulic dredging.

The option to leave the sediment in place is mainly associated with the option of retaining the dam structure, while the other sediment management options are associated with the dam removal alternatives.

### **17.2.1 Leave Dam in Place**

The simplest decommissioning option is usually to leave the dam in place. This option will not be feasible when dam removal is desired for environmental purposes such as restoring migratory pathways or when it will result in unsafe conditions. The dam engineering associated with this decommissioning option is directed at removal and closure of appurtenant structures such as power houses, turbines, and power lines. Because engineering requirements to retire the dam structure are often minimal, this option may result in immediate savings, but may imply an indefinite commitment to maintain, supervise, and operate certain elements of the facility. For example, maintenance and operation of gates for flood control may be required to ensure the safety of downstream communities. This option may also be desirable when the reservoir sediments contain contaminants which are costly to remove and which should not be released downstream.

The sediment management strategy that is intuitively associated with this decommissioning option can be fairly simple, i.e., leaving the deposited sediment in place. However, the long-term consequences of sediment accumulation must be considered. Future deposition of sediment may raise the bed elevation in the river reaches upstream of the full supply elevation of the reservoir pool and may also accumulate before the dam, causing problems to communities and infrastructure, such as increased flooding, blockage of water intakes, or reduced capacity of infrastructure such as bridges to pass floods, and may also affect the structure of the dam itself. When the reservoir continues to accumulate sediment, adverse consequences downstream due to the cutoff of the sediment supply will continue. Future dam removal will become increasingly difficult if sediments continue to accumulate.

### **17.2.2 Partial Dam Removal**

Under partial removal, or breaching, only a portion of the dam structure is removed. The breach may extend to the original stream thalweg, or the new crest may be established at some level between the existing crest and the original thalweg. Figure 17.2 illustrates the concept of partial breaching. Breaching lowers the pool elevation, exposing and potentially eroding sediment deposits in the dewatered portion of the pool, while sediment closer to the dam and below the new crest level will remain trapped behind the dam. When only a part of the dam is removed, the remaining section of the dam may still have a retarding effect on flow at high discharges. This can reduce the flow velocity during large events and cause continued sediment deposition in the reach upstream of the partially breached dam. Sediments eroded from the delta area may also deposit behind the breached dam.

### **17.2.3 Complete Dam Removal**

Complete removal of a dam occurs when the entire structure is removed in a relatively short period of time, restoring the original cross-sectional shape of the valley at the dam

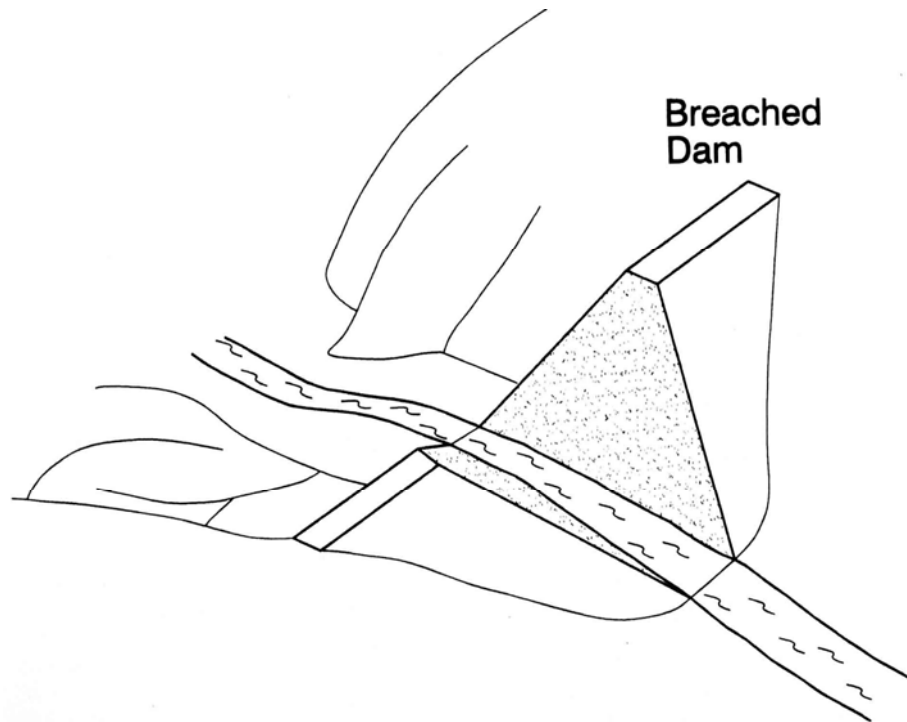


**FIGURE 17.2** Partial breaching of a dam.

location. The duration of the dam removal process will depend on the size and complexity of the structure, but may require only a few months for smaller dams. Figure 17.3 illustrates complete dam removal.

#### **17.2.4 Staged Breaching**

Staged breaching can be used with either partial or complete removal of a dam, and entails the gradual lowering of the crest of the dam over a period of time until the final intended geometry is achieved. The total duration of the staged removal may be months or years, and the time step between drawdown stages will depend on factors including the volume of sediment deposits and the rate they can be removed. If frequent high-discharge floods occur, and the volume of sediment that must be removed is relatively small and easily eroded, then the duration between successive stages can be short. If the flood discharges are low, the sediment volume to be removed is large, and the sediment is difficult to erode, the duration between successive stages may be longer. The rate of lowering will often depend on the rate at which the downstream channel can accept the sediment load, and particularly the limitations imposed by the downstream river channel morphology, infrastructure, ecosystems, and other factors sensitive to increased sediment loading. Staged breaching or removal is well-suited to the gradual release of sediment downstream by natural erosion.

Staged breaching can be implemented on a variety of dam structure types, but is riskier when applied to earth embankment dams as opposed to more robust structures,

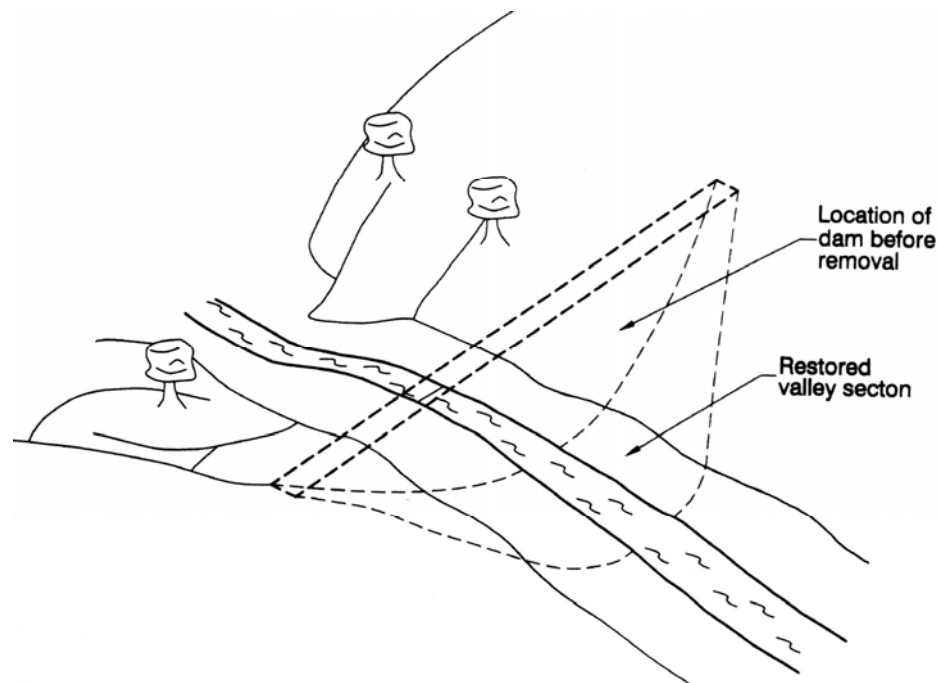


**FIGURE 17.3** Complete dam removal.

such as concrete dams. Figure 17.4 is a schematic illustration of the staged removal process. When staged removal of a dam is applied to earth embankment dams, armoring of the crest or inclusion of an auxiliary spillway may be required for the duration of the project. Should no auxiliary spillway be provided, flows will discharge over the crest of the structure, exposing it to the erosive power of the water and potentially creating a dam safety hazard due to embankment failure. Armoring of the crest may be required to safeguard against such events.

### **17.3 SEDIMENT MANAGEMENT OPTIONS**

---

There are four basic sediment management options. Some of these options can be combined in a single project. For example, it may be feasible to allow part of the sediment to erode naturally during the initial phases of the decommissioning project, with channeling and stabilization being implemented during the later phases. Another option might be to allow natural erosion to occur in the early phases of a project, with complete removal of sediment taking place during the last phase. Selection of the optimal strategy will depend on factors including cost, potential for downstream flooding due to sediment release, impact to downstream infrastructure, water quality, and other environmental considerations. The sediment management options outlined below are by no means exhaustive. Unique project conditions may lead to the use of innovative techniques, which may or may not be a combination of the options outlined below.

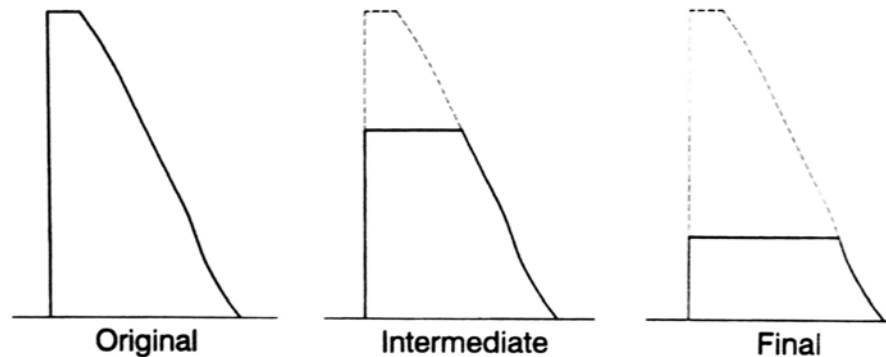


FIGURE 17.4 Staged removal of a dam structure, in section view.

### 17.3.1 Leave Sediment in Place

If it is feasible to leave the dam in place, the option of also leaving the sediment in place may be the cheapest solution, at least initially. Nondisturbance of the sediments has the important advantage of avoiding the release of a large sediment volume to the environment downstream of the dam. In some cases it may also be desired to leave sediments in place due to the presence of pollutants, or concerns that removal of contaminated sediment from a reservoir and disposal to an upland site could generate leachate that might contaminate groundwater.

To leave sediments in place it is necessary that they not be scoured and remobilized by the river system, implying that areas of sediment deposition continue to be impounded and that the dam remains in place. Sediments may remain trapped upstream of a dam using a partial breaching which lowers but does not empty the pool. Predominantly coarse material within the dewatered upstream part of the pool may be eroded and transported closer to the dam, prograding over and burying finer sediment deposits in deeper areas of the pool near the dam. However, if the reservoir is breached to the level of the original thalweg, significant erosion of sediment will occur. Attempts to leave the sediment in place during partial or complete removal of a dam are not likely to be successful if the lowered pool level allows scouring velocities to be generated in the area of deposits, unless the channel is artificially armored or lined.

If sediment inflow and outflow are nearly balanced before decommissioning, there may be little additional long-term impact from leaving the dam in place. However, if this balance has not been achieved and the dam remains in place, then sediments will continue to accumulate and can potentially generate adverse long-term consequences because of aggradation upstream of the dam, deposition against the structure, and continued degradation of the reach below the dam due to the interruption in sediment supply. From the standpoint of sediment management, in general it is desirable to undertake decommissioning in a manner that accelerates the reestablishment of the sediment balance across the impounded reach, instead of continuously accumulating sediment which may create future problems, and which only further delays the reestablishment of the natural sediment regime along the river.

The long-term response of the fluvial system can be investigated with empirical methods or computer modeling. The investigation commences by establishing sediment characteristics, estimating sediment yield, and simulating sediment transport. Simple empirical approaches to estimate the ability of the reservoir to retain sediment as a function of storage capacity and inflow were developed by Brune (1953) and Churchill

(1948). An empirical method for distributing the trapped sediment within the impoundment was developed by Borland and Miller (1958) and is applicable to deposits below the maximum pool level. The method presented by Annandale (1987) can also analyze backwater deposits above the maximum pool level. The selection of the numerical modeling approach will depend on the nature of the problem.

### 17.3.2 Natural Erosion

Natural erosion can occur when a dam is either partially or completely removed; it is conceptually similar to the creation of a flushing channel by the permanent drawdown of the pool. This sediment management option can be combined with other techniques. For example, the first phase of the project may entail removal of sediment by natural erosion, followed by channel stabilization during phase 2 of the project.

Natural erosion has the potential advantage of low initial cost, but needs to be executed in a controlled manner. Uncontrolled erosion may produce adverse conditions in river reaches below the dam. Erosion of fines can produce a wide range of adverse downstream environmental consequences, and the release of large volumes of coarse sediment can infill downstream channels and cause problems such as flooding and impairment of navigation. The savings achieved at the reservoir by using natural erosion need to be balanced against the costs that may be experienced downstream because of the increased sediment loading.

An alternative approach is to control sediment release by removing the dam in stages, lowering the dam crest elevation by stages to allow sediment deposits to be eroded and discharged downstream in an incremental manner. The objective is to develop a chronology of staged breaching that will limit the rate of sediment release to satisfy environmental and other downstream restrictions. The process of staged dam removal continues in steps until the final elevation has been achieved or free flow through the river system has been reestablished, depending on the project objectives. When staged dam removal is used, the staging should be developed to cause natural erosion during floods having a relative high frequency (short return interval).

Natural erosion will not remove all the sediment from a reservoir, even with complete dam removal, and in a heavily sedimented, shallow, wide reservoir, natural erosion may remove only a small part of the total deposit. Conversely, in a narrow river or gorge-type reservoir, natural erosion can remove most of the sediment. The lowered water level within the reservoir that results from lowering the dam crest will create a channel-floodplain configuration in areas of sediment deposition, but unlike flushing, lowering the crest will permanently expose previously deposited sediments. Revegetation will help stabilize and dewater these deposits, and the sediment deposits in these stabilized and vegetated floodplains will remain in place and will not be eroded and transported downstream.

The rate of dam lowering and sediment release will be determined by rate-limiting processes within the reservoir, such as the inflow and erodibility of deposits, plus the rate of sediment release that can be tolerated by downstream aquatic ecosystems or infrastructure. Because both the amount and characteristics (e.g., grain size, erodibility) of the deposits vary as a function of elevation within the impounded area, each stage of the dam breaching process will not necessarily proceed at the same rate. Progress may also be influenced by hydrologic conditions such as flood or drought, or other unknowns which cause the rate of sediment release to depart from predictions.

Development of a sediment management plan that uses the concept of natural erosion will require field investigation to determine transport and entrainment characteristics of the deposits. Field information may be systematically analyzed by

computer simulation of the intended plan. Computer models such as HEC-6, FLUVIAL-12 and GSTARS that have the ability to simulate the scour and deposition of sediment can be helpful in the evaluation of potential management plans. Models such as these can help evaluate and compare various staged dam removal strategies, the cross-sectional shape of the dam crest during each successive phase of dam removal, and the timing of each consecutive stage of dam crest lowering. A stochastic approach based on historical hydrologic sequences that may be modified for this purpose is presented by Annandale (1996). However, experience with dam removal is quite limited, and methods of predicting the rate of retrogressive erosion under a dam removal scenario are far from precise. Significant departure from predicted conditions should be anticipated unless field trials are conducted or there is experience from a similar site to work from.

### 17.3.3 Channeling and Stabilization

Sediment management by channeling and stabilization may be used concurrently with the partial breaching and complete dam removal options, or as the last phase of a staged dam removal process. The objective is to leave a significant amount of the sediment in the reservoir pool, passing flow through a stabilized channel that will not erode the deposits. The procedure is to first drain the reservoir, partially breach or completely remove the dam, and excavate a channel through the sediment deposits upstream of the dam. Because erosion of the deposits will begin as soon as the pool is lowered, dredging may be used to evacuate the channel prior to or during pool lowering to minimize sediment release. Excavated sediments may be discharged to an upland disposal site, or may be discharged to another portion of the reservoir where they will be stabilized and protected against future erosion.

Channel design is a key element to this sediment management strategy, and the design criteria will depend on the conditions specific at each project. Since the objective of decommissioning is to abandon the project insofar as possible, a primary design objective is to provide a channel configuration that will either be stable in the long run or evolve into an acceptable configuration in a short time as sediment inflow and outflow come into balance across the previously impounded river reach. The development of a suitable sediment balance along any channel design is critical to the long-term success of this strategy. In general, the best option is to redevelop a "natural" channel configuration through the deposits, using channel widths and slopes which produce a stable channel configuration, thereby minimizing or eliminating the need for costly bank stabilization.

If the dam is removed, the channel would normally be reestablished along the original stream thalweg. However, since sediment deposits are deepest along the thalweg, this option may also result in the removal of large volumes of sediment. In the case of partial dam removal, a portion of the pool area near the dam may continue to be impounded after decommissioning, and a new channel planform may be developed across the area near the dam. This planform may be developed by channeling if the pool is lowered to the point that deposits are exposed, or it may develop naturally as the remaining pool fills with sediment in areas where the original deposits continue to be submerged. In the case of partial breaching, the breach would normally be located to discharge into the existing downstream channel, even though a new channel planform may be developed in the still-impounded reach above the dam.

A major objective of decommissioning is to return the fluvial system to a self-maintaining natural condition. This implies the use of environmental design approaches which seek to restore natural stream geometry, including the development of streambank configurations that enhance the potential for the growth of stabilizing riparian vegetation and which encourages overbank flooding which nurtures riparian wetlands. The channel

layout will represent a meandering stream, possibly with a gravel bed and planted bank vegetation to provide shade, food supply, and habitat. This approach contrasts sharply with the conventional engineering approach involving the design of a straight flood channel to pass floods downstream as quickly as possible. However, in some cases the traditional design approach may be suitable. Both design options are schematically illustrated in Fig. 17.5.

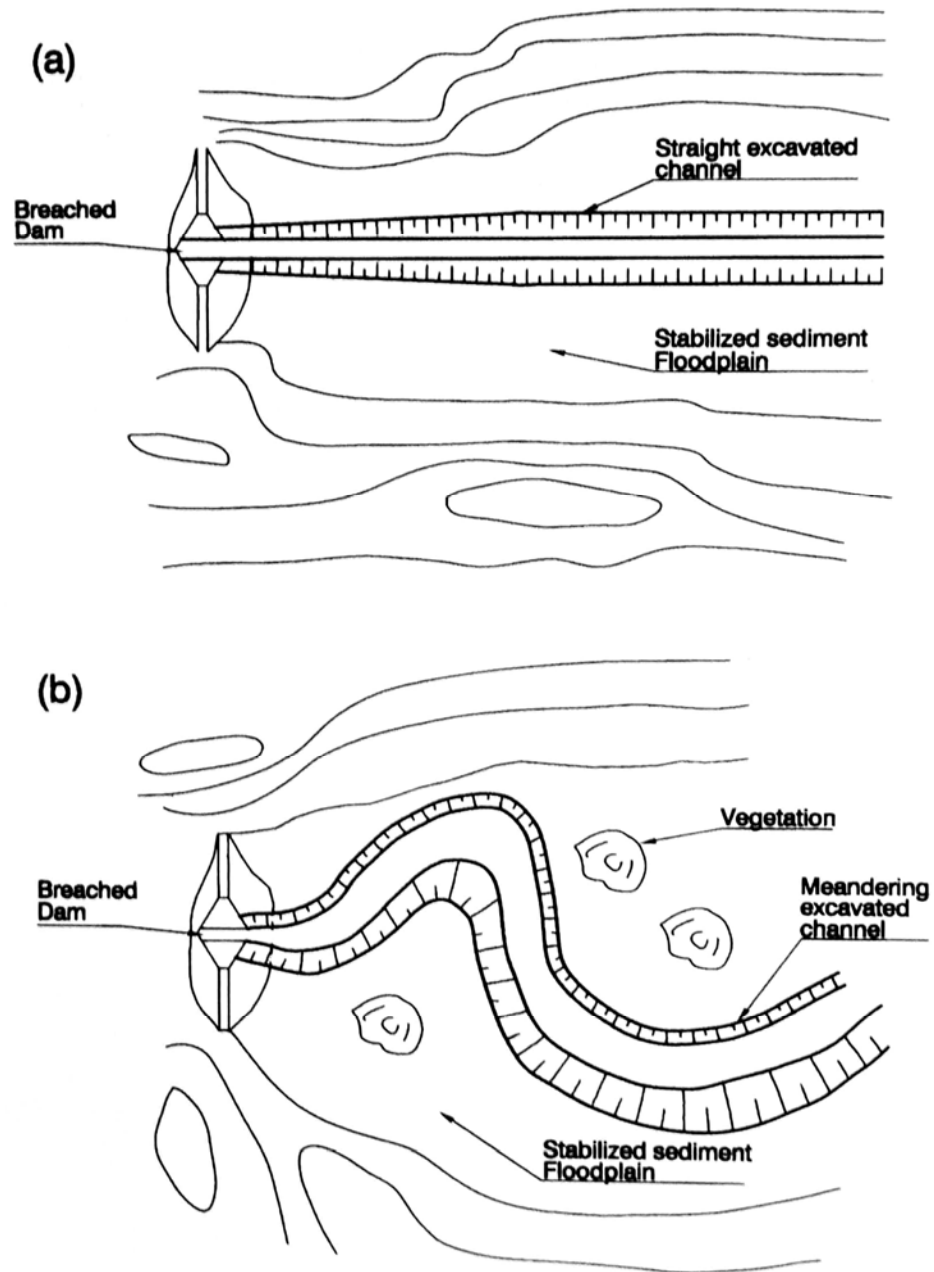


**FIGURE 17.5** (a) Conventional engineered channel through sediment deposits. (b) Natural channel design through sediment deposits.

It may be necessary to stabilize the channel banks using either conventional stabilization techniques, such as riprap, or bioengineering approaches. The choice of suitable stabilization techniques will depend on the nature of the deposits, and, in poorly consolidated deposits near the dam, the use of conventional materials such as riprap may not be feasible. The floodplain sediments on either side of the channel may also benefit from vegetative stabilization by seeding with grasses or tree planting.

Another channeling and stabilization option is to keep the dam in place and route the river around it. This may be a feasible option in cases where the dam and reservoir are located in an oxbow. The bypass channel around Nagel Dam in South Africa for the purpose of sediment bypass is shown in Fig. 13.9. This same strategy may be used to bypass flow around a structure that is to be decommissioned, leaving the dam and sediments in place.

#### **17.3.4 Complete Removal of Sediment**

Complete removal of sediment from a reservoir to be decommissioned can be performed by either conventional earth moving techniques or hydraulic dredging (Chap. 16).

Conventional excavation takes place in the dry and requires that the reservoir be drained and sediments dewatered sufficiently for access and handling before excavation begins. The sediment is then removed with conventional equipment such as dozers and front-end loaders, and loaded onto trucks or conveyers for transport to the disposal site. The viability of the approach is a function of the time it takes for the sediment to dry, the availability of disposal sites, the quality of the sediment, and the possibility of draining the reservoir. Because sediments will be eroded downstream while the reservoir is emptied (as in flushing), environmental restrictions may limit the possibility of draining the reservoir, or may require draining and excavation by phases. If contaminants have collected to the point that the sediment is considered a hazardous material, special handling and disposal measures will be required.

Mechanical dredging with a clamshell or dragline can be conducted without dewatering the reservoir, but is best suited for coarse sediment and relatively small impoundments; it is poorly suited for the handling of fines. For the removal of large volumes of sediment that is sand-size or smaller, hydraulic dredging will generally be the preferred option. The dredging system will typically consist of a barge-mounted pumping unit, suction line with a cutterhead, and a discharge line extending to the disposal area. The disposal area consists of a diked holding pond in which the sediment is allowed to settle, and the clear supernatant water is then discharged back into the environment (Fig. 16.3). The settled material can be either left in place or hauled to the final disposal site.

### **17.4 DECISION FACTORS**

---

Many cost, legal, and environmental factors enter into decisions pertaining to the feasibility of decommissioning a dam. They include water and sediment quality and impacts on the fluvial system, existing infrastructure, flood management, ecological, and social issues.

#### **17.4.1 Water and Sediment Quality**

Pollutants from both point and nonpoint sources can be sorbed onto sediment particles, particularly fines, and deposited in reservoirs as the sediment accumulates.

Contaminants may include agricultural chemicals such as pesticides, runoff or point-source discharge from upstream industrial areas which may contain heavy metals or toxic organic compounds, products from mine drainage or tailings, or products from industrial or other spills. Some constituents may not be classified as toxins, but nevertheless may have extremely deleterious effects on downstream ecosystems, such as sediment containing high nutrient levels or organics which will exert a significant oxygen demand.

Contaminants immobilized within reservoir sediments may not have a deleterious impact on the water quality discharged downstream of reservoirs as long as the sediments are not disturbed. This is particularly true of older sediments, which may contain toxic substances (such as pesticides) that are no longer being discharged to the environment, and which have become entombed beneath more recent clean sediments. Dam removal may mobilize these contaminated sediments.

Should the sediments contain unacceptable concentrations of pollutants, such as those on the U.S. Environmental Protection Agency Priority Pollutant List, or should the sediments be classified as hazardous material, it may be more costly, more harmful to the environment, or both, to decommission in a manner that disturbs and remobilizes the contaminated sediments. Testing of sediments through the entire depth of the deposit to be disturbed should be undertaken for contents such as heavy metals (arsenic, beryllium, cadmium, zinc, etc.); volatile solids (acrolein, bromoform, benzene, etc.); base/neutral compounds (acenaphthene, benzidine, chrysene, etc.); acidic compounds (4-chloro-3-methylphenol, phenol, etc.); and pesticides (Aldrin, Chlordane, etc.). To better define the chemical composition of the sediment, it is also common to test for total Kjeldahl nitrogen, nutrient level, and total organic carbon. The toxicity characteristics leaching procedure (TCLP) can be used to determine whether the sediment has the potential for contaminants to leach out.

The type and levels of contaminants in the sediments, together with the characteristics and sensitivity of the downstream areas that would be affected by sediment release, will play an important role in determining whether it is feasible to decommission by either partial or complete removal of the structure in a manner that mobilizes sediment. Should dam removal be required despite presence of problem sediments, the sediment properties will play a major role in determining the dam removal and sediment management strategy.

In reservoirs that trap fine suspended sediments, dam removal will impact the turbidity downstream. A temporary increase in turbidity will occur while the new channel is being established through the reservoir, and a long-term increase in turbidity will occur as a result of eliminating the sediment-trapping function previously provided by the dam. Elimination of storage above the dam will also affect the streamflow and temperature budget of the stream, with the direction and magnitude of this change being highly site specific.

An increase in downstream turbidity can impact the entire aquatic food chain by shading primary producers, smothering benthos, clogging spawning gravels, and heavily affecting filter feeders. Changes in visibility affect the ability of sight predators to detect their prey, which can significantly alter the structure of the biological community, favoring some species and potentially eliminating others. Dam construction can also change a turbid warm-water stream into a clear cold-water stream, as in the case of the Colorado River below Lake Powell where the predam water temperature range was 0° to 28°C and the postdam temperature range is 8° to 9°C. This change had a significant impact on the aquatic life in the river, leading to the establishment of a new ecosystem. After the stream ecosystem and society (especially anglers and recreational boaters) become adjusted to clear-water conditions, a change back to natural but turbid conditions may be considered undesirable. In many other areas, clear-

water conditions may occur naturally, but increased sediment loads have occurred because of disturbance and accelerated erosion in upstream watersheds. The maintenance of downstream aquatic or marine ecosystems that rely on clear-water conditions may depend on continued sediment trapping by the dam, and dam removal would subject the downstream ecosystems to turbidity stress.

Prediction of the impact of turbidity and temperature changes on aquatic life and habitat is a complicated issue: positive impacts on certain species may have negative impacts on others. Biological assessment, modeling, and monitoring of the affected reach may be required, and biological impacts may be an important parameter in selecting the optimal mix of potential decommissioning actions.

### 17.4.2 Fluvial Morphology

Dam decommissioning can affect the morphology of the fluvial system both upstream and downstream of the reservoir. If the dam is not removed and sediments remain in place, the pattern of long-term sediment accumulation will continue until a full sediment balance is achieved across the impounded reach. Not only will continued sediment deposition eventually fill the reservoir pool, but it can also cause significant deposition above the pool level, thereby creating problems such as increased upstream flood levels and waterlogging of riparian soils as the streambed is progressively elevated by continued deposition. The extent of deposition above the maximum normal level can be significant. An example of sediment deposition above the full supply level is presented in Fig. 17.6, which shows profiles for the original river bed and subsequent sediment deposits upstream of Welbedacht Dam along the impounded reach of the Caledon River, on the border between the Kingdom of Lesotho and the Republic of South Africa. The high rate of sediment discharge into this reservoir led to rapid loss of capacity. The large sediment volumes deposited above the full supply elevation of the reservoir led to frequent over-

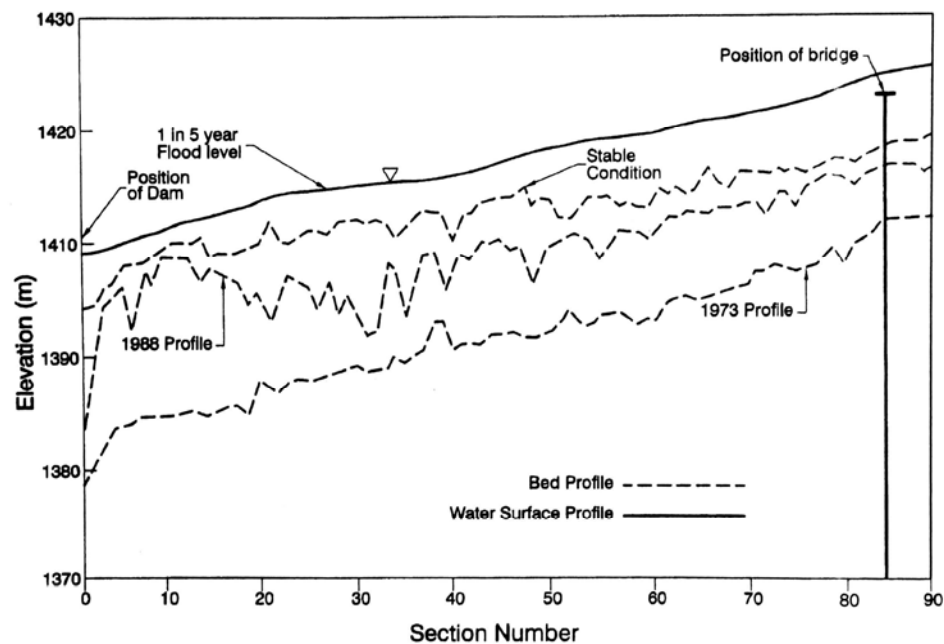


FIGURE 17.6 Sediment deposition upstream of Welbedacht Dam, South Africa.

topping of a bridge structure located approximately 25 km upstream of the dam, and frequent flooding in the town of Wepener located on a tributary to the Caledon River. Conversely, the partial or complete removal of the dam will lower the base level for the stream above the dam, potentially causing erosion to extend above the pool level.

Impacts to the river below the dam can be severe, especially when the dam is partially or completely removed and sediments are released to the downstream channel. The magnitude and duration of the impacts will depend on the sediment volume released relative to the transport capacity in the river. Fine sediment released to a high-gradient stream may have a large initial impact in terms of water quality, but if the sediment deposits are quickly eroded from the reservoir and the fines are rapidly flushed out of the downstream channel, the impact will be short-lived. However, coarse material is typically flushed through a river system at a much slower rate, and sandy sediment released by dam removal may be transported along the downstream channel as a slow-moving sediment wave. Observations of fluvial behavior of rivers below dams which have failed indicate that sediment can require many years to move through the river system. The sand wave released by removal of the Newaygo Dam on the Muskegon River, Michigan (Simons and Simons, 1991) moved downstream a distance of about 14 km during the first 9 years, and an estimated 50 to 80 years will be required for the sediment slug that was released from this dam to be flushed through the river system. The downstream impacts of sediment release can be reduced by channelization or staged dam removal, respectively, to lessen the total volume or the rate of sediment release to the downstream channel.

The slow downstream migration of a sand wave or slug can produce a variety of problems in the river system including channel changes, impairment of navigation, elevation of the river bed and flood levels, and blockage of tributaries. The greatest reduction in the cross-sectional area of the stream occurs at the apex of the sand dune, with less influence at other locations. If a sand bar is stable for sufficient time for brush and small trees to grow, the sand can become trapped in the channel and flood levels can rise due to reduced channel capacity plus increased channel friction due to the vegetation. If sufficient sediment is released, the increased sediment load can alter the river planform, causing meandering and braiding or more frequent lateral movement of the river. Any marked acceleration of lateral migration attributable to dam removal can become a costly problem in areas where riverbank property, infrastructure, or bridge crossings are affected and require protection. Elimination of reservoir storage may increase downstream flood peaks, which will tend to increase the sediment transport capacity below the former dam site and accelerate channel erosion processes.

### **17.4.3 Existing Infrastructure**

Movement of a sand wave through a river system, and its associated effects on river morphology, can also have an impact on existing infrastructure. The infrastructure most likely to be affected include bridges, water intakes, outfalls, and navigation channels. Bridges can be affected by an increase in the stream bed elevation due to the release of coarse sediment from the previously impounded area, decreasing both flood conveyance capacity and navigational clearance beneath the structure.

### **17.4.4 Flood Management**

The impact of dam decommissioning on flood management depends on the selected dam removal and sediment management options. Should the decommissioning plan call for the dam and sediment to remain in place, the owner might be required to staff the

facility to ensure that flood management benefits historically provided by the dam continue to be offered. The owner may also be required to monitor sediment deposition at the upstream limit of the pool and to amend the flood management operation as required to minimize flood hazard to communities upstream of the pool in the reach affected by streambed aggradation. Should the decommissioning plan call for partial or complete dam removal, with sediment release that results in morphological changes in the river reach below the dam site, a flood management plan may call for monitoring and improvements to levee and related flood control systems downstream if downstream bed aggradation is anticipated.

#### **17.4.5 Aquatic Habitat and Life**

Depending on the size of the project and the sensitivity of the downstream river reach, intensive biological studies may be required to determine the impact of changes in water quality on aquatic life along the fluvial system affected by the dam. The decommissioning and removal of a dam will influence the fluvial environment in a number of ways, including changes in benthos, flow duration, and peak discharge. Effects on the environment include changes in temperature, turbidity, and degradation of spawning gravel due to deposition of fine sediments.

Should reservoirs having significant effects on turbidity or temperature be removed by decommissioning, the downstream ecosystem will be affected. Similarly, reduction in the turbidity of water can affect a variety of processes, including photosynthesis, and the predominance of certain kinds of predators. Reduced turbidity will favor sight predators, and can have a significant impact on the balance of aquatic life. Should turbidity increase after decommissioning, it will change both the ability of sight predators to prey on other fish and will also affect plant life. However, these impacts may be offset by many environmental benefits, such as the restoration of the stream migration corridor by elimination of the barrier imposed by the dam.

#### **17.4.6 Social Effects**

Social effects of dam decommissioning include the impacts of reduced efficiency of flood protection, impacts on cultural resources and impacts to shoreline properties.

#### **17.4.7 Legal Issues**

Legal issues involving sedimentation can be wide and varied. In the United States the taking issue is among the more relevant. It relates to the taking of property, or rendering it unusable, by reason of increased flood hazard, the effects of erosion and sedimentation, obstruction of land drainage, and impairment or loss of water rights. These issues are covered by case law and the Tucker Act, which allows legal action against the United States government for damages caused by improvements built by the government.

#### **17.4.8 Cost**

Cost is a major factor determining the feasibility of dam decommissioning and selection of the appropriate sediment management plan. Generally, dams are more costly

to remove than to construct, and sediment management is one of the major cost components of decommissioning.

## **17.5 EXAMPLES**

---

Decommissioning with concurrent dam removal is a relatively new topic, and dam removal in particular is controversial. In cases where owners decide that decommissioning with concurrent dam removal makes economic sense, decommissioning and removal is likely to take place on a voluntary basis. In other cases, for example, when agencies such as the Federal Energy Regulatory Commission demand dam removal, owners may be less willing to comply. This section first briefly contrasts the responses of Edwards Manufacturing Co., Inc. and of Consumers Power Company to a FERC request for dam removal. While many reasons for the differences in response may exist, one of the obvious differences is that the hydroelectric plant owned by Edwards Manufacturing was still operating at the time of request for dam removal, whereas the Consumers Power Company hydroelectric facilities at Stronach Dam had already been decommissioned for many years and dam removal was the only remaining decommissioning issue. The second part of this section contrasts sediment removal issues at the urban North Avenue Dam in downtown Milwaukee, with the issues at the Elwha and Glines Canyon dams on the Olympic Peninsula in Washington state.

### **17.5.1 Edwards Manufacturing**

Edwards Manufacturing (FERC, 1995) owns a hydroelectric facility on the Kennebec River near Augusta, Maine. Upon application for project relicensing, resource agencies and the Kennebec Coalition (an environmental group) argued that fish passage at the site was inadequate. This resulted in a demand for decommissioning of the project and dam removal. Edwards Manufacturing wishes to continue operation of the plant and proposed alternatives for fish passage, such as installation of fish ladders. FERC is currently issuing annual licenses that allow Edwards Manufacturing to continue operation of the plant, a process which will continue until the property is taken over or a new license is issued. The owner has not developed any plans for decommissioning and dam removal, and the case is the subject of a continuing legal battle.

### **17.5.2 Stronach Dam**

Stronach Dam, owned by the Consumers Power Company, is located in the Pine River, within the Manistee National Forest in Manistee County, Michigan. The dam consists of an earth embankment approximately 10 m high with a concrete core. The original project was constructed in 1911 and 1912. The dam is located at the foot of the rapids over which the Pine River descends from the high valley banks to the river bottom. The Pine River is characterized by a high sediment load, and by 1930 the pond above Stronach Dam was almost completely filled with sediment. Conditions worsened because of continued sediment accumulation, and in 1953 the hydroelectric plant was retired and the generators and auxiliary equipment were removed. The trash racks were blocked and most of the flashboards were removed to reduce the headwater elevation.

No removal of sediment occurred since decommissioning of the hydroelectric equipment, and by 1996 the original surface area of 27 ha had tilled almost entirely with

sediment. Both the dam owners and resource agencies agreed that removal of the dam structure would have significant ecological, recreational, scenic, and aesthetic benefits, and the owner subsequently requested permission from FERC to remove the structure (FERC, 1996). FERC issued a new license for operation of the Tippy Project, of which Stronach Dam is a part, while at the same time approving a settlement agreement to remove Stronach Dam. The major components of the Stronach Dam removal project are structural modification to allow staged drawdown and removal of sediment by natural erosion, dam removal, stream stabilization, site restoration, monitoring of wetland habitat, and studies of fisheries on the Pine River.

The dam removal plan submitted by Consumers Power Company consists of three stages: (1) construction of a temporary water drawdown structure; (2) pond drawdown, and (3) demolition of selected structures and restoration of the Pine River. During stage 1, a steel A-frame structure equipped with stoplogs will be erected concurrently with removal of part of the powerhouse through which flow will be discharged. Construction is expected to require 6 months. Stage 2 of the project will last 6.5 years and will entail the staged removal of stoplogs at a rate of 0.15 m every three months. The objective is to achieve a gradual release of sediment from the pond by natural erosion, at a rate that minimizes detrimental effects in the river reach below the dam. Stage 3 of the project entails removing the temporary A-frame structure, the embankment, and concrete core wall of the dam to create a channel through which the river can flow, as well as the remaining appurtenant structures. The new river channel through the deposits will be protected against continued erosion in appropriate locations by riprap.

### **17.5.3 North Avenue Dam, Milwaukee, Wisconsin**

The 5 m tall North Avenue Dam is located on the Milwaukee River about 5 km upstream of Lake Michigan, and passes through downtown Milwaukee (Fig. 17.7). The dam creates a small (33 ha) impoundment that is about 3.7 km long and averages only 87 m in width. Maximum water depth is about 3 m. The Milwaukee River was first dammed in 1835 near the site of the present dam, to control water levels in the Milwaukee River for a canal scheme which was never completed. The current dam forms an artificial boundary between the river and the Milwaukee River Estuary, which was first dredged in 1857 to allow large vessels to enter the river. Subsequent dredging allowed vessels to reach an area just below the existing dam.

Despite the dam's small size, complex issues are associated with its management (Woodward-Clyde Consultants, 1994). Surface water quality within the impoundment is seriously degraded by low dissolved oxygen, high heavy metal concentrations, high turbidity, high temperature, and high populations of algae and bacteria. Fish kills have occurred within the impoundment. The dam constitutes a migration barrier to fish and the sediments represent a source of contaminants which impair water quality and recreational use of the river. After many decades of trapping sediments and contaminants, today's sediment deposits are contaminated with heavy metals, polychlorinated biphenyls (PCBs), polycyclic aromatic hydrocarbons (PAHs), and a variety of oxygen-demanding materials.

The dam's gates had previously been opened to temporarily draw down the reservoir in 1954, 1970, and 1985. In 1990 the dam's gates were opened and the reservoir was drawn down to replace a water main and a bridge. When the gates were opened the river ran along its original course, exposing about 18 ha (45 acres) of contaminated sediment deposits along either side, an area that was called the sediment flats. About 20 m<sup>3</sup> of urban debris such as auto parts and building materials, plus more than 2000 tires, were removed from the sediment flats, which were then revegetated to control erosion. After the impoundment was drawn down,

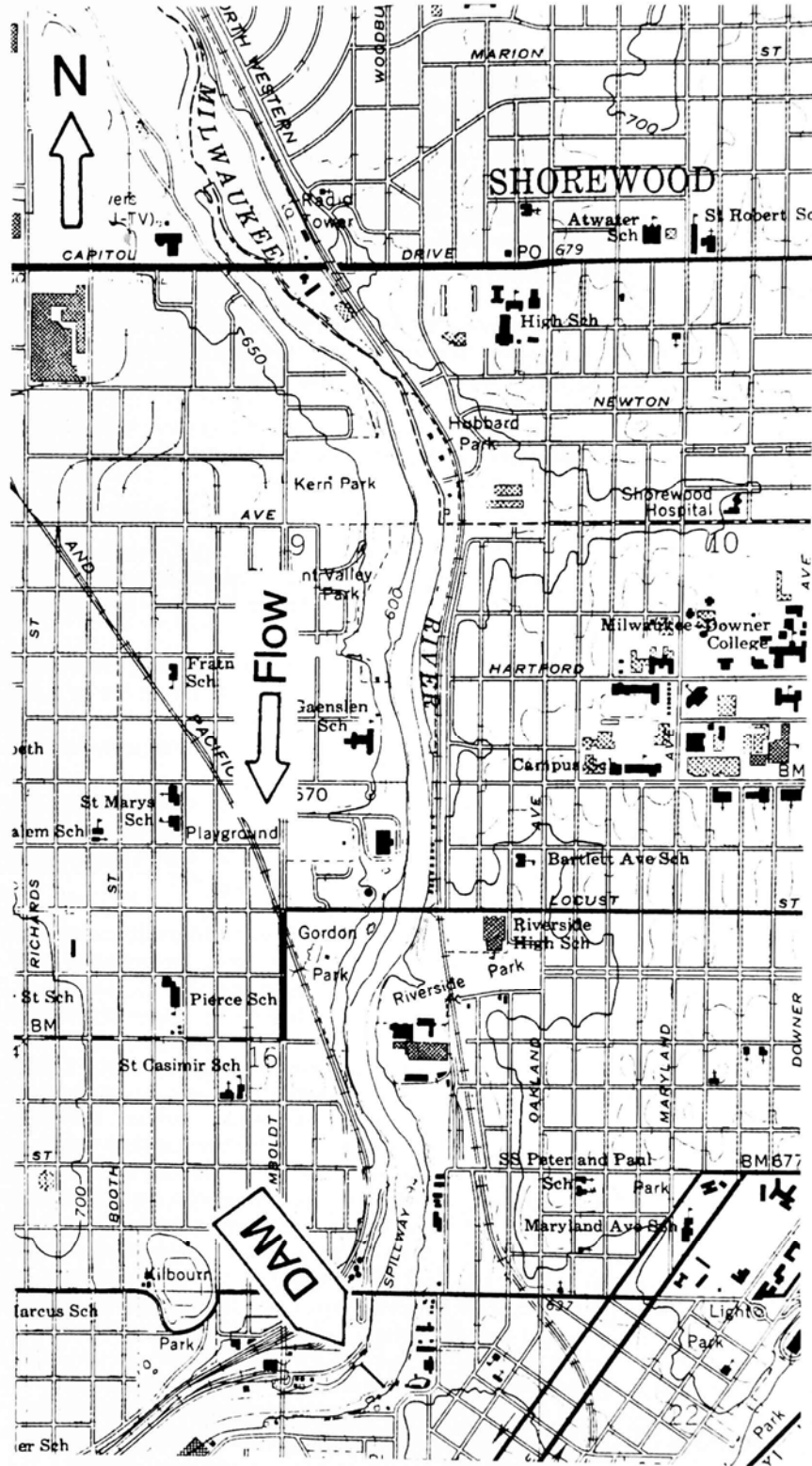


FIGURE 17.7 Location map for North Avenue Dam, Milwaukee, Wisconsin (USGS topographic quadrangle).

the Wisconsin Dept. of Natural Resources recommended that the reservoir's gates remain open until completing a study to determine the potential effects on the Milwaukee River of either keeping the impoundment or removing the dam.

Among the issues of importance at this site was that of contaminated sediment ownership, due to the potential environmental liabilities and long-term management costs. It was determined that the riparian property owners were also owners of the sediment, whether it was submerged by the impoundment or exposed as a result of opening gates or removing the dam.

Five management alternatives were considered, with capital costs ranging from \$114,000 to \$15.8 million. Annual operation costs under all alternatives were similar, between \$138,000 and \$253,000. Each of the five alternatives are briefly described below, and the capital costs are indicated.

1. Close the dam's gates to impound water, submerging sediment flats, with no additional remedial action other than minor repairs (\$114,000).
2. Leave the dam's gates open, exposing the sediment flats, with no additional remedial action other than minor repairs (\$114,000).
3. Close the dam's gates to impound water, but remedial actions would be taken to cap the submerged contaminated sediments to minimize health and environmental risks (\$15.8 million).
4. Remove the gated portion of the dam to the level of the original river channel and remove portions of the spillway on either side of the gates to create a trapezoidal cross section. Portions of the dam would remain in place to hold upstream sediments in place. Sediment management activities would include sediment consolidation, bank and channel stabilization, and revegetation (\$5.7 million).
5. Completely remove the dam. This would expose a 4 m tall "wall" of sediments, which would be graded back to a stable angle and protected with geomembrane and riprap. Other sediment management activities would include sediment consolidation, bank and channel stabilization, and revegetation (\$6.5 million).

Alternatives involving drawdown of the impoundment also included modification to an existing industrial water supply intake dewatered by the drawdown, protection of a utility crossing, and activities for wildlife and recreational enhancement.

Each alternative was evaluated with respect to its effect on the following resource parameters: water quality (dissolved oxygen, bacteria, and toxins); stream hydraulics and flooding; sediment quality; recreational use (canoeing/kayaking, sculling, hiking, disabled access, fishing access, birding, and view aesthetics); land use, value and ownership; aquatic and riparian wildlife; utilities and infrastructure; cultural resources; groundwater; and cost. The first two alternatives were discarded because they would not meet the project's water quality objectives; contaminants would continue to be released from the sediments. The fourth alternative, which was recommended for implementation, was not only the least costly of the alternatives considered acceptable from the standpoint of water quality, but would also provide enhanced public recreational access because the revegetated and stabilized sediment flats would become public property. It would provide a more diverse ecological environment and improve water quality. Partial removal of the dam would also eliminate a barrier to fish migration and allow recreational navigation through the breached dam by canoe and kayak.

The riparian land along the length of the reservoir consists of a number of different public and private properties, and the privately owned parcels tend to restrict recreational access to the river and reservoir. It was recommended that private landowners cede their ownership of contaminated sediment flats to the State. It was

further recommended that both the City and County of Milwaukee, who are also riparian landowners, perform sediment management work on their sediment flats plus privately owned sediment flats, once the suitable deeds or easements were in hand. Upon completion of remediation, all sediment flats would be deeded to the State so that it would fall under unified ownership and operation and would provide unrestricted public access. However, Milwaukee County would continue to own upland areas, where it would maintain park and recreational facilities.

#### 17.5.4 Glines Canyon and Elwha Hydroelectric Dams, Washington State

The Elwha and Glines Canyon hydropower dams are located on the Elwha River on Washington's Olympic Peninsula. Summary characteristics are given in Table 17.1. Pool

**TABLE 17.1** Summary Characteristics of Darns on Elwha River.

	Elwha	Glines Canyon
Year completed	1912	1927
Dam height (m)	32	64
Crest length (m)	137	82
Reservoir name	Lake Aldwell	Lake Mills
Reservoir surface area (ha)	108	168
Original reservoir volume ( $10^6\text{m}^3$ )	10.0	49.4
Accumulated sediment in 1989 ( $10^6\text{m}^3$ )	3.2	8.3
Installed hydropower capacity (MW)	14.8	13.1
Average gross energy production (GWh/yr)	70	102

*Source:* FERC (1991).

levels vary little and both dams are operated essentially as run-of-river facilities. Upper portions of the Elwha River are within Olympic National Park and represent some of the most outstanding scenic and ecological resources in the United States. It is also designated a world biosphere reserve and a World Heritage Park by UNESCO. Glines Canyon Dam and its reservoir, Lake Mills, lie entirely within Olympic National Park (Fig. 17.8).

The generalized variation in grain size within the deposits above Glines Canyon Dam is presented in Fig. 17.9. Trapping of bed material within the reservoirs has caused significant coarsening of the riverbed below the dams (Fig. 17.10), and dam construction has also contributed to coastal erosion. Prior to the dams, the Elwha delivered about  $30,000\text{ m}^3/\text{yr}$  of coarse sediment to its delta. Longshore currents subsequently transported this sediment eastward to Ediz Hook, with a travel time on the order of 10 years between the delta and Ediz Hook (see location map in Fig. 17.8). Erosion in the area of the river delta due to reduced sediment supply was first noticed in the period from 1926 to 1940, and has also contributed significantly to subsequent shoreline erosion along the western end of Ediz Hook.

Anadromous fish are those that migrate from freshwater to saltwater and then return. In the Elwha the principal anadromous fish of historical significance are coho, chinook, pink, and chum salmon, and steelhead trout. The Elwha fisheries were generally described as prolific until dam construction began in 1910, but declined

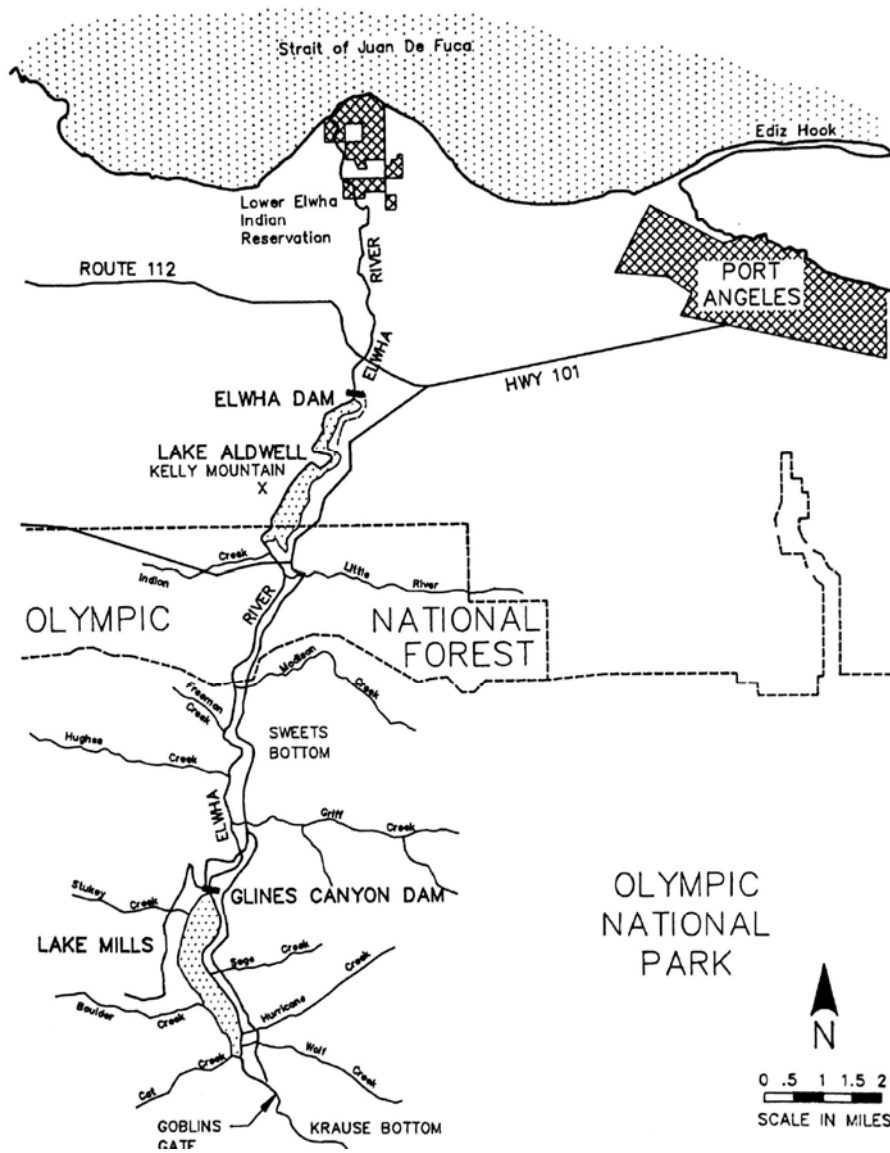


**FIGURE 17.8** Location map for Elwha and Glines Canyon Dams and adjacent areas (FERC, 1991).

dramatically thereafter. In addition to physically blocking migration, coarsening of the below-dam riverbed has also made this zone less suitable for spawning.

The Lower Elwha Klallam Tribe has a reservation along the lower river, and has repeatedly stressed the importance of the river and its anadromous fish resource as the most significant single aspect of their cultural identity. For the aboriginal Klallam, the

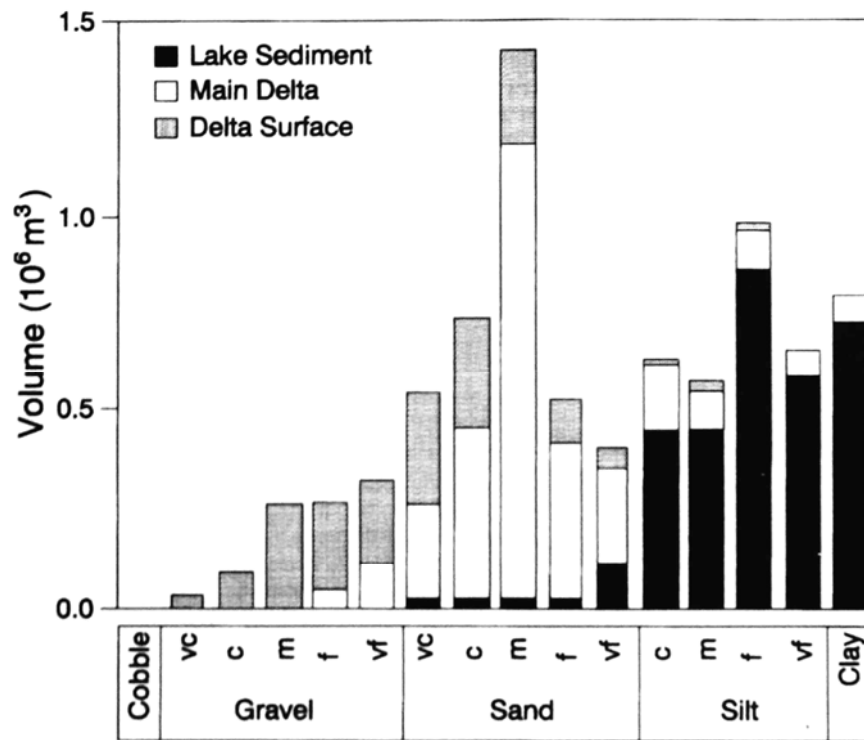


**FIGURE 17.9** Grain size variation of sediment trapped above Glines Canyon Dam, as a function of location within the reservoir (after FERC, 1991).

anadromous fishery was the most important source of food, both for immediate consumption and long-term storage. In 1855 the United States Government granted fish harvest rights to the Klallams and other signatories of the Point No Point Treaty, in exchange for territorial claims. Subsistence and commercial fishing continued to be their primary activity until dam construction, which decimated the fishery. Removal of the dams would increase fisheries and help to restore these rights, as well as provide more species and locally increased populations for both commercial and sport fishing.

Environmental benefits of fisheries restoration will also extend to many other species. Salmon die after spawning, and following removal of both dams it was expected that over 400,000 kg/yr of salmon carcasses would be returned to the river system for consumption by other wildlife. At least 22 different bird and mammal species have been documented to feed on the carcasses of coho salmon. Additionally, the increased population of fry and juvenile salmon will support other predators.

Both dams were submitted to the Federal Energy Regulatory Commission (FERC) for relicensing, which has been opposed by the Elwha Klallam Tribe and environmental interests favoring restoring the Elwha's natural habitat. The draft environmental impact statement (EIS) prepared by FERC (1991) to address the relicensing issue provides the information used in this example. The EIS evaluated the applicant's proposal for continued operation of the dams, with mitigation measures to provide fish passage for some species, against alternatives incorporating the removal of either or both dams.

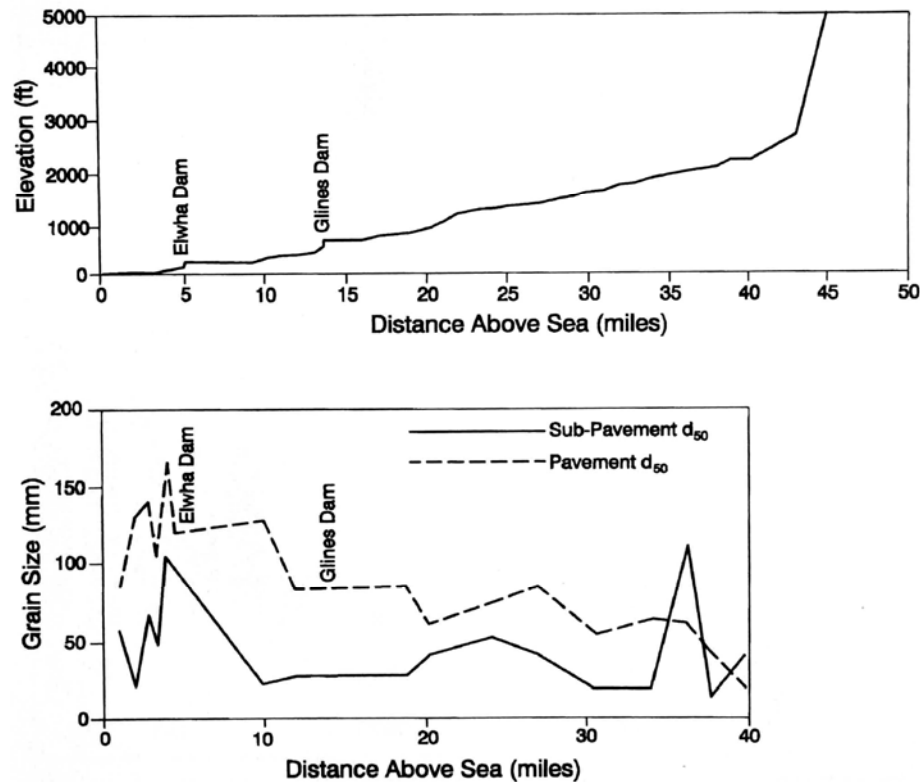


FIGURE 17.10 Longitudinal profiles for Elwha River Showing (top) elevation profile, and (bottom)  $d_{50}$  grain size of bed material (after FERC, 1991).

Three primary resource objectives in this case were: (1) restoration of wild, self-sustaining runs of anadromous fish; (2) restoration of natural conditions within Olympic National Park, and (3) provision of renewable hydroelectric power. The restoration of wild, self-sustaining runs of anadromous fish is a principal resource objective in the Elwha River because the Elwha watershed provides unique opportunities for such restoration, and because restoration of anadromous docks is a regional priority. FERC's analysis revealed the hydropower production and environmental enhancement objectives to be mutually exclusive.

Four alternatives were considered: (1) the applicant's proposed modification of both dams to facilitate fish passage, (2) removal of Glines Canyon Dam only, (3) removal of Elwha Dam only, and (4) removal of both dams. At the Elwha Dam the applicant proposed the installation of fish ladders for upstream passage, screening of intakes, and provision of a bypass system to facilitate the outmigration of juveniles to the ocean. At the taller Glines Canyon Dam fish passage would be accomplished using a fish barrier weir and a trap-and-haul system. However, these techniques would increase the populations of only 2 of the 5 anadromous fish species affected by the dams.

While removal of the dams was greatly preferred from the environmental standpoint, it represents a large cost in terms of foregone electrical power production. The value of foregone power associated with dam removal was computed as the difference between

**TABLE 17.2** Economic Analysis Summary, Net Present Value Cost of the Alternatives.

Alternative	Incremental costs (thousands of 1996 dollars)*		
	Capital and O&M Cost	Value of lost Generation †	Total Cost
Applicant's dam retention proposal	\$ 35,583	\$ 3,530	\$ 39,113
Removal of both dams	80,855	164,221	245,076
Glines Canyon removal with retention of Elwha	84,383	99,960	184,343
Elwha removal with retention of Glines Canyon	35,088	67,881	102,969

\*Present value of costs occurring over the 50-year period of analysis.

†Lost generation valued at the 50-year levelized cost of the region's long-term marginal generating resource.

Source: FERC, 1991.

the cost of hydropower production at the two dams, and the cost of producing a comparable amount of power from a coal-fired power plant. The power cost was twice as large as the cost of dam removal itself (Table 17.2).

Management of the accumulated sediment is a key issue associated with dam removal. Because the watershed is in pristine condition and has never been logged, there are no issues related to sediment contamination. However, the release of nutrients and organic matter associated primarily with fine sediments could have deleterious water quality effects downstream, including decreased oxygen levels and increased nutrient levels. Fine sediments and organics may cause water quality problems at drinking water intakes and at the fish hatchery intake. Ranney collector wells installed 20 m below the bed of the Elwha River and used to supply the City of Port Angeles could also be clogged by fine sediment and require backflushing.

Both reservoirs have sizable delta deposits of coarse sediment, which must also be managed. While it is desired to reestablish the transport of coarse material along the river system, it is not desired to release these sediments rapidly. This could smother spawning areas below the dam, cause downstream flooding, and interfere with intakes.

The proposed strategy is to excavate a new river channel through the existing sediment deposits, and to store the excavated sediment on top of the existing sediment deposits in other areas of the reservoir. Drawdown and sediment stabilization activities would be performed during periods of lower flow, March to October. Delta sediments, consisting mostly sands and gravels, would be placed in terraces located within the existing upper reservoir area but away from the future river channel. A dragline operating from the surface of the delta would excavate the channel along which the river will flow within the dewatered reservoir. This channel alignment is illustrated in Fig. 17.11. Once substantial surfaces are exposed by drawdown, conventional earthmoving equipment would be used. Trucks would haul excavated material to the terrace surfaces, where it would be deposited at slopes of about 4.5:1 (horizontal:vertical).

Most coarse material that washed further downstream in the reservoir during the progressive drawdown would continue to be trapped in the lowered pool, from which it could be excavated as levels continue to drop. However, most of the fines which are eroded are expected to be flushed through the system and into the ocean as wash load. Silt present on the reservoir bottom in the area near the dam would not be moved by mechanical means. Instead, the silt that remains trapped outside the

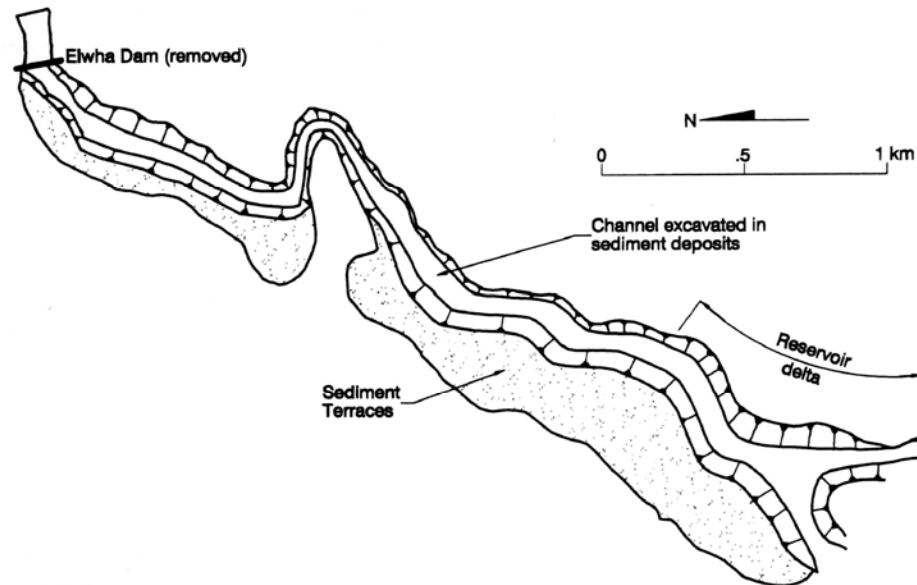


**FIGURE 17.11** Alignment of proposed channel to be excavated through sediment deposits above Elwha Dam, if the dam is removed. Sediments excavated from the channel will be deposited on top of the existing off-channel sediment deposits in the reservoir (after FERC, 1991).

scour channel would be allowed to remain in place. After drawdown, it would be protected by erosion control blankets and revegetated.

The proposed construction sequence for dam removal takes into account the need to minimize sediment release. At Elwha Dam a 4.1 m diameter diversion tunnel would be constructed for dewatering the reservoir below the level of the power intakes, and a cofferdam would divert the entire river flow into the diversion and away from the dam area to allow demolition to be performed under dry conditions. Floods exceeding the diversion capacity would be temporarily stored in the reservoir and, if large enough, discharged over the dam. A similar procedure would be used at the Glines Canyon Dam.

A revegetation program would be undertaken in both reservoirs to establish a cover of native species on the disposal terraces as soon as possible. Terraces would be carefully graded to reduce erosion, and tributary streams would be carefully routed across the erodible terraces. Terraces would be seeded and mulched in the early fall of the year in which they are constructed, and areas affected by winter erosion would be replanted in the spring. Areas of poor cover would be reseeded in the fall. The seed mix would consist of sterile forms of fast-growing grass and cover species as well as native pioneer grasses and forbs. Willow wattling would be planted in highly erodible areas. Replanting would not be performed during the dry summer months when there would be little opportunity for plant establishment on the coarse well-drained sediments.

Excavation and terracing of sediment would be carried out for 2 years in Lake Aldwell, and for 3 years at Glines Canyon, prior to dam removal. It is expected that 4 to 10 years would be required for the sediment terraces to become stabilized with good vegetative cover and mulch. Thereafter, sediment levels within the river would be dominated by natural sediment delivery from the upper watershed rather than

erosion of reservoir deposits. Over a period of centuries the Elwha River channel would migrate laterally and erode away the terraces through natural processes.

River erosion and additional sediment management alternatives for the Elwha River, including a slurry pipeline to the coast and mechanical excavation and hauling, have been described by Randle and Lyons (1995).

## **17.6 CLOSURE**

---

As dams age, decommissioning and removal is becoming an issue of increasing importance. Sediment management during and after dam removal is a major technical and cost component of decommissioning projects. Various strategies for dam removal and sediment management exist. These methods will become more refined, and newer approaches will be developed as engineers become more experienced in dam removal and the concurrent management of sediment.

---

## CHAPTER 18

---

# ENVIRONMENTAL AND REGULATORY ISSUES

---

### 18.1 INTRODUCTION

---

Dams are the greatest point source of hydrologic disturbance to rivers (Petts, 1984). They alter the flow of water, sediment, nutrients, energy, and biota and also modify channel morphology, thereby interrupting and altering most of the river's important ecological processes. The impact of dams often extends hundreds of kilometers downstream, and they may also influence estuarine and coastal ecosystems far below the dam site. Even hydrologically small dams can create large impacts when they block migration, trap bed material, divert a significant portion of the flow (especially low flow), or are sufficiently numerous on a river to significantly reduce peak discharges. Channel morphology and habitat conditions below a dam are particularly affected by the reduced magnitude and frequency of flood flows, and the trapping of coarse bed material in the reservoir. Riparian wetlands and anadromous fisheries are particularly susceptible to impact.

In concept, the partial or complete restoration of the sediment balance along an impounded river is environmentally desirable. Ligon et al. (1995) stated that the best means to preserve the morphology and biota of rivers is to design reservoirs that pass coarse sediment on a regular basis, consistent with the frequency of natural sediment transport events. Unfortunately, the coarse bed material is the most difficult fraction of the inflowing load to pass through the impoundment. Many factors complicate sediment management, making it difficult, costly, or virtually impossible to replicate natural patterns of sediment discharge along an impounded river. Downstream interests may oppose a return to the natural preimpoundment sediment transport regime. Large flows required to sustain channel morphology may cause property damage because of human encroachment onto floodplains. New aquatic species and human uses may have become adapted to the clear cold water in the reach below the dam, in what was formerly a turbid warm-water stream. Anglers, recreationists, landowners, operators of municipal and industrial intakes, and regulatory agencies may oppose increased sediment discharge to the reach below the dam. Owners of downstream dams will not want to experience increased sediment loading, shortened useful life, and increased sediment management costs in their own reservoirs.

This chapter first reviews environmental impacts of dams related to sediment management. Next, the types of environmental impacts to be anticipated from each of several types of sediment management activities are outlined, along with general mitigation strategies. Sediment will be released any time a reservoir is emptied through a bottom outlet, whether the emptying is for sediment flushing or for another purpose such as the repair of a gate. Thus, the discussion of reservoir emptying

is widely applicable and not limited only to emptying for sediment flushing. The chapter closes with a discussion of coarse sediment management below dams. Environmental issues associated with sediment excavation and dredging are discussed in Chap. 16.

Petts (1984) provides a comprehensive overview of the physical and biological characteristics of impounded rivers and the environmental impacts of dams. Below-dam impacts have been summarized by Williams and Wolman (1984) and Collier et al. (1995). An overview of dam-related environmental issues from the perspective of the World Bank are discussed by Dixon et al. (1989). Goldsmith and Hilyard (1984, 1985) respectively, reviewed the environmental impacts of large dams and presented a compendium of case studies worldwide. A more recent overview of the adverse environmental and social impacts of large dams is presented by McCully (1996). The International Rivers Network ([www.internationalrivers.org](http://www.internationalrivers.org)), 2150 Allston Way, Suite 300, Berkeley, CA 94704-1378, issues a newsletter and publications describing the environmental impacts of dams.

## 18.2 ENVIRONMENTAL EFFECTS OF DAMS

---

### 18.2.1 Dams and Environmental Impacts

Dams generate large and long-term socioeconomic benefits, but can also generate large and long-term environmental impacts. The term *environmental impact* broadly include economic, environmental, and social impacts not directly considered in the economic accounting of project benefits and costs, plus those ecological and social impacts for which it is difficult or inappropriate to establish a monetary value. The evaluation of environmental impacts is important because a dam will contribute to net economic development only if total benefits exceed total costs. Failure to include environmental impacts in an analysis does not make these impacts and their deleterious economic and social effects disappear (Dixon et al., 1989).

Certain types of environmental impacts may be directly measured or predicted: soil erosion and sedimentation, the land occupied by the dam and reservoir, salinization and waterlogging in newly irrigated or riparian areas, changes in stream hydrology, health effects, fishery effects, wetland impacts, and recreational impacts. However, the valuation of these attributes can be highly problematic. What per-hectare value should be assigned to a forest which serves as ecological habitat? An important characteristic which imparts high ecological value, such as remoteness, may give it low economic value and underscores the difficulty of establishing comparative values.

The difficulty of rendering a full and accurate accounting of environmental impact lies not only in their inherent nonmarket nature, but also in the technical uncertainty associated with impact prediction. Dams can create large direct impacts hundreds of kilometers downstream, and possibly many years removed in time. Project proponents may not want to render a full accounting of project impacts, if they can reap the benefits of the dam while environmental costs are borne by others. Consultants hired by proponents to undertake environmental studies tend to become part of the pro-project team. For example, the environmental assessment of the 900-MW Pangu hydroelectric dam of Chile's Biobio River has been criticized as "a propagandistic justification for the project." The environmental study characterized all downstream effects as "negligible, even though the proposed operating schedule as a peaking operation would cause daily channel dewatering during 137 days per year and violent fluctuations in stage, severely impacting the aquatic ecosystem. Potentially large downstream social and economic impacts were also ignored, even though the river flow serves as a drinking water source to 550,000 people, dilutes untreated domestic and industrial sewage

discharged into the river, and is an important source of irrigation (Meier, 1995). The upper Biobio is also considered one of the finest recreational whitewater rivers in the world.

Despite environmental impacts, dams have been built in large numbers worldwide, and continue to be built, because they also generate large economic and social benefits (Veltrop, 1992). Egypt's Aswan High Dam has been a focal point of environmental criticism for many years because of impacts such as the inundation of archaeological sites, increase in schistosomiasis infection, trapping of nutrients that affect fisheries in the Mediterranean, erosion of the delta coastline (Fig. 2.4), clogging of irrigation canals by aquatic weeds, riverbed degradation, and loss of annual silt and nutrient deposition on farmlands. However, Egypt has worked to solve the problems, and has reaped large benefits from the dam which annually produces 7 billion kWh of electricity, has eliminated disastrous floods, provided a stable irrigation supply that insulated Egypt from the disastrous 9-year (1979/80 to 1987/88) drought and resulting famine that affected sub-Saharan Africa, greatly increased agricultural productivity by changing from annual irrigation (one crop a year) to perennial irrigation (two crops a year), has improved navigation both above and below the dam, and has created a new fishery with 34,000 tons of annual harvest from the 6500-km<sup>2</sup> lake.

As much as we might like to eliminate dams and return rivers to pristine conditions, to do so would undermine the basis of modern hydraulic society. The next-best option is to:

- Minimize dam construction;
- Conduct research and monitoring necessary to document and understand environmental impacts and to develop viable mitigation strategies; and
- Decommission obsolete dams in a manner that is both cost-effective and environmentally sound.

Sediment management represents an important aspect of environmental impact assessment and mitigation work, and maximizing the sustainable benefits from existing structures though sediment management is one way to minimize the need for new dam construction in the future. In some cases dam construction can aid environmental protection. For example, the watershed above a dam may be acquired and designated as parkland in which development is strictly prohibited. This protects habitat for ecological purposes, while also protecting the reservoir from the high sediment loads that would result from deforestation.

Dam building is but one of many damaging activities that accompanies the spread of high-density human occupation into all environments. Pristine rivers will exist only to the extent that dam building is permanently prohibited within their watersheds. Thus, while it may be impractical to stop dam building, it is certainly appropriate that dam construction should be prohibited in certain rivers, and existing operations altered or dams removed from others.

### **18.2.2 Economic Quantification of Environmental Impacts**

Projects are evaluated by government agencies and lending institutions within the formal economic framework of a benefit-cost analysis. A project will be viable only when the present value of the project benefits exceeds the present value of its costs. A discount rate is applied to the projected stream of both benefits and costs over time, to determine the present value of each so that they may be compared.

Although the magnitude of environmental impacts may be difficult to quantify in economic terms, in the end these impacts must be compared against the project economic benefits. This makes it useful to quantify certain environmental impacts in economic terms. Methods used to quantify environmental and other indirect project impacts have been summarized by Dixon et al. (1989). Several approaches based on *market prices* may be used to establish an economic value for project impacts:

- *Productivity changes* can be used to evaluate a variety of on-site and off-site economic costs, such as changes in forestry, agricultural, and fisheries production.
- The *opportunity cost* approach is based on the concept that the cost of not using a site for a reservoir can be estimated by what has to be given up to avoid dam construction at that particular site. This may be paraphrased as "the cost of preservation." and is useful for evaluating ecological or cultural values that are difficult to express in monetary terms. It may be appropriate for the evaluation of options such as thermal versus hydropower or of alternative sites for the same type of facility.
- The *preventive expenditure* or *mitigation expenditure* approach seeks to establish the minimum value that people place on the environment, by establishing how much individuals or communities are willing to spend to prevent damage to the environment or to themselves.
- A *cost-effectiveness* approach may be used to evaluate projects which, in purely economic terms, may not have positive economic benefits. An example might be a rural water supply project in which water cost is subsidized for social or health reasons. The analysis seeks to select the least-cost alternative for achieving the stated goal. Selection should be based on both economic and environmental criteria.

Another approach that can be used to evaluate monetary impacts is the *cost-analysis technique*. The *replacement cost* approach estimates the cost required to replace productive assets damaged or eliminated by a proposed project. For instance, the damage to an instream fishery might be estimated from the cost of establishing mitigation measures, such as fish ladder and hatcheries. The cost of social displacement would be evaluated from resettlement costs. Unlike the preventive expenditure approach, which seeks to establish the cost of preventing damage, the replacement cost approach looks at the financial burden incurred in repairing the damage. This approach assumes that whatever is damaged can be replaced, at a cost, which is not necessarily true. For example, hatchery-bred fish are considered genetically inferior to wild populations. The *infrastructure relocation cost* approach is a variation of the replacement cost approach. It may be used to evaluate the cost of relocating infrastructure such as intakes or roads which may be affected by dam construction.

There may be no tangible value or market price associated with important environmental parameters, such as clean air, visual aesthetics, and recreational quality. In this case it is necessary to use *surrogate market prices*, using the market price for another good or service to estimate the value of the nonmarket quality of the environment:

- The *land value approach* is based on the concept of using the variation in land prices as the basis for valuation of a nonmarket commodity such as a visual amenity (e.g., lakefront versus interior house lots).
- *Travel cost* may be used to evaluate the value of an amenity, based on the concept that the true price paid by the consumer consists of the ticket price (which may be zero) plus the expense incurred to reach and use the facility. This approach has been extensively used in developed countries to evaluate recreational goods and services such as parklands. Thus, the economic value

of a site such as the Grand Canyon (once a proposed dam site) is measured not by the gate receipts of the park, but by the much larger cost to reach it.

Despite economic analysis, many types of environmental impacts remain inherently nonquantifiable in dollar terms. As discussed in Chap. 2, a discount rate of around 7 percent will produce a negligible value for virtually any economic impact more than 50 years in the future. Thus, economic analysis is totally unsuited to the evaluation of long-term issues concerning non-replaceable resources, such as the long-term survival of species and ecosystems, or the welfare of future human generations. Also, environmental effects are often "external" to many economic decisions because they do not directly affect either buyer or seller in a significant manner, but are borne by third parties. Society has expressed its value for environmental protection through the political system (legislation and regulatory standards) because it has not been adequately expressed through economic markets.

### 18.2.3 Hydroperiod Modification

One of the primary purposes of dams is to modify hydroperiod, and this is also one of the greatest instruments of environmental impact. Petts (1984) defined five types of hydroperiod modifications caused by dams:

**1. Reduced peak discharges.** From the aspect of channel morphology, the most significant hydrologic changes associated with dams is the reduction in peak discharge, which inevitably occurs below an impounding reservoir whether a flood control pool is provided or not. In a study of 21 dams in the United States, Williams and Wolman (1984) found that peak discharges were reduced from 3 to 91 percent of the pre-impoundment peaks. The reduction in peak discharge along the Colorado River is illustrated in Fig. 18.1.

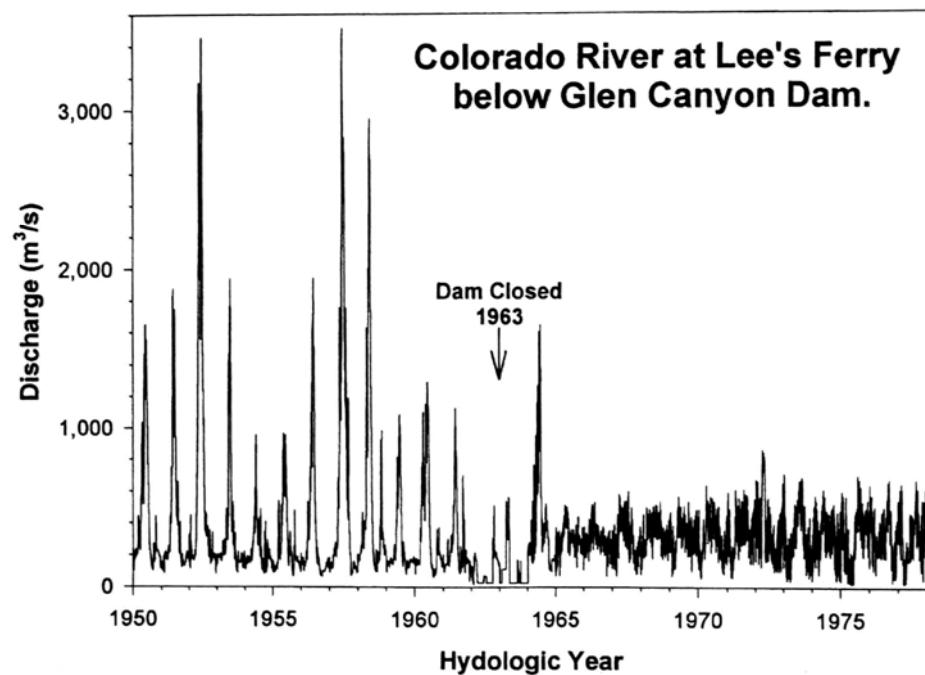


**Figure 18.1** Mean daily flow of the Colorado River at Lee's Ferry, reflecting the impact of constructing Glen Canyon Dam upstream (USGS data published on CD-ROM by EarthInfo).

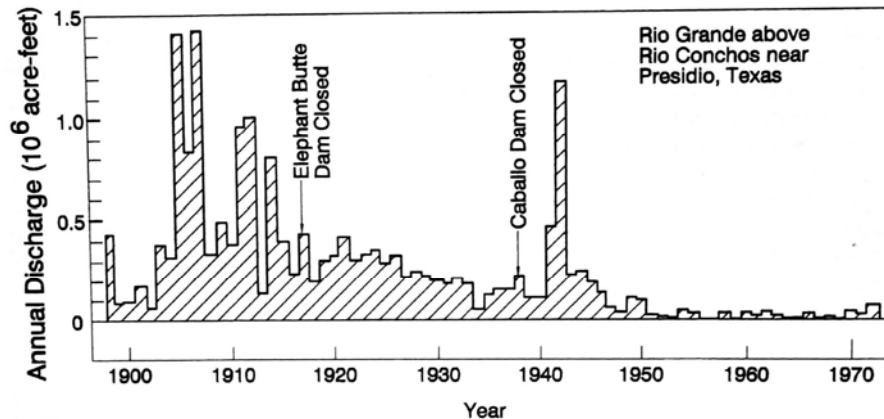


**FIGURE 18.2** Stream flow reduction in the Rio Grande near Presidio, Texas, due to upstream dam construction and increasing irrigation diversions (Collier *et al.*, 1995).

**2. Reduction in total runoff.** Dams which divert water to offstream uses will reduce the total downstream flow, as illustrated in Fig. 18.2. Other well-known examples are the diversion of most Colorado River water to irrigation and urban uses, and the diversion of water to irrigation which has caused desiccation of the Aral Sea. Hydropower production does not reduce total flow, but may divert flow into another basin where hydroturbines are located, or may divert water around the reach of the river between the dam and the power plant. A flood control reservoir will not reduce total streamflow.

**3. Reduced seasonal flow variability.** Reservoirs often convert highly variable natural flows into more stable flows lacking significant seasonal variation, as illustrated by the data from the Colorado River in Fig. 18.1.

**4. Imposition of flow pulses.** Hydropower reservoirs operated for generation of peak power can produce pulsed flows below the dam (Fig. 18.3). Pulsed flows can increase bank erosion, can represent a life-threatening situation for anglers and others in the river, and can be highly detrimental to aquatic species. However, daily releases can optimize conditions for recreational activities such as whitewater rafting and kayaking.

**5. Altered seasonal timing of downstream releases.** Reservoirs can significantly alter the timing of flows along a river. Hydropower reservoirs, for example, may capture spring snowmelt and release this water during the summer months, producing a seasonal flow pattern unlike the natural condition.

All dams produce at least some of these hydrologic changes in varying degrees.

One of the river systems affected by dams is the Colorado River in the Grand Canyon, dammed by upstream construction of Glen Canyon Dam in 1966. To combat the deleterious effects of flow regulation on the below-dam ecosystem and channel morphology, an experimental 1275 m/s flood was initiated in March 1996 by releases from Glen Canyon Dam, to simulate pre-impoundment hydrologic processes along the Grand Canyon reach below the dam. The controlled flood release had the following objectives: disrupt life cycles of nonnative fish; rejuvenate backwater habitats for native fishes; redeposit sand bars at higher elevations, followed by a decreasing erosion rate, to preserve and restore camping beaches used by river rafters; reduce near-shore vegetation; and provide water to old high-water zone vegetation. As constraints, it was desired to avoid significant impacts to the trout fishery, endangered species, cultural resources, and economic conditions. Initial analysis of the

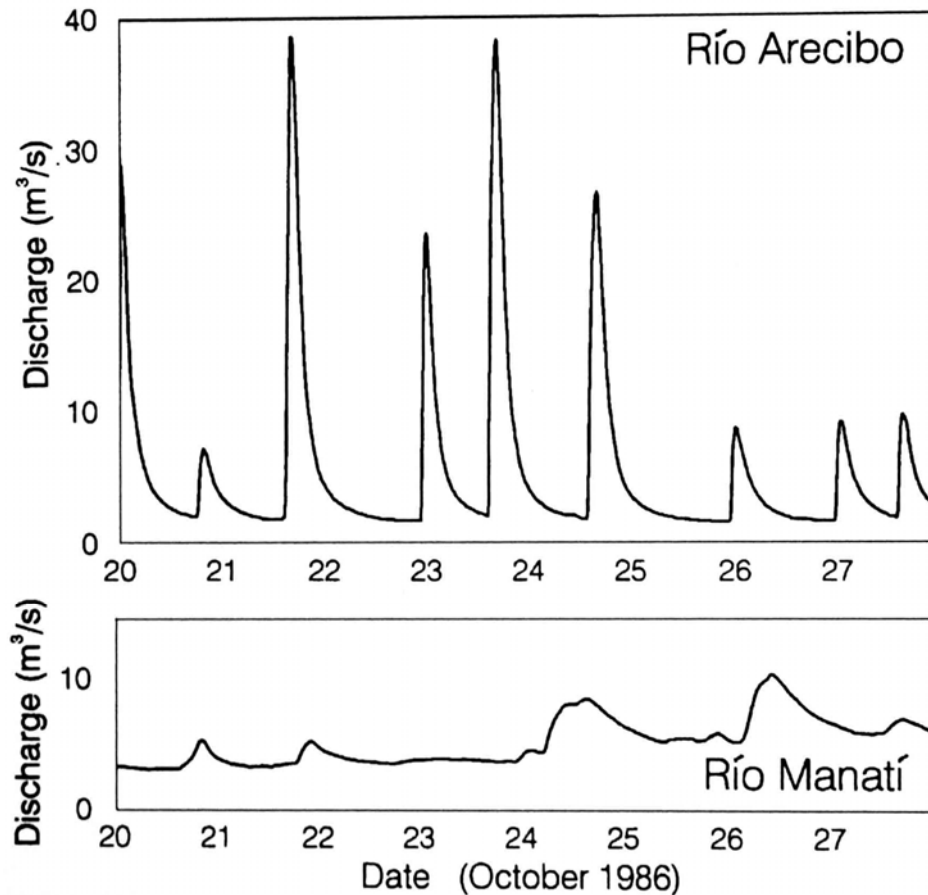


**FIGURE 18.3** Daily pulsed flow below the Dos Bocas hydropower dam on Río Arecibo as compared to the adjacent and similar but free-flowing Río Manatí, both on Puerto Rico's north coast. Base flow at the Arecibo gage station is maintained by groundwater seepage from the limestone aquifer (*constructed from USGS data*).

results indicate that the release was successful in meeting its objectives. Information on "Grand Canyon Environmental Studies" is posted on the Internet by the U.S. Geological Survey (<http://www.gcmrc.gov/>) and may be consulted for information on the many environmental studies that are being conducted related to the management of Glen Canyon Dam.

#### 18.2.4 Environmental Consequences of Sediment and Its Management

Dams control sediment movement along impounded rivers, and the operation of dams and reservoirs can itself be heavily influenced by sediment management problems. Major issues potentially related to sedimentation and sediment management are summarized in Table 18.1.

The environmental impacts of sediment management are determined by comparing the proposed condition against some baseline condition. Since the river reach below a dam represents an environment substantially altered from natural conditions, it is necessary to determine whether sediment management impacts should be

**TABLE 18.1** Environmental Issues Related to Sediment and Its Management

Type of impact	Description
Within- reservoir impacts	
Loss of storage capacity	Reduction in firm yield causing water rationing, reduced hydropower and flood control benefits.
Contaminated sediment	Reservoir can trap and bury contaminated sediment, effectively removing it from the biotic environment. Contaminated sediments can cause lake quality to deteriorate. Sediment removal can remobilize contaminated sediment.
Organic sediment deposition	Oxygen demand exerted by organic sediment contributed from upstream or primary producers within a lake can make bottom waters anaerobic.
Turbidity	Turbid water reduces depth of photic zone, decreases primary productivity. Reduced visibility interferes with fish feeding. Reduced clarity makes lake as aesthetically unpleasant for recreation.
Navigation	Sediment fills navigation channels and locks. Interferes with boating, fishing, and marina access
Wildlife	If sedimented areas become wetlands, significant wildlife benefits may occur. Fine sediment deposition can reduce nesting habitat for fish.
Air pollution	Exposure of fine sediment to winds during drawdown can create dust storms.
Upstream of reservoir	
Deposition above pool elevation	Upstream deposition increases flood levels; reduces navigational clearance below bridges; causes water table to rise inducing soil waterlogging and salinization; and can increase evaporative losses. Deposition above pool level reduces the rate of storage loss by reducing sedimentation in the active pool
Downstream of dam	
Reduced coarse sediment load	Riverbed may incise and accelerate bank erosion. Lowered base level may initiate erosion along tributary channels and desiccate wetlands. Riverbed will coarsen and may become unsuitable for spawning. Bridge, pier, and river training works may be undermined, shoreline structures may be threatened, and deposits of contaminated river sediment may be remobilized.
Lower flood peaks	Reduced peak discharge can lead to reduction in channel size and vegetative encroachment, reducing downstream channel conveyance. Reduction of char net capacity will offset the effectiveness of upstream flood control reservoirs
Reduced fine sediment load	Reduced sedimentation and dredging in navigational channels. Increased erosion along riparian lands, loss of sediment-dependent wetlands, reduced nutrient and sediment inputs to floodplains and riparian wetlands, and loss of delta and ocean shoreline replenished by river sediments. Downstream water clarity benefits water-based recreation and sediment-sensitive species, including coastal ecosystem such as coral reefs.
Sediment release	Timing and magnitude of sediment release may influence most types of downstream environmental, social, and economic activities associated with the river.

*Source:* Modified from Qum (1982) and Scheuerlein (1995).

compared against conditions in the pre-impoundment river or the modified post-impoundment river. The selection of a baseline condition for impact assessment will have considerable bearing on the methodology and results of impact analysis, and should be considered carefully.

Increased levels of suspended sediment impact downstream aquatic ecosystems. Periphyton, algal growth on submerged surfaces, is the base of the aquatic food chain in many streams, and many benthic invertebrates graze periphyton. Increased suspended sediment levels reduces light penetration and photosynthetic activity. High levels of suspended sediment in conjunction with high discharge can scour algae off streambed substrates. Grazing benthic invertebrates can be impacted by reduced food supply (periphyton), and filter feeders are affected because suspended sediment can clog feeding structures and reduce food intake, thereby stressing or killing the organisms. Benthic invertebrates may also be damaged by scour, and all benthic organisms can be smothered if a significant amount of sediment is deposited on the stream bottom. Suspended sediment affect salmonid fishes by: (1) stressing or killing living fish, (2) interfering with development of eggs or larvae, (3) modifying movement and migration, and (4) reducing the food supply. The stress to which aquatic organisms are subjected is related to both the suspended sediment concentration and the duration of exposure (Newcombe and MacDonald, 1991).

### 18.2.5 Morphologic Impact Downstream of Dams

Stream morphology below dams is affected by both the interruption of sediment transport and the reduction in peak discharge. The typical pattern is for the streambed to incise and become armored below the dam in response to the elimination of bed material load. The zone immediately below the spillway or outlet works may be scoured to bedrock (Fig. 18.4), and structures on alluvial material below dams may



**Figure 18.4.** Photograph of area of scoured bedrock immediately downstream of Nizam Sagar Dam, Andhra Pradesh, India (G.Morris).



**FIGURE 18.5** Streambed degradation and resultant bridge scour about 2.5 km below Patillas Dam, Puerto Rico (*G. Morris*).

Be subject to damage by scour (Fig. 18.5). Armoring and degradation can extend for tens or hundreds of kilometers downstream as the sediment-deficient river entrains material from the streambed and banks. The armored bed below Dos Bocas Dam is shown in Fig. 18.6. Bed degradation extended 300 km below Sariyar Dam in Turkey (Simons and Senturk, 1992). Sediment release by pass-through or reservoir flushing will not counteract riverbed degradation unless it discharges sediment large enough to constitute bed material in the downstream reach.

The suspended sediment load along the Nile in different years illustrates the changes along this formerly sediment-laden sand-bed river resulting from dam construction. Under pre-impoundment conditions, the river deposited sediment moving downstream during the annual flood. After dam construction, year-round releases of clear water resulted in sediment loads that were very low, but increased moving downstream as the clear water entrained sediment from bed and banks (Fig. 18.7). Degradation along the Nile has been limited to less than a meter in the 27 years following dam construction because of factors such as the reduction in peak flood discharge, armoring, and the presence of several barrages along the length of the river which provide grade control (Hammad, 1972; Moattassem and Abdelbary, 1993). The amount of bed degradation along the Nile has been lower than predicted by a number of different researchers (Shalash, 1983). In other cases the rate and amount of degradation below a dam can be significant.

The impacts of dam construction on stream channels below dams were analyzed by Williams and Wolman (1984) on the basis of pre- and post-impoundment measurements at 287 cross sections below 21 dams on alluvial rivers, mostly located in the semiarid area of the western United States. Bed degradation varied from negligible to about 7.5 m at the studied cross sections, with most degradation occurring during the first 10 or 20 years after dam closure. Trends in channel degradation at streamgage stations are illustrated in Fig. 18.8, showing that channel changes proceed irregularly over time at some sites, and proceed regularly at

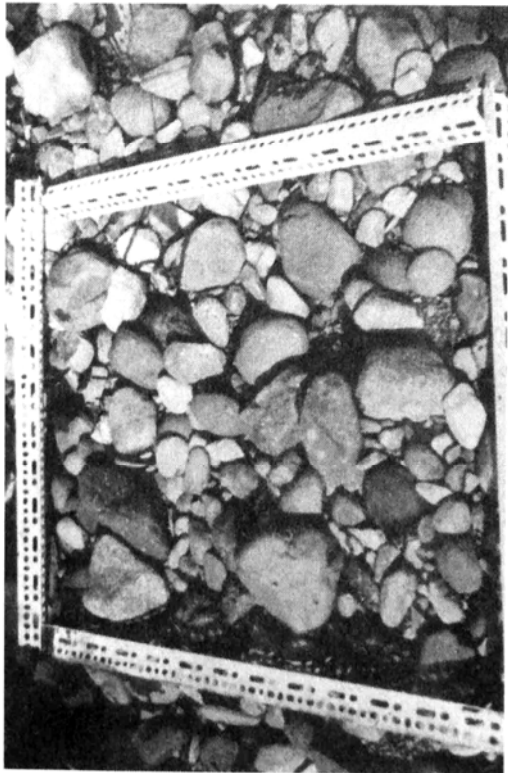
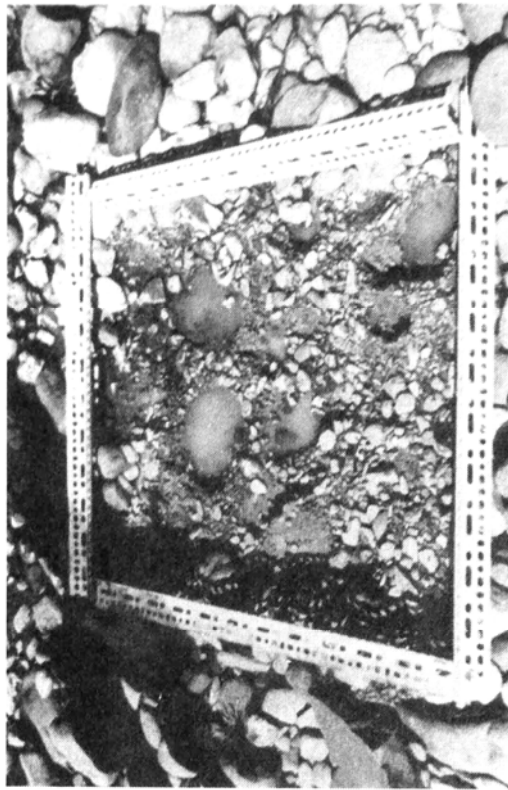


**FIGURE 18.6** Removal of surface armor layer to reveal finer underlying sediment in Rio Arecibo, Puerto Rico, about 12 river kilometers below Dos Bocas Dam (*G. Morris*).

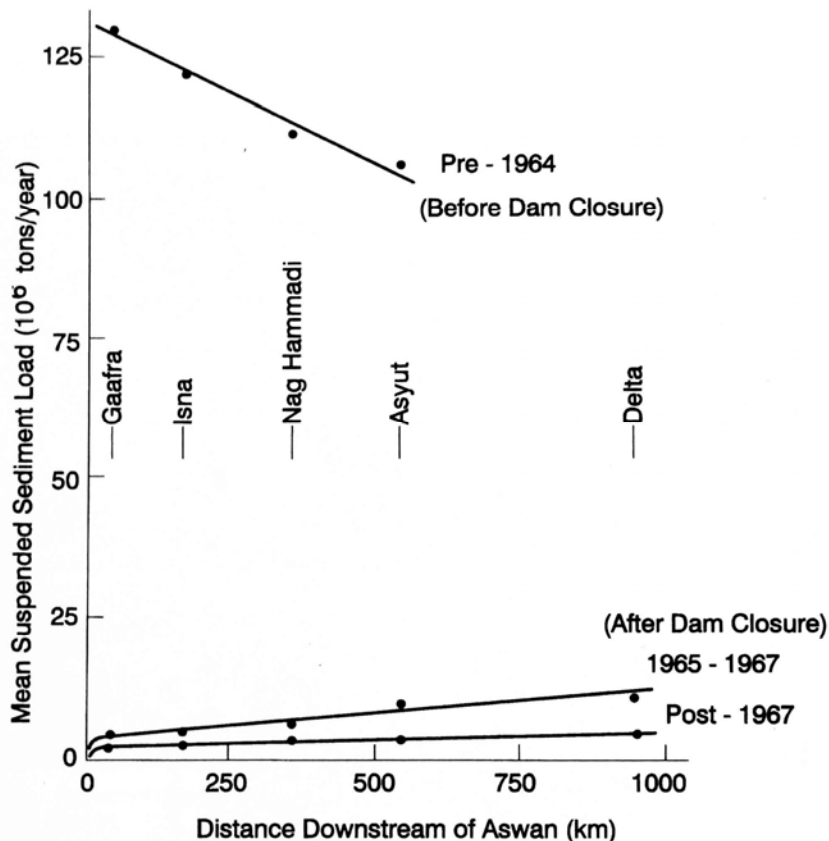


**FIGURE 18.7** Response of the Nile River to sediment trapping at the Aswan High Dam. (adapted from Moattassem and Abdelbary, 1993). After dam construction the suspended sediment load transported by the river was dramatically reduced, and the river's sediment load now gradually increases moving downstream because of sediment entrainment from the riverbed and banks. Sediment entrainment from the riverbed declines over time due to armoring. The Nile has no tributary inflow downstream of Aswan.

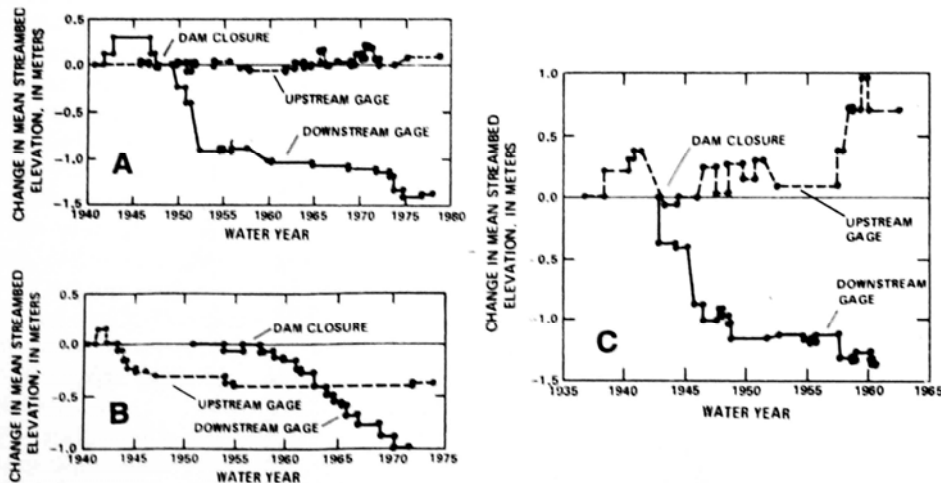


**FIGURE 18.8** Timewise rate of streambed degradation below dams, as compared to streambed elevations above the dam. The location of the downstream gage is given. (a) Smoky Hill River 1.3 km below Kanopolis Darn, Kansas. (b) Chattahoochee River 4 km below Buford Dam, Georgia. (c) Red River 4.5 km below Denison Dam, Oklahoma. (Williams and Wolman, 1984.)

others. Channel changes at gages both upstream and downstream of the reservoir were plotted to separate dam effects from any underlying trends.

Streambed degradation will be limited by armoring, reduced peak discharges, sediment inflow from tributaries, and grade control points along the bed such as bars, bedrock, or artificial sills and barrages. The river below a dam will evolve toward a new equilibrium condition, typically influenced by more than one of these factors. The reduction in peak discharge not only reduces the rate of transport, thereby prolonging the period of channel adjustment, but it will also reduce the size of sediment required to armor the bed. The bed will degrade until enough coarse material has been uncovered to stabilize the surface for the post-impoundment slope and discharge conditions. Mathematical modeling is the most appropriate method for evaluating these parameters and their impact on the evolution of the streambed below the dam.

In some cases, coarse sediment constituting as little as 1 percent of the bed sediment may effectively control the bed profile, as in the Colorado River below Glen Canyon Dam where the profile is controlled by cobble bars (Pemberton, 1976). For example, Crystal Rapid in the Grand Canyon is created by a field of boulders and smaller debris discharged by a small but steep tributary during storms. At high flows (1600 m<sup>3</sup>/s) this formation produces gigantic standing waves and an adrenalin rush for rafters.

Channel width can increase, decrease, or remain constant below the dam. In the 21 rivers studied by Williams and Wolman, channel width decreased by as much as 90 percent and increased as much as 100 percent at different cross sections. Channels below dams are often affected by the encroachment of vegetation when large channel-forming discharges are reduced or eliminated. Large flows are necessary to scour sediments and vegetation from channels, and when flood flows are reduced the channel width may also be expected to reduce in size, other things being equal. Encroaching vegetation can block part of the channel resulting in reduced channel conveyance, faster flow velocities in the channel thalweg, and greater channel depth. On the Republican River in Nebraska, vegetation decreased the channel capacity by 50 to 60 percent in some reaches. Examples of vegetative encroachment below dams are illustrated in Fig. 18.9. The period of low flows when a reservoir is initially filling may be particularly critical, since pioneer vegetation can rapidly encroach onto bars and "lock" a formerly braided stream into a fixed channel (Lagasse, 1980).

Ligon et al, (1995) described the reduction of the braided reaches of the McKenzie River in Oregon as a result of flow regulation by two Corps of Engineer dams, which have reduced peak discharges by over 50 percent. Channel simplification and stabilization, with vegetative encroachment, has substantially reduced the area of gravels suitable for salmon spawning. It has also reduced the area of sloughs, backwaters, and traces of former channels created by meander cutoffs, habitat required for rearing juveniles.

In the rivers studied by Williams and Wolman, the bed material initially coarsened as degradation proceeded, but this pattern could change during later years. Armoring has occurred in the reach immediately below main stem dams on the Missouri River, and sediment size along the Mississippi River was also expected to coarsen as a result of upstream dam construction, especially from construction of the dams along the Missouri in the 1950s, its greatest sediment contributor. However, contrary to expectations, 505 samples at 417 locations along the river, taken by techniques and at locations duplicating the extensive sampling performed in 1932, showed that thalweg sediments in 1989 were somewhat finer than in 1932 (Queen et al., 1991).

Although less common, the riverbed below a dam or barrage can also aggrade as a result of dam construction. This can occur when a large sediment load is passed

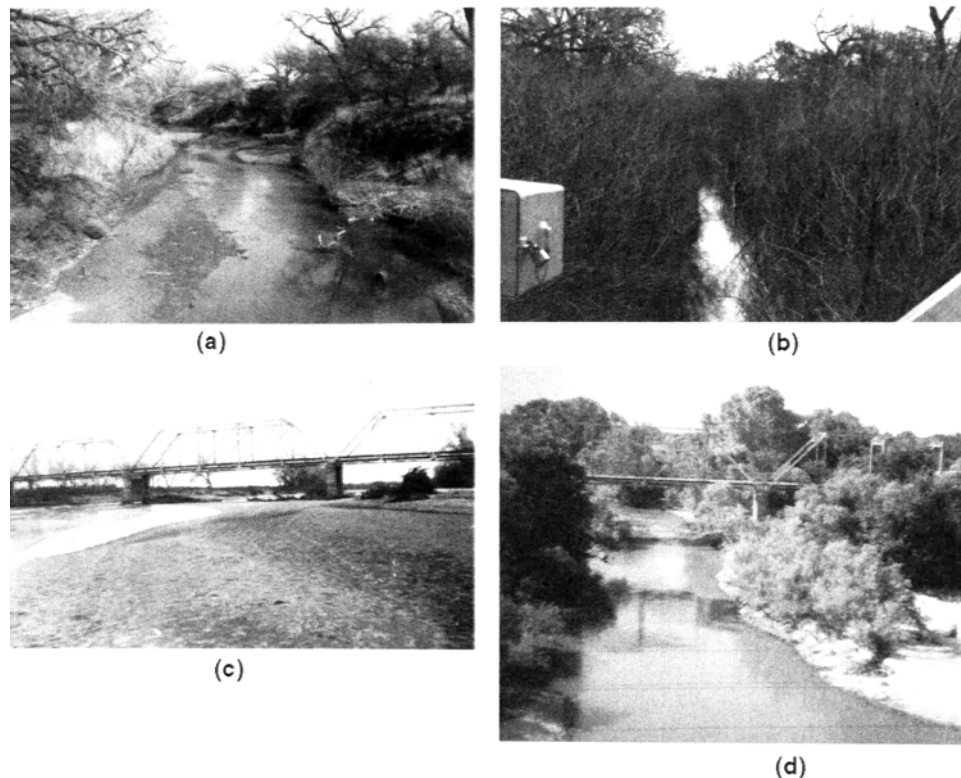


**FIGURE 18.9** Encroachment of vegetation into stream channels below dams as a result of eliminating flood peaks which maintained the channel. Washita River 1.4 km below Foss Dam, Oklahoma (a) in February 1950, and (b) in February 1970. Foss Dam was closed in 1961. North Canadian River 0.8 km below Contort Dam, Oklahoma (c) in 1938, and (d) in 1980. Canton Dam was closed in 1948. (Witrams and Wonnou, 1984)

downstream but much of the water is diverted out of the river, or if a high concentration flow is released at a low discharge rate as discussed in the Sanmenxia case study (Sec. 24.9). Deposition can also occur when tributaries below the dam deliver large quantities of sediment, or large grain sizes, to a river which has reduced discharge because of upstream dam construction. For example, deltaic deposits have been formed where tributaries and arroyos deliver coarse sediment to the Río Grande below Cochiti Dam, in northern New Mexico, because the regulated post-impoundment discharges are generally not capable of transporting the coarser sediment load and volume delivered to the channel below the dam. The coarsening of the surface bed material along the Río Grande following construction of Cochiti Dam is illustrated in Fig. 18.10. Farther downstream, below Elephant Butte Reservoir, flow in the Río Grande is inadequate to transport even fine sediment, and the river channel has gradually filled in (Fig. 18.11).

### 18.3 ENVIRONMENTAL IMPACTS OF SEDIMENT ROUTING

Sediment routing techniques (Chap. 9) can be used to mimic natural sediment flows along a river while producing adverse environmental impacts that are small or negligible compared to techniques such as emptying and flushing. Although off-stream reservoirs

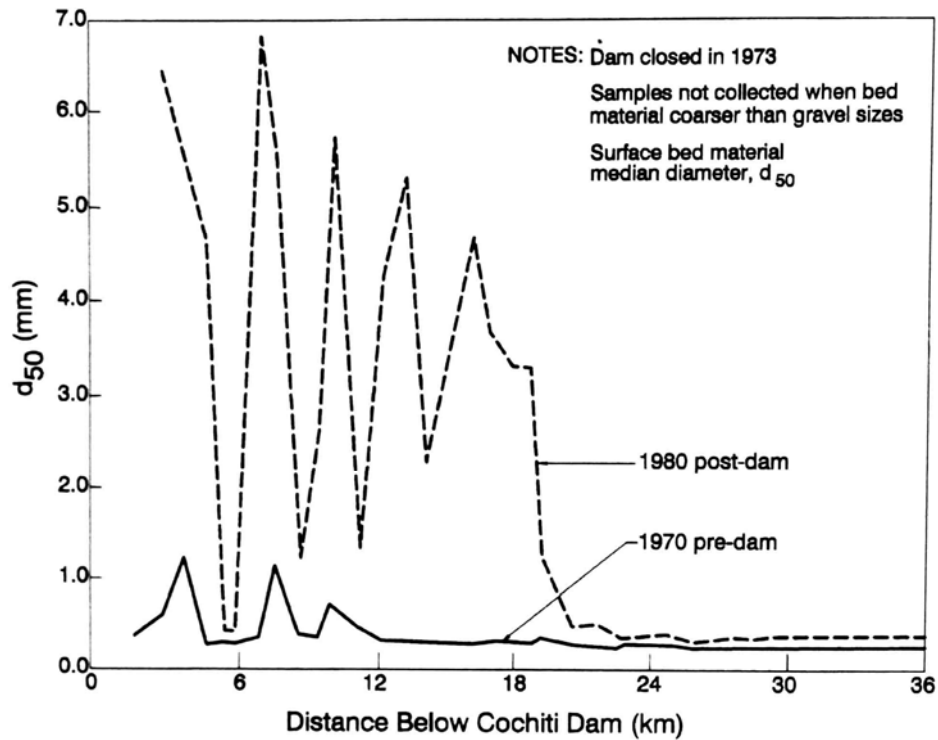


**FIGURE 18.10** Coarsening of bed material in Río Grande in northern New Mexico below Cochiti dam resulting from trapping of sediment and reduction of peak flows by the dam, and the continued delivery of coarse sediment by steep tributary arroyos along the river. (Lagasse, 1980.)

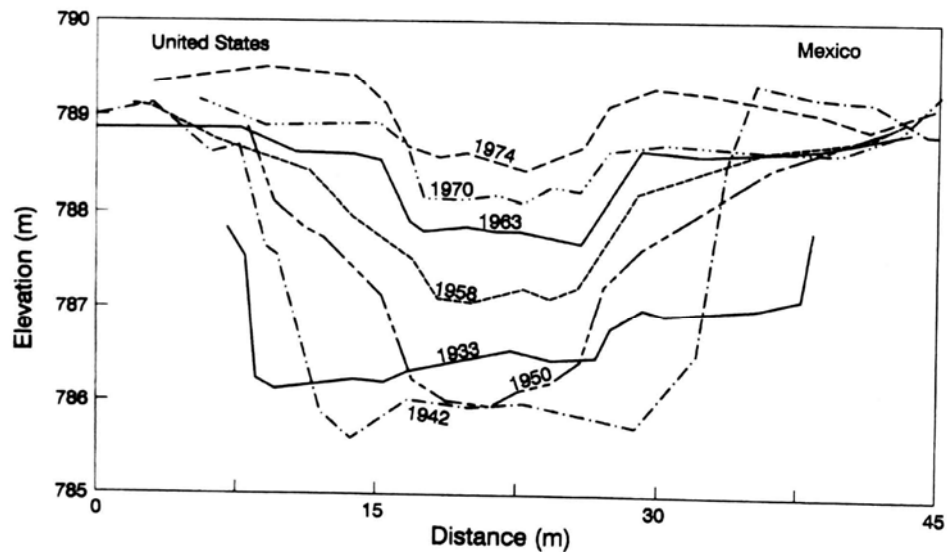


**FIGURE 18.11** Narrowing and aggradation of Río Grande at Presidio, Texas, as a result of the dramatic reduction in flow shown in Fig. 18.2, combined with the continued input of sediment from tributary arroyos. (Collier et al., 1995.)

and sediment pass-through are well-adapted to reproducing many aspects of the natural pattern of sediment movement, they are not without potential impacts.

### **8.3.1 Venting Turbid Density Currents**

Passing the inflow of fine sediment through a reservoir as a turbid density current, which is vented through the dam, can produce suspended sediment concentration below the dam similar to that in the upstream inflow. In general this may be considered an environmentally benign strategy since the suspended sediment concentration and timing will be correlated to conditions above the pool. Because the turbidity current normally passes through the reservoir in a relatively short period of time, the vented current may remain oxygenated even though water within the reservoir hypolimnion is anaerobic (recall Fig. 4.6). Nevertheless several limitations and potential problems are associated with this technique.

Turbidity currents cannot transport coarse sediment under normal conditions, and to release of a turbidity current will not solve downstream problems caused by the lack of bed material. Turbid water may enter a reservoir during floods large enough to mobilize and clean stream gravels. However, the turbidity current may be vented from the dam at a discharge too low to mobilize downstream gravels. Repeated releases of turbid water without flows adequate to mobilize and flush gravels will lead to the clogging of spawning gravels and water supply infiltration galleries. This can be mitigated by releasing clear water at a discharge sufficient to mobilize and cleanse gravels. If venting is initiated at a site where it was not previously performed, the increase in turbidity as compared to the established post-impoundment conditions below the dam may be considered an environmental problem, adversely impacting users and aquatic ecosystems adapted to the clear-water condition below the dam

### **18.3.2 Off-Stream Reservoir**

A river intake diverts flow into an off-stream reservoir, while allowing floods to pass the intake unimpeded. This type of reservoir maintains the continuity of bed material transport along the river as well as the peak discharges below the dam. It also presents a lesser migration barrier since the intake may consist of a low structure forming a pool of quiescent water small enough that it will neither disorient migrating species nor support a large population of predators. The intake structure should be designed to minimize entrainment of migrating species, depending on the characteristics of each river and the species of concern. For instance, river shrimp in the Caribbean use estuaries as a nursery area, and the juveniles migrate upstream along freshwater streams where they will mature and reproduce. The migrating juveniles, about 1 cm in length, swim along the margins of streams where both current and predation is reduced. An intake withdrawing water from one side of the stream will entrain and kill half of the migrants. In this environment an intake structure should be located at the center of the stream to prevent entrainment of the migrating shrimp.

### **18.3.3 Seasonally Empty Reservoir**

A reservoir may be operated to supply water seasonally, remaining empty during the first part of the flood season and allowing natural flood flows to scour and release sediment. A single-purpose flood detention reservoir will be empty almost continuously, whereas an irrigation reservoir may be empty for only a few weeks each year. This wide range in possible operating conditions makes it difficult to make generalizations about the impacts of these types of structures. A normally impounded reservoir having large low-

level outlets and empty long enough to pass significant floods through the empty impoundment with little attenuation (thereby preserving the transport of bed material), may have relatively small impacts. Conversely, a normally empty flood control reservoir which greatly attenuates downstream peak flows may trap a significant amount of bed material and affect below-dam morphology. An irrigation reservoir on a sediment-laden stream that is emptied for only a few weeks per year can produce impacts very similar to sediment flushing.

A seasonally empty reservoir should be expected to produce water quality patterns similar to any other reservoir emptying, but the magnitude of the downstream impacts may be minimized by several factors: (1) the reservoir will trap less sediment during the impounding period; (2) it can be emptied during a wet period when a large flow is available for dilution and transport; and (3) anoxic bottom conditions may never occur, thereby improving the quality of released bottom water.

#### 18.3.4 Sediment Routing on Isar River

Environmental impacts from sediment routing may be caused not only by sediment release, but also by contaminants released from the interstitial water in sediment deposits. Two important contaminants associated with the discharge of reservoir sediments are ammonia, which is lethal to aquatic life at high concentrations, and the biological and chemical oxygen demand exerted by organic material and reduced chemical forms. Westrich and Al-Zoubi (1992) describe the design and environmental mitigation strategy for sediment routing through a low (7.6 m) hydroelectric dam on the Isar River in the alpine area of southern Germany. This reservoir is about 150 m wide and 1800 m long and the original riverbed slope was about 2.5 percent.

During 30 years of impounding operations, the 0.83-Mm<sup>3</sup> reservoir lost 43 percent of its capacity because of the accumulation of sediments ranging in size from silts to gravels. Streambed degradation below the dam lowered groundwater levels and desiccated riparian wetlands in national parklands. It was desired to undertake sediment routing to reestablish the pre-dam sediment transport pattern, but it was not desired to flush a significant amount of the accumulated sediment out of the reservoir. Analysis of sediments and pore water indicated the presence of several agricultural chemicals, but the most critical limiting factors were considered to be high ammonium concentration (20 to 40 mg/L) in the interstitial water, the need to limit the increase in suspended sediment concentration across the reservoir to not more than 5 g/L, and potentially high oxygen demand by bacterial decomposition of organics plus the chemical oxidation of reduced FE-II and sulfide compounds found in the sediments. The rapid first-phase oxygen consumption rate in the water released from the dam was to be limited to 0.4 mg O<sub>2</sub>/L within 2 hours. A minimum pore water dilution factor of 100 was adopted to control oxygen and ammonia levels. Surface sediment deposits in some areas of the impounded reach consisted of silt size material that could be readily resuspended, and it was also necessary to ensure that bed shear stress in these areas remained low enough to minimize resuspension.

The objective was to approximately reestablish the morphology of the original river channel along the length of the sediment deposits above the dam, enabling floods to transport sediments along this channel without disturbing floodplain sediments. The strategy adopted was to dredge (rather than hydraulically scour) a main channel through the deposits. During flood periods, water level at the dam would be lowered about 2.5 m to enhance transport capacity through the dredged channel, while simultaneously reducing flow velocity and transport capacity over the submerged floodplain due to shallowing of the water depth. To determine the alignment of the channel, the grain size  $d_{50}$  isolines were interpreted as transport capacity isolines within the reservoir,

and the dredged channel was located along the line of highest transport capacity as identified by the largest-diameter material in the sediment deposits. This had two effects: because the channel was dredged along the line of coarser sediment deposits, it reduced the potential for erosion and entrainment of fines; it also placed the channel along the line of maximum flow already developed within the impounded reach. The channel was designed to gradually increase bed shear stress in the downstream direction. It was dredged as a 10 m wide trapezoidal section with a bed slope of 2.5 percent to match the original bed slope of the river, and 4:1 (horizontal:vertical) side slopes. The design discharge was  $300 \text{ m}^3/\text{s}$ . A flood of  $228 \text{ m}^3/\text{s}$  was passed through the completed system in June 1991 during a 12-h 2.5-m drawdown. Suspended sediment downstream of the dam increased by only  $2 \text{ g/L}$ , and dissolved oxygen levels remained near saturation. However, some erosion of the bed occurred as a result of this event (Fig. 18.12) and about  $26,000 \text{ m}^3$  of sediment was transported out of the reservoir.

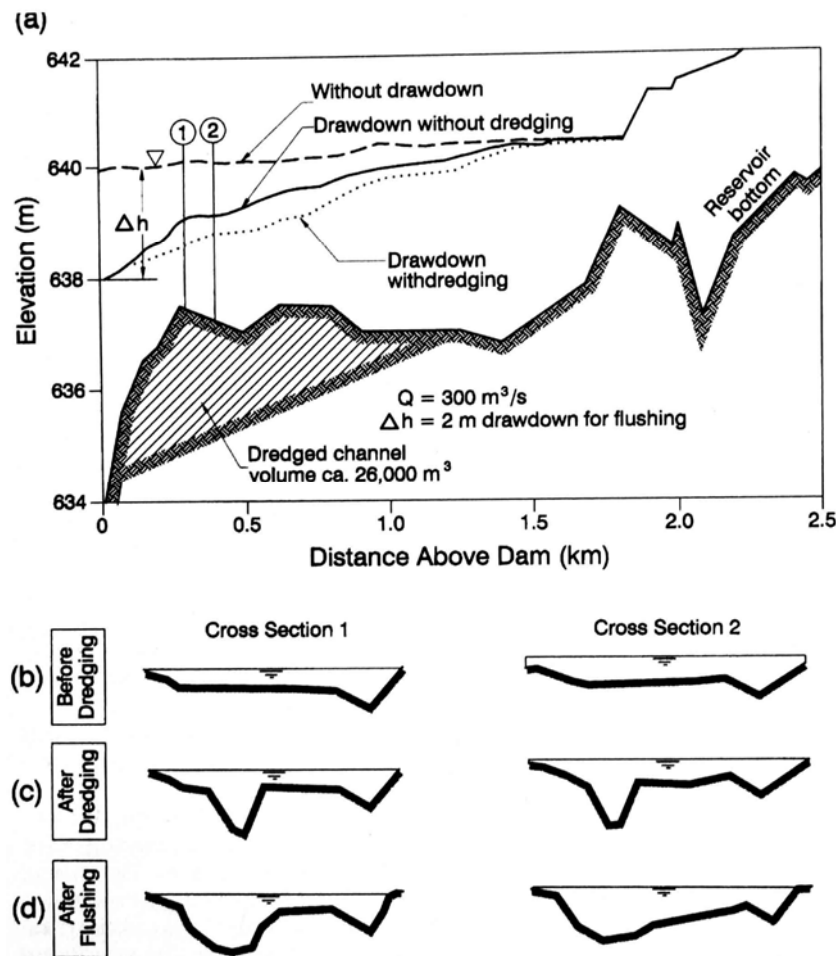


**FIGURE 18.12** Channel for routing sediment through Isar River Reservoir, Germany. (a) Longitudinal profile of reservoir showing the effect of drawdown on water surface profiles, and pre- and post-dredging thalweg and water surface profiles. (b) Pre-flushing cross section. (c) Flushing channel excavated by dredging. (d) Dredged channel modified by the first flushing event. (Modified from Westrich and Al-Zoubi, 1992.)

## 18.4 RESERVOIR EMPTYING AND FLUSHING

---

The largest and most intractable downstream environmental impacts associated with sediment release from reservoirs are caused by reservoir emptying and flushing. The types of impacts described in this section will occur any time a reservoir is emptied, but with wide differences in severity. Material in this section relies heavily on experience in France and Switzerland as reported by Electricité de France (EDF, 1995), Gerster and Rey (1994), and discussions with Petitjean and Bouchard (1995).

There are two opposing schools of thought on the subject of reservoir emptying. One proposes that downstream environmental impacts should be minimized by keeping the trapped sediment within the pool. While this is feasible initially, sediment cannot accumulate indefinitely and at some point in time sediment must be discharged or removed by dredging. The opposing school of thought is to allow sediments to escape during emptying, but to mitigate deleterious effects.

### 18.4.1 Water Quality during Reservoir Emptying

Probably the most comprehensive analysis of the downstream impacts of reservoir emptying has been undertaken by Electricité de France, which operates about 500 dams and has published guidelines for reservoir emptying (Electricité de France, 1995). French law requires reservoir emptying at larger dams for safety inspection at 10-year intervals, resulting in 10 to 15 emptyings annually at EDF facilities. Even though the objective of these emptyings is not to preserve reservoir capacity, bottom sediments are flushed out as an inevitable consequence of the emptying, and sediment management techniques are employed. French reservoirs typically do not have large amounts of sediment accumulation; sediment concentrations and downstream loadings can be much higher at reservoirs with high sediment loads, or many decades of accumulation. When large volumes of sediment are to be removed by flushing, there may be no practical method for mitigating downstream impacts except by timing the flushing release.

Monitoring of French reservoirs by EDF revealed the characteristic sequence of water quality changes illustrated in Fig. 18.13 and described below.

1. Opening of the bottom gate releases sediment immediately in front of the outlet, causing a relatively small perturbation in the quality of the released water as sediments are eroded to create a scour hole. Sediment that accumulates in front of the gate will typically be transported as wash load through the downstream channel by the higher quality water that continues to be released after the initial scouring.

2. Water quality remains steady or changes gradually until the end of the emptying process. During this period, deposits eroded from the channel scoured in the upper area of the reservoir are transported toward the dam, but little sediment is released.

3. At the final stage of emptying, the establishment of riverine flow along the length of the reservoir and through the bottom outlet causes dramatic and rapid changes in water quality as bottom muds are washed out of the empty pool. Suspended solids concentrations are measured in tens of grams per liter, dissolved oxygen levels are depressed and may reach zero as anaerobic bottom water is released and the organic muds exert an oxygen demand, and ammonia concentration increases. This drainage of bottom muds represents the most severe water quality problem posed by emptying, and peak suspended sediment concentrations on the order of 100 g/L can occur (Petitjean and Bouchard, 1995). The concentration and duration of the release depend on factors such as the amount and characteristics of the sediment deposits and the discharge rate.

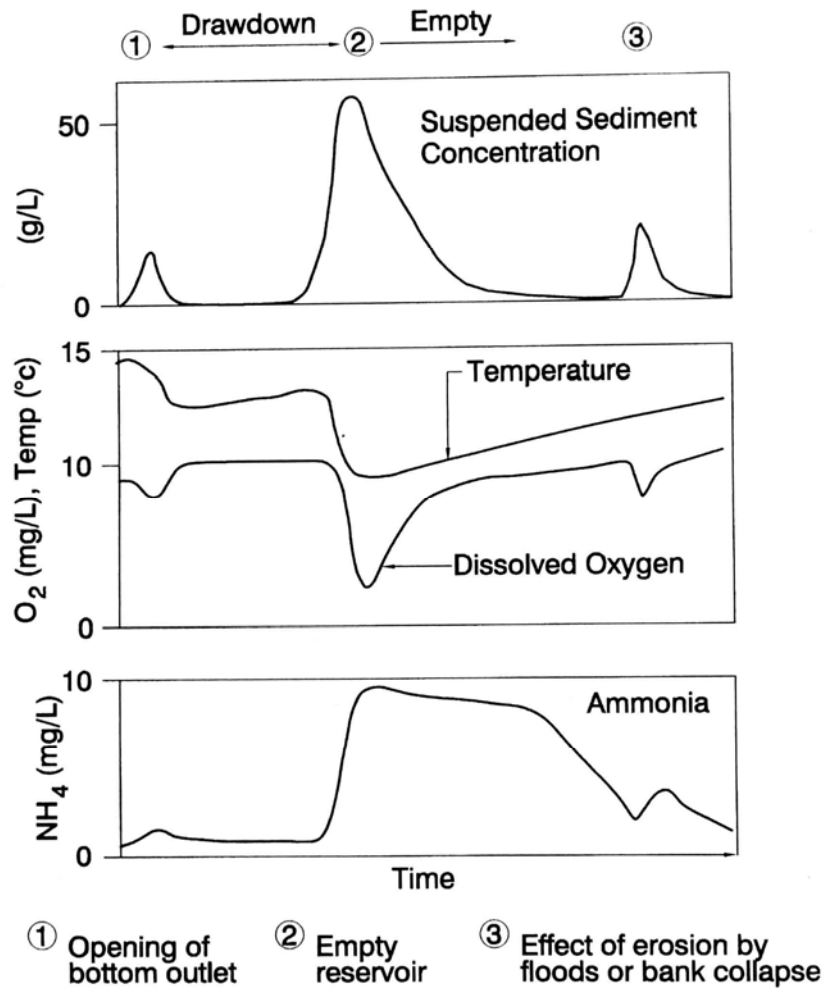


**FIGURE 18.13** Sequence of water quality changes that accompany the release of water during reservoir emptying (*Electricité de France, 1995*).

4. Following release of the bottom mud, water quality tends to improve throughout the duration of the empty period. Bank slides, small floods which scour sediment, and rainfall erosion of exposed sediment can temporarily increase sediment discharge during the empty period.

This general sequence is also reflected in the available data from reservoirs emptied for sediment flushing, as illustrated in case studies for Gebidem, Cachi, Sefid-Rud, and Heisonglin.

#### 18.4.2 Fisheries Impacts

Virtually all the fish in a reservoir will be flushed downstream or killed during emptying, and fish nests will be desiccated. Fish downstream of the dam can be affected by:

1. Physical blockage of gills by high sediment concentration, essentially causing suffocation;
2. Reduced dissolved-oxygen levels;
3. Washout of nests and fry if unseasonably large flows are released during flushing;
4. Modification of the benthos due to sediment deposition;
5. Modification of the aquatic population structure;
6. Disruption of the aquatic food chain and elimination of food sources, especially on the benthos; and
7. Incorporation of toxic substances into the food chain if reservoir sediments containing toxins are released during flushing (agricultural chemicals, mine tailings, etc.).

The physical stresses induced by flushing can produce fish kills, reduce resistance to disease, reduce growth rates, and cause genetic problems if toxins are present. Release of a large sediment volume at high concentration will kill virtually all stream biota.

Drastic fish mortality has been observed downstream of French reservoirs which are drained, primarily because of reduction in dissolved oxygen and high suspended-solids concentration. Garric et al. (1990) studied the effects of emptying the Saint Hilaire reservoir on water quality and fish mortality in the Isère River. Comparison of laboratory and field data suggests that hypoxia (oxygen deficiency) was the major cause of fish mortality during dam draining, with larval stages being much more susceptible than adults. Ammonia concentrations were never high enough to be considered a contributing factor, and temperature and pH values during the draining were not significantly affected. It was concluded that a better knowledge of fish acclimatization to depressed oxygen levels could lead to the adoption of a progressive draining protocol to let fish better adapt to hypoxia before being submitted to an anoxic period.

The dissolved oxygen concentration in the river below the dam during flushing is determined by: (1) the oxygen level in the hypolimnic water that is released through the bottom outlet, (2) the oxygen demand exerted by the sediment that is released with the water, and (3) the rate of reaeration within the stream by gas transfer from the atmosphere plus photosynthetic activity by aquatic algae and bottom plants. These parameters are influenced by a variety of factors, including temperature. The saturated oxygen content is lower in warm water than in cold water, and the higher rate of biological activity in warm water consumes the limited oxygen supply more quickly. This makes it increasingly difficult to sustain dissolved oxygen levels as water temperature increases.

#### **18.4.3 Predicting Downstream Water Quality**

Oxygen and suspended sediment concentration below a dam during flushing may be estimated by modeling which includes parameters for the transport rate, reaeration rate, and the reduction in sediment concentration due to deposition. The initial oxygen concentration, that of the hypolimnic water, must be known, and the oxygen consumption kinetics of the sediment must be determined for the temperatures that will prevail during flushing. When a range of sediment sizes are present, the oxygen consumption by sediment should be determined for the fines; coarse sediments exert little oxygen demand. The timewise variation in sediment concentration over the duration of flushing will also need to be computed.

Fish mortality increases as a function of decreased dissolved oxygen levels, increased suspended-sediment concentration, and increased exposure time (Fig. 18.14). Ideally,

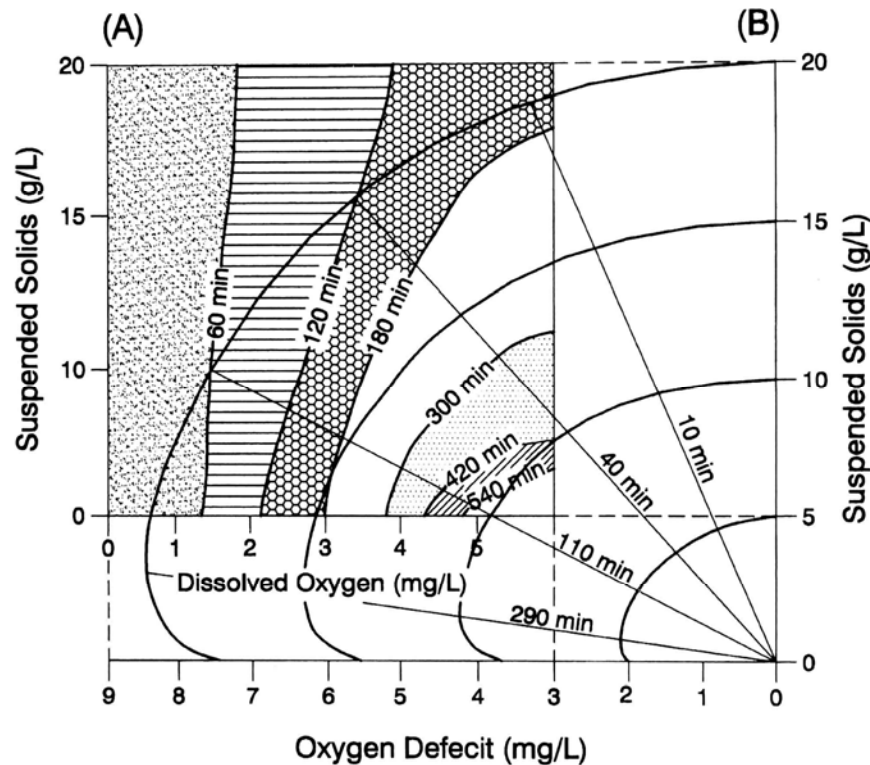


**FIGURE 18.14** (a) Isolines for 10 percent mortality of trout alevins as a function of dissolved oxygen, suspended sediment concentration, and exposure duration (Garric *et al.*, 1990). (b) Superposition of predicted oxygen deficit and suspended concentration due to flushing on data for trout mortality (Gerster and Rey, 1994).

modeling could determine the sediment concentrations and dissolved oxygen levels at different points below the dam as a function of the flushing regime, and this information could be used to predict impacts and optimize flushing procedures. In practice, computations of this nature provide only rough approximations of field conditions. One of the principal parameters to be analyzed is sediment release during flushing. Present state-of-the-art modeling with ample field data, including reservoir borings, allows the volume of sediment release to be predicted within the range of about -50 to + 200 percent of the actual discharge when cohesive sediments are present. Greater errors should be expected if less effort is dedicated to field data collection and modeling activities. A large part of the uncertainty is attributable to the difficulty in specifying erosion rate and equilibrium conditions for cohesive materials with complex bedding (Petitjean and Bouchard, 1995). Impacts to the benthos are more difficult to predict. Planning of reservoir emptying should consider the uncertainty in predicting water quality conditions, and in sensitive areas these plans should include contingencies to stop the release and flush the stream with clear water.

#### 18.4.4 Reservoir Ecosystem

Reservoir ecosystems typically develop through a series of successional stages as the system matures. After first filling, the water nutrient conditions stabilize, fast-growing pioneer species give way to more diversity, and species populations grow and stabilize with respect to their age-class distribution. Emptying a reservoir eliminates large compo-

nents of the ecosystem, including virtually all fish and those benthic species unable to dig into mud and survive the dewatering period. During the first years following emptying, the fish face an ecosystem abundant in food, water quality is good because of oxidation of sediments during emptying, and interspecies competition is weak. Studies in French reservoirs recovering from emptyings followed by 10 years of impoundment revealed that fish populations in these manipulated ecosystems tend to be characterized by unequal population distributions: both older and younger age classes were overrepresented, whereas the intermediate age classes were underrepresented. This phenomenon becomes more pronounced as the ecosystem ages. The initial restocking after refilling is a primary determinant of the "trajectory" along which the lacustrine ecosystem develops during the impounding interval.

#### **18.4.5 Water Supplies**

Reservoir emptying and flushing can have a large impact on municipal, industrial, and irrigation water supply intakes. An alternative water supply source will need to be provided for intakes located in the reservoir when it is empty. Downstream intakes and diversion channels can be physically clogged by high sediment concentrations, as can heat exchangers at industrial facilities drawing cooling water from the river. The solids-handling facilities at filter plants can be overloaded, especially in facilities designed for operation with water normally having low suspended solids. Fine sediment can clog infiltration galleries beneath the streambed. The water may be anaerobic with high concentrations of dissolved iron and manganese, and organics such as methane may react with chlorine to create chlorinated hydrocarbons. Taste and odor problems may be anticipated. It may be necessary to temporarily close water supply intakes, implying an alternative water source (e.g., from a storage basin). The period of water supply disruption can be estimated by water quality monitoring below the dam, dilution by tributary inflow, and hydraulic travel time.

#### **18.4.6 Timing, Coordination, and Public Relations**

Some irrigation reservoirs are heavily drawn down or emptied on an annual basis, in which case emptying for sediment flushing or pass-through should be conducted in conjunction with the existing drawdown schedule, extending or modifying it as necessary. In reservoirs not normally subject to heavy drawdown, the following factors should be considered.

- Emptying can be performed only when inflows are significantly less than the discharge capacity of the bottom outlet. It should be possible to pass the river flow with little or no backwater upstream of the bottom outlet.
- Maximum sediment release will occur when emptying coincides with high flows that will scour sediment deposits. When it is desired to minimize sediment release during emptying, avoid periods of high streamflow.
- Emptying should be timed to minimize impacts to beneficial uses and the environment. In some cases it will be important that the reservoir refill quickly. In others it may be desirable to avoid periods of recreational use in the reservoir or downstream river, to avoid ecologically sensitive periods such as spawning, or to coincide with specific hydrologic conditions in a downstream river to provide dilution flows [e.g., see Gehidem case study (Chap. 21)]. Particular attention should also be given to life cycles of benthic organisms which occupy the base of the aquatic food chain.

There may be other activities that can be facilitated when the reservoir is empty, and, with advance coordination, multiple benefits can be achieved. Activities facilitated in an empty reservoir may include: any work in and around the dam and hydropower facilities; rehabilitation of intakes, screens and gates; excavation of navigation channels; repairing of marinas, boat ramps, and beach areas; bank stabilization; photogrammetric reservoir surveys; sampling of sediment deposits; and timber harvest areas near the lake.

In areas of France dependent on reservoir-based recreation, and where emptying impacts the recreational season, alternative recreational events have been staged such as fishing competition as the lake is being lowered, dirt bike racing in the empty reservoir, concerts, and visits to villages submerged by the reservoir. Unorganized recreational activity on the bottom of Folsom Reservoir in California is shown in Fig. 18.15.



**FIGURE 18.15** Off-road vehicle recreational use of the bottom of Folsom Reservoir, California, during drawdown as a result of prolonged drought (G. Morris).

Fish kills are a highly visible indicator of environmental damage. When a reservoir is drained, the fish within the reservoir are either flushed downstream (where many of them die) or they are crowded into the shrinking reservoir pool until it empties. After emptying, dead fish may be found on the banks of the drained reservoir and along the downstream river. At French reservoirs, intensive fishing is performed prior to and during draining with the objective of catching all fish in the reservoir. Despite the promotion of recreational fishing contests during this period, it has been found necessary to contract commercial fishermen to attain the high catch efficiency that is desired. At the end of the drawdown period, when many fish are being flushed out the bottom outlet, discharge is directed across a bar screen which catches the fish. These fish are sold or given away to local residents. The banks of the reservoir and downstream river are patrolled to remove all dead or dying fish. If the reservoir remains empty for an appreciable period during the

summer, the exposed banks may be seeded with fast-growing grass to reduce rainfall erosion and enhance the aesthetic appearance. After refilling, the reservoir is restocked with fish.

The coordination and communication required prior to emptying is site-dependent. EDF begins planning and coordinating emptyings about 30 months in advance. Emptyings are generally timed to coincide with the driest part of the year, and the empty period may last for several weeks, depending on the programmed maintenance work. Refilling may be further delayed by low water. In Costa Rica the annual flushing of Cachi Reservoir is planned about 6 months in advance and scheduled to coincide with a long weekend when electrical demand is low. Because flushing occurs annually and there is little development in the area, coordination efforts in Costa Rica are minimal compared to France.

Potentially affected users, regulatory agencies, and government authorities bordering the lake and downstream should be identified and contacted. These may include: operators of all water intakes; wastewater plant operators who may depend on dilution flows of a stated quality to meet instream water quality standards: national, state, and local agencies regulating water quality and aquatic life; and political representatives such as mayors. It is also important to contact recreational users such as marinas, fishing clubs, and tourist associations and to coordinate emptying to minimize impacts to their members and clients insofar as possible. Emptying dates should be coordinated to minimize impacts to seasonal recreational users, especially when seasonal recreation is a major economic activity in the area. Because of the numerous reservoir drainings performed each year, EDF has prepared a public relations video which describes the emptying process and typical mitigation activities.

#### **18.4.7 Water Quality Mitigation Measures for Flushing**

Reservoir emptying can reduce oxygen levels downstream by: (1) the release of oxygen-depleted hypolimnetic water, (2) the oxygen demand exerted by organic sediment, and (3) increased turbidity which shades instream primary producers. In some cases, low dissolved oxygen can be mitigated by artificial oxygenation. Fish have improved tolerance to suspended sediment if dissolved oxygen levels are high, and to a certain extent high sediment levels can be compensated by aeration. However, if the oxygen demand exerted by released sediment exceeds the natural reaeration rate along the river, oxygen depletion may occur downstream despite adequate oxygen levels at the dam. At reservoirs in France it has been found that dissolved oxygen levels can be elevated about 2 to 3 mg/L by reaerating with atmospheric oxygen, and 6 to 8 mg/L can be achieved when reaeration is performed with pure oxygen. Either floating or submerged aerators may be used. In air bubble systems, best results are achieved by using the smallest possible bubble size and the deepest possible placement depth (over 2 m) to maximize oxygen transfer. However, a bubbler should not be installed directly on the bottom where it may be smothered by sediments. Aeration systems may also be installed upstream of the dam to improve hypolimnetic water quality prior to release.

Releases containing a high suspended-sediment concentration can be captured and treated in either off-stream or on-stream settling basins below the dam. Sediment trapped in an off-stream settling basin may be removed by dredging, or dewatered and then trucked away, thereby restoring basin capacity for the next flushing event. Sediment trapped in an on-stream basin located within the river channel below the dam may be scoured and transported downstream by hydraulic

action during subsequent flood events, which would also provide dilution water. Sedimentation basins may operate in a continuous flow-through mode, with sediment-laden water continuously entering the basin and clarified water being continuously discharged. Alternatively, they may be operated in batch mode by filling a basin with muddy water, allowing it to settle, and releasing the clarified supernatant. Design procedures for settling basins are given in Chap. 16.

If the stream normally sustains a low flow, it will be necessary to maintain the low flow by using water of adequate quality from another source while the muddy water is being diverted into settling basins. Options include the controlled release of clarified and oxygenated water from previously filled settling basins or the construction of a small reserve impoundment within the main reservoir which would supply clear water to the stream by canal or pipeline when muddy flow is diverted (Fig. 18.16). A

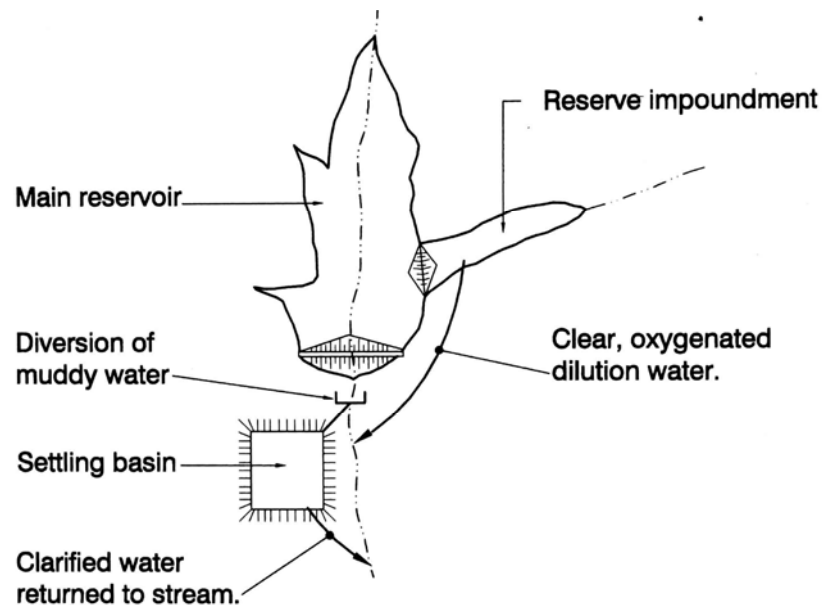


**FIGURE 18.16** Potential use of reserve impoundment and sedimentation basin to mitigate downstream effects of reservoir emptying.

reserve storage compartment may have additional uses as well, including the provision of dilution water during flushing, even when muddy water is not being diverted into settling basins. After the release of muddy water, the bed and banks of the stream will typically be covered with a layer of fine sediment (Fig. 21.10). A large clear water release following the release of muddy water may be used to scour and flush fines downstream.

#### 18.4.8 Monitoring

Monitoring should be conducted before, during, and after flushing. Pre-flushing water quality data should be available for the downstream river, and the vertical stratification condition in the reservoir should be monitored to determine the temperature and dissolved oxygen levels in the bottom water to be released. Sampling and analysis of reservoir sediments is required to determine the oxygen uptake

kinetics of the fine sediment and the chemical characteristics of the interstitial water.

Routine monitoring during flushing should focus on parameters such as suspended sediment concentration and grain size, dissolved oxygen, temperature, forms of nitrogen, total and orthophosphate, and pH. Additional parameters may be required, depending on site conditions. Data collection should normally focus on: (1) monitoring water quality to control the operation of water supply intakes, (2) the collection of information that will help predict the impacts of future flushing operations, and (3) data required for the validation of predictive models. In monitoring water supply intakes, parameters such as turbidity would normally be used in addition to suspended sediment, since the processing of suspended sediment samples is time-consuming, even with filtration and microwave drying. Selected cross sections may be surveyed before and after flushing to determine the depth and grain size of sediment deposition, and gravels may be sampled to monitor the entrainment of fines.

Reservoir emptying and flushing can have large impacts on the benthic community in the downstream river because of both water quality changes and sediment deposition. The population and species composition of the benthos can change seasonally, and long-term monitoring is required to understand seasonal effects and separate them from the effects of reservoir emptying. The choice of monitoring points is important, and monitoring stations should be established at several points below the dam representative of different stream environments. For example, monitoring results will be biased if all sampling stations are located in pools or near the shoreline where sediment deposition is most likely, or in midchannel riffles where sediment deposition is least likely. Aquatic ecosystems on regulated rivers are heavily impacted by the changes in hydroperiod, sediment transport, peak discharge, temperature, migration barriers, and other effects of the dam. It may be difficult to separate these effects from those caused by reservoir emptying and flushing, and it may be difficult to find a representative paired river (control) for the purpose of comparative long-term monitoring (Electricité de France, 1995).

#### **18.4.9 Flushing at Spencer Dam, Nebraska**

Biological impacts and mitigation recommendations for sediment flushing at the small (1 MW) low-head Spencer hydro station on the sand-bed Niobrara River, Nebraska, were reported by Hesse and Newcombe (1982). The dam, located 63.3 km upstream of the Niobrara's discharge into the Missouri River, operates as a run-of-river hydropower station. Mean annual flow at the dam site is 1.3 m<sup>3</sup>/s, and the river transports mostly sands. The low dam has no bottom outlet, and flushing is conducted by opening radial gates and allowing sands and fines to be scoured and discharged over the gated spillway (Fig. 18.17). After about a week of flushing, the gates are closed and the impoundment is refilled. Although the dam is very small, and the volume of sediment release is not large, the impacts on water quality and stream ecology are significant.

Water quality along the entire 63-km reach of the Niobrara between the dam and the Missouri River confluence is affected by the flushing. A comparison of flushing flows to ambient conditions at a station 60 km below the dam shows that flushing caused: a turbidity increase of 400 percent [240 versus 56 Jackson turbidity units (JTU)]; a 15-fold increase in settleable solids; a 4-fold increase in suspended solids; and a 2-fold increase in dissolved solids.

The impoundment was flushed 22 times in 5 years. Significant fish kills were reported in four of these instances, affecting nearly 30 species. Fish were most affected in the immediate vicinity of the dam, and the documented fish kills occurred during



**FIGURE 18.17** Spencer Dam on Niobrara River, Nebraska. View looking downstream across sand sediment deposits being scoured from the empty pool (*G. Morris*).

the summer and fall, when the largest fish populations occur in the zone below the dam. One kill of 22,47 individuals was counted (of which 18,000 were minnows). This undercounts actual fish loss, since fish stranded behind rocks and depressions during flushing were quickly buried by up to a meter of sediment, and other fish in extreme distress floated downriver. For most species, young-of-the-year and yearlings were the most affected. Fish were affected by depressed oxygen levels (but not anoxia), high suspended-sediment levels, high flow velocities, and physical smothering by sediment, and the exact cause of death was difficult to establish. The impacts of sediment release on the stream ecosystem extend well beyond the flushing period itself because the benthos becomes smothered. As a result, macroinvertebrates were even more acutely affected than fish, disrupting the aquatic food chain.

The following management techniques were recommended to minimize downstream impacts.

1. Time flushing to avoid spawning periods, April 15 to September 15 on Niobrara River.
2. Flush less frequently (annually) to maximize recolonization of the stream by insect macroinvertebrates.
3. Refill the reservoir slowly so that stream flow below the dam is not reduced below 6 percent of natural mean monthly flow.
4. Establish mitigation programs to offset fish loss.
5. Develop a fish ladder or bypass system.
5. Monitor to evaluate effects of the recommended actions.

Hotchkiss proposed a continuous sand bypass system at Spencer Dam which would discharge sandy sediment on an essentially continuous basis, as opposed to the highly irregular release caused by flushing.

## 18.5 MANAGEMENT OF COARSE SEDIMENT

Most dams, including those managed for sediment pass-through, continue to act as efficient gravel traps. A continuous supply of gravels below the dam may be required to prevent channel incision, and to maintain aquatic habitat and spawning areas. Artificial means will usually be required to deliver gravel to the river below a dam.

### 18.5.1 Gravel Replenishment below Dams in California

When the transport of spawning-size gravels along a stream is interrupted by dam construction, the gradual coarsening of the bed below the dam can reduce the areas available for spawning. Artificial gravel-feeding techniques used in California have been reviewed by Kondolf and Matthews (1993).

Ideally the gravel would be excavated from the deposition areas in the reservoir delta and discharged below the dam. However, because delta deposits may be far from the dam and lack good access, it may be less costly to obtain replenishment gravels from a nearby quarry. Replenishment gravels should not be obtained from an active river channel, lest gravel replenishment in the target river promote degradation in another river.

The cost of gravel replenishment is highly sensitive to scale economies and the proximity to an appropriate gravel source. Costs of gravel replenishment projects are summarized in Table 18.2. The least costly procedure is to discharge gravel regularly at a single site, replenishing the supply point as the gravel is transported into the downstream reach by the river. An example of this type of gravel replenishment operation is illustrated in Fig. 18.18. It is much more costly to replace gravel along an entire river reach, which also involves impacts caused by access by heavy equipment along the replenishment reach. When spawning habitat is to be maintained, the gravel emplaced in the river should be free of fines or sands which impart turbidity and can clog spawning beds.

### 18.5.2 Grain Feeding in the Rhine River

A series of 10 barrages have been constructed along the reach of the Rhine River extending 17.5 km downstream from Basel, at the Swiss border, to Karlsruhe,

**TABLE 18.2** Gravel Replenishment Projects in California

Reservoir and river	Year	Volume, m <sup>3</sup>	Total cost, \$	Unit cost, \$/m <sup>3</sup>
Camanche, Mokelumne River	1990	76	\$ 20,000	\$ 263
Camanche, Mokelumne River	1992	230	6,300	27
Keswick, Sacramento River	1988	76,410	250,000	3
Keswick, Sacramento River	1989	68,769	200,000	3
Los Padres, Carmel River	1990	612	82,000	134
Iron Gate, Klamath River	1985	1,666	136,000	82
Courtwright, Helms Creek*	1985	5	12,000	2,400
Trinity, Trinity River	1989	1,490	22,000	15
Folsom, American River	1991	764	30,000	39
Grant Lake, Rush Creek	1991	917	18,000	20

\*At Courtwright, a helicopter was used to drop gravel into a narrow gorge by hopper.

*Source:* Kondolf and Matthews (1993).

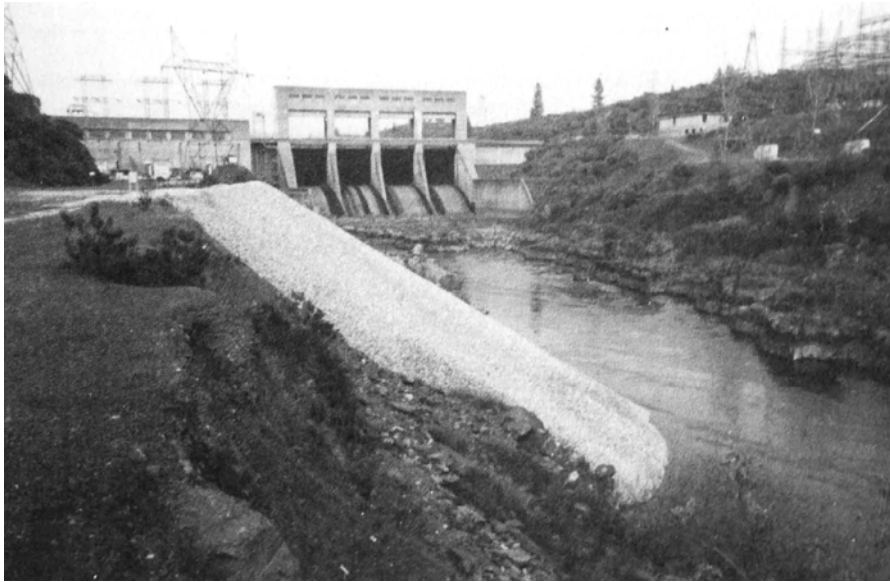


**FIGURE 18.18** Gravel replenishment below Keswick Dam on Sacramento River, California (Kondolf and Matthews, 1993).

Germany. The first barrage was constructed in 1928 at the upstream end of this reach, and the most recent and most downstream barrage, Iffezheim, was closed in 1977. These barrages trap part of the suspended load and all the bed material load, consisting of sands and gravels. Although the river flows freely below Iffezheim, its course is fixed by a series of river training works, resulting in the gradual incisement of the channel. Lowering of downstream water levels reduces navigation clearance at the exit from the locks, and erosion of coarse bed material can expose finer-grained underlying formations to scour, producing an irregular bottom profile. The navigational depth along this reach of the Rhine is 2.1 m, plus only 0.4 m of additional clearance to the bottom, and even slight scouring of the bed can change the profile sufficiently to interfere with navigation.

Four methods were considered to stabilize the bed geometry below the Iffezheim barrage: (1) continued construction of additional barrages farther downstream, (2) continued construction of groynes, (3) bed armoring, and (4) artificial grain feeding. While the first three methods could control bed erosion and water levels in the treated area, the erosion problem would continuously reappear farther downstream and the treatment area would need to be continuously extended. The first three alternatives would also tend to interfere with easy and safe navigation, and would meet environmental opposition. As a result, artificial grain feeding was initiated at Iffezheim after its closure in 1977.

Grain feeding is conducted by excavating sands and gravels from a floodplain quarry upstream of the barrage, which are placed onto a hopper-bottom scow that is locked downstream. The bed material is discharged to the riverbed below the barrage by opening the hopper bottom while the scow is traveling downstream at high speed, resulting in a deposition pattern 50 to 300 m long and 10 to 20 m wide (Fig. 18.19). To reduce travel distance, the gravel is obtained from a quarry near the lock rather than being dredged from deposits near the upstream limit of the pool. On the average, 150,000 m<sup>3</sup> of coarse material is deposited below Iffezheim each year. The grain size is matched against the original material in the riverbed to allow the continued downstream transport, and the rate is adjusted to maintain navigational

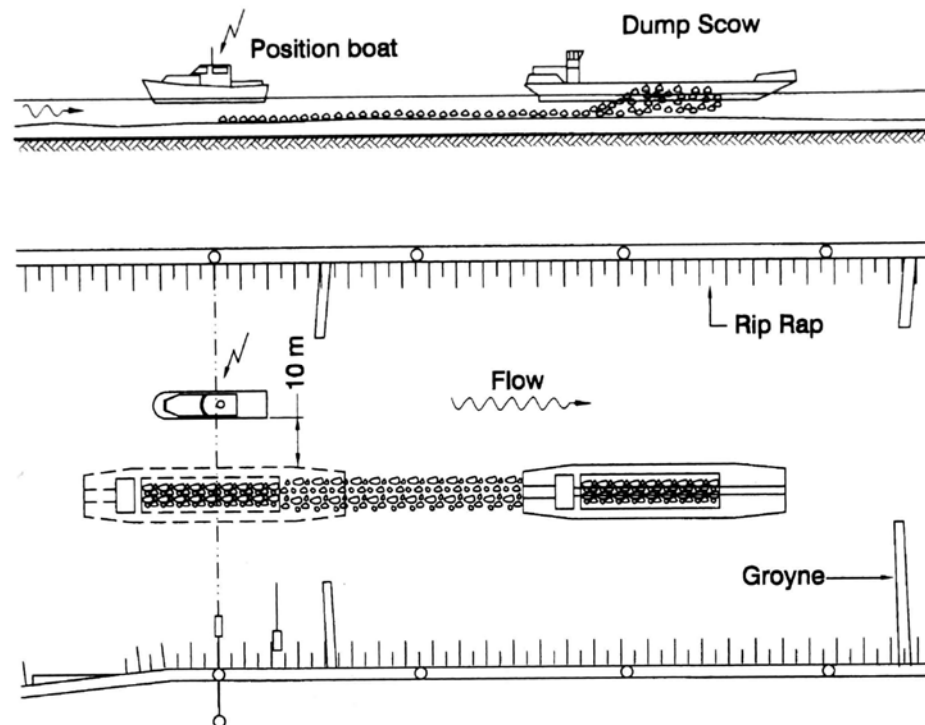


**FIGURE 18.19** Grain feeding below Iffezheim barrage on the Rhine River near Karlsruhe, Germany (after Kuhl, 1992).

clearance. Navigation conditions along the 18-km reach downstream of the dam are monitored at 38 water level gages. Cross sections are measured daily in the area of grain feeding, every fortnight in the 2-km reach below the feeding area, and annually in the 18-km reach below the barrage. Overall, about 6000 cross sections are measured each year. The effect of grain feeding has been examined by both physical (Nestmann, 1992) and numerical modeling (Siebert, 1992).

Grain feeding has successfully stabilized the bed of the Rhine to date in the reach immediately below Iffezheim, and it has not been necessary to construct additional barrages downstream to maintain navigation depth (Kuhl, 1992). However, reaches further downstream have not been stabilized by the gravel feeding at Iffezheim, and additional grain feeding at downstream locations will probably be required in the future to compensate for reduced delivery of bed material from regulated tributaries (Golz, 1992).

## 18.6 FLUSHING FLOWS FOR COARSE SEDIMENT MANAGEMENT

### 18.6.1 Importance of Gravel Flushing

Salmon and related species use gravel beds for spawning. The  $d_{50}$  size for salmonid spawning gravels is usually between 14.5 and 35 mm, but may include beds with  $d_{50}$  values in the range of 5.4 to 78 mm (Kondolf and Wolman, 1993). Permeable gravels are

essential not only for the spawning success of a number of fish species, but also as habitat for a variety of crustaceans and insects which sustain stream diversity and productivity. Fish explore the pool and riffle sequence to locate a site suitable for spawning, excavate a pit, deposit eggs, and, in some species, backfill with permeable gravel. After an incubation period of 1 or 2 months, the eggs hatch and the alevins (hatchlings still attached to their yolk sac) spend another 1 or 2 months in the intergravel environment until the yolk sac is fully absorbed before emerging as fry. The accumulation of fine sediment in the gravel diminishes the flow of oxygenated water and reduces the rate of removal of metabolic wastes produced by the eggs, and dramatically reduces survival of both eggs and alevin. Coarser sediment such as sand which fills the interstices near the surface of the bed can trap fry within the gravel matrix, preventing their migration into open water, and can also fill the interstices used by juvenile fish to escape from predators.

The depth of infiltration into a gravel bed by fines depends on the sizes of the fines relative to the grains composing the bed matrix. Fine sediment is carried deep into the bed and accumulates by plain sedimentation within the void spaces. Larger grains may penetrate only the armor layer, creating a seal by particle bridging within the upper layer of the subarmor. Observations in tilting flumes indicate that sedimentation within gravel beds occurs first in the pools and the tail of bars, gradually moving upstream to the head of the bars. The fine sediments that accumulate in gravels may be removed by large flows which mobilize the bed and wash out the fines. This cleansing process begins at the head of gravel bars and moves downstream, in reverse order to the clogging process (Diplas and Parker, 1985).

Gravels are maintained free of fines by high-discharge flushing flows which occur during flood season and mobilize the bed. These large flows are also important for maintaining the overall channel capacity and preventing the encroachment of riparian vegetation into the active channel, which can further reduce the amount of gravel available for spawning. Dam construction reduces or eliminates the flood flows needed to flush finer sediment from gravel beds and maintain channel morphology, and also eliminates the supply of gravels from upstream. These negative impacts are only partially offset by fine sediment trapping within the reservoir, which will reduce the rate of gravel clogging. However, in the absence of flushing flows, even low concentrations of fine sediment will eventually clog the bed. Diminished peak flows below a dam can also allow sediment to accumulate in pools used for rearing of fish, and will change a complex braided stream into a single narrow channel with loss of habitat.

Flushing flows to maintain spawning gravels below dams should: (1) mobilize gravels to flush out fines, (2) be large enough to maintain channel morphology and prevent vegetative encroachment, and (3) prevent significant downstream transport of gravel which would deplete spawning beds. These objectives are not complementary. Large discharges which flush gravels and maintain the channel also transport gravels downstream, exacerbating the problem of gravel loss and bed coarsening.

Benthic invertebrates, mainly aquatic insects having a lifespan of about 1 year, are the major food source for anadromous fish. Because these invertebrates cannot move from one location to another when the water level drops, the lowest flows of the year delimit the areas where these organisms are most numerous. Continuously submerged gravel riffles contribute the most food to fish production (Nelson et al., 1987). The lack of flushing flow can allow encroachment by vegetation, narrowing and deepening of the channel, affecting not only the availability of spawning gravels, but also reducing food-producing areas and related habitat. Hydroperiod modification which desiccates the streambed, as well as reservoir flushing that smothers this habitat, can have disastrous consequences on benthic fauna and all species that depend on them for food.

### 18.6.2 Factors Affecting Habitat Rehabilitation

Dam construction and other activities impacting rivers have severely affected river biota, and considerable attention has focused on the management of coarse sediments below dams to rehabilitate habitat. Many factors have contributed to the continuing decline of salmon and other ecological changes affecting regulated rivers. Ligon et al. (1995) state that, despite possibly 10,000 to 15,000 research articles on salmonid biology and ecology, there is little consensus on the relative importance of dams, commercial harvest, hatchery-reduced genetic fitness, oceanic conditions, predation, habitat degradation due to timber harvest, stream degradation by cattle, and other factors which affect fish populations and survival. Because conditions will vary from one river to another, it is dangerous to make generalized statements or use a generic approach to habitat restoration. The conditions limiting populations of salmon or any other species of concern in one river may be quite distinct from the limiting conditions in another river.

Without a clear understanding of the role of dams and other factors influencing the decline of any aquatic species or habitat, including a sound understanding of the geomorphic and sediment transport conditions in the target stream reach, there is considerable potential for rehabilitation to be misdirected. For example, Kondolf et al. (1996) reviewed the implementation of the Four Pumps Agreement, passed in response to the near extinction of salmon in California's Sacramento-San Joaquin River system. Of the \$33 million allocated between 1986 and 1995, 45 percent was directed to increase populations of striped bass, an introduced species that preys on young salmon. Another \$5.6 million was allocated to hatcheries, apparently in conflict with the Agreement's guideline that priority funding be given to natural production, since hatchery fish are known to have a deleterious effect on natural runs through competition and genetic introgression. Another \$3.4 million was allocated to spawning habitat enhancement projects, although studies showed that spawning habitat was not a critical limiting factor in this system. Projects to reconstruct spawning riffles were planned and designed without full understanding of the geomorphic and ecological effects of upstream dams that modified flow and eliminated gravel supply, and of instream gravel mining pits that trap bed material and induce channel incision. Instream mining pits also provide habitat for largemouth and smallmouth bass, principal predators of juvenile salmon. A survey of three reconstructed riffles showed that the artificially placed gravels had washed away within 1 to 4 years, and in some places the post-project bed was even lower than it was before gravel placement.

### 18.6.3 Planning Flushing Flows

The periodic release of large flows to flush fine sediment from gravel beds is necessary to maintain spawning beds. Reiser et al. (1988) outlined a four-step procedure for analyzing flushing flows:

- 1. Define purpose and objectives.** Prior to undertaking flushing, it is essential to clearly establish the target sediment grain size and the flushing objectives (e.g., cleaning of surface sediment, deep cleansing of gravels, maintenance of channel morphology).

- 2. Timing.** Flushing flows should be scheduled considering factors such as the life history of important species in the river, the natural flow variation prior to impoundment, and water availability. Properly timed flushing flows can cleanse gravels in preparation for spawning, but a later release may wash out eggs and fry. Recreational benefits (rafting, kayaking) and seasonal variation in water cost (lost power generation benefits) may also be important. Flushing flows timed to

coincide with high runoff events in undammed tributaries can minimize the release required from the dam.

**3. Flushing discharge.** In undertaking gravel flushing, the objective is to mobilize the sediment bed and remove fines, while minimizing the net downstream transport of gravel, and the optimal flushing domain may be very narrow. However, there is no standardized method for computing flushing flows. Reiser et al. (1988) enumerated 16 different published analytical and field techniques used to estimate flushing flow, and reported that different techniques can give flushing flows differing by as much as 800 percent. Because stream hydraulic characteristics are irregular, at a given discharge a portion of the gravel beds in the stream will be flushed. In streams where spawning gravels occur in patches, hidden from the areas of maximum current flow by boulders or stream morphology, mean hydraulic and bed shear conditions along the stream give little indication of conditions in the spawning gravel. This makes it difficult to establish more than approximate values for flushing flows using analytical techniques. In such cases, the effects of different flushing discharges should be monitored to determine the optimal flow rate. An example of this procedure is described by Reiser et al. (1989).

**4. Flushing effectiveness.** The effectiveness of flushing flows should be evaluated by field inspection and quantification. These observations will be the basis for recommending adjustments in the discharge and duration of subsequent flushing flows. Several methods may be used to monitor flushing effectiveness. The initiation of motion may be monitored by gravel tracers, stones colored with bright waterproof paint which are placed on a gravel bed and monitored for movement. Tracer stones found at a downstream point, or not found at all after a given flow, have been mobilized. This technique is useful for determining the discharge corresponding to the initiation of motion in different areas of the stream. Scour depth can be determined using scour chains in different locations (Fig. 8.20a), and net changes in bed configuration can be quantified from before and after cross-section surveys. The change in size distribution of sediment within the gravel bed can be determined by bulk sampling (Fig. 18.20b) or the freeze core technique. Bed surface conditions can be documented by photography.

#### 18.6.4 Analytical Flushing Flow Computations for Gravel Cleansing

Flushing discharge can be estimated by the criterion of incipient sediment motion based on Shields parameter. Gessler (1971) determined that a given particle will have a 5 percent probability of movement for a Shields parameter value of 0.024, and a 50 percent probability for a parameter value of 0.047. From flume studies of graded sands and gravels (0.25 to 64 mm), Wilcock and McArdell (1993) found that complete mobilization of a size fraction occurs at roughly twice the shear stress necessary for incipient motion of that fraction. Thus, as a first estimate, bed shear stress values between 1 and 2 times the critical bed shear stress  $\tau_{CR}$  might be suitable for flushing without causing excessive downstream transport of gravel. In some cases it may be desired to remove finer sediments from the surface of a coarse armor layer, without mobilizing the armor layer itself. The bed shear  $\tau$  to achieve superficial flushing may be estimated by:

$$\tau_{surfaceflush} = 2/3 \tau_{CR}$$

where  $\tau_{CR}$  = critical bed shear stress for the armor layer (Milhous and Bradley, 1986). Average bed shear stress values may be related to discharge by using stream cross

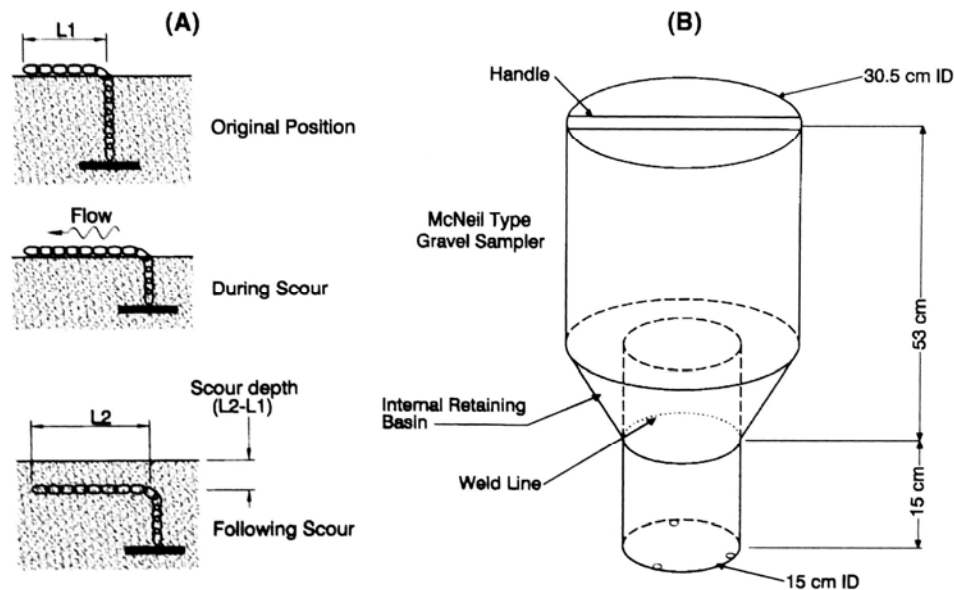


**FIGURE 18.20** Tools useful for determining flushing impacts. (a) Use of scour chain to determine depth of bed mobilization during a flushing event. (b) McNeil type gravel sampler for bulk sampling. The stainless steel sampler is pushed into the gravel to the weld line and gravel is scooped by hand from the core into the outer ring.

sections and hand computation by the Manning equation and the average stream slope along the reach, or by using a hydraulic model. The initiation of sediment motion is discussed in Chap. 9. In the evaluation of flushing flow in the North Fork Feather River, several transport equations were used to select the recommended flushing flow discharge and duration, as described in Sec. 22.9. For more complex cases, sediment transport modeling would be recommended.

Computations using the Shields parameter assume conditions of loose, noncohesive sediment. Sand-embedded gravels, especially with a cemented organic crust or containing clay, may require mechanical loosening by heavy equipment for flushing to be successful.

### 18.6.5 Gravel Flushing in Trinity River, California

An example of the complexities of gravel management in Northern California's Trinity River below Lewiston Dam is presented by Nelson et al. (1987). Chinook salmon and steelhead trout are the species of critical concern.

Eighty percent of the average runoff from the upper watershed has been diverted from the basin for hydropower and irrigation, and the annual flood peak has decreased from 525 to 73  $\text{m}^3/\text{s}$ . Extensive clearcutting and logging road construction in the watershed disturbed the erodible soils, increasing the delivery of coarse sand to the river. The reduced flows are unable to transport this sediment, and sands have filled pools, buried cobble substrate, and clogged spawning gravels, thereby degrading the habitat for anadromous salmonids which were formerly abundant in this reach. Reduced flows also allowed riparian vegetation to encroach into formerly active channel areas, producing a deeper and narrow channel which reduced the area of shallow riffles important for food production. Sediment-related stream rehabilitation

measures considered for this stream include watershed rehabilitation to reduce sediment inflow, construction of debris dams to trap sand, mechanical loosening of compacted sediments, artificial replenishment of depleted gravels, removal of encroaching riparian vegetation, and flushing. Because of the large volume of flushing water required, and the high opportunity cost of lost water due to foregone power production and irrigation, flushing was considered a high-cost option.

Using tracer gravel particles, Kondolf and Matthews (1993) found that a 5-day flushing flow release of 170 m<sup>3</sup>/s would mobilize most of the gravels, but did not significantly alter the sand:gravel ratio because the duration was not sufficient to flush sands out of the river system. Flushing flows exceeding 240 m<sup>3</sup>/s are not considered feasible because they would accelerate gravel loss below the dam and would also exceed the 100-year flood level computed for post-dam conditions. The sustained releases that would be required to flush the sand out of this system are extremely costly because of the value of the water. Dredging of sand accumulation from pools was recommended as an alternative.

## **18.7 CLOSURE**

---

The environmental impacts of dams and their disruption of riverine sediment transport processes vary tremendously from one site to another, and the nature of the problem and mitigation options may be extremely complex. The regulatory environment is similarly variable, with water quality and sediment management issues potentially falling within the purview of multiple regulatory jurisdictions (federal, state, and local), and multiple users (water supply, recreation, fisheries, power production, irrigation, navigation, flood control, and upstream land uses). In some areas of the world, dam building is still being undertaken on a large scale, but in areas such as the United States, where impoundment capacity equals about 60 percent of annual runoff, the critical issue is no longer dam building but improved management of the existing infrastructure (Collier et al., 1995). Sediment management is not only essential for the sustained utilization of reservoir storage, but also is equally important for the maintenance of acceptable environmental conditions in rivers below dams.

---

## CHAPTER 19

---

# CASE STUDY: CACHÍ HYDROPOWER RESERVOIR, COSTA RICA

---

### 19.1 PROJECT OVERVIEW

---

#### 19.1.1 Project Description

The 54-Mm<sup>3</sup> Cachí hydropower reservoir was constructed on the Reventazón River in Costa Rica in 1966 (Fig. 19.1). It was first emptied for flushing in 1973, and over the next 18 years it was flushed 14 times. Flushing maintained the power intake free of sediment and reduced the reservoir trap efficiency from 82 to 27 percent. Flushing operations at this reservoir have been both well-documented and very successful in preserving storage capacity. This case study description is based on investigations conducted jointly by the department of Physical Geography, Uppsala, Sweden, and the Instituto Costarricense de Electricidad (ICE), which owns and operates the project, and on the first author's observation of the 1990 flushing event and discussions with Alexis Rodríguez, Ake Sundborg, and Margaret Jansson.

Cachí Dam is a single-purpose hydroelectric facility. The dam is a 76 m tall and 184 m long concrete arch structure with two radial crest gates and a 3.8-m-diameter power tunnel running 6.2 km to the power house. Three Francis-type impulse turbines are installed with 100.8 MW of capacity and 246 m of usable head. The dam has a single bottom outlet with two bottom gates. There is a vertical sluice at the upstream end and a radial gate at the downstream end of the outlet tunnel through the dam. Guides for an emergency sluice gate are provided at the upstream entrance to the bottom outlet. The bottom outlet was placed near the thalweg of the original river channel and immediately adjacent to the intake screen, a location that facilitates flushing of sediment from in front of the intake. Pertinent elevations are:

Full reservoir level	990 m
Spillway crest	980 m
Minimum generating level	960 m
Power intake sill level	936 m
Sill of bottom outlet	921.5 m

This is the first major hydroelectric project on the Reventazón River. Several others downstream of the Cachí site are in the planning stage.

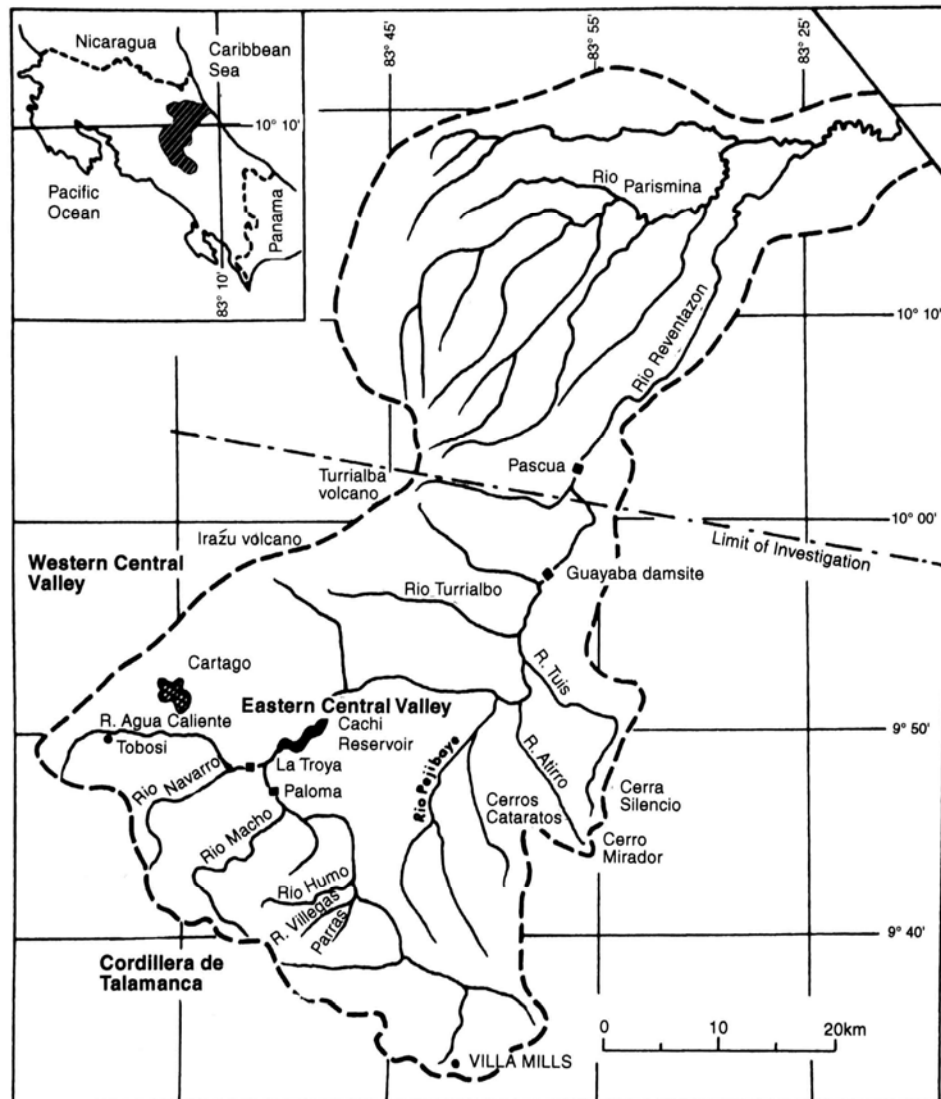


**FIGURE 19.1** Location map of Cachí reservoir on Rio Reventazón, Costa Rica, showing the tributary streams and gaging stations (*Ramírez et al., 1992*).

The reservoir had an original capacity of  $54 \text{ Mm}^3$  in 1966 and a surface area of 324 ha. It is approximately 6 km long with maximum and minimum widths of 1.5 and 0.13 km, respectively. A narrow section about 4 km upstream from the dam divides the pool into "upper" and "lower" basins. The floor of the lower basin of the impoundment consists of a series of relatively flat river terraces, onto which fine sediment is depositing, with a deep river channel maintained by flushing. In contrast, the upper basin is filling with sand and coarser material which is not removed by flushing. During drawdown for flushing the river exhibits a braided pattern across these coarse delta deposits in the upper basin. The bathymetric map (Fig. 19.2) illustrates these features. Figure 19.3 is a photograph of the reservoir looking upstream from the dam during the 1990 flushing event, showing the deep incised channel and natural river terraces on either

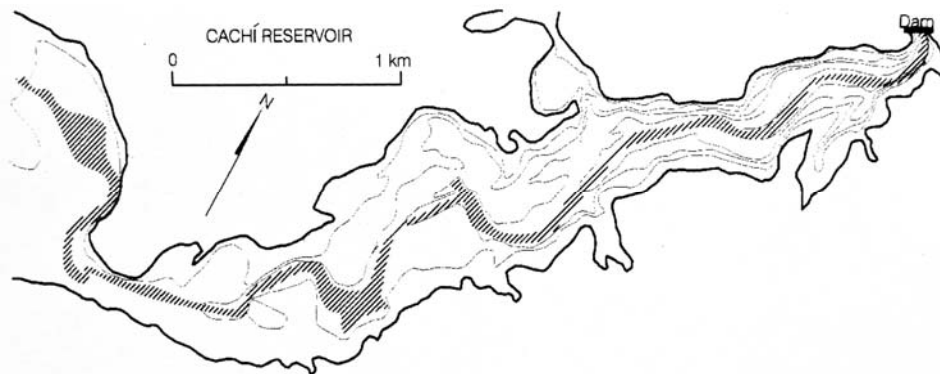


**FIGURE 19.2** Bathymetric map of Cachí reservoir lower basin with contour lines on 10-m intervals (Erlingsson, 1992b).



**FIGURE 19.3** Photograph of empty Cachí reservoir during flushing looking upstream from the dam, showing channel and river terrace near the dam (G. Morris).

side. Figure 19.4, a photograph of the lower portion of the pool looking upstream from the reservoir's right-hand bank, illustrates the configuration of the broad flat terrace that is normally submerged.

The reservoir has an extensive growth of water hyacinths (*Eichornia crassipes*), a floating macrophyte that can exceed 0.5 m in height and forms a dense floating mat across the water surface. ICE personnel indicated that prevailing winds usually pushed the hyacinths into the lake's upper basin, and, during the 1990 flushing most of the upper basin surface outside the active channel was covered with hyacinths trapped there by the falling water level. Hyacinths were largely absent from the main (lower) basin.



**FIGURE 19.4** Photograph of left side of Cachí reservoir during flushing showing broad flat terrace. The main flushing channel is in the background at a lower level and is barely discernible (*G. Morris*).

### 19.1.2 Hydrology

The dam controls 785 km<sup>2</sup> of the upper Río Reventazón watershed. The watershed is mountainous and rainfall varies from 1500 to 7000 mm/yr, generally increasing with elevation. Precipitation is well-distributed throughout the year, with September and October being the wettest months. At the Cachí station the diurnal temperature ranges typically from 14 to 27°C with about a 3° variation in the average monthly temperature between the coldest and hottest month. Watershed soils are derived primarily from volcanic ash, with sedimentary deposits found on valley floors. As a result of humid conditions the watershed is heavily vegetated. About 55 percent of the watershed is forested, primarily at higher (more moist) elevations and on steep slopes. Another 43 percent is divided about evenly between pasture and crops. The principal crop is coffee, covering almost 10 percent of the watershed, with sugar cane and vegetables covering most of the remaining crop acreage. Urban uses account for 1.3 percent of total land use.

Two hydrologic stations, La Troya and Palomo on the Río Navarro and Río Reventazón respectively, gage 82 percent of the watershed tributary to the dam. Runoff station data are summarized in Fig. 19.5 and Table 19.1.

## 19.2 FLUSHING

---

### 19.2.1 Operational Procedures

The power intake at Cachí Dam is located near the original riverbed elevation. A portion of the suspended load entering the reservoir is transported by turbidity currents to the area of the dam, and within several years of construction, sediments accumulating

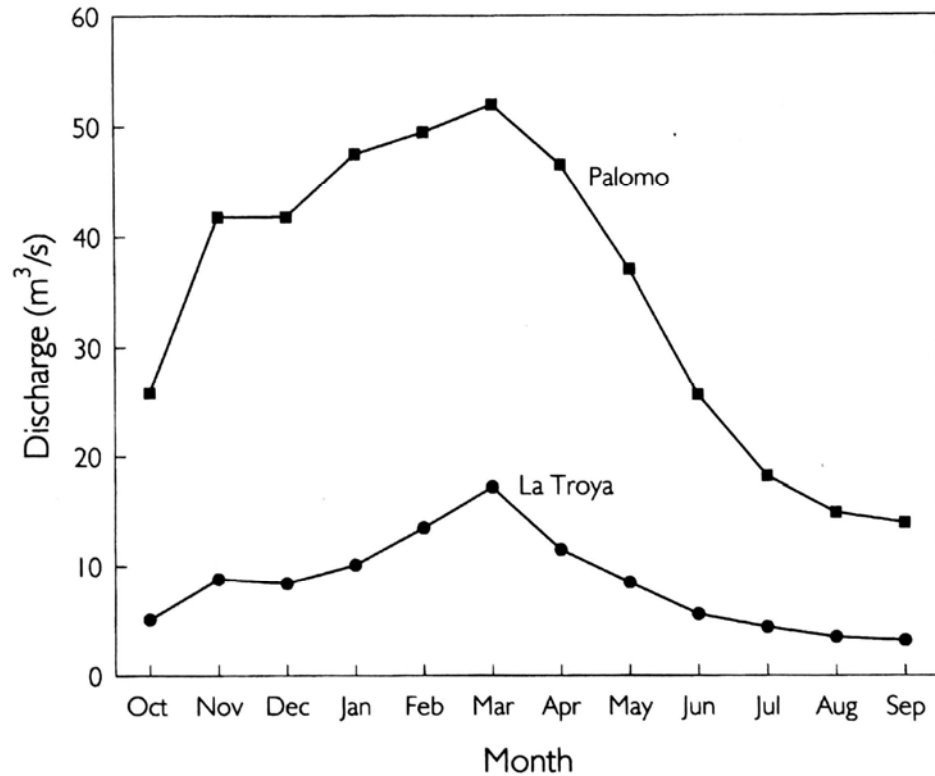


**FIGURE 19.5** Mean annual runoff at the two streamgauge stations tributary to Cachí reservoir. Period of record is August 1971 through August 1990 (after Ramírez *et al.*, 1992).

**TABLE 19.1** Summary Characteristics of Streamgauge Stations

Station	Drainage Area Km <sup>2</sup>	Mean annual runoff M <sup>3</sup> /3	Mean Runoff Depth mm/yr	Peak Discharge M <sup>3</sup> /3	Min Discharge M <sup>3</sup> /3
La Troya	274.6	8.5	976	340	1.6
Palomo	371.1	34.4	2920	593	5.4

near the dam began to be drawn into the turbines and interfere with hydropower production.

The reservoir was emptied for the first time in October 1973 to flush the accumulated sediments through the bottom gate, which was located immediately adjacent to the intake screen (Fig. 19.6). Because of the success of the first flushing operation, it was decided to repeat this operation every year during the wet season when the reservoir could be refilled quickly, and from 1973 to 1990 the reservoir was flushed 14 times.

Flushing occurs in three stages: slow drawdown, rapid drawdown, and free flow. During the slow drawdown period the reservoir level is lowered from 990 m to 965 m at the rate of 1 m/day, with turbines operating at full capacity. If inflow is too large to achieve the drawdown schedule by turbine flow alone, the discharge is augmented by



**FIGURE 19.6** View from the darn during flushing looking down on the flushing channel and power intake at Cachí reservoir. The intake is located adjacent to the thalweg in an area affected by turbidity currents. This location facilitates sediment removal from in front of the intake during flushing, as shown (*G. Morris*).

opening the crest gates when water levels are above the spillway crest, or opening the bottom outlet at lower water levels.

When the water level reaches 965 m, the turbines are stopped and the bottom gate is opened to initiate the rapid drawdown phase and evacuate the remaining water from the reservoir, a process which may require 5 to 10 hours. This is followed by the free-flow phase, which occurs when the pool has been completely drawn down and the river flows freely along the original river channel and through the bottom outlet. Free flow typically lasts 2 to 3 days, and during this period inspection and maintenance is performed on the power tunnel and other facilities. The bottom gate is then closed and the reservoir is refilled to the 990 level, which requires 16 to 21 days depending on inflow and power generation requirements.

The amount of sediment released in each stage of flushing varies widely from one event to another (Table 19.2), reflecting year-to-year variation in sediment inflow and accumulation along the flushing channel, different periods between flushing events, flushing duration (as long as 15 days in one year because of maintenance requirements), and operation of the bottom gate during drawdown. The power intake is at a higher elevation than the bottom outlet, and when drawdown occurs through the turbines relatively little sediment is evacuated during the drawdown phase. However, when high inflow requires the use of the bottom outlet to maintain the drawdown schedule, more sediment is released during drawdown. Thus, use of the bottom outlet during drawdown increases sediment release during this phase.

During the drawdown period, sediment deposits in the upper portion of the reservoir are scoured and transported downstream, where they become redeposited within the still-submerged portion of the river channel. As water levels continue to decline, this material is again exposed to scour and is transported closer to the dam. During a flushing event, an individual particle may be scoured and redeposited several times before reaching the dam.

**TABLE 19.2** Tons of Sediment Released by 14 Flushing Events at Cachí Reservoir, by Flushing Stage

Date	Slow drawdown	Rapid drawdown	Free flow	Total flushing
October 1973	nd	nd	nd	nd
August 1974	186,200	225,200	nd	(411,400)
October 1975	nd	nd	nd	nd
October 1977	nd	40,700	44,000	(84,700)
May 1980	nd	19,500	5,000	(24,500)
October 1981	14,600	348,900	113,400	476,900
October 1982	5,800	111,600	250,900	386,300
September 1983	28,700	402,400	114,300	545,400
October 1984	23,300	604,600	32,600	665,500
June 1985	nd	nd	nd	nd
July 1987	nd	nd	nd	nd
September 1988	61,600	627,000	577,100	1,265,700
September 1989	42,400	144,300	295,500	482,200
October 1990	27,200	278,700	347,100	653,000

nd = no data. The data in parentheses are estimates.

*Source:* Ramírez and Rodríguez (1992).

Scouring of sediment from the upper reaches of the reservoir and redeposition within the submerged river channel near the dam during the slow drawdown period creates a large supply of relatively fine sediment that is released as a slug of highly concentrated flow when the reservoir is fully emptied by opening the bottom gate for rapid drawdown. Peak sediment concentrations exceeding 400 mg/L have been measured downstream of the dam, occurring at the end of rapid drawdown and the beginning of the free flow phase, when riverine flow scours deposits near the dam. Extremely high suspended sediment concentration also makes this the period of maximum sediment evacuation. Even though rapid drawdown and free flow typically last more than 48 hours, about half the sediment release occurs in only 4 hours.

The suspended sediments released from the dam continue downstream and into the Caribbean Sea, forming a plume of turbid fresh water overlying the seawater. No studies have been undertaken on the effect of the sediment on downstream biology, but anecdotal information from Costa Rican observers indicates that the concentrated sediment release causes extreme mortality to all types of river biota.

### 19.2.2 Sedimentation Studies at the Reservoir

To construct a sediment budget for the reservoir, suspended-sediment data have been collected since 1972 by ICE at both the La Troya and Palomo gage stations upstream of the reservoir, and during flushing events intensive sampling was made at the El Congo station several kilometers downstream of the dam. The river passes through a steep narrow gorge between the dam and El Congo and there is little opportunity for either gain or loss of suspended sediment along this reach. Thus, the suspended-sediment data at El Congo is considered representative of the material released from the dam.

The ICE manual sampling program was based on depth-integrated water samples collected from verticals at each of the three stations using a USD 49 sampler operated from a funicular carriage. The samples were analyzed separately by drying at 110°C on 24-mm glass fiber filters in perforated porcelain crucibles, and the mean sediment concentration was computed. Sediment release during flushing was computed from suspended sediment measurements taken at intervals of 1 hour or less at the El Congo gage. At all gage stations, the bed material consisted of cobbles and bed load was not measured at any station.

Suspended sediment samples at the two upstream gages were collected frequently soon after the gage station was installed, but afterward sampling frequency declined to once or twice a month. More important, there were few data from high-inflow events. Sediment samples at the two inflow stations were used to develop sediment rating curves, the mean sediment concentration being converted into tons per day of sediment load according to the instantaneous discharge. The sediment load was plotted against instantaneous discharge on log-log paper and a straight line was fitted by eye. The annual load was computed by applying this rating curve to the series of mean daily discharges at each station. However, when the sediment inflow measured at the two upstream gage stations was compared against the sediment discharged during flushing at the downstream El Congo station, it was found that sediment discharged by flushing was typically 3 to 4 times larger than the estimated long-term sediment inflow, clearly an impossibility. Measurements at the El Congo station downstream of the dam were essentially continuous during flushing events and were considered accurate. Because flushing events lasted only a few days and were adequately sampled, the problem appeared to lie with underestimation of the inflowing load.

The problem with the sediment balance, coupled with ICE's interest in developing more detailed information on the sediment dynamics of the system and the possibility of

improving management of the reservoir flushing, led to the collaborative research effort between ICE and the University of Uppsala. Several types of studies were undertaken.

1. **Sediment inflow.** Historical suspended sediment data were analyzed to determine the accuracy of the sediment rating curves. During 1989-1990, an intensive data collection program was undertaken, including the use of recording turbidimeters, to improve the database for estimating the inflowing sediment load.
2. **Deposition and erosion patterns.** Patterns of sediment deposition in the reservoir were analyzed from air photos, historical measurements of sedimentation plates, x-ray radiographic analysis of sediment cores, side-scan sonar, subbottom profiling, and repeated depth soundings.
3. **Sediment flushing.** The October 1990 flushing event was observed and sediment release was measured by water sampling and turbidimeters.
4. **Sediment budget.** Data collected during 1989-90 were used to construct a detailed sediment budget across the reservoir for a one-year period.
5. **Synthesis.** A generalized theoretical and mathematical model for sedimentation processes in reservoirs was presented (Sundborg, 1992b), illustrated by data from Cachí.

### 19.3 SEDIMENT INFLOW

---

Historical data were reanalyzed and additional data collection was undertaken to better define the inflowing sediment concentration, as reported by Jansson (1992a).

#### 19.3.1 Rating Curve Analysis

Several types of problems could be responsible for underestimating the inflowing load into Cachí Reservoir. One possible problem was that sediment rating curves fitted by eye did not correctly represent the gage station dataset. The existing datasets from each of the two inflow gage stations were analyzed by fitting the following types of least squares regressions:

- Regression on the logs of all individual values.
- Regression of logged means. The mean sediment load was determined for discharge intervals and a regression was run on the logs of these means. The ICE samples were collected at regular timewise intervals, resulting in numerous sediment samples at low flows and very few at high flows. The data were also highly scattered. Replacement of multiple datapoints within each discharge interval by a single mean value reduced the apparent scatter in the dataset, and also eliminated the influence of the numerous low-flow data points on the shape of the overall regression curve, since numerous low-flow datapoints were replaced by a single value for the mean in each discharge class.
- Two regressions, on either individual values or means. Because the relationship between discharge and sediment load appeared discontinuous, two separate regression equations were developed for low and high discharge

values to improve the fit to the data. The transition point from one equation to another was selected by eye.

- Power function regression on all values.
- Power function regression on means.
- Two power function regressions on either individual values or means.

Some of the resulting curves are illustrated in Fig. 19.7.

The goodness of fit for these datasets cannot be determined by the regression coefficient. First, a regression coefficient on the logged variables says little about the correlation for the unlogged variables. Furthermore, in a sediment rating curve, the data points at higher discharges are more important (and typically less numerous) than the data points at low discharge values. The more numerous data points

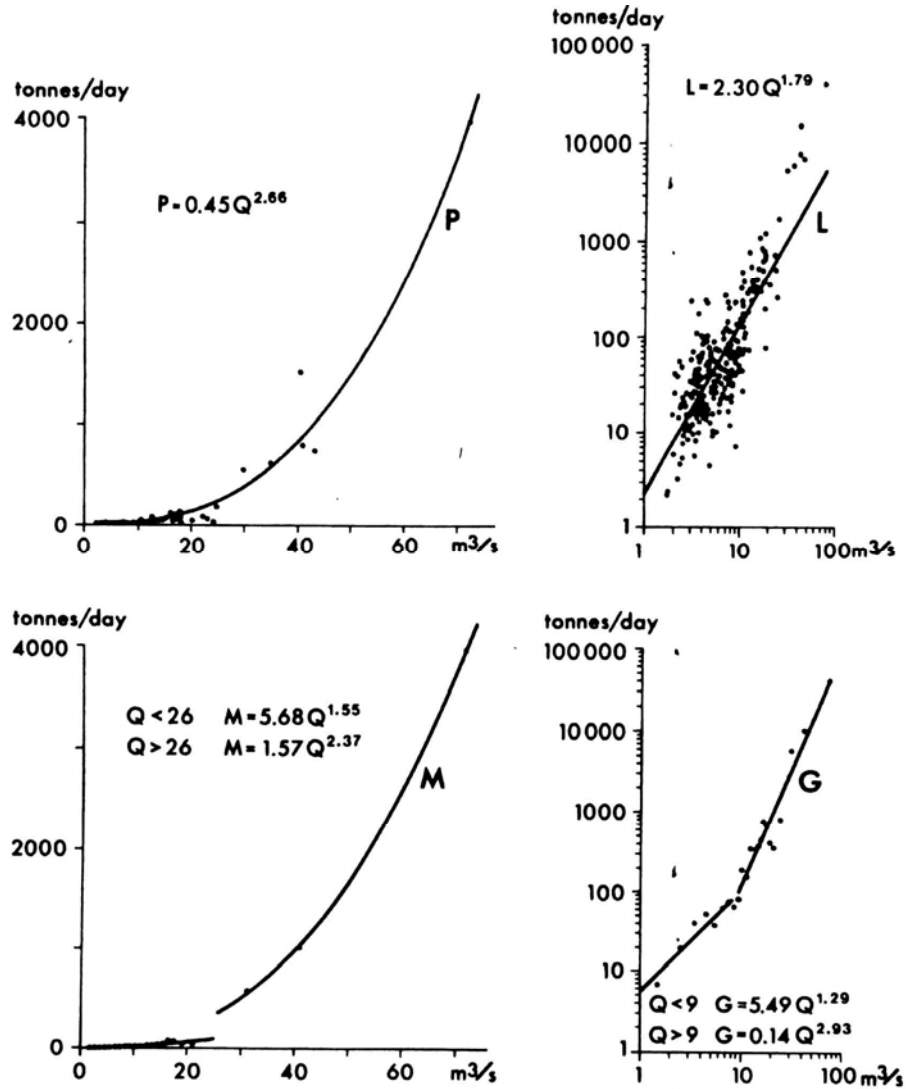


FIGURE 19.7 Several types of sediment rating curve equations derived at the La Troya station on Río Navarro (Jansson, 1992a).

at low discharge can weight the least square regression so it does not adequately represent the higher discharge values.

To determine the goodness of fit, the total load was computed by assigning a 24-hour duration for each sample data point and computing the total load in tons for the sample dataset as the sum of the loads on the sampled days. When the fitted rating curve is applied to all the individual discharge values in the dataset, it should produce a total load value very close to the computed sum of loads from the original dataset. The results, summarized in Table 19.3, show that although the visually fitted curve somewhat overestimated sediment load, it was considerably more accurate in describing the dataset than several of the mathematically fitted equations. This exercise showed that the problem with the sediment balance across the reservoir could not be attributed to an error in curve fitting.

### 19.3.2 Analysis of Computational Increment

The sediment rating curve had been developed from instantaneous values of concentration and discharge, but the load computations were made by applying the rating curve to the record of average daily (not instantaneous) discharges. Hydrographs on small, steep streams rise and fall rapidly, and mean daily discharge values reflect actual discharges only approximately. Since sediment load increases as a power function of discharge, applying an instantaneous-value rating curve to average daily flows will underestimate sediment load.

To determine the severity of this error, the load was recomputed with hourly and half-hourly discharge data from the arbitrarily selected inter-flushing period of 1982-1983, using several different rating equations. The results for La Troya (Table 19.4) showed that the use of average daily discharges underestimated sediment load by about 25 to 30 percent compared to computations with hourly data. There was little difference between the total load computed for hourly versus half-hourly data. A similar result was obtained using the Palorno data.

**TABLE 19.3** Percentage of Sampled Sediment Load Explained by Different Sediment Rating Equation

Type of Equation	% of measured load at inflow gage	
	La Troya	Palomo
ICE visual curve	109	115
Regression on all logged values	33	50
Two regressions on all logged values	—	83
Regression on logged means	61	102
Two regressions on logged means	89	108
Two regressions on logged means	101	—
Power function regression on all values	107	113
Two power function regressions on all values	—	113
Power function regression on means	113	—
Two power function regressions on means	106	133

*Note:* At La Troya, two regressions on logged means were developed for two different transition points. The La Troya data covered discharges only up to 72 m<sup>3</sup>/s because of lack of data (a single point) at higher discharges.

**TABLE 19.4** Variation in Sediment Load Estimates for Rio Navarro at La Troya. as a Function of Discharge Interval Used in Load Computations

Type of model	Sediment load, tons		
	Daily water discharge	Hourly water discharge	Half hour discharge
Regression on all logged values	28,753	36,015	35,814
Two regressions on logged means	46,037	63,520	64,725
Two regressions, logged means	53,065	73,815	75,229
Power function regression on all values	59,072	78,046	79,272
ICE visual fitted equation	61,493	80,380	81,674

*Note.* Data corresponds to the period October 11, 1982 through September 18, 1983. For discharges in excess of 72 m<sup>3</sup>/s, the equation load = 273Q<sup>1.16</sup> was used, representing a line through the two available data points at 72 and 458 m<sup>3</sup>/s, respectively.

### 19.3.3 Field Data Collection Program

The combination of improved rating equations and the use of hourly instead of daily discharge data produced a relatively small (about 30 percent) improvement in the estimate of the inflowing load, leaving a discrepancy on the order of 250 percent between the inflowing sediment load and flushing release. This indicated that the available dataset did not accurately reflect the sediment transport process in the river system. Even though the dataset extended back to 1971, an apparently significant record length, there were two important deficiencies in the dataset: (1) because of regular diurnal variations in discharge the sediment data were mostly collected from the recession limb of hydrographs, and there were few data points from the rising limb; and (2) the data did not adequately characterize high-discharge events responsible for most sediment delivery.

### 19.3.4 Diurnal Variation in Discharge

Suspended sediment samples were normally collected around 10:00 A.M. However, the hydrograph record (Fig. 19.8) revealed the importance of regular afternoon rainstorms which caused discharge to increase quickly in the late afternoon and recede at night. Water quality sampling at 10:00 A.M. coincided with the end of the receding hydrograph, a period of minimum sediment discharge.

### 19.3.5 Critical Discharge Classes

Streamflow varies over a wide range, and a flow-duration analysis will reveal that some discharge intervals are much more important than others in terms of both water and sediment discharge. It is essential that a sediment rating curve properly reflect sediment loads over the range of discharges responsible for most of the sediment transport, which is characteristically not the most frequent discharge class. With the

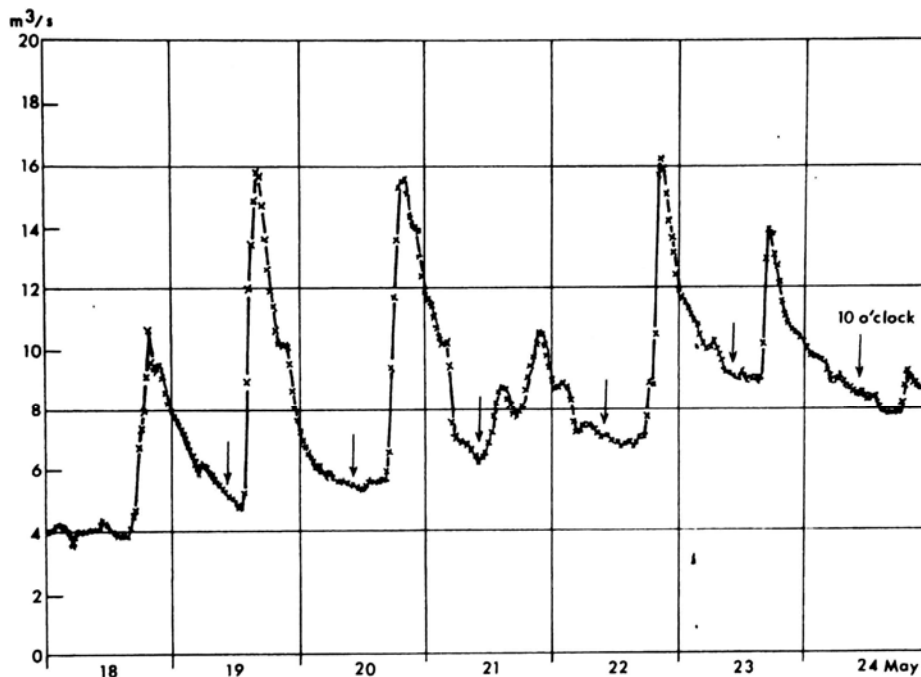


**FIGURE 19.8** Discharge hydrograph at La Troya for 1 week. Peak discharges in this watershed characteristically occur in the evening. Thus, suspended sediment samples collected around 10:00 each morning typically correspond to the falling limb of the hydrograph, when sediment concentrations are lowest (*Jansson, 1992a*).

Palomo gage as an example, hourly discharge data for 1989-1990 were divided into 10  $\text{m}^3/\text{s}$  discharge classes and analyzed to produce the flow-duration graph in Fig. 19.9. The 10- to 20- $\text{m}^3/\text{s}$  discharge class was represented with the greatest frequency, but the 40- to 50- $\text{m}^3/\text{s}$  class produced the greatest volume of water discharge.

The three sediment rating curves shown in Fig. 19.9a were applied to the hourly discharge data to estimate the relative importance of each discharge class with respect to suspended sediment load, producing the values of sediment load in each class summarized in Fig. 19.9b. Sediment loads were computed by applying the rating curve to the mean discharge value within each water discharge class, and then multiplying by the discharge duration for that class. Despite the large difference in sediment loads at peak discharges given by the three rating curves, this has relatively little effect on the total sediment load because the highest flows occur infrequently. Sediment load computations at Palomo are most sensitive to discharges in the range of 30 to 200  $\text{m}^3/\text{s}$ , and particular attention must be given to accurately fitting the sediment rating curve within this range.

### 19.3.6 Turbidity Measurement

Intensive sampling was conducted during the 1989-1990 inter-flushing period to generate a representative dataset for computing new sediment rating curves. Given the difficulty of collecting representative suspended sediment data from small watersheds

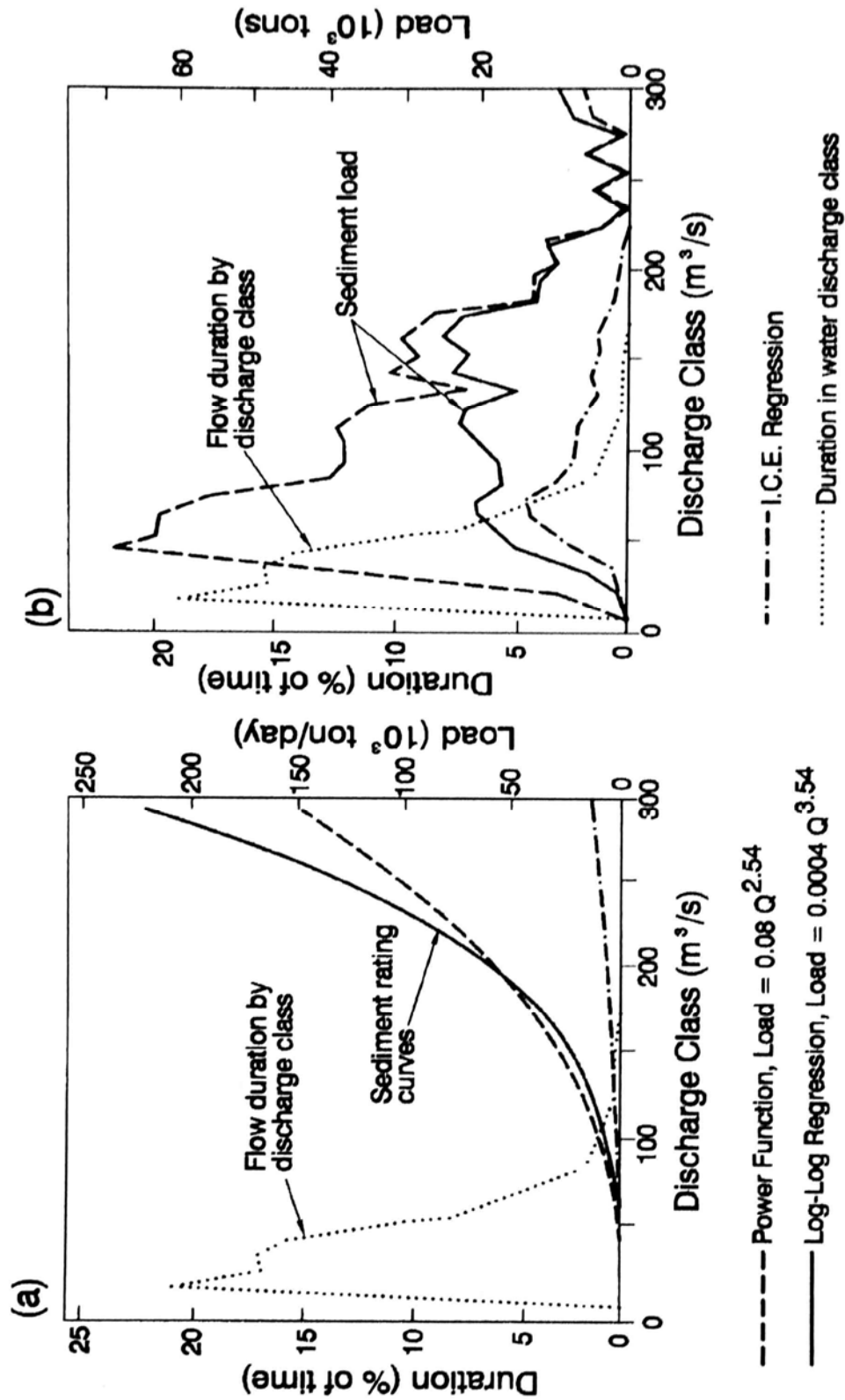


**FIGURE 19.9** (a) Flow duration curve at Palomo gage based on hourly discharge data during 1989–1990 and three different sediment rating curves in tons/day as a function of discharge. (b) Flow duration as a function of discharge interval and total sediment load as a function of discharge interval computed for each of three sediment rating curves (Jansson, 1992a).

with fast-rising peaks, turbidimeters were used to continuously record sediment concentration. Two types of turbidimeters were used, the Hach Surface Scatter 6 turbidimeter and the Monitek Clam 52 LE. Submersible pumps were used to deliver water to the turbidimeters (Fig. 19.10). Data were collected by data loggers at intervals of approximately 5 to 6 minutes and analyzed with an electronic spreadsheet. Both types of turbidimeters experienced problems with clogging by heavy sediment loads and debris, failure of pumps and transformers, and other logistical problems. The Hach instrument, with its smaller water delivery tube, was more prone to clogging by leaves and the husks of coffee beans discarded to the river during coffee harvest season. The larger interior chamber in the Monitek instrument was less prone to clogging, but produced low flow velocities that allowed sediment to settle out at high concentrations (e.g., in measuring sediment concentrations downstream of the dam during flushing).

The turbidimeters were calibrated (NTU versus suspended solids) by using suspended sediment data collected from the stream over a range of discharges while the turbidimeters were operating. A power function regression was developed for the Hach instrument having the form:

$$\text{Concentration} = 0.59 \text{ NTU}^{1.30} \quad (19.1)$$

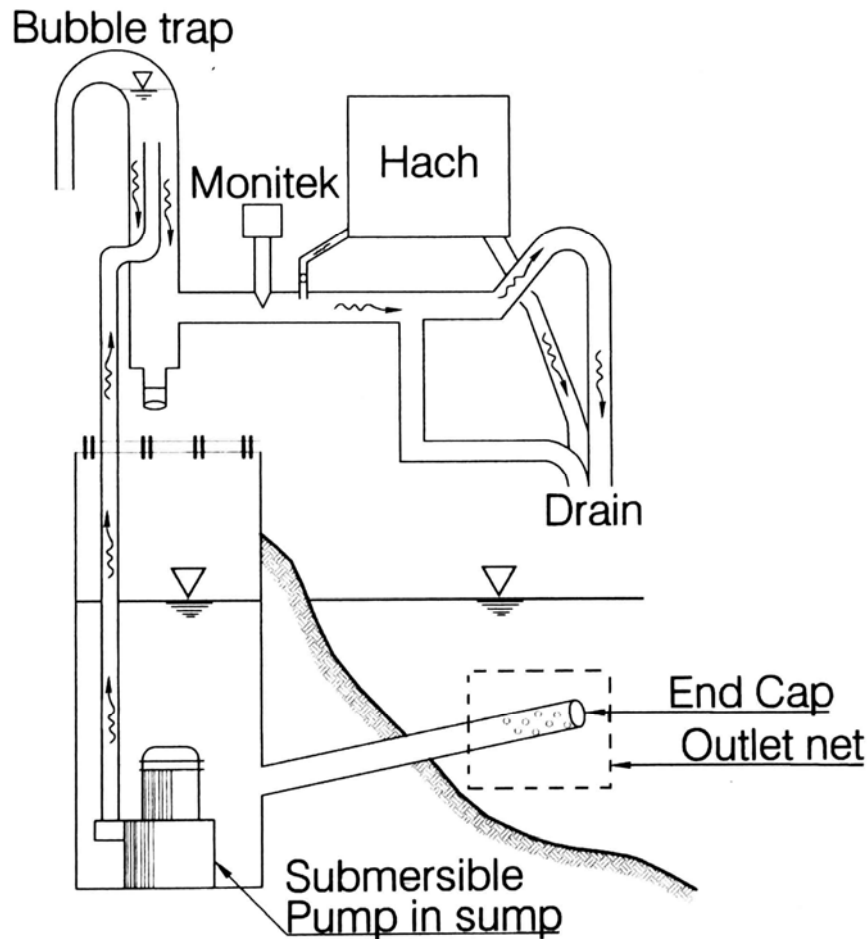


FIGURE 19.10 Sample collection arrangement for turbidity monitors (Jansson, 1992a).

The calibration curve for the Monitek instrument was of the form:

$$\text{Concentration} = 1.22 \text{ PPM} + 71 \quad (19.2)$$

where PPM is the Monitek instrument reading.

Because the instruments continuously report turbidity values, even though these values may be spurious, it was necessary to scan the data for reasonableness to search for periods of clogging. Sudden declines in turbidity, or periods when turbidity remained essentially stable despite significant changes in discharge, were taken as signals of clogging. For example, Fig. 19.11a shows a short-duration turbidity spike at Palomo which produces an open discharge-concentration loop. This could be caused by high sediment discharge from an area near the gage station (e.g., farms) with little sediment contribution from the upper watershed. It could also be caused by clogging of the turbidimeter intake during the event. Because these events with extremely short turbidity peaks seemed to occur primarily during the coffee processing season, and were otherwise atypical, it was thought to represent a period of spurious readings due to clogging of the turbidimeter, and these data were discarded. Figure 19.11b shows a more typical event at this same gage station.

At La Troya, the turbidity at low flows was affected by waste discharge from an upstream factory and by in-stream mining, both of which caused turbidity spikes with no increase in discharge. To avoid the irregular turbidity readings caused by waste discharges and mining, the sediment rating curve at La Troya was constructed by using data only from the rising and falling limbs of hydrographs when sediment concentrations exceeded 1000 mg/L. The resulting dataset at La Troya contained 5763 data points at 6-min intervals, representing 23 different runoff events between September 1989 and October 1990 (Fig. 19.12). At La Troya gage the discharge peaks typically preceded the turbidity peak, generating a counter-clockwise loop and a high degree of scatter in the dataset. At Palomo the opposite pattern was observed; the highest turbidities occurred on the rising limb creating a clockwise loop.

### 19.3.7 Interpretation of Turbidity Data

The correlation of turbidity data to suspended solids is problematic. The relationship varies as a function of the monitoring site, stage, type of instrument, calibration, grain

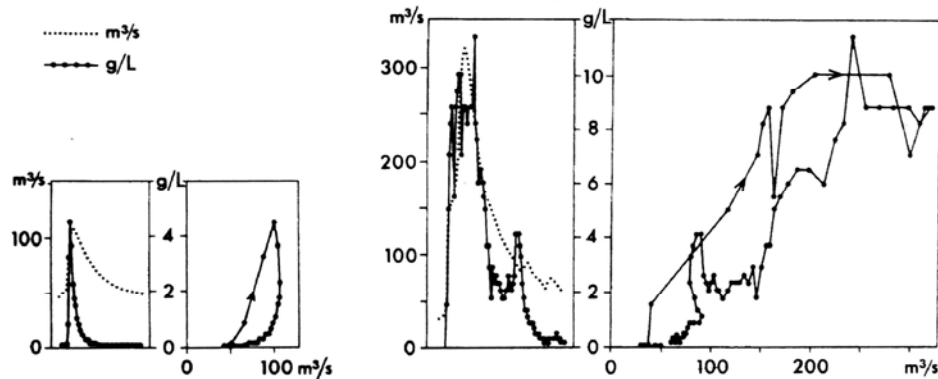


**FIGURE 19.11** (Left) Short-duration turbidity spike at Palomo gage station which creates an open discharge-concentration loop, probably caused by clogging of the turbidimeter during coffee harvest season. (Right) More typical discharge-concentration relationship at Palomo outside of coffee harvest season when clogging is not a problem (Jansson, 1992a).

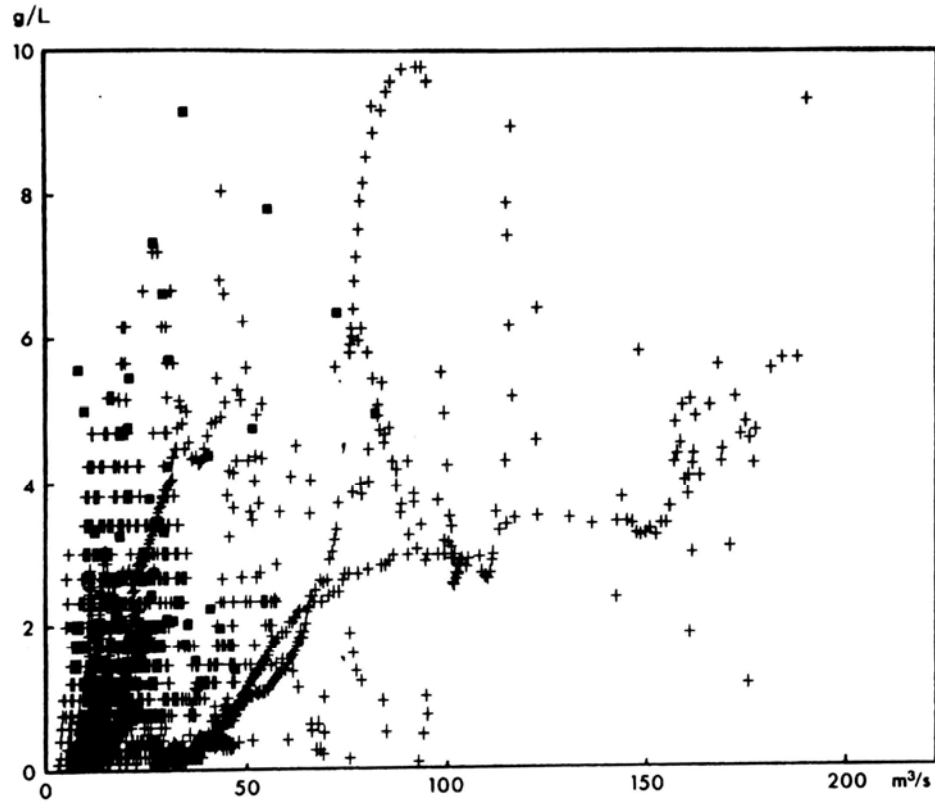


**FIGURE 19.12** Concentration versus discharge dataset at La Troya based on turbidimeter measurements and used to construct sediment rating curves. In places the traces of rising or falling hydrographs from individual events are discernible (*Masson, 1992a*).

size distribution, and other parameters. Furthermore, turbidimeters collect point samples and the relative depth of the fixed measurement point will vary as a function of stage. It was intended to continuously measure both streamflow and turbidity, and compute the sediment load by using a correlation between suspended solids and turbidity. However, numerous field problems intervened and the turbidity record was far from complete, making it necessary to construct a rating curve from the turbidity data. Despite problems and limitations, continuous turbidity measurements were obtained from both the rising and falling limbs of several hydrographs, and these data provided a more representative dataset than the water quality sampling program with its population of data points taken mostly from the falling limb.

To evenly distribute the regression weighting factor across the full range of the available data, the dataset was divided into  $2\text{-m}^3/\text{s}$  discharge intervals and the mean value of the concentration data points falling within each discharge class was computed. Three rating curves were computed from these means. A power regression on the mean values gave:

$$L = 4.10 Q^{1.91} \quad (19.3)$$

The other two equations were developed after discarding the mean value for the highest discharge class in the dataset, since it contained only one observation. After removing the highest data point the power regression on the means became:

$$L = 28.77 Q^{1.51} \quad (19.4)$$

A log transformation of the means, a log-log regression, gave:

$$L = 14.18 Q^{1.645} \quad (19.5)$$

In these equations  $L$  = sediment load in tons/day and  $Q$  = water discharge in  $m^3/s$ .

The resulting sediment rating curves at La Troya are shown in Fig. 19.13, along with the mean load values in each water discharge class. Table 19.5 compares the load computed by each equation against the load computed using the 5763 points in the original dataset, and also shows the total load for the 1980-1990 period computed by each equation. This table illustrates the importance of equation-selection on the load computations.

A similar procedure was followed to develop a rating curve at Palomo which had 6140 data points representing the rising and falling limbs of 22 distinct and significant runoff events, plus several low-flow intervals between individual events. The longest continuous record was a 10-day period in October. Data from this station were affected by periodic releases from the El Macho upstream hydropower station, which increased discharge with no corresponding increase in turbidity. Two sediment rating equations were developed from the means, a power function and a log-log regression. The two equations were first tested by comparing the total sediment load predicted by the

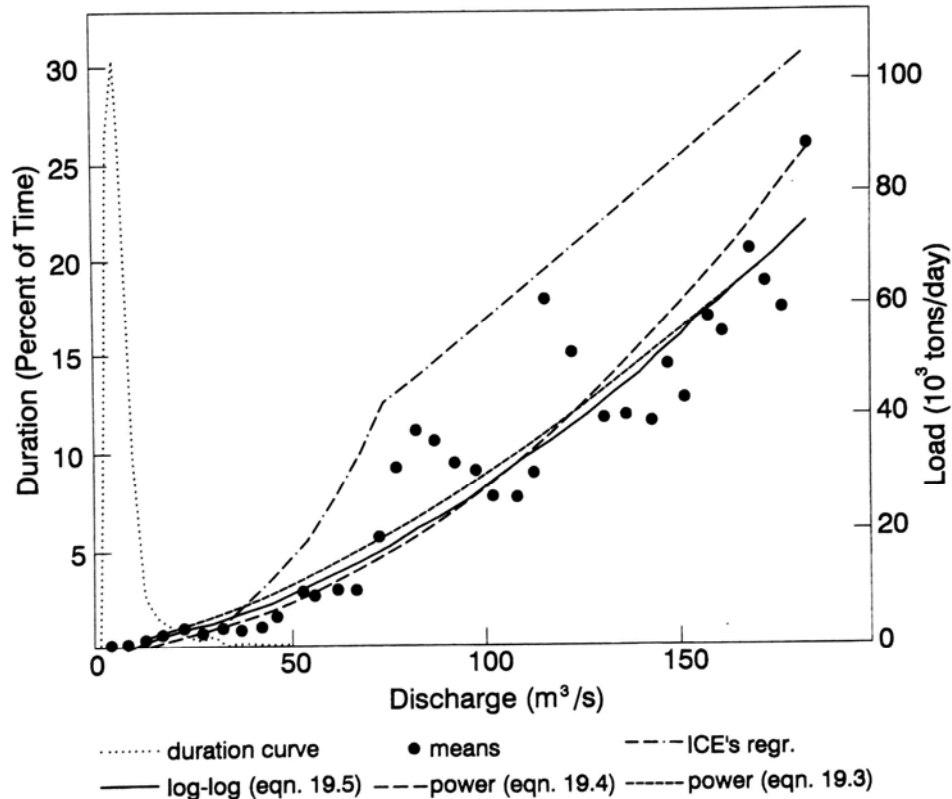


**FIGURE 19.13** Sediment rating curves at La Troya based on turbidity data. Each circle is the mean for a discharge interval (*Masson, 1992a*).

**TABLE 19.5** Sediment Load Computed by Various Rating Curves Applied to Original Dataset from which the Equations Were Derived, and for the 1989-1990 Period

Load computed for dataset	Power [Eq. (19.3)]	Power [Eq. (19.4)]	Log-log [Eq. (19.5)]	ICE's equation
Load for original dataset*:				
Tons	47,846	69,132	57,243	78,612
% of ICE equation	61	188	73	100
Load for 1989-1990 inter-flushing period:				
Tons	167,241	312,421	238,695	222,047
% of ICE equation	75	141	107	100

\*The load computed from the dataset values was 57,667 tons.

equations against the measured load in the dataset. At this station there were some manually collected water quality data at very high water discharges, which were much lower than the sediment load values predicted by the rating curves. Therefore, these additional data points were added to the record obtained by the turbidimeter to augment the sparse record at high discharges and the regressions were recomputed. The log-log regression fit the data very well, except that it appeared to overestimate values at higher discharges. Therefore, an eye-fitted line was used for discharges over 206 m<sup>3</sup>/s.

### 19.3.8 Unsampled Area

The soils, drainage density, and land use indicated that the sediment yield from the unsampled area near the reservoir would probably be similar to the yield from the watershed tributary to the La Troya gage station. Therefore, the sediment discharge from the ungaged area was based on the sediment yield at La Troya with a correction for watershed area.

### 19.3.9 Conclusions Concerning Sediment Inflow

The original ICE equation provided a reasonable estimate of the sediment load at the La Troya gage station. However, the load at the Palomo gage was seriously underestimated at discharges over 100 m<sup>3</sup>/s, and this was the primary factor responsible for the large discrepancy in the sediment balance across the reservoir. At Palomo the rating curve had a clockwise loop, meaning that suspended sediment concentrations on the rising limb were much higher than on the falling limb, which provided most of the data points for the original rating curve. The original sediment rating curve had been derived from a nonrepresentative dataset.

## 19.4 SEDIMENT DEPOSITION AND EROSION

Various procedures were used to quantify the amount and pattern of sediment deposition and erosion within the reservoir.

### 19.4.1 Sedimentation Plates

In 1976, ICE set out five sedimentation plates in different parts of the reservoir and returned in subsequent years to measure deposition depth over each plate. From this, deposition was computed by apportioning the reservoir area among the plates with Thiessen polygons. In 1981, additional plates were set out, for a total of 39 measurement points. However, as burial depth increased the plates became more difficult to find, resulting in lost plates and incomplete data.

### 19.4.2 Topographic Survey

In June 1985, the reservoir was emptied for 15 days and a survey crew mapped the topography of the flat terraces and measured total sediment depth. It was estimated that  $1.03 \text{ Mm}^3$  of sediment had accumulated on  $1.027 \text{ km}^2$  of terraces in 19 years of impounding, for an average deposition depth of 1.0 m.

### 19.4.3 Grain Size Analysis

Twenty-eight samples of surface sediment were collected from the right-hand terraces when the reservoir was emptied in 1983, and grain size was determined by the densitometer method (ASTM-D422). The results, summarized in Fig. 19.14, show that grain size on the terraces declined moving downstream, from an average of 0.70 mm in the upper basin to less than 0.015 mm near the dam. The main channel was not sampled.

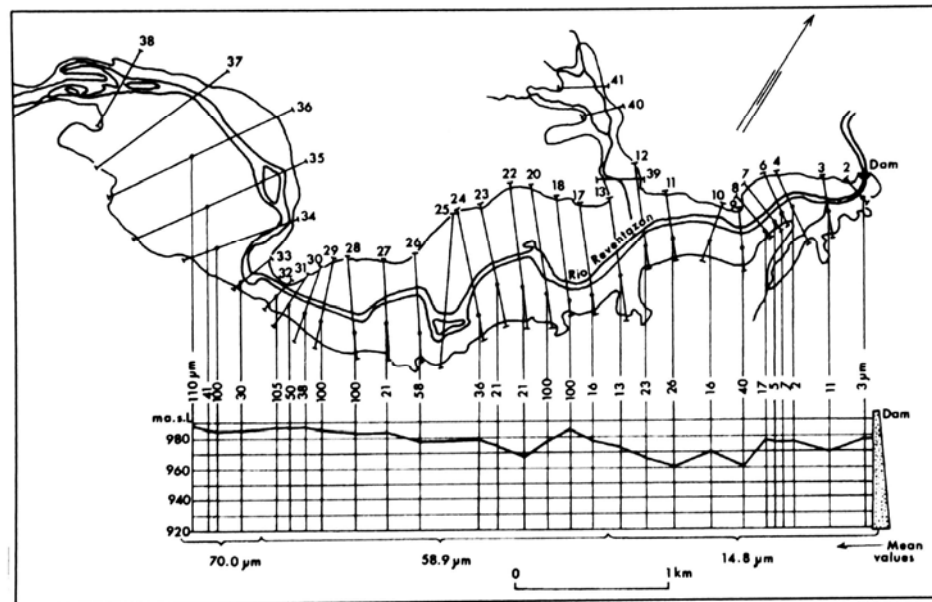


FIGURE 19.14 Elevation and median grain size of sediments on the surface of right-hand terraces (Ramírez et al., 1992).

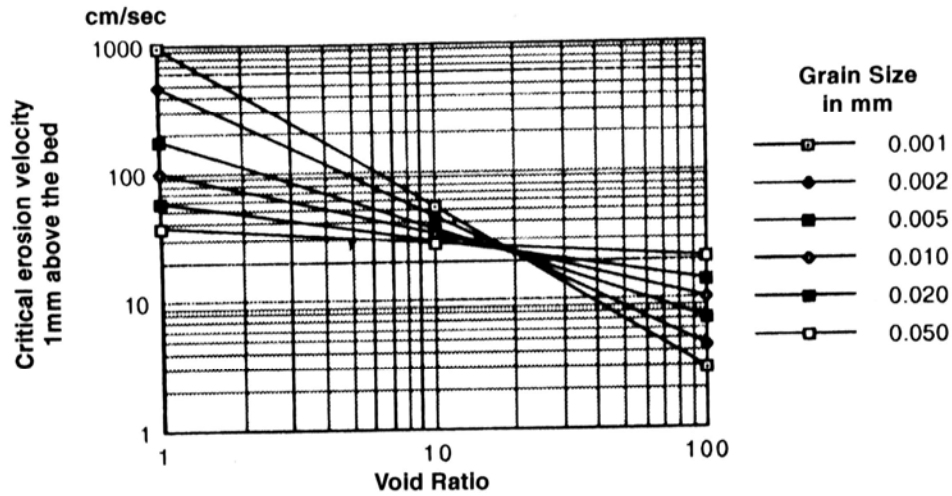


FIGURE 19.15 Preliminary calculated relationship between critical erosion velocity and void ratio as a function of grain size (Axelsson, 1992).

#### 19.4.4 X-Ray Analysis

Reservoir sediments were analyzed by x-ray radiographic techniques (Axelsson, 1992) using 15 shallow cores (0.2 to 0.5 m deep) collected with a valved gravity corer plus nine surficial grab samples. Rectangular cores, 30 × 60 mm, were collected, since either square or rectangular cores of uniform thickness are required for quantitative interpretation of radiographic images. Unextruded cores with adjoining bottom water were transported, stored, and then irradiated in the upright position at a laboratory in San José, Costa Rica. A seven-step aluminum wedge was irradiated simultaneously with the cores for density calibration.

The x-ray image density varies as a function of the density of the material in the core. Flushing and air drying exposes the soft sediment to desiccation, creating an alternating sequence of denser surface crusts sandwiched between softer subcrustal material. By taking cores at intervals of months or years, and by correlating the sedimentary sequences between cores, it is possible to determine contemporary rates of sedimentation. However, only one set of cores was available at Cachí, and sediment accumulation rates could not be determined by radiography because the sediment sequence could not be correlated over time.

Air drying of the sediment and formation of a surface crust during drawdown substantially reduces the erodibility of the sediments. Axelsson developed from a variety of sources a preliminary relationship between critical erosion velocity and void ratio in the sediments, as related to grain size (Fig. 19.15). Void ratios in Cachí reservoir ranged from 20 in gas-rich organic layers to less than 2 in the hard crusts formed on exposure during flushing. Newly deposited silt and clays at Cachí had void ratios often exceeding 5.

#### 19.4.5 Side-Scan Sonar

Dual-frequency (104 and 435 kHz) side-scan sonar in conjunction with an electronic positioning system were used to produce a side-scan sonar mosaic of the entire lower portion of the reservoir (Erlingsson, 1992a). The survey was accomplished by making three passes along the axis of the reservoir on three parallel tracks 150 m apart. The strength of the reflected side-scan sonar signal causes gray-scale differences in the sonar-

graph images, and the resulting sonargraph is a 16 gray-scale map which reflects both bottom topography and bottom material. Factors that influence signal strength include angle of incidence, grain size of the bottom material, mineral composition, porosity, gas bubbles in the sediment, and bottom flora and fauna. A single track in the shallow water in the upper portion of the reservoir was made without the positioning system, but the return signal strength was extremely weak because of the coarse-grain material.

Hydrogen sulfide ( $H_2S$ ) gas bubbles are formed in the sediments by the anaerobic decomposition of organic matter. Cachí sediments are relatively high in organic material, with loss-on-ignition values averaging about 4 percent and reaching 10 percent in soft sediments. These organics are derived primarily from hyacinth and lake plankton detritus. The warm temperatures in this tropical reservoir accelerate the rate of organic decomposition and the formation of gas bubbles. The bubbles create sharp density interfaces within the sediments, strongly scattering acoustic signals. Boat traffic can also generate acoustic noise that interferes with sonar, and at Cachí (where there was no boat traffic) the sonar sometimes picked up strong acoustical interference from the hydropower plant.

The bottom characteristics at a number of locations were known from the sediment cores, making it possible to correlate the following bottom conditions against gray-scale units on the sonargraph: median grain size, wet bulk density (related to porosity), and depth to visible gas in the x-ray films of the cores. Through a series of regression correlations, it was determined that variation in grain size was the most important gray-scale parameter, giving a correlation coefficient of  $R^2 = 0.71$  for an exponential regression. Finer sediments gave a stronger echo (darker image). Variations in wet bulk density and gas content were poorly correlated to gray-scale value. Bottom flora was absent in the reservoir (water hyacinths float on the surface) and tube worms were present at very few locations, so biotic factors were ignored. Organic detritus caused low wet bulk density values.

In the sonargraphs, it was found that the thalweg generally became darker in the downstream direction, interpreted as a decrease in grain size and wet bulk density. The sonargraph showed a dark gray meander along the thalweg, interpreted as a zone of deeper sediment deposition by turbidity currents. Despite small grain size, terraces showed lighter gray-scale values, interpreted as reflection from gas within 15 cm of the sediment-water interface and signal attenuation by deposits overlying the gas layer.

#### **19.4.6 Subbottom Profiler**

The higher frequency sonar is reflected strongly in the immediate vicinity of the water-sediment interface, thereby registering the bottom of the reservoir. The lower-frequency (14 kHz) subbottom profiler signal penetrates farther and is reflected from boundaries within the sediment deposit, plus backscatter within the sediments. When a subbottom profiler is used in a reservoir, the three principal boundaries of interest are (1) the sediment-water interface, (2) the boundary between the surface crust formed by desiccation during the most recent drawdown (flushing) and the overlying recently deposited material, and (3) the boundary between the original bottom and the material deposited since impoundment. Deposition depth is determined as the difference between these boundaries. Because of the presence of gas, the acoustic signals penetrated to only about 10 cm, even in the thalweg where deposition depth was known to be much deeper. This abundance of gas made it impossible to obtain usable readings of deposition depth by acoustic methods.

### 19.4.7 Repeated Depth Soundings

Two depth sounding surveys were made of the reservoir before and after the October 1990 flushing to determine the amount of material eroded from the reservoir and the areas where erosion occurs during flushing. The surveys were performed with a 192-kHz echo sounder, a total survey station giving the distance and bearing to the boat every second, and a portable computer which calculated position on the national grid and stored the information on disk. Survey cross sections ran perpendicular to the reservoir axis at 100-m intervals. Depth data were recorded on paper, digitized, edited graphically, and then converted into files of depth as a function of time. Depth errors were expected to be on the order of 0.1 m. The total survey station was accurate to within 0.1 m, but the positioning prism on the boat was mounted 4.5 m ahead of the sonar transducer. To minimize this positioning error, the travel time of 4.5 m at the survey speed of 2.8 knots was computed and the corresponding time delay was added into the depth data prior to merging with the coordinate data file. Because heavy subbottom profiling equipment was carried in the boat during the first survey only, there was a difference in the vessel draft of about 3 cm, which was compensated for. Coordinate data and time-delayed depth data were merged to create a file of x, y, z datapoints, and all data values within each 10- x 10-m grid along the survey lines were averaged to determine the average depth within each grid during each of the two surveys. There were 542 grid boxes having datapoints for both surveys, and depth differences were computed for these locations.

From the 542 coincident grid boxes, it was found that most erosion occurred along the thalweg with erosion depths typically in the 0.5- to 1.5-m range, similar to the deposition depth. Most of the sediment delivered to the reservoir was deposited along the main channel and subsequently removed by flushing. About 750,000 m<sup>3</sup> of material was eroded from the main channel in the surveyed area (the lower reservoir basin), equivalent to about 300,000 tons dry weight of sediment using a bulk density of 0.4 g/cm<sup>3</sup>. Erosion from the unsurveyed upper reservoir basin was estimated at 50,000 to 100,000 tons by interpretation of side-scan sonar and subbottom profiling. Total erosion during flushing was estimated at 350,000 to 400,000 tons.

River terraces submerged by the reservoir are elevated 5 to 10 m above the channel thalweg. They showed either a consistent increase in sediment accumulation of 0.1 to 0.2 m, or a pattern of alternating positive and negative changes. The largest net accumulation (0.1 to 0.2 m) occurred on terraces covered with hyacinths during flushing. Hyacinths prevented desiccation of surface sediments and also contributed organic debris. Accumulation depth was greatest on lower terraces adjacent to the channel, or close to the river inflow. The rate of sediment accumulation was small on the larger and higher terraces. Turbidity currents transporting the inflowing fines along the main channel probably play a large role in this distribution pattern. The Swedish team observed a turbidity current during a rainstorm when the reservoir was full. The plunge point was observed to occur in the narrow region separating the upper and lower reservoir, based on changing water color and hyacinth movement.

## 19.5 SEDIMENT RELEASE

---

### 19.5.1 Erosion Processes Observed during Flushing

Sundborg (1992a) reported on the erosional processes observed during drawdown and flushing. The upper basin has a rather flat and shallow bottom and is normally covered with water hyacinths. It contains beds of sandy or gravelly material from delta deposits, and relatively small amounts of erosion were observed from this area during flushing. In the main basin minor gullies were formed across the terraces during the slow draw-down phase, and on terrace slopes there was a tendency for sediments to be eroded by wave action. However, there were no traces of any generalized erosion of sediment from

the surface of the terraces, except for the small gullies draining tributaries which reached a maximum width and depth of about 2 to 3 m.

Most of the inflowing sediment is deposited along the main channel, which is also the zone of maximum erosion. The slow drawdown exposed channel sediments to scouring action, and finer sediments were transported toward the dam. Each opening of the bottom gates during slow drawdown released highly turbid water for a short period, discharging fine-grained material that had been eroded from along the thalweg and transported to the dam during the previous day's drawdown.

During the rapid drawdown phase (from 960 m to 921 m over a period of about 10 hours) the erosion and release of thalweg sediments was spectacular. This was especially true during the last few meters of the drawdown when the water level declines rapidly because of the reduced water surface area. So much sediment was being eroded and transported during this period that hyperconcentrated flows were observed along the flushing channel. Scars formed by sediment slumping were observed within the reservoir after flushing. A photograph looking downstream along the left bank of the main channel during flushing is shown in Fig. 19.16.

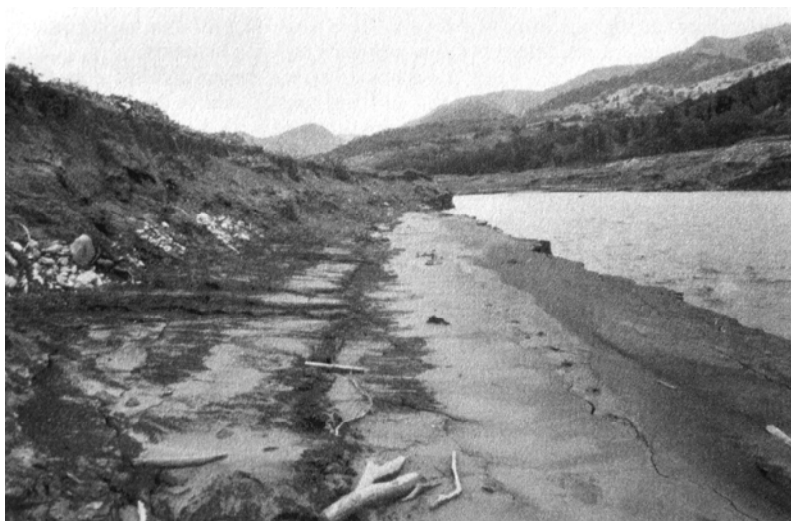


**FIGURE 19.16** Photo looking downstream along main channel during flushing, illustrating higher river terrace on the left, recent sandy deposits being eroded with visible tension cracks, and the main channel on the right which has already eroded to the original armor layer in the river (*G. Morris*).

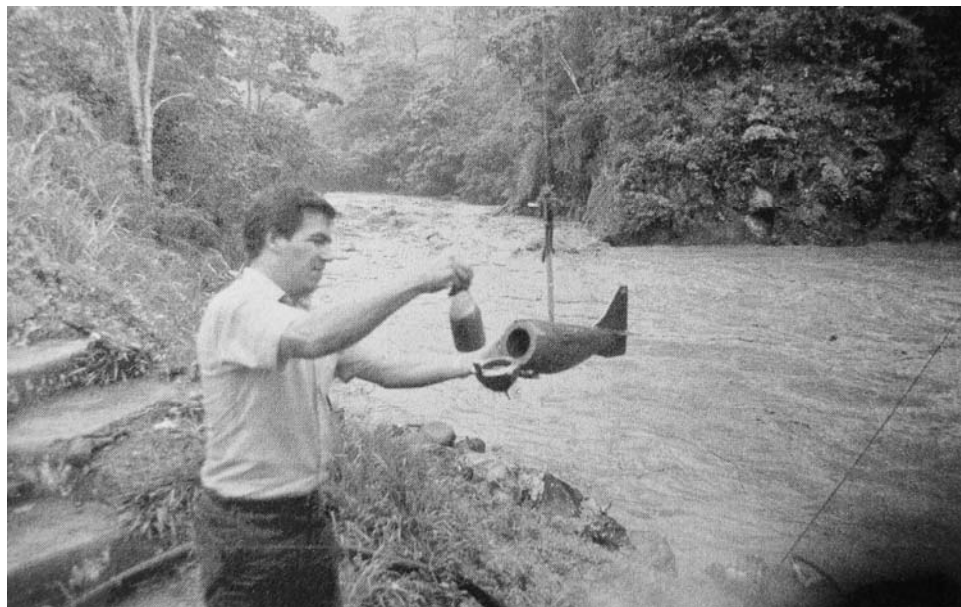
The turbid water released from the reservoir, as monitored from a light aircraft, was observed to flow downstream to the ocean where it creates a stratified plume of turbid water extending into the Caribbean Sea. Substantial amounts of sediment were deposited on low floodplain areas and bars between the dam and the ocean. These deposits would be eroded during subsequent floods.

### 19.5.2 Sediment Release during Flushing

Jansson (1992*b*) summarized the monitoring of sediment outflow during flushing. ICE monitored sediment discharge during flushing events by taking depth-integrated water samples at 15- to 30-min intervals at the El Congo gage during the rapid drawdown and free-flow periods (Fig. 19.17). The slow drawdown phase was sampled only intermittently, as relatively small amounts of sediment are released during that phase. Because the flushing period was controlled by gate operations and could easily be



(a)



(b)

**FIGURE 19.17** Suspended solids measurement at El Congo station downstream of Cachí reservoir during flushing. (a) Funicular carriage with sampler hanging beneath. (b) removal of sample bottle containing sediment. (*G. Morris*)

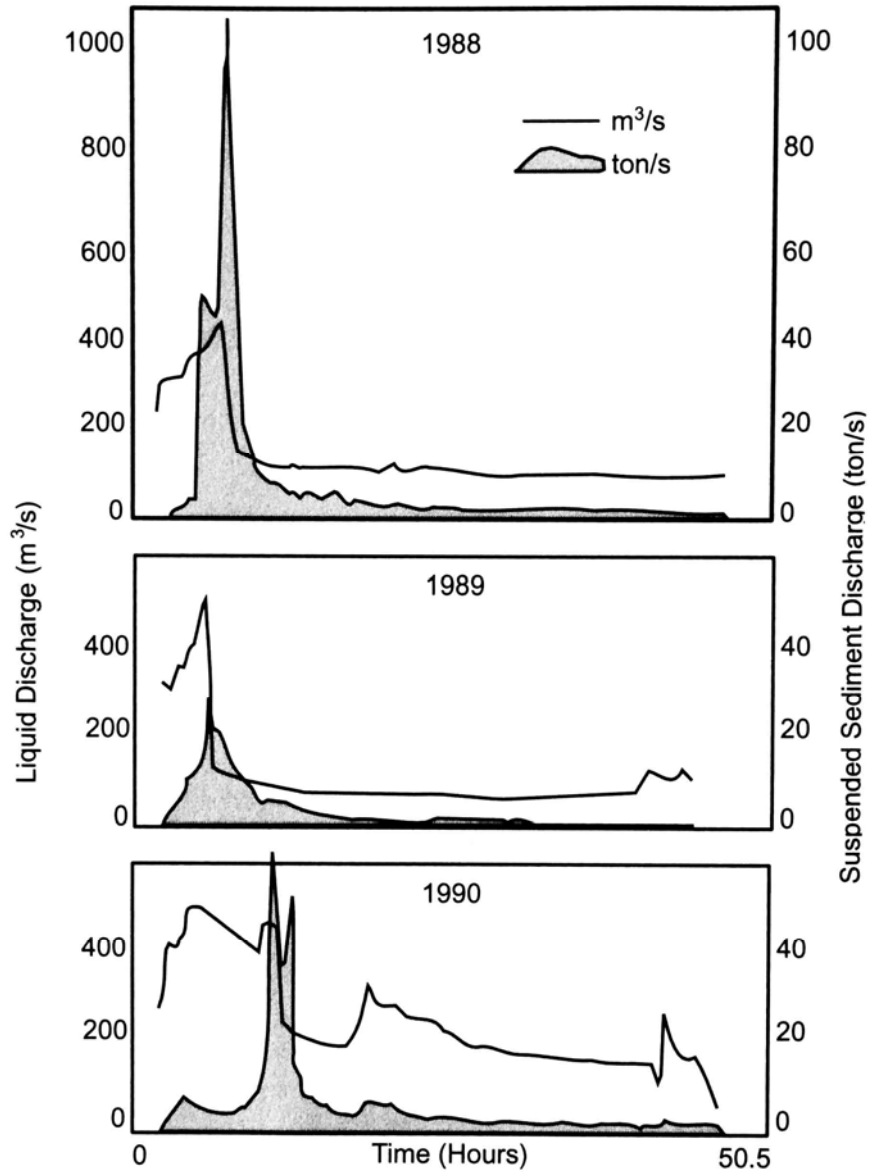


**FIGURE 19.18** Discharge and sediment load at El Congo station downstream of Cachi reservoir during 50.5 hours of flushing in three different years (after Jansson, 1992b).

easily monitored, reliable data on sediment release were obtained without use of turbidimeters. The water discharge and sediment load during 50.5 hours of rapid drawdown and free flow for three flushing events are shown in Fig. 19.18. Sediment discharge during each period for the 1990 flushing is given below:

Slow evacuation	27,000 tons	4%
Rapid evacuation	278,700 tons	43%
Free flow	<u>347,100 tons</u>	<u>54%</u>
Total	652,800 tons	100%

The sediment discharge computed from water sampling was over 50 percent higher than the erosion estimate of 350,000 to 400,000 tons computed from depth soundings before and after the flushing event.

The highest sediment concentrations (exceeding 400 g/L during the 1988 flushing) and most of the sediment discharge occurs at the end of the rapid drawdown and start of the free-flow phase, when high velocities erode the material that has been transported to and accumulated along the channel near the dam. The percentage of total sediment outflow that occurred during the peak 4-hour period in the 1988, 1989, and 1990 flushing events has been computed from these load graphs as 62, 51, and 44 percent respectively.

Turbidimeter monitoring of sediment released during the 1990 flushing was discontinuous because of clogging and other mechanical problems. However, sufficient data were collected to reveal that the calibration curve of turbidity versus suspended solids changed from the rapid drawdown to the free-flow period, apparently because of the change in the grain size distribution of the transported sediments. Sediment monitoring at the Angustura station, downstream of El Congo, also revealed that sediment concentration tends to decrease downstream because of settling plus dilution from tributaries.

## 19.6 SEDIMENT BUDGET

Reservoir sediment budgets were prepared for the studied flushing period (September 16, 1989 to October 13, 1990) and for an average hydrologic year (Table 19.6), classifying the sediment inflow by source (Sundborg and Jansson, 1992).

**TABLE 19.6** Sediment Inflow into Cachí Reservoir by Source

Sediment source	1989-1990, ton/yr	Average year, ton/yr
Suspended load:		
La Troya	265,000	326,000
Palomo	450,000	259,000
Ungaged area	110,000	162,000
El Llano dredging	28,000	—
Bed load:		
All sources	<u>66,000</u>	<u>60,000</u>
Total Load	919,000	807,000

*Note:* Dredging at the small El Llano reservoir upstream contributed sediment during the intensive study period. *Source:* Sundborg and Jansson (1992).

The fate of the sediment entering the reservoir during an average hydrologic year is summarized in Table 19.7. Of the average inflow of 807,000 tons/year, 148,000 tons is released through normal hydropower and gate operations for an average release efficiency of only 18% (trap efficiency of 82%) in the absence of flushing. With annual flushing operations the sediment release efficiency is increased to 73%. Most of the inflowing fines are transported along and deposited within the flushing channel by turbidity currents, and essentially all these in-channel deposits are removed by flushing. Only the coarse bed material and the fines deposited on terraces remain trapped.

**TABLE 19.7** Sediment Loading and Release at Cachí Reservoir during an Average Hydrologic Year

Sediment Distribution	tons/year	% of total
Throughflow	148,000	18
Deposited on terraces	167,000	21
Bed load trapped in reservoir	60,000	7
Turbidity current deposits removed by flushing	<u>432,000</u>	<u>54</u>
Total	807,000	100

*Source:* Sundborg and Jansson (1992).

## 19.7 CLOSURE

Studies at Cachí demonstrate the effectiveness of regular flushing for sediment removal. They also demonstrate the difficulty of accurately measuring sediment yield in small flashy streams, and provide an excellent example of use of turbidimeters under difficult field conditions. Despite sophisticated methods used to determine the annual sediment balance across the reservoir by bathymetric measurements, only 350,000 to 400,000 tons of sediment removal was computed in the bathymetric study, as opposed to 652,000 tons based on suspended-sediment measurements downstream of the dam. Sampling during the 1990 flushing event was carefully planned and supervised by technical personnel from ICE and the Swedish team, and the suspended sediment data at El Congo during flushing are felt to be the most accurate of all the datasets. This underscores the problem of short-interval bathymetric comparisons which attempt to measure small changes in sediment depth. Although better results might be achieved in a reservoir with a more regular bottom, as opposed to the steep terrace faces that occur in Cachí, the sources of error in bathymetric measurements are such that they should be used with utmost caution in studies involving small increments in deposition depth. While bathymetric studies continue to be the most convenient and accurate method for determining long-term deposition patterns, and represent the benchmark against which fluvial sediment studies should be compared, they have important limitations for short-term studies.

---

## CHAPTER 20

---

# LOÍZA RESERVOIR CASE STUDY

---

The Loíza case study illustrates sediment management strategies developed at a municipal reservoir based on a combination of sediment pass-through and dredging. Sediment pass-through at this site requires real-time hydrograph prediction. The history of this site also illustrates the consequences of failing to address sedimentation issues in a timely fashion, a problem that may become increasingly common as urban areas continue to grow, reservoirs age, and sedimentation progresses. This case study has been compiled from published documents and the first author's involvement with this site.

### 20.1 PROJECT HISTORY

---

The 8680-km<sup>2</sup> island of Puerto Rico lies approximately 1600 km southeast of Miami, Florida. The island's topography is rugged, consisting mostly of hilly and mountainous lands surrounded by a narrow coastal plain, and 55 percent of the island's land surface has slopes exceeding 35 percent. The climate is tropical and moist, rainfall averages about 1900 mm/yr, and the average temperature is 25°C. With a 1995 population of 3.7 million, the island wide population density was 426/km<sup>2</sup>. Most of the population is located along the coastal plains, and about 1.5 million reside in the metropolitan area of greater San Juan, the capital city.

Loíza (Carraízo) Reservoir (Fig. 20.1), owned and operated by the Puerto Rico Aqueduct and Sewer Authority (PRASA), produces about half of the total 7.4 m<sup>3</sup>/s (170 × 10<sup>6</sup> gal/day) municipal water supply for the San Juan area. It had an original volume of 26.8 Mm<sup>3</sup>. Between closure in March 1953 and the most recent survey in November 1994, Loíza reservoir had lost 53 percent of its capacity because of sedimentation; its total volume had been reduced to 14.2 Mm<sup>3</sup> (Webb and Soler-Lopez, 1997). Reservoir sedimentation has long been recognized to be a problem in Puerto Rico. Bogart et al. (1964) stated, "Loss of reservoir capacity is the major problem caused by sediment in Puerto Rico. Several reservoirs are almost completely filled with sediment and some larger reservoirs are losing capacity rapidly." Rapid sedimentation of Loíza Reservoir was identified as a serious problem by Quinones (1980) and also by several engineering studies during the 1970s and 1980s.

Drought and water rationing affected San Juan in 1964, 1967-1968, 1974, 1977, 1994, and 1995. Fluvial sediment monitoring at U.S. Geological Survey (USGS) gage stations upstream of Loíza Reservoir was initiated in 1984, but attention was not focused on the deteriorating conditions at the reservoir until 1989, when failure of both the primary and backup electrical systems during hurricane Hugo resulted in overtopping of the dam when the crest gates could not be opened (Fig. 20.2). Discharge over the non-overflow portion of the dam flooded the 3.5-m<sup>3</sup>/s (80×10<sup>6</sup> gal/day) raw water pump station, leaving



**FIGURE 20.1** Loíza Reservoir, Puerto Rico. Much of the water surface near the dam is covered with water hyacinth, *Eichornia crassipes* (G. Morris).

about 750,000 people in San Juan without water for 8 days (Morris and Krishna, 1991). Sediment management activities were initiated soon thereafter with a reconnaissance level analysis of both Loíza and La Plata reservoirs, the development of a sediment routing procedure, and the initiation of planning and permitting procedures for a large-scale (6-Mm<sup>3</sup>) dredging project. However, a change of administration in 1993 resulted in temporary abandonment of all phases of this project.

A severe drought began in 1994 which affected all surface water sources supplying San Juan, and more than 1.5 million persons were subjected to water rationing for a period extending from May until September. Total municipal water production was less than half of normal, and withdrawals from Loíza reservoir dropped to less than 40 percent of normal. The entire water distribution system was pressurized on a rotating basis, each sector receiving water service for up to 8 hours every second day. Extensive use was made of tank trucks to distribute water to hotels and to consumers (Fig. 20.3). As water levels dropped, an emergency project was undertaken to dredge a channel through the shallowest part of the reservoir, about 3 km above the dam, to prevent the pool from becoming divided into two separate areas as water levels dropped. For lack of a suitable disposal site in the mountainous area surrounding the lake, the dredged sediment was placed below the normal pool level in a tributary arm of the lake. This hastily organized work was not completed under the short timetable established in the contract and terminated in litigation. A small amount of coarse sediment was subsequently removed from a normally submerged sand bar by the National Guard with conventional earthmoving equipment, but in general the deposits were too fine and weak to be worked by land equipment.

In 1995, drought conditions and water rationing returned again, and it was decided to reactivate the large-scale dredging plan and permitting process. In 1996, large-scale dredging was contracted, but by 1997 sediment pass-through had not yet been implemented.



**FIGURE 20.2** Overtopping of Loíza Dam during hurricane Hugo, 1989 (G. Morris).



**FIGURE 20.3** Use of tank trucks to distribute water in San Juan during 1994 drought (G. Morris).

To provide the additional water supply needed to eliminate overdrafting at both Loíza and La Plata Reservoirs, a contract for the design and construction of a  $4.4 \text{ m}^3/\text{s}$  ( $100 \times 10^6$  gal/day) aqueduct to connect Dos Bocas and Caonillas hydropower reservoirs to the metropolitan water supply system was also awarded in 1996. These existing reservoirs, constructed in 1942 and 1948 respectively, had by 1996 lost 43 percent and 12 percent of their capacity to sedimentation. With its heavy dependence on reservoirs, sediment management is required for Puerto Rico to sustain long-term water supplies.

## 20.2 HYDROLOGY

Loíza Dam is a concrete gravity structure 29 m tall with eight 10-m-tall radial crest gates and a spillway design capacity of  $8830 \text{ m}^3/\text{s}$ . There are three inoperative 1.1-m-diameter (42-in) low-level drains and no bottom sluice (Fig. 20.4). Bogart et al. (1964) reported that, during the initial years of impounding the 1.1-m-diameter outlets at the base of the

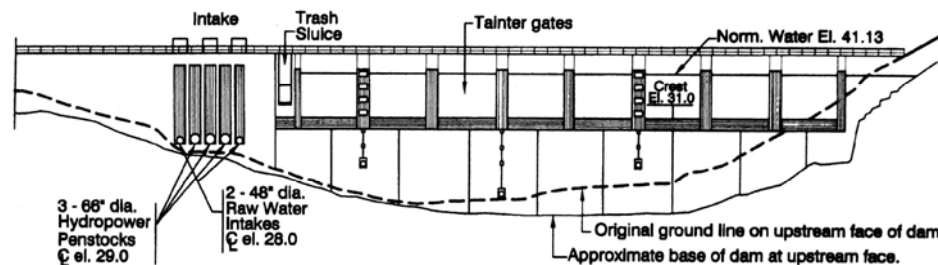
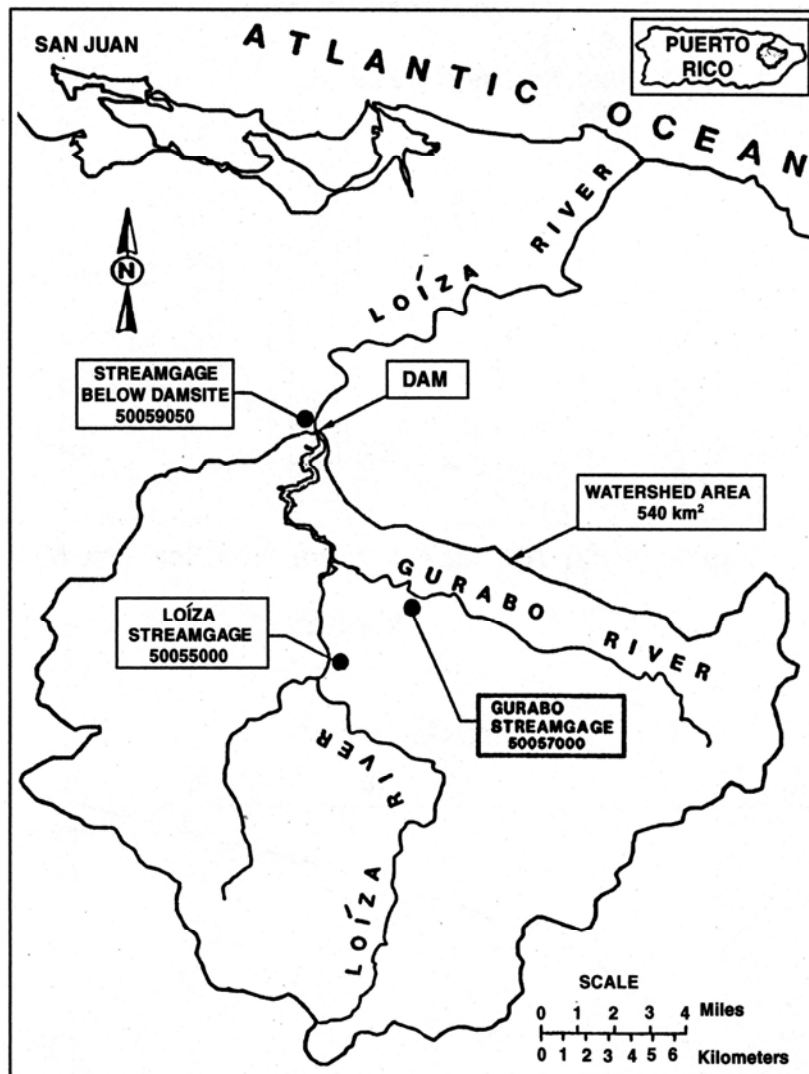


FIGURE 20.4 Water face of Loíza Dam (P. R. Water Resources Authority, 1979).

dam were opened during runoff events to vent turbidity currents. The effectiveness of this measure in releasing sediment was never documented, but it was probably not large. Each drain had only a single gate valve. Sediment releasing was discontinued after some years for fear that submerged debris may become lodged in the valve, preventing closure and draining the reservoir, a problem which actually occurred at the Guayabal irrigation reservoir on the island's south coast.

The dam impounds  $534 \text{ km}^2$  (71 percent) of the Loíza River watershed, the largest in Puerto Rico (Fig. 20.5). Rainfall within the watershed averages  $1900 \text{ mm}/\text{yr}$ , of which about  $841 \text{ mm}$  (44 percent) appears as runoff. As seen in Fig. 20.6a, runoff is usually well-distributed throughout the year. The reservoir is hydrologically small, and the original total storage volume of  $26.8 \text{ Mm}^3$  equaled only 6 percent of mean annual runoff, equivalent to a runoff depth of  $50 \text{ mm}$ , across the tributary watershed.

The storage-yield curve at Loíza dam (Fig. 20.6b) shows that a significant increase in firm yield can be achieved from a relatively small increment in storage. This is advantageous from the standpoint of sediment control, since substantial water supply benefits can be achieved while maintaining a relatively small storage volume free of sediment. Despite the limited storage capacity, this reservoir normally diverts to municipal use a constant flow equal to 25 percent of the mean annual flow of the Loíza River at the dam site, a withdrawal rate that exceeds the reservoir firm yield and which leads to severe rationing during drought.



**FIGURE 20.5** Location map of Loíza watershed USGS, gage stations, and reservoir.

## 20.3 SEDIMENTATION

### 20.3.1 Sediment Yield

Sediment yields in Puerto Rico are high, typically around 1000 to 2000 t/km<sup>2</sup>/yr, as illustrated in Table 20.1 which is based on data from reservoir surveys, corrected for trap efficiency by Brune's curve, and on estimated values of deposit bulk density. Despite intensive urban development within the watershed, the specific sediment yield from the Loíza watershed is the lowest of all island reservoirs, probably because of the lower slopes in the broad and gently sloping valley along Rio Gurabo. However, because of its small hydrologic size, the reservoir experiences a high 1.2 percent annual rate of storage loss.

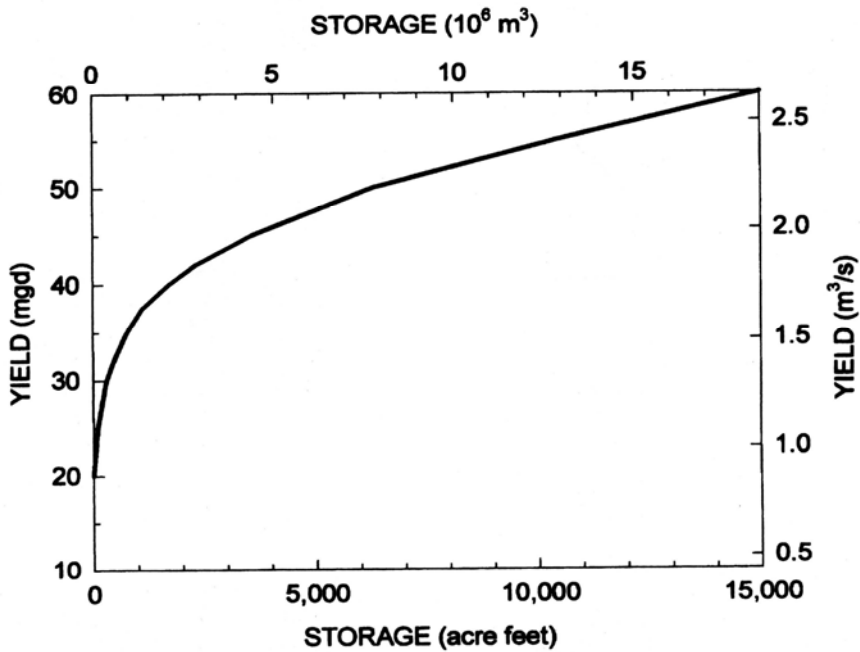
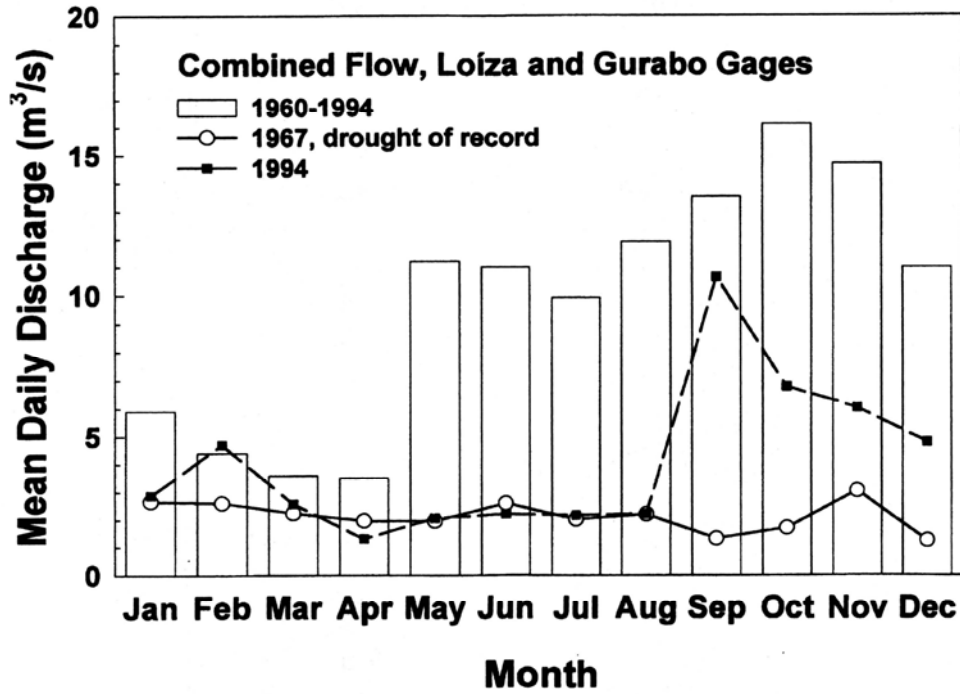


FIGURE 20.6 (Top) Seasonality of runoff at Loíza and Gurabo gage stations, as reported by the USGS. (Bottom) Storage-yield curve for firm yield of Loíza Reservoir constructed from gage data from 1959 through 1994. The drought of record occurred in 1967.

**TABLE 20.1** Sedimentation at Reservoirs in Puerto Rico

Site	Year constructed	Original volume, $10^6 \text{ m}^3$	Original C:I ratio	Watershed area, $\text{km}^2$	Specific sediment yield, $\text{t}^3/\text{km}^2/\text{yr}$	Annual storage loss, %
Caonillas	1948	59.0	0.36	211.4	659	0.3
Luchetti	1952	18.2	0.86	44.8	2651	0.6
Carite	1913	13.9	0.41	20.5	2026	0.3
Guayabal	1913	18.6	0.50	111.1	1817	0.9
Matrullas	1934	3.7	0.35	11.4	1534	0.5
Guineo	1931	2.3	0.49	4.1	1236	0.2
Garzas	1943	5.8	0.39	16.1	1159	0.3
Cidra	1946	6.6	0.55	22.3	1227	0.4
Dos Bocas	1942	37.5	0.09	310.8	1000	0.8
Patillas	1914	17.6	0.26	65.3	916	0.3
La Plata	1974	28.0	0.10	448.1	2331	1.3
Guajataca	1928	45.1	0.56	63.7	1637	0.1
Loco	1951	1.8	0.24	21.8	761	0.9
Loíza	1954	26.8	0.08	533.5	715	1.2

*Source:* Compiled from individual bathymetric studies performed by USGS in various years.

Streamflow and sediment yield throughout Puerto Rico are highly episodic, typical of small watersheds where rainfall and runoff events are intense and of short duration. This creates a runoff pattern characterized by low base flows punctuated by intense events of short duration. Most of the sediment load entering Loíza reservoir is contributed by these infrequent storm events. Sediment delivery is significantly more concentrated in time than discharge (Fig. 20.7). Although rainy periods associated with storm systems may last up to a week, even the largest runoff events have steep hydrographs and durations of less than 24 hours, as illustrated by the September 5, 1960 flood caused by the passage of hurricane Donna, which produced the peak discharge of record (Fig. 20.8).

Continuous suspended sediment measurements at the USGS gage stations on the Gurabo and Loíza Rivers, gaging 72 percent of the watershed above the dam, indicated that 65 percent of the total 7-year (1984-1990) sediment inflow was contributed on only 10 days, and 17 percent of the total sediment inflow was attributed to a single storm during that period (Table 20.2). This high concentration of sediment discharge in a short period of time is typical of streams throughout Puerto Rico.

### 20.3.2 Sediment Deposits

Sediments deposited in Loíza Reservoir grade from clays to fine gravels moving upstream from the dam. Deep borings revealed most of the sediment in the reservoir consists of fines; only about 20 percent is sand-size, and a trace of gravel occurs upstream. The lake is highly eutrophic because of nutrient inputs from both nonpoint and point sources in the tributary watershed, and the organic content of sediments is high. Shallow sampling of sediments by Quinones (1980) performed during a drought period in 1974 revealed an organic content (loss on irrigation) in the range of 8 to 12 percent over most of the reservoir. However, the organic fraction averaged over the entire deposit depth is significantly lower. Figure 20.9 illustrates the thalweg profile showing the

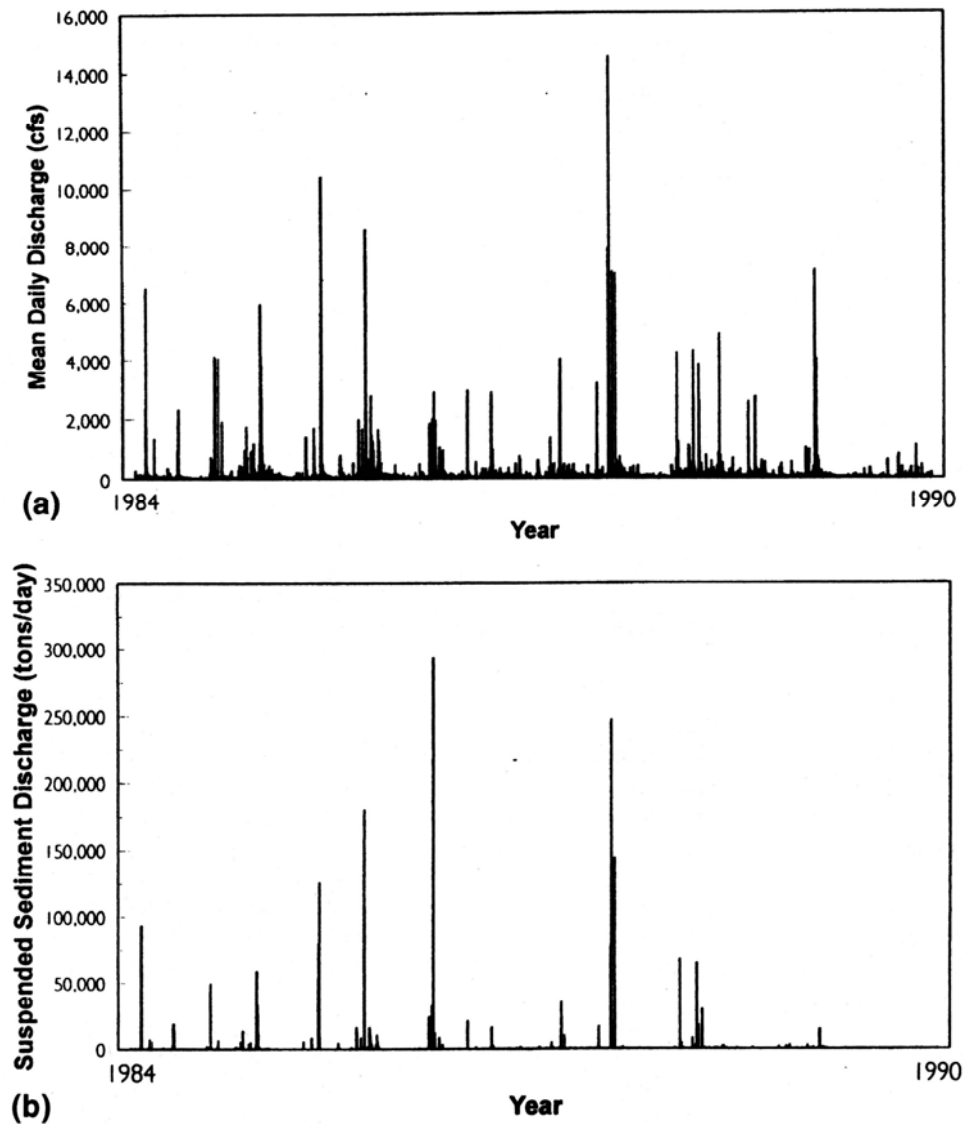


**FIGURE 20.7** Daily discharge of (a) water and (b) sediment from Loíza plus Gurabo streamgages in U.S. customary units (plotted from USGS data).

longitudinal pattern of sediment deposition and the grain size variation based on shallow (less than 1 m) surface cores. The entire dead storage pool had been sedimented by 1990 and the remaining active pool volume was controlled by the crest gates. At Loíza Reservoir, sediment deposits reduced the overall storage capacity in the reservoir, prevented utilization of the lowest water supply intake, and elevated the top of the dead pool, as illustrated by the shift in the stage-storage curves shown in Fig. 20.10. The localized deposits about 3 km above the dam (Fig. 20.9) further inhibited the ability to lower the pool without creating water quality problems by scouring anaerobic organic sediments. There is no delta at the upstream limit of the reservoir in the thalweg profile, as confirmed by visual inspection at low pool level.

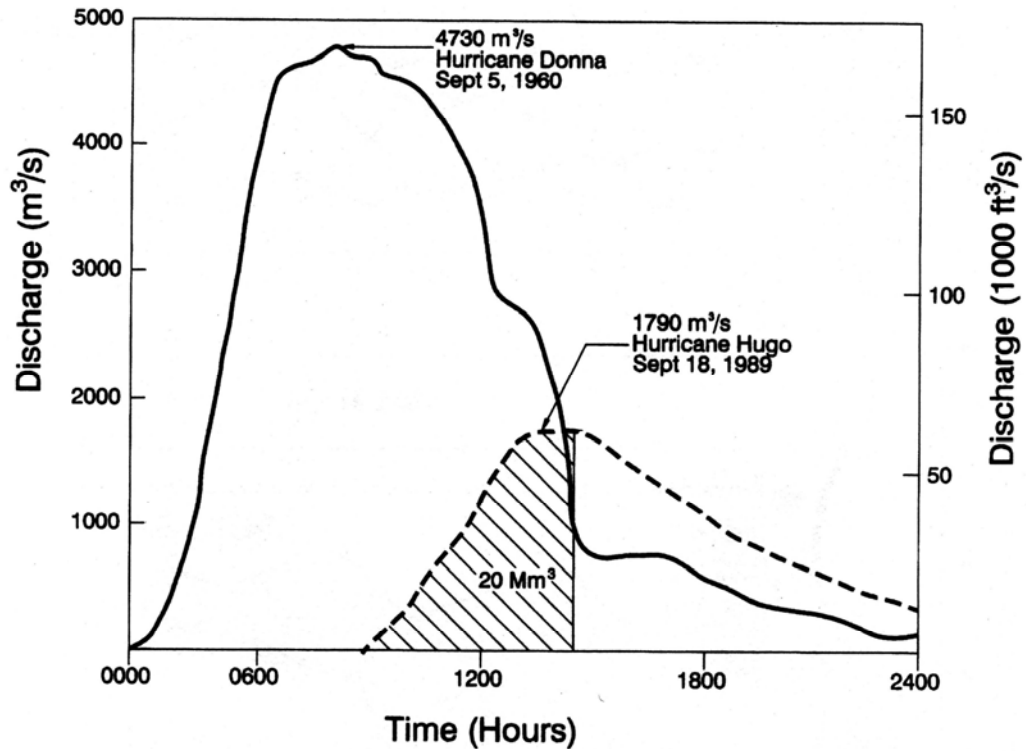


**FIGURE 20.8** Discharge hydrographs at the Loíza dam site for hurricane Donna, the peak discharge of record, and hurricane Hugo. The total usable reservoir volume of 20 Mm<sup>3</sup> (without sedimentation), superimposed on the rising limb of the Hugo hydrograph, is significantly smaller than the volume under either storm hydrographs (after P. R. Water Resources Authority, 1979 & USGS data)

**TABLE 20.2** Total Daily Discharge of Water and Suspended Sediment, Ranked by Sediment Load, Sum of Gurabo and Loíza Streamgages

Daily rank	Water discharge		Suspended-sediment load	
	Daily discharge, m <sup>3</sup> /s	Cumulative percentage*	Daily load, m <sup>3</sup> /s	Cumulative percentage*
1	34,300	3.5	913,000	17.7
2	16,750	5.2	558,000	28.6
3	15,980	6.8	510,300	38.5
4	5,960	7.4	303,300	44.4
5	17,360	9.1	231,800	48.9
6	21,780	11.3	216,600	53.1
7	21,300	13.5	208,200	57.2
8	12,480	14.7	166,500	60.4
9	13,070	16.0	126,000	62.8
10	7,580	16.8	111,500	65.0

\*Cumulative percent of the 7-year total.  
 Source: Computed from USGS data.

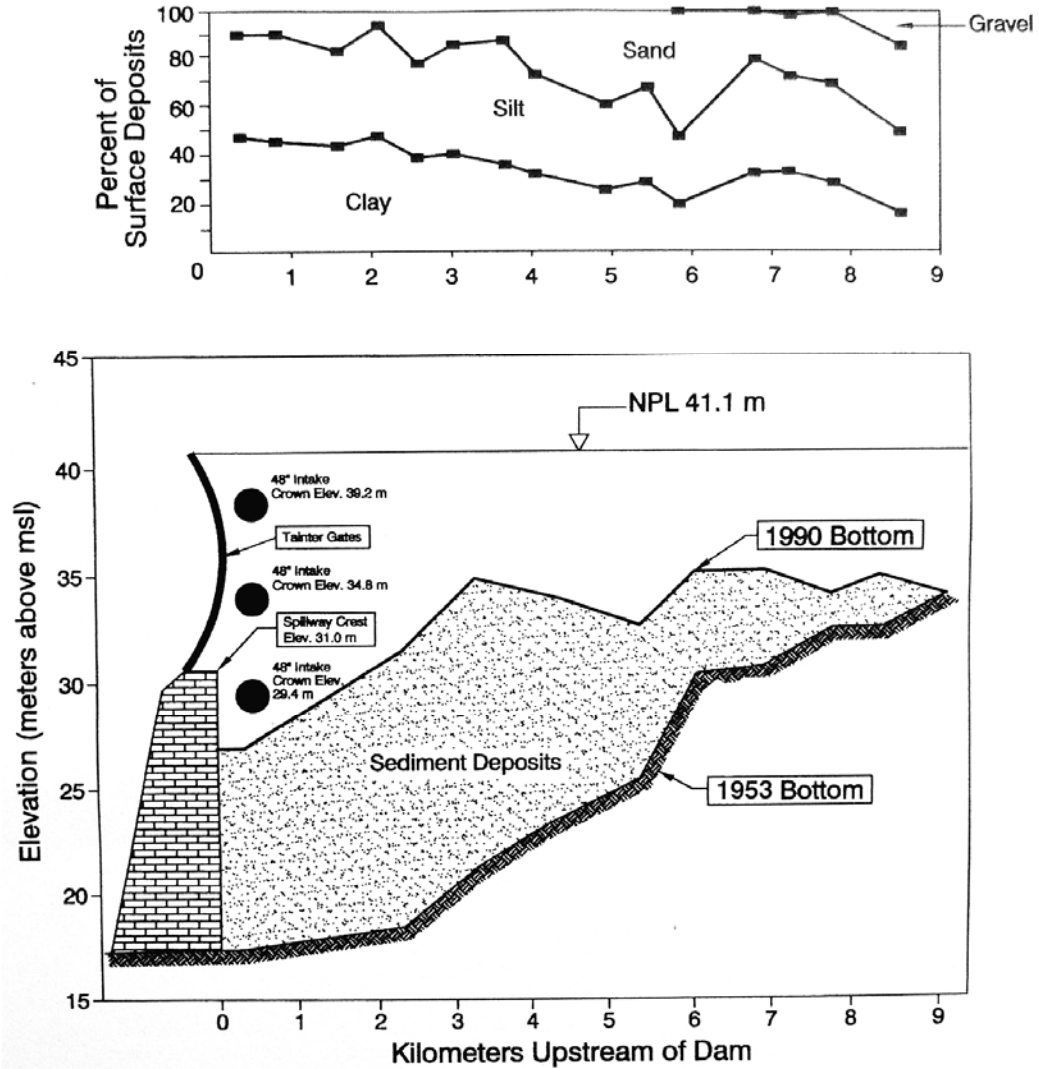


**FIGURE 20.9** Thalweg profile along Loíza Reservoir showing sediment deposit profile and grain size variation. The location of the three 48-inch diameter potable water supply intakes are also shown (adapted from PRASA, 1992).

Deposits in the upper reservoir exposed during drought revealed a riverine-type cross section and normally submerged bars of sandy sediment, but insignificant deposition of coarse sand or gravels. The supply of coarse material has been reduced by the extensive instream mining of sand and gravel in the river reaches above the dam. Bedrock is exposed along much of the reach of Rio Loíza extending upstream from the dam, and instream mining has lowered the bed of Rio Gurabo, its principal tributary.

A geotechnical drilling rig was mounted on a barge and used to obtain fully penetrating core samples. Layered deposits occur in the middle section of the reservoir (Fig. 20.11) but the sediments closer to the dam are more uniformly fine-grained. The sand layers represent coarse material transported deeper into the impoundment during larger floods, and the fines above and below the sand lenses represent deposits from both stratified and nonstratified flow during smaller runoff events, plus organic deposition from primary production in the eutrophic lake (water hyacinth and algae).

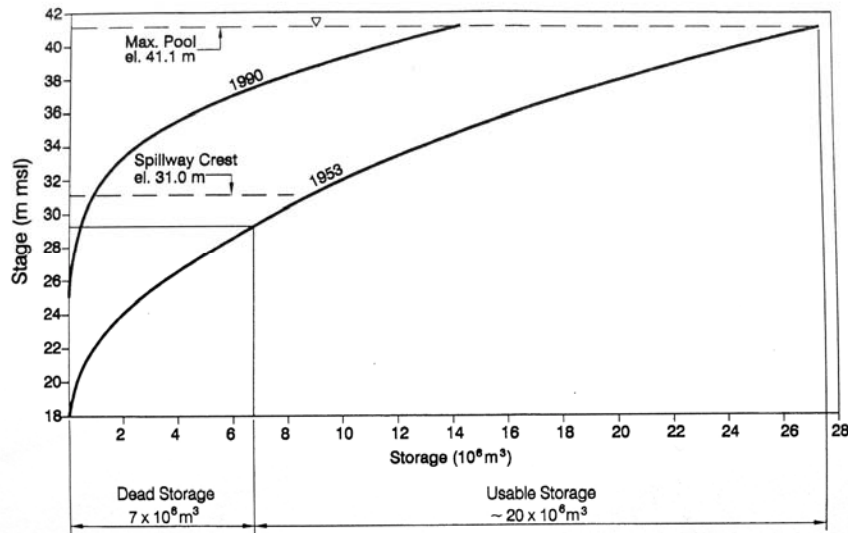


FIGURE 20.10 Change in the stage-storage relationship at Loíza Reservoir (adapted from PRASA, 1992).

### 20.3.3 Sediment Discharge during Runoff Event

Discharge and suspended-sediment concentrations upstream and downstream of the reservoir during a significant runoff event are illustrated in Fig. 20.12 with data from hurricane Hugo collected at the three U.S. Geological Survey gage stations. Inflowing sediment concentration in both the Gurabo and Loíza Rivers peaked before discharge peaked and then dropped rapidly, with maximum inflow concentrations of 5.5 and 4.5 g/L at the Gurabo and Loíza gages respectively. However, concentrations below the dam site remained relatively steady at about 1 g/L. The inflowing streams delivered most of the sediment load and deposited it within the reservoir during the rising limb of the hydrograph. Sediment yield was relatively low during the Hugo event, attributed by Gellis (1993) to sediment trapping resulting from blockage of stream channels by wind-blown woody debris.

### 20.3.4 Rate of Storage Loss

At Loíza Reservoir, the rate of storage loss may be computed by two methods: by repeated bathymetric surveys (Fig. 20.13) and by measuring the difference in fluvial sediment delivery at gage stations above and below the dam installed in 1984.

From fully penetrating cores and the 1991 bathymetry performed by the USGS, the bulk densities of the reservoir sediments were determined as follows:

More than 5 km above dam, deposit volume = 2.0 Mm<sup>3</sup>, density = 960 kg/m<sup>3</sup>

Less than 5 km above dam, deposit volume = 8.9 Mm<sup>3</sup>, density = 1200 kg/m<sup>3</sup>

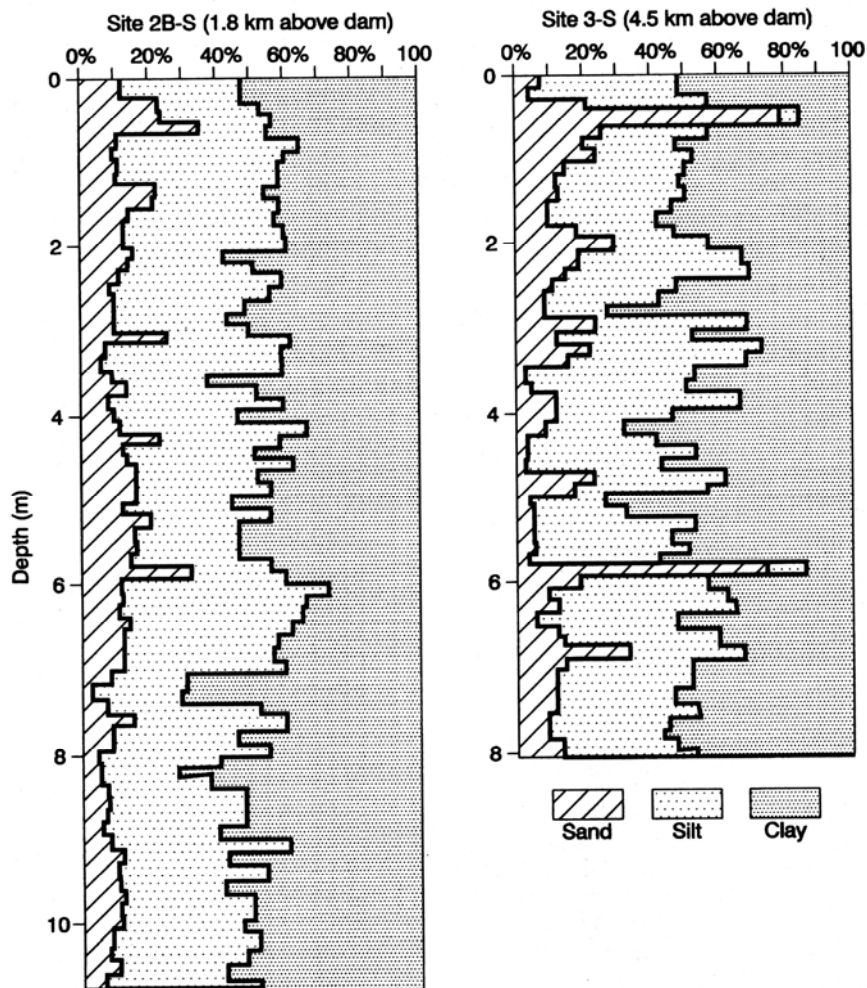


**FIGURE 20.11** Vertical profiles of sediment deposits at Loíza dam showing layering about 4.5 km above the dam, but more uniform fine-grained material closer to the dam (*adapted from PRASA, 1992*).

The average bulk density for all sediment deposits in the reservoir is  $1,156 \text{ kg/m}^3$ . Applied to the recent rate of storage loss of  $0.175 \text{ Mm}^3/\text{yr}$  (Fig. 20.13), this bulk density corresponds to the trapping of 202,000 t/yr of sediment in the reservoir.

Suspended sediment data from USGS gages at Gurabo, Loíza, and below dam site (located as in Fig. 20.5) are summarized in Table 20.3 for calendar years 1987-1994, the period with suspended sediment data for all three locations. Because the Caribbean wet season extends from September through November, data are presented in calendar years rather than the U.S. water year used by the USGS, which ends September 30. The bed load in this system is not large, and load computations based on suspended load should give a rather accurate estimate of the total sediment inflow into the reservoir.

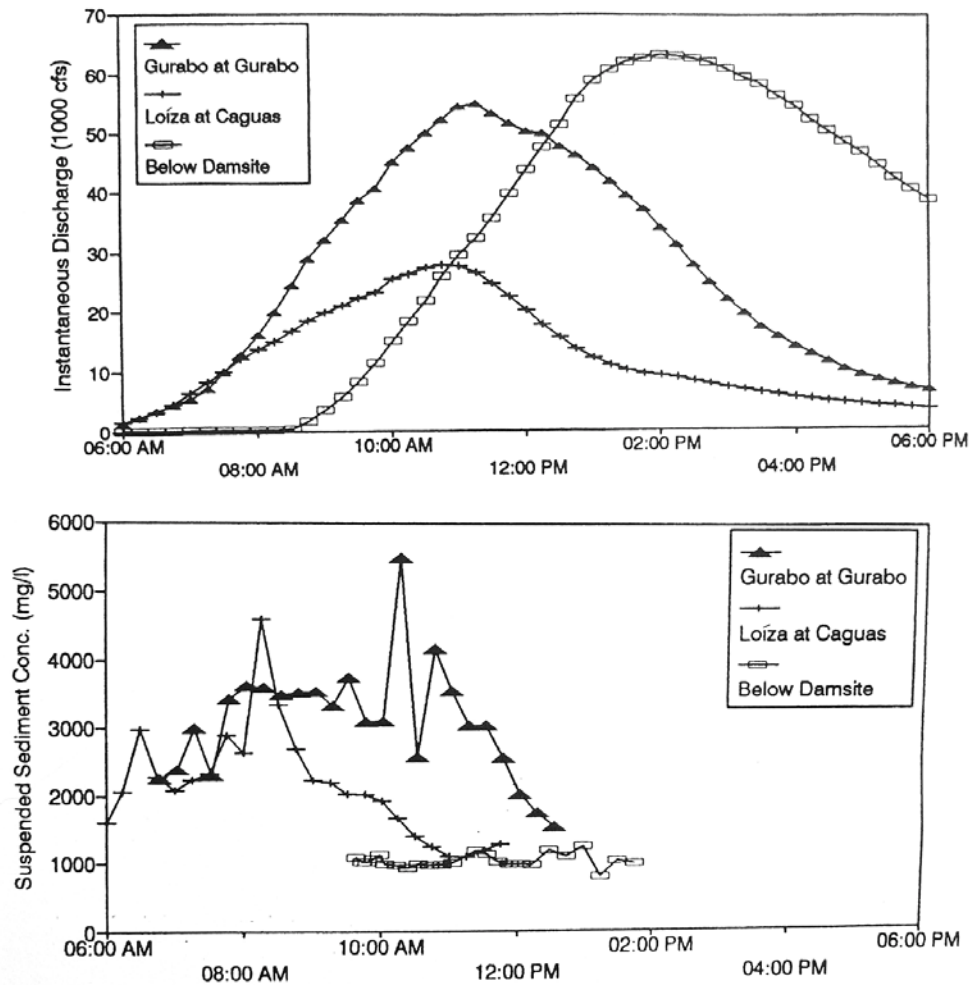


**FIGURE 20.12** Hydrographs of runoff (top), and suspended-sediment concentration (bottom) registered at USGS gage stations during hurricane Hugo. See Fig. 20.5 for gage locations.

The area tributary to the Loíza and Gurabo streamgages comprises 72 percent of the watershed tributary to the dam, making it necessary to adjust the sediment inflow at these two gage stations to include the ungaged area tributary to the dam. Because the ungaged area is primarily steep lands, much of which drains directly into streams tributary to the reservoir itself, and because portions of the ungaged area are affected by urban development which can generate high sediment loads, it seems logical to adjust the gaged sediment yield by a factor of 1.39. based on the ratio of total to gaged watershed areas. However, on the basis of water yield, adjusted for withdrawals at the dam, the below-dam gage station plus diversions at the dam account for only 110 percent of the inflow at the upstream gages, for an adjustment factor of 1.10 for the total load entering the reservoir. The values in Table 20.3 have been computed by using the adjustment factor of 1.10 to determine sediment inflow, from which sediment discharge below the dam is subtracted, to compute average sediment trapping of 433,700 t/yr. This rate of sediment accumulation based on fluvial data is more than double the rate of accumulation based on bathymetric measurements, despite using the lower adjustment factor and ignoring bed load.

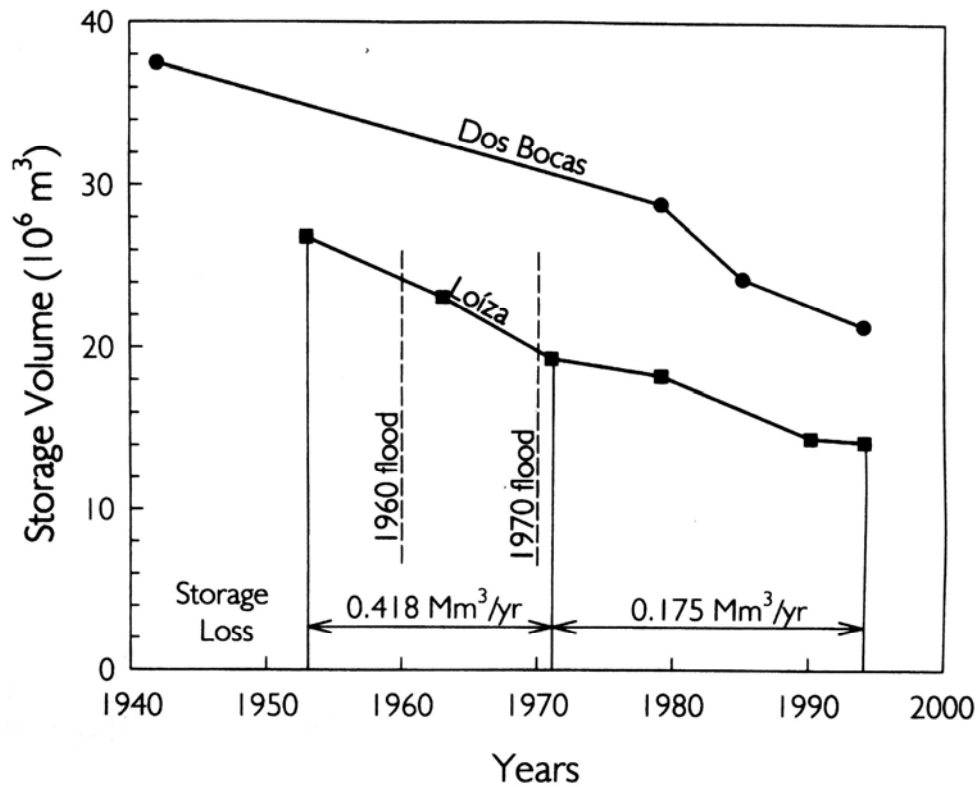


**FIGURE 20.13** Trends in storage loss at Loíza and Dos Bocas Reservoirs, Puerto Rico, based on repeated bathymetric surveys. Both reservoirs are in north coast watersheds (data from Webb and Soler-Lopez, 1997; Webb and Gomez-Gomez, 1994).

**TABLE 20.3** Suspended Sediment Trapped in Loíza Reservoir Based on USGS Fluvial Gage station Data

Calendar year	Loíza load, t/yr	Gurabo load, t/yr	Adjusted load, t/yr	Release below dam, t/yr	Total trapped, t/yr	Trap efficiency, %
1987	557,505	1,656,516	2,435,423	244,244	2,191,179	90
1988	251,341	134,633	424,572	63,925	360,647	85
1989	117,253	201,103	350,191	73,829	276,362	79
1990	73,820	25,232	108,957	14,148	94,809	87
1991	46,337	15,317	67,819	15,726	52,093	77
1992	373,616	46,769	462,423	157,273	305,149	66
1993	135,625	41,528	194,869	64,376	130,493	67
1994	51,258	11,198	68,702	9,857	58,845	86

Source: Computed from USGS fluvial gage station data.

The source of these discrepancies is probably related to measurement problems in 1987, which contributed most of the computed sediment inflow during two sparsely sampled storm events. The bathymetric and fluvial estimates of trapped sediment agree rather closely if the 1987 fluvial data are discarded. This illustrates the potential difficulty in measuring sediment yield in flashy streams.

### 20.3.5 Trends in Sediment Yield

Reforestation and erosion control have long been proposed for sediment management in Puerto Rico. At the time of Spanish occupation in 1508, the entire island was forested, but by 1828 forest cover had been reduced to about 66 percent of the island's area (Wadsworth, 1950). Forest inventories summarized by Birdsey and Weaver (1987) show that the total forested area in Puerto Rico had declined to a low of 12 percent of the island's area in the late 1940s, with about half of this area being shade coffee plantings. This dramatic denudation of forest area reflected the extensive cultivation of steep erodible hillsides either by hand or by oxen, a practice that was commonplace into the 1960s. Erosion from steep hillside farms has been a major source of erosion contributing to reservoir sedimentation (Noll, 1953). Improving economic conditions since the 1950s led to the gradual abandonment of hillside farming and reforestation of the slopes. By 1984, forest cover of all types, including areas of shade coffee production, covered 34 percent of the island. Most of the increase in forest cover occurred in the island's steep interior area, where most hillside farms have been abandoned and are in secondary forest or pasture. During this same period, urban development has focused primarily on the coastal plain, largely bypassing the watersheds tributary to reservoirs, with the notable exception of the Loíza watershed, which had a 1990 population density exceeding 500 persons/km<sup>2</sup>.

Given the small steep watersheds, gravel bed rivers, predominance of easily transported fine-grained sediment, and the limited opportunity for and evidence of sediment deposition on the narrow valley floors above most reservoirs, the sediment delivery ratio is expected to be very high. Under these conditions a significant decline in erosion due to the abandonment of hillside farms and dramatic increase in forest cover would be expected to produce a noticeable, if not dramatic, decline in the rate of reservoir storage loss, except possibly in watersheds affected by extensive sediment-producing construction activity.

The longest continuous fluvial sediment record in Puerto Rico (1968 to present) monitors discharge and load from the 47.7-km<sup>2</sup> Rio Tanama watershed on the north coast. No trends are evident in this dataset based on construction of a double mass curve of water and sediment. Longer-term trends in sediment yield may be analyzed using reservoir resurvey data. Repeated bathymetric survey data are available at only a few sites in Puerto Rico. Data from Loíza and Dos Bocas reservoirs, both on the island's north coast and with similar watershed sizes, reflect contrasting trends in sedimentation (Fig. 20.13). The Dos Bocas watershed has experienced extensive reforestation and relatively little urban development, yet there has been no apparent decline in the rate of sediment accumulation. In contrast, the Loíza basin has experienced considerable urban expansion, including both housing and highway development on sloping soils with virtually no erosion control practices. (See Figs. 12.4 and 12.13.) Nevertheless, the Loíza data show an apparent decline in sediment yield as a function of time: the rate of reservoir storage depletion averaged 0.418 Mm<sup>3</sup>/yr from 1953 to 1971, but only 0.175 Mm<sup>3</sup>/yr from 1971 to 1994. It is not clear to what extent this reflects differences in hydrology; there has not been a major flood in the Loíza basin since October 1970, whereas Dos Bocas experienced a large flood in 1985.

## **20.4 SCREENING OF SEDIMENT CONTROL STRATEGIES**

---

Sediment management activities were initiated by compiling the available data and conducting a screening analysis to identify the most feasible control options.

### **20.4.1 Reservoir Replacement**

Can Loíza Reservoir be replaced? The existing dam occupies the only feasible dam site on the main stem of Rio Loíza. The two main tributaries, Loíza and Gurabo, join at the upstream limit of the impoundment, and proposed dam sites further upstream above the valley floor would control only a small fraction of the total watershed tributary to the existing dam. There is limited opportunity to raise the pool elevation because it would increase flood hazard to upstream urban areas, and with the base of the dam only 15 m above sea level and extensive urbanization downstream, there is little opportunity for a new downstream site. Other existing and potential reservoir sites are found elsewhere on the island, but, in addition to development costs they would incur, these alternative sites would eventually face sedimentation problems. Furthermore, both the Loíza and La Plata watersheds are ideally located from the standpoint of supplying water to San Juan, and the entire water treatment and distribution system has been developed from these two points of supply.

A new water supply with an ultimate firm yield of 4.4 m<sup>3</sup>/s (100 mgd) is being developed from the existing Dos Bocas and Caonillas hydropower reservoirs in the Arecibo watershed, 60 km west of San Juan. However, Rio Arecibo does not have enough water to allow existing reservoirs to be abandoned, and sedimentation is also a problem in the Arecibo reservoirs. Dos Bocas Reservoir, impounded in 1942, and Caonillas Reservoir, impounded in 1948, have respectively lost 43 and 12 percent of their capacity to sedimentation. Using and then abandoning reservoir sites is not a sustainable water supply strategy in Puerto Rico.

### **20.4.2 Upstream Sediment Detention Basins**

Sediment trapping at upstream detention basins was considered, but the combination of fine sediment sizes and high discharges would require large basins. Further, sediment trapping is only a temporary measure unless combined with sediment removal, and sediment removal from the reservoir would probably not be materially more difficult or costly than removal from detention basins. Given the high cost of land and high population density, upstream sediment trapping was considered infeasible.

### **20.4.3 Sediment Flushing**

Full drawdown of the reservoir for flushing was considered infeasible without costly structural modification to the dam because of the lack of bottom sluicing capacity. It is also incompatible with the requirement to maintain the reservoir in continuous service to provide water for San Juan. Finally, there is no possibility of obtaining environmental permits for reservoir flushing at this site.

### **20.4.4 Venting Turbid Density Currents**

Turbidity current venting was not considered a viable option. Preliminary computations indicated that Loíza Reservoirs was too shallow to generate flow stratification during

major events, although smaller freshets can plunge upon entering the reservoir. Also, low-level outlets were too small and the broad flat deposits are not conducive to maintaining density current motion.

#### **20.4.5 Explosive Mobilization**

The use of explosives to mobilize sediment so it would be carried away during floods was considered, as described in Sec. 16.3.6. However, there were too many uncertainties associated with this technique for it to be considered. One important problem was the possibility of leaving explosive material in place for a period of more than a year if a flood did not occur during the target wet season.

#### **20.4.6 Sediment Pass-Through**

Loíza Reservoir is highly elongated, and the 10-m-tall radial gates control virtually the entire useful storage pool, suggesting that sediment pass-through may be feasible. The reservoir has always been operated to maintain the highest possible pool level to ensure adequate water supplies, thereby maximizing both detention time and sediment deposition within the impounded reach. However, if the dam's radial gates are fully opened during flood events, the reservoir will behave like a river, producing high flow velocities which minimize the deposition of fine sediments. The original usable reservoir capacity of 20 Mm<sup>3</sup> is smaller than the volume of the major storm events that deliver high sediment loads (Fig. 20.8). This pointed to the possibility of opening the reservoir's gates at the onset of a storm event, allowing the flood to pass through the impounded reach at high velocity, and closing the gates to refill the impoundment with the volume contained in the recession portion of the hydrograph. Sediment pass-through was selected as a prospective management strategy at Loíza Reservoir.

#### **20.4.7 Dredging**

Sediment pass-through at Loíza Reservoir is not expected to remove previously deposited sediment and will not be effective in transporting coarse sediment beyond the dam. Sediment removal is required to recover and maintain storage capacity. Dry excavation is not considered feasible because the reservoir needs to remain in service. However, even if the reservoir could be withdrawn from service, dry excavation would still not be feasible because: (1) draining the reservoir would create flushing conditions with unacceptable downstream environmental impacts, (2) the poorly consolidated fine sediment deposits in the submerged river channel, which comprise the majority of the deposits, are poorly suited to dry excavation, and (3) with only 1.1-m-diameter low level outlets, the work area in the reservoir would be inundated by even small runoff events. Thus, hydraulic dredging was the only option considered feasible.

### **20.5 MODELING OF SEDIMENT ROUTING**

---

The HEC-6 sediment transport model (U.S. Army, 1991) was used to quantify the effectiveness of sediment routing (Morris and Hu, 1992). Loíza Reservoir has highly one-dimensional geometry, and HEC-6 was the only U.S. model capable of handling the full range of grain sizes important at this site, sand through clay. Two models were con-

structed. One model simulated the reach from the dam upstream for a distance of 14.8 km along the Loíza River, plus a 5.2-km-long branch along the Gurabo River. This covered the impounded reach, extending approximately 9 km upstream of the dam, plus the riverine reaches between the pool and the two gage stations. The second model covered the reach between the ocean and the dam, a distance of 28 km, and was oriented to addressing environmental issues related to the possible settling of material from the reservoir into the downstream river and riverine estuary. Modeling indicated that downstream deposition should be insignificant for any grain size transported past the dam.

### **20.5.1 Inflow Hydrographs**

An inflow hydrograph containing time steps ranging from one day during high-flow periods to 30 days during low-flow periods was developed from the 30-year record of average daily streamflow at the Loíza and Gurabo River gage stations. The one-day time step matched the shortest time interval for which published sediment load and discharge data were available from the USGS.

### **20.5.2 Sediment Characteristics**

A rating curve specifying the total daily sediment load and its grain size characteristics as a function of daily discharge was developed from the 5-year record of daily sediment load. This relationship was then applied to the entire 30-year gage record. The percentage of sediment in each of the size classes was specified to vary as a function of discharge; at low flow all inflowing sediment was specified to be of clay-sized particles, whereas at high flows coarse silts and sands become more important. The initial grain size distribution of the bed within each reach of the model was specified by using data from shallow gravity cores in the reservoir plus bed material samples from the Loíza and Gurabo Rivers above the reservoir.

### **20.5.3 Model Calibration**

The model was calibrated by simulating the historical deposition pattern and grain size distribution in the reservoir. Calibration analysis could not be started from the original (1953) reservoir bathymetry because streamgaging did not start until 1959. Therefore, the calibration analysis was initiated with the 1963 bathymetry and was run until 1985 using the gage station discharge data and the rating curve, and the resulting deposition pattern was compared to the 1985 bathymetry. It was initially not possible to match the 1985 bathymetry, but when the 1990 bathymetry became available several months after these simulations were performed, it was discovered that the 1985 bathymetry was erroneous and the model was successfully calibrated to the 1990 data.

Initially the model underestimated clay deposition. A similar problem had been encountered with the HEC-6 model at the Martins Fork Reservoir (Martin, 1988). Settling tests conducted with native water demonstrated the presence of strong flocculation that caused the clay fraction to settle at velocities more typical of silts. The program code was modified to allow the clay settling rate to be user-specified, and excellent calibration results were achieved using the modified model and 1990 bathymetry. Historical deposition patterns were matched very closely in terms of both the deposit pattern and the average grain size distribution in the reservoir deposits obtained from the shallow cores (Fig. 20.14).

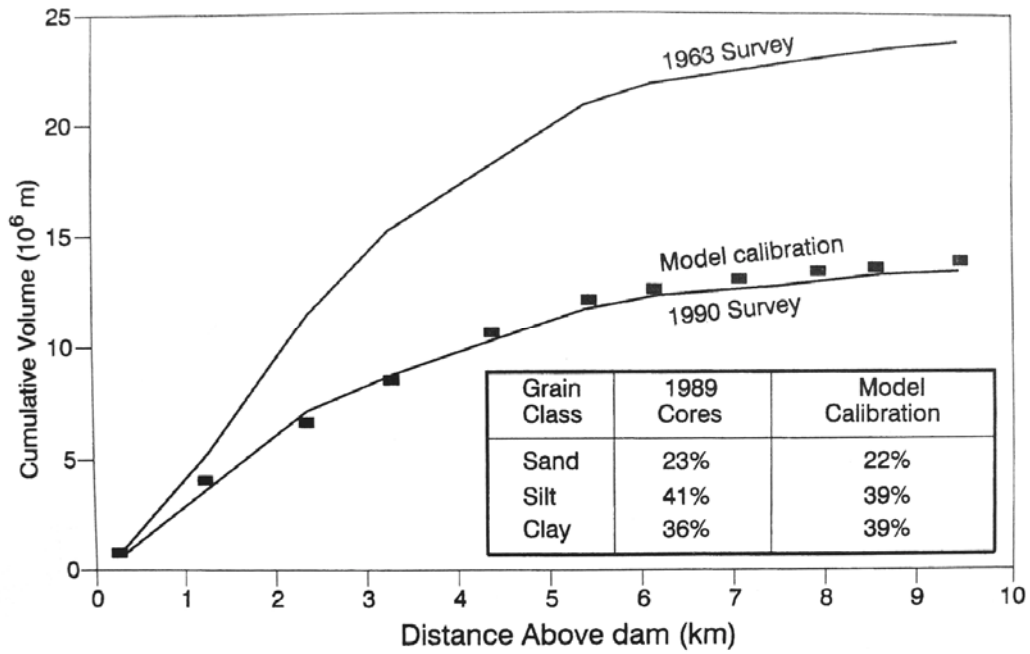


FIGURE 20.14 HEC-6 model calibration at Loíza Reservoir. Model results are shown as solid squares (Morris and Hu, 1992).

### 20.5.4 Modeling Results

The bed shear stress profile along the reservoir for a discharge of 708 m<sup>3</sup>/s (25,000 ft<sup>3</sup>/s) is shown in Fig. 20.15, which compares high-pool (historical) operating conditions against low-pool (sediment pass-through). The pass-through operation increases bed shear values by more than a full order of magnitude over much of the reservoir.

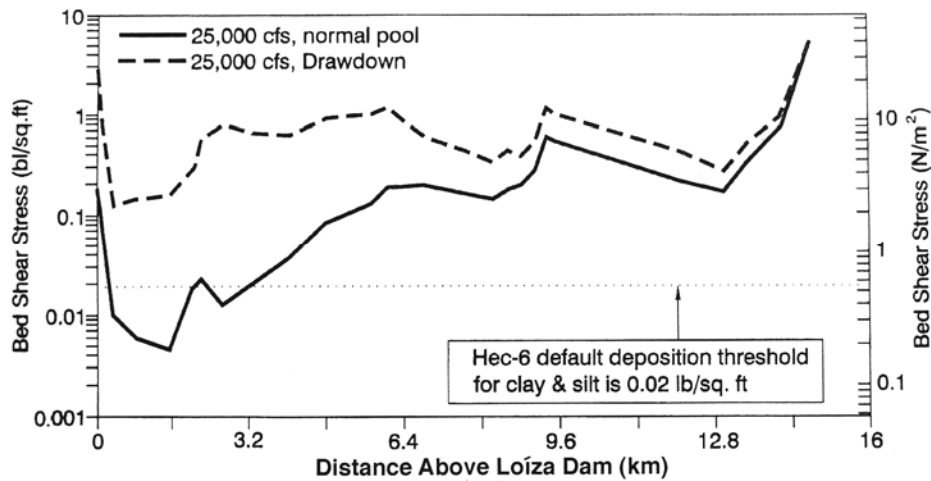
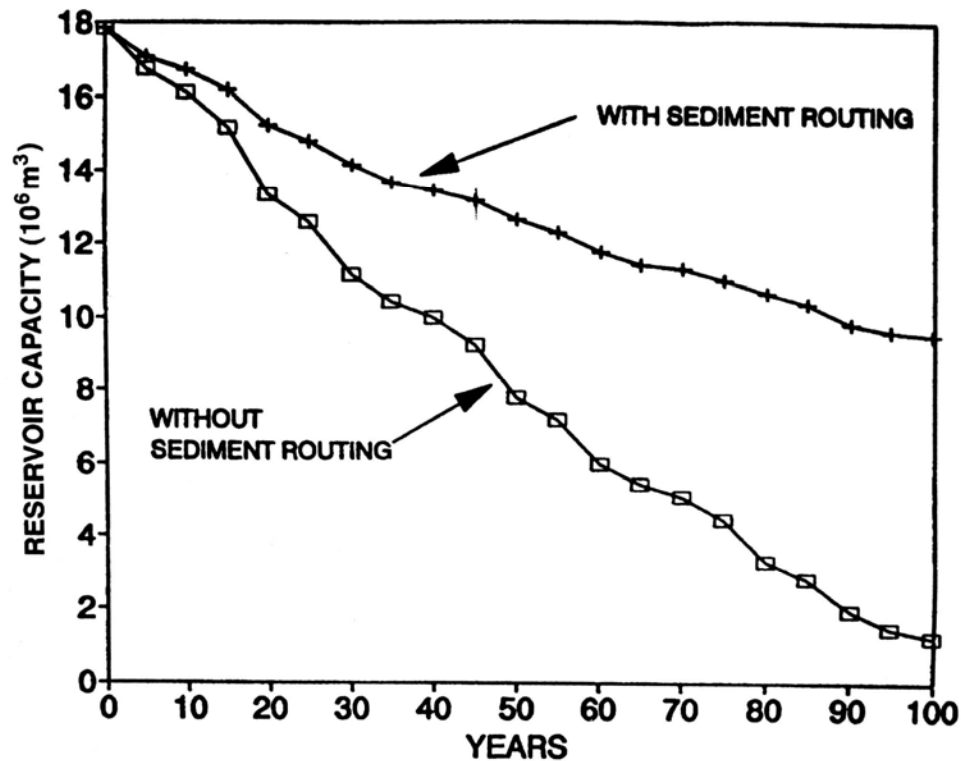


FIGURE 20.15 Bed shear stress along the impounded reach of Loíza Reservoir showing the effect of sediment pass-through routing.



**FIGURE 20.16** Effect of sediment pass-through routing in reducing the rate of sediment accumulation.

The impact of sediment pass-through on bed shear values decreases moving upstream from the dam as the backwater profile becomes increasingly controlled by channel friction along the narrow reservoir. However, successive bathymetric measurements indicate that by 1990 the reservoir had already reached an equilibrium profile in the narrow upstream reach, and most sediment was accumulating in the portion of the reservoir within about 4 km of the dam. One-hundred-year simulations indicated that by changing the operating strategy from continuous high-pool operation to sediment pass-through during flood periods will decrease sediment accumulation by 65 percent (Fig. 20.16). Sediment pass-through should be capable of transporting most flood-borne silts and clays through the reservoir, but most sand-size particles will continue to be trapped, as will fines delivered during small inflow events.

## 20.6 OPERATIONAL MODEL

### 20.6.1 Operational Constraints

Implementation of sediment pass-through at Loíza Reservoir is complicated by several operational constraints. The tributary watershed is small and steeply sloping, and peak runoff will reach the dam within several hours of the receipt of rainfall in the watershed. Although Loíza Reservoir is too small to have significant flood control benefits, there are flood-prone communities downstream of the dam and it is essential that reservoir operations not increase flood damage above levels which would have occurred in the absence

of the dam. On at least one previous occasion, gate operation at Loíza Dam magnified discharge below the dam during a runoff event by, releasing water faster than it entered the reservoir, causing downstream flooding that would not otherwise have occurred.

Because of the downstream flooding hazard, releases from the reservoir should not exceed bankfull capacity of about 1700 m<sup>3</sup>/s unless reservoir inflow exceeds this amount, in which case reservoir discharge should not exceed inflow. The bankfull capacity is variable and depends on the sandbar configuration at the river mouth where it discharges to the Atlantic Ocean, and adjacent to the flood-prone coastal community of Loíza Aldea. The river mouth becomes completely blocked with beach sand during dry periods, and releases should be made from the dam as early as possible to wash out the river mouth bar. Maximum sediment routing effectiveness also requires the earliest possible reservoir drawdown, to the lowest level possible, and for the longest duration possible. Early release of water from storage is critical because the rate of reservoir drawdown is determined by the difference between discharge and inflow. As inflow increases, the drawdown rate must decline to prevent downstream flooding, and, when inflow exceeds downstream bank full discharge, the reservoir level cannot be lowered further because it would require that discharge exceed inflow. It is also essential to completely refill the reservoir at the end of the flood for the water supply.

### 20.6.2 Model Development

A sediment routing system was developed within these constraints by using the sediment pass-through strategy based on hydrograph prediction outlined in Sec. 13.4 and Fig. 13.6. All modeling was implemented in a 386 25-Mhz microcomputer. Prediction of the 24-hour storm runoff hydrograph from tributary areas and hydraulic routing through the reservoir was undertaken with the BRASS model (Morris et al., 1992). This model was used to forecast the total water volume tributary to the dam consisting of: (1) the runoff in the tributary watershed which has not yet reached the reservoir, plus (2) the water volume in the reservoir.

The BRASS model was originally developed by the U.S. Army Corps of Engineers (1981) and has been described by McMahan et al. (1984) and Colon and McMahan (1987). The model includes a hydrologic module and a hydraulic module which incorporates the DWOPER (Dynamic Wave Operational) one-dimensional unsteady flow hydraulic model, which solves the St. Venant equations. Originally designed to operate at 1-hour intervals, the model was modified to use the 15-minute time increment needed to simulate the response of the relatively small and steep Loíza watershed. Another modification allowed reporting of the total water volume above the dam in both the hydrologic and hydraulic modules. The DWOPER model was used to perform hydraulic flood routing through the river-reservoir reach instead of a hydrologic flow routing method because highly variable flow conditions may occur in the reservoir over a storm period. Within hours, a reach may alternate from impounding to free flow to impounding again because of early drawdown, passage of the flood, and subsequent refilling.

The model predicts runoff hydrographs based on the Soil Conservation Service unit hydrograph method which uses a soil "curve number" that is adjusted according to antecedent moisture conditions. Real-time rainfall data are available from two independent networks of reporting gages within the watershed. The primary data source is the Enhanced ALERT (Automated Local Evaluation in Real Time) system, which incorporates tipping bucket raingages and VHF radio telemetry. The USGS data collection platforms, which also have tipping bucket raingages and report via satellite, are available as backup telemetry.

The operational system delivered to the authority uses a customized BASIC language system manager software shell which automatically reads and interprets program output files. It includes graphical display of water surface and velocity profiles, discharge hydrographs, summary data on reservoir and runoff volume, recommendations for gate operation, and access to all program input and output options. The system manager was programmed to compute the gate openings required to maintain the maximum permissible discharge subject to the limited capacity in the downstream channel plus water storage constraints. Gate operating limitations such as opening and closing speed and out-of-service gates are incorporated. Hard copy reports and graphics can be printed out during and at the end of the event. Multiple preprogrammed graphics display parameters are provided such as gage status, rainfall intensity, water surface profile, and observed and predicted hydrographs. The Spanish-language menu system allowed the operator to manage the hundreds of program and data files contained in the system.

### **20.6.3 Model Input**

For runoff computations, the watershed tributary to the dam was divided into 14 subbasins. Thiessen polygons are drawn for each raingage, antecedent soil moisture is calculated for the 5 days prior to a storm event, and curve number values for each subbasin are adjusted accordingly. Each subbasin receives a weighted portion of the rainfall reported by neighboring raingages, and the resulting discharge hydrograph from each subbasin is computed and routed into the hydraulic model. The hydraulic model contains 55 cross sections extending approximately 13.5 km upstream of the dam along the Loíza River, and 4.7 km upstream along the Gurabo river from its confluence with the Loíza river. The system is designed to operate in real-time based on rainfall actually received at reporting raingages; computations are not dependent on rainfall prediction, although the model is capable of predicting reservoir hydraulics from forecast rainfall.

### **20.6.4 Model Calibration**

At the time of model construction, very few ALERT raingage data were available in the Loíza watershed. Calibration was conducted with the only significant set of continuous rainfall and discharge data available prior to June 1991, that for hurricane Hugo on September 18, 1989. This was not a particularly heavy rainfall event and the 1800-m<sup>3</sup>/s peak discharge at the dam had a return interval of under 5 years. Model calibration focused on hindcasting three hydrographs: runoff hydrographs at the Gurabo and Loíza gages, and the discharge hydrograph immediately below the dam. Extensive convergence testing of the DWOPER model was undertaken, challenging the hydraulic module with extreme fast-rising hydrographs and sudden opening and closure of gates, making adjustments as necessary until the model was capable of continuous computation without convergence error through events more extreme than those considered physically possible in the watershed.

### **2.6.5 Model Operation**

Periods of heavy rainfall across the Loíza watershed are associated with large-scale weather systems such as tropical depressions and frontal systems which can be forecast. During these periods it is necessary to continuously monitor the total tributary volume of water upstream of the dam. As rainfall is received in the watershed the total volume tributary to the dam (predicted 24-hour inflow hydrograph plus reservoir storage) will

exceed the total reservoir storage capacity. When this occurs, it is possible to release water from the reservoir with confidence that the reservoir can be refilled, as long as the total tributary volume always equals or exceeds the total reservoir capacity. As the storm continues to develop, drawdown can continue until the reservoir is fully drawn down with all gates open and the water level at the dam is determined by weir flow over the gated spillway. When rainfall diminishes, the gates are progressively closed to store water in the reservoir. Thus, sediment routing procedures may be initiated at the beginning of all significant rainfall events, and the extent of drawdown will be determined by the magnitude of the storm that eventually develops. Simulations showed that the reservoir can be completely drawn down with approximately 3 hours of lead time.

The hydraulic BRASS model has a limitation in that there is no opportunity within a model run to adjust the reservoir volume using real-time field observations during an event. An option is to continuously compute storage volume from reporting level gages at different points along the reservoir instead of using a hydraulic model. Hydrologic computations would continue to be performed according to the previously developed methodology.

## 20.7 SEDIMENT REMOVAL

---

Sediment pass-through at Loíza Reservoir can substantially reduce sedimentation but cannot prevent it. HEC-6 sediment transport modeling indicated that sands, which constitute about 20 percent of the sediment load, will continue to be trapped in the reservoir, and fines delivered during smaller runoff events will also be trapped. Sediment removal is required to maintain reservoir capacity or to recover previously lost capacity. Hydraulic dredging is both technically and economically feasible, but dredging alone as the sole means to control future sedimentation is unnecessarily costly. As much sediment as possible should be passed through the reservoir by sediment routing to reduce both the economic and environmental costs of dredging, and to reduce dredging frequency. Dredging options were discussed in the project environmental documents (PRASA, 1992, 1995).

### 20.7.1 Dredging Volume

Two types of dredging activities were analyzed: (1) maintenance dredging and (2) restoration dredging. Maintenance dredging would focus in the upstream portion of the reservoir where the existing deposits consist largely of sand-size particles. Approximately  $2 \text{ Mm}^3$  of sediments would be removed by dredging, creating a trap to capture the coarse fraction of the inflowing sediments which cannot be transported through the reservoir during pass-through events, essentially stabilizing present reservoir capacity. It is preferable to have these sediments accumulate in an area near disposal sites upstream of the reservoir rather than to transport sediment into the main part of the impoundment. There is a strong market for sand in Puerto Rico with prices in excess of  $\$10/\text{m}^3$ . An additional consideration was the possibility of marketing sand trapped in this upper area of the reservoir.

Restoration dredging would entail the removal of about  $6 \text{ Mm}^3$  of material, returning the active pool of the reservoir to near its original capacity. Sediments more than 2 m below the invert elevation of the lowest water supply intake would not be removed and most of the dead storage pool would remain sedimented. The restoration dredging alter

native was preferred, since it would immediately create about a  $0.26 \text{ m}^3/\text{s}$  ( $6 \times 10^6$  gal/day) increase in firm yield and also produce the longest time interval before the next dredging.

### 20.7.2 Spoil Disposal Options

There are no easy disposal options at Loíza reservoir. Lands in the vicinity of the reservoir are steeply sloping. Flat coastal lands between the dam and the sea are either urbanized, are protected wetlands, or have been designated as river floodway by the Federal Emergency Management Agency (FEMA). The nearest potential downstream land disposal site would require about 15 km of pipeline from the dam site. Use of this site would also require a floodway revision in a hydraulically complex floodplain area.

Disposal to the Atlantic Ocean was considered and rejected under two different options. One option would entail a pipeline to the coast extending offshore to a new ocean disposal site to be designated. Another ocean disposal option would involve a pipeline to a coastal site, where the sediment would be dewatered and transferred onto barge which would dump it into the currently designated dredged material deep ocean disposal site located in the vicinity of San Juan harbor. Both options would require a pipeline in excess of 20 km long and would involve long permitting lead times. Additionally, if an economically viable land disposal site is available, the U.S. Environmental Protection Agency (EPA) is not likely to grant an ocean disposal permit.

Upland sites upstream of the reservoir are available but again require rather long pumping distances. The three disposal areas currently under consideration vary in distance from 12 to 21 km from the dam (Fig. 16.11). Most sediment is deposited in the wider portion of the impoundment within 3 km of the dam rather than the narrow upstream reach, and over half the disposal volume occurs in the most distant disposal site. In addition to pumping friction losses, the upstream disposal areas require static pumping heads up to 30 m. The volume of dredged material will initially exceed that of in situ sediment because of water entrainment. At Loíza Reservoir, containment area volume requirements were estimated for initial bulking factors of 1.5 to 1.8 and a final bulking factor of 1.2.

### 20.7.3 Sediment Sampling

A two-part sediment sampling program was undertaken in the reservoir to analyze the possible presence of contaminants. A preliminary sampling and analysis program was conducted on 19 sediment samples which were subjected to the elutriate and modified elutriate analysis tests. These tests mix sediment with water to simulate the dredging process, then allow the water to settle. The concentration of chemicals found in the settled water simulates the quality of water that will be discharged from a dredged material containment area. Supernatant filtration removes fine sediment and the associated contaminants. This gives an indication of the fraction of the contaminants associated with particulate material, and also approximates the quality of water that could be produced if the undiluted containment area discharge were used to supply a potable water filtration plant. The preliminary sampling and analysis program indicated that concentrations of inorganics in the elutriate that exceeded water quality standards included cadmium, copper, chromium, lead, mercury, nickel, silver, zinc, and cyanide. However, high concentrations were found only in the unfiltered elutriate samples, indicating that the contaminants were associated with sediment particles and were not generally present in dissolved form. It was concluded that removal of sediment from the

water column by filtering or other means (e.g., additional natural sedimentation within the reservoir) would reduce potential water quality impacts to acceptable levels.

## **20.8 PROJECT COSTS AND IMPLEMENTATION**

---

The total implementation cost of sediment routing at Loíza is less than \$1 million. No structural modifications are required at the dam. The cost of dredging 6 Mm<sup>3</sup>, including construction and management of diked containment areas, received a low bid of \$42 million in 1995. This does not include land acquisition costs, which may run \$8 million. Engineering, testing, and permitting are estimated to cost an additional \$2 million. The total dredging cost is anticipated at about \$8.70/m<sup>3</sup>.

## **20.9 CLOSURE**

---

The Loíza case study illustrates the application of real-time hydrologic modeling to optimize sediment routing within a highly constrained operational environment, in conjunction with reservoir dredging. It also illustrates that in some cases significant sediment control benefits can be achieved without structural modification, and with minimal environmental impact, by simply changing operating procedures during storm events. Finally, this case history illustrates the consequences of failing to take timely actions to solve sedimentation problems, and the potentially torturous path toward implementation.

---

## CHAPTER 21

---

# GEBIDEM DAM AND RESERVOIR

---

The Gebidem hydroelectric reservoir in Switzerland is an example of one of several sites in the Alps region where flushing for sediment control has been conducted on a regular basis. This case study is based on annual operating reports of flushing activities kindly provided by the owner, Electra Massa, and a site visit to observe the empty reservoir and modifications to the outlet structure in the company of Gian Rechsteiner, in addition to the cited literature and reports.

### 21.1 INTRODUCTION

---

The Gebidem arch dam began impounding in 1968 on the Massa River, a tributary to the Rhone just upstream of Brig, Switzerland. Because of topographic limitations imposed by the 5 percent stream slope and narrow gorge, the 120-m-tall arch dam with a 327 m crest length impounds only  $9 \times 10^6 \text{ m}^3$  of water and the reservoir is only 1.5 km long. The facility operates either in a daily peak load mode or continuously, depending on the inflow. The power plant has a 340-MW nominal generating capacity at  $55 \text{ m}^3/\text{s}$  and 743 m head, and the tailrace discharges directly to the Rhone. A location map is shown in Fig. 21.1.

Sixty-five percent of the 200-km<sup>2</sup> watershed tributary to the dam is occupied by the d'Aletsch Glacier, the largest in Europe. Glacial activity produces a sediment yield equivalent to a denudation rate of 2.5 mm/yr averaged across the watershed, more than an order of magnitude higher than is typical of unglaciated mountain areas in Switzerland. The total sediment load entering the reservoir is about 400,000 m<sup>3</sup>/yr of cohesionless material, mostly in sizes ranging from very fine sand through gravel, and about 20 percent of the total load is composed of sediments between 1 and 100 mm in diameter. Because a conventionally operated reservoir at this site would fill with sediment in about 20 years, sediment management was incorporated from the initial design stage.

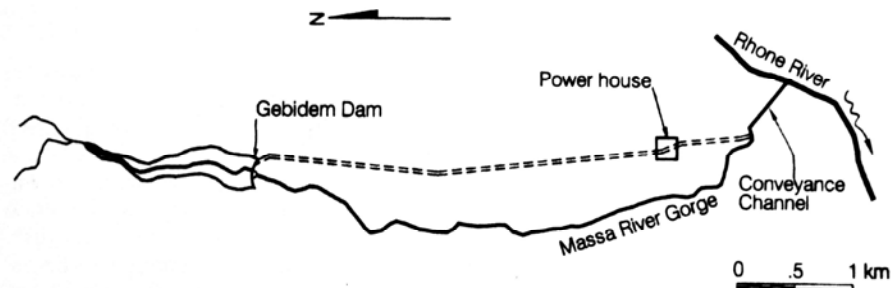
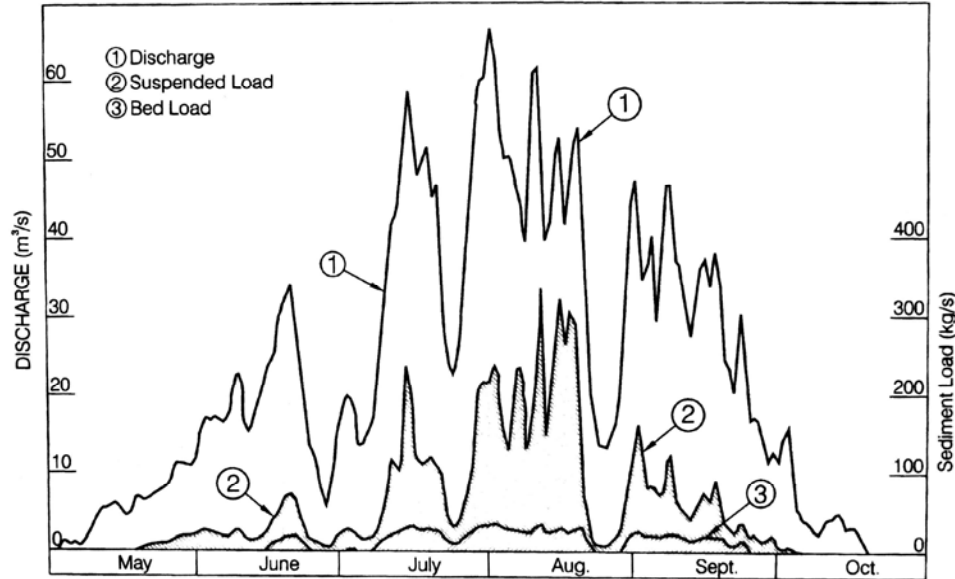


FIGURE 21.1 Location map of Gebidem darn.



**FIGURE 21.2** Discharge of water and solids in Massa River at Gebidem dam site, 1958 (after Oberle et al., 1967).

The Massa River between the glacier and the Rhone can be divided into three reaches: a 5-km upper reach averaging 5.5 percent slope, a steep middle reach 1 km long at 20 percent slope, and a lower reach 0.8 km long at 0.8 percent slope. The dam was located in the middle of the upper reach. Because of its low slope, the reach of the Massa River immediately upstream of its confluence with the Rhone was channelized by a rectangular concrete section to facilitate sediment conveyance into the Rhone. A sand and gravel operator subsequently constructed a small dam in the gorge immediately upstream of the channel to capture part of the sediment for classification and sale as commercial aggregate.

Typical of glacial-fed streams, discharge at the dam site is seasonal and is dominated by snowmelt, glacial melt, and summer storms. Winter flows, from November through April, are negligible. The hydrograph in Fig. 21.2 illustrates the pattern of both liquid and solid discharge observed in 1958 during the six warm months when there was appreciable flow.

## 21.2 ALTERNATIVES CONSIDERED

A variety of sediment management alternatives were initially considered, but based on a screening analysis which eliminated a number of options, three alternatives were subject to more detailed analysis at this site: (1) sediment bypass, (2) periodic dredging, and (3) emptying and flushing. Under the sediment bypass alternative, the sediment-laden flows would be discharged through a large-diameter free-flow tunnel exiting downstream of the dam. The dredging alternative would involve use of a pumping suction dredge discharging downstream through outlets located at various levels in the dam. Oberle et al. (1967) noted that the venting of turbidity currents was among the alternatives originally considered, but that the grain size of the inflowing sediment was considered to be generally too large. Under the flushing alternative the sediment would be scoured out

**TABLE 21.1** Cost and Water Use for Three Sediment Management Alternatives Considered at Gebidem Dam

Alternative	Capital cost, 10 <sup>6</sup> francs	Unit cost of sediment removal, francs/m <sup>3</sup>	Water use, 10 <sup>6</sup> m <sup>3</sup> /yr
1. Sediment bypass	9	3.8	24
2. Dredging	3.7	2.0	10
3. Flushing	Small	0.8	8

Source: Ullmann (1970).

through the low-level sluices designed for emptying the reservoir. Flushing was the least costly alternative to implement because it would use planned engineering works (the emptying outlet) and would require essentially no other structural work. This alternative also used the least amount of water. The costs and water use associated with each alternative are compared in Table 21.1.

Two physical models were constructed to test and aid in the design of the system. A 1:30 scale model of most of the reservoir area was used to examine sediment scour along the entire length of the reservoir, and a 1:15 scale model of a single low-level sluice examined the entrance shape and the placement of deflectors and water jet pipes for disaggregating sediment that may accumulate in front of the outlet. Bed material up to 40 cm in diameter was simulated.

Two types of sediment flushing operations were considered and analyzed in the modeling, pressure scour, and free-flow scour. Under the pressure scour option, the reservoir is drawn down to the minimum operating level and then the bottom outlets are opened to allow the development of a conical scour hole in front of the outlet while maintaining the minimum operating level (Fig. 15.8). Sediments from the upper portion of the reservoir are carried toward the dam during the drawdown, but the only sediments evacuated are about 25,000 to 30,000 m<sup>3</sup> of material in the area of the semi-conical scour hole in front of the outlets. While the scour hole can be evacuated in only 2 to 3 hours, it takes 20 to 30 hours to refill the hole with sediment. To discharge the anticipated 400,000 to 500,000 m<sup>3</sup>/yr of sediment inflow, 10 to 15 drawdowns would be required annually.

The adopted flushing alternative was to completely empty the reservoir and allow free flow through the bottom outlets for a period of 2 to 4 days. Water use during the flushing was originally estimated at 6 to 8×10<sup>6</sup> m<sup>3</sup>, but in practice it has averaged less than 3×10<sup>6</sup> m<sup>3</sup>. Because of regular flushing, there has not been a problem of excessive sediment accumulation in front of the bottom gates, and the water jet pipes provided for dislodging sediment are not used.

### 21.3 CONFIGURATION OF LOW-LEVEL OUTLET

The dam was designed with two flushing tunnels located directly beneath the intake structure and near the original streambed elevation (Fig. 21.3). This figure also shows the new multiple-level intake tower that was retrofitted in 1995-1996. The low-level outlet originally contained two gates: a downstream sector gate (radial gate) and an upstream flap gate to serve as an emergency gate that can be closed for maintenance of the sector gate and discharge tunnel. These gates were selected for their robust design and ability to pass coarse sediment. Neither type of gate requires guide channels or mechanical surfaces

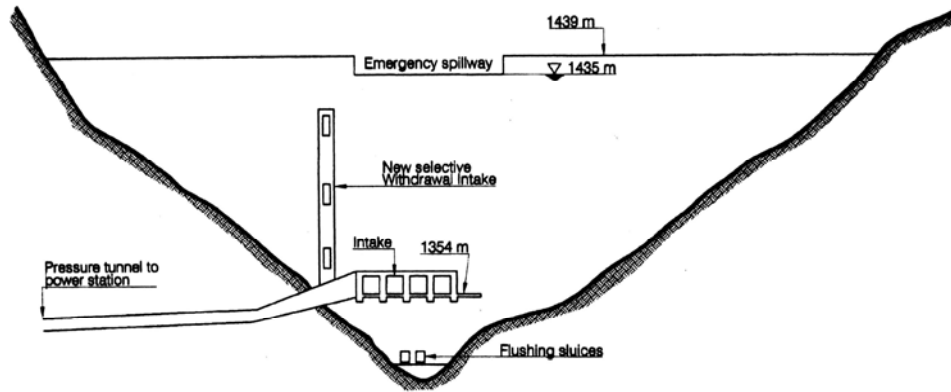


**FIGURE 21.3** Water face of Gebidem dam showing location of flushing outlets in relation to the intake structure.

in the flushing channel, other than the flat surfaces for gate seals (Stutz, 1967). So that it resists erosion, the entire perimeter of the flushing tunnel was lined with steel plate. The hydropower intake was located above the flushing sluices so that sediment is removed from the area beneath the intake during each flushing.

After 25 years of operation, erosion had become significant in the gate seal on the bottom outlet. Suspended sands were able to enter the power intake, and fine sediment that entered the power intake was causing excessive wear on turbine runners. In 1995-1996 two construction modifications were performed to correct these problems. A third gate was added to modulate discharge during flushing operations, allowing the two original gates to be used only in fully open or fully closed mode. When these gates are used in partially open mode to regulate flow, the sediment erodes their seals and compromises their water tightness. Erosion of the seal at the modulating gate would not be a problem because it would never be used as a watertight closure. The new regulating gate is a vertical sluice installed immediately upstream of the sector gate, which was relocated a short distance downstream to make space. The modified gate arrangement is shown in Fig. 21.4. The second modification was to replace the existing fixed-level intake with an intake tower having multiple ports to allow withdrawals from higher levels in the water column where both the concentration and grain size of sediment will be smaller.

## 21.4 FLUSHING OPERATIONS

The reservoir first impounded water during a partial filling in 1968. It was flushed in June of that year and between May and July in every subsequent year. Flushing has maintained the entire reservoir virtually free of sediment accumulation because of its narrow gorge-type geometry (Fig. 21.5). Flushing is conducted during the late spring and early summer, prior to late summer floods, when two conditions occur: (1) the flow of the Massa River is relatively low (less than  $20 \text{ m}^3/\text{s}$ ) and dilution flow in the Rhone is relatively large (more than  $40 \text{ m}^3/\text{s}$ ) but not near flood stage; and (2) the  $0^\circ\text{C}$  isotherm is located around 3000 m, which corresponds to stable meteorological conditions. The large flow in the Rhone is required to dilute and transport the sediment delivered from the flushing. Ideally

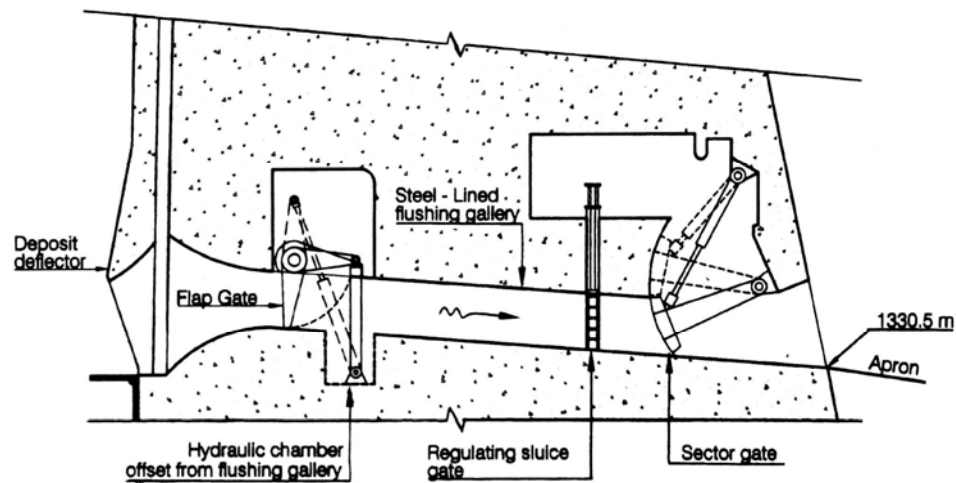


**FIGURE 21.4** Gate configuration at Gebidem dam.



**FIGURE 21.5** General view of reservoir upstream of Gebidem dam in 1995, after 27 years of operation with annual flushing (*G. Morris*).

the Rhone discharge would be 10 times the flow of the Massa, but this condition is rarely met. Although the designated flushing period is the same every year, the exact date to begin flushing is established only 1 day in advance, when the proper hydrologic and meteorological conditions have coincided. Monetary penalties may be assessed for downstream fish kills, and high suspended-sediment concentrations also interfere with downstream municipal water intakes. Suspended-sediment concentrations in the Rhone are monitored at several sites during each flushing event.

Prior to flushing, the reservoir is brought to its minimum operational level by releasing water through the turbines. Flushing is initiated with the gradual opening of first one gate, then the second, over a period of approximately 2 hours, increasing discharge from an initial rate of about  $10 \text{ m}^3/\text{s}$  to a final rate of about  $60 \text{ m}^3/\text{s}$ . Between 3 and 6 hours after initiation of gate opening the reservoir has been completely emptied and free

flow flushing through the outlet begins, typically at discharges between 10 and 20 m<sup>3</sup>/s. In some years the gates are closed for periods of about 20 minutes, then fully reopened; the resulting rising and lowering water level facilitates flushing of deposits in the vicinity of the dam. Some characteristics of flushing events are summarized in Table 21.2. The column labeled "Gate operations" in the table refers to the number of times the bottom gates were closed and reopened during the flushing event to facilitate sediment removal. The amount of solids flushed from the reservoir are not monitored every year, but are computed by assuming 6 percent solids concentration in the flushing discharge, a value established by field sampling during early flushing events. Thus, the values for sediment removed are, in many years, only rough estimates.

More detailed measurements were made during the 1991 flushing event to construct a sediment budget. The original data for sediment concentration are reported in units of milliliters per liter of settleable solids as measured in an Imhoff cone, and have been adjusted to grams per liter by using the conversion factor of 1 mL/L = 1.32 g/L, measured in the Rhone at Lonoza during the 1995 flushing. Discharge and concentration data at the dam (Fig. 21.6) reflect the high initial sediment concentration characteristic of flushing operations. Because of settling of sediments within the gorge, the maximum suspended solids concentration measured at the channel in the flat downstream reach was 304 g/L, only 51 percent of the maximum value registered at the dam. The highest suspended solids concentration measured in the Rhone at the Brigerbad Bridge was 47 g/L, compared to 2 g/L in the Rhone above the confluence with the Massa. Two-thirds of the total sediment discharge occurred during the first 5 hours of this 95.5-hour event (Fig. 21.7). Different portions of the reservoir are eroded during the early and later parts of the flushing, as illustrated in Fig. 21.8, which is based on photogrammetric surveys of the reservoir during the flushing. A sediment balance based on monitoring at various points is shown in Table 21.3, showing that much of the material flushed from the reservoir is deposited in the gorge below the dam, and is not washed downstream until later in the summer. A sand and gravel operator removes an unquantified volume of sediment from the system for commercial use. The delta region of the reservoir may be experiencing the gradual accumulation of material too large to be transported through the impounded reach

**TABLE 21.2** Summary of Flushings at Gebidem Dam

Year	Water used, 10 <sup>6</sup> m <sup>3</sup>	Duration, hours	Mean purge flow, m <sup>3</sup> /s	Gate operations	Solids removed, 10 <sup>6</sup> m <sup>3</sup>	Solids concentration, %
1982	2.38	56	11.8	0	0.143	6.0
1983	3.38	48	19.6	2	0.175	5.2
1984	2.97	68	12.1	6	0.178	6.0
1985	2.50	49	14.2	0	0.150	6.0
1986	3.53	45	21.8	0	0.212	6.0
1987	3.20	45	19.8	13	0.192	6.0
1988	2.93	79	10.3	13	0.176	6.0
1989	2.49	49	14.1	1	0.150	6.0
1990	3.18	40	22.1	12	0.191	6.0
1991	2.35	96	6.8	0	0.270	11.5
1992	3.28	151	6.0	61	0.197	6.0
1993	2.48	101	6.8	?	0.260	10.5

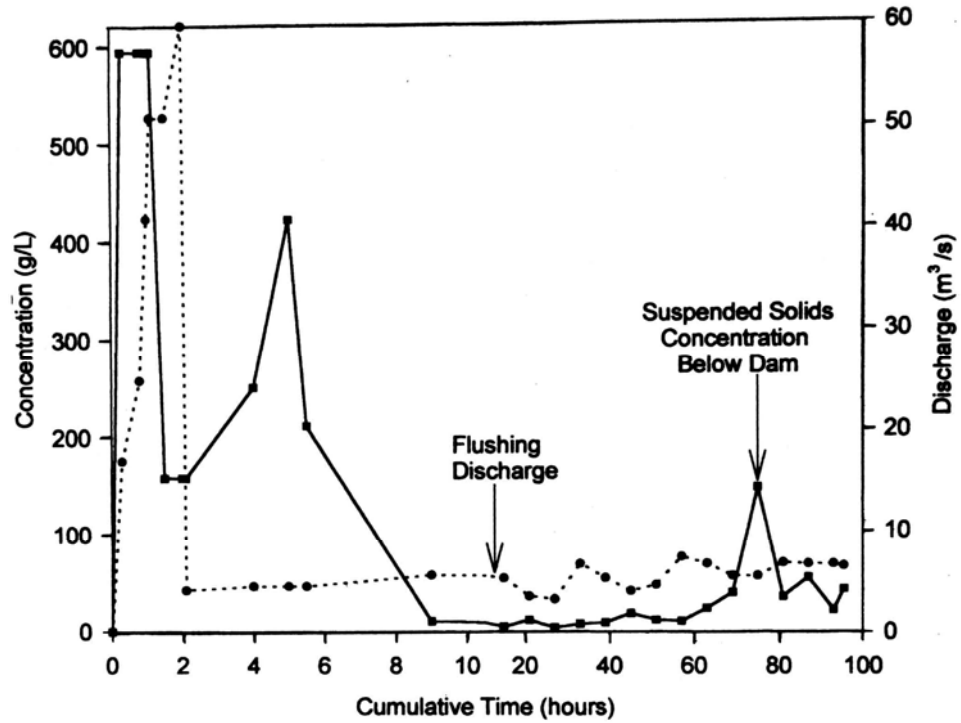


FIGURE 21.6 Discharge hydrograph and suspended sediment concentration at the outlet from the dam during the 1991 flushing event (data from *Electra Massa*).

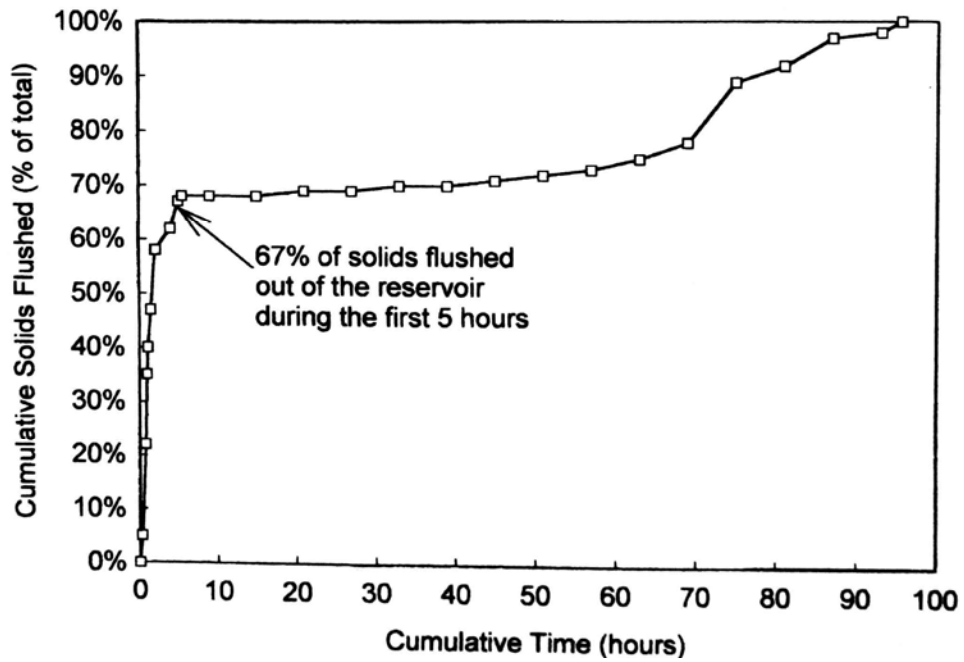
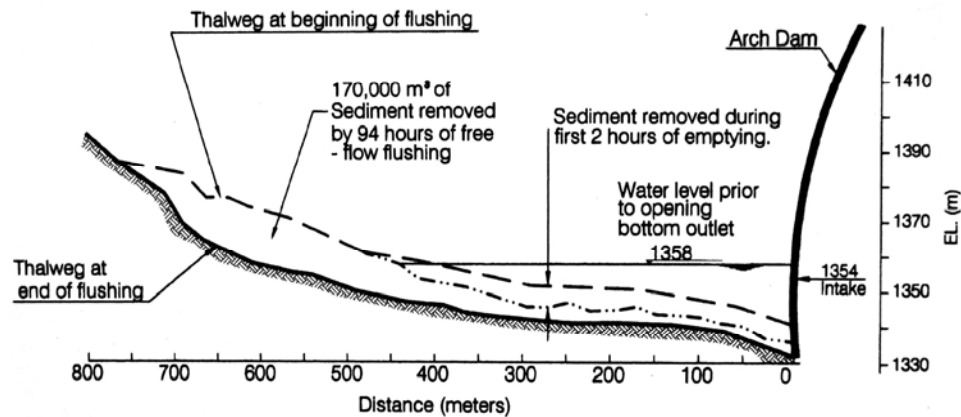


FIGURE 21.7 Cumulative sediment discharge from Gebidem dam during 1991 flushing event (data from *Electra Massa*).



**FIGURE 21.8** Thalweg profile upstream of Gebidem dam, 1991 flushing event, showing the areas of sediment removal during different parts of the flushing period (data from *Electra Massa*).

**TABLE 21.3** Sediment Balance, 1990-1991, Gebidem Darn

Parameter	Volume, m <sup>3</sup>
Annual sediment release, 1990-1991:	
Sediment released by flushing (95.5 hours)	270,000
Sediment passing through turbines (12 months)	70,000
Fate of sediment flushed:	
Deposited in gorge	81,000
Deposited in aggregate works	32,000
Delivered to Rhone	157,000
Delivered to Rhone by turbines (12 months)	<u>70,000</u>
<b>Total</b>	<b>340,000</b>

impounded reach by the low-discharge flushing flows. However, there are no data on the long-term accumulation of coarse material in the delta area.

## 21.5 DOWNSTREAM IMPACTS

Discharge and suspended solids data from the Rhone River during the 1991 flushing event are shown in Fig. 21.9. The same short-duration high-solids peak that occurs at the dam is reflected in the Rhone data, but sediment concentrations are an order of magnitude lower because of upstream deposition and dilution (Table 21.4). The peak sediment concentration in the Rhone occurred during the initial flushing period, when the flushing discharge of 60 m<sup>3</sup>/s exceeds the Rhone discharge of 50 m<sup>3</sup>/s. Thus, most of the reduction in peak concentration is due to upstream sedimentation rather than dilution.

The combination of sediment release and reduced discharge due to diversion for power production has heavily impacted the Massa gorge downstream of the dam. The photograph of the gorge downstream of the dam in Fig. 21.10 shows both the constricted

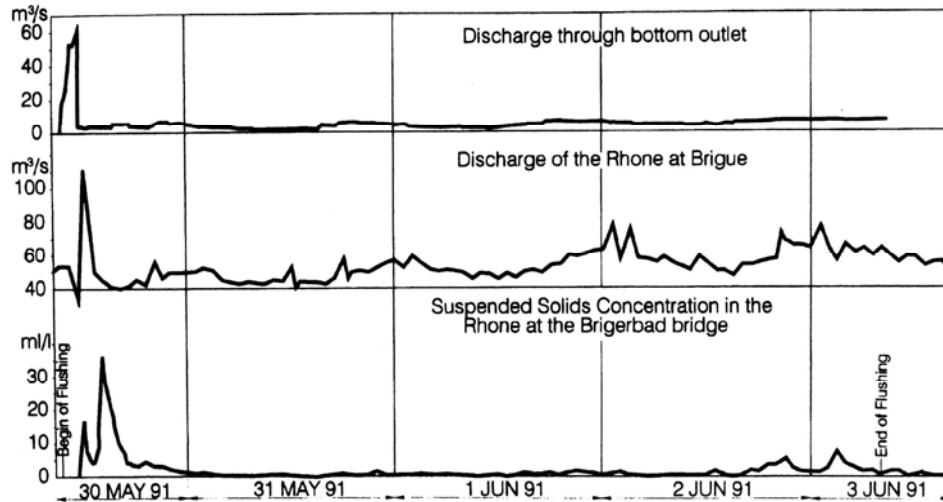


**FIGURE 21.9** Hydrographs and sediment concentration in the Rhone River during the 1991 flushing event (after *Electra Massa* 1992).

**TABLE 21.4** Peak Downstream Sediment Concentrations during Flushing

Measurement point	Time	Concentration, g/L
Base of the dam	0915	450
Conveyance channel	1330	230
Rhone above Massa confluence		2
Rhone at Naters	1345	37
Rhone at Brigerbad bridge	1400	47

nature of the gorge reach and the deposition of fine sediment. After many years of operation without difficulty, during the 1990 flushing the conveyance channel became two-thirds filled with coarse sediment, and during the 1992 flushing it became completely filled. Seventy percent of the sediment deposited in the conveyance channel was sized between 1 and 32 mm in diameter (Boillat, 1994), which is much coarser than the total load of the Massa, of which only 20 percent consists of grains larger than 1 mm. The massive deposition in the conveyance channel represents the coarsest part of the load, which gradually accumulated along the length of the gorge over the years, and which also probably deposited in the conveyance channel in smaller amounts during previous years but went unnoticed. Massive deposition occurred once the gorge had reached a new equilibrium condition with respect to the coarser sediment, and this coarse material was exported in large quantities to the downstream conveyance channel.

According to Stutz (1967), physical modeling was used to design the conveyance channel and analyze the effects of the localized sediment discharge on the Rhone. The conveyance channel reportedly had adequate capacity and impacts on the Rhone were insignificant. The volume of flushing flows used over the past decades have been as little as half the volume considered for release under the original studies. Through both physical and numerical modeling, Boillat (1994) concluded that the problem of deposition could not be solved by modifying the channel, and recommended increasing flows to increase transport capacity through the channel. Because of this problem the

amount of water required for flushing is not determined by sediment removal from the reservoir, but by the transport-limited conveyance channel downstream of the dam.



**FIGURE 21.10** Photo of sediment in the gorge 200 m downstream of dam showing a layer of fine sand deposited over cobbles and boulders (*G. Morris*).

The Rhone is a fast-flowing gravel-bed river which has been severely altered by channelization along virtually its entire reach above Lake Geneva. It has also suffered from a long history of extensive aggregate extraction. The release of flushing sediments into the Rhone appears to have no significant long-term adverse impact on current river morphology. On the contrary, it helps maintain sediment contributions to the river. However, the temporary high suspended-sediment loads and deposition of fine sediment on the bed has caused some temporary inconveniences at downstream water supply intakes, and fish kills in the Rhone River have also been associated with flushing.

---

## CHAPTER 22

---

# NORTH FORK FEATHER RIVER, CALIFORNIA, U.S.A.

---

### 22.1 INTRODUCTION

---

Along the steep canyon reach of the North Fork Feather River draining the Sierra Nevada mountains above Lake Oroville, California, the Pacific Gas and Electric Company (PG&E) operates a chain of three small hydropower dams; moving downstream along the river they are Rock Creek, Cresta, and Poe. About 40 percent of the 4587-km<sup>2</sup> watershed area tributary to Rock Creek dam is regulated; most sediment is delivered from the unregulated 2657 km<sup>2</sup> East Branch tributary which enters a short distance above Rock Creek Reservoir (Fig. 22.1).

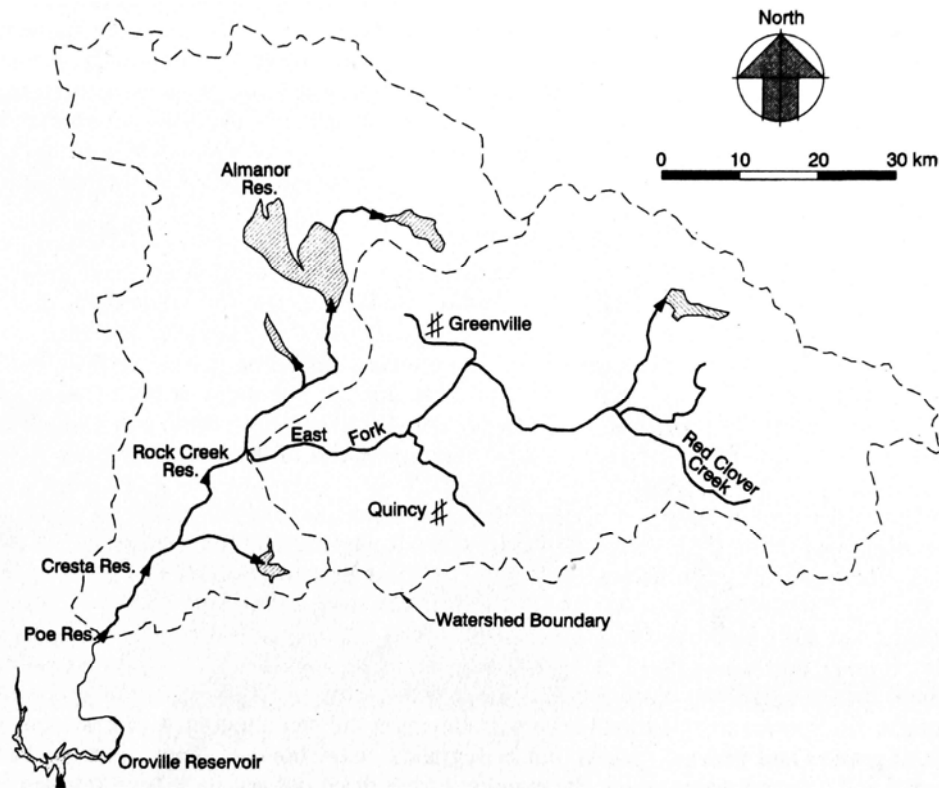


**FIGURE 22.1** Location map of watershed boundaries and reservoirs, North Fork Feather River.

After 30 years of operation, the accumulation of coarse sediment and the environmental issues related to sediment management began to interfere with the operation of these power stations. Sediment management at Rock Creek and Cresta Dams was not contemplated when they were constructed, and the original gate design is not well-suited to the passage of coarse sediment. Sediment-related problems at all three dams has led to a number of studies and remedial actions both in the watershed and at the dams.

This case study provides an example in which the owner, PG&E, has employed a two-pronged approach to address sedimentation problems, working to reduce sediment yield from upstream by supporting a watershed management program while simultaneously working to develop remedial measures at the dams. Demonstration erosion control projects initiated in the watershed in 1986 have catalyzed watershed restoration activities across the entire East Branch and Middle Fork watersheds, an area of 8345 km<sup>2</sup>. This case study focuses on the watershed management activities, which parallel many other similar activities nationwide. At the dams a sediment routing strategy has been developed which can produce a sediment equilibrium along the chain of reservoirs, but at this writing the sediment routing system at Rock Creek and Cresta Dams has not yet been initiated. Data from this case study have been drawn from site visits, interviews, published documents, and other material kindly provided by numerous contributors.

## 22.2 GENERAL DESCRIPTION

---

### 22.2.1 Site Description

The North Fork Feather River upstream of Lake Oroville is a steep channel incised in a granitic gorge with an average slope of 0.009. The river has a riffle and pool sequence and generally contains cobble and boulder size material. Gravels occur locally, primarily in sheltered areas or eddies. Some reaches contain large boulders (several meters in diameter) delivered to the channel as debris flows or dropped from the steep canyon walls. Once highly regarded as a trout stream, a combination of watershed degradation, road and railroad construction, and hydropower development have greatly impacted the fishery.

The river profile showing the location of Rock Creek, Cresta, and Poe Dams is presented in Fig. 22.2. The three dams serve as forebays to power tunnels and have very little flow regulation function; they are used to produce peaking power except during periods of high discharge when they run continuously. All three dams are low structures with crest gates. The smallest and most downstream dam, Poe, has underflow radial gates which are well-suited to the passage of sediment. The dams at both Cresta and Rock Creek are almost identical, and both are fitted with overspill drum gates which are unsuited for sediment passage (Fig. 22.3). Characteristics of the dams are summarized in Table 22.1.

The Feather River drains the Sierra Nevada Mountains, and elevations in the study watershed vary from 424 m at Poe dam to 667 m at Rock Creek to 3182 m on Lassen Peak, the highest point in the watershed. Much of the East Branch watershed is at elevations above 1200 m, and contains numerous valleys with deep sedimentary deposits. Parent material consists primarily of volcanics, and the overlying soils on slopes tend to be coarse, well-drained, and relatively shallow. The vegetation consists primarily of mixed conifer forests including yellow pine, Jeffrey pine, ponderosa pine, sugar pine, white fir, and Douglas fir. Species composition varies with elevation and precipitation. Meadows contain mixed grasses and wetland species, but in degraded valley bottoms where channels have eroded and lowered water tables, the meadows have dried out and have been invaded by drought-resistant species with little forage value, such as sagebrush.

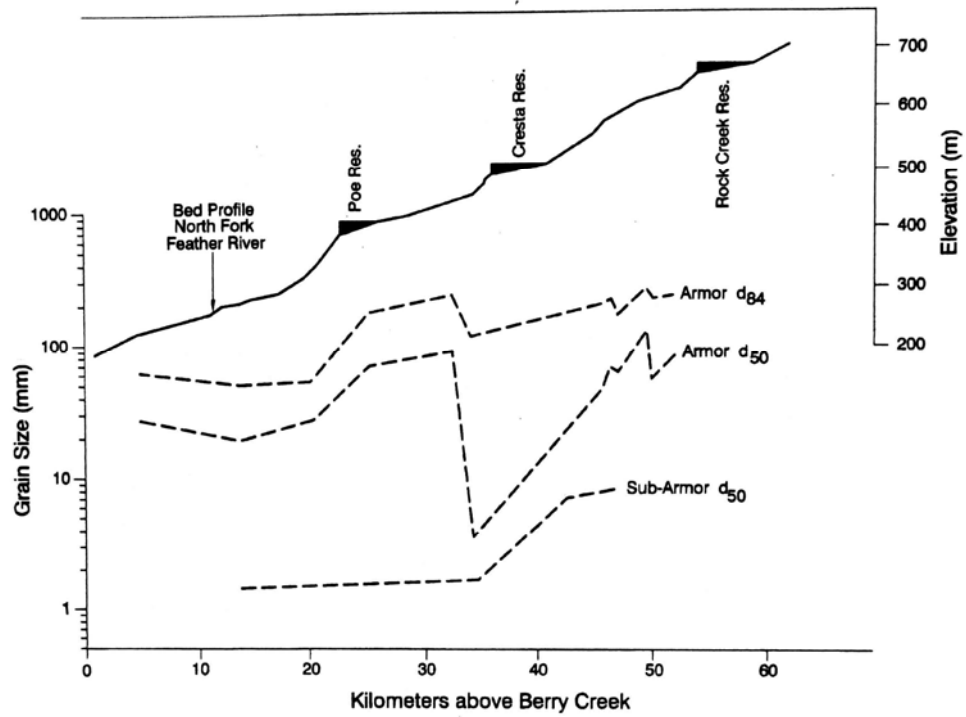


FIGURE 22.2 Profile along North Fork Feather River showing reservoirs and grain size of material on river bars (modified from Resource Consultants and Engineers, 1992).

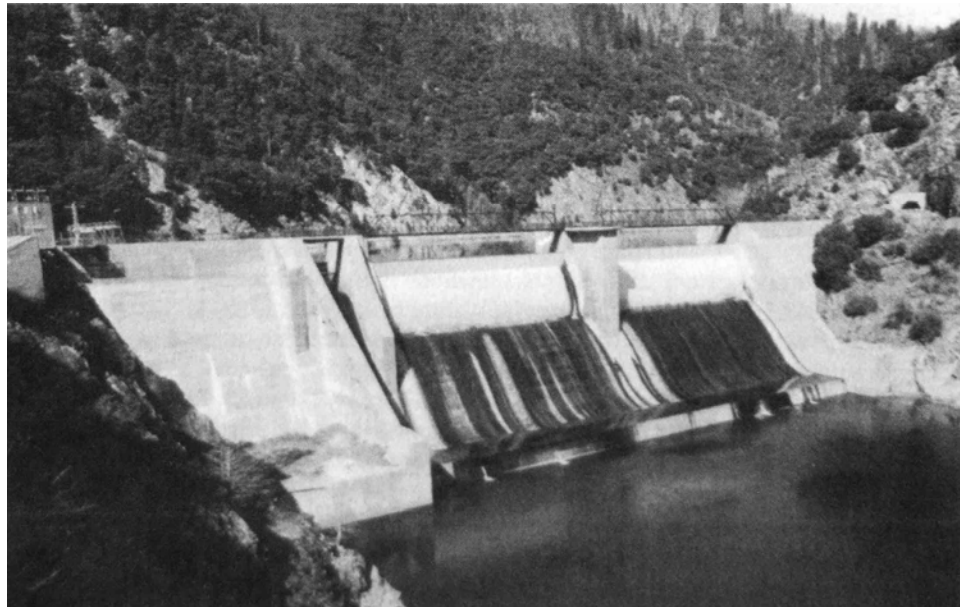


FIGURE 22.3 Photograph of Rock Creek Dam (G. Morris).

**TABLE 22.1** Characteristics of PG&E Hydro Dams on North Fork Feather River

Parameter	Rock Creek	Crests	Poe
Year completed	1950	1949	1958
Original volume. $10^6 \text{ m}^3$	5.4	5.1	1.42
Most recent bathymetry	1994	1994	1993
Sediment accumulation. $10^6 \text{ m}^3$	3.1	2.45	.338
Pool length, km	4.5		
Max. turbine discharge, $\text{m}^3/\text{s}$	94	110	
Generating capacity, MW	112	70	120

Over 50 percent of the annual precipitation of 1100 mm falls in December, January, and February, primarily as snow above an elevation of 1800 m and a mixture of rain and snow at lower elevations. However, warm winter storms can produce rain at elevations as high as 3000 m. Summer months account for less than 3 percent of the annual precipitation. Runoff and sediment transport is associated primarily with snowmelt, which normally extends into early summer, or winter storms. Maintenance of summer base flows in the unregulated East Fork streams depends heavily on the drainage of shallow groundwater, including the annual cycle of water storage and release from wet meadows along valley floors. Flow along the impounded North Fork reach is regulated by releases from Lake Alomar.

### 22.2.2 Geomorphology

A geomorphic evaluation of the North Fork Feather River and the three reservoirs was conducted to better characterize the behavior of the system and its sediment transport characteristics (Resource Consultants and Engineers, 1992).

Within the area of the three dams, the North Fork passes along a channel incised in granodiorite, and exhibits a step-pool geomorphic configuration characteristic of steep channels with bedrock control. Sediment transport along the stream is limited by the rate of sediment supply from the tributaries, and the stream profile is determined by bedrock lithology. This pattern is in sharp contrast to lowland streams which typically exhibit a smooth, concave, longitudinal profile that flattens in the downstream direction, indicating that the channel is in equilibrium with sediment supplied from the bed. Also unlike lowland or alluvial streams in which the size of the material transported decreases regularly moving downstream, a pattern of regular changes in grain diameter is not readily apparent along the North Fork. Instead, the grain size in any given section of the channel reflects primarily the grain size delivered from tributaries plus local hydraulic controls within the step-pool system. Wide variations in grain size can occur over short distances, with finer material, including limited amounts of gravels suitable for spawning, accumulating only behind flow obstructions. Grain size analysis using Wolman counts for surface material and bulk sampling for subpavement below the armor layer showed that the channel bars were heavily armored, as evidenced by the large difference in grain size in the armor layer and the subpavement (Fig. 22.2). A minimum of 50 percent of the subpavement samples consists of fine gravel to very coarse sand, but this size material is essentially absent on the surface of the bars. Comparison with historical air photos showed that the location of boulder/cobble bars in the system has

remained relatively constant. The core materials in these bars are remnants of deposition from previous high-energy hydrologic regimes or catastrophic events.

### 22.2.3 Sediment Management History

In the early 1980s it was already apparent to PG&E that sedimentation would affect the North Fork Feather River system. Sedimentation issues include both the operational problems caused by sediment accumulation as well as the environmental issues associated with sediment management techniques that would further impact the stream and its fishery. One of the major issues was the historical degradation of spawning habitat because of loss of gravel beds (most of the river bed is today too coarse for spawning), combined with the smothering impact that would be caused by releasing significant quantities of material smaller than 0.84 mm in diameter. Most of the sediment trapped in the reservoirs fell into this undesirable size range.

Initial sediment management efforts focused on erosion control in the degraded East Branch watershed. The Plumas National Forest manages 84 percent of the East Branch watershed, private timber holdings constitute an additional 11 percent, private agricultural holdings are 4 percent, and the, remaining 1 percent comprises all remaining private and public ownership including all urban areas. More than a century of activities such as mining, logging, and overgrazing had degraded 60 percent of the watershed. Most sediment was derived from erosion and gullying within destabilized stream channels, plus logging roads, and 80 percent of the sediment yield was estimated to be the product of accelerated erosion (Clifton, 1994).

In 1984 PG&E began an effort to develop a long-term plan to manage sediment at its reservoirs, surveying the watershed to diagnose erosion problems and initiating a series of meetings with government agencies responsible for controlling erosion upstream of the dams. It was apparent that watershed management could be achieved only in a coordinated and cooperative manner, and in 1985 PG&E and 12 other agencies and institutions joined to create a Coordinated Resource Management (CRM) group organized under the terms of a formal memorandum of understanding. Five more institutions have subsequently joined. The CRM goals set forth in the memorandum are to: identify erosion sources, coordinate between public and private landowners, implement erosion control projects where practical, ensure project cost-effectiveness for contributors, and develop a cooperative regional erosion control plan (Plumas Corp., 1996).

A rain-on-snow event in February 1986 produced a peak discharge of 2265 m<sup>3</sup>/s at Rock Creek Dam, about an 80-year return interval flood, which buried the low-level outlets at Rock Creek dam beneath sediment and dramatically underscored the system's vulnerability to continued sedimentation. Deposits in both Rock Creek and Cresta Reservoirs had been surveyed in 1984, and by resurveying in 1986 the effect of this large event on sediment accumulation was documented. The flood caused the net erosion of 417,000 m<sup>3</sup> of sediment from Rock Creek Reservoir and a net accumulation of 230,000 m<sup>3</sup> of sediment in Cresta Reservoir. However, at Cresta the flood also caused a significant redistribution of deposits as sediments were scoured from the upper part of the reservoir and transported toward the dam: a net deposition of 421,000 m<sup>3</sup> occurred in the lower 1.45-km reach of Cresta Reservoir. Because of the smaller size of Poe Reservoir and the use of underflow spillway gates, sediment accumulation did not create operational problems. Sediment inflow and outflow had already come into balance at Poe Reservoir.

Sediment accumulation decreases the overall reliability of hydropower operations, interferes with spillway gate operations, accelerates wear on powerhouse turbines, and generally increases maintenance requirements. Sediments can also obstruct the low-

level dam outlets, fishwater release piping, and piping for operating the spillway drum gates. A sudden buildup of sediment and debris during a large flood could place the bar racks at the intake structures in jeopardy of plugging and collapse. Damages of this type could require months to repair and, in addition to repair costs, represent a significant loss of power revenue (Harrison, 1991).

While watershed restoration presented an attractive long-term strategy to reduce sediment yield by possibly 50 percent over a 30-year period, it could not solve the immediate sedimentation problem which threatened the dams. This prompted the development of dredging plans at Rock Creek and Cresta Reservoirs during the late 1980s. Because of the extremely high cost of dredging, and because it would not provide a long-term solution to the sedimentation problem, PG&E continued to work on alternatives, and by the mid-1990s had developed a sediment routing plan based on pass-through during floods. All these strategies are described in this case study.

## **22.3 WATERSHED MANAGEMENT**

---

### **22.3.1 Land Use History**

The East Branch watershed consists of forested mountains and grassy intermountain valleys. The discovery of gold in California in 1849, and the subsequent discovery of gold in the Feather River, initiated mining, grazing, timber harvesting, their associated road and railroad construction in the watershed, and wildfires, all leading to watershed degradation and increased erosion. In the twentieth century the construction of hydropower dams and diversions further affected fluvial sediment transport along the Feather River system.

### **22.3.2 Erosion History**

An erosion inventory was performed to reconstruct the erosion history in the watershed and determine the primary sources of sediment from within the East Branch watershed (River Basin Planning Staff, 1989). Aerial photographs, field surveys, oral histories, and historical sources were used to reconstruct the history of stream channels in the study area. This reconstruction suggested that before 1850 the natural creeks in the valleys were probably heavily vegetated and overflowed with discharges less than the 5-year flood. The combination of small channel sections and the hydraulic resistance offered by riparian vegetation forced flood flow onto overbank areas where sediment tends to be deposited and flows are usually too shallow to cause erosion. Riparian vegetation was extremely important in stabilizing the channels of smaller tributaries, reducing erosion by retarding flow velocity and anchoring soils.

Logging, grazing, clearing of stream channels, placer mining, levee construction, stream diversions, irrigation, and drainage ditches all contributed to increases in peak discharge and sediment yield from the watershed. Riparian vegetation was destroyed by processes including channel clearing, overgrazing, mechanical damage by livestock, and desiccation resulting from the declining water table as streams eroded and base levels in meadows dropped due to incision. The regrowth of riparian vegetation was suppressed by continued cattle grazing and the repeated removal of collapsed bank material by streamflow, thereby exposing new banks to erosion attack. As channels incised and eroded, their hydraulic capacity increased, allowing larger flows to be transported through the channel and eliminating the detention storage effects of overflow onto the riparian meadows. This flow channelization caused peak discharges to increase, further accelerating the channel erosion process. In many areas, disturbance

related to human activity has caused an estimated 0.15 to 0.30 m loss of topsoil from both upland and meadow areas, and contributed to the creation of large and small gullies that have formed in almost every meadow and run the full length of many valleys (Clifton, 1994).

Air photo interpretation suggests that channel incision had largely reached its maximum depth throughout the watershed by about 1940, after which time erosion caused the deep channels to widen as steepened banks collapsed and attempted to stabilize. The impact of large storms was particularly dramatic. For example, erosion during the February 1986 flood, an 80-year event that was initiated as rain falling on snow, caused Indian Creek to almost double in width (Table 22.2).

**TABLE 22.2** Channel Erosion History of Indian Creek, East Branch North Fork Feather River

Air photo year	Length, km	Width, m	Channel area, ha
1941	13.4	24	33
1982 (preflood)	13.0	48	63
1987 (postflood)	13.5	90	121

*Source:* River Basin Planning Staff (1989).

Road construction was identified as another major source of erosion. Although the watershed is rural in character, the 84 percent that is managed as national forest lands contains about 1600 ha of unpaved road surface and more than one "problem" stream crossing per kilometer of road (Clifton, 1996). Much of the erosion from roads is attributed to the difficulty of revegetating cut and fill slopes because of steep slopes, low moisture levels on the bare slopes, and low nutrient levels. Road cuts remain steep because of the continued removal of dry gravel and sediment deposited at the base of the slope, to prevent blockage of the road drainage system. Roads also intercept natural downslope drainage patterns and focus water along drainage channels, greatly limiting the opportunity for redeposition of finer material once it has become entrained.

The history of Wolf Creek (Plumas Corp., 1996) is illustrative of some of the factors that combined to degrade streams in the area. Wolf Creek travels 19 km through dense mixed conifer forest before meandering along the valley floor for 3.2 km and passing through the town of Greenville. A wagon road built along Wolf Creek in 1863 was improved in the 1930s to become State Highway 89, and in 1931 the Western Pacific Railway was constructed alongside the creek for a distance of 8 km above Greenville. Together, they contributed 125 acres of impermeable surface to the valley floor, focused runoff, and contributed sediment as the unvegetated cut and fill slopes began to erode. Logging roads were constructed throughout the lower watershed in the 1940s and contributed more sediment. (With present timber harvest methods, including helicopter logging of most Forest Service lands, the present impact of timber harvest is considered small.) During the 1940s and 1950s, two lumber mills operated in the Wolf Creek floodplain, and in the late 1950s a cedar mill dam on the creek failed, releasing a flood wave that scoured creek bottom sediments and lowered the creek bed by 2 m in the area of Greenville. In 1955, the Army Corps of Engineers dynamited 1.5 m of bedrock from the lower end of Indian Valley below Greenville to help ranchers drain marshy fields so livestock grazing could begin earlier in the season, leading to further downcutting of the

channel crossing the valley. In the 1960s, a 40-year-old irrigation dam was removed, further accelerating erosion. The Corps of Engineers unsuccessfully attempted to stabilize the stream by straightening it in three places and removing riparian vegetation. In 1978 the county constructed floodwalls along the creek banks, which were undermined during a flood only 2 years later.

### 22.3.3 Erosion Inventory

An erosion inventory was performed for mid-1980s conditions in the East Branch watershed to quantify the sediment contribution from each source and better focus erosion control efforts. Because of generally excellent vegetative cover across the watershed, the combination of sheet, rill, and gully erosion from the sloping soils accounted for only 4 percent of the total erosion in the watershed. Roads, on the other hand, accounted for nearly 57 percent of the total erosion. The remaining 39 percent was derived from streambank erosion, primarily in smaller tributaries (Table 22.3). Because most erosion is derived from channel processes which allow eroded sediment to be transported efficiently, the sediment delivery ratio in this watershed is high.

### 22.3.4 Coordinated Resources Management Group

To address the pervasive erosion problems throughout the watershed, the CRM group first undertook the rehabilitation of a 1.6-km reach of Red Clover Creek, described below. This first project was undertaken to demonstrate cost-effective erosion control measures and to test the ability of the group to cooperatively plan, fund, and implement projects. In the following 10 years, more than 33 restoration projects have been executed using funds and in-kind contributions from PG&E, landowners, agencies, and state and federal grants.

The adoption of a formal Coordinated Resource Management framework has an important advantage in that it can involve the local Resource Conservation District personnel, and it also permits federal staff (e.g., Forest Service personnel), who are

**TABLE 22.3** Sources of Erosion in East Branch North Fork Feather River

Erosion source	Erosion in watershed, %	Sediment load at Rock Creek Res., %	Delivery ratio, %
Sheet and rill, all sources	2.5	0.8	20
Gully erosion, all sources	1.5	1.5	62
Roads:			
Surfaces	0.6	0.5	51
Cut slopes	36.7	30.0	51
Fill slopes	19.6	16.0	51
Streambanks:			
Major streams	5.8	8.4	90
Tributary streams	<u>33.3</u>	<u>42.8</u>	<u>80</u>
Total erosion, %	100	100	
Total erosion, t/yr	$1.62 \times 10^6$	$1.01 \times 10^6$	62

*Source:* River Basin Planning Staff (1989).

normally limited to federal lands, to work on cooperative projects on private lands (Clifton, 1994). Approximately 200 CRM groups have been formed in California to cooperatively address watershed management problems. These groups represent largely grass roots coalitions to address specific local watershed issues and implement workable solutions. Because participation is voluntary, all parties must perceive individual benefit from watershed restoration, and that cooperation with others will enhance the opportunity for solving watershed problems. This strategy promotes an integrated approach to watershed restoration that embodies the principles of ecosystem management (Lindquist and Harrison, 1995).

Because it is based on voluntary cooperation, the East Branch CRM must necessarily develop a consensus among the participants, and it does not interfere with the activities or roles of polarized interest groups or agency mandates related to current resource management practices. CRM participants adhere to the following guidelines (Clifton, 1994):

- The CRM works on cumulative watershed effects on both public and private lands and in multiple land uses. It does not work exclusively on specific land areas or use patterns. While executed projects have primarily focused on stream erosion problems, they have also included improved grazing management and stabilization of mine tailings.
- All decisions are reached by consensus.
- Enlightened self-interest and long investment horizons are necessary to achieve solutions that are both economically and environmentally sustainable.
- Education, innovation, and demonstration projects are used to encourage cooperation and participation, instead of regulatory approaches.
- All affected interests necessary to implement a long-term comprehensive solution are involved near the beginning of the process.
- Public and private landowners take the lead on projects on their lands. The landowners develop goals, worst-case scenarios, and land use history information. All participants, including technicians, investors, and regulators make a three-part promise to: (1) attempt to solve shared problems, (2) prevent landowner and participant fears from being realized, and (3) monitor and document project successes and failures.

The cumulative watershed effects for the East Branch CRM are water quality, fuel hazard, desertification, and biodiversity problems that: cannot always be solved in a reasonable time by management changes alone; are caused by multiple and cumulative effects over decades involving many people, most of whom are now gone; require comprehensive long-term strategies as opposed to a piecemeal approach; are causing increasing costs and conflicts among resource users; and involve long-term monitoring.

The overall organizational structure of the East Branch CRM is illustrated in Fig. 22.4. The executive committee provides overall policy guidance, liaison with Washington, and dispute arbitration. The steering committee provides public access, ensures program continuity from year to year, and approves and forwards project concepts to the management committee for execution. The management committee is part of the executive committee and is responsible for day-to-day operations. There are five types of subcommittees. The project subcommittee, chaired by the Feather River Resource Conservation District, is responsible for nominating projects for implementation. This procedure helps keep control of project proposals at the local level. The finance subcommittee identifies potential funding sources and aids in preparation of funding applications when necessary. The design subcommittee defines overall project design objectives and principles and provides expertise in specific areas as required. The monitoring subcommittee designs and oversees monitoring activities. There are several

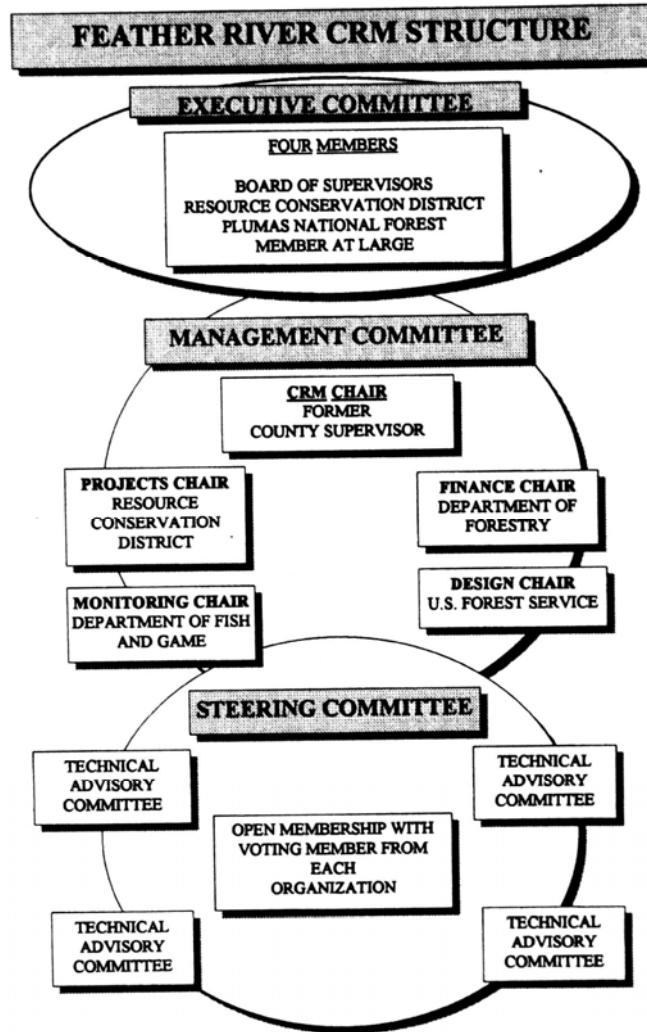


**FIGURE 22.4** Organizational structure of Coordinated Resource Management group, East Branch North Fork Feather River (*Clifton, 1994*).

technical assistance committees composed of interdisciplinary teams of resource specialists, landowners, and managers, which provide technical expertise and direction through the planning, execution, and monitoring phase of individual projects.

## 22.4 SAMPLE STREAM RESTORATION ACTIVITIES

### 22.4.1 Red Clover Creek Demonstration Project

The Red Clover Creek demonstration project, constructed in 1986 and 1987, is an example of instream channel rehabilitation. This project was described by Lindquist et al. (1995).

Prior to 1880, the Red Clover Creek had a narrow, small stable channel including a well-developed riparian zone with hardwoods, willows, and sedges that protected streambanks. Flood flows overflowed out of the narrow channel and onto the adjacent meadows, thereby reducing the flood peak, dissipating erosive energy into

shallow overbank flow, and recharging the water table in the riparian meadow wetland area. However, by 1985 the loss of riparian vegetation and the process of channel degradation had produced an actively eroding channel 15 to 18 m wide with vertical bank cuts up to 3 m tall, eroding about 490,000 m<sup>3</sup> of sediment out of the channel system in the process. As a result of channel incision and widening, the groundwater table was lowered, dewatering soils and converting wet riparian meadows into dry sagebrush-dominated lands. Prior to the project, the demonstration area was composed primarily of xeric species of undesirable shrubs and grasses such as sagebrush, rabbitbrush, and cheatgrass. Two project objectives were established: stabilize streambanks to reduce erosion and raise the water table to restore meadow habitat.

Rehabilitation activity on the 1.6-km demonstration reach of Red Clover Creek consisted of four major elements:

1. A 28-ha riparian corridor was fenced, and grazing and vehicles were excluded.
2. Four rock check dams were constructed to establish higher water levels and control erosion.
3. Streambanks were stabilized by wood revetment and revegetated using native species including aspen, alder, willow, and grasses.
4. Monitoring of water table, vegetation, fisheries, wildlife habitat, and channel morphology was conducted over a 10-year period.

The structural elements of this project are located in Fig. 22.5.

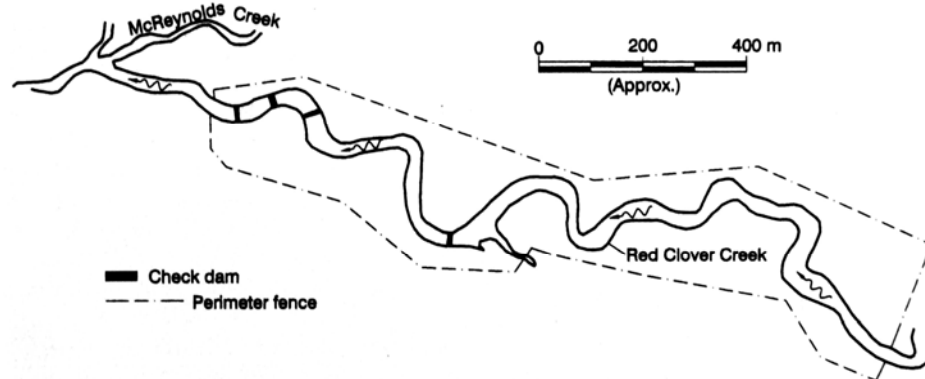


**FIGURE 22.5** Location map of restoration activities on Red Clover Creek.

The total structural height of the check dams was 2 to 3 m, and they were keyed about 3 m into the streambanks to ensure the abutments would not wash out. The four dams required 1920 m<sup>3</sup> of rock, blasted from a nearby outcrop, plus local soil which was compacted to form the impermeable core. To reduce discharge velocity the aprons extending downstream of the spillway crest were constructed at a flat 10:1 (horizontal:vertical) slope. Spillways were designed for the 10-year discharge. In the meandering stream it was important to orient spillways in a direction that did not discharge against and erode downstream channel banks.

Channel morphology was monitored for evidence that the channel was stabilizing, but geomorphic data were of insufficient detail to quantify changes. Because large changes did not occur, the 10-point cross sections taken at the beginning of the project did not offer sufficient detail to monitor results. Very little sediment, possibly a few hundred cubic meters, accumulated behind the check dams during the monitoring

period. Because of the slow changes which normally occur, some types of monitoring (*e.g.*, geomorphic change) should be scheduled at multiyear rather than annual intervals, or following large flood events.

The check dams immediately elevated groundwater levels, which allowed the rapid establishment of riparian and wetland vegetation. There was a dramatic increase in vegetation biomass and diversity within about 60 m of the stream, and vegetation changed to more desirable mesic (moist) species, as opposed to the xeric (dry) species previously dominating in the area. The before and after photographs taken at a permanent photo point (Fig. 22.6) illustrate the dramatic recovery in riparian vegetation. No change in vegetation occurred away from the channel in control areas unaffected by the raised water table.

In the fenced control area downstream of the last check dam and thus not affected by increased groundwater levels, a remarkable improvement in vegetation was observed after 4 years. The channel narrowed and began to meander, riparian vegetation reestablished along the banks, fish became established, and bank stability improved. This suggested that grazing exclusion alone may be sufficient for stream rehabilitation under favorable circumstances. Although natural rehabilitation is relatively slow, it is much less costly than the construction and maintenance of structural measures such as check dams.

During the first 8 years of the project, there was no grazing within the 28-ha enclosure. At the end of this period vegetation was thriving within the enclosure, in contrast to conditions outside the enclosure where heavy grazing removed most vegetation and left soils vulnerable to erosion. During the ninth year, late-season grazing within the enclosure was planned for a 5-day period, but the cattle were left in the enclosure for several weeks, denuding the vegetation and trampling channel banks. Although significant regrowth occurred during the following summer, mechanical damage to stream-banks from the cattle was still evident one year later and slow to heal.

Avian species diversity increased by 21 percent and avian density increased by 96 percent in the demonstration area as compared to the control area, with a total of 94 species observed. Seventeen waterfowl species were observed in the demonstration area, compared to nine in the control area, and waterfowl use was 700 percent greater than in the control. Over a 4-year study period from 1988-1991, there were 588 ducklings produced in the demonstration area compared to 23 in the control area. The project area also provided refuge for threatened or at-risk avian species. Trout populations increased, but no areas suitable for spawning were produced by the project.

The establishment of a beaver population hindered stream rehabilitation. A beaver dam was constructed on top of check dam 4, elevating the water level more than originally intended. This caused the stream to overflow its banks, flood meadows, and then reenter the stream farther downstream, causing bank failure and headcutting. Also, beaver depredation of willows and other hardwoods for food and dam-building materials hindered revegetation. Control of the beaver population is essential in the early project phase before vegetation has become well-established.

Project costs and funding sources are itemized in Table 22.4. The table does not include the personnel costs of participating state and federal agencies or the value of donated materials.

Several practical conclusions emerged from the project. The use of permanent photo points provided an effective qualitative documentation of trends over time, but low-altitude infrared aerial photography was most useful for monitoring vegetative changes. Native seed mixes were found to germinate more slowly than commercial seeds, but provided effective erosion protection, and their use is encouraged. Check dams are



(a)

(a)



(b) (b)

**FIGURE 22.6** Red Clover Creek: (a) before restoration and (b) after restoration (D. Lindquist).

**TABLE 22.4** Red Clover Creek Demonstration Project, Cost Sharing

Project Cooperator	Funding, \$
Pacific Gas and Electric Co.:	
Design and construction	11,500
10 years monitoring: biology, geomorphology, groundwater	100,000
Private landowner:	
Donated rock, excluded cattle	-
California Department of Forestry:	
Check dam construction, cultural resource study	41,000
California Department of Fish and Game:	
Fencing, design assistance	20,000
U.S. Forest Service, Plumas National Forest:	
Rock blasting, design, donated trees for revetment	-
U.S. Department of Agriculture, Natural Resource Conservation Service:	
Check dam design	-
<b>Total (does not include personnel costs for agencies or donations)</b>	<b>185,590</b>

*Source:* Plumas Corp. (1996).

expensive, require regular maintenance, and are not a panacea to correct erosion problems. Improved grazing management, revegetation, and exclusion fencing of the riparian corridor can dramatically improve degraded channels on some sites and should always be evaluated as an alternative to more costly structural measures. The first several years following installation are critical because vegetation has not yet become established and it can easily be washed out by large floods. Maintenance expenditures should be anticipated.

### 22.4.2 Big Flat Meadow Restoration Project

Restoration work in Big Flat Meadow, which had been severely degraded by gullyng of Cotton Creek, was performed in 1995 with revegetation in 1996. This project exemplifies channel replacement and is described by Plumas Corp. (1996).

Continuous grazing under permit was initiated in Cottonwood Creek in 1910, and severe erosion was evident by the 1930s. By 1990 the stream had gullied to a depth of 5 m in some places where it crossed Big Flat Meadow and large volumes of sediment were exported because of channel erosion. Dewatering of riparian areas due to stream incision, steep banks, and continued mechanical damage by cattle all combined to prevent restabilization of streambanks. As the meadow dried out and vegetation changed from grasses to sagebrush, average meadow forage production dropped to 10 kg/ha from values formerly in the 17- to 28-kg/ha range. Nevertheless, grazing pressure since 1957 continued to be high, between 93 and 200 percent of the allowable use.

The agencies and individuals in the CRM group worked cooperatively to undertake the Big Flat Meadow rewatering project to restore the original geomorphic conditions of a stable meandering channel-floodplain system. The project had four major objectives: (1) reduce the amount of sediment exported and improve downstream water quality, (2) restore spawning and rearing habitat for rainbow trout by augmenting summer base flow, (3) elevate groundwater levels to restore wetland conditions in the meadow, and (4) demonstrate stream restoration technology that can be applied to other

degraded sites. The rewatering project restored 19 ha of meadow, increasing the grazing resource for both cattle and wildlife.

Project design included both structural and nonstructural measures. The structural measures consisted of creating a 1.2 km shallow meandering channel crossing the meadow along a new alignment, with rock pools in the steepest sections of the new channel to protect against gullying. The gullied channel was backfilled and converted into a chain of seven ponds to create wildlife habitat. The overall configuration of the meadow in the original and restored conditions is shown in the aerial photos in Fig. 22.7*a* and *b*, and the changes in the channel cross section are illustrated in Fig. 22.8. Nonstructural measures focused on revegetation by replanting and reduction of grazing. Changes in the total grazing allotment were relatively small, a 12 percent reduction from 1268 to 1118 animal unit months per year. The most important change was a substantial (85 percent) reduction of grazing pressure in the riparian areas and improved pasture rotation (see Table 22.5). Cost sharing for the project is summarized in Table 22.6.

## 22.5 COST AND BENEFIT OF WATERSHED RESTORATION

It is difficult to determine both the cost and the benefit of watershed restoration. The published dollar costs for projects do not include the personnel cost of agency staff, nor is volunteer time shown as a cost. Benefits are far more difficult to quantify. Obvious benefits include reduced sedimentation at the downstream dams. The computation of sediment reduction benefits to PG&E (and ultimately to their utility customers) are described below, but do not include any benefits at the large Oroville Reservoir further downstream, where all sediments eventually deposit but which does not belong to PG&E. Other directly tangible



(a)

**FIGURE 22.7** (a) Oblique aerial photo of Big Flat Meadow with the gullied pre-project Cottonwood Creek.



(b)

**FIGURE 22.7** (b) Oblique aerial photo of Cottonwood Creek showing new alignment of the low-flow channel, with the gullied channel refilled and converted into a chain of ponds. (C. Clifton).

benefits include increased forage in meadows. Less economically tangible but no less important are benefits to overall ecosystem integrity, wildlife, and biodiversity. Only some of these environmental benefits can be translated into direct economic benefits through recreational activities (such as trout fishing). Recreational use of Plumas National Forest amounts to 2.3 million visitor-days per year. The East Branch also provides inflow into California's State Water Project. (Clifton, 1994).

### 22.5.1 Overview of Project Costs

More than 30 projects have been completed under the purview of the CRM group. Cost data on 10 projects involving the rehabilitation of significant lengths of streams have been summarized in Table 22.7.

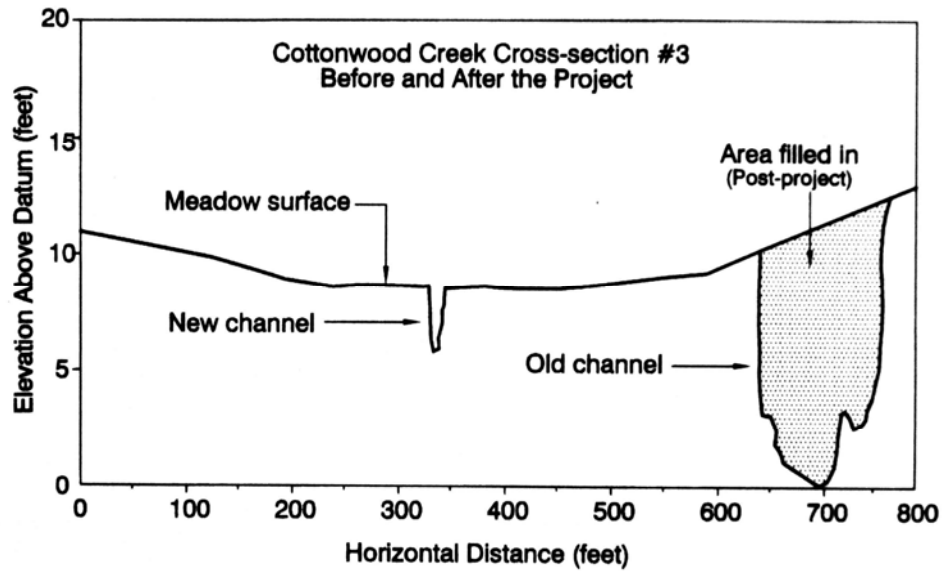


**FIGURE 22.8** Cross section of Cottonwood Creek in Big Flat Meadow, showing the replacement of the original severely eroded stream with a new shallow low-flow (1.1 m<sup>3</sup>/s capacity) channel which will overflow onto the meadow during high discharges, and which promotes higher groundwater levels because of the higher channel invert elevation (Plumas Corp., 1996).

**TABLE 22.5** Grazing Management Changes, Big Flat Meadow Area

	Preproject	Postproject
Allowed grazing	317 AU for 4 months	317 AU for 3 months and 167 AU for 1 month
Total AU months	1268	1118
Riparian pasture use	2-3 weeks/yr	2-3 days/yr
Grazing system	Two-pasture deferred grazing	Five-pasture rotation with 4.8-km new fence

AU = animal units. Each AU is equivalent to a cow-calf pair or 5 sheep.

Source: Plumas Corp. (1996).

### 22.5.2 PG&E Economic Justification for Watershed Protection Activities

Between 1984 and 1995 PG&E invested approximately \$1.1 million to partially fund administration of the CRM group by the Plumas County Development Corp. and to implement projects contributing directly to the reduction of sediment reaching Rock Creek and Cresta Reservoirs. Originally this investment was easily justified by the exclusion of sediment which would otherwise need to be removed from reservoirs by costly dredging. However, development of an economical sediment routing strategy which is expected to eliminate the need for maintenance dredging undercut this basis for justifying expenditures in the watershed program. Harrison and Lindquist (1995) exam-

**TABLE 22.6** Big Flat Meadow Rewatering Project, Cost Sharing (Plumas Corp., 1996).

Project cooperator	Funding, \$
U.S. Forest Service, Plumas National Forest:	
Construction funding	30,000
Design and assessment work	5,590
Rock, 350 1-m boulders	10,000
Aerial photos and mapping	13,000
Fencing	10,000
Pacific Gas and Electric Co.:	
Revegetation	13,000
Hydrologic monitoring	25,000
State Water Resources Control Board:	
Construction funding	70,000
Grazing permittee:	
Fencing	2,000
Plumas County Community Development Commission:	
Design	7,000
Total (funds and in-kind contributions)	\$ 185,590

**TABLE 22.7** Cost of Stream Rehabilitation in Plumas County

Site	Year	Cost, \$	Length treated, m	Unit cost, \$/m
Red Clover Creek 1	1986	172,000	1,610	107
Poco Creek	1986-1989	128,000	366	350
Wolf Creek I, 2, 3	1989-1990	850,000	2,938	289
Greenhorn Creek	1991	406,000	854	476
Clarks Creek	1992-1994	24,000	610	39
Haskins Creek	1993	40,000	244	164
Red Clover Creek 2	1994-1995	39,000	793	49
Big Flat Meadows	1995	189,000	1,235	153
Jamison Creek	1995	180,000	610	295
Poplar Creek	1994-1995	35,000	122	287
Total or average		2,063,000	9,380	220

Source: Plumas Corp. (1996).

-ined the potential economic benefits to PG&E from improved watershed management, in the absence of savings from reduced dredging.

On the anticipation that 15 watershed projects completed or proposed during 1991 could produce a 5 or 6 percent reduction in sediment yield, it was estimated that a 50 percent reduction in sediment yield at the downstream reservoirs is reasonably achievable within the next 30 years. The downstream benefits of watershed restoration were based on this scenario.

- Suspended sediment is estimated to increase annual overhaul costs by approximately \$150,000 (in 1995 dollars) for the six turbines in the North Fork Feather River

system. Assuming turbine wear declines in proportion to reduced sediment inflow, annual savings of \$75,000 may be achieved at the end of 30 years.

- Erosion of turbines by sediment reduces their efficiency. Assuming a 1 percent efficiency degradation due to sediment, a 0.5 percent increase in efficiency achieved by a 50 percent reduction in suspended sediment would increase power generation by about  $9 \times 10^6$  kWh/yr at the three power stations.
- Improved watershed management can increase base flow and change the shape of runoff hydrographs by reducing the storm peak. This effect was assumed to reduce the amount of spills in the system by 5 percent at the end of 30 years, which represents only 0.4 percent of the average  $2 \times 10^9$  m<sup>3</sup>/yr inflow to Rock Creek reservoir. This represents an additional  $8.3 \times 10^6$  m<sup>3</sup> of water available for power generation, equivalent to an additional  $6.7 \times 10^6$  kWh annually.

In summary, watershed protection could eventually result in an additional  $15.7 \times 10^6$  kWh/yr, much of this valuable peaking power, plus \$75,000/yr in reduced turbine maintenance costs.

## **22.6 RESERVOIR SEDIMENTATION**

---

Bathymetry in the vicinity of Rock Creek Dam (Fig. 22.9) shows the scour of sediment deposits on the outside of the bend, and the scour cone at the existing small-capacity low-level outlet pipes. Sediments deposited in both Rock Creek and Cresta Reservoirs contain a large percentage of silt-size material, and at both sites the sediments are predominately in the sub-0.84 mm (medium sand) size range which is most deleterious to spawning gravels. Release of the fine sediments presently stored behind the dams would adversely affect fisheries. The Feather River was heavily mined for gold during the nineteenth century. Analysis of some of the initial sediment samples from the reservoir revealed a significant gold content, raising the interesting possibility that the reservoir sediments might be an economic resource rather than a liability. However, a subsequent boring and assay program revealed that the amount of gold in the reservoir was not significant (Alpha Geotechnical, 19876).

## **22.7 RESERVOIR DREDGING**

---

Sediment control efforts initially focused on the dredging of accumulated sediments from the reservoir rather than on establishing equilibrium conditions across the impounded reaches. An environmental impact report was prepared for the proposed dredging which described the selected dredging strategy, several dredging alternatives, and project environmental requirements (Planning Associates, 1991). The most important dredging limitations at this site are the stringent water quality requirements and the lack of suitable large-volume disposal sites. The canyon floor is narrow, with a railroad running along one bank and State Highway 70 running along the other bank and frequent tunnels on both routes. The removal and disposal of a large volume of sediment would require a sediment storage area below the canyon reach and a sediment transport distance exceeding 40 km. Disposal options evaluated included long-distance trucking, rail transport, and slurry pipeline. All were very costly. Consequently, a small-volume dredging job was proposed which would not exceed the fill capacity at the Rogers Flat area, located in the canyon between Rock Creek and Cresta Reservoirs. Because sediment inflow and discharge had already stabilized at Poe Reservoir, no dredging was proposed there.

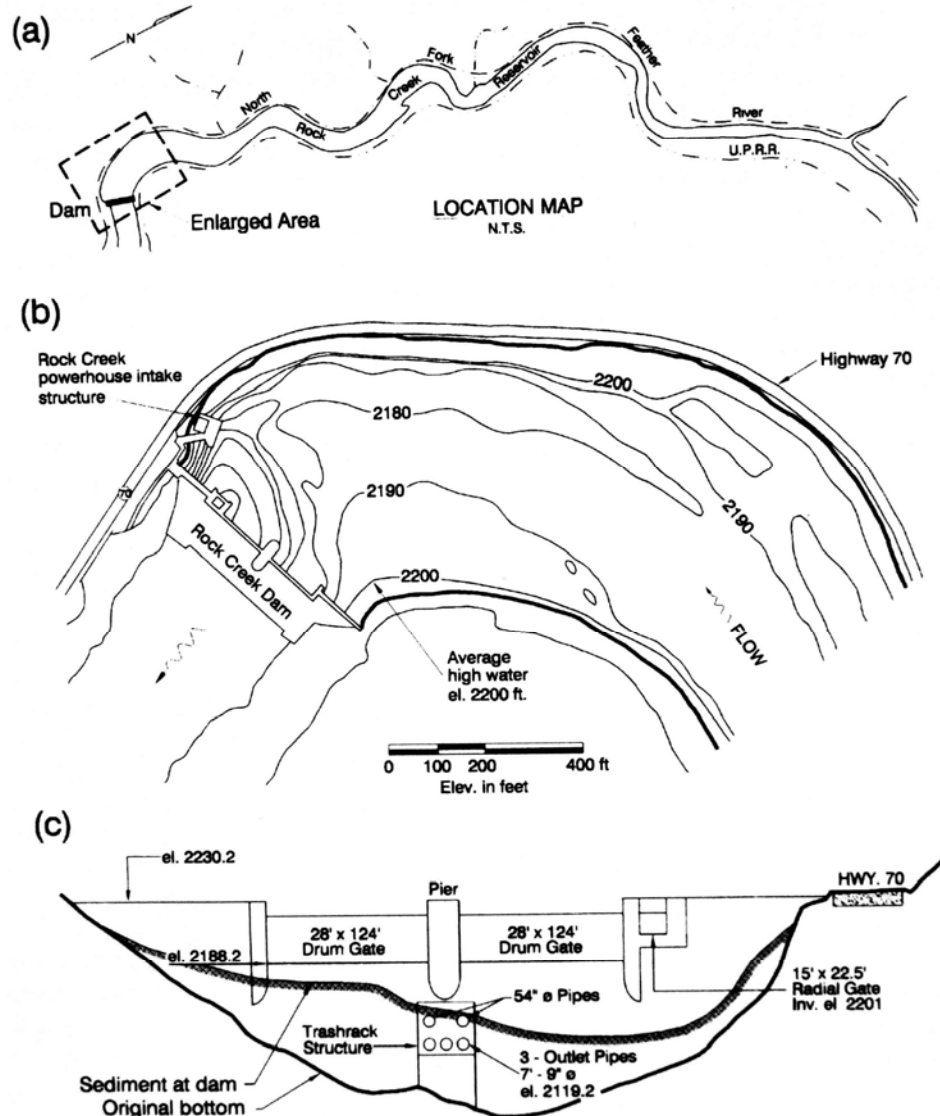


**FIGURE 22.9** Rock Creek Reservoir: (a) geometry and (b) bathymetry near the dam showing scour on the exterior of the curve. (c) Configuration of Rock Creek Dam, upstream face, showing gate arrangement and sediment accumulation. (modified from *Planning Associates*, 1991).

The proposed dredging project involved the removal of 380,000 m<sup>3</sup> of sediment that had accumulated in front of the powerhouse tunnel intakes and the low-level outlets at each dam by a barge-mounted crane with a 7.6-m<sup>3</sup> (10-yd<sup>3</sup>) clamshell bucket. The sediment was to be loaded onto receiving barges, dewatered, off-loaded onto trucks, and then hauled over the highway to create an engineered fill at Rogers Flat. The proposed fill area would cover about 7.5 ha and would be about 21 m tall. Dredging was anticipated to require 1 year, with an additional 6 months for mobilization and take-down.

To minimize disturbance to aquatic habitat, the mean daily turbidity level generated by dredging operations was limited to not more than 25 NTU over ambient, as measured

at designated compliance points downstream of the project. An absolute suspended solids limit of 80 mg/L (project plus ambient) was also established. Provision was made for determining suspended solids compliance from turbidity data once the relationship between NTU and mg/L was established in the field. Several monitoring stations were specified, including one not more than 90 m downstream of the off-loading facility on the side of the reservoir with the highest turbidity. Provision was also made for the release of a flushing flow at the end of the project to remove sediment from spawning gravels and other important aquatic habitats, in accordance with procedures previously developed by Bechtel (1987), if recommended by a qualified independent fisheries biologist or hydrologist qualified in fluvial geomorphology.

Sampling of benthic invertebrate populations and streambed sediment accumulation by Coleman-Haynes substrate samplers was required. Three sampling stations were specified: a control station in a riffle area upstream of the dams and sites about 300 m downstream of each of the two dams. These samplers were to be left in place for an 8-week period, removed and inventoried, and a new sampler set out. Sampling was to begin 8 weeks prior to start of dredging. Data to be reported were substrate volume, identification and counts of organisms, and dry weight and grain size distribution of fine sediment collected in the sampler.

Dust was to be controlled on dirt roads by watering, and on the paved road by sweeping rather than watering to prevent turbid runoff from entering the river. Special requirements were also established for items such as monitoring a golden eagle nest near Rock Creek Reservoir, removal of fuel from a crane that had been previously sunk in Rock Creek Reservoir, protection of riparian vegetation, noise, burning, employee parking, provision of alternative recreation sites, and cultural resources.

Although the use of large-scale reservoir dredging has been discarded, the installation of the outlets for sediment pass-through will require that about 103,000 m<sup>3</sup> of material be dredged from the upstream side of the new outlets. During 1994, a one month test dredging program was performed in Cresta Reservoir, removing about 8000 m<sup>3</sup> of material from the vicinity of the powerhouse intake while monitoring water quality parameters (Creek and Sagraves, 1995). The dredging system used in the test was a submerged slurry pump which suspended sediment by using a strong hydraulic vortex to draw a water-sediment mixture into the pumping system, rather than a cutterhead. The system complied with the water quality requirements established by the California Regional Water Quality Control Board of not more than 25 NTU turbidity increase or more than 80 mg/L total suspended solids, absolute. It was concluded that the system was capable of dredging sandy material without significant water quality impacts.

## **22.8 SEDIMENT ROUTING**

---

PG&E is preparing to implement sediment pass-through to route the inflowing fluvial sediments through all three dams along the North Fork of the Feather River, without scouring and releasing the large volume of the fine sediment which has accumulated behind the dams over the past 40 years or more. This project seeks to maintain reliable hydropower operations at Rock Creek and Cresta despite sediment accumulation. The specific objectives of the sediment management are:

1. Avoid plugging and collapse of trash racks;
2. Restore reliable operation of the primary hydraulic control system for the spillway drum gates;

3. Reduce sediment-caused turbine wear at powerhouses;
4. Minimize buildup of sediments within drum gate flotation chambers in the dams;
5. Eliminate the need for costly major dredging projects;
6. Eliminate sediment buildup in the vicinity of the power intake and bottom outlets;
7. Maintain long-term storage capacity equivalent to an average pool depth of about 3 m for daily hydropower peaking storage.

Although the dams make it impossible to precisely reestablish the natural (predam) sediment discharge relationship, sediment routing mimics the natural sediment discharge relationship more closely than does any other type of sediment management procedure. A modeling program was undertaken to design the physical and operational characteristics of the sediment routing required to achieve these objectives. Modeling procedures are described by Harrison et al. (1995) and Chang et al. (1995).

The reservoirs will be operated to reestablish, as nearly as possible, the pre-impoundment pattern of sediment transport along the river. The fines presently trapped behind the dam should not be released downstream in significant quantities. However, sediment routing will create a scour cone upstream from each low-level outlet which would release fine sediment. To prevent this release, the scour cone volume will be dredged prior to the first flushing event.

### 22.8.1 Modeling Approach

Sediment passage required that both Rock Creek and Cresta Dams be reconstructed to incorporate in each dam large low-level outlets that could be opened to reduce the pool elevation in the reservoir and release sediments. These outlets would be used in conjunction with the existing low-level outlet pipes. Hydraulic design required two types of sediment transport modeling activities. Physical modeling was used to determine the three-dimensional characteristics of the scour hole in the vicinity of the proposed outlet works and to ensure the outlets had adequate capacity to discharge sediment under conditions of extreme loading. A one-dimensional numerical model of the river, including all three dams, was used to develop the operating rule that would allow a sediment balance to be achieved. Both the physical and numerical modeling was performed as an iterative process.

### 22.8.2 Physical Modeling

A 1:50 scale physical model was constructed under the direction of Albert Molinas at Colorado State University to simulate the downstream plunge pool, dam, and reservoir bathymetry 460 m upstream of each dam (Fig. 22.10). Polystyrene pellets of cylindrical shape with specific gravity of 1.04 were used to model sediment with 3-mm (prototype) grain size. Calibration was performed with data from the 1986 flood.

The physical model was exercised to determine the stage-discharge rating curves for the existing and each proposed gate configuration, and this relationship was used as the downstream boundary condition in the reach of the mathematical model extending upstream from each dam. It was also used to observe the configuration of flushing cones and the entrainment of sediment near the dam for alternative outlet configurations. The volume of existing sediment in the anticipated flushing cones ranged from 25,000 to 40,000 m<sup>3</sup> at Cresta and 10,000 to 31,000 m<sup>3</sup> at Rock Creek. Sediment in the area of the flushing cones will be dredged out for two reasons: to

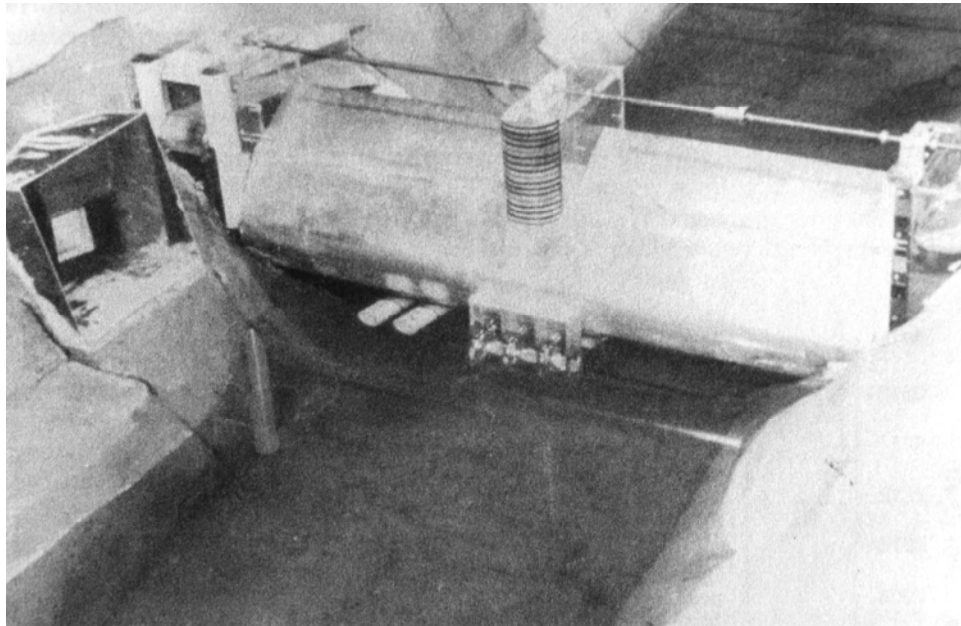


**FIGURE 22.10** Physical model of dam at 1:50 scale (W. Lee).

prevent the sudden collapse of sediment when operation begins, and to eliminate the release of fine sediment into the river downstream of the dams. The dredging volume will be specified as 50 percent larger than the predicted cone volume to provide a margin of safety. The modeled flushing cone configuration was determined by the outlet elevation, exit velocity, outlet size, and sediment angle of repose, and was nearly independent of the reservoir operating rules tested.

Three types of sensitivity analysis were performed:

1. A sediment wave test simulated an upstream landslide which could potentially bury low-level outlets.
2. The critical velocity required to produce incipient motion of the sediment bed was determined to be about 0.76 m/s.
3. Plate tests performed to determine the ability of the flow to induce motion of various sizes of particles during sediment pass-through events, indicated that gravel up to 17 mm in diameter may be mobilized and transported through the reservoir.

The model was also run with 0.1-mm (model-size) sand to validate the use of lightweight plastic pellets to simulate reservoir sediments, producing results very similar to those for plastic pellets.

### 22.8.3 Numerical Modeling

Numerical modeling of the entire river reach including the three dams was reported by Chang et al. (1995) and by Chang and Fan (1996) using the FLUVIAL-12 model described by Chang, 1988. Numerical simulations were used to identify an operating rule that would produce long-term sediment equilibrium and would also be simple for the operators to implement. The 1986 flood event was used to calibrate the numerical model, and validated the use of Yang's formula for both sand and gravel transport. The calibrated model was then run to test different operating rules with the 30-year historical

hydrograph, which was compressed by eliminating all discharges less than  $57 \text{ m}^3/\text{s}$ , since these had an insignificant impact on sediment transport.

Numerical modeling indicated that discharges of  $283 \text{ m}^3/\text{s}$  and  $368 \text{ m}^3/\text{s}$  respectively were required to initiate effective sediment pass-through at Cresta and Rock Creek. These discharges have an average return interval of 1.3 years (30 events in 38 years of gage record). The operating rule curve developed at Rock Creek Reservoir is presented in Fig. 22.11. At discharges below  $368 \text{ m}^3/\text{s}$ , the reservoir is operated in normal impounding mode

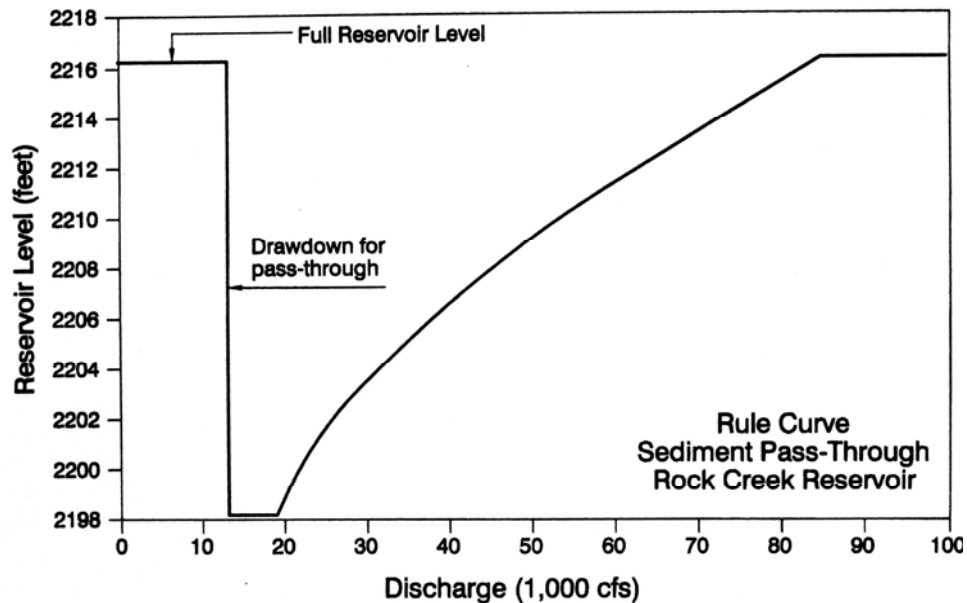


FIGURE 22.11 Operating rule curve proposed at Rock Creek Dam (after Chang *et al.*, 1995).

and power is produced. When the critical discharge is reached, low-level outlets are opened as required to achieve and maintain a 5.5-m drawdown until full outlet capacity is reached, after which the water level rises with increasing discharge. This operational sequence is reversed during flow recession. The existing drum gates may also be exercised to achieve the initial drawdown, and power inlets are closed during drawdown to prevent sediment from entering the turbines. Poe Dam will continuously operate at its normal pool level.

Because low flows carry little sediment, there will be relatively little accumulation within the reservoirs between routing events. However, to stabilize storage capacity there will necessarily be some net export of sediment during a routing event, but its environmental impact will be minimal because of dilution and the ability of the sediment pass-through discharge to transport sediment through the downstream channel.

The spatial variation in sediment delivery along a river reach may be visualized by plotting cumulative sediment delivery over a specified time interval as a function of distance along the reach (Fig. 22.12). In graphs of this type, if the plotted sediment delivery line tends upward while moving downstream along the river, this represents increasing sediment delivery because of the scouring of channel sediment. Declining sediment delivery, on the other hand, indicates an area of sediment deposition. The essentially uniform longitudinal plot of sediment delivery along the North Fork Feather River under the proposed operating process shows that depositional and erosional processes along the entire reach, including the reservoirs, are well-balanced in the long term, even though each reservoir still undergoes periods of net erosion and net deposition at different

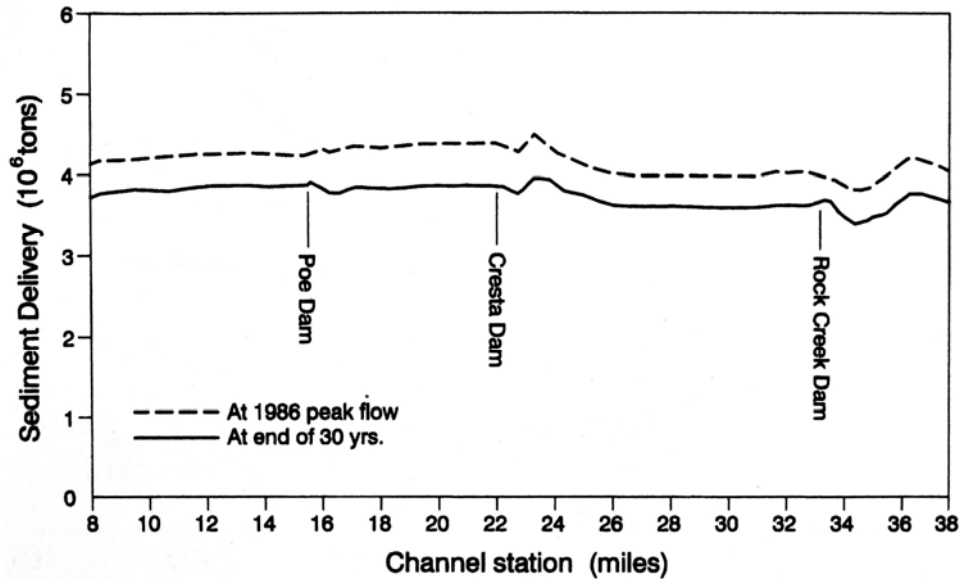


FIGURE 22.12 Long-term sediment delivery along North Fork Feather River under the proposed operating rule (after Chang *et al.*, 1995).

times. One particular feature of the FLUVIAL-12 model is its ability to simulate patterns of transverse scour, once properly calibrated. This feature enabled the transverse configuration of the bed in the curved reach of Rock Creek Reservoir upstream of the dam to be simulated (Fig. 22.13).

#### 22.8.4 Selected Project Configuration

The project configuration recommended for construction consists of:

1. Installation of a new 5.18-m-diameter low-level outlet pipe at Rock Creek dam;
2. Installation of a new 4.27-m-diameter low-level outlet pipe at Cresta dam;
3. Modification of trash racks at existing low-level outlet pipes at both dams to improve sediment pass-through;
4. Limited dredging at both reservoirs to excavate scour cones upstream of the new low-level outlets; and
5. Implementation of sediment pass-through operating rule during high flows.

The dredging volumes recommended at Rock Creek and Cresta are 46,000 m<sup>3</sup> and 57,000 m<sup>3</sup> respectively, compared to dredging 382,000 m<sup>3</sup> from each reservoir as previously planned, and future maintenance dredging is eliminated. It is proposed that dredged material be discharged into an upstream area of each reservoir from which it would subsequently be entrained and transported downstream during pass-through operations. An alternative plan involves trucking of dredged material to Roger's Flat.

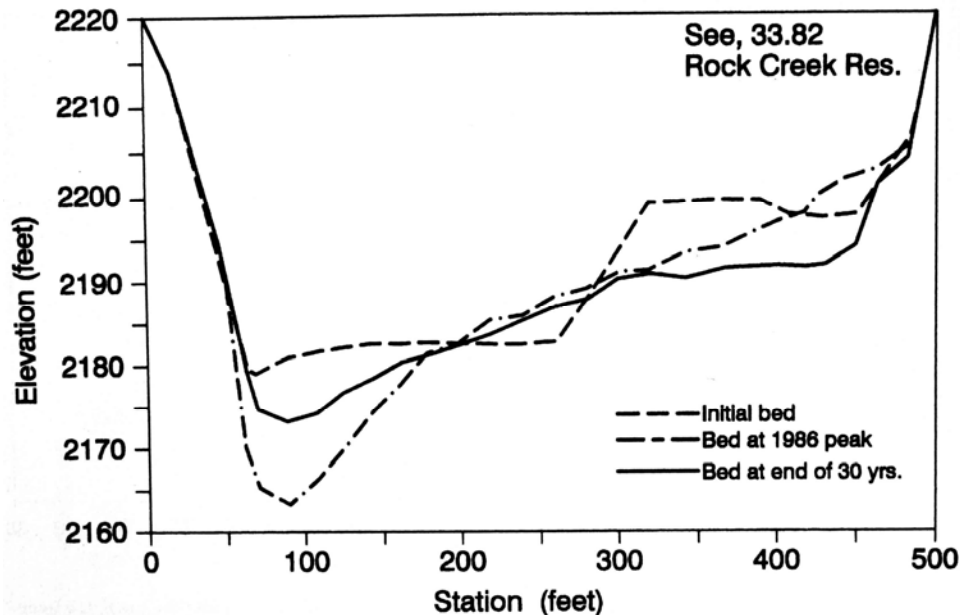


FIGURE 22.13 Simulation of long-term and flood impacts on cross-section geometry in the curved reach upstream of Rock Creek Dam, view looking upstream (after Chang *et al.*, 1995).

## 22.9 SEDIMENT PROBLEMS AT POE DAM

Although sediment problems at Poe Dam were insignificant from the standpoint of hydropower generation, some problems have occurred as a result of environmental issues. In February of 1988, spillway gates at Poe Reservoir were opened to drawdown the pool to allow the repair of a leaking gate. Discharge during this release peaked at about  $50 \text{ m}^3/\text{s}$ , and as the pool was drawn down it became apparent that a significant amount of fine sediment was being sluiced from the reservoir and into the river channel downstream. The gates were closed and drawdown was halted. This action revealed that the pool immediately downstream of the dam had filled completely with fine sediment, and two additional pools further downstream had partially filled with fine sediment. The  $d_{50}$  grain size decreased moving downstream along the three pools: 0.21 mm, 0.20 mm, and 0.13 mm. Mechanical removal of the fine sediment was considered, but because of poor access to the two downstream pools and because the sediment was spread out in a thin layer (less than 0.6 m thick) over a rather large area, mechanical removal might cause more environmental harm than good.

As an alternative to mechanical removal, the release of clear water to flush  $3800 \text{ m}^3$  of sediments downstream into the large Oroville Reservoir about 12 km downstream was evaluated. Four equations were used to estimate sediment transport as a function of discharge (Table 22.8). The Meyer-Peter and Muller equation reports only bedload and underreports total sand transport at larger discharges when much of the sand is transported as suspended load. The transport values from the other three equations were averaged to develop a relationship between discharge and transport capacity, which was then used to estimate the time and water volume required to flush the sediment (Table 22.9). Although a high discharge could quickly remove the sands, it would also flush spawning gravels out of the system. With spawning-size gravels in limited supply, and

**TABLE 22.8** Sediment Transport Capacity,  $m^3/s$ , as a Function of Discharge for Four Transport Equations

Discharge $m^3/s$	Meyer-Peter and Muller	Ackers and White	Brownlie	Engelund and Hansen
14	24	1	8	8
28	145	57	105	114
57	609	1025	966	1317
85	1258	4176	3094	4815
113	1982	9943	6386	10,555

*Source:* Ramey (1988).

**TABLE 22.9** Flushing Duration and Water Required to Remove  $3800 m^3$  of Sand

Discharge, $m^3/s$	Average transport capacity, $m^3/day$	Flushing duration, days	Volume of water used, $10^6 m^3$
14	5	714	874
28	92	42	102
57	1102	3.5	17
85	4025	1.0	7.0
113	8961	0.4	4.2

*Source:* Ramey (1988).

their resupply being prevented by trapping at the upstream dams, it was important that the release not further encourage the flushing of this resource out of the river system. The recommended maximum flushing flow in this case was  $70 m^3/s$  ( $2500 ft^3/s$ ), a discharge adequate to superficially cleanse gravel deposits without causing major movement of the gravels themselves (Bechtel, 1990).

---

## CHAPTER 21

---

# CASE STUDY: SEFID-RUD RESERVOIR, IRAN

---

### 23.1 INTRODUCTION

---

Sefid-Rud Reservoir in Iran demonstrates the implementation of sediment control at a large 1760-Mm<sup>3</sup> reservoir which has floodplain-foothill (Type II) geometry. The dam is located on Sefid-Rud River, a tributary to the Caspian Sea, immediately downstream of the confluence of Qezel Owzan and Shahrud Rivers and about 250 km northwest of Teheran. The geometry of the watershed and the reservoir, which has a major and a minor branch, is shown in Fig. 23.1. The reservoir was constructed in 1962 to supply 2800 Mm<sup>3</sup> of regulated flow to irrigate 250,000 ha of rice during a 6-month summer irrigation season. It also has a 87.5-MW hydropower station. Sedimentation was a serious problem and caused storage loss at the rate of 36.5 Mm<sup>3</sup>/yr, equivalent to an annual rate of 2.1 percent. Because of rapid storage loss, in 1980 reservoir operation was changed to incorporate desilting operations following 17 years of conventional operation.

Detailed and comprehensive data on all phases of sediment management at this reservoir, including flushing and supplemental erosion of deposits by using both lateral and longitudinal (diversion) channels has been reported by Esmail Tolouie (1989, 1993). These reports, photography, and additional comments kindly provided by Tolouie, have been the basis for this case study.

### 23.2 SITE CHARACTERISTICS

---

#### 23.2.1 Dam and Reservoir

The dam is a buttress-gravity concrete structure with a maximum height of 106 m and a crest length of 425 m. The installed powerhouse capacity is 87.5 MW and the minimum hydropower operating level is 240 m. The general configuration of the dam showing the location of the outlets is presented in Fig. 23.2. There are three bottom outlets on the right side and two bottom outlets on the left side (looking downstream), with total combined capacities of 430 m<sup>3</sup>/s and 550 m<sup>3</sup>/s respectively. Bottom outlets are near the original streambed elevation and the design does not incorporate a dead storage pool. High-level "morning glory" and auxiliary spillways are also provided.

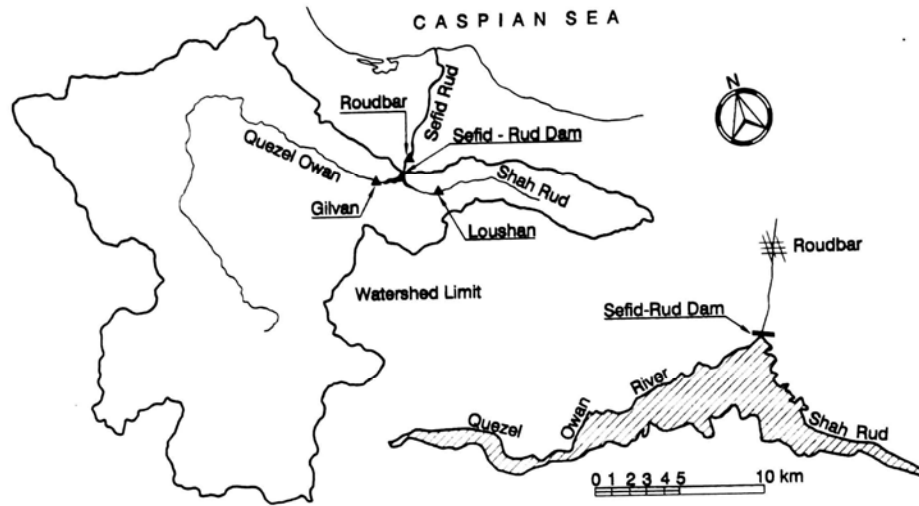


**FIGURE 23.1** Location and planview geometry of Sefid-Rud Reservoir (after Tolouie, 1989, and Parhami, 1986).

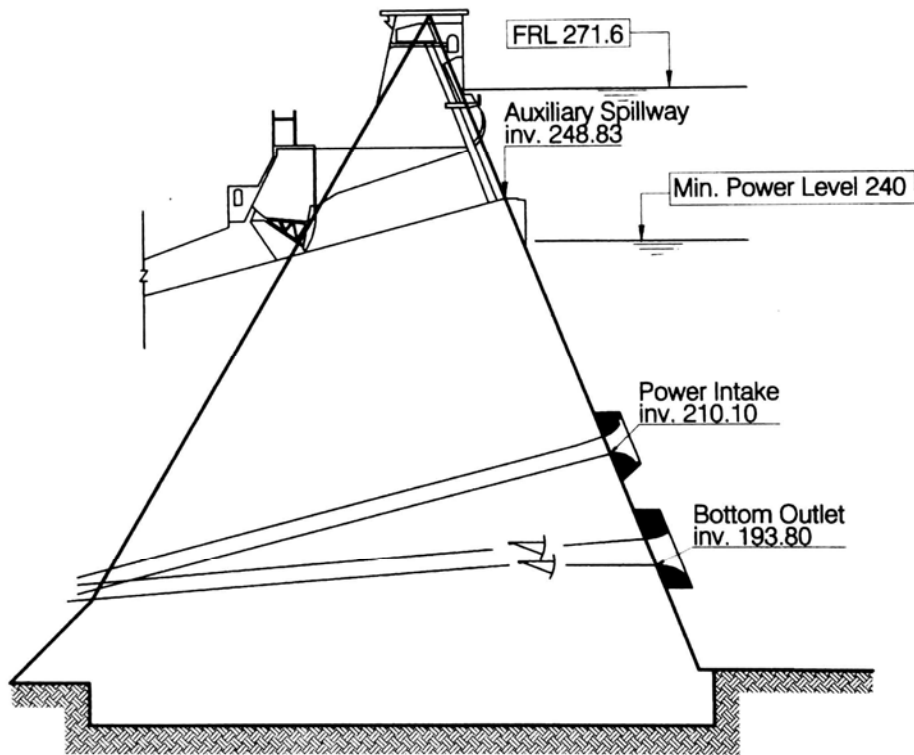


**FIGURE 23.2** Section view of Sefid-Rud Dam showing gate locations (after Tolouie, 1989).

### 23.2.2 Water and Sediment Inflow

Streamflow and suspended sediments are measured at the Gilevan and Loushan stations just upstream of the reservoir on the Qezel Owzan and Shah Rud Rivers respectively, and at the Roudbar station on the Sefid-Rud River 3 km downstream of the dam (see Fig. 23.1 for locations). Measurements are made at least twice weekly during low-flow periods and several times daily during high floods. Stage-discharge curves for gaging stations are prepared from velocity measurements and the curves are updated annually after spring floods. Sediment discharge is measured with a USDH-48 depth-integrating sampler at a single vertical, the location of which is adjusted after each high flood as required to obtain a sample representative of the entire cross section. During high floods and desilting, sampling is performed at five to seven points across the river at hourly intervals between 0700 and 1800. Bed load is not measured, but the sum of bed load plus the contribution from the ungaged area tributary to the reservoir is estimated as 15 percent of the measured load.

The 56,200-km<sup>2</sup> watershed tributary to the dam consists of semiarid lands generally receiving from 250 to 400 mm/yr of precipitation. The average elevation within the watershed is about 1800 m and is composed primarily of unconsolidated to consolidated clastics (sand, gravel, clay, and their consolidated equivalents), with limited exposures of pyroclastics and crystalline silicate rocks. Sediments delivered to the reservoir come from the following sources: sheet erosion 5 percent, gully erosion 25 percent, badlands 57 percent, and channel erosion 16 percent (Sogreah Consulting Engineers, 1974). Average annual inflow is 5008 Mm<sup>3</sup>, equivalent to 89 mm of runoff from the tributary watershed. The original reservoir volume was equivalent to a runoff depth of 31 mm from the tributary watershed, producing a capacity:inflow ratio of 0.36 at closure. Prior to commencement of desilting operations, the trap efficiency was about 73 percent, with most sediments released as density currents. Characteristics of the reservoir and tributary streams are summarized in Table 23.1.

Monthly flow and suspended sediment data reported by Tolouie from 1963 through 1987 show water and sediment discharge to be closely correlated in time (Fig. 23.3). A double mass diagram of water and sediment inflow (Fig. 23.4) clearly shows the large discharge of both water and sediment during the extremely wet water year 1968-1969, and reduced sediment yield in the 2 years following the wet year. This short period of reduced yield probably reflects temporary exhaustion of the sediment supply because the

**TABLE 23.1** Summary Characteristics of Tributaries to Sefid-Rud Reservoir

	Qezel Owzan River	Shahrud River	Reservoir total
Watershed area, km <sup>2</sup>	49,300	5,070	56,200*
Mean annual flow, Me/yr	3824	1183	5008
Capacity, Mm <sup>3</sup>	630	370	1760
Original stream slope	0.0033	0.0061	—
Total river length, km	500	180	—
Reservoir length, km	20.0	10.5	—
Sediment yield, 10 <sup>6</sup> t/yr	41.6	8.8	50.4
Specific sediment yield, t/km <sup>2</sup> /yr	832	1469	900
Mean suspended sediment concentration, g/L	10.9	7.5	
Suspended sediment, sand, %	33	44	
Suspended sediment, silt, %	47	46	
Suspended sediment, clay, %	20	10	

\*Includes 1830 km<sup>2</sup> of ungaged area around the reservoir.  
*Source:* Tolouie (1989).

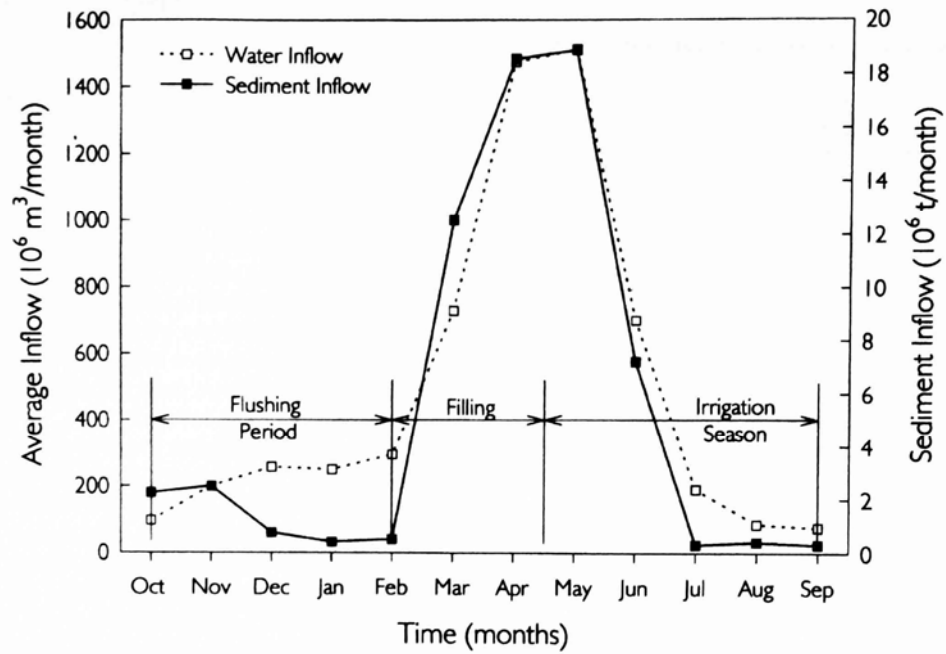


**FIGURE 23.3** Mean monthly inflow of water and suspended sediment into Sefid-Rud Reservoir, 1963-1987 (data from Tolouie, 1989).

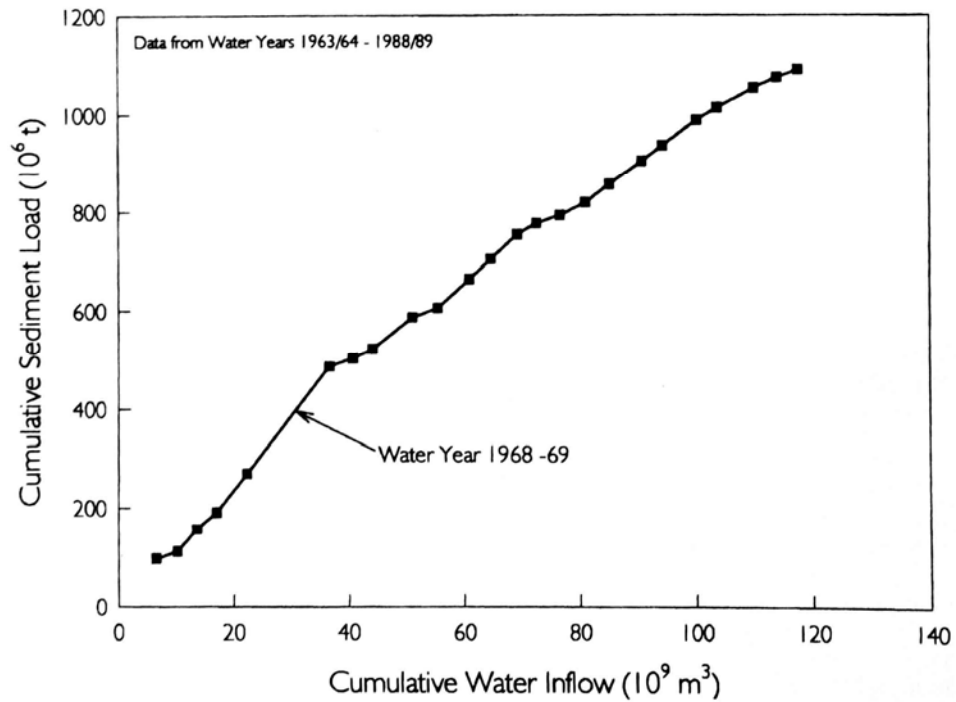


**FIGURE 23.4** Double mass curve of water and sediment inflow at Sefid-Rud Reservoir. 1968-1969 was an extreme-discharge year, contributing 3 times the average annual runoff and 5 times the average annual sediment load (data from Tolouie, 1993).

readily mobilized sediment was delivered to the reservoir during 1968-1969. The high discharge during that year had a return interval of 200 years on the Qezel Owzan River and 1000 years on the Shahrud River.

During conventional impounding, the grain size of suspended sediment discharged from the dam was significantly finer than the inflow. However, when flushing operations began the average grain size of the discharged suspended solids became larger than the inflow (Fig. 23.5). Tolouie (1996) indicated that this increase in grain size during flushing could be attributed to several factors:

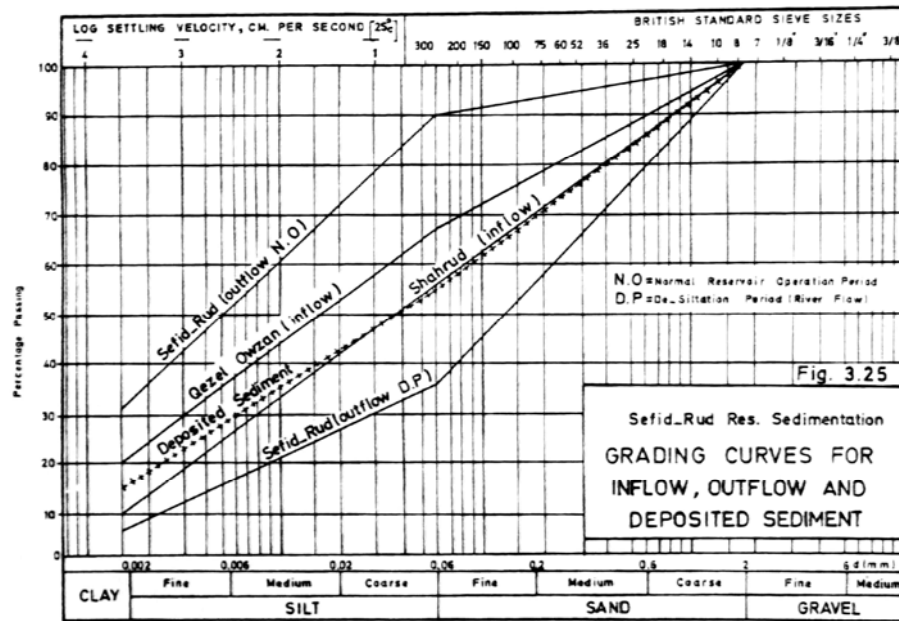


**FIGURE 23.5** Grain size distribution of suspended sediments entering and leaving Sefid-Rud Reservoir and of sediment deposits. The grain size discharged below the dam increased significantly as a result of flushing (Tolouie, 1989).

Extensive piping occurred at Sefid-Rud during the flushing period, which eroded the sandy sediment layers into the flushing channel while the overlying cohesive sediment layers slumped in place.

1. Consolidated blocks of cohesive sediment were frequently transported as bed load and were not sampled as part of the suspended load. Bed load transport was not measured.
2. Because the sill elevation of the bottom outlet is located very close to the original thalweg elevation of the river, coarse material can be transported very effectively despite reduced discharge during the flushing season. Sand and gravel deposited in the upper reaches of the main channel by floods during the impounding period are almost completely removed during the next flushing operation, whereas fines continued to deposit on the submerged floodplain.

### 23.2.3 Sediment Deposits

No borings were made through the deposits prior to desilting. After 6 years of desilting operations which dewatered and compacted the sediments to an unknown degree, 250 borings were made. The borings revealed that the average composition of the deposits

was 41 percent sand and 59 percent clayey silt. Specific weights averaged  $1.20 \text{ t/m}^3$  for clayey sediments and  $1.45 \text{ t/m}^3$  for sandy layers, or about  $1.3 \text{ t/m}^3$  overall, reported to agree well with estimates of  $1.25$  and  $1.34 \text{ t/m}^3$  made by the Trask (1931) and (Lane and Koelzer, 1953) methods respectively. Nine of the deep borings made through the sediments between 7 and 20 km above the dam were reported by Tolouie (1989). The profile for borehole 7, reproduced in Fig. 23.6, shows the alternating layers of sand and fines encountered in most of the reported borings. The deepest boring reported by Tolouie penetrated 22 m of layered sediment deposits. Deposits near the dam consisted entirely of cohesive sediments without lenses of coarser material.

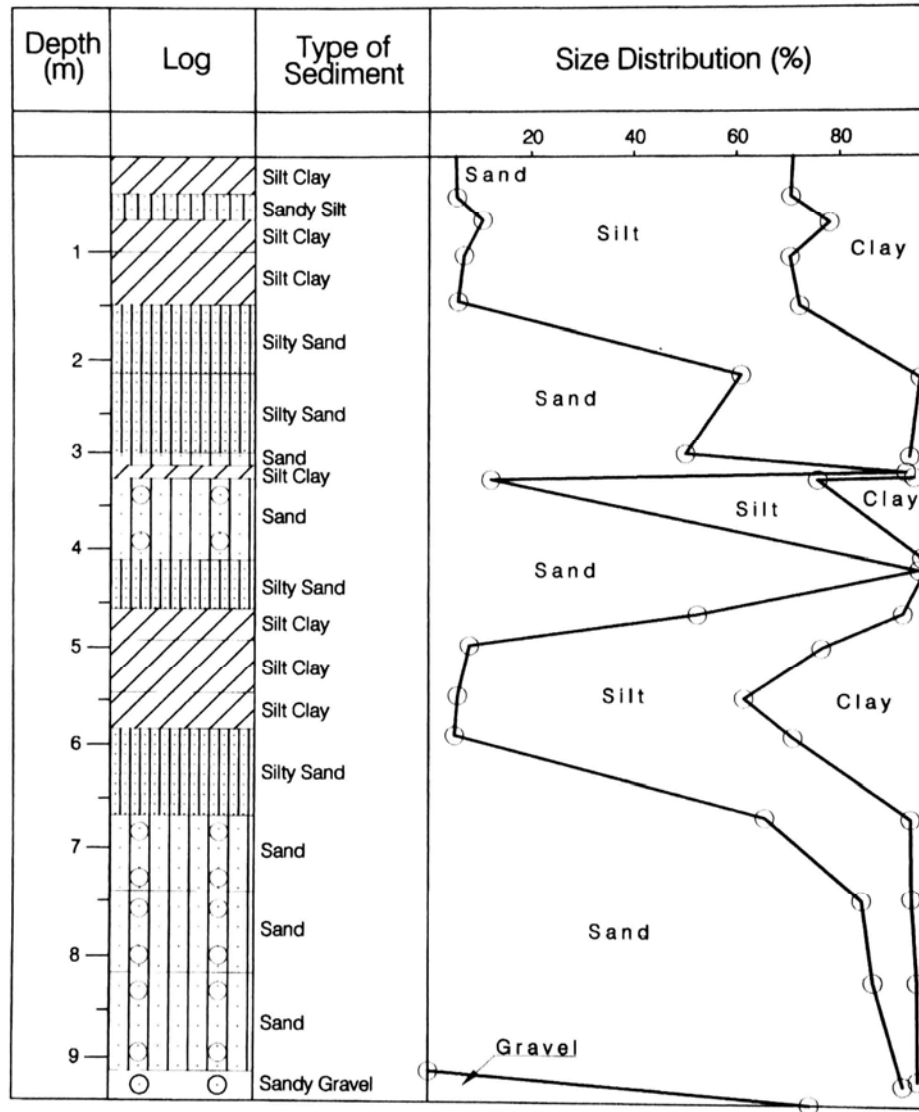


**FIGURE 23.6** Vertical profiles through sediment deposits more than 5 km from the dam in borehole 7 showing the presence of alternating layers of sandy noncohesive and clayey cohesive sediments. This layering is largely absent closer to the dam because coarse sediments were not transported that far into the reservoir (after Tolouie, 1989).

### 23.2.4 Turbid Density Currents

The reservoir geometry, particularly along the steep Shahrud River, in combination with large-capacity bottom outlets near the original river bed and 15 m below the power intakes, is conducive to the venting of turbid density currents. Despite the 12 m high cofferdam located 150 m upstream of the main dam, which interfered with density current movement, and the low priority given to the release of density currents, 27 percent of the inflowing suspended sediment was released over the 1963-1980 period, primarily as density currents. The effect of bottom sluice operation on sediment release is illustrated in Table 23.2, showing the release of as much as 36 percent of the inflowing sediment load during an individual flood event. The average  $d_{50}$  and  $d_{90}$  diameters for sediment vented through the Sefid-Rud Dam by turbid density currents were 0.007 and 0.080 mm, respectively, which is coarser than the values reported for turbid density currents in Chinese reservoirs. On January 1, 1976, a turbidity current was observed to enter the reservoir at a point 15 km upstream of the dam in the Qezel Owzan River, and was vented on January 4 through bottom outlets, resulting in an average forward velocity of 0.058 m/s in the turbidity current. During this same period the Qezel Owzan inflow averaged 412 m<sup>3</sup>/s with an average sediment concentration of 6.35 g/L.

## 23.3 SEDIMENT CONTROL ALTERNATIVES

### 23.3.1 Hydraulic Dredging

Dredging was initially considered for sediment removal at Sefid-Rud, and the recommended scheme entailed the removal of up to 700 Mm<sup>3</sup> of sediment, to be deposited in terraces constructed of hydraulic fill to maximum heights on the order of 20 to 30 m, without use of a retaining wall. The dredging system would consist of a floating hydraulic cutterhead dredge, floating and overland pipeline, booster pump stations, and hydrocyclones for separation of the coarse fraction for terrace construction by hydraulic fill (Fig. 23.7). The terraces would be located between 40 and 120 m above the average reservoir elevation, and maximum digging depth would be 35 m, on the basis of a maximum fluctuation in reservoir level of about 30 m during normal operation. Twelve dredging units plus three standby units, with an annual dredging capacity of 70×10<sup>6</sup> tons, were proposed. At the time of its proposal in 1985, dredging was estimated to require a capital investment of \$155 million, which would be recovered after 20 years at an interest rate of 8 percent.

**TABLE 23.2** Role of Bottom Outlets in Venting Turbid Density Currents, Sefid-Rud Reservoir

Date	Operation mode*	Average flow rate		Average reservoir level, m	Discharge averaged sediment concentration		Sediment release efficiency, %
		Inflow, m <sup>3</sup> /s	Discharge m <sup>3</sup> /s		Inflow, g/L	Outflow, g/L	
Apr. 1-2, 1973	P	290	109	259	4.1	0.1	0.9
Apr. 9-10, 1973	P + B	484	145	264	13.0	10.0	23.0
Apr. 17-18, 1973	P	420	127	267	4.4	0.1	0.8
Oct. 5, 1973	P	321	280	272	7.4	0.2	2.3
Oct. 14-15, 1973	P + B	415	385	273	13.0	5.0	36.0

\*P= power intakes open, P + B = power intakes + one bottom outlet open.

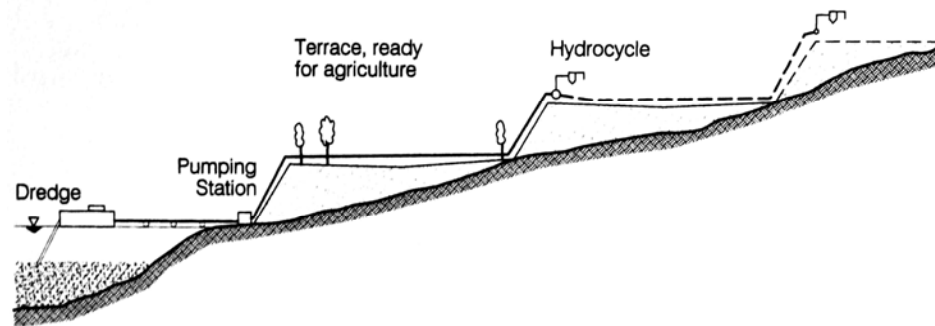


**FIGURE 23.7** Schematic diagram of dredging strategy considered but not implemented at Sefid-Rud Reservoir (after Tolouie, 1993).

Dredging with discharge to the river downstream of the dam was not considered feasible because, during the irrigation season, the dredged sediment would be carried downstream and deposit behind irrigation barrages and diversion dams, or within the system of irrigation canals. This would only move the sedimentation problem from one location to another.

Although it was not considered technically or economically feasible to undertake large-scale dredging at Sefid-Rud, dredging is considered the only feasible method of removing cohesive sediment deposits within 3 km of the dam. This area is characterized by difficult access due to the unconsolidated deposits, and the sediments consist of nonlayered cohesive material. One alternative in this area is for a cutterhead dredge to pump sediments by pipeline into the main flushing channel, from which they would be washed out during subsequent flushing. Use of a short pipeline discharging to the flushing channel minimizes pumping head and dredging cost.

### 23.3.2 Siphon Dredging

A siphon dredge differs from a conventional hydraulic dredge only in that a pump is not used; the slurry is moved by the difference in static head between the reservoir and the discharge point below the dam (Fig. 16.6a). Discharge distance is limited by the head available between the reservoir water level and the toe of the dam. In the case of SefidRud, the dredge would be able to work to a distance of about 2 to 3 km from the dam. However, a siphon dredge was considered too costly for use at this site.

### 23.3.3 Explosives

Another alternative was the use of explosives to destabilize banks along the flushing channel during drawdown to increase the amount of sediment removed by flushing. In areas of low bank elevation, continuous cable charges could be installed at depths up to 3 m by cable-laying equipment in which the cable drum has been replaced with an explosives tank. In areas of higher banks, 100-mm holes could be drilled for placement of explosives (Fig. 23.8). Waterproof explosives would be required. This method was estimated to be capable of removing 30 to 50 Mm<sup>3</sup> of additional sediment over the course of two flushing events.

### 23.3.4 Venting Turbid Density Currents

The venting of turbid density currents was the primary means of releasing sediment during normal impounding. Although venting of turbid density currents can retard sediment accumulation, it cannot stop deposition or recover capacity. Thus, density current release was not considered a feasible solution.

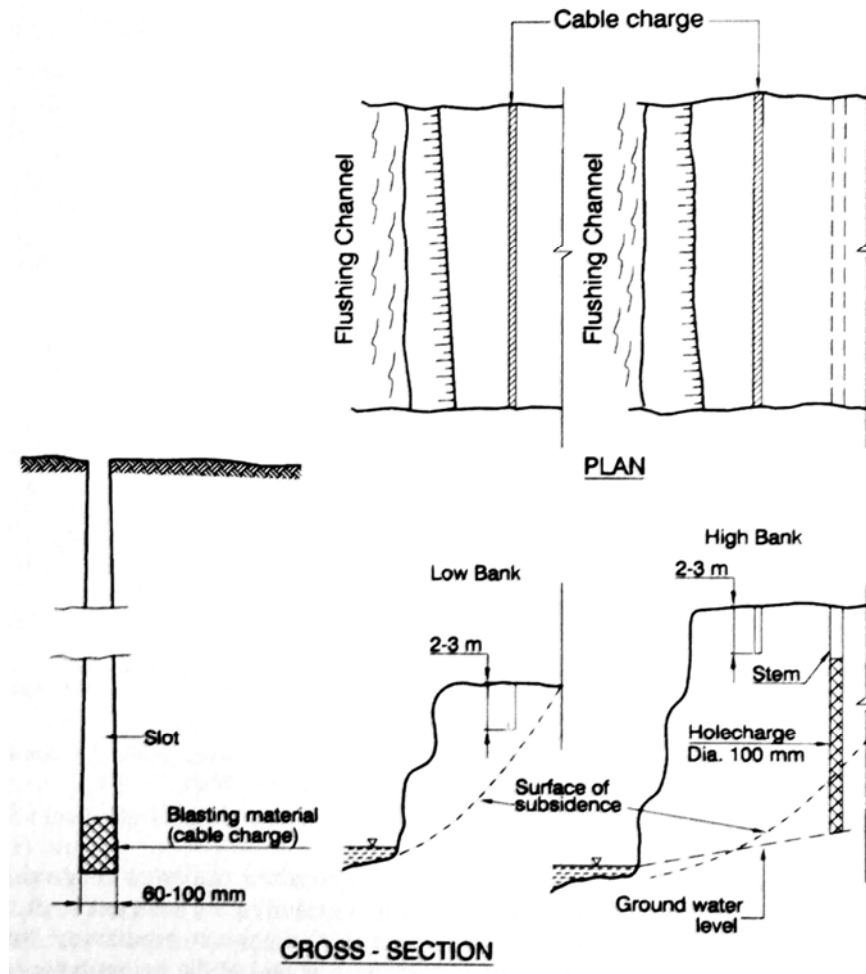


**FIGURE 23.8** Proposed use of explosives at Sefid-Rud Reservoir to enhance bank failure and widen the flushing channel (after Tolouie, 1993).

### 23.3.5 Sediment Bypassing

Sediment bypass would release inflow on those days of high sediment discharge during flood events. However, the topographic features at Sefid-Rud are not conducive to construction of a bypass channel around the reservoir. The hydrologic size of the reservoir is too large to effectively pass sediment through the impoundment, and a large fraction of the inflowing load is sand that would settle quickly and be more difficult to bypass. Thus, bypassing was not considered a viable alternative.

### 23.3.6 Emptying and Flushing

The sediment management technique selected for utilization was to seasonally empty and flush the reservoir, which entailed the change in operating rule shown in Fig. 23.9.

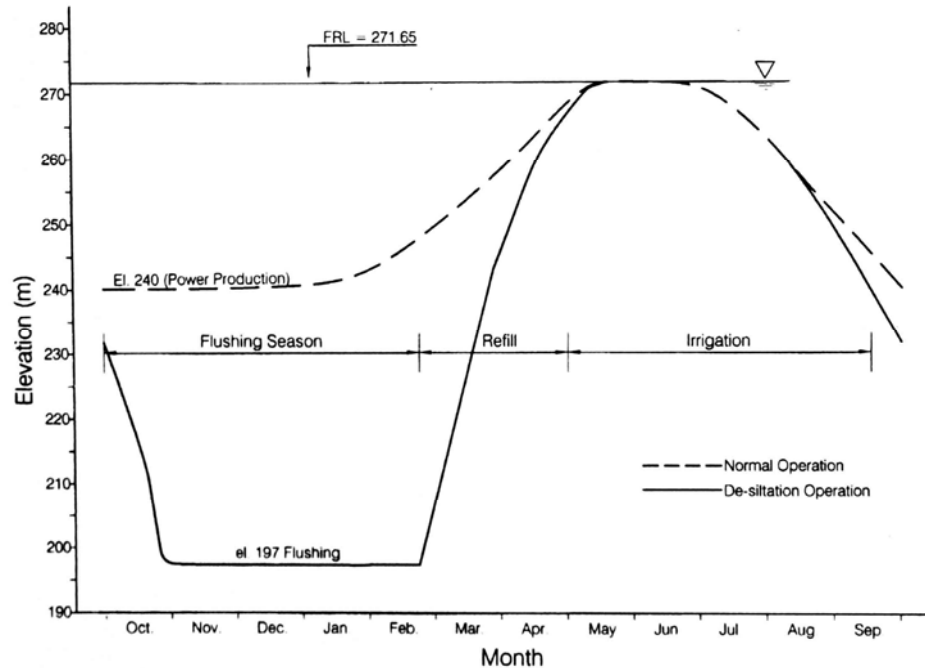


**FIGURE 23.9** Operation curve at Sefid-Rud Reservoir showing water levels for conventional impounding and the modification for flushing operation (after Tolouie, 1993).

Under the original operating rule, which did not consider sediment removal, filling occurred during the winter wet season and irrigation deliveries were made during the months of April through September. For continued hydropower production, the minimum operating level was maintained at 240 m after the end of the irrigation season. To undertake flushing, instead of maintaining a minimum elevation of 240 m for power generation during the nonirrigation season, the reservoir is emptied and the river discharges freely through bottom outlets, scouring a flushing channel through the deposits. This technique can be implemented without interfering with the primary operational objective, which is irrigation service. This reservoir does not have carryover storage from one year to the next. Flushing also does not require costly, sophisticated, and energy-intensive equipment such as required for dredging, and is economical to implement. Tolouie (1993) cited the estimated unit cost of sediment removal by the proposed dredging project as a minimum of  $\$3.00/\text{m}^3$ , as compared to  $\$0.10/\text{m}^3$  for flushing.

## 23.4 RESERVOIR FLUSHING

### 23.4.1 Reservoir Operation

Sediment control was initiated in water year 1980-1981 by emptying and flushing the reservoir from October to February, the period of low flow. In some years flushing began as early as mid-September or as late as mid-November, but refilling was always initiated in the first or second week of February. It would be highly desirable to delay closure of the bottom gates to allow large spring discharges to scour the deposits and

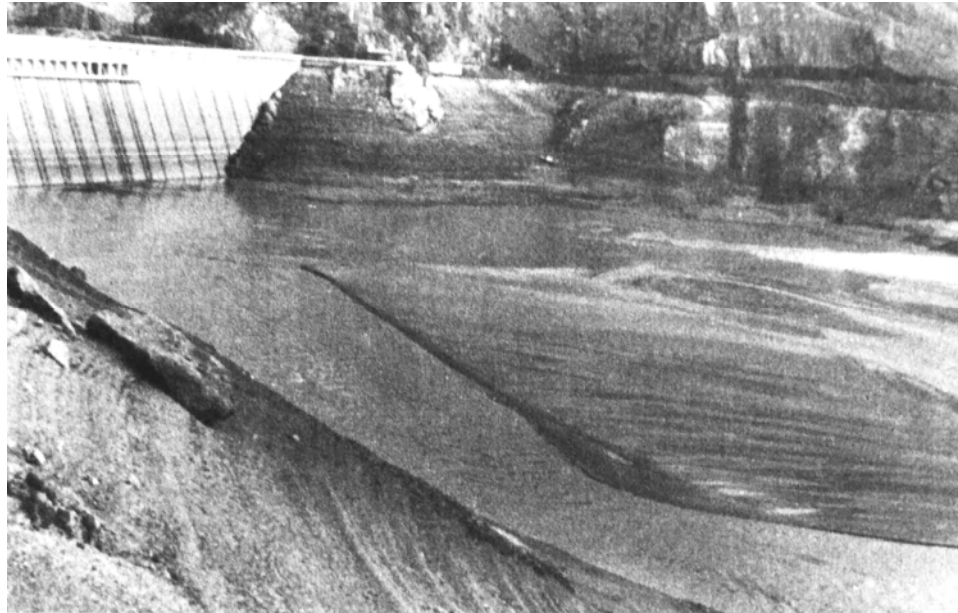


**FIGURE 23.10** Photograph of upstream side of Sefid-Rud Dam during partial drawdown in 1981-1982 (*E. Tolouie*).

widen the main flushing channel, but the uncertainty of filling the reservoir dictates closure in February.

During the first 2 years of flushing (1980-1981 and 1981-1982), the reservoir was not completely drawn down for fear that unstable sediments near the dam would slump and block the bottom outlets. Figure 23.10 shows the appearance of the deposits upstream of the dam during the 1981-1982 partial drawdown. The gabion cofferdam, which had not been demolished after dam construction and had become buried in sediments, was exposed when sediment deposits near the dam were scoured away. For 3 months during the first flushing season water overflowed the cofferdam crest and eroded the downstream face, endangering its stability. During the early part of the subsequent flushing season, the sediment plug in a broken section of the cofferdam was eroded through, and by the third year enough sediment had been washed away from the area near the dam to allow complete drawdown. Flushing created a main channel through the deposited sediment, generally following the original thalweg of the Qezel Owzan and Shahrud Rivers. Selected statistics on each of the flushing periods conducted through 1990 are summarized in Table 23.3.

The initial years of erosion and expansion of the main channel produced very high sediment yields and rapid recovery of storage capacity. As illustrated in Fig. 23.11, the total benefit of flushing consists of the volume of sediment removed plus the volume of deposition prevented. At Sefid-Rud this was equivalent to  $320 \text{ Mm}^3$  of reservoir volume over the first 10 years of flushing. The  $320 \text{ Mm}^3$  of sediment removal required  $10.667 \text{ Mm}^3$  of water, an average of  $33 \text{ m}^3$  of water for each  $1 \text{ m}^3$  of sediment removed and an average suspended sediment concentration of  $48 \text{ g/L}$ , as in Table 23.3. However, these average values can be misleading because of large year-to-year differences in sediment removal. Large variations also occur during flushing events; suspended sediment concentration is highest when flushing starts and declines rapidly.

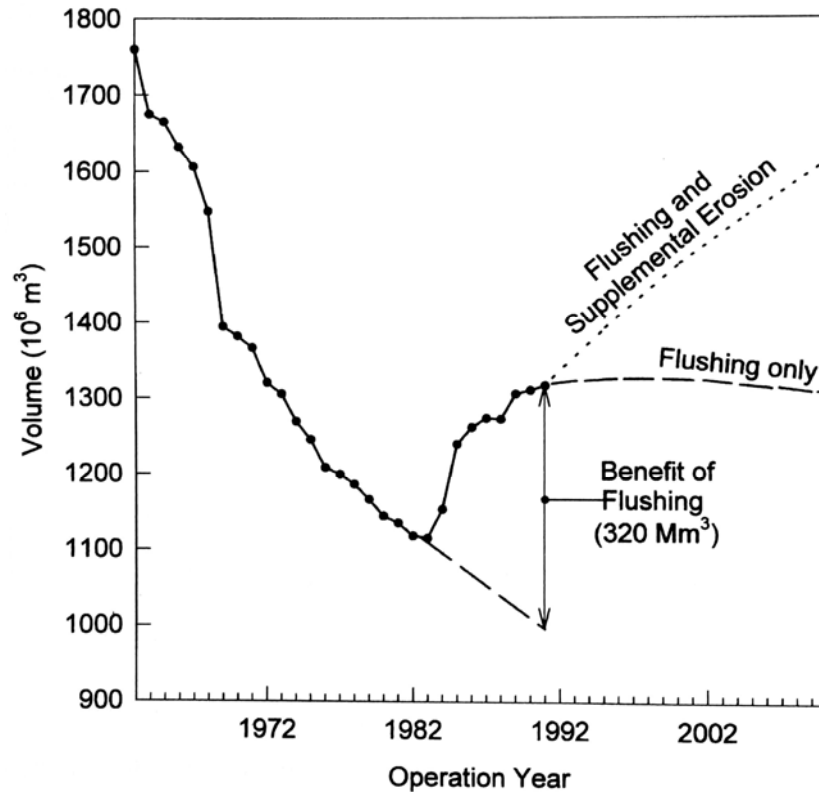


**FIGURE 23.11** Recovery of reservoir storage as a result of flushing. The total benefit of flushing is the sum of the storage recovered plus the storage loss avoided. Predicted long-term storage recovery using flushing alone compared to flushing plus supplemental floodplain erosion by using longitudinal diversion channels (*adapted from Toulouie, 1993*).

**TABLE 23.3** Flushing Statistics

Flushing period	Drawdown flushing duration, days	Empty flushing, days	Water volume used to flush		Sediment Removed, 10 <sup>6</sup> t	Average suspended sediment concentration in flushing flow g/L
			10 <sup>6</sup> m <sup>3</sup>	% of annual inflows		
1980-1981	61	0	536	10	24	45
1981-1982	65	0	390	11	12	31
1982-1983	117	10	1,513	26	52	34
1983-1984	16	80	795	23	68	85
1984-1985	19	138	1,810	29	142	78
1985-1986	18	129	1,131	29	46	41
1986-1987	17	85	942	26	27	29
1987-1988	24	86	1,812	22	57	31
1988-1989	9	113	1,057	31	54	51
1989-1990	5	103	681	22	32	47
Total	351	744	10,667	21	514	48

The capacity elevation curves and thalweg profiles shown in Figs. 23.12 and 23.13 illustrate the rapid storage loss and subsequent recovery achieved with flushing. Because of channel formation, significant capacity was recovered at all active storage levels within the reservoir. Sediments were eroded during flushing by three processes: sheet erosion, channel erosion, and bank failure. Only the latter two processes were significant.

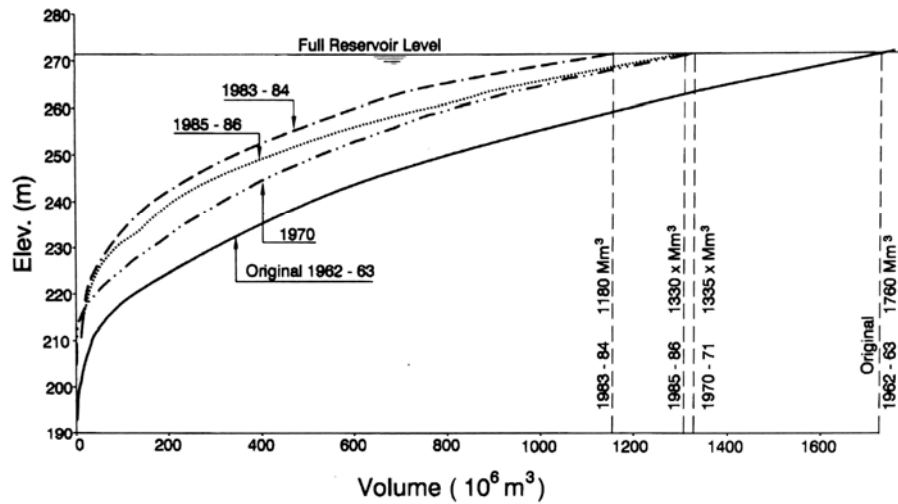


**FIGURE 23.12** Variation in sediment storage with time at Sefid-Rud illustrated by capacity elevation curves (after Tolouie, 1993).

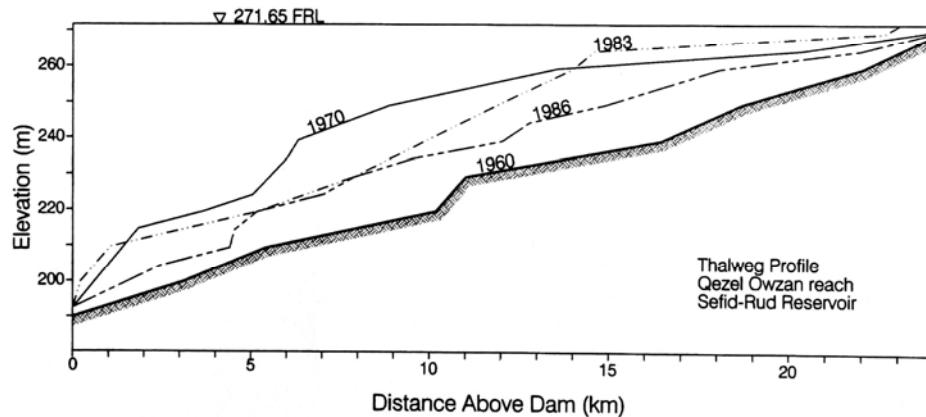


**FIGURE 23.13** Thalweg profiles along Qezel Owzan River for different years, showing the upstream progression of the flushing channel (after Tolouie, 1993).

#### 23.4.2 Sheet Erosion

During the desiltation operation in 1980-1981 the most important type of erosion was sheet flow and scour of recently deposited, unconsolidated fine sediments from within 5 km of the dam. This was the first year of drawdown, and sediments on the top of the bed below 240 m had not been previously dewatered. Because of the high rate of sheet

erosion during the first flushing event, during the second year of flushing the reservoir level was raised and lowered several times between pool elevations 215 and 220 m to accelerate sheet erosion, but after 2 months, sediment concentration in the discharge had dropped to only 0.9 g/L and the procedure was stopped. Overall, sheet erosion was of little importance after the first flushing event and was always limited to only a small fraction of the sediments deposited on the submerged floodplains during the preceding impounding period.

### 23.4.3 Channel Erosion

The most important sediment removal process was channel erosion. Soon after the first complete drawdown in 1982-1983, main channels were eroded, extending upstream from the bottom outlets along both the Qezel Owzan and Shahrud Rivers, and these channels quickly deepened and widened as flushing continued. Because of the presence of cohesive sediments, very steep banks were formed. Massive bank slides occurred during the first month after complete drawdown and the magnitude of channel erosion was very sensitive to changes in flow rate. If the channel became relatively stabilized at one discharge, a subsequent larger discharge would renew accelerated bed and bank erosion. The photograph in Fig. 23.14 illustrates the general appearance of the flushing channel in layered sediments during the active erosion period, showing collapsing banks of cohesive material after erosion of underlying sandy deposits by piping.

Referring to the sequence of thalweg profiles in Fig. 23.13, one can see that channel deepening initially occurred near the dam and moved upstream by retrogressive erosion.

### 23.4.4 Turbidity Currents

During impounding, the main flushing channels within the deposits produced a submerged gorge along which turbidity currents could travel, thereby improving the potential to release sediments through bottom outlets at the dam. However, because sediment can be removed by flushing, priority was not given to venting turbidity currents. Sediments in turbidity currents deposited in the channels are removed by flushing.

### 23.4.5 Outflow Sediment Concentration

Instantaneous suspended-sediment concentrations as high as 670 g/L were measured downstream of the dam during flushing. The concentration and amount of sediment transported out of the reservoir depends on sediment delivered from the watershed and deposited in the flushing channel, the rate of sediment entrainment from the deposits, and the sediment transport capacity of the streamflow. The main channel was formed during the first 3 years of flushing, and these years were the period of maximum sediment export and increase in reservoir capacity. After the main channel has become relatively stable, most sediment removal involved material deposited in the channel since the previous flushing, or material eroded from the floodplain deposits using auxiliary methods such as lateral or longitudinal erosion (diversion channels). Although the greatest volume of sediment is removed during the initial period of main channel formation, the data in Table 23.4 indicate that the maximum sediment concentrations occur after the main channel has been formed. This is caused by the rapid mobilization of unconsolidated sediment deposited along the main channel during the preceding impounding period.



(a)



(b)

**FIGURE 23.14** (a) Photograph of main channel formation showing erosion of sand sublayer by seepage. (b) Bank collapse due to erosion of the sand sublayer, forming terraces and gullies.

**TABLE 23.4** Maximum Daily Suspended Sediment Release during Each Flushing Season, Sefid-Rud Reservoir

Date	Pool elevation, m	Inflow		Outflow		Drawdown rate, m/day	Max. daily ave. SS concentration, g/L
		Water m <sup>3</sup> /s	SS, 10 <sup>3</sup> t/day	Water, m <sup>3</sup> /s	SS, 10 <sup>3</sup> t/day		
Nov. 9, 1980	216	61	31	105	967	3.9	107
Oct. 3, 1981	223	28	1	160	981	2.6	71
Oct. 10, 1982	229	239	503	182	1927	0.3	122
Dec. 14, 1983	201	136	70	154	2342	4.1	176
Dec. 3, 1984	205	205	106	266	7918	6.1	344
Oct. 4, 1985	210	27	0.5	165	2905	8.6	204
Nov. 20, 1986	197	81	14	129	3256	11.2	292
Nov. 20, 1987	198	87	7	213	5617	16.5	305
Oct. 24, 1988	200	89	41	135	4639	6.0	398

The reservoir attained full drawdown for the first time in February 1983.

SS = suspended solids

Source: After Toulouie (1993).

The variation in pool elevation, water discharge and sediment discharge during 1982-1983, the first year in which complete emptying was achieved, is illustrated in Fig.

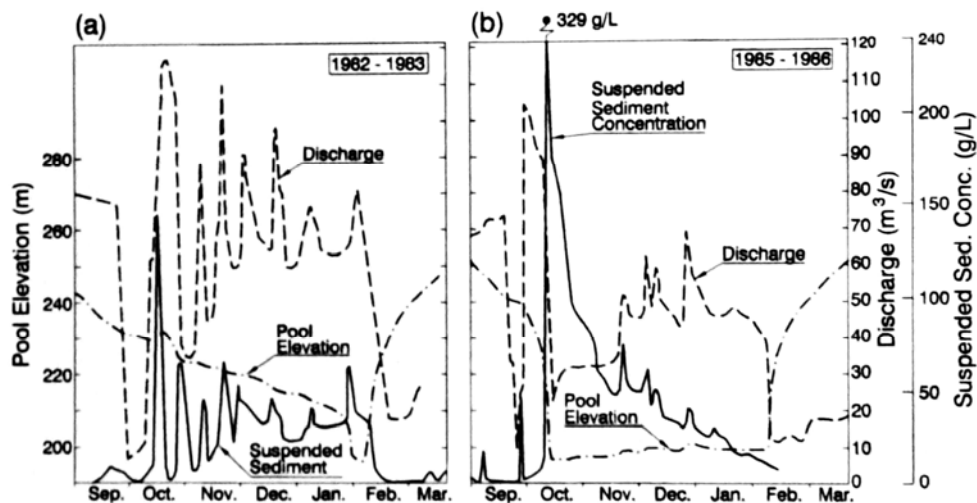


**FIGURE 23.15** Variation in pool level, discharge, and sediment concentration during two flushing events, Sefid-Rud Reservoir: (a) during first year (b) after stabilization. (after Toulouie, 1989).

23.15a. The maximum instantaneous suspended-solids concentrations of 150 g/L downstream of the dam occurred during this first full drawdown event when a large discharge occurred after a period of gate closure, and probably included a significant amount of material that had accumulated in front of the outlets. As the pool was lowered and discharge varied, suspended sediment spikes downstream of the dam closely tracked the discharge spikes, with erosion within the reservoir generally increasing as a function of

discharge. A final sediment concentration peak occurred when full drawdown was achieved. A high rate of sediment discharge and continuously elevated suspended sediment concentrations occurred throughout this entire flushing period while the main channel was being formed.

The situation was quite different only 3 years later during the 1985-1986 flushing season when the main channel had become more stabilized (Fig. 23.15b). In that year, the reservoir level was dropped from 220 to 196 m over only a few days creating a very high rate of sediment release. Suspended-solids concentration exceeded 150 g/L for about 1 week and reached a maximum value of 329 g/L. However, the solids content of the water released from the dam declined steadily, despite increasing discharge over the flushing period. Similar behavior was observed during subsequent years, except in 1989-1990, when the concentration of the flushing flow increased in February because of erosion of the Shahrud diversion channel. It is characteristic of flushing that, even though sediment discharge can equal sediment inflow on an annual basis, the seasonality of sediment release differs from the seasonality of sediment inflow. At Sefid-Rud most sediment is delivered to the reservoir by wet season floods, but most sediment is released as a highly concentrated flow during the dry season.

#### **23.4.6 Downstream Impacts**

Barrages and intakes are installed on the Sefid-Rud River downstream of the dam to divert reservoir releases to irrigators. These intakes and canals cannot tolerate heavy sediment loads, since this would create serious sedimentation problems within the irrigation system. To prevent serious downstream sedimentation problems, the sediment concentration of water released from Sefid-Rud Dam during the irrigation season (April - September inclusive) should not exceed 5 g/L. The sluices on irrigation barrages remain fully open during the October through February flushing season, passing sediment-laden river flow with minimum interruption. Since flows during the flushing period are typically less than 150 m<sup>3</sup>/s, there is insignificant backwater at these downstream structures. Irrigation intakes remain shut to exclude the muddy water from delivery canals. Tolouie (1993) reported that this procedure avoided operational problems below the dam caused by sediment flushing. No information is available on changes in channel morphology or other impacts downstream of the dam.

#### **23.4.7 Long-Term Storage Recovery**

The bed of the main channel created by flushing enlarged until a stable width was achieved. However, the resulting channel was narrow compared to the total deposit width, and sediment continued to be deposited on the submerged floodplain during impounding periods. Thus, for flushing alone the reservoir capacity at first increased rapidly, then increased more slowly, and in the future the capacity will start to decrease once again (Fig. 23.11). Therefore two additional methods were investigated to remove floodplain deposits on either side of the main channel: (1) lateral erosion by piping and (2) longitudinal erosion or diversion channels. These two techniques are discussed in the following sections.

### **23.5 LATERAL EROSION BY PIPING**

---

Sediments in the upper reaches of the reservoir had been deposited in thick alternating layers of cohesive and noncohesive material as shown in the boring data (Fig. 23.6). Cohesive deposits were 2 to 4 m thick, and desiccation and compaction during

annual drawdowns enhanced their resistance to surface erosion and gullying. However, in areas near the main flushing channel, thick layers of cohesive sediments were observed to collapse, forming a series of terraces at different elevations. This collapse was apparently caused by piping and washout of the sandy sediments from beneath the cohesive deposits. Drainage of the sand sublayer and the subsequent sliding to form terraces and gullies is shown in the photographs in Fig. 23.14, looking along the main channel.

The observed process of bank collapse suggested that *lateral erosion* might be accomplished by subsurface piping rather than superficial gullying. A field experiment was conducted during the 1985-1986 flushing season to attempt to artificially induce piping through the sandy sediment layers, causing the overlying cohesive sediment layer to collapse and erode. The experiment was performed by digging a pit 2 m in diameter and 4 m deep down to the sandy deposits, about 40 m away from the edge of the main channel. During flushing this pit was maintained full of water by pumping at a maximum rate of about 5 L/s. After 5 days a sand boil was observed at the foot of the main channel bank, and after 15 days the top layer of cohesive sediment had collapsed completely to create a gully 3 to 10 m deep and 6 to 15 m wide (Fig. 23.16). From this field experiment, it was concluded that a hydraulic gradient of 0.25 to 0.33 between the pit and the water surface in the main channel was adequate to initiate piping in these deposits.



**FIGURE 23.16** Photograph of gully created as a result of lateral erosion by piping (E. Tolouie).

### 23.6 DIVERSION CHANNEL TECHNIQUE

The concept of *longitudinal erosion*, termed a *diversion channel* by Tolouie (1993), is similar to lateral erosion except that a pilot channel is constructed parallel to the main channel rather than perpendicular to it. The channel is fed by water, either from a tributary or from the main river, which is diverted into the channel by a diversion dam.

An initial test of the diversion channel concept was made during the 1987-1988 flushing season, using a 5-km diversion channel with a slope  $s = 0.005$  and water diverted from the Siahpush River, a smaller tributary. For flows between 1.2 and 2.2  $\text{m}^3/\text{s}$  the outflow sediment concentration was normally increased by about 40  $\text{g/L}$ , and during a period with 3.8  $\text{m}^3/\text{s}$  of flow the outflow concentration was increased by 107  $\text{g/L}$  compared to the inflow. On the basis of this success, during the next year a diversion channel system was constructed along the right side of the Shahrud River reach, the smaller of the two main tributaries to Sefid-Rud Dam.

### 23.6.1 Components of the System

The Shahrud diversion system consisted of two main parts: an earthen diversion dam and a pilot channel. The layout of the system and other features are shown in Fig. 23.17, which also illustrates the meandering configuration that developed along the main flushing channel.

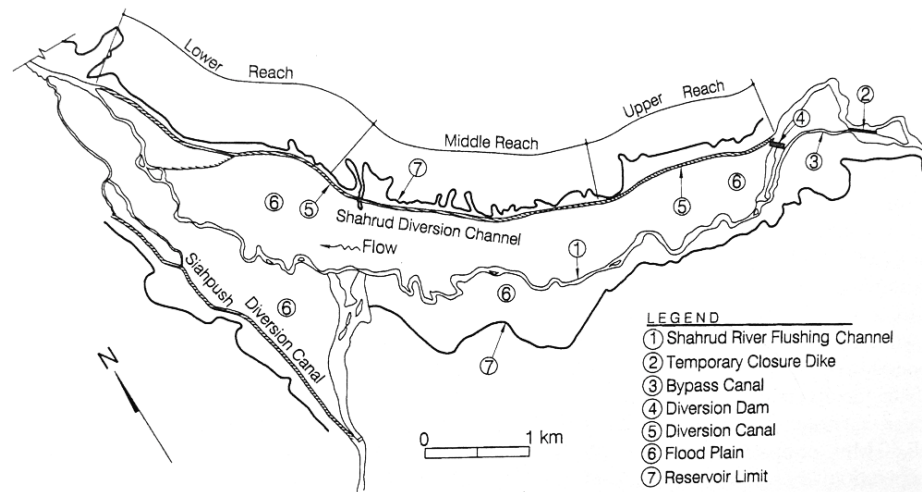


**FIGURE 23.17** Schematic layout of Shahrud reach of Sefid-Rud Reservoir showing longitudinal diversion channels, diversion dam, and other features. Note the meandering planform of the flushing channel.

Construction and operation of the diversion channel was undertaken in the following steps:

1. Construct a pilot channel to define the route of the longitudinal channel to be eroded.
2. Construct a stream bypass around the site of the diversion dam.
3. Construct an earthen diversion dam to deliver all streamflow into the pilot diversion channel.
4. When the diversion dam is completed, close the bypass and begin filling the diversion dam.
5. Begin diverting water into the pilot canal at a rate high enough so that overtopping of the earthen diversion dam is prevented, but without allowing the pilot channel to overflow and thereby cause lateral erosion into the main channel.

The initial stage of this operation is critical, when the diversion channel consists only of the small pilot section not yet enlarged by erosion. To prevent overtopping of the diversion channel and consequent breaching, an overflow section along the left bank of the pilot channel was provided about 500 m downstream from the inlet to allow excess flow to spill back into the main channel, in an area that was accessible and observable by operating personnel.

### 23.6.2 Diversion Dam

Several geotechnical and hydraulic considerations influenced siting of the diversion dam. The dam site needed to be in an area where piping through the adjacent beds was not anticipated, since this could cause an abutment to be washed out. The diversion dam was designed as a nonoverflow structure; no spillway or outlets were provided other than the diversion channel. To prevent overtopping and erosion of the diversion dam by flood flows exceeding the capacity of the diversion channel after it had been enlarged by erosion, the diversion dam was designed to be submerged every year by the rising reservoir pool prior to spring floods. This dictated the maximum height of the diversion structure with respect to the pool elevation.

The river bypass around the diversion dam site was dug in the form of a pilot channel on the left bank, taking off from an area where the river was wide and braided with a gravel and cobble bed. The pilot bypass channel was sized for a hydraulic capacity of about  $1 \text{ m}^3/\text{s}$  capacity, and when the channel had been excavated, the river was closed by an 800-m-long dike about 2 m high with a 2-m top width. The amount of flow discharged into the bypass channel gradually increased as the dike was extended farther across the riverbed, gradually eroding the pilot channel so that, upon closure, the total Shahrud River discharge of  $12 \text{ m}^3/\text{s}$  could flow through the diversion channel. Two weeks were required to construct the river bypass system.

The diversion dam was an earthen structure 80 m long with a maximum height of 8 m above the riverbed and a 5-m crest width. The foundation was stripped, abutments were trimmed, and mixed soil was placed in 0.3-m layers and compacted with six passes of a bulldozer. The crest of the dam was set at 269 m, about the same level as the adjacent floodplain. Dam construction required about  $8500 \text{ m}^3$  of material consisting of clayey silt excavated from nearby sediment deposits. As necessary, layers of cohesive sediment excavated from the diversion channel were mixed in to achieve the desired fill specification. The dam was constructed in 2 months (November 1988 through January 1989) and provided about  $0.40 \text{ Mm}^3$  of upstream storage, which stored inflow during the initial days of pilot channel operation when it could not accept the full Shahrud discharge.

### 23.6.3 Diversion Channel

The location of the diversion channel was selected near the right-hand margin of the floodplain to provide access and workability for construction machinery. The canal was 7.6 km long with an average slope  $s = 0.0054$ . A canal could not be constructed in the bottom portion of the lower reach because the unconsolidated silts and clays in this area had almost no strength and would not support construction equipment. Therefore, in this area discharge was simply allowed to flow across the deposits. Construction of the pilot diversion channel required 2 months with two bulldozers and two mechanical shovels (backhoes). Figure 23.18 illustrates a portion of the channel prior to diversion.

### 23.6.4 Operational Results

The most critical phase of longitudinal erosion by a pilot diversion channel is the initial scouring, when flow is initiated through the pilot channel but insignificant erosion and



**FIGURE 23.18** Photograph of upper reach of pilot diversion channel prior to erosion (*E. Tolouie*).

deepening of the channel has occurred. The Shahrud bypass was closed and filling of the impounded reach upstream of the diversion dam was initiated. Flow through the pilot channel was initiated on January 19, 1989 with a discharge of only  $1 \text{ m}^3/\text{s}$ , but after 10 days the river inflow had raised the water level behind the diversion dam to 266 m, and on January 28 discharge into the diversion channel was increased to  $5 \text{ m}^3/\text{s}$  to prevent overtopping of the diversion dam. As erosion continued to enlarge the diversion channel, the flow was increased, until by February 4 the entire  $12 \text{ m}^3/\text{s}$  discharge from the Shahrud River was being diverted.

Retrogressive erosion was the principle mechanism for scouring the diversion channel. The shallow pilot channel followed the slope of the floodplain deposits and its terminus was well above the thalweg elevation of the main channel. Retrogressive erosion was initiated immediately in the weak and unstable deposits where the diversion channel discharged into the main channel, and thence propagated rapidly upstream. Two mechanisms were observed by which retrogressive erosion accelerated erosion: plunging flow occurred at the upstream headwall, causing intense undercutting in an action similar to that associated with gullying, and flow acceleration in the reach extending as far as 200 m upstream from the point of plunging flow caused visibly accelerated erosion and turbidity increase. The erosional pattern was affected by two thick layers of cohesive sediment which formed erosion-resistant layers, as illustrated in Fig. 23.19a. Erosion proceeded upstream along the upper clay layer at about 100 m/day, but at a slower rate along the lower layer. However, in the lower reach of the channel where the deposits were not well consolidated and stratification was largely absent, erosion by layers was not detected. The appearance of the area of active retrogressive erosion, the "nickpoint," is shown in Fig. 23.20.

Only small bank slides occurred in the middle and upper reaches during the initial phase of diversion, with only  $1 \text{ m}^3/\text{s}$  of flow and a small bottom slope. However, when discharge was increased to  $5 \text{ m}^3/\text{s}$ , the erosion rate increased dramatically and frequent

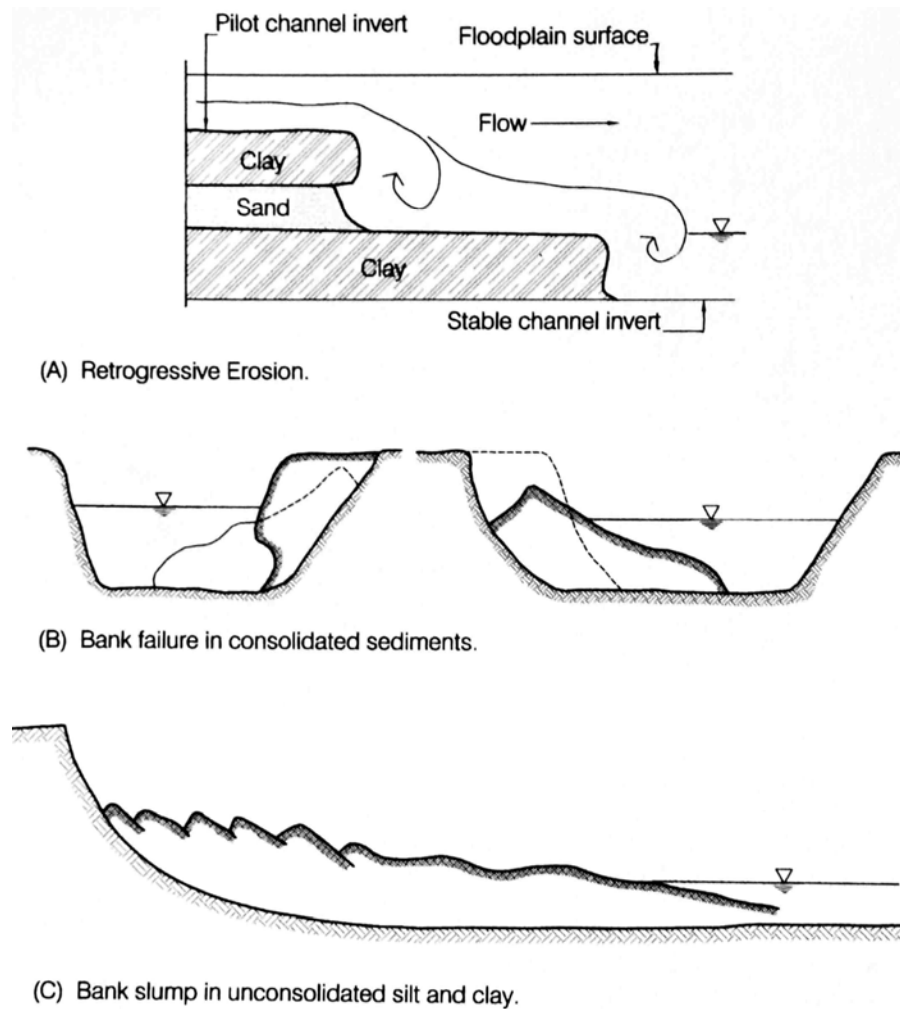


**FIGURE 23.19** Erosion patterns observed in Shahrud diversion channel: (a) retrogressive erosion in layered sediment, (b) block failures in middle reach, and (c) slumping of weak deposits in the lower channel. (after Tolouie, 1993).

deep slides were observed, at the rate of about one per minute. This continued until the canal became partially submerged by reservoir impounding in February, and resumed again when the reservoir was lowered for flushing in the subsequent year.

Banks slid into the eroding channel by slumping in areas of poorly consolidated and saturated sediments, or as the collapse of larger blocks in areas of more consolidated sediment (Fig. 23.19b and c). There was a noticeable increase in bank sliding as discharge increased. Blocks of consolidated clays that fell into the channel were transported downstream as bed load, and thus part of the load of fines was not sampled by suspended load measurements. The photograph in Fig. 23.21 shows the massive slumping process along the lower part of the diversion channel, as contrasted to the higher bank angles characteristic along the middle reach shown in Fig. 23.22. Bank sliding was particularly evident when the diversion channel emerged as the reservoir was emptied for the 1989-1990 flushing because of factors such as higher pore pressure in the saturated bank material and seepage. The diversion channel appeared to have



**FIGURE 23.20** Retrogressive erosion "nickpoint," view looking upstream (*E. Tolouie*).



**FIGURE 23.21** Slumping of poorly consolidated fine sediment in the lower reach of the longitudinal diversion channel (*E. Tolouie*).

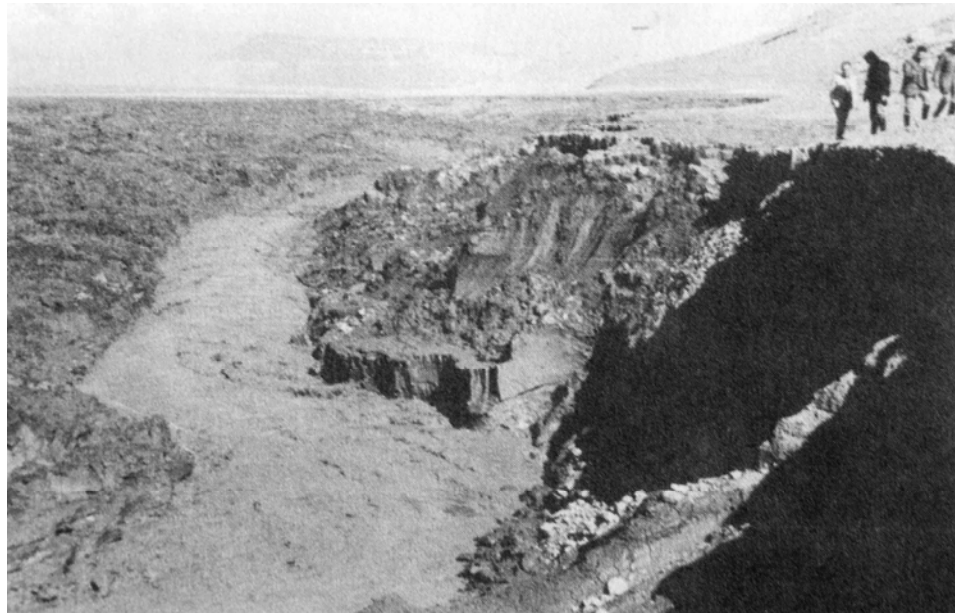


**FIGURE 23.22** Steep banks of consolidated sediment in the middle reach of the diversion channel during active erosion period (*E. Toulouie*).

reached a stable geometric configuration by late December 1989, after about 95 days of diversion flow.

Fifty cross-section measurements of the diversion channel taken in January 1990, after it appeared to have stabilized, showed it to have an irregular geometry. Most of the cross sections had a combined section geometry consisting of a deeper main channel with a shallower and wider terraced channel on either one or both sides, created by the layers of cohesive sediment within the deposits. Channel top width varied from about 50 m to 200 m. The final stable condition in the middle reach is shown in Fig. 23.23, illustrating the deep main channel bordered by flat terraces and the pronounced tendency to create a meandering planform.

### 23.6.5 Prediction of Channel Width

Toulouie (1993) used many regime and tractive force equations to compute the equilibrium width of the diversion channel based on the soils data available from the extensive boring program, discharge, and slope. The diversion channel geometry at Sefid-Rud consisted of a terrace section in which the slope was defined by the top of the thick cohesive sediment layer, and a deeper section whose slope was fixed by the main channel elevations at the beginning and the end of the diversion channel. These two slopes were used to compute the widths within the upper and lower channel sections. The computational procedure is given in Chap. 15.

In general, it was found that the regime-type equations underestimated the width of the eroded channel, apparently because the canals from which regime equations were derived are quite different from the conditions in sediment deposits. More reasonable results were achieved with tractive force methods. However, considerable field data are



**FIGURE 23.23** Stabilized channel configuration in the middle reach of the diversion channel. Notice the flat terraces created by clay layers in the deposits. (*E. Toluie*).

needed to make effective predictions, and the presence of layered cohesive sediments and the presence of some cohesive material in nominally noncohesive deposits are important factors which significantly complicate the analysis.

### 23.6.6 Long-Term Capacity

Toluie (1993) modeled the effect of flushing alone, as well as the use of diversion channels to control sediment accumulation at Sefid-Rud. From field experience, it was assumed that one flushing season would be adequate to scour a diversion channel to a stable configuration. Thus, at the beginning of each flushing season a new diversion channel pilot channel would be dug and eroded. It was assumed that the emptying period would begin in October, but diversion into the new channel would not begin until November of each year. At Sefid-Rud it was estimated that about 90 percent of the original reservoir capacity ( $1600 \text{ Mm}^3$ ) can be recovered and maintained through a combination of flushing and diversion channels. Figure 23.11 compares 30-year projections of storage capacity for flushing alone against flushing plus supplemental erosion using longitudinal diversion channels, with 75 percent of the flushing season inflow used to erode the new channels.

## 23.7 ECONOMIC ANALYSIS

---

An economic analysis was performed to compare a variety of sediment management alternatives (Toluie, 1989). The analysis started in the year 1963 (first year of dam operation) and considered the capital cost of the dam and appurtenant facilities as sunk costs and thus excluded from the analysis. Income streams from both irrigation and hydropower were either reduced or increased over time because of the change in

reservoir storage volume caused by sediment accumulation or removal. Hydropower benefits were eliminated during the period October through February in the alternatives which incorporated flushing. At Sefid-Rud the elimination of hydropower benefits over this period is not a major economic consideration, since irrigation benefits are more than 10 times the benefit from hydropower

A total of 10 alternatives were examined, divided among four basic categories. The first category (alternative 1) was continued conventional operation with no sediment management. The second category (alternatives 2 and 3) considered only the operation of bottom outlets to vent turbidity currents, discharging as much water as possible from the bottom of the reservoir rather than over high-level spillways. The third category (alternatives 4 and 5) considered flushing with or without discharge through bottom outlets. The fourth category considered flushing plus additional measures. The alternatives are summarized in Table 23.5. The economic analysis was performed over a period that started in 1963 and ended when 75 percent of the capacity had been lost, or after 100 years. Under the first two categories (alternatives 1, 2, and 3) the reservoir is rendered unusable by sedimentation within 100 years, but under all others reservoir life exceeds the 100-year period used for the analysis. The reservoir was assumed unusable when 75 percent of its original capacity was sedimented. Construction of diversion channels was not considered in this analysis because this technique had not been developed and tested when the economic analysis was undertaken. All economic values were expressed in terms of 1963 dollars and the present value of all future income and costs were determined for a discount rate of 4 percent. Under all cases (except alternative 1), reservoir desilting was assumed to begin in the eighteenth year of reservoir

**TABLE 23.5** Economic Analysis of Sediment Control Alternatives at Sefid-Rud

Alternative	Category	Spillage through bottom outlets		Ave. annual desilting efficiency,	Reservoir half-life, years	Base year cost of measures, million \$	Base year cumulative net benefit, million \$
		Vol. of annual spillage,	Ave. susp. sediment conc., g/L				
I	Normal operation	0	0	25	27	-	2458
2	Sluicing surplus water	50	10	36.3	28	20	2515
3	during spring floods	90	15	56.8	31		2705
4	Flushing*	0	0	96.5	-	-	3079
5		90	15	105.9	-	20	3122
6	Flushing, 60 g/L	0	0	114.1	-	46.3	3135
7	with coin- 65 g/L	0	0	121.9	-	35.9	3167
8	plementary 70 g/L	0	0	129.7	-	30.8	3185
9	measures 70 g/L	0	0	133.1	-	47	3180
10	75 g/L	0	0	137.1	-	26	3198

\*Shows average sediment concentration of flushing discharge

Source: Toluie (1989).

operation, and all alternatives incorporate the continual loss of reservoir storage through the seventeenth year under normal operation. Because of the high rate of sedimentation at this reservoir, it was considered economically advantageous to intensely manage the reservoir for sediment control to stabilize its capacity. If this same economic analysis were performed with the present time as the base year, instead of 1963 when the reservoir entered into operation, the net benefit from flushing would be much higher than shown in Table 23.5.

### **23.8 CLOSURE**

---

Tolouie (1993) concluded that flushing plus longitudinal diversion is an inexpensive and practical method to recover and maintain reservoir capacity which can be implemented using simple technology at sites where flushing is possible. With a combination of flushing and diversion, it may be possible to maintain reservoir capacity equivalent to a C:I ratio of 0.3. Because high sediment release efficiency is obtained during the first 3 years of flushing, diversion should not be undertaken during this initial flushing period. While the amount of sediment that can be removed increases as a function of the flow diverted into the channels, experience at Sefid-Rud suggests that, because of operational constraints, it will probably not be possible to divert more than 75 percent of inflow during the flushing period into diversion channels.

---

## CHAPTER 24

---

# CASE STUDY: SANMENXIA RESERVOIR

---

### 24.1 INTRODUCTION

---

The Yellow River (Huanghe) drains China's semiarid loess plateau, which is composed of thick aeolian deposits of silty soils. As a result of high erodibility and gully, intensive land use, inadequate soil conservation practices, and virtually limitless sediment supply, the sediment load carried through the Samen Gorge by the Yellow River is the greatest of all the world's rivers. After passing through the gorge reach, the river has historically deposited about 33 percent of its load on the alluvial floodplain and another 43 percent on the delta prior to discharging to the Yellow Sea (Long and Zhang, 1981).

The Sanmenxia Dam, constructed during 1957-1960, is the first dam built on the middle reach of the silt-laden Yellow River. The 96-m-high concrete gravity dam controls a drainage area of 688,400 km<sup>2</sup>, or 92 percent of the entire Yellow River basin (Fig. 24.1). The maximum historical floods at the dam site were 22,000 m<sup>3</sup>/s in 1933 and 36,000 m<sup>3</sup>/s in 1843. The dam was planned as a multiple-use project for flood control, hydropower, irrigation, navigation, and ice jam control. It was originally designed with a full reservoir level of 360 m and 64.7 km<sup>3</sup> of storage, inundating 3500 km<sup>2</sup> of floodplain and requiring the relocation of 870,000 persons. To reduce these impacts, the dam was built to an elevation of 350 m with a maximum pool elevation of 340 m in the initial stage of operation. Construction began in 1957, the river was closed in November 1958, and the dam was completed in September 1960. According to the original plans, two sediment control measures were to be implemented. (1) The reservoir was to continuously impound water and release 35 percent of the sediment inflow as turbidity currents through 12 outlets at 300 m. (2) Total sediment inflow was to be reduced 3 percent annually by soil conservation works, resulting in a 60 percent reduction of sediment inflow after 20 years. These numbers subsequently proved to be extremely optimistic. Furthermore, the amount of sediment inflow and the severity of upstream backwater deposition had also been underestimated (Dai, 1991).

Severe sediment accumulation problems became evident immediately after impounding began; 1.8 billion metric tons of sediment accumulated during the first 18 months after closure, representing a release efficiency of only 7 percent (93 percent trap efficiency). Sedimentation not only threatened to eliminate all project benefits in a short time, but sediment deposits were also raising the bed elevation and flood levels in the Yellow River as far as 260 km upstream of the dam. This threatened additional agricultural lands and riverside industrial areas in the city of Xian located on the Wei River, and it potentially required relocation of an additional million persons. These were unacceptable impacts. The project could not even be abandoned without removing the dam, and establishment of a sediment balance became the highest priority objective.

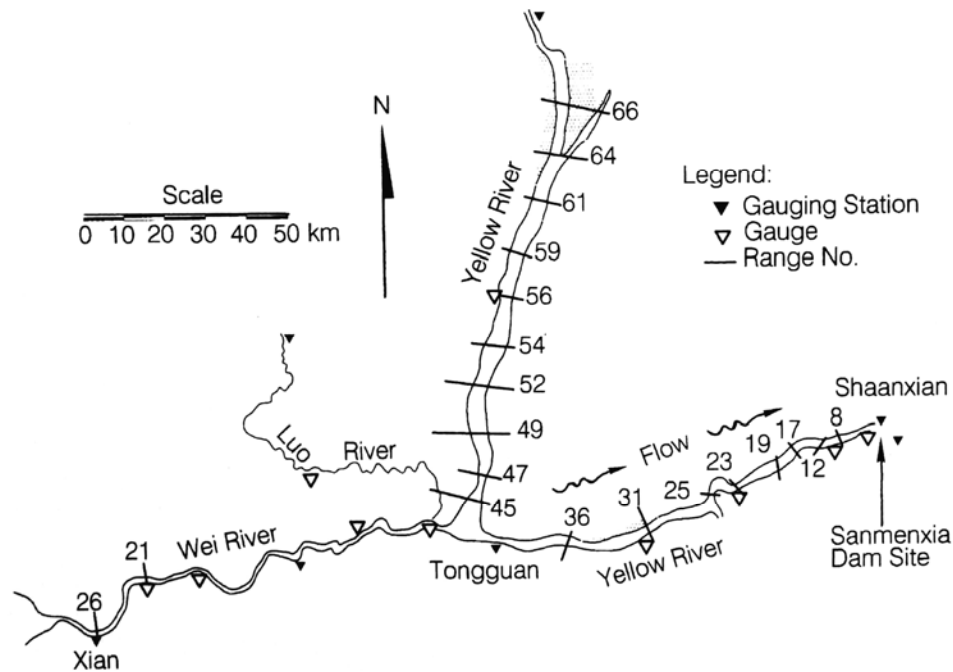


**FIGURE 24.1** Location map of Sanmenxia Reservoir, on the Yellow River, China (after Long and Zhang, 1981).

To achieve balance between sediment inflow and outflow, the dam was extensively reconstructed to provide high-capacity bottom outlets and reservoir operation was substantially changed. Sediment balance was finally achieved after 1970, making Sanmenxia the first major reservoir in the world where this was accomplished (Fig. 24.2). This project not only demonstrates the perils of giving inadequate consideration to sediment management in the planning and design of a reservoir, but it also shows that a sediment balance can be achieved across an impounded reach even in a large reservoir on a river with an extreme sediment load. Although project benefits are much smaller than the unrealistic values originally planned, the benefits are permanent. A principal objective of dam construction, flood detention to protect the downstream floodplains, has been achieved.

This case study describes sediment management strategies that were implemented and also the complex river sedimentation behavior that was influenced by dam construction. Because of the extreme silt loads and the highly erodible nature of the alluvial silts, river adjustment processes occur quickly in this system and are useful indicators of the types of responses that may occur in other systems over longer time periods. This case study is based on the second author's involvement in this project since the 1950s, site visit and interviews by the first author in 1987, plus the cited literature.

## 24.2 HYDROLOGIC SETTING

Most rainfall in central China occurs in late summer, generating surface runoff, erosion, and extremely high rates of sediment transport during July and August. Before dam construction, the annual runoff at Shaanxian station near the dam site averaged 43,100  $\text{Mm}^3$  and the sediment load consisted mostly of silts with a median grain diameter  $d_{50}$  of 0.03 mm. Sediment discharge averaged 1.6 billion tons per year, equivalent to an

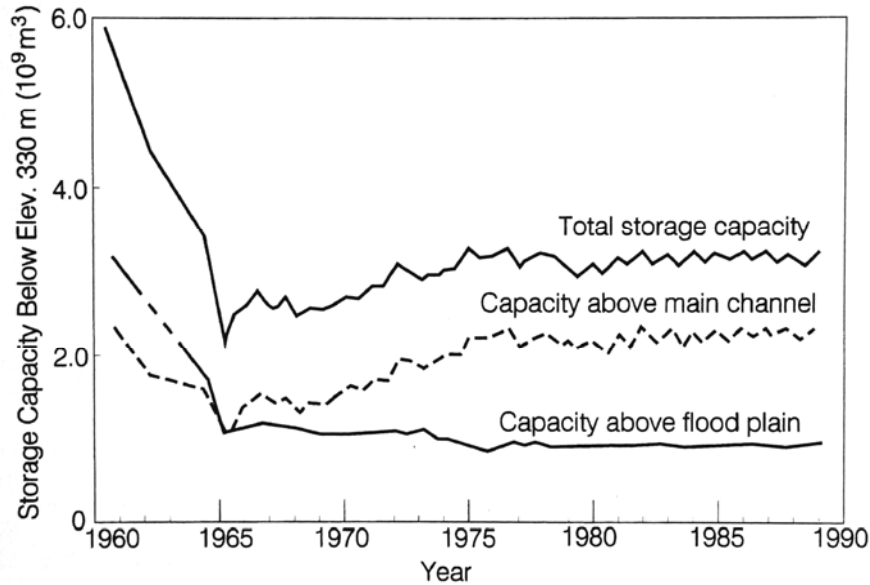


**FIGURE 24.2** Summary of the sedimentation history of Sanmenxia Reservoir (after Pan, 1990). The initiation of emptying and flushing in 1966 using large-capacity low-level outlets recovered storage capacity in the main channel area by scouring of the deposits. In contrast, the floodplain areas continued to accumulate sediment and lose capacity, although at a greatly reduced rate.

annual sediment yield of  $2300 \text{ t/km}^2$  and a mean suspended-sediment concentration of  $38 \text{ g/L}$ . July and August account for about 60 percent of total sediment yield but only 30 percent of the annual runoff (Table 24.1). Sediment concentrations as high as  $941 \text{ g/L}$  have been measured in the Yellow River near the dam site.

**TABLE 24.1** Monthly Variation of Discharge and Sediment Transport at Shaanxian Hydrologic Station, 1919-1959

Monthly mean	Discharge, $\text{m}^3/\text{s}$	Sediment transport, $10^6 \text{ t}$	Sediment concentration, $\text{kg}/\text{m}^3$
January	463	12.1	9.8
February	570	14.4	10.4
March	768	26.5	12.9
April	855	27.8	12.5
May	855	31.9	13.9
June	1080	79.8	28.5
July	2230	356	59.6
August	2880	611	79.2
September	2560	259	39.1
October	2100	121	21.4
November	1240	48.9	15.2
December	570	16.8	11.0
Yearly means	1353	1605	37.6

*Source:* Shaanxi Provincial Institute of Hydraulic Research and Qinghua University (1978).

Sanmenxia Dam is situated in the downstream portion of the gorge reach of the Yellow River and upstream of flood-threatened plains. The dam site is 114 km downstream of the ancient stronghold of Tongguan, situated immediately downstream of the confluence of the Yellow and Wei Rivers (Fig. 24.1). The Yellow River is only 1 km wide at Tongguan, but upstream it expands to more than 10 km in width at the confluence with the Wei River. The constricted river reach at Tongguan acts as a hydraulic control section that influences river stage, flow velocity, and thus the sediment transport capacity in the reaches of both the Yellow and Wei Rivers upstream of Tongguan. During floods, the stage at Tongguan rises rapidly and creates backwater conditions extending tens of kilometers upstream, thereby limiting sediment transport capacity and promoting sediment deposition upstream of the constricted Tongguan reach. This backwater reduces flow velocity and causes sediments to deposit in both the Yellow and Wei Rivers. At the end of the flood season, lower flows and reduced water levels cause these deposits to be scoured and moved downstream into the narrow Tongguan reach. Thus the bed elevation at Tongguan varies seasonally; it is scoured by high-velocity flow during the flood season, and during the nonflood season it is refilled by sediment that was deposited in the upstream reach during the preceding flood. Historical records indicate that the average bed elevation at Tongguan aggraded about 14 m during the 1800 years preceding dam construction, or about 0.008 m/yr, but no net change in the bed elevation at Tongguan was detected between 1948 and 1960. However, impounding by Sanmenxia Dam caused the bed elevation at Tongguan to rise 4.5 m between 1960 and 1961. Because the bed elevation and stage at Tongguan exert hydraulic control on both the Yellow and Wei Rivers upstream, the control of sediment accumulation at Tongguan is the key to limiting deposition and controlling backwater further upstream.

### 24.3 SUMMARY OF SEDIMENT CONTROL MEASURES

---

Water and sediment at Sanmenxia are regulated to achieve the following objectives:

1. Control extreme floods;
2. Provide irrigation, ice jam control, and power supply benefits;
3. Limit upstream backwater deposition above Tongguan;
4. Limit the amount of sediment deposition in the Lower Yellow River downstream of the dam; and
5. Preserve long-term useful storage capacity.

Sediment controls were implemented in stages, and two decades were required to bring sediment inflow and discharge into balance and control the bed elevation at Tongguan. This was achieved by extensively reconstructing the dam to increase the discharge capacity of low-level outlets, and by changing the operating rule to impounding during the nonflood season, and emptying and flushing during the flood season from July to October each year, thereby limiting deposition and scouring out deposited sediments.

The general layout of Sanmenxia Dam showing the location of deep sluices used for sediment release is presented in Fig. 24.3. Upstream and downstream views of the dam during drawdown and flushing are shown in Fig. 24.4, and a view of the top of the dam showing vertical sluice gates and the gantry for gate placement is presented in Fig. 24.5. The capacities of sediment sluices installed in the dam are summarized in Table 24.2.

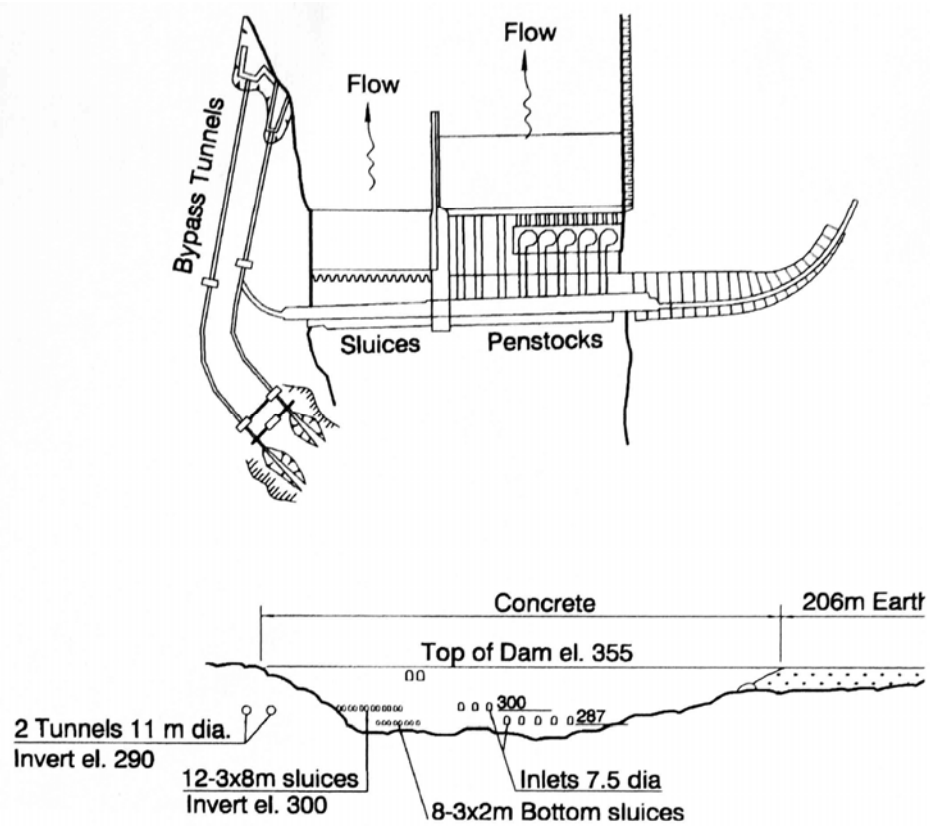


**FIGURE 24.3** General layout of Sanmenxia Dam showing the location of deep sluices and penstocks used for sediment release (after Chinese National Committee on Large Dams, 1987).



**FIGURE 24.4** (a) Upstream face of Sanmenxia Dam during sediment flushing, showing low pool and low level sluices in the foreground (*G. Morris*).



**FIGURE 24.4** (b) Downstream face of Sanmenxia Dam during sediment flushing showing flow exiting from the sediment sluices (G. Morris).

The effectiveness of sediment control achieved at each stage of reconstruction was analyzed and used as the basis for designing the next stage improvements. Sediment inflow and outflow were brought into balance during the fourth stage, and subsequent work focused on increasing project benefits while maintaining the sediment balance across the impounded reach. The six stage of dam reconstruction and operation to date are outlined in Table 24.3 and are described in more detail below.

**Stage 1.** Impounding began in September 1960. According to the original project design, the dam was intended to maintain a pool elevation of 340 m for multipurpose benefits, but serious deposition was already occurring when the water level reached 335.5 m. Six months after closure, sediment accumulation caused backwater effects to extend upstream about 250 km from the dam, that is, 136 km upstream from Tongguan, and the bed elevation at Tongguan rose by 4.5 m. The floodplain adjacent to the downstream reach of the Wei River is an important agricultural area, and the industrial area of Xian is situated on the south bank of the Wei River about 150 km upstream of Tongguan. It was realized that both would be partially flooded because of backwater deposition if sedimentation were not controlled.

**Stage 2.** Reservoir operation was changed after 1962 to maintain lower water levels year-round by using the outlets at 300 m contained in the original design, but the rate of deposition was still high because the outlet capacity was too small and the elevation was too high for efficient sediment release. An additional  $3.39 \times 10^9$  tons of sediment had deposited by June 1966. The original design did not have



**FIGURE 24.5** Vertical sluice gate (right foreground) and gantry for gate placement. (G. Morris).

**TABLE 24.2** Outlets in Sanmenxia Dam

Outlet	Dimensions	Total number	Serial number	Invert elevation, m	Starting year of operation
Deep sluices	3 x 8 m	12	1-12	300	1960
Penstock	Diameter = 7.5 m,	1	5	287	1966
sluices*	exit gate 2.6 x 3.4m	3	6-8	300	1966
Tunnels	Diameter = 11m,	2	1-2	290	1967 and
	8 x 8 m radial gate				1968
Bottom sluices	3 x 8 m	3	1-3	280	1970
		5	4-8	280	1971
		2	9-10	280	1990

\*Penstocks 5 through 8 were converted to discharge floodwater in 1966. Penstocks 5 was converted back to power generation in 1978.

**Source:** Shaanxi Provincial Institute of Hydraulic Research and Qinghua University (1978).

TABLE 24.3 Stages of Operation at Sanmenxia Dam

Stage	Date	Sluicing capacity at 315 m elevation, m <sup>3</sup> /s	Mode of operation	Outlets	Number of flood seasons	Annual deposition in Sanmenxia Reservoir, 10 <sup>9</sup> m <sup>3</sup>	Annual sediment entering lower Yellow River, 10 <sup>4</sup> t	Annual deposition in lower Yellow River, 10 <sup>4</sup> t	Annual deposition in delta region, 10 <sup>4</sup> t
	July 1950– June 1960		Pre-impoundment		10		1.80	0.37	0.95
I	Sept. 1960– Mar. 1962	3080	Storing water	12 deep sluices	1	1.75	0.14	-0.98	0.90
II	Apr. 1962– Jul. 1966	3080	Detention and flood flushing	12 deep sluices	4	0.49	0.88	-0.16	0.97
III	July 1966– June 1970	6070	Detention and flood flushing	12 deep sluices, 2 tunnels, and 4 penstocks	4	0.40	1.86	0.36	1.09
IV	July 1970– Oct. 1973	9390	Detention and flood flushing	12 deep sluices, 2 tunnels, 4 penstocks, and 8 bottom sluices	4	0.03	1.47	0.46	0.46
V	Nov. 1973– Oct. 1978	9390	Sediment regulation	12 deep sluices, 2 tunnels, 4 penstocks, and 8 bottom sluices	5	0.01	1.36	0.25	0.78
VI	Nov. 1978		Sediment regulation	12 deep sluices, 2 tunnels, 3 penstocks, and 10 bottom sluices (2 of which began operating in July 1990)					

Source: Shaanxi Provincial Institute of Hydraulic Research and Qinghua University (1978).

adequate sluicing capacity to prevent backwater during flood periods, and it became evident that greatly increased low-level sluice capacity would be required to control the bed elevation at Tongguan. Enhanced sluicing would also decrease the degradation in the Yellow River below the darn, which was now suffering from the reduction in sediment supply caused by the darn.

**Stage 3.** Additional sluicing capacity was provided by excavating two 11 m diameter bypass tunnels around the left abutment of the darn with an invert elevation of 290 m, and controlled by 8 x 8 m radial gates. Four of the eight power intakes were converted to sediment sluices and the pool level was lowered during the flood season. These measures increased the release efficiency to 82.5 percent, but the bed elevation at Tongguan was not lowered and deposition in the lower Wei River was still serious. It was determined that additional low-level sluicing capacity was required.

**Stage 4.** In the fourth stage of reconstruction, eight of the original twelve river diversion outlets at elevation 280 m, used for river diversion during dam construction but subsequently filled with concrete, were reopened with jackhammers and blasting. Reservoir operation was changed to flood detention and sediment sluicing; all outlets remained continuously open and the dam acted as an uncontrolled detention reservoir. The addition of bottom sluice capacity allowed lower pool levels to be maintained during the flood season, resulting in a net removal of sediment by scouring out some of the deposits. Sediment release efficiency reached 105 percent of inflow, and the bed elevation at the Tongguan control section fell by nearly 2 m. In 1973 five generating sets of 50 MW each were installed, replacing the eight original 125-MW units. This represented less than one-quarter the design generating capacity, a result of lower pool elevation and conversion of some penstocks to sediment sluicing.

**Stage 5.** After sediment balance had been achieved and the bed elevation was under control at Tongguan, reservoir operation was modified to increase project benefits by impounding clear water during the nonflood season and releasing muddy water by drawdown flushing during the flood season. As currently operated, all outlets are opened and the reservoir is emptied starting in July, the beginning of the flood season, allowing riverine flow to occur along the length of the impoundment for the purpose of sediment pass-through routing and flushing. High-capacity bottom sluices allow the pool elevation to be maintained at a low level during the flood season, minimizing backwater deposition at Tongguan and thereby restricting further upstream deposition in the Wei River. The history of bed elevation at Tongguan is shown in Fig. 24.6.

Impounding part of the year provides water for irrigation, hydropower, and ice jam control. Sediments deposited in the channel during the nonflood season are scoured from the reservoir by high discharges at low pool elevations during the flood season. Sediments flushed from the reservoir during the flood season are transported downstream by higher discharges than were possible before dam reconstruction. This mode of operation not only minimizes deposition within the reservoir, it also increases sediment transport capacity in the Yellow River downstream of the dam, and avoids the deposition of released sediment downstream of the darn.

**Stage 6.** Serious abrasion in the bottom outlets was repaired, decreasing the cross-sectional area of outlets and reducing low-level sluicing capacity. To compensate, two additional bottom outlets were opened and began operating in July 1990 to increase discharge capacity. Generating units were installed in two penstocks previously used for sediment sluicing, to increase power production. The reopening of the last two bottom outlets is presently being considered to further increase discharge capacity. Since 1980, hydropower generation has been halted during the flood season to avoid turbine abrasion by high sediment concentrations.

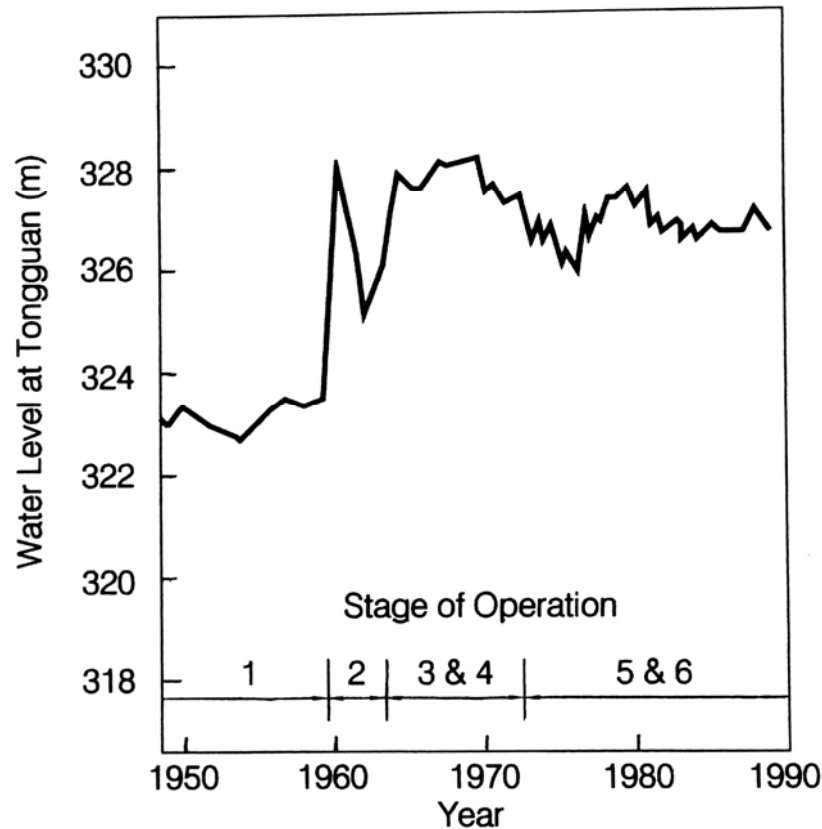


**FIGURE 24.6** Variation in water level at Tongguan at a discharge of  $1000 \text{ m}^3/\text{s}$ , showing the impact of dam construction and operation on bed elevation. The variation in water surface at a given discharge is used to represent the variation in bed elevation because continuous bed measurements were not taken (after Pan, 1990).

## 24.4 SEDIMENT MANAGEMENT FEATURES

### 24.4.1 Deposition and Flushing

The longitudinal pattern of sediment deposition is illustrated in Fig. 24.7, which shows the rapid buildup of sediment along the entire length of the reservoir after closure. Rapid deposition near the dam was caused by three factors: (1) high inflow sediment load. (2) turbidity currents transported sediment-laden water to the vicinity of the dam during periods of high pool elevation, and (3) limited reservoir drawdowns scoured sediments from the upstream area of the impoundment, which were redeposited closer to the dam upon encountering the backwater pool. At times the scoured sediments also plunged and formed a turbidity current which deposited sediments near the dam.

During impounding, sediments are deposited along the main channel and also on the submerged floodplain. Flushing flow scours the main channel and removes new deposits from this area, but does not remove sediment from the floodplain. Sediments deposited in the main channel are scoured during each subsequent flushing operation, but sediments deposited on the submerged floodplain accumulate continuously. The strategy used at

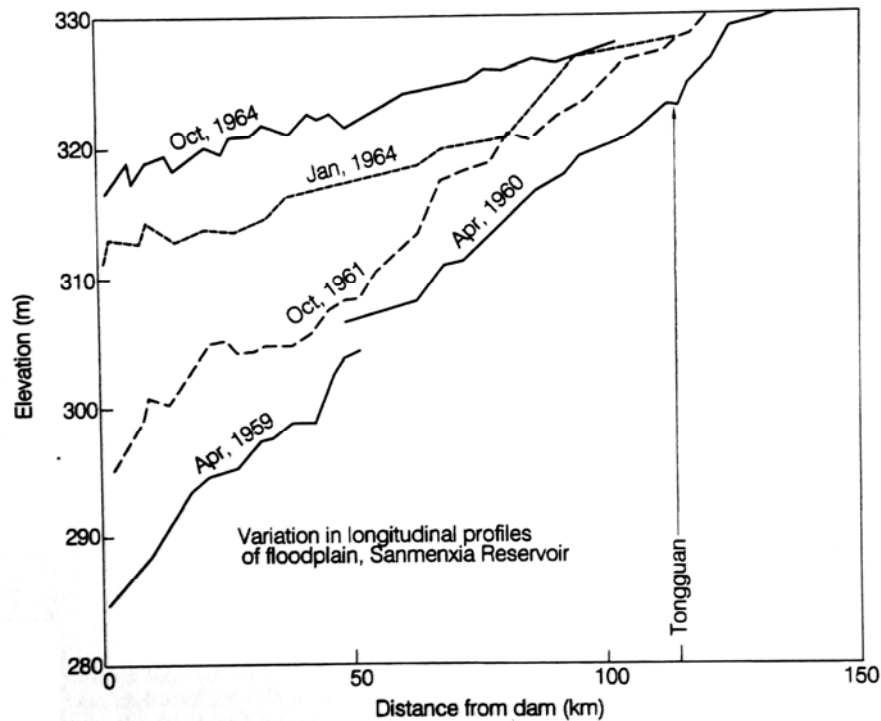


**FIGURE 24.7** Longitudinal floodplain profiles in Sanmenxia Reservoir (after Fan, 1985).

Sanmenxia was to provide low-level outlets large enough to discharge sediment-transporting floods through the dam with minimum backwater, only rarely inundating the floodplain with sediment-laden flood water. The profile in Fig. 24.8 shows that thalweg deposits attained depths exceeding 20 m near the dam between 1960 and 1964, but by 1973 the pre-impoundment thalweg profile had been reestablished as a result of reopening of low-level outlets and seasonal flushing. As the reservoir is operated today, impounding begins and the floodplain is inundated starting at the end of the flood season in October, when suspended-solids concentrations are lower and little sediment accumulates on the submerged floodplain. The historical effect of this operation on storage capacity was summarized in Fig. 24.2, which showed that storage capacity in the main channel area was increased by flushing at the same time that storage continued to decline in the floodplain area.

## 24.5 DELTA DEPOSITION AND EROSION

Siltation occurs in both longitudinal and transverse directions to form a reservoir delta or submerged floodplain at the upstream end of the backwater reach created by a dam. After closure in 1960, the delta started to form and advanced downstream toward the dam. Figure 24.9 illustrates the cross section changes at Range 35 in Sanmenxia Reservoir during the building of deltaic floodplain deposits. Range 35 is 90.2 km upstream of the dam, at a point where the river gorge widens from an upstream section only a few hundred meters in width.

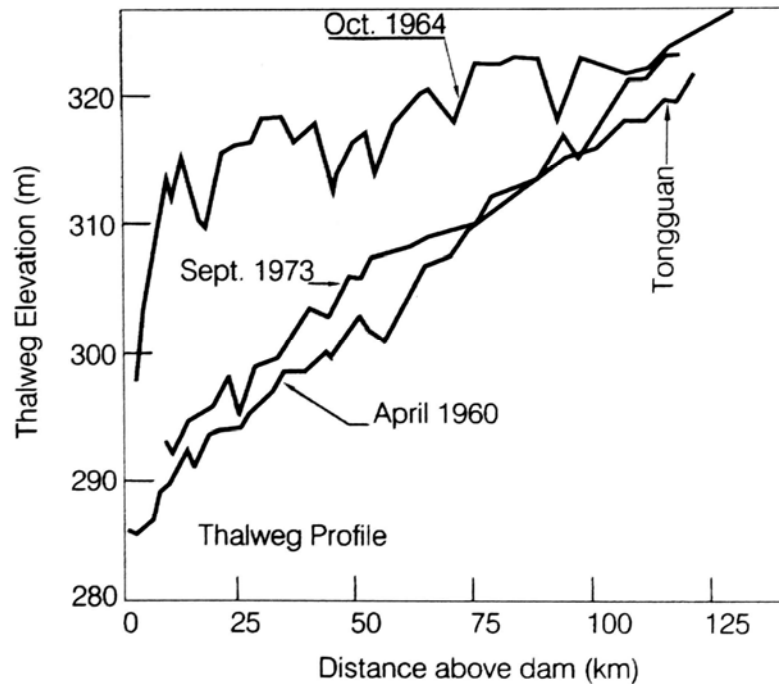


**FIGURE 24.8** Thalweg profiles in Sanmenxia Reservoir showing the rapid deposition of sediment along the entire length of the reservoir, particularly near the dam, and reestablishment of the pre-impoundment profile by flushing (after Fan, 1985).

From July 17 through August 8, 1961, the river discharged at a rate of 2200 to 4760 m<sup>3</sup>/s into range 35 which, at that time, was about 2 m deep and 1500 m wide. In response to both siltation and scour, by August 8 a submerged floodplain more than 1200 m wide had been created and a main channel had been scoured that was less than 300 m wide and over 4 m deep. The successive measurements at range 35 suggest that, in addition to moving longitudinally, sediment also moved laterally from the main channel and onto floodplain deposits. Cross-section measurements on August 5 show the formation of a natural levee, suggestive of the lateral movement of sediment from the main channel onto the floodplain. Isolines of sediment concentration (Fig. 24.10) exhibit a gradient that decreased laterally from the main channel onto the floodplain.

While the dam was still under construction in 1959 and the 12 diversion outlets at 280 m were being used to release floodwater, the backwater pool extended up to 40 km above the dam. During this period, the area between 30 and 40 km upstream of the dam was subject to alternating episodes of delta deposition followed by scour. High-water levels during the July-August flood season caused deposition to concentrate at the upstream end of the pool, but during the low-flow period both discharge and water level decreased and scoured the previously deposited material. Erosion occurred in most parts of the reservoir during low-flow periods, and the entrainment of sediment from the bed caused sediment concentration in the discharge to exceed inflow. Cross sections measured during the depositional and erosional phases are presented in Fig. 24.11. Unlike cross sections from reservoirs which are subjected exclusively to depositional processes and which consequently have a flat bottom, these cross sections exhibit the development of the main channel and floodplain configuration typical of cross

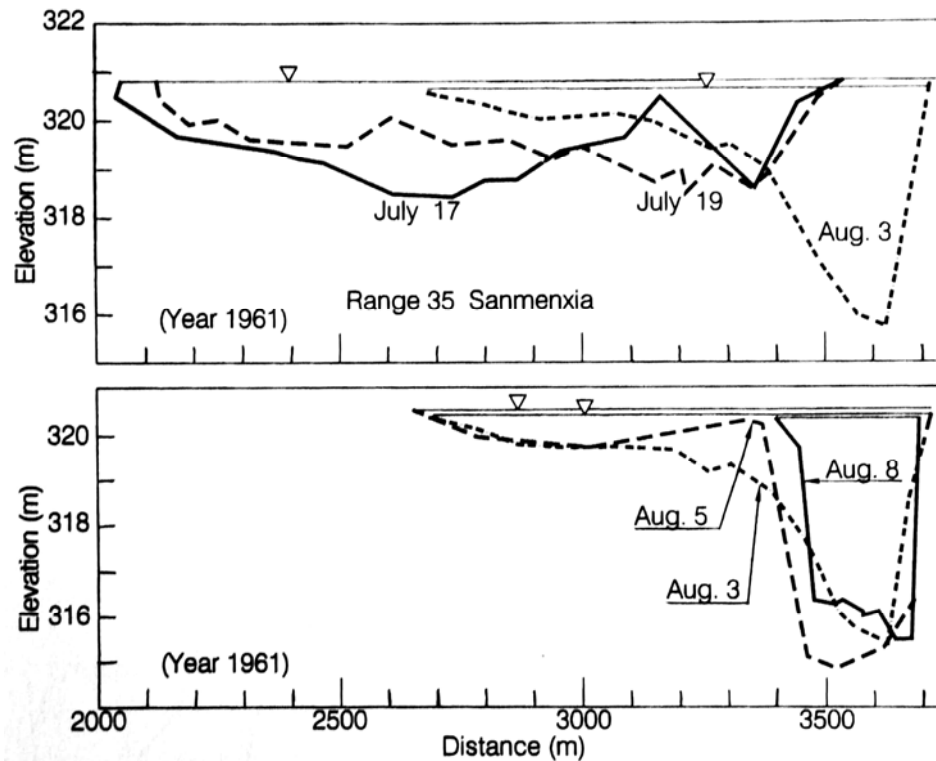


**FIGURE 24.9** Cross-section changes at range 35 in Sanmenxia Reservoir during building of deltaic floodplain deposits (*Fan and Morris, 1992a*).

sections affected by alternating periods of deposition and scour. This pattern was absent only in the narrower reaches where the scour channel extended across the full width of the reservoir.

## 24.6 TURBIDITY CURRENTS

Extensive measurements of flow patterns in turbidity currents at Sanmenxia documented the transition from nonstratified flow, propagation along the length of the reservoir, velocity and sediment concentration profiles at different stages and discharges, unsteady flow characteristics of turbidity currents, timewise variation in the location of the clear-muddy water interface, and the venting efficiency of turbidity current release through low-level outlets (Fan, 1985, 1986, 1991). Turbid density currents, including data from Sanmenxia reservoir, are discussed in Chap. 14.

Turbidity currents first occurred in the backwater reach prior to completion of the dam. The longitudinal profile of a turbidity current along a 65-km impounded reach, caused by the plunging of river inflow having a high suspended-sediment concentration, is summarized in Fig. 24.12. The figure shows the transition of inflow to stratified flow downstream of the plunge point, travel along the reservoir, and the creation of a muddy lake between Range 12 and the dam site. A different situation was observed on July 30, 1962, when the reservoir was at a low water level of 314 m, creating a 40-km impounded reach. In this case, the river inflow was not highly turbid, but reservoir drawdown caused the river to scour and entrain previously deposited sediment between Ranges 31 and 41, thereby creating high sediment concentrations and a turbid current that was vented through the dam. This

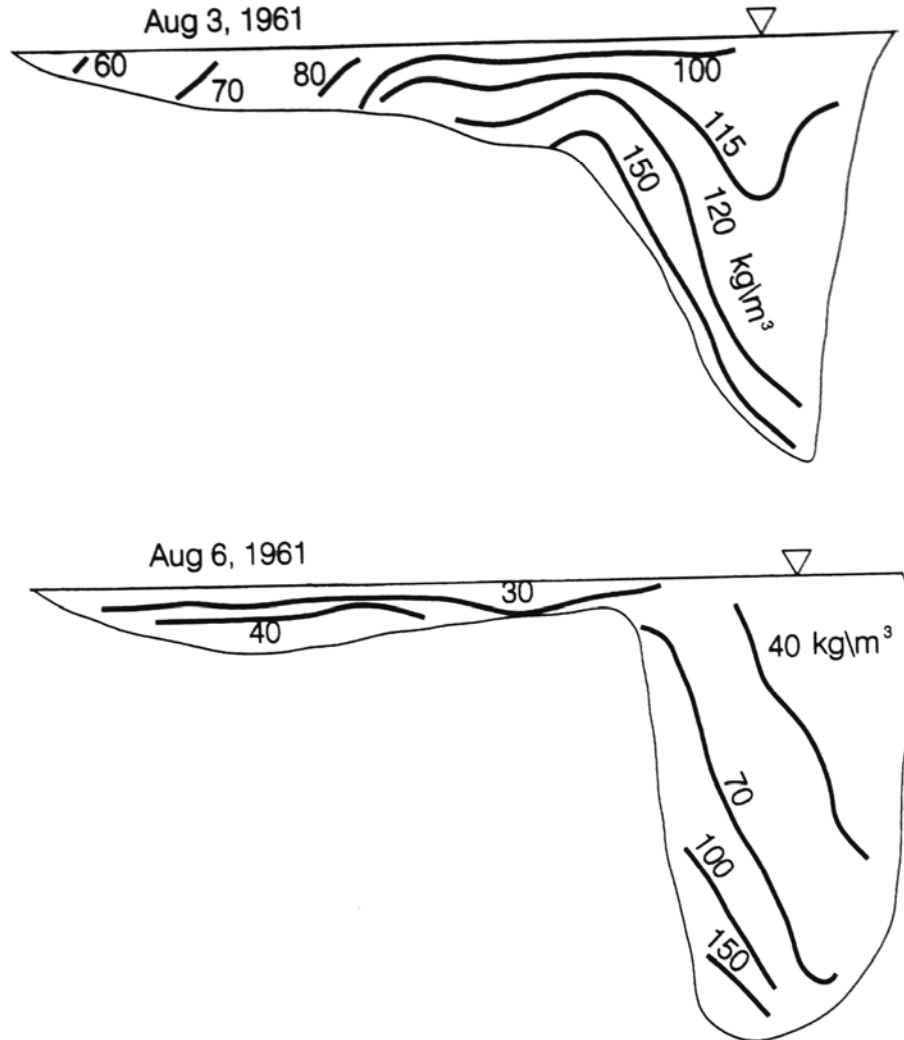


**FIGURE 24.10** Concentration isolines for suspended sediment showing a gradient that decreased laterally from the main channel to the floodplain (*Fan and Morris, 1992a*).

demonstrated that a turbidity current may be created by the entrainment of previously deposited sediment during reservoir drawdown, even when inflow conditions would not otherwise have produced flow stratification. Thus, during reservoir drawdown, turbidity currents may be created within the impounded reach, independent of the sediment load contributed by the river.

## 24.7 DEPOSITION ALONG WEI RIVER

Historical data from the Wei River indicate that the river channel along the lower reach had remained in a state of quasi-equilibrium for more than 2000 years before dam con-

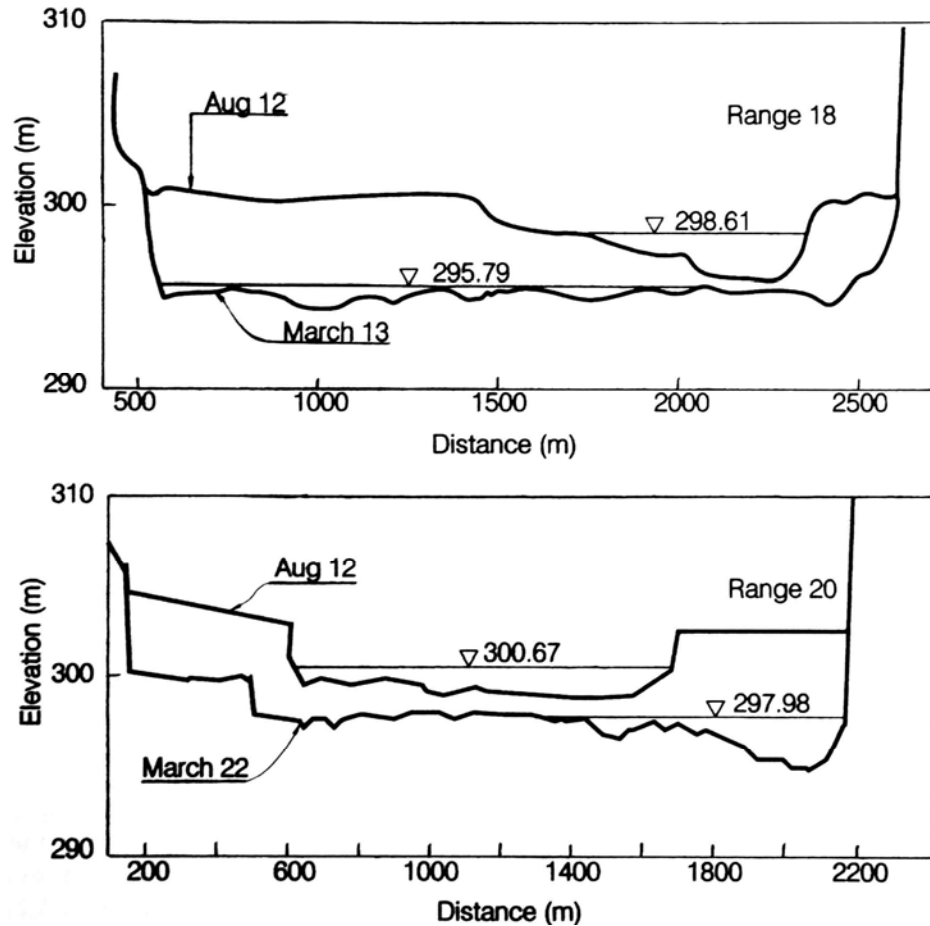
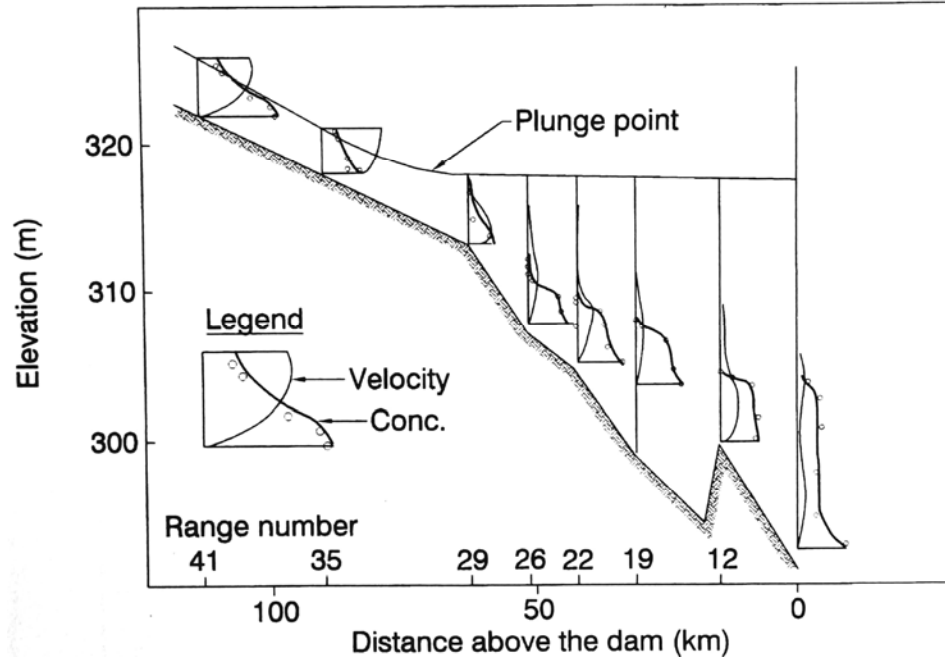


FIGURE 24.11 Development of channel and floodplain configuration in Sanmenxia Reservoir (Fan, 1985).

struction. Archaeologists discovered sediment deposits less than 1 m deep overlying wells built in the Qin Dynasty (221-206 B.C.) on the floodplain of the Lower Reach of the Wei River. Before dam construction the bed material in the Lower Reach of the Wei River consisted of sands, with fines being transported as wash load. Because the confluence of the Wei and Yellow Rivers is only a few kilometers upstream of Tongguan, sediment deposition and backwater at Tongguan affect the Wei River. The upstream limit of sediment deposition during floods historically shifted over a distance of tens of kilometers along both the Wei and Yellow Rivers in response to alternating deposition and scour events and the stage at Tongguan. Following dam construction, three conditions caused serious deposition upstream along the Wei River: (1) backwater from the dam, (2) upstream movement of turbid density currents from the Yellow River, and (3) deposition from a sediment-laden tributary, the Luo River, as located in Fig. 24.1.

#### 24.7.1 Backwater Deposition

Backwater from the dam caused sediments transported along the Wei River to settle as far as 250 km upstream of the dam during the initial impounding period, as illustrated



**FIGURE 24.12** Turbidity current along the 65-km impounded reach downstream of Range 29 during August 16-18, 1961 (Shaanxi Provincial Institute of Hydraulic Research and Qinghua University, 1978).

by comparing the June 1960 pre-impoundment profile along Wei River against the November 1961 profile (Figure 24.13a). The next measurement in October 1962 showed that, although the level near the mouth of the Wei River had lowered, deposition remained in the river channel as far as 250 km upstream.

### 24.7.2 Local Deposition from Luo River

Submerged deposits may be formed in two areas along the lower Wei River: upstream of the confluence with the Yellow River or at the tributary Luo River located 19 km upstream of the Yellow River confluence. Deposits created by the intrusion of sediment-laden water from the Yellow River upstream along the Wei River can be eroded quickly by subsequent discharge from the Wei River, but deposits farther upstream created by deposition from the Luo River require much longer to remove. Serious deposition from the Luo River occurred during August and September 1967, when high water levels (above 330 m) were maintained at Tongguan by five flood periods of 5000 m/s along the Yellow River. During this period, both the Wei and Luo Rivers had low discharges, but the Luo River discharge was hyperconcentrated, with a monthly mean concentration of  $538 \text{ kg/m}^3$ . The resulting sand bar in the Wei River channel is shown in Fig. 24.13b. The subsequent October 1968 measurement along the Wei River showed that the Luo River bar had been mostly washed out of the lower river reach, but upstream of about km 190, the bed levels in 1968 were even higher than they had been in 1967 when the mouth bar was formed. This illustrates the lag times involved in sediment profile adjustments, which may result in the continuing accumulation of sediment in an upstream reach at the same time the downstream reach is eroding. In 1961-1962 and again in 1968-1969, the zone of channel deposition moved upstream along

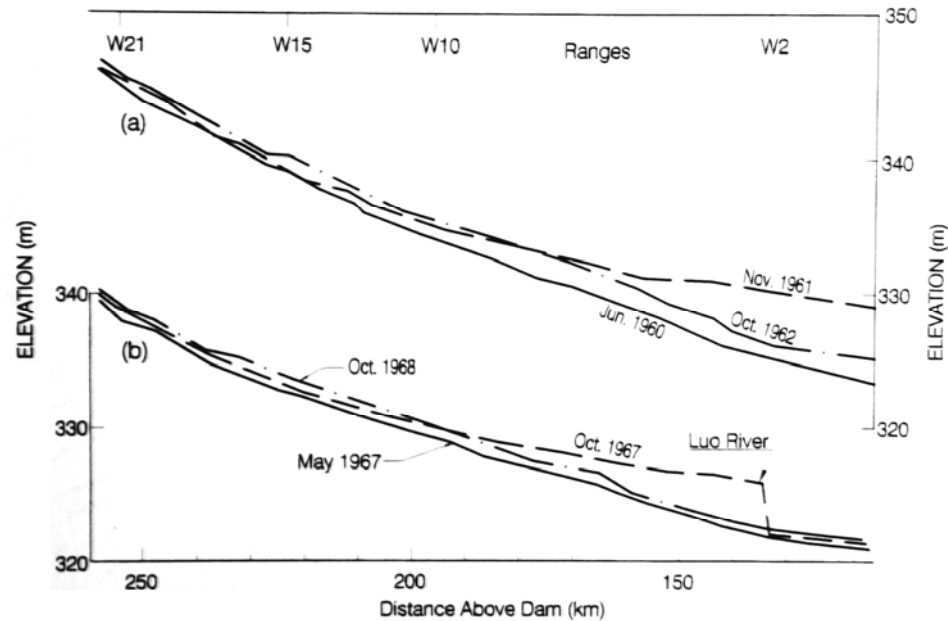


**FIGURE 24.13** Longitudinal deposition in river channel with retrogressive deposition in the Lower Reach of Wei River, (a) 1960-1962 and (b) 1967-1969, in terms of water level at  $Q = 200 \text{ m}^3/\text{s}$  (Zhang and Long, 1980).

the Wei River (retrogressive deposition). The upstream movement of the deposit limit, and the downward erosion through previous deposits, were at different times observed to occur simultaneously or alternately.

### 24.7.3 Turbidity Current from Yellow River

High flows in the Yellow River that create backwater conditions upstream of Tongguan can cause turbid water in the Yellow River to plunge and flow upstream along the Wei River. Some of the velocity profiles measured during these events showed surface water from the Wei River flowing downstream while silt-laden bottom water from the Yellow River traveled upstream. Deposition from the turbidity current moving upstream along the Wei River causes bottom sediment to be sorted from coarse to fine proceeding upstream, opposite to the sorting direction imposed by normal flow. More complex deposition patterns occur when hyperconcentrated flow from the Luo River also plunges beneath the Wei River. Prior to dam construction, the Yellow River flowed upstream into the Wei River and formed a river-mouth bar at intervals of about 10 years: in 1932, 1942, 1954, and 1959. The greater the flood of the Yellow River relative to the discharge of the Wei River, the more serious the deposition. Backwater effects from dam construction caused flow reversal to occur more frequently.

## 24.8 RETROGRESSIVE EROSION

When bottom outlets are opened and a reservoir is emptied for flushing, the area in front of the bottom outlets will typically be scoured first. This creates steep-gradient,

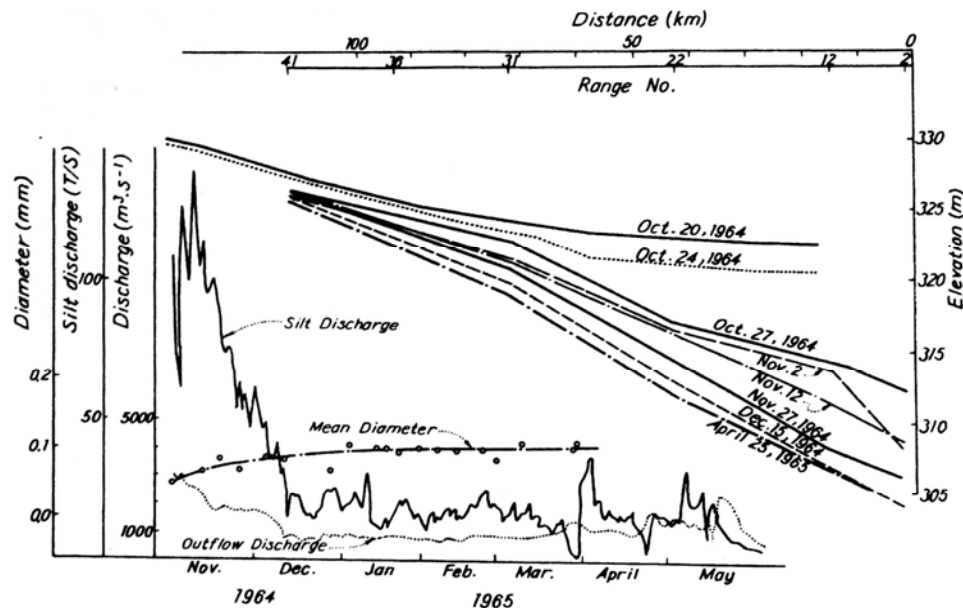


**FIGURE 24.14** Development of retrogressive erosion by flushing in Sanmenxia Reservoir as indicated by the sequence of reservoir water-level profiles (Fan, 1985).

super-critical flow, and a zone of extremely active erosion which moves upstream as the eroded material is carried away. During the 1964 flushing event, retrogressive erosion was observed to begin near Sanmenxia Dam and eventually extended more than 100 km upstream, the greatest length of retrogressive erosion documented in a reservoir. Development of the longitudinal erosion pattern is indicated by the sequence of reservoir water level profiles given in Fig. 24.14. The time-wise variation in water level and sediment concentration at various points during retrogressive erosion are illustrated in Fig. 24.15. Outflow sediment concentration increased rapidly as soon as drawdown was initiated and declined gradually thereafter. Most of the net increase in sediment concentration occurred between km 42.3 and the dam.

## 24.9 SEDIMENT DISCHARGE DOWNSTREAM

Below Sanmenxia Dam, the Yellow River emerges from the 130-km-long gorge reach at Mengin and flows 858 km across an alluvial plain to the sea. These alluvial plains, the traditional heartland of the Chinese civilization, have been the site of catastrophic floods for millennia, and records of major flood control efforts date back over 2000 years. Effective flood control measures in the form of an immense system of dikes have been constructed only since the 1950s. Because of the continuous accumulation of sediment along the alluvial riverbed contained within flood-control levees, the base elevation of the river has gradually risen and now stands above the adjacent floodplains.

Figure 24.16 illustrates the timewise pattern of sediment accumulation in the Yellow River downstream of Sanmenxia dam, showing the gradual accumulation of sediment in the downstream reach prior to dam closure in 1960. During 1960-1964 the reservoir operated at a high trap efficiency and released clear water, causing a net erosion of sediments from the Lower Yellow River. This erosion posed danger to the earthen dikes because more constant, clear water discharges produced

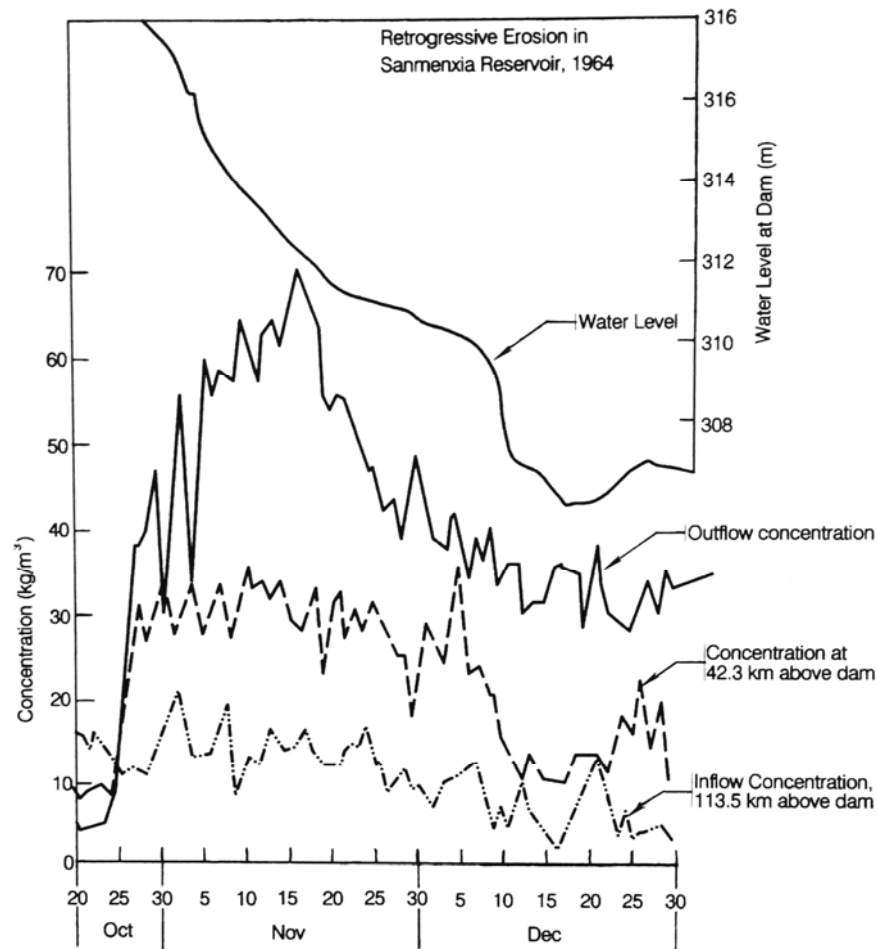


**FIGURE 24.15** Timewise variation in water level and sediment concentration at various points during retrogressive erosion (*Shaanxi Provincial Institute of Hydraulic Research and Qinghua University, 1978*).

prolonged and concentrated scour in some areas, creating danger of bank collapse. In contrast, the irregular sediment-laden flows prior to dam closure caused areas of maximum scour to shift and be dissipated over longer sections of dike. Scour depth decreased moving downstream along the Yellow River as the entrainment of sediment from the river bed and banks gradually brought transport capacity into balance with the available supply. This adjustment is evident from the longitudinal variation in sediment concentration for different dates, shown in Fig. 24.17.

During the period of dam reconstruction, from 1964 through 1973, the reservoir was operated for flood detention and sediment flushing with outlets open all year. However, the limited flood discharge capacity of the outlets also limited sediment transport capacity. During this period, high-concentration, low-discharge releases from the dam exceeded the transport capacity in the downstream channel, and the years 1965 through 1973 were characterized by serious sediment deposition along the reach 300 to 400 km downstream of the dam. During this period 67 percent of the

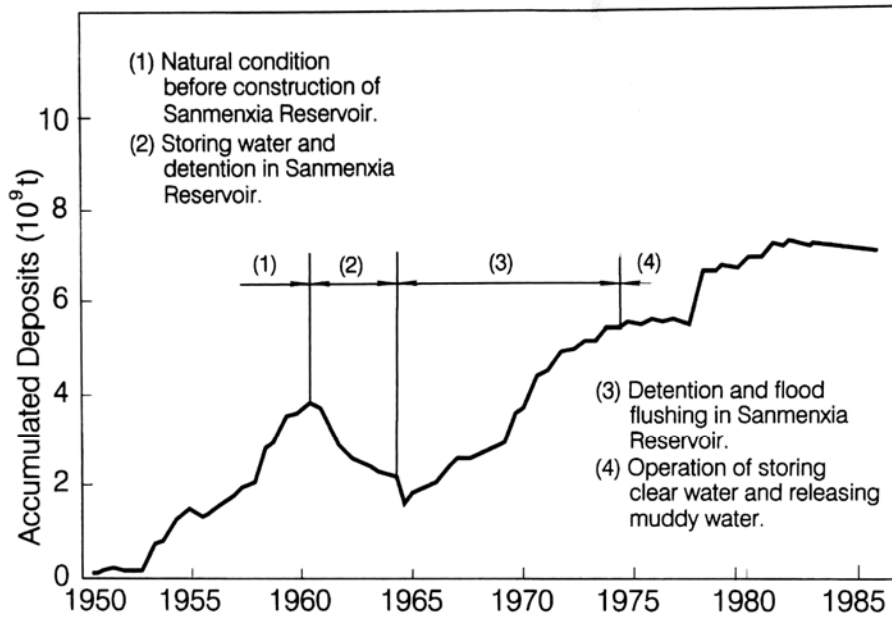


**FIGURE 24.16** Timewise pattern of sediment accumulation in the Yellow River downstream of Sanmenxia Dam, showing the gradual accumulation of sediment in the downstream reach prior to dam closure in 1960 and the dramatic reversal of this trend after closure of the dam (after Pan, 1990).

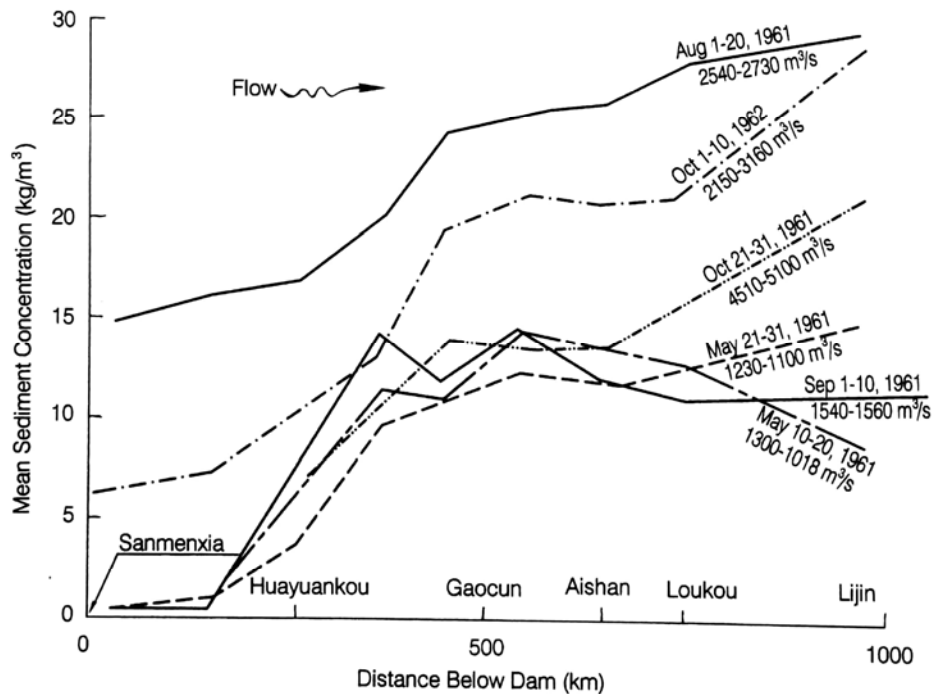


**FIGURE 24.17** Increase in suspended solids concentration downstream of Sanmenxia dam during the initial impounding period, caused by scour of material from the bed of the Yellow River by the clear water released from the dam (after Pan, 1990).

deposition occurred in the channel of the Yellow River and only 33 percent on the floodplain. Siltation in the main channel of the Lower Yellow River has serious flood control consequences, and prevention of deposition in the main channel is the key problem of river regulation and flood protection along the lower reach. Only after reopening of the eight bottom outlets at 280 m, opening of two tunnels at 290 m, and reconstruction of four penstocks could both sediment and water be discharged at the rates required to better stabilize conditions downstream of the dam, as occurred after 1973. Between March 1973 and October 1985, more than 90 percent of the sediment deposition downstream of the dam occurred on the floodplain, and erosion occurred in the channel, which is generally beneficial from the standpoint of flood protection along the Lower Yellow River. However, channel deposition continues to occur at low river discharge, and sediment regulation in the Lower Yellow River is still a problem that is not fully solved.

### **24.10 CLOSURE**

---

The Sanmenxia case study illustrates the potential complexity of sediment management issues both upstream and downstream of a dam, and the use of an incremental approach to solve difficult problems. The sediment problem was not sufficiently understood to enable effective management until after years of intensive research and practical experience had been gained. The knowledge gained at Sanmenxia formed the basis for the design and management of subsequent reservoirs where sedimentation has been considered from the early design stage, including the Shialongdi and Three Gorges Projects in China.

It is also important to note that at Sanmenxia sediment management was not merely an issue of achieving a sediment balance across the storage reach to preserve reservoir capacity. It also required achievement of a sediment balance in the upper backwater reach above Tongguan, and along the downstream reach extending to the ocean, to prevent flooding due to sediment deposition. In all, Sanmenxia Dam seriously affected the sediment balance and flooding problems along some 1300 km of the Yellow River and its tributary, the Wei River, from the ocean upstream to the vicinity of Xian.

---

## CHAPTER 25

---

# CASE STUDY: HEISONGLIN RESERVOIR, CHINA

---

### 25.1 OVERVIEW

---

Prior to the revolution in 1949 there were very few reservoirs in China. With chronic food shortages, high population, and limited arable land, one of the first tasks of the new government was to undertake widespread water resource development, giving heavy emphasis to the construction of reservoirs for irrigation and flood control. The middle and late 1950s saw the construction of numerous reservoirs, but in the highly erodible loess region of northern China, the area drained by the Yellow River, these reservoirs rapidly began filling with sediment. In some cases the rate of siltation was astounding. The Xinghe Reservoir in Shaanxi Province required 2 years to construct but only one year to fill with sediment, and the 21.8-Mm<sup>3</sup> Laoying Reservoir in Shaanxi Province silted up before the irrigation canal was completed. It was quickly evident that water could not be managed without simultaneously managing sediment (Xia, 1984). As a result of the severe reservoir sedimentation problems, during 1960-1961 engineers and officials in Shaanxi Province evaluated the situation at all reservoirs in the province. It was decided to utilize Heisonglin Reservoir as an experimental site to intensely study the sedimentation phenomena and develop sediment management techniques which could then be applied to other reservoirs within the region.

Results at Heisonglin have been impressive: the reservoir capacity is stabilized with a capacity:inflow ratio of approximately 0.20, and 100 percent of the inflow can be diverted to irrigation use. At Heisonglin Reservoir, a combination of seasonal drawdown, flushing, and turbidity current venting is used, and it was at this site that the lateral erosion technique was first developed. The primary operational focus is on sediment routing, but because of limited discharge capacity, flood retention periods up to several days' duration, and heavy inflowing sediment loads, a significant part of the inflowing sediment is temporarily deposited within the main channel and the hydrographs are typical of flushing operations. The Chinese have classified Heisonglin as a flushing operation. This case study is based on a site visit and discussions with Xia Mai-ding and operational personnel at the reservoir in 1987 and subsequent written communication, in addition to the cited literature.

### 25.2 SITE DESCRIPTION

---

Heisonglin Reservoir occupies a valley with a slope of about 1 percent, located in a hilly region on the upstream reach of the Yeyu River, a tributary of the Wei River. The earth dam, completed in May 1959, impounds water for irrigation and flood protection. Water

deliveries are made to the river below the dam through a single 2 x 1.5 m low-level outlet installed on the right side of the dam with a discharge capacity of 10 m<sup>3</sup>/s. The outlet is controlled by two vertical sluices arranged in series in an intake tower. Irrigators withdraw water from the river downstream of the dam using high-capacity river diversions which were in use long before dam construction, and were thus sized to divert high discharges of sediment-laden water produced by the intermittent summer storms characteristic of the region.

A hydrologic station 7.5 km upstream of the dam was established in 1961; it gages 286 km<sup>2</sup> (77 percent) of the 370 km<sup>2</sup> watershed tributary to the reservoir. The inflowing sediment load consists mostly of noncohesive silts with a  $d_{50}$  of 0.025 mm. General characteristics of the reservoir are presented in Table 25.1 and the general layout is given in Fig. 25.1.

**TABLE 25.1** Summary Characteristics of Heisonglin Reservoir

Parameter	Value
Total reservoir volume at 764.5 m spillway crest	$8.6 \times 10^6 \text{ m}^3$
Dead pool	$0.7 \times 10^6 \text{ m}^3$
Mean annual inflow (1961-1972)	$14.2 \times 10^6 \text{ m}^3$
Mean annual sediment inflow (1961-1972)	$0.71 \times 10^6 \text{ tons}$
Mean annual sediment yield (1961-1972)	$2475 \text{ ton/km}^2$
Sediment size ( $d_{50}$ )	0.025 mm
Watershed area	$370 \text{ km}^2$

*Source:* Ren (1986); Xia and Ren (1980).

The mean sediment concentration at the inflow gage station is 50 g/L and peak inflowing sediment concentrations exceed 800 g/L (Zhang et al., 1976). Sediment discharge is both irregular and highly concentrated in time: 87 percent of the annual sediment load enters the reservoir during July and August, yet these same 2 months contribute only 25 percent of average annual runoff (Fig. 25.2). Summer flood events at Heisonglin are caused by short intense summer rainstorms having steep rising and falling hydrographs and durations on the order of several hours. These events produce extremely high rates of gully erosion in the hilly loessal soils. The relationship between peak flood discharge and the average suspended-sediment concentration at the inflow gage station during flood events is shown in Fig. 25.3.

Between May 1959 and June 1962, the first 3 years following construction when the reservoir was operated in continuous impounding mode, 1.62 Mm<sup>3</sup> of sediment accumulated in the reservoir, representing a storage loss of 6 percent per year and a trap efficiency estimated at 76 percent on the basis of long-term sediment inflow of 0.71 Mt/yr. At this rate the reservoir would become completely silted up after 16 years of operation. Starting in 1962, reservoir operation was changed to incorporate seasonal emptying during the flood season while continuing to impound water during nonflood season when sediment loads were smaller by employing the strategy, "Store the clear water and discharge the muddy water." Turbid density currents were also released. These measures reduced trap efficiency to about 15 percent but the reservoir continued to lose capacity. As a result of additional work, the lateral erosion technique was developed and first implemented at this site in 1980 by Xia Mai-Ding and coworkers (Xia, 1986). This technique was found to be capable of arresting sediment accumulation and recovering a

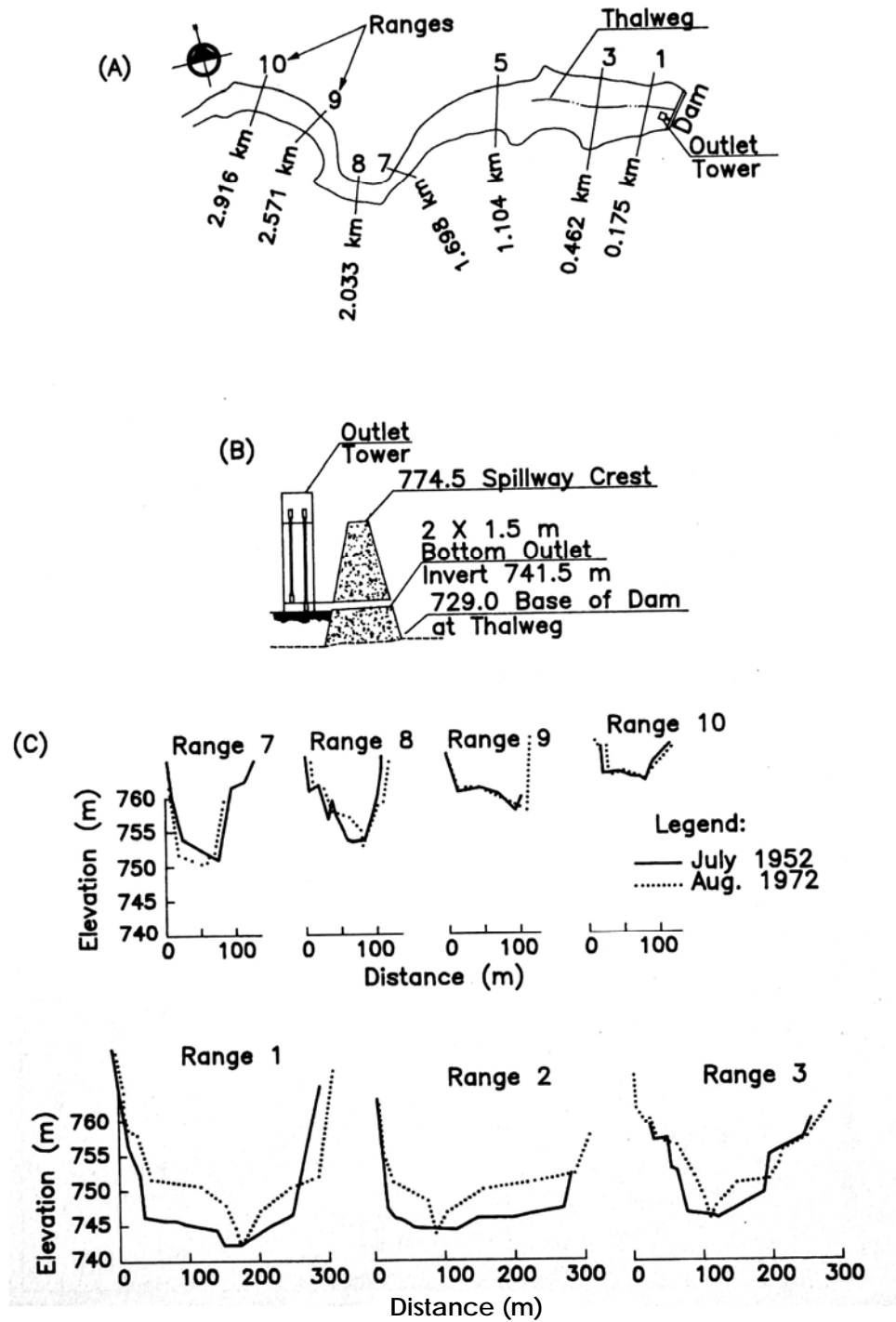


FIGURE 25.1 Geometry of Heisonglin Dam and Reservoir, Shaanxi Province, China. (a) Plan view showing range locations; (b) sketch of dam cross section; (c) selected ranges (after Ren, 1986).

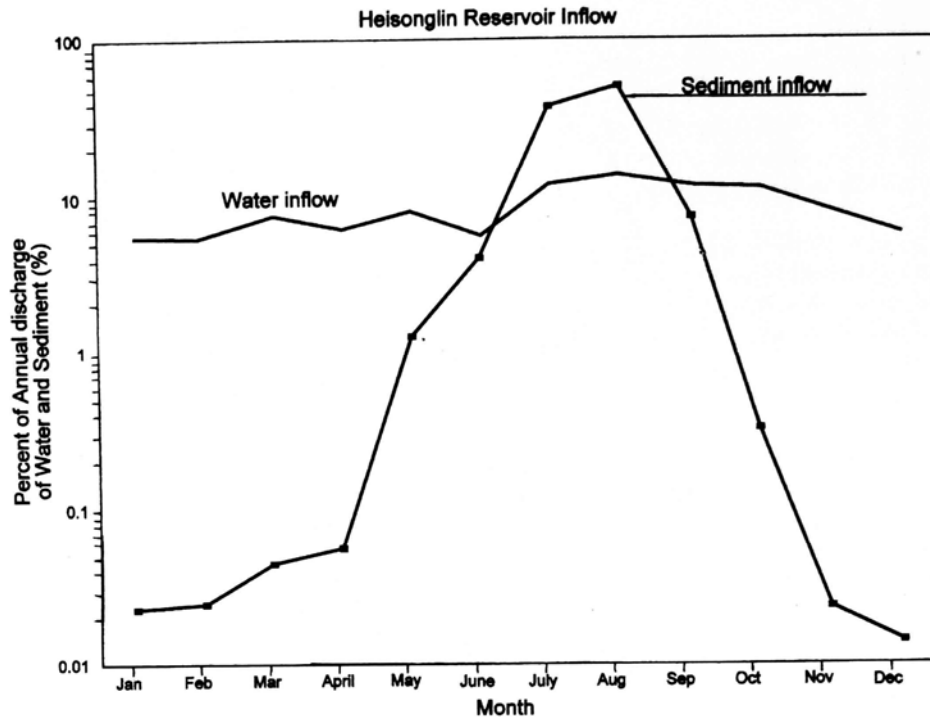


FIGURE 25.2 Annual variation in water and sediment inflow, Heisonglin Reservoir, 1961–1978. Notice that the y axis uses a log scale (after Xia and Ren, 1980).

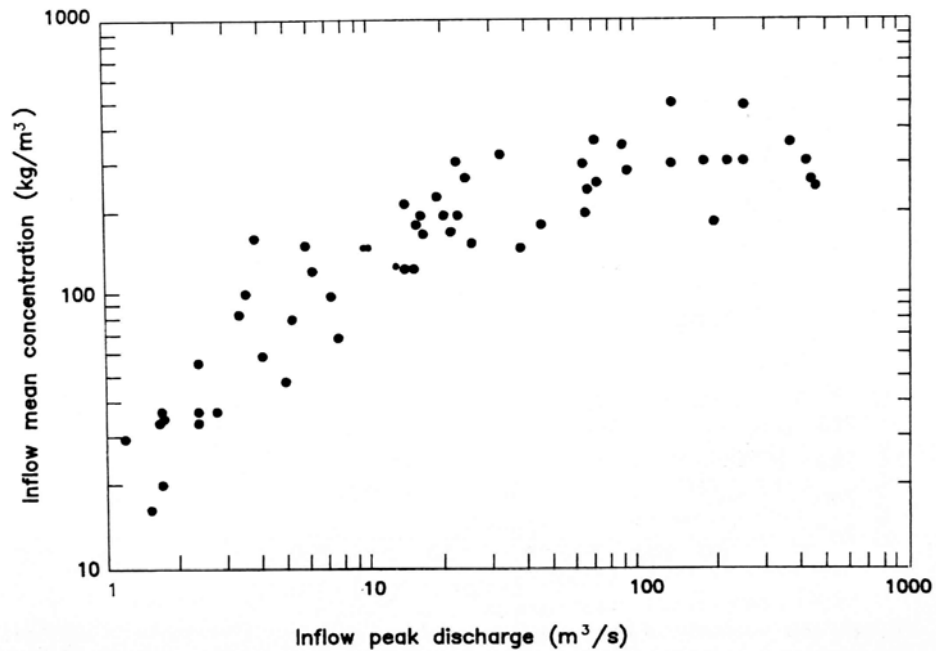
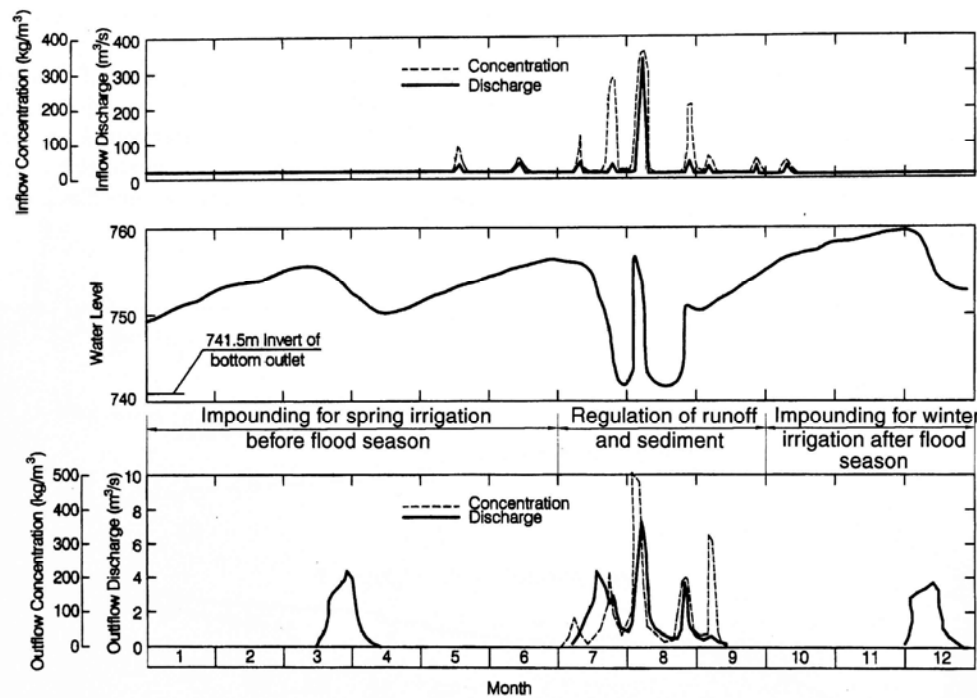


FIGURE 25.3 Mean suspended-sediment concentration in inflowing floods versus peak discharge, Heisonglin Reservoir (after Northwest Institute of Hydraulic Research et al., 1983).

Portion of lost storage capacity. The stable long-term capacity that can be maintained at Heisonglin by all sediment management techniques is about 2.5 to 3.0 Mm<sup>3</sup>, or 20 percent of mean annual inflow.

### 25.3 SEDIMENT MANAGEMENT STRATEGIES

The original operating mode of Heisonglin Reservoir was for continuous impounding. Sediment management was initiated by modifying this operating mode to incorporate seasonal emptying during July and August when most sediment enters the impoundment. Turbid density currents were also vented whenever possible. Reservoir operations during an annual cycle incorporating seasonal drawdown are summarized in Fig. 25.4.



**FIGURE 25.4** Annual operational cycle for Heisonglin Reservoir incorporating seasonal emptying (after Northwest Institute of Hydraulic Research, 1983).

During the early part of the summer flood season when both flow and suspended solids concentration are low, the reservoir impounds water but turbidity currents are released downstream for irrigation. The middle flood season, July and August, is characterized by intense rainstorms, and both flows and suspended-sediment concentrations are high. During this period the reservoir is emptied and operated to release floods at the maximum capacity of downstream irrigation diversions. Because the silts settle slowly in the high-concentration fluid, if the flood can be discharged within 2 days, about 70 percent of the sediment can normally be released (Xia, 1987). In addition, as the reservoir is emptied at the end of each flood and riverine flow is again established, deposited silt is scoured out by flushing action. At the end of the flood season, the base flow is high and suspended-sediment concentration is low, and during this period the reservoir impounds water for winter irrigation deliveries in December. The reservoir

impounds water and is again emptied for spring irrigation deliveries in late March. Impounding then continues again until summer irrigation deliveries in July, after which the reservoir remains empty for flood season sediment release.

Although the reservoir remains empty during the July and August flood season, it still captures floodwater and diverts all inflow to irrigation. Between floods, the river flows freely through the reservoir, exits the open bottom outlet, and is diverted into irrigation intakes farther downstream along the river. Seasonal floods that exceed the capacity of the irrigation intakes are temporarily impounded and released to irrigators at the maximum capacity of the downstream irrigation diversions, thereby minimizing the period of floodwater detention and sediment deposition in the reservoir. Lateral erosion is also performed during this drawdown period. The exception to this procedure occurs during dry years, when the reservoir continuously impounds and sediment-laden inflows are released as density currents. Between 1962 and 1978, a total of 61 Mm<sup>3</sup> of water containing 13 Mt of sediment was released to irrigators during the seasonal drawdown period. The average suspended solids in the released water was about 210 g/L.

Procedures for lateral erosion were developed which allowed part of the lost flood-plain storage to be recovered, and, when used in conjunction with other methods, allows a sustainable sediment balance to be achieved (Fig. 25.5). Lateral erosion by a discharge of 0.2 m<sup>3</sup>/s carried away 4000 m<sup>3</sup>/day of sediment deposits from the reservoir. By using this flow rate for approximately 40 days per year, in combination with seasonal emptying, it was possible to develop an equilibrium between sediment inflow and discharge (Xia, 1993).

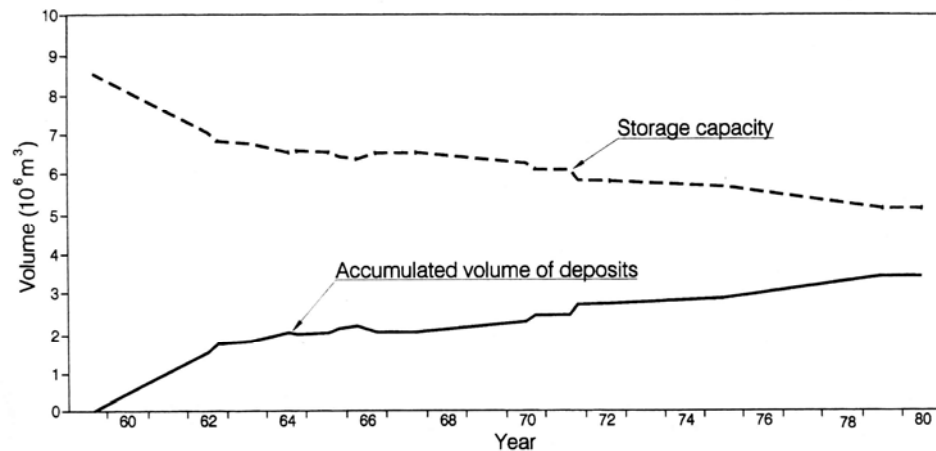


**FIGURE 25.5** Variation in storage capacity, Heisonglin Reservoir (after Northwest Institute of Hydraulic Research, 1972b).

## 25.4 WARPING

A unique feature of Heisonglin is that, not only is a sediment balance achieved in the reservoir, but both water and sediment are diverted to beneficial use. Operation of the dam is guided by the slogan, "Release not a drop of water nor a particle of sediment to Wei River." The ability to irrigate during the summer flood season with water having sediment concentrations of hundreds of grams per liter is an essential aspect of sediment management at Heisonglin and other reservoirs in the loess region of China. Irrigation with high or hyperconcentrated (typically over 200 g/L) flows of muddy water, a practice termed *warping*, has been used for at least 2000 years in China; the use of muddy flows containing several parts of silt per 10 parts of volume is described in the Han Dynasty

(206 B.C. - 25 A.D.) "Record of Ditches" archives. The silt-laden water enhances soil fertility by providing nutrients, increasing organic matter content, and improving moisture retention in coarse soils. Crop yields per hectare in the Heisonglin area almost doubled between 1958, when dam construction started, and 1974, with most of the yield increase occurring after warping was initiated (Zhang et al., 1976). Maximum application depth of muddy water depends on the crop, ranging from 5 to 7 cm for corn and Chinese sorghum, and from 3 to 6 cm for cotton (Cheng and He, 1989). Warping also offers the benefit of diverting to the land sediment that would otherwise flow into downstream reservoirs. Warping is facilitated at Heisonglin and other sites in the Yellow River basin where traditional river diversions for irrigation were already adapted to using the high-concentration flows that naturally occurred in the region, and peasants applied muddy water to their fields prior to dam construction.

## 25.5 DEPOSITION PATTERNS

Because of the short length of the reservoir, steep gradient, and high inflowing sediment concentration, during impounding periods turbidity currents travel to the dam and create a submerged muddy lake. Sediments depositing from the muddy lake created longitudinal floodplain deposits that were nearly horizontal in the reach near the dam. After seasonal emptying was initiated, sediment continued to deposit in the same longitudinal pattern, but with two important differences: the rate of the accumulation was lower, and a main flushing channel was scoured through the deposits. During impounding and flood detention periods, sediments were deposited on the floodplain and within the channel. Drawdown and emptying eroded and flushed sediments out of the main channel, but the floodplain deposits on either side of the channel remained and the surface of the floodplains rose continuously. The resulting pattern of sediment accumulation is illustrated in Fig. 25.6, and the change in one channel cross section during an annual cycle is illustrated in Fig. 25.7, which shows

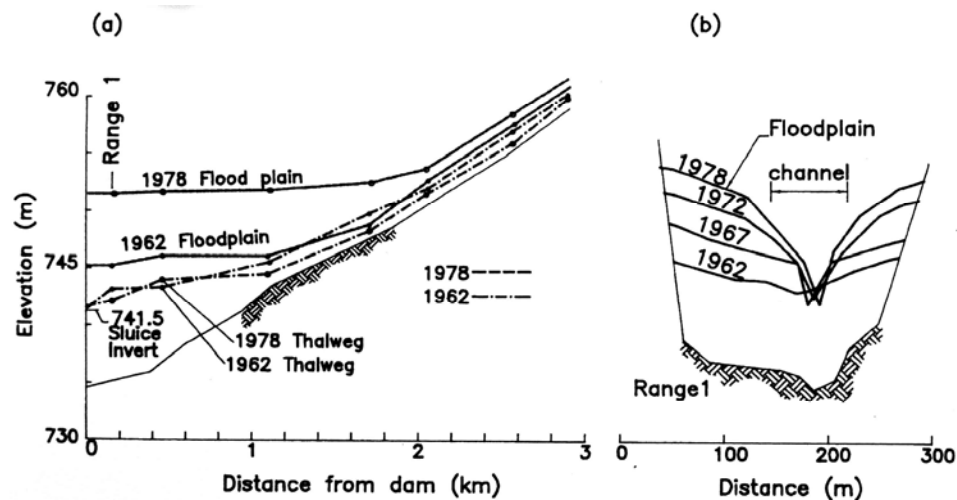


**FIGURE 25.6** Timewise pattern of sediment accumulation in Heisonglin Reservoir illustrated using (a) longitudinal profiles along the flushing channel thalweg and the floodplain and (b) successive cross sections at range 1. There is continual accumulation of sediments on the floodplains, but the main channel is maintained by flushing (after Xia and Ren, 1980).

the alternating periods of deposition and scour within the channel. In the narrow upstream portion of the reservoir, the main channel occupies the entire reservoir width, preventing flood-plain formation in this zone (see ranges 7 to 10 in Fig. 25.1).

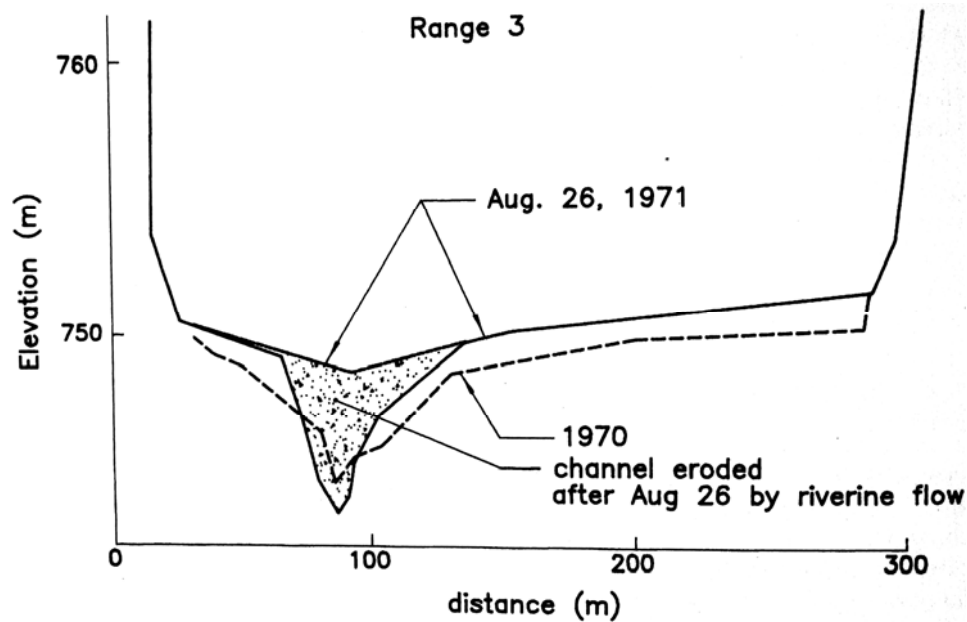


**FIGURE 25.7** Sequence of sediment deposition and scour at range 3, Heisonglin Reservoir. The sediments deposited in the main channel during the detention phase of the large August 20, 1971, flood (shown in Fig. 25.8) were subsequently scoured out by river base flow. However, the floodplain level rises continuously (after Northwest Institute of Hydraulic Research, 1972a).

## 25.6 SEDIMENT FLUSHING AND ROUTING

### 25.6.1 Drawdown Flushing

When the reservoir is emptied in July, the declining water levels initiate the erosional processes associated with flushing, including bank sloughing, progressive erosion of deposits along the main channel, and the progressive transport of sediments toward the bottom outlet. A large and highly concentrated discharge of sediment occurs at the transition from drawdown to flushing. Thereafter, smaller amounts of sediment are removed by base flow and the small inflow events that can be released through the bottom outlet with little backwater behind the dam, since flow runs along the already-eroded main channel. At Heisonglin, the events with low peak discharges contribute relatively little sediment. Flushing with large flood flows to widen the main channel cannot be performed at Heisonglin because it is not compatible with the operational objective at this site, which is to detain inflow and then release it at a low discharge rate, allowing the diversion of all water for irrigation.

### 25.6.2 Detention Flushing

When floods entering the reservoir storage pool during the drawdown period exceed the release rate to irrigators, the pool becomes partially filled with silt-laden water for periods

of hours or days. Some of the main characteristics of temporary flood detention at Heisonglin are shown in Fig. 25.8, which illustrates hydrograph behavior and reflects the depositional and erosional processes during detention flushing of the large flood on August 20-21, 1971. The flood contained  $5.92 \text{ Mm}^3$  of water and  $1.48 \text{ Mt}$  of sediment, for an average concentration of  $250 \text{ g/L}$ , and the reservoir was empty before the flood. Because of the large flood volume and limited discharge rate, 6 days were required to release the floodwaters.

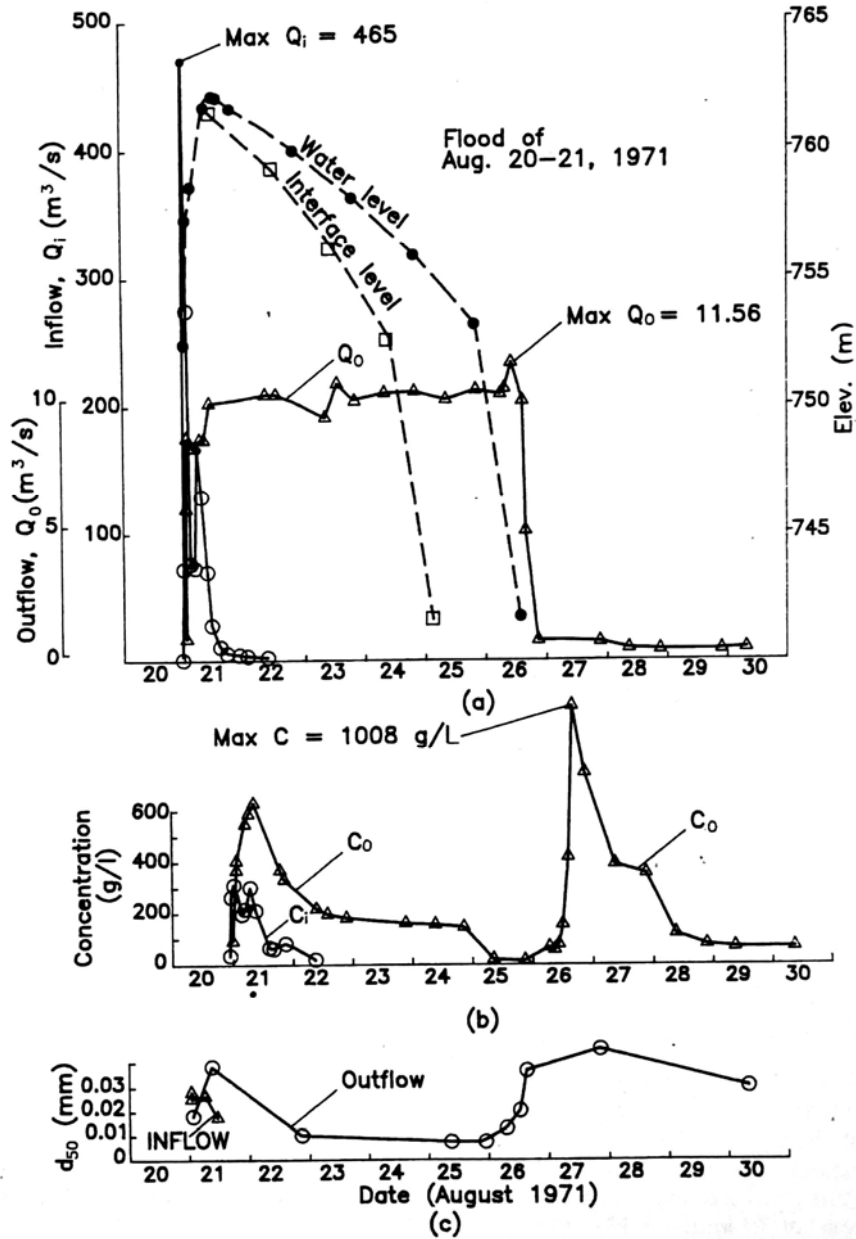


**FIGURE 25.8** Characteristics of inflow and discharge at Heisonglin Reservoir during a large detention flushing event. The volume of this flood equaled 42 percent of the mean annual discharge (after Xia and Ren, 1980).

Sediment continuously accumulated in the reservoir during the detention period, and both sediment concentration and grain size in the discharge declined until the reservoir was emptied on August 26, at which time both concentration and grain size values suddenly peaked. In parts *b* and *c* of Fig. 25.8 it is seen that suspended solids concentration and  $d_m$  were larger in the discharge from the dam than at the inflow station, at both the beginning and the end of the event. Four factors may have contributed to this phenomenon:

- The rapid settling of coarser grains can create a hyperconcentrated bottom layer within the muddy lake. Because the outlet is at the lowest elevation in the reservoir, and as long as discharge is not so great that overlying clear water will be aspirated, the discharge concentration will reflect conditions in this concentrated bottom layer.
- Higher sediment discharge values at the beginning of the event may reflect the scouring of channel deposits along the reach between the inflow hydrologic station and the reservoir as the flood discharge increased, which would cause the inflowing sediment concentration measured at the hydrologic station to be smaller than the concentration actually entering the reservoir.

A vertical concentration profile was measured through the portion of the floodwaters overlying the left floodplain at range 1 on August 23 (Table 25.2). Although the mean concentration of  $110 \text{ kg/m}^3$  measured within the muddy lake at range 1 is less than the outflow concentration of approximately  $180 \text{ kg/m}^3$  that same day (Fig. 25.8), the liquid mud at 9.22 m depth was highly concentrated and contained larger grains because of the accelerated settling of layer particles. Settling is retarded in this hyperconcentrated bottom layer of liquid mud, and the drainage of this concentrated liquid mud from the submerged floodplain into the main channel may have contributed additional sediment to the channel.

**TABLE 25.2** Vertical Profile during Detention Flushing, Aug. 23, 1971, Range 1, Heisonglin Reservoir

Water depth, m	Concentration, g/L	$d$ , mm	Notes
2.56	177	0.0070	Turbidity interface
3.81	112	0.0082	
4.81	120	0.0082	
5.82	98	0.0094	
6.82	112	0.0076	
9.22	894	0.0160	Mud bottom

*Source:* Ren (1986).

- When the reservoir was emptied on August 26, the outflow suspended-solids concentration and grain size both increased because of the scouring of sediments from the channel. On August 27 a base flow of about  $1 \text{ m}^3/\text{s}$  flowed along the flushing channel, continuing to scour sediments and discharge a hyperconcentrated flow of relatively coarse material for another day. This riverine flow was responsible for the scouring illustrated in Fig. 25.7.

As the flood entered the empty reservoir, a nonsubmerged muddy lake was formed initially, which was transformed into a submerged muddy lake as a result of settling. The falling interface between the muddy water and overlying clear water shown in Fig. 25.8a resulted from hindered settling and the separation of clear water from the muddy lake. During the

flood,  $1.4 \text{ Mm}^3$ , or 23 percent of the inflow flood volume, seeped from the muddy lake and into the overlying clear water, as computed from the rate of lowering of the water level, the turbidity interface, and the outflow discharge. The muddy water interface fell by 0.03 to 0.05 m/h, which was faster than the water level (Table 25.3).

**TABLE 25.3** Settling of Turbidity Interface Measured August 21-24, 1971, Heisonglin Reservoir

Time of observation	Water level in reservoir, m	Depth of interface, m	Interface settling rate, m/h	Amount of clear water seeped, $10^3 \text{ m}^3$
Aug. 21, 11:30	1761.98	0.6	-	324
Aug. 22, 11:00	1760.62	1.41	0.034	620
Aug. 23, 11:00	1758.80	2.56	0.047	1050
Aug. 24, 10:34	1756.69	4.05	0.063	1460

*Source:* Northwest Institute of Hydraulic Research (1972b).

Previous flume experiments and field data (Fan, 1980) showed that the interface settling velocity is inversely proportional to the suspended-solids concentration of the muddy suspension. For loessal silts, the settling velocity of the interface ( $V_z$ , cm/s) may be expressed as a function of suspended solids concentration ( $C$ , g/L) by the following formula:

$$V_z = 0.02C^{-2/3} \quad (25.1)$$

For the mean concentration of 110 g/L on August 23, the interface settling velocity may be computed as  $V_z = 0.00087 \text{ cm/s} = 0.031 \text{ m/h}$ , which is of the same order of magnitude as the average interface settling rate of 0.048 m/h observed in the field (Table 25.3). As the sediment thickness in the muddy lake decreased, clear water was aspirated into the bottom outlet and diluted the outflow concentration (Fig. 25.8).

The coarsest materials in a muddy lake settle first, thereby sorting the deposits from individual flood events. Floodplain sediments deposited by the August 20, 1971, event were sampled as a function of depth, showing that grain size in the deposit increased with depth because coarse particles settled faster and became concentrated toward the bottom of the deposit (Fig. 25.9). Deposit depth was relatively uniform from range 1 to 8 and decreased further upstream.

## 25.7 TURBIDITY CURRENT VENTING

In dry years characterized by low runoff during the early flood season, the reservoir was not emptied but sediment was released by venting turbidity currents. Hydrographs for two turbidity current venting events are shown in Figs. 25.10 and 25.11. Both events involved relatively small inflowing floods in which the inflowing sediment-laden water plunged beneath the already-impounded water and accumulated as a submerged muddy lake behind the dam, where it was gradually released through the bottom outlet. There is a 1.5-hour hydraulic travel time over the 7.5 km from the inflow gage station to the dam. Of this distance, the first 5.8 km is above the plunge point and flow is nonstratified. During the larger 1964 event (Fig. 25.10) the peak outflow sediment concentration slightly exceeded peak inflow concentration. This may be a result of either scour and entrainment of sediment downstream of the inflow gage station or increased sediment concentration due to settling within the muddy lake. In the smaller event (Fig. 25A1), the

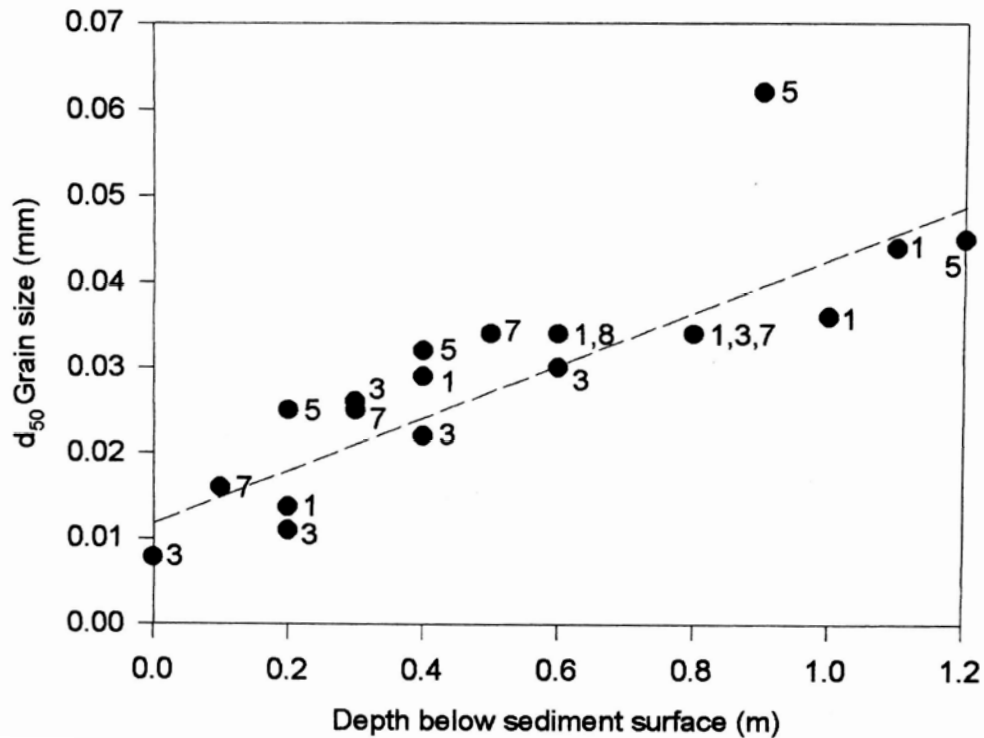


**FIGURE 25.9** Increase in grain size with depth in floodplain deposits due to differential settling rates of sediments from a single flood event at Heisonglin Reservoir. Numbers indicate range locations for the samples (after Ren, 1986).

density current was released almost as soon as it reached the reservoir without creating an appreciable muddy lake, and the discharge concentration was lower than the maximum inflowing sediment concentration. This reduction of outflow concentration as compared to inflow concentration is typical of turbidity current hydrographs measured in larger reservoirs. Figure 25.12 shows vertical profiles of velocity, concentration, and sediment grain size within the main channel during turbidity current venting. Grain size was nearly constant within the turbidity current except near the clear water interface where the sediment particles became much finer.

## 25.8 LATERAL EROSION

Experiments were initiated at Heisonglin to attempt to create a longitudinal channel running parallel to the existing flushing channel for hydraulic scouring of floodplain deposits, but relatively low rates of erosion were obtained because of the low longitudinal slope. However, the accidental overflow of this longitudinal channel initiated lateral erosion which quickly scoured a gully across the deposits. From this it was recognized that erosion of the deposits would proceed much faster by directing the flow along the high lateral slopes from the side of the reservoir toward the main channel, as opposed to a longitudinal channel of lower slope running parallel to the existing main channel (Xia, 1987). Because of the high gradient that can be achieved by

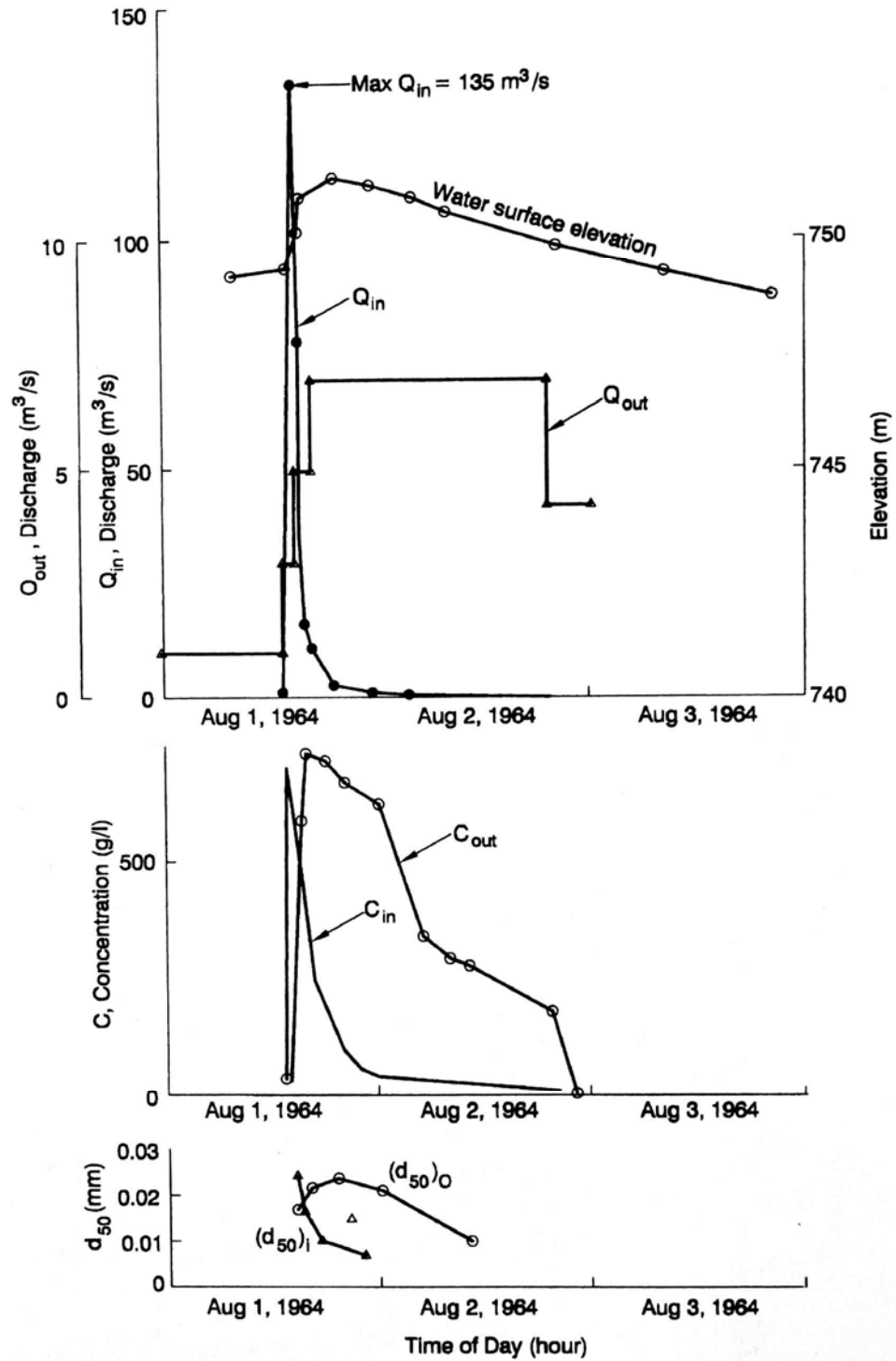


**FIGURE 25.10** Characteristics of flood inflow and density current discharge at Heisonglin Reservoir, August 1-3, 1964 (Northwest Institute of Hydraulic Research et al., 1972a).

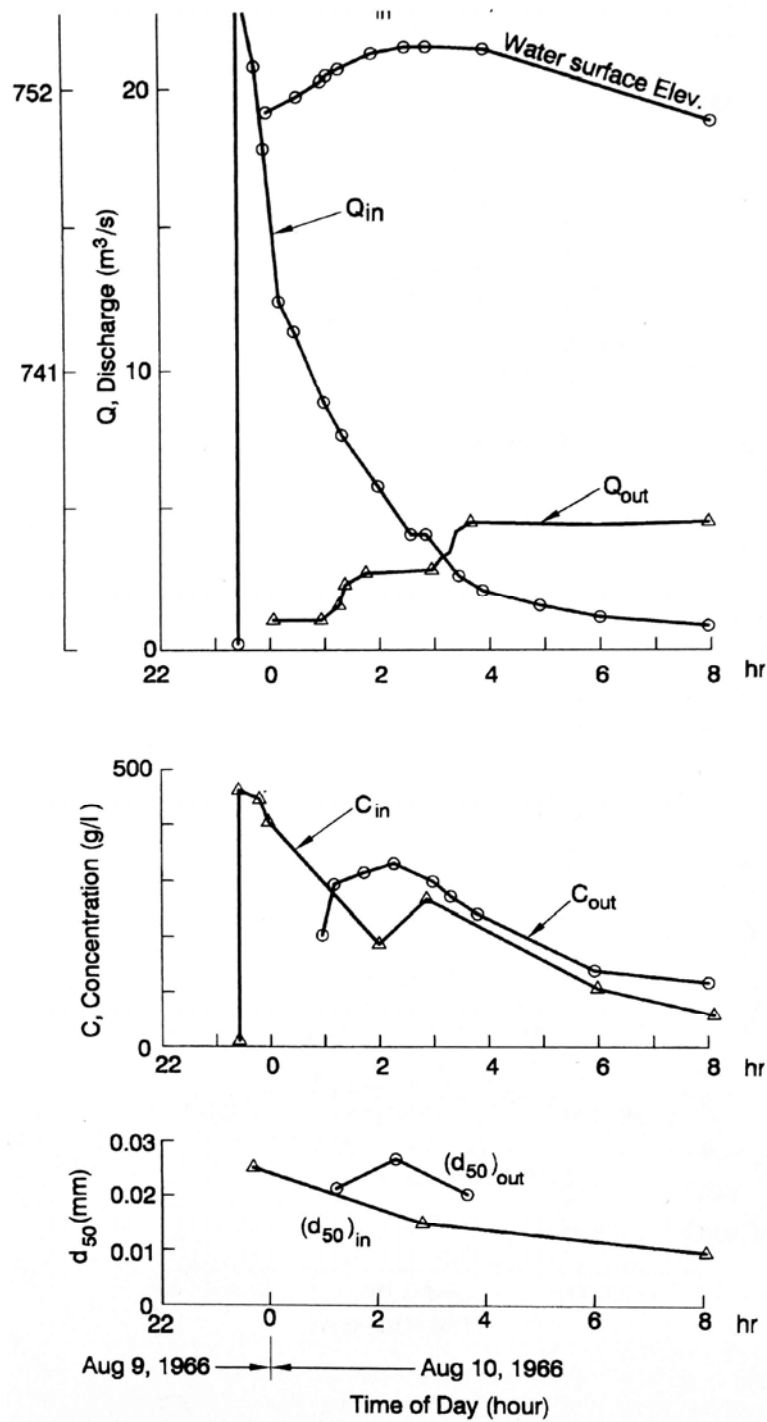


**FIGURE 25.11** Characteristics of flood inflow and density current discharge at Heisonglin Reservoir, August 9-10, 1966 (Ren, 1986).

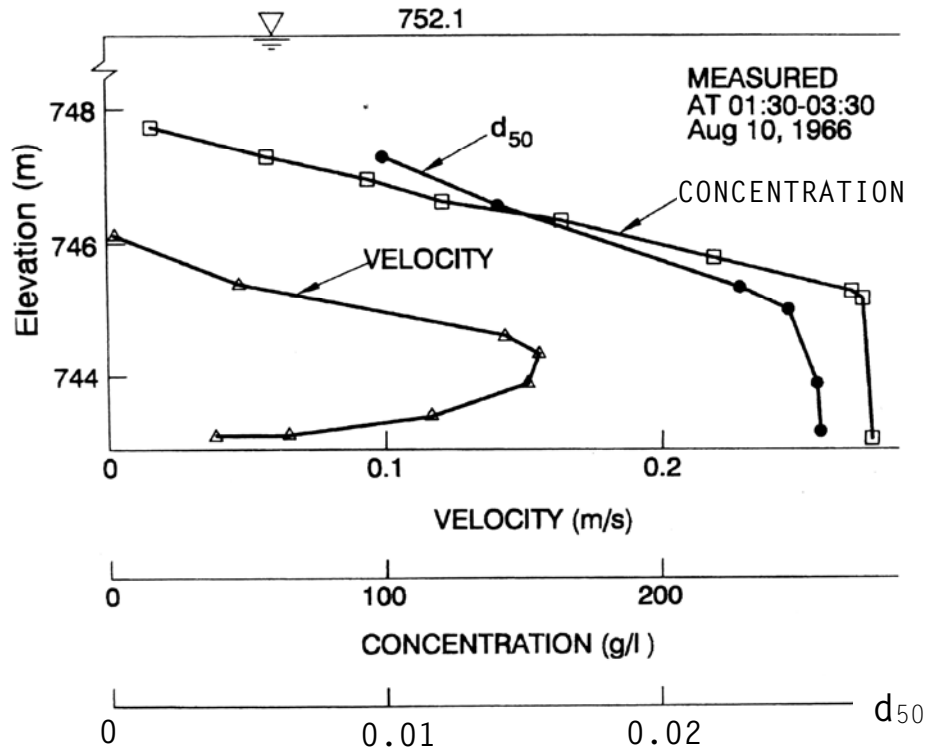


**FIGURE 25.12** Vertical profile in the flushing channel at range 1 in Heisonglin Reservoir showing the passage of a turbidity current (*Ren, 1986*).

lateral drainage, even small discharges were highly effective in eroding deposits of noncohesive silt. The lateral erosion technique was applied for a total of 6.8 months during the 1980-1985 period by using a flow of 0.2 m/s, and 816,000 m<sup>3</sup> of deposits was eroded into the main channel (Xia, 1993). This corresponds to a flushing efficiency (sediment:water) ratio of 0.23. The achievement of this high flushing efficiency is to a large part due to the highly erodible nature of the silt deposits at Heisonglin.

The layout for lateral erosion at Heisonglin was illustrated schematically in Fig. 15.14. It consists of a stream diversion at the upstream end of the reservoir, a delivery channel constructed on contour around the periphery of the floodplain deposits, and a series of outlet points. The flow path extending laterally across the floodplain was initially directed by workers with shovels, and the initial pilot channel was subsequently scoured to a width and depth of many meters by the flow. Photographs of lateral channel erosion are shown in Fig. 25.13. The delivery channel was initially excavated in the sediment at the edge of floodplain deposits, but once it was functioning, plans were made to reconstruct the delivery canal with concrete and to provide movable gates at each lateral outlet (Xia, 1987).

## 25.9 VARIATION IN SEDIMENT RELEASE EFFICIENCY

Sediment release efficiency is defined as the ratio of sediment discharged to sediment inflow over a given period, the complement of the trap efficiency. Because of the short

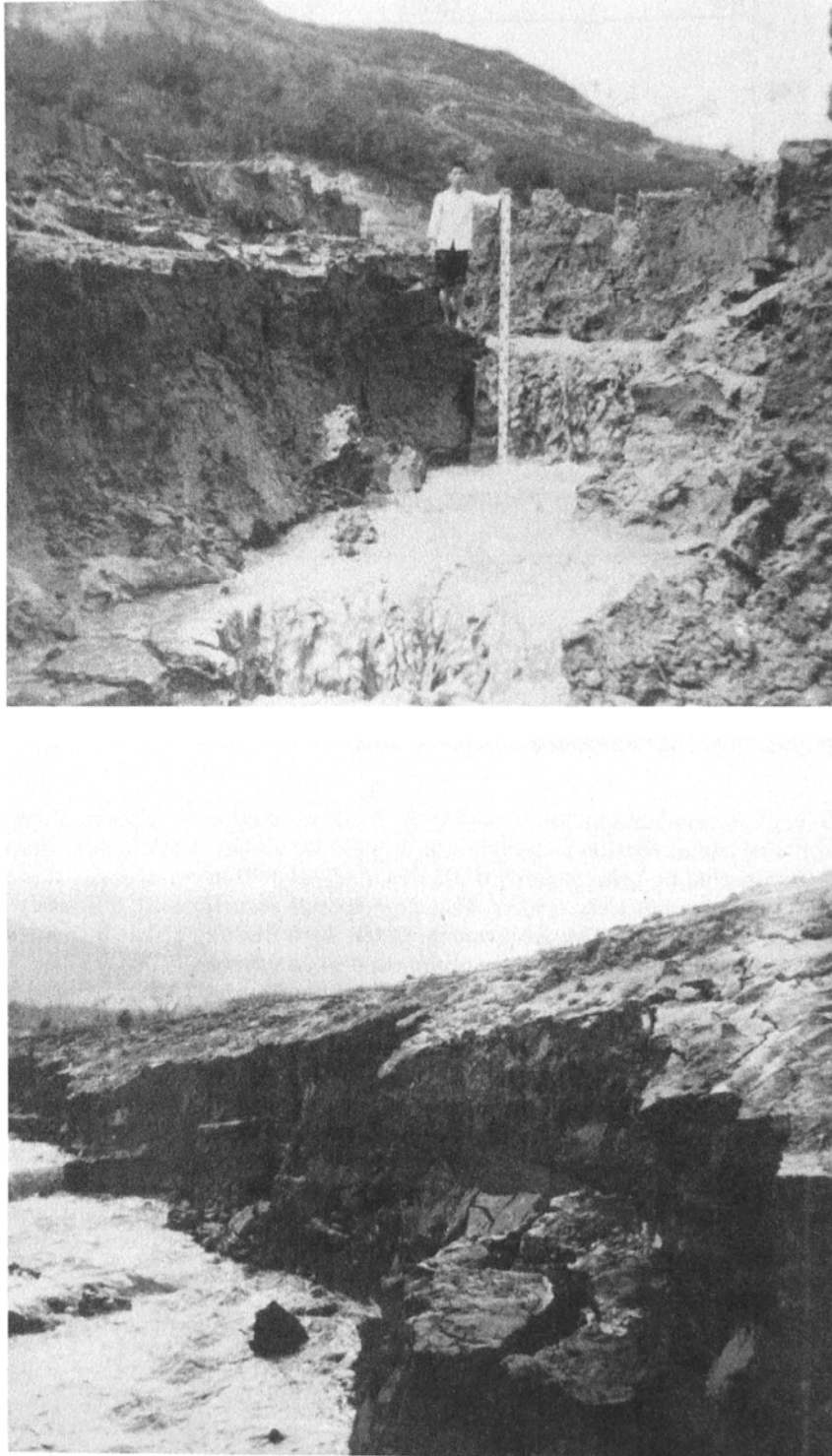


**FIGURE 25.13** Lateral erosion channels at Heisonglin Reservoir. (*Top*) Retrogressive erosion. (*Bottom*) Bank slumping.

length of the reservoir, steep slope, well-defined thalweg maintained by flushing, and high inflow concentration of fine sediments, the release efficiency is relatively high at Heisonglin, usually in the range of 50 to 60 percent. However, release efficiency has varied widely for individual events, ranging from 39 to more than 100 percent for detention flood flushing, and from 36 to 92 percent for turbidity current venting (Table 25.4). Factors affecting release efficiency are discussed below.

### 25.9.1 Turbidity Currents

Three periods of turbidity current events during 1964 had sediment release efficiencies of 38, 66, and 91 percent. The release efficiency during the July 11 event was low, only 38 percent, because the bottom outlet was not opened on time. This allowed suspended sediment in the muddy lake to settle out and become trapped. As illustrated in Fig. 25.14, the outlet opened 2 hours after the flood peak, the initial opening was for only a small discharge of  $2.0 \text{ m}^3/\text{s}$  for a period of 12 hours, and it was followed by a discharge of only  $4.8 \text{ m}^3/\text{s}$ . Conditions for turbidity current venting were also unfavorable for the July 19, 1965, flood, when the outlet discharge was initially limited to  $0.35 \text{ m}^3/\text{s}$ , although the inflow discharge peaked at  $23.6 \text{ m}^3/\text{s}$ . The release efficiency was only 36 percent.

The August 1, 1964, event achieved a release efficiency of 91 percent. As shown in Fig. 25.10, the outlet was opened immediately and discharge was quickly increased to  $7 \text{ m}^3/\text{s}$ . Both inflow and outflow were hyperconcentrated, inhibiting the settling of coarser sediments. It is also possible that some sediments deposited in the delta region by the floods of July 11 and 16 of that year were eroded from the area downstream of the inflow gaging station by the August event, since the reservoir water level was lower in August than in July. Together these factors explain the unusually high flushing efficiency for this turbidity current event.

### 25.9.2 Flood Detention Flushing

The release efficiency for flood detention followed by flushing is typically higher than for turbidity current flushing, even though the period that muddy water is detained in the reservoir may be longer than for turbidity current venting. Detention flushing is more efficient because sediment deposited in the main channel during the detention period is removed when the reservoir attains full drawdown and flushing occurs as riverine flow is established, as was illustrated in Fig. 25.7. This scouring does not occur when a turbidity current is vented because the reservoir is not emptied, and the sediments from the turbidity current settling into the main channel are not discharged until the subsequent emptying and flushing period.

Under detention flushing the reservoir is initially empty. The flood discharge flows along the main channel to the dam where a muddy lake is created, which then expands in the upstream direction and overflows the floodplain. As illustrated in Fig. 25.8, the surface of the muddy water initially corresponds to the water surface, but the interface between clear and muddy water becomes submerged as sedimentation proceeds. Detention time is a critically important factor affecting flushing efficiency. Sediment release efficiency is reduced when the floodplain remains submerged by muddy water for a prolonged period and accumulates sediment deposits because of large floods, delayed discharge, or a low rate of discharge. Sediment deposits having a mean thickness of  $0.8 \text{ m}$  settled onto the floodplain during the large flood on August 4, 1970, which had a peak inflow of  $370 \text{ m}^3/\text{s}$  and a volume of  $2.715 \text{ Mm}^3$ . Discharge from the low-level outlet averaged

**TABLE 25.4** Sediment Release Efficiency for Flood Detention Flushing and Density Current Venting, Heisonglin Reservoir

Mode of operation (a)	Date of flood	Inflow			Outflow			Sediment release efficiency, * %		
		$Q_{\max}$ , m <sup>3</sup> /s	$C_{\max}$ , g/L	Total water, 10 <sup>3</sup> m <sup>3</sup>	Total sediment, 10 <sup>3</sup> t	$Q_{\max}$ , m <sup>3</sup> /s	$C_{\max}$ , g/L		Total water, 10 <sup>3</sup> m <sup>3</sup>	Amount of sediment, 10 <sup>3</sup> t
Flood detention flushing	Aug. 10, 1964	92.2	427	830.5	243.4	7.6	540	930	207.2	85
	Sept. 2, 1964	11.5	856	990.2	28.8	9.75	900	1246	41.1	142
	Aug. 9, 1969	215	585	3210	1000	6.54	418	2479	389.5	39
	Jul. 24, 1970	63.4	415	414	83.65	5.8	514	389	74.7	90
	Aug. 4, 1970	370	438	3260	1180	8.79	606	2550	757.6	64
	Aug. 27, 1970	55	238	461	57	6.82	420	316.5	64	112
	Aug. 19, 1971	19.3	369	145	29.2	4.54	403	130.5	31.3	108
	Aug. 20, 1971	465	314	5927	1484	10.75	621	4880	862	58
Venting of turbidity currents	Aug. 16, 1972	21.3	774	120	49	3.22	630	153.8	40.9	84
	Jul. 11, 1964	132	534	880	237.9	4.8	582	779	116.9	38
	Jul. 16, 1964	35.5	224	574	78.8	7.3	338	629	67.2	66
	Aug. 1, 1964	135	731	721	268.9	7	749	835	308.8	91
	Jul. 19, 1965	23.6	389	500	61.4	6.5	573	371.5	28.3	36
	Aug. 9, 1966	23.2	472	152	51.3	4.6	340	189	25.6	50
	Jul. 21, 1971	18.1	456	134	30.9	3.96	227	236.5	18.25	59
	Aug. 1, 1972	30.9	430	1067	34.6	5.1	273	160.8	18.67	54

\*Release efficiency is the ratio of sediment inflow:outflow.

Source: Shaanxi Provincial Institute of Hydraulic Research and Qinghua University (1978).

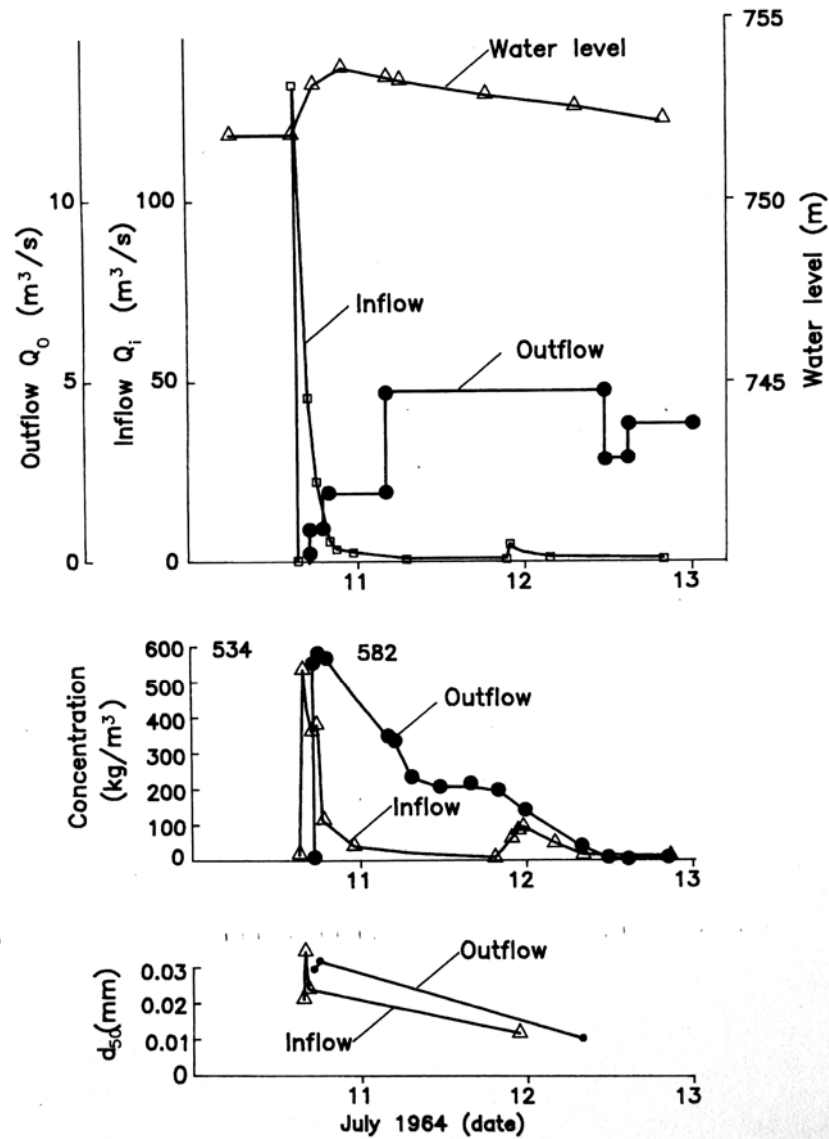


**FIGURE 25.14** Characteristics of flood inflow and density current discharge at Heisonglin Reservoir, China, July 11-13, 1964 (*Northwest Institute of Hydraulic Research et al., 1972a*).

only 7.7 m<sup>3</sup>/s, resulting in a detention time of 92 hours and producing a flushing release efficiency of only 64 percent. Similarly, the large flood of August 20, 1971, having a peak discharge of 465 m<sup>3</sup>/s and an outlet discharge of 8.5 m<sup>3</sup>/s, produced a relatively low flushing release efficiency of 58 percent because of prolonged detention over the floodplain. The flood of August 9, 1969, with a peak flow of 215 m<sup>3</sup>/s, was detained for a prolonged period because the outlet discharge was held at only 2.8 m<sup>3</sup>/s until the inflow flood reached its maximum water level, and only 6.5 m<sup>3</sup>/s thereafter. Release efficiency was only 39 percent, the lowest of record for detention flood flushing at Heisonglin.

Some low-discharge floods shown in Table 25.4 had sediment release efficiencies approaching or exceeding 100 percent. These high efficiencies occur when small volume events do not overflow onto the floodplain and when sediments deposited during previous events are scoured out. This is illustrated by two inflow events during 1964 shown in Table 25.4. The high-discharge high-concentration event on August 10 overflowed the floodplain and deposited sediment which was not washed out at the end of the event. The subsequent flood on September 2 had much lower values of peak discharge and sediment concentration, although it had a larger volume, and it flowed through the main channel without inundating the floodplain. The combination of low sediment inflow and the erosion of previously deposited material from the main channel produced a flushing efficiency of 142 percent for this event.

## **25.10 CLOSURE**

---

Heisonglin Reservoir is located in a rural area of China. The sediment control operations at this reservoir and reported in this case study were conducted without computers or sophisticated telemetering equipment, by locally trained dam operators, at a reservoir equipped with only the most basic types of equipment. The sediment load entering the reservoir is extreme, and storage capacity was being lost at the annual rate of 6 percent before sediment management was initiated. These are not the types of conditions under which one would expect to stabilize reservoir volume at a capacity:inflow ratio of 20 percent, without dredging, and while continuously diverting 100 percent of all inflow (water plus sediment) to irrigation. Yet this was achieved at Heisonglin. This demonstrates that successful sediment management depends first and foremost on the understanding and application of basic concepts, combined with the systematic pursuit of clearly established goals.

## REFERENCES

---

- Abdeihadi, M. L., 1995. "Environment and Socio-economic Impacts of Erosion and Sedimentation in North African Countries." pp. 1141-1152 6th Intl. Symp. River Sedimentation. Central Board of Irrigation and Power, New Delhi.
- Adams, J., 1979. "Gravel Size Analysis from Photographs," *J. Hydraulics Div. ASCE*, 105 (HY10): 1257-1285.
- Adams, J., 1980. "High Sediment Yields from Major Rivers of the Western Southern Alps. New Zealand," *Nature*, 287: 88-89.
- Adams, P. W., 1991. *Maintaining Woodland Roads. The Woodland Workbook*. Oregon State University Extension Service, Extension Circular 1139.
- Aldridge, B. N., and Garrett, J. M., 1973. "Roughness Coefficients for Stream Channels in Arizona," USGS Open File Report.
- Allen, P. B., 1981. "Measurement and Prediction of Erosion and Sediment Yield," ARM-S-15. U.S. Department of Agriculture, Washington, D.C.
- Allen, P. B., and Petersen, D. V., 1981. "A Study of the Variability of Suspended Sediment Measurements," pp. 203-218, *Erosion and Sediment Transport Measurement Symp.*, IAHS Publ. 133, Wallingford, U.K.
- Alonso, C. V., 1980. "Selecting a Formula to Estimate Sediment Transport Capacity in Non-vegetated Channels," pp. 426-439. In W. G. Knisel (editor), *CREAMS (A Field Scale Model for Chemicals, Runoff, and Erosion from Agricultural Management System)*. U.S. Department of Agriculture, Conservation Research Report No. 26.
- Alpha Geotechnical, 1987a. "Sediment Study and Gold Assay Results, Rock Creek Reservoir, Plumas County, California," Report to Pacific Gas and Electric Co., San Francisco.
- Alpha Geotechnical, 1987b. "Sediment Study and Gold Assay Results, Cresta Reservoir, Plumas County, California," Report to Pacific Gas and Electric Co., San Francisco.
- Altunin, S. T., 1964. *Barrages and Reservoirs*. Kolof Press, Moscow (in Russian).
- Amirtharajah, A., and O'Melia, C. R., 1990. "Coagulation Processes: Destabilization. Mixing and Flocculation." In F. W. Pontun (editor), *Water Quality and Treatment*. McGraw-Hill, New York.
- Anderson, D., 1987. "The Economics of Afforestation: A Case Study in Africa," World Bank Occasional Paper No. 1, Washington, D.C.
- Anderson, M. P., Ward, D. S., Lappala, E. G., and Prickett, T. A., 1992. "Computer Models for Subsurface Water," Chap. 22. In D. R. Maidment (editor), *Handbook of Hydrology*. McGraw-Hill, New York.
- Annandale, G. W., 1987. *Reservoir Sedimentation*. Elsevier Science Publishers, New York.
- Annandale, G. W., 1994. "Taking the Scour out of Water Power," *Intl. Water and Dam Construction* (November).
- Annandale, G. W., 1995. "Erodibility," *J. Hydraulic Research. IAHR*, 33 (5): 471-494.
- Annandale, G. W., 1996. "Prediction of Sediment Distribution in a Dry Reservoir: A Stochastic Modeling Approach," pp. 1.85-1.92, *Proc. 6th Federal Interagency Sedimentation Conf.*, Las Vegas.

- Anonymous, 1995. "The food crisis that isn't and the one that is," *The Economist*, (Nov): 41. APHA (American Public Health Association), 1985. *Standard Methods for the Examination of Water and Wastewater*. APHA, Washington, D.C.
- Arcement, G. J. J., and Schneider, V. R., 1989. "Guide for Selecting Manning's Roughness Coefficients for Natural Channels and Flood Plains," USGS Water Supply Paper 2339, Washington, D.C.
- Ariathurai, R., and Krone, R. B., 1976. "Finite Element Model for Cohesive Sediment Transport," *J. Hydraulics Div. ASCE*, 102 (HY3): 323-338.
- ASCE, undated. Guidelines for Retirement of Dams and Hydroelectric Facilities (in preparation). ASCE. New York.
- ASCE Committee on Sedimentation, 1982. "Relationships between Morphology of Small Streams and Sediment Yield," *J. Hydraulics Div., ASCE*, 108 (HY11): 1328-1365.
- Ashida, K., and Egashira, S., 1975. "Basic Study on Turbidity Currents," *J. Hydraulic and Sanitary Engineering Div. ASCE*, 7: 83-85.
- AWWA (American Water Works Association), 1995. "Electronic Watershed Management Reference Manual," CD-ROM ver. 1.0, Denver.
- Axelsson, V., 1992. "X-ray Radiographic Analysis of Sediment Cores from the Cachí Reservoir." In M. B. Janson and A. Rodríguez (editors), *Sedimentological Studies in the Cachí Reservoir, Costa Rica*, UNGI Report No. 81. Department of Physical Geography, Uppsala University, Sweden.
- Barendregt, R. W., and Ongley, E. D., 1977. "Piping in the Milk River Canyon, Southeastern Alberta: A Contemporary Dryland Geomorphic Process," pp. 233-243, *Erosion and Solid Matter Transport in Inland Waters Symp.*, IAHS Publ. 122, Wallingford, U.K.
- Barnes, H. H., 1967. "Roughness Characteristics of Natural Channels," USGS Water-Supply Paper 1849, Washington, D.C.
- Basson, M. S., Allen, R. B., Pegram, G. G. S., and Van Rooyen, J. A., 1994. *Probabilistic Management of Water Resource and Hydropower Systems*. Water Resources Publications, Littleton, Colorado.
- Baurne, G., 1984. "'Trap-dams': Artificial Subsurface Storage of Water," *Water International*, 9 (1): 2-9.
- Beach, T., and Dunning, N. P., 1995. "Ancient Maya Terracing and Modern Conservation in the Pet & Rain Forest of Guatemala," *J. Soil and Water Conservation*, 50 (2): 138-145.
- Bechtel Construction Inc., 1987. "Evaluation of the Effect of Reduced Spill and Recommended Flushing Flows below Rock Creek and Cresta Dams in the North Fork of the Feather River," Report to Pacific Gas and Electric Co., San Francisco.
- Bechtel Construction Inc., 1990. "Flushing Flow Evaluation: The North Fork of the Feather River below Poe Dam." Report to Pacific Gas and Electric Co., San Francisco.
- Becker, A., and Serban, P., 1992. "Hydrological Models for Water-Resources System Design and Operation," Operational Hydrology Report No. 34, WMO-No. 740, World Meteorological Organization, Geneva.
- Bell, H. S., 1942. "Stratified Flow in Reservoirs and Its Use in Preventing of Silting," USDA, Misc. Publ. 491, USGPO, Washington, D.C.
- Benson, M. A., and Dalrymple, T., 1967. "General Field and Office Procedures for Indirect Discharge Measurements" *U.S. Geological Survey Techniques of Water-Resources Investigations*, Book 3, Chap. A1.
- Berga, L., 1995. "Criteria for Design Flood Assessment," pp. 607-618, *Research and Development in the Field of Dams*. Conf. Proc. Swiss National Committee on Large Dams, Crans-Montana, Switzerland.
- Berrini, P., 1996. Personal communication. Cochran and Wilken Consulting Engineers. Springfield, Illinois.
- Bhowmik, N. G., Adams, J. R., and Demissie, M., 1988. "Sediment of Four Reaches of the Mississippi and Illinois Rivers," pp. 11-20, *Sediment Budgets*, IAHS, Publ. 174, Wallingford, U.K.

- Bhowmik, N. G., Fitzpatrick, W. P., Helfrich, J., and Krug, E. C., 1988. "Lake Dredging in Illinois and a Preliminary Assessment of Pre-Dredging Conditions at Lake Springfield," Report by Illinois State Water Survey to Illinois Department of Energy and Natural Resources (ILENR/RE-WR-88/22), Springfield.
- Birdsey, R. A., and Weaver, P. L., 1987. "Forest Area Trends in Puerto Rico," Research Note SO- 331, USDA, Southern Forest Experimental Station, New Orleans.
- Biswas, A. K., 1991. "Water for Sustainable Development in the 21st Century: A Global Perspective," *Water International*, 6 (4): 219-224.
- Blanton, J. O., 1982. "Procedures for Monitoring Reservoir Sedimentation." U.S. Bureau of Reclamation, Denver.
- Bogart, D. B., Arnow, T., and Crooks, J. W., 1964. "Water Resources of Puerto Rico, A Progress Report." Water Resources Bulletin No. 4, USGS, San Juan.
- Boillat, J. L., 1994. "Barrage de Gebidem, Modifications du Chenal de Chasse de le Massa. Étude Expérimentale sur Modèle Hydraulique," École Polytechnique Fédérale de Lausanne.
- Boillat, J. L., and DeCesare, G., 1994. "Dichtestromungen im Bereich des Grundablasses de Staueses Luzzone - Modellversuch," *Symp. Operation, Maintenance and Renovation of Danis and High Pressure Systems*. Graz, Austria.
- Bollinne, A., 1985. "Adjusting the Universal Soil Loss Equation for Use in Western Europe," pp. 206-213. In S. A. El-Swaify, W. C. Moldenhauer, and A. Lo (editors), *Soil Erosion and Conservation*. Soil Conservation Society of America, Ankeny, Iowa.
- Borg, J. E., 1993. "Hydraulic Models," pp. 3.1-3.22. In V. J. Zipparro and H. Hasen (editors). *Davis' Handbook of Applied Hydraulics*, 4th ed., McGraw-Hill, New York.
- Borland, W. M., and Miller, C. R., 1958. "Distribution of Sediment in Large Reservoirs," *J. Hydraulics Div. ASCE*, 84 (HY2).
- Borland, W. M., 1971. "Reservoir Sedimentation," Chap. 29. In H. W. Shen (editor), *River Mechanics*. Water Resources Publications, Fort Collins, Colo.
- Bosh, J. M., and Hewlett, J. D., 1982. "A Review of Catchment Experiments to Determine the Effect of Vegetation Changes on Water Yield and Evapotranspiration," *J. Hydrology*, 55: 3-23. Boss International, 1993. *ARSP User's Manual*, Madison, Wis.
- Bouchard, J. P., Cordelle, M., Labadie, G., and Lorin, J., 1989. "Numerical Simulation of Mud Erosion in Reservoirs by Floods, Application to Reservoirs on the Durance River." Tech. Session B, *IAHR 23rd Congress*, Ottawa.
- Bouchard, J. P., 1993. "Étude de la Sédimentation dans la Retenue de Kembs," Electricité de France, Department Laboratoire National d'Hydraulique, Chatou.
- Bouchard, J. P., 1995. "Mud Investigations and Management, Simulation of Reservoir Sediments," *Proc. 6th Intl. Symp. River Sedimentation*, Central Board of Irrigation and Power, New Delhi. Bouvard, M., 1988. "General Report Q93: Design Flood and Operational Flood Control," *16th Intl. Congress on Large Dams*. ICOLD, Paris.
- Bouvard, M., 1992. *Mobile Barrages and Intakes on Sediment Transporting Rivers*, IAHR Monograph. A. A. Balkema, Rotterdam.
- Boyce, R. C., 1975. "Sediment Routing with Sediment-Delivery Ratios," pp. 61-65. In *Present and Prospective Technology for Predicting Sediment Yields and Sources*. ARS-S-40. USDA Sedimentation Lab., Oxford, Miss.
- Brady, N. C., 1974. *The Nature and Properties of Soils*. Macmillan, New York.
- Brakensiek, D. L., Osborn, H. B., and Rawls, W. J. (editors), 1979. *Field Manual for Research in Agricultural Hydrology*. Agricultural Handbook No. 224. U.S. Department of Agriculture, Washington, D.C.
- Brandt, C. J., 1990. "Simulation of the Size Distribution and Erosivity of Raindrops and Throughfall Drops," *Earth Surface Processes and Landforms*, 15: 687-698.
- Brown, L. R., 1995. *Who Will Feed China? Wake-up Call for a Small Planet*, The Worldwatch Environmental Alert Series. W. W. Norton. New York.
- Brown, E. T., Stallard, R. F., Larsen, M. C., Raisbeck, G. M., and Yiou, F., 1995. "Denudation Rates Determined from the Accumulation of In Situ-produced Be-10 in the Luquillo Experimental Forest, Puerto Rico," *Earth and Planetary Science Letters*, 129: 193-202.

- Brownlie, W. R., 1981. "Prediction of Flow Depth and Sediment Discharge in Open Channels," Report KH-R-43A, W. M. Keck Laboratory, California Institute of Technology, Pasadena. Brownlie, W. R., 1983. "Flow Depth in Sand-Bed Channels," *J. Hydraulic Engineering*, 109 (7): 959-990.
- Bruce, J. P., 1992. "Meteorology and Hydrology for Sustaining Development," WMO Report No. 769, World Meteorological Organization, Geneva.
- Brune, G. M., 1953. "Trap Efficiency of Reservoirs," *Trans. Am. Geophysical Union*, 34 (3): 407-418.
- Bu, N., Su, F., and Shang, R., 1980. "Sediment Problems in Liujiaxia and Yangouxia Reservoirs," pp. 737-752, *Proc. Intl. Symp. River Sedimentation*. Guanghai Press. Beijing.
- Buckler, J. H., Skelly, T. M., Luepke, M. J., and Waken, G. A., 1988. "Case Study: The Lake Springfield Sediment Removal Project," *Lake and Reservoir Management*, 4 (1): 143-152. Bureau of Reclamation, 1948. "Lake Mead Density Current Investigations, 1937-1946," 3 vol., Boulder City, Nevada.
- Bureau of Reclamation, 1987. "Test Designations," *Earth Manual*, Denver, Colorado.
- Bureau of Reclamation, 1987. *Design of Small Dams*. U.S. Government Printing Office, Denver. Bureau of Reclamation, 1994. "Operation of Glen Canyon Dam: Draft Environmental Impact Statement," Salt Lake City.
- Buntash, R. J. C., Ferral, R. L., and McGuire, R. A., 1973. "A Generalized Streamflow Simulation System: Conceptual Modeling for Digital Computers," U.S. Department of Commerce, National Weather Service, Sacramento.
- Burns, M., and McArthur, R., 1996. "Sediment Deposition in Jennings Randolph Reservoir, Maryland and West Virginia." pp. 10.16-10.21, *Proc. 6th Federal Interagency Sedimentation Conf.*, Las Vegas.
- Burrell, G. N., 1951. "Constant-Factor Method Aids Computation of Reservoir Sediment," *Civil Engineering*, 21: 51-52.
- Butcher, D. P., Labadz, J. C., Potter, A. W. R., and White, P., 1992. "Assessment of Catchment Erosion in the Southern Pennines, United Kingdom, Using Reservoir Sedimentation Monitoring." pp. 443-454. *Erosion and Sediment Transport Monitoring Programmes in River Basins*, IAHS Publ. 210, Wallingford, U.K.
- Calixte, J. P., Jones, J. W., Beinroth, F. H., and Perez, L. R., 1992. "A Prototype of AEGIS: Agricultural and Environmental Geographic Information System." In *Proc. 31st Caribbean Food Crop Society*, St. Thomas. USVI.
- Campbell, I. A., 1985. "The Partial Area Concept and Its Application to the Problem of Sediment Source Areas." pp. 128-138. In M. El-Swaify and A. Lo (editors), *Soil Erosion and Conservation*. Soil Conservation Society of America, Ankeny, Iowa.
- Campbell, B. L., Loughran, R. J., and Elliott, G. L., 1988. "A Method for Determining Sediment Budgets Using Caesium-137," pp. 171-179, *Proc. Symp. Sediment Budgets*, IAHS Publ. 174, Wallingford, U.K.
- Canfield, D. E., and Bachmann, R. W., 1981. "Prediction of Total Phosphorus Concentrations, Chlorophyll-a and Secchi Disk in Natural and Artificial Lakes," *Can. J. Fish and Aq. Sci.*, 38: 414-423.
- Cao, S., 1981. "Laboratory Studies on Retrogressive Erosion of Fine Sediment Deposits," Master Thesis, IWHR, Beijing.
- Cao, R., Ren, S., and Lu, Y., 1984. "Analysis of Conditions of Formation and Maintenance of High Sediment Concentration Density Currents," *J. Sediment Research* (2): 59-64.
- Cassidy, R. A., 1989. "Water Temperature, Dissolved Oxygen, and Turbidity Control in Reservoir Releases." In J. A. Gore and G. E. Petts (editors), *Alternatives in Regulated River Management*. CRC Press, Boca Raton, Fla.
- Castle, G. H., 1963. "Determination of Reservoir Deposits by Reconnaissance Methods," *Proc. Federal Interagency Sedimentation Conf.* USDA-ARS Misc. Pub. 970.
- Chang, H. H., 1980. "Geometry of Gravel Streams," *J. Hydraulics Div. ASCE*, 106 (HY9): 1443-1455.

- Chang, H. H., 1988. *Fluvial Processes in River Engineering*. John Wiley and Sons. New York.
- Chang, H. H., Harrison, L. L., Lee, W., and Tu, S., 1995. "Fluvial Modeling for Sediment-pass-through Operations of Reservoirs," Proc. Hydraulics Div. Meeting at San Antonio. ASCE, New York.
- Chang, H. H., 1996. "Reservoir Erosion and Sedimentation for Model Calibration," *6th Federal Interagency Sedimentation Conf.*, Las Vegas.
- Changjiang Water Resources Commission, 1994. "The Three Gorges Project," When, China.
- Chapel, P. D., and Larson, S. J., 1996. "Evaluation of Selected Information on Splitting Devices for Water Samples," USGS Water-Resources Investigations Report 95-4141.
- Chen, B. -F., and Hung, T. -K., 1993. "Dynamic Pressure of Water and Sediment on Rigid Dam." *ASCE. J. Mechanical Engineering*, 19 (7): 1411-1433.
- Chen, C. -T., and Millero, F. L., 1977. "The Use and Misuse of Pure Water PVT Properties for Lake Water," *Nature*, 226: 707-708.
- Chen, J., and Zhao, K., 1992. "Sediment Management in Nanqin Reservoir," *Intl. J. Sediment Research*, 7 (3): 71-84.
- Chen, J., 1994. "Sedimentation Studies at Three Gorges," *Intl. Water Power and Dam Construction* (August): 54-58.
- Cheng, Y., and He, Z., 1989. "Effects and Technical Measures of Warping in Some Irrigation Districts of Shanxi Providence," pp. 1532-1538, *Proc. 4th Intl. Symp. River Sedimentation*, vol. 2, China Ocean Press, Beijing.
- Childers, D., Gao, H., and Zhou, G., 1989. "Field Comparison of Bedload Samplers from the United States of America and the People's Republic of China," pp. 1309-1316, *Proc. 4th Intl. Symp. River Sedimentation*, vol. 2. Beijing.
- Chinese National Committee on Large Dams, 1987. *Large Dams in China, History, Achievement, Prospect*. China Water Resources and Electric Power Press, Beijing.
- Chow, V. T., 1959. *Open-Channel Hydraulics*. McGraw-Hill, New York.
- Church, M. A., McLean, D. G., and Wolcott, J. F., 1987. "River Bed Gravels: Sampling and Analysis," pp. 43-118. In C. R. Thorne, J. C. Bathurst, and R. D. Hey (editors), *Sediment Transport in Gravel-Bed Rivers*. John Wiley and Sons, New York.
- Churchill, M. A., 1948. Discussion of "Analysis and Use of Reservoir Sedimentation Data," by L. C. Gottschalk, pp. 139-140, *Proc. Federal Inter-Agency Sedimentation Conf.*, Denver.
- City of Santa Barbara Public Works Department, 1987. "Gibraltar Lake Restoration Project," Final Report, Submitted to U.S. Environmental Agency Clean Lakes Program, Washington, D.C.
- Clark, E. H., 1985. "The Off-site Costs of Soil Erosion," *J. Soil and Water Conservation*, 40 (1): 19-22.
- Clark, E. H., Haverkamp, J. A., and Chapman, W., 1985. "Eroding Soils: The Off-farm Impacts," The Conservation Foundation, Washington, D.C.
- Clausner, J. E., 1989. "Jet Pump Bypassing, Nerang River Entrance. Australia," DRP-3-01, Dredging Research Program, U.S. Army Engineer Waterways Experiment Station, Vicksburg.
- Clausner, J. E., 1990. "Fixed Sand Bypassing Plant-An Update," DRP-3-03, Dredging Research Program, U.S. Army Engineer Waterways Experiment Station, Vicksburg.
- Clifton, C. C., 1994. "East Branch North Fork Feather River Erosion Control Strategy." Plumas National Forest, Quincy, Calif.
- Clifton, C. C., 1996. Personal communication. Plumas National Forest, Quincy, Calif.
- Coboum, J.: 1989. "Is Cumulative Watershed Effects Analysis Coming of Age?" *J. Soil and Water Conservation*, 44 (4): 267-270.
- Colacicco, D., Osborn, T., and Klaus, A., 1989. "Economic Damage from Soil Erosion," *J. Soil and Water Conservation*, 44 (1): 35-39.
- Cole, G. E., 1994. *Textbook of Limnology*. Waveland Press, Prospect Heights, 111.
- Coleman, J. M., 1982. *Deltas: Processes of Deposition and Models for Exploration*. International Human Resources Corporation, Boston.
- Coleman, D. J., and Scatena, F. N., 1986. "Identification and Evaluation of Sediment Sources," pp. 3-18, *Drainage Basin Sediment Delivery*, IAHS Publ. 159, Wallingford, U.K.

- Collier, M., Webb, R. H., and Schmidt, J. C., 1995. "Dams and Rivers: A Primer on the Downstream Effects of Dams," USGS Circular 1126, Denver.
- Colon, R., and McMahon, G. F., 1987. "BRASS Model: Application to Savannah River System Reservoirs," *ASCE J. Water Resources Planning and Management*, 113 (2): 177-190.
- Comite Francaise des Grands Barrages, 1976. "Problemas de Sedimentation dans les Retenues," pp. 537-562, *Trans 14th ICOLD*, Q54, R. 34, v. 3.
- Committee on Hydropower Intakes, 1995. Guidelines for Design of Intakes for Hydroelectric Plants. ASCE, New York.
- Condolios, E., and Chapus, E. E., 1963. "Designing Solids-Handling Pipelines," *J. Chem. Eng.* (June 24): 131-138.
- Cook, M. G., 1988. "Soil Conservation on Steep Lands in the Tropics," pp. 18-22. In W. C. Moldenhauer and N. W. Hudson (editors), *Conservation Farming on Steep Lands*. Soil and Water Conservation Society, Ankeny, Iowa.
- Cooke, G. D., Welch, E. B., Peterson, S. A., and Newroth, P. R., 1993. *Restoration and Management of Lakes and Reservoirs*. Lewis Publishers, Boca Raton, Fla.
- Copeland, R. R., 1991. "Comparison of Sediment Transport Functions," pp. 8.7-8.13, *Proc. 5th Federal Interagency Sedimentation Conf.*, Las Vegas.
- Cowan, W. L., 1956. "Estimating Hydraulic Roughness Coefficients." *Agricultural Engineering*, 37 (7): 473-475.
- Crayu, A., 1946. "Loi de la Hauteur Limite d'Aspiration dan Deux Fluides de Densitis Differentes," *Comptes Rendus. Academie de Sciences, Paris*, T. 222: 1159-1160.
- Creek, K. D., and Sagraves, T. H., 1995. "EDDY Pump Dredging: Does it Produce Water Quality Impacts?" pp. 2246-2252, *Waterpower '95, Proc. Intl. Conf. Hydropower at San Francisco*. ASCE, New York.
- Crowder, B. M., 1987. "Economic Costs of Reservoir Sedimentation: A Regional Approach to Estimating Cropland Erosion Damages," *J. Soil and Water Conservation*. 42 (3): 194-197.
- CTIC (Conservation Technology Information Center), 1996. "Tales from Two Watershed Groups, from Flooding Concern to Comprehensive Plan," *CTIC Partners*, 14 (5): 3-4. West Lafayette, Ind.
- Cuesta, M. D., 1994. "Economic Analysis of Soil Conservation Projects in Costa Rica." In E. Lutz, S. Pagiola, and C. Reiche (editors), *Economic and Institutional Analysis of Soil Conservation Projects in Central America and the Caribbean*. World Bank Environmental Paper No. 8, Washington, D.C.
- Dabney, S. M., Meyer, L. D., Harmon, W. C., Alonso, C. V., and Foster, G. R., 1995. "Depositional Patterns of Sediment Trapped by Grass Hedges," *Trans. ASCE*. 38 (6): 1719-1729.
- Dal, D., 1991. "River Sedimentation Problems in China." In *Water Conservancy of China*. Water Resources and Electric Power Press, Beijing.
- Danielevsky, A., 1993. "Dust Storms Caused by Reservoirs," Engineering Solutions to Environmental Challenges, *13th Annual USCOLD Lecture*, Denver.
- Dawdy, D. R., and Vanoni, V. A., 1986. "Modeling Alluvial Channels," *Water Resources Research*, 22 (9): 712-812.
- Day, T. J., 1988. "Evaluation of Long Term Suspended Sediment Records for Selected Canadian Rivers," pp. 189-195. *Sediment Budgets*, IAHS Publ. 174, Wallingford, U.K.
- DeCesare, G., 1995. Personal communication. Ecole Polytechnique Fdddral de Lausanne, Switzerland.
- Dedkov, A. P., and Moszherin, V. I., 1992. "Erosion and Sediment Yield in the Mountain Regions of the World," *Erosion, Debris Flows and Environment in Mountain Regions*, IAHS Publ. 209, Wallingford, U.K.
- Dendy, F. E., Champion, W. A., and Wilson, R. B., 1973. "Reservoir Sedimentation Surveys in the United States." In W. C. Ackermann, G. F. White, and E. B. Worthington (editors), *Man-made Lakes: Their Problems and Environmental Effects*, Geophysical Monograph No. 17. American Geophysical Union, Washington, D.C.

- Dendy, F. E., and Bolton, G. C., 1976. "Sediment Yield-Runoff-Drainage Area Relationships in the United States," *J. Soil and Water Conservation*, 31 (6): 264-266.
- Dendy, F. E., Allen, P. B., and Piest, R. F., 1979. "Sedimentation," Chap. 4. In *Field Manual for Research in Agricultural Hydrology*. Agricultural Handbook No. 224. USDA, Superintendent of Documents, Washington, D.C.
- DeRoo, A. P. J., Wesseling, C. G., Gremers, N. H. D. T., Offermons, R. J. E., Ritsema, C. J., Van Ostindie, K., 1994. "LISEM: A New Physically-based Hydrological and Soil Erosion Model in a GIS-environment, Theory and Implementation," pp. 439-448, *Variability in Stream Erosion and Sediment Transport*, IAHS Publ. 224, Wallingford, U.K.
- Dewald, C. L., Henry, J., Bruckerhoff, S., Richie, J., Dabney, S., Shepherd, D., Douglas, J., Wolf, D., 1996. "Guidelines for Establishing Warm Season Grass Hedges for Erosion Control," *J. Soil and Water Conservation*, 51 (1): 16-20.
- Dhawan, B. D., and Satya Sai, K. J. S., 1991. "Economic Linkages Among Irrigation Sources: A Study of the Beneficial Role of Canal Seepage," pp. 124-133. In R. Meinzen-Dick and M. Svendsen (editors), *Future Directions for Indian Irrigation-Research and Policy Issues*. International Food Policy Research Institute, Washington, D.C.
- Dillaha, T. A., Ross, B. B., Mostaghimi, S., Heatwole, C. D., and Shanholtz, V. O., 1988. "Rainfall Simulation: A Tool for Best Management Practice Education." *J. Soil and Water Conservation*, 43 (4): 288-290.
- Diplas, P., and Parker, G., 1985. "Pollution of Gravel Spawning Grounds due to Fine Sediment," Project Report No. 240, St. Anthony Falls Hydraulic Laboratory, U. of Minnesota, Minneapolis.
- Dissmeyer, G. E., and Foster, G. R., 1980. "A Guide for Predicting Sheet and Rill Erosion on Forest Land," Tech. Publ. SA-TP I I, USDA, Forest Service, Washington, D.C.
- Dissmeyer, G., 1982. "How to Use Fabric Dams to Compare Erosion from Forestry Practices," Forestry Report SA-FR 13, USDA, Forest Service, Atlanta.
- Dixon, J. A., Talbot, L. M., and LeMoigne, G. J. M., 1989. "Dams and the Environment: Considerations in World Bank Projects," World Bank Technical Paper No. 110. Washington, D.C.
- Dorough, W. G., and Ried, J. R., 1991. "Shoreline Erosion Process, Lake Sakakaea," pp. 15.1-5.8, *5th Federal Interagency Sedimentation Conf.*, Las Vegas.
- Dou, G., 1977. "A Similarity Theory Concerning the Design of Total Sediment Transport Models with Reference to a Particular Project," Bulletin of Nanjin Institute of Hydraulic Research, No. 3, pp. 1-20.
- Driscoll, F. G., 1986. *Groundwater and Wells*. Johnson Division, St. Paul, Minn.
- Du, G., and Zhang, Z., 1989. "The Erosion of Cohesive Sediments in Reservoirs," *Selected Scientific Papers I.W.H.R.* 29: 152-163. (in Chinese).
- Dunne, T., 1979. "Sediment Yield and Land Use in Tropical Catchments," *J. Hydrology*, 42: 281-300.
- Duquenois, H., 1956. "New Methods of Sediment Control in Reservoirs." *Water Power* (May): 174-180.
- Durand, R., 1953. "Basic Relationship of the Transportation of Solids in Experimental Research," *Proc., Intl. Assoc. Hydraulic Research*, U. Minnesota.
- Eads, R. E., and Thomas, R. B., 1983. "Evaluation of a Depth Proportional Intake Device for Automatic Pumping Samplers," *Water Resources Bulletin* 19 (2): 289-292.
- Eakin, H. M., and Brown, C. B., 1939. "Siltng of Reservoirs," Technical Bulletin No. 524, U.S. Department of Agriculture. Washington. D.C.
- EDF (Electricité de France), 1995. "Guide Vidange. Document d'Aide a la Preparation et a la Realisation des Vidages d'Ouvrages Hydriluliques." Paris.
- Edwards, T. K., and Glysson, G. D., 1988. "Field Methods for Measurement of Fluvial Sediment," USGS Open-file Report 86-531, Reston, Va.
- Eftekhazadeh, S., and Laursen, E. M., 1990. "A New Method for Removing Sediment from Reservoirs," *Hydro Review*, 9 (1): 80-84.

- Einstein, H. A., 1964. "River Sedimentation." In V. T. Chow (editor), *Handbook of Applied Hydraulics*. McGraw-Hill, New York.
- EI-Swaify, S. A., and Dangler, E. W., 1982. "Rainfall Erosion in the Tropics: A State-of-the-Art," pp. 1-25. In *Soil Erosion and Conservation in the Tropics*. Am. Soc. Agronomy, Madison. Emmett, W. W., 1976. "Bedload Transport in Two Large Gravel-Bed Rivers, Idaho and Washington," *3d Federal Interagency Sedimentation Conf.*, Water Resources Council. Washington, D.C.
- Engelman, R., and Leroy, P., 1994. "Sustaining Water: Population and the Future of Renewable Water Supplies," Population Action International, Washington, D.C.
- Erlingsson, U., 1992a, "Survey with Side-scan Sonar and Sub-bottom Profiler." In M. B. Janson and A. Rodriguez (editors), *Sedimentological Studies on the Cachí Reservoir, Costa Rica*, UNGI Report No. 81. Department of Physical Geography, Uppsala University. Sweden.
- Erlingsson, U., 1992b, "Repeated Depth Soundings." In M. B. Jansson and A. Rodriguez (editors), *Sedimentological Studies in the Cachí Reservoir, Costa Rica*, UNGI Rapport 81, Dept. of Physical Geography, Uppsala Univ., Sweden.
- Ervin, D. E., 1993. "Conservation Policy Alternatives: An Overview," *J. Soil and Water Conservation*, 48 (4): 299-303.
- Evenari, M., Shanan, L., and Tadmor, N., 1971. *The Negev: The Challenge of a Desert*. Harvard University Press, Cambridge, Mass.
- Ezzat, M. N., 1993. "Nile Water Flow, Demand and Water Development," *Intl. Symp. High Aswan Dam: Vital Achievement Fully Controlled*. Egyptian National Committee on Large Dams, Cairo. Falkenmark, M., and Lindh, G., 1993. "Water and Economic Development," pp. 80-91, in P. H. Gleick (editor) *Water in Crisis*. Oxford University Press, New York.
- Fan, J., and Jiao, E., 1958. "Preliminary Analysis of Density Currents in Guanting Reservoir," *J. Sediment Research*, 3 (4). (in Chinese).
- Fan, J., Wang, H., Huang, Y., Wu, D., and Shen, S., 1959. *Studies on Density Current and Their Applications*. Water Resources and Electric Power Press, Beijing (in Chinese).
- Fan, J., 1960. "Experimental Studies on Density Currents," *Scientia Sinica*, Chinese Academy of Sciences, 9 (2): 275-303 (in Chinese).
- Fan, J., Wang, H., Shen, S., and Wu, D., 1962. "An Approximate Method for Calculating Density Currents in Reservoirs." *Scientia Sinica*, 11 (5): 707-722 (in Russian).
- Fan, J., 1980. "Analysis of the Sediment Deposition in Density Currents," *Scientia Sinica*, 23 (4): 526-538.
- Fan, J., and Jiang, R., 1980. "On Methods for the Desiltation of Reservoirs" Com. 15, *Intl. Seminar of Experts on Reservoir Desiltation*, Tunis.
- Fan, J., 1985. "Methods of Preserving Reservoir Capacity," pp. 65-164. In S. Bruk (editor), *Methods of Computing Sedimentation in Lakes and Reservoirs*. UNESCO, Paris.
- Fan, J., 1986. "Turbid Density Currents in Reservoirs," *Water International*, 11 (3): 107-116. Fan, J., 1991. "Density Currents in Reservoirs," Workshop on Management of Reservoir Sedimentation, New Delhi.
- Fan, J., and Morris, G. L., 1992a, "Reservoir Sedimentation. I: Delta and Density Current Deposits," *J. Hydraulic Engineering ASCE*, 118 (3): 354-369.
- Fan, J., and Morris, G. L., 1992b, "Reservoir Sedimentation. II: Reservoir Desiltation and Long-term Storage Capacity," *J. Hydraulic Engineering ASCE*, 118 (3): 370-384.
- Fan, J., 1995. "An Overview of Preserving Reservoir Storage Capacity," *Proc. 1995 Intl. Workshop on Reservoir Sedimentation at San Francisco*. Federal Regulatory Commission, Washington, D.C.
- Fan, S. S., 1988. "Twelve Selected Computer Stream Sedimentation Models Developed in the United States," Interagency Advisory Committee on Water Data, Subcommittee on Sedimentation, published by Federal Energy Regulatory Commission, Washington, D.C.
- Fang, D., and Cao, S., 1996. "An Experimental Study on Scour Funnel in Front of a Sediment Flushing Outlet of a Reservoir," pp. 1.78-1.84, *Proc. 6th Federal Interagency Sedimentation Cont.*, Las Vegas.

- Farrel, G. J., and Stefan, H. G., 1986. "Bouyancy Induced Plunging Flow into Reservoirs and Coastal Regions," Project Report No. 241, St. Anthony Falls Hyd. Lab., U. of Minnesota.
- Faulkner, D., and McIntyre, S., 1996. "Persisting Sediment Yields and Sediment Delivery Changes," *Water Resources Bulletin*. 31 (4): 817-829.
- Federal Highway Administration. 1975. "Design of Stable Channels with Flexible Linings," Hydraulic Engineering Circular No. 15, Dept. of Transportation, Washington. D.C.
- FERC (Federal Energy Regulatory Commission), 1991. "Draft Environmental Impact Statement. Clines Canyon and Elwha Hydroelectric Projects, Washington," FERC/EIS-0059D, Washington, D.C.
- FERC (Federal Energy Regulatory Commission), 1994. Project Decommissioning at Relicensing, Policy Statement, Docket No. RM93-23-000, issued December 14, 1994. Washington. D.C.
- FERC (Federal Energy Regulatory Commission), 1995. Edwards Manufacturing Co., Inc. and the City of Augusta, Maine (Project No. 2389-009) and Project Decommissioning at Relicensing (Docket No. RM93-23-000), January 1995, Washington. D.C.
- FERC (Federal Energy Regulatory Commission), 1996. Consumers Power Company, Order Approving Stronach Dam Removal Plan and Amending License, Project No. 2580-040, -043, -044, -045, and -046, Michigan, March 19, 1996, Washington, D.C.
- Ferguson, R. I., 1986. "River Loads Underestimated by Rating Curves," *Water Resources Research*, 22 (1): 74-76.
- Fernández-Ordóñez, J., 1984. *Catálogo de Noventa Presas y Azudes Españoles Anteriores a 1900*. Comisión de Estudios Históricos de Obras Públicas y Urbanismo, Madrid.
- Finkner, S. C., Nearing, G. R., Foster, G. R., and Gilley, J. E., 1989. "A Simplified Equation for Modeling Sediment Transport Capacity," *Trans. ASAE*, 32 (5): 355-359.
- Fitzpatrick, W., Bogner, W., and Bhowmik, N., 1985. "Sedimentation Investigations of Lake Springfield, Illinois," Contract Report, Illinois State Water Survey.
- Ford, D. E., and Johnson, M. C., 1983. "An Assessment of Reservoir Density Currents and Inflow Processes." Technical Report E-83-7. U.S. Army Corps of Engineers, Vicksburg, Miss.
- Ford, D. E., 1990. "Reservoir Transport Processes." In K. W. Thornton, B. L. Kimmel, and F. E. Payne (editors), *Reservoir Limnology*. John Wiley and Sons, New York.
- Forel, F. A., 1885. "Les Ravins Sous-lacustres de Fleuves Glaciaires." *Comptes Rendus, Academie de Sciences*, Paris, T. 101: 725-728.
- Foster, G. R., McCool, D. K., Renard, K. G., and Moldenhauer, W. C., 1981. "Conversion of the Universal Soil Loss Equation to SI Metric Units," *J. Soil and Water Conservation*, 36 (6): 355-359.
- Foster, I. D. L., Millington, R., and Grew, R. G., 1992. "The Impact of Particle Size Controls on Stream Turbidity Measurements: Some Implications for Suspended Sediment Yield Estimation," pp. 51-62, *Erosion and Sediment Transport Monitoring Programmes in River Basins*, IAHS Publ. 210, Wallingford, U.K.
- Foster, I. D. L., and Charlesworth, S. M., 1994. "Variability in the Physical, Chemical and Magnetic Properties of Reservoir Sediments: Implications for Sediment Source Tracing," pp. 153-160, *Proc. Symp. Variability in Stream Erosion and Sediment Transport*, IAHS Publ. 224, Wallingford, U.K.
- Fread, D. L., 1988. "The NWS DAMBRK Model: Theoretical Background and User Documentation," Office of Hydrology, NWS, U.S. Department of Commerce, Silver Spring, Md.
- Fredericks, D. J., Norris, V., and Perrens, S. J., 1988. "Estimating Erosion Using Caesium-137: Measuring Caesium-137 Activity in a Soil," pp. 225-231, *Proc. Symp. Sediment Budgets*, IAHS Publ. 174, Wallingford, U.K.
- French, R. H., 1985. *Open-Channel Hydraulics*. McGraw-Hill, New York.
- Frenette, M., and Julien, P. Y., 1986. "Advances in Predicting Reservoir Sedimentation," *Proc. 3d Intl. Symp. River Sedimentation*, U. Mississippi, Oxford.
- Froehlich, W., and Walling, D. E., 1994. "Use of Chernobyl-derived Radiocaesium to Investigate Contemporary Overbank Sedimentation on Flood Plains of Carpathian Rivers," pp. 161-169, *Erosion and Sediment Transport Monitoring Programmes in River Basins*. IAHS Publ. 210, Wallingford, U.K.

- Galay, V., 1987. *Erosion and Sedimentation in the Nepal Himalaya*. Water and Energy Commission Secretariat, Kathmandu.
- Galay, V. I., and Okaji, T., 1995. "Erosion from the Kulekhani Watershed Nepal During the July 1993 Rainstorm." In H. Schreier, P. B. Shah, and S. Brown (editors). *Challenges in Mountain Resource Management in Nepal*. Water and Energy Commission Secretariat, Kathmandu.
- Gariel, P., 1946. "Sur la Loi de la Hauteur Limite d'Aspiration dans Deux Fluides de Densite Differentes," *Comptes Rendus. Academie de Sciences, Paris*, T. 222: 781-783.
- Gariel, P., 1949. "Recherches Experimentales sur l'Ecoulement de Couches Superposes de Fluide de Densites Differentes," *La Houille Blanche* (1).
- Garric, J., Migeon, B., and Vindimian, E., 1990. "Lethal Effects of Draining on Brown Trout. A Predictive Model Based on Field and Laboratory Studies." *Water Resources Research*, 24 (1): 59-65.
- Gatwood, E., Petersen, J., and Casey, K., 1992. "Los Angeles District Method for Prediction of Debris Yield." U.S. Army Corps of Engineers, Los Angeles District.
- Gee, M., 1992. "Guidelines for the Calibration and Application of Computer Program HEC-6," Training Document No. 13. U.S. Army Corps of Engineers, Hydrologic Engineering Center, Davis, Calif.
- Geiger, A. F., 1963. "Developing Sediment Storage Requirements for Upstream Retarding Reservoirs." pp. 881-885. *Proc. Federal Interagency Sedimentation Conf.* USDA-ARS Misc. Pub. 970.
- Gellis, A., Hereford, R., Schumm, S. A., and Hayes, B. R., 1991. "Channel Evolution and Hydrologic Variations in the Colorado Basin: Factors Influencing Sediment and Salt Loads," *J. Hydrology*, 124: 317-344.
- Gellis, A., 1991. "Decreasing Trends of Suspended Sediment Concentrations at Selected Streamflow Stations in New Mexico." In C. T. Ortega-Klett (editor), *Proc. 36th Annual New Mexico Water Conf.* New Mexico State U., Las Cruces.
- Gellis, A., 1993. "The Effects of Hurricane Hugo on Suspended-Sediment Loads, Lago Loíza Basin, Puerto Rico." *Earth Surface Processes and Landforms*, 18: 505-517.
- Gellis, A. C., Cheama, A., Laahty, V., and Lalio, S., 1995. "Assessment of Gully-control Structures in the Río Nutria Watershed, Zuni Reservation, New Mexico," *Water Resources Bulletin*, 31 (4): 633-646.
- Gerster, S., and Rey, P., 1994. "Conséquences écologiques des curages de bassins de retenue," Cahier de l'Environnement No. 219, Office Fédéral de l'Environnement, des Forêts et du Paysage, Berne, Switzerland.
- Gessler, J., 1971. "Beginning and Ceasing of Sediment Motion," Chap. 7. In H. W. Shen (editor), *River Mechanics*, vol. I, Hsieh Wen Shen, Fort Collins, Colo.
- Gilbert, A., 1996. "NPDES Stormwater Permit Requirements in the Southeastern US," *Erosion Control*, 3 (5): 48-53.
- Gilmour, D. A., 1977. "Logging and the Environment, with Particular Reference to Soil and Stream Protection in Tropical Rainforest Situations," pp. 223-235. In *Guidelines for Watershed Management*. FAO, Rome.
- Gippel, C. J., 1995. "Potential of Turbidity Monitoring for Measuring the Transport of Suspended Solids in Streams," *Hydrological Processes*, 9: 83-97.
- Gist, W. S., Scott, S., Stonestreet, E., and Copeland, R. R., 1996. "In-channel Sediment Basins: An Alternative to Dam Style Debris Basins," pp. V.99-V.106, *Proc. 6th Federal Interagency Sedimentation Conf.*
- Gleick, P. H., 1993. "Water and Energy," pp. 67-79. In Peter H. Gleick (editor), *Water in Crisis*. Oxford University Press, New York.
- Glymph, L. M. 1957. "Importance of Sheet Erosion as a Source of Sediment," *Trans. Am. Geophysical Union*, 35 (6): 903-907.
- Glysson, G. D., 1987. "Sediment Transport Curves," USGS Open-file Report 87-218, Reston, Va.
- Gogus, M., and Yalcinkaya, F., 1992. "Reservoir Sedimentation in Turkey," pp. 909-918, *5th Intl. Symp. River Sedimentation*, Karlsruhe.

- Goldman, S. J., Jackson, K., and Bursztynsky, T. A., 1986. *Erosion and Sediment Control Handbook*. McGraw-Hill, New York.
- Goldsmith, E., and Hildyard, N., 1984, 1985. *The Social and Environmental Effects of Large Dams*, vol. 1: Overviews, vol. 2: Case Studies. Wadebridge Ecological Centre, Cornwall, U.K.
- Golz, E., 1992. "Recent Morphologic Development of the Rhine River," pp. 95-103, *5th Intl. Symp. River Sedimentation*, Karlsruhe.
- Gong, S., and Jiang, D., 1979. "Soil Erosion and Its Control in Small Watersheds of the Loess Plateau," *Scientia Sinica*, 22 (11): 1302-1313.
- Gorbach, C. A., and Baird, D. C., 1991. "Case History: Channel Aggradation above a Reservoir," pp. 4.115-4.122, *5th Federal Interagency Sedimentation Conf.*, Las Vegas, Nevada.
- Gorbach, C., 1996. "Rio Puerco Sedimentation and Water Quality Study," Albuquerque Area Office, Bureau of Reclamation.
- Gordon, N. D., McMahon, A., and Finlayson, B. L., 1992. *Stream Hydrology: An Introduction for Ecologists*. John Wiley and Sons, New York.
- Graf, W. H., 1971. *Hydraulics of Sediment Transport*. McGraw-Hill, New York.
- Graf, W. H., 1984. "Storage Losses in Reservoirs," *Water Power and Dam Construction*, 36 (4): 37-40.
- Graf, W. L., 1993. "Landscapes, Commodities, and Ecosystems: The Relationship Between Policy and Science for American Rivers," Chap. 2. In *Sustaining Our Water Resources*. National Academy Press, Washington, D.C.
- Grant, G. E., and Wolff, A. L., 1991. "Long-term Patterns of Sediment Transport after Timber Harvest, Western Cascade Mountains, Oregon, USA," pp. 31-40, *Sediment and Stream Water Quality in a Changing Environment: Trends and Explanation*, IAHS Publ. 203, Wallingford, U.K.
- Griffiths, G. A., 1979. "High Sediment Yield from Major Rivers of the Western Southern Alps, New Zealand," *Nature*, 282: 61-63.
- Grimshaw, D. L., and Lewin, J., 1980. "Source Identification for Suspended Sediments," *J. Hydrology*, 47: 151-163.
- Grimshaw, R. G., and Helfer, L., 1995. "Vetiver Grass for Soil and Water Conservation, Land Rehabilitation, and Embankment Stabilization," World Bank Technical Paper No. 273, Washington, D.C.
- Grover, N. C., and Howard, C. S., 1938. "The Passage of Turbid Water Through Lake Mead," *Trans. ASCE*, 103: 720-790.
- Gunkel, R. C. et al., 1984. "A Comparative Study of Sediment Quality in Four Reservoirs," Technical Report E-84-2, U.S. Army Engineer Waterways Experiment Station, Vicksburg, Miss.
- Guo, Z., and Li, D., 1984. "Experience on Water and Sediment Management in Hengshan Reservoir," *Water and Hydropower Technology* (5): 54-60 and 64 (in Chinese).
- Gurnell, A. M., Clark, M. J., Hill, C. T., and Greenhalgh, J., 1992. "Reliability and Representativeness of a Suspended Concentration Monitoring Programme on a Remote Alpine Proglacial River," pp. 191-200, *Erosion and Sediment Transport Monitoring Programmes in River Basins*, IAHS Publ. 210, Wallingford, U.K.
- Guy, H. P., 1969. "Laboratory Theory and Methods for Sediment Analysis," *Techniques of Water Resources Investigations of the U.S. Geological Survey*. Book 5, Chap. C1, USGS, Reston, Va.
- Guy, H. P., and Norman, V. W., 1970. "Field Methods for Measurements of Fluvial Sediment," *Techniques of Water Resources Investigations of the U.S. Geological Survey*. Book 3, Chap. C2, USGS, Reston, Va.
- Gvelessiani, L. G., and Shimaltsel, N. P., 1968. "Reservoir Silting at Hydroelectric Station," *Energy*, Moscow (in Russian).
- Haan, C. T., Barfield, B. J., and Hayes, J. C., 1994. *Design Hydrology and Sedimentology for Small Catchments*. Academic Press, New York.
- Hach, C. C., Vanous, R. D., and Heer, J. M., 1990. "Understanding Turbidity Measurement," Technical Information Series No. 11, Hach Company, Loveland, Colo.
- Hadley, R. F., and Shown, L. M., 1976. "Relation of Erosion to Sediment Yield," pp. 1.132-1.139, *Proc. 3d Federal Interagency Sedimentation Conf.*, Water Resources Council, Washington, D.C.

- Haliburton, T. A., 1978. "Guidelines for Dewatering/Densifying Confined Dredged Material." Tech. Report DS-78-I I. U.S. Army Engineering Waterways Experiment Station, Vicksburg, Miss.
- Hamel, J. V., and Sekela, J. E., 1995. "Shoreline Erosion Study and Management Policy, Berlin Lake, Ohio." pp. 173-186. In *15th Annual USCOLD Lecture Series*, USCOLD, Denver. Hammad, H. Y., 1972. "River Bed Degradation After Closure of Dams." *J. Hydraulics Div. ASCE*, 98 (HY4): 591-607.
- Hann, C. T., Barfield, B. J., and Hayes, J. C., 1994. *Design Hydrology and Sedimentology for Small Catchments*. Academic Press, New York.
- Happ, S. C., 1975. "Valley Sedimentation as a Factor in Sediment-yield Determination." pp. 57-60. In *Present and Prospective Technology for Predicting Sediment Yields and Sources*, USDA, Agricultural Research Service, ARS-S-40, Washington. D.C.
- Harrison, L. L., 1991. "North Fork Feather River Erosion Control Program," pp. 199-208. *Waterpower '91*. ASCE, New York.
- Harrison, L. L., Lee, W. H., and Tu, S., 1995. "Sediment Pass-through, An Alternative to Reservoir Dredging," pp. 2236-2245, *Waterpower '95*. ASCE, New York.
- Harrison, L. L., and Lindquist, D. S., 1995. "Hydropower Benefits of Cooperative Watershed Management," *Waterpower '95*. ASCE, New York.
- Harrison, L. L., and Weinrib, H. P., 1996. "EDDY Pump Dredging Demonstration at Cresta Reservoir," *North American Water and Environment Congress '96*. CD-ROM. ASCE, New York. Heede, B. H., and Mufich, J. G., 1974. "Field and Computer Procedures for Gully Control by Check Dams," *J. Environmental Management* (2): 1-49.
- Heede, B. H., 1975. "Stages of Development of Gullies in the West," pp. 155-161 In *Present and Prospective Technology for Predicting Sediment Yields and Sources*. ARS-S-40. USDA Sedimentation Lab., Oxford, Miss.
- Heede, B. H., 1976. "Gully Development and Control: The Status of Our Knowledge," USDA Forest Service Research Paper RM-169, Rocky Mountain Forest and Range Experiment Station, Fort Collins, Colo.
- Heede, B. H., 1983. "Control of Rills and Gullies on Off-Road Vehicle Traffic Areas." In R. H. Webb and H. G. Wilshire (editors), *Environmental Effects of Off-Road Vehicles: Impacts and Management in Arid Regions*. Springer-Verlag, New York.
- Heinemann, H. G., and Dvorak, V. I., 1963. "Improved Volumetric Survey and Computational Procedures for Small Reservoirs," Proc. Federal Interagency Sedimentation Conf., USDA Misc. Publ. 970, Washington, D.C.
- Herbich, J.B. (editor), 1992. *Handbook of Dredging Engineering*. McGraw-Hill Co., New York.
- Hereford, R., 1987. "Sediment-yield History of a Small Basin in Southern Utah, 1937-1976: Implications for Land Management and Geomorphology," *Geology*, 15 (Oct): 954-957.
- Hesse, L. W., and Newcomb, B. A., 1982. "Effects of Flushing Spencer Hydro on Water Quality. Fish and Insect Fauna in the Niobrara River, Nebraska," *N. American J. Fisheries Management*, 2: 45-52.
- Hill, P. R., 1996. "Conservation Tillage: A Checklist for U.S. Farmers," Conservation Technology Information Center, West Lafayette, Ind.
- Hillebrenner, G., 1993. "Roller-Compacted Concrete Dams." In V. J. Ziparo and H. Hansen (editors), *Davis' Handbook of Applied Hydraulics*. McGraw-Hill, New York.
- Hirshleifer, J., DeHaven, J. C., and Milliman, J. W., 1970. *Water Supply: Economics Technology and Policy*. University of Chicago Press, Chicago.
- Holeman, J. N., 1981. "The National Erosion Inventory of the Soil Conservation Service, U.S. Department of Agriculture, 1977-1979." pp. 315-319, *Erosion and Sediment Transport Measurement Symp.*, IAHS Publ. 133, Wallingford, U.K.
- Holmes, R. R., and Oberg, K. A., 1996. "Sediment and Hydraulic Data Collected During the Upper Mississippi River System Flood of 1993," pp. 8.38-8.44, 6th *Federal Interagency Sedimentation Conf.*, Las Vegas.
- Horne, A. J., and Goldman, C. R., 1994. *Limnology*. McGraw-Hill, New York.
- Hotchkiss, R. H., and Xi, H., 1995. "Designing a Hydrosuction Sediment Removal System," pp. 165-174, 6th *Intl. Symp. River Sedimentation*, Central Board of Irrigation and Power, New Delhi.

- Hubbel, D. W., 1987. "Bed Load Sampling and Analysis," pp. 89-118. In C. R. Thome, J. C. Bathurst, and R. D. Hey (editors), *Sediment Transport in Gravel-Bed Rivers*. John Wiley and Sons, New York.
- Hudson, N. W., 1988. "Conservation Practices and Runoff Water Disposal on Steep Lands." pp. 117-128. In W. C. Moldenhauer and N. W. Hudson (editors), *Conservation Fanning on Steep Lands*. Soil and Water Conservation Society, Ankeny, Iowa.
- Hudson, N., and Cheatle, R. J., 1993. *Working with Fanners for Better Land Husbandry*. Soil and Water Conservation Society, Ankeny, Iowa.
- Hwang, J. S., 1985. "The Study and Planning of Reservoir Desilting in Taiwan," *Water International*, 10 (1): 7-13.
- Hwang, J. S., no date, "A Proposed Desilting Reservoir System: the Nan-Hwa Reservoir Project," mimeo report. TPWCB. Taiwan.
- Hydrocomp Inc., 1985. "Sediment and Turbidity in Rock Creek Reservoir," Report to Pacific Gas and Electric Co., San Francisco.
- Hyson, J., Adamus, P., Tibbets, S., and Darnell, R., 1982. "Handbook for Protection of Fish and Wildlife from Construction of Farm and Forest Roads," U.S. Fish and Wildlife Service, FWS/OBS 82118.
- IBSNAT Project, 1989. Decision Support System for Agrotechnology Transfer (DSSAT). User's Guide. IBSNAT Project, University of Hawaii, Honolulu.
- ICOLD, 1984. *World Register of Darns*. International Commission on Large Dams, Paris. ICOLD, 1988. *World Register of Dams*, Update. International Commission on Large Dams, Paris.
- Interagency Committee, 1957. "Some Fundamentals of Particle Size Analysis, A Study of Methods Used in Measurement and Analysis of Sediment Loads in Streams," Report No. 12, Subcommittee on Sedimentation, Interagency Committee on Water Resources. St. Anthony Falls Hydraulic Laboratory, Minneapolis.
- Ippen, A. T., and Drinker, P. A., 1962. "Boundary Shear Stress in Curved Trapezoidal Channels," *J. Hydraulics Div. ASCE*, 88 (HY5): 143-180.
- ISO (International Standards Organization), 1977a. "Method for Measurement of Suspended Sediment," ISO Standard 4363. Geneva.
- ISO (International Standards Organization), 1977b. "Requirements for Suspended Sediment Samplers," ISO Standard 3716, Geneva.
- Jackson, M., 1988. "Amish Agriculture and No-till: The Hazards of Applying the USLE to Unusual Farms," *J. Water and Soil Conservation*, 43 (6): 483-486.
- James, D. L., and Lee, R. R., 1971. *Economics of Water Resources Planning*. McGraw-Hill, New York.
- James, W. F., and Kennedy, R. H., 1987. "Patterns of Sedimentation at DeGray Lake, Arkansas." In R. H. Kennedy and J. Nix (editors), *DeGray Lake Symp.*, U.S. Army, Waterways Experiment Station, Vicksburg, Miss.
- James, W. F., and Kennedy, R. H., 1987. "Dissolved Oxygen Status of DeGray Lake, Arkansas." In R. H. Kennedy and J. Nix (editors), *DeGray Lake Symp.*, U.S. Army Waterways Experiment Station, Vicksburg, Miss.
- Jansen, R. B., 1983. *Dams and Public Safety*, U.S. Bureau of Reclamation, Denver.
- Jansson, M. B., 1988. "A Global Survey of Sediment Yield," *Geogr. Ann.* 70, ser. A (1-2): 81-98.
- Jansson, M. B., 1992a, "Suspended Sediment Inflow to the Cachi Reservoir." In M. B. Jansson and A. Rodriguez (editors), *Sedimentological Studies on the Cachi Reservoir, Costa Rica*, UNGI Report No. 81. Department of Physical Geography, Uppsala University, Sweden.
- Janson, M. B., 1992b, "Suspended Sediment Outflow from the Cachi Reservoir during the Flushing in 1990." In M. B. Janson and A. Rodríguez (editors), *Sedimentological Studies in the Cachi Reservoir, Costa Rica*, UNGI Report No. 81. Department of Physical Geography, Uppsala University, Sweden.
- Jantawat, S., 1985. "An Overview of Soil Erosion and Sedimentation in Thailand," pp. 10-14. In S.A. El-Swaify, W. C. Moldenhauer, and A. Lo (editors), *Soil Erosion and Conservation*. Soil Conservation Society of America, Ankeny, Iowa.
- Jarecki, E. A., and Murphy, T. D., 1963. "Sediment Withdrawal Investigation-Guernsey Reservoir," Proc. Federal Interagency Sedimentation Conf., Misc. Publ. 970. U.S. Department of Agriculture, Washington, D.C.

- Jiang, J., 1992. "Unit Stream Power and Riverbed Evolution," *Proc. 5th Intl. Symp. River Sedimentation*, Karlsruhe.
- Jin, L., 1992. "Local Scour Upstream of a Bottom Sluice Gate in Reservoirs," pp. 791-798, *Proc. 5th Intl. Symp. River Sedimentation*, Karlsruhe.
- Jones, S., 1996. Personal communication. Placer County, Calif.
- Jowett, I., 1984. "Sedimentation in New Zealand Hydroelectric Schemes." *Water International*. 9 (1984): 172-176.
- Julien, P. Y., 1995. *Erosion and Sedimentation*. Cambridge University Press. Cambridge, U.K. Kadlec, R. H., and Knight, R. L., 1995. *Treatment Wetlands*. Lewis Publishers, Boca Raton, Fla.
- Kellerhals, R., and Bray, D. I., 1971. "Sampling Procedures for Coarse Fluvial Sediments," *J. Hydraulics Div. ASCE*, 97 (HY8): 1165-1180.
- Kellogg, R. L., TeSelle, G. W., and Goebel, J., 1994. "Highlights from the 1992 National Resources Inventory," *J. Soil and Water Conservation*, 49 (6): 521-527.
- Kelso, M. M., Martin, W. C., and Mack, L., 1973. *Water Supplies and Economic Growth in an Arid Environment: An Arizona Case Study*. University of Arizona Press, Tucson.
- Kemper, D., Dabney, S., Kramer, L., and Dominick, D., 1992. "Hedging Against Erosion," *J. Soil and Water Conservation*, 47 (4): 284-288.
- Kennedy, R. H., and Nix, J., 1987. *Proc. of Symposium on DeGray Lake, Arkansas*. Technical Report E-87-4, U.S. Army Waterways Experiment Station, Vicksburg, Miss.
- Kereselidze, N. B., Kutavaya, V. I., and Tsagareli, Y. A., 1985. "Siltation and Flushing Mountain Reservoirs, Exemplified by the Rioni Series of Hydroelectric Stations," *Gidrotekhnicheskije, Stroitelstvo* (9): 50-54.
- Khafagy, A. A., and Fanos, A. M., 1993. "Impacts of Irrigation Control Works on the Nile Delta Coast," pp. 307-325. In *High Aswan Dam: Vital Achievement Fully Controlled* Egyptian National Committee on Large Dams, Cairo.
- Kimmel, B. L., Lind, O. T., and Paulson, L. J., 1990. "Reservoir Primary Production." In IC W. Thornton, B. L. Kimmel, and F. E. Payne (editors), *Reservoir Limnology*. John Wiley and Sons, New York.
- King, C., 1957. "First Report on the Desilting Experiments of the Gen-San-Pee Reservoir," HsinYin Regional Mill, Taiwan Sugar Corp.
- King, H. W., and Brater, E. F., 1963. *Handbook of Hydraulics*, 5th ed., McGraw-Hill, New York. Klaassen, G. J., 1995. "Lane's Balance Revisited," *6th Intl. Symp. River Sedimentation*, Central Board of Irrigation and Power, New Delhi.
- Kondolf, G. M., and Matthews, W. V. G., 1993. "Management of Coarse Sediment on Regulated Rivers," Report No. 80, California Water Resources Center, U. Calif., Davis.
- Kondolf, G. M., and Wolman, M. G., 1993. "The Sizes of Salmonid Spawning Gravels," *Water Resources Research*, 27 (7): 2275-2285.
- Kondolf, G. M., 1995. "Managing Bedload Sediments in Regulated Rivers: Examples from California, USA," *Geophysical Monograph* 89: 165-176.
- Kondolf, G. M., Vick, C. J., and Ramirez, T. M., 1996. "Salmon Spawning Habitat Rehabilitation in the Merced, Tuolumne, and Stanislaus Rivers, California: An Evaluation of Project Planning and Performance," Report No. 90, California Water Resources Center, U. Calif., Davis.
- Krone, R. B., 1962. "Flume Studies of the Transport of Sediment in Estuarial Shoaling Processes," Report to U.S. Army Corps of Engineers, San Francisco District, by Hydraulic Engineering Laboratory, U. Calif., Berkeley.
- Krumbein, W. C., 1934. "Size Frequency Distributions of Sediments," *J. Sediment and Petrology*, 4: 65-77.
- Kuelegan, G. H., 1938. "Laws of Turbulent Flow in Open Channels." U.S. Department of Commerce, NBS, Vol. 21.
- Kuhl, D., 1992. "14 Years of Artificial Grain Feeding in the Rhine Downstream the Barrage Iffezheim," pp. 1121-1129, *5th Intl. Symp. River Sedimentation*. Karlsruhe.
- Kumar, S., 1995. Los Angeles County Flood Control District, Personal communication.
- Laften, J. M., Lane, L. J., and Foster, G. R., 1991. "WEPP A New Generation of Erosion Prediction Technology." *J. Soil and Water Conservation*, 46 (1): 34-38.

- Laften, I. M., Elliot, W. J., Simonton, J. R., Holzhey, C. S., and Kohl, K. D., 1991. "WEPP Soil Erodibility Experiments for Rangeland and Cropland Soils," *J. Water and Soil Conservation*, 46 (1): 39-44.
- Lagasse, P. F., 1980. "An Assessment of the Response of the Rio Grande to Dam Construction, Cochiti to Isleta Reach," Technical Report for the U.S. Army Engineer District, Albuquerque Corps of Engineers. Albuquerque, N.M.
- Lai, J. S., and Shen, H. W., 1996. "Flushing Sediment Through Reservoirs," *J. Hydraulic Research*, 34 (2): 237-255.
- Laird, J. R., and Harvey, M. D., 1986. "Complex-response of a Chaparral Drainage Basin to Fire," pp. 165-183. *Drainage Basin Sediment Delivery*, IAHS Publ. 159, Wallingford, U.K.
- Lajczak, A., 1995. "Proposed Model for Long-term Course of Mountainous Reservoir Sedimentation and Estimating the Useful Life of Dams," pp. 699-711, *6th Intl. Symp. River Sedimentation*. Central Board of Irrigation and Power, New Delhi.
- Lai, H., Jones, J. W., and Beinroth, F. H., 1990. "Regional Agricultural Planning Information and Decision Support System," pp. 51-60. In *Proc. on Application of Geographic Information Systems. Simulation Models, and Knowledge-based Systems for Landuse Management*, Virginia Polytechnic Institute and State University, Blacksburg.
- Lal, R., 1994. "Soil Erosion by Wind and Water: Problems and Prospects." In R. Lal (editor), *Soil Erosion Research Methods*. Soil and Water Conservation Society, Ankeny, Iowa.
- LaMarche, V. C., 1968. "Rates of Slope Degradation as Determined from Botanical Evidence. White Mountains, California," USGS Prof. Paper 352-I. Reston, Va.
- Lane, E. W., 1947. "Report of the Subcommittee on Sediment Terminology." *Trans. American Geophysics Union*, 28 (6): 936-938.
- Lane, E. W., and Koelzer, V. A., 1943. "Density of Sediments Deposited in Reservoirs," Report No. 9. In *A Study of Methods Used in Measurement and Analysis of Sediment Loads in Streams*. Hydraulic Lab, U of Iowa.
- Lane, E. W., 1953. "Progress Report on Studies on the Design of Stable Channels by the Bureau of Reclamation," *Proc. ASCE*, 79: 280.1-280.31.
- Lane, E. W., 1954. "Some Hydraulic Engineering Aspects of Density Currents," Hyd. Lab. Report No. Hyd-373, U.S. Bureau of Reclamation, Denver.
- Lane, E. W., 1955. "Design of Stable Channels." *Trans. ASCE*, 120: 1234-1279.
- Langbein, W. B., and Schunun, S. A., 1958. "Yield of Sediment in Relation to Mean Annual Precipitation," *Trans. Am. Geophysical Union*. 29 (6): 1076-1084.
- Lara, J. M., 1962. "Revision of Procedures to Compute Sediment Distribution in Large Reservoirs," U.S. Bureau of Reclamation, Denver, Colo.
- Lara, J. M., and Pemberton, E. L., 1963. "Initial Unit Weight of Deposited Sediments." pp. 818-845. *Proc. Federal Interagency Sedimentation Conf.*, USDA-ARS Misc. Publ. 970.
- Lora, J. M., 1973. "A Unique Sediment Depositional Pattern." In *Man-made Lakes: Their Problems and Environmental Effects*, Geophysical Monograph 17. American Geophysical Union., Washington, D.C.
- Laronne, J. B., 1990. "Probability Distribution of Event Sediment Yield in the Northern Negev, Israel." In J. Boardman, I. D. L. Foster and J. A. Dearing (editors), *Soil Erosion on Agricultural Land*. John Wiley and Sons, New York.
- Laronne, J. B., Ried, I., Yitshak, Y., and Frostick, L. E., 1992. "Recording Bedload Discharge in a Semiarid Channel, Nahal Yatir, Israel," pp. 79-86, *Erosion and Sediment Transport Monitoring Programmes in River Basins*, IAHS Publ. 210, Wallingford, U.K.
- Larsen, M. C., 1991. "Mass Movement Disturbance and Denudation in a Humid-Tropical Montane Forest, Puerto Rico," *Geological Soc. Am.*, Abstracts and Programs. 23 (5): A256.
- Larsen, M. C., and Torres-Sanchez, A. J., 1992. "Landslides Triggered by Hurricane Hugo in Eastern Puerto Rico, September 1989," *Caribbean J. Science*, 28 (3-4): 113-125.
- Larsen, M. C., and Simon, A., 1993. "Rainfall Intensity-Duration Threshold for Landslides in a Humid-Tropical Environment, Puerto Rico," *Geografiska Annaler* 75, A (1-2): 13-21.
- Lavelle, J. W., and Mofjeld, H., 1987. "Do Critical Stresses for Incipient Motion and Erosion Really Exist?" *ASCE J. Hydraulic Engineering*, 113 (3): 370-385.

- Laws, J. O., and Parsons, D. A., 1943. "The Relationship of Raindrop-size to Intensity," *Trans. Am. Geophys. Union*, 24 (452-460).
- Leopold, L. M., Wolman, M. G., and Miller, J. P., 1964. *Fluvial Processes in Geomorphology*. W. H. Freeman, San Francisco.
- Leopold, L. B., 1970. "An Improved Method for Size Distribution of Stream Bed Gravel," *Water Resources Research*, 6 (5): 1357-1366.
- Lewis, J., 1996. "Turbidity-controlled Suspended Sediment Sampling for Runoff-event Load Estimation," *Water Resources Research*, 32 (7): 2299-2310.
- Li, C., and Jin, D., 1981. *River Model Experiments*. Communication Press (in Chinese).
- Li, Y. H., 1976. "Denudation of Taiwan Island since the Pliocene Epoch," *Geology*, 4: 105-107.
- Li, Z., 1992. "The Effects of Forest in Controlling Gully Erosion." pp. 429-437, *Erosion. Debris Flows and Environment in Mountain Regions*. IAHS Publ. 209, Wallingford, U.K.
- Ligon, F. K., Dietrich, W. E., and Trush, W. J., 1995. "Downstream Ecological Effects of Dams," *Bioscience*, 45 (3): 183-192.
- Lijklema, L., Aalderink, R. H., Blom, G., and AnDuin, E. H. S., 1994. "Sediment Transport in Shallow Lakes: Two Case Studies Related to Eutrophication." In J. V. DePinto, W. Lick, and J. F. Paul (editors), *Transport and Transformation of Contaminants near the Sediment-Water Interface*. Lewis Publishers, Boca Raton, Fla.
- Lin, B., Dou, G., Xie, J., Dai, D., Chen, J., Tang, R., Zhang, R., 1989. "On Some Key Sedimentation Problems of Three Gorges Project (TGP)," *Intl. J. Sediment Research*, 4 (1): 57-74.
- Lin, B., Dou, G., Xie, J., Dai, D., Chen, J., Tang, R., Zhang, R., 1993. "On Some Sedimentation Problems of Three Gorges Project (TGP) in the Light of Recent Findings." In S. S. Fan and G. L. Morris (editors), *Notes on Sediment Management in Reservoirs: National and International Perspectives*. Federal Energy Regulatory Commission, Washington, D.C.
- Lindquist, D. S., Harrison, L. L., and Bowie, L. Y., 1995. "Red Clover Creek Erosion Control Demonstration Project: Ten Year Research Summary," Cost Reduction Projects Report 95-30924022. Pacific Gas and Electric Co., San Francisco.
- Lindquist, D. S., and Harrison, L. L., 1995. "Watershed Restoration in the Northern Sierra Nevada: A Coordinated Resource Management Approach," *Conf Water Resources Planning and Management*. ASCE, New York.
- Liu, Y., 1987. "Cavitation in Sediment-Laden Flow," in *Selected Papers of Researches on the Yellow River and Present Practices*, Yellow River Commission, Beijing.
- Livesey, R. H., 1975. "Corps of Engineers Methods for Predicting Sediment Yield," In *Present and Prospective Technology for Predicting Sediment Yields and Sources*. ARS-S-40. USDA Sedimentation Lab., Oxford, Miss.
- Locher, F. A., and Wang, J. S., 1995. "Operation Procedures for Sediment Bypassing at Cowlitz Falls Dam." pp. 75-90. In *15th Annual USCOLD Lecture Series*, USCOLD, Denver.
- Long, Y., and Zhang, Q., 1981. "Sediment Regulation Problems in Sanmenxia Reservoir," *Water Supply and Management*, 5 (4/5): 351-360.
- Long, Y., 1989. "Manual on Operational Methods for the Measurement of Sediment Transport," Operational Hydrology Report No. 29, World Meteorological Organization, Geneva.
- Lowe, J. I., and Fox, I., 1995. "Sediment Management Schemes for Tarbela," pp. 1-15, *15th Annual USCOLD Lecture Series*, USCOLD, Denver.
- Lopez-Vargas, G., and Pfo-Camey, A., 1994. "Practical Experiences and Lessons Learned by Vecinos Mundiales from Soil Conservation Work in Rural Communities of Honduras," pp. 201-207. In E. Lutz, S. Pagiola, and C. Reiche (editors), *Economic and Institutional Analysis of Soil Conservation Projects in Central America and the Caribbean*. World Bank Environmental Paper No. 8. Washington, D.C.
- Lu, Y., 1995. "Three Gorges Project on the Yangtze River," *Annual Meeting of ICOLD Executive Committee*, Oslo, Norway.
- Lull, H. W., 1959. "Soil Compaction on Forest and Range Lands," USDA Misc. Pub. 768. Washington, D.C.

- Lutz, E., Pagiola, S., and Reiche, C., 1994. "Lessons from Economic and Institutional Analysis of Soil Conservation Projects in Central America and the Caribbean," pp. 3-18. In E. Lutz, S. Pagiola, and C. Reiche (editors), *Economic and Institutional Analysis of Soil Conservation Projects in Central America and the Caribbean*. World Bank Environmental Paper No. 8, Washington, D.C.
- Lyons, J., 1996. "A Survey of Reservoir Shoreline Erosion Problems at Bureau of Reclamation Reservoirs," *6th Federal Interagency Sedimentation Conf.*, Las Vegas.
- MacArthur, R. C., Harvey, M. D., and Sing, E. F., 1990. "Estimating Sediment Delivery and Yield on Alluvial Fans," TP-130, U.S. Army Corps of Engineers, Hydrologic Engineering Center, Davis, Calif.
- MacArthur, R. C., and MacArthur, T. B., 1992. "International Survey of Levee Freeboard Procedures," *Water Forum '92*. ASCE, New York.
- MacArthur, R. C., Hamilton, D., and Gee, D. M., 1995. "Application of Methods and Models of Prediction of Land Surface Erosion and Yield," Training Document No. 36. U.S. Army Corps of Engineers, Hydrologic Engineering Center, Davis, Calif.
- Mahmood, K., 1987. "Reservoir Sedimentation: Impact, Extent, Mitigation," World Bank Technical Report No. 71, Washington, D.C.
- Malta, H., 1993. "Influence of Heterogeneous Sediment Transport on the Function of Sediment Control of a Check Dam," pp. 277-284, *Sediment Problems: Strategies for Monitoring, Prediction and Control*, IAHS Publ. 217, Wallingford, U.K.
- Mann, P. C., and Clark, D. M., 1993. "Marginal Cost Pricing: Its Role in Conservation," *J. AWWA*, 85 (8): 71-78.
- Martin, W. D., 1988. "Martins Fork Lake Sedimentation Study: Hydraulic Model Investigation," Technical Report HL-88-21, U.S. Army Corps of Engineers, Waterways Experiment Station, Vicksburg, Miss.
- McCuen, R. H., 1993. *Statistical Hydrology*. Prentice Hall, Englewood Cliffs, N.J.
- McCully, P., 1996. *Silenced Rivers-The Ecology and Politics of Large Danis*. Zed Books Ltd., N.J.
- McHenry, J. R., 1974. "Reservoir Sedimentation," *Water Resources Bulletin*, 10 (2): 329-337.
- McHenry, J. R., and Ritchie, J. C., 1980. "Dating Recent Sediments in Impoundments," pp. 1279-1289. In *Surface Water Impoundments*, ASCE, New York.
- McIntire, J., 1993. "A Review of the Soil Conservation Sector in Mexico," pp. 107-128. In E. Lutz, S. Pagiola, and C. Reiche (editors), *Economic and Institutional Analysis of Soil Conservation Projects in Central America and the Caribbean*. World Bank Environment Paper No. 8, Washington, D.C.
- McIntyre, S. C., Naney, I. W., Lance, J. C., and Denton, G. M., 1986. "Sedimentation in Reelfoot Lake," Report by Water Quality and Watershed Research Lab., USDA-ARS, for Tennessee Department of Health and Environment, Nashville.
- McKibben, B., 1995. "An Explosion of Green," *Atlantic Monthly*, 275 (4): 61-83.
- McLaughlin, R. T. J., 1959. "The Settling Properties of Suspensions," *J. Hydraulics Div. ASCE*, Proc. Paper 2311 (HY-12): 9-41.
- McMahon, G. F., Fitzgerald, R., and McCarthy, B., 1984. "BRASS Model: Practical Aspects," *J. Water Resources Planning and Management*. 110 (I): 75-89.
- McMahon, T. A., and Mein, R. G., 1986. *River and Reservoir Yield*. Water Resources Publications, Littleton, Cob.
- McNown, J. S., and Lin, P. N., 1952. "Sediment Concentration and Fall Velocity," pp. 401-411, *2d Midwestern Conf. Fluid Mechanics*, Ohio State U.
- Meade, R. H., and Parker, R. S., 1984. "Sediment in Rivers of the U.S.," *National Water Summary*, USGS, Reston, Va.
- Meadowcroft, I. C., Bettess, R., and Reeve, C. E., 1992. "Numerical Modeling of Reservoir Sedimentation." In N. M. Parr, J. A. Charles, and S. Walker (editors), *Water Resources and Reservoir Engineering*. Thomas Telford, London.
- Megahan, W. F., 1975. "Sedimentation in Relation to Logging Activities in the Mountains of Central Idaho," pp. 74-82. In *Present and Prospective Technology for Predicting Sediment Yields and Sources*. ARS-S-40. USDA Sedimentation Lab., Oxford, Miss.

- Megahan, W. F., 1977. "Reducing Erosional Impacts of Roads," pp. 237-261. In *Guidelines for Watershed Management*. FAO, Rome.
- Megahan, W. F., 1981. "Nonpoint Source Pollution from Forestry Activities in the Western United States: Results of Recent Research and Research Needs," pp. 92-151. In U.S. Forestry and Water Quality: What Course in the 80's? Water Pollution Control Federation Meeting, Washington, D.C.
- Megahan, W. F., 1983. "Guidelines for Reducing Negative Impacts of Logging." In L. S. Hamilton and P. N. King (editors), *Tropical Forest Watersheds: Hydrologic and Soil Response to Major Uses of Conversions*. Westview Press, Boulder, Colo.
- Meier, C. I., 1995. "A Critical Review of the Pangué Dam Project EIA, Biobio River, Chile," pp. 51-55, *Water Resources Engineering*, vol. 1, Proc. Hydraulics Div. Annual Conf. ASCE, New York.
- Metha, A. J., Hayter, E. J., Parker, W. R., Krone, R. B., and Teeter, A. M., 1989. "Cohesive Sediment Transport is Process Description," *ASCE J. Hydraulic Engineering*, 115 (8): 1076-1093.
- Meyer, L. D., 1985. "Interrill Erosion Rates and Sediment Characteristics," pp. 167-177. In S. A. El-Swaify, W. C. Moldenhauer, and A. Lo (editors), *Soil Erosion and Conservation*. Soil Conservation Society of America, Ankeny, Iowa.
- Meyer, L. D., 1994. "Rainfall Simulations for Erosion Research," pp. 83-103. In R. Lal (editor), *Soil Erosion Research Methods*. Soil and Water Conservation Service, Ankeny, Iowa.
- Michon, X., Goddet, J., and Bonnefille, R., 1955. "Étude Théorique et Expérimentale des Courants de Densité, I and II," National Hydraulic Laboratory, Chatou, France.
- Migniot, C., 1968. "Étude des Propriétés Physiques de Différents Sédiments Très Fins at de Leur Comportement Sous des Actions Hydrodynamiques," *Houille Blanche* (7): 591-620.
- Migniot, C., 1982. "Dynamique Sédimentaire Estuarienne: Matériaux Cohésifs et Non Cohésifs," Laboratoire Central d'Hydraulique de France, Maisons-Alfort.
- Milhous, R. T., and Bradley, J. B., 1986. "Physical Habitat Simulation and the Moveable Bed," pp. 1976-1983, *Proc. Water Forum '86*. ASCE, New York.
- Miller, C. R., 1953. "Determination of the Unit Weight of Sediment for Use in Sediment Volume Computations," U.S. Bureau of Reclamation, Denver.
- Miller, A. J., and Shoemaker, L. L., 1986. "Channel Storage of Fine-Grained Sediment in the Potomac River," pp. 287-303, *Drainage Basin Sediment Delivery*, IAHS Publ. 159, Wallingford, U.K.
- Milliman, J. D., and Meade, R. H., 1983. "World-Wide Delivery of Sediment to the Oceans," *J. Geology*, 91 (1): 1-21.
- Mizuyama, T., 1993. "Structural and Non-Structural Debris-flow Countermeasures." In H. W. Shen, S. T. Su, and F. Wen (editors), *Hydraulic Engineering '93*. vol. 2. ASCE, New York. Moattassem, M. E., and Abdelbary, M. R., 1993. "Bed Degradation and Channel Shifting in the Nile River After Aswan High Dam," In *Intl. Symp. High Aswan Dam: Vital Achievement Fully Controlled*. Egyptian National Committee on Large Dams, Cairo.
- Mohrman, J., and Ewing, R., 1991. "Postfire Suspended Sediment in Yellowstone Park," pp. 4.175-4.182, *Proc. 5th Federal Interagency Sedimentation Conf.*, Las Vegas.
- Moldenhauer, W. C., and Hudson, N. W. (editors), 1988. *Conservation Farming on Steep Lands*. Soil and Water Conservation Society, Ankeny, Iowa.
- Molinas, A., and Yang, C. T., 1986. *Computer Program User's Manual for GSTARS (Generalized Stream Tube model for Alluvial River Simulation)*. U.S. Bureau of Reclamation, Denver. Molinas, A., and Yang, C. T., 1991. "Effects of Parameter Selection on Sediment Modeling," pp. 94-100. In *Proc. 5th interagency Sedimentation Conf.* Las Vegas.
- Montgomery, R., Ford, A. W., Poindexter, M. E., and Bartos, M. J., 1978. "Guidelines for Dredged Material Disposal Area Reuse Management," Tech. Report DS-78-12, U.S. Army Engineering Waterways Experiment Station, Vicksburg.
- Morgan, R. P. C., 1995. *Soil Erosion and Conservation*, 2d ed. Longman Group, Essex, U.K.

- Morin, J., Benyamini, Y., and Michaeli, A., 1981. "The Effect of Raindrop Impact on the Dynamics of Soil Surface Crusting and Water Movement in the Profile." *J. Hydrology*, 52: 321-326.
- Morris, G. L., and Krishna, J. H., 1991. "Hurricane Hugo and Its Effects on Water Supplies in the U.S. Virgin Islands and Puerto Rico," Water Resources Research Center, Caribbean Research Institute. U. Virgin Islands, St. Thomas.
- Morris, G. L., and Hu, G., 1992. "HEC-6 Modeling of Sediment Management in Loíza Reservoir, Puerto Rico," pp. 630-635. In M. Jennings and N. Bhowmik (editors), *Hydraulic Engineering, Water Forum '92*. ASCE, New York.
- Morris, G. L., Colón, R., Laura, R., and Anderson, G. T., 1992. "BRASS Modeling of Loíza Reservoir, Puerto Rico, for Sediment Management Operations," *Water Forum '92*. ASCE. New York.
- Morris, G. L., and Ancalle, C., 1994. "Análisis del Río Maniqui en San Borja: Hidrología, Hidráulica y Transporte de Sedimentos," Reporte a Servicio Nacional de Caminos, La Paz, Bolivia.
- Moths, G. L., 1995a. "Reservoirs and the Sustainable Development of Water Resources," pp. 17-28. In *15th Annual USCOLD Lecture Series*, USCOLD, Denver.
- Morris, G. L., 1995b. "Reservoir Sedimentation and Sustainable Development in India: Problem Scope and Remedial Strategies," pp. 53-61, *6th Intl. Symp. River Sedimentation*. Central Board of Irrigation and Power, New Delhi.
- Morris, G. L., 1996. "Design Analysis of Sediment-Excluding Off-Stream Reservoir, Río Fajardo, Puerto Rico." pp. V.78-V.84, *6th Federal Interagency Sedimentation Conf.*, Las Vegas.
- Mudroch, A., and MacKnight, S. D., 1991. *Handbook of Techniques for Aquatic Sediments Sampling*. Lewis Publications, Boca Raton. Fla.
- Murthy, B. N., 1977. *Life of Reservoir*: Central Board of Irrigation and Power, New Delhi.
- Mutchler, C. K., Murphree, C. E., and McGregor, K. C., 1994. "Laboratory and Field Plots for Erosion Research." In R. Lal (editor), *Soil Erosion Research Methods*. Soil and Water Conservation Society, Ankeny, Iowa.
- Napier, T., 1990. "The Evolution of U.S. Soil-Conservation Policy: From Voluntary Adoption to Coercion." In J. Boardman, I. D. L. Foster, and J. A. Dearing (editors). *Soil Erosion on Agricultural Land*. John Wiley and Sons, New York.
- Napier, T. L., Camboni, S. M., and El-Swaify, S. A. (editors), 1994. *Adopting Conservation on the Farm: An International Perspective on the Socioeconomics of Soil and Water Conservation*. Soil and Water Conservation Society, Ankeny, Iowa.
- National Research Council. Board on Science and Technology for International Development, 1993. *Vetiver Grass. A Thin Green Line Against Erosion*. National Academy Press, Washington, D.C.
- Natural Resources Conservation Service, 1995. "Summary Report 1992 Natural Resource Inventory," U.S. Department of Agriculture, Washington, D.C.
- Natural Resources Conservation Service, no date. "Sedimentation" Sec. 3, *National Engineering Handbook*. USDA, Washington, D.C.
- Nelson, R. W., Dwyer, J. R., and Greenberg, W. E., 1987. "Regulated Flushing in a Gravel-Bed River for Channel Habitat Maintenance: A Trinity River Fisheries Case Study," *Environmental Management*, 11(4): 479-493.
- Nestmann, F., 1992. "Improvement of the Upper Rhine, TW Iffezheim," pp. 1130-1152, *5th Symp. River Sedimentation*, Karlsruhe.
- Newcombe, C. P., and MacDonald, D. D., 1991. "Effects of Suspended Sediments on Aquatic Ecosystems." *North American J. Fisheries Management*, 11: 72-82.
- Nimlos, T. J., and Savage, R. F., 1991. "Successful Soil Conservation in the Ecuadorian Highlands," *J. Soil and Water Conservation*, 46 (5): 341-343.
- Nizery, A., and Bonnin, I., 1953. "Observations Systématiques de Courants de Densité dans une Retenue Hydro-electrique." pp. 369-386, *Proc. Minnesota Intl. Hydraulics Convention*.

- Noll, J. J., 1953. "The Silting of Caonillas Reservoir, Puerto Rico," USDA, Soil Conservation Service, Washington, D.C.
- Nordin, C. F., 1963. "A Preliminary Study of Sediment Transport Parameters, Rio Puerco near Bernalillo, New Mexico," USGS Prof. Paper 462-C. Washington, D.C.
- Nordin, C. F., 1964. "Aspects of Flow Resistance and Sediment Transport, Rio Grande near Bernalillo New Mexico." USGS Water-Supply Paper 1498-H. Washington, D.C.
- Northwest Institute of Hydraulic Research, Institute of Water Conservancy and Hydroelectric Power Research and Shanxi Institute of Hydraulic Research, 1983. *Sediment Problems in Design and Management of Medium and Small-Sized Reservoir*. Science Press. Beijing (in Chinese).
- Northwest Institute of Hydraulic Research and Administrative Bureau of Yeyu River, 1972a. "Preliminary Analysis on Operation Mode of Storing Clear Water and Releasing Muddy Water for Warping Used in Heisonglin Reservoir," *Selected Papers on Reservoir Sedimentation* (in Chinese).
- Northwest Institute of Hydraulic Research and Administrative Bureau of Yeyu River, 1972b. "Preliminary Experience of the Heisonglin Reservoir Management," pp. 169-183. In *Proc. Symp. Reservoir Sediment Measurement and Research*, Sanmenxia (in Chinese).
- Novotny, V. et al., 1979. "Simulation of Pollutant Loadings and Runoff Quality," U.S. Environmental Protection Agency, Chicago, Ill.
- Novotny, V., Simsim, G. V., and Chesters, V., 1986. "Delivery of Pollutants from Non-point Sources." pp. 133-140, *Proc. Symp. Drainage Basin Sediment Delivery*, IAHS Publ. 159, Wallingford, U.K.
- Novotny, V., and Olem, H., 1994. *Water Quality, Prevention, Identification and Management of Diffuse Pollution*. Van Nostrand Reinhold, New York.
- Obando, M. E., and Montalvin, D., 1994. "Technical and Economic Analysis of Soil Conservation Projects in Nicaragua," pp. 75-80. In E. Lutz, S. Pagiola, and C. Reiche (editors), *Economic and Institutional Analysis of Soil Conservation Projects in Central America and the Caribbean*. World Bank Environmental Paper No. 8. Washington, D.C.
- Oberle, R., Dubas, C., Gardet, A., Charpie, J., and Decoppet, H. P., 1967. "Protection contre l'Ensemblement du Bassin d'Accumulation de l'Aménagement Hydroélectrique de la Massa," pp. 665-688, *9th ICOLD*, Q.33, R.37.
- Odgaard, A. J., and Wang, Y., 1991. "Sediment Management with Submerged Vanes," *J. Hydraulic Engineering*, 117 (3): 267-302.
- Odum, E. P., 1971. *Fundamentals of Ecology*. W. P. Saunders, Philadelphia.
- Oglesby, R. T., Carlson, C. A., and McCann, J. A., 1972. *River Ecology and Man*. Academic Press, New York.
- Okada, T., and Baba, K., 1982. "Sediment Release Plan at Sakuma Reservoir," pp. 41-64, *14th ICOLD*, Q.54, R.4.
- Olive, L. J., and Rieger, W. A., 1988. "An Examination of the Role of Sampling Strategies in the Study of Suspended Sediment Transport." pp. 259-268, *Sediment Budgets*, IAHS Publ. 174, Wallingford, U.K.
- Olsen, N. R. B., Jimenez, O., Lovoll, A., and Abrahamsen, L., 1994. "Calculation of Water and Sediment Flow in Hydropower Reservoirs," *J. AHR Intl. Conf on Modeling, Testing and Monitoring of Hydropower Plants*, Budapest.
- Orvis, C. J., 1989. "Elephant Butte Reservoir 1988 Sedimentation Survey," Bureau of Reclamation, Denver.
- Osborn, T., 1993. "The Conservation Reserve Program: Status, Future and Policy Options," *J. Soil and Water Conservation*, 48 (4): 271-278.
- Osterman, D. A., and Hicks, T. L., 1988. "Highly Erodible Land: Farmer Perceptions versus Actual Measurements," *J. Soil and Water Conservation*. 43 (2): 177-181.
- Otsubo, K., and Muraoka, K., 1988. "Critical Shear Stress of Cohesive Bottom Sediments," *ASCE J. Hydraulic Engineering*, 114 (10): 1241-1256.
- Owens, P., and Slaymaker, O., 1994. "Post-glacial Temporal Variability of Sediment Accumulation in a Small Alpine Lake," pp. 187-195, *Variability in Stream Erosion and Sediment Transport*, IAHS Publ. 224, Wallingford, U.K.

- Owens, L. B., Edwards, W. M., and Vankeuren, R. W., 1996. "Sediment Losses from a Pastured Watershed Before and After Stream Fencing," *J. Soil and Water Conservation*. 51 (1): 90-94.
- Page, D., and Smith, G. F., 1993. "Interactive Forecasting with the National Weather Service River Forecast System," *Proc. Intl. Conf. Hydro Science and Engineering*, Washington, D.C.
- Pan, X., 1990. "A Summary on Erosion and Sedimentation in Sanmenxia Reservoir and Its Downstream Reaches on the Yellow River," Yellow River Commission, Beijing (in Chinese).
- Pansic, N., Austin, R. J., and Finis, M., 1995. "Sediment Management for Dam Decommissioning," pp. 29-46. In *15th Annual USCOLD Lecture Series*, USCOLD, Denver.
- Parhami, F., 1986. "Sediment Control Methods in Sefid-Rud Reservoir," pp. 1047-1055. In *Proc. 3d Intl. Symp. River Sedimentation*, U. Mississippi, Oxford.
- Partheniades, E., 1962. "A Study of Erosion and Deposition of Cohesive Soils in Salt Water," Ph.D. Diss., U. California. Berkeley.
- Partheniades, E., 1965. "Erosion and Deposition of Cohesive Soils," *J. Hydraulics Div. ASCE*. 91 (HY 1): 105-138.
- Partheniades, E., 1986. "The Present State of Knowledge and Needs for Future Research on Cohesive Sediment Dynamics," In *Proc. 3d Intl. Symp. River Sedimentation*, U. Mississippi, Oxford.
- Paul, T. C., and Dhillon, G. S., 1988. "Sluice Dimensioning for Desilting Reservoirs." *Water Power and Dam Construction* (May): 40-44.
- Peart, M. R., and Walling, D. E., 1986. "Fingerprinting Sediment Source: The Example of a Drainage Basin in Devon, U.K.," pp. 41-56. *Proc. Symp. Drainage Basin Sediment Delivery*, IAHS Publ. 159, Wallingford, U.K.
- Peart, M. R., 1989. "Methodologies Currently Available for the Determination of Suspended Sediment Sources: A Critical Review," pp. 150-157. In *Proc. 4th Intl. Symp. on River Sedimentation*, vol. 2. China Ocean Press, Beijing.
- Pemberton, E. L., 1976. "Channel Changes in the Colorado River Below Glen Canyon Dam," *3d Federal Interagency Sedimentation Conf.*, Water Resources Council, Washington, D.C.
- Pendergast, J., 1992. "RCC at 10," *Civil Engineering*, 62 (10): 44-47.
- Perez, L. R., Beinroth, F. H., and Jones, J. W., 1993. "AEGIS: Agricultural and Environment Geographic Information System," In *Proc. 32d Caribbean Food Crop Society*, Santo Domingo.
- Perrier, J., and Fruchart, F., 1995. "Expérience de la Compagnie Nationale de Rhone dans le Domaine de Erosion (choc, abrasion)." pp. 533-541, *Conf. Proc. Research and Development in the Field of Dams*. Swiss National Committee on Large Dams, Crans-Montana, Switzerland.
- Petersen, M. S., 1986. *River Engineering*. Prentice Hall, Englewood Cliffs, N.J.
- Petitjean, A., and Bouchard, J.-P., 1995. Personal communication. Electricité de France. Hydraulic Laboratory, Chateau.
- Petts, G. E., 1984. *Impounded Rivers: Perspectives for Ecological Management*. Wiley-Interscience, New York.
- Piest, R. F., Kramer, L. A., and Heinemann, H. G., 1975. "Sediment Movement from Loessial Watersheds," pp. 130-141. In *Present and Prospective Technology for Predicting Sediment Yields and Sources*. ARS-S-40. USDA Sedimentation Lab., Oxford, Miss.
- Piest, R. F., Bradford, J. M., and Spomer, R. G., 1975. "Mechanisms of Erosion and Sediment Movement from Gullies," pp. 162-176. In *Present and Prospective Technology for Predicting Sediment Yields and Sources*. ARS-S-40. USDA Sedimentation Lab., Oxford, Miss.
- Planning Associates. 1991. "Rock Creek-Cresta Dredging Project," Plumas County EIR No. 50, Quincy, Calif.
- Plate, E. J., 1993. "Sustainable Development of Water Resources: A Challenge to Science and Engineering," *Water International*. 18 (2): 84-94.
- Plumas Corp., 1996. Fact Sheets 1, 2, 3, 5 and 6. The Feather River Coordinated Resource Management Group, U. California Cooperative Extension, Quincy, Calif.
- Plumas County Water Agency. 1990. "Preliminary Feasibility Analysis of Alternative Sediment Management Options for Ralston Afterbay Reservoir," Foresthill, Calif.
- Postel, S., 1989. "Water for Agriculture: Facing the Limits." Worldwatch Paper 93. Worldwatch Institute, Washington, D.C.

- Postel, S., 1993. "Water and Agriculture," pp. 56-66. In Peter H. Gleick (editor), *Water in Crisis*. Oxford University Press, New York.
- PRASA (Puerto Rico Aqueduct and Sewer Authority), 1992. "Declaración de Impacto Ambiental Preliminar, Dragado del Lago Loíza," San Juan.
- PRASA (Puerto Rico Aqueduct and Sewer Authority), 1995. "Supplementary Preliminary Environment Impact Statement for the Carraízo Reservoir Dredging Project," San Juan. Prendergast, J., 1993. "Engineering Sustainable Development," *Civil Engineering*, 63 (10): 39-42.
- Przedwojski, B., Blazewski, R., and Pilarczyk, K. W., 1995. *River Training Techniques: Fundamentals, Design and Applications*. A. A. Balkema, Rotterdam.
- PSIAC (Pacific Southwest Interagency Committee), 1968. Report of the Water Management Subcommittee, "Factors Affecting Sediment Yield and Measures for Reduction of Erosion and Sediment Yield," mimeo.
- Puerto Rico Water Resources Authority, 1979. "Loíza Dam, Trujillo Alto, Puerto Rico: Phase 1- Inspection Report," National Dam Safety Program, San Juan.
- Qian, N., 1980. "Preliminary Study on the Mechanism of Hyperconcentrated Flow in Northwest Region of China," pp. 244-267, *Selected Papers, Symp. Sediment Problems on the Yellow River*, vol. 4 (in Chinese).
- Qian, N., 1982. "Reservoir Sedimentation and Slope Stability; Technical and Environmental Effects," pp. 639-690. In *Proc. 14th ICOLD Congress*, Río de Janeiro.
- Qian, N., Ren, Z., and Zhide, Z., 1987. *River Fluvial Mechanics*. Science Publishing House, Beijing (in Chinese).
- Queen, B. S., Rentschler, R. E., and Nordin, C. F., 1991. "Mississippi River Sediment Size Changes, 1932 to 1989," *5th Federal Interagency Sedimentation Conf., Las Vegas*.
- Quiñones-Aponte, V., 1991. "Water Resources Development and Its Influence on the Water Budget for the Aquifer System in the Salinas to Patillas Area, Puerto Rico," In F. Gómez-Gómez, V. Quiñones-Aponte, and A. I. Johnson (editors), *Aquifers of the Caribbean Islands*. American Water Resources Association, Bethesda, Md.
- Quiñones-Márquez, F., 1980. "Limnology of Lago Loíza, Puerto Rico," USGS Water Resources Investigations 79-97, San Juan.
- Ramey, M. P., and Beck, S. M., 1990. "Flushing Flow Study, North Fork of the Feather River Below Poe Dam," Pacific Gas and Electric Co., San Francisco.
- Ramírez, C., Machado, P., and Rodríguez, A., 1992. "The Reventazón River Basin: Natural Conditions and Technical Development." In M. B. Jansson and A. Rodríguez (editors), *Sedimentological Studies on the Cachí Reservoir, Costa Rica*, UNGI Report No. 81. Department of Physical Geogaphy, Uppsala U., Sweden.
- Ramírez, C., and Rodríguez, A., 1992. "History of the Cachí Reservoir." In M. B. Jansson and A. Rodríguez (editors). *Sedimentological Studies on the Cachí Reservoir*, Costa Rica. UNGI Report No, 81, Department of Physical Geography, Uppsala U., Sweden.
- Randle, T. J., and Lyons, J. K., 1995. "Elwha River Restoration and Sediment Management," pp. 47-62. In *15th Annual USCOLD Lecture Series*, USCOLD, Denver.
- Raudkivi, A. J., 1993. *Sedimentation: Exclusion and Removal of Sediment from Diverted Water*. IAHR Hydraulic Structures Design Manual No. 6., A. A. Balkema, Rotterdam.
- Reiser, D. W., Ramey, M. P., and Wesche, T. A., 1988. "Flushing Flows," pp. 91-135, *Alternatives in Regulated River Management*. CRC Press, Boca Raton, Fla.
- Reiser, D. W., Ramey, M. P., Beck, S., Lambert, T. R., and Geary, R. E., 1989. "Flushing Flow Recommendations for Maintenance of Salmonid Spawning Gravels in a Steep, Regulated Stream," *Regulated Rivers: Research and Management* (3): 267-275.
- Ren, Z., 1986. "Experience on Operation Mode on Storing Clear Water and Releasing Muddy Water from Warping in Heisonglin Reservoir," In *Collected Papers of the Northwest Institute of Hydraulic Research*, vol. 2, Yangling (in Chinese).
- Renard, K. G., Laften, J. M., Foster, G. R., and McCool, D. K., 1994. "The Revised Universal Soil Loss Equation." In R. Lal (editor), *Soil Erosion Research Methods*. Soil and Water Conservation Society, Ankeny, Iowa.

- Renfro, G. W., 1975. "Use of Erosion Equations and Sediment-Delivery Ratios for Predicting Sediment Yield," pp. 33-45. In *Present and Prospective Technology for Predicting Sediment Yields and Sources*. ARS-S-40. USDA Sedimentation Lab., Oxford, Miss.
- Replogle, J. A., and Johnson, L. C., 1963. "Improved Measuring and Sampling Equipment for Sediment-laden Runoff," *Trans. ASCE*, 6 (3): 259-261.
- Resource Consultants and Engineers (RCE), 1992. "Geomorphological Assessment of Rock Creek and Reservoir System," report prepared for Pacific Gas and Electric Co., San Francisco.
- Rhoton, F. E., and Meyer, L. D., 1987. "Sediment Size Distributions Predicted for Selected Soils," *J. Soil and Water Conservation*, 42 (2): 127-129.
- Richardson, J. F., and Zaki, W. N., 1954. "Sedimentation and Fluidization, Pt. 1," *Trans. Institute Chemical Engineers*, 32: 35-53.
- Rickson, R. J., 1995. "Simulated Vegetation and Geotextiles." In R. P. C. Morgan and R. J. Rickson (editors), *Slope Stabilization and Erosion Control: A Bioengineering Approach*. E&FN Spon, London.
- Ritchie, J. C., McHenry, I. R., and Gill, A. C., 1973. "Dating Recent Reservoir Sediments," *Limnology and Oceanography*, 18 (2): 254-263.
- Ritchie, J. C., and McHenry, J. R., 1985. "Comparison of Three Methods for Measuring Recent Rates of Sediment Accumulation," *Water Resources Research*, 21 (1): 99-103.
- Ritchie, J. C., Cooper, C. M., and McHenry, R., 1986. "Sediment Accumulation Rates in Lakes and Reservoirs in the Mississippi River Valley," *3d Intl. Symp. on River Sedimentation*, U. Mississippi, Oxford.
- River Basin Planning Staff, 1989. "East Branch North Fork Feather River Erosion Inventory Report," USDA, Soil Conservation Service, Davis, Calif.
- Robertson, R. A., and Colletti, J. P., 1994. "Off-site Impacts of Soil Erosion on Recreation: The Case of Lake Red Rock Reservoir in Central Iowa," *J. Soil and Water Conservation*, 49 (6): 576-581.
- Rogers, C. S., 1990. "Response of Coral Reefs and Reef Organisms to Sedimentation," *Marine Ecology Progress Series*, 62: 185-202.
- Rooseboom, A., 1992. "Sediment Transport in Rivers and Reservoirs: A South African Perspective," Report to Water Research Commission of South Africa, by Sigma Beta Consulting Engineers, Stellenbosch.
- Rosgen, D., 1996. *Applied River Morphology*. Wildland Hydrology, Pagosa Springs, Colorado.
- Rubey, W. R., 1931. "Settling Velocities of Gravel, Sand and Silt Particles," *American J. Science*, 21: 325-338.
- Saaty, T. L., 1990. *Multicriteria Decision Making: The Analytical Hierarchy Process*. RWS Publication, Pittsburgh.
- Salas, J. D., Delleur, J. W., Yevjevich, V., and Lane, W. L., 1980. *Applied Modeling of Hydrologic Time Series*. Water Resources Publications, Littleton, Colo.
- Sanders, J. H., Southgate, D. D., and Lee, J. G., 1995. "The Economics of Soil Degradation: Technological Change and Policy Alternatives," SMSS Tech. Monograph 22, World Soil Resources. NRCS, USDA, Washington, D.C.
- Sanderson, W. H., 1992. "Dredging Contacts," pp. 9.100-9.118. In J. B. Herbich (editor), *Handbook of Dredging Engineering*. McGraw-Hill, New York.
- Sanmenxia Reservoir Hydrologic Experimental Station and IWHR, 1962. "Report on Density Currents Observed During 1961 in Sanmenxia Reservoir," Beijing (in Chinese).
- Saynor, M. H., Loughran, R. J., Erskine, W. D., and Scott, P. F., 1994. "Sediment Movement on Hillslopes Measured by Caesium-137 and Erosion Pins," pp. 87-93, *Variability in Stream Erosion and Sediment Transport*, IAHS Publ. 224, Wallingford, U.K.
- Scatena, F. N., and Larsen, M. C., 1991. "Physical Aspects of Hurricane Hugo in Puerto Rico," *Blotropica*, 23 (4a): 317-323.
- Scheuerlein, H., 1995. "Downstream Effects of Dam Construction and Reservoir Operation," pp. 1101-1108. *6th Intl. Symp. on River Sedimentation*, Central Board of Irrigation and Power, New Delhi.

- Schick, A. P., Lekach, J., and Hassan, M. A., 1987. "Bed Load Transport in Desert Floods: Observations in the Negev." In C. R. Thorne, J. C. Bathurst, and R. D. Hey (editors), *Sediment Transport in Gravel-Bed Rivers*. John Wiley and Sons, New York.
- Schiller, R. E. J., 1992. "Sediment Transport in Pipes." pp. 6.39-6.55. In J. B. Herbich (editor). *Handbook of Dredging Engineering*. McGraw-Hill Co., New York.
- Schnitter, N. I., 1994. *A History of Dams, the Useful Pyramids*. A. A. Balkema, Rotterdam.
- Schueler, T., 1987. "Controlling Urban Runoff: A Practical Method for Planning and Designing Urban BMPs," Metropolitan Washington Council of Governments, Washington, D.C.
- Schueler, T. R., Kumble, P. A., and Haraty, M. A., 1992. "A Current Assessment of Urban Best Management Practices, Techniques for Reducing Non-Point Source Pollution in the Coastal Zone," Metropolitan Washington Council of Governments, Washington, D.C.
- Schueler, T. R., 1993. "Design of Stormwater Wetland Systems: Guidelines for Creating Diverse and Effective Stormwater Wetlands in the Mid-Atlantic Region," Metropolitan Washington Council of Governments, Washington, D.C.
- Schumm, S. A., Harvey, M. D., and Watson, C. C., 1988. *Incised Channels: Morphology, Dynamics and Control*. Water Resources Publications, Littleton, Colo.
- Schwab, G. O., Fangmeir, D. D., Elliot, W. J., and Frevert, R. K., 1993. *Soil and Water Conservation Engineering*. 4th ed., John Wiley and Sons, New York.
- Senturk, F., 1994. *Hydraulics of Dams and Reservoirs*. Water Resources Publications, Highlands Ranch, Colo.
- Shaanxi Provincial Institute of Hydraulic Research and Faculty of Hydraulic Engineering, Quinghua U., 1978. *Reservoir Sedimentation*. Water Resources and Electric Power Press, Beijing.
- Shahin, M., 1989. "Review and Assessment of Water Resources in the Arab Region," *Water International*, 14 (4): 206-219.
- Shahin, M. M. A., 1993. "An Overview of Reservoir Sedimentation in some African River Basins," pp. 93-100, *Sediment Problems: Strategies for Monitoring, Prediction and Control*, IAHS Publ. 217, Wallingford, U.K.
- Shalash, S., 1983. "Degradation of the River Nile." *Water Power and Dam Construction* (July): 37-58.
- Shangle, A. K., 1991. "Hydrographic Surveys of Indian Reservoirs." Report by Central Water Commission for Workshop on Management of Reservoir Sedimentation, New Delhi.
- Shanholtz, V. O., Flagg, J. M., Metz, C. D., Desai, C. J., and Kleene, 1990. "Information Support Systems Laboratory (and VIRGIS Project) Overview," pp. 265-276, *Proc. Application of Geographic Information Systems, Simulation Models, and Knowledge-based Systems for Landuse Management*. Virginia Polytechnic Institute and State University, Blacksburg.
- Shaxson, T. F., 1988. "Conserving Soil by Stealth." In W. C. Moldenhauer and N. W. Hudson (editors), *Conservation Farming on Steep Lands*. Soil and Water Conservation Society, Ankeny, Iowa.
- Shiklomanov, I. A., 1993. "World Fresh Water Resources." In Peter H. Gleick (editor), *Water in Crisis*. Oxford University Press, New York.
- Shown, L. M., 1970. "Evaluation of a Method for Estimating Sediment Yield," USGS Prof. Paper 700-B, pp. 245-249.
- Sidle, R. C., and Hornbeck, J. W., 1991. "Cumulative Effects: A Broader Approach to Water Quality Research," *J. Soil and Water Conservation*, 46 (4): 268-271.
- Siebert, W., 1992. "Simulation of Erosion and Deposition of Coarse Material Below Iffezheim-Barrage, Rhine," pp. 1153-1174, *5th Intl. Symp. River Sedimentation*, Karlsruhe.
- Siever, R., 1988. *Sand*. W. H. Freeman, New York.
- Simons, D. B., and Richardson, E. V., 1966. "Resistance to Flow in Alluvial Channels," USGS Prof. Paper 422-1.
- Simons, D. B., and Simons, R. K., 1987. "Differences Between Gravel- and Sand-bed Rivers," pp. 3-15. In C. R. Thorne, J. C. Bathurst, and R. D. Hey, (editors), *Sediment Transport in Gravel-bed Rivers*. John Wiley and Sons, New York.

- Simons, R. K., and Simons, D. B., 1991. "Sediment Problems Associated with Dam Removal, Muskegon River, Michigan," *ASCE National Hydraulics Conf.*, Nashville, Tenn.
- Simons, D. B., and Senturk, F., 1992. *Sediment Transport Technology*. Water Resources Publications, Littleton, Colo.
- Simons Li & Assoc. Inc., 1982. *Engineering Analysis of Fluvial Systems*, Fort Collins, Colo.
- Singh, B., and Shan, C. R., 1971. "Plunging Phenomena of Density Currents in Reservoirs," *La Houille Blanche* (1): 59-64.
- Sinniger, R. O., DeCesare, G., and Martini, O., 1994. "Apports de Sédiments dans une Retenue par Courant de Densité - Measures in situ," pp. 85-98, *Trans. 18th ICOLD*, Q.69, R.7.
- Skelly, T. M., 1996. Personal communication. City of Springfield, Ill.
- Smith, R. M., and Stamey, W. L., 1965. "Determinating the Range of Tolerable Erosion." *Soil Science*, 100 (6): 414-424.
- Smith, N., 1971. *A History of Dams*. Citadel Press, Secaucus, N.J.
- Sogreah Consulting Engineers, 1974. Soil Conservation Studies in Sefid-Rud Catchment (in French).
- Soil Conservation Service, 1983. "Hydraulic Proportioning of Two-Way Covered Baffle Inlet Riser," Tech. Release No. 70, Washington, D.C.
- Sombroek, W. G., 1985. "Introduction to the Subject," pp. 1-7. *Intl. Symp. on Assessment of Soil Surface Sealing*. Ghent, Belgium.
- Stall, I. B., and Lee, M. T., 1980. "Reservoir Sedimentation and Its Causes in Illinois." *Water Resources Bulletin*, 16 (5): 874-880.
- Stanley Consultants, 1989. "Lake Francis Case Aggradation Study, 1953-1986," U.S. Army Corps of Engineers, Omaha.
- Stelczer, K., 1981. *Bed-load Transport Theory and Practice*. Water Resources Publications, Littleton, Colorado.
- Stonestreet, S. E., 1994. "San Timoteo Creek, California, Sedimentation Study: Numerical Model Investigation of In-Channel Sediment Basins," Misc. Paper HL-94-6. U.S. Army Corps of Engineers, Los Angeles District, Los Angeles.
- Strahler, A. N., 1957. "Quantitative Analysis of Watershed Geomorphology," *Trans. Am. Geophys. Union*, 38: 913-920.
- Strand, R. I., and Pemberton, E. L., 1987. "Reservoir Sedimentation," In *Design of Small Dams*. U.S. Bureau of Reclamation, Denver.
- Stutz, R. O., 1967. "The Bitsch Hydroelectric Scheme," *Water Power*, part 1, Nov. 1967, pp. 445-454, part 2, Dec. 1967, pp. 487-493.
- Styczen, M. E., and Morgan, R. P. C., 1995. "Engineering Properties of Vegetation." pp. 5-58. In R. P. C. Morgan and R. J. Rickson (editors). *Slope Stabilization and Erosion Control: A Bioengineering Approach*. E&FN Spoil. London.
- Summer, W., Klaghofer, E., Abi-Zeid, I., and Villeneuve, J. P., 1992. "Critical Reflections on Long Term Sediment Monitoring Programmes Demonstrated on the Austrian Danube," *Erosion and Sediment Transport Monitoring Programmes in River Basins*, IAHS Publ. 210, Wallingford, U.K.
- Summer, W., Stritzinger, W., and Zhang, W., 1994. "The Impact of Run-of-river Hydropower Plants on the Temporal Suspended Sediment Transport Behavior," pp. 411-419, *Variability in Stream Erosion and Sediment Transport*, IAHS Publ. 224. Wallingford, U.K.
- Sundborg, A., and Jansson, M. B., 1992. "Present and Future Conditions of Reservoir Sedimentation." In M. B. Jansson and A. Rodríguez. (editors), *Sedimentological Studies on the Cachí Reservoir, Costa Rica*. UNGI Report No. 81. Department of Physical Geography, Uppsala University, Sweden.
- Sundborg, A., 1992a, "Erosion Processes in the Cachí Reservoir during the Flushing Period in 1990," pp. 9-26. In M. A. Jansson and A. Rodríguez (editors), *Sedimentological Studies in the Cachí Reservoir, Costa Rica*, UNGI Report No. 81. Department of Physical Geography, Uppsala University, Sweden.

- Sundborg, A., 1992b, "Sedimentation in the Cachí Reservoir Illustrated by Mathematical Modeling." In M. B. Jansson and A. Rodríguez (editors), *Sedimentological Studies in the Cachí Reservoir, Costa Rica*, UNGI Rapport Nr. 81. Department of Physical Geography, Uppsala University, Sweden.
- Sutherland, R. A., and Bryan, R. B., 1988. "Estimation of Colluvial Reservoir Life from Sediment Budgeting, Katorin Experimental Basin, Kenya," pp. 549-560, *Sediment Budgets*, IAHS Publ. 174, Wallingford, U.K.
- Svendsen, M., 1991. "Sources of Future Growth in Indian Irrigated Agriculture." In R. Meinzen-Dick and M. Svendsen (editors), *Future Directions for Indian Irrigation: Research and Policy Issues*. International Food Policy Research Institute, Washington, D.C.
- Svendsen, M., and Rosegrant, M. W., 1994. "Irrigation Development in Southeast Asia Beyond 2000: Will the future be like the past?" *Water International* 19 (1): 25-35.
- Taconi, P., and Billi, P., 1987. "Bed Load Transport Measurement by the Vortex-tube Trap on Virginio Creek, Italy." In C. R. Thorne, J. C. Bathurst, and R. D. Hey (editors), *Sediment Transport in Gravel-Bed Rivers*. John Wiley and Sons, New York.
- Tang, R., and Lin, W., 1987. "A Study on Sedimentation Problems of the Gezhouba Project," *Intl. J. Sediment Research*, 1: 69-101.
- Tang, R., 1990. "Physical Modeling of Sediment," pp. 183-221, *The Gezhouba Project Series No. 2*. Water Resources Power Press, Beijing (in Chinese).
- Tejwani, K. G., 1984. "Reservoir Sedimentation in India: Its Causes, Control and Future Course Action," *Water International* 9 (4): 150-154.
- Thevenin, J., 1960. "La Sedimentation des barrages-reservoirs en Algerie et les moyens mis en oeuvre pour preserver les capacites." pp. 1277-1293, *Annales de l'institute Technique du Batiment a des Travaux*, no. 156.
- Thomas, W. A., and McAnally, W. H. J., 1985. "User's Manual for the Generalized Computer Program System Open-channel Flow and Sedimentation TABS-2," U.S. Army Waterways Experiment Station, Vicksburg, Miss.
- Thomas, R. B., 1985. "Estimating Total Suspended Sediment Yield with Probability Sampling," *Water Resources Research* 21 (9): 1381-1388.
- Thomas, R. B., and Lewis, J., 1993. "A Comparison of Selection at List Time and Time-Stratified Sampling for Estimating Suspended Sediment Loads," *Water Resources Research* 29 (4): 1247-1256.
- Thomas, R. B., and Lewis, J., 1995. "An Evaluation of How-Stratified Sampling for Estimating Suspended Sediment Loads," *J. Hydrology* 170: 27-45.
- Thornton, K. W., Kennedy, R. H., Magoun, A. D., and Saul, G. E., 1982. "Reservoir Water Quality Sampling Design," *Water Resources Bulletin* (18): 471-480.
- Thornton, K. W., 1990. "Perspectives on Reservoir Limnology," pp. 1-13. In K. W. Thornton, B. L. Kimmel, and F. E. Payne (editors), *Reservoir Limnology*. John Wiley and Sons, New York.
- Toffaletti, F. B., 1963. "Deep River Velocity and Sediment Profiles and Suspended Sand Load," pp. 207-228, *Proc. Federal Interagency Sed. Conf.* USDA-ARS Misc. Publ. 970.
- Tolouie, E., 1989. "Reservoir Sedimentation and De-siltation," M.Phil. Thesis, U. Birmingham, U.K.
- Tolouie, E., 1993. "Reservoir Sedimentation and De-siltation," Ph.D. Thesis, U. Birmingham, U.K.
- Tolouie, E., 1996. Personal communication. Tehran.
- Torres, P. A., 1997. "Prediction of Flow Resistance Due to Vegetation," M.E. Thesis, U. Puerto Rico, Mayaguez.
- Trask, P., 1931. "Compaction of Sediment," *Bull. American Association of Petroleum Geologists*, 1S (11): 271-276.
- Trimble, S. W., 1974. *Man-Induced Soil Erosion on the Southern Piedmont, 1700-1970*. Soil Conservation Society of America, Ankeny, Iowa.
- Trimble, S. W., 1977. "The Fallacy of Stream Equilibrium in Contemporary Denudation Studies," *American J. Science*, 277: 876-887.

- Trimble, S. W., 1981. "Changes in Sediment Storage in Coon Creek Basin, Driftless Area, Wisconsin, 1853-1975." *Science*. 214 (9): 181-183.
- Trocino, I., 1991. Personal communication. Shock Wave Advanced Technology, Inc., Sherman Oaks, Calif.
- Tsuji, G. Y., Vehara, G., and Balas, S., 1994. "DSSAT (Decision Support System for Agrotechnology Transfer)," vol. 3, U. Hawaii, Honolulu.
- Turner, T. M., 1995. Personal communication. Turner Consulting, Sarasota, Fla.
- Turner, T. M., 1996. *Fundamentals of Hydraulic Dredging*, 2d ed. ASCE, New York.
- U.S. Army Corps of Engineers, 1981. "BRASS, Basin Runoff and Streamflow Simulation Model: User's Manual," Savannah District, Savannah, Ga.
- U.S. Army Corps of Engineers, 1982. HEC-5 Simulation of Flood Control and Conservation Systems." Hydrologic Engineering Center, Davis, Calif.
- U.S. Army Corps of Engineers, 1986. "Mount St. Helens, Washington: Toutle, Cowlitz and Columbia Rivers," Sedimentation Design Memorandum No. 3, Portland District.
- U.S. Army Corps of Engineers, 1987. "Confined Disposal of Dredged Material," EM 1110-2-5027, Washington, D.C.
- U.S. Army Corps of Engineers, 1988. "GRASS: Geographic Resource Analysis Support System," Ver. 3.0, Construction Engineering Research Laboratory, Champaign, Ill.
- U.S. Army Corps of Engineers, 1989. "Sedimentation Investigations of Rivers and Reservoirs," Engineering Manual 1110-2-4000, Washington, D.C.
- U.S. Army Corps of Engineers, 1990. "HEC-2 Water Surface Profiles, User's Manual." U.S. Army Corps of Engineers, Hydrologic Engineering Center, Davis, Calif.
- U.S. Army Corps of Engineers, 1991. "HEC-6 Scour and Deposition in Rivers and Reservoirs, User's Manual," Hydrologic Engineering Center, Davis, Calif.
- U.S. Army Corps of Engineers, 1992. "Debris Method: Los Angeles District Method for Prediction of Debris Yield," Los Angeles.
- U.S. Army Corps of Engineers, 1992. "UNET: One-dimensional Unsteady Flow Through a Full Network of Open Channels," Hydrologic Engineering Center, Davis, Calif.
- U.S. Army Corps of Engineers, 1995. "HEC-RAS River Analysis System, User's Manual," Hydrologic Engineering Center, Davis, Calif.
- U.S. Department of Agriculture, 1977. "Procedure for Determining Rates of Land Damage, Land Depreciation and Volume of Sediment Produced by Gully Erosion," pp. 125-141. In *Guidelines for Watershed Management*, FAO Conservation Guide No. 1, Rome.
- U.S. Department of Interior, 1994. "The Elwha River Report, Restoration of the Elwha River Ecosystem and Native Anadromous Fisheries," report submitted pursuant to PL 102-495 by Department of the Interior and Department of Commerce, Washington. D.C.
- U.S. EPA (U.S. Environmental Protection Agency), 1986. "Methodology for Analysis of Detention Basins for Control of Urban Runoff Quality," EPA440/5-87-001.
- U.S. Forest Service, 1980. "An Approach to Water Resources Evaluation of Non-point Silvicultural Sources: A Procedural Handbook," In EPA-600/8-80-012, Environmental Protection Agency, Washington, D.C.
- Ullmann, F., 1970. "Particular Features of the Gebidem Dam of the Massa Hydroelectric Scheme," *World Dams Today*. pp. 199-206.
- Urbonas, B., and Stahre, P., 1993. *Stormwater Best Management Practices and Detention*. PTR Prentice Hall, Englewood Cliffs, N.J.
- Urlapov, G. A., 1977. "Irrigation Reservoir that Silts up Insignificantly," *Soviet Hydrology: Selected Papers*. 16 (3): 256-258.
- USCOLD, 1978. *Environmental Effects of Large Dams*. ASCE, New York.
- U.S. Geological Survey (USGS), 1978. "Sediment," Chap. 3, *National Handbook of Recommended Methods for Water Data Acquisition*. U.S. Geological Survey, Reston, Va.
- Van Den Wall Bake, G. W., 1986. "The Siltation and Erosion Survey in Zimbabwe: Drainage Basin Sediment Delivery." pp. 69-80, *Drainage Basin Sediment Delivery*. IAHS Publ. 159. Wallingford, U.K.
- Vanoni, V. A., Brooks, N. H., and Kennedy, J. F., 1960. "Sediment Transportation and Channel Stability," Report No. KH-R-I. W. M. Keck Laboratory of Hydraulics and Water Resources, California Institute of Technology, Pasadena.

- Vanoni, V. A., 1975. *Sedimentation Engineering*. ASCE, New York.
- Varma, C. V. J., Rao, A. R. G., and Natarajan, S., 1992. "Sedimentation of Indian Reservoirs. An Assessment," pp. 919-923, *Proc. 5th Intl. Symp. River Sedimentation*. Karlsruhe.
- Veltrop, J. A., 1992. "The Role of Dams in the 21st Century," U. S. Committee on Large Dams, Denver.
- Vieux, B. E., and Kang, Y. T., 1990. "GRASS Waterworks: A GIS Toolbox for Watershed Hydrologic Modeling," In *Proc. on Application of Geographic Information Systems, Simulation Models, and Knowledge-based Systems for Landuse Management*. Virginia Polytechnic Institute and State University, Blacksburg.
- Vitousek, P. M., Ehrlich, P. R., Ehrlich, A. H., and Matson, P. A., 1986. "Human Appropriation of the Products of Photosynthesis," *Bioscience*, 36: (6) 368-373.
- Wada, A., 1995. "Japan's Experience in Reservoir Sediment Management," Intl. Reservoir Sedimentation Workshop, San Francisco. Federal Energy Regulatory Commission, Washington, D.C.
- Wadsworth, F., 1990. "Notes on the Climax Forests of Puerto Rico and Their Destruction and Conservation Prior to 1900." *Caribbean Forester*, 11 (1): 38-47.
- Walkotten, W. J., 1976. "An Improved Technique for Freeze-Sampling Streambed Sediments." Res. Note PNW-281, USDA Forest Service. Pacific Northwest Forest and Range Experimental Station. Portland, Ore.
- Walling, D. E., 1977. "Limitations of the Rating Curve Technique for Estimating Suspended Sediment Loads, with Particular Reference to British Rivers," pp. 34-48. *Erosion and Solid Matter Transport in inland Waters Symp.*, IAHS Publ. 122, Wallingford, U.K.
- Walling, D. E., and Kleo, A. H., 1979. "Sediments Yields of Rivers in Areas of Low Precipitation: A Global View," pp. 479-493, *The Hydrology of Areas of Low Precipitation*, IAHS Publ. 128, Wallingford, U.K.
- Walling, D. E., and Webb, B. W., 1981. "The Reliability of Suspended Sediment Load Data," pp. 177-194, *Erosion and Sediment Transport Measurement Symp.*, IAHS Publ. 133, Wallingford, U.K.
- Walling, D. E., 1983. "The Sediment Delivery Problem," *J. Hydrology*, 65: 209-237.
- Walling, D. E., 1984. "The Sediment Yields of African Rivers," pp. 265-283, *Challenges in African Hydrology and Water Resources Planning*, IAHS Publ. 144, Wallingford, U.K.
- Walling, D. E., and Webb, B. W., 1988. "The Reliability of Rating Curve Estimates of Suspended Sediment Yield: Some Further Comments," pp. 337-350, *Sediment Budgets*, IAHS Publ. 174, Wallingford, U.K.
- Walling, D. E., and Quine, T. A., 1992. "The Use of Caesium-137 Measurements in Soil Erosion Surveys," pp. 143-152, *Erosion and Sediment Transport Monitoring Programmes in River Basins*, IAHS Publ. 210, Wallingford, U.K.
- Walling, D. E., and Woodward, J. C., 1992. "Use of Radiometric Fingerprints to Derive Information on Suspended Sediment Sources," pp. 153-164, *Erosion and Sediment Transport Monitoring Programmes in River Basins*, IAHS Publ. 210, Wallingford, U.K.
- Walling, D. E., 1994. "Measuring Sediment Yield from River Basins." In R. Lal (editor), *Soil Erosion Research Methods*. Soil and Water Conservation Society, Ankeny, Iowa.
- Wan, Z., and Wang, Z., 1994. *Hyperconcentrated Flow*, IAHR Monograph, A. A. Balkema, Rotterdam.
- Wang, W. C., Tsai, C. T., Hsu, S. K., and Hsieh, C. D., 1995. "Evaluation of Alternatives for Reservoir Sediment Removal: A Case Study," pp. 381-387. In 15th Annual USCOLD Lecture Series, USCOLD, Denver.
- Ward, T. J., 1985. "Sediment Yield Modeling of Roadways," pp. 188-199. In S. A. El-Swaify, W. C. Moldenhauer, and A. Lo (editors), *Soil Erosion and Conservation*. Soil Conservation Society of America, Ankeny, Iowa.
- Washburn, E. W., 1928. *International Critical Tables of Numerical Data, Physics, Chemistry and Technology*, National Research Council of USA. McGraw-Hill, New York.

- Webb, R. M. T., and Gómez-Gómez, F., 1996. "Sedimentation Survey of Lago Dos Bocas, Puerto Rico. August 1994," Water-Resources Investigations Report 95-4214, USGS, San Juan.
- Webb, R. M. T., and Soler-López, L. R., 1997. "Sedimentation History of Lago Loíza 1953-1994." USGS, San Juan.
- Weiss, E. B., 1993. "Intergenerational Fairness and Water Resources" pp. 3-10. In *Sustaining Our Water Resources*. Water Science and Technology Board 10th Anniversary Symp. National Academy Press, Washington, D.C.
- Wenner, C. G., 1988. "The Kenyan Model of Soil Conservation," pp. 197-206, *Conservation Farming on Steep Lands*. Soil and Water Conservation Society, Ankeny, Iowa.
- Westrich, B., and Al-Zoubi, S., 1992. "Planning and Designing a Flushing Channel for River Reservoir Sediment Management." pp. 861-867, *Proc. 5th Intl. Symp. River Sediment Management*. Karlsruhe.
- Wetzel, R. G., 1983. *Limnology*. Saunders College Publishing, New York.
- White, C. M., 1940. "The Equilibrium of Grains on the Bed of a Stream," *Proc. Royal Society, Series A, Mathematical and Physical Sciences*, 174 (958).
- White, F. M., 1979. *Fluid Mechanics*. McGraw-Hill, New York.
- Whitlock, B., and Loughran, R. J., 1994. "Sediment Production and Storage in an Urbanizing Basin: Lake Macquarie, New South Wales, Australia," pp. 103-110. *Variability in Stream Erosion and Sediment Transport*. IAHS Publ. 224, Wallingford. U.K.
- Wilcock, P. R., and McArde, B. W., 1993. "Surface-based Frictional Transport Rates: Mobilization Thresholds and Partial Transport of a Sand-gravel Sediment," *Water Resources Research*, 29 (40): 1297-1312.
- Wilkins, D. C., and Hebei, S. J., 1982. "Erosion, Redeposition and Delivery of Sediment to Midwestern Streams," *Water Resources Research*, 18 (4): 1278-1282.
- Williams, D. T., and Julien, P. Y., 1989. "Applicability Index for Sand Transport Equations," *J. Hyd. Div. ASCE*, 115 (11): 1578-1581.
- Williams, D. T., 1990. "Review and Selection of Sediment Transport Functions," Mimeo, *Sediment Transport in Rivers and Reservoirs Short Course*, Hydrologic Engineering Center, Davis, Calif.
- Williams, D. T., Austin, D. N., and Theisen, M. S., 1996. "Erosion Protection of Channels Using Permanent Geosynthetic Reinforcement Matting," pp. 111.54-61, 6th Federal Interagency Sedimentation Conf., Las Vegas.
- Williams, G. P., and Wolman, M. G., 1984. "Downstream Effects of Dams on Alluvial Rivers," USGS Prof. Paper 1286, Washington, D.C.
- Williams, G. P., 1989. "Sediment Concentration Versus Water Discharge During Single Hydrologic Events in Rivers," *J. Hydrology*. 111: 89-106.
- Williams, J. R., 1984. "The Physical Components of the EPIC Model," pp. 272-284. In S. A. El-Swaify, W. C. Moldenhauer, and A. Lo (editors), *Soil Erosion and Conservation*. Soil Conservation Society of America, Ankeny, Iowa.
- Willis, J., Tuttle, J., Bowie, A., and Darden, R., 1989. "Seasonal Effects on Sediment Transport," pp. 730-737, *Proc. 4th Intl. Symp. River Sedimentation*, Beijing.
- Winterstein, T. A., 1986. "Effects of Nozzle Orientation on Sediment Sampling," pp. 20-28, 4th Federal Interagency Sedimentation Conf.
- Wischmeier, W. H., and Smith, D. D., 1958. "Rainfall Energy and its Relation to Soil Loss," *Trans. American Geophysical Union*, 39 (2): 285-291.
- Wischmeier, W. H., and Smith, D. D., 1965. Predicting Rainfall-erosion Losses from Cropland East of the Rocky Mountains. *Agricultural Handbook No. 282*. USDA, Washington, D.C.
- Wischmeier, W. H., 1976. "Use and Misuse of the Universal Soil Loss Equation," *J. Soil and Water Conservation*, 31(1): 5-9.
- Wisconsin Department of Natural Resources, 1990. "Forest Practice Guidelines for Wisconsin," Madison.

- WMO (World Meteorological Organization), 1981a. "Measurements of River Sediments," Operational Hydrology Report No. 16, WMO No. 561, Geneva.
- WMO (World Meteorological Organization), 1981b. "Guide to Hydrological Practices," WMO No. 168, Geneva.
- WMO (World Meteorological Organization). 1990. "Simulated Real-Time Intercomparison of Hydrological Models," Operational Hydrology Report No. 38, WMO-No. 779, Geneva. Wolman, M. G., 1954. "A Method of Sampling Coarse River-bed Material," *Trans. American Geophysical Union*, 35: 951-956.
- Woodward-Clyde Consultants, 1994. "North Avenue Dam Feasibility Study, Milwaukee, Wisconsin," Report prepared for State of Wisconsin, Department of Natural Resources, Madison.
- Wright, J. C., 1967. "Effect of Impoundments on Productivity, Water Chemistry, and Heat Budgets of Rivers," *Reservoir Fishery Resources*, Am. Fish. Soc., Washington, D.C.
- Wu, C. M., 1991. "Reservoir Capacity Preserving Practice in Taiwan," pp. 10.75-10.81, *Proc. 5th Federal Interagency Sedimentation Conf.*, Las Vegas.
- Wuhan College of Hydropower, 1982. *Fluvial and Sedimentation Engineering*. Water Resources Publishing, Beijing (in Chinese).
- Xia, M., and Ren, Z., 1980. "Methods of Sluicing Sediment from Heisonglin Reservoir and Its Utilization Downstream," *Proc. Intl. Symp. River Sedimentation*, vol. 2. Guanghai Press. Beijing (in Chinese).
- Xia, M. (editor). 1983. *Sediment Problems in Design and Operation of Medium and Small Size Reservoirs*. Science Press, Beijing (in Chinese).
- Xia, M., 1984. "Sediment Regulation in Reservoirs on Heavily Sediment-laden Rivers," *Yellow River* (5): 3-8 (in Chinese).
- Xia, M., 1986. "New Desilting Method Used in Heisonglin Reservoir: Lateral Erosion on Floodplain," In *Collected Research Papers, Northwest Institute of Hyd. Res.*, vol. 2, part 2, Yangling.
- Xia, M., 1987 and 1993. Personal communication. Northwest Institute of Hyd. Res., Yangling. Xia, M., 1989. "Lateral Erosion, A Storage Recovery Technique for Silted-up Reservoirs," pp. 1143-1149, *Proc. 4th Intl. Symp. River Sedimentation*, Beijing.
- Yalin, M. S., and Karahan, E., 1979. "Inception of Sediment Transport," *J. Hydraulics Division ASCE*, 105 (HY11): 1433-1443.
- Yang, C. T., 1973. "Incipient Motion and Sediment Transport," *J. Hyd. Div. ASCE*, 99 (10): 1679-1704.
- Yang, C. T., 1979. "Unit Stream Power Equations for Total Load," *J. Hydrology*, 40: 123-138.
- Yang, C. T., 1983. "Rate of Energy Dissipation and River Sedimentation," pp. 575-585, *2d Intl. Symp. River Sedimentation*, Nanjing, China.
- Yang, C. T., 1984. "Unit Stream Power Equation for Gravel," *J. Hyd. Div. ASCE*, 110 (HY12): 1783-1798.
- Yang, C. T., and Wan, S., 1991. "Comparisons of Selected Bed-Material Load Formulas," *ASCE J. Hydraulic Engineering*, 117 (8): 973-989.
- Yang, C. T., 1996. *Sediment Transport: Theory and Practice*. McGraw-Hill, New York.
- Yang, M., and Wang, G., 1996. "Formulas for Incipient Motion of Mud with Various Densities," *Intl. J. Sediment Research*, 11 (1): 34-42.
- Yuzyk, T. R., Gunner, W. D., and Churchland, L. M., 1992. "A Comparison of Methods used to Measure Suspended Sediment in Canada's Federal Monitoring Programs," pp. 289-297, *Erosion and Sediment Transport Monitoring Programmes in River Basins*, IAHS Publ. 210, Wallingford, U.K.
- Zarn, B., 1992. "Numerical Simulation of Sediment Management in Reservoir Planning along the River Rhine Upstream of Lake Constance," pp. 853-860, *Proc. 5th Intl. Symp. River Sedimentation*, Karlsruhe.
- Zhang, H., Xia, M., Chen, S. -J., Li, Z. -W., and Xia, H. -B., 1976. "Regulation of Sediments in Some Medium and Small-sized Reservoirs on Heavily Silt-laden Streams in China." pp. 1223-1243, *12th ICOLD*. Q.47. R.32, Mexico City.

- Zhang, Q., and Long, Y., 1980. "Sediment Problems of Sanmenxia Reservoir," pp. 707-716, *Proc. Intl. Symp. River Sedimentation*. vol. 2., Guanghai Press. Beijing (in Chinese).
- Zhang, C., Tang, Z., Feng, J., and Zhou, B., 1992. "Review about Measures of Sand Drainage and Reducing Silt at the Hongqi Reservoir," pp. 815-819. *Proc. 5th Intl. Symp. River Sedimentation*, Karlsruhe.
- Zhang, G., 1993. "An Experimental Study on the Form of Headwater Erosion in Reservoirs," *J. Sediment Research* (3): 86-94 (in Chinese).
- Zhang, R., and Qian, N., 1995. *Reservoir Sedimentation*, Lecture Notes of the Training Course on Reservoir Sedimentation. IRTCES, Beijing.
- Zhou, Z., 1993. "Remarks on Reservoir Sedimentation in China," pp. 153-160. In S. S. Fan and G. Morris (editors), *Notes on Sediment Management in Reservoirs: National and International Perspectives*. Federal Energy Regulatory Commission, Washington, D.C.

# APPENDIXES

---

- A. Properties of Water, International Units
- B. Properties of Water, U.S. Customary or British Units
- C. Gravitational Constant
- D. Unit Prefixes
- E. Greek Alphabet
- F. International and Derived Units of Measure
- G. Units of Measure in British or U.S. Conventional Units
- H. Table of Unit Conversions
- I. Density of Water or Water-Sediment Mixtures
- J. Stream Power

## **A. PROPERTIES OF WATER, INTERNATIONAL UNITS**

Temperature °C	Specific Weight $\gamma$ (kN/m <sup>3</sup> )	Density $\rho$ (kg/m <sup>3</sup> )	Viscosity $\mu \times 10^3$ (N-s/m <sup>2</sup> )	Kinematic viscosity $\nu \times 10^6$ (m <sup>2</sup> /s)
0	9.805	999.8	1.781	1.785
4	9.807	1000.0	1.567	1.567
10	9.804	999.7	1.307	1.306
15	9.798	999.1	1.139	1.139
20	9.789	998.2	1.002	1.003
25	9.777	997.0	0.890	0.893
30	9.764	995.7	0.798	0.800
40	9.730	992.2	0.653	0.658

## B. PROPERTIES OF WATER, U.S. CUSTOMARY OR BRITISH UNITS

Temperature °F	Specific Weight $\rho$ (lb/ft <sup>3</sup> )	Density $\rho$ (slugs/ft <sup>3</sup> )	Viscosity $\mu \times 10^3$ (lb-s/ft <sup>2</sup> )	Kinematic viscosity $\nu \times 10^6$ (ft <sup>2</sup> /s)
0	62.42	1.940	3.746	1.931
4	62.43	1.941	3.229	1.664
10	62.41	1.940	2.735	1.410
15	62.37	1.938	2.359	1.217
20	62.30	1.936	2.050	1.059
25	62.22	1.934	1.799	0.930
30	62.11	1.931	1.595	0.826
40	62.00	1.927	1.424	0.739

## C. GRAVITATIONAL CONSTANT

The gravitational constant  $g$  has a defined value of  $9.806 \text{ m/s}^2$  or  $32.17 \text{ ft/s}^2$ . Its true value varies slightly as a function of location and elevation.

## D. UNIT PREFIXES

Multiple	Prefix	Symbol	Example
$10^9$	giga	G	Gigawatt
$10^6$	mega	M	Megaton
$10^3$	kilo	k	kilometer
$10^2$	hecto	h	hectare
$10^{-1}$	deci	d	Decimeter
$10^{-2}$	centi	c	centimeter
$10^{-3}$	milli	m	millimeter
$10^{-6}$	micro	$\mu$	micrometer
$10^{-9}$	nano	n	nanogram

## E. GREEK ALPHABET

A	$\alpha$	alpha	N	$\nu$	nu
B	$\beta$	beta	$\xi$	$\xi$	xi
$\Gamma$	$\gamma$	gamma	O	o	omicron
$\Delta$	$\delta$	delta	$\Pi$	$\pi$	pi
E	$\epsilon$	epsilon	P	$\rho$	rho
Z	$\zeta$	zeta	$\Sigma$	$\sigma, \varsigma$	sigma
H	$\eta$	eta	T	$\tau$	tau
$\Theta$	$\theta$	theta	Y	$\upsilon$	upsilon
I	$\iota$	iota	$\Phi$	$\phi$	phi
K	$\kappa$	kappa	X	$\chi$	chi
$\Lambda$	$\lambda$	lambda	$\Psi$	$\psi$	psi
M	$\mu$	mu	$\Omega$	$\omega$	omega

## F. INTERNATIONAL AND DERIVED UNITS OF MEASURE

Parameter	Unit and symbol	Equivalence
International System of Measures, Selected Units:		
Length	meter, m	
Mass	kilogram, kg	
Time	second, s	
Temperature	degree Kelvin, K	
Selected Supplementary and Derived Units:		
Mass	gram, g	$10^{-3}$ kg
	ton, t	1000 kg
Length	kilometer, km	1000 m
	centimeter, cm	0.01 m
	millimeter, mm	$10^{-3}$ m
	micron, $\mu\text{m}$	$10^{-6}$ m
	Ångstrom, Å	$10^{-10}$ m
Temperature	degree centigrade, °C	
Area	Hectare, ha	$10^4$ m <sup>2</sup>
	km <sup>2</sup>	$10^6$ m <sup>2</sup>
Volume	liter, L	$10^{-3}$ m <sup>3</sup>
	hectare-meter	$10^4$ m <sup>3</sup>
	million m <sup>3</sup> , Mm <sup>3</sup>	$10^6$ m <sup>3</sup>
	cubic kilometer	$10^9$ m <sup>3</sup>
Density	kg/m <sup>3</sup>	1000 g/cm <sup>3</sup>
	g/cm <sup>3</sup>	0.001 kg/m <sup>3</sup>
Force	Newton, N	1 kg•m/s <sup>2</sup>
Pressure	Pascal, Pa	1 N/m <sup>2</sup>
Kinematic viscosity*	m <sup>2</sup> /s	
Dynamic or absolute viscosity	N s/m <sup>2</sup>	
Work, energy	Joule, J	1 N•m
	calorie, cal	4.1868 J
Power	Watt, W	1 J/s
Time	day, d	86,400 s

NOTE: For additional explanations see Sec. 3.5.3 for power and energy, and Sec. 9.1 for pressure, viscosity, mass and weight.

\*Kinematic viscosity is dynamic viscosity divided by fluid density.

## G. UNITS OF MEASURE IN BRITISH OR U.S. CONVENTIONAL UNITS (FPS SYSTEM)

	Unit and abbreviation	Equivalence
Length	foot, ft	12 inches
	mile, mi	5280 ft
	yard, yd	3 ft
Area	acre, ac	43,560 ft <sup>2</sup>
	square mile, mi <sup>2</sup>	640 ac
Volume	U.S. gallon, gal	0.13368 ft <sup>3</sup>
	U.S. gallon	0.8327 British gallon
	cubic foot, ft <sup>3</sup>	7.4806 gal
	acre-foot	43,560 ft <sup>3</sup>
Mass	pound, lb	
	slug	32.174 lb
	short ton	2000 lb
Force	poundal, pdl	1.0 ft•lb/s <sup>2</sup>
	pound-force, lbf	32.17 pdl
Pressure	lbf/in <sup>2</sup> , psi	
Dynamic viscosity	pdl s/ft <sup>2</sup>	
Work, Energy	foot-pound, ft•lbf	
	1 BTU	778.2 ft•lbf
Power	Horsepower, hp	550 ft•lbf/s

NOTE: The *slug* is the unit of mass in the British system, and corresponds the mass that can be accelerated by 1 ft/s<sup>2</sup> by applying 1 pound-force. Under the force of gravity, one slug produces 32.17 pounds of force. The term *pound (lb)* is also used as a unit of mass in the British system, and is differentiated from the *pound-force (lbf)* unit. The *poundal (pdl)* is also used as a force unit in the British system.

## H. TABLE OF UNIT CONVERSION FACTORS

To convert Col. A to Col. B,  $B = A \cdot F_A = A/F_B$   
 To convert Col. B to Col. A,  $A = B \cdot F_B = B/F_A$

Col. A	Col. B	$F_A$	$F_B$
<b>LENGTH</b>			
feet, ft	meters, m	0.3048	3.2808
inches, in	centimeters, cm	0.3937	2.540
miles, mi	kilometers, km	1.6093	0.6214
<b>AREA</b>			
square foot, ft <sup>2</sup>	square meters, m <sup>2</sup>	0.0929	10.764
acres, ac	hectares, ha	0.4047	2.471
square mile, mi <sup>2</sup>	square kilometer, km <sup>2</sup>	2.590	0.3861
square mile, mi <sup>2</sup>	hectares, ha	259.0	0.00386
<b>VOLUME</b>			
cubic feet, ft <sup>3</sup>	cubic meters, m <sup>3</sup>	0.0283	35.31
gallons, gal	liters, L	3.785	0.2642
gallons, gal	cubic meters, m <sup>3</sup>	0.00378	264.2
acre-feet, af	cubic meters, m <sup>3</sup>	1233.5	0.0008107
thousand acre-feet	million cubic meters, Mm <sup>3</sup>	1.2335	0.8107
<b>FLOW RATE or DISCHARGE</b>			
cubic feet/s, cfs, cusec	cubic meters/s, m <sup>3</sup> /s	0.0283	35.31
cubic feet/s, cfs, cusec	million gallons/d, mgd	0.6463	1.547
million gal/d, mgd	cubic meters/s, m <sup>3</sup> /s	0.0438	22.82
million gal/d, mgd	gal/min, gpm	694	0.00144
gallons/min, gpm	liters/s, L/s	0.0631	15.85
<b>MASS</b>			
slug	kilogram, kg	14.59	0.0685
pound-mass, lb	kilogram, kg	0.45359	2.2046
short ton	tons, t	0.9072	1.1023
<b>FORCE</b>			
pound-force, lbf	Newtons, N	4.4482	0.2248
<b>PRESSURE OR STRESS</b>			
g/m <sup>2</sup>	Pascal, N/m <sup>2</sup>	0.009806	102.0
lbf/ft <sup>2</sup>	Pascal, N/m <sup>2</sup>	47.88	0.0209
lbf/in <sup>2</sup>	Pascal, N/m <sup>2</sup>	6895	1.450 × 10 <sup>-4</sup>
dynes/cm <sup>2</sup>	Pascal, N/m <sup>2</sup>	0.1	10
<b>WORK or ENERGY (the product of force and distance)</b>			
ft-lbf	Joule, J	1.3558	0.7376
<b>POWER (the rate of energy dissipation)</b>			
Horsepower, hp	watt, W	745.7	0.00134
ft-lbf/s	watt, W	1.356	0.7376
<b>TEMPERATURE</b>			
°C = (F - 32)/1.8			
°F = 1.8 C + 32			
°K = C + 273.15			

## I. DENSITY OF WATER OR WATER-SEDIMENT MIXTURES

---

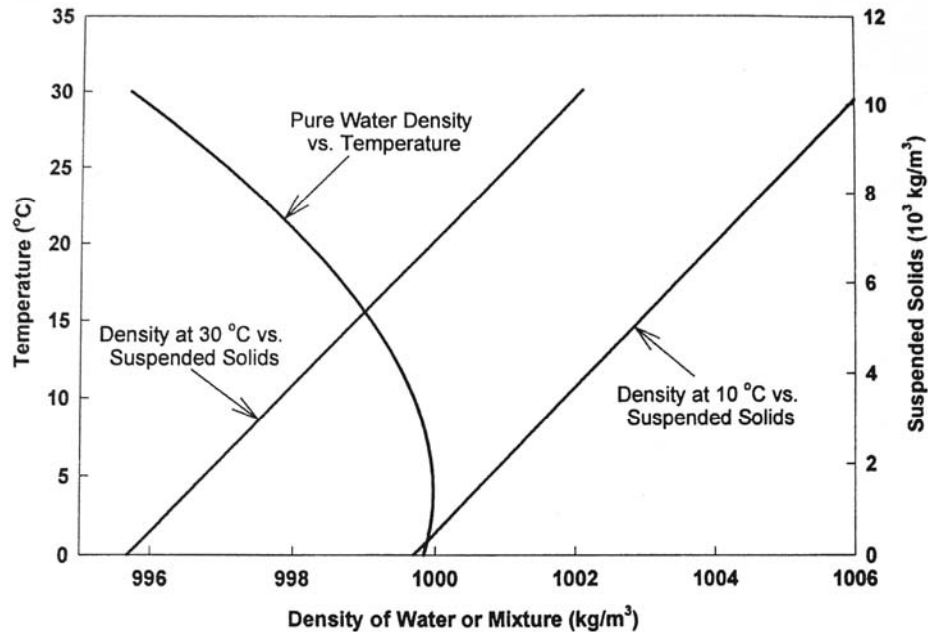


**FIGURE App I.1** Density of pure water vs. temperature, and of water-sediment mixtures as a function of suspended solids concentration at two different water temperatures. These graphs are computed from the equations given in Section 4.2.3.

## J. STREAM POWER

---

Stream power is an important concept in sediment transport, and is the basis for several methods to estimate the initiation of erosion, to determine the rate of transport of bed material load (see Secs. 9.7.5, 9.7.6, and 9.9.3). Chang (1988) has hypothesized that the geomorphic form of alluvial channels evolves in a way that minimizes stream power per unit channel length. This appendix presents basic stream power relations, using the definitions and units presented below and in Sec. 9.1.

$D$  = depth (m)

$B$  = breadth (width) of channel (m)

$\Delta E$  = change in energy grade line (m)

- $L$  = channel length (m)  
 $P$  = total power expenditure or rate of energy dissipation (W)  
 $Q$  =  $DBV$  = total discharge ( $\text{m}^3/\text{s}$ )  
 $q$  =  $Q/B$  = discharge per unit channel width ( $\text{m}^3/\text{s m} = \text{m}^2/\text{s}$ )  
 $S$  = slope of energy grade line (dimensionless)  
 $V$  = velocity (m/s)  
 $\gamma$  = gamma, the unit weight of fluid ( $\text{N}/\text{m}^3$ )  
 $\tau$  =  $\gamma DS$  = bed shear stress

Units are given in brackets [W = watts].

The rate of energy dissipation or the power of expenditure by flowing water is given by:

$$P = \gamma Q \Delta E \quad [\text{W}] \quad (J.1)$$

Thus, the total power expended by  $1 \text{ m}^3/\text{s}$  of water dropping through a 0.5 m vertical fall may be computed as:

$$P = (9810 \text{ N}/\text{m}^3)(1 \text{ m}^3/\text{s})(0.5 \text{ m}) 4905 \text{ W}$$

For flow along a channel let  $\Delta E = SL$  and  $Q = DBV$  so that:

$$P = \gamma QSL = \gamma(DBV)(SL) \quad [\text{W}] \quad (J.2)$$

Although in streams the bed slope or the water surface slope can be used to approximate the energy slope, this approximation may lead to unacceptable error when varying flow is being analyzed.

The rate of energy dissipation per unit of channel length may be computed by rearranging Eq. (J.2)

$$P/L = \gamma QS = [\text{W}/\text{m}] \quad (J.3)$$

The rate of energy dissipation may be computed per unit area of channel bed by rearranging Eq. (J.2) and substituting  $\tau = \gamma DS$

$$P/(BL) = \gamma DSV = \tau V \quad [\text{W}/\text{m}^2] \quad (J.4)$$

The rate of energy dissipation per unit weight of water is termed *unit stream power* and may also be obtained by rearranging Eq. (J.2)

$$P/(\gamma DBL) = VS \quad [\text{m}/\text{s}] \quad (J.5)$$